Ocean Engineering: A Wiley Series

EDITOR:
MICHAEL E. McCORMICK, Ph.D.
U.S. Naval Academy
ASSOCIATE EDITOR:
RAMESWAR BHATTACHARYYA, Dr.-Ing.
U.S. Naval Academy

Michael E. McCormick	Ocean Engineering Wave Mechanics
John B. Woodward	Marine Gas Turbines
H. O. Berteaux	Buoy Engineering
Clarence S. Clay and Herman Medwin	Acoustical Oceanography: Principles and Applications
Rameswar Bhattacharyya	Dynamics of Marine Vehicles

DYNAMICS OF MARINE VEHICLES

RAMESWAR BHATTACHARYYA
Director of Naval Architecture
U.S. Naval Academy
Annapolis, Maryland

A WILEY-INTERSCIENCE PUBLICATION

JOHN WILEY & SONS, New York · Chichester · Brisbane · Toronto

Copyright © 1978 by John Wiley & Sons, Inc.

All rights reserved. Published simultaneously in Canada.

Reproduction or translation of any part of this work beyond that permitted by Sections 107 or 108 of the 1976 United States Copyright Act without the permission of the copyright owner is unlawful. Requests for permission or further information should be addressed to the Permissions Department, John Wiley & Sons, Inc.

Library of Congress Cataloging in Publication Data:

Bhattacharyya, Rameswar.
Dynamics of marine vehicles.

(Ocean engineering, a Wiley series)
"A Wiley-Interscience publication."
Includes bibliographical references and index.
1. Ships—Seakeeping. I. Title.

VM156.B49 623.8'1 78-950
ISBN 0-471-07206-0

Photosetting by Thomson Press (India) Limited, New Delhi
Printed in the United States of America

10 9 8 7 6 5 4 3 2 1

This book is dedicated
to the memory of my revered teacher

PROFESSOR GEORG P. WEINBLUM
University of Hamburg, Germany

for his affection, encouragement, and inspiration.

SERIES PREFACE

Ocean engineering is both old and new. It is old in that man has concerned himself with specific problems in the ocean for thousands of years. Ship building, prevention of beach erosion, and construction of offshore structures are just a few of the specialties that have been developed by engineers over the ages. Until recently, however, these efforts tended to be restricted to specific areas. Within the past decade an attempt has been made to coordinate the activities of all technologists in ocean work, calling the entire field "ocean engineering." Here we have its newness.

Ocean Engineering: A Wiley Series has been created to introduce engineers and scientists to the various areas of ocean engineering. Books in this series are so written as to enable engineers and scientists easily to learn the fundamental principles and techniques of a specialty other than their own. The books can also serve as text books in advanced undergraduate and introductory graduate courses. The topics to be covered in this series include ocean engineering wave mechanics, marine corrosion, coastal engineering, dynamics of marine vehicles, offshore structures, and geotechnical or seafloor engineering. We think that this series fills a great need in the literature of ocean technology.

MICHAEL E. MCCORMICK, EDITOR
RAMESWAR BHATTACHARYYA, ASSOCIATE EDITOR
November 1972

CONTENTS

1. Introduction 1
2. Simple Harmonic Motion 4
3. Sinusoidal Water Waves 13
4. Uncoupled Heaving, Pitching, and Rolling Motions 35
5. Irregular Seaway 101
6. Motion in an Irregular Seaway 121
7. Dynamic Effects 137
8. Motion in Three-Dimensional Irregular Seaway 171
9. Coupled Heaving and Pitching Motions 183
10. Nonlinear Rolling Motion (Uncoupled) 208
11. Powering in a Seaway 220
12. Loads Due to Motion 240
13. Wave Loads 249
14. Motion Stabilization 278
15. Model Tests, Full-Scale Trials, and Scale Effects 308
16. Seakeeping Considerations in Design 331
17. Seakeeping of Advanced Marine Vehicles 396

Appendix A. Seakeeping Tables for Extended Series 60 Ships in Head Seas 427

Appendix B. Symbols 476

Glossary of Seakeeping Terms 478

Conversion Table 482

Abbreviations for References 484

References 485

Index 491

PREFACE

This book is based on lecture notes prepared for students of naval architecture, marine engineering, and ocean engineering at the University of Michigan, the U.S. Naval Academy, the Catholic University of America, the University of Veracruz, Mexico, and the Technical University at Guayaquil in Ecuador, over a period of 10 years. It must be emphasized that the literature presently available on the dynamics of marine vehicles is either more scientifically oriented or scattered in various publications not easily accessible to the common reader.

Primarily the book is intended as a textbook for a first course in seakeeping, and emphasis is therefore placed on the fundamentals of the subject matter. Through the use of numerous figures, tables, and solutions of exemplary problems, the aim is to help the reader in understanding the basic principles and to demonstrate the applicability of the methods outlined in the text, since I am strongly of the opinion that any treatise on an engineering discipline should consider its primary goal to be oriented toward numerical results. However, after the fundamentals have been grasped in this way, the reader can go on to study the advanced developments made in recent years for the purpose of obtaining more scientific, if not more accurate, solutions to actual problems.

The book is self contained; all essential material related to the topics covered has been defined and derived in the text. Also, the various chapters have been arranged in such a way that the reader becomes acquainted with the various topics step by step, and I followed strictly a course that would qualify the book to be self-taught with a basic knowledge of calculus. The chapters have been arranged to present a sequence of the physical phenomena necessary for a complete understanding of dynamics of marine vehicles (e.g., simple waves, linearized motion, nonlinear motion, coupled motion, the seaway, motions in an irregular seaway), and each chapter can be well understood with the knowledge acquired from studying the preceding chapters.

Along with the sophisticated marine systems, the design procedures for marine vehicles should not be limited to stability, structure, resistance, and propulsion; an integrated design criterion should also include a study of motion and maneuvering. It is not only desirable but also feasible to make accurate quantitative predictions of the seakeeping and maneuverability qualities of a marine vehicle when geometrical descriptions of the hull form, the weight distribution, and the necessary seaway conditions are available. To do this requires a good understanding of the fundamentals of the subject, the theories making it possible to justify all the assumptions necessary for quantitative answers, and a proper skill and ingenuity in the complex design process. This book has been written also with the idea that a design engineer will have ample opportunity to understand the basic principles and to follow the proper steps to improve the hull form for his specific design.

I should like to express my indebtedness to all the authors of the various publications listed in the bibliography. They have provided me with the necessary knowledge to write this book. Specifically I express my sincere gratitude to Rear Admiral R. W. King, USN (Ret.), and Professor M. E. McCormick of the U.S. Naval Academy, without whose encouragement and initiative this book could not have been written. Acknowledgments are due also to the students who have taken my course at the University of Michigan, the U.S. Naval Academy, the Catholic University of America, and the University of Veracruz in Mexico; especially Mr. D. Goldstein of the Naval Ship Engineering Center, Mr. F. Agdern of the Naval Facility Engineering Command, Ensign M. C. Tracy, and Señor R. Hernandez Valdes of the University of

Veracruz helped me throughout in the preparation of the manuscript.

I am grateful to Mrs. I. E. Johnson for superb typing and the necessary secretarial help from the very beginning. Particular thanks go also to Mrs. D. V. Christensen and Mrs. V. E. Stafford for their expert editorial assistance.

Any suggestions or corrections from readers in regard to any part of this book will be highly appreciated.

RAMESWAR BHATTACHARYYA

Annapolis, Maryland
January 1978

Acknowledgment is due to the following Organizations:

Royal Institution of Naval Architects

Figures 11–19, 13–11, 14–7, 14–18, 14–20b, 14–21, 14–23, 16–6, 16–12, 16–15, 16–16, 16–21, 16–29, 16–30, 16–41, 16–43, 16–44, 16–61, 16–62, 16–65, 16–67, 16–68, 17–10b

Tables 16.1 to 16.6, 16.8 to 16.10

Institution of Marine Engineers

Figure 17–10a

Association Technique Maritime at Aéronautique

Figure 9–13

Society of Naval Architects of Japan

Figures 4–27, 11–9, 11–10, 11–15 to 11–18, 15–18, 15–19

North East Coast Institution of Engineers and Shipbuilders

Figures 15–17, 16–1, 16–23

Schiffstechnik

Figure 9–14

Schiffbautechnische Gesellschaft

Figures 16–24 to 16–28

Royal Institution of Engineers (The Netherlands)

Figures 11–8, 16–18

Hamburgische Schiffbauversuchsanstalt

Figures 4–4, 4–6

Handbuch der Werften

Figures 4–5, 4–8, 4–21, 4–22

International Shipbuilding Progress

Figures 4–26, 4–28, 7–24, 9–6 to 9–8, 9–11, 13–2, 13–5, 13–6, 16–2 to 16–5, 16–7, 16–19, 16–20, 16–31, 16–32, 16–35, 16–36, 16–38

Society of Naval Architects and Marine Engineers

Figures 4–10, 4–23, 4–24, 4–31, 4–35, 4–39, 4–40, 6–4, 6–8, 6–9, 7–12, 7–19, 7–29, 8–3 to 8–6, 8–9 to 8–11, 9–5, 11–3a, 11–6, 13–7 to 13–10, 14–3a, 14–13, 16–2, 16–3, 16–5, 16–10, 16–13, 16–14, 16–17, 16–33, 16–34, 16–39, 16–40, 16–46, 16–48, 16–49, 16–51, 16–55 to 16–58, 16–63, 17–3 to 17–7, 17–15

Davidson Laboratory

Figure 17–14

Dynamics of Marine Vehicles

Chapter

One

INTRODUCTION

Ships are built for the purpose of carrying men, material, and/or weapons upon the sea. In order to accomplish its mission, a ship must possess several basic characteristics. It must float in a stable upright position, move with sufficient speed, be able to maneuver at sea and in restricted waters, and be strong enough to withstand the rigors of heavy weather and wave impact. To design a ship with these features, the naval architect must have an understanding of ship dynamics.

With a simple knowledge of hydrostatics a naval architect can produce a ship that will float upright in calm waters. However, ships rarely sail in calm water. Waves, which are the main source of ship motions in a seaway, affect the performance of a ship considerably and the success of a ship design depends ultimately on its performance in a seaway. Unfortunately, however, the prediction of ship motions, resistance and power, and structural loads in an actual seaway is such a complex problem that the naval architect is usually forced to select the hull form and ship dimensions on the basis of calm water performance without much consideration of the sea and weather conditions prevailing over the route on which the ship is to operate.

To study the effects of waves on ship dynamics it is logical that we should also understand ocean waves, which are not regular but highly complex in nature. Statistical means have been adopted to study this irregular behavior of the seaway and also to obtain ship motion characteristics.

It is not the motion characteristics per se that are important in the study of ship behavior in a seaway but rather the dynamic effects caused by the motions themselves. These effects are the shipping of green water on the deck, the emergence of the forefoot leading to slamming, and the effects of acceleration due to pitch, heave, or roll, or all combined.

When the relative movement of the bow and local wave surface become too great, water is shipped over the forecastle. The shipping of green water can have a very detrimental effect if watertight integrity is not maintained. Many of the electrical systems can be so damaged that they may not be functional. The freezing of green water on contact can stop a piece of apparatus on the weather decks from functioning and may seriously impair the fighting quality of a warship. Also, in an earlier stage, spray is driven over the forward portion of the ship by the wind. Both conditions (spray and green water) are undesirable and can be improved by increasing the freeboard.

Under some conditions, the pressures exerted by the water on a ship's hull may become excessive and slamming may take place. Slamming is characterized by a sudden change in the vertical acceleration of the ship, followed by a vibration of the hull girder in its natural frequency. The conditions leading to slamming are high relative velocity between the ship and the water surface, shallow draft, and small deadrise.

Repeated slams will not only damage the ship structure and other components, but also will have a considerable effect on the personnel operating the ship. This is especially important in respect to the satisfactory operation of naval vessels, the mission of which is to act as a floating platform for weapon systems. The platform, therefore, should be as stable

as possible. The area between 10 and 25% of the length from the bow is the one most likely to suffer high pressures leading to damage.

In the design of ships, speed is an important factor. However, there is a loss of speed while a vessel is under way in a sea, because of the increase in motion resistance and the loss of propeller efficiency. This results in higher fuel consumption and thereby limits the cruising range. The heavier the seaway, the greater is the loss of speed. To overcome this loss it is often necessary to improve the resistance and propulsion characteristics of the vessel, as well as to design the machinery plant for adequate reserve power. Although model tests can predict with reasonable accuracy the still water resistance and propulsion performance of a ship, their determination in a seaway is still the subject of research. The maximum speed that can be attained by a ship is governed, not necessarily by the available power, but mostly by the accelerations experienced in a seaway.

To reduce the dynamic effects, various means of motion stabilization have been adopted. Bilge keels, damping tanks, and fins are a few examples. Knowledge of the phenomenon of resonance between regular waves and the rolling motion has led to the use of successful roll damping devices, but not much progress toward dampening the pitching motion adequately has yet been made because of the large forces involved. Consideration of motion stabilization is particularly important for passenger ships, as well as many types of naval vessels. Structural failure in severe seas is not infrequent even with modern technology.

The relative importance of the various aspects of ship performance in a seaway varies from design to design, depending on what the operators require of the ship. The following general items, must be investigated when designing seaworthy ships:

a. Excessive motions, which are undesirable since they may impair stability and cause discomfort to the crew and passengers. Also, in warships most weapon systems require a stable platform for proper functioning.

b. Additional stresses caused by the ship's bending or by wave impacts in a seaway.

c. Inertial forces causing damage to equipment, armament structures, and so forth.

d. Shipping and spraying of green water, causing equipment breakdown and degradation of liability.

e. Slamming.

f. Speed reduction and the conditions under which the propeller will start racing, thereby overloading the propelling machinery and hence increasing the fuel consumption per mile or dropping off the cruising range.

g. Ship-handling quality.

The various problems encountered in regard to ship motions may be investigated in four different ways:

1. Analytically, that is, on a theoretical basis.
2. Experimentally, by means of model tests in controlled environments.
3. Empirically, through statistical observations.
4. Directly, as with trials of ships after they are built.

Both theoretical and experimental studies help the designers to determine the influences of various ship features on seakeeping characteristics, knowledge that is extremely valuable in designing a ship. Therefore one of the most important studies in naval architecture is the investigation of ship performance in rough water. Both merchant and naval vessels must maintain a high degree of seakeeping quality in many different types of weather and still attain their mission—the merchant ship from the commercial point of view, and the naval vessel with regard to optimum operational ability. For the purpose of design one should be able to estimate the dynamic forces to which a ship may be subjected and the motions that result therefrom. Theoretical studies, model results, and full-scale data are all necessary to provide reliable design criteria.

In recent years, research on ship motions has made considerable advances in the area of theoretical development, as well as in experimental facilities. However, no quantitative index has yet been found to compare the seakeeping qualities of ships, as is possible in comparing the resistance or propulsion characteristics of one hull form with another by means of simple coefficients.

The introduction of advanced marine vehicles, such as planing crafts, hydrofoil boats, and air cushion vehicles has necessitated further studies in seakeeping in order to achieve the maximum results from these special vehicles. Intensive investigations are now under way to determine experimentally the effects of parametric variations in motions, bottom pressures, and power requirements on models of planing boats, surface effect ships (SESs), and so on. In addition, scale effect studies on high-performance vessels are being looked into to correlate test results from models of different scales and full-scale trials.

Therefore, the responsibility of a ship designer includes the development of technology for measuring, predicting, and improving the various qualities that govern ship dynamics. This also includes the application of this technology to specific designs, the identification of design faults, and the correction and improvement of such designs. The specifics will depend on the particular design, but it is essential that the designer have some means of judging the expected performance.

In theoretical investigations the problem of determining the motions of a ship consists of deriving simple analytical expressions for the surface of the seaway and determining the ship motions for such a seaway. Theoretical studies can offer the following:

a. General information regarding the most relevant characteristics of the behavior of a ship in a seaway.
b. A prediction of the motion of a ship in any given seaway.
c. An insight into the acceptable values of motions, accelerations, and so on.
d. A knowledge of the average performance to be expected, including stability and resistance.
e. Basic ideas regarding motion stabilization and ways to achieve it.
f. Guidelines for model tests and full-scale trials.

However, since ship motion is rather complex, it cannot be completely treated by analytical means alone; therefore model experimentation and ship trials are carried out in order to predict ship performance. Sophisticated methods of model tests have been developed in various experimental facilities throughout the world and extensive ship trials are conducted in order to correlate model and ship results. This is especially important for naval ships. However, before new ships, including hydrofoils, SESs, and hovercrafts, can be employed effectively in their design environment (open sea and at speed), the human habitability factor must be addressed.

It is to a basic and fundamental discussion of such means that the later chapters are devoted.

Chapter

Two

SIMPLE HARMONIC MOTION

2.1 INTRODUCTION

Motions of a body can be described as either translational or rotational. These motions, according to Newton's law, take place continuously in one direction only unless disturbed by some external force. The direction of motion can also be alternating; that is, motion can progress in one direction and then reverse after an interval of time. Such a motion is known as *oscillatory*. An oscillatory motion is common in nature, and, since it was originally studied in relation to music, is also called a *harmonic motion*. Since most harmonic motions are rather complicated, a simplified treatment is adopted here using some simple oscillatory motions, which are then called *simple harmonic motions*.

In the case of simple harmonic motion, when a body is displaced from its equilibrium position, a force that is inherent in the body tends to bring it back to its original equilibrium position. This force, known as the *restoring force*, is directly proportional to the displacement of the body from its equilibrium position. When displaced from its equilibrium position, the body moves back toward this position with an acceleration under the action of the restoring force, that is, the body moves faster and faster as it nears its equilibrium position. However, as the body comes closer to this position, the restoring force decreases and the acceleration toward the equilibrium position diminishes. When the body finally reaches its equilibrium position, the restoring force and acceleration vanish, but by then the body has attained its maximum velocity. If there is no force to stop the body at its equilibrium position, it will move past this position in the opposite direction. Again a restoring force acting toward the equilibrium position comes into play, but in the opposite direction. As the body continues to move further, the displacement and the restoring force, as well as the acceleration, increase until the velocity becomes zero, that is, the body reaches its maximum displacement from its equilibrium position. Now, under the influence of the restoring force, the body gains velocity continuously until it reaches the equilibrium position and moves past this position again.

If there is no resistance or damping during this oscillatory motion, the body will oscillate indefinitely, and the maximum displacement of the body on either side of its equilibrium position will remain constant. The time taken to reach from one extreme point to the one on the other side and back is known as the *period* of the motion.

In a simple harmonic motion, displacement, velocity, and acceleration change constantly at every instant. This kind of motion can be represented by another kind of motion with a constant speed: motion around a circle.

This topic is discussed in the following section.

2.2 EQUATIONS OF SIMPLE HARMONIC MOTION

If a point is considered to be moving along the circumference of a circle with uniform speed, the motion of the projection of the point on the diameter of the circle is defined as the simple harmonic motion.

In Fig. 2.1 let us suppose that point P is moving along the circumference of a circle having a radius z_a. If P has a constant angular velocity of ω radians

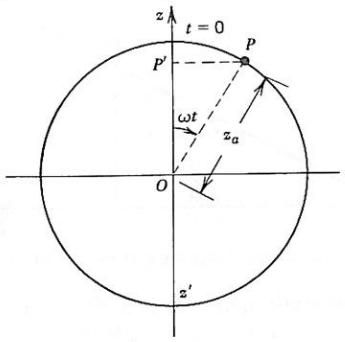


Figure 2.1 Definition of simple harmonic motion.

per unit time, P' is the projection of P on the diameter of the circle zz'. While P rotates along the circumference of the circle, P' moves from z to z' and again back to z. The motion of P' is known as simple harmonic motion. Now

$$\text{Displacement of } P' \text{ from } O = OP' = z = z_a \cos \omega t \quad (2.1)$$

$$\text{Velocity of } P' = \frac{dz}{dt} = -z_a \omega \sin \omega t \quad (2.2)$$

$$\text{Acceleration of } P' = \frac{d^2z}{dt^2} = -z_a \omega^2 \cos \omega t \quad (2.3)$$

Figure 2.2 shows displacement, velocity, and acceleration. The amplitude of P', its maximum displacement from the middle position, is z_a. The period of motion, the time required for P' to reach z' from z and move back to z again, is the same as the time required for P to make a complete rotation:

$$T = \frac{2\pi z_a}{\omega z_a} = \frac{2\pi}{\omega}$$

$$\text{Characteristic frequency} = \frac{1}{T}$$

$$\text{Angular frequency} = \omega = \frac{2\pi}{T}$$

Note the following:

a. The maximum velocity occurs when $v = z_a \omega \sin \omega t$ is maximum, that is, when $\sin \omega t = \pm 1$. This occurs when P' is at the midpoint from its two extreme positions, or when the body is at its equilibrium position.

b. The maximum acceleration occurs when the expression $\cos \omega t = \pm 1$, that is, when the body is at its extreme position from the position of equilibrium.

c. As already mentioned, the restoring force in a simple harmonic motion is directly proportional to the displacement of the body from its position of equilibrium, that is,

$$f = cz$$

where f is the restoring force, c is a constant, and z is the displacement of the body from O, which is the position of equilibrium. When the body is at its equilibrium position, z is zero and so is the restoring force f. When the body is at its extreme position (i.e., $z = z_a$), the restoring force is maximum and equal to cz_a.

Therefore, as the body moves from its position of equilibrium to one extremity, it acts against a force that is zero at first and then increases gradually to a maximum value of cz_a. Then from (2.3) we see that the maximum acceleration is $-\omega^2 z$. It is noted that the amplitude z_a does not come into this equation, or into the equation for period $T = 2\pi/\omega$. Therefore one can say that, since ω^2 does not refer to any particular circle, a whole set of simple harmonic motions, even ones of different amplitudes, will have the same period.

Hence the simple harmonic can be redefined as follows:

"Simple harmonic motion is motion in a straight line if at each instant the acceleration is directly proportional to its distance from a fixed reference point in the straight line and acts toward that point."

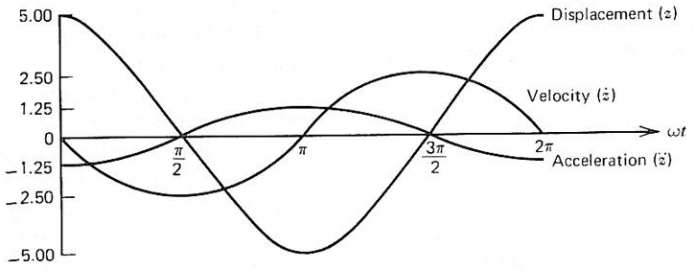


Figure 2.2 Displacement, velocity, and acceleration of a simple harmonic motion.

Also,

"Whatever be the amplitude of motion, the period is determined only by the acceleration at unit displacement [i.e., putting $z = 1$ in (2.3)]."

The preceding discussion has dealt with simple harmonic motion in a straight line, that is, oscillatory translational motion along the diameter zz' of the circle in Fig. 2.1, where the body oscillates in a straight line, but oscillatory rotational motion, that is, the motion of a body moving back and forth along a circular arc, can also be simple harmonic motion. In that case the restoring force is the restoring moment, the angular acceleration is proportional to the angular displacement and oppositely directed, the angular motion is simple harmonic, and again the period is independent of the angular amplitude.

Example 2.1

A simple harmonic motion $z = z_a \cos \omega t$ has an amplitude of 5 ft and a circular frequency of 0.5 rad/sec. Show with the help of a diagram how the displacement, velocity, and acceleration of this simple harmonic motion should vary with time.

Solution

Angular velocity: $\omega = 0.5$ rad/sec (given)

Amplitude of motion: $z_a = 5$ ft (given)

Displacement: $z = z_a \cos \omega t = 5 \cos 0.5t$

Velocity: $\dfrac{dz}{dt} = -\omega z_a \sin \omega t = -2.5 \sin 0.5t$

Acceleration: $\dfrac{d^2z}{dt^2} = -\omega^2 z_a \cos \omega t = -1.25 \cos 0.5t$

See Fig. 2.2.

When the body begins to move away from its equilibrium position, it possesses only kinetic energy. Since it loses velocity as it goes further from the neutral position, the kinetic energy is decreasing and potential energy is taking its place. When the body comes to a complete stop at its extreme position, all the energy the body possesses is potential.

The kinetic energy of an oscillating body, directly as a function of time, is expressed as

$$\begin{aligned} E_K &= \tfrac{1}{2}mv^2 \\ &= \tfrac{1}{2}m(\omega^2 z_a^2 \sin^2 \omega t) \qquad \text{from (2.2)} \end{aligned} \tag{2.4}$$

where m is the mass of the body, v is its velocity, and z_a is its amplitude or maximum displacement.

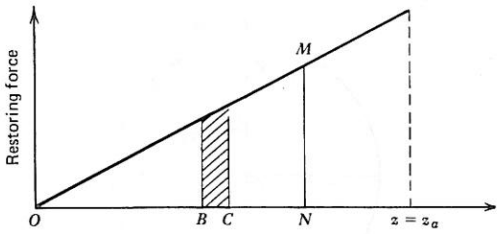


Figure 2.3 Restoring force as a function of displacement.

The potential energy of a body, as a function of time (or displacement), is calculated by equating the work done against the restoring force F, expressed as

$$\begin{aligned} F &= -ma \\ &= -m(-\omega^2 z_a \cos \omega t) \qquad \text{from (2.3)} \\ &= m\omega^2 z \end{aligned} \tag{2.5}$$

As stated before, the restoring force is directly proportional to the displacement of the body from the reference point or the equilibrium position as shown in Fig. 2.3. In this figure the shaded area represents the work done or the increase of potential energy corresponding to the small change in displacement from B to C. With the same argument the increase in potential energy of a body from its equilibrium position to any displacement z (i.e., $ON = z$) is given by the area of the triangle OMN or

$$\begin{aligned} E_p &= \tfrac{1}{2}zF \\ &= \tfrac{1}{2}zm\omega^2 z \end{aligned}$$

Since $z = z_a \cos \omega t$,

$$\begin{aligned} E_p &= \tfrac{1}{2}m\omega^2 z^2 \\ &= \tfrac{1}{2}m\omega^2 z_a^2 \cos^2 \omega t \end{aligned} \tag{2.6}$$

Adding (2.4) and (2.6), we obtain the total energy:

$$E_K + E_p = \tfrac{1}{2}m\omega^2 z_a^2$$

or

$$= \frac{2\pi^2 m z_a^2}{T^2} \tag{2.7}$$

where T is the period of oscillation. We see from (2.7) that the sum of the kinetic and potential energies remains constant with time (or displacement); that is, Fig. 2.4 shows the distribution of both kinetic and potential energies while the total energy remains constant. We can also see from (2.7) that the total energy of a simple harmonic motion is directly proportional to the mass and the square of the amplitude and inversely proportional to the square of the period (or directly proportional to the square of the frequency).

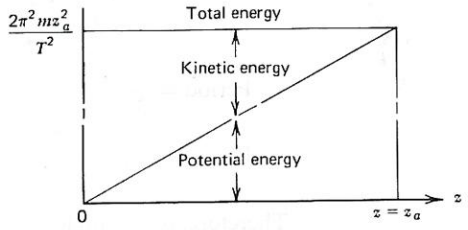


Figure 2.4 Distribution of kinetic and potential energies.

Phase Difference

We saw in Fig. 2.1 that, if point P starts rotating in the clockwise direction from position z, the time t when P is at z equals zero and the displacement of OP' for the simple harmonic motion is given as

$$OP' = z = OP\cos\omega t$$
$$= z_a\cos\omega t$$

However, if P starts its motion from Q, as in Fig. 2.5, then the time t when P is at Q equals zero and

$$OP' = z = OP\cos(\omega t + \varepsilon)$$
$$= z_a\cos(\omega t + \varepsilon)$$

Figure 2.6 shows the two curves drawn on the same axes for comparison, where

$$z_a = 2, \qquad \varepsilon = \frac{\pi}{3}, \qquad \theta = \omega t$$

We notice that the two curves have the same shape and size but are moved or shifted in relation to each other in the direction of the θ-axis. Both functions have the same amplitude and the same period in θ, but they are different in phase. In any general case we say that, if $z = z_a\cos(\theta + \varepsilon)$, the constant angle ε is called the *phase angle* of the function with respect to $z = z_a\cos\theta$. Generally, the range of ε is restricted, so that $-\pi \leqslant \varepsilon \leqslant \pi$. The phase shift is $-\varepsilon$, which is the condition for the argument of the cosine function to be zero.

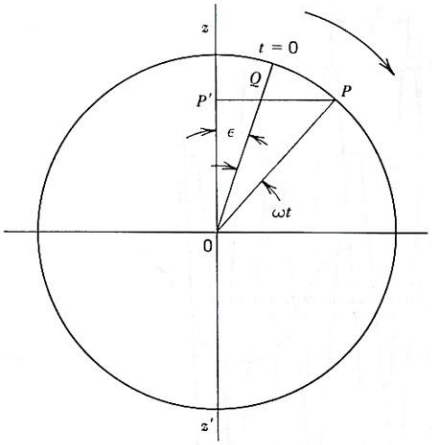


Figure 2.5 Phase difference in a simple harmonic motion.

Note: If we compare $z_a\cos 3\theta$ and $z_a\cos(3\theta + \pi/4)$, the phase angle is $\pi/4$. However, this is not the shift of the graph to the left from the graph of $z_a\cos 3\theta$. The left shift is given by $3\theta + \pi/4 = 0$ or $\theta = -(\pi/12)$. If ε is positive (as in Fig. 2.6, $\varepsilon = \pi/3$), the function $z_a\cos(\theta + \varepsilon)$ is said to lead the function $z_a\cos\theta$, where the corresponding zeros of $z_a\cos(\theta + \varepsilon)$ occur *before* or to the *left* of the zeros of $z_a\cos\theta$. If ε is negative, $z_a\cos(\theta + \varepsilon)$ *lags* the function $z_a\cos\theta$.

With the above explanation, it is said that $z_a\sin\theta = z_a\cos(\theta - \pi/2)$ lags $z_a\cos\theta$ by $\pi/2$, and $z_a\cos\theta = z_a\sin(\theta + \pi/2)$ leads $z_a\sin\theta$ by $\pi/2$. Note also that a lead by π has the same effect as a lag by π. The following conclusions can be drawn from Fig. 2.6:

a. A change in the amplitude leaves the period in θ and the phase angle unchanged.

b. A change in the period in θ leaves the amplitude and the phase angle unchanged.

c. A change in the phase angle leaves the amplitude and the period in θ unchanged.

The amplitude, the period in θ, and the phase angle are independent properties of the functions,

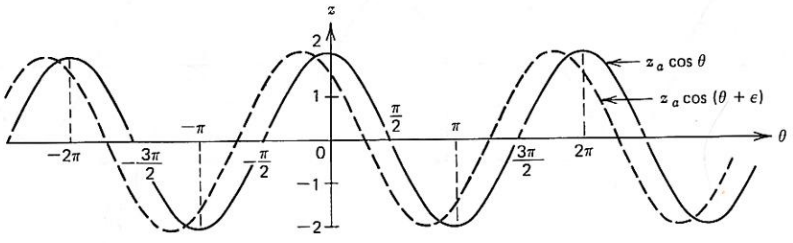


Figure 2.6 Two simple harmonic motions with a phase difference of ε

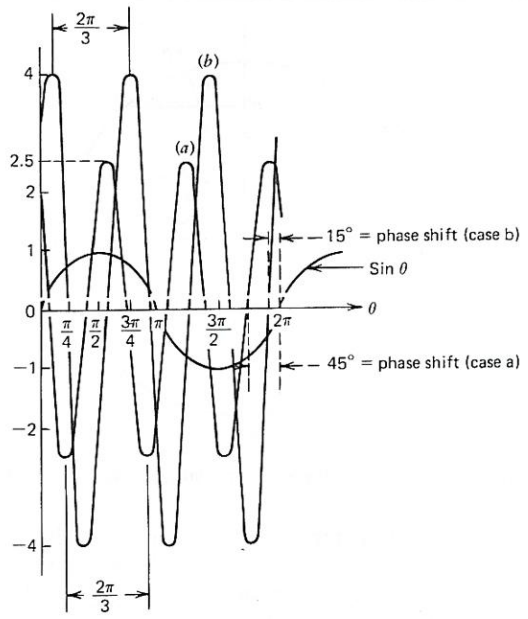


Figure 2.7 Phase shift.

whereas the phase shift in θ is dependent on both the phase angle and the period in θ but is independent of the amplitude.

Example 2.2

Find the amplitude, the period, the phase angle, and the phase shift relative to $\sin\theta$ of:

a. $2.5\sin 3(\theta + \pi/4)$.

b. $4\sin(3\theta + 45°)$.

Solution (see also Fig. 2.7.):

a. $2.5\sin 3\left(\theta + \dfrac{\pi}{4}\right)$ Amplitude $= 2.5$

Phase Shift: $3\theta + 3\dfrac{\pi}{4} = 0$

or $\theta = -\dfrac{\pi}{4}$

$\text{Period} = \dfrac{2\pi}{3}$

Phase angle: $3\theta + \dfrac{3\pi}{4}$

Therefore, phase angle $= \dfrac{3\pi}{4}$

b. $4\sin(3\theta + 45°)$ Amplitude $= 4$

Phase shift: $3\theta + 45° = 0$

or $\theta = -\dfrac{45°}{3}$

$= -15°$

$\text{Period} = \dfrac{2\pi}{3}$

Phase angle $= 45°$

In Fig. 2.8 the harmonic curves are shown as each having the same amplitude and period but a different origin of time. In Fig. 2.8*a* time is measured when point P' is in a position $z = z_a$. In Fig. 2.8*c* time is measured when P' is in the equilibrium position (i.e., $z = 0$); here, as in Fig. 2.8*b*, time is measured when t_0 units of time have elapsed after P' has passed the extreme position $z = z_a$ in the clockwise direction, or

$$\varepsilon = \omega t_0$$

$$t_0 = \frac{\varepsilon}{\omega} = \frac{\varepsilon T}{2\pi}$$

As can be seen from Fig. 2.8, all three diagrams describe identical curves except that they are shifted in relation to each other along the abscissa, that is, the t-axis. As said before, this relative shift is known as the phase shift, and when this is multiplied by the angular velocity ω (which is the same as the circular frequency), the phase angle ε, in terms of radians, is obtained. Note again that the period T is the same

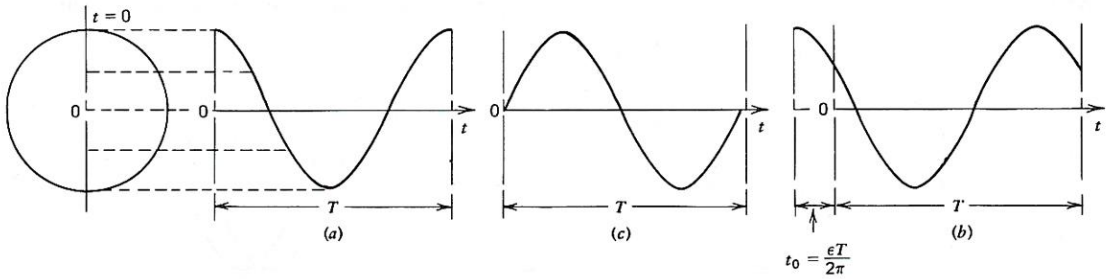


Figure 2.8 Identical harmonic motions shifted in relation to each other.

in all three diagrams in Fig. 2.8. If this is not the case, the curves cannot be compared to each other. Therefore the phase angle is applicable only if harmonic motions of the same frequency are considered. Thus, if we compare (2.1) and (2.2), we have

$$z = z_a \cos \omega t$$

$$\dot{z} = -\omega z_a \sin \omega t$$

$$= \omega z_a \cos\left(\omega t + \frac{\pi}{2}\right)$$

This means that the velocity of P' is a harmonic function with the same frequency as displacement. As shown in Fig. 2.2, the amplitude of the acceleration is ω^2 times larger than that of the displacement and the phase angle is 180°, whereas the frequency in all three cases remains the same.

Example 2.3

The simple harmonic motion of a body is expressed as

$$z = z_a \cos \omega t$$

and the period $T = 2$ sec. If the body is held fixed for a time $t = 0.5$ sec and then is released, and if the time is measured from the same starting point as before, find the expression for the continuing harmonic motion.

Solution:

As explained, the phase angle ε is described as

$$\varepsilon = \omega t_0$$

$$= \frac{2\pi}{T} t_0 = \frac{2\pi}{2} \times 0.5 = \frac{\pi}{2}$$

Therefore the simple harmonic motion will be

$$z = z_a \cos\left(\omega t + \frac{\pi}{2}\right)$$

2.3 VECTOR REPRESENTATION

As mentioned earlier, the simple harmonic motion of any oscillating body can be represented by the projection of the end point of a radial vector on the diameter of the circle (see Fig. 2.9). Any one of the projections of P will represent the harmonic motion. If, for example, $t = 0$ when P is at z and P rotates in the clockwise direction, the vertical projection will be $z_a \cos \omega t$ and the horizontal one will be $z_a \sin \omega t$. The latter may be represented by the vertical

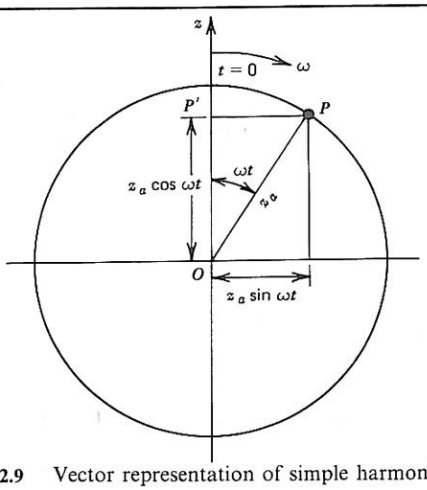


Figure 2.9 Vector representation of simple harmonic motion.

vector with a phase angle of $-(\pi/2)$ since

$$z_a \sin \omega t = z_a \cos\left(\omega t - \frac{\pi}{2}\right)$$

For example, from (2.1), (2.2), and (2.3) the rotating vectors for displacement, velocity, and acceleration may be described as in Fig. 2.10.

If we differentiate the displacement vector z_a, we see that the velocity vector length is multiplied by ω and advances by an angle of 90°. The vector representation is useful if we are to add and subtract the simple harmonic motions with phase differences. The resultant vector will represent the resultant motion both in amplitude and in phase.

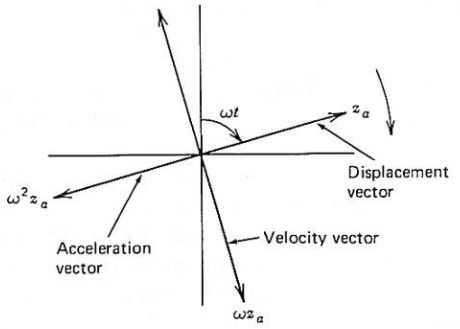


Figure 2.10 Vector representation of displacement, velocity, and acceleration.

2.4 ADDITION OF SIMPLE HARMONIC MOTIONS

When two simple harmonic motions have the same period, they can differ only in amplitude and in phase.

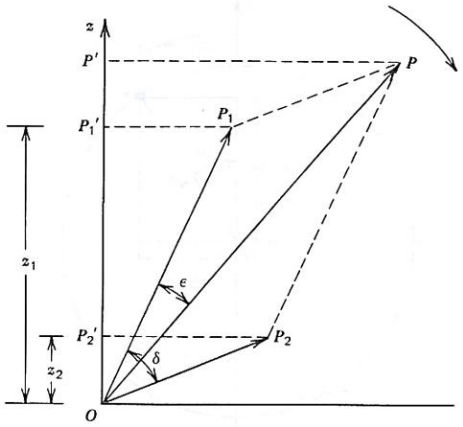


Figure 2.11 Vector addition of two simple harmonic motions.

Let A_1 and A_2 be the amplitudes of two simple harmonic motions represented by OP_1 and OP_2, plotted from a fixed point O (see Fig. 2.11). Let us suppose that the second motion, OP_2, is leading OP_1 and the phase angle between the two is δ. Let us also suppose that each motion is rotating in a clockwise direction with a constant angular velocity $\omega = 2\pi/T$, where T is the period for both motions.

The projections of P_1 and P_2 on the reference line (Oz) are P_1' and P_2', respectively. They describe the simple harmonic motions to be added. Both P_1' and P_2' have the same period T, while their amplitudes are a_1 and a_2, respectively. The second motion leads the first one by the phase angle δ.

Both of the simple harmonic motions are on the same straight line Oz and about the same point O, the resultant displacement at any time being the sum of two individual displacements z_1 and z_2. In Fig. 2.11, z_1 and z_2 are represented by OP_1' and OP_2'.

If we now draw the parallelogram OP_1OP_2, from the parallelogram law we have $OP' = z$, which is the sum of z_1 and z_2 since $OP' = OP_1' + OP_2'$. The amplitude of the resultant motion, a, is then represented by the length OP, since OP' is the projection of the rotating vector OP on the reference line.

We can also obtain the same result analytically instead of graphically. Let the combined motion be $a\cos(\omega t + \varepsilon)$. But

$$z = z_1 + z_2 = a_1 \cos \omega t + a_2 \cos(\omega t + \delta)$$

since

$$a_2 \cos(\omega t + \delta) = a_2 \cos \delta \cos \omega t - a_2 \sin \delta \sin \omega t$$

Therefore

$$\begin{aligned} \text{combined motion} &= (a_1 + a_2 \cos \delta) \cos \omega t \\ &\quad - a_2 \sin \delta \sin \omega t \\ &= a \cos(\omega t + \varepsilon) \\ &= a \cos \varepsilon \cos \omega t \\ &\quad - a \sin \varepsilon \sin \omega t \end{aligned}$$

or

$$a \cos \varepsilon = a_1 + a_2 \cos \delta \tag{2.8}$$

and

$$a \sin \varepsilon = a_2 \sin \delta \tag{2.9}$$

Squaring (2.8) and (2.9) and adding them, we have

$$\begin{aligned} a^2 &= (a_1 + a_2 \cos \delta)^2 + (a_2 \sin \delta)^2 \\ &= a_1^2 + a_2^2 \cos^2 \delta + 2a_1 a_2 \cos \delta + a_2^2 \sin^2 \delta \\ &= a_1^2 + a_2^2 + 2a_1 a_2 \cos \delta \end{aligned}$$

or

$$a = \sqrt{a_1^2 + a_2^2 + 2a_1 a_2 \cos \delta} \tag{2.10}$$

Also, dividing (2.9) by (2.8) gives

$$\varepsilon = \tan^{-1}\left(\frac{a_2 \sin \delta}{a_1 + a_2 \cos \delta}\right) \tag{2.11}$$

where the resultant motion leads the lagging component (represented by OP_1) by the phase angle ε.

It is, therefore, shown that the graphical representation of this case is very suitable for determining the amplitude as well as the phase angle of the resultant motion. In addition, we have learned that the resultant motion of two harmonic motions is also harmonic and has the same frequency as the individual motions. Note, however, that the resultant motion is not a harmonic motion if the frequencies of the individual motions are not the same.

Example 2.4

A resultant motion is obtained by superimposing two displacements, namely,

$$z_1 = 8 \sin \omega t$$

$$z_2 = 7 \cos\left(\omega t - \frac{\pi}{4}\right)$$

Find the amplitude of the resultant motion and its phase angle in relation to the displacement of the first motion.

$$\begin{aligned} z_1 &= \text{the lagging component} \\ &= 8 \sin \omega t \\ &= 8 \cos\left(\frac{\pi}{2} - \omega t\right) = 8 \cos\left(\omega t - \frac{\pi}{2}\right) \end{aligned}$$

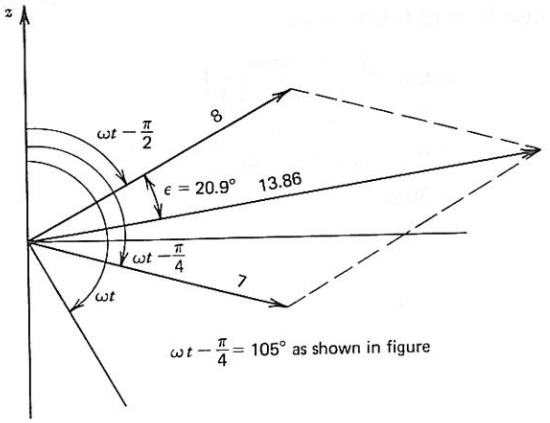


Figure 2.12 Vector addition of simple harmonic motions for Example 2.4

$$z_2 = \text{the leading component} = 7\cos\left(\omega t - \frac{\pi}{4}\right)$$

Therefore,

$$\delta = \text{the phase angle between the leading and lagging components} = \left(\omega t - \frac{\pi}{4}\right) - \left(\omega t - \frac{\pi}{2}\right) = \frac{\pi}{4}$$

Graphical Solution:

A graphical solution is obtained as shown in Fig. 2.12. Another graphical approach would be to draw both z_1 and z_2 as a function of t or ωt; the resultant motion could be obtained by superimposing the two harmonic motions z_1 and z_2 as shown in Fig. 2.13. Note that the accuracy of the results will depend on the accuracy of the graphical construction.

ωt	$\sin \omega t$	$\cos\left(\omega t - \frac{\pi}{4}\right)$	z_1	z_2	$z_1 + z_2$
0	0.0	0.707	0.0	4.949	4.949
$\frac{\pi}{4}$	0.707	1.0	5.656	7.00	12.656
$\frac{\pi}{2}$	1.0	0.707	8.0	4.949	12.949
$\frac{3\pi}{4}$	0.707	0.0	5.656	0.0	5.656
π	0.0	− 0.707	0.0	− 4.949	− 4.949
$\frac{5\pi}{4}$	− 0.707	− 1.0	− 5.656	− 7.0	− 12.656
$\frac{3\pi}{2}$	− 1.0	− 0.707	− 8.0	− 4.949	− 12.949
$\frac{7\pi}{4}$	− 0.707	0.0	− 5.656	0.0	− 5.656
2π	0.0	0.707	0.0	4.949	4.949
3π	0.0	− 0.707	0.0	− 4.949	− 4.949

Analytical Solution:

If we have both the lagging and leading components as the cosine functions, we can substitute the given values into (2.10) and (2.11) for both the amplitude a of the resulting motion and the phase angle ε between the resultant motion and the lagging component, that is,

$$a = \sqrt{a_1^2 + a_2^2 + 2a_1a_2\cos\delta}$$

where a_1 is the amplitude of the lagging component = 8, a_2 is the amplitude of the leading component = 7, and δ is the phase angle between the

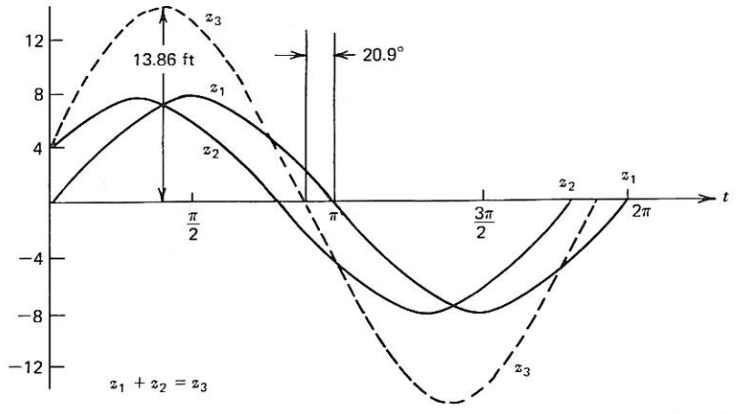


Figure 2.13 Graphical addition of simple harmonic motions for Example 2.4.

motion of the lagging component and that of the resulting motion.

Hence

$$a = \sqrt{(8^2 + 7^2 + 2 \times 8 \times 7 \times \cos 45°)}$$
$$= 13.86$$

Also from (2.11), we have

$$\varepsilon = \tan^{-1}\left(\frac{a_2 \sin \delta}{a_1 + a_2 \cos \delta}\right)$$
$$= \tan^{-1} \frac{7 \sin 45°}{8 + 7 \cos 45°} = \tan^{-1} 0.382$$
$$= 20.9°$$

Chapter

Three

SINUSOIDAL WATER WAVES

3.1 DESCRIPTION

Like, solids, fluids can also have translational, rotational, and oscillatory motions. Translational motion of water is present when rivers flow, rotational motion in a whirlpool, and oscillatory motion in the distortion of the shape that travels outward. Such a moving shape distortion of the water surface is known as a *water wave.*

When a stone falls into water, its weight pushes down the water with which it comes into contact and a depression takes place. Since water is incompressible (for all practical purposes), room is made for the water pushed down by lifting the water in the immediate vicinity around the central depression. Because of the gravitational effect of the earth, the ring of raised water falls back, and the weight of the raised water, acting like that of the stone, pushes water below, causing a larger ring around the center of the disturbance. As this process continues, the raised water surface continues to travel outward from the center. However, since the total mass of water raised by the stone must be spread out through an ever-increasing circumference, the height of the ring of the raised water will be less and less as it goes farther away from the center of disturbance.

The center of disturbance is not the source of only *one wave* traveling outward since, as the ring of raised water is formed, it pushes the water not only outward, but inward as well. The water at the center rises and again drops, acting like a second stone and producing a second wave traveling outward. However, each successive wave is lower than the one before, since each rise and fall of water causes some of the energy to be consumed because of the internal friction of water and the production of some heat. Ultimately all the waves die out and the water surface becomes smooth again, but the tempera-

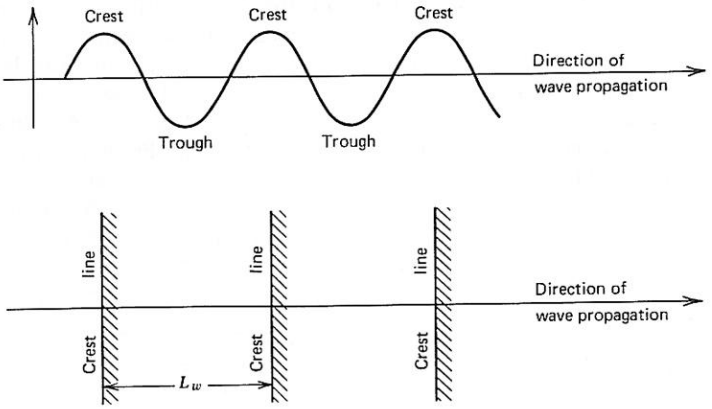


Figure 3.1 Free surface for a regular seaway.

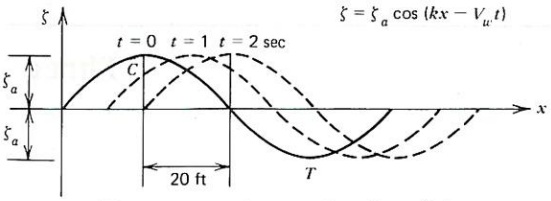


Figure 3.2 Wave propagation as a function of time.

ture of the water is increased slightly to account for the kinetic energy of the falling stone.

Thus an initial disturbance is needed in order to generate the propagating waves. However, although the waves propagate outwardly across the surface of the water as described above, the mass of water does not move with the wave. When waves in the sea arrive at a beach, we notice the up and down motion of water particles that did not come from the sea along with the wave, that is, the water particles were there before the waves arrived. Therefore the wave is not the water itself; it is the disturbance of the sea surface that travels. The process is known as *wave propagation.*

A water wave is a transverse disturbance, since the motion of particles is apparently in one direction (i.e., up and down) and the direction of propagation of the disturbance is at a right angle to the direction of motion, as shown in Fig. 3.1. Note that in a long-crested seaway the crest lines are also at right angles to the direction of wave propagation.

An idealized water wave is a sinusoidal curve, that is, either a sine curve or a cosine curve, that travels outward. An example is shown in Fig. 3.2. The *wave crest* is defined as the point at which the water surface has the highest elevation. The point at which the disturbance is greatest in the downward direction is called the *trough.* The vertical distance between the maximum disturbance and the undisturbed water surface is known as the *amplitude* of the wave, as indicated by ζ_a.

The distance from one crest to the next (or from one trough to the next) is known as the *wavelength,* L_w (Fig. 3.1). As seen in Fig. 3.2, the crest C moves toward the right with time (it is the shape of the disturbance, not the water itself, that moves), and the distance traveled by C per second is called the *phase velocity* of the wave, V_w. In Fig. 3.2 point C is shown to have moved a distance of 20 ft in 2 sec; hence the velocity of this wave is 10 ft/sec.

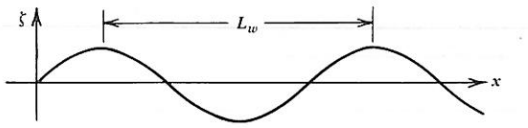


Figure 3.3 Wave amplitude and wavelength.

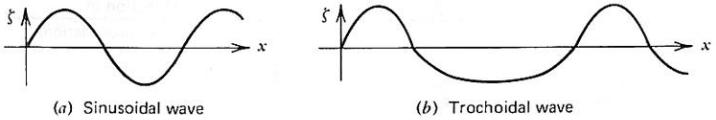
The number of crests (or troughs) passing a given point in 1 sec is known as the *characteristic frequency* f, which is the same as the velocity of the wave divided by its wavelength.

Waves can be classified in various ways. As mentioned above, a *sinusoidal wave* has a symmetrical shape in regard to both the crest and the trough (Fig. 3.3). Another type of wave with shape variation, known as a *trochoidal wave*, has a sharp, narrow crest and a relatively flat, broad trough (Fig. 3.4).

Waves can also be classified from the point of horizontal motion of the wave profile. A *progressive wave* is one that moves horizontally in relation to the water surface. If the profile merely oscillates up and down at one place and does not move transversely, the wave is called a *standing wave.*

In the theoretical investigation of seakeeping, the seaway is thought of as a regular train of waves defined by simple equations. The actual appearance of the sea surface is quite different from this idealized concept. However, in spite of its strong limitations, the theoretical seaway provides certain relationships that observations have shown to be valid. These involve the velocity, period, and length of waves. These theoretical relationships are discussed in the next section.

The assumption of two-dimensional irrotational motion satisfying *La Place's equation,* for which the influence of the acceleration of gravity is taken into account, results in the simple sinusoidal equation of the wave surface. The relationship of simple harmonic motion can be illustrated in the case of wave motion by plotting the distance OP' of Fig. 2.1 as a function of time t. This is shown in Fig. 3.5*a*, where ζ is plotted as the ordinate against t along a horizontal axis. Point P_1 is obtained by plotting a horizontal line through P to the required value at $t = 1$ sec. As P travels around the circle, a curve $P_0P_1P_2 \ldots P_7P_8P_9$ is obtained by plotting horizontal lines from different positions of P. The distance



(*a*) Sinusoidal wave (*b*) Trochoidal wave

Figure 3.4 Comparison of sinusoidal and trochoidal wave profiles.

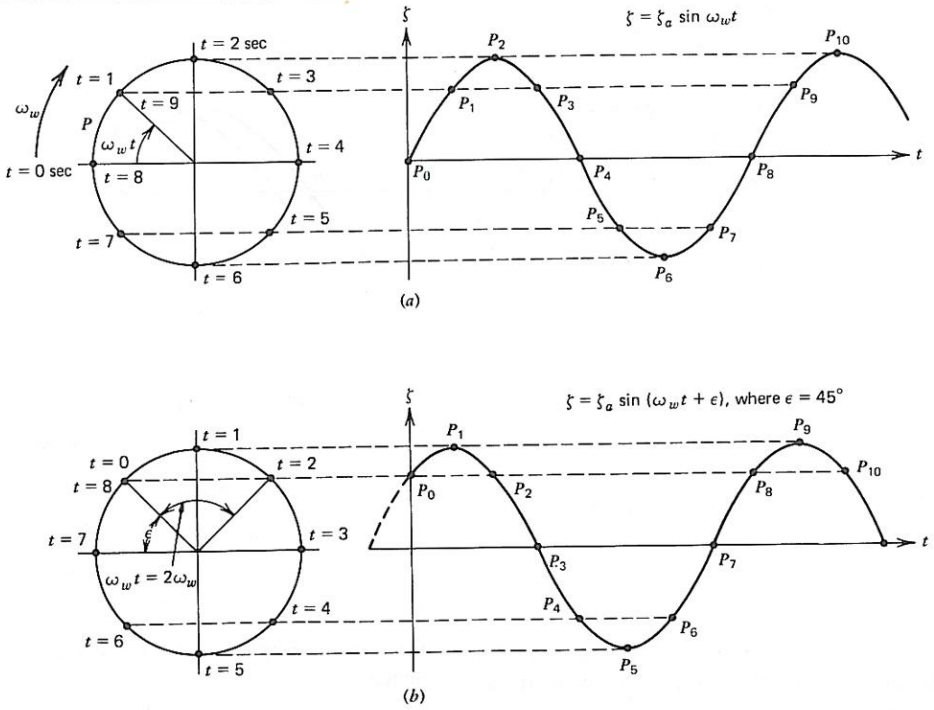


Figure 3.5 Sinusoidal wave from a radius vector.

between the corresponding points on the sinusoidal wave (e.g., P_0 and P_8 or P_1 and P_9, etc.) corresponds to the period T. It was mentioned previously that the water surface at any position appears to rise up and down during the formation of waves. In the case of sinusoidal waves such an elevation can be defined as simple harmonic motion and described analytically as

$$\zeta = \zeta_a \sin \omega_w t \tag{3.1}$$

or, more generally,

$$\zeta = \zeta_a \sin (\omega_w t + \varepsilon) \tag{3.2a}$$

where ζ_a = wave amplitude

ε = phase angle that shifts the curve along the t-axis

ω_w = circular frequency of the wave

t = a measure of time

These equations are shown graphically in Figs. 3.5*a* and 3.5*b*, which are sine curves.

Let us now develop a general equation for a simple water wave that progresses at any *velocity* V_w. We consider first a *stationary* sinusoidal wave, that is, a wave that can be represented by a sine or cosine curve as shown in Fig. 3.6. The equation of this curve is written as

$$\zeta = \zeta_a \sin kx \tag{3.3a}$$

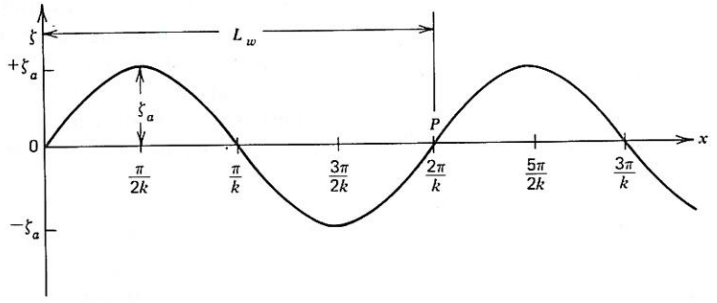


Figure 3.6 Sine (or cosine) representation of a wave.

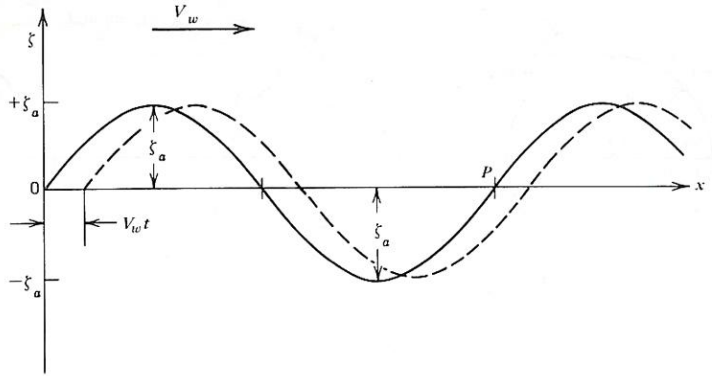


Figure 3.7 Propagation of a sine wave after time t.

where

$$k = \frac{2\pi}{L_w}, \text{ known as the } \textit{wave number}$$

Thus

$$\zeta = \zeta_a \sin \frac{2\pi}{L_w} x \tag{3.3b}$$

Notice, however, that the curve described by (3.3) is a stationary one and does not move forward like a progressive wave in water.

Consider the progressive wave in Fig 3.7. Let us assume that the dotted curve is the new position of the wave after t seconds and may be described by the equation

$$\zeta = \zeta_a \sin \theta$$

where θ should contain x.

It is known that θ is zero when $x = V_w t$ and again when $t = 0$; thus, when $t = 0$, θ must be kx as shown in (3.3). This is possible only if

$$\theta = k(x - V_w t)$$

or

$$\theta = \frac{2\pi}{L_w}(x - V_w t)$$

since

$$k = \frac{2\pi}{L_w}$$

Thus the equation of a sinusoidal wave traveling at a velocity V_w in the positive x-direction is given as

$$\zeta = \zeta_a \sin \frac{2\pi}{L_w}(x - V_w t) \tag{3.2b}$$

which shows that the wave starts from the position of the solid line in Fig. 3.7 and moves toward the right.

The wave equation can also be given in terms of wave frequency ω_w. After a period of time T, we have the value of ζ at $x = x_0$ as given by the expression

$$\zeta = \zeta_a \sin (kx - 2\pi)$$

or at any other time t we have

$$\zeta = \zeta_a \sin\left(kx - \frac{2\pi t}{T}\right)$$

But from simple harmonic motion $2\pi t/T = \omega_w t$; hence

$$\zeta = \zeta_a \sin(kx - \omega_w t) \tag{3.4a}$$

or, in general form,

$$\zeta = \zeta_a \sin(kx - \omega_w t + \delta) \tag{3.4b}$$

where δ = any arbitrary *phase angle*.

If we observe a wave passing a fixed point on the free surface, x is constant and so is kx. Let us then assume that

$$\beta = kx + \delta$$

Then the general equation of wave motion becomes [from (3.4)]

$$\zeta = \zeta_a \sin(-\omega_w t + \beta)$$

or

$$\zeta = -\zeta_a \sin(\omega_w t - \beta)$$

that is, the water particles within a wave undergo a simple harmonic motion, but the phase of one particle differs from that of another, as one moves along x since β contains kx.

Alternatively, (3.4) can be considered at any instant of time, and $\omega_w t$ then becomes a constant. If

$$\varepsilon = \delta - \omega_w t$$

(3.2) and (3.4) are identical. Thus (3.4) describes the motion of an individual particle at all times at any point on the axis, or the positions of the particles at all places along the x – axis at any instant of time.

Figure 3.2 therefore can be considered to be the displacement of any particle at a fixed position on the x-axis, and this depends on the time elapsed, since it began somewhere on the left of the axis. This figure also shows the form of the wave profile at any instant.

It has been shown that the simplified wave profile is sinusoidal. Although a sinusoidal wave is not to be expected in a sea, an irregular seaway can be thought of as being formed by the superposition of a great number of sinusoidal waves. Therefore in the following section the properties of simple (i.e., sinusoidal) waves are discussed.

3.2 VELOCITY, LENGTH AND PERIOD OF WAVES

Without placing any restriction on the magnitude of *water depth*, h, relative to wavelength, sinusoidal waves have been studied and the wave velocity (known also as the *phase velocity* or *celerity*) has been found to be

$$V_w = \left(\frac{gL_w}{2\pi}\tanh\frac{2\pi h}{L_w}\right)^{\frac{1}{2}} \tag{3.5}$$

where V_w is the wave velocity or celerity, L_w is the wavelength, and h is the water depth.

If, however, the water depth is very much less in magnitude than the wavelength (i.e., $h/L_w \to 0$), then

$$\tanh\frac{2\pi h}{L_w} \to \frac{2\pi h}{L_w} = kh$$

Substituting this relation in (3.5), we have

$$V_w = \sqrt{gh} \tag{3.6}$$

this means that in *shallow water* all waves travel with the same velocity regardless of their wavelengths.

On the other hand, when the water depth becomes large in comparison with the wavelength, that is, when h/L_w is very large, then

$$V_w = \sqrt{\frac{gL_w}{2\pi}} \tag{3.7}$$

since $\tanh x \to 1$ when $x \to \infty$. Equation 3.7 shows that, unlike shallow water waves, deep water waves propagate at speeds depending on their lengths.

Although the above equations have been derived on the basis of a number of assumptions and approximations [150]*, the results are found to agree very well with actual cases. The only major assumption made is that the amplitude of the wave is very small.

*Number in brackets refer to items in the bibliography at the end of the book.

Example 3.1

A wave in deep water has the following dimensions:

$$L_w = 20 \text{ ft}, \qquad \zeta_a = 1 \text{ ft}$$

Find the velocity and the wave profiles at different time intervals, namely, $t = 0$, 0.1, 0.2, 0.3, and 1 sec.

Solution:

From (3.7)

$$V_w = \frac{gL_w}{2\pi} = \frac{32.2 \times 20}{2 \times \pi} = 10.1 \text{ ft/sec}$$

and from (3.2b)

$$\zeta = \zeta_a \sin\frac{2\pi}{L_w}(x - V_w t)$$

from which the following table is obtained.

t = 0 sec		t = 0.1 sec		t = 0.2 sec		t = 0.3 sec		t = 1 sec	
x	ζ	x	ζ	x	ζ	x	ζ	x	ζ
[ft]	[ft]	[ft]	[ft]	[ft]	[ft]	[ft]	[ft]	[ft]	[ft]
0	0	1	0	0	−0.59	3	0	0	0
2	0.59	3	0.59	2	0	5	0.59	2	−0.59
4	0.97	5	0.97	4	0.59	7	0.97	4	−0.97
5	1.00	6	1.00	6	0.97	8	1.00	5	−1.00
6	0.97	7	0.97	7	1.00	9	0.97	6	−0.97
8	0.59	9	0.59	8	0.97	11	0.59	8	−0.59
10	0	11	0	10	0.59	13	0	10	0
12	−0.59	13	−0.59	12	0	15	−0.59	12	0.59
14	−0.97	15	−0.97	14	−0.59	17	−0.97	14	0.97
15	−1.00	16	−1.00	16	−0.97	19	−0.97	15	1.00
16	−0.97	17	−0.97	17	−1.00	21	−0.59	16	0.97
18	−0.59	19	−0.59	18	−0.97	23	0	18	0.59
20	0	21	0	20	−0.59			20	0
				22	0				

The values in the table are plotted in Fig. 3.8.

As mentioned earlier, wavelength is measured from crest to crest or trough to trough. If T_w is the time required for a particle at a certain crest to reach the next crest, then

$$L_w = V_w T_w$$

where L_w = wavelength
V_w = wave speed = $\sqrt{gL_w/2\pi}$
T_w = wave period

or

$$T_w = \sqrt{\frac{2\pi L_w}{g}}$$
$$= 0.442\sqrt{L_w} \text{ in fps units}$$
$$= 0.800\sqrt{L_w} \text{ in cgs units}$$

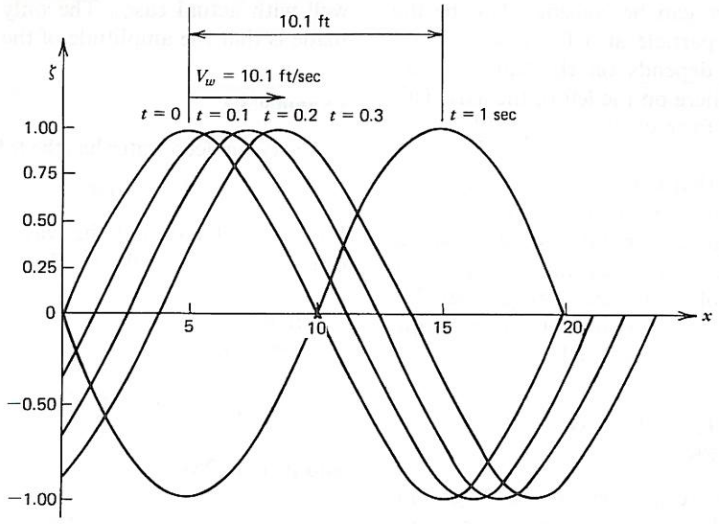


Figure 3.8 Propagation of a sine wave as given in Example 3.1.

Table 3.1 is obtained from the relationship of length, velocity, and period of waves.

TABLE 3.1

Length [ft]	Period [sec]	Velocity [ft/sec]	Velocity [knots]
5	0.99	5.05	3.0
10	1.40	7.14	4.2
20	1.97	10.1	6.0
50	3.10	16.0	9.5
100	4.40	22.7	13.4
200	6.20	32.0	19.0
400	8.80	45.3	26.8
600	10.80	55.0	32.8
800	12.50	64.1	37.9
1000	14.00	71.6	42.4
2000	19.80	101.5	60.0

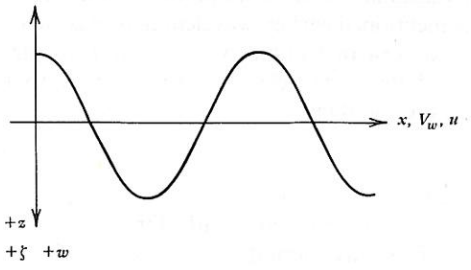


Figure 3.9 Coordinate system for a sinusoidal wave.

From the relationship of velocity, length, and period of waves, the equation for the sinusoidal wave can be expressed as

$$\zeta = \zeta_a \cos k(x - V_w t)$$

$$= \zeta_a \cos\left(kx - \frac{2\pi}{L_w}\sqrt{\frac{gL_w}{2\pi}}\,t\right)$$

$$= \zeta_a \cos(kx - \omega_w t)$$

since $\omega_w = 2\pi/T_w$.

The various characteristics of sinusoidal water

TABLE 3.2 PROPERTIES OF HARMONIC WAVES IN DEEP WATER

Elevations of Lines of Equal Pressure (at a depth z)	ζ_z	$= \zeta_a e^{-kz} \cos k(x - V_w t)$
Surface Profile (i.e. elevation of line of equal pressure at $z = 0$) (first approximation)	$\zeta = \zeta_0$	$= \zeta_a \cos k(x - V_w t)$ $= \zeta_a \cos(kx - \omega_w t)$
Horizontal Water velocity	u	$= k\zeta_a V_w e^{-kz} \cos k(x - V_w t)$
Vertical Water Velocity	w	$= k\zeta_a V_w e^{-kz} \sin k(x - V_w t)$
Wave Velocity or Celerity	V_w	$= \frac{L_w}{T_w} = \frac{g}{\omega_w} = \left(\frac{gL_w}{2\pi}\right)^{1/2}$
Wavelength	L_w	$= \frac{2\pi V_w^2}{g} = \frac{2\pi g}{\omega_w^2} = \frac{gT_w^2}{2\pi}$
Wave Number	k	$= \frac{2\pi}{L_w} = \frac{\omega_w^2}{g} = \frac{g}{V_w^2} = \frac{4\pi^2}{gT_w^2}$
Wave Period	T_w	$= \left(\frac{2\pi L_w}{g}\right)^{1/2}$
Pressure	p	$= \rho g(z - \zeta)$ or $p = \rho g z - \zeta_a \rho g e^{-kz} \cos(kx - \omega_w t)$ where $\rho g z$ is hydrostatic pressure
Maximum Wave Slope (first approximation)	$\alpha_M = k\zeta_a$	$= \frac{2\pi\zeta_a}{L_w} = \frac{\pi h_w}{L_w}$
Energy per unit wave Surface	E	$= \frac{1}{2}\rho\zeta_a^2 g$

TABLE 3.3 PROPERTIES OF HARMONIC WAVES IN WATER OF ANY DEPTH

Elevations of Lines of Equal Pressure	$\zeta = \zeta_a \dfrac{\sinh k(-z+h)}{\sinh kh} \cos k(x - V_w t)$
Surface Profile (i.e. elevation of line of equal pressure at $z = 0$)	$\zeta_0 = \zeta_a \cos k(x - V_w t)$
Horizontal water velocity	$u = \zeta_a V_w k \dfrac{\cosh k(-z+h)}{\sinh kh} \cos k(x - V_w t)$
Vertical water velocity	$w = \zeta_a V_w k \dfrac{\sinh k(-z+h)}{\sinh kh} \sin k(x - V_w t)$
Wave Velocity or Celerity	$V_w = \left(\dfrac{gL_w}{2\pi} \tanh kh\right)^{1/2}$
Pressure	$p = \rho g z - \zeta_a \rho g \dfrac{\cosh k(-z+h)}{\cosh kh} \cos k(x - V_w t)$

where ρgz is hydrostatic pressure, and h is depth of water

Note: For very shallow water (i.e., for $h < L_w/20$) $V_w = \sqrt{gh}$ and for deep water (i.e., $h > L_w/2$), $V_w = (gL_w/2\pi)^{1/2}$.

waves are given for deep water in Table 3.2 and for water of any depth in Table 3.3. The notations for Tables 3.2 and 3.3 are explained in Fig. 3.9.

The origin of coordinates ($x = 0$, $z = 0$, at $t = 0$) is taken at the still water level under the *wave crest*. The x-coordinates, the wave velocity (or celerity) V_w, and the horizontal component u of the water velocity are positive to the right. The ordinate for z and ζ is positive in the downward direction; that is, below the stillwater level z and ζ have positive values. The vertical component w of the water velocity is positive in the upward direction. The water depth h is taken as a positive quantity.

Note: At the bottom, that is, when $z = h$,

$$\zeta = 0 \qquad \text{since } -z + h = 0$$

and

$$w = 0$$

that is, a particle at the bottom moves along a straight line coincident with the bottom, as, of course, should be the case. In other words, the vertical velocity is zero.

Example 3.2

a. What is the speed and period of a deep-sea wave 1000 ft long?

b. A wave is 1000 ft long and 40 ft high, and the depth of water is 150 ft. Calculate the velocity of the wave and the amplitudes of the water particles at the bottom of the channel. Compare the speed of the wave with that of a deep-sea wave of the same dimensions.

Solution:

a. $L_w = 1000$ ft. From Table 3.2

$$T_w = \left(\frac{2\pi L_w}{g}\right)^{1/2} = \left(\frac{2\pi \times 1000}{32.2}\right)^{1/2} = 13.96 \text{ secs}$$

and

$$V_w = \frac{gT_w}{2\pi} = \frac{32.2 \times 13.96}{2\pi} = 71.6 \text{ ft/sec}$$

b. $L_w = 1000$ ft, $h_w = 40$ ft, $h = 150$ ft. Since h, the water depth, is not greater than $L_w/2$, we would consider this problem as a shallow water one. From Table 3.3

$$V_w = \left(\frac{gL_w}{2\pi} \tanh kh\right)^{1/2}$$

where

$$k = \frac{2\pi}{L_w} = \frac{2\pi}{1000} = 6.28 \times 10^{-3}$$

or

$$V_w = \left[\frac{32.2 \times 1000}{2\pi} \tanh(6.28 \times 10^{-3}) \times 150\right]^{1/2}$$
$$= 61.9 \text{ ft/sec}$$

Now

$$\text{Amplitude at the free surface} = \zeta_a = \frac{h_w}{2} = 20 \text{ ft}$$

For any depth the vertical displacement is

$$\zeta = \zeta_a \frac{\sinh k(-z+h)}{\sinh kh} \cos k(x - V_w t)$$

and the amplitude is

$$\zeta_{\max} = \zeta_a \frac{\sinh k(-z+h)}{\sinh kh}$$

where, in this case, $\cos k(x - V_{wt}) = 1$.

However, since at the bottom $-z + h = 0$, $\sinh k(-z+h)$ becomes zero in the numerator, as does the amplitude of the waves at the bottom. But, the water particles at the bottom have a horizontal displacement according to the equation

$$\xi = \zeta_a \frac{\cosh k(-z+h)}{\sinh kh} \cos k(x - V_w t)$$

and the amplitude of the horizontal displacement is

$$\xi_{\max} = \zeta_a \frac{\cosh k(-z+h)}{\sinh kh}$$

At the seafloor,

$$\xi_{\max} = \zeta_a \frac{\cosh 0}{\sinh kh} = \frac{\zeta_a}{\sinh kh}$$

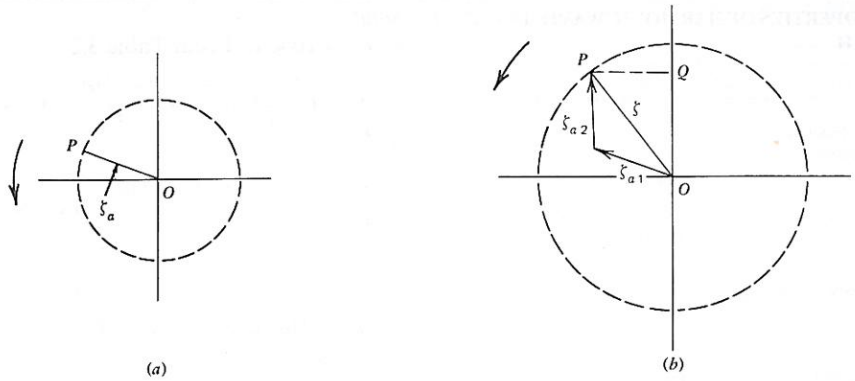


Figure 3.10 Vector addition of two sinusoidal waves.

Since cosh 0 = 1.0,

$$\zeta_{\max} = \zeta_a \operatorname{cosech} kh$$
$$= 20 \times \operatorname{cosech} 0.942$$
$$= 20 \times 0.917 = 18.34 \text{ ft}$$

Wave speed V_w in shallow water is 61.9 ft/sec, almost five-sixth as much as that in deep water, which is 71.6 ft/sec.

Note:

a. If we consider h to be smaller than $L_w/20$, which is considered to be the upper limit of the shallow water (i.e., 50 ft), we can use (see Table 3.3)

$$V_w = \sqrt{gh}$$
$$= \sqrt{32.2 \times 50} = 40 \text{ ft/sec}$$

b. If the path of a particular particle is traced through a complete cycle, it will be found that in deep water all particles describe circular paths having radii that are ζ_a (the maximum) at the surface and decrease with depth; that is, at a depth z the radius is $\zeta_a e^{-kz}$, where z should be measured to the center of the circular path described by the particle.

In shallow water the particles move in ellipses with horizontal and vertical semiaxes that diminish with increasing depth. At the bottom the vertical semiaxis is zero, and the particles oscillate back and forth on straight lines.

3.3 ADDITION OF WAVE TRAINS

If two wave trains happen to arrive at the same time, we have a *superposition* of these wave trains. This addition of wave trains can be regarded as the addition of two simple harmonic motions. To illustrate, let us consider two wave trains as follows:

$$\zeta_1 = \zeta_{a_1} \cos(kx - \omega_w t - \varepsilon_1)$$

and

$$\zeta_2 = \zeta_{a_2} \cos(kx - \omega_w t - \varepsilon_2)$$

Note that two simple harmonic motions can be added if their circular frequencies ω_w and wave numbers k are the same.

Therefore, the combined elevation is

$$\zeta = \zeta_{a_1} \cos(kx - \omega_w t - \varepsilon_1) + \zeta_{a_2} \cos(kx - \omega_w t - \varepsilon_2)$$

This combination is shown in Fig. 3.10.

3.4 STANDING WAVE

Standing waves are formed by the superposition of two trains of waves of the same amplitude traveling

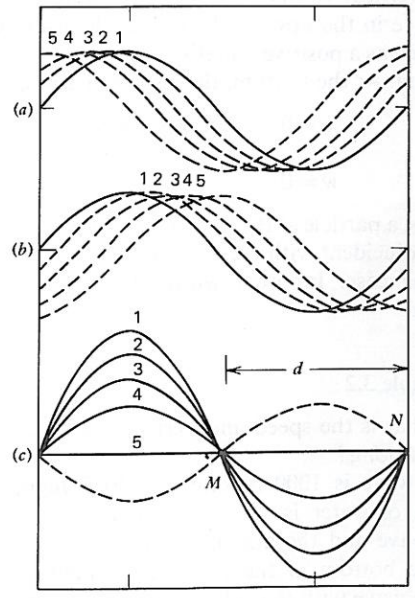


Figure 3.11 A standing wave.

in opposite directions. Standing waves merely oscillate up and down without progressing in either direction. In Fig. 3.11*a* the curves describe five successive positions of progressive wave A at different times, moving toward the left. The curves in Fig. 3.11*b* show the position of another wave B for the same times. Wave B has the same amplitude and length as A but is moving in the opposite direction to A. Figure 3.11*c* shows the addition of the displacements of both waves, A and B, for the same times. At position 1 the displacement of the combined wave is maximum. At position 5 the crest of one wave is added to the trough of the other. The resultant wave then has no displacement from the undisturbed water surface. As A and B continue to move, the resultant wave oscillates below the line between L and M and above line between M and N. Such a wave is known as a *standing wave*, as no direction of travel is involved in the motion of the combined wave.

Analytically, a standing wave can be represented in simplified form as the sum of two sine waves, ζ_1 and ζ_2, traveling in opposite directions:

$$\zeta_1 = \zeta_a \sin \omega_w \left(t - \frac{x}{V_w} \right)$$

and

$$\zeta_2 = \zeta_a \sin \omega_w \left(t + \frac{x}{V_w} \right)$$

Therefore, $\zeta = \zeta_1 + \zeta_2$

$$= \zeta_a \sin \omega_w \left(t - \frac{x}{V_w} \right) + \zeta_a \sin \omega_w \left(t + \frac{x}{V_w} \right)$$

$$= \left(2\zeta_a \cos \frac{2\pi x}{L_w} \right) \sin \omega_w t \qquad (3.8)$$

Now $\zeta = 0$, for all values of t, if

$$x = \tfrac{1}{4}L_w, \tfrac{3}{4}L_w, \ldots, \left(\frac{2n+1}{4} \right) L_w$$

Also, at each point x, we have a harmonic motion because of the expression $\sin \omega_w t$ in (3.8). On the other hand, the amplitude of the motion changes from one point to the other by the factor

$$2\zeta_a \cos \frac{2\pi x}{L_w}$$

The points of zero amplitude (i.e., the nodes) are obtained from

$$\cos \frac{2\pi x}{L_w} = 0$$

or the distance between two nodes is given by

$$d = \frac{L_w}{2}$$

Example 3.3 Standing Wave

In (3.8) assume that $L_w = 20$ ft and $\zeta_a = 0.25$ ft and determine the elevation of the standing wave as a function of time.

Solution

$$T_w = \sqrt{\frac{2\pi L_w}{g}} \triangleq 1.975 = 2 \text{ sec}$$

Therefore $\omega = \pi$ and $\zeta = 0.5 \cos 0.1\pi x \sin \pi t$. Results obtained from this equation are presented in the following table and in Fig. 3.12.

	$t = 0$ sec	$t = 0.1$ sec	$t = 0.2$ sec	$t = 0.3$ sec	$t = 0.4$ sec	$t = 0.5$ sec
x [ft]	ζ [ft]	ζ [ft]	ζ [ft]	ζ [ft]	ζ [ft]	ζ [ft]
0	0	0.15	0.29	0.40	0.48	0.50
2	0	0.13	0.24	0.33	0.39	0.41
3	0	0.09	0.17	0.24	0.28	0.29
5	0	0	0	0	0	0
7	0	−0.09	−0.17	−0.24	−0.28	−0.29
8	0	−0.13	−0.24	−0.33	−0.39	−0.41
10	0	−0.15	−0.29	−0.40	−0.48	−0.50
12	0	−0.13	−0.24	−0.33	−0.39	−0.41
13	0	−0.09	−0.17	−0.24	−0.28	−0.29
15	0	0	0	0	0	0
17	0	0.09	0.17	0.24	0.28	0.29
18	0	0.13	0.24	0.33	0.39	0.41
20	0	0.15	0.29	0.40	0.48	0.50

Note: The same ζ values are obtained for
$t = 0.6$ *sec as for* $t = 0.4$
$t = 0.7$ *sec as for* $t = 0.4$
$t = 0.8$ *sec as for* $t = 0.3$
$t = 0.9$ *sec as for* $t = 0.1$
$t = 1.0$ *sec as for* $t = 0$
etc.

Example 3.4

Show that a combination of two standing waves out of phase by $\pi/2$ produces a progressive wave.

Solution:

Let the equation of standing wave 1 be

$$\zeta_1 = 2\zeta_a \cos \frac{2\pi x}{L_w} \sin \omega t.$$

The equation of standing wave 2, out of phase by

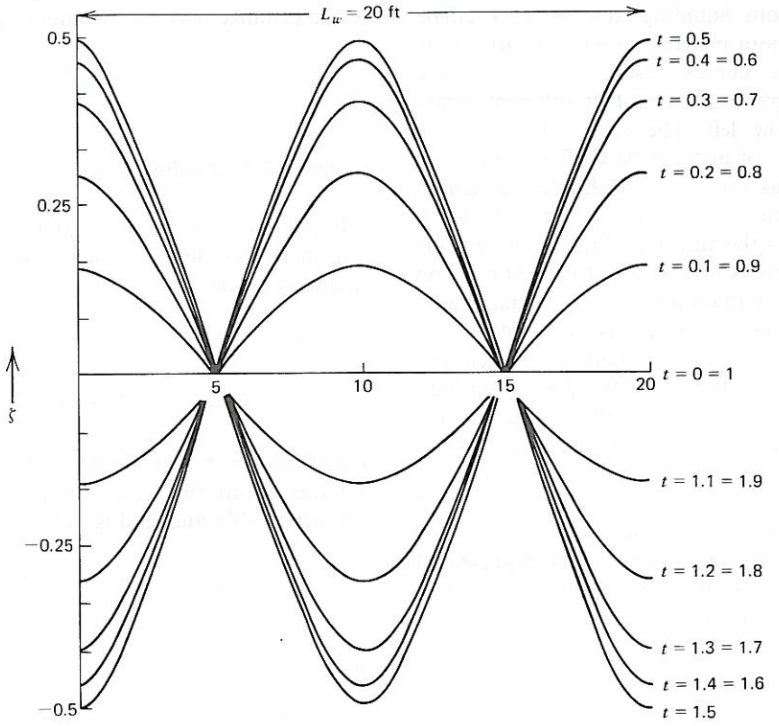


Figure 3.12 Standing wave of Example 3.3.

by $\pi/2$ from the first wave, is then

$$\zeta_2 = 2\zeta_a \sin\frac{2\pi x}{L_w}\cos\omega t$$

Therefore, using trigonometric identities, we have

$$\zeta_1 + \zeta_2 = 2\zeta_a \sin\left(\frac{2\pi x}{L_w} + \omega t\right)$$

From Table 3.2 we obtain

$$\omega = \frac{2\pi}{T_w} = \frac{2\pi}{L_w}\cdot V_w$$

Let $A = 2\zeta_a$. Therefore the equation of the combined wave is

$$\zeta = A\sin\frac{2\pi}{L_w}(x + V_w t)$$

This is an equation for the progressive wave of amplitude A.

In the discussion of wave motion thus far, only the motions of particles lying on the surface have been considered, but motion is not confined to the free surface. The amplitude of motion at a point decreases as the distance of the point from the free surface increases. At a distance of a few wavelengths from the free surface wave motion is negligible, although, in the stricter sense, the whole fluid mass is involved in wave motion.

3.5 DEPTH EFFECTS

The radius of the orbit of a particle in deep water decreases rapidly with its depth from the surface. This is expressed analytically as

$$\frac{\zeta_z}{\zeta_a} = e^{-kz}$$

where ζ_z = wave amplitude at a depth below surface
ζ_a = wave amplitude at the surface
z = mean depth of the particle below the surface
k = wave number $= 2\pi/L_w$

Therefore

$$\frac{\zeta_z}{\zeta_a} = e^{-[(2\pi/L_w)z]}$$

Table 3.4, which is calculated from this equation, shows that at a water depth equal to twice the wavelength the disturbance due to a surface wave is almost nonexistent (see Fig. 3.13). The expression

TABLE 3.4 DECREASE OF WAVE DISTURBANCE WITH DEPTH

$\frac{\text{Depth of Water}}{\text{Wavelength}} = \frac{z}{L_w}$	Ratio of Wave Amplitudes $= \frac{\zeta_z}{\zeta_a}$
0.01	0.9391
0.02	0.8819
0.03	0.8283
0.04	0.7778
0.05	0.7304
0.1	0.5335
0.2	0.2846
0.3	0.1518
0.5	0.0432
1.0	0.00187
2.0	0.0000035

for wave profile at any depth is therefore given as

$$\zeta = \zeta_z \cos k(x - V_w t)$$
$$= \zeta_a e^{-kz} \cos k(x - V_w t)$$

or by *first approximation*

$$\zeta = \zeta_a e^{-kz} \cos(kx - \omega_w t)$$

The water particles on the surface during wave motion are not absolutely still but possess a velocity of constant magnitude while rotating steadily. When a water particle is on the wave crest, it moves forward with the wave, whereas a particle moves backward, in the opposite direction of the wave motion, when it is in the trough of a wave. The wave particles move vertically downward or upward when the wave passes through the undisturbed water level (see Fig. 3.14).

In the case of deep water sinusoidal waves, which have, strictly speaking, very small amplitude, the paths of the water particles are circular, but for waves of finite amplitude the water particles possess forward velocity for a longer period of time than backward velocity. That is the reason why in reality the paths of the water particles are not closed but advance steadily in the direction of wave motion (see Fig. 3.15a), although the velocity of water particles is very much less than that of waves. The motion of

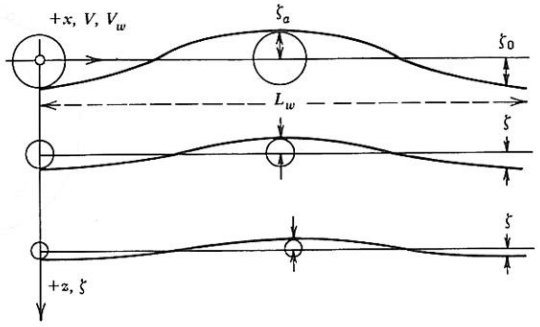


Figure 3.13 Wave profiles at different depths.

water particles follows the same pattern below the free surface as on the surface (see Fig. 3.15b). The velocities of water in the horizontal and vertical directions are given as

$$u = k\zeta_a V_w e^{-kz} \cos k(x - V_w t) \quad \text{(horizontal direction)}$$

$$w = k\zeta_a V_w e^{-kz} \sin k(x - V_w t) \quad \text{(vertical direction)}$$

One can see from these equations that the disturbance of water particles diminishes with increasing depth from the free surface.

3.6 PRESSURE IN A WAVE

For many problems the most important aspect of waves is the distribution of pressure below the surface. It is convenient to compute the pressure in relation to horizontal lines of constant pressure in still water.

Pressure at any point under waves in water of any depth (assuming that the wave height is small—strictly speaking, infinitesimal) is

$$\rho g(z - \zeta) \tag{3.9}$$

where z is to be measured downwards from the still water line, and ζ, known as the elevation of lines of equal pressure in a wave, is either positive or negative, depending on whether the wave profile is in the

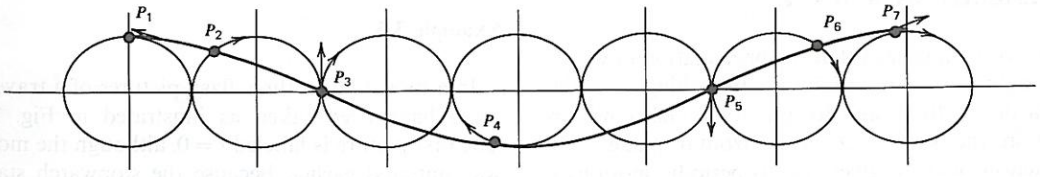


Figure 3.14 Motion of water particles in a wave.

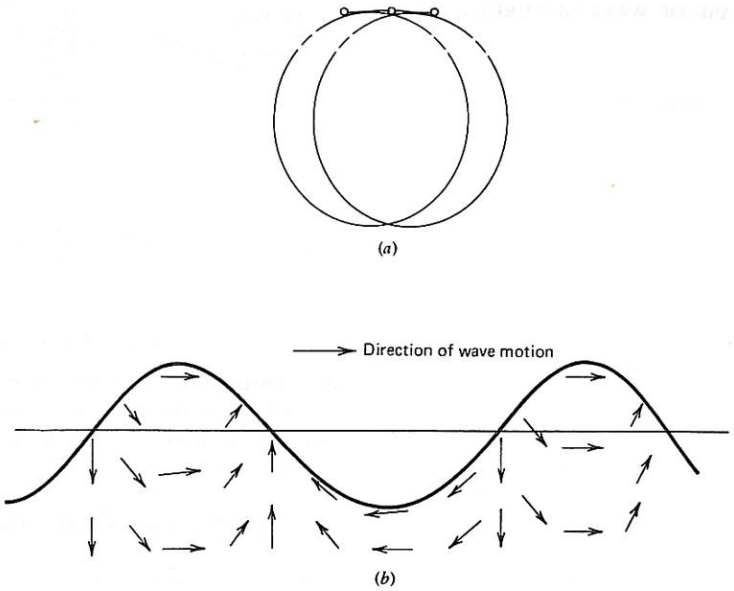


Figure 3.15 Water particles during wave motion. (*a*) Water particles in a forward-moving wave. (*b*) Motion of water particles in a wave.

trough or crest region, (see Fig. 3.9) and is expressed by

$$\zeta = \zeta_a \frac{\cosh k(-z+h)}{\cosh kh} \cos k(x - V_w t) \quad (3.10)$$

where h is the depth of water. In deep water (large h) the ratio $\cosh k(-z+h)/\cosh kh$ approaches e^{-kz}, and

$$\zeta = \zeta_a e^{-kz} \cos k(x - V_w t) \quad (3.11)$$

These expressions show that contours of equal pressure at any depth are cosine curves which are functions of time when observed at a fixed point x_0, or functions of distance x at a particular instant t_0. Since e^{-kz} decreases as z increases, the contours of equal pressure are attenuated with depth, approaching zero amplitude as $z \to \infty$. Moreover, these contours are the same as those generated by the orbital motions of the individual particles, as illustrated in Fig. 3.14.

3.7 ENERGY IN A WAVE

It must be emphasized that the propagation of waves is brought about essentially by two things: (a) the inertia of the fluid, and (b) gravity, which tends to maintain the surface as a horizontal plane. The interaction of these gives rise to periodic motion; a wave system possesses both kinetic and potential energies. The kinetic energy is due to the fact that the water particles have an orbital motion, and the potential energy is due to the elevation of the water level. For a sinusoidal wave the potential energy is given as

$$\bar{E}_p = \tfrac{1}{4}\rho g \zeta_a^2 L_w \text{ per foot of breadth}$$

or

$$E_p = \tfrac{1}{4}\rho g \zeta_a^2 \quad \text{per unit of area of wave surface} \quad (3.12)$$

Similarly, the kinetic energy can be expressed as

$$E_k = \tfrac{1}{4}\rho g \zeta_a^2 \text{ per unit area of wave surface} \quad (3.13)$$

Therefore the total energy for a sinusoidal wave is the sum of (3.12) and (3.13), given as

$$\bar{E} = \tfrac{1}{2}\rho g \zeta_a^2 L_w \text{ per foot of breadth}$$

or it can be said that the total energy per unit area of the wave surface is

$$E = \tfrac{1}{2}\rho g \zeta_a^2$$

Example 3.5

In a model basin three flash pictures of a traveling wave have been taken as illustrated in Fig. 3.16. The first picture is labeled $t = 0$, although the motion was initiated earlier, because the stopwatch started at this time.

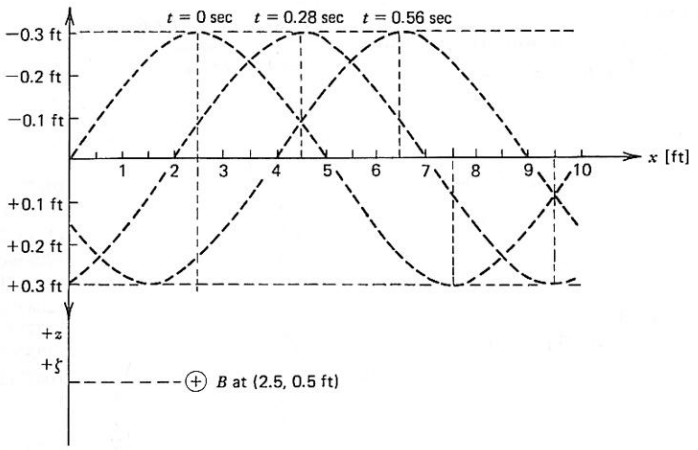


Figure 3.16 Sinusoidal wave motion of Example 3.5.

Determine:

a. The wave speed and period.
b. The wavelength and frequency.
c. The mathematical expression for the wave.
d. The total energy.
e. The pressures at $B(x = 2.5$ ft and $z = +0.5$ ft) for $t = 0$ (i.e., a wave crest), for $t = 0.28$ sec, or when a wave trough is above B. Compare these pressures with the values for the same depths of water if there were no waves.

Solution:

From the data in Fig. 3.16 we have

a. Wave speed:

$$V_w = \frac{\text{Distance}}{\text{Time}} = \frac{4 \text{ ft}}{0.55 \text{ sec}} = 7.15 \text{ ft/sec}$$

Period:

$$T_w = \sqrt{\frac{2\pi L_w}{g}} = \sqrt{\frac{2\pi \cdot 10}{32.2}} = 1.396 \text{ sec}$$

b. Wavelength:

$$L_w = \frac{2\pi V_w^2}{g} = \frac{2\pi(7.15)^2}{32.2} = 10 \text{ ft}$$

Frequency:

$$f_w = \frac{1}{T_w} = \sqrt{\frac{g}{2\pi L_w}} = \sqrt{\frac{32.2}{2\pi \times 10}} = 0.715 \text{ Hz/sec}$$

Thus the circular frequency is $\omega_w = 2\pi f = 4.49 \text{ sec}^{-1}$.

c. Mathematical expression for the wave:

The equation for the surface profile of a wave as given in Tables 3.2 and 3.3 is expressed as

$$\zeta_0 = \zeta_a \cos(kx - \omega t)$$

At $t = 0$ and $x = 0$

$$\zeta_0 = \zeta_a$$

But the first wave profile shows that, at $t = 0$, $\zeta_0 = 0$. Therefore there is a *phase difference* of $\pi/2$, that is,

$$\zeta_0 = \zeta_a \cos\left[\frac{\pi}{2} - (kx - \omega t)\right]$$
$$= \zeta_a \sin(kx - \omega t)$$

Since

$$\zeta_a = 0.3 \text{ ft}, \qquad k = \frac{2\pi}{L_w} = \frac{2\pi}{10} = 0.628,$$

and $\omega = 4.49$ (from the solution of part a)

the equation of the wave can be written as

$$\zeta_0 = 0.3 \sin(0.628x - 4.49t)$$

d. Total energy:

$$\bar{E} = \tfrac{1}{2}\rho g \zeta_a^2 L_w \text{ per foot of breadth}$$

or

$$E = \tfrac{1}{2}\rho g \zeta_a^2 \text{ per square foot of surface}$$

Therefore

$$\bar{E} = \tfrac{1}{2}\rho g \zeta_a^2 L_w$$
$$= \tfrac{1}{2}(1.9905)(32.2)(0.3)^2 \times 10$$
$$= 29.0 \text{ lb per foot of breadth of the wave}$$

e. Pressure at any point in crest is expressed (from Table 3.2) as

$$p = \rho g z + \rho g \zeta_a e^{-kz} \cos(kx - \omega t)$$

Since we have established that the surface profile can be expressed by a sine function, the pressure at any point in the wave should be expressed by

$$\begin{aligned} p &= \rho g z + \zeta_a \rho g e^{-kz} \sin(kx - \omega t) \\ &= \rho g[z + \zeta_a e^{-kz} \sin(kx - \omega t)] \\ &= 64.4[z + 0.3e^{-0.628z} \sin(0.628x - 4.49t)] \end{aligned}$$

since

$$\rho = 2, \quad \zeta_a = 0.3, \quad g = 32.2,$$
$$k = 0.628, \quad \text{and} \quad \omega_w = 4.49$$

Now for $t = 0$ (i.e., for the first wave profile), the pressures at all values of x from 0 to 10 ft and $z = 0.5$ (i.e., at a depth 0.5 ft from the still water level) are calculated in Table 3.5.

Note: The point ($z = 0.5$, $x = 2.5$) is under the crest, and the point ($z = 0.5$, $x = 7.5$) is under the trough, when $t = 0$. Therefore point B, which is under the crest at $t = 0$, has a pressure of 46.3114 psf, whereas when B is under the trough (when $t = T/2$, i.e., when $t = 0.7$ sec), the pressure at B will be the same as that at the point ($x = 7.5$ ft when $t = 0$ sec), that is, 18.0886 psf (see Fig. 3.17).

For any other point at any depth from the still water level and at any time, the pressure can be calculated by using the equation in part e, as was done for Table 3.5.

If B has the same height of water in still water as in the case of the crest above, the pressure will be

$$\begin{aligned} p &= \rho g(z + \zeta_a) \\ &= 64.4(0.5 + 0.3) = 64.4 \times 0.8 \\ &= 51.52 \text{ psf} \end{aligned}$$

If B has the same height of water in still water as in the case of the trough above, the pressure will be

$$\begin{aligned} p &= \rho g(z - \zeta_a) \\ &= 64.4(0.5 - 0.3) = 64.4 \times 0.2 \\ &= 12.88 \text{ psf} \end{aligned}$$

TABLE 3.5 $z = 0.5$ ft, t = 0 sec, $k = \dfrac{2\pi}{L_w} = 0.628$, $\omega = 4.49$ sec^{-1}

x	$\zeta_a e^{-kz} \sin(kx - \omega t)$	Pressure [psf]
0	0	32.2
0.5	0.0677121	36.5607
1.0	0.128796	40.4945
1.5	0.177272	43.6163
2.0	0.208396	45.6207
2.5	0.219121	46.3114
3.0	0.208396	45.6207
3.5	0.177272	43.6163
4.0	0.128796	40.4945
4.5	0.0677121	36.5607
5.0	0	32.2
5.5	−0.0677121	27.8393
6.0	−0.128796	23.9055
6.5	−0.177272	20.7837
7.0	−0.208396	18.7793
7.5	−0.219121	18.0886
8.0	−0.208396	18.7793
8.5	−0.177272	20.7837
9.0	−0.128796	23.9055
9.5	−0.0677121	27.8393
10.0	0	32.2

Therefore the difference in pressures for the same depth at the same point is

$$46.31 - 51.52 = -5.21 \text{ psf under a crest}$$

and

$$18.09 - 12.88 = +5.21 \text{ psf under a trough}$$

This difference was first pointed out by Smith [112] and is known as the *Smith effect*.

3.8 GROUP VELOCITY

Wave groups may be formed by superimposing two trains of waves having the same amplitudes but

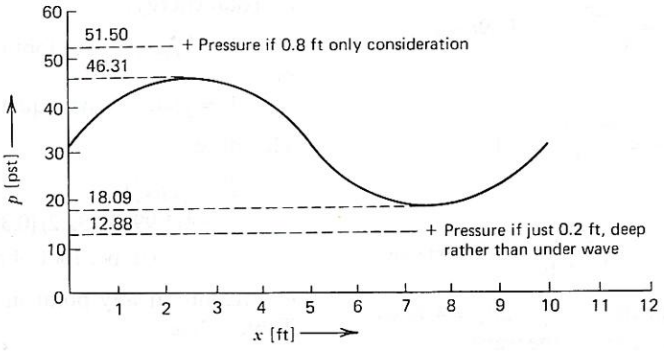


Figure 3.17 Change of pressure during wave motion.

different wavelengths and therefore unequal velocities. Let us now consider two trains of regular waves, for example,

$$\zeta_1 = \zeta_a \sin(k_1 x - \omega_1 t) \tag{3.14}$$

and

$$\zeta_2 = \zeta_a \sin(k_2 x - \omega_2 t) \tag{3.15}$$

(Note that different wavelengths correspond to different k and ω values.)

The combination of the two waves yields

$$\begin{aligned}\zeta^* &= \zeta_1 + \zeta_2 \\ &= \zeta_a[\sin(k_1 x - \omega_1 t) + \sin(k_2 x - \omega_2 t)] \\ &= 2\zeta_a \sin\left(\frac{k_1 + k_2}{2} x - \frac{\omega_1 + \omega_2}{2} t\right) \\ &\quad \times \cos\left(\frac{k_1 - k_2}{2} x - \frac{\omega_1 - \omega_2}{2} t\right)\end{aligned} \tag{3.16}$$

Comparing (3.16) with (3.14) or (3.15), we notice that through (3.16) we have a wave motion with a displacement proportional to

$$\sin\left(\frac{k_1 + k_2}{2} x - \frac{\omega_1 + \omega_2}{2} t\right)$$

and a variable amplitude of

$$\zeta_a^* = 2\zeta_a \cos\left(\frac{k_1 - k_2}{2} x - \frac{\omega_1 - \omega_2}{2} t\right)$$

Now ζ_a^* is maximum when

$$\frac{k_1 - k_2}{2} x - \frac{\omega_1 - \omega_2}{2} t = 0 + 2n\pi, \quad n = \pm 1, \pm 2, \ldots$$

and ζ_a^* is zero when

$$\frac{k_1 - k_2}{2} x - \frac{\omega_1 - \omega_2}{2} t = \frac{\pi}{2} + n\pi, \qquad n = \pm 1, \pm 2, \ldots$$

If k_1 and k_2 are very nearly equal, the cosine term of (3.16) changes very slowly with x; therefore the wave at any instant has the form of a sine curve where the amplitude changes between the minimum value of zero and the maximum value of $2\zeta_a$. The free surface will therefore look like a series of *groups* of waves separated by bands of nearly smooth water at equal intervals of time, as illustrated in Fig. 3.18.

The *group velocity* in water of any depth is given by the expression

$$V_w^* = \tfrac{1}{2} V_w + \frac{gh}{2V_w} \operatorname{sech}^2\left(\frac{2\pi h}{L_w}\right) \tag{3.17}$$

For the deep water case the ratio h/L_w is rather large,

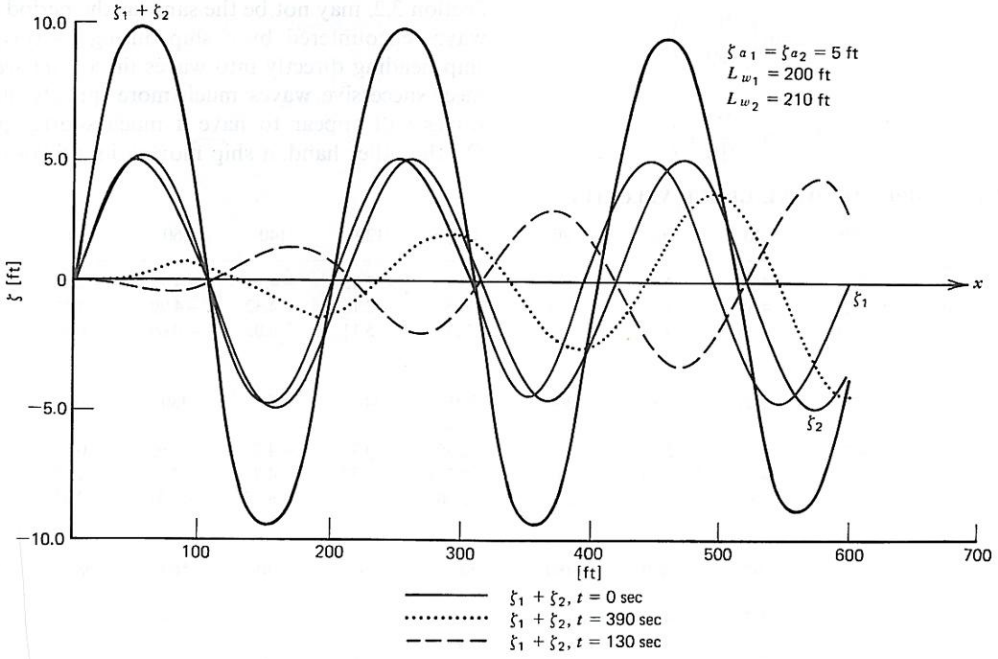


Figure 3.18 Group wave of Example 3.6.

and so

$$V_w^* = \tfrac{1}{2} V_w$$

since $\operatorname{sech}^2(2\pi h/L_w) \to 0$. This means that the component waves will appear at the rear of the group, will travel through it at double the velocity of the group, and will disappear in front. This is often observed in deep water.

The group velocity is of great physical importance, since it is identical with the rate of transmission of energy in waves. In other words, an isolated group of waves cannot advance through still water unless its energy is transmitted at the velocity of the group [150].

In the case of shallow water wave speed is independent of wavelength, that is, $V_w = \sqrt{gh}$ and h/L_w is very small, and (3.17) is stated as

$$V_w^* = \tfrac{1}{2} V_w + \tfrac{1}{2} V_w = V_w$$

In other words, in shallow water the velocity of a group of waves and that of the component waves are the same. For this reason one does not see waves appearing and disappearing when one looks at waves from the beach. At the beach the sea is so shallow that the waves and the wave groups travel forward at the same speed.

Example 3.6 Wave Group

Let, for $t = 0$, $\zeta_1 = 5.0 \sin\left(\dfrac{2\pi}{200} x\right)$

and

$$\zeta_2 = 5.0 \sin\left(\frac{2\pi}{210} x\right)$$

where

$$\zeta_{a_1} = 5.0 \text{ ft}$$

$$L_{w_1} = 200 \text{ ft}$$

$$\zeta_{a_2} = 5.0 \text{ ft}$$

and

$$L_{w_2} = 210 \text{ ft}$$

Find the elevation of the group wave.

Solution

Results of the combination of ζ_1 and ζ_2 are presented in Table 3.6 and also shown in Fig. 3.18.

The wave groups for $x = 0$ ft and for various t values ranging from 0 to 390 sec are illustrated in Fig. 3.19, which indicates that the node created at $x = 0$ by the combination $(\zeta_{a_1} + \zeta_{a_2})_{x=0}$ will occur every 260 sec. If we plot $(\zeta_{a_1} + \zeta_{a_2})$ at other x values, the nodes will again appear at 260 sec intervals, although at different values of t from those for $x = 0$. It is also observed from Fig. 3.19 that the envelope of a group wave is wavy instead of consisting of two parallel straight lines, as is the case with component waves.

TABLE 3.6 EXAMPLE OF WAVE GROUP VELOCITY

x	0	20	40	60	80	100	120	140	160	180	200
ζ_1	0	2.95	4.7	4.7	2.95	0	− 2.95	− 4.7	− 4.7	− 2.95	0
ζ_2	0	2.81	4.65	4.88	3.41	0.755	− 2.16	− 4.32	− 4.99	− 3.92	− 1.49
$\zeta_1 + \zeta_2$	0	5.76	9.35	9.58	7.83	0.755	− 5.11	− 9.02	− 9.69	− 6.87	− 1.49

x	220	240	260	280	300	320	340	360	380	400	420
ζ_1	2.95	4.7	4.7	2.95	0	− 2.95	− 4.7	− 4.7	− 2.95	0	2.95
ζ_2	1.45	3.89	4.98	4.34	2.19	0.714	− 3.37	− 4.87	− 4.66	− 2.85	− 0.04
$\zeta_1 + \zeta_2$	4.40	8.59	9.68	7.29	2.19	− 3.66	− 8.07	− 9.57	− 7.41	− 2.85	2.91

x	440	460	480	500	520	540	560	580	600
ζ_1	4.7	4.7	2.95	0	− 2.95	− 4.7	− 4.7	2.95	0
ζ_2	2.78	4.64	4.88	3.44	0.79	− 2.12	− 4.3	− 4.99	− 3.95
$\zeta_1 + \zeta_2$	7.48	9.34	7.83	3.44	− 2.16	− 6.82	− 9.00	− 7.94	− 3.95

3.9 A SHIP IN WAVES

The absolute period of the waves, as described in Section 3.2, may not be the same as the period of the waves encountered by a ship during its travels. A ship heading directly into waves (in a *head sea*) will meet successive waves much more quickly and the waves will appear to have a much shorter period. On the other hand, a ship moving in a *following sea*

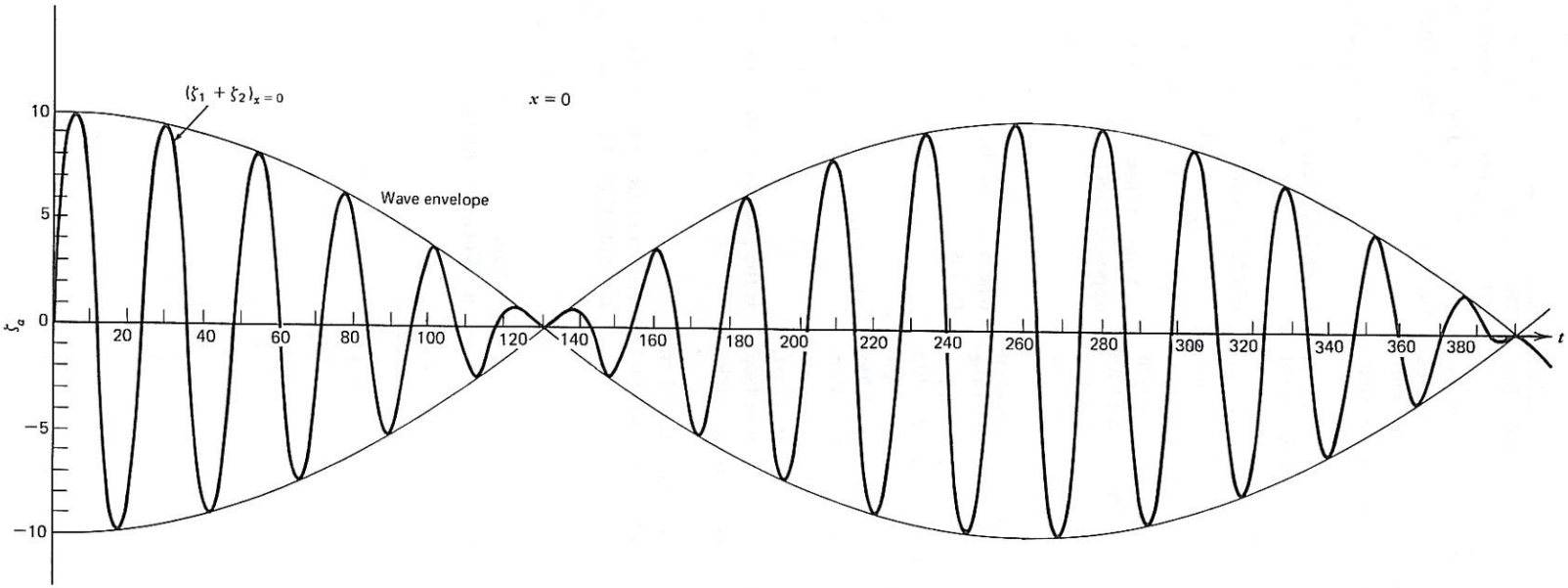


Figure 3.19 Group wave as a function of time.

will move away from the waves, which will then appear to have a longer period. If the waves approach a moving ship from the broadside, there will be no difference between the absolute period of the waves and the apparent period experienced by the ship. The period of waves thus encountered by the ship, known as the *encountering period* T_e, is a function of the absolute period of the wave, the ship speed, and the angle between the direction of wave travel and the direction in which the ship is heading.

The encountering period T_e (or the encountering frequency $\omega_e = 2\pi/T_e$) is the important consideration in regard to ship motion in waves, since the encountering period tells how the ship meets the waves, which then affect the motion of the ship. Therefore, in all ship calculations, the encountering period (or frequency) should be considered instead of the absolute wave period (or frequency).

The *encountering angle* μ, that is, the angle between the direction of wave travel and the direction of the ship's heading, is measured in a clockwise manner from the direction of wave travel. When the ship is heading into a train of regular waves, the angle μ is considered to be 180°, as shown in Fig. 3.20*a*. Similarly, it is shown in the figure that the encountering angles μ for the following and the *beam sea* are are 0° and 90°, respectively. It should be noted that, because of the symmetry of the ship on the sea surface, one should consider only the encountering angles from 0° to 180°.

The expression for frequency of encounter when a vessel is traveling at an angle μ from the advance of the waves is now derived. Let

L_w = length of wave

V_w = speed of wave

and

V = speed of ship

The component of V in the direction of the waves if $V \cos \mu$, while the relative speed of ship to waves is $V_w - V\cos \mu$. The time required by the ship to travel from one crest to the next is

$$T_e = \frac{L_w}{V_w - V \cos \mu} \tag{3.18a}$$

which is the period of encounter. But

$$L_w = V_w T_w$$

where T_w is the wave period. Therefore

$$T_e = \frac{V_w T_w}{V_w - V \cos \mu} = \frac{T_w}{1 - (V/V_w) \cos \mu}$$

Note: When ship and waves are traveling in opposite directions, cos μ is negative. Hence

$$\frac{2\pi}{\omega_e} = \frac{2\pi/\omega_w}{1 - (V/V_w) \cos \mu}$$

where ω_w is the circular frequency of the waves, that is,

$$\omega_w = \frac{2\pi}{T_w}$$

Therefore

$$\omega_e = \omega_w \left(1 - \frac{V}{V_w} \cos \mu\right)$$

is the circular frequency of encounter. Also,

$$V_w = \frac{g}{\omega_w}$$

Therefore the relationship between the frequency of encounter and the wave frequency is

$$\omega_e = \omega_w \left(1 - \frac{\omega_w V}{g} \cos \mu\right) \tag{3.18b}$$

Note:

a. When $\mu = 90°$ (i.e., $\cos \mu = 0$), then $\omega_e = \omega_w$.

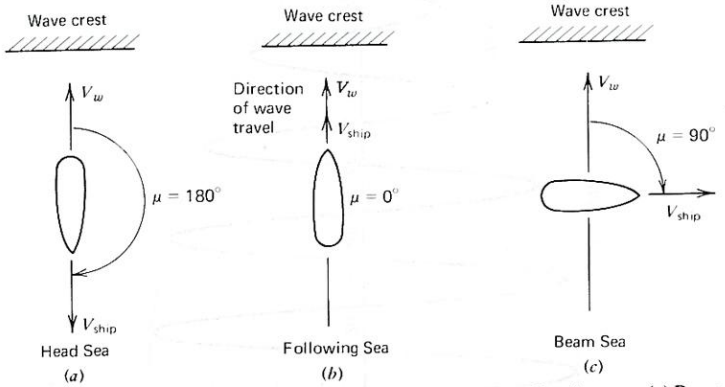


Figure 3.20 Definition of heading angles. (*a*) Head sea. (*b*) Following sea. (*c*) Beam sea.

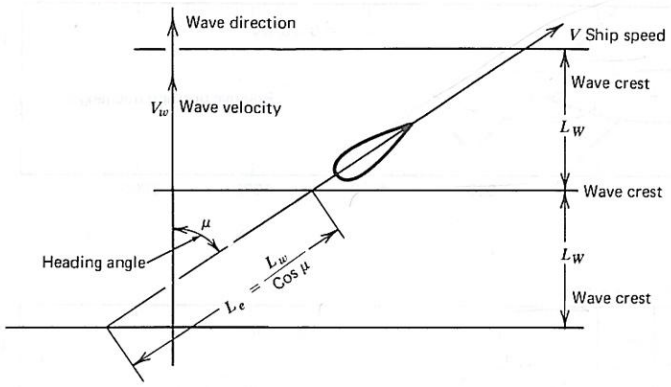


Figure 3.21 Vessel moving in a regular wave train.

b. Effective wavelength $= (L_w)_e = L_w/\cos\mu$ (Fig. 3.21).

Now we have two kinds of frequencies, one being the absolute wave frequency ω_w and the other the frequency of encounter ω_e. In the study of ship motions it is essential that we always convert the absolute wave frequency into the frequency of encounter because the latter is the frequency that the ship experiences and to which it reacts. The ship speed and wave direction must be accounted for in the frequency of encounter. The physical significance of the encountering frequency ω_e can be described as follows.

From (3.18a) we obtain

$$\omega_e = \frac{2\pi(V_w - V\cos\mu)}{L_w} \tag{3.18c}$$

or from (3.18b) we have

$$\omega_e = \omega_w(1 - \eta) \tag{3.18d}$$

where

$$\eta = \frac{\omega_w V\cos\mu}{g}$$

Now, consider the following:

a. When ω_e is zero, the ship remains in the same position relative to the wave profile. This is possible when $\eta = 1$ or $V_w - V\cos\mu = 0$, that is, when the waves and the ship (component of ship speed in direction of waves) are moving at the same speed. See Fig. 3.22*a*.

b. When ω_e is negative, the ship overtakes the waves, which then appear to come off the bow of the ship, although the opposite is actually the case. This occurs when $\eta > 1$ or when $V_w - V\cos\mu < 0$, that is, $V\cos\mu$ has the same direction and sign but is of larger magnitude than V_w. Such sea conditions are described as *following seas* ($0° < \mu < 90°$ and $270° < \mu < 360°$). (See Fig. 3.22*b*.)

c. When ω_e is positive, $V_w - V\cos\mu > 0$, V_w and $V\cos\mu$ may be of the same sign; however, V_w is greater than $V\cos\mu$ (i.e., $0 < \eta < \frac{1}{2}$), and the waves approach the ship from aft and travel so rapidly that ω_e is only slightly less than ω_w. (See Fig. 3.22*c*.) On the other hand, V_w and $V\cos\mu$ may be of the same sign and the waves may still approach the ship from aft, but they may travel so slowly compared to the ship that ω_e will tend to be small ($\frac{1}{2} < \eta < 1$). (See Fig. 3.22*d*.) Such sea conditions are defined as *overtaking seas*, that is, when $0° < \mu < 90°$ or $270° < \mu < 360°$.

d. V_w and $V\cos\mu$ may be of opposite direction and sign, and then $V_w + V\cos\mu$ is positive and large. For this case the waves approach the ship from the bow, and ω_e is everywhere greater than ω_w ($\eta < 0$). (See Fig. 3.22*e*.) Such a case is known as the *ahead sea* condition and corresponds to $90° < \mu < 270°$. The frequency of encounter attains its maximum value when

$$\frac{d\omega_e}{d\omega_w} = 0$$

that is, when

$$1 - \frac{2\omega_w}{g} V\cos\mu = 0$$

since

$$\omega_e = \omega_w - \frac{\omega_w^2}{g} V\cos\mu$$

or when $\eta = \frac{1}{2}$, or when ~~$V/V_w \cos\mu = \frac{1}{2}$~~.

In other words, the maximum encountering frequency is obtained when the component of the ship speed in the direction of wave travel, $V\cos\mu$, is half of the wave speed, V_w.

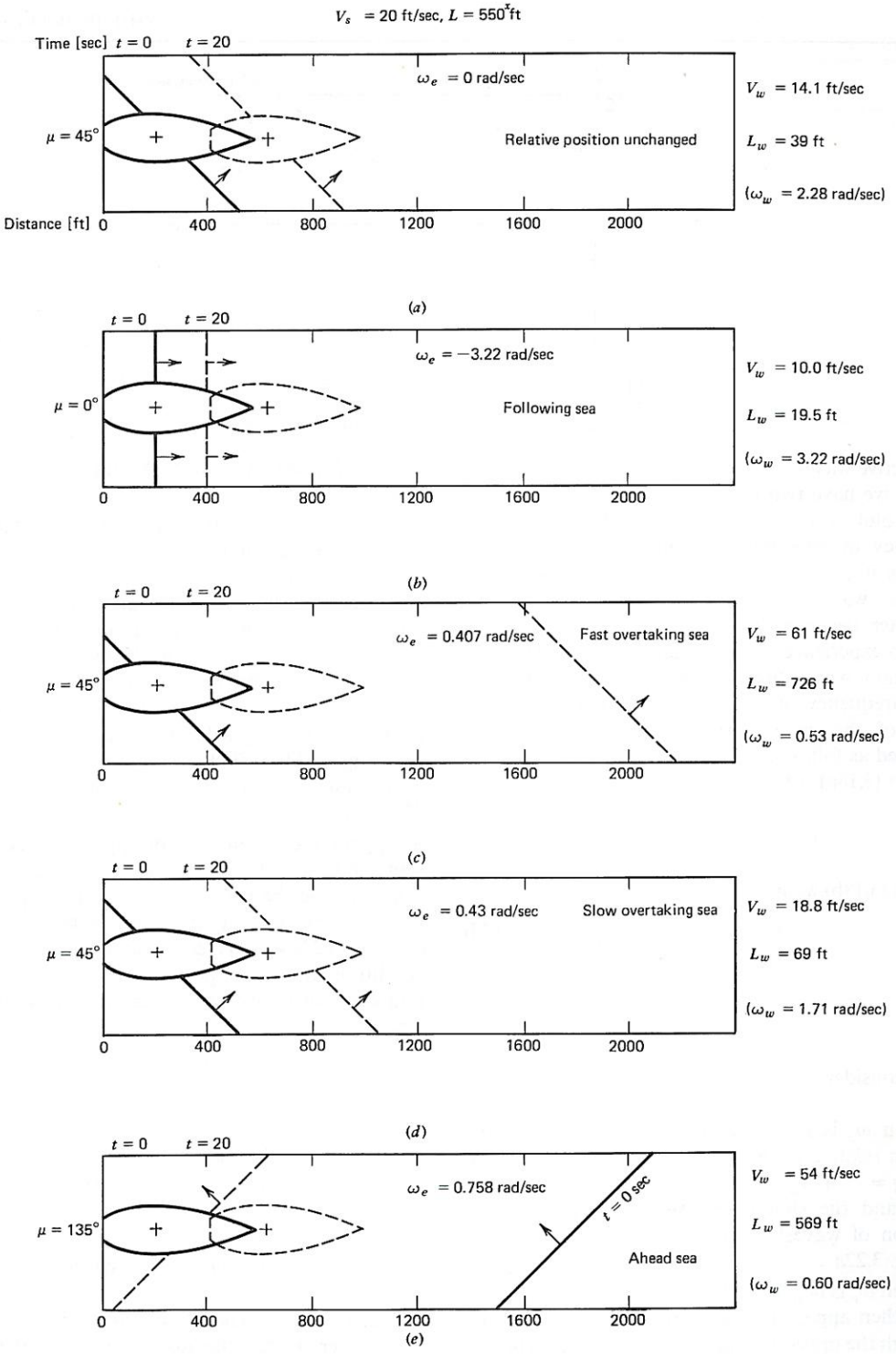


Figure 3.22 Relative positions of a vessel in various wave trains.

Example 3.7

A 500 ft long ship is proceeding through a regular train of waves at an angle of 40° to the line of wave crests. The bow of the ship meets the successive waves every 15 sec, and a wave crest takes 10 sec to pass from bow to stern. Find the speed of the ship.

Solution:

In this problem $\mu = 90° - 40° = 50°$

$$L = 500 \text{ ft}$$

and the component of V in the wave direction = $V \cos \mu$. Therefore relative speed of ship to waves in the direction of wave travel is $V_w - V \cos \mu$. If t is the time interval of a wave crest as observed at the bow and stern positions perpendicular to wave advance, then

$$t = \frac{\text{Encountering length}}{\text{Relative speed of ship to wave}}$$

$$= \frac{L \cos \mu}{V_w - V \cos \mu} = 10 \text{ sec}$$

from which

$$(V_w - V \cos \mu) \times 10 = 500 \cos \mu$$

$$= 321.5 \text{ ft}$$

or

$$V_w - V \cos \mu = 32.15 \text{ ft}$$

If T_e is the time interval between successive crests as observed at the bow and stern positions perpendicular to the wave advance, then

$$\text{Encountering period} = T_e = \frac{\text{Wavelength}}{\text{Relative speed of ship to waves}}$$

or

$$T_e = \frac{L_w}{V_w - V \cos \mu}$$

$$= 15 \text{ sec}$$

from which

$$L_w = T_e(V_w - V \cos \mu)$$

$$= 15 \times 32.15$$

$$= 482.25 \text{ ft}$$

Therefore $V_w = \sqrt{\frac{gL_w}{2\pi}} = 49.71$ ft/sec

Again,

Relative speed $= V_w - V \cos \mu = 32.15$ ft/sec

$$- V \cos \mu = 32.15 - 49.71$$

$$= - 17.56 \text{ ft/sec}$$

from which

$$- V = \frac{- 17.56}{\cos 50°}$$

$$= - 27.32 \text{ ft/sec}$$

or

$$V = 16.17 \text{ knots}$$

Note:

a. In this example the encountering length is $L_e = L \cos \mu$, where L is the distance between the bow and the stern; however, L could be any distance on board the ship.

b. The procedure as outlined in this example is actually followed to estimate the velocity and length of waves from actual observations in a seaway.

3.10 WAVE SLOPE

a. The surface wave profile has been considered as a simple harmonic wave:

$$\zeta_0 = \zeta_a \cos k(x - V_w t)$$

$$= \zeta_a \cos (kx - \omega_w t)$$

The *slope* of the wave surface α is obtained by differentiating ζ_0 with respect to x at any fixed time (say, $t = 0$); thus, if

$$\zeta_0 = \zeta_a \cos kx$$

then

$$\alpha = \frac{d\zeta_0}{dx} = - k\zeta_a \sin kx$$

Note that the angle α is variable and is sinusoidal, as is the wave profile itself.

The *maximum wave slope* α_M is therefore obtained when $\sin kx = + 1.0$ or $- 1.0$ (neglecting the sign of the slope), or when $kx = \frac{1}{2}\pi, \frac{3}{2}\pi, \frac{5}{2}\pi, \frac{7}{2}\pi$, etc. Thus

$$\alpha_M = \frac{d\zeta_0}{dx} = k\zeta_a$$

$$= \frac{2\pi}{L_w} \zeta_a$$

or

$$\alpha_M = \frac{\pi h_w}{L_w} \tag{3.19}$$

where h_w is the wave height (from trough to crest).

b. For a ship moving with speed V and at angle μ

to the wave direction

$$\begin{aligned}\zeta &= \zeta_a \cos(k_e x - \omega_e t) \\ &= \zeta_a \cos\left(\frac{2\pi}{L_w} x - \omega_e t\right) \\ &= \zeta_a \cos\left(\frac{2\pi}{L_w} x \cos\mu - \omega_e t\right)\end{aligned} \tag{3.20}$$

where $L'_w = L_w/\cos\mu$.

Now the maximum slope in this case is

$$\alpha'_M = \left(\frac{d\zeta}{dx}\right)_{\max}$$

where ζ is expressed by (3.20), or

$$\alpha'_M = \alpha_M \sin\mu$$

where α'_M = effective maximum wave slope

α_M = maximum wave slope
$= 2\pi\zeta_a/L_w$ as in (3.19)

The following should be noted:

When the waves are coming broadside to the ship (i.e., $\mu = 90°$), α'_M is the same as α_M.

Chapter

Four

UNCOUPLED HEAVING, PITCHING, AND ROLLING MOTIONS

4.1 GENERAL

A ship moving on the surface of a sea is almost always in oscillatory motion. The different kinds of oscillatory motions that a ship experiences can be described with the help of Figure 4.1, which shows the six kinds of motion, three linear and three rotational about the three principal axes. Accordingly,

a = surging — motion backwards and forwards in the direction of ship travel.

b = swaying — athwartship motion of the ship.

c = heaving — motion vertically up and down.

d = rolling — angular motion about the longitudinal axis. When the ship rolls, it lists alternately from starboard to port and then back to starboard.

e = pitching — angular motion about the transverse axis. When a ship pitches, it trims alternately by the bow and by the stern.

f = yawing — angular motion about the vertical axis.

Only three kinds of motion, namely, heaving, rolling, and pitching, are purely oscillatory motions, since these motions act under a restoring force or moment when the ship is disturbed from its equilibrium position. In the case of surging, swaying, or yawing, the ship does not return to its original equilibrium position if disturbed from it unless the exciting forces or moments that cause such a disturbance act alternately from the opposite directions.

Although in reality a ship experiences all six kinds

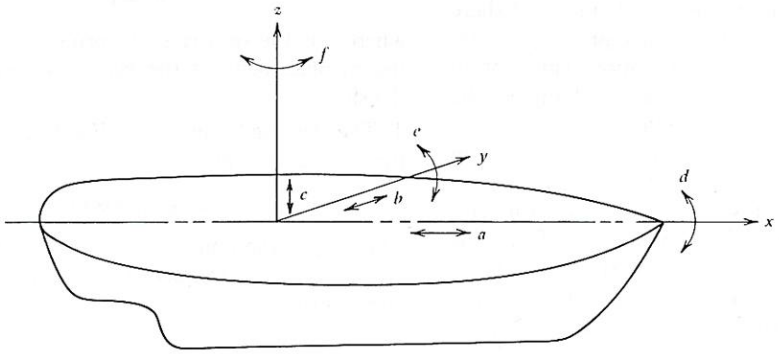


Figure 4.1 The x, y, and z-axes of a ship.

of motion simultaneously, only one motion at a time will be treated in the following sections. However, it must be borne in mind that any one kind of motion is not independent of the others; in the first approximation coupling between the motions is neglected in order to simplify the problem. If a body is free to move in space, it is said to have six degrees of freedom of motion; whereas, if a body is so restrained that it can move only in two directions or rotate only about two axes, it is said to have two degrees of freedom. However, for the sake of simplicity only one degree of freedom is considered in this chapter.

4.2 HEAVING

Let us suppose that a ship is forced down deeper into water from its equilibrium position and then suddenly released. Since its buoyant force is then greater than its weight, the ship will move vertically upward. When the equilibrium position is reached, the ship continues rising because of its momentum; however, now the ship's weight is greater than the buoyant force. This will tend to slow the motion. When the velocity is finally zero, the ship reaches its extreme position, and since the weight is now greater than the buoyant force the ship will move vertically downward. The downward velocity will increase until the equilibrium position is reached, when the buoyancy will again become equal to the weight. However, because of momentum the ship will move further down until the extreme position is reached, that is, the position from which the ship started. But the ship will not stay there because of the inequality of the forces. This is again a simple harmonic motion as discussed in Chapter 2. As described in that chapter, this oscillatory motion, known as *heaving*, will continue indefinitely if there is no damping force, which, when present, always acts in the opposite direction of motion. This motion is known as *free oscillation*; if there is damping, the motion is termed *damped oscillation.*

In the case of free oscillation, the difference in displacement of the ship to its upper extreme position from the equilibrium position is the same in magnitude as the difference in displacement from the equilibrium position to its lower extreme position. This magnitude is known as the *amplitude of the heaving motion.* The time required for one complete cycle of motion is termed the *heaving period.* Since the free heaving motion is a simple harmonic motion, the period of oscillation is independent of the amplitude and is thus known as the *natural period.* The frequency of motion is likewise called the *natural frequency* of the ship.

However, when damping is present, the amplitude of the heaving motion gradually decreases until the ship finally stops at its equilibrium position. The period will be slightly greater in the case of damped oscillation.

Now suppose that the ship is being oscillated vertically up and down by a fluctuating force that is periodic in nature. For a certain amount of time the motion will be rather irregular; such a motion is known as *transient oscillation.* But because of damping, the irregularities soon disappear and a steady-state oscillation takes their place. This is known as *forced oscillation*, in which the amplitude and frequency of motion are dependent on the amplitude and frequency of the exciting force. The damping will also affect the amplitude of forced oscillation. In this case of forced, damped oscillations the following four elements are of importance:

1. The inertial force, which is present when the ship is in oscillatory motion, is

$$F_a = -a\ddot{z}$$

where a is the virtual mass (ship mass plus added mass), and $\ddot{z} = d^2z/dt^2$ is the vertical acceleration.

2. The damping force, which always resists the motion, is

$$F_b = b\dot{z}$$

where b is the damping constant, and $\dot{z} = dz/dt$ is the velocity.

3. The restoring force, which always tends to bring the ship back to its equilibrium position, is

$$F_c = cz$$

where c is the restoring or spring constant, and z is the displacement of the center of gravity (CG) of the ship.

4. The exciting (or encountering) force, which acts on the mass of the ship, is

$$F = F_0 \cos \omega_e t$$

where F_0 is the amplitude of the encountering force, ω_e is the circular frequency of the encountering force, and t is time.

However, the forces must be in equilibrium; thus the equation of motion can be written as

$$F_0 \cos \omega_e t - a\ddot{z} - b\dot{z} - cz = 0$$

or

$$a\ddot{z} + b\dot{z} + cz = F_0 \cos \omega_e t \tag{4.1}$$

Note: When $F_0 = 0$ and $b = 0$, the oscillation is known as *free, undamped heaving motion.* When $F_0 = 0$, the motion is called *free, damped oscillation.* When all the forces act, the motion is termed *forced, damped heaving motion.*

Free, Undamped Heaving Motion ($F_0 = 0, b = 0$)

From the condition of equilibrium, we have

$$a\ddot{z} + cz = 0$$

and the solution for this differential equation is

$$z = A \sin \omega_z t + B \cos \omega_z t \tag{4.2}$$

or

$$z = A \sin(\omega_z t - \beta) \tag{4.2a}$$

where A and B are constants that can be determined from the initial conditions, ω_z is the natural frequency of the heaving motion, that is,

$$\omega_z = \frac{2\pi}{T} = \sqrt{\frac{c}{a}} \tag{4.3}$$

T_z is the heaving period, and β is the phase angle.

Note that the natural heaving period T_z is considered to be a constant and does not depend on the amplitude of motion. This may be true for small and moderate motions. The natural period is an important factor in determining a ship's heaving motion in a seaway.

Free damped Heaving Motion ($F_0 = 0$)

In this case the condition of equilibrium is

$$a\ddot{z} + b\dot{z} + cz = 0$$

The solution for this equation is given (provided that $b < \sqrt{2ac}$) by

$$z = e^{-\nu t}(C_1 \cos \omega_d t + C_2 \sin \omega_d t) \tag{4.4}$$

or

$$z = e^{-\nu t} A \sin(\omega_d t - \delta) \tag{4.5}$$

where $\nu = b/2a$ is the decaying constant, ω_d is the circular frequency of the damped oscillation, that is,

$$\omega_d = \sqrt{\omega_z^2 - \nu^2} \tag{4.6a}$$

ω_z is the natural circular frequency of the undamped oscillation, and C_1 and C_2, or A and δ, are constants to be determined from the initial conditions.

The damped period is given by

$$T_d = \frac{2\pi}{\omega_d} \tag{4.6b}$$

which is greater than T_z since $\omega_d < \omega_z$. Free, damped heaving motion is illustrated in Fig 4.2.

Note: If damping is very large (i.e., $\nu > \omega_z$), the motion is no longer oscillatory and is known as *aperiodic.* This is of no interest for us, since in ship motions ν is always very small in relation to ω_z.

As mentioned above, the constants C_1 and C_2 can be found by prescribing the initial conditions. For example, when $t = 0$,

(a) $z = z_a$ and also (b) $\dfrac{dz}{dt} = 0$

Consider (a): if $t = 0$ in (4.4), then

$$z_a = C_1$$

and

$$z = e^{-\nu t}(z_a \cos \omega_d t + C_2 \sin \omega_d t)$$

Consider (b):

$$\frac{dz}{dt} = \nu e^{-\nu t}(C_1 \cos \omega_d t + C_2 \sin \omega_d t) + \omega_d e^{-\nu t}(C_1 \sin \omega_d t + C_2 \sin \omega_d t)$$

We have already specified that, at $t = 0$, $dz/dt = 0$

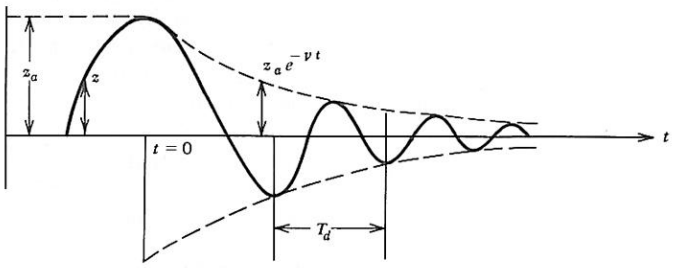


Figure 4.2 Free damped oscillation.

or $0 = -\nu C_1 + \omega_d C_2$, from which

$$C_2 = \frac{\nu C_1}{\omega_d} = \frac{\nu z_a}{\omega_d}$$

since $C_1 = z_a$ and, therefore,

$$z = e^{-\nu t}\left(z_a \cos \omega_d t + \frac{\nu z_a}{\omega_d} \sin \omega_d t\right)$$

or

$$z = z_a e^{-\nu t}\left(\cos \omega_d t + \frac{\nu}{\omega_d} \sin \omega_d t\right)$$

Forced Heaving Motion

In this case, for the equilibrium condition the equation of motion is

$$a\ddot{z} + b\dot{z} + cz = F_0 \cos \omega_e t \tag{4.7a}$$

The solution of the equation is

$$z = e^{-\nu t}(C_1 \cos \omega_d t + C_2 \sin \omega_d t) + z_a \cos(\omega_e t - \varepsilon_2) \tag{4.7b}$$

or

$$z = Ae^{-\nu t} \sin(\omega_d t - \beta) + z_a \cos(\omega_e t - \varepsilon_2)$$

where z_a is the amplitude of the forced motion, and ε_2 is the phase angle of the forced motion in relation to the exciting force. According to (4.7b), the motion is the sum of two oscillations; the first term describes a free, damped oscillation [compare with (4.4)], and the second term an oscillation with the same circular frequency as that of the exciting force for heaving. As long as both oscillations are effective, the result is called a *transient motion*. However, the first oscillation decays more or less quickly, depending on the magnitude of ν. For the steady condition the amplitude of the forced heaving motion z_a is given by

$$z_a = z_{st} \cdot \mu_z$$

where z_{st} = static heaving amplitude $= \dfrac{F_0}{c}$

$$\mu_z = \text{magnification factor} = \frac{z_a}{z_{st}} = \frac{1}{\sqrt{(1-\Lambda^2)^2 + 4\kappa^2\Lambda^2}} \tag{4.8a}$$

$$\Lambda = \text{tuning factor} = \frac{\text{Frequency of encounter}}{\text{Natural frequency}} = \frac{\omega_e}{\omega_z} \tag{4.8b}$$

$$\kappa = \text{nondimensional damping factor} = \frac{\nu}{\omega_z} \tag{4.8c}$$

$$\nu = \frac{b}{2a} \text{ as in (4.5)}$$

$$\omega_z = \sqrt{\frac{c}{a}} \text{ as in (4.3)}$$

$$\varepsilon_2 = \text{phase angle between the exciting force and the motion} = \tan^{-1} \frac{2\kappa\Lambda}{1-\Lambda^2}$$

If it is assumed that a wave of a certain length and amplitude passes along rather slowly, so that the ship is in position to balance itself statically on the wave at every instant of its passage, the ship will then rise and fall slowly with the encountering frequency so as to keep balance between weight and buoyancy, and a static amplitude, z_{st}, will result. If the wave is now considered to move at its correct velocity, a dynamic amplitude, namely z_a, will be produced. The ratio of the amplitude in the dynamic case to that in the static case is called the *magnification factor*. By plotting $\mu = z_a/z_{st}$ to a base of Λ we obtain the figure for dynamic response, as shown in Fig. 4.3. The maximum response is obtained when the quantity under the root sign of (4.8a) is a minimum. The condition for this is obtained by differentiating with respect to Λ and equating to zero. Thus, when $\Lambda = \sqrt{1 - 2\kappa^2}$, then

$$\mu = \mu_{\max}$$

For a very undamped heaving motion (i.e., when κ is very small), Λ_Z for $\mu_{\max}$ is nearly equal to unity. This condition, that is, when the encountering frequency of the exciting force is equal to the natural frequency of heaving for the ship, is considered to be a critical one.

Also it can be seen from Fig 4.3 that for larger and larger damping the maximum response tends to shift more and more toward the left, that is, $\mu_{\max}$ is obtained for Λ somewhat less than unity.

In any case it is recommended that tuning factors near 1.0 be avoided if possible; in other words, for a given wave height, more moderate and less objectionable motions are expected at speeds far removed from synchronism. Such is the case when the ship speed is high and the effective wave lengths are short (i.e., $\Lambda < 1.0$).

It is true that a ship's seakeeping is dependent mainly on the forced oscillations, but the free oscillations are also important for two reasons:

1. The natural frequency of a ship, which is evaluated from the free oscillations, determines the value

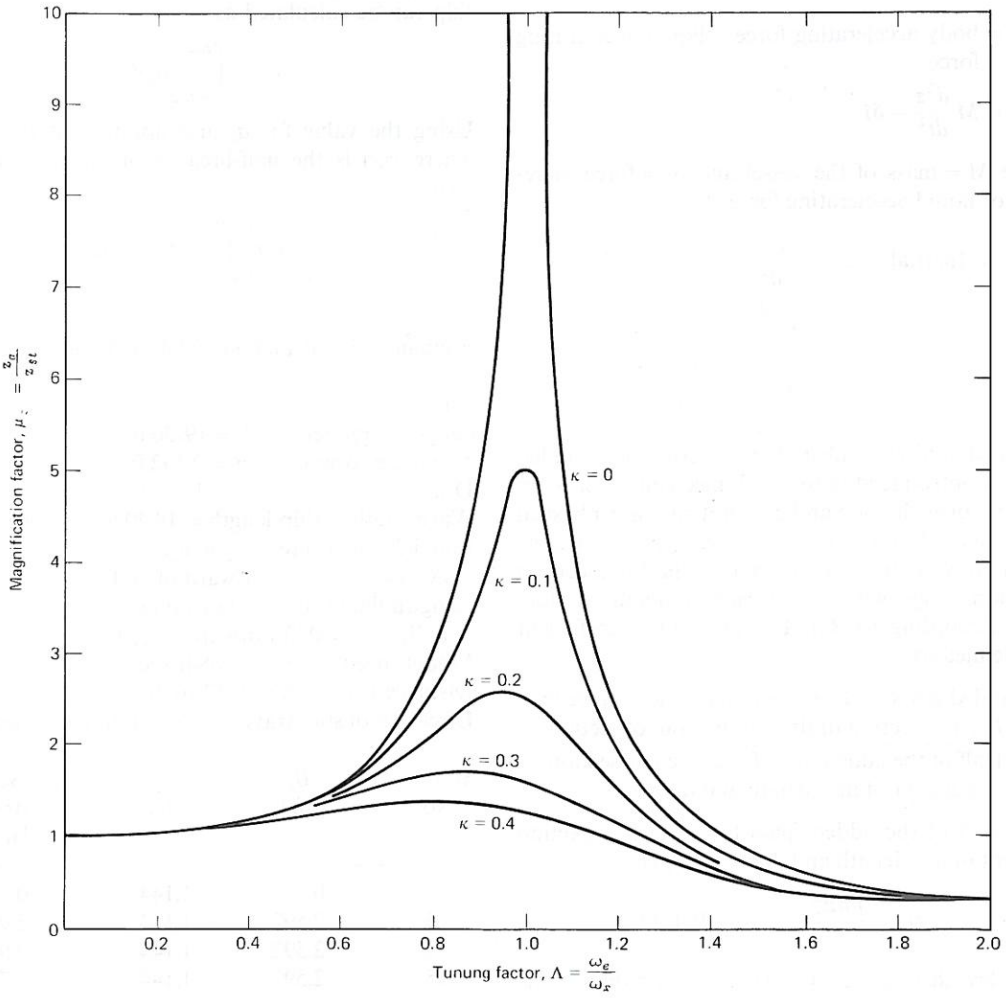


Figure 4.3 Magnification factor versus tuning factor.

of the tuning factor, $\Lambda = \omega_e/\omega_z$, and this is important in finding the region of resonance (i.e., $\Lambda = 1.0$, where the motion is largest).

2. Even in regular seas the transient motion that may cause a large amplitude is dependent on the free (though damped) oscillations. In an irregular seaway, the transient motions may take place at random.

Attempts are therefore made to reduce free oscillations as far as practicable, especially by introducing high damping, as in motion stabilization.

Once the forces for inertia, damping, restoring, and exciting are known, the various expressions for the motion can be easily determined. In other words, before we can determine the heaving motion, we must evaluate the various force coefficients, namely, a, b, c, and F_0 of the equation of heaving motion, equation 4.7a.

Inertial Force

A body having an accelerated motion in a continuous medium of fluid experiences a force that is greater than the mass of the body times the acceleration. Since this increment of force can be defined as the product of the body acceleration and a quantity having the same dimension as the mass, it is termed *added mass.* This concept is needed to discuss the inertial force of a ship; thus the inertial force is

$$a\frac{d^2z}{dt^2} = \text{body accelerating force} + \text{liquid accelerating force}$$
$$= M\frac{d^2z}{dt^2} + \delta I$$

where M = mass of the vessel and δI = force increment or liquid accelerating force. Thus

$$\text{Inertial force} = a\frac{d^2z}{dt^2} = M\frac{d^2z}{dt^2} + \delta I$$
$$= M\frac{d^2z}{dt^2} + a_z\frac{d^2z}{dt^2}$$
$$= (M + a_z)\frac{d^2z}{dt^2}$$

One should remember that the concept of added mass is introduced into fluid mechanics for convenience of evaluation and does not have any physical significance. For example, one should not imagine that a body accelerating in an ideal fluid in a certain direction drags with it a certain amount of fluid mass. According to Ref. 135, an inertial coefficient C is defined as

$$C = \frac{\text{Added mass of the section of unit length, beam } B_n, \text{ and section draft } T_n \text{ to bottom of section}}{\text{Half of the added mass for a circular section segment of unit length and diameter } B_n}$$

Now, half of the added mass for a circular section segment of unit length and diameter B_n is

$$\tfrac{1}{2}\rho\pi r^2 = \frac{\rho\pi B_n^2}{8} \qquad \text{from Ref. 135}$$

where breadth $B_n = 2r$. For shapes other than semicircular ones, the added mass of a ship section, a_n, is found to be [135]

$$a_n = C\frac{\rho\pi B_n^2}{8}$$

The coefficient C for Lewis-form sections is obtained from Fig. 4.4 as a function of the draft/beam ratio, and the area coefficient of the section (defined as section area divided by beam × draft), as well as a function of circular frequency of oscillation. It is assumed that the added masses for sections other than those of the mathematical Lewis form will not differ appreciably as long as the beam, draft, and area of each section are equal in both cases. For conventional hull forms the Lewis-form representation of a section that has the correct beam, draft, and area, but not shape, has been found to be quite satisfactory. Therefore the added mass of the total ship can be calculated as

$$a_z = \int_{-L/2}^{L/2} a_n\,dx$$

Using the value for a_n and noting that $B_n = 2y(x)$, where $y(x)$ is the half-breadth of the waterline, we have

$$a_z = \rho\frac{\pi}{2}\int_{-L/2}^{L/2} Cy^2(x)\,dx$$

Example 4.1 Calculation of Added Mass

Given:

Length of model $L = 19.20$ ft
Maximum beam $B = 2.592$ ft
Draft $T = 1.144$ ft
Wavelength = ship length = 19.20 ft
Longitudinal center of gravity
LCG = + 0.48 ft (forward of ⊗)
Longitudinal center of buoyancy
LCB = + 0.48 ft (forward of ⊗)
Model speed $u = 4.788$ ft/sec
Displacement $\Delta = 2837.76$ lb
Direction of ship travel $\mu = 180°$ (i.e., head sea)

Station No.	B_n [ft]	T_n [ft]	S_n, = Sectional Area [ft²]
0	0	1.144	0
5	2.592	1.144	2.944
10	2.592	1.144	2.944
15	2.592	1.144	2.752
20	0	1.144	0

Find the added mass for heaving, in terms of the model mass.

Solution:

From Table 3.2 the wave frequency is

$$\omega_w = \sqrt{\frac{2\pi g}{L_w}} = \left(\frac{2 \times 3.1416 \times 32.2}{19.20}\right)^{1/2}$$
$$= 3.245 \text{ rad/sec}$$

and the encountering frequency is

$$\omega_e = \omega_w - \frac{\omega_w^2}{g}u\cos\mu$$
$$= 4.811 \text{ rad/sec}$$

where u is the model speed in feet per second.

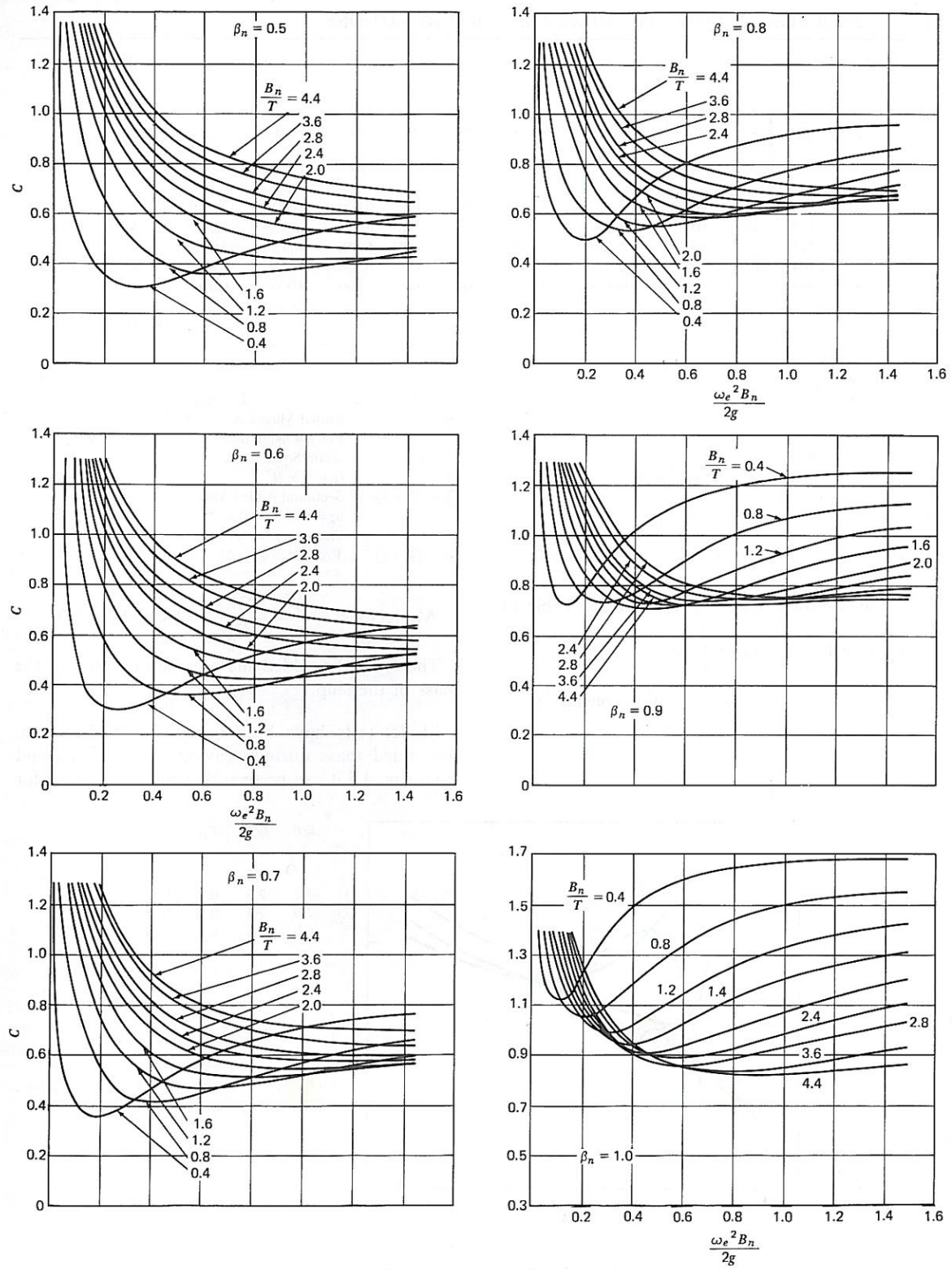


Figure 4.4 Added mass coefficients for two-dimensional floating bodies in heaving motion. [89]

TABLE 4.1

Station Number	B_n [ft]	T_n [ft]	S_n [ft]	$\frac{\omega_c^2}{2g} \times B_n$	B_n/T_n	$B_n \times T_n$	β_n	C	B_n^2	$\frac{\rho\pi}{8} \times B_n^2$	a_n	Simpson's Multiplier	Product
①	②	③	④	⑤	⑥	⑦	⑧	⑨	⑩	⑪	⑫	⑬	⑭
0	0.000	1.144	0.000	0.000	0.000	0.000	0.000	0.00	0.000	0.000	0.000	1	0.000
5	2.592	1.144	2.944	0.932	2.266	2.965	0.993	0.98	6.718	5.113	5.011	4	20.044
10	2.592	1.144	2.944	0.932	2.266	2.965	0.993	0.98	6.718	5.113	5.011	2	10.022
15	2.592	1.144	2.752	0.932	2.266	2.965	0.928	0.84	6.718	5.113	4.295	4	17.180
20	0.000	1.144	0.000	0.000	0.000	0.000	0.000	0.00	0.000	0.000	0.000	1	0.000
												SUM	47.246

Description of Table 4.1

Column Number	*Description*
①	Station Number
②	Beam at Station, B_n[ft]
③	Draft at Station, T_n[ft]
④	Sectional Area at Station, S_n[ft^2]
⑤	$(\omega_c^2/2g) \times B_n$
⑥ = ② ÷ ③	Beam Draft Ratio, B_n/T_n
⑦ = ③ × ②	$B_n \times T_n$
⑧ = ④ ÷ ⑦	Sectional Area Coefficient, $\beta_n = S_n/(B_n \times T_n)$
⑨	Added Mass Coefficient, C, obtained from Fig. 4.4 using the values from ⑤, ⑥, and ⑧
⑩ = ②^2	Beam Squared, B_n^2
⑪	$(\rho\pi/8) \times B_n^2$
⑫ = ⑨ × ⑪	Sectional Added Mass Coefficient, $a_n = C \times (\rho\pi/8) \times B_n^2$
⑬	Simpson's Multiplier
⑭ = ⑫ × ⑬	Product = ⑫ × ⑬

The data for this example are presented in Table 4.1.

$$\text{Added mass for heaving} = \int a_n d\xi$$

$$= \tfrac{1}{3} \times \text{station spacing}(s) \times \text{SUM}$$

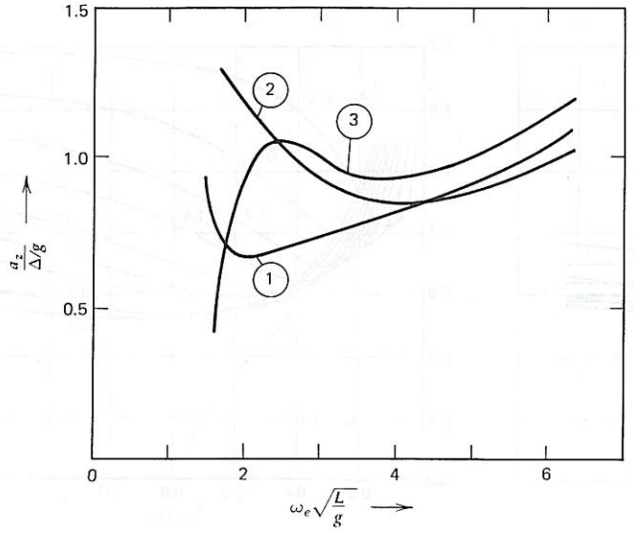
$$= \tfrac{1}{3} \times 4.8 \times 47.246$$

$$= 75.6 \text{ lb-sec}^2/\text{ft}$$

$$\text{Model mass} = \frac{\Delta}{g} = \frac{2837.76}{32.2} = 88.13 \text{ lb-sec}^2/\text{ft}$$

Therefore the added mass is 0.86 or 86% of the mass of the ship.

Model tests have been conducted to determine the added mass during heaving motion [71], and from Fig. 4.5 it can be seen that the added mass for



	L/B	B/T	C_B	C_{WP}	C_M
①	7.5	2.5	0.6	0.706	0.977
②	7.0	2.5	0.7	0.785	0.986
③	6.5	2.5	0.8	0.871	0.994

L	Length of ship
B	Beam
T	Draft
C_B	Block coefficient
C_{WP}	Waterplane coefficient
C_M	Midship section coefficient

Figure 4.5 Nondimensional added mass for heaving [71].

heaving is of the same order of magnitude as the mass of the ship itself. Therefore in the calculation of heaving motion the added mass should be found with sufficient accuracy.

In general, the added mass coefficient for heaving increases with an increase in the block coefficient, C_B, and beam length ratio, B/L.

Damping Force

The damping force always acts in the opposite direction to the motion of the ship and produces a gradual reduction in the amplitude of motion. To determine the effect of damping, the equation of motion must include the damping force, which in our simplified case is

$$F_b = -b\frac{dz}{dt}$$

where b is the coefficient for the damping force in heaving. This damping coefficient normally depends on the following factors:

a. Type of oscillatory motion.
b. Encountering frequency of oscillation.
c. Form of vessel.

The damping force, as considered in our simplified equation of motion, is linearly proportional to the velocity of oscillation, dz/dt. This can be justified, since the damping due to friction and eddymaking is quite small in comparison with that due to wavemaking.

As in the case of added mass, the damping coefficient b can be calculated by the method of strip theory. Because the damping in heaving is caused mainly by the waves generated by the heaving motion of the ship, the damping coefficient per unit length is directly related to the amplitude of the waves. In Ref. 89 the damping coefficient per unit length, b_n, is given by

$$b_n = \frac{\rho g^2 \bar{A}^2}{\omega_e^3}$$

where ω_e is the frequency of the radiated waves (in this case the encountering frequency), and

$$\bar{A} = \frac{\text{Amplitude of the radiated waves}}{\text{Amplitude of the heaving motion}} = \frac{\bar{\zeta}_a}{z_a}$$

The amplitude ratio $\bar{A}$ can be obtained from Fig. 4.6; therefore the total damping coefficient can be calculated by integrating b_n over the entire length of the ship, that is,

$$b = \int_{-L/2}^{L/2} b_n\, dx$$

Example 4.2

Calculate the damping coefficient b for the same values used in Example 4.1.

Solution:

The data are presented in Table 4.2.

TABLE 4.2

Station Number ①	$\frac{\omega_e^2}{2g} \times B_n$ ②	B_n/T_n ③	β_n ④	$\bar{A}$ ⑤	$(\bar{A})^2$ ⑥	b_n ⑦	Simpson's Multiplier ⑧	Product ⑨
0	0.000	0.000	0.000	0.000	0.000	0.000	1	0.000
5	0.932	2.266	0.993	0.570	0.325	5.866	4	23.464
10	0.932	2.266	0.993	0.570	0.325	5.866	2	11.732
15	0.932	2.266	0.928	0.660	0.436	7.869	4	31.476
20	0.000	0.000	0.000	0.000	0.000	0.000	1	0.000
							SUM	66.670

Description of Table 4.2

Column Number	*Description*
①	Station Number
②	$(\omega_e^2/2g) \times B_n$
③	Beam Draft Ratio, B_n/T_n
④	Sectional Area Coefficient, β_n
⑤	Amplitude Ratio for Two-Dimensional Body in Heaving Motion, $\bar{A}$, found by entering Fig. 4.6 with the values from columns ②, ③, and ④
⑥	$(\bar{A})^2$
⑦	Sectional Damping Coefficient, $b_n = \rho g^2 \bar{A}^2/\omega_e^3$
⑧	Simpson's Multiplier
⑨	Product = ⑦ × ⑧

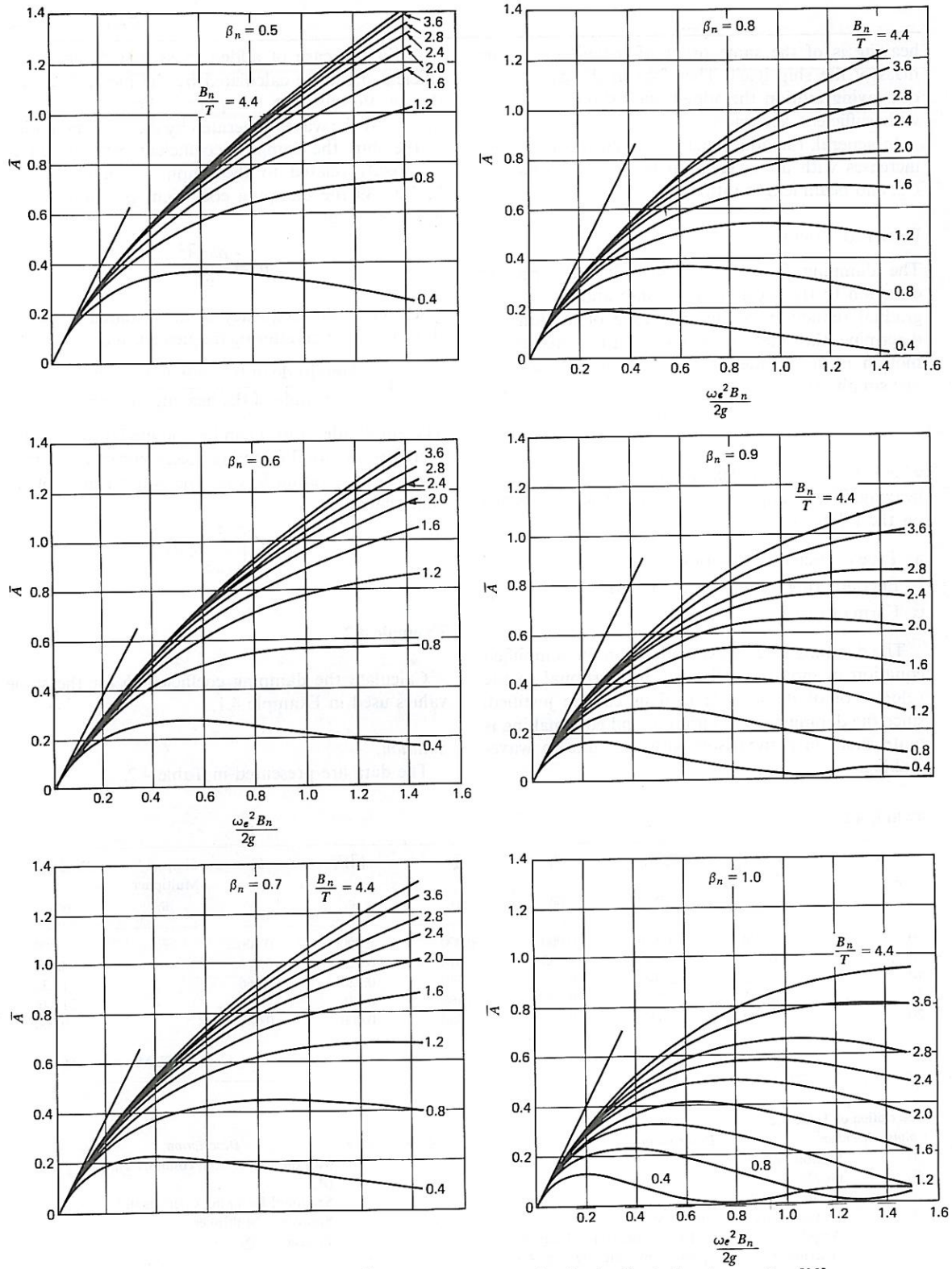


Figure 4.6 Amplitude ratios $\bar{A}$ for two-dimensional floating bodies in heaving motion [89]. Here β_n is sectional area coefficient, B_n is breadth of each section, and T is draft.

The damping coefficient for heaving is

$$b = \int b_n dx$$
$$= \tfrac{1}{3} \times s \times \text{SUM}$$
$$= \tfrac{1}{3} \times 4.8 \times 66.67$$

or

$$b = 106.67 \text{ lb-sec/ft}$$

It should be noted that damping is very important in the evaluation of amplitude of motion near synchronism, whereas it has less effect on the amplitude of motion at frequencies that are further away from synchronism. However, the damping has a greater effect on the phase lag of motions at frequencies different from the synchronous one.

In strip theory the interaction between adjacent sections is ignored. However, the results obtained from such calculations agree well with experimental ones. There are three different methods of obtaining damping by model tests [242]:

1. Free oscillations in calm water.
2. Forced oscillations in calm water.
3. Forced oscillations in regular waves.

Method 1 is not very accurate, since there is a large amount of damping in heaving motion and an extinction curve cannot be determined accurately. By using method 2 all the factors determining the damping force can be determined accurately. This is especially the case with the exciting forces generated by an oscillator. Although method 3 represents a more realistic situation, it is difficult to determine the exciting force accurately and therefore this method can deliver results only for a more qualitative study. In any event the values of the damping coefficient can be different in the three experimental procedures, since the physical conditions in these procedures are different.

Determination of the damping coefficient by method 2 follows.

Experimental Determination of Damping. The amplitude of the exciting force (here the driving force) F_0 can be kept constant for a wide range of frequencies both above and below the natural frequency of heaving, and a diagram may be obtained experimentally as shown in Fig. 4.7. In reality only a part of this diagram is obtained by the test, and the scale of the ordinates is not important. The maximum value of the magnification factor μ_z is measured and put equal to $1/2\kappa$. A line is drawn parallel to the base having an ordinate value of $\sqrt{2}/2 = 0.707$ times the maximum ordinate or equal to $\sqrt{2}/4\kappa$. The horizontal line crosses the dynamic response curve at two values of Λ, namely, Λ_1 and Λ_2. Now from (4.8)

$$\frac{1}{\mu_z^2} = (1 - \Lambda^2)^2 + 4\kappa^2\Lambda^2$$
$$= \left(\frac{4\kappa}{\sqrt{2}}\right)^2$$
$$= 8\kappa^2$$

Solving for Λ, we obtain

$$\Lambda_1^2 = 1 - 2\kappa^2 - 2\kappa\sqrt{1 + \kappa^2}$$

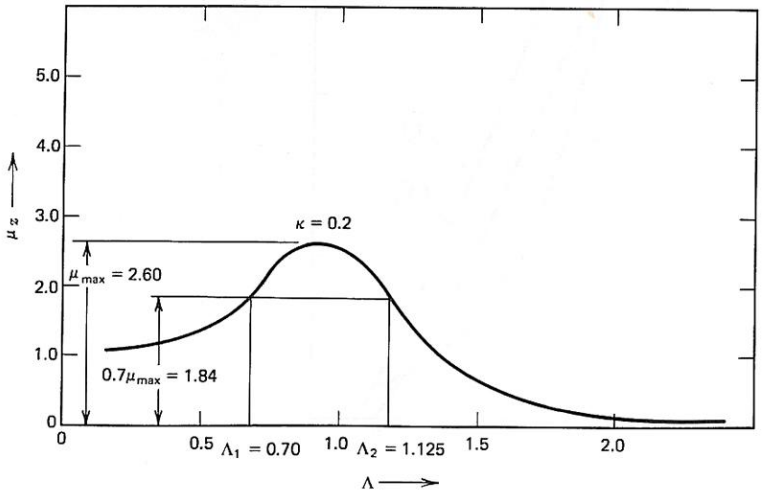


Figure 4.7 Plot of magnification factor versus turning factor.

and

$$\Lambda_2^2 = 1 - 2\kappa^2 + 2\kappa\sqrt{1+\kappa^2}$$

Thus

$$\Lambda_2^2 - \Lambda_1^2 = 4\kappa\sqrt{1+\kappa^2}$$

Since the damping factor κ usually has a small value in ship motion, we can neglect the value of κ^2 and get

$$\Lambda_2^2 - \Lambda_1^2 = 4\kappa$$

Again, as both Λ_1 and Λ_2 are approximately equal to 1.0, we may write

$$\Lambda_1 + \Lambda_2 \simeq 2$$

or

$$\Lambda_2^2 - \Lambda_1^2 = (\Lambda_2 + \Lambda_1)(\Lambda_2 - \Lambda_1) = 4\kappa$$

or

$$2(\Lambda_2 - \Lambda_1) = 4\kappa$$

so that

$$\kappa = \frac{\Lambda_2 - \Lambda_1}{2}$$

In Fig. 4.7 we read the values of Λ_1 and Λ_2 as 0.700 and 1.125, respectively. Therefore the nondimensional damping coefficient κ for this particular case is determined as

$$\kappa = \frac{\Lambda_2 - \Lambda_1}{2} = \frac{1.125 - 0.700}{2} = 0.21$$

The experimentally obtained damping force coefficient obtained by the forced oscillation method in calm water is shown in Fig. 4.8. The results have been plotted nondimensionally.

Both theoretical and experimental investigations enable us to draw the following conclusions:

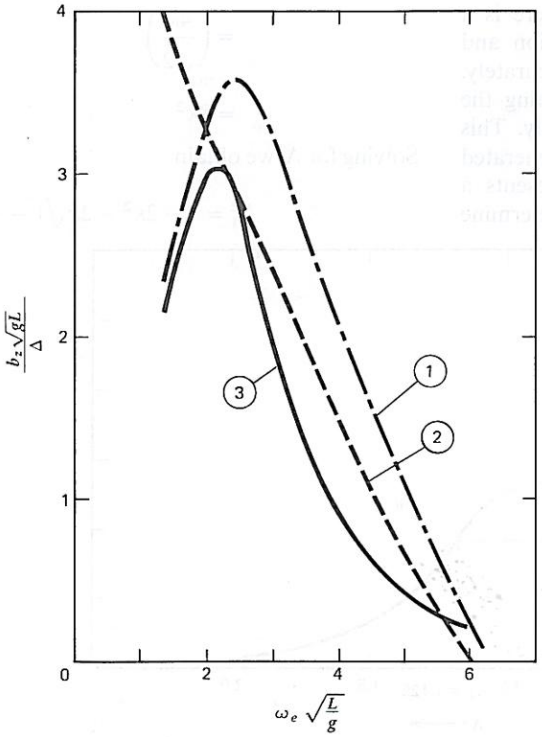
a. The damping force coefficient is proportional to the square of the waterplane area.

b. Ships with V-type sections experience more damping than do U-type ships for the same load waterplane.

c. The nondimensional damping coefficient, when plotted to a base of $\omega_e\sqrt{B/g}$, reaches a maximum value and then decreases rapidly (see Fig. 4.8). In the region of resonance, where damping plays a very important role, this decrement in damping does not appear to have a large effect.

d. The higher the speed of advance, the lower is the wave damping.

In general, it can be said that the damping coefficient increases as B/L increases but decreases with increase in the block coefficient, C_B, of the vessel.



	L/B	B/T	C_B	C_W	C_θ
①	7.5	2.5	0.6	0.706	0.977
②	7.0	2.5	0.7	0.785	0.986
③	6.5	2.5	0.8	0.871	0.994

Figure 4.8 Nondimensional damping coefficient for heaving motion [124].

Restoring Force

The restoring force for heaving is given as the additional buoyancy force that acts on a body when it is submerged to a deeper draft. If it is assumed that there is no significant change in the waterplane area during heaving (i.e., the ship is said to be wall-sided near the load waterline), the restoring force is given as the amount of water displaced, which is equal to specific weight times additional submerged volume. Thus

$$cz = \rho g A_{WP} z$$

where the product of A_{WP} (the area of load waterplane) and z (the additional immersion of the ship) is equal to the excess of displacement volume. Therefore

$$c, \text{ the restoring force coefficient} = \rho g A_{WP} = \rho g L B C_{WP} \quad (4.9)$$

where C_{WP} is the waterplane area coefficient.

The restoring force is obtained directly from offsets as

$$c = \rho g \int_{-L/2}^{+L/2} 2y(x)\,dx \quad (4.9a)$$

where $y(x)$ is the half-breadth at section x.

If the restoring force coefficient is absent, as in surging, swaying, and yawing motions, the motion is nonoscillatory in the real sense, and therefore neither resonance nor the magnifications of amplitudes are possible in such modes of motion; however, oscillatory motions do take place because of the reversal of the exciting force.

Example 4.3

Find the restoring force coefficient for heaving for the model described in Example 4.1.

TABLE 4.3

Station No.	B_n [ft]	$c_n = \rho g B_n$ [lb/ft²]	Simpson's Multiplier	Product
0	0	0	1	0
5	2.592	161.78	4	647.12
10	2.592	161.78	2	323.56
15	2.592	161.78	4	647.12
20	0	0	1	0
			SUM	1617.80

Solution:

The restoring force coefficient for heaving is

$$c = \tfrac{1}{3} \times s \times \text{SUM}$$
$$= \tfrac{1}{3} \times 4.8 \times 1617.8$$
$$= 2588 \text{ lb/ft}$$

where s is the station spacing.

Note: $\rho = 1.9384$ lb-sec²/ft for fresh water at 59° F.

Example 4.4

Given:

Ship length	$L = 420$ ft
Beam	$B = 56$ ft
Draft	$T = 20$ ft
Block coefficient	C_B = waterplane coefficient C_{WP}
Added mass	= 90% of ship mass

Assuming that there is no damping, do the following:

a. Calculate the heaving period in still water.

b. Derive the expression for heaving oscillation in still water if the initial displacement from the equilibrium position and the velocity of the heaving motion at the instant of time $t = 0$ are 0 and 5.52 ft/sec, respectively.

c. Calculate the maximum force exerted on the deck of a ship by a winch that weighs 4 tons.

d. Show by diagrams how the displacement, velocity, and acceleration change with time.

Solution:

a. From (4.3) the natural heaving period T_z is given by

$$T_z = 2\pi \sqrt{\frac{a}{c}}$$

where a is the virtual mass, and c is the restoring force coefficient. Now

$$a = M + a_z = M + 0.9M = 1.9\frac{\Delta}{g}$$

and

$$c = \rho g A_{WP}$$

from (4.9). Thus

$$T_z = 2\pi \sqrt{\frac{1.9\Delta}{g \cdot \rho g A_{WP}}} = 2\pi \sqrt{\frac{1.9LBTC_B \cdot \rho g}{g \rho g L B C_{WP}}} = 2\pi \sqrt{\frac{1.9T}{g}}$$
$$= 6.81 \text{ sec}$$

See Fig. 4.9*a*.

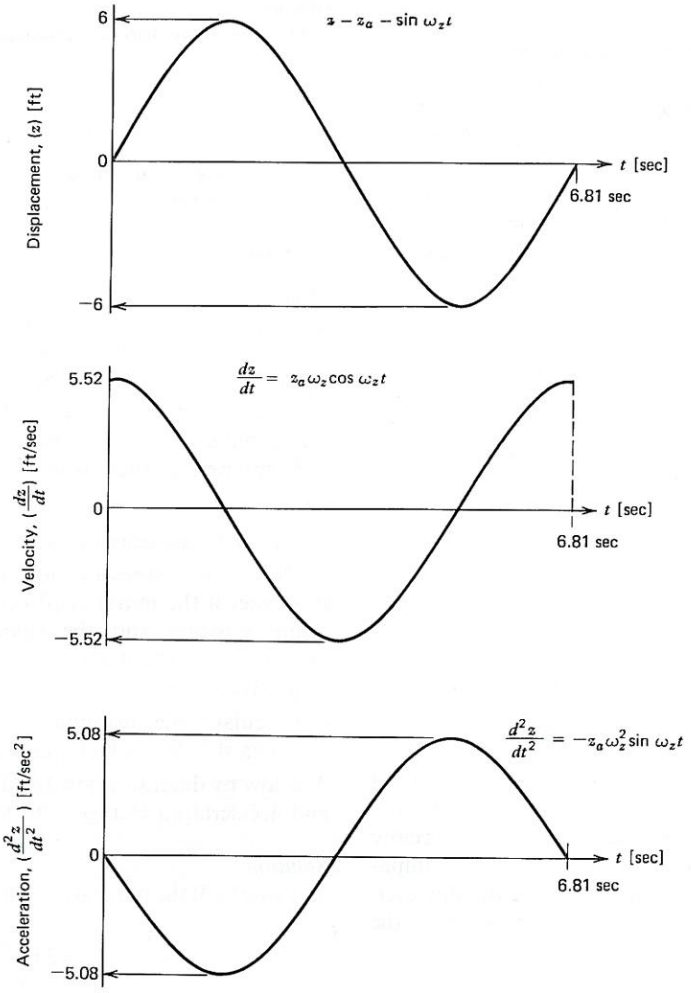


Figure 4.9 Displacement, velocity, and acceleration of heaving motion.

b. The general solution for undamped heaving in still water is given as

$$z = A \sin \omega_z t + B \cos \omega_z t$$

From (4.1):

1. When $t = 0$, $z = 0$ and $B = 0$.

2. Again, when $t = 0$, $dz/dt = 5.52$ ft/sec, or, differentiating (4.1), we have

$$\frac{dz}{dt} = \{A\omega_z \cos \omega_z t - B\omega_z \sin \omega_z t\}\Big|_{t=0} = A\omega_z$$

Substituting the value of dz/dt for $t = 0$, we get

$$5.52 = A\omega_z$$

or

$$A = \frac{5.52}{\omega_z}$$

Since

$$\omega_z = \frac{2\pi}{T_z} = \frac{2\pi}{6.81} = 0.92$$

$$A = 6$$

Hence the expression for heaving motion in still water is

$$z = 6 \sin 0.92t$$

This is shown in Fig. 4.9*b*.

c. The force exerted by the winch on the deck is the addition of the gravity force and the inertial force due to heaving motion, where the inertial force is

Here m is the mass of the winch, and d^2z/dt^2 is the heaving acceleration. Since the mass of the winch does not change, the maximum force of the winch on the deck takes place when the inertial force is maximum, that is, when the acceleration d^2z/dt^2 is maximum.

Differentiating (4.1) twice, we have

$$\frac{d^2z}{dt^2} = -A\omega_z^2 \sin \omega_z t - B\omega_z^2 \cos \omega_z t$$
$$= -A\omega_z^2 \sin \omega_z t$$

since $B = 0$ in this particular case; the heaving acceleration is shown in Fig. 4.9*c*.

We see from this equation that d^2z/dt^2 is maximum when $-\sin \omega_z t = 1$, or

$$\frac{d^2z}{dt^2} = A\omega_z^2$$
$$= 6(0.92)^2$$
$$= 5.08 \text{ ft/sec}^2$$

Since g or an acceleration of 32.2 ft/sec^2 gives a force of 4 tons to the winch, an acceleration of 5.08 ft/sec^2 gives a force of (4/32.2) × 5.08 or 0.63 ton; the total force is then 4 + 0.63 or 4.63 tons.

d. Figure 4.9 shows diagramatically displacement, velocity, and acceleration of heaving motion as functions of time.

Example 4.5

a. Show that, if the linear dimensions of a ship and those of its geometrically similar model are in the ratio of λ (the scale factor), the natural heaving period of the ship is $\sqrt{\lambda}$ times that of the model.

b. If a 16.8 ft long model of a ship (length 420 ft) has a heaving period of 1.362 sec, find the heaving period of the ship.

Solution:

a. The natural heaving period of the ship is

$$T_Z = 2\pi \sqrt{\frac{C\Delta}{g\rho g A_{WP}}} \qquad (4.9b)$$

where C is the ratio of the virtual mass and the ship mass. Thus

$$T_z = 2\pi \sqrt{\frac{CLBTC_B\rho g}{g\rho g LBC_{WP}}}$$
$$= 2\pi \sqrt{\frac{CTC_B}{gC_{WP}}}$$
$$= 2\pi \sqrt{\frac{C(\lambda T_m)C_B}{gC_{WP}}}$$

where T_m is the model draft. Finally

$$T_z = \sqrt{\lambda} 2\pi \sqrt{\frac{C(\lambda T_m)C_B}{gC_{WP}}}$$
$$= \sqrt{\lambda} T_z \text{ (model)}$$

since C, C_B, g, and C_{WP} are the same for both ship and model.

b. The scale factor is

$$\lambda = \frac{420}{16.8} = 25$$

Therefore

$$T_z \text{ (ship)} = \sqrt{\lambda}\, T_z \text{ (model)} = \sqrt{25} \times 1.362 = 6.81 \text{ sec}$$

EXCITING FORCE

To determine the exciting force for ship motions, water waves must be studied, since they are the only source of ship excitation in a seaway. Let $\zeta = \zeta_a \cos \omega_e t$. The exciting force for the heaving motion is obtained by integrating the additional buoyancy due to waves along the ship. Therefore the exciting force on a section of a ship of unit length is given by

$$\rho g 2y\zeta\, dx$$

where ζ is the ordinate of the effective wave profile; that is, the effective wave is considered to be a subsurface wave profile, or

$$\zeta = \zeta_a e^{-k'T_m} \cos(k'x - \omega_e t)$$

where k' is the effective wave number, $2\pi/L_w'$, that is, $k \cos \mu$, k being the normal wave number, $2\pi/L_w$; μ is the direction of the ship's heading in relation to the waves; and T_m is the mean depth of the effective wave from the free surface.

Note that for any arbitrary heading angle μ the heaving exciting force is found by introducing the effective wavelength, $L_w' = L_w/\cos \mu$, in place of the absolute wavelength, L_w. For the beam sea case ($\mu = 90°$ or $270°$) $L_w' \to \infty$, and the exciting force amplitude F_0 becomes maximum and is given as

$$F_0 = 2\rho g \zeta_a BLC_{WP}$$
$$= 2\rho g \zeta_a A_{WP}$$

However, in the calculations of the exciting force for heaving, the ship is supposed to remain stationary as far as the vertical motion is concerned, and the waves are assumed to pass along the ship gradually. Hence the exciting force is the excess buoyancy

force at any instant of time:

$$F = F_0 \cos \omega_e t \tag{4.11a}$$

and F_0, the amplitude of the total exciting force, is obtained by integrating the bouyancy force of individual sections.

Let us suppose that the ship is wall sided in the region of the load waterline (LWL) and that, while the wave approaches the ship, the time t is recorded when the wave crest is amidships. Then the wave at any position x from the midship section is given by (4.10). Now the exciting force for heaving is calculated by assuming that the ship remains still as far as vertical motion is concerned and the waves pass slowly by the ship. The exciting force for heaving is then the additional buoyancy force at any instant and can be expressed as

$$F = \int_{-L/2}^{L/2} \rho g 2y(x)\zeta \, dx \tag{4.11b}$$

Substituting the expression for wave profile and expanding the cosine term, as well as assuming the ship to be symmetrical about the midship section, we obtain the exciting force for heaving [242] as

$$F = \int_{-L/2}^{L/2} (\rho g_2 y \zeta_a e^{-k'T_m} \cos k'x \, dx) \cos \omega_e t \tag{4.11c}$$

However, if the surface wave profile is taken to be the effective wave profile (this assumption means a greater exciting force and the design will therefore be on the safer side), the expression for the exciting force becomes

$$F = \left(2\rho g \zeta_a \int_{-L/2}^{L/2} y \cos k'x \, dx\right) \cos \omega_e t \tag{4.12a}$$
$$= F_0 \cos \omega_e t$$

Note that the exciting force F is positive if it acts in the positive direction, that is, downward.

Comparing (4.10) and (4.12a), we find the phase angle between the wave profile and the heaving force due to waves to be

$$\varepsilon_1 = 0^\circ \tag{4.12b}$$

The amplitude of the exciting force can be expressed nondimensionally as

$$f_0 = \frac{F_0}{\rho g \zeta_a LB}$$
$$= \frac{2}{LB} \int_{-L/2}^{L/2} y(x) \cos(kx \cos \mu) dx \tag{4.13}$$

Note: For the beam sea condition (i.e., $\mu = 90^\circ$ or 270°) the exciting force for heaving reaches the maximum value.

Example 4.6 Calculation of the Amplitude of the Exciting Force for Heaving for The Ship Model Described in Example 4.1

From that example the following data are available:

μ $= 120^\circ$
LCG = at ⊗
L $= L_w = 19.2$ ft
B $= 2.592$ ft
ζ_a $= 0.20$ ft
ρ $= 1.93$ lb-sec^2/ft^4

Find f_0 and F_0.

Solution:
From the above values, the wave number is

$$k = \frac{2\pi}{L_w} = \frac{6.28}{19.20} = 0.327 \text{ ft}^{-1}$$

and the dimensionless force amplitude is

$$f_0 = \frac{2}{LB} \int_{-L/2}^{L/2} y(x) \cos(kx \cos \mu) dx$$

The numerical values of f_0 and F_0 are determined with the help of Table 4.4.
Thus

$$\text{Integral} = \tfrac{1}{3} \times s \times \text{SUM} = \tfrac{1}{3} \times 4.8 \times 9.92 = 15.87$$

Therefore

$$f_0 = \frac{2}{LB} \times \text{integral} = \frac{2}{LB} \times 15.87 = 0.638$$

or

$$F_0 = \rho g \zeta_a LB f_0 = 396.2 \text{ lb.}$$

Note: If more stations than the five taken in this example are considered, more accurate result can be obtained for F_0.

The typical exciting force coefficient for heaving, f_0, as a function of the ratio of encountering wavelength to ship length for different values of the waterplane area coefficient is given in Fig. 4.10. The following conclusions are drawn about the heaving force [242]:

a. The heaving force is small when the effective wavelength is less than half of the ship's length.

b. When the ratio of effective wavelength to ship length is equal to the waterplane area coefficient, the heaving force seems to be zero.

TABLE 4.4

Station No. ①	$y = \frac{B_n}{2}$ ②	Cos μ ③	x ④	$k' = kx \cos \mu$ ⑤	Cos (kx cos μ) ⑥	y cos ($k'x$ cos μ) ⑦	Simpson's Multiplier ⑧	Product ⑨
0	0	− 0.5	9.6	− 1.570	0.000	0.000	1	0.000
5	1.296	− 0.5	4.8	− 0.785	0.707	0.916	4	3.664
10	1.296	− 0.5	0	0.000	1.000	1.296	2	2.592
15	1.296	− 0.5	− 4.8	0.785	0.707	0.916	4	3.664
20	0	− 0.5	− 9.6	1.570	0.000	0.000	1	0.000
							SUM	9.920

Description of Table 4.4

Column Number	*Description*
①	Station Number
②	Offset (half-breadth of waterplane), y = $B_n/2$
③	Cos μ
④	Distance from LCG, x
⑤	kx cos μ = effective wave number k'
⑥	Cos (kx cos μ)
⑦	y Cos ($k'x$ cos μ)
⑧	Simpson's Multiplier
⑨	Product = ⑦ × ⑧

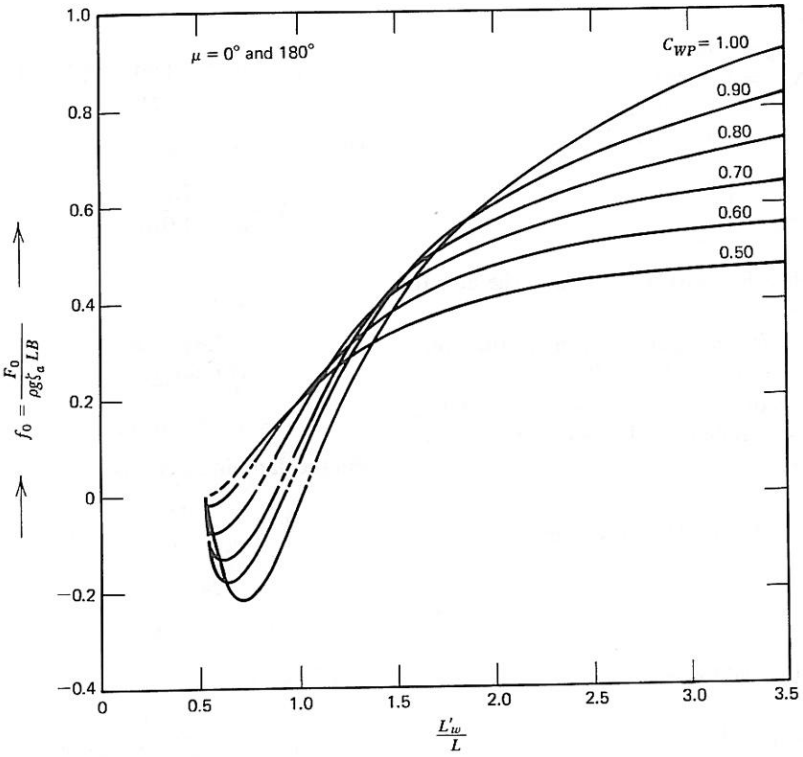


Figure 4.10 Exciting force coefficient for heaving, f_0 [242].

c. The heaving force is small or moderate when the effective wavelength is equal to the ship's length.

d. As the effective wavelength approaches infinity, the nondimensional heaving force approaches the value of the waterplane area coefficient.

If it is assumed, as mentioned earlier, that the waves pass along the ship very slowly, the vertical

displacement of any section in the wave is termed *static heave* and is given by

$$\frac{F}{c} = z_{st}\cos\omega_e t$$

The static heave amplitude is then

$$z_{st} = \frac{F_0}{c}$$

where F is the exciting force for heaving, that is,

$$F = F_0\cos\omega_e t$$

$$= 2\rho g\zeta_a e^{-kT_m}\int y\cos(kx - \omega_e t)dx$$

Example 4.7

Given:

$L = 450\,\text{ft}$
$B = 70\,\text{ft}$
$C_{WP} = 0.80$
$\Delta = 12{,}500$ tons
$\omega_e = 1.18$ rad/sec
$\rho = 1.99\,\text{lb-sec}^2/\text{ft}^2$

Wave amplitude $\zeta_a = 10\,\text{ft}$.
and also these facts:

1. The added mass for heaving is 80% of the actual mass of the ship.
2. The coefficient for damping is given in the non-dimensional form as $b\sqrt{gL}/\Delta = 1.70$.
3. The amplitude of the exciting force for heaving motion is given nondimensionally as $f_0 = F_0/\rho g\zeta_a LB = 0.17$ (see Fig. 4.10).

Find the heaving amplitude of the ship.

Solution:

a.

$$\text{Inertial force} = \frac{\Delta' d^2z}{g\,dt^2}$$

where the virtual mass is

$$a = \frac{\Delta'}{g} = 1.80\frac{\Delta}{g}$$

$$= 1.80 \times \frac{12{,}500}{32.2} \times 2240$$

$$= 1{,}565{,}222\,\text{lb-sec}^2/\text{ft}$$

b. Since

$$\frac{b\sqrt{gL}}{\Delta} = 1.70$$

the damping coefficient is

$$b = \frac{1.70\Delta}{\sqrt{gL}} = \frac{1.70 \times 12{,}500}{\sqrt{32.2 \times 450}} = 176.53\ \text{ton-sec/ft}$$

$$= 395{,}427\ \text{lb-sec/ft (by multiplying by 2240)}$$

c. The restoring force coefficient is

$$c = 1.99 \times 32.2 \times (450 \times 70 \times 0.80)\ [\text{from (4.9)}]$$
$$= 1{,}614{,}766\ \text{lb/ft}$$

d. The dimensionless exciting force is

$$f_0 = \frac{F_0}{\rho g\zeta_a LB} = 0.17$$

so that

$$F_0 = 0.17 \times 1.99 \times 32.2 \times 10 \times 450 \times 70$$
$$= 3{,}431{,}377\,\text{lb}$$

The tuning factor is

$$\Lambda = \frac{\omega_e}{\omega_z} = \frac{1.180}{1.016} = 1.61$$

$$\omega_z = \sqrt{\frac{c}{a}}$$

$$= \sqrt{\frac{1{,}614{,}766}{1{,}565{,}222}}$$

$$= 1.016\ \text{rad/sec}$$

and the damping factor is

$$k = \frac{\nu}{\omega_z} = \frac{0.126}{1.016} \qquad \text{where } 2\nu = \frac{b}{a}$$

$$= 0.124$$

The heaving amplitude

$$z_a = z_{st}\cdot\mu_z$$

$$= \frac{F_0}{c} \times \frac{1}{\sqrt{(1-\Lambda^2)^2 + 4\kappa^2\Lambda^2}}$$

$$= \frac{3{,}431{,}377}{1{,}614{,}766}$$

$$\times \frac{1}{\sqrt{[1-(1.161)^2]^2 + 4 \times (0.124)^2 \times (1.161)^2}}$$

$$= 4.70\,\text{ft}$$

Example 4.8

With the data given in Example 4.7 find the following:

a. The phase relationship between the wave motion and the heaving motion.

b. The maximum heaving acceleration in a regular seaway.

c. The relative motion (i.e., displacement) of the ship with respect to the wave.

d. The magnitude of the maximum resultant relative motion (i.e., displacement) of the ship with respect to the wave surface.

Solution:

a. The phase angle between the wave motion and the heaving motion is expressed as

$$\varepsilon = \varepsilon_1 + \varepsilon_2$$

where ε_1 is the phase angle between the wave motion and the exciting force caused by waves, and ε_2 is the phase angle between the exciting force and the heaving motion.

Now

$$\varepsilon_1 = 0 \text{ from (4.12b)}$$

and from (4.7b)

$$\varepsilon_2 = \tan^{-1}\left(\frac{2\kappa\Lambda}{1-\Lambda^2}\right)$$

$$= \tan^{-1}\left(\frac{2 \times 0.124 \times 1.161}{1-(1.161)^2}\right)$$

$$= -39.6^\circ$$

Note: The investigation of phase angles is a rather important aspect of the study of ship motions, since, as will be shown later, both deck wetness and the added resistance of a ship in waves depend on the ship's relative position with respect to the waves.

It should also be noted that, if the frequency of encounter is very nearly equal to the natural frequency of heaving, the phase lag prediction may become extremely uncertain, since in this resonance region the damping influences the heaving motion appreciably. On the other hand, if the damping is very small, the phase lag is 0° below resonance and 180° above resonance. Near the resonance zone the motion amplitude is also very sensitive to damping; therefore motion predictions near resonance are not always satisfactory.

b. The equation of heaving motion of a ship in a train of regular waves is expressed as

$$z = z_a \cos(\omega_e t - \varepsilon)$$

so that

$$\frac{dz}{dt} = -z_a \omega_e \sin(\omega_e t - \varepsilon)$$

and

$$\frac{d^2z}{dt^2} = -z_a \omega_e^2 \cos(\omega_e t - \varepsilon)$$

The magnitude of d^2z/dt^2 is maximum when $\cos(\omega_e t - \varepsilon) = -1.0$; thus

$$\frac{d^2z}{dt^2} = z_a \omega_e^2$$

$$= 4.70 \times (1.18)^2$$

$$= 6.54 \text{ ft/sec}^2$$

c. Let the equation of wave motion about any fixed point on the calm waterline be given as

$$\zeta = \zeta_a \cos \omega_e t$$

The heaving motion of the same point for the steady-state condition is then

$$z = z_a \cos(\omega_e t - \varepsilon)$$

where ε is the phase angle between the wave motion and the motion of the ship. Thus the relative motion (or displacement) of the point can be expressed as

$$s = \zeta - z$$

$$= \zeta_a \cos \omega_e t - z_a \cos(\omega_e t - \varepsilon)$$

$$= \zeta_a[\cos \omega_e t - \frac{z_a}{\zeta_a} \cos(\omega_e t - \varepsilon)]$$

d. The maximum relative motion of the ship is obtained when

$$\frac{ds}{d(\omega_e t)} = 0$$

or, differentiating, we have

$$\omega_e \zeta_a[-\sin \omega_e t + \frac{z_a}{\zeta_a} \sin(\omega_e t - \varepsilon)] = 0$$

Since $\zeta_a \neq 0$, the expression inside the brackets is zero, that is,

$$-\sin \omega_e t + \frac{z_a}{\zeta_a} \sin(\omega_e t - \varepsilon) = 0$$

from which

$$-\sin \omega_e t + \frac{z_a}{\zeta_a}(\sin \omega_e t \cos \varepsilon - \cos \omega_e t \sin \varepsilon) = 0$$

Now, inserting the values of z_a, ζ_a, and ε, we have

$$-\sin \omega_e t + \frac{4.7}{10}[\sin \omega_e t \times \cos(-39.6°) - \cos \omega_e t \times \sin(-39.6°)] = 0$$

or

$$-0.638 \sin \omega_e t + 0.299 \cos \omega_e t = 0$$

or

$$1 = \frac{0.638 \sin \omega_e t}{0.299 \cos \omega_e t}$$

from which

$$\tan \omega_e t = 0.469$$

Thus

$$\omega_e t = 25.11° \text{ (or } 205.11°)$$

and

$$s \text{ is maximum when } \omega_e t = 25.11°$$

The maximum resultant relative motion is obtained by inserting this value of $\omega_e t$ into the equation for the relative motion, that is,

$$s = 10[\cos 25.11° - \frac{4.7}{10}\cos(25.11° + 39.60°)] = 7.04 \text{ ft}$$

Note also that by drawing curves for ζ, z, and s it is seen that at $\omega_e t = 25°$ and 205° the maximum relative motion of 7.04 ft is obtained. Also note that in Fig. 4.11 the motion curve precedes the wave curve since $z = z_a \cos[\omega_e t - (-39.6°)]$, that is, the phase angle

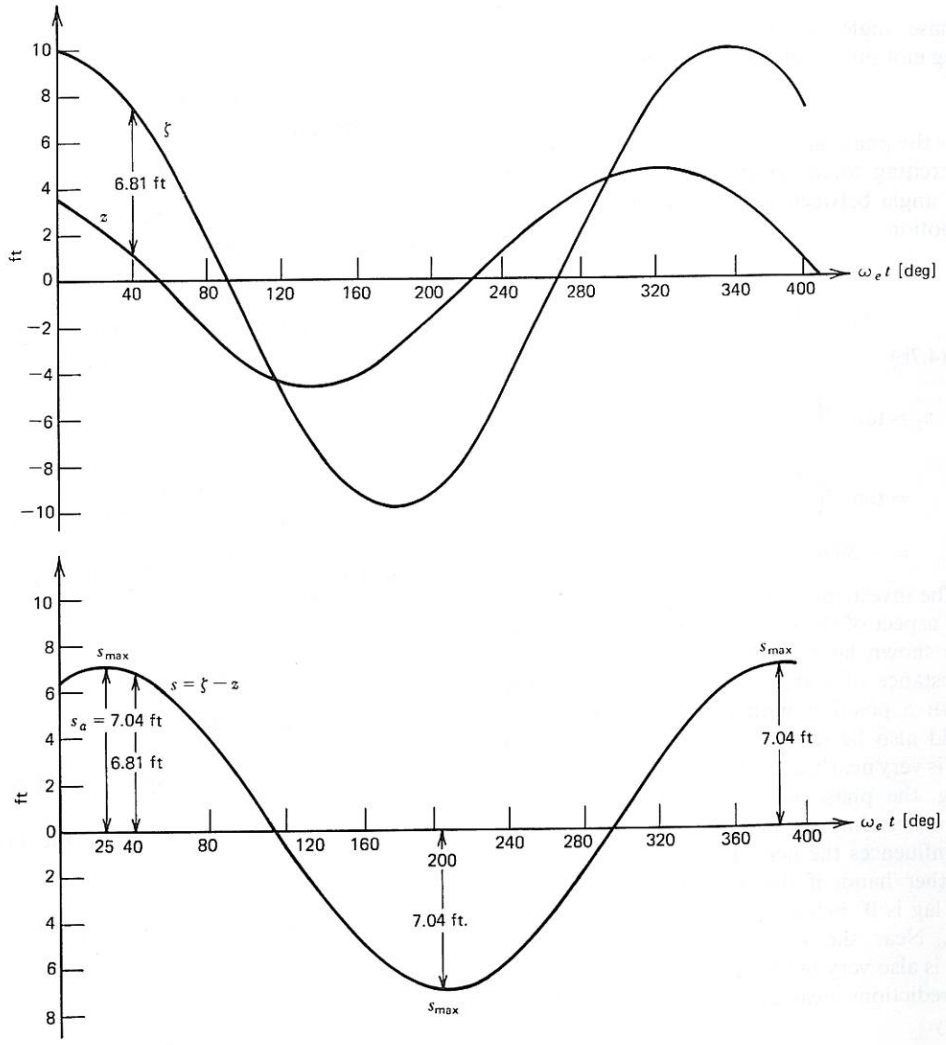


Figure 4.11 Motion relative to free surface.

is positive in relation to the wave curve (see Section 2.2).

Ship Model Correlation

From the dynamical analysis (see Table 4.5) the following relations hold between the ship and the model:

$$L = \lambda l, \qquad M = \lambda^3 m$$

where

$$\lambda = \frac{\text{Length of ship}}{\text{Length of model}} = \text{scale factor}$$

M and L are ship quantities, and m and l are model quantities.

Consider two ships (or one ship and one model) that are exactly similar in all respects except dimensions; in other words, if the relation between any linear dimensions of one ship and the corresponding dimension of the other ship is λ (i.e., $L_1 = \lambda L_2$), prove that the periods for small oscillations are in the ratio of $\lambda^{1/2}$, or $T_1 = \lambda^{1/2} T_2$. (T_1 and L_1 are for the larger hull, and T_2 and L_2 for the smaller one.) We know from Example 4.5 that

$$T_1 = \frac{2\pi k_1}{\sqrt{g\overline{GM}_1}}$$

and

$$T_2 = \frac{2\pi k_2}{\sqrt{g\overline{GM}_2}}$$

since

$$\lambda = \frac{\text{Dimension}_1}{\text{Dimension}_2}$$

Then

$$T_1 = \frac{2\pi\lambda k_2}{\sqrt{g\lambda\overline{GM}_2}} = \frac{\lambda 2\pi k_2}{\lambda^{1/2}\sqrt{g\overline{GM}_2}} = \lambda^{1/2} T_2$$

Note: In place of a model a geometrically similar ship can also be considered (using the appropriate scale factor) for finding the physical dimensions of quantities occurring in ship dynamics.

4.3 ACCELERATED ROTATIONAL MOTION

If a purely rigid body has an accelerated rotational motion, the acceleration of any particle of the body at a perpendicular distance r from the axis of rotation has two components:

1. The first is $r\alpha$, along the direction of instantaneous velocity.
2. The second is $r\omega^2$, directed toward the axis.

Here the instantaneous angular velocity is

$$\alpha = \frac{d\omega}{dt} = \frac{d^2\phi}{dt^2}$$

TABLE 4.5 PHYSICAL DIMENSIONS OF QUANTITIES IN SHIP DYNAMICS
Based on mass, length and time as fundamental units.

Quantity	Measure Formula	Quantity	Measure Formula
Mass	M	Volume and first moment of area	L^3
Length	L	Second moment of area	L^4
Time	T	Density	ML^{-3}
Speed or velocity	LT^{-1}	Mass per unit area	ML^{-2}
Acceleration	LT^{-2}	Mass moment	ML
Momentum and impulse	MLT^{-1}	Moment of inertia and product of inertia	ML^2
Force, thrust, resistance	MLT^{-2}	Stress and pressure	$ML^{-1}T^{-2}$
Energy and work	ML^2T^{-2}	Strain	$M^0L^0T^0$
Power	ML^2T^{-3}	Elastic modulus	$ML^{-1}T^{-2}$
Moment of force of Torque	ML^2T^{-2}	Flexural rigidity of a beam, EI	ML^3T^{-2}
Angular momentum or moment of momentum	ML^2T^{-1}	Torsional rigidity of a shaft, GJ	ML^3T^{-2}
		Linear stiffness (moment per radian)	MT^{-2}
Angle	$M^0L^0T^0$	Angular stiffness (moment per radian)	ML^2T^{-2}
Angular velocity or of circular frequency, ω		Linear flexibility or receptance (displacement	
Revolution, η	T^{-1}	per unit force)	$M^{-1}T^2$
Angular acceleration	T^{-2}	Viscosity	$ML^{-1}T^{-1}$
Area	L^2	Kinematic viscosity	L^2T^{-1}

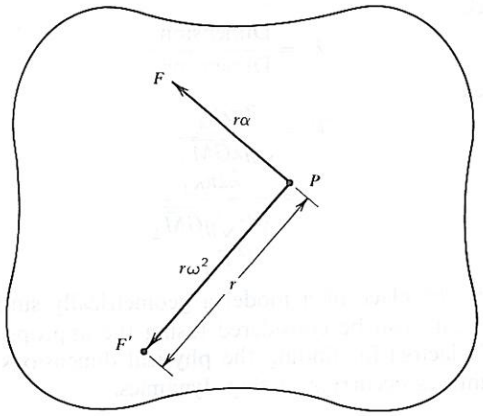


Figure 4.12 Two components of acceleration of a particle in accelerated rotational motion.

See Fig. 4.12. The component forces acting on the particle in two directions, as shown by arrows in Fig. 4.12, are

$$F = \text{mass} \times \text{acceleration} = mr\alpha$$

and

$$F' = \text{mass} \times \text{acceleration} = mr\omega^2$$

If we consider the body to be composed of different particles, it is clear that the resultant force on each individual particle has all directions parallel to the plane of rotation. It is, therefore, meaningless to add all these forces, although the contribution of each particle must be added to the total rotational effect of the body. Thus we add the moments of forces about the axis of rotation. Therefore the sum of moments of forces F and F' about the axis of rotation is given by

$$Fr = mr\alpha r = mr^2\alpha$$

The total moment of all the forces about the axis of rotation is

$$\begin{aligned}\Sigma F_i r_i &= \Sigma(m_i r_i^2)\alpha \\ &= \Sigma(m_i r_i^2)\frac{d^2\phi}{dt^2} \\ &= I\frac{d^2\phi}{dt^2}\end{aligned}$$

where I is the moment of inertia of the body about the axis of rotation, that is, $\Sigma(m_i r_i^2)$.

The quantity $\Sigma(m_i r_i^2)$ depends on the distribution of the mass of the body, as well as on the axis of rotation, and it is referred to as the *moment of inertia of the body about the particular axis.* Therefore it must be remembered that, although the total mass $M = \Sigma m_i$ of a body is a single-valued quantity, the moment of inertia of a body may have different values, depending upon the particular axis in question. In other words, there is no such thing as the moment of inertia of a body; rather, there are moments of inertia, each referring to a particular axis, such as the moment of inertia of a ship about the x-axis (i.e., for rolling), the moment of inertia of the same ship about the y-axis (for pitching), and similarly about the z-axis (for yawing), and all these values are different from each other. Now, if I is the moment of inertia about a particular axis of a body of total mass M, a related length k is defined by the dimensionally homogeneous equation

$$I = Mk^2$$

where k is called the *radius of gyration of the ship about a particular axis.* Therefore we may have radii of gyration for three different rotational motions: namely, rolling, pitching, and yawing. Thus, if we have the proper radius of gyration, the moment of inertia about a particular axis is obtained from the relation

$$I = \frac{\Delta}{g}k^2$$

In practice, the radius of gyration of a vessel about any axis is obtained by considering the total weight of the vessel as the sum of many small weights and then adding the products of each small weight and the square of its distance from the particular axis concerned, that is,

$$k^2 = \frac{\Sigma(w_i r_i^2)}{\Delta}$$

where w_i is the weight of the ith element, r is the

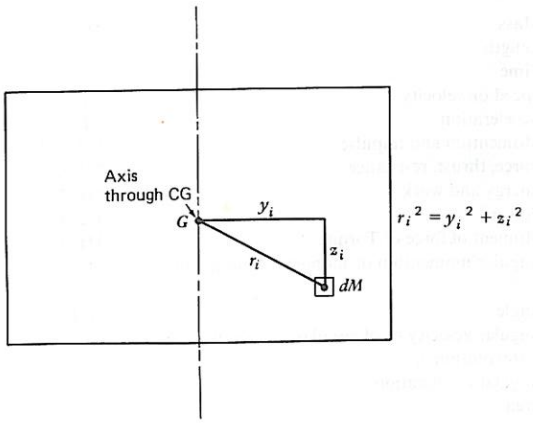


Figure 4.13 Radius of gyration for rolling.

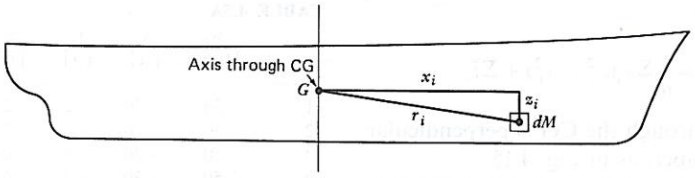


Figure 4.14 Radius of gyration for pitching.

direct distance of the ith element from the axis of rotation, and Δ is the total weight of the vessel.

Radius of Gyration for Different Angular Motions

Radius of Gyration for Rolling

The moment of inertia for rolling is (see Fig. 4.13)

$$I_{xx} = Mk_{xx}^2 = \int dM\, r_i^2$$

$$= \int dM\,(y_i^2 + z_i^2)$$

since $r_i^2 = y_i^2 + z_i^2$.

Thus

$$I_{xx} = \frac{1}{g}\Sigma[w_i(y_i^2 + z_i^2)] + \Sigma I_i$$

where w_i = weight of the ith element

y_i = transverse distance of the CG of the ith element from the axis through the ship (i.e., from the rolling axis)

z_i = vertical distance of the CG of the ith element from the axis through the CG of the ship

I_i = moment of inertia of the ith element about its own CG

Note that the axis of rolling is through the CG of the ship and perpendicular to the plane of this page. However, if the ship is subdivided into sufficiently small weights, the radius of gyration can be found from

$$I_{xx} = \frac{\Delta}{g}k_{xx}^2 = \frac{1}{g}\Sigma[w_i(y_i^2 + z_i^2)]$$

from which

$$k_{xx} = \sqrt{\frac{\Sigma w_i(y_i^2 + z_i^2)}{\Delta}} \tag{4.14}$$

Radius of Gyration for Pitching

With reference to Fig. 4.14, the pitching moment of inertia is

$$I_{yy} = Mk_{yy}^2 = \int dM\, r_i^2 = \int dM\,(x_i^2 + z_i^2)$$

since $r_i^2 = x_i^2 + z_i^2$, or

$$I_{yy} = \frac{\Delta}{g}k_{yy}^2 = \frac{1}{g}\Sigma[w_i(x_i^2 + z_i^2)] + \Sigma I_i$$

However, if the ship is subdivided into sufficiently small weights, the radius of gyration can be found from

$$I_{yy} = \frac{\Delta}{g}k_{yy}^2 = \frac{1}{g}\Sigma[w_i(x_i^2 + z_i^2)]$$

that is,

$$k_{yy} = \sqrt{\frac{\Sigma[w_i(x_i^2 + z_i^2)]}{\Delta}} \tag{4.15}$$

Radius of Gyration for Yawing

The yawing moment of inertia is

$$I_{zz} = Mk_{zz}^2 = \int dM\, r_i^2 = \int dM\,(x_i^2 + y_i^2)$$

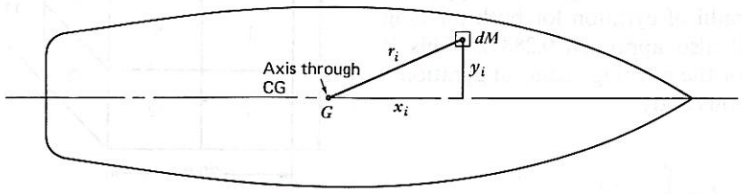


Figure 4.15 Radius of gyration for yawing.

since $r_i^2 = x_i^2 + y_i^2$, or

$$I_{zz} = \frac{\Delta}{g} k_{zz}^2 = \frac{1}{g} \Sigma w_i (x_i^2 + y_i^2) + \Sigma I_i$$

The axis of yawing through the CG is perpendicular to the plane of the paper, as in Fig. 4.15.

Again, if the ship is subdivided into sufficiently small weights, the radius of gyration can be found from

$$I_{zz} = \frac{\Delta}{g} k_{zz}^2 = \frac{1}{g} \Sigma [w_i (x_i^2 + y_i^2)]$$

that is,

$$k_{zz} = \sqrt{\frac{\Sigma [w_i (x_i^2 + y_i^2)]}{\Delta}} \tag{4.16}$$

Example 4.9

A homogeneously loaded barge ($\Delta = 600$ tons) is considered to have 12 uniform divisions, each weighing 50 tons. Find the radius of gyration for rolling, pitching, and yawing if the weights are considered to be centered at the CG of each division, that is, assuming that the mass moment of inertia of each division about its own CG can be neglected. See Fig. 4.16.

Solution:

The loads and the positions of their CGs are listed in Table 4.5A.

TABLE 4.5A

	w_i [tons]	x_i [ft]	y_i [ft]	z_i [ft]	x_i^2 [ft²]	y_i^2 [ft²]	z_i^2 [ft²]
1	50	−30	−5	2.5	900	25	6.25
2	50	0	−5	2.5	0	25	6.25
3	50	+30	−5	2.5	900	25	6.25
4	50	+30	+5	2.5	900	25	6.25
5	50	0	+5	2.5	0	25	6.25
6	50	−30	+5	2.5	900	25	6.25
7	50	−30	−5	−2.5	900	25	6.25
8	50	0	−5	−2.5	0	25	6.25
9	50	+30	−5	−2.5	900	25	6.25
10	50	+30	+5	−2.5	900	25	6.25
11	50	0	+5	−2.5	0	25	6.25
12	50	−30	+5	−2.5	900	25	6.25

$y_i^2 + z_i^2$ [ft²]	$x_i^2 + z_i^2$ [ft²]	$x_i^2 + y_i^2$ [ft²]	$w_i(y_i^2 + z_i^2)$ [ton-ft²]	$w_i(x_i^2 + z_i^2)$ [ton-ft²]	$w_i(x_i^2 y_i^2)$ [ton-ft²]	I_i
31.25	906.25	925	1,562.5	45,312.5	46,250	0
31.25	6.25	25	1,562.5	312.5	1,250	0
31.25	906.25	925	1,562.5	45,312.5	46,250	0
31.25	906.25	925	1,562.5	45,312.5	46,250	0
31.25	6.25	25	1,562.5	312.5	1,250	0
31.25	906.25	925	1,562.5	45,312.5	46,250	0
31.25	906.25	925	1,562.5	45,312.5	46,250	0
31.25	6.25	25	1,562.5	312.5	1,250	0
31.25	906.25	925	1,562.5	45,312.5	46,250	0
31.25	906.25	925	1,562.5	45,312.5	46,250	0
31.25	6.25	25	1,562.5	312.5	1,250	0
31.25	906.25	925	1,562.5	45,312.5	46,250	0
		SUMS	18,750	363,750	375,000	0

Equations 4.14, 4.15, and 4.16 yield, respectively,

$$k_{xx}^2 = \frac{18{,}750}{600} = 31.25, \text{ i.e., } k_{xx} = 5.59 \text{ ft}$$

$$k_{yy}^2 = \frac{363{,}750}{600} = 606.25, \text{ i.e., } k_{yy} = 24.62 \text{ ft}$$

$$k_{zz}^2 = \frac{375{,}000}{600} = 625.00, \text{ i.e., } k_{zz} = 25.00 \text{ ft}$$

Note: Since the barge is homogeneous, it may be considered to be made up of many more small boxes than just 12, as shown in the above example. Then the radius of gyration for rolling, k_{xx}, would approach $0.2887B$, and the radii of gyration for both pitching and yawing would also approach $0.2887L$. This is illustrated below for the pitching radius of gyration.

For a homogeneous body

$$I = \int m_n \xi^2 d\xi$$

and

$$k_{yy}^2 = \frac{I}{M} = \frac{\int m_n \xi^2 d\xi}{M}$$

For the determination of pitching radius of gyra-

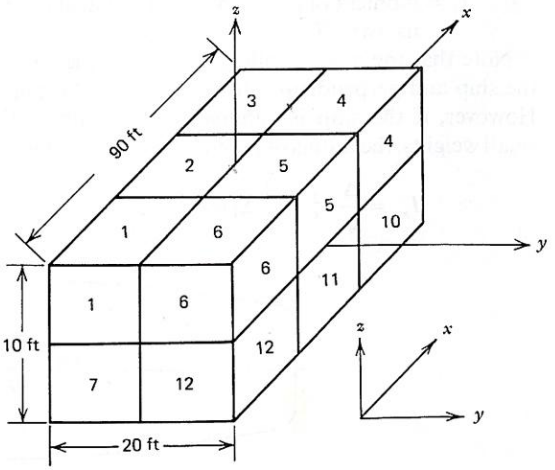


Figure 4.16 Barge of 12 uniform divisions.

TABLE 4.5B

Station No.	m_n [ton-sec^2/ft^2]	ξ Distance from Pitching Axis	$m_n\xi^2$	Simpson's Multiplier	Product
0	$\frac{600}{32.2 \times 90}$	45	$\frac{40{,}500}{32.2 \times 3}$	1	$\frac{40{,}500}{32.2 \times 3}$
1	$\frac{600}{32.2 \times 90}$	0	0	4	0
2	$\frac{600}{32.2 \times 90}$	45	$\frac{40{,}500}{32.2 \times 3}$	1	$\frac{40{,}500}{32.2 \times 3}$
				SUM	$\frac{81{,}000}{32.2 \times 3}$

Therefore $I_{yy} = \frac{1}{3} \times 45 \times \frac{81{,}000}{32.2 \times 3}$
$= 12{,}577.64$ ton-sec^2-ft

tion, k_{yy} we have the values shown in Table 4.5B.

Therefore

$$I_{yy} = \tfrac{1}{3} \times 45 \times \frac{81{,}000}{32.2 \times 3}$$
$$= 12577.64 \text{ ton-sec}^2/\text{ft}$$

or

$$k_{yy} = \sqrt{\frac{I_{yy}}{M}} = \sqrt{\frac{1277.6}{600/32.2}}$$
$$= 25.9807 \text{ ft (i.e., } 0.2887L)$$

where

$$\text{M} = \frac{600}{32.2} \text{ ton-sec}^2/\text{ft}$$

Example 4.10

A model weighing 7.50 lb should be ballasted to 11.50 lb in order to have a displacement corresponding to that of the prototype. However, after ballasting the model, as shown in Fig. 4.17, it is found that the pitching radius of gyration is 12 in., whereas that of the prototype is $0.25L$. If the length of the model is 5 ft, and if the equal weights are to be equidistant from the CG so that the CG will remain at the original location, how far away from the CG should the weights be located?

Solution:

The desired mass moment of inertia should be

$$\frac{11.5}{g} \times (0.25\,L)^2 = \frac{11.5}{g} \times (0.25 \times 60 \text{ in.})^2$$
$$= \frac{2590 \text{ lb-in.}^2}{g \text{ ft/sec}^2}$$

The mass moment of inertia of the ballasted model is

$$\frac{11.5}{g} \times 12^2 = \frac{1655 \text{ lb-in.}^2}{g \text{ ft/sec}^2}$$

The decrease in the moment of inertia is

$$\frac{2590}{g} - \frac{1655}{g} = \frac{935 \text{ lb-in.}^2}{g[\text{ft/sec}^2]}$$

The contribution of two weights (each weighing 2 lb) to the total moment of inertia is

$$\frac{2}{g} \times 10^2 + \frac{2}{g} \times 10^2 = \frac{400 \text{ lb-in.}^2}{g[\text{ft/sec}^2]}$$

However, the weights should produce a moment of inertia of 935 lb-in.$^2/g$[ft/sec^2] more; that is, the

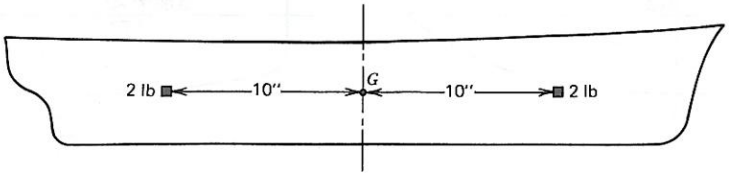


Figure 4.17 Determination of pitching gyradius of a model.

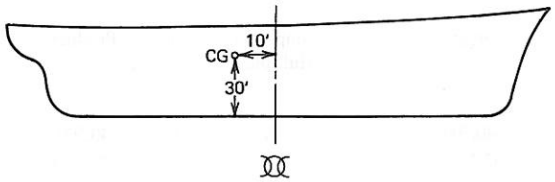


Figure 4.18 Illustration of vessel in Example 4.11.

total moment of inertia due to the weights should be

$$\frac{400}{g}+\frac{935}{g}=\frac{1355\ \text{lb-in.}^2}{g[\text{ft/sec}^2]}$$

$$m_1r_1^2+m_2r_2^2=\frac{1335\ \text{lb-in.}^2}{g[\text{ft/sec}^2]}$$

since

$$m_1=m_2=\frac{2\ \text{lb}}{g[\text{ft/sec}^2]}$$

and

$$r_1=r_2=r\ \text{in.}$$

then

$$r^2\frac{(2+2)}{g}=\frac{1335\ \text{lb-in.}^2}{g[\text{ft/sec}^2]}$$

or

$$r=18.3\ \text{in.}$$

This means that the weights should be placed at a distance of 18.3 in. apart from the CG.

Example 4.11

From Fig. 4.18,

$L = 500$ ft
$B = 70$ ft
$\Delta = 13{,}000$ tons
$CG = 10$ ft aft of ⊠ and 30 ft above keel and on the centerline of the ship
$k_{xx} = 0.40$ of the ship's beam
$k_{yy} = 0.25$ of the ship's length
$k_{zz} = 0.25$ of the ship's length

A weight of 200 tons located at a position 100 ft forward of ⊠, 50 ft above keel, and 5 ft on starboard is shifted to a different position that is 50 ft forward of ⊠, 20 ft above keel, and 10 ft on starboard. What will be the new CG, K_{xx}, k_{yy}, and k_{zz}?

Solution:

A shift of weight can be considered in two steps

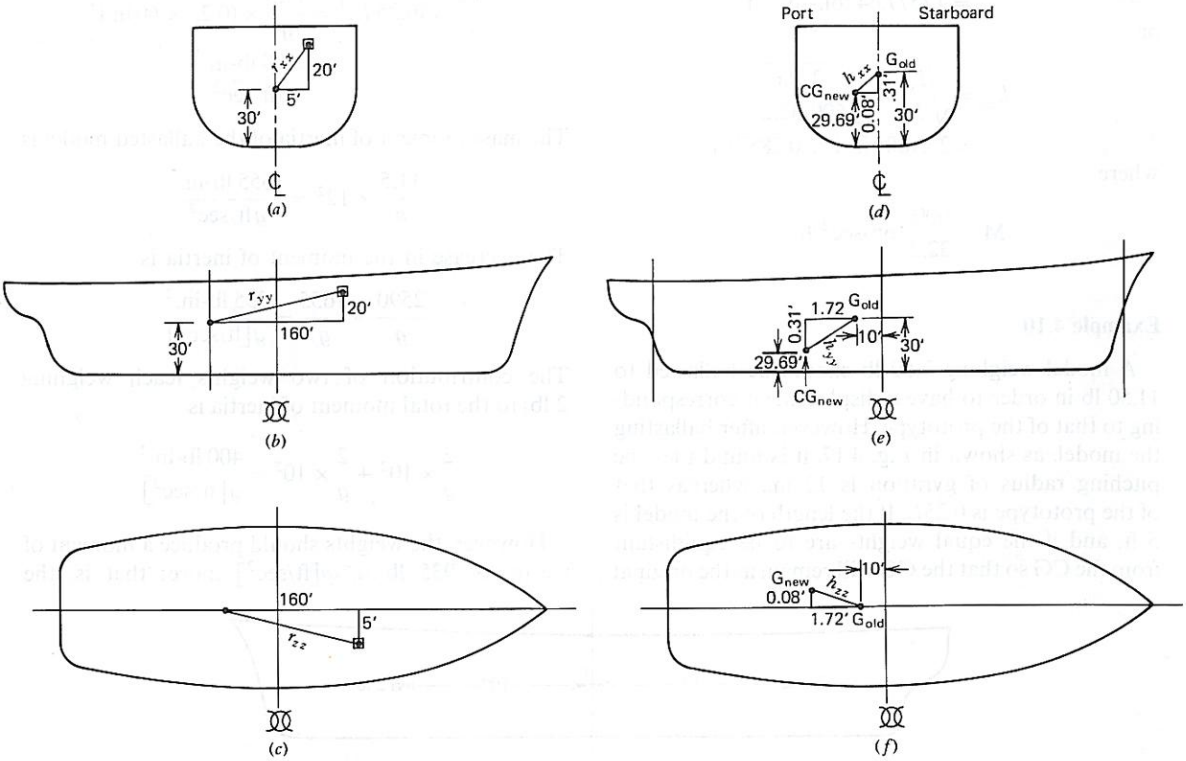


Figure 4.19 Rolling, pitching, and yawing radii of gyration for Example 4.11.

in the determination of the radius of gyration: (a) weight removal, and (b) addition of the same weight at its new location.

a. *Removal of weight*

The weight of 200 tons is considered to be removed from its original position. Thus, referring to Fig. 4.19*a*,

$$\begin{aligned}(I_{xx_{\text{new}}})_{\text{new (CG)}} &= (I_{xx})_{\text{original}} - mr_{xx}^2 \\ &= Mk_{xx}^2 - mr_{xx}^2 \\ &= \frac{13{,}000}{32.2} \times (0.4 \times 70)^2 \\ &\quad - \frac{200}{32.2} \times [(20)^2 + 5^2] \\ &= 313{,}882 \text{ ton-sec}^2\text{-ft}\end{aligned}$$

and from Fig. 4.19*b*

$$\begin{aligned}(I_{yy_{\text{new}}})_{\text{old CG}} &= (I_{yy})_{\text{original}} - mr_{yy}^2 \\ &= \frac{13{,}000}{32.2} \times (125)^2 \\ &\quad - \frac{200}{32.2} \times [(110)^2 + (20)^2] \\ &= 6{,}230{,}590 \text{ ton-sec}^2\text{-ft}\end{aligned}$$

and, referring to Fig. 4.19*c*,

$$\begin{aligned}(I_{zz_{\text{new}}})_{\text{old CG}} &= (I_{zz})_{\text{original}} - mr_{zz}^2 \\ &= \frac{13{,}000}{32.2} \times (125)^2 \\ &\quad - \frac{200}{32.2} \times [(110)^2 + 5^2] \\ &= 6{,}232{,}919 \text{ ton-sec}^2\text{-ft}\end{aligned}$$

Because of the removal of the weight the new CG of the vessel should be determined. Taking the moment about the forward perpendicular, we have

$$\text{New (CG)}_x = \frac{13{,}000 \times 260 - 200 \times 150}{13{,}000 - 200}$$
$$= 261.72 \text{ from the forward perpendicular}$$

Thus the shift of $(\text{CG})_x$ is 1.72 ft.

Taking the moment about the centerline, we have

$$\text{New (CG)}_y = \frac{13{,}000 \times 0 - 200 \times (+5)}{13{,}000 - 200}$$
$$= -0.08 \text{ ft (port)}$$

that is, a shift of $(\text{CG})_y$ of 0.08 ft.

Taking the moment about the baseline, we have

$$\text{New (CG)}_z = \frac{13{,}000 \times 30 - 200 \times 50}{13{,}000 - 200}$$
$$= 29.69 \text{ ft above baseline}$$

Thus the shift of $(\text{CG})_z$ is $(30 - 29.69) = 0.31$ ft, and

$$(I_{xx_{\text{new}}})_{\text{new CG}} = (I_{xx_{\text{new}}})_{\text{new (CG)}} - (M - m)h_{xx}^2$$

where h_{xx} is the direct distance of the x-axis through the new CG and the x-axis through the old CG (Fig. 4.19*d*), that is,

$$h_{xx}^2 = (\text{shift of } G_y)^2 + (\text{shift of } G_z)^2$$

Therefore

$$\begin{aligned}(I_{xx_{\text{new}}})_{\text{new CG}} &= 313{,}882 - \frac{(13{,}000 - 200)}{32.2} \\ &\quad \times [0.32)^2 + (0.08)^2] \\ &= 313{,}841 \text{ ton-sec}^2\text{-ft}\end{aligned}$$

and

$$(I_{yy_{\text{new}}})_{\text{new CG}} = (I_{yy_{\text{new}}})_{\text{new CG}} - (M - m)h_{yy}^2$$

where h_{yy} is the direct distance of the y-axis through the new CG and the y-axis through the old CG (Fig. 4.19*e*), that is,

$$h_{yy}^2 = (\text{shift of } G_z)^2 + (\text{shift of } G_x)^2$$

Therefore

$$\begin{aligned}(I_{yy_{\text{new}}})_{\text{new CG}} &= 6{,}230{,}590 - \frac{(1300 - 200)}{32.2} \\ &\quad \times [(1.72)^2 + (0.31)^2] \\ &= 6{,}229{,}376 \text{ ton-sec}^2\text{-ft}\end{aligned}$$

and

$$(I_{zz_{\text{new}}})_{\text{new CG}} = (I_{zz_{\text{new}}})_{\text{old CG}} - (M - m)h_{zz}^2$$

where $h_{zz} \pm$ is the direct distance of the z-axis through the new CG and the z-axis through the old CG (Fig. 4.19*f*), that is,

$$h_{zz}^2 = (\text{shift of } G_x)^2 + (\text{shift of } G_y)^2$$

Therefore

$$\begin{aligned}(I_{zz_{\text{new}}})_{\text{new (CG)}} &= 6{,}232{,}919 - \frac{(1300 - 200)}{32.2} \\ &\quad \times [(1.72)^2 + (0.08)^2] \\ &= 6{,}231{,}740 \text{ ton-sec}^2\text{-ft}\end{aligned}$$

b. *Additions of Weight*

The weight of 200 tons is now considered to be placed at its new position. Thus, from Fig. 4.20*a*,

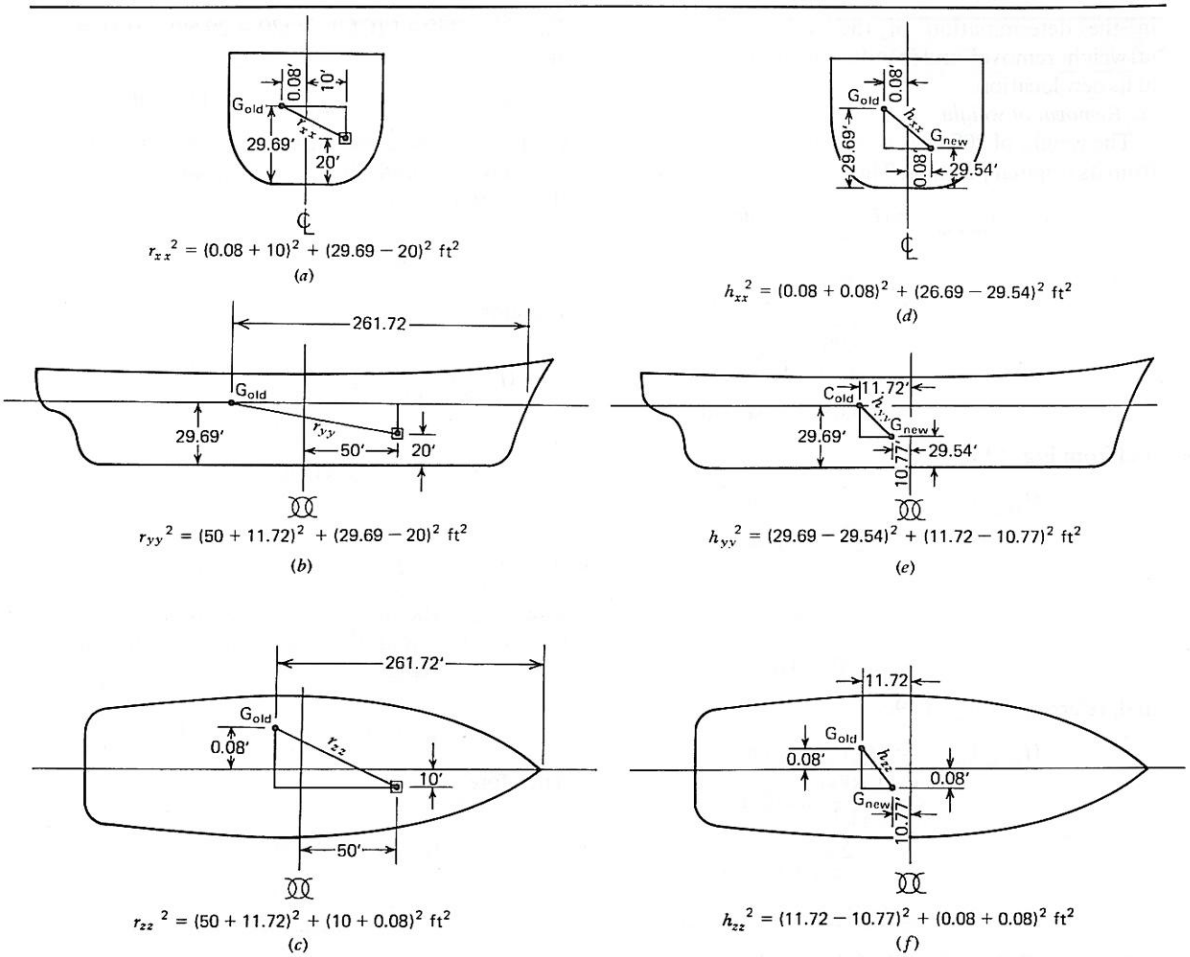


Figure 4.20 Shift of center of gravity in each direction.

$$(I_{xx_{\text{new}}})_{\text{old CG}} = (I_{xx})_{\text{original}} + mr_{xx}^2$$
$$= 313{,}841 + \frac{200}{32.2} \times [(10.08)^2 + (9.69)^2]$$
$$= 315{,}055 \text{ ton-sec}^2\text{-ft}$$

From Fig. 4.20*b*,

$$(I_{yy_{\text{new}}})_{\text{old CG}} = (I_{yy})_{\text{original}} + mr_{yy}^2$$
$$= 6{,}229{,}376 + \frac{200}{32.2} \times [(61.72)^2 + (9.69)^2]$$
$$= 6{,}253{,}620 \text{ ton-sec}^2\text{-ft}$$

and from Fig. 4.20*c*,

$$(I_{zz_{\text{new}}})_{\text{new CG}} = (I_{zz})_{\text{original}} + mr_{zz}^2$$
$$= 6{,}231{,}740 + \frac{200}{32.2} \times [(61.72)^2 + (10.08)^2]$$
$$= 6{,}256{,}032 \text{ ton-sec}^2\text{-ft}$$

But, because of the addition of weight, the CG of the ship is changed. Taking the moment about the forward perpendicular, we have

$$\text{New (CG)}_x = \frac{12{,}800 \times 261.72 + 200 \times 200}{12{,}800 + 200}$$
$$= 260.77 \text{ ft from the forward perpendicular}$$

that is, a shift of $(\text{CG})_x$ of $(11.72 - 10.77) = 0.95$ ft.

Taking the moment about the centerline, we have

$$\text{New(CG)}_y = \frac{12{,}800 \times (-0.08) + 200 \times 10}{12{,}800 + 200}$$
$$= +0.08 \text{ ft (i.e., starboard)}$$

and the shift of $(CG)_y$ is $(0.08 + 0.08) = 0.16$ ft.

Taking the moment about the baseline, we have

$$\text{New } (CG)_z = \frac{12{,}800 \times 29.69 + 200 \times 20}{12{,}800 + 200}$$
$$= 29.54 \text{ ft above the baseline}$$

The shift of $(CG)_z$ is $(29.69 - 29.54) = 0.15$ ft.

Returning to the moments of inertia, we have, from Fig. 4.20*d*,

$$(I_{xx_{\text{new}}})_{\text{new (CG)}} = (I_{xx_{\text{new}}})_{\text{old CG}} - (M + m)h_{xx}^2$$

where

$$h_{xx}^2 = (\text{shift of } G_y)^2 + (\text{shift of } G_z)^2$$

Therefore

$$(I_{xx_{\text{new}}})_{\text{new (CG)}} = 315{,}055 - \frac{12{,}800 + 200}{32.2} \times [(0.16)^2 + (0.15)^2]$$
$$= 315{,}036 \text{ ton-sec}^2\text{-ft}$$

and from Fig. 4.20*e*,

$$(I_{yy_{\text{new}}})_{\text{new (CG)}} = (I_{yy_{\text{new}}})_{\text{old CG}} - (M + m)h_{yy}^2$$

where

$$h_{yy}^2 = (\text{shift of } G_z)^2 + \text{shift of } G_x)^2$$

Therefore

$$(I_{yy_{\text{new}}})_{\text{new (CG)}} = 6{,}253{,}620 - \frac{12{,}800 + 200}{32.2} \times [(0.15)^2 + (0.95)^2]$$
$$= 6{,}253{,}247 \text{ ton-sec}^2\text{-ft}$$

while from Fig. 4.20*f*,

$$(I_{zz_{\text{new}}})_{\text{new (CG)}} = (I_{zz_{\text{new}}})_{\text{old CG}} - (M + m)h_{zz}^2$$

where

$$h_{zz}^2 = (\text{shift of } G_x)^2 + (\text{shift of } G_y)^2$$

Therefore

$$(I_{zz_{\text{new}}})_{\text{new CG}} = 6{,}256{,}032 - \frac{(12{,}800 + 200)}{32.2} [(0.95)^2 + (0.16)^2]$$
$$= 6{,}255{,}657 \text{ ton-sec}^2\text{-ft}$$

Since

$$\frac{\Delta}{g} k_{xx}^2 = I_{xx}$$

then

$$k_{xx} = \sqrt{\frac{I_{xx}g}{\Delta}} = \sqrt{\frac{315{,}036 \times 32.2}{13{,}000}}$$
$$= 27.93 \text{ ft}$$

Similarly,

$$k_{yy} = \sqrt{\frac{I_{yy}g}{\Delta}} = \sqrt{\frac{6{,}253{,}247 \times 32.2}{13{,}000}}$$
$$= 124.45 \text{ ft}$$

and

$$k_{zz} = \sqrt{\frac{I_{zz}g}{\Delta}} = \sqrt{\frac{6{,}255{,}567 \times 32.2}{13{,}000}}$$
$$= 124.48 \text{ ft}$$

Also, as calculated earlier,

(G_x) New = 10.77 ft aft of ⊗

(G_y) New = 0.08 ft on starboard

(G_z) New = 29.54 ft above baseline

4.4 PITCHING

As mentioned before, a ship may undergo a simple harmonic motion about either a transverse axis (i.e., *y*-axis) or a longitudinal axis (i.e., *x*-axis) if it is displaced from its equilibrium position and then released, or if it is given an initial velocity away from its equilibrium position. (See Fig. 4.1.) It has also been noted that we should always refer to the moments of forces, rather than the forces, when we describe angular motions like pitching and rolling.

As in the case of heaving, the following four moments act in pitching and rolling motions:

1. Inertial moment.
2. Damping moment.
3. Restoring moment.
4. Exciting moment.

Pitching motion is described in this section; rolling motion, in section 4.5.

The equation of motion of pitching can be written as

$$a\frac{d^2\theta}{dt^2} + b\frac{d\theta}{dt} + c\theta = M_0 \cos \omega_e t$$

where:

a. Inertial moment $= a\dfrac{d^2\theta}{dt^2}$

Here a is the virtual mass moment of inertia, and $d^2\theta/dt^2$ is the angular acceleration of pitching.

b. Damping moment $= b\dfrac{d\theta}{dt}$

Here b is the damping moment coefficient, and $d\theta/dt$ is the angular velocity.

The damping moment is again considered to be linearly proportional to the angular velocity for the sake of simplicity, as in the case of heaving.

c. Restoring moment $= c\theta$

Here c is the restoring moment coefficient, and θ is the angular displacement in pitching.

Again the restoring moment is considered to be linearly proportional to the pitching displacement. This is true only for small angles of pitching.

d. The exciting moment, $M_0 \cos \omega_e t$, is considered to be fluctuating with an encountering frequency of ω_e.

If we can determine the various values of a, b, c, and M_0 we shall be able to determine the motion characteristics for pitching. It should be noted, however, that the coefficients, a, b, c, and M_0 of pitching are not the same as those of heaving or rolling. Therefore they should be determined separately for the different kinds of motion.

Determination of Coefficients for Pitching Motion

The virtual mass moment of inertia for pitching, a, is the vessel moment of inertia for pitching plus the added mass moment of inertia for pitching, that is,

$$a = I_{yy} + \delta I_{yy} = \frac{\Delta}{g} k_{yy}^2 + \delta I_{yy} \qquad (4.16a)$$

where δI_{yy} is the added mass moment of inertia for pitching, and k_{yy} is the radius of gyration for pitching.

The virtual mass moment of inertia for pitching, a, can also be defined as

$$\begin{aligned} a &= (\text{virtual mass}) \times (\text{radius of gyration})^2 \\ &= (M + \delta M) \times k_{yy}^2 \\ &= \frac{\Delta'}{g} k_{yy}^2 \end{aligned}$$

where Δ'/g is the virtual mass.

The mass moment of inertia of a ship for the pitching motion, I_{yy}, can be roughly estimated from the moment of inertia of the area under the ship's sectional area curve, that is,

$$I_{yy} \simeq \rho \int_{-L/2}^{L/2} A(x) x^2 \, dx \qquad (4.17b)$$

where $A(x)$ is the sectional area.

Here it is assumed that the longitudinal distribution of mass is the same as of the longitudinal distribution of displacement; thus the vertical distribution is neglected, and it is also assumed that the CG of the ship is at the midship section. Note that for the normal ship form the radius of gyration for the pitching motion is

$$k_{yy} = 0.24L \text{to } 0.26L$$

where L is the length of the ship.

The added mass moment of inertia for pitching can be determined by experiment or by the method of strip theory, that is, the ship is considered to have different sections, for each of which the added mass is obtained. Then the added mass moment of inertia is obtained from the added mass, as is the ship's moment of inertia from the ship mass. Thus

$$\delta I_{yy} = \int_{-L/2}^{L/2} a_n x^2 \, dx \qquad (4.17c)$$

where a_n is the added mass for each section as determined in Section 4.2, and x is the distance of each section from the LCG.

Equation 4.17c can be written as

$$\delta I_{yy} = \rho \frac{\pi}{2} \int_{-L/2}^{L/2} C x^2 y^2 \, dx$$

where C is the added mass coefficient, the values of which are obtained from Fig. 4.4.

Example 4.12

Find the added mass moment of inertia of a ship model for which the added mass was determined in Example 4.1. The data for this example are given in Table 4.6.

Solution:

From the values in Table 4.6, the added mass moment of inertia for pitching is

$$\begin{aligned} A &= \int a_n \xi^2 \, d\xi \\ &= \tfrac{1}{3} \times s \times \text{SUM} \\ &= \tfrac{1}{3} \times 4.8 \times 855.3 = 1368.5 \text{ lb-ft-sec}^2 \end{aligned}$$

where s is the station spacing.

Figure 4.21 shows the values for added inertia for pitching. From the figure one can see that the added inertia is of the same order of magnitude as the inertia of the actual ship, and therefore in the determination of pitching motion added inertia should be taken into consideration.

DAMPING COEFFICIENT FOR PITCHING

The damping coefficient for pitching can also be obtained by the method of strip theory, that is, determined for each section and then integrated

TABLE 4.6

Station No. ①	a_n [from Example 4.1] ②	ξ [ft] ③	ξ^2 [ft^2] ④	$a_n\xi^2$ [slugs-ft^2] ⑤	Simpson's Multiplier ⑥	Product ⑦
0	0.000	9.12	83.174	0.000	1	0.00
5	5.0011	4.32	18.662	93.515	4	374.06
10	5.0011	− 0.48	0.230	1.152	2	2.30
15	4.295	− 5.28	27.878	119.736	4	478.94
20	0.000	− 10.08	101.606	0.000	1	0.00
					SUM	855.30

Description of Table 4.6

Column Number	*Description*
①	Station Number
②	Added Mass for Each Section, a_n, obtained from ⑫ of Table 4.1.
③	Lever Arm, ξ, distance of each section from LCG
④	Lever Arm Squared, $\xi^2 = ③ \times ③$
⑤	$a_n\xi^2 = ② \times ④$ = Added Mass Moment of Inertia of Each Section
⑥	Simpson's Multiplier
⑦	Product = ⑤ × ⑥

over the entire length, as follows:

$$b_{\text{pitching}} = \int_{-L/2}^{L/2} b_{n\ \text{heaving}} \times \xi^2 \, d\xi$$

where b_n is the damping force coefficient for each strip along the ship's length, and ξ is the distance of the individual strip from the LCG (same as the LCB) position.

Example 4.13

Find the damping coefficient for pitching motion of the ship model for which the data are given in Example 4.1. The relevant data are presented in Table 4.7.

Solution:

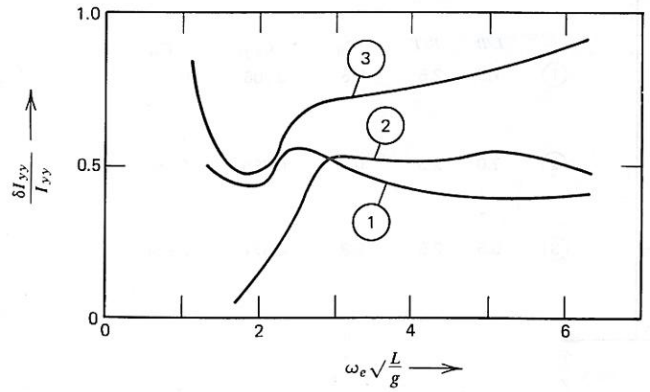
From the data of Table 4.7, the damping coefficient for pitching is

$$b = \int b_n \xi^2 d\xi$$
$$= \tfrac{1}{3} \times s \times \text{SUM}$$
$$= \tfrac{1}{3} \times 4.8 \times 1316.17$$
$$= 2105.9 \text{ft-lb-sec}$$

The damping for the pitching motion is increased by the following:

(1) Increase of beam
(2) Decrease of draft
(3) Decrease of vertical prismatic coefficient (i.e., increase of V-form).

On the other hand, there is a rapid reduction in damping with an increase in frequency of oscillation. Such a high frequency, however, generally occurs



	L/B	B/T	C_B	C_{WP}	C_M
①	7.5	2.5	0.6	0.706	0.977
②	7.0	2.5	0.7	0.785	0.986
③	6.5	2.5	0.8	0.871	0.994

Figure 4.21 Nondimensional added mass moment of inertia for pitching motion [124].

TABLE 4.7

Station No.	b_n (from Example 4.2) [lb-sec^2]	ξ [ft]	ξ^2 [ft^2]	$b_n\xi^2$ [lb-sec]	Simpson's Multiplier	Product
①	②	③	④	⑤	⑥	⑦
0	0.000	9.12	83.174	0.00	1	0.00
5	5.866	4.32	18.662	109.47	4	437.88
10	5.866	− 0.48	0.230	1.35	2	2.70
15	7.869	− 5.28	27.878	218.89	4	875.59
20	0.000	− 10.08	101.606	0.00	1	0.00
					SUM	1316.17

Description of Table 4.7

Column Number	*Description*
①	Station Number
②	Sectional Damping Coefficient, $b_n = \rho g^2 \bar{A}^2/\omega_e^3$ [$\bar{A}$ from Fig. 4.6]
③	ξ = Lever Arm (i.e., distance of individual section from the LCG position)
④	Lever Arm Squared, ξ^2
⑤	$b_n\xi^2 = ④ \times ②$
⑥	Simpson's Multiplier
⑦	Product = ⑤ × ⑥

outside the domain of resonance, where damping is of not much significance.

Figure 4.22 shows the experimentally obtained nondimensional damping coefficient for pitching motion [72, 73].

Restoring Moment Coefficient

The restoring moment for pitching can be expressed in the simple form as

$$c\theta = \rho g\theta \int_{-L/2}^{L/2} x^2 y(x)\,dx = \rho g\theta I_Y$$

where c is the restoring moment coefficient, and I_y is the moment of inertia of the load waterplane area.

Thus, since $\overline{BM}_L \simeq I_y/\nabla$,

$$c\theta = \rho g\theta \nabla \overline{BM}_L$$

or

$$c\theta = \rho g \nabla \overline{GM}_L \theta$$

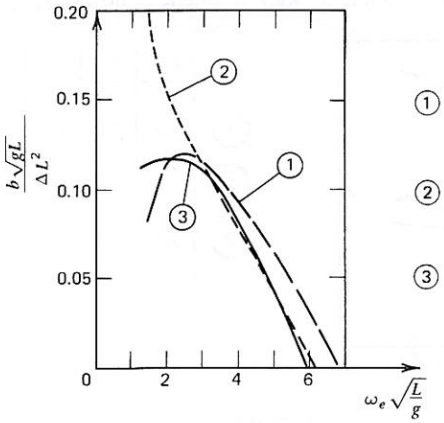
for small angles of inclination, and therefore

$$c = \rho g \nabla \overline{GM}_L = \Delta \overline{GM}_L$$

Note, however, that the restoring moment coefficient determined in this manner is valid only so long as the restoring moment for pitching can be considered to be linearly proportional to the angle of inclination θ.

Example 4.14

Determine the restoring moment for the model



	L/B	*B/T*	C_B	C_{WP}	C_M
①	7.5	2.5	0.6	0.706	0.977
②	7.0	2.5	0.7	0.785	0.986
③	6.5	2.5	0.8	0.871	0.994

Figure 4.22 Nondimensional damping coefficient [124].

TABLE 4.8

Station No.	B_n [ft]	$C_n = \rho g B_n$ [lb/ft²]	ξ^2 [ft²]	$C_n\xi^2$ [lb]	Simpson's Multiplier	Product
0	0	0	83.174	0	1	0
5	2.592	161.78	18.662	3019.14	4	12,076.6
10	2.592	161.78	0.230	37.21	2	74.4
15	2.592	161.78	27.878	4510.10	4	18,040.4
20	0	0	101.606	0	1	0
					SUM	30,191.4

described in Example 4.1. The data for this example are given in Table 4.8.

Solution:

The restoring moment coefficient for pitching is

$$\begin{aligned} c &= \tfrac{1}{3} \times s \times \text{SUM} \\ &= \tfrac{1}{3} \times 4.8 \times 30{,}191.4 \\ &= 48{,}306.2 \text{ ft-lb} \end{aligned}$$

Pitching Motion in Calm Water

The equation of motion for pitching in calm water is

$$a\frac{d^2\theta}{dt^2} + b\frac{d\theta}{dt} + c\theta = 0 \tag{4.18a}$$

or

$$I'_{yy}\frac{d^2\theta}{dt^2} + b\frac{d\theta}{dt} + \Delta\overline{GM}_{L\theta} = 0 \tag{4.18b}$$

or

$$\frac{d^2\theta}{dt^2} + \frac{b}{I'_{yy}}\frac{d\theta}{dt} + \frac{\Delta\overline{GM}_L}{I'_y}\theta = \theta \tag{4.18c}$$

This equation can also be written as

$$\ddot{\theta} + 2v\dot{\theta} + \omega_\theta^2\theta = 0 \tag{4.18d}$$

where

$$2v = \frac{b}{a} = \frac{b}{I'_{yy}} \tag{4.18e}$$

and

$$\omega_\theta^2 = \frac{c}{a} = \frac{\Delta\overline{GM}_L}{I'_{yy}} \tag{4.18f}$$

Here ω_θ is the natural frequency (circular) for pitching.

The expression for the natural pitching period, T_θ, is given as

$$T_\theta = \frac{2\pi}{\omega_\theta}$$

$$= 2\pi\sqrt{\frac{I'_{yy}}{\Delta\overline{GM}_L}} \tag{4.19a}$$

Now, the solution of (4.18d) is written as

$$\theta = e^{-vt}(C_1\cos\omega_d t + C_2\sin\omega_d t) \tag{4.18g}$$

or

$$\theta = e^{-vt}A\sin(\omega_d t - \delta) \tag{4.18h}$$

where ω_d is the damped frequency $= \sqrt{\omega_\theta^2 - v^2}$.

As mentioned in Section 4.2, the motion is not oscillatory in nature if $v \geqslant \omega_\theta$, and is called aperiodic. This case is of no interest in the study of motions of marine vehicles.

The damped pitching period can then be expressed as

$$\begin{aligned} T_d &= \frac{2\pi}{\omega_d} \\ &= \frac{2\pi}{\sqrt{\omega_\theta^2 - v^2}} \qquad \text{since } \omega_d = \sqrt{\omega_\theta^2 - v^2} \\ &= T_\theta\frac{1}{\sqrt{1 - (v/\omega_\theta)^2}} \end{aligned} \tag{4.19b}$$

where $T_\theta = 2\pi/\omega_\theta$ is the natural pitching period as given by (4.19a). We see that the period increases with damping; however, the damping is very small in ship motion, and therefore the increase in the period is negligible.

Example 4.15

Given:

$$\begin{aligned} L &= 500 \text{ ft} \\ k_{yy} &= 0.25L \\ GM_L &= 500 \text{ ft} \\ \Delta &= 15{,}000 \text{ tons} \end{aligned}$$

If the added mass moment of inertia is about 90% of the mass moment of inertia of the ship, find the natural pitching period.

Solution:

The natural circular frequency is

$$\omega_\theta = \sqrt{\frac{c}{a}}$$

where $a = I'_{yy}$ and $c = \Delta\overline{GM}_L$.

Now $$I'_{yy} = 1.90 I_{yy} = 1.90 \times \frac{\Delta}{g} k_{yy}^2$$

Thus

$$\omega_\theta = \sqrt{\frac{\Delta \overline{GM}_L g}{1.9 \Delta k_{yy}^2}} = \sqrt{\frac{500 \times 2.2}{1.90 \times (125)^2}}$$

and

$$T_\theta = \frac{2\pi}{\omega_\theta} = \frac{2\pi}{0.736}$$
$$= 8.52 \text{ sec}$$

Pitching Periods

The natural pitching period is comparatively small and is generally close to the heaving period and almost half of the rolling period. However, the pitching period is more important than the others in view of the dynamic effects, namely, deck wetness, slamming, and vertical accelerations. The pitching period can be increased by increasing the longitudinal radius of gyration, k_{yy}, that is, by moving weights toward both ends of the vessel. However, for all conventional vessels k_{yy} is fairly constant and is about $0.24L$ to 0.26 L , where L is the length of the ship.

An improvement in the longitudinal stability will reduce the natural pitching period. Full ends, a flare at the bow, and flatness at the stern have a considerable damping effect on the pitching motion.

To avoid resonance the pitching period is kept as small as possible so that T_θ/T_e remains very small. This small value makes it possible for the ship to pitch with the waves, that is, the bow and stern should rise and fall with the waves, thereby reducing the possibility of the dynamic effects.

For different sizes of geometrically similar ships, the nondimensional quantity for the pitching period, $T_\theta((L/g)$, is constant. In Fig. 4.23 the pitching periods for both merchant and naval ships are given as functions of another nondimensional quantity, the displacement/length ratio, $\Delta/(L/100)^3$ [127]. A simplified formula for the pitching period can be obtained from the scattered points of Fig. 4.23 as follows:

$$\frac{T_P}{\sqrt{L}} = C \sqrt{\frac{\Delta}{(0.01L)^3} \cdot \frac{L}{g}}$$

where C = constant = 0.009 to 0.01. Typical values of pitching periods for various kinds of ships are given in Table 4.9.

Example 4.16

From the data presented in Example 4.15 find the

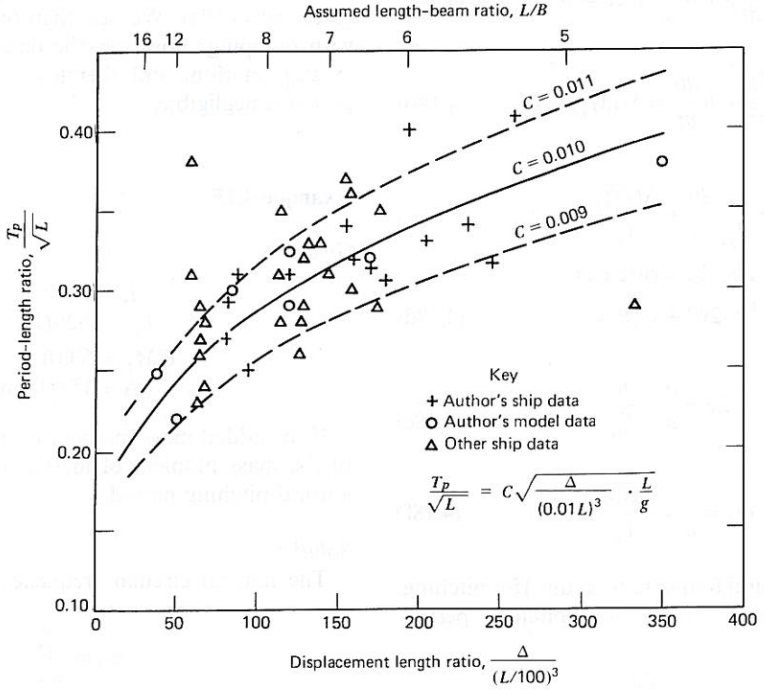


Figure 4.23 Pitching period as a function of displacement/length ratio [127].

TABLE 4.9

Type of Ship	Δ [tons]	L [ft]	T_θ [from Fig. 4.23]
Icebreaker	5,301	279	5.3–6.5
Command	2,800	300	4.5–5.5
Submarine	6,900	410.5	5.2–6.4
Aircraft carrier	75,700	1040	7.4–9.0
Cruiser (heavy)	17,500	664	5.9–7.2
Cruiser (light)	14,600	600	5.8–7.1
Frigate	5,800	512.5	4.5–5.6
Destroyer	5,155	493	4.4–5.5
Destroyer escort	3,425	414.5	4.4–5.2
Battleship	59,000	860.0	7.6–9.0
Inshore fire support	1,500	245	4.0–5.0
Amphibious command	19,290	620	6.2–7.7
Amphibious assault	39,300	820	6.8–8.5
Amphibious cargo	20,700	575.5	6.2–7.8
Amphibious transport	15,200	465.0	6.2–7.7
Amphibious dock	16,900	570.0	5.9–7.1
Landing ship dock	11,270	510	5.4–6.7
Landing ship tank	8,392	522.3	5.2–6.1
Landing craft (utility)	360	115	3.3–4.1
Landing craft (mechanized)	113	75.6	2.9–3.4
Petrol gunboat	245	164.5	2.9–3.4
River petrol boat	8	32	1.2–2.2
Minesweeper	9,040	440	5.6–6.9
Ammunition ship	20,500	565	6.4–7.8
Store ship	15,500	459.2	6.2–7.7
Oiler	40,000	640	7.3–8.8
Destroyer tender	20,500	643	5.8–7.3
Hospital ship	15,400	496	6.0–7.5
Submarine tender	22,250	643.7	6.3–7.6

pitching motion at $t = 0$ sec and exactly after 1, 2, and 3 periods, if the coefficient for the damping moment during pitching motion is known to be 2,500,000 ft-ton-sec and the initial conditions are specified as

$$\theta = 5^\circ \text{ and } \frac{d\theta}{dt} = 0 \text{ at } t = 0 \text{ sec}$$

Solution:

The equation of motion for damped pitching in calm water is given as

$$\theta = e^{-\nu t} A \sin(\omega_d t - \delta)$$

from (4.18). Furthermore,

$$\omega_\theta = \frac{2\pi}{T_\theta} = \frac{2\pi}{8.53} = 0.737 \text{ sec}^{-1}$$

$$2\nu = \frac{b}{I'_{yy}} = \frac{2{,}500{,}000}{1.9 \times (15{,}000/32.2) \times (125)^2} = 0.181 \text{ sec}^{-1}$$

$$\omega_d = \sqrt{(0.737)^2 - (0.091)^2} = 0.731 \text{ sec}^{-1}$$

$$T_d = \frac{2\pi}{\omega_d} = 8.60 \text{ sec}$$

Now, at $t = 0$, $\theta = 5^\circ$ so that from (4.18h)

$$\theta = 5 = A \sin(-\delta) = -A \sin \delta$$

Differentiating (4.18h), we have

$$\frac{d\theta}{dt} = e^{-\nu t} A \omega_d \cos(\omega_d t - \delta) - \nu e^{-\nu t} A \sin(\omega_d t - \delta)$$

At $t = 0$, $d\theta/dt = 0$ so that

as $$0 = A\omega_d \cos(-\delta) - \nu A \sin(-\delta)$$

or

$$\tan \delta = -\frac{\omega d}{\nu} = -\frac{0.731}{0.090} = -8.12$$

from which

$$\delta = -84.8^\circ \text{ or } -1.48 \text{ rad}$$

and therefore

$$A = -\frac{5}{\sin \delta} = 5.021$$

The equation of pitching motion can, therefore, be written as

$$\theta[\text{rad}] = e^{0.091t} \times 5.021 \sin(0.731t + 1.48)$$

By inserting different values of t into the equation, Table 4.10 was prepared.

Exciting Moment for Pitching Motion

The exciting moment for pitching is due to the unbalanced moment caused by the waves about the transverse axis of the ship. As in the case of heaving, the pitching moment can easily be developed by means of the hydrostatic pressure distribution (but without any Smith correction; see Chapter 3), that is,

$$M_\theta = \rho g \int_{-L/2}^{L/2} 2y\zeta x dx \tag{4.19c}$$

Now, substituting the free surface expression $\zeta = \zeta_a \cos(kx \cos \mu - \omega_e t)$ and assuming that the ship is symmetrical about the midship section, we have

$$M_\theta = \left[2\rho g \zeta_a \int_{-L/2}^{L/2} y(x) \times \sin(kx \cos \mu) dx \right] \sin \omega_e t \tag{4.19d}$$

TABLE 4.10

Period [sec]	t[sec]	θ[rad]	θ[deg]
0	0	0.0873	5
1	8.6	0.0402	2.30
2	17.2	0.0183	1.05
3	25.8	0.0082	0.48

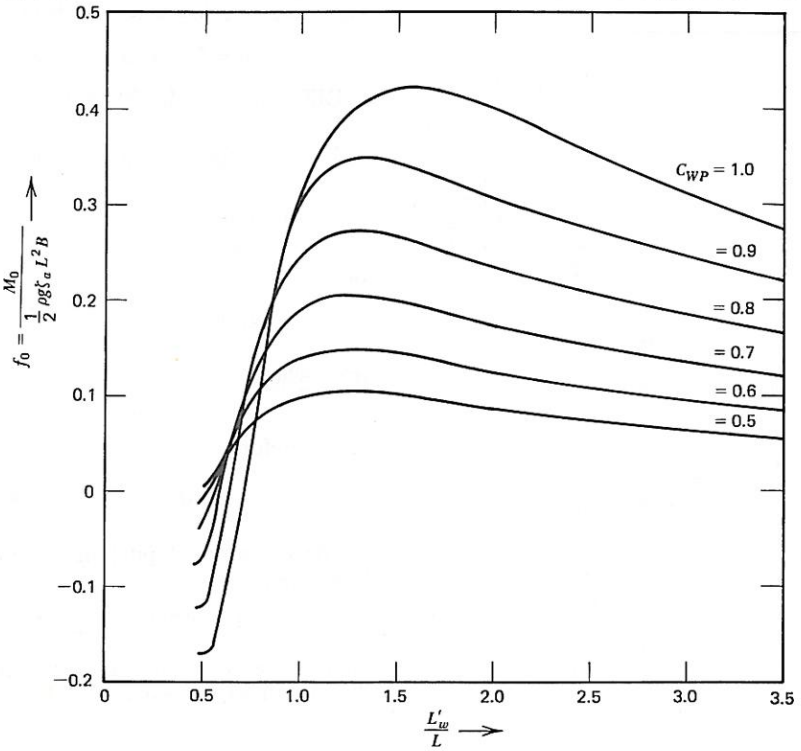


Figure 4.24 Coefficient for pitching exciting moment [242].

Let us now assume that

$$M_\theta = M_0 \sin \omega_e t$$

or

$$M_\theta = M_0 \cos(\omega_e t - \varepsilon_1)$$

where M_0 is the amplitude of the exciting moment, and ε_1 is the phase angle of the exciting moment relative to the waves. Thus

$$M_0 = 2\rho g \zeta_a \int_{-L/2}^{L/2} y(x) \times \sin(kx \cos \mu)\, dx \quad (4.19e)$$

and $\varepsilon_1 = +90°$.

The nondimensional amplitude of the exciting moment for pitching is given as

$$f_0 = \frac{M_0}{\frac{1}{2}\rho g \zeta_a B L^2} = \frac{4}{BL^2} \int_{-L/2}^{L/2} y(x) \times \sin(kx \cos \mu)\, dx \quad (4.19f)$$

Note that for the beam sea condition (i.e., for $\mu = 90°$ or 270°) the exciting moment for pitching, M_θ, becomes zero.

Figure 4.24 shows how the nondimensional amplitude of the exciting moment for pitching, f_0, varies with the ratio of effective wavelength to ship length and the waterplane area coefficients of some simplified hull forms.

Example 4.17

Using the data from Example 4.16 calculate the exciting moment for the pitching motion.

The required data are presented in Table 4.11.

Solution:

The value of the integral of (4.19f) is

$$(\tfrac{1}{3})(4.8)(-35.18) = -56.288\, ft^3$$

Thus the nondimensional amplitude of the exciting moment of (4.19f) is

$$f_0 = \frac{4}{BL^2}(\text{integral}) = \frac{4}{2.592 \times (19.2)^2}(-56.288) = -0.2356$$

and the amplitude of moment is

$$M_0 = \tfrac{1}{2}\rho g \zeta_a B L^2 f_0 = (\tfrac{1}{2})(1.9384)(32.2)(0.2)(2.592) \times [(19.2)^2](-0.2356) = -1405.12 \text{ ft-lb}$$

TABLE 4.11

Station No. ①	$y = B_n$ [ft] ②	ξ [ft] ③	$y\xi$ [ft²] ④	$k\xi\cos\mu$ [–] ⑤	$\sin(k\xi\cos\mu)$ [–] ⑥	$y\xi\sin(k\xi\cos\mu)$ [ft²] ⑦	Simpson's Multiplier ⑧	Product [ft²] ⑨
0	0	9.6	0	– 1.570	– 1.000	0.000	1	0.00
5	1.296	4.8	6.22	– 0.785	– 0.707	– 4.400	4	– 17.59
10	1.296	0	0	0	0	0.000	2	– 0.00
15	1.296	– 4.8	– 6.22	0.785	0.707	– 4.400	4	– 17.59
20	0	– 9.6	0	1.570	1.000	0	1	0.00
							SUM	– 35.18

Description of Table 4.11

Column Number	*Description*
①	Station Number
②	Half-Breadths of Waterplane
③	Distance from LCG, ξ
④	$y\xi$
⑤	$k\xi\cos\mu$, where k = wave number $= 2\pi/L_w = 2\pi/19.2 = 0.327$
	$\cos\mu = \cos 120^\circ = -0.5$
⑥	$\sin$ ⑤
⑦	$y\xi\sin(k\xi\cos\mu) = \xi y\sin k$
⑧	Simpson's Multiplier
⑨	Product = ⑦ × ⑧

By performing numerical calculations, we can reach the following conclusions [242]:

a. When the effective wavelength is less than half the ship's length, the pitching moment is small.

b. When the effective wavelength equals the ship's length, the pitching moment is high. It attains its maximum value, which is dependent on the form (especially the waterplane coefficient), for $1.0 < L'_w/L < 1.5$.

c. The asymptotic value of the pitching moment as the effective wavelength approaches infinity is zero, since for constant wave height and infinite length the wave slope tends to disappear.

Pitching in Waves

The equation of motion for pitching in waves is

$$I'_{yy}\frac{d^2\theta}{dt^2} + b\frac{d\theta}{dt} + c\theta = M_0\sin\omega_e t \qquad (4.19g)$$

or

$$\frac{d^2\theta}{dt^2} + \frac{b}{I'_{yy}}\frac{d\theta}{dt} + \frac{\Delta\overline{GM}_L}{I'_{yy}}\theta = \frac{M_0}{I'_{yy}}\sin\omega_e t \qquad (4.19h)$$

This equation is similar to the one for heaving and leads to a similar solution:

$$\theta_a = \theta_{st}\cdot\mu_\theta$$

where θ_{st} is the static pitch angle due to the application of the maximum pitching moment, that is,

$$\theta_{st} = \frac{M_0}{c} = \frac{M_0}{\Delta\overline{GM}_L}$$

and

$$\mu_\theta = \frac{1}{\sqrt{(1-\Lambda^2)^2 + 4\kappa^2\Lambda^2}} \qquad (4.19i)$$

is the magnification factor for pitching motion, where

$$\Lambda = \frac{\omega_e}{\omega_\theta} \qquad (4.19j)$$

and

$$\kappa = \frac{\nu}{\omega_\theta} \qquad (4.19k)$$

is the nondimensional damping coefficient.

The solution of (4.19g) is, then,

$$\theta = Be^{-\nu t}\sin(\omega_d t + \gamma) + C\sin(\omega_e t - \varepsilon_2) \qquad (4.19l)$$

which, for a steady-state condition (when the first term dies out with time t), is

$$\theta = \theta_a\sin(\omega_e t - \varepsilon_2) \qquad \text{since } C = \theta_a \qquad (4.19m)$$

or

$$\theta = \frac{\theta_{st}}{\sqrt{(1-\Lambda^2)^2 + 4\kappa^2\Lambda^2}}\sin(\omega_e t - \varepsilon_2) \qquad (4.19n)$$

We see that ε_2 is the phase angle between the exciting moment and the pitching motion and

$$\tan\varepsilon_2 = \frac{2\kappa\Lambda}{1-\Lambda^2} \qquad (4.19o)$$

The same type of response curve is obtained as for heaving, and the maximum pitching amplitude is obtained when

$$\Lambda = 1 - 2\kappa^2$$

Once again for lightly damped systems, resonance can be said to occur at $\Lambda \approx 1$. However, it would seem that with the values of κ normally obtained for ship hull forms resonance would probably occur at $\Lambda = 0.85$ to 0.90.

The total phase angle between the wave and the pitching motion is

$$\begin{aligned}\varepsilon &= \varepsilon_1 + \varepsilon_2 \\ &= 90^\circ + \varepsilon_2\end{aligned}$$

where $0 \geqslant \varepsilon_2 \geqslant -180^\circ$.

Example 4.18

Given:

$$L = 450 \text{ ft}$$
$$B = 70 \text{ ft}$$
$$\overline{GM}_L = 450 \text{ ft}$$
$$C_{WP} = 0.80$$
$$k_{yy} = 110 \text{ ft}$$
$$\mu = 180^\circ \text{ (i.e., head sea)}$$
$$\zeta_a = 10 \text{ ft}$$
$$\rho = 1.99 \text{ lb-sec}^2/\text{ft}^4$$
$$\omega_e = 1.18 \text{ rad/sec}$$

Assume the added mass of inertia to be 54% of the mass moment of inertia of the ship, and the nondimensional damping coefficient of pitching motion, $b\sqrt{gL}/\Delta L^2$, to be 0.154. From Fig. 4.24 the nondimensional amplitude of the pitching moment is

$$f_0 = \frac{M_0}{\frac{1}{2}\rho g \zeta_a L^2 B} = 0.25$$

Find both the amplitude of the pitching motion and the phase differences between the wave and the pitching motions. Draw a figure showing the wave motion, exciting moment for pitching, and pitching motion as functions of $\omega_e t$.

Solution:

The pitching moment of inertia is

$$I'_{yy} = I_{yy} + \delta I_{yy} = I_{yy} + 0.54 I_{yy} = 1.54 I_{yy}$$

or

$$\begin{aligned}I'_{yy} &= 1.54 \frac{\Delta}{g} k_{yy}^2 = 1.54 \times \frac{12{,}500}{32.2} \times (110)^2 \\ &= 7{,}233{,}000 \text{ ton-sec}^2\text{-ft}\end{aligned}$$

Since $b\sqrt{gL}/\Delta L^2 = 0.154$, the damping coefficient for pitching, b, becomes

$$\begin{aligned}b &= \frac{0.154 \Delta L^2}{\sqrt{gL}} = \frac{0.154(12{,}500)(450)^2}{\sqrt{32.2 \times 450}} \\ &= 3{,}240{,}000 \text{ ft-ton-sec}\end{aligned}$$

The amplitude of the pitching moment, M_0, is

$$\begin{aligned}M_0 &= f_0(\tfrac{1}{2})\rho g \zeta_a L^2 B \\ &= 0.25(\tfrac{1}{2}) \times 1.99 \times 32.2 \times 10 \times 450^2 \times 70 \\ &= 506{,}250 \text{ ft-tons} \qquad \text{(after dividing by 2240)}\end{aligned}$$

Thus the static pitch deflection is

$$\theta_{st} = \frac{M_0}{c} = \frac{M_0}{\Delta \overline{GM}_L} = \frac{506{,}250}{12{,}500 \times 450} = 0.09 \text{ rad}$$

Also,

$$2\nu = \frac{b}{I'_{yy}} = \frac{3{,}240{,}000}{7{,}233{,}000} = 0.448$$

$$\omega_0 = \sqrt{\frac{c}{a}} = \sqrt{\frac{12{,}500 \times 450}{7{,}233{,}000}} = 0.882 \text{ rad/sec}$$

$$\kappa = \frac{\nu}{\omega_0} = \frac{0.224}{0.882} = 0.254$$

and

$$\Lambda = \frac{\omega_e}{\omega_0} = \frac{1.18}{0.882} = 1.338$$

The amplitude ratio is, then,

$$\begin{aligned}\frac{\theta_a}{\theta_{st}} = \mu_0 &= \frac{1}{\sqrt{(1-\Lambda^2)^2 + 4\kappa^2\Lambda^2}} \\ &= \sqrt{0.624 + 4 \times (0.254)^2 \times (1.338)^2} \\ &= 0.960\end{aligned}$$

from which

$$\begin{aligned}\theta_a &= \mu_0 \cdot \theta_{st} \\ &= 0.960 \times 0.09 \\ &= 0.086 \text{ rad (or } 4.93^\circ)\end{aligned}$$

The phase angle between the wave motion and the pitching motion is

$$\varepsilon = \varepsilon_1 + \varepsilon_2$$

where ε_1 is the phase angle between the wave motion and the exciting moment for pitching, and ε_2 is the phase angle between the exciting moment for pitching and the pitching motion. Now from (4.19e)

$$\varepsilon_1 = 90^\circ$$

and from (4.19p)

$$\varepsilon_2 = \tan^{-1}\left(\frac{2\kappa\Lambda}{1-\Lambda^2}\right)$$

$$= \tan^{-1}\left[\frac{2 \times 0.254 \times 1.338}{1-(1.338)^2}\right]$$

$$= -41^\circ$$

so that

$$\varepsilon = \varepsilon_1 + \varepsilon_2 = 90^\circ - 41^\circ = 49^\circ$$

the equation of wave motion is

$$\zeta = \zeta_a \cos \omega_e t$$

and the equation of the exciting moment for pitching is

$$M_\theta = M_\theta \sin \omega_e t$$

$$= M_0 \cos(\omega_e t - 90^\circ)$$

The equation of pitching motion is expressed as

$$\theta = \theta_a \sin(\omega_e t - \varepsilon_2)$$

that is,

$$\theta = \theta_a \sin(\omega_e t + 41^\circ)$$

or

$$\theta = \theta_a \cos(\omega_e t - 49^\circ)$$

The phase relationship between the wave motion and the exciting moment for pitching is 90°, that is, the maximum exciting moment occurs after the maximum wave motion by an angle of 90°.

Similarly, the phase relationship between the exciting moment and the pitching motion is +41°, that is, the maximum pitching motion takes place 41° earlier than the maximum pitching moment. Therefore the maximum pitching motion is to be expected at an angle of 90° − 41° or, as illustrated in Fig. 4.25, 49° after the wave motion.

The model results for heave and pitch of three Series 60 hull forms in regular head seas for different speeds are presented in nondimensional form in Fig. 4.26. This figure also shows the phase relationship between the pitching and heaving motions, with heave following pitch. One should notice the considerable differences in motion amplitudes among the three hull forms. In most cases the hull form with $C_B = 0.80$ has the smallest pitch amplitudes. The

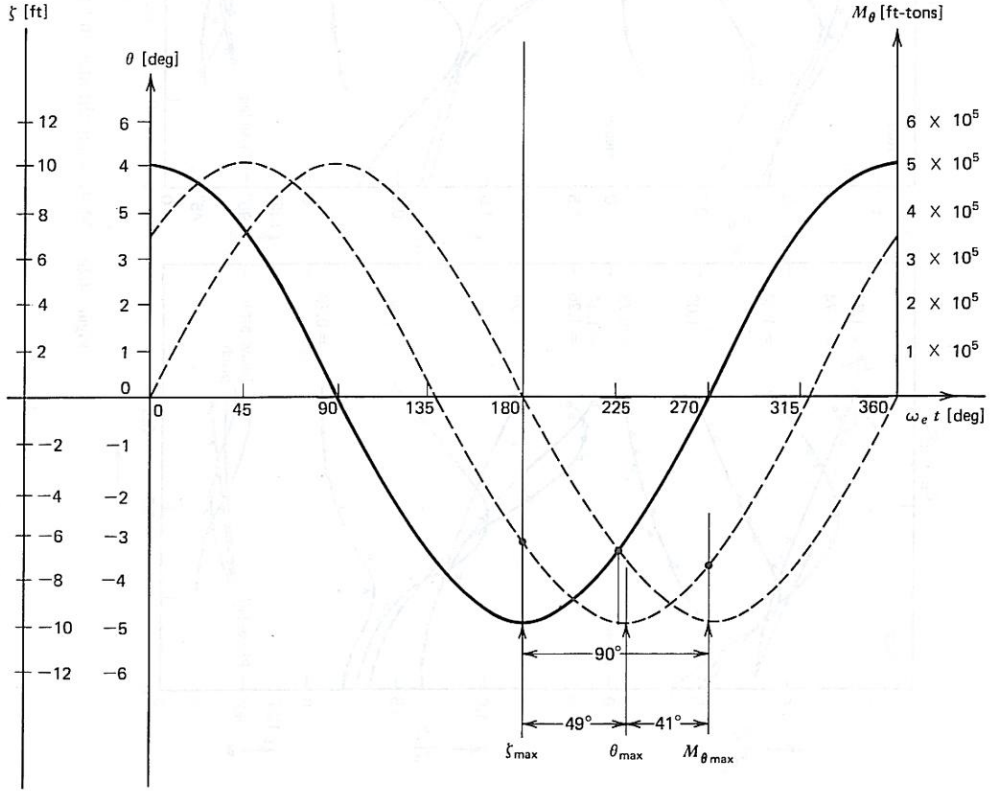


Figure 4.25 Wave elevation, pitching exciting moment, and pitching motion as functions of $_e t$.

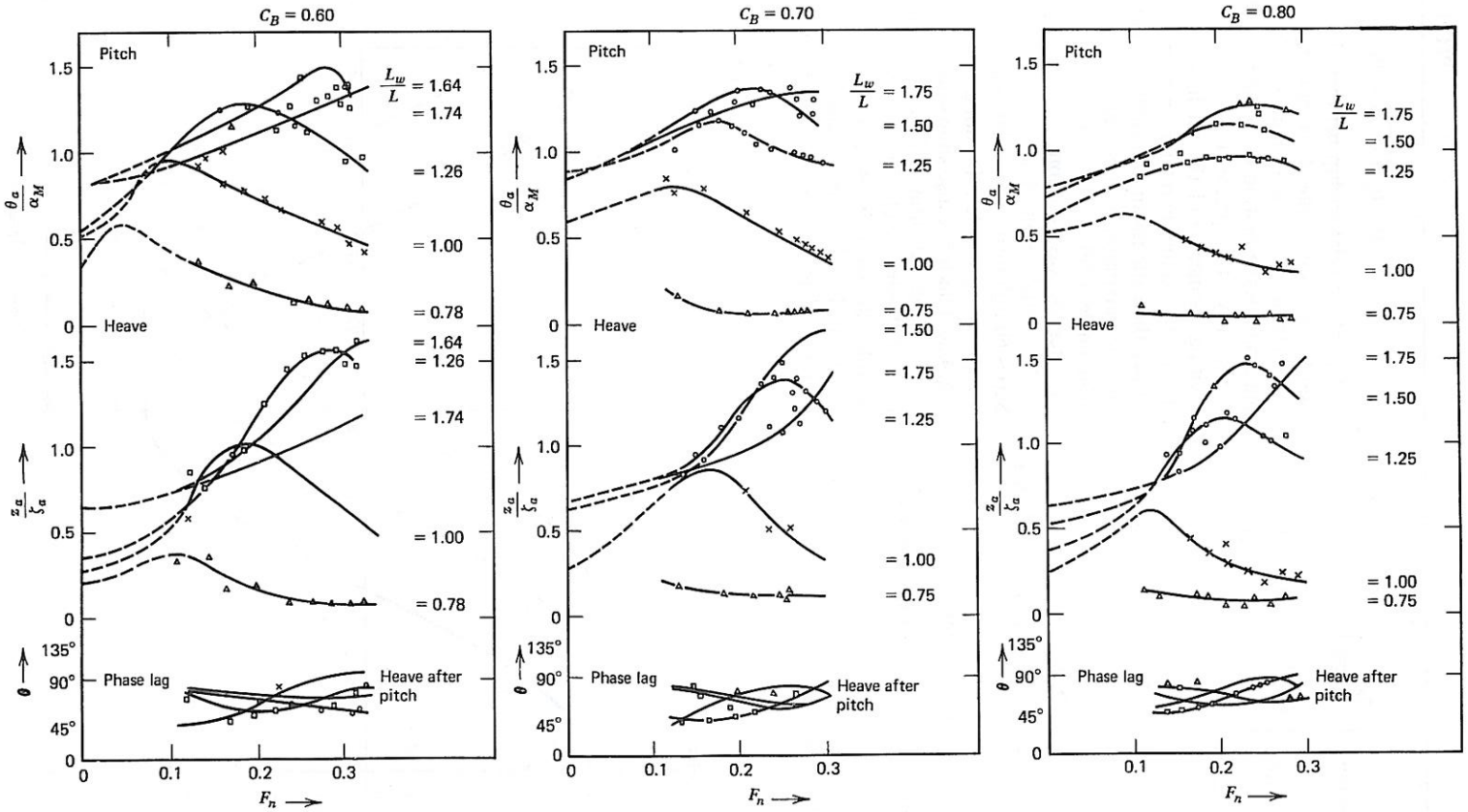


Figure 4.26 Motion amplitudes and phase angles in regular waves [73].

TABLE 4.12 [73]

F_n	$C_B = 0.60$		$C_B = 0.70$		$C_B = 0.80$	
	ω_z [sec^{-1}]	ω_θ [sec^{-1}]	ω_z [sec^{-1}]	ω_θ [sec^{-1}]	ω_z [sec^{-1}]	ω_θ [sec^{-1}]
0.15	7.2	7.0	6.5	6.9	6.2	6.7
0.20	7.0	7.1	6.5	6.7	6.2	6.5
0.25	7.0	7.2	6.7	6.9	6.2	6.6
0.30	7.1	7.2	6.8	6.8	6.2	6.9

heave amplitudes are also smaller for this hull form except in the case of excessive model speed. The reduction in heave and pitch is quite appreciable, especially for wavelength equal to or less than $1.25L$. Another interesting phenomenon is the small variation in the phase lag.

Table 4.12 summarizes the approximate natural frequency values obtained for these Series 60 model forms.

4.5 ROLLING

The equation of motion for rolling is analogous to that for pitching and is expressed as

$$a\frac{d^2\phi}{dt^2} + b\frac{d\phi}{dt} + c\phi = M_0 \cos \omega_e t \qquad (4.19q)$$

where $a(d^2\phi/dt^2)$ is the inertial moment and a is the virtual mass moment of inertia for rolling, $d^2\phi/dt^2$ is the angular acceleration of rolling, $b(d\phi/dt)$ is the damping moment and b is the damping moment coefficient, and $d\phi/dt$ is the angular velocity.

In the simplified case the damping moment is considered to be linearly proportional to the angular velocity $d\phi/dt$. Also, in (4.19q) $c\phi$ is the restoring moment, c is the restoring moment coefficient, and ϕ is the angular displacement of rolling.

As in the case of pitching motion, the exciting moment $M_0 \cos \omega_e t$ is thought of as fluctuating with the wave encountering frequency ω_e.

If now the various coefficients can be assessed for the rolling motion, the rolling motion of a ship can be determined. However, it should be emphasized here that the coefficients for the rolling motion are different from those for pitching or heaving.

Determination of Coefficients for Rolling Motion

The virtual mass moment of inertia for rolling is the moment of inertia of the actual mass of the vessel plus the added mass moment of inertia; thus

$$\begin{aligned} a &= I_{xx} + \delta I_{xx} \\ &= \frac{\Delta}{g} k_{xx}^2 + \delta I_{xx} \end{aligned} \qquad (4.19r)$$

where k_{xx} is the radius of gyration for rolling, and δI_{xx} is the added mass moment of inertia for rolling. The value of a can be found experimentally or by using analytical expressions. By both analytical and experimental investigations it has been found that the added mass moment of inertia for rolling is about 20% of the mass moment of inertia of the actual ship. The coefficient a can also be expressed as

$$\begin{aligned} a = I'_{xx} &= I_{xx} + \delta I_{xx} \\ &= \frac{\Delta}{g} k_{xx}^2 + \frac{\delta\Delta}{g} k_{xx}^2 \\ &= \left(\frac{\Delta + \delta\Delta}{g}\right) k_{xx}^2 \\ &= \frac{\Delta'}{g} k_{xx}^2 \end{aligned} \qquad (4.19s)$$

where Δ' is the virtual displacement of the ship for rolling, that is,

$$\Delta' = \Delta + \delta\Delta$$

which is the sum of the actual weight and the added weight.

Note: When no data are available, the added weight can be taken as about 10 to 20% of the actual displacement of the ship.

Figure 4.27 shows the experimental results of the added radius of gyration, which is defined from (4.19r), that is,

$$\begin{aligned} a &= I_{xx} + \delta I_{xx} \\ &= \frac{\Delta}{g} k_{xx}^2 + \frac{\Delta}{g} k_{xx}'^2 \\ &= \frac{\Delta}{g}(k_{xx}^2 + k_{xx}'^2) = \frac{\Delta}{g} k_{xx}''^2 \end{aligned} \qquad (4.19t)$$

Thus k_{xx} is the radius of gyration of the ship about the x-axis (see Section 4.3), k'_{xx} is the added radius of gyration about the x-axis (see Fig. 4.27), and k''_{xx} is the virtual radius of gyration. The quantity k''_{xx} is often expressed as a fraction of the beam of the ship and is normally in the range of $0.33B \leqslant k''_{xx} \leqslant 0.45B$.

From experimental results with models of various kinds of ships the following two formulas are derived in (Ref. 115) for estimating the virtual radius of gyration for the rolling motion:

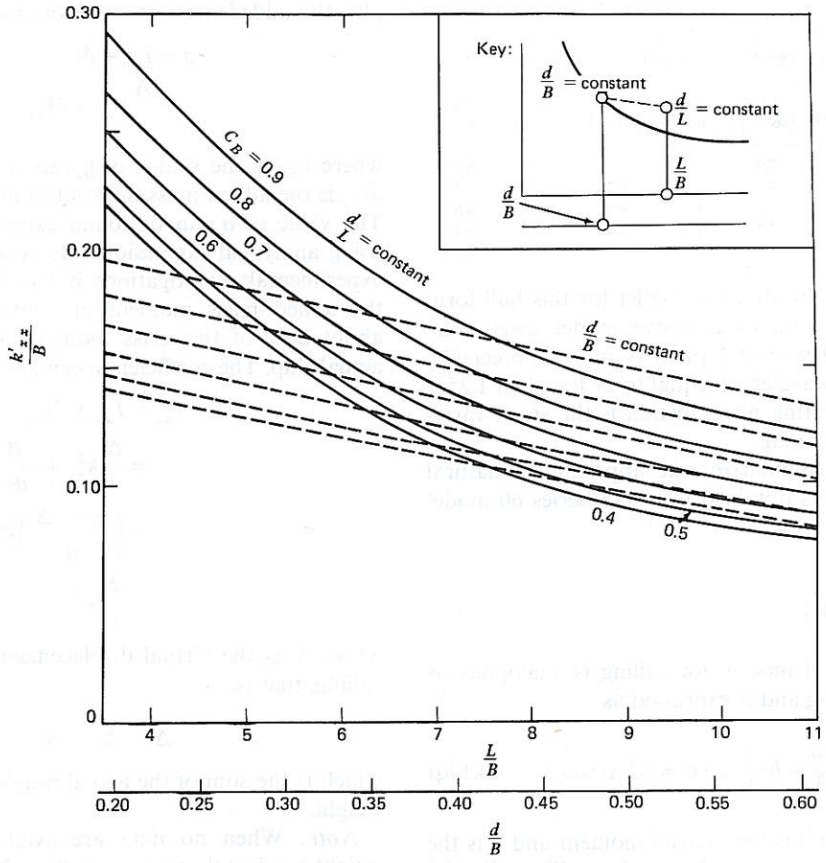


Figure 4.27 Added radius of gyration for rolling [202].

1. For ordinary merchant ships

$$\left(\frac{k''_{xx}}{B}\right)^2 = f\left[C_B C_u + 1.10 C_u (1 - C_B)\left(\frac{H_e}{T} - 2.20\right) + \frac{H_e^2}{B^2}\right] \tag{4.19u}$$

where k''_{xx} = virtual radius of gyration about the x-axis through the CG of the ship
C_B = block coefficient
C_u = upper deck area coefficient = Area/(Length × Breadth)
H_e = effective depth of the ship superstructure $= D + (A/L_{pp})$
D = depth to main deck (molded)
A = projected lateral area of superstructures and deck houses above the main deck
L_{pp} = length between perpendiculars
T = draft (molded)
B = ship's beam

and

f = constant, depending on the type of ship, where
f = 0.125 for passenger, cargo, and passenger–cargo vessels
= 0.133 for tankers
= 0.177 for whale catchers
= 0.200 for bonito fishing vessels

2. For warships

$$\left(\frac{k''_{xx}}{B}\right)^2 = f\left[C_B C_u + 1.10 C_e (1 - C_B)\left(\frac{H_n}{d} - 2.20\right) + \frac{H_n^2}{B_u^2}\right]$$

where B = molded breadth of the ship
d = mean draft (molded draft, if the ship has a block keel)
B_u = maximum breadth under water
C_e = exposed deck area coefficient

$H_n = D + A_n/L_{pp}$
D = depth from the top of the keel to the upper deck (i.e., molded)
A_n = sum of the projected lateral areas of the forecastle, under the bridge and gun
f = 0.177 for battle ships
= 0.172 for cruisers, destroyers, and torpedo boats

It should be noted here that a very accurate determination of the added moment of inertia for rolling is not essential, since the added mass moment of inertia is much smaller than the mass moment of inertia of the ship itself for the rolling motion.

Damping Moment Coefficient

The damping forces acting on a ship during rolling motion can be due to any combination of the following:

a. Waves generated.
b. Water friction on the ship surface or eddymaking.
c. Bilge keels, skeg, and other appendages.
d. Resistance between the ship and the air.
e. energy loss because of heat generated during the rolling motion.
f. Surface tension.

The effects due to causes a, b, and c are significant, whereas those due to causes d, e, and f are considered to be very small. As in the case of heaving and pitching motions, the damping coefficient is very important in rolling motion, especially because the roll damping coefficient is relatively small and the magnification factor may reach a value between 5 and 10.

The damping coefficient b, due to wavemaking during the rolling motion, can also be calculated by the strip method. The damping coefficient per unit length is expressed as

$$b_n = \frac{\rho g^2}{\omega_e^3}\left(\frac{B_n}{2}\right)^2 \bar{A}_\phi^2 \tag{4.19w}$$

where $\bar{A}_\phi$ is defined as

$$\bar{A}_\phi = \frac{\zeta_a}{\phi_a(B_n/2)} = d_\phi\left(\frac{\omega_e^2 B_n}{2g}\right)^2$$

By using the strip method the total damping moment coefficient b is obtained from the expression

$$b = \int b_n d\xi$$

Figure 4.28 gives for LEWIS sections [135] the values of d_ϕ as a function of individual section coefficient β and s_n, where

$$S_n = \frac{B_n}{2T_n}$$

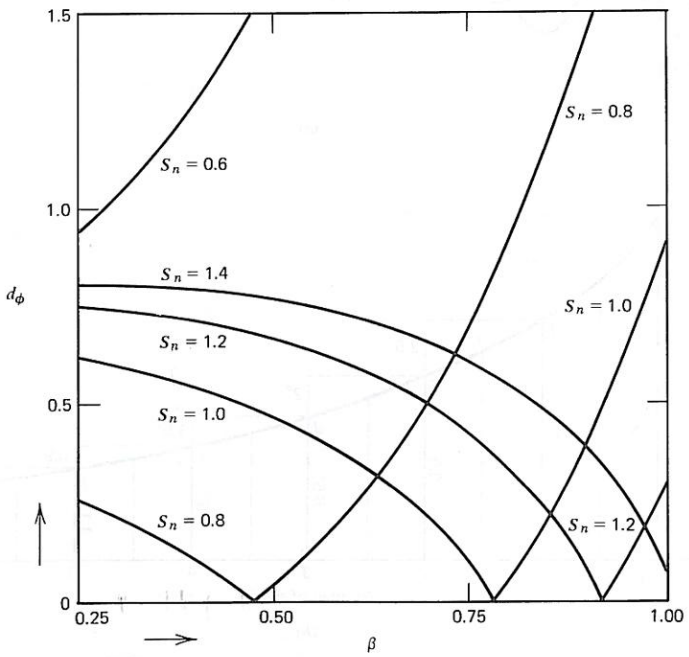


Figure 4.28 Coefficient $d\phi$ for the determination of roll damping

TABLE 4.13

Station No.	B_n [ft]	B_n^2 [ft²]	$\frac{B_n^2}{4}$ [ft²]	S_n $\frac{②}{2.288}$	β_n [−]	d_ϕ (from Fig.4.28)	$\bar{A}_\phi$	$\bar{A}_\phi^2$	b_n	Simpson's Multiplier	Product
①	②	③	④	⑤	⑥	⑦	⑧	⑨	⑩	⑪	⑫
0	0	0	0	0	0	0	0	0	0	1	0
5	2.592	6.718	1.680	1.133	0.993	0.50	2.9157	8.5025	258	4	1032
10	2.592	6.718	1.680	1.133	0.993	0.50	2.9159	8.5025	258	2	516
15	2.592	6.718	1.680	1.133	0.993	0.50	2.9159	8.5025	258	2	1032
20	0	0	0	0	0	0	0	0	0	1	0
										SUM	2580

The values in this figure are valid for $(\omega_e^2 B_n/2g)$ less than 0.3.

Example 4.19

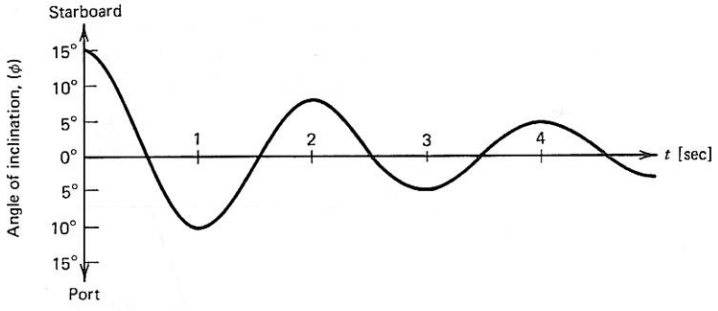
Using the data from Example 4.1, calculate the coefficient of damping for rolling motion. The relevant values are presented in Table 4.13.

Solution:

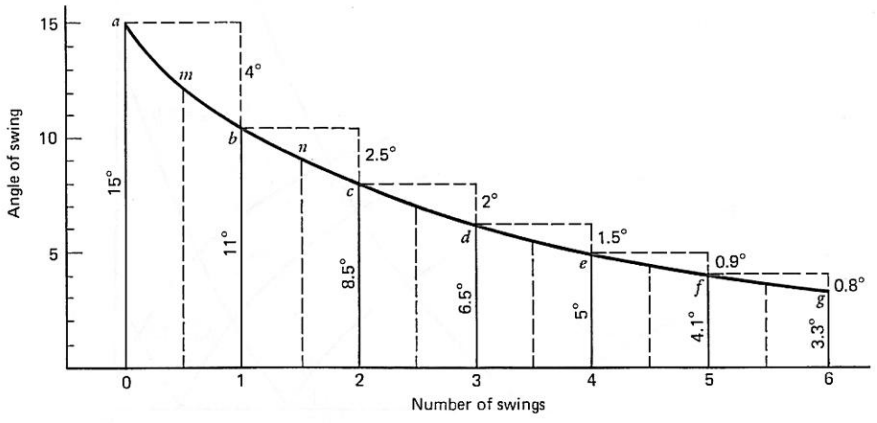
$$b = \int b_n \, d\xi$$

where

$$b_n = \frac{\rho g^2}{\omega_e^3}\left(\frac{B_n}{2}\right)^2 \bar{A}_\phi^2$$



(*a*)



(*b*)

Figure 4.29 (*a*) Roll motion as a function of time. (*b*) Curve of declining angles.

Therefore

$$b = \tfrac{1}{3} \times 5 \times \text{SUM}$$
$$= \tfrac{1}{3} \times 4.8 \times 2580$$
$$= 4128 \text{ ft-lb-sec}$$

Note for column ⑩, that is,

$$\bar{A}_\phi = d_\phi \left(\frac{\omega_e^2 B_n}{2g}\right)^2 = \left[\frac{(4.811)^2 B_n}{64.4}\right]^2$$
$$= 0.1292 B_n^2 \, d_\phi$$

Therefore

$$b_n = \frac{\rho g^2}{\omega_e^3} \cdot \frac{B_n^2}{4} (\bar{A}_\phi)^2$$
$$= \frac{1.94(32.2)^2}{(4.811)^3 \times 4} B_n^2 \bar{A}_\phi^2 = 4.526 B_n^2 \bar{A}_\phi^2$$
$$= 4.526③ \times ⑨$$

Since frictional effect plays a significant role in roll-damping, the damping due to wavemaking alone may not be sufficiently accurate. In the first place, the bilge keels or other appendages fitted to a ship may contribute significantly to the total roll damping effect caused by the generation of eddies. Second, the ship's speed is also a contributing factor in roll damping, which has been found to be as much as three times larger when the ship is in motion than when it is not under way. Lastly, if the angle of roll is large, the linear damping law [roll damping moment $= b(d\phi/dt)$ is not valid.

Damping Coefficient from Experiment in Calm Water

Consider a ship that experiences successive amplitudes of roll port and starboard, which are

$$15°, 11°, 8.5°, 6.5°, 5°, 4.1°, 3.3°, 2.6°$$

Then Fig. 4.29*a* can be drawn to a base of time. With the direction of inclination ignored, a curve drawn through point *a*, which represents the original inclination, and points *b*, *c*, *d*, and so on, which represent the inclinations at the ends of the successive rolls to left and right, is shown in Fig. 4.29*b*. This curve is known as the *curve of declining angles*. Now, it is seen that the difference between two successive ordinates, such as 1*b* and 2*c*, is the decrease in inclination for a single roll due to damping. If preferred,

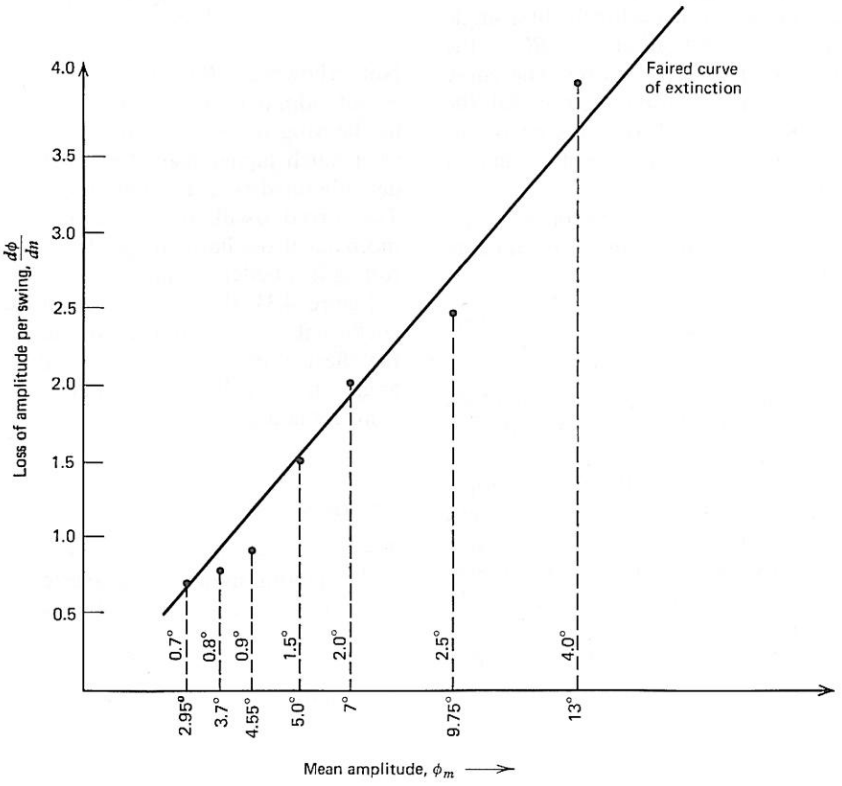


Figure 4.30 Curve of extinction.

TABLE 4.14

$\delta\phi$ [deg]	ϕ [deg]	ϕ_m [deg]
	15	
4		13
	11	
2.5		9.75
	8.5	
2		7
	6.5	
1.5		5.75
	5.0	
0.9		4.55
	4.1	
0.8		3.7
	3.3	
0.7	2.6	2.95

ordinates may be interpolated like those drawn at m and n, and the decrease for a single roll to angle $1b$ may be determined from them.

In Fig. 4.30 the decrease of inclination for a single roll is presented as an ordinate and the total inclination as an abscissa, the inclination being the mean angle of roll, calculated in Table 4.14.

Thus Aa (i.e., 4°) is the decrease for the first single roll from the mean inclination of 13°, Bb is the decrease for the second roll, and so on. The curve through the points thus determined is called the *curve of extinction of rolling*. From this curve the decrease for a single roll from any angle of inclination is readily determined.

In Ref. 11 it is suggested that the curve of extinction for ships can, in general, be represented by an equation having the form

$$\Delta\phi \text{ per swing} = K_1\phi \tag{4.20}$$

in which ϕ represents the angle of inclination at the beginning of a roll, and $\Delta\phi$ is the loss of amplitude for the next single roll from side to side. Equation 4.20 is called the *extinction equation.*

Since the line is supposed to go through the origin and since there is only one arbitrary constant, one observation is required to determine the equation of the curve. In other words, by taking any representative point on the faired curve of extinction, the coefficient K_1 can be determined. For example, let $\phi_m = 7°$; then $K_1\ 7° = 2.1$ or $K_1 = 0.3$ from (4.20).

Therefore

$$-\frac{d\phi}{dn} = 0.3\phi_m$$

Hence, for $\phi = 10°$,

$$-\frac{d\phi}{dn} = 0.3 \times 10 = 3°$$

and for $\phi = 5°$,

$$-\frac{d\phi}{dn} = 0.3 \times 5 = 1.5°$$

and so on.

Note: These two predicted points (for 10° and 5°) lie very close to the curve drawn through the experimental points in Fig. 4.30.

The value of K_1 does not depend on the unit of ϕ, which may be given in either radians or degrees.

Also it can be shown [132] that

$$-\frac{d\phi}{dn} = \frac{\pi^2 b}{T_\phi \Delta\overline{GM}_T}\phi_m \tag{4.21a}$$

where b is the damping coefficient.

Therefore, comparing (4.20) and (4.21a) gives

$$K_1 = \frac{\pi^2 b}{T_\phi \Delta\overline{GM}_T}$$

or

$$b = \frac{K_1 T_\phi \Delta\overline{GM}_T}{\pi^2}$$

Note, however, that this experimental approach is not adopted for the determination of damping for heaving or pitching motion, since the damping is of much higher magnitude in these motions and data obtained experimentally are not accurate enough. The forced oscillator technique, which employs a mechanical oscillator to produce exciting forces for rolling is a better method.

Figure 4.31 shows the nondimensional damping coefficient k of two models A and B, and illustrates the effect of bilge keels, speed, and amplitude of roll angle on the roll damping moment (k was derived from extinction curves).

Restoring Moment Coefficient c

The restoring moment of a ship for rolling motion is the righting moment (transverse) at any particular angle of inclination and is expressed as

$$c\phi = \Delta\overline{GZ} \tag{4.21b}$$

For small angles of inclination [ϕ in radians]

$$\begin{aligned} c\phi &\simeq \Delta\overline{GM}_T \sin\phi \\ &\simeq \Delta\overline{GM}_T \\ &= \rho g \Delta\overline{GM}_T \phi \end{aligned} \tag{4.21c}$$

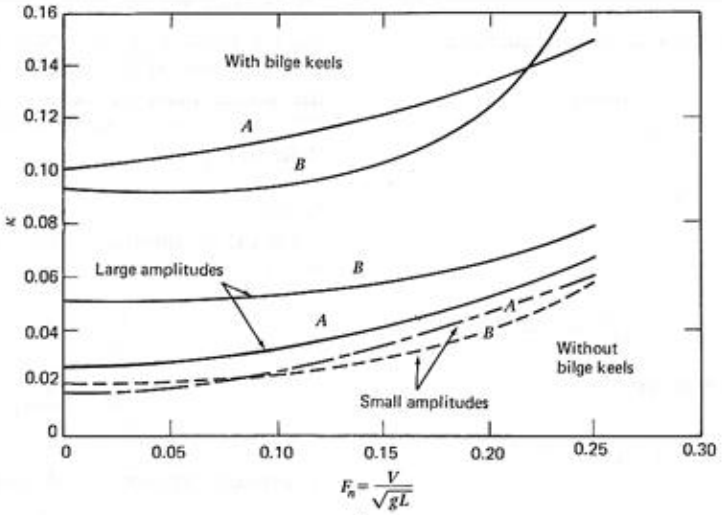


Figure 4.31 Roll damping coefficient, as a function of Froude number [242].

so that

$$c = \rho g \nabla \overline{GM}_T \tag{4.21d}$$

However, (4.21d) is valid only for small amplitudes of rolling displacement (say, to 10° if the curve of righting moment is linearly proportional up to an inclination of 10°).

Rolling in Calm Water

The equation of motion for rolling in calm water is

$$a\frac{d^2\phi}{dt^2} + b\frac{d\phi}{dt} + c\phi = 0 \tag{4.22a}$$

or, inserting the expressions for a, b, and c,

$$I'_{xx}\frac{d^2\phi}{dt^2} + b\frac{d\phi}{dt} + \Delta\overline{GM}_T\phi = 0 \tag{4.22b}$$

from which

$$\frac{d^2\phi}{dt^2} + 2v\frac{d\phi}{dt} + \omega_\phi^2\phi = 0 \tag{4.23}$$

where

$$2v = \frac{b}{a} = \frac{b}{I'_{xx}}$$
$$\omega_\phi^2 = \frac{c}{a} = \frac{\Delta\overline{GM}_T}{I'_{xx}} \tag{4.24}$$

and

$$T_\phi = \frac{2\pi}{\omega_\phi} = 2\pi\sqrt{\frac{I'_{xx}}{\Delta GM_T}} \tag{4.25}$$

Solving this last differential equation, we obtain

$$\phi = e^{-vt}(C_1\cos\omega_d t + C_2\sin\omega_d t) \tag{4.24a}$$

or

$$\phi = e^{-vt}A\sin(\omega_d t - \delta) \tag{4.24b}$$

where

$$\omega_d = \sqrt{\omega_\phi^2 - v^2} \tag{4.24c}$$

Let us now see how the damping of rolling motion affects the magnitude of the period. The damped rolling period is

$$T_d = \frac{2\pi}{\omega_d} = \frac{2\pi}{\sqrt{\omega_\phi^2 - v^2}} = T_\phi\frac{1}{\sqrt{1-(v/\omega_\phi)^2}} \tag{4.26}$$

where T_ϕ is the period without damping, as given by (4.25). It follows then that the period increases with damping, but this increase is almost negligible since damping is very small in rolling motions.

Example 4.20A

A certain ship 450 ft long has a displacement of 12,500 tons and a radius of gyration about the longitudinal axis of 30.8 ft. The transverse metacentric height is 5.79 ft. Find the natural and the damped period of roll if the coefficient for the roll damping moment is assumed to be 32,000 ft-ton-sec and the added mass to be 20% of the actual mass of the ship.

Solution:

From (4.25) the natural circular frequency is

$$\omega_\phi = \sqrt{\frac{\Delta \overline{GM}_T}{I'_{xx}}}$$

where

$$I'_{xx} = \frac{\Delta'}{g} k_{xx}^2 = \frac{1.2\Delta}{g} k_{xx}^2$$

Thus

$$\omega_\phi = \sqrt{\frac{\Delta \overline{GM}_T g}{1.2\Delta k_{xx}^2}} = 0.405 \text{ sec}^{-1}$$

from which the natural period is

$$T_\phi = \frac{2\pi}{\omega_\phi} = \frac{2\pi}{0.405} = 15.51 \text{ sec}$$

Also,

$$\nu = \frac{b}{2I'_{xx}} = 0.0362 \text{ sec}^{-1}$$

Hence, from (4.26) the damped roll period is,

$$T_d = 15.51 \frac{1}{\sqrt{1 - \left(\frac{0.0362}{0.405}\right)^2}} = 15.52 \text{ sec}$$

Example 4.20B

Given:

$\Delta = 20{,}000$ tons
$\overline{GM}_T = 4$ ft
$T_\phi = 20$ sec

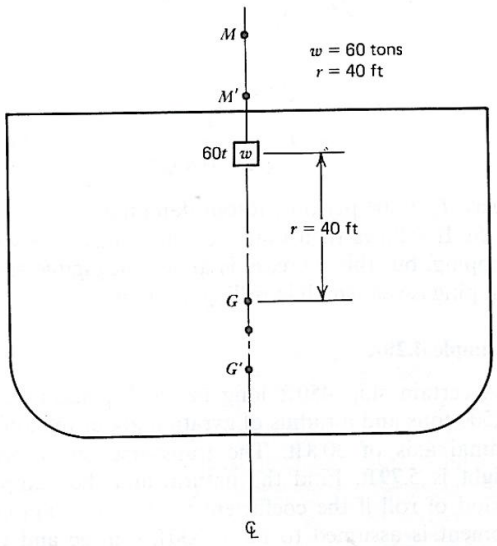


Figure 4.32 Change in gyradius due to weight removal.

Calculate T_ϕ when a weight of 60 tons is removed from a position 40 ft directly above the CG. It is assumed that $\overline{GM}_T$ remains unchanged and that the added mass moment of inertia for rolling is 20% of the mass moment of inertia of the ship. Refer to Fig. 4.32.

Solution:

On the assumption that no damping exists, (4.22b) is

$$I'_{xx} \frac{d^2\phi}{dt^2} + \Delta \overline{GM}_T \phi = 0$$

or

$$\frac{d^2\phi}{dt^2} + \frac{\Delta \overline{GM}_T}{I'_{xx}} \phi = 0$$

The natural frequency is obtained from

$$\omega_\phi^2 = \frac{\Delta \overline{GM}_T}{I'_{xx}}$$

and the rolling period is

$$T_\phi = \frac{2\pi}{\omega_\phi} = 2\pi \sqrt{\frac{I'_{xx}}{\Delta \overline{GM}_T}}$$

Hence $I'_{xx} = 810{,}000$, using the values for Δ and $\overline{GM}_T$ given. But $I'_{xx} = 1.20 I_{xx}$ since the added moment of inertia is 20% of the ship's moment of inertia. Thus

$$I_{xx} = 675{,}000 \text{ ton-sec}^2\text{-ft}$$

The new I_{xx} about the original CG of the ship is

$$I_{xx} = I_{xx} - m r_{xx}^2$$
$$= 675{,}000 - \frac{60}{32.2} \times (40)^2$$
$$= 675{,}000 - 2981 = 672{,}019 \text{ ton mass-sec}^2\text{-ft}$$

where

$$m = \frac{w}{g} = \frac{60}{32.2}$$

and

$$r_{xx} = r = 40 \text{ ft}$$

Furthermore,

$$\overline{CG}' = \frac{w \times r}{\Delta - w} = \frac{60 \times 40}{19{,}940} = 0.12 \text{ ft}$$

and

$$\text{New } I_{xx} \text{ about the new CG} = 672{,}019 - \frac{19{,}940}{32.2} \times (0.12)^2$$
$$= 672{,}010 \text{ ton mass-ft-sec}^2$$

TABLE 4.15 TYPICAL ROLLING PERIODS

Type of ships	T_ϕ [sec]
Passenger	20 –25
Cargo-Passenger	10.5–14.5
Cargo	9 –13
Tanker	9 –10
Fishing boat	5.5– 7.0
Whale boat	9 –11.5
Battleship	14.5–17.0
Cruiser	12.0–13.0
Destroyer	9 – 9.5
Torpedo boat	7 – 7.5

while

New I'_{xx} = 1.20 × (new I_{xx}) = 806,412 ton mass-sec^2-ft

and the new period is

$$T_\phi = 2\pi\sqrt{\frac{I'_{xx_{\text{new}}}}{\Delta_{\text{new}} \times \overline{GM}_T}} = 2\pi\sqrt{\frac{806{,}412}{19{,}940 \times 4}}$$
$$= 19.98 \text{ sec}$$

Typical rolling periods for various types of marine vehicles are given in Table 4.15.

Example 4.21

A ship having a displacement of 10,000 tons rolls with a period of 10 sec and has a metacentric height (transverse) of 4 ft. Its sister ship has a displacement and a metacentric height of 12,000 tons and 4.25 ft, respectively. The weight distribution in both cases is similar in all respects. (The added mass for rolling is 16% of the ship mass.)

a. Calculate the period of the sister ship without added mass.

b. Calculate the period of the sister ship with added mass.

Solution:

a. $T_1 = \lambda^{1/2}T$

$$\frac{\Delta_1}{\Delta} = \frac{12{,}000 \text{ tons}}{10{,}000 \text{ tons}} = \lambda^3 = \frac{6}{5}$$

Therefore

$$\lambda = 1.062$$

or

$$\lambda^{1/2} = 1.031$$

Then

$$T_1 = 1.031 \times 10$$

or

$$= 10.31 \text{ sec}$$

b. $T_1 = \lambda^{1/2}T$

$$\frac{\Delta_1}{\Delta} = \frac{1.16 \times 12{,}000}{1.16 \times 10{,}000} = \frac{6}{5} = \lambda^3$$

Therefore

$$\lambda = 1.062$$

$$\lambda^{1/2} = 1.031$$

Thus

$$T_1 = 10.31 \text{ sec}$$

It is obvious that consideration of the added mass does not change the relationship of periods between two sister ships.

Example 4.22

A ship has a radius of gyration (about the rolling axis) of 30.8 ft, a transverse metacentric height ($\overline{GM}$) of 4.84 ft, and a displacement of 15,000 tons. If the coefficient for the roll damping moment expression, b [where damping moment = $b(d\phi/dt)$], has a value of 32,000 ft-ton-sec while the ship is rolling in still water, determine the amplitude of roll after three complete oscillations if the ship was initially inclined at 7° (i.e., when $t = 0$, $\phi = 7°$ and $d\phi/dt = 0$). The added mass moment of inertia is 20% of that of the ship in this case of rolling.

Solution:

From (4.22b)

$$\frac{d^2\phi}{dt^2} + \frac{bg}{\Delta' k_{xx}^2}\frac{d\phi}{dt} + \frac{\Delta g \overline{GM}}{\Delta' k_{xx}^2}\phi = 0$$

where

$$\Delta' = \Delta + \delta\Delta = 1.2\Delta$$

The solution is

$$\phi = e^{\nu t}(C \cos \omega_d t + D \sin \omega_d t)$$

where

$$2\nu = \frac{b}{I'_{xx}} = \frac{32{,}000 \times 32.2}{1.2[15{,}000 \times (30.8)^2]} = 0.0603 \text{ sec}^{-1}$$

or

$$\nu = 0.0301 \text{ sec}^{-1}$$

and

$$\omega_\phi^2 = \frac{\Delta g GM_T}{\Delta' k_{xx}^2} = \frac{32.2 \times 4.84}{1.20 \times 949} = 0.137 \text{ rad/sec}^2$$

The damped rolling frequency is

$$\omega_d = \sqrt{\omega_\phi^2 - \nu^2} = \sqrt{0.137 - 0.0009} = 0.369 \text{ rad/sec}$$

At $t = 0$, $\phi = 7°$, so

$$7 = C$$

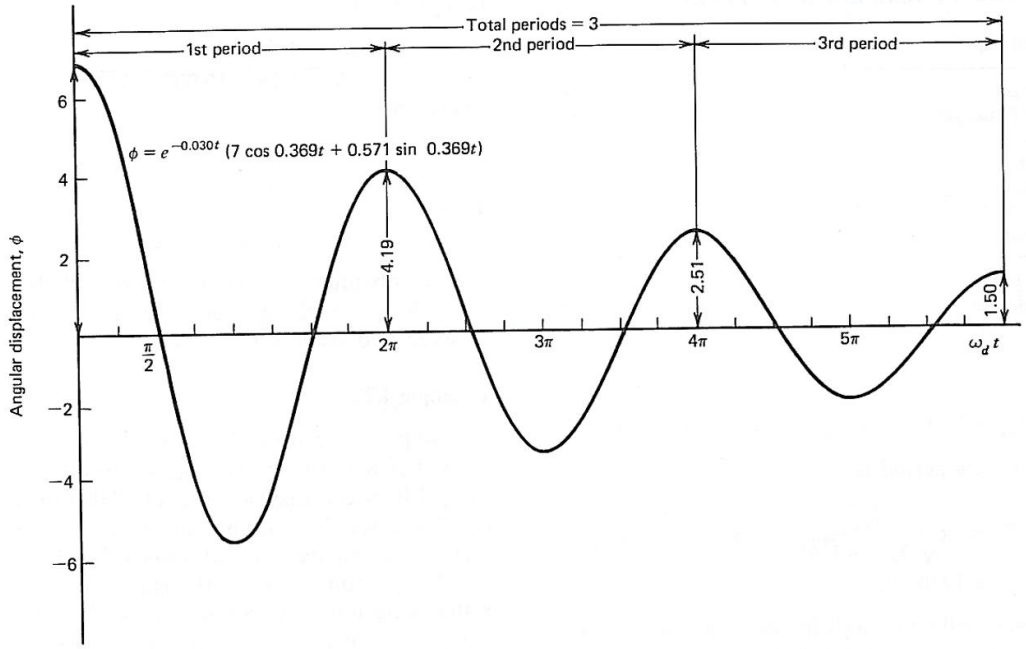


Figure 4.33 Damping effect on roll in calm water.

Again at $t = 0, d\phi/dt = 0$; therefore

$$0 = e^{-\nu t}(\omega_d C \sin \omega_d t + D\omega_d \cos \omega_d t) - \nu e^{-\nu t}(C \cos \omega_d t + D \sin \omega_d t)$$

or

$$0 = D\omega_d - C\nu$$

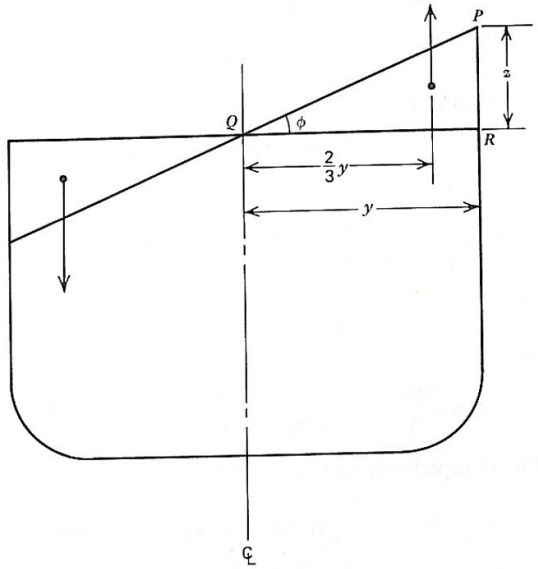


Figure 4.34 Roll exciting moment due to change in buoyant force.

Thus

$$D = \frac{C\nu}{\omega_d} = \frac{7 \times 0.0301}{0.369} = 0.571$$

and the solution of the equation is

$$\phi = e^{-0.0301t}(7 \cos 0.369t + 0.571 \sin 0.369t)$$

or

$$T_d = \frac{2\pi}{\omega_d} = \frac{6.28}{0.369} = 17.00 \text{ sec}$$

after 3 periods, that is, after 3×17 sec (or $\omega_d t = 0.369 \times 3 \times 17$ rad),

$$\phi = e^{-0.0301 \times (17 \times 3)}[7 \cos(0.369 \times 17 \times 3) + 0.571 \sin(0.369 \times 17.00 \times 3)]$$

or

$$\phi = e^{-1.54}(7 + 0) = 1.50°$$

Figure 4.33 shows the decay of rolling amplitude with time t.

Exciting Moment for Rolling

The exciting moment for rolling is due to the change in the buoyant force while the ship is in the wave. This moment is calculated by integrating for each ship section the difference in buoyancy of the triangles

drawn as in Fig. 4.34. The slope of the free surface is

$$\tan \phi = \frac{z}{y}$$

so that

$$z = y \times \text{slope}$$

Thus the area of PQR is $\frac{1}{2}y \times y \times$ slope, and the moment of buoyancy for this triangle is ρg (volume) $\times \frac{2}{3}y$. For both triangles the rolling moment is

$$\begin{aligned}\Delta M_\phi &= 2\rho g\,(\text{volume}) \times \tfrac{2}{3}y \\ &= 2\rho g(\tfrac{1}{2}y^2 \tan\phi\, dx)\tfrac{2}{3}y \\ &= \tfrac{2}{3}\rho g y^3 \frac{\partial \zeta}{\partial y}\, dx \\ &= [\tfrac{2}{3}\rho g y^3 k\zeta_a \sin\mu \cos(kx\cos\mu)\, dx]\sin\omega_e t\end{aligned}$$

Since

$$\zeta = \zeta_a \cos(kx\cos\mu - \omega_w t)$$

then

$$\begin{aligned}\frac{\partial \zeta}{\partial y} &= \text{wave slope} \\ &= \alpha'_M \cos(kx\cos\mu) \\ &= k\zeta_a \sin\mu \cos(kx\cos\mu)\end{aligned}$$

The *moment* is, then,

$$M_\phi = \left[\tfrac{2}{3}\rho g k\zeta_a \sin\mu \int_{-L/2}^{L/2} \cos(kx\cos\mu) y^3\, dx\right]\sin\omega_e t \tag{4.26a}$$

If we assume that

$$M_\phi = M_0 \sin(\omega_e t + \varepsilon_1)$$

the amplitude is

$$M_0 = \tfrac{2}{3}\rho g k\zeta_a \sin\mu \int_{-L/2}^{L/2} \cos(kx\cos\mu) y^3\, dx \tag{4.26b}$$

and the phase angle between exciting moment and wave elevation is

$$\varepsilon_1 = -\frac{\pi}{2} \tag{4.26c}$$

since

$$\sin\theta = \cos\left(\theta - \frac{\pi}{2}\right).$$

The nondimensional amplitude of the exciting moment is

$$f_0 = \frac{M_0}{\rho g k\zeta_a LB^2 T} = \tfrac{2}{3}\frac{\sin\mu}{LB^2T}\int_{-L/2}^{+L/2} \cos(kx\cos\mu) y^3\, dx \tag{4.26d}$$

For beam seas ($\mu = 90°$) the amplitude of the rolling moment is

$$M_0 = \rho g \nabla k\zeta_a \overline{GM}_T \tag{4.26e}$$

Since $\frac{2}{3}\int y^3\, dx$ is the transverse moment of inertia of the waterplane area,

$$M_0 = \rho g \nabla \alpha_M GM_T$$

or

$$M_\phi = \Delta\alpha_M \overline{GM}_T \sin\omega_e t = c\alpha_M \sin\omega_e t$$

where c is the restoring moment coefficient $= \Delta\overline{GM}_T$.

Note: For the sake of simplicity, the rolling moment M_ϕ for any angle of wave direction other than that for a beam sea is taken to be

$$M_\phi = c\alpha'_M \sin\omega_e t \tag{4.26g}$$

where

$$\alpha_M = \alpha'_M \sin\mu \tag{4.26h}$$

The rolling moment coefficient f_0 has been plotted in Fig. 4.35 against the wave direction for several waterplane area coefficients and L'_w/L ratios.

Example 4.23

Calculate the exciting moment for rolling of the ship for which the data are given in Example 4.1. Assume that the longitudinal center of buoyancy is at the midship section and also that $\mu = 120°$ (see Example 4.6).

Solution:

From the data in Example 4.1 Table 4.15A is prepared:

Therefore the integral becomes

$$\tfrac{1}{3} \times s \times \text{SUM} = \tfrac{1}{3} \times 4.8 \times 16.666 = 26.666$$

TABLE 4.15A

Station	x	y	y^3	$kx\cos\mu$	$\text{Cos}(kx\cos\mu)$	$y^3\cos(kx\cos\mu)$	Simpson's Multiplier	Product
0	9.6	0	0	−1.570	0	0	1	0
5	4.8	1.296	2.177	−0.785	0.707	1.539	4	6.156
10	0	1.296	2.177	0	1.000	2.177	2	4.354
15	−4.8	1.296	2.177	0.785	0.707	1.539	4	6.156
20	−9.6	0	0	1.570	0	0	1	0
							SUM	16.666

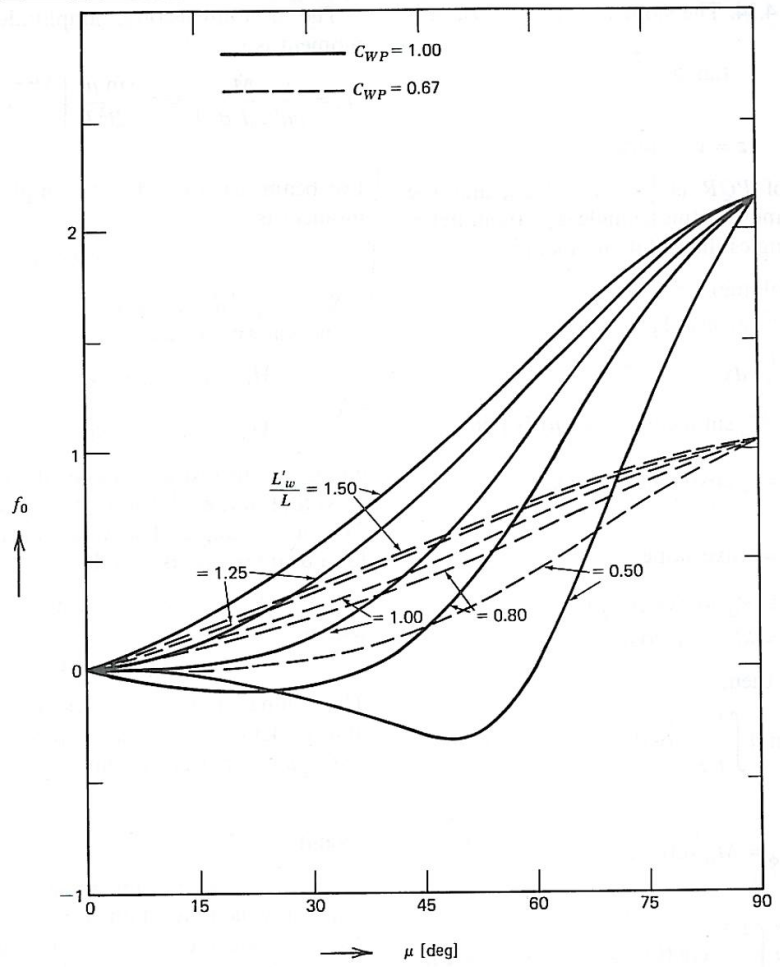


Figure 4.35 Coefficient for roll exciting moment [242].

The nondimensional exciting moment amplitude for rolling is

$$f_0 = \tfrac{2}{3}\frac{\sin\mu}{LB^2T} \times \text{integral}$$
$$= \tfrac{2}{3} \times \frac{0.866}{19.2 \times (2.592)^2 \times 1.144} \times 26.666$$
$$= 0.1043$$

and the exciting moment amplitude for rolling is

$$M_0 = \rho g k \zeta_a L B^2 T \cdot f_0$$
$$= 1.93 \times 32.2 \times 0.327 \times 0.2 \times 19.2 \times (2.592)^2 \times 1.144 \times 0.1043$$
$$= 62.6 \text{ ft-lb}$$

Rolling in a Regular Seaway

For rolling in a regular seaway the equation of motion becomes

$$I'_{xx}\frac{d^2\phi}{dt^2} + b\frac{d\phi}{dt} + \Delta\overline{GM}\phi = \Delta\overline{GM}\alpha'_M \sin\omega_e t$$

or

$$\frac{d^2\phi}{dt^2} + \frac{bg}{\Delta' k_{xx}^2}\frac{d\phi}{dt} + \frac{\Delta\overline{GM}_T}{\Delta' k_{xx}^2}\phi = \frac{\Delta\overline{GM}_T}{\Delta' k_{xx}^2}\alpha'_M \sin\omega_e t \tag{4.27}$$

For beam seas ω_e can be replaced by ω_w, which is the actual wave frequency, since $\omega_e = \omega_w$ for $\mu = 90°$. When a ship is found to be rolling heavily, the proper procedure is to alter course and/or speed. This will alter the encountering frequency (or encountering

period) and destroy synchronism, which is nearly always the cause of such rolling.

The general solution for this kind of differential equation is

$$\phi = e^{-\nu t}(C\cos\omega_d t + D\sin\omega_d t) + \left(\frac{\alpha'_M\omega_\phi^2}{\sqrt{(\omega_\phi^2-\omega_e^2)^2+4\nu^2\omega_e^2}}\right) \times \sin\left[\omega_e t - \tan^{-1}\left(\frac{2\nu\omega_e}{\omega_\phi^2-\omega_e^2}\right)\right] \tag{4.27a}$$

or

$$\phi = e^{-\nu t}(C\cos\omega_d t + D\sin\omega_d t) + \phi_a\sin(\omega_e t - \varepsilon_2) \tag{4.27b}$$

where

$$\omega_d = \sqrt{\omega_\phi^2 - \nu^2} \tag{4.28}$$

$$\phi_a = \frac{\alpha'_M\omega_\phi^2}{\sqrt{(\omega_\phi^2-\omega_e^2)^2+4\nu^2\omega_e^2}} \tag{4.29}$$

and

$$\varepsilon_2 = \tan^{-1}\left(\frac{2\nu\omega_e}{\omega_\phi^2-\omega_e^2}\right) \tag{4.30}$$

From (4.27a) or (4.27b) it can be seen that the rolling motion in a regular seaway is composed of two forms of oscillations—natural and forced. Natural oscillations have the frequency of the rolling of the vessel in still water, ω_d, and, as a result of the presence of the factor $e^{-\nu t}$, gradually die out with time. Forced oscillations are presented by the encountering frequency due to the exciting force. The amplitude ϕ_a and the phase angle ε_2 of the forced oscillations do not change with time and do not depend on the initial conditions of the motion. Therefore for the steady-state condition

$$\phi = \phi_a\sin(\omega_e t - \varepsilon_2) \tag{4.30a}$$

Now, comparing this equation with the exciting moment for rolling, we see that there is a phase difference between the motion and the exciting moment. This phase difference ε_2 is given by (4.30). Note that, when $\nu = 0$ (i.e., when there is no damping), the ship motion takes place at the same time as the exciting moment.

As in the cases of heaving and pitching, Λ and κ are now introduced and defined for the rolling motion. The tuning factor is

$$\Lambda = \frac{\omega_e}{\omega_\phi}$$

and the nondimensional damping coefficient is

$$\kappa = \frac{\nu}{\omega_\phi}$$

Note that for conventional ship forms the value of κ lies between 0.035 and 0.10. From (4.8a) the rolling amplitude is

$$\phi_a = \frac{\alpha'_M}{\sqrt{(1-\Lambda^2)^2+4\kappa^2\Lambda^2}} \tag{4.30b}$$

and the phase angle is obtained from (4.30):

$$\tan\varepsilon_2 = \frac{2\kappa\Lambda}{1-\Lambda^2} \tag{4.30c}$$

From (4.30b) the magnification factor μ_ϕ is

$$\mu_\phi = \frac{\phi_a}{\phi_{st}} = \frac{\phi_a}{\alpha'_M} = \frac{1}{\sqrt{(1-\Lambda^2)^2+4\kappa^2\Lambda^2}} \tag{4.31}$$

Since

$$\phi_{st} = \frac{F_0}{c} = \alpha'_M$$

μ_ϕ is also called the *magnification factor* and has a maximum value between 5 and 10. If there is no damping, ν and κ are both equal to zero, and

$$\mu_\phi = \frac{\phi_a}{\alpha'_M} = \frac{1}{1-\Lambda^2}$$

The magnification factor μ_ϕ, which is shown in Fig. 4.36 as a function of $\Lambda = \omega_e/\omega_\phi$, shows the following characteristics:

a. At $\Lambda = 0$, we get for all values of κ

$$\mu_\phi = \frac{\phi_a}{\alpha'_M} = 1$$

b. At $\Lambda = \infty$ (i.e., for extremely small periods of encounter), we get the magnification factor

$$\mu_\phi = \frac{\phi_a}{\alpha'_M} = 0$$

c. At $\Lambda = 1$ (i.e., at resonance), we have

$$\mu_\phi = \frac{\phi_a}{\alpha'_M} = \frac{1}{2\kappa} \tag{4.32}$$

d. To determine the location of the maximum magnification factor, let

$$y = \left(\frac{\phi_a}{\alpha'_M}\right)^2 \quad \text{and} \quad x = \Lambda^2$$

From (4.31)

$$y = \frac{1}{(1-x)^2+4\kappa^2 x}$$

For the maximum of y the first derivative of y is

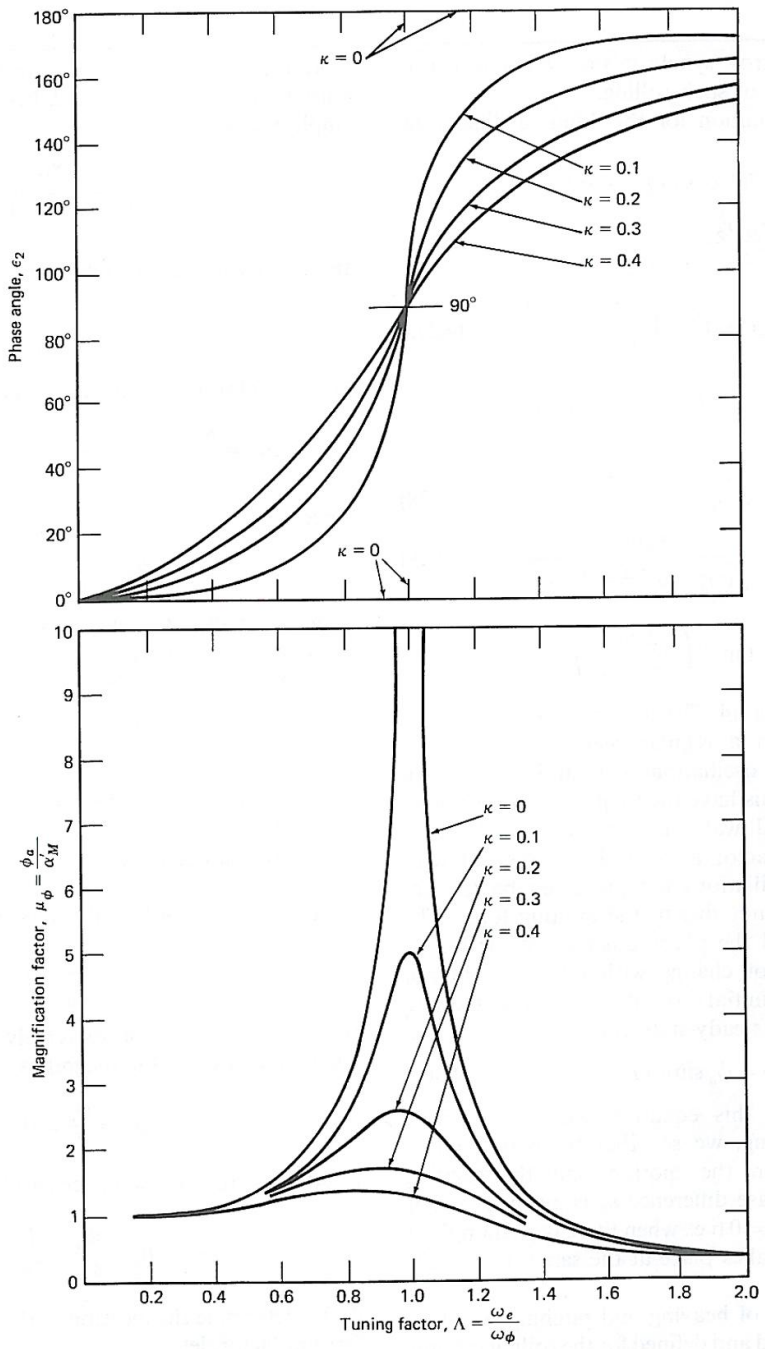


Figure 4.36 Magnification factors and phase angles between exciting moment and rolling motion.

set equal to zero, and we obtain

$$\frac{dy}{dx} = -\frac{-2(1-x)+4\kappa^2}{[(1-x)^2+4\kappa^2 x]^2} = 0$$

from which

$$-2(1-x)+4\kappa^2 = 0$$

and

$$x = 1-2\kappa^2$$

or

$$\Lambda = \sqrt{1-2\kappa^2} \tag{4.33}$$

Thus the maximum of the magnification factor does not coincide with the position of resonance (i.e., $\omega_e/\omega_\phi = 1$) but occurs to the left of it, depending on the magnitude of the nondimensional damping coefficient κ.

Knowing the position of the maximum magnification factor, we can determine its magnitude by substituting (4.33) into (4.31). Therefore

$$(\mu_\phi)_{\max} = \left(\frac{\phi_a}{\alpha'_M}\right)_{\max} = \frac{1}{\sqrt{[1-(1-2\kappa^2)]^2+4\kappa^2(1-2\kappa^2)}} = \frac{1}{2\kappa\sqrt{1-\kappa^2}} \tag{4.34}$$

Equations 4.33 and 4.34 show that a large amount of damping not only lowers the peak amplitude of the forced oscillation but also makes it occur at a lower value of Λ than in the case with less damping. When $k > 1/\sqrt{2}$ or 0.707, there are no peaks in Fig. 4.36.

Note: As the damping factor κ for rolling motion is usually small in comparison to unity, one may, in practice, consider that the location and magnitude of the maximum magnification factor coincide with those for the resonant region. Compare with (4.32).

Example 4.24

Given:

$T_\phi = 15$ sec
$V = 35$ knots
$L_w = 900$ ft

Determine the heading of the ship relative to the waves when the largest rolling would be expected

Solution;

The largest rolling motion occurs when synchronism takes place, namely, when

$$\Lambda = \frac{\omega_e}{\omega_\phi} \approx 1.0$$

that is, when

$$\omega_e = \omega_\phi$$

where

$$\omega_e = \omega_w\left(1-\frac{\omega_w}{g}V\cos\mu\right)$$

and μ is the heading angle relative to the waves. Thus

$$\omega_\phi = \frac{2\pi}{T_\phi} = \frac{2\pi}{15} = 0.419 \text{ rad}$$

Also

$$\omega_\phi = \omega_e = \omega_w - \frac{\omega_w^2}{g}V\cos\mu$$

Thus

$$\cos\mu = \frac{(\omega_w-\omega_\phi)g}{\omega_w^2 V}$$

For deep water waves

$$\omega_w = \sqrt{\frac{2\pi g}{L_w}} = \sqrt{\frac{2\pi \times 32.2}{900}} = 0.474 \text{ rad/sec}$$

and, since $V = 35 \times 1.689$ ft/sec,

$$\cos\mu = \frac{(0.474-0.419)\times 32.2}{(0.474)^2 \times 35 \times 1.689} = 0.133$$

or

$$\mu = 82.5^\circ \text{ or } -82.5^\circ$$

The rolling motion in a seaway can be drastically reduced by changing the ship's heading in the ranges of 0 to 45° and 135 to 180°. Therefore, as mentioned previously, if for any reason a ship rolls heavily in a seaway, the proper action is to change the course and/or speed of the ship. The encountering frequency is thereby altered, and the synchronism, which is normally the main reason for heavy rolling in a seaway, will be destroyed.

The equations given in this section are to be used for computation of the AMPLITUDES and PHASES of rolling for vessels oriented at any angle to the direction of wave travel, provided that the amplitudes of the motions do not exceed the limits of linearity, that is, ϕ_a/α'_M remains the same for all values of

ζ_a, although giving the same value of

$$\alpha'_M\left(=\frac{2\pi\zeta_a}{L_w}\right)$$

The phase angle ε_2 depends on the damping factor κ as well as on the frequency ratio (or tuning factor) Λ, as is shown in Fig. 4.36. It is interesting to note that for $\Lambda = 1$ the phase angle is 90° regardless of the damping factor, and for small values of κ it varies very rapidly in the neighborhood of $\Lambda = 1$. The figure also shows that for small values of Λ the displacement ϕ is nearly in phase with the exciting moment, but as the frequency of forced oscillation increases so also does the phase angle ε_2. For very high frequencies (i.e., as $\Lambda \to \infty$) ε_2 approaches 180° regardless of the amount of damping.

Example 4.25

A certain ship encountered two trains of regular waves of wavelengths 300 and 600 ft, respectively, during its voyage in a beam sea. However, if the maximum wave slopes in both cases were 5°, what were the amplitudes of rolling motion on those two occasions if the natural period of rolling of the ship is known to be 15 sec?. Consider the motion to be both undamped and forced.

Solution:

For the steady-state condition the rolling motion is obtained from (4.30a),

$$\phi = \phi_a(\sin \omega_e t - \varepsilon_2)$$

where ϕ_a is the amplitude of rolling motion. From (4.30b)

$$\phi_a = \alpha'_M \frac{1}{1-\Lambda^2}$$

assuming that there is no damping. For the beam sea condition (i.e., $\mu = 90°$)

$$\omega_e = \omega_w$$

Also

$$\alpha'_M = \alpha_M$$

a. For 300 ft length, deep water waves have a period of

$$T_w = \sqrt{\frac{2\pi L_w}{g}} = \sqrt{\frac{6.28 \times 300}{32.2}} = 7.65 \text{ sec}$$

so that

$$\omega_w = \frac{2\pi}{T_w} = \frac{6.28}{7.65} = 0.821 \text{ rad/sec}$$

and

$$\omega_\phi = \frac{2\pi}{T_\phi} = \frac{6.28}{15} = 0.419 \text{ rad/sec}$$

$$\Lambda = \frac{\omega_w}{\omega_\phi} = 1.959$$

and

$$\phi_a = \alpha'_M \frac{1}{1-\Lambda^2} = 0.0874\left(\frac{1}{1-3.838}\right)$$

$$= -0.0308$$

or,

$$\phi_a = 0.0308 \text{ rad} = 1.77°$$

b. For 600 ft length of waves the wave period is

$$T_w = \sqrt{\frac{2\pi L_w}{g}} = \sqrt{\frac{6.28 \times 600}{32.2}} = 10.8 \text{ sec}$$

so that

$$\omega_w = \frac{2\pi}{T_w} = \frac{2\pi}{10.8} = 0.582 \text{ rad/sec}$$

$$\omega_\phi = \frac{2\pi}{T_\phi} = \frac{2\pi}{15} = 0.419 \text{ rad/sec}$$

and

$$\Lambda = \frac{\omega_w}{\omega_\phi} = 1.389$$

The rolling amplitude is

$$\phi_a = \alpha'_M \frac{1}{1-\Lambda^2} = 0.0874\left[\frac{1}{1-(1.389)^2}\right]$$

$$= 0.094 \text{ rad} = 5.4°$$

Example 4.26

A ship is heading at an angle of 150° relative to the wave direction at a speed of 20 knots.

a. Plot the magnification factors for rolling against the tuning factors for wave frequencies ω_w ranging from 0 to 2.00 at an interval of 0.10. The relevant dimensions of the ship are as follows:

$$L = 450 \text{ ft}$$
$$k_{xx} = 30.8 \text{ ft}$$
$$\overline{GM} = 5.79 \text{ ft}$$
$$\Delta = 12{,}500 \text{ tons}$$

The added mass is 20% of the mass of the ship, and the damping moment is $32{,}000(d\phi/dt)$ ft-ton.

b. Find the amplitude of the maximum rolling motion the ship will experience if the wave height is taken to be 60 ft.

Solution:

a. The natural rolling frequency is, from (4.25),

$$\omega_\phi = \sqrt{\frac{\Delta\overline{GM}_T}{I'_{xx}}} = \sqrt{\frac{\Delta\overline{GM}_T g}{1.2\Delta k_{xx}^2}} = \sqrt{\frac{5.79 \times 32.2}{1.2 \times (30.8)^2}}$$

The damping factors are

$$\nu = \frac{b}{2a} = \frac{b}{2I'_{xx}} = \frac{32{,}000}{2(\Delta'/g)k_{xx}^2} = \frac{32{,}000}{2[(1.2 \times 12{,}500)/32.2]}$$
$$= 0.0362 \text{ sec}^{-1}$$

and

$$\kappa = \frac{\nu}{\omega_\phi} = \frac{0.0362}{0.405} = 0.089$$

The magnification factor is

$$\mu_\phi = \frac{1}{\sqrt{(1-\Lambda^2)^2 + 4\kappa^2\Lambda^2}} = \frac{\phi_a}{\phi_{st}}$$

where the tuning factor is

$$\Lambda = \frac{\omega_e}{\omega_\phi} = \frac{\omega_e}{0.405}$$

The encountering frequency is

$$\omega_e = \omega_w\left(1 - \frac{\omega_w}{g}V\cos\mu\right)$$

With $V = 20$ knots $= 20 \times 1.689 = 33.78$ ft/sec and $\mu = 150°$, the numerical values are presented in Table 4.16. The magnification factor is shown in Fig. 4.37.

b. The rolling amplitude is given by the expression

$$\phi_a = \mu_\phi \phi_{st}$$

TABLE 4.16

ω_w [rad/sec] ①	$\eta = \frac{\omega_w V}{g}\cos\mu$ ②	$\omega_e = \omega_w(1-\eta)$ [rad/sec] ③	$\Lambda_\phi = \frac{\omega_e}{\omega_\phi}$ ④	$\mu_\phi = \frac{\phi_a}{\phi_{st}}$ ⑤
0.00	0	0	0	1.0
0.10	− 0.091	0.109	0.269	1.078
0.20	− 0.182	0.236	0.583	1.497
0.30	− 0.272	0.382	0.942	4.923
0.40	− 0.363	0.545	1.346	1.179
0.50	− 0.454	0.727	1.795	0.445
0.60	− 0.545	0.927	2.288	0.235
0.70	− 0.635	1.145	2.827	0.143
0.80	− 0.726	1.381	3.410	0.094
0.90	− 0.817	1.635	4.038	0.065
1.00	− 0.908	1.908	4.711	0.047
1.10	− 0.999	2.198	5.428	0.035
1.20	− 1.089	2.507	6.191	0.027
1.30	− 1.180	2.834	6.998	0.021
1.40	− 1.271	3.179	7.850	0.016
1.50	− 1.362	3.543	8.747	0.013
1.60	− 1.453	3.924	9.689	0.011
1.70	− 1.634	4.324	10.676	0.009
1.80	− 1.725	5.177	11.707	0.007
1.90	− 1.725	5.177	12.783	0.006
2.00	− 1.816	5.681	13.904	0.005

where μ_ϕ is the magnification factor for rolling, and ϕ_{st} is the static rolling amplitude, that is,

$$\phi_{st} = \frac{M_0}{c} = \frac{\Delta\overline{GM}_T\alpha'_M}{\Delta\overline{GM}_T} = \alpha'_M = \alpha_M \sin\mu$$
$$= 0.5\alpha_M$$

since

$$\sin\mu = \sin 150° = 0.5$$

Thus ϕ_a is maximum when the magnification factor μ_ϕ is maximum.

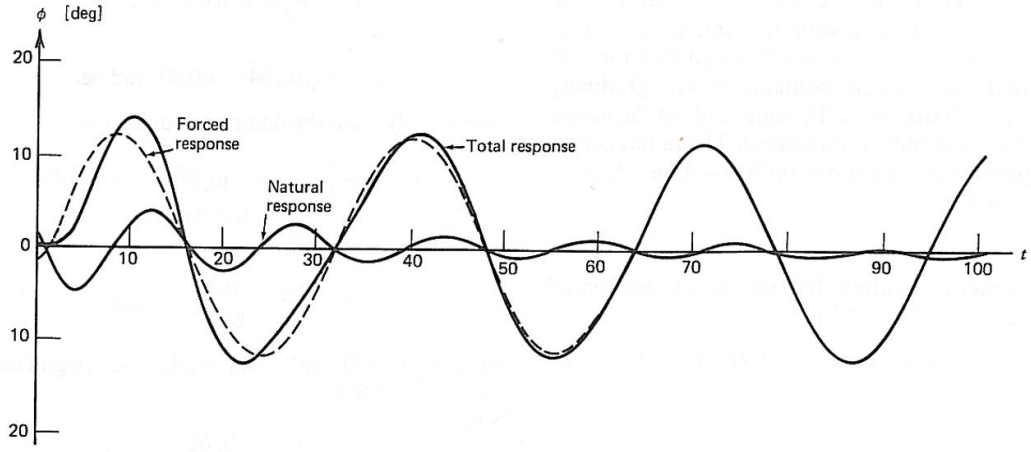


Figure 4.37 Ratio of roll and wave amplitude to tuning factor.

Now μ_ϕ is maximum at a position

$$\Lambda = \sqrt{1 - 2\kappa^2} = \sqrt{1 - 2 \times (0.089)^2}$$
$$= 0.992$$

From (4.31), when the value of Λ is 0.992, the value of μ_ϕ is 5.64.
Thus

$$(\phi_a)_{\max} = 5.64\phi_{st} = 5.64 \times 0.5\alpha_M$$
$$= 2.82\alpha_M$$

where α_M, the maximum wave slope, has to be determined for $\Lambda = 0.992$. By plotting ω_w against Λ, we have $\omega_w = 0.312$ for $\Lambda = 0.992$. Also, the wavelength is

$$L_w = \frac{2\pi g}{\omega_w^2} = \frac{2\pi \times 32.2}{(0.312)^2}$$
$$= 2078 \text{ ft}$$

and

$$\alpha_M = \frac{2\pi\zeta_a}{L_w} = \frac{2\pi \times 30}{2078}$$
$$= 0.091 \text{ rad}$$

so that

$$(\phi_a)_{\max} = 2.82 \times \alpha_M = 2.82 \times 0.091$$
$$= 0.257 \text{ rad } (14.73°)$$

Example 4.27

The equation of rolling motion of a ship is expressed as

$$\frac{d^2\phi}{dt^2} + 0.0724\frac{d\phi}{dt} + 0.164\phi = \alpha'_M\omega_\phi^2 \sin\omega_e t$$

If the maximum effective wave slope α'_M can be considered to be a constant, namely, $\pi/20$ rad, for a certain encountering frequency of 0.20 rad/sec, show that the natural oscillations will gradually disappear with time while the amplitude of the forced oscillations will remain unaffected. The initial conditions specified are as follows: both $\phi = 0$, and $d\phi/dt = 0$ when $t = 0$.

Solution:

The general solution for the given differential equation is given by (4.27b):

$$\phi = e^{-\nu t}(C_1 \cos\omega_d t + C_2 \sin\omega_d t) + \phi_a \sin(\omega_e t - \varepsilon_2)$$

where

$$\omega_d = \sqrt{\omega_\phi^2 - \nu^2}$$
$$\phi_a = \mu_\phi\alpha'_M$$

$$\mu_\phi = \frac{1}{\sqrt{(1 - \Lambda^2)^2 + 4\kappa^2\Lambda^2}}$$

and

$$\varepsilon_2 = \tan^{-1}\left(\frac{2\kappa\Lambda}{1 - \Lambda^2}\right)$$

From the initial conditions:

a. When $t = 0$, $\phi = 0$, that is, the ship is in an upright position when it is hit by the waves. Thus

$$\phi = 0 = C_1 - \phi_a \sin\varepsilon_2$$

or

$$C_1 = \phi_a \sin\varepsilon_2$$

b. At $t = 0$, $d\phi/dt = 0$. Differentiating (4.27), we have

$$\frac{d\phi}{dt} = -\nu e^{-\nu t}(C_1 \cos\omega_d t + C_2 \sin\omega_d t)$$
$$+ e^{-\nu t}(-\omega_d C_1 \sin\omega_d t + \omega_d C_2 \cos\omega_d t)$$
$$+ \phi_a\omega_e \cos(\omega_e t - \varepsilon_2)$$

Thus, at $t = 0$, $d\phi/dt = 0$, and

$$0 = -\nu(C_1) + (\omega_d C_2) + \phi_a\omega_e \cos(-\varepsilon_2)$$

or

$$C_2 = \frac{\nu C_1 - \phi_a\omega_e \cos\varepsilon_2}{\omega_d}$$

Using the value of C_1 previously obtained, we get

$$C_2 = \frac{\phi_a(\nu \sin\varepsilon_2 - \omega_e \cos\varepsilon_2}{\omega_d}$$

Using the given values of the coefficients of the equation of motion, we obtain for the damping and rolling frequencies

$$\nu = \frac{0.0724}{2} = 0.0362 \text{ sec}^{-1}$$

and

$$\omega_\phi = \sqrt{0.164} \quad = 0.405 \text{ rad/sec}$$

respectively; thus the damped frequency is

$$\omega_d = \sqrt{\omega_\phi^2 - \nu^2} = \sqrt{(0.405)^2 - (0.0362)^2}$$
$$= 0.403 \text{ rad/sec}$$

The tuning factor is

$$\Lambda = \frac{\omega_e}{\omega_\phi} = \frac{0.20}{0.405} = 0.494$$

since $\omega_e = 0.20$ and from (4.31), the magnification factor $\mu_\phi = 1.314$.
Since

$$\kappa = \frac{\nu}{\omega_\phi} = \frac{0.0362}{0.405} = 0.089$$

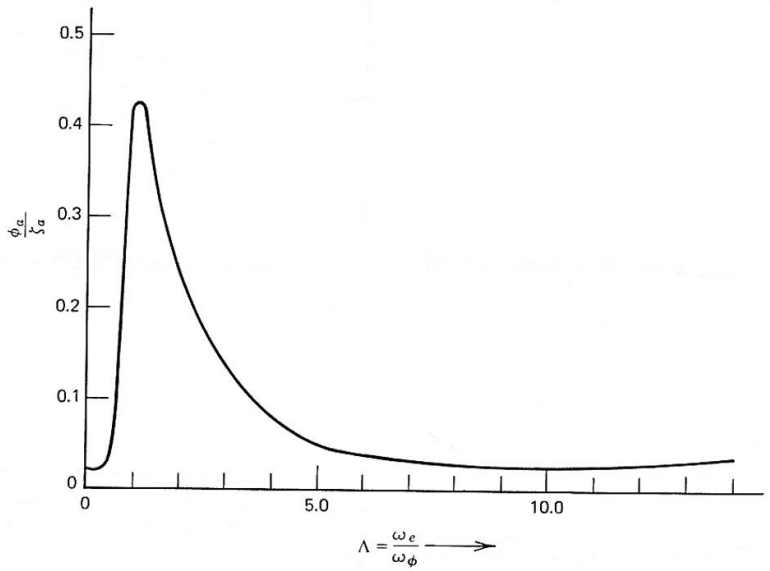


Figure 4.38 Natural, forced, and total response for rolling motion as functions of time.

the amplitude is

$$\phi_a = \mu_\phi \phi_{st} = \mu_\phi \alpha'_M = 1.314 \times \frac{\pi}{20}$$
$$= 0.206\,\text{rad (or } 11.83^\circ)$$

where

$$\phi_{st} = \frac{M_0}{c} = \alpha'_M$$

Furthermore, from (4.30),

$$\varepsilon_2 = \tan^{-1}\left(\frac{2\kappa\Lambda}{1-\Lambda^2}\right) = \tan^{-1}(0.11675)$$
$$= 0.116 \text{ rad (or } 6.659^\circ)$$

and therefore $C_1 = 0.024$ and

$$C_2 = \frac{\phi_a(v\sin\varepsilon_2 - \omega_e\cos\varepsilon_2)}{\omega_d}$$
$$= \frac{0.206(0.0362 \times 0.116 - 0.20 \times 0.993)}{0.403}$$
$$= -0.099$$

Now, using the values of v, C_1, C_2, ω_d, ϕ_a, and ε_2, we have the equation of rolling:

$$\phi = e^{-0.0362t}(0.024\cos 0.403t - 0.099\sin 0.403t)$$
$$+ 0.206\sin(0.200t - 0.116)$$

With, now, time $t = 0$, 10, 20, 100 sec, Table 4.17 has been prepared and Fig. 4.37 has been drawn.

Ratio of Response Amplitude to Wave Amplitude (ϕ_a/ζ_a)

In Fig. 4.36 the magnification factor $\mu(=\phi_a/\alpha'_M)$ has been plotted on a base of the tuning factor $\Lambda(=\omega_e/\omega_\phi)$. For a particular tuning factor the value of μ_ϕ is constant. Therefore ϕ_a is linearly proportional to α'_M.

The rolling amplitude ϕ_a can also be determined (per foot of wave amplitude) by means of the following expression:

$$\frac{\phi_a}{\zeta_a} = \frac{\phi_a}{\alpha'_M}\alpha'_M\frac{1}{\zeta_a}$$
$$= \mu_\phi \frac{2\pi\zeta_a}{L_w}\sin\mu\frac{1}{\zeta_a}$$

TABLE 4.17

t[sec]	$e^{-0.0362t}$	[rd]	Damped Rolling $e^{-0.0362t}(\ )$ [deg]	Forced Rolling 0.206 sin [deg]	ϕ[deg]
①	②	③	④ = ② × ③	⑤	⑥ = ④ + ⑤
0	1.000	0.024	1.37	− 1.37	0
10	0.696	0.062	2.46	11.23	13.69
20	0.485	− 0.102	− 2.83	− 7.98	− 10.81
30	0.338	0.067	1.29	− 4.59	− 3.30
40	0.235	0.018	0.24	− 11.80	− 12.04
50	0.164	− 0.083	− 0.84	− 5.23	− 6.07
60	0.114	0.095	0.61	− 7.44	− 6.83
70	0.079	− 0.030	− 0.14	11.43	11.29
80	0.055	− 0.056	− 0.18	− 2.07	− 2.25
90	0.038	0.101	0.23	− 9.71	− 9.48
100	0.027	− 0.072	− 0.11	10.15	10.04

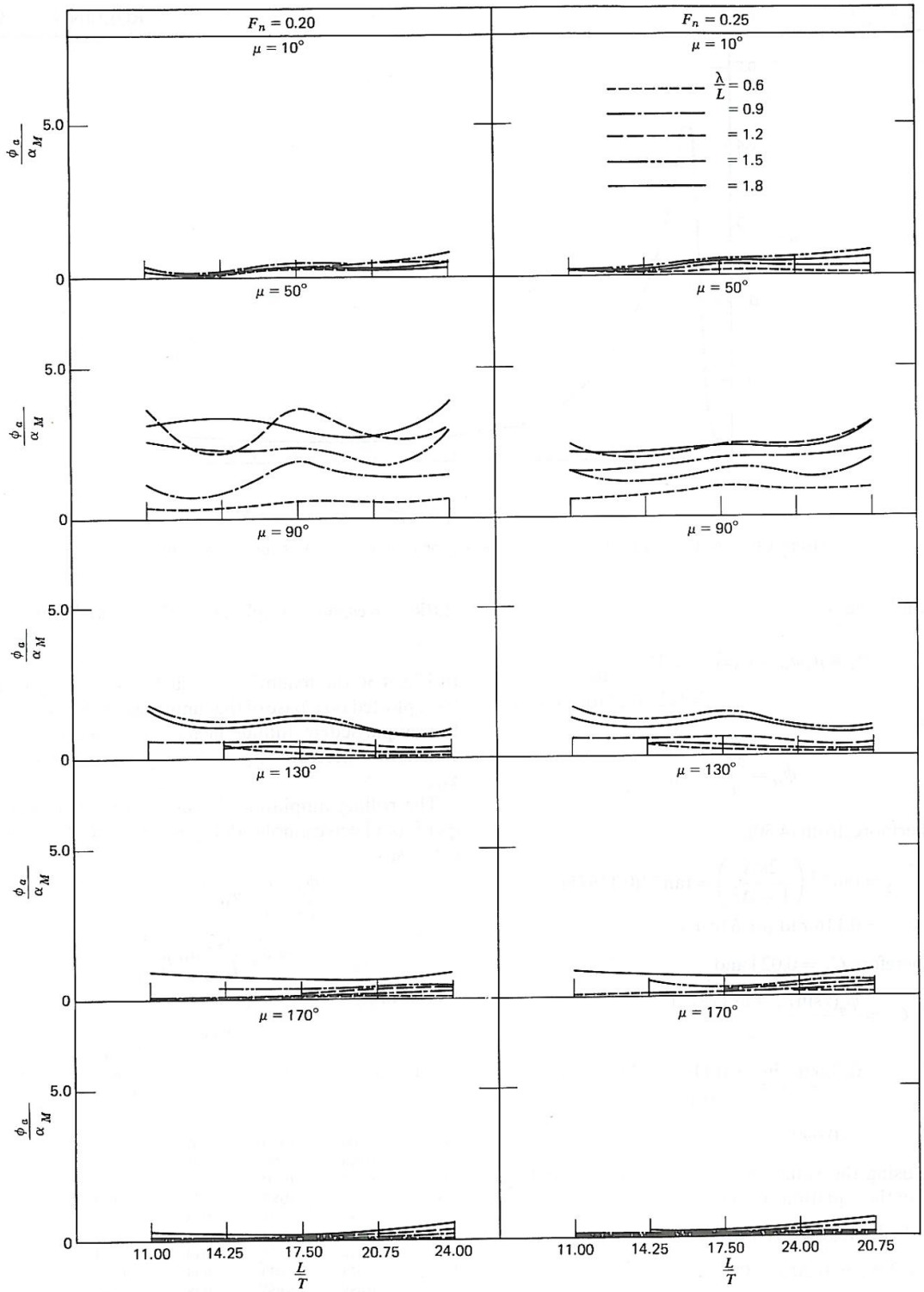


Figure 4.39 Roll amplitude as a function of length draft ration [226a].

TABLE 4.18

ω_e [rad/sec] ①	$\mu = \frac{\phi_a}{\alpha'_M}$ [—] ②	$\frac{\omega_w^2}{g}$ [ft^{-1}] ③	$\frac{\omega_w^2}{g}\sin 150°$ [ft^{-1}] ④	$\left(\frac{\omega_w^2}{g}\sin 150°\right)57.3$ [ft^{-1}] ⑤	$\frac{\phi_a}{\zeta_a}$ [ft^{-1}] ⑥
0.24	1.50	0.001	0.0005	0.029	0.044
0.38	4.96	0.003	0.0015	0.086	9.424
0.55	1.18	0.005	0.0025	0.143	0.169
0.73	0.45	0.008	0.0040	0.230	0.104
0.93	0.23	0.011	0.0055	0.316	0.073
1.14	0.14	0.015	0.0075	0.430	0.060
1.38	0.09	0.020	0.0100	0.573	0.052
1.64	0.07	0.026	0.0130	0.745	0.052
1.91	0.05	0.031	0.0155	0.888	0.045
2.20	0.04	0.038	0.0190	1.090	0.045
2.51	0.03	0.045	0.0225	1.290	0.039
2.83	0.02	0.053	0.0265	1.520	0.030
3.18	0.02	0.061	0.0305	1.750	0.035
3.54	0.01	0.070	0.0350	2.008	0.020
3.92	0.01	0.080	0.0400	2.295	0.023
4.32	0.01	0.090	0.0450	2.580	0.026
4.74	0.01	0.101	0.0505	2.895	0.029
5.18	0.01	0.112	0.0560	3.210	0.032
5.63	0.01	0.124	0.0620	3.560	0.036

where $\alpha'_M = \alpha_M \sin\mu$, and since

$\phi_a/\alpha'_M = \mu_\phi$. Furthermore,

$$\frac{\phi_a}{\zeta_a} = \mu_\phi \frac{2\pi}{L_w}\sin\mu$$

$$= \mu_\phi \frac{\omega_w^2}{g}\sin\mu \qquad \text{since } \frac{\omega_w^2}{g} = \frac{2\pi}{L_w}$$

$$= \mu_\phi \frac{\omega_w^2}{g}\,57.3\sin\mu$$

if ϕ_a is to be in degrees.

The above equation shows that, for a fixed wave frequency, ϕ_a is linearly proportional to wave amplitude ζ_a, since μ_ϕ and g in the equation do not change when the frequency is constant. However, this linear relationship between ϕ_a and ζ_a is, strictly speaking, not valid except for waves of small amplitudes.

Note: Instead of μ_ϕ (the amplitude of motion per unit wave slope), a quantity like ϕ_a/ζ_a (the amplitude of motion per foot of wave amplitude) can be drawn to a base of the tuning factor, as given in Fig. 4.38.

Again, by multiplying the abscissa Λ of Fig. 4.37 by ω_ϕ, a figure can be obtained in which the ordinate denotes the amplitude of motion per foot of wave amplitude on a base of frequency of encounter.

Example 4.28

Find the linear relationship of the rolling motion to the wave amplitude, at different encountering frequencies, for the ship described in Example 4.1, and plot the values to a base of the encountering frequencies.

Solution:

The relevant quantities are presented in Table 4.18.

Figure 4.39 shows the experimental results of nondimensional rolling motion ϕ_a/α_M as a function of L/T and the ship's heading angle relative to the wave travel. For both speeds, with Froude numbers of $F_n = 0.20$ and 0.25, it is noticed that the following quartering sea produces the largest rolling motion.

4.6 SHIP SPEED ZONES

In the preceding sections it was shown that the amplitude of motion of either heave, pitch, or roll in a seaway depends on the tuning factor Λ. Since the encountering frequency, as described in Section 3.9, depends on both the ship's speed and the ship's heading, a ship may have different values of the tuning factor, depending on the speed and direction of travel, which therefore have influence in the determination of its motion characteristics.

The relationship between the nondimensional ship speed, the direction of travel, and the tuning factor for the heaving motion can be derived as follows: [144]. From (3.19) we have

$$\omega_e = \frac{2\pi(V_w - V\cos\mu)}{L_w}$$

or

$$\omega_e = \omega_w - \frac{\omega_w^2}{g}V\cos\mu \tag{4.35}$$

so that

$$V\cos\mu = \frac{(\omega_w - \omega_e)g}{\omega_w^2}$$

and

$$\frac{V}{g^{1/2}L^{1/2}}\cos\mu = \frac{1}{\omega_w}\frac{g^{1/2}}{L^{1/2}} - \frac{\omega_e}{\omega_z}\frac{\omega_z}{\omega_w}\frac{g^{1/2}}{L^{1/2}} \tag{4.36}$$

or

$$F_n\cos\mu = \frac{1}{(2\pi)^{1/2}}\left(\frac{L_w}{L}\right)^{1/2} - \frac{\Lambda_z}{2\pi}\frac{\omega_z}{g^{1/2}}\frac{L_w}{L^{1/2}}\frac{L^{1/2}}{L^{1/2}}$$

$$= \frac{1}{(2\pi)^{1/2}}\left(\frac{L_w}{L}\right)^{1/2} - \frac{\Lambda_z}{2\pi}\left[\omega_z\left(\frac{L}{g}\right)^{1/2}\right]\frac{L_w}{L} \tag{4.37}$$

where the expression inside the brackets on the

right-hand side of (4.37), that is, $\omega_z(L/g)^{1/2}$, is termed the *nondimensional frequency parameter*. Similarly, for the pitching and rolling motions, similar expressions are derived, for example:

For the *pitching motion*

$$F_n \cos\mu = \frac{1}{(2\pi)^{1/2}}\left(\frac{L_w}{L}\right)^{1/2} - \frac{\Lambda_\theta}{2\pi}\left[\omega_\theta\left(\frac{L}{g}\right)^{1/2}\right]\frac{L_w}{L} \tag{4.38}$$

and for the *rolling motion*

$$F_n \cos\mu = \frac{1}{(2\pi)^{1/2}}\left(\frac{L_w}{L}\right)^{1/2} - \frac{\Lambda_\phi}{2\pi}\left[\omega_\phi\left(\frac{L}{g}\right)^{1/2}\right]\frac{L_w}{L} \tag{4.39}$$

As mentioned in Section 3.9, (4.35) describes three different sea conditions for consideration. These conditions are as follows [144]:

1. *Ahead seas* ($90° < \mu < 270°$; $V_w - V\cos\mu$ is large and positive). In this case the absolute value of the second term on the right-hand side of (4.37) must be greater than that of the first term.
2. *Overtaking seas* ($0° < \mu < 90°$ and $270° < \mu < 360°$; $V_w - V\cos\mu$ is positive). To achieve this condition the absolute value of the second term of the right-hand side of (4.37) must be smaller than that of the first term.
3. *Following seas* ($0° < \mu < 90°$ and $270° < \mu < 360$; $V_w - V\cos\mu$ is negative). In the following sea condition both the encountering frequency ω_e and the tuning factor Λ have the opposite sense (and sign) to those in the other two sea conditions. For following seas and second term on the right-hand side of (4.37) becomes positive and the ship speed is rather high. Note that, when $\omega_e = 0$, the relative positions of the ship and the wave remain the same, since both the ship and the wave then move at the same speed (i.e., $\Lambda = 0$).

One can see from the plot of the magnification factor to the base of the tuning factor in Fig. 4.36 that ship motions in waves are considerably affected by the following items:

a. Magnitude of the exciting force.
b. Zone of resonance.
c. Magnitude of damping.

Again, since the magnitude of the exciting force is such an influential consideration, it is important to study three different regions of ship operation in waves:

TABLE 4.19

Zone of Operation	Tuning Factor, Λ
Subcritical	< 0.75
Critical	1.00
Supercritical	> 1.20

Note: The tuning factor Λ may have either a positive or a negative value. If Λ is negative, the case is an important one of the following sea.

1. Subcritical zone.
2. Critical zone.
3. Supercritical zone.

Table 4.19 describes the three different zones of operation.

It is seen from the table that there are overlapping regions between subcritical and critical zones, as well as between critical and supercritical zones, where the motions could be more severe than in purely subcritical or supercritical conditions. However, it is obvious that moderate motions are to be expected at both subcritical and supercritical zones.

The following general conclusions are stated in Ref. 144 regarding the zones of operations.

In head sea cases, conventional ships up to a length of 1000 ft enter the critical zone of heaving and pitching motions when their speeds are high. Ships having higher values for natural frequency of heave and pitch can move faster before attaining the critical zone than ships with lower natural frequencies.

Conventional ships are always in the subcritical zone in astern seas, and so have relatively less severe motions in such seas. In following sea operations normal ships can reach the critical zone if they can attain speeds much higher than the normal maximum speeds.

It is also rather difficult for conventional ships to attain the supercritical zone of operation in head sea conditions.

On the other hand, at such high speeds in the supercritical zone of operation resonance may take place, and heavy motions are to be expected if the vessel meets some significant waves in following seas (see Fig. 4.40). Moreover, if the ship is required to reduce its speed, it will enter the critical zone and thus may experience the most severe motions.

Figure 4.40 shows that, if the nondimensional frequency parameter of pitch (or heave), $\omega_0\sqrt{L_0/g}$, was reduced to a value of 0.75, a 400 ft ship would always be operating in the supercritical zone, whatever the speed might be, in head seas, and at speeds up to

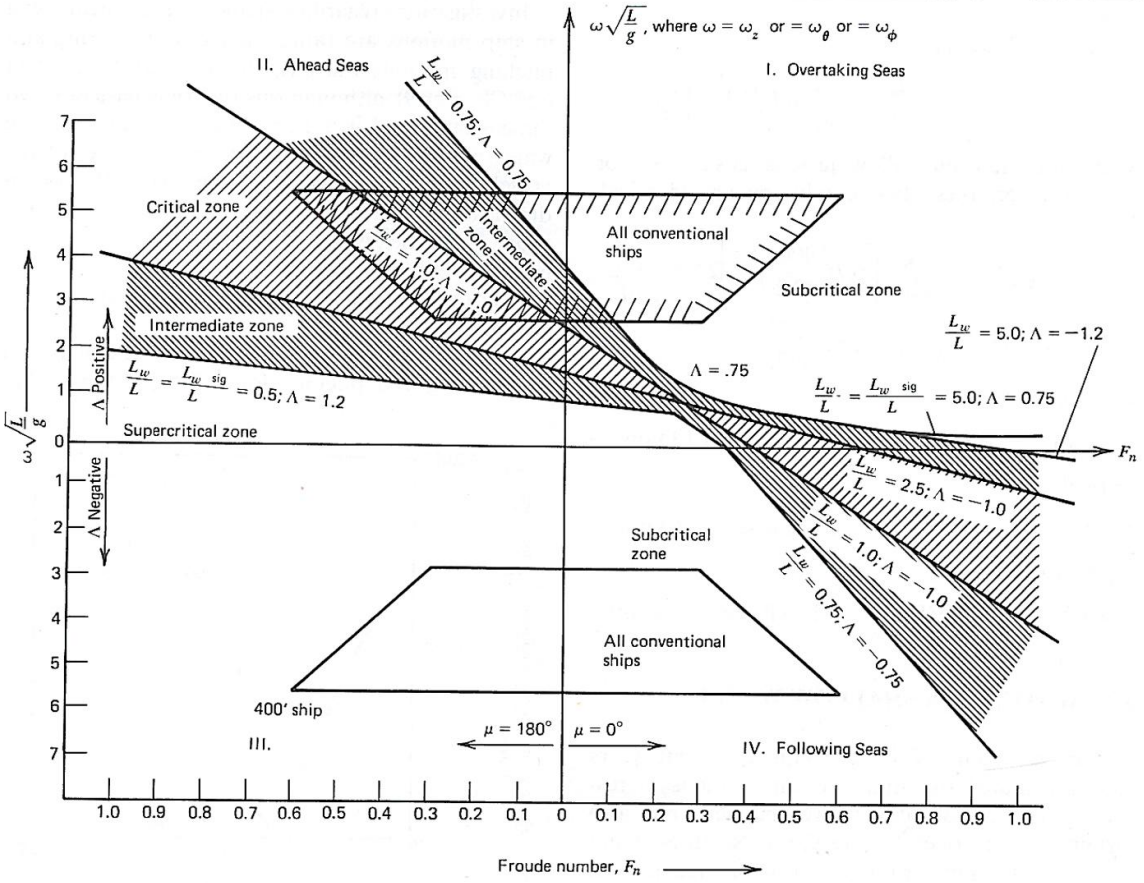


Figure 4.40 Subcritical, critical, and supercritical speed zones for a 400 ft ship [144].

12 knots ($F_n = 0.175$) in overtaking seas. It would not enter the critical zone in overtaking seas until a speed of 18.5 knots was reached ($F_n = 0.275$) and would leave the critical zone at a speed of 22 knots ($F_n = 0.325$).

With further increase in speed this ship would still not be able to reenter the subcritical zone. For speed between 22 and 35 knots ($F_n = 0.325$ to 0.515) the ship would operate in the intermediate zones: first in overtaking, and then in following, seas. At a still higher speed (above 35 knots) the ship would enter the critical zone in following seas and remain in this region for all practical limits of speed.

If, however, the nondimensional pitch or heave frequency parameter, $\omega_\theta\sqrt{L/g}$ or $\omega_z\sqrt{L/g}$, could be increased to 6.0 (rather too high for conventional vessels) for a 400 ft ship, it would be possible for the ship to operate in the subcritical zone at all speeds in overtaking seas and at speed up to 12 knots (i.e., $F_n = 0.18$) in head seas. Also, the vessel would not attain the critical zone in the head sea condition until a speed of 37 knots (i.e., $F_n = 0.55$) was reached.

However, neither value of the frequency parameter discussed above ($\omega_\theta\sqrt{L/g} = 0.75$ or 6.0) is possible for conventional ships unless they are drastically modified. High frequency parameters, in general, correspond to long, lean, fast vessels like destroyers; tugs, trawlers, and other short, slow ships have low frequency parameters.

Example 4.29

Given:

$$L = 400 \text{ ft}$$

$$\omega_\theta = 0.70$$

$$L_w/L = 2.5$$

Find the ship's speed for subcritical, critical, and supercritical operations in the head sea condition.

Solution:

From (4.38) we have

$$F_n \cos\mu = \frac{1}{\sqrt{2\pi}}\sqrt{\frac{L_w}{L}} - \frac{\Lambda_\theta}{2\pi}\left[\omega_\theta\left(\frac{L}{g}\right)^{1/2}\right]\frac{L_w}{L}$$

where, for head and following seas, $\cos\mu = +1$ or -1; however, these two conditions are identical. Thus

$$F_n = \frac{1}{\sqrt{6.28}}\sqrt{2.5} - \frac{\Lambda_\theta}{6.28}\left[0.7\left(\frac{400}{32.2}\right)^{1/2}\right]2.5 = \frac{V}{\sqrt{gL}}$$

$$= 0.63094 - \Lambda_\theta(0.98216) = \frac{V}{113.49}$$

Subcritical:

$\Lambda < 0.75$, $F_n < 0.106$, $V < 11.99$ ft/sec (7.1 knots)

Critical:

$\Lambda = 1.0$, $F_n = 0.351$, $V = 39.86$ ft/sec (23.6 knots)

Supercritical:

$\Lambda > 1.2$, $F_n > 0.548$, $V > 62.15$ ft/sec (36.7 knots)

4.7 MOTIONS IN SHALLOW WATER

The development of larger ships in recent years has necessitated the study of ship motions in restricted water. Not only many channels, but also certain areas in open seas (e.g., the North Sea), are considered shallow for the operation of huge tankers. To avoid grounding as well as to allow for proper maneuvering, it is important to study the hydrodynamic coefficients for the vertical as well as the horizontal motions in shallow water.

From full-scale operations it has been found that the effect of shallow water on vessel motions is felt when the depth of water is less than four times the draft of the marine vehicle, and the shallow water effect becomes significant when the ratio of water depth to vessel draft is two or less.

The effect of shallow water on ship motion is due to two factors:

1. The incident waves are affected because of the shallow water, and hence the exciting force due to waves in shallow water is different from that due to deep water waves.
2. The hydrodynamic coefficients themselves also differ because of the nearness of the bottom of the channel.

Investigations regarding shallow water phenomena in ship motions are rather sparse. For heaving and pitching motions the strip theory may be applied (see Chapter 9), although this theory is basically two dimensional, and it is necessary to assume that the water will flow entirely underneath the keel of the vessel. But for the shallow water case the three-dimensional effect becomes significant, since the water flows below the keel as well as around the ends. For the extreme case in which the ship is almost resting on the bottom, water flows only around the ship ends.

The transfer function for the wave excited load for heaving and pitching for a 200,000 ton tanker

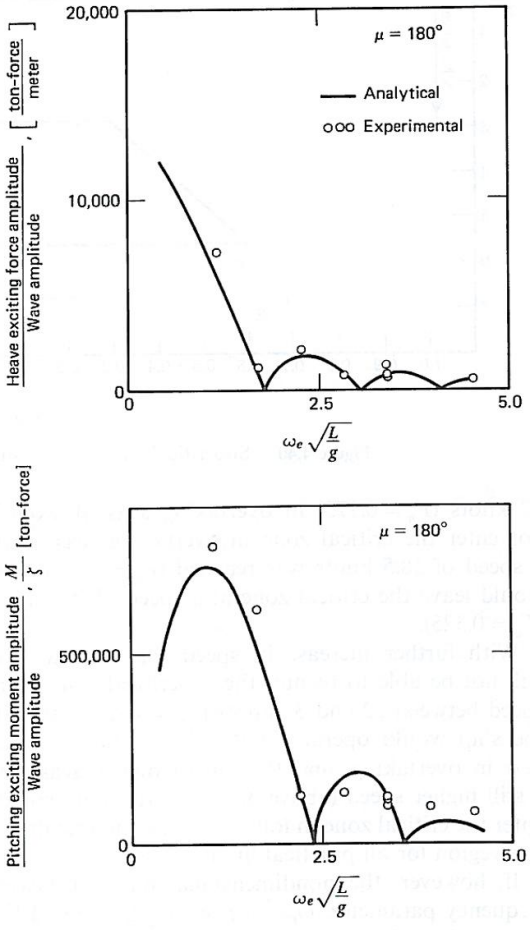


Figure 4.41 Heave exciting force amplitude/wave amplitude and pitch exciting moment amplitude/wave amplitude ratio [219].

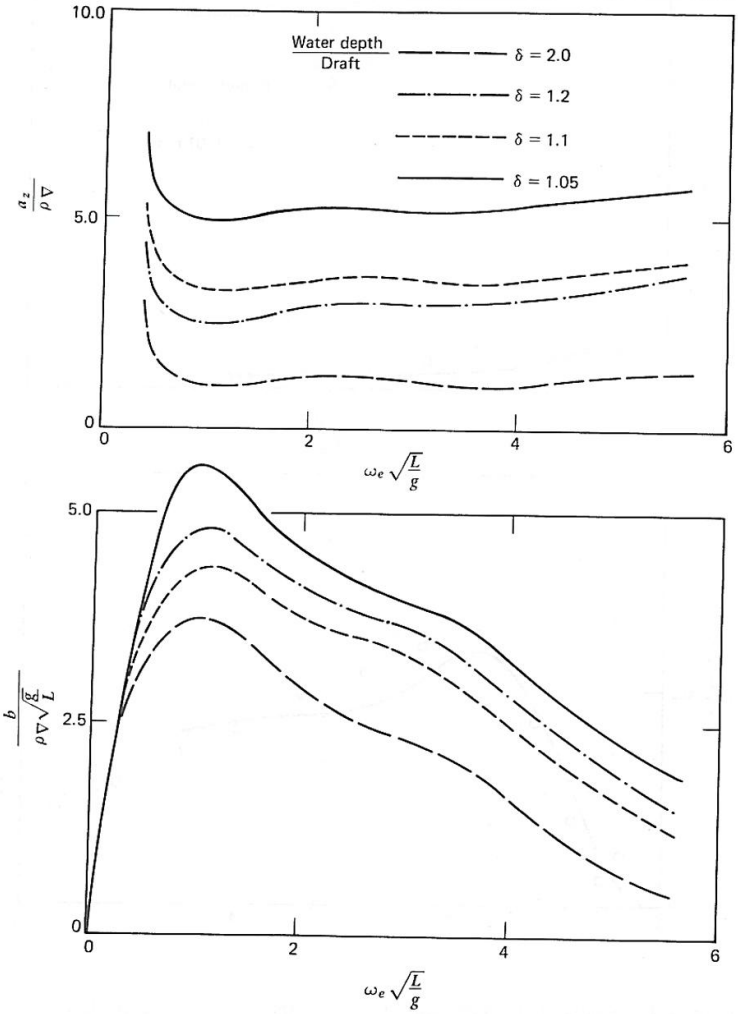


Figure 4.42 Added mass and damping in heave for different water depths [219].

in head seas is shown in Fig. 4.41. Both the exciting force for heaving and the exciting moment for pitching have been made nondimensional with the help of the following equations [see also (4.13) and (4.19f)]:

$$(f_0)_{\text{heaving}} = \frac{F_0}{\rho g \zeta_a L B}$$

$$(f_0)_{\text{pitching}} = \frac{M_0}{\frac{1}{2}\rho g \zeta_a L^2 B}$$

where $L = 310$ m and $B = 47.20$ m.

The nondimensional added mass or added mass moment of inertia and the damping coefficients for both heaving and pitching motions are presented in Figs. 4.42 and 4.43. It should be noted that the heave damping increases with water depth, and similar results should be expected also for the pitching motion. The claim is made in Ref. 219 that both heaving and pitching motions are also linearly proportional to wave amplitude in shallow water.

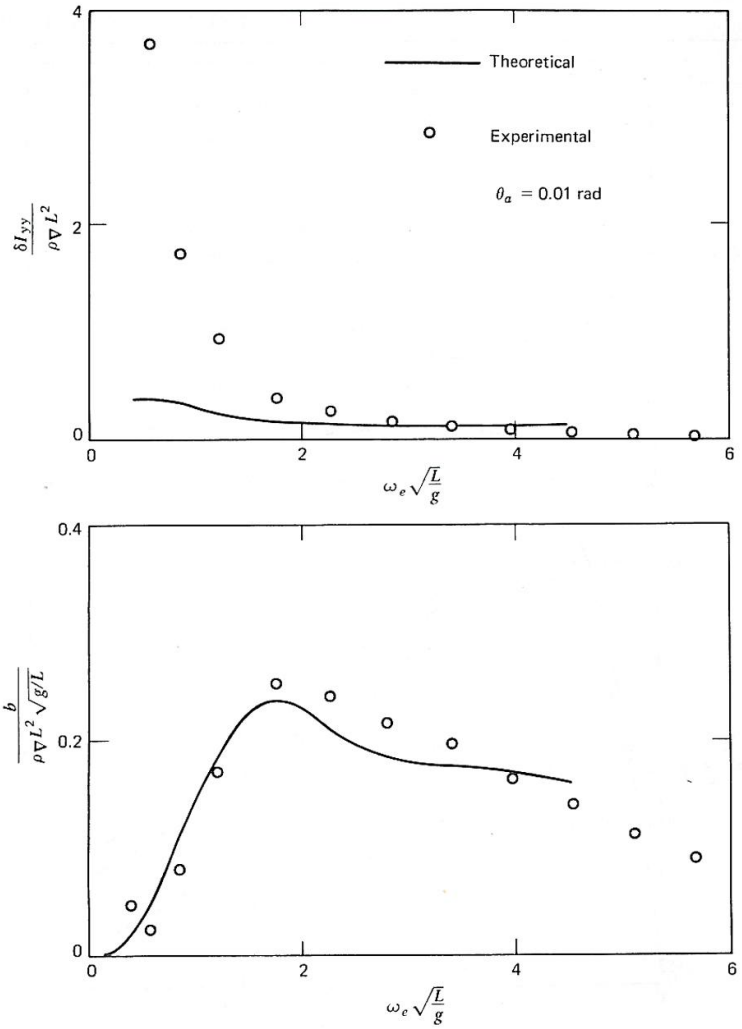


Figure 4.43 Added mass moment of inertia and damping in pitch (water depth/drift = 1.2) [219].

Chapter

Five

IRREGULAR SEAWAY

5.1 CLASSIFICATION OF SEAS

In the preceding chapters ship motions due to long-crested waves of regular sinusoidal form have been studied because these were all that could be handled by analytical methods. However, a treatment of ship motion purely for regular waves is, to a considerable extent, academic in nature, since an actual sea does not have a regularly corrugated surface, and the wave pattern is rather complex and extremely irregular.

Although an actual sea surface is very irregular, oceanographers have been able to predict by statistical means how often various wave heights may occur over a certain period of time for a particular sea surface of a given amount of energy. Since in an irregular seaway the sea surface constantly changes, a few new terms regarding wave height will be defined in this chapter in order to perform a statistical study of the seaway.

The irregular wave surface varies from time to time and place to place, depending on the wind speed or the *Beaufort number*, which is a means of estimating and reporting wind speeds. This system was devised in the early nineteenth century by Admiral Beaufort of the British Navy. The *sea state* is the condition of the surface of the seas (e.g., calm water, white caps). By observing the surface, an individual can derive a Beaufort number and hence a wind speed. Pictured in Fig. 5.1 are some of the various sea states and the wind speeds that accompany these states. These sea states are also described in Table 5.1. In the case of sinusoidal waves the amplitude, period, and so on remain the same, but for an irregular seaway these properties constantly change from time to time and place to place. For an irregular seaway the disturbance of the sea surface at any given point as a function of time is shown in Fig. 5.2*a*, where the following symbols are used:

$\tilde{\zeta}$ = wave elevation (i.e., instantaneous displacement of the sea surface from the position of rest or the reference line).

$\tilde{\zeta}_a$ = apparent wave amplitude (i.e., distance of the crest of the wave from the position of rest or the reference line)

$\tilde{h}_w$ = apparent wave height (i.e., vertical distance between a successive crest and a trough)

$\tilde{T}_z$ = apparent zero-crossing period (i.e., time elapsing between two successive upward crossings of zero in a record)

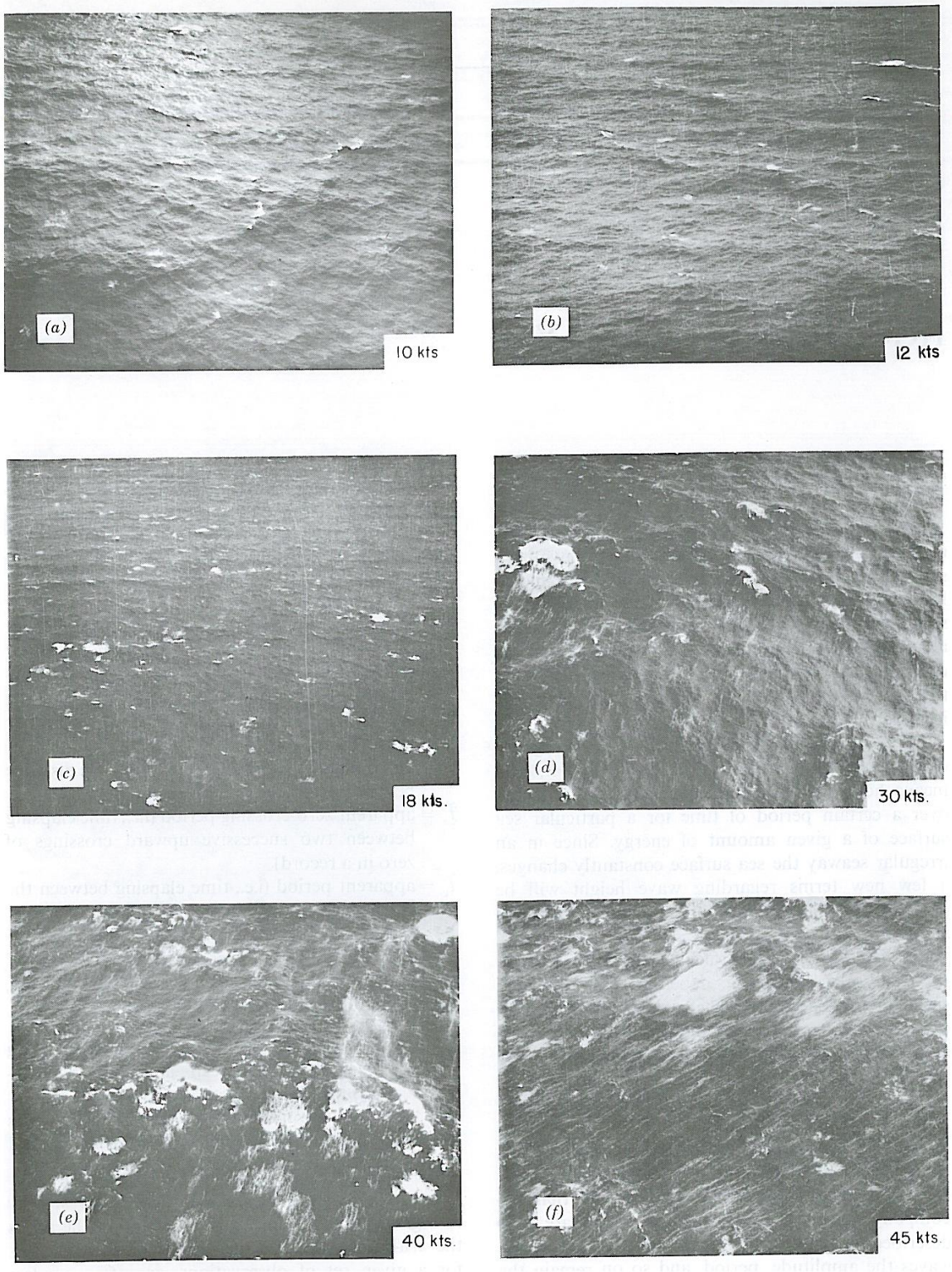
$\tilde{T}_c$ = apparent period (i.e., time elapsing between the occurrence of two successive crests)

The elevation of an irregular seaway is plotted to a base of x at a given instant of time in Fig. 5.2*b*, where:

$(\tilde{L}_w)_z$ = apparent wavelength of zero up-crossing (i.e., distance between adjacent zero up-crossings in the direction of advance)

$(\tilde{L}_w)_c$ = apparent wavelength between adjacent crests (i.e., horizontal distance between adjacent crests in the direction of advance)

The *average wave height* of an irregular seaway at a given time and in a given location of the sea is the arithmetic mean of the heights of all the waves for a given set of observations, except waves less than 1 ft in height. The *characteristic wave height*,


(a)
10 kts
(b)
12 kts
(c)
18 kts.
(d)
30 kts.
(e)
40 kts.
(f)
45 kts.

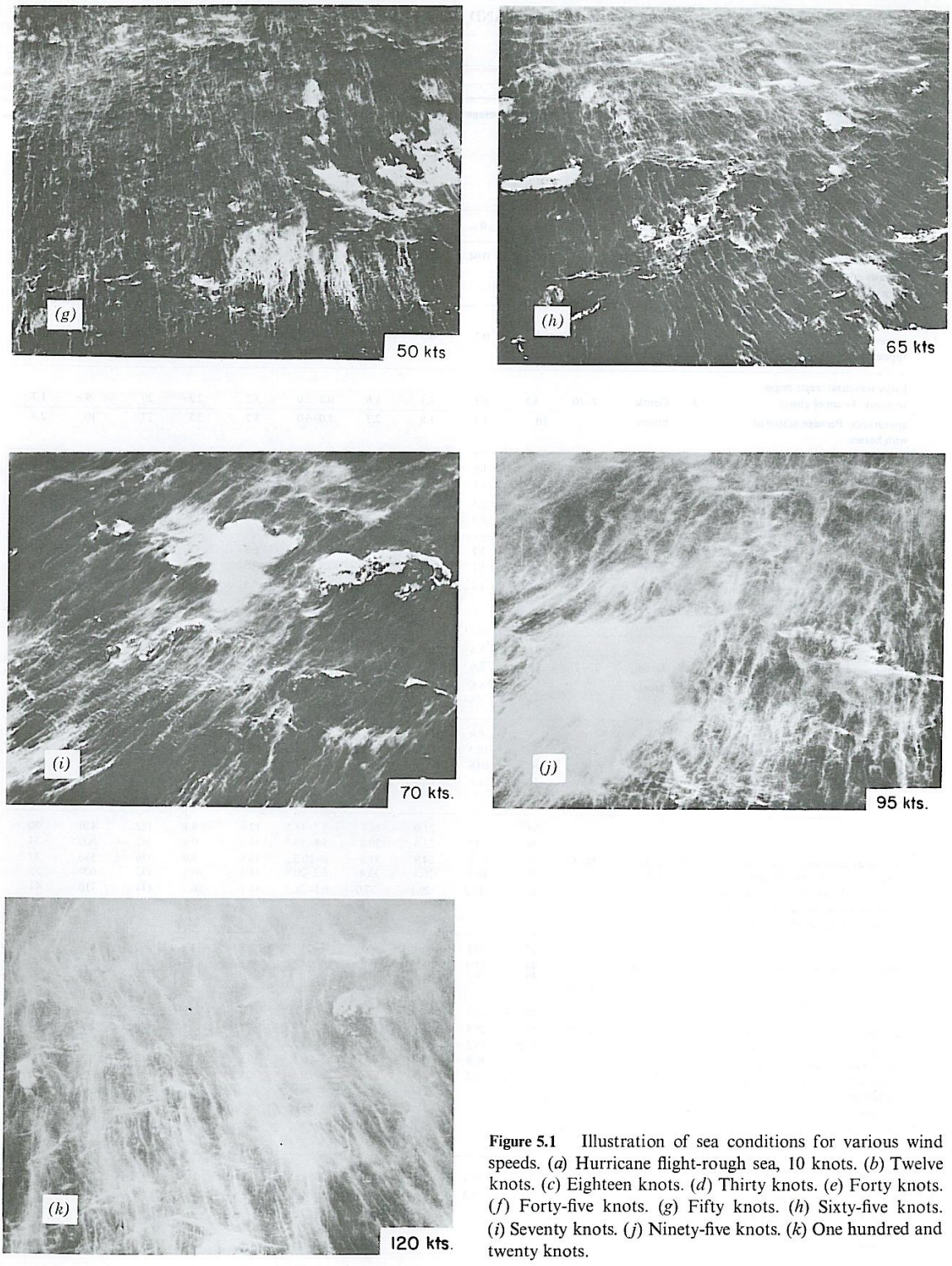


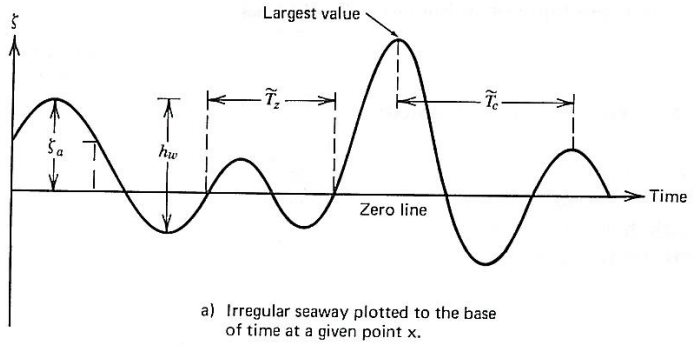
Figure 5.1 Illustration of sea conditions for various wind speeds. (*a*) Hurricane flight-rough sea, 10 knots. (*b*) Twelve knots. (*c*) Eighteen knots. (*d*) Thirty knots. (*e*) Forty knots. (*f*) Forty-five knots. (*g*) Fifty knots. (*h*) Sixty-five knots. (*i*) Seventy knots. (*j*) Ninety-five knots. (*k*) One hundred and twenty knots.

TABLE 5.1 DEFINITIONS OF SEA CONDITIONS: WAVE AND SEA FOR FULLY ARISEN SEA**

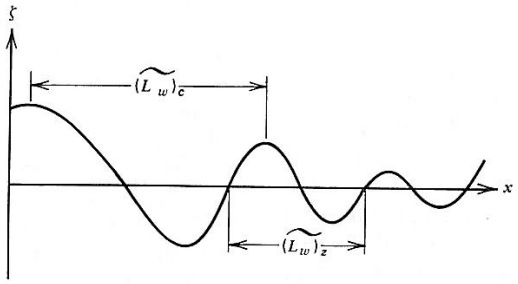
Sea — General		Wind				Sea								
Sea State	Description	(Beaufort) Wind force	Description	Range (knots)	Wind Velocity (knots)	Wave Height: Average	Wave Height: Significant	Wave Height: Average of One-Tenth Highest	Significant Range Periods [sec]	Periods of maximum Energy of Spectra $T_{max} = T_c$	Average Period $\bar{T}_z$	Average Wavelength $\bar{L}_w$ [ft unless otherwise indicated]	Minimum Fetch (nautical) miles)	Minimum Duration [hr unless otherwise indicated]
	Sea like a mirror	U	Calm	1	0	0	0	0	—	—	—	—	—	—
0	Ripples with the appearance of scales are formed, but without foam crests.	1	Light airs	1–3	2	0.04	0.01 0.01	0.09	1.2	0.75	0.5	10 in	5	18 min
1	Small wavelets; short but pronounced crests have a glossy appearance, but do not break.	2	Light breeze	4–6	5	0.3	0.5	0.6	0.4–2.8	1.9	1.3	6.7 ft	8	39 min
	Large wavelets; crests begin to break. Foam of glossy	3	Gentle	7–10	8.5	0.8	1.3	1.6	0.8–5.0	3.2	2.3	20	9.8	1.7
	appearance. Perhaps scattered with horses.		breeze		10	1.1	1.8	2.3	1.0–6.0	3.2	2.7	27	10	2.4
2					12	1.6	2.6	3.3	1.0–7.0	4.5	3.2	40	18	3.8
	Small waves, becoming larger;	4	Moderate		13.5	2.1	3.3	4.2	1.4–7.6	5.1	3.6	52	24	4.8
	fairly frequent white horses.		breeze	11–16	14	2.3	3.6	4.6	1.5–7.8	5.3	3.8	59	28	5.2
3					16	2.9	4.7	6.0	2.0–8.8	6.0	4.3	71	40	6.6
					18	3.7	5.9	7.5	2.5–10.0	6.8	4.8	90	55	8.3
4	Moderate waves, taking a more	5	Fresh	17–21	19	4.1	6.6	8.4	2.8–10.6	7.2	5.1	99	65	9.2
	pronounced long form; many white horses are formed (chance of some spray).		breeze		20	4.6	7.3	9.3	3.0–11.1	7.5	5.4	111	75	10
5					22	5.5	8.8	11.2	3.4–12.2	8.3	5.9	134	100	12
	Large waves begin to form;	6	Strong	22–27	24	6.6	10.5	13.3	3.7–13.5	9.0	6.4	160	130	14
	white crests are more extensive		breeze		24.5	6.8	10.9	13.8	3.8–13.6	9.2	6.6	164	140	15
6	everywhere (probably some spray).				26	7.7	12.3	15.6	4.0–14.5	9.8	7.0	188	180	17
					28	8.9	14.3	18.2	4.5–15.5	10.6	7.5	212	230	20
	Sea heaps up, and white foam from	7	Moderate	28–33	30	10.3	16.4	20.8	4.7–16.7	11.3	8.0	250	280	23
	breaking waves being to be blown		gale		30.5	10.6	16.9	21.5	4.8–17.0	11.5	8.2	258	290	24
7	in streaks along the direction of the wind (Spindrift begins to be seen).				32	11.6	18.6	23.6	5.0–17.5	12.1	8.6	285	340	27
					34	13.1	21.0	26.7	5.5–18.5	12.8	9.1	322	420	30
7					36	14.8	23.6	30.0	5.8–19.7	13.6	9.6	363	500	34
	Moderate high waves of greater	8	Fresh	34–40	37	15.6	24.9	31.6	6–20.5	13.9	9.9	376	530	37
	length; edges of crests break into		gale		38	16.4	26.3	33.4	6.2–20.8	14.3	10.2	392	600	38
	spindrift. The form is blown in well-marked streaks along the direction of the wind. Spray affects visibility.				40	18.2	29.1	37.0	6.5–21.7	15.1	10.7	444	710	42
8					42	20.1	32.1	40.8	7–23	15.8	11.3	492	830	47
	High waves. Dense streaks of foam	9	Strong		44	22.0	35.2	44.7	7–24.2	16.6	11.8	534	960	52
	along the direction of the wind. Sea		gale	41–37	46	24.1	38.5	48.9	7–25	17.3	12.3	590	1110	57
	begins to roll. Visibility affected.													
	Very high waves with long over-				40	26.2	41.9	53.2	7–5–26	18.1	12.9	650	1250	63
	hanging crests. The resulting foam	10	Whole*	48–55	50	28.4	45.5	57.8	7–5.27	18.8	13.4	700	1420	69
	is in great patches and is blown in		gale		51.5	30.2	48.3	61.3	8–28.2	19.4	13.8	736	1560	73
	dense white streaks along the direction of the wind. On the whole, the				52	30.8	49.2	6.25	8–28.5	19.6	13.9	750	1610	75
	surface of the sea takes on a white				54	33.2	53.1	67.4	8–29.5	20.4	14.5	810	1800	81
9	appearance. The rolling of the sea becomes heavy and shocklike. Visibility is affected.													
	Exceptionally high waves. Sea completely covered with long white patches of foam lying in direction of wind. Everywhere edges of wave crests are blown into froth. Visibility affected.	11	Storm*	56–63	56 59.5	35.7 40.3	57.1 64.4	72.5 81.8	8.5–31 10–32	21.1 22.4	15 15.9	910 985	2100 2500	88 101
	Air filled with foam and spray. Sea white with driving spray. Visibility very seriously affected.	12	Hurricane*	64–71	> 64	> 46.6	74.5	94.6	10–35	24.1	17.2	—	—	—

* For hurricane winds (and often whole gale and storm winds) required durations and reports are barely attained. Seas are therefore not fully arisen.

† Revised December 1964 by L. Moskowitz and W. Pierson. Used courtesy of The Navy Oceanographic Office.



a) Irregular seaway plotted to the base of time at a given point x.



b) Irregular seaway plotted to the base of x at a given instant of time.

Figure 5.2 (*a*) Irregular seaway plotsed to a base of time at a given point x. (*b*) Irregular seaway plotted to a base of x at a given instant of time.

or *significant wave height*, $(h_w)_{1/3}$, of an irregular seaway at any given time and in a given location in the sea is the arithmetic mean of the heights of the one-third highest waves for a given record. Again, waves less than 1 ft in height are ignored. Similarly, the average of the 10% highest waves, $(h_w)_{1/10}$, is the average of the heights of the one-tenth highest waves for the same observation, and the average of the 1% highest waves, $(h_w)_{1/100}$, is the average of the heights of the one-hundredth highest waves for the same wave record.

Example 5.1

The Wave Height Characteristics from Wave Records are obtained as shown in Table 5.2.

The average height, the significant height, the

TABLE 5.2

Wave Height	Number of Waves Having Heights of ①	Approximate Percent	Cumulative Number of Waves observed Reading from Top of 2	① × ②	① × ② for One-Third Highest Waves	① × ② for One-Tenth Highest Waves	① × ② for One-Hundredth Highest Waves
①	②	③	④	⑤	⑥	⑦	⑧
1	4	4	4	4			
2	40	39	44	80			
3	31	30	75	93	21(= 3 × 7)		
4	25	25	100	100	100	32(= 4 × 8)	
5	2	2	102	10	10	10	5(= 5 × 1)
SUM	102	100		287	131	42	5

average of the one-tenth and one hundredth highest waves can be determined as follows:

Solution:

From Table 5.2 the following data are obtained:

Average height = 287/102 = 2.81 ft

Significant height = 131/34 = 3.85 ft (considering $\frac{1}{3} \times 102$ or 34 waves)

Average of the one-tenth highest waves = 42/10 = 4.2 ft (consider $\frac{1}{10} \times 102$ or 10 waves)

Average of the one-hundred highest waves = 5/1 = 5 ft (considering $\frac{1}{100} \times 102$ or 1 wave only)

Height of the highest wave = at least 5 ft

Note: in calculating the average of the one-third highest waves of the total we need to consider only 102/3 (i.e., 34) highest waves. The results of the last two rows plus ⑦ waves from the third row of column ② will be considered in the evaluation of the column for the significant height, that is, for ⑥. Similarly, in finding the average of the one-tenth highest waves, only 102/10 (i.e., 10 out of 102 waves) should be considered for column ⑦. The value of the fifth row of column ② will give only ② waves, and therefore another eight waves from the fourth row of the same column are to be considered in the evaluation of ⑦.

Although the behavior of a ship in an irregular seaway should be related to the significant wave height of the irregular seaway in a statistical study, as is standard practice in oceanography, a more severe seaway, $(h_w)_{1/10}$, is often considered for the seakeeping design.

5.2 IRREGULARITY OF THE SEAWAY AND THE HISTOGRAM

The degree of irregularity of a seaway can be determined by the shape of a histogram, that is, a frequency function for the individual wave characteristics at a given time or in a given place. For the preparation of the histogram the wave record is grouped into equally spaced intervals of time, say 60 sec, and the mean wave elevations for all of these intervals are tabulated in increasing order. (See Fig. 5.3). Next, the values of ζ_a are divided into groups of equal elevations, and the number in each elevation group is divided by the total number in the sample. The percentage value in each group is then plotted as shown in the histogram in Fig. 5.4.

TABLE 5.3

Mean Elevation [ft]	Number of Groups	Percentage of Occurrence
1.5 to 2.5	26	13
2.5 to 3.5	22	11
3.5 to 4.5	20	10
− 1.5 to − 2.5	30	15
− 2.5 to − 3.5	24	12
etc.		

Assume that we have an actual record of wave elevations for 200 min, similar to Fig. 5.3. From the wave record there are 26 intervals with mean elevations of 1.5 to 2.5 ft, 22 intervals with mean elevations of 2.5 to 3.5 ft, 20 intervals with mean elevations of 3.5 to 4.5 ft, and so on.

There are 200 one minute intervals. Experience has shown that the histogram of the wave elevations takes the shape of a Gaussian or normal distribution, as shown by the dotted line in Fig. 5.4. Table 5.3 has been made for the histogram of the wave elevation.

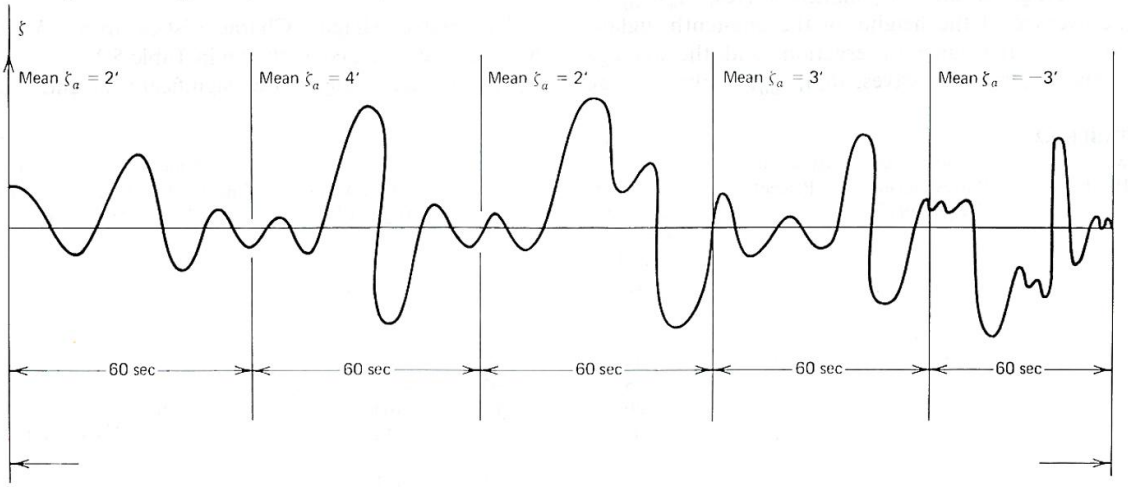


Figure 5.3 Record of wave elevations over a period of time.

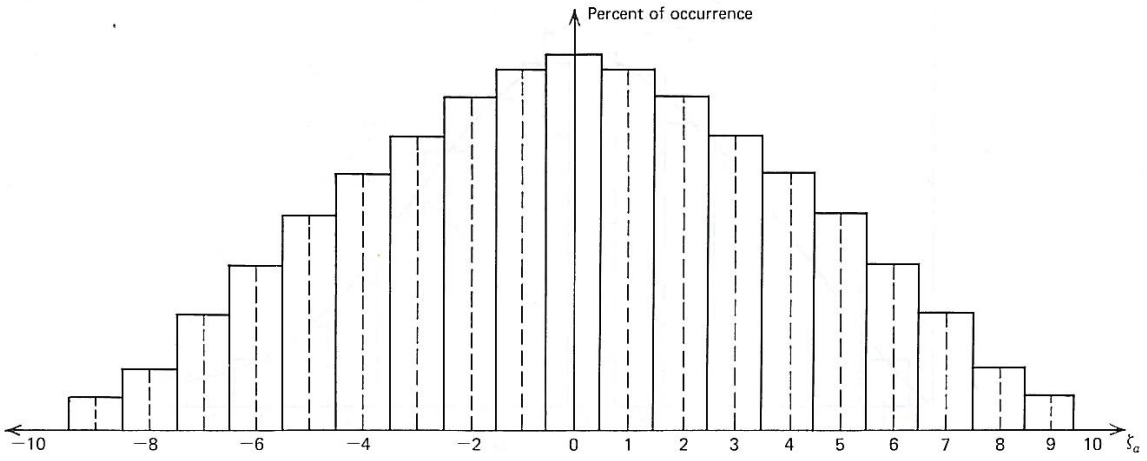


Figure 5.4 Frequency function of wave elevations.

Similarly, a histogram or frequency function of the *apparent wave periods* of an irregular seaway can be prepared from a table in which all the $\tilde{T}_z$ values from the wave record are tabulated in order of increasing period. The values of apparent period, $\tilde{T}_z$, are then grouped between 0.5 and 1.5 sec, 1.5 and 2.5 sec, and so on, showing the number of zero up-crossings in each group. By dividing the number of zero up-crossings for each group by the total number of zero up-crossings available from the record, the percentage is calculated and drawn as in Fig. 5.5*a*.

It has been found by taking innumerable wave records that a comparatively regular seaway will yield a high, narrow histogram, whereas an irregular seaway will produce a low, wider histogram. The location of the *center of gravity* of the histogram in relation to the y-axis gives the *average value* of the apparent wave period $\bar{\tilde{T}}$, that is,

$$T = \frac{\int p\tilde{T}_z \, d\tilde{T}_z}{\int p \, d\tilde{T}_z}$$

where p is the percentage of occurrence.

Another way of using the histogram is to plot the cumulative distribution diagram (see Fig. 5.5*b*) by taking the cumulative number of observations that fall below a series of increasing values of $\tilde{T}$, $\tilde{h}_w$, or $\tilde{\zeta}_a$, converting them to percentages, and drawing them against the base values. The significant value or the average value of the one-tenth or one-hundredth highest values can be readily obtained by using the cumulative distribution.

It has been found by experience that the theoretical Rayleigh curve fits the histograms for the wave height (double amplitude) very well. The Rayleigh distribution is expressed by the following equation:

$$p(H_i) = \frac{2H_i}{\bar{H}^2} e^{-H_i^2/\bar{H}^2} \tag{5.1}$$

where $p(H_i)$ is the probability density per foot or the percentage of times that any particular wave height H_i will appear, with $0 < p < 1$. If $p = 0$, H_i will never occur, whereas $p = 1$ means that H_i will occur with every experiment. Furthermore, $\bar{H}^2$ is the average of all the wave heights squared (i.e., the square of wave heights), defined by

$$\bar{H}^2 = \frac{\Sigma[(H_i)^2 \times f(H_i)]}{\Sigma[f(H_i)]}$$

where $f(H_i)$ is the number of occurrences of H_i.

This is very easily illustrated in Example 5.2.

Example 5.2

The following wave heights were recorded over a 24 hr period:

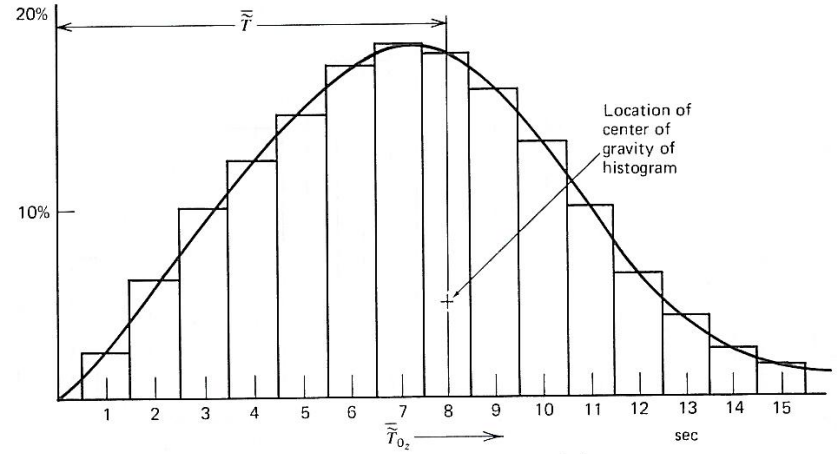
Height (ft)	0–5	5–10	10–15	15–20	20–25
Number of waves	5600	7200	1920	960	320

Plot the wave height histogram along with the theoretical Rayleigh distribution.

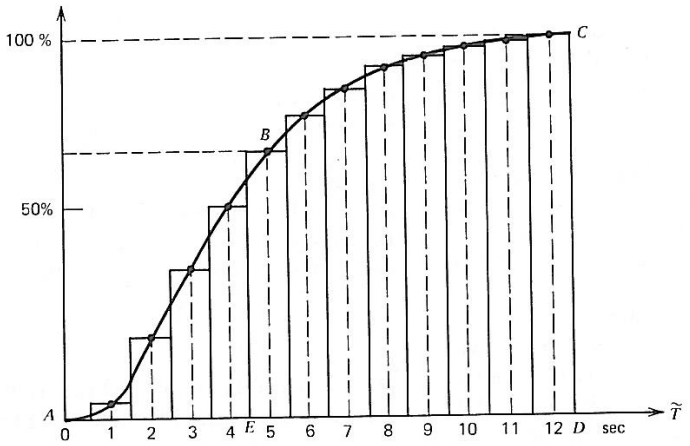
Solution:

The histogram data are shown in Table 5.4.

The values of column ⑤, obtained by dividing ④ by 5, which is the interval of wave height record, determine the ordinates for the wave histogram. Note, however, that, when the wave records are



a) Histogram of apparent wave periods



b) Cumulative distribution diagram

Figure 5.5 (*a*) Histogram of apparent wave periods. (*b*) Cumulative distribution diagram.

grouped into 1 ft intervals, column ⑤ will have the same values as ④.

A sample calculation for Rayleigh distribution is as follows. The mean square of wave heights is

$$\bar{H}^2 = \frac{\Sigma[(H_i)^2 \times f(H_i)]}{\Sigma[f(H_i)]}$$

$$= \frac{(2.5)^2 \times 5600 + (7.5)^2 \times 7200 + (12.5)^2 \times 1920 + (17.5)^2 \times 960 + (22.5)^2 \times 320}{16{,}000}$$

$$= 73.72 \text{ ft}^2$$

Thus the root mean square (rms) of wave heights $= \bar{H} = 8.59$ ft.

Now, according to the theoretical Rayleigh distri-

TABLE 5.4 HISTOGRAM DATA

Wave Record	Mean Height H_i	Occurrence	Percent Occurrence	Percent Occurrence per Foot of Wave Height (from record)
①	②	③	④ = ③/SUM × 100	⑤
0–5	2.5	5,600	35	7
5–10	7.5	7,200	45	9
10–15	12.5	1,920	12	2.4
15–20	17.5	960	6	1.2
20–25	22.5	320	2	0.4
	SUM	16,000		

TABLE 5.5

Wave Record	Mean Height, H_i [ft]	Rayleigh Ord. $p(H_i)$
0–5	2.5	0.0623
5–10	7.5	0.0949
10–15	12.5	0.0407
15–20	17.5	0.0075
20–25	22.5	0.0006

bution in (5.1), the probability for a wave height of 2.5 ft is

$$p\{2.5\} = \frac{2(2.5)}{73.72} e^{-(6.25/73.72)}$$
$$= 0.0623 \text{ or } 6.23\%$$

Similarly, the other probability values are calculated as shown in Table 5.5, and plotted in Fig. 5.6.

Note: The total area under the Rayleigh distribution curve should equal 1.0 (i.e., the total probability should be 1.0).

From 5.6 we have

Area from 2.5 to 22.5 $= \frac{1}{3}h\Sigma$ Product, using the Simpson rule for integration
$= \frac{1}{3}(5)(0.0623 \times 1 + 0.0949 \times 4 + 0.0407 \times 2 + 0.0075 \times 4 + 0.0006 \times 1)$
$= 0.92$

Area from 0 to 2.5 $= \frac{1}{12}(2.5)[5(0) + 8(0.0623) - 0.0966]$, using the 5, 8, -1 rule for integration
$= 0.08$

Total area $= 0.92 + 0.08 = 1.0$

which should be the probability for all waves.

From its definition one can see that $\bar{H}$, being the average over the entire area of the sea, should very closely represent the average energy of the sea, that is,

$$\frac{\rho g \bar{H}^2}{8} = \frac{\rho g}{8}(h_{w_1}^2 + h_{w_2}^2 + \ldots)$$
$$= \text{Energy} \tag{5.2}$$

Therefore, if the area under the histogram curve is known, one can directly relate $\bar{H}$ to the Rayleigh distribution formula and determine from this the probability of occurrence of different wave heights. Thus the probability that $h > H_i$ is

$$p\{h > H_i\} = 1 - \int_0^{H_i} \frac{2H_i}{\bar{H}^2} e^{-H_i^2/\bar{H}^2}$$
$$= e^{-H_i^2/\bar{H}^2}$$

For example, if $H_i = 10$ ft, then $p = e^{-(100/73.72)} = 0.258$. There is a probability of 0.258 that the wave height will be greater than H_i or 10 ft. In other words, out of a number of waves N, $Ne^{-H_i^2/\bar{H}^2}$ waves will be higher than H_i.

From such a formulation one can find the average wave height, or the average height of the one-third highest waves, or the average height of the one-tenth highest waves, and so on. For example, in the preceding example the average wave height is

$$(H)_0 = 0.89(\bar{H}^2)^{1/2} \tag{5.3a}$$

the average height of the one-third highest waves is

$$(H)_{1/3} = 1.41(\bar{H}^2)^{1/2} \tag{5.3b}$$

and the average height of the one-tenth highest waves is

$$(H)_{1/10} = 1.80(\bar{H}^2)^{1/2} \tag{5.3c}$$

These expressions are valid, however, only if the Rayleigh distribution is correct. Some corrections are required if the actual distribution differs from

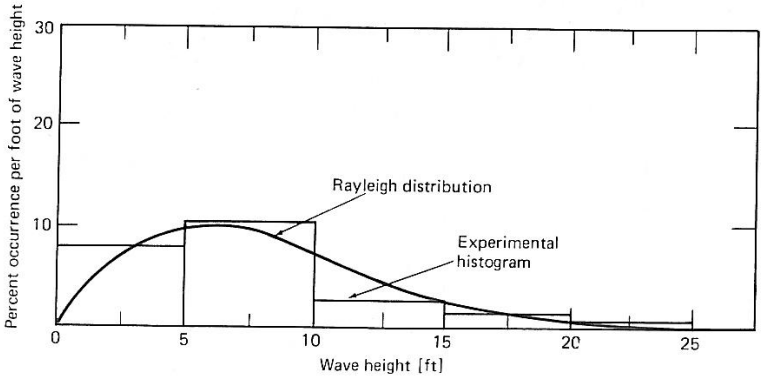


Figure 5.6 Wave histogram and theoretical Rayleigh distribution.

TABLE 5.6

Height [ft] ①	Number of Waves ②	Cumulative Number of Waves ③	Number × Height ④ = ① × ②
2.5	5,600	5,600	14,000
7.5	7,200	12,800	54,000
12.5	1,920	14,720	24,000
17.5	960	15,680	16,800
22.5	320	16,000	720
SUM	16,000		116,000

the Rayleigh one, as will be shown later.

Table 5.6 has been compiled in accordance with Table 5.4 in order to compare the actual values of the average wave heights with those predicted by the Rayleigh law. Average wave height is 116,000/16,000 = 7.25 ft. According to the Rayleigh distribution, average wave height is 0.89 × 8.59 = 7.65 ft. One can see that the theoretical Rayleigh distribution fits the example rather well.

The histograms as described above can define only one characteristic of the irregular seaway, namely, either period, height, or amplitude. Only the wave energy spectrum method of describing a seaway takes into account both the frequency and the wave amplitude. This is discussed in the following section.

5.3 WAVE SPECTRUM

An irregular wave pattern can be generated if a large number of sinusoidal waves of different wavelengths

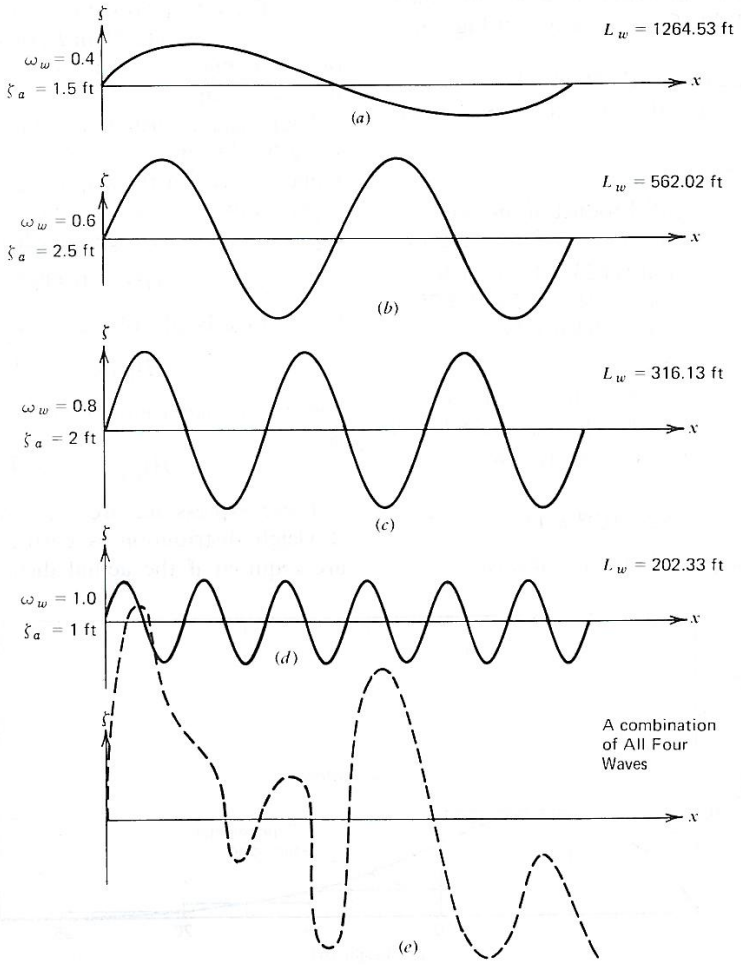


Figure 5.7 Addition of four sinusoidal waves.

and heights are superimposed on each other. The resulting wave shows no definite pattern for either wave height, wavelength, or wave period. This is illustrated in Fig. 5.7 by considering four sinusoidal waves, each having its own particular wavelength and wave height. The combination of four waves, shown in Fig. 5.7*e*, is of extremely irregular shape in regard to both wavelength and wave height.

Not only does the superposition of many sinusoidal waves create an extremely irregular seaway, but also the pattern of the seaway is never repeated from one time to another. There is, however, only one way to take into account the irregularity of the waves, and that is to determine the total energy. This is obtained by adding together the energies of all of the small, regular sinusoidal waves that produce the seaway by their superposition. The severity of the seaway is then measured by the total energy content of all the waves present.

As mentioned in Section 3.7, the energy of a sinusoidal wave is given as

$$\tfrac{1}{2}\rho g\zeta_a^2$$

per square foot of sea surface. Therefore the total energy per square foot of surface of all the waves, with amplitudes $\zeta_{a_1}, \zeta_{a_2}, \ldots, \zeta_{a_n}$, is given by

$$E_T = \tfrac{1}{2}\rho g(\zeta_{a_1}^2 + \zeta_{a_2}^2 + \ldots + \zeta_{a_n}^2) \qquad (5.4)$$

Thus any given seaway can be described by the energy distribution versus the different frequencies (or wavelengths or wave periods) for various wave components. The frequency distribution of energy is called the *energy spectrum* for the particular seaway, as illustrated in Example 5.3.

Example 5.3

Find the energy distribution of an irregular seaway composed of four different waves having the following characteristics:

Wave number	1	2	3	4
Length [ft]	1265	562	316	202
Height [ft]	3	5	4	2

Solution:

The circular frequency expression is

$$\omega_w = \sqrt{\frac{2\pi g}{L_w}}$$

from which

$$\omega_1 = 0.4, \qquad \omega_2 = 0.6 \qquad \omega_3 = 0.8,$$

and $\omega_4 = 1.0\ \text{sec}^{-1}$

Thus the total energy per square foot of the wave surface

$$E_T = \frac{\rho g}{2}(\zeta_{a_1}^2 + \zeta_{a_2}^2 + \zeta_{a_3}^2 + \zeta_{a_4}^2)$$
$$= \frac{62.4}{2}[(1.5)^2 + (2.5)^2 + 2^2 + 1^2]$$
$$= 70.2 + 195 + 124.8 + 31.2$$
$$= 421.2\ \text{lb/ft}$$

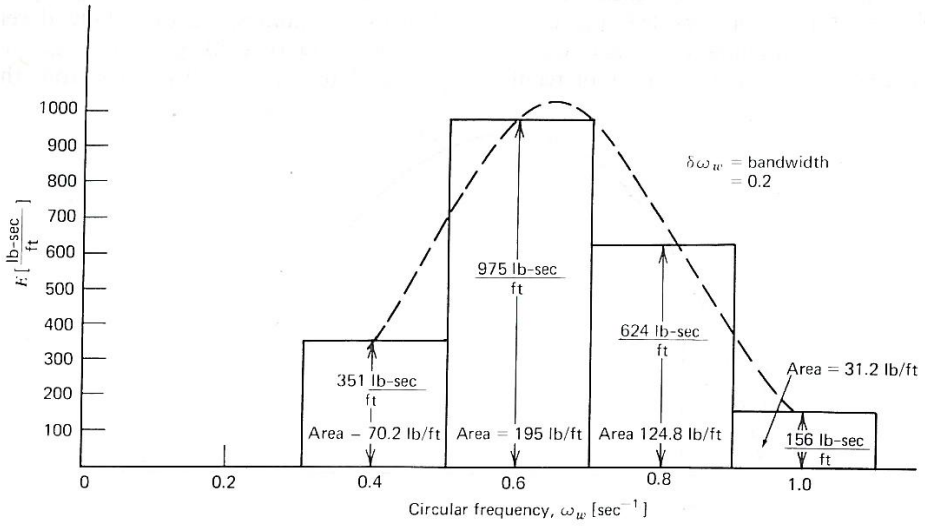


Figure 5.8 Energy spectrum for four waves.

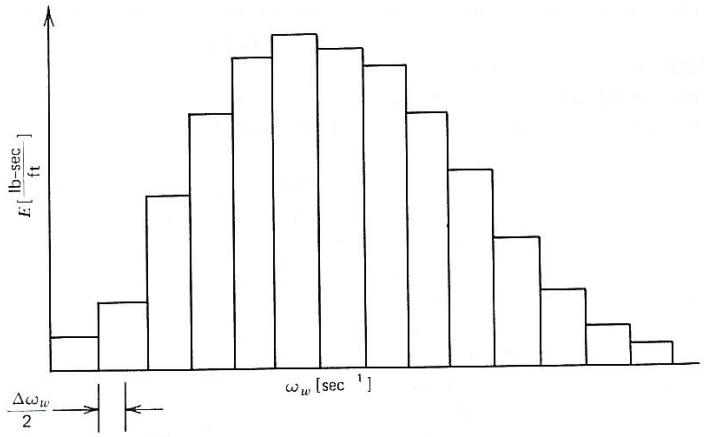


Figure 5.9 Approach toward final spectrum.

where $\rho g = 62.4\,\text{lb/ft}^3$ for fresh water.

The distribution of this total energy according to the frequency of waves is given in Fig. 5.8, where the ordinates are obtained by dividing the individual energy content by the bandwidth, which is 0.2 in this particular example.

Note that the dimension of energy (see Table 4.5) is lb-ft. Since the area under the total curve should give this dimension, the ordinates represent lb-sec/ft, since the abscissa has the dimension of sec^{-1}.

The total area under the energy spectrum gives the total energy of all the wave components. Note that the energy due to each frequency has been given a small bandwidth $\delta\omega_w$ in order to obtain a continuous curve, as shown by the dotted line of Fig. 5.8. Since the real sea is made up of all frequencies and the wave pattern itself is never repeated, the energy spectrum has to be a continuous curve, composed of the contributions of an infinite number of regular waves, having all different wavelengths and very small amplitudes, as Fig. 5.9 shows.

The energy spectrum in Fig. 5.10 covers the entire range of frequency; the bandwidth $\delta\omega_w$ is decreased, and the number of individual wave trains increases until it reaches infinity. At the same time the energy content of each individual wave component is also decreased; however, the total amount of energy available in the seaway remains the same. This continuous curve between $\omega_w = 0$ and $\omega_w = \infty$ actually represents the energy spectrum of the waves.

It is to be noted that for a given *wind speed* the waves that are first generated are short; the longer wavelengths are generated when the wind continues to blow. Ultimately a *fully developed sea* is produced which is stable and does not change as the wind continues to blow. Thus the energy spectrum also changes continuously until a fully developed sea is formed. During its growth longer waves are produced (i.e., the contributions from the shorter

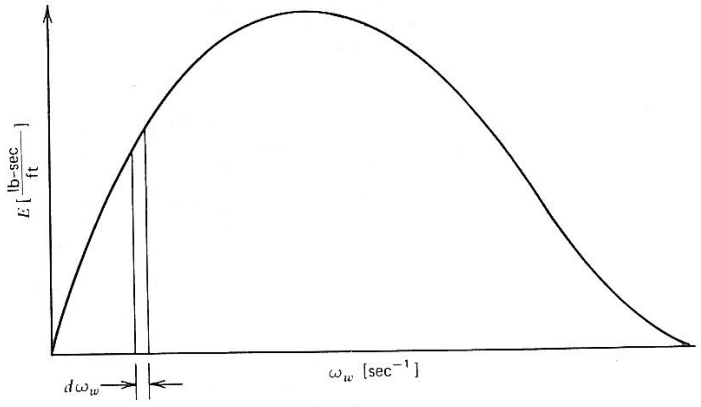


Figure 5.10 Final energy spectrum.

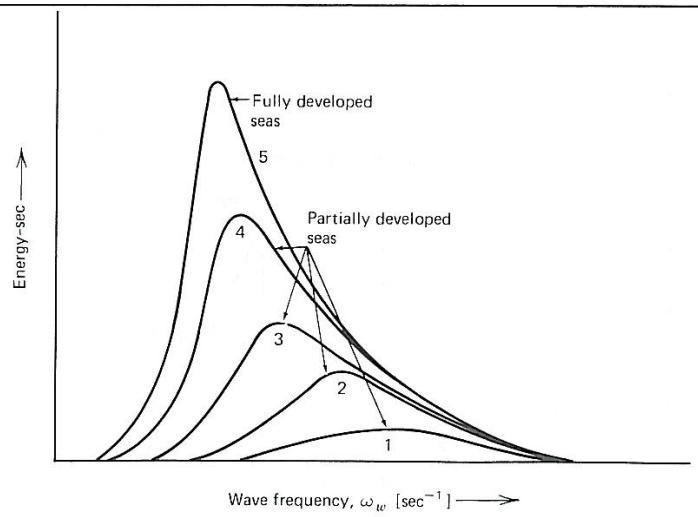


Figure 5.11 Energy build-up of partially and fully developed seas.

frequencies become predominant), as is shown in Fig. 5.11. This figure also shows that, along with the generation of longer waves, the maximum value of the energy spectrum shifts toward the lower frequency side. This is also the case for a fully developed sea when it is experiencing increasing wind speed. See Fig. 5.12.

We have seen that (5.4) represents the energy in waves and that the area under the curve in Fig. 5.8 yields the same quantity. Now, instead of drawing a spectrum as in Fig. 5.8 that is, from (5.4), one can draw a different figure in which the ordinates represent

$$\tfrac{1}{2}(\zeta_{a_1}^2 + \zeta_{a_2}^2 + \ldots + \zeta_{a_n}^2) \tag{5.5}$$

Note: ρg is divided out, and the area under the curve of the new figure, generally denoted as m_0, is later multiplied by ρg to obtain the energy. The new figure is called the *wave spectrum*, and the ordinates are represented by the symbol $S_\zeta(\omega_w)$, which is called the *spectral density of wave energy*. The wave spectrum for example 5.3 is shown in Fig. 5.13.

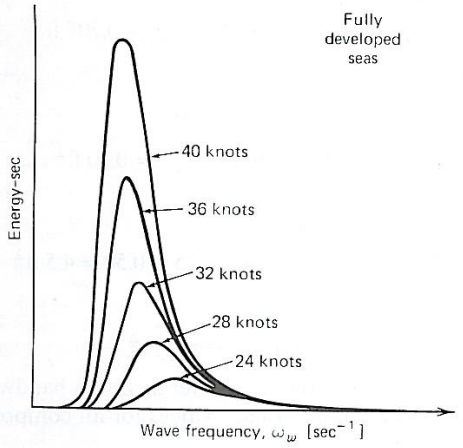


Figure 5.12 Energy spectra of fully developed seas for various wind speeds.

In Example 5.3,

$$\tfrac{1}{2}(\zeta_{a_1}^2 + \zeta_{a_2}^2 + \zeta_{a_3}^2 + \zeta_{a_4}^2) = \tfrac{1}{2}[(1.5^2) + (2.5)^2 + 2^2 + 1^2] = 6.755 \text{ ft}^2$$

Therefore the total area under the wave spectrum in Fig. 5.13 should have a value of 6.755, which, when multiplied by ρg, that is, about 62.4 lb/ft^3 (for fresh water), gives the energy, which is 421.2 lb/ft as before. As in the case of the energy spectrum, the ordinates of the wave spectrum are obtained by dividing the individual $\frac{1}{2}$(amplitude)^2 values by the bandwidth, which is 0.2 in this particular example.

In conclusion it should be noted that there is a limit on the number of waves to be considered in obtaining the maximum wave height from the Rayleigh distribution. Although we may obtain a very high wave if the wave record is made for a very long time, the probability of occurrence for the extremely high wave is very low. Therefore often a record of 1000 waves is considered to be sufficiently representative for the determination of the wave spectrum, and the "most probable" value of the one-thousandth highest waves is taken to be the most probable largest value [152].

Sometimes it is not the number or observations but the period of time that is considered in obtaining a wave record for statistical evaluation, for example,

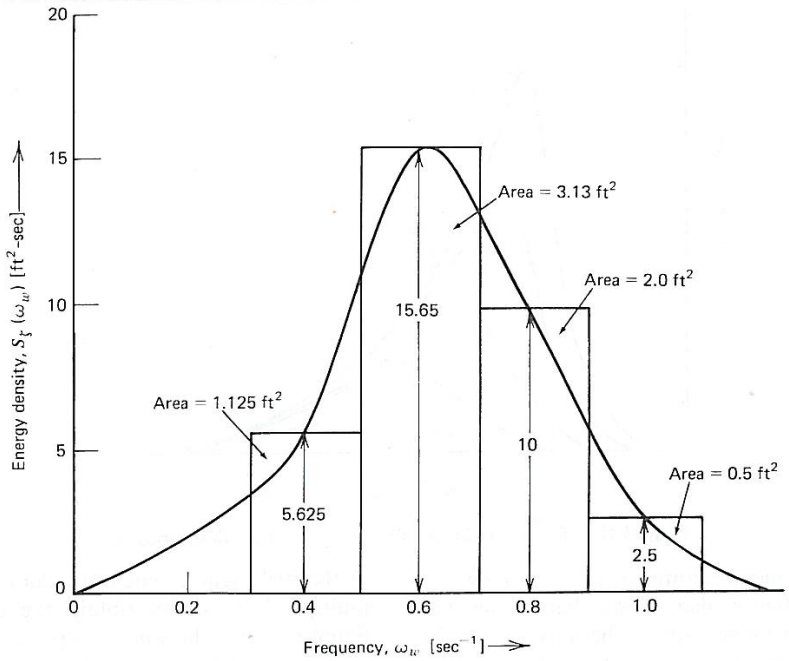


Figure 5.13 Wave spectrum for four waves.

the total number of waves passing a point within an hour, or the total number passing a point during a longer period of time. The total number of waves is obtained by dividing 1 hr by the significant wave period.

5.4 PREDICTION OF AN IRREGULAR SEAWAY

To be able to define a seaway it is necessary to take sample records of the wave heights and the frequency of the particular seaway concerned over a limited period of time. Although the wave pattern will never be repeated, the statistical characteristics of the sea state, that is, the energy spectrum or wave spectrum, will remain the same. This is the advantage of statistical investigations. In other words, the sinusoidal components that approximate a record for a particular sea state are the same regardless of time and place and differ from one record to another only in the phase orientation, thereby keeping the energy of the wave system constant.

Although a spectral density curve may be drawn from just one wave record, it is often preferred to obtain the average wave characteristics for any given area by taking many samples of wave records. The spectral density curve may also be approximated by an analytical expression based on probability theory.

The procedure for plotting a spectral density curve to a base of wave frequency is illustrated below. Let us suppose that a record has been made of four component waves of wave frequency, ω_w, between 0.75 and 0.85 (i.e., $\omega_w = 0.8 \pm 0.05$), and that $\delta\omega_w = 0.85 - 0.75 = 0.1$ is the bandwidth. The wave amplitudes of the wave record are

$$\zeta_{a_1} = 0.866, \qquad \zeta_{a_2} = 1.414,$$
$$\zeta_{a_3} = 1.118, \qquad \text{and} \qquad \zeta_{a_4} = 0.707 \text{ ft}$$

Thus

$$\zeta_{a_1}^2 = 0.75, \qquad \zeta_{a_2}^2 = 2.00,$$
$$\zeta_{a_3}^2 = 1.25, \qquad \text{and} \qquad \zeta_{a_4}^2 = 0.50 \text{ ft}^2$$

Therefore

$$\sum^{\delta\omega_w} \zeta_{a_i}^2 = 0.75 + 2.00 + 1.25 + 0.50 = 4.5 \text{ ft}^2$$

and

$$S(\omega_w)\,\delta\omega_w = \tfrac{1}{2} \sum^{\delta\omega_w} \zeta_{a_i}^2$$

or the area under the curve over a certain bandwidth is the sum of $\frac{1}{2}$(amplitude)^2 values for all component waves. Thus

$$S(\omega_w)\,\delta\omega_w = \tfrac{1}{2}(4.5) = 2.25 \text{ ft}^2$$

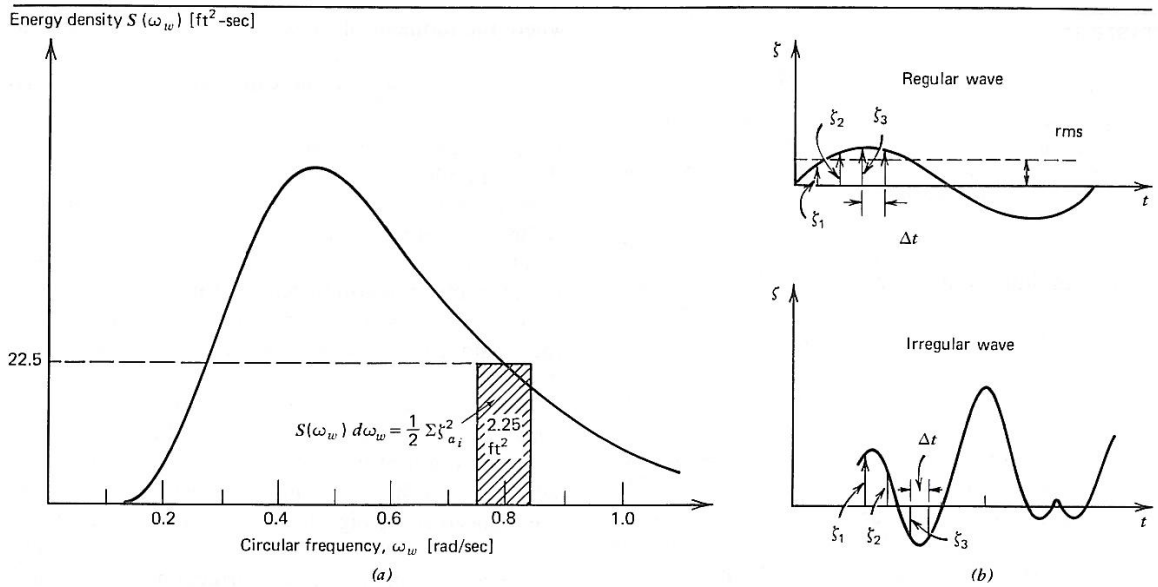


Figure 5.14 (*a*) Energy density for a particular frequency band. (*b*) Surface elevation at equal intervals of time.

which is the area under the energy density curve for ω_w between 0.75 and 0.85 sec^{-1}. Since $\delta\omega_w = 0.1$ sec^{-1}, that is, 0.85 − 0.75 in our records,

$$S(\omega_w) = \frac{2.25}{0.1} = 22.5 \text{ ft}^2\text{-sec}$$

This value obtained for energy density has been plotted in Fig. 5.14*a*.

Now the total energy $E = \rho g m_0$ per square foot of wave surface, where m_0 is the area under the energy density spectrum, or, dimensionally, $E = (ML^{-3})(LT^{-2})(L^2)$ or $E = (ML^{-2}T^{-2})$ for the total wave surface. This is the dimensional expression for energy as given in Table 4.6.

Note that it is not the energy spectrum of the seaway that has a Gaussian form; it is the seaway record (histogram) for *wave elevation* that is Gaussian. The histogram for the *wave heights* of an irregular seaway is considered to be more or less a Rayleigh distribution. The energy spectrum may have any functional form.

To use the principle of the energy spectrum for engineering studies, the *quantitative values of the wave spectrum for different sea regions and for different climatic conditions should be known.*

Although there are differences between different wave spectrum formulas, the ordinate of the curve is generally taken as the *spectral density*, which is used to represent the full energy of the component waves. Since the energy of the component waves is directly related to the square of their amplitudes, *the spectral density can be referred directly to the square of the amplitude of the waves.* The notation for the spectral density is $S_\zeta(\omega_w)$, and the area under the curve is equivalent to the statistical *variance.* Furthermore the significant height is obtained by the relation

$$(h_w)_{1/3} = 4.0\sqrt{\text{area}} \qquad \text{or} \qquad (h_w)_{1/3} = 4.0\sqrt{m_0}$$

where

$$m_0 = \int_0^\infty S_\zeta(\omega_w)\,d\omega_w \tag{5.6}$$

is the area under the curve of the wave spectrum. The factor 4.0 is obtained on the basis that the histogram for wave height follows the mathematical approximation given by the Rayleigh distribution, which characterizes a rather narrow wave spectrum. Again,

$$S_\zeta(\omega_w)/\delta\omega_w = \tfrac{1}{2}(\zeta_{a_1}^2 + \zeta_{a_2}^2 + \ldots) \tag{5.7}$$

for the particular value of bandwidth $\delta\omega_w$, as mentioned before. The wave spectrum so obtained not only gives the various average values (the significant amplitude, average amplitude of the one-tenth highest waves, etc.) but is also used for the extreme values, as will be shown later.

The following useful information can be derived from a wave spectrum:

a. The range of frequencies that are important for the contribution of energy to the seaway.
b. The frequency at which the maximum energy is supplied.
c. The content of energy at different frequency bands.
d. The existence of a swell at low frequencies.

TABLE 5.7

	Amplitude	Height
Average wave:	$1.25\sqrt{m_0}$	$2.50\sqrt{m_0}$
Average of one-third highest waves:	$2.00\sqrt{m_0}$	$4.00\sqrt{m_0}$
Average of one-tenth highest waves:	$2.55\sqrt{m_0}$	$5.09\sqrt{m_0}$
Average of one-hundredth highest waves:	$3.34\sqrt{m_0}$	$6.67\sqrt{m_0}$

From a known wave spectrum one can obtain the wave amplitudes or heights by using the simple formulas given in Table 5.7. The area under a wave spectrum, as described earlier, is

$$\int_0^\infty S_\zeta(\omega_w)\,d\omega_w = m_0 \tag{5.8}$$

where m_0 is the value of wave elevations squared, or $\sqrt{m_0}$ is the root mean square (rms) value of the wave elevations in an irregular seaway. The rms of wave elevations from the zero line measured at constant Δt does not give the peak deviation (or mean amplitude), but it does give a mean (statistical average) of the deviations from the zero line i.e., $m_0 = (1/n)\Sigma\zeta_n^2$ where n is the number of measurements. It is to be noted that Δt should be less than half the minimum time between successive crests and n should be large [see Fig. 5.14*b*]. Thus the area under the wave spectrum yields the mean of the deviations squared (i.e., m_0), and hence the rms value of the irregular wave response is $\sqrt{m_0}$. The significant wave amplitudes or other averages are multiples of rms (i.e., a constant $\times\sqrt{m_0}$). Such multipliers depend on the assumed probability distribution. For example, for the Rayleigh distribution the amplitude and height of the average of all, the one-third highest, the one-tenth highest, or the one-hundredth highest waves are given in Table 5.7. Also, if the wave height histogram follows the Rayleigh distribution, the mean of the wave height squared is related to the area under the wave spectrum as

$$\bar{H}^2 = 8m_0$$

As the formulas of Table 5.7 have been derived for a *narrow frequency spectrum* (i.e., for *Rayleigh distribution* of the wave height histogram), oceanographers have introduced a correction factor (CF):

$$\text{CF} = (1-\varepsilon^2)^{1/2} \tag{5.9}$$

by which the above constants should be multiplied to take into account the broadness of the spectrum. The *broadness parameter* is found from the *even moments* of the spectrum and is given by the expression

$$\varepsilon^2 = \frac{m_0 m_4 - m_2^2}{m_0 m_4} \tag{5.10}$$

where the moment of the area under the spectrum is

$$m_n = \int_0^\infty \omega_w^n S_\zeta(\omega_w)\,d\omega_w \tag{5.11}$$

Here n is any integer, and m_n is the nth moment of the area under the spectrum.

Note that the physical significance of m_0 and m_2 is that they represent the vertical velocity and vertical acceleration of wave motion, respectively. The form of the spectrum is completely determined by knowing all the moments of the area of the spectrum about the origin, as necessary for the broadness parameter given in (5.10).

In the case of *swells*, the high frequencies are not very prominent and the height distribution (wave height histogram) approaches the theoretical Rayleigh law. On the other hand, in *wind-generated* seas (wide band spectra) the high frequencies are rather important, and the wave height distribution approaches the *Gaussian law*; hence the correction factor should be used to find the statistical averages for wave amplitudes or heights for wind-generated seas. Note that the value of ε usually lies between 0 and 1.0.

In general, the following factors determine the shape of a wave spectrum:

a. Wind speed (the most significant parameter).
b. Wind duration.
c. Fetch (distance over which the wind blows).
d. Location of other storm areas from which the swell may travel.

The expression for the average number of zero up-crossings per second, N_0, is also given in terms of moments of the area under the spectrum:

$$N_0 = \frac{1}{2\pi}\sqrt{\frac{m_2}{m_0}} \tag{5.12}$$

and the average zero-crossing period, $\tilde{T}_z$, is given as

$$\tilde{T}_z = \frac{1}{N_0} = 2\pi\sqrt{\frac{m_0}{m_2}} \tag{5.13}$$

where the zero-crossing period is the average time interval between successive upward or downward crossings of the line representing the mean water level.

Also, the crest-to-crest period $\tilde{T}_c$ is defined as

$$\tilde{T}_c = 2\pi\sqrt{\frac{m_2}{m_4}}$$

which is the average time between successive crests or troughs in the record.

In an irregular seaway, crests and troughs occur from time to time below and above, respectively, the mean water level; therefore the crest-to-crest period $\tilde{T}_c$ has a value less than that of $\tilde{T}_z$, which is the zero-crossing period. Since $\tilde{T}_z$ does not include the effect of important ripples, it is therefore considered to be more closely related to visual estimates of period than is $\tilde{T}_c$.

Another important characteristic for the irregular seaway is the average apparent wavelength $(\tilde{L}_w)_z$, which is also defined in terms of the spectral moments:

$$(\tilde{L}_w)_z = 2\pi g \sqrt{\frac{m_0}{m_4}} \tag{5.15}$$

Standard Wave Spectrum (Recommended by the International Towing Tank Conference)

When the wave spectrum of a particular sea is not available, International Towing Tank Conference (ITTC) spectral formulation should be used as follows:

a. $$S(\omega_w) = \frac{A}{\omega_w^5} e^{-B/\omega_w^4} \tag{5.16}$$

Here ω_w is the circular frequency in radians per second, and $A = 8.10 \times 10^{-3} g^2$, where g is the acceleration of gravity in appropriate units.

Also, $S(\omega_w)$ is in cm^2-sec units when $B = 3.11 \times 10^4 / H_{1/3}^2$, where $H_{1/3}$ is the significant wave height in centimeters, or $S(\omega_w)$ is in ft^2-sec units when $B = 33.56/(H)_{1/3}^2$, where $H_{1/3}$ is the significant wave height in feet.

b. If statistical information is available on both the characteristic wave period and the significant wave height, then

$$A = 173(H)_{1/3}^2/T_1^4, \qquad B = 691/T_1^4$$

where the significant wave period T_1 is given as

$$T_1 = 2\pi \sqrt{\frac{m_0}{m_1}}$$

The data suggest that this period can be taken as the observed period.

Furthermore, the significant wave height is $(H)_{1/3} = 4.0\sqrt{m_0}$, that is, the significant height is 4.0 × variance.

c. Although a wide variation in significant wave heights exists for a given wind speed, the approximate relationship between wind speed and significant height in the open ocean, to be used when only wind speed is known, is tentatively defined by a curve (Fig. 5.15) having the following ordinates:

Wind Speed [knots]	Significant Wave Height [ft]
20	10
30	17.2
40	26.5
50	36.6
60	48.0

The "wind speed" is taken to be that which is "sensed" by personnel on board ship.

Example 5.4

a. Using the ITTC formulation, plot a wave spectrum for a wind speed of 31 knots.

b. Find the significant wave height from this spectrum if the assumption that the wave height histogram follows the Rayleigh distribution is not valid.

Solution:

Since wind speed = 31 knots, the significant wave height $H_{1/3}$ is 18.5 ft from Fig. 5.15. The spectral density is

$$S(\omega_w) = \frac{A}{\omega_w^5} e^{-B/\omega_w^4}$$

where $A = 8.10 \times 10^{-3} g^2 = 8.385$ ft^2-sec, and $B = 33.56/(H)_{1/3}^2 = 0.09806$.

Substituting the values of A and B, we obtain Table 5.8 for the wave spectrum (see Fig. 5.16); Table 5.9 has been prepared for the calculation of the correction factor (CF) to be used for the broadness of the wave spectrum.

The variance is then

$$m_0 = \tfrac{1}{3} \times \Delta\omega_w \times \text{SUM}_0 = \tfrac{1}{3} \times 0.1 \times 646.92 \text{ ft}^2 = 21.564 \text{ ft}^2$$

Furthermore,

$$(H)_{1/3} = 4.0\sqrt{m_0} = 4\sqrt{21.564} = 18.50 \text{ ft}$$

$$(H)_{\text{average}} = 2.506\sqrt{m_0} = 2.506 \times 4.65 = 11.67 \text{ ft}$$

and

$$(H)_{1/10} = 5.090\sqrt{m_0} = 5.090 \times 4.65 = 23.65 \text{ ft}$$

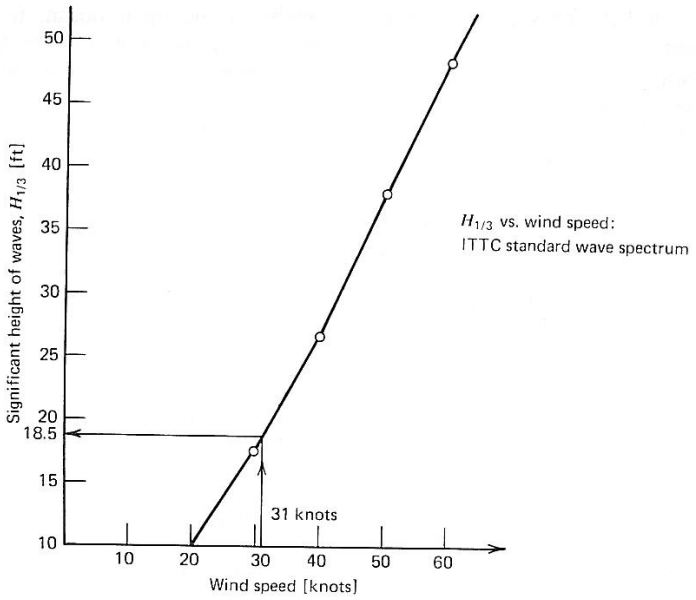


Figure 5.15 Significant wave height versus wind speed [106].

Also

$$(H)_{1/100} = 6.671\sqrt{m_0} = 6.671 \times 4.65 = 31.00 \text{ ft}$$

$$m_2 = \tfrac{1}{3} \times \Delta\omega_w \times \text{SUM}_2 = \tfrac{1}{3} \times 0.1 \times 327.14 = 10.91 \text{ ft}^2/\text{sec}^2$$

$$m_4 = \tfrac{1}{3} \times \Delta\omega_w \times \text{SUM}_4 = \tfrac{1}{3} \times 0.1 \times 285.48 = 9.52 \text{ ft}^2/\text{sec}^4$$

$$N_0 = \frac{1}{2\pi}\sqrt{\frac{m_2}{m_0}} = \frac{1}{2\pi}\sqrt{\frac{10.91}{21.56}} = \frac{1}{2\pi}(0.507)^{1/2}$$

$$= 0.1132 \text{ sec}^{-1}$$

$$\tilde{T}_{\text{average}} = \frac{1}{N_0} = \frac{1}{0.1132} = 8.83 \text{ sec}$$

$$\tilde{T}_c = 2\pi\sqrt{\frac{m_2}{m_4}} = 2\pi\sqrt{\frac{10.91}{9.52}} = 7.2 \text{ sec}$$

$$(L_w)_z = \tilde{L}_{\text{average}} = 2\pi g\sqrt{\frac{m_0}{m_4}} = 2\pi \times 32.2\sqrt{\frac{21.56}{9.52}}$$

$$= 304.5 \text{ ft}$$

Energy $= \rho g m_0 = 62.4 \times 21.56 = 1342$ lb-sec/ft (per

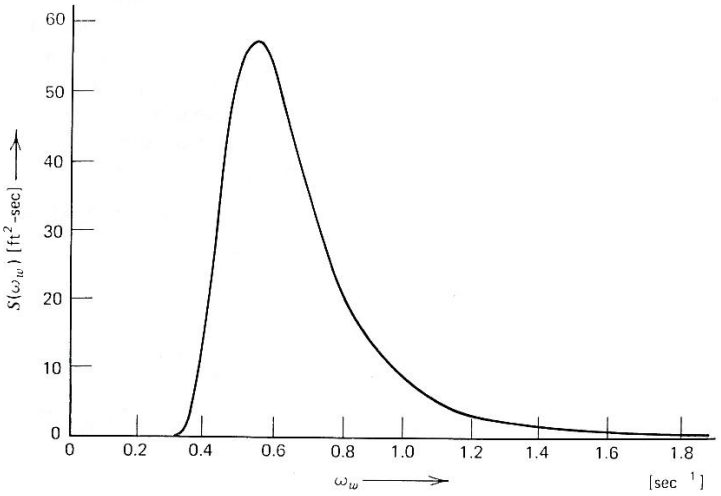


Figure 5.16 Wave spectrum for a significant wave height of 18.5 ft.

TABLE 5.8

ω_w [sec^{-1}] ①	$B\sqrt{\omega_w^4}$ ②	e^{-B/ω_w^4} ③	$S(\omega_w)$ [ft^2-sec] ④
0.20	61.286	0	0
0.30	12.106	0	0.02
0.40	3.830	0.022	17.80
0.50	1.569	0.208	55.97
0.60	0.757	0.469	50.68
0.70	0.408	0.665	33.22
0.80	0.239	0.787	20.17
0.90	0.149	0.861	12.25
1.00	0.098	0.907	7.61
1.10	0.067	0.935	4.88
1.20	0.047	0.954	3.22
1.30	0.034	0.966	2.19
1.40	0.026	0.975	1.52
1.50	0.019	0.981	1.09
1.60	0.015	0.985	0.79
1.70	0.012	0.988	0.59
1.80	0.009	0.991	0.44
1.90	0.008	0.993	0.34
2.00	0.006	0.994	0.26

square foot of sea surface). Thus

$$\varepsilon^2 = \frac{m_0 m_4 - m_2^2}{m_0 m_4}$$

$$= \frac{21.56 \times 9.52 - (10.91)^2}{21.56 \times 9.52}$$

from which the correction factor is

$$\text{CF} = (1 - \varepsilon^2)^{1/2}$$
$$= (1 - 0.42)^{1/2}$$
$$= 0.76$$

Finally, the significant wave amplitude is

$$(\zeta_a)_{1/3} = 2\sqrt{m_0} \times \text{CF} = 2 \times \sqrt{21.564} \times 0.76 = 7.5 \text{ ft}$$

so that the significant wave height is 15 ft.

The average, significant, and other wave heights are obtained statistically by applying the correction factor. However, the CF is taken to be 1.0 when standard ITTC formulation is used for wave spectra for a given significant wave height, since it is assumed by ITTC that the wave height (double amplitude) histogram follows the Rayleigh distribution.

5.5 MOST PROBABLE LARGEST WAVE AMPLITUDE

The expected value of the most probable largest amplitude in a record of n waves is obtained statistically, as given by Ref. 139, using (5.17). The most probable largest amplitude is

$$\sqrt{2 \log_e n} \times \sqrt{m_0} \times \text{CF} \qquad (5.17)$$

where n is the total number of observations, m_0 is

TABLE 5.9 WAVE CHARACTERISTICS FROM ITTC STANDARD SPECTRUM, $(h_w)_{1/3}$ = 18.5 ft.

ω_w [sec^{-1}] ①	$S(\omega_w)$ ②	Simpson's Multiplier ③	Product ② × ③ ④	ω_w^2 ⑤	$\omega_w^2 S(\omega_w)$ ⑥	Simpson's Multiplier ⑦	Product ⑥ × ⑦ ⑧	ω_w^4 ⑤^2 ⑨	$\omega_w^4 S(\omega_w)$ ⑨ × ② ⑩	Simpson's Multiplier ⑪	Product ⑨ × ⑪ ⑫
0.20	0	1	0	0.04	0	1	0	0.0	0	1	0
0.30	0.02	4	0.08	0.09	0.00	4	5.70	0.01	0.00	4	0
0.40	17.80	2	35.60	0.16	2.85	2	55.96	0.03	0.53	2	1.06
0.50	55.97	4	233.88	0.25	13.99	4	36.50	0.06	3.36	4	13.44
060	50.68	2	101.36	0.36	18.25	2	65.12	0.13	6.59	2	13.18
0.70	33.22	4	132.88	0.49	16.28	4	25.82	0.24	7.97	4	31.88
0.80	20.17	2	40.34	0.64	12.91	2	39.68	0.41	8.27	2	16.54
0.90	12.25	4	49.00	0.81	9.92	4	15.22	0.66	8.09	4	32.36
1.00	7.61	2	15.22	1.00	7.61	2	23.60	1.00	7.61	2	15.22
1.10	4.88	4	19.52	1.21	5.90	4	9.28	1.46	7.12	4	28.28
1.20	3.22	2	6.44	1.44	4.64	2	14.80	2.07	6.67	2	13.34
1.30	2.19	4	8.76	1.69	3.70	4	5.96	2.86	6.26	4	25.04
1.40	1.52	2	3.04	1.96	2.98	2	9.80	3.84	5.84	2	11.68
1.50	1.09	4	4.36	2.25	2.45	4	4.04	5.06	5.52	4	22.08
1.60	0.79	2	1.58	2.56	2.02	2	6.84	6.55	5.17	2	10.34
1.70	0.59	4	2.36	2.89	1.71	4	2.86	8.35	4.93	4	19.72
1.80	0.44	2	0.88	3.24	1.43	2	4.92	10.50	4.62	2	9.24
1.90	0.34	4	1.36	3.61	1.23	4	1.04	13.03	4.43	4	17.72
2.00	0.26	1	0.26	4.00	1.04	1		16.00	4.16	1	4.16
		SUM_0	646.92 ft^2-sec			SUM_2	327.14 ft^2-sec^{-1}			SUM_4	285.48 ft^2-sec^{-3}

TABLE 5.10

Number of Waves	Most Probable Largest Wave Amplitude
1	$1 \times \sqrt{m_0}\,\mathrm{CF}$
10	$2.24 \times \sqrt{m_0}\,\mathrm{CF}$
100	$3.07 \times \sqrt{m_0}\,\mathrm{CF}$
1000	$3.74 \times \sqrt{m_0}\,\mathrm{CF}$
10,000	$4.30 \times \sqrt{m_0}\,\mathrm{CF}$
100,000	$4.81 \times \sqrt{m_0}\,\mathrm{CF}$

the area under the wave spectrum (variance), and CF is the correction factor, $(1 - \varepsilon^2)^{1/2}$

For different values of n, Table 5.10 shows the results using (5.17).

For example, if the wave height (double amplitude) histogram follows the ideal Rayleigh distribution (which means that the correction factor is unity), then, for a value of $m_0 = 80.70\ \mathrm{ft}^2$, out of 50 waves one would have an amplitude of 25.5 ft, or out of a total of 1000 waves one should attain an amplitude of 33.6 ft.

Statistical estimation of the most probable largest values of wave amplitudes is useful in practical design consideration.

Chapter

Six

MOTION IN AN IRREGULAR SEAWAY

6.1 RESPONSE IN AN IRREGULAR SEAWAY

The response of a ship in an irregular seaway follows the same statistical laws as do the waves. Records of ship responses show patterns similar to those of wave records. Therefore, instead of having a graph for the square of each component wave amplitude as a function of frequency, one can have a graph of the square of the rolling (or any other motion) amplitude that the particular wave component of that amplitude and frequency would produce. The resulting spectrum, known as the *response spectrum*, will give similar statistical properties, when the proper statistical factors are applied, to those obtained in the case of sea waves.

Example 6.1

The rolling amplitudes (double, i.e., peak to peak) of a ship in an irregular seaway were measured, and the results are presented in Table 6.1.

Find the average, significant, average of one-tenth highest, and average of one-hundredth highest rolling motions.

Solution:

From the measured rolling angles, Table 6.2 is constructed.

$$\text{Average roll} = \frac{\text{SUM}_4}{\text{SUM}_2} = \frac{767}{100} = 7.67^\circ$$

Since $\frac{1}{3}(\text{SUM}_2) = 33$,

$$\text{Significant roll} = \frac{\text{SUM}_5}{33} = \frac{402}{33} = 12.2^\circ$$

Similarly, $\frac{1}{10}(\text{SUM}_2) = 10$; therefore the average of the one-tenth highest rolls is

$$\frac{\text{SUM}_6}{10} = \frac{160}{10} = 16^\circ$$

Finally, $\frac{1}{100}(\text{SUM}_2) = 1$; therefore the average of the one-hundredth highest rolls is

$$\frac{\text{SUM}_7}{1} = \frac{20}{1} = 20^\circ$$

Histogram for the double amplitude of motion can be obtained either for heaving or pitching or rolling, as in Fig. 6.1. The theoretical Rayleigh approximation for the motion is defined as:

TABLE 6.1

Double Amplitude of Rolling Angle [deg]	Number of Occurrence
1	1
2	4
3	7
4	10
5	13
6	8
7	12
8	10
9	8
10	7
11	5
12	2
13	4
14	3
15	1
16	0
17	2
18	2
19	0
20	1

TABLE 6.2

Amplitude of roll, ϕ_i [deg] ①	Number of Cases ②	Cumulative Number of Cases ③	① × ② ④	① × ② for One-Third largest Roll Amplitudes ⑤	① × ② for One-Tenth Largest Roll Amplitudes ⑥	① × ② for One-Hundredth largest Roll Amplitudes ⑦
1	1	1	1			
2	4	5	8			
3	7	12	21			
4	10	22	40			
5	13	35	65			
6	8	43	48			
7	12	55	84			
8	10	65	80			
9	8	73	72	54(= 9 × 6)		
10	7	80	70	70		
11	5	85	55	55		
12	2	87	24	24		
13	4	91	52	52	13(13 × 1)	
14	3	94	42	42	42	
15	1	95	15	15	15	
16	0	95	0	0	0	
17	2	97	34	34	34	
18	2	99	36	36	36	
19	0	99	0	0	0	
20	1	100	20	20	20	20
	SUM$_2$ 100		SUM$_4$ 767	SUM$_5$ 402	SUM$_6$ 160	SUM$_7$ 20

$$p(x_i) = \frac{2x_i}{\bar{x}^2} e^{-(x_i^2/\bar{x}^2)} \qquad (6.1a)$$

where $p(x_i)$ is the percentage of times that any particular double amplitude of motion, x_i, will appear, that is, the double amplitude of heaving, pitching, or rolling. In (6.1a) $\bar{x}^2$ is the mean value of the squares of the double amplitudes, that is,

$$\bar{x}^2 = \frac{\sum_{i=1}^{n} x_i^2 f(x_i)}{\sum_{i=1}^{n} f(x_i)}$$

Hence $\bar{x}$ is the root mean square (rms) of the double amplitude of motion, and n is the total number of x_i. The function $f(x_i)$ is the number of occurrences for each mean value of the double amplitude of motion.

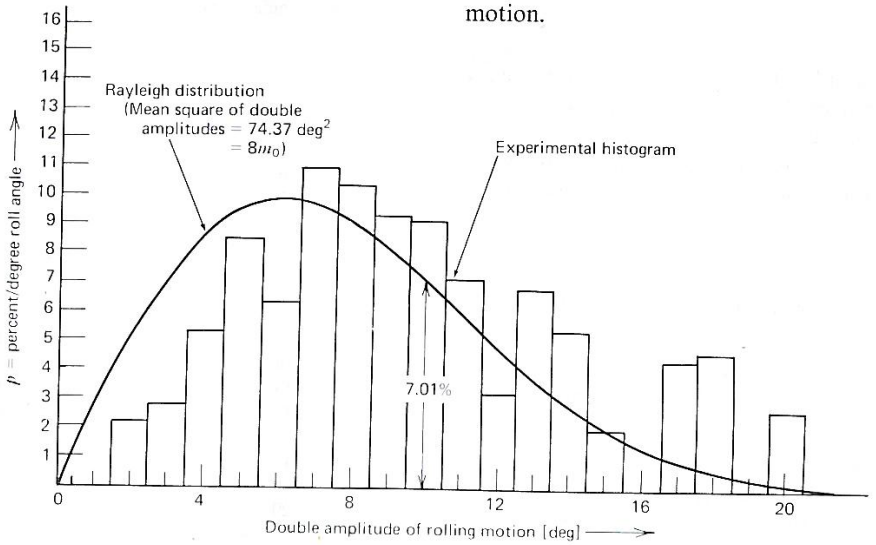


Figure 6.1 Histogram of rolling motion (double amplitude).

TABLE 6.3

ϕ_i ①	$f(\phi_i)$ ②	ϕ_i^2 ③	$\phi_i^2 \cdot f(\phi_i)$ ④	*Number of Occurrences,* $f(\phi_i)$ ⑤	① × ⑤ ⑥	Percent Occurrences ⑥ 767 ⑦
1	1	1	1	1	1	0.13
2	4	4	16	4	8	1.04
3	7	9	63	7	21	2.74
4	10	16	160	10	40	5.22
5	13	25	325	13	65	8.47
6	8	36	288	8	48	6.26
7	12	49	588	12	84	10.95
8	10	64	640	10	80	10.43
9	8	81	648	8	72	9.39
10	7	100	700	7	70	9.13
11	5	121	605	5	55	7.17
12	2	144	288	2	24	3.13
13	4	169	676	4	52	6.78
14	3	196	588	3	42	5.48
15	1	225	225	1	15	1.96
16	0	256	0	0	0	0
17	2	289	578	2	34	4.43
18	2	324	648	2	36	4.69
19	0	361	0	0	0	0
20	1	400	400	1	20	2.61
SUM	100		7437		767	

The Rayleigh distribution can also be expressed in terms of the motion spectrum as

$$p(x_i) = \frac{2x_i}{8m_0} e^{-(x_i^2/8m_0)} \tag{6.1b}$$

where $8m_0$ is the mean value of the squares of x_i (i.e., $\bar{x}^2$), m_0 is the area under the response spectrum for motion:

$$m_0 = \int_0^\infty S(\omega_e)\, d\omega_e \tag{6.2}$$

and $S(\omega_e)$ is the spectral density of the motion.

Example 6.2

For the data given in Example 6.1, draw the histogram, as well as the theoretical Rayleigh distribution, for the rolling motion.

Solution:

The histogram of the rolling amplitudes (double) is obtained in Table 6.3.

Thus $\bar{\phi}^2$ is the mean square of double rolling amplitudes, that is,

$$\bar{\phi}^2 = \frac{7437}{100} = 74.37 \text{ deg}^2$$

and $\bar{\phi}$ is the mean or rms, which is $\sqrt{74.37} = 8.62°$, that is, the mean rolling amplitude is 4.31°, since the amplitude is half of the double amplitude.

The Rayleigh distribution is given as

$$p(\phi_i) = \frac{2\phi_i}{\bar{\phi}^2} e^{-(\phi_i^2/\bar{\phi}^2)} \tag{6.3}$$

For example,

$$p(10°) = \frac{2 \times 10}{74.37} e^{-100/74.37} = 0.0701 \text{ or } 7.01\%$$

The results of Table 6.3 are presented with those obtained from (6.3) in Fig. 6.1.

It was pointed out in Section 5.2 that the Rayleigh distribution fits well with the histogram for double wave amplitudes, that is, wave heights. Similarly, the Rayleigh distribution is a good fit for the double amplitude of ship response, for example, the double amplitude of rolling or pitching motion, or the double amplitude of the wave bending moment. Note that the constants of the formulas for significant amplitude and other averages are based on the rms of the Rayleigh distribution.

6.2 PREDICTION IN AN IRREGULAR SEAWAY

Ship motion in an irregular seaway is determined by means of the following steps:

1. For the particular seaway in which the vessel is to operate a suitable wave spectrum is chosen.
2. Next the wave spectrum is transformed into a spectrum where the frequency of encounter is considered, instead of the absolute wave frequency. However, the area under the modified spectrum is the same as that under the original spectrum, since the total energy remains the same.
3. A plot is obtained in which the ordinates represent the amplitude of motion (either pitch, roll, or heave) to a base of encountering frequency distribution. This can be obtained analytically or by experimentation with regular or irregular waves in a tow tank.
4. The diagram obtained is step 3 is modified so that the ordinates represent the ratio of the square of the motion amplitude divided by the square of the wave amplitude. This diagram is termed the *response amplitude operators* (*RAO*) or simply the *transform spectrum.*

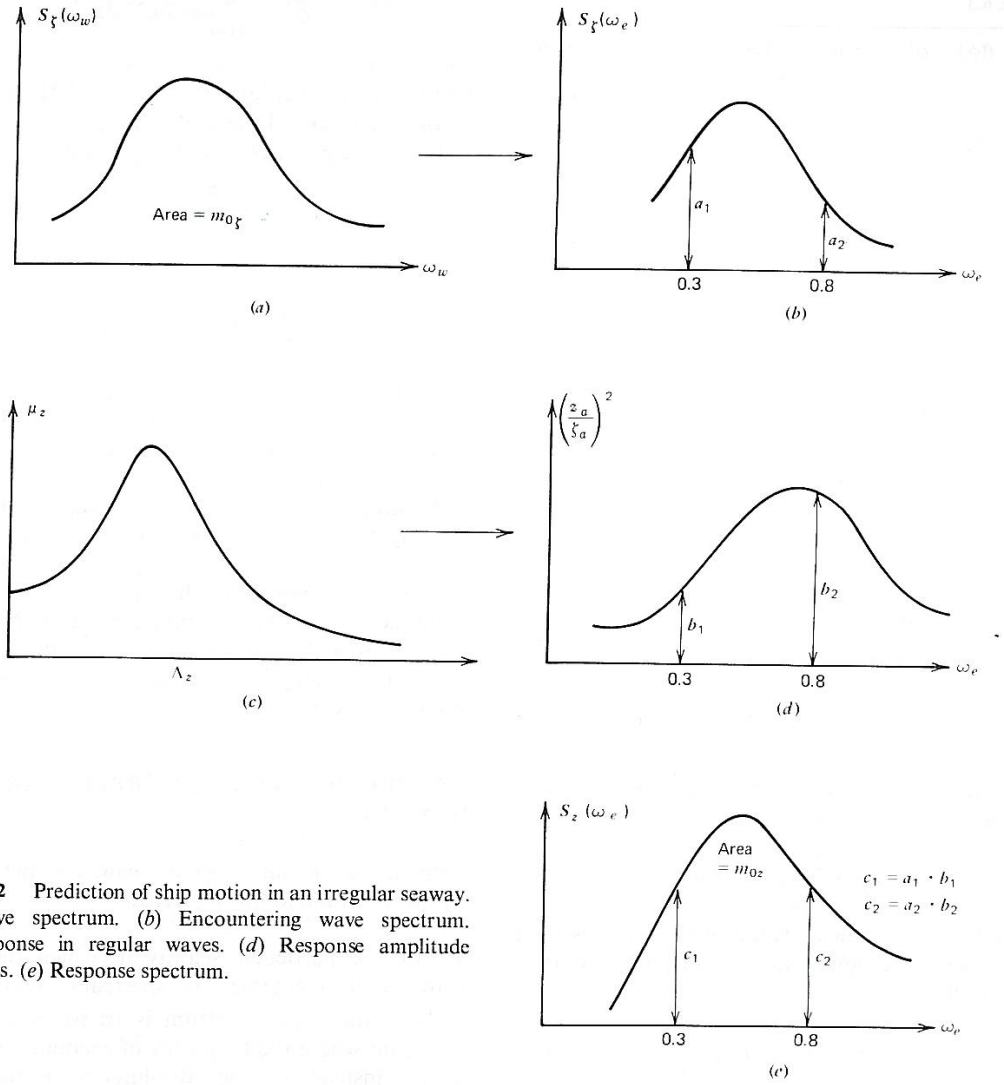


Figure 6.2 Prediction of ship motion in an irregular seaway. (*a*) Wave spectrum. (*b*) Encountering wave spectrum. (*c*) Response in regular waves. (*d*) Response amplitude operators. (*e*) Response spectrum.

5. The motion amplitude spectrum is obtained by multiplying the ordinates of the transformed wave spectrum by the ordinates of the RAO for the corresponding frequencies of encounter.

6. Finally, the area under the motion amplitude spectrum is determined in order to obtain the necessary motion characteristics (e.g., average, average of one-third highest, or average of one-tenth highest motion amplitudes), as in the case of waves, using the same formulations given in Section 5.4.

These six steps can be explained with the help of Fig. 6.2.

It must first be noted, however, that the above method is valid for ship response in an irregular seaway only if the responses are linearly proportional to the wave excitation (i.e., the wave amplitude). This assumption is quite reasonable if the seaway is moderate and only moderate responses are expected. Numerous model experiments have shown that, although in principle the ship responses are nonlinear, the nonlinearities can be ignored in practice. Hence the linear technique for the prediction of ship responses provides a very useful means for *seakeeping design*. The various steps for the prediction of ship response by statistical means as described above will now be explained with the help of Example 6.3.

Step 1

A standard wave spectrum, like that of the ITTC, is selected for design prediction of ship motion characteristics if no particular sea spectrum is to be preferred. On the other hand, if a ship is to be designed for a particular seaway (e.g., for the Atlantic Ocean), the wave spectrum for that seaway should be selected instead of the standard ITTC spectrum. The spectral density $S_\zeta(\omega_w)$ for a significant wave height of 18.5 ft was evaluated in Example 5.4 according to the ITTC formulation.

Step 2

It is necessary to transform the wave spectrum obtained in step 1 into the spectrum that would be obtained by a wave meter moving with the ship, that is, the wave spectrum should be recognized in terms of the frequencies of encounter instead of the absolute frequencies. Thus the wave spectrum as encountered by the ship is obtained.

As given in Chapter 3, the circular frequency of encounter is obtained by using the following formulation:

$$\omega_e = \omega_w - \frac{\omega_w^2 V}{g} \cos \mu \tag{6.4}$$

For the wave spectrum the abscissa values for ω_w should now be replaced by the ω_e values as obtained by (6.4). Then the corresponding values of the ordinate, $S(\omega_e)$, should be obtained as

$$S(\omega_e) = S(\omega_w) \frac{1}{[1 - (4\omega_e V/\mathrm{g}) \cos \mu]^{1/2}} \tag{6.5a}$$

or, in terms of ω_w, as

$$S(\omega_e) = S(\omega_w) \frac{1}{1 - (2\omega_w V/g) \cos \mu} \tag{6.5b}$$

and plotted as the ordinate for the encountering wave spectrum with ω_e as the abscissa.

Note that *the change in the ordinate value is necessary so that the total area will be the same under the encountering wave spectrum as under the original wave spectrum; in other words, the total energy and significant height of the seaway do not change if the recording of the seaway is made at a moving instead of a stationary point.*

Proof: The energy for the total surface should remain the same, or

$$\int S(\omega_e)\, d\omega_e = \int S(\omega_w)\, d\omega_w \tag{6.6}$$

Now

$$\omega_e = \omega_w - \frac{\omega_w^2 V}{g} \cos \mu$$

and

$$\text{Thus} \qquad \frac{d\omega_e}{d\omega_w} = 1 - \frac{2\omega_w V}{g} \cos \mu$$

$$S(\omega_e)\, d\omega_w \left(1 - \frac{2\omega_w V}{g} \cos \mu\right) = S(\omega_w)\, d\omega_w$$

or

$$S(\omega_e) = \frac{S(\omega_w)}{1 - (2\omega_w V/g) \cos \mu}$$

In terms of ω_e we can write

$$S(\omega_e) = S(\omega_w) \frac{1}{[1 - (4\omega_e V/g) \cos \mu]^{1/2}}$$

It should be pointed out that in the case of a *head sea* ($\mu = 180°$) the energy is spread out over a wider band of higher frequencies than for a *stationary point spectrum*, whereas, for a *following sea*, at moderate negative velocities, energy tends to be concentrated in narrower bands at low frequencies, the spectral density becoming infinite at the frequency of encounter:

$$\omega_{e\,\max} = -\tfrac{1}{4} \frac{g}{V}$$

Note: $V < 0$, so $\omega_{e\,\max} > 0$.

This singularity in the spectral density is integrable, so that the energy in any given band of frequencies is finite. Following sea spectra are *double valued* in the range of frequencies for which it is possible to encounter waves of two wavelengths at the same frequency of encounter, and extend into the "negative frequency" range. The physical interpretation of "negative frequency" for following seas is merely that the waves are propagating with velocity $V_w < |V|$ and are being overtaken by the moving point. The negative spectral density is seen to pose no problem when it is considered that, in integrating the energy content in any frequency band, a path of increasing values of ω_e is followed, so that the product $S(\omega_e) \cdot \omega_e$ is always positive. For example, one can write

$$m_0 = \int_0^\infty S(\omega)\, d\omega$$

$$= \int_0^{\omega_{e\,\max}} [S(\omega_e)]\, d\omega_e + \int_{\omega_{e\,\max}}^{-\infty} [S(\omega_e)]\, d\omega_e$$

In the final form of this variance equation the first integration is carried out from left to right in the upper half of the plane $S(\omega_e)$ versus ω_e, and the second

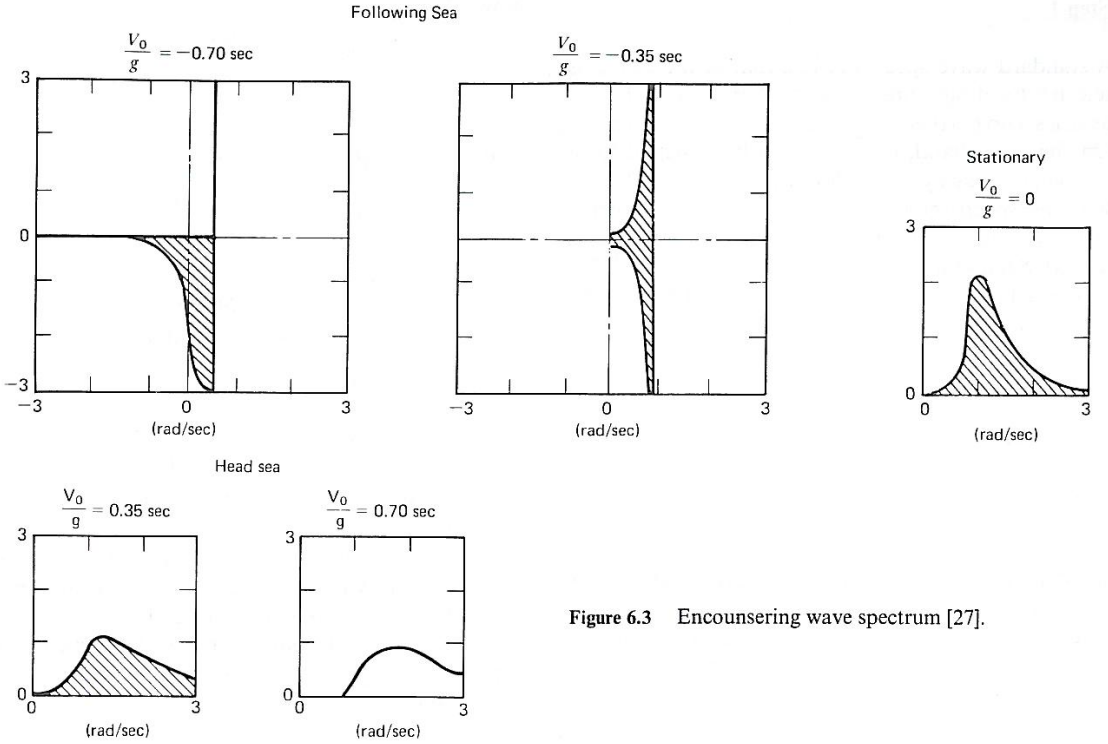


Figure 6.3 Encounsering wave spectrum [27].

is carried out from right to left in the lower half-plane.

Some examples are given in Fig. 6.3 for a state 3 sea (see Table 5.1) and for speeds appropriate to slow surface vessels.

It should be pointed out that, when a vehicle travels at much higher speeds (*e.g., air cushion vehicles and hydrofoil crafts*), *there is little practical difference between head and following sea.* The respective frequency spectra resemble reflections about the origin of one another. *The following sea spectrum still has the singular "spikes" near the origin, although the spikes contain practically no energy.*

Example 6.3

Given:

$$L = 450 \text{ ft}$$

$$k_{xx} = 30.8 \text{ ft}$$

$$\overline{GM}_T = 5.79 \text{ ft}$$

$$\Delta = 12{,}500 \text{ tons}$$

The added mass for rolling is 20% of the mass of the ship, and the damping moment is 32,000 $(d\phi/dt)$ ft-tons.

If the ship is traveling with a speed of 20 knots at an angle of 150° to the line of wave crests in a seaway of significant wave height 18.5 ft, determine the significant rolling motion.

Solution:

$$\omega_e = \omega_w(1 - \eta)$$

where $$\eta = \frac{\omega_w V}{g} \cos \mu$$

$$V = 20 \text{ knots} = 20 \times 1.689 = 33.78 \text{ ft/sec}$$

$$\mu = 150°$$

$$\cos \mu = -0.8660$$

$$g = 32.2 \text{ ft/sec}^2$$

Thus

$$\omega_e = \omega_w(1 + 0.909\omega_w)$$

now $S_\zeta(\omega_e)$ is obtained by using the equation

$$S_\zeta(\omega_e) = \frac{S_\zeta(\omega_w)}{[1 - (4\omega_e V/g)\cos \mu]^{1/2}}$$

The values of ω_e and $S_\zeta(\omega_e)$ as calculated from ω_w and $S_\zeta \omega_w)$, respectively, are given in Table 6.4.

TABLE 6.4

ω_w [sec^{-1}] ①	$\eta = \frac{\omega_w V}{g}\cos\mu$ ②	$\omega_e = \omega_w(1-\eta)$ [sec^{-1}] ③	$S_\zeta(\omega_w)$ [ft^2-sec] ④	$S_\zeta(\omega_e)$ [ft^2-sec] ⑤
0.20	− 0.18	0.24	0	0
0.30	− 0.27	0.38	0.02	0.01
0.40	− 0.36	0.55	17.80	10.31
0.50	− 0.45	0.73	55.97	29.34
0.60	− 0.55	0.93	50.68	24.26
0.70	− 0.64	1.14	33.22	14.63
0.80	− 0.73	1.38	20.17	8.23
0.90	− 0.82	1.64	12.25	4.65
1.00	− 0.91	1.91	7.61	2.70
1.10	− 1.00	2.20	4.88	1.63
1.20	− 1.09	2.51	3.22	1.01
1.30	− 1.18	2.83	2.19	0.65
1.40	− 1.27	3.18	1.52	0.43
1.50	− 1.36	3.54	1.09	0.29
1.60	− 1.46	3.92	0.79	0.20
1.70	− 1.55	7.32	0.59	0.14
1.80	− 1.64	4.74	0.44	0.10
1.90	− 1.73	5.18	0.34	0.08
2.00	− 1.82	5.63	0.26	0.06

Step 3

Example 4.28 showed how the ratio of rolling amplitude and wave amplitude against encountering frequency can be obtained analytically for this particular case. The values calculated in Example 4.28 are shown in Table 6.5.

TABLE 6.5

ω_w[sec^{-1}] ①	ω_e[sec^{-1}] ②	$\frac{\phi_a}{\zeta_a}$[deg/ft] ③
0.20	0.24	0.044
0.30	0.38	0.424
0.40	0.55	0.169
0.50	0.73	0.104
0.60	0.93	0.073
0.70	1.14	0.060
0.80	1.38	0.052
0.90	1.64	0.052
1.00	1.91	0.045
1.10	2.20	0.045
1.20	2.51	0.039
1.30	2.83	0.030
1.40	3.18	0.035
1.50	3.54	0.020
1.60	3.92	0.023
1.70	4.32	0.026
1.80	4.74	0.029
1.90	5.18	0.032
2.0	5.63	0.036

Step 4

Table 6.5 is now changed to Table 6.6 by changing the ordinate value from ϕ_a/ζ_a to $(\phi_a/\zeta_a)^2$.

TABLE 6.6

ω_e [sec^{-1}] ①	$\frac{\phi_a}{\zeta_a}$ [deg/ft] ②	RAO $= \left(\frac{\phi_a}{\zeta_a}\right)^2$ [deg^2/ft^2] ③
0.24	0.044	0.0019
0.38	0.424	0.1789
0.55	0.169	0.0282
0.73	0.104	0.0108
0.93	0.073	0.0057
1.14	0.060	0.0038
1.38	0.052	0.0028
1.64	0.052	0.0022
1.91	0.045	0.0018
2.20	0.045	0.0014
2.51	0.039	0.0012
2.83	0.030	0.0010
3.18	0.035	0.0008
3.54	0.020	0.0007
3.92	0.023	0.0006
4.32	0.026	0.0005
4.74	0.029	0.0004
5.18	0.032	0.0004
5.63	0.036	0.0003

The response amplitude operators are functions that give the amplitude of the oscillating motion of the ship in a regular seaway of unit amplitude. Therefore the RAOs are different for different kinds of motion.

It should be mentioned here that the RAOs *can be determined either analytically or by model tests. In the latter case the models are run in regular waves of different wavelengths but of constant wave amplitude.* The RAOs are obtained directly by relating the amplitude of each motion to the wave amplitude taken from the simultaneous recordings of motions and wave amplitudes.

The frequencies of waves would again be considered as the frequencies of encounter in the computations for irregular seaways.

The tests should be carried out for a wide range of wave frequencies and directions for each model speed of interest.

The ratios of maximum model heave to wave height, and of maximum pitch to wave slope, and the corresponding *phase lags* can be measured readily. The plots of these quantities versus frequencies of wave encounter will give directly the ship response functions needed for the application of the method. It should be pointed out that, although the data so obtained are given separately for heave and pitch,

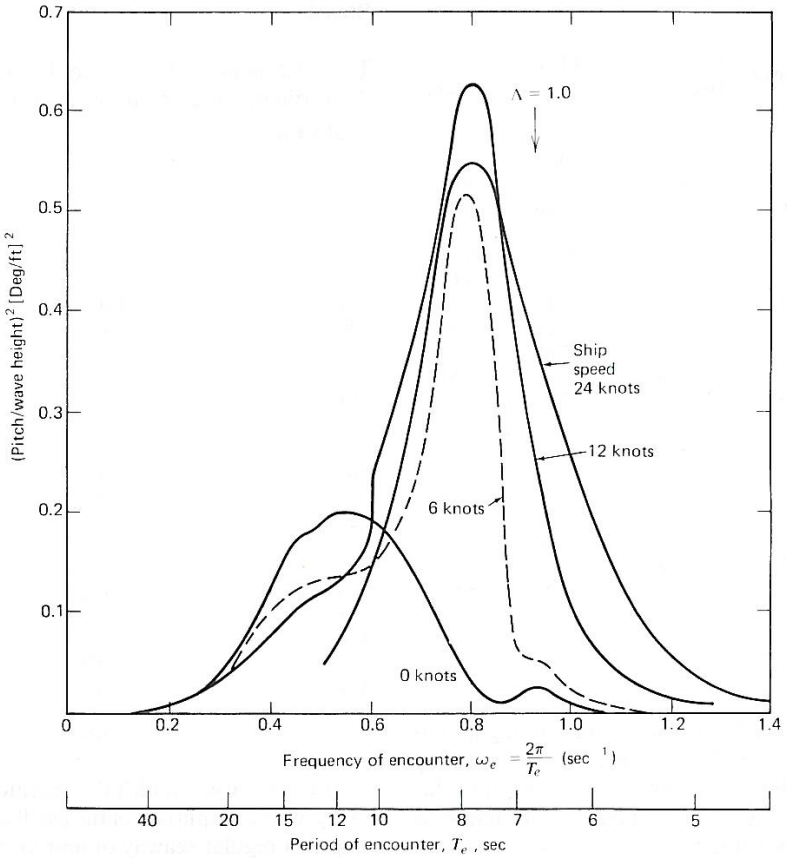


Figure 6.4 Typical response amplitude operators of pitching for a 500 ft ship [127].

they are taken from the records of the actual coupled motion and therefore do not contain the error due to noncoupling. *The analytically obtained pitch and heave amplitudes (e.g., using the strip theory) can also be used* in a similar manner.

The solution of equations of motion given in Chapter 4 enables us to determine the motion responses of a particular ship in terms of heave, pitch, or roll amplitude per foot of wave height as a function of encountering frequency.

Finding the response to a regular sinusoidal wave is a comparatively deterministic process, but in summing (or integrating) these responses we carry the *stochastic nature* of the seaway over to the ship motions.

The *fundamental assumption* made in this method of motion studies in an irregular seaway is that the sum of the responses of a ship to a number of simple sine waves is equal to the response of the ship to the sum of the waves. If this assumption is not valid, then the method given in Ref. 194 is also not valid. However, it has been found by model tests that this assumption is justifiable for average motions that are not too severe.

A plot of the RAOs for the pitching motion as functions of ship speeds is shown in Fig. 6.4.

Step 5: Ship Responses

The linear superposition technique used for calculations of ship response in an irregular seaway is based on two fundamental assumptions:

1. *The response of a vessel to any individual regular wave component is a linear function of the amplitude of this component*, and is assumed to be the response that would be experienced had the vessel been subjected to a train of these same regular waves for a long time previously. The response of the vessel is assumed to be simple harmonic (i.e., sinusoidal), and to have a frequency equal to the frequency of

encounter with the train of waves. If the wave amplitude were doubled, the amplitude of ship motion response would also be doubled.

Let us assume that ship response is linearly proportional to wave amplitude, that is, a certain wave

$$a_i \sin \omega_i t$$

will cause a response

$$b_i \sin(\omega_i t + \varepsilon_i)$$

where

$$b_i = a_i H(\omega_i)$$

and $H(\omega_i)$ is the frequency response function.

2. *The response of a vessel to any individual wave component is independent of its response to any other wave component.* This means that the response of the vessel to the seaway is the sum of its responses to the individual wave components that comprise the seaway. In other words, the effect of the seaway on a ship is found by summing the effects of the separate wave systems on the ship.

The spectral density function of ship response is equal to the product of the spectral density function of the waves and the response amplitude operator. For example, for rolling motion,

$$S_\phi(\omega_e) = S_\zeta(\omega_e) \cdot |H(\omega_e)|^2 \qquad (6.7)$$

where $S_\zeta(\omega_e)$ = density function of wave spectrum [ft^2-sec]

$S_\phi(\omega_e)$ = spectral density function of ship response for rolling [deg^2-sec]

TABLE 6.7

ω_e [sec^{-1}] ①	$S_\zeta(\omega_e)$ (from Table 6.4) [ft^2-sec] ②	RAO $= \left(\frac{\phi_a}{\zeta_a}\right)^2$ (from Table 6.6) [deg^2/ft^2] ③	$S_\phi(\omega_e)$ [deg^2-sec] ④
0.25	0.0	0.40×10^{-2}	0.00×10^{-2}
0.50	6.0	3.80×10^{-2}	22.80×10^{-2}
0.75	32.5	0.92×10^{-2}	29.90×10^{-2}
1.00	20.0	0.47×10^{-2}	9.40×10^{-2}
1.25	11.0	0.32×10^{-2}	3.52×10^{-2}
1.50	6.4	0.25×10^{-2}	1.60×10^{-2}
1.75	3.5	0.18×10^{-2}	0.63×10^{-2}
2.00	2.0	0.14×10^{-2}	0.28×10^{-2}
2.25	1.3	0.11×10^{-2}	0.14×10^{-2}
2.50	1.0	0.10×10^{-2}	0.10×10^{-2}
2.75	0.6	0.10×10^{-2}	0.06×10^{-2}

and $|H(\omega_e)|^2$ = response amplitude operator, as follows:

a. For rolling motion, RAO $= \left(\frac{\phi_a}{\zeta_a}\right)^2 \left[\frac{\text{deg}^2}{\text{ft}^2}\right]$

b. For pitching motion, RAO $= \left(\frac{\theta_a}{\zeta_a}\right)^2 \left[\frac{\text{deg}^2}{\text{ft}^2}\right]$

c. For heaving motion, RAO $= \left(\frac{z_a}{\zeta_a}\right)^2 \left[\frac{\text{ft}^2}{\text{ft}^2}\right]$

d. For relative bow motion, RAO $= \left(\frac{s_a}{\zeta_a}\right)^2 \left[\frac{\text{ft}^2}{\text{ft}^2}\right]$

Etc.

In other words, the ordinates of the motion spectrum are obtained by multiplying the ordinates of

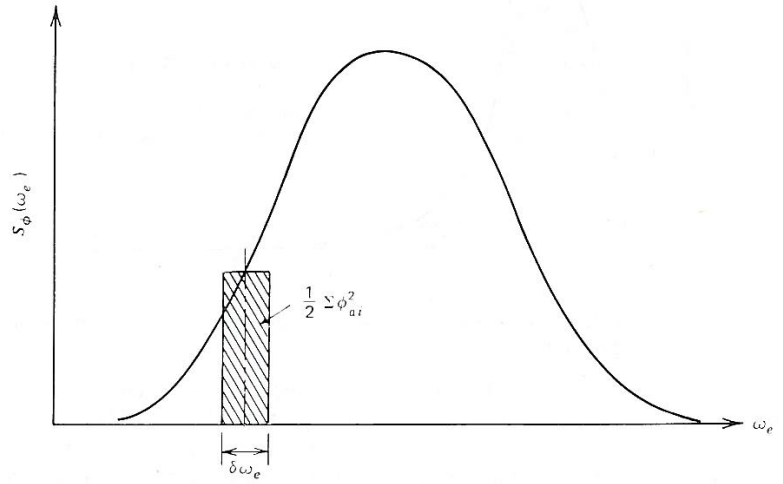


Figure 6.5 Response spectrum for rolling motion.

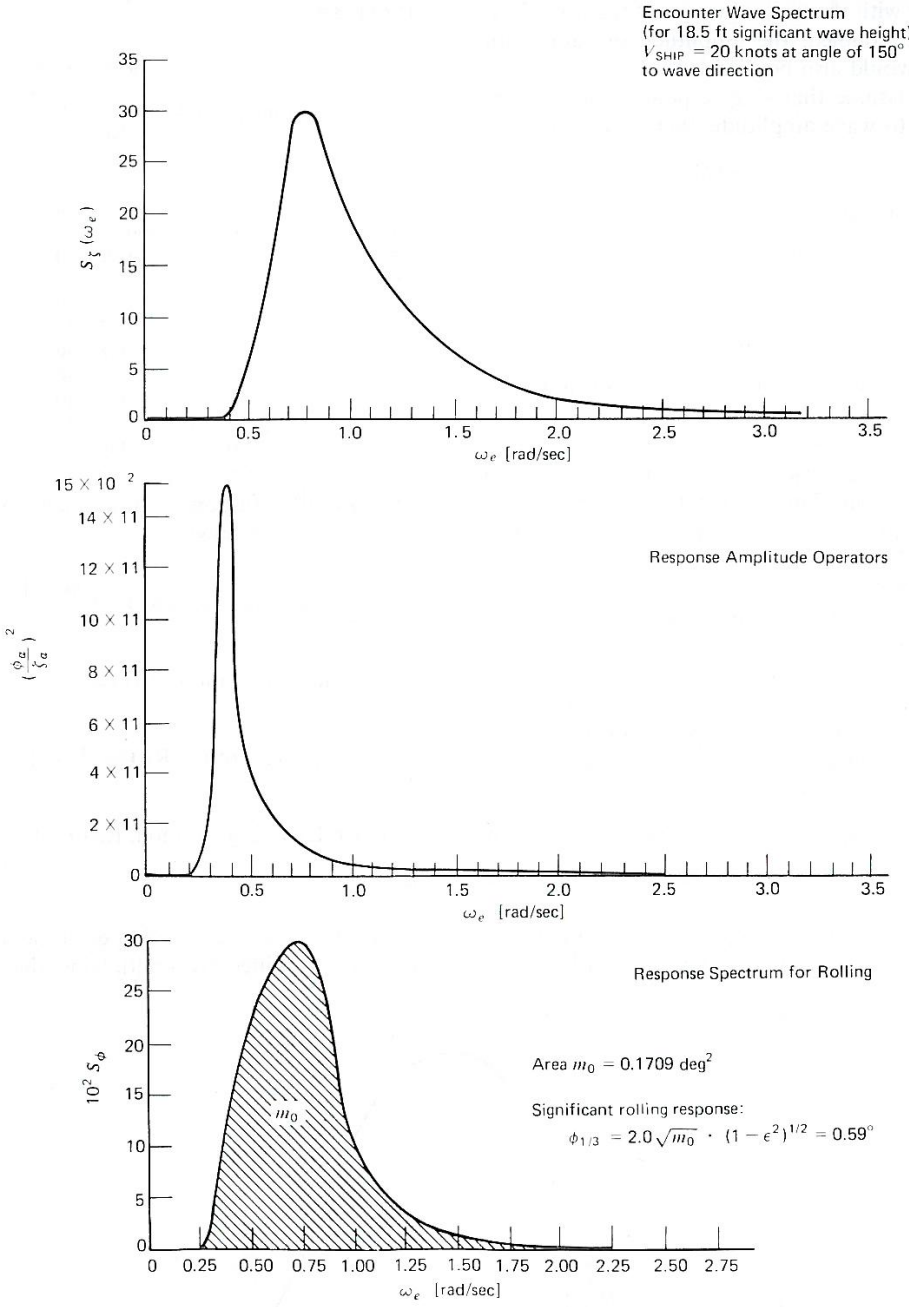


Figure 6.6 Typical plots of wave spectrum, response amplitude operators, and response spectrum for rolling motion.

the encountering wave spectrum by the RAOs for the corresponding frequencies of encounter ω_e. See Table 6.7.

Note that, in order to distinguish the wave spectrum from the response spectrum, the ordinates of the wave spectrum are denoted by S_ζ and those of the roll spectrum by S_ϕ. The area of the rectangle at $\omega_e = 0.8$ in the roll amplitude spectrum is shown in Fig. 6.5. This area represents half of the square of the amplitude of roll produced by this wave component,

or approximately by the band of wave frequencies $\delta\omega_e$. In other words, this area represents half of the squared rolling amplitudes $\frac{1}{2}\Sigma\phi_n^2$ due to $\frac{1}{2}\Sigma\zeta_a^2$ present in the bandwidth of encountering frequency between $\omega_e - (\delta\omega_e/2)$ and $\omega_e + (\delta\omega_e/2)$, that is, this spectrum for rolling is analogous to the wave spectrum the ordinates of which represent $\frac{1}{2}\Sigma\zeta_a^2$.

Equation 6.7 is very significant, since any of the three quantities that it contains can be calculated if the other two are known. Consider the following (see Fig. 6.6):

a. If $S_\zeta(\omega_e)$ and $|H(\omega_e)|^2$ (i.e., the spectral density of the waves and the RAO of the ship) are known, with the help of (6.7) the spectral density of the ship motion can be calculated. If, for instance, the RAO, that is, $|H(\omega_e)|^2$, has been determined by means of a calculation or a model test, the ship motions can be predicted for any given seaway.

b. If S_ζ and S_ϕ are known, the spectral densities of the waves and of the motion are known. Then with the help of (6.7) the RAO of the ship can be determined. This is especially important because the response characteristic of the ship (the RAO) can then be determined during one run of the model in an irregular wave system; otherwise, many runs would be necessary in regular waves of different lengths.

c. If S_ϕ and $|H(\omega_e)|^2$ are known, this is a case in which measurements for response spectrum are carried out on board the ship. The spectral density of the sea can then be calculated with the aid of (6.7).

In view of the fact that measurements of wave height are difficult to carry out, this method may be useful for obtaining seaway data; however, (6.7) applies only to a one-dimensionally irregular seaway when no, or practically no, spreading of the seaway components in other directions takes place.

The most direct approach to verify the superposition principle for ship responses is to conduct model tests in different sea conditions. In each test the wave and motion spectra are measured, and, from these the RAO of the ship can be calculated. If different conditions generate the same RAO, the ship can be described as responding "separately" to each frequency component, the total response being the sum of the responses to the various frequencies. Alternatively, one may use the RAO obtained from one test, together with the wave spectrum from a second test, to predict the motion spectra in the second test. Comparison of these predictions with measured spectra then provides an indication of the degree of validity of the superposition technique.

More specifically, suppose that the energy density of the wave heights at the center of gravity of the ship is given by $S_\zeta(\omega_e)$ and that the RAO for roll is given by $(\phi_a/\zeta_a)^2$. Again, the spectrum must be properly adjusted so that "frequency" is really frequency of encounter. Then the response spectrum of the rolling motion will be

$$S_\phi = S_\zeta(\omega_e)\cdot\left(\frac{\phi_a}{\zeta_a}\right)^2 \tag{6.8}$$

If both spectra are known, this equation yields the magnitude ϕ_a/ζ_a. (Note that the RAO will depend on the angle of incidence of the waves, as well as on ω_w.) In a single test the quantity ϕ_a/ζ_a can always be found from (6.8); however, defining such a ratio of two energy spectra implies nothing about the physical processes involved. In a second test with a different $S_\phi(\omega_e)$, the same ϕ_a/ζ_a will be obtained only if the ship responds "separately" and linearly to each frequency component. Thus a simple direct means is avaliable for checking the principle of superposition and thus the linearity of the whole process.

However, only ϕ_a/ζ_a is found by this procedure. Such a result is to be expected, since the calculation of an energy spectrum from a given test record obscures all phase information. *But for some purposes phase information is necessary; for example, if we want to predict bow emergence, the occurrence of slamming, deck wetness, and so on, we must be able to relate the instantaneous ship position and attitude to the simultaneous free surface deformation.*

Step 6

The significance of the motion spectrum is that it completely defines the motion behavior of a ship in an irregular seaway. *The information that can be gained about waves from a wave spectrum can similarly be obtained for motion from a motion spectrum.*

For example, from the above roll amplitude spectrum, information concerning the average roll amplitude, the average of the one-third highest roll amplitudes or the highest roll amplitude can be obtained as in the case of waves, since the double amplitude distribution of the rolling motion follows the theoretical *Rayleigh distribution.* If the area under the roll amplitude spectrum is denoted by m_0, then, when the rms value of the roll response is $m_0^{1/2}$,

Average roll amplitude,

$$(\phi)_{av} = 1.253m_0^{1/2} \tag{6.9a}$$

Mean of one-third highest amplitudes,

$$(\phi)_{1/3} = 2.000 m_0^{1/2} \tag{6.9b}$$

Mean of one-tenth highest amplitudes,

$$(\phi)_{1/10} = 2.545 m_0^{1/2} \tag{6.9c}$$

Mean of one-hundredth highest amplitudes,

$$(\phi)_{1/100} = 3.336 m_0^{1/2} \tag{6.9d}$$

The numerical constants in (6.9) are the same as in the case of the statistical constants for the wave amplitude expressions. Thus the assumption is made that the "peak-to-peak" (i.e., double amplitude) values of rolling motion follow a Rayleigh distribution.

Since the rms of motion/rms of wave ratio is taken to be the same as amplitude of motion/amplitude of wave or the double amplitude of motion/double amplitude of wave ratio, the area under the response spectrum delivers the mean of the squared responses, as that under the wave spectrum represents the mean of the deviations squared from the zero line. Hence

$$\text{rms of motion} = \sqrt{\text{area under response spectrum}}$$
$$= \sqrt{m_0}$$

since the area under the wave spectrum for a bandwidth of $\Delta\omega_e$, when multiplied by a scalar number for the same frequency band of RAO plot, yields an area representing $\frac{1}{2}\Sigma$ (response amplitude)^2, and the total area under the response spectrum represents the mean square value of the response deviations from the zero line.

Again, as in the case of the wave spectrum, a correction factor introduced in Ref. 139 can be used to take into account the broadness of the motion amplitude spectrum. Thus

Average roll amplitude
$$= 1.253 m_0^{1/2} \times (1 - \varepsilon^2)^{1/2} \tag{6.10a}$$

Mean of one-third highest roll amplitudes
$$= 2.000 m_0^{1/2} \times (1 - \varepsilon^2)^{1/2} \tag{6.10b}$$

Mean of one-tenth highest roll amplitudes
$$= 2.545 m_0^{1/2} \times (1 - \varepsilon^2)^{1/2} \tag{6.10c}$$

Mean of one-hundredth highest roll amplitudes
$$= 3.336 m_0^{1/2} \times (1 - \varepsilon^2)^{1/2} \tag{6.10d}$$

where the correction factor parameter is

$$\varepsilon^2 = \frac{m_0 m_4 - m_2^2}{m_0 m_4} \tag{6.11}$$

and

$$m_n = \int_0^\infty \omega^n S_\phi(\omega_e)\, d\omega_e \tag{6.12}$$

where n is any integer.

Computation of the significant rolling motion involving the correction for the broadness of the response spectrum is illustrated in Table 6.8, using the values of Example 6.3.

In the case of rolling, the motion amplitude spectrum is rather narrow, and the correction $(1 - \varepsilon^2)^{1/2}$ tends to equal 1.0, that is, only a slight correction is necessary.

Figure 6.7 illustrates the response spectrum for the rolling motion, as well as the second and fourth moments of the response spectrum. From (6.11)

$$\varepsilon^2 = \frac{m_0 m_4 - m_2^2}{m_0 m_4} = \frac{0.1709 \times 0.1398 - (0.1101)^2}{0.1709 \times 0.1398}$$

TABLE 6.8 AREAS AND MOMENTS OF RESPONSE SPECTRUM FROM EXAMPLE 6.3

ω_e [sec^{-1}] ①	$S_\phi(\omega_e)$ [deg^2-sec] ②	Simpson's Multiplier ③	Product ④	ω_e^2 [sec^{-2}] ⑤	$\omega_e^2 S_\phi(\omega_e)$ [deg^2 – sec^{-1}] ⑥	Simpson's Multiplier ⑦	Product ⑧	$\omega_e^2 S_\phi(\omega_e)$ [deg^2-sec^{-3}] ⑨	Simpson's Multiplier ⑩	Product ⑪
0.25	0.00×10^{-2}	1	0.00×10^{-2}	0.0625	0×10^{-2}	1	0	0	1	0
0.50	22.80×10^{-2}	4	91.20×10^{-2}	0.2500	5.7×10^{-2}	4	22.8×10^{-2}	1.425×10^{-2}	4	5.700×10^{-2}
0.75	29.90×10^{-2}	2	59.80×10^{-2}	0.5625	16.819×10^{-2}	2	33.638×10^{-2}	9.461×10^{-2}	2	18.922×10^{-2}
1.00	9.40×10^{-2}	4	37.60×10^{-2}	1.0000	9.400×10^{-2}	4	37.600×10^{-2}	9.400×10^{-2}	4	37.400×10^{-2}
1.25	3.52×10^{-2}	2	7.04×10^{-2}	1.5625	5.500×10^{-2}	2	11.000×10^{-2}	8.594×10^{-2}	2	17.188×10^{-2}
1.50	1.60×10^{-2}	4	6.40×10^{-2}	2.2500	3.600×10^{-2}	4	14.400×10^{-2}	8.100×10^{-2}	4	32.400×10^{-2}
1.75	0.63×10^{-2}	2	1.26×10^{-2}	3.0625	1.929×10^{-2}	2	3.858×10^{-2}	5.908×10^{-2}	2	11.816×10^{-2}
2.00	0.28×10^{-2}	4	1.12×10^{-2}	4.0000	1.120×10^{-2}	4	4.480×10^{-2}	4.480×10^{-2}	4	17.920×10^{-2}
2.25	0.14×10^{-2}	2	0.28×10^{-2}	5.0625	0.709×10^{-2}	2	1.418×10^{-2}	3.589×10^{-2}	2	7.178×10^{-2}
2.50	0.10×10^{-2}	4	0.40×10^{-2}	6.2500	0.625×10^{-2}	4	2.500×10^{-2}	3.906×10^{-2}	4	15.624×10^{-2}
2.75	0.06×10^{-2}	1	0.06×10^{-2}	7.5625	0.454×10^{-2}	1	0.454×10^{-2}	3.433×10^{-2}	1	3.433×10^{-2}
		SUM_0	205.16×10^{-2}			SUM_2	132.148×10^{-2}		SUM_4	167.781×10^{-2}

$m_0 = \frac{1}{3} \times \Delta\omega_e \times SUM_0 = \frac{1}{3} \times 0.25 \times 205.16 \times 10^{-2} = 0.1709 \text{deg}^2$
$m_2 = \frac{1}{3} \times \Delta\omega_e \times SUM_2 = \frac{1}{3} \times 0.25 \times 132.148 \times 10^{-2} = 0.1101 \text{ deg}^2\text{-sec}^{-2}$
$m_4 = \frac{1}{3} \times \Delta\omega_e \times SUM_4 = \frac{1}{3} \times 0.25 \times 167.781 \times 10^{-2} = 0.1398 \text{ deg}^2\text{-sec}^{-4}$

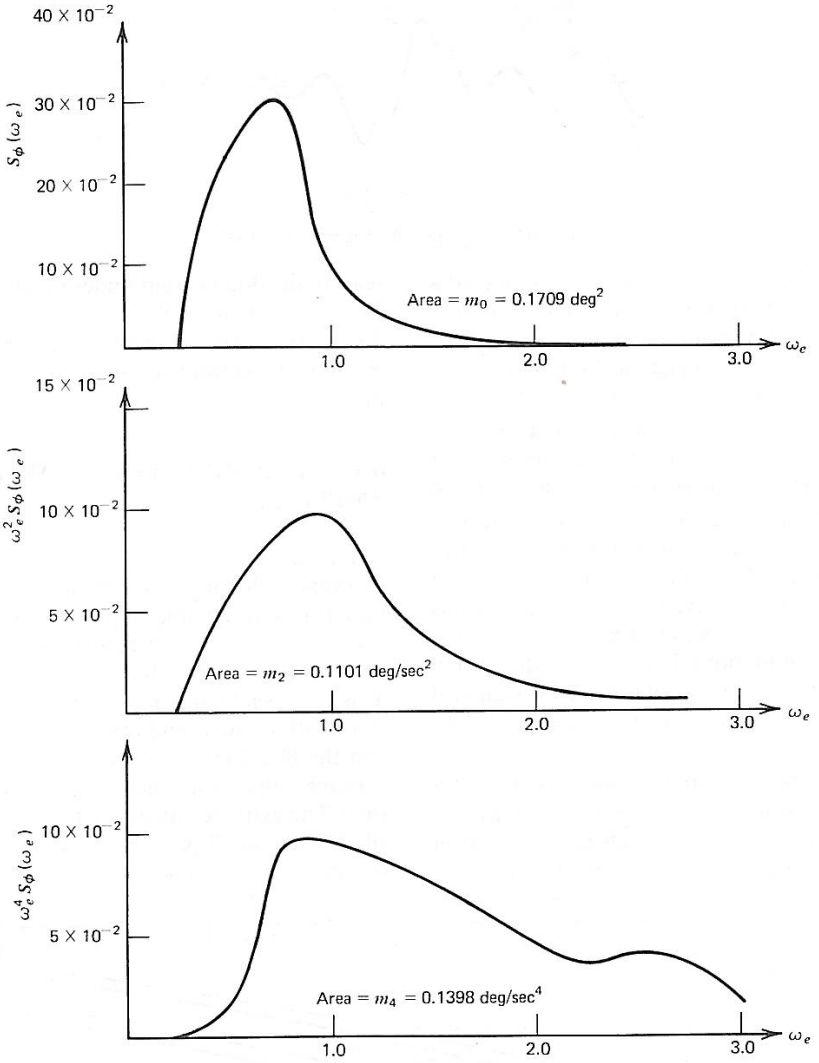


Figure 6.7 Area and second and fourth moments of area under the response spectrum.

so that the correction factor is

$$(1-\varepsilon^2)^{1/2} = (1-0.494)^{1/2} = 0.711$$

The amplitude of the significant rolling motion then

$$= 2.0\sqrt{m_0}(1-\varepsilon^2)^{1/2} = 2.0\sqrt{0.1709} \times 0.711$$
$$= 0.59^\circ$$

and the mean of the one-hundredth highest amplitudes

$$= 3.336\sqrt{m_0}(1-\varepsilon^2)^{1/2} = 3.336\sqrt{0.1709} \times 0.711$$
$$= 0.98^\circ$$

The following remarks can be made regarding the energy spectrum method [127]:

a. When a particular seaway has a broad range of component (encountering) frequencies, the wave components that are long enough to produce appreciable regular wave responses have appreciable effects and are known as important components.

b. Large responses are to be expected from the important component waves having the greatest heights (i.e., near the modified wave spectrum peak).

c. Large responses are to be expected also from the important nearly synchronous components.

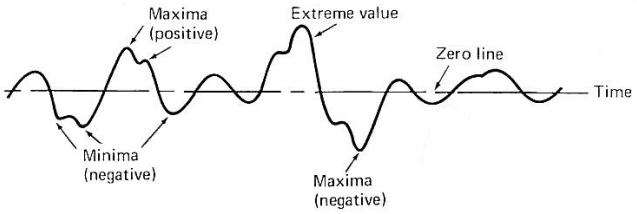


Figure 6.8 A random process $X(t)$ [169].

d. When the motion in an irregular seaway includes responses to important nearly synchronous components, the average amplitude of these responses depends primarily on the magnification factors.

e. Since small ships operate in coastal waters, appropriate coastal wave spectra should be used for the determination of motion characteristics for small vessels operating in particular coastal regions.

f. The motion characteristics of a conventional vessel (i.e., having a length of 300 ft or above) will not change appreciably even if different wave spectra are used for the statistical evaluation of ship motions as long as the significant wave height is used for the comparison of ship motions. However, for the prediction of ship motions from model results a standard formulation for the wave spectrum (e.g., ITTC or ISSC) is preferred.

g. The linear superposition technique for the prediction of ship motions in an irregular seaway has been found to be valid if the RAOs are obtained in relatively mild, regular waves. For the irregular seaway the double amplitudes of motions, even when severe, seem to follow the Rayleigh probability distribution. Therefore even the severe motions in an irregular seaway can be predicted by the spectral method.

6.3 EXTREME VALUE OF MOTION AMPLITUDE

For many random phenomena in the study of the seakeeping characteristics of ships, it is of considerable importance to be able to predict the highest (i.e., the extreme) value of an irregular phenomenon that is expected to occur within a specified period of time. This is especially true in the design considerations for ship motions, wave-induced forces on ship structures, and the like. Figure 6.8 shows the occurrence of the extreme value of a random process as a function of time. The extreme value is obtained when an arbitrarily chosen small probability is exceeded. Figure 6.8 shows that maxima may occur anywhere and also

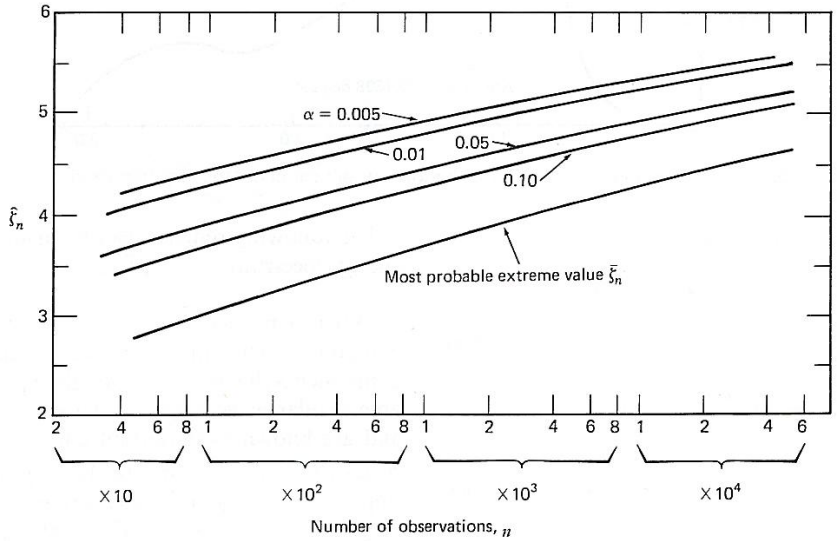


Figure 6.9 Extreme values $\hat{\zeta}_n$ (amplitude) for the Rayleigh distribution ($\varepsilon = 0$) as a function of probability of being exceeded, α [169].

that several maxima can occur during one cycle as defined by zero crossings. On the other hand, the extreme value is defined as the largest value of the maxima that may occur in an observation. In some cases it may be more meaningful to express the extreme value in terms of time rather than as a function of the number of observations.

Figure 6.9 shows the extreme value $\hat{\zeta}_n$ for the Rayleigh distribution for $\alpha = 0.005$, 0.01, 0.05, and 0.10 (where α is the probability that the extreme value exceeds a specified value), together with the most probable largest value $\bar{\zeta}_n$, which is the nondimensional most probable largest value in n observations. For a bandwidth parameter $\varepsilon \leqslant 0.9$, the nondimensional extreme value is obtained by means of equation [169]

$$\hat{\zeta}_n = \left[2 \log_e \left(\frac{\sqrt{1-\varepsilon^2}}{1+\sqrt{1-\varepsilon^2}} \right) \frac{2n}{\alpha} \right]^{1/2} \tag{6.13}$$

The dimensional extreme value of the amplitude is therefore obtained by multiplying $\hat{\zeta}_n$ by $\sqrt{m_0}$, where m_0 is the area under the density spectrum of the random process under consideration.

An extreme value $\hat{\zeta}_n$, defined in this case as the nondimensional extreme value in n observations, for which the probability that the extreme value will exceed $\hat{\zeta}_n$ is α, is determined for a desired probability of being exceeded. Although the decision concerning which probability value should be taken in practice depends on the designer's discretion, a probability of 0.01 appears to be appropriate. See Fig. 6.9.

The most probable largest value of a random process having an arbitrary bandwidth parameter ε, as given in Ref. 169, is

$$\bar{\zeta}_n = \left[2 \log_e \left(\frac{2\sqrt{1-\varepsilon^2}}{1+\sqrt{1-\varepsilon^2}} n \right) \right]^{1/2} \sqrt{m_0} \tag{6.14}$$

for $\varepsilon \leqslant 0.9$. Note that for a narrow band random process (i.e., $\varepsilon = 0$) or for a Rayleigh distribution (6.14) agrees with the equation given in Ref. 139. (See Section 5.5.)

Extreme Values as a Function of Time

The extreme values of a random process are given as functions of the number of observations. For practical design purposes, however, it is often more significant to obtain the extreme value in terms of time instead of the number of observations n, where n can be expressed as a function of time by the following equation:

$$n = (60)^2 \left(\frac{T}{4\pi} \right) \left(\sqrt{\frac{m_2}{m_0}} + \sqrt{\frac{m_4}{m_2}} \right) \tag{6.15a}$$

or

$$n = (60)^2 \left(\frac{T}{4\pi} \right) \left(\frac{1+\sqrt{1-\varepsilon^2}}{\sqrt{1-\varepsilon^2}} \right) \sqrt{\frac{m_2}{m_0}} \tag{6.15b}$$

where T is time in hours. Then the amplitude of the extreme value as a function of time T is given by [169]

$$\hat{\zeta}_n = \left\{ 2 \log_e \left[\frac{(60)^2 T}{(2\pi)\alpha} \sqrt{\frac{m_2}{m_0}} \right] \right\}^{1/2} \sqrt{m_0} \tag{6.16}$$

for small α and the amplitude of the most probable largest value as a function of time T is given as [169]

$$\bar{\zeta}_n = \left\{ 2 \log_e \left[\frac{(60)^2 T}{2\pi} \sqrt{\frac{m_2}{m_0}} \right] \right\}^{1/2} \sqrt{m_0} \tag{6.17}$$

Note that the extreme value, or the most probable largest value as given in (6.16) or (6.17) as a function of time T, is not a function of the broadness parameter ε, but is dependent on the area and the second moment of the energy density spectrum of the random process under consideration.

Example 6.4

For a 520 ft ship the following data are available for pitching motion:

$$\text{Time} = 23.5 \text{ min}$$
$$m_0 = 6.522 \text{ deg}^2$$
$$m_2 = 3.562 \text{ deg}^2\text{-sec}^{-2}$$
$$m_4 = 2.276 \text{ deg}^2\text{-sec}^{-4}$$

Find out the most probable largest pitching motion.

Solution:

By means of (6.15a) the number of observations is found:

$$n = 172$$

Therefore, using (6.17), the most probable largest pitching motion is

$$3.20\sqrt{m_0} = 8.15^\circ$$

However, the observed extreme value of the pitching amplitude, as recorded during observations, is 9.45°, which is 16% more than the predicted value of 8.15°.

This is expected, since the probability of occurrence of a value greater than the most probable value is rather high. Therefore the extreme value with a certain probability α should be estimated rather than the most probable largest value. If α is selected as 0.01, this means that only one among 100 sister ships operating in similar environmental conditions may have a pitching motion (or bending moment) greater than the predicted value in a specified period of time. The chance that the extreme value will exceed the most probable largest value is high, and theoretically this probability for a random process having a narrow band spectrum is 0.63. Therefore the most probable largest value is not suitable for the design consideration. On the other hand, the extreme value for $\alpha = 0.01$ is between 35 and 40% greater than the most probable largest value and therefore can be used for the design requirement [169].

In conclusion, it can be said that the significant values of the motions of a ship are most useful as design criteria. Statistical prediction of a ship's motion is the only reasonable way of expressing the random motion. However, it should be emphasized that the prediction is based on a linear theory of ship motions that may not be valid for extreme sea conditions. Fortunately, ship motions have been found to be linear in many wave conditions, so that an assumption of linearity may be valid. With this assumption the significant value and other statistical characteristics of motions can be obtained, and the time history of the motion is not necessary.

Chapter

Seven

DYNAMIC EFFECTS

7.1 GENERAL

In the preceding chapters the motions of heave, pitch, and roll were dealt with. All these motions, along with their associated effects, are known as *dynamic effects*, which, again, can be further classified into vertical and rolling effects. Vertical effects deal with the heaving and pitching motions and their related effects, whereas, rolling effects include those of the angular "rolling" motions. In general, the dynamic effects in connections with ship motion may be listed as follows:

1. *Shipping of green water* over the bow, especially at deep drafts.
2. *Slamming* or sudden impact on the bottom of the forefoot, particularly at ballast drafts.
3. *Acceleration effects*, especially vertical accelerations (due to pitch and heave) at critical points, such as accommodation areas, bridge deck, or machinery space. Vertical and lateral accelerations may also result from rolling motion.
4. *Speed loss* in a seaway. In addition to the available power, deck wetness and slamming can be deciding factors in sustained sea speed.
5. *Free racing* of the engine due to propeller shaft emergence.

The study of dynamic effects involved chiefly the following investigations:

a. Frequencies of occurrence of deck wetness and slamming.
b. Magnitude of impact pressure caused by slamming.
c. Response of ship bottom plating to slam impact.
d. Hull response (stress and acceleration) due to slamming.
e. Freeboard and deck wetness.
f. Severity of green water on the deck.
g. Determination of added resistance in a seaway operation.

7.2 VERTICAL MOTION

With reference to Fig. 7.1 for notation, the *vertical motion* of any point along the ship length in a train of regular waves is a simple harmonic motion. Hence the expression for the vertical motion of the CG of the vehicle is given by

$$z = z_a \sin \omega_e t \tag{7.1}$$

or

$$z_\xi = (z_\xi)_a \sin \omega_e t \tag{7.2}$$

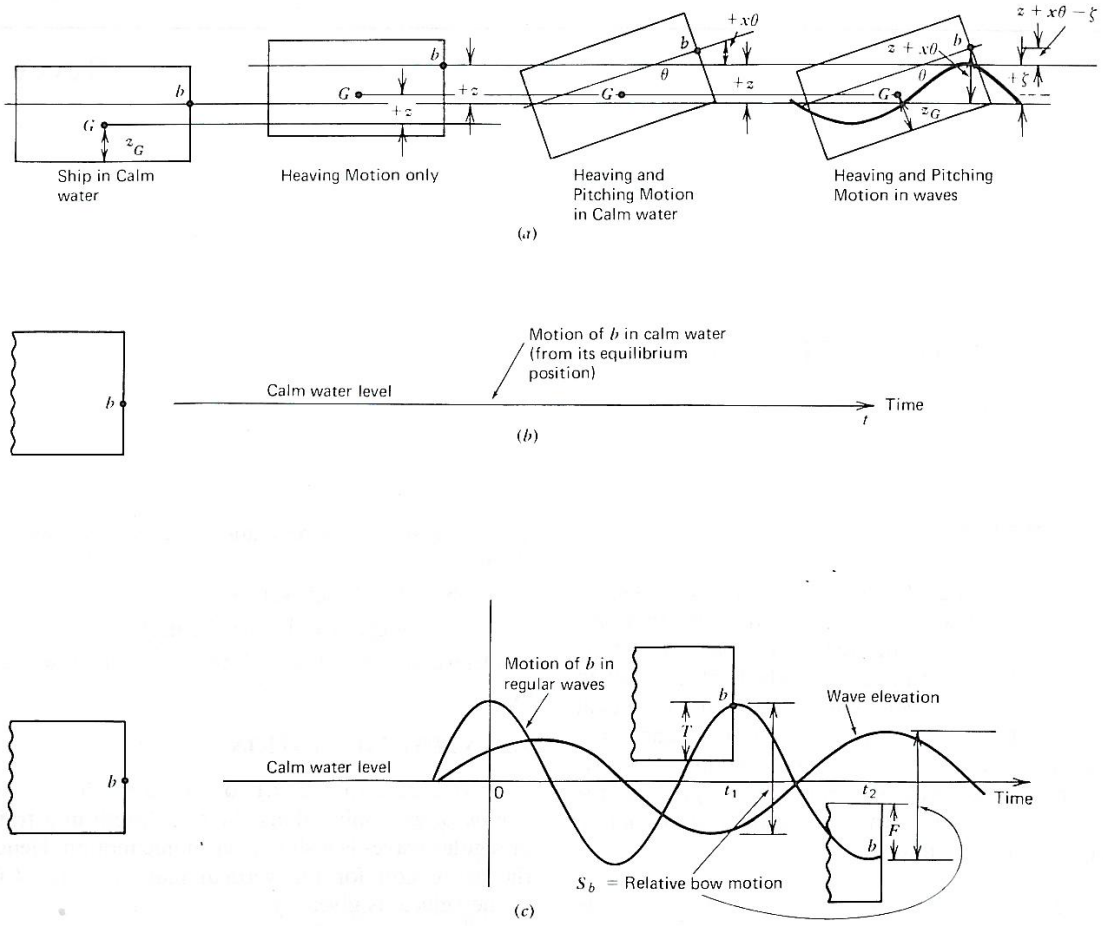
for any point at a distance of ξ from the CG of the ship.

If a ship is assumed to be moving in a *regular seaway*, the bow motion, denoted by z_b, is given by

$$\begin{aligned} z_b &= z + \xi \sin \theta \\ &\approx z + \xi\theta \text{ for small angle of pitch} \end{aligned} \tag{7.3}$$

where ξ is the horizontal distance of the point under consideration from the ship CG, the *pitching angle* θ is in radians and assumed to be small, and z is the *heaving motion*. Both z and θ are positive when the bow is displaced upward. One should note that for a different co-ordinate system the expression for z_b will also be different. For example, the bow motion corresponding to the co-ordinate system of Fig. 9.1 is known to be as follows:

$$z_b = z - \xi\theta.$$



Notes: 1. At time t_1 the bow will emerge, since the motion of point b (i.e., displacement) relative to wave elevation is greater than draft T.

2. At time t_2 the deck edge will immerse into water, since the motion of point b (i.e., displacement) relative to wave elevation is greater than freeboard F.

Figure 7.1 Relative bow motion.

When the point b, located at the intersection of the bow and the load waterline, is at the still water level, we say that there is no bow motion (i.e., $z_b = 0$). Similarly, when the bow (i.e., point b) is above the still water level, $z_b > 0$; and when b is below the still water level, $z_b < 0$.

Bow emergence takes place when z_b is greater than draft T; similarly, if $z_b < -F$ (where F = freeboard), the deck will go into water.

In a regular seaway the heaving and pitching motions are expressed as

$$z = z_a \cos(\omega_e t + \varepsilon_z) \tag{7.4}$$

and

$$\theta = \theta_a \cos(\omega_e t + \varepsilon_\theta) \tag{7.5}$$

where ε_z is the phase angle for heaving motion relative to wave motion, and ε_θ is the phase angle for pitching motion relative to wave motion. Therefore the bow motion z_b is given as

$$\begin{aligned} z_b &= z + \xi\theta \\ &= z_a \cos(\omega_e t + \varepsilon_z) + \xi\theta_a \cos(\omega_e t + \varepsilon_\theta) \\ &= (z_b)_a \cos(\omega_e t + \varepsilon_b) \end{aligned} \tag{7.6}$$

where

$$(z_b)_a = \sqrt{z_a^2 + (\xi\theta_a)^2 + 2z_a\xi\theta_a \cos(\varepsilon_z - \varepsilon_\theta)} \tag{7.7}$$

and

$$\tan \varepsilon_b = \frac{z_a \sin \varepsilon_z + \xi\theta_a \sin \varepsilon_\theta}{z_a \cos \varepsilon_z + \xi\theta_a \cos \varepsilon_\theta} \tag{7.8}$$

(see section 2.4).

The determination of forefoot emergence or deck immersion should be based on the bow motion in relation to the wave elevation at the bow.

If the ship is heading into waves, then, in the coordinate system moving with the ship, the wave elevation is described as [see also (3.20)]

$$\zeta = \zeta_a \cos(k_e x - \omega_e t) \tag{7.9}$$

where k_e is the effective wave number, that is, $2\pi/(L_w)_e$ and $(L_w)_e = L_w/\cos\mu$.

The water elevation at the bow at any given instant of time is given by

$$\zeta_b = \zeta_a \cos(k_e \xi - \omega_e t) \tag{7.10}$$

Example 7.1

Given:

L = 450 ft
μ = 180° (i.e., head sea condition)
L_w = 420 ft
ξ = distance of bow from ship CG = 225 ft
h_w = 20 ft
T = 25 ft
F = freeboard = 20 ft
V_s = 20 knots (33.78 ft/sec)

Also obtained either from computations (see Example 4.7, 4.8) or experimental results are the following:

$z_a = 5$ ft
$\theta_a = 0.15$ rad
$\varepsilon_z = -40°$
$\varepsilon_\theta = 15°$

Determine the vertical motion of the bow.

Solution:

The frequency of encounter is

$$\omega_e = \omega_w\left(1 - \frac{\omega_w V}{g}\cos\mu\right) = 1.2 \text{ rad/sec}$$

where

$$\omega_w = \sqrt{\frac{2\pi g}{L_w}} = 0.694 \text{ rad/sec}$$

The vertical motion of the bow Z_b is computed in Table 7.1 and shown in Fig. 7.2. The amplitude of the resultant bow motion can be obtained analytically as follows:

$$(z_b)_a = \sqrt{z_a^2 + (\xi\theta_a)^2 + 2z_a\xi\theta_a\cos(\varepsilon_z - \varepsilon\theta)}$$

where

$$\varepsilon_b = \tan^{-1}\frac{z_a \sin\varepsilon_z + \xi\theta_a \sin\varepsilon_\theta}{z_a\cos\varepsilon_z + \xi\theta_a\cos\varepsilon_\theta}$$

$$= \tan^{-1}\frac{5\sin(-40°) + 225 \times 0.15\sin(15°)}{5\cos(-40°) + 225 \times 0.15\cos(15°)}$$

$$= 8.62° \text{ (or } 0.15 \text{ rad)}$$

Also,

$$z_b = (z_b)_a \cos(\omega_e t + \varepsilon_b)$$

Therefore,

$$z_b = (z_b)_a \cos(\omega_e t + 8.62°)$$

and

z_b is maximum when $\cos(\omega_e t + 8.62°)$ is 1.0 or when

$\omega_e t + 8.62° = 0°$ or 360°

or

$\omega_e t = -8.62°$ or 351.38°

TABLE 7.1

t [sec]	$\omega_e t$ [rad]	$z = z_a \cos(\omega_e t + \varepsilon_z)$ $= 5\cos(\omega_e t - 0.698)$ [ft]	$\xi\theta = \xi\theta_a \cos(\omega_e t + \varepsilon_\theta)$ $= 225 \times 0.15\cos(\omega_e t + 0.262)$ [ft = rad]	$z_b = z + \xi\theta$ [ft]
①	②	③	④	⑤ = ③ + ④
$0/\omega_e$	0	3.83	32.60	36.4
$0.25\pi/\omega_e$	0.25π	4.98	16.86	21.8
$0.50\pi/\omega_e$	0.50π	3.21	− 8.75	− 5.5
$0.75\pi/\omega_e$	0.75π	− 0.44	− 92.23	− 29.67
π/ω_e	1.00π	− 3.83	− 32.60	− 36.43
$1.25\pi/\omega_e$	1.25π	− 4.98	− 16.86	− 21.84
$1.50\pi/\omega_e$	1.50π	− 3.21	8.75	5.54
$1.75\pi/\omega_e$	1.75π	0.44	29.23	29.67
$2.00\pi/\omega_e$	2.00π	3.83	32.59	36.42
$2.25\pi/\omega_e$	2.25π	4.98	16.86	21.84
$2.50\pi/\omega_e$	2.50π	3.21	− 8.75	− 5.54

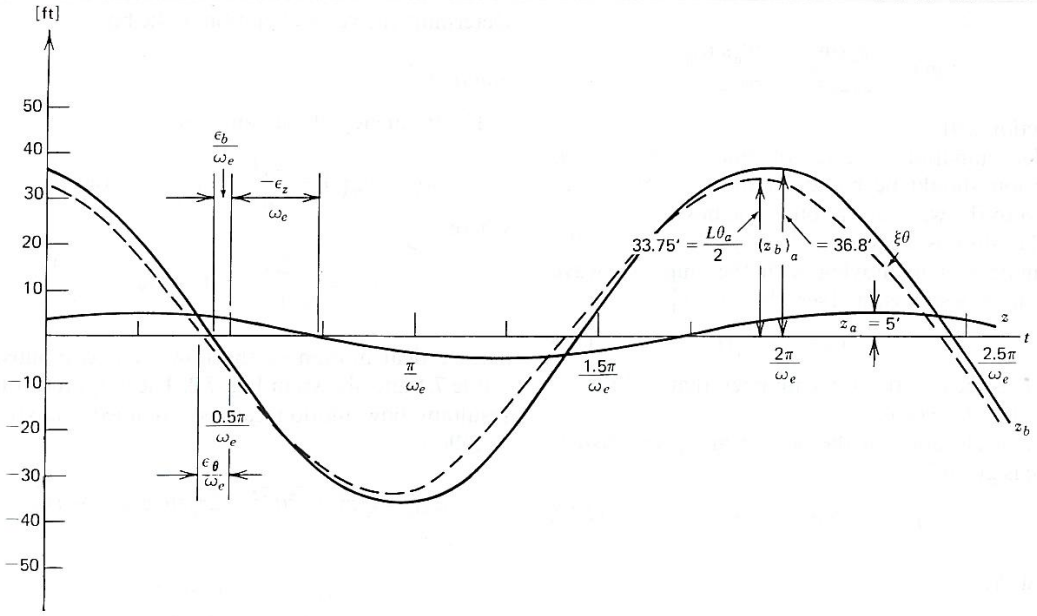


Figure 7.2 Absolute bow motion (i.e., motion of point *b*).

Thus, for

$$\omega_e t = 351.38°,$$
$$z_b = z_a \cos(\omega_e t + \varepsilon_z) + \xi\theta_a \cos(\omega_e t + \varepsilon_\theta)$$
$$= 5\cos(351.38° - 40°) + 225 \times 0.15\cos(351.38° + 15°)$$
$$= 36.8\,\text{ft}$$
$$= (z_b)_a$$

that is,

$$z_b = 36.8\cos(\omega_e t + 0.15)$$

and this is evaluated in Table 7.2.

Vertical Velocity

The *vertical velocity* in a train of regular waves is also a simple harmonic motion. Since motion in regular waves is a simple harmonic motion and is expressed as

$$z_\xi = (z_\xi)_a \sin \omega_e t \tag{7.11}$$

the vertical velocity is

$$\dot{z}_\xi = \omega_e (z_\xi)_a \cos \omega_e t \tag{7.12}$$

The amplitude of the vertical velocity $\dot{z}_\xi$ at any point along the length of the ship is given by the expression

$$(\dot{z}_\xi)_a^2 = (\dot{z})_a^2 + \xi^2(\dot{\theta})_a^2 + 2(\dot{z})_a(\dot{\theta})_a \xi \cos\varepsilon \tag{7.13}$$

where

$(\dot{z})_a$ = amplitude of heaving velocity at the CG [ft/sec]
$(\dot{\theta})_a$ = amplitude of pitching velocity at the CG [deg/sec]
ξ = longitudinal distance of the point in question from the CG [ft]
ε = phase lag of heave after pitch [deg]

For the case of regular waves, if the amplitude of heaving motion or of the vertical motion at any

TABLE 7.2

$\omega_e t$ [rad]	$t = \frac{\omega_e t}{\omega_e} = \frac{①}{1.2}$ [sec]	$Z_b = 36.8\cos(\omega_e t + 0.15)$ [ft]
①	②	③
0	0	36.4
0.125π		
0.250π	0.208π	21.8
0.500π	0.417π	− 5.5
0.750π	0.625π	− 29.6
1.000π	0.833π	− 36.4
1.250π	1.042π	− 21.8
1.500π	1.250π	+ 5.5
1.750π	1.458π	+ 29.6
2.000π	1.667π	+ 36.4
2.250π	1.875π	+ 21.8
2.500π	2.083π	− 5.5

Note: The forefoot has emerged when $z_b - T$ is positive.

point is known, the amplitude of the corresponding velocity can be found by using the expression

$$(\dot{z})_a = \omega_e z_a$$

or

$$(\dot{z}_\xi)_a = \omega_e (z_\xi)_a \tag{7.14}$$

The vertical velocity at the bow in relation to the water surface is known as the *relative vertical velocity*, and the amplitude of the relative vertical velocity is expressed by the symbol $\dot{s}_a$.

Vertical Acceleration

Like vertical velocity, the *vertical acceleration* of any point along the length of a ship in a regular train of waves is harmonic in nature. Therefore the expression for the acceleration is given by

$$\ddot{z} = \ddot{z}_a \sin \omega_e t \tag{7.15a}$$

for the CG of the ship or by

$$\ddot{z}_\xi = (\ddot{z}_\xi)_a \sin \omega_e t$$

for any point at a distance of ξ from the CG of the ship.

The amplitude of vertical acceleration $(\ddot{z}_\xi)_a$ at any point along the ship length is given by

$$(\ddot{z}_\xi)_a^2 = (\ddot{z})_a^2 + \xi^2 (\ddot{\theta})_a^2 + 2(\ddot{z})_a (\ddot{\theta})_a \xi \cos \varepsilon \tag{17.15b}$$

where $(\ddot{z})_a$ is the amplitude of heaving acceleration at the CG, and $(\ddot{\theta})_a$ is the amplitude of pitching acceleration at the CG. For the case of *regular waves*, if the amplitude of heave or the vertical motion at any point is known, the amplitude of the corresponding acceleration is determined as follows:

$$(\ddot{z})_a = \omega_e^2 (z_a)$$

or

$$(\ddot{z}_\xi)_a = \omega_e^2 (z_\xi)_a \tag{7.15c}$$

The vertical acceleration at the bow in relation to the water surface is known as the *relative bow acceleration*, and the amplitude of the relative bow acceleration is expressed by the symbol $\ddot{s}_a$.

For most practical applications it is assumed that motion, velocity, and acceleration amplitudes (double) follow the *Rayleigh distribution*; that is, the probability that a certain pitch amplitude θ_a exceeds a value θ_a^* is given by

$$p\{\theta_a \geqslant 0_a^*\} = e^{-[(\theta_a^*)^2/2m_{0\theta}]} \tag{7.16}$$

where $m_{0\theta}$ is the variance of the pitch angles, which is the area under the response spectrum for the pitching motion.

7.3 RELATIVE BOW MOTION

The study of relative bow motion (or displacement) is of particular interest in regard to the seakeeping quality of a vessel because of two derived quantities:

1. Foredeck immersion, as an index of shipping of water.
2. Forefoot emergence, as a rough indication of the possibility of slamming.

For a particular forward freeboard or draft these quantities can easily be worked out statistically from the response spectra.

The immersion and emergence of the bow or the relative bow motions in waves are determined by the vertical distance between the wave surface at any location at the bow or stern and the at-rest waterline at the same region, as shown in Fig. 7.1*a*. The relative bow motion is normally defined as the motion at the fore perpendicular or very near it (Fig. 7.1*b*).

When the heaving and pitching motions are known in both amplitude and phase in relation to the wave surface, the relative motion (i.e., the vertical displacement of any point at any location in relation to the wave surface) can be determined by the following expression:

$$s_\xi = z_\xi - \zeta_\xi \tag{7.17}$$

where s_ξ is the relative motion of the point in question, which is located at a distance of ξ from the CG of the ship in the x-direction; z_ξ is the vertical motion of the point (i.e., $z + \xi\theta$); and ζ_ξ is the wave motion at the point under consideration. Then the position of the bow in relation to the waves is given as

$$s_b = z_b - \zeta_b \tag{7.18}$$

When $z_b > \zeta_b$, we have $s_b > 0$. Thus, when the bow elevation is greater than the wave elevation, point b (Fig. 7.1) will be above water, whereas when the bow elevation is less than the wave elevation, point b will submerge. Therefore, if the immersion of point b exceeds the magnitude of *freeboard*, the deck will immerse into water; similarly, if the emergence of point b exceeds the magnitude of draft, forefoot emergence will take place. Now, using the expressions for ζ_b and z_b, we have [see (7.10)]

$$\begin{aligned} s_b &= z_b - \zeta_b \\ &= (z_b)_a \cos(\omega_e t + \varepsilon_b) - \zeta_a \cos(k_e \xi - \omega_e t) \\ &= (z_b)_a \cos(\omega_e t + \varepsilon_b) \\ &\quad - \zeta_a \cos\left(\frac{2\pi\xi}{L_w} + \omega_e t\right) \text{for head sea conditions} \end{aligned} \tag{7.19}$$

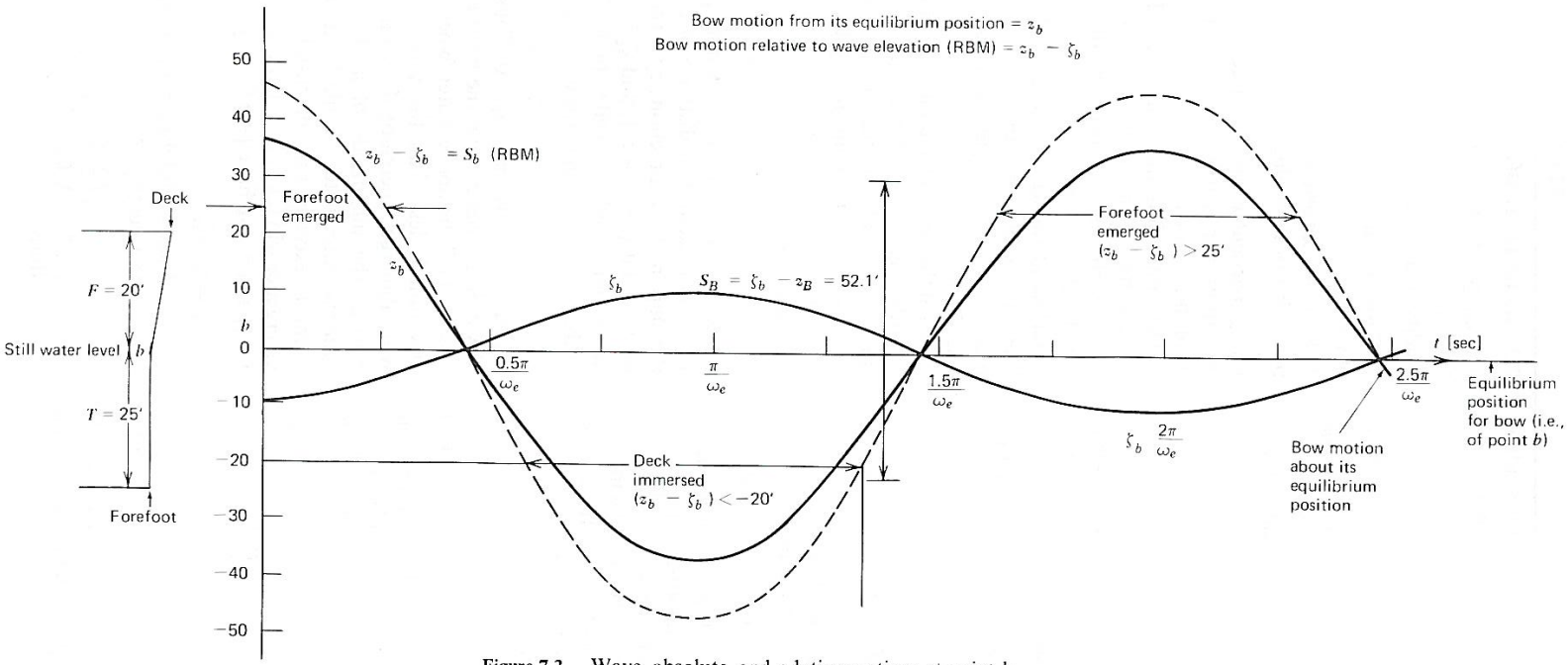


Figure 7.3 Wave, absolute, and relative motions at point b.

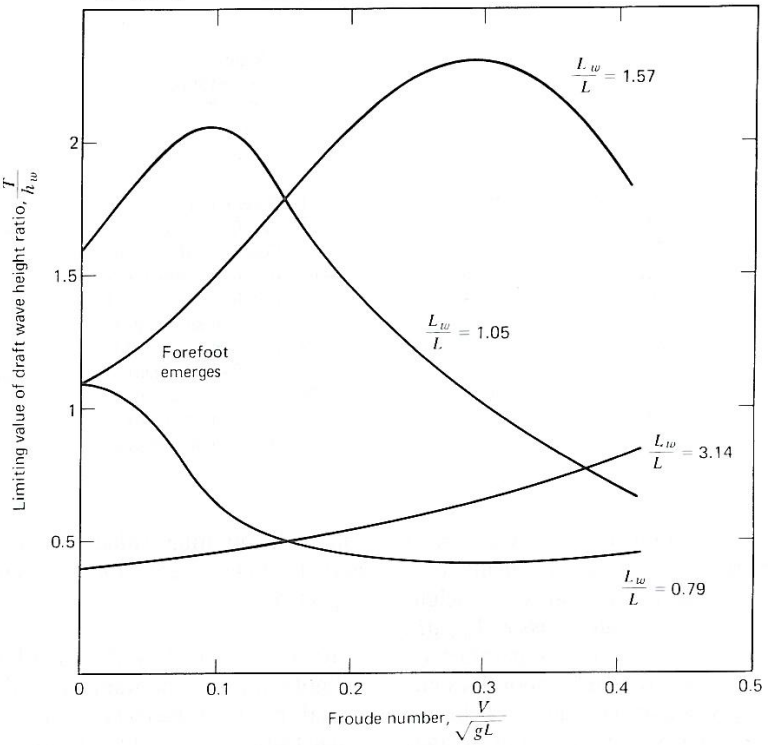


Figure 7.4 Condition for forefoot emergence [203].

or

$$s_b = (s_b)_a \cos(\omega_e t + \varepsilon_s)$$

where

$$(s_b)_a = \sqrt{(z_b)_a^2 + (\zeta_a)^2 - 2(z_b)_a \zeta_a \cos(k_e \xi - \varepsilon_b)} \quad (7.20)$$

and

$$\tan \varepsilon_s = \frac{\zeta_a \sin(k_e \xi) - (z_b)_a \sin \varepsilon_b}{\zeta_a \cos(k_e \xi) - (z_b)_a \cos \varepsilon_b} \quad (7.21)$$

Figure 7.2 can, therefore, be extended to include the wave motion as illustrated in Fig. 7.3, which shows the bow motion from the equilibrium position z_b, the wave motion, ζ_b, and the relative bow motion, s_b.

Consider the relative bow motion, using the values from Example 7.1. Thus, from (7.20)

$$(s_b)_a = \sqrt{36.8^2 + 10^2 - 2 \times 36.8 \times 10 \cos\left(\frac{2\pi}{420} \times 225 - 0.15\right)}$$

$$= 46.78 \text{ ft.}$$

$$\tan \varepsilon_s = \frac{10 \sin[\pi(450/420)] - 36.8 \sin(0.15 \text{ rad})}{10 \cos[\pi(450/420)] - 36.8 \cos(0.15 \text{ rad})}$$

$$= 0.168$$

or

$$\varepsilon_s = 9.529^\circ \text{ (or } 0.166 \text{ rad)}$$

Therefore the elevation of the wave surface at the bow above the forefoot is obtained from (7.19), that is,

$$s_b = 46.78 \cos(\omega_e t + 0.166)$$

The values from this expression are tabulated in Table 7.3.

When the wave crest is at the midship section (i.e., when $t = 0$), then

$$s_b = 46.14 \text{ ft}$$

or

$$s_b - T = 46.14 - 25 = +21.14 \text{ ft}$$

Since $s_b - T$ is positive, the forefoot will emerge from the water. (See Fig. 7.1.) Similarly, at $t = \pi/\omega_e$, we have $s_b = -46.14$ ft from Table 7.3, or

$$s_b + F = -26.14 \text{ ft}$$

Since the result is again negative, bow immersion takes place in this case.

Note: Column ④ can also be obtained from the plots of ζ_b and z_b.

TABLE 7.3

t [sec] ①	$\omega_e t$ [rad] ②	$\omega_e t + \varepsilon_s$ ② + 0.166 [rad] ③	$S_b =$ 46.78 cos $(\omega_e t + 0.166)$ [ft] ④	Relative Forefoot Motion, $S_b - T$ [ft] ⑤	Relative Deck Motion, $F + S_b$ [ft] ⑥
0	0	0.166	46.14	21.2 (forefoot emerged)	66.2 (deck above water)
$\pi/4\omega_e$	0.25π	0.951	27.15	2.1 (forefoot emerged)	47.1 (deck above water)
$\pi/2\omega_e$	0.50π	1.737	− 7.75	− 32.7 (forefoot submerged)	12.3 (deck above water)
$3\pi/4\omega_e$	0.75π	2.522	− 38.10	− 63.1 (forefoot submerged)	− 18.1 (deck below water)
π/ω_e	1.00π	3.308	− 46.14	− 72.2 (forefoot submerged)	− 26.2 (deck below water)
$5\pi/4\omega_e$	1.25π	4.093	− 27.15	− 52.1 (forefoot submerged)	− 7.1 (deck below water)
$3\pi/2\omega_e$	1.50π	4.878	7.75	− 17.3 (forefoot submerged)	27.7 (deck above water)
$7\pi/4\omega_e$	1.75π	5.664	38.10	13.1 (forefoot emerged)	58.1 (deck below water)
$2\pi/\omega_e$	2.00π	6.449	46.14	21.2 (forefoot emerged)	66.2 (deck below water)
$9\pi/4\omega_e$	2.25π	7.235	27.15	2.1 (forefoot emerged)	47.1 (deck above water)
$5\pi/2\omega_e$	2.50π	8.020	− 7.75	− 32.7 (forefoot submerged)	12.3 (deck above water)

Note: Column ④ can also be obtained from the plots of ζ_b and z_b.

For the head sea condition, Fig. 7.4 is a typical sketch obtained from simple analytical calculations, showing the limiting value of the draft/wave height ratio as a function of the *Froude number*, $V/\sqrt{gL}$, with wavelength to ship length as parameters. As can be seen from this figure, the forefoot does not emerge if the limiting value of the draft/wave height ratio T/h_w, as obtained from the curves is smaller than the actual T/h_w.

Example 7.2

Given:

$L = 400\,\text{ft}$
$T = 25\,\text{ft}$
$V_s = 20$ knots
$L_w = 628\,\text{ft}$
$h_w = 20\,\text{ft}$
$\mu = 180°$ (i.e., head sea)

Determine whether or not the forefoot of the ship emerges.

Solution:

$$\text{Froude number, } F_n = \frac{V}{\sqrt{gL}} = \frac{20 \times 1.689}{\sqrt{32.2 \times 400}} = 0.3$$

$$\text{Ratio of wavelength of ship length, } \frac{L_w}{L} = \frac{630}{400} = 1.57$$

From Fig. 7.4, the limiting value of the ratio is

$$\frac{T}{h_w} = 2.3$$

However, the actual value of T/h_w is $25/20 = 1.25$. Since the limiting value (2.3) is greater than the actual value (1.25), forefoot emergence can be expected.

If the speed of this ship is voluntarily reduced to 7 knots, the Froude number F_n (i.e., the nondimensional speed parameter) becomes 0.1, and the limiting value from Fig. 7.4 is 1.5. The forefoot is still expected to emerge. However, if the draft of the ship is increased so that $T/h_w > 1.5$ (i.e., $T > 30\,\text{ft}$), the forefoot will not emerge. Thus the probability of bow emergence increases with reduction in the draft of the ship.

On the other hand, the speed at which the forefoot will not emerge (with the draft given originally as 25 ft) is about 3 knots.

Phase Difference between Wave Motion and Bow Motion

If the wave motion and the bow motion are 180° out of phase, they oppose each other. On the other hand, if the phase difference is 0° or 360°, the bow will move along with the wave, that is, it will ride the wave. If the phase angle is 180°, the downward-moving bow will meet an upward-moving wave, and this is a rather critical condition.

For the regular head sea condition, the simplified analytical solution gives the phase difference between the wave motion and the bow motion, as shown in Fig. 7.5. Coupling between heave and pitch should not be neglected in such calculations, since phase relations between the wave and bow motions are greatly influenced by the coupling effects.

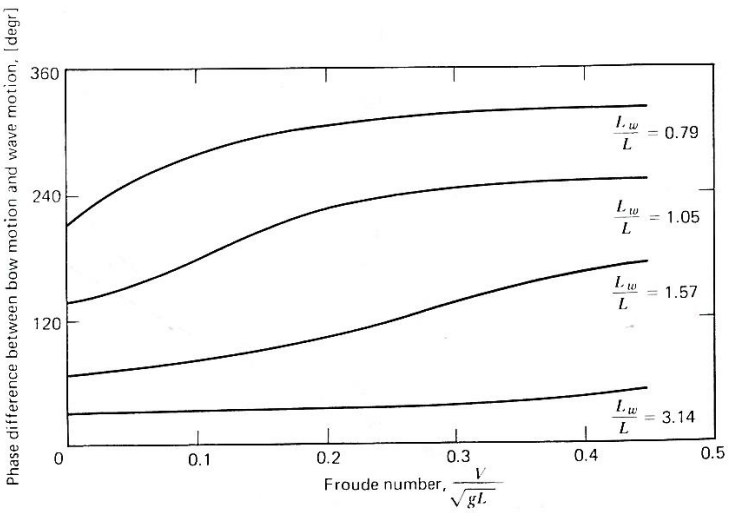


Figure 7.5 Phase difference between bow and wave motions [203].

Relative Bow Velocity (in Head Seas)

The relative velocity of a ship is an important consideration in the determination of the dynamic effects of a ship. Therefore let us consider the vertical velocity of the wave at the bow (say at point b in Fig. 7.1). From (7.10)

$$\zeta_b = \zeta_a \cos\left(2\frac{\pi}{L_e}\xi - \omega_e t\right) \tag{7.22}$$

since $\mu = 180°$ and the vertical velocity of the wave for any heading is given by

$$\dot{\zeta}_b = +\omega_e \zeta_a \sin\left(2\frac{\pi}{L_e}\xi - \omega_e t\right) \tag{7.23}$$

$$= -\omega_e \zeta_a \sin\left(\omega_e t + \frac{2\pi}{L_w}\xi\right) \qquad \text{for } \mu = 180°$$

where $\dot{\zeta}$ is the wave velocity, and ω_w is the wave frequency. Let us assume here that $\dot{\zeta}_b$ is positive when the motion is in the upward direction. Now the resultant velocity of the bow due to heaving and pitching motion is [see (7.6)]

$$\dot{z}_b = z + \xi\dot{\theta}$$
$$= -(z_b)_a \omega_e \sin(\omega_e t + \varepsilon_b) \tag{7.24}$$

assuming linear motions. In (7.24), z_b is also to be positive when the motion is in the upward direction. The velocity of the bow relative to that of the wave is the time derivative of (7.19), that is,

$$\dot{s}_b = \dot{z}_b - \dot{\zeta}_b$$

and for the head sea condition (i.e., $\mu = 180°$)

$$\dot{s}_b = -(z_b)_a \omega_e \sin(\omega_e t + \varepsilon_b) + \omega_e \zeta_a \sin\left(\omega_e t + \frac{2\pi}{L_w}\xi\right)$$
$$= (\dot{s}_b)_a \cos(\omega_e t + \varepsilon_{\dot{s}}) \tag{7.25}$$

where

$$(\dot{s}_b)_a = \sqrt{\omega_e^2 (z_b)_a^2 + \omega_e^2 \zeta_a^2 - 2(z_b)_a \zeta_a \omega_e^2 \cos\left(\frac{2\pi}{L_w}\xi - \varepsilon_b\right)} \tag{7.26}$$

and

$$\tan \varepsilon_{\dot{s}} = \frac{(z_b)_a \omega_e \cos \varepsilon_b - \omega_e \zeta_a \cos[(2\pi/L_w)\xi]}{-(z_b)_a \omega_e \sin \varepsilon_b + \omega_e \zeta_a \sin[(2\pi/L_w)\xi]} \tag{7.27}$$

It is found by both theoretical investigations and model tests that bow emergence is always associated with a large relative bow velocity. Since, however, the relative bow velocity depends on the phase difference between the wave velocity at the bow and the bow velocity, it is obvious that a large relative bow velocity occurs when the phase difference between these two velocities is 180°, since the velocities will then tend to oppose each other.

Example 7.3

The data from Example 7.1 yield the following:

$$\dot{z}_b = -36.8\omega_e \sin(\omega_e t + 0.15)$$
$$\dot{z}_b = -36.8\omega_e \sin(\omega_e t + 0.15)$$

and

$$\zeta_b = 10\cos(\omega_e t + 1.071\pi)$$

$$\dot{\zeta}_b = 10\omega_e \sin(\omega_e t + 1.071\pi)$$

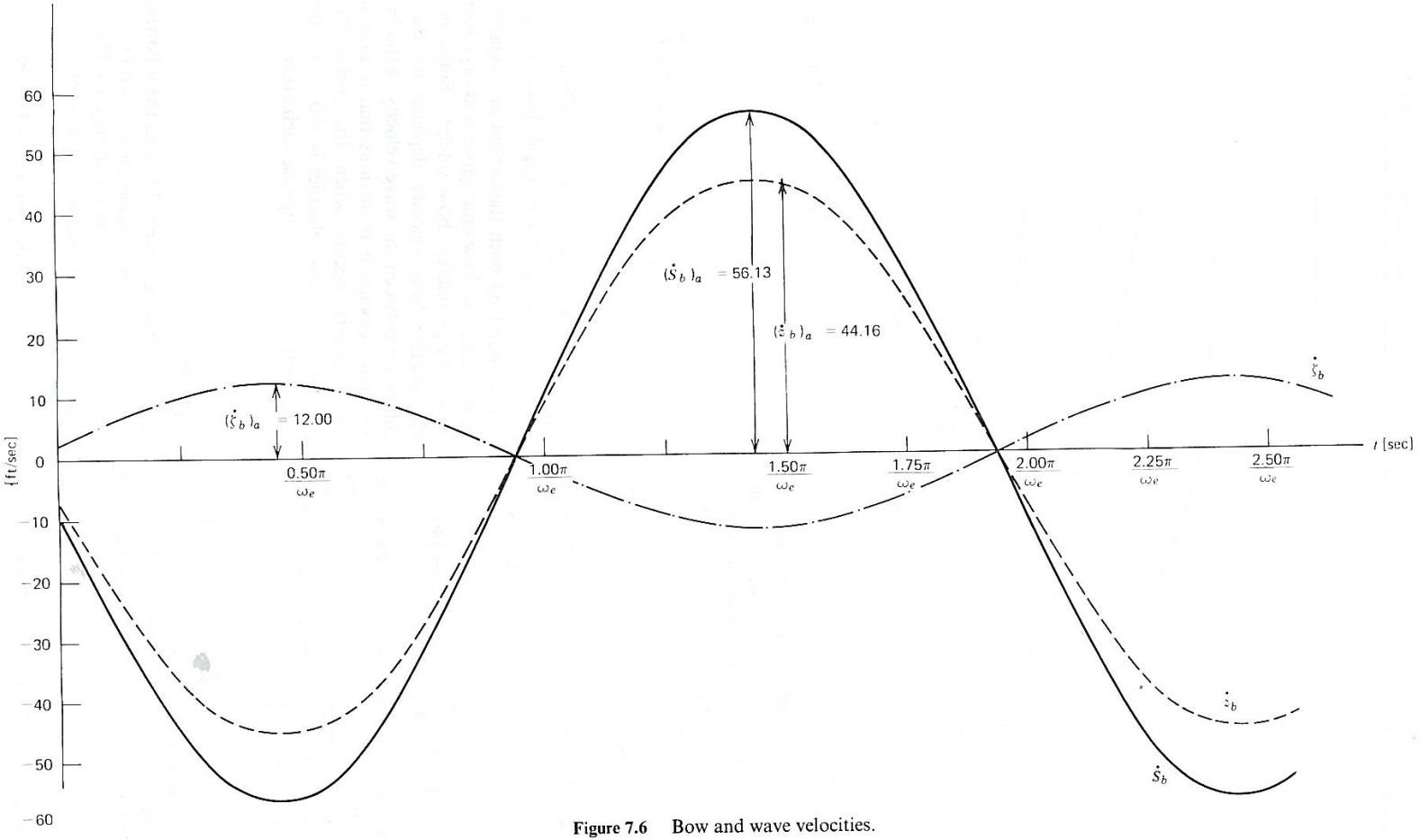


Figure 7.6 Bow and wave velocities.

TABLE 7.4

t [sec] ①	$\omega_e t$ [rad] ②	$\dot{z}_b =$ $-44.16\sin(\omega_e t + 0.15)$ [ft/sec] ③	$\dot{\zeta}_b =$ $-12.00\sin(\omega_e t + 1.071\pi)$ [ft/sec] ④	$\dot{S}_b =$ $56.13\cos(\omega_e t + 1.7365)$ [ft/sec] ⑤
0	0	− 6.61	2.66	− 9.27
$0.25\pi/\omega_e$	0.25π	− 35.55	10.16	− 45.71
$0.50\pi/\omega_e$	0.50π	− 43.66	11.70	− 55.36
$0.75\pi/\omega_e$	0.75π	− 26.20	6.39	− 32.59
π/ω_e	1.00π	6.61	− 2.66	9.27
$1.25\pi/\omega_e$	1.25π	35.55	− 10.16	45.71
$1.5\pi/\omega_e$	1.5π	43.66	− 11.70	55.36
$1.75\pi/\omega_e$	1.75π	26.20	− 6.39	32.59
$2.00\pi/\omega_e$	2.00π	− 6.61	2.67	− 9.27
$2.25\pi/\omega_e$	2.25π	− 35.55	10.16	− 45.71
$2.50\pi/\omega_e$	2.50π	− 43.66	11.70	− 55.36

Note: The values of column ⑤ may also be obtained by substracting ④ from ③.

where

$$\omega_e = 1.200 \text{ rad/sec}$$

Therefore

$$\dot{z}_b = -44.16\sin(\omega_e t + 0.15)$$

and

$$\dot{\zeta}_b = -12.00\sin(\omega_e t + 1.071\pi)$$

Find the amplitude of relative bow velocity.

Solution:

From (7.26) and (7.27), respectively, we have

$$(\dot{s}_b)_a = \sqrt{(1.2)^2(36.8)^2 + (1.2)^2(10)^2 - 2 \times 36.8 \times 10 \times (1.2)^2 \cos\left(\frac{\pi 450}{420} - 0.15\right)}$$

$$= 56.13 \text{ ft/sec}$$

and

$$\tan\varepsilon_{\dot{s}} = \frac{36.8 \times 1.2\cos(0.15) - 1.2 \times 10\cos(\pi/450/420)}{-36.8 \times 1.2\sin(0.15) + 1.2 \times 10\sin(\pi 450/420)} = -5.97$$

or

$$\varepsilon_{\dot{s}} = 99.5°(1.736 \text{ rad})$$

Figure 7.6 contains plots of the bow velocity, $\dot{z}_b$, the vertical wave velocity at the bow, $\dot{\zeta}_b$, and the relative bow velocity, $\dot{s}_b$, as calculated in Table 7.4.

In the design process it is often asked how large

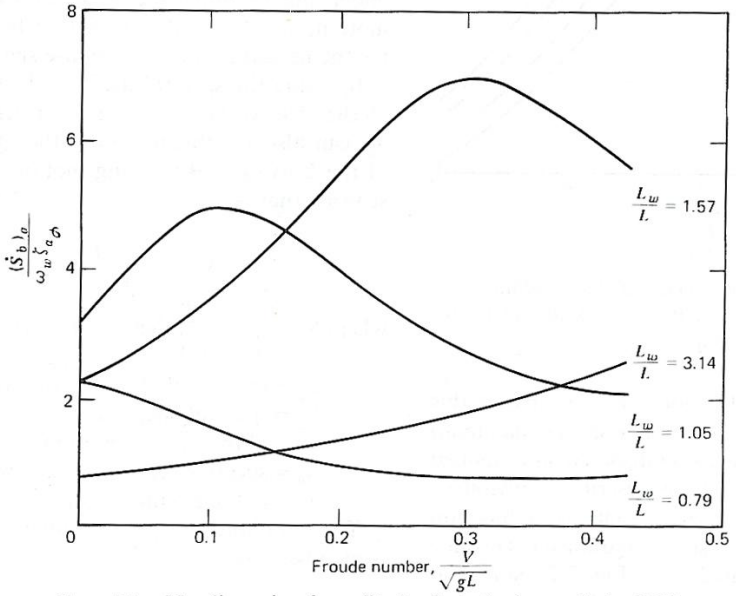


Figure 7.7 Nondimensional amplitude of relative bow velocity [137].

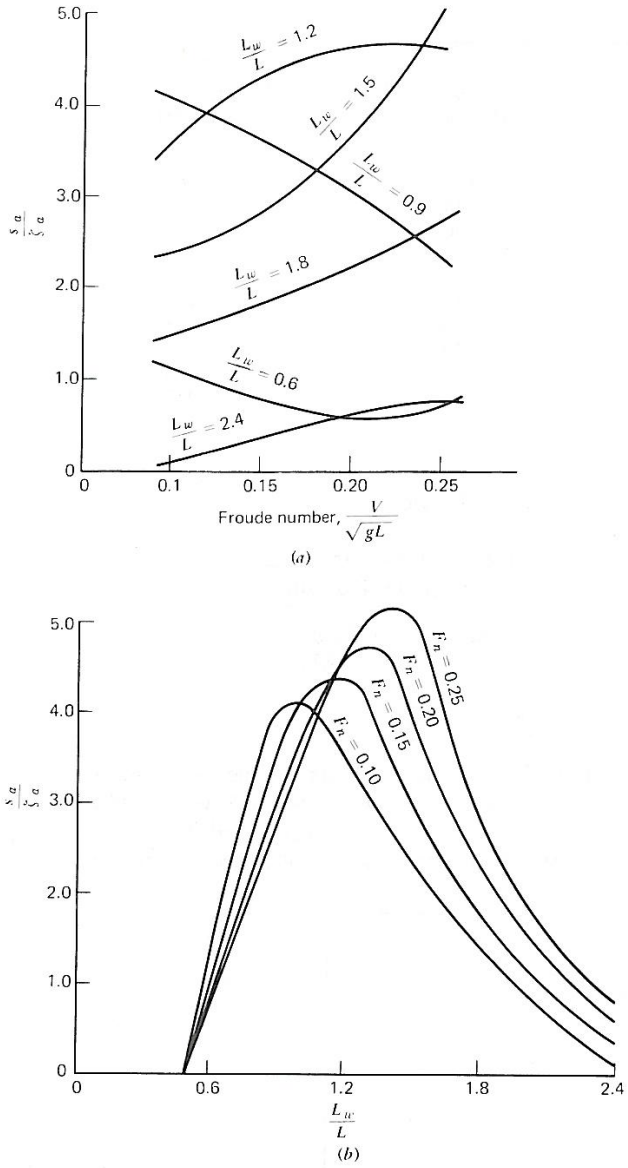


Figure 7.8 Typical response curves (*a*) for constant wavelength/ship length ratio L_w/L (for $C_B = 0.70$) and (*b*) for constant speed (C_B = p.70) [80].

the relative bow velocity should be. To answer this question consider Fig. 7.7, which shows maximum relative velocity (nondimensional), based on simplified formulations similar to those described previously. The maximum relative bow velocity as a function of the nondimensional speed parameter (Froude number) can be estimated from Fig. 7.7. Note that for a given ship certain critical speeds are associated with certain given waves. These critical speeds occur at the "humps" in the speed curves. For $L_w/L = 1.57$ or 1.05, either a decrease or an increase (from the critical) will reduce the relative velocity. For short waves ($L_w/L = 0.79$) an increase in relative bow velocity is recommended, whereas for long waves ($L_w/L = 3.14$) a reduction in relative velocity is desirable.

Typical results for the nondimensional relative bow motion amplitude from model tests in regular waves are given in Fig. 7.8.

Relative Bow Motion in an Irregular Seaway

From model tests in an irregular seaway and full-scale trials the relative bow motion has been formed to follow the same statistical laws as do heaving, pitching, and rolling motions. Histograms as well as the theoretical Rayleigh distributions of relative bow motion, immersion, and emergence at a particular ship speed are shown in Figs. 7.9*a*, 7.9*b*, and 7.9*c*.

The response spectrum for the relative bow motion in an irregular seaway is obtained as in the case of heaving, rolling, or pitching motions, that is by multiplying the ordinate of the encountering wave spectrum by that of the RAO for the same encountering frequency, where the RAOs can be obtained by regular wave tests or by analytical studies in regular waves.

The amplitude of the significant relative bow motion is equal to $2.0\sqrt{m_{0s}}\text{CF}$, where m_{0s} is the area under the response spectrum for the relative bow motion, and CF is the correction factor to account for the broadness of the response spectrum.

By using the spectral method, the spectral density of the relative bow motion in an irregular seaway, S_s, can also be obtained from the spectral densities of the heaving and pitching motions in an irregular seaway, that is,

$$S_s = S_z + \frac{\pi L}{L_w} S_\theta - S_\zeta \tag{7.28}$$

where S_s = spectral density for the relative bow motion
S_ζ = spectral density for the wave spectrum
S_z = spectral density for the response spectrum of the heaving motion
S_θ = spectral density for the response spectrum of the pitching motion

The amplitude of the relative vertical velocity is expressed as

$$(\dot{s})_a = \omega_e s_a \tag{7.29}$$

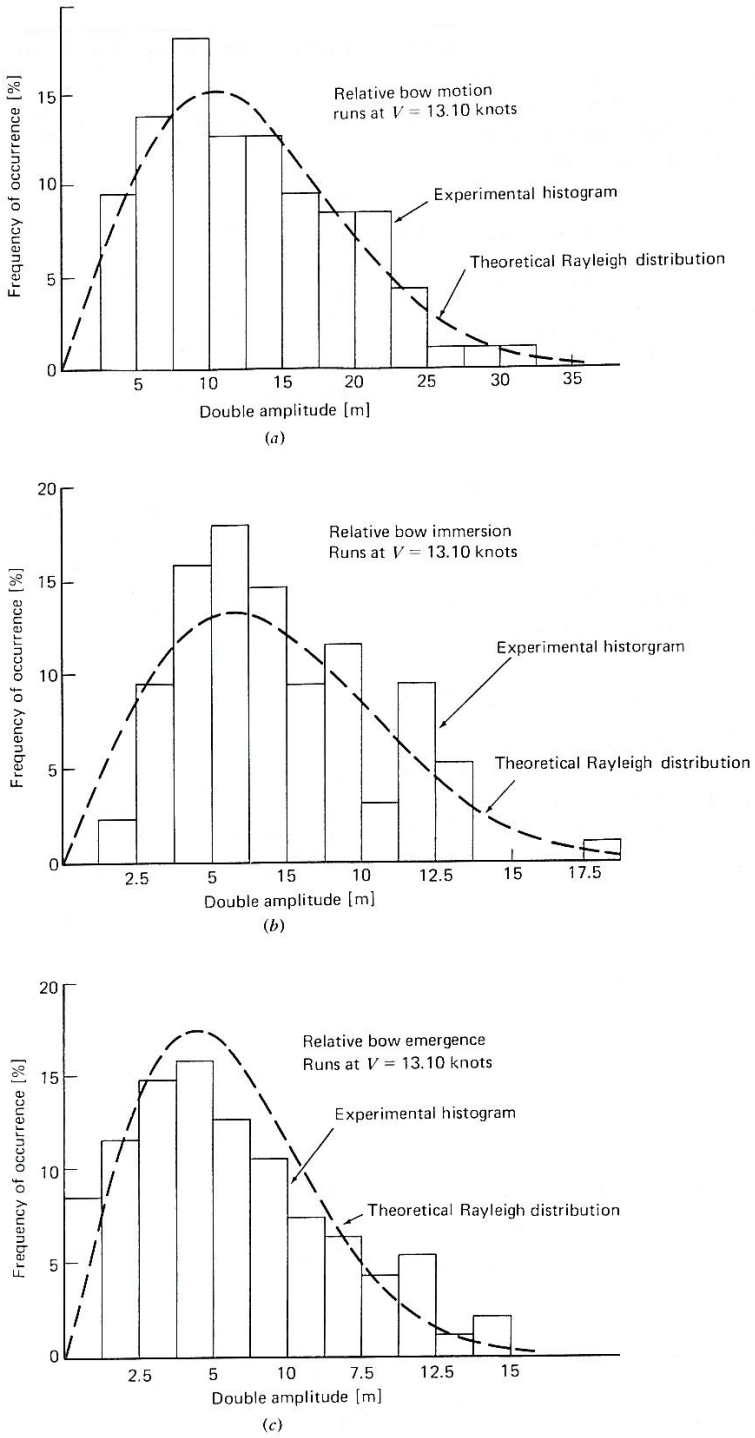


Figure 7.9 Histograms and Rayleigh distributions for (*a*) relative bow motion, (*b*) relative bow immersion, and (*c*) relative bow emergence [167].

Therefore, for the computation of vertical velocity in a regular seaway, the ordinates of the curve for the RAOs for the relative vertical velocity can be obtained from the RAO of the relative vertical motion by multiplying the ordinate for each frequency by the square of the particular frequency value, that is,

$$\text{RAO(for velocity)} = \text{RAO(for motion)}\,\omega_e^2 \quad (7.30)$$

where both RAOs are, themselves, functions of ω_e. However, it is easier to modify the response spectrum directly by making the same multiplications; that is, the area under velocity spectrum is

$$\int S_s(\omega_e)\,d\omega_e = \int \omega_e^2 S_s(\omega_e)\,d\omega_e = m_{2s} \quad (7.31)$$

which is the second moment of the motion spectrum area.

For the computation of acceleration in an irregular seaway the ordinates of the RAO for acceleration can be obtained by multiplying the ordinates of the RAO for motion by the fourth power of the particular frequency, that is,

$$\text{RAO(for acceleration)} = \omega_e^4\,\text{RAO(for motion)} \quad (7.32)$$

where both RAOs are functions of the frequency of encounter; as mentioned before, it is easier to modify the response spectrum for the vertical motion directly by making the same multiplications. Then the area under the acceleration spectrum is

$$\int S_{\ddot{s}}(\omega_e)\,d\omega_e = \int \omega_e^4 S_s(\omega_e)\,d\omega_e = m_{4s} \quad (7.33)$$

which is the fourth moment of the area under the motion spectrum.

Example 7.4

Find the significant relative bow motion of a 400 ft ship steaming at 20 knots into head seas in a long-crested seaway with a significant wave height of 18.5 ft.

The following values are available for the ship from tests in regular waves of a corresponding model:

$\frac{L_w}{L}$	$\left(\frac{s_a/L}{2\pi\zeta_a/L_w}\right)^2$ (nondimensional RAO for relative bow displacement)
0.5	0.0086
0.75	0.0477
1.00	0.2424
1.25	0.2500
1.80	0.1592
3.00	0.0791

Solution:

Figure 7.10*a* shows the plot of $S_\zeta(\omega_w)$; Fig. 7.10*b*, $S_\zeta(\omega_e)$.

Figure 7.10*c* shows $(s_a/\zeta_a)^2$ versus ω_e.

Table 7.7 is prepared to find the ordinates of the response spectrum from the values of $S_\zeta(\omega_e)$ and $(s_a/\zeta_a)^2$ as obtained from Tables 7.5 and 7.6, respectively.

TABLE 7.5 ENCOUNTERING WAVE SPECTRUM

ω_w [sec^{-1}] ①	$S_\zeta(\omega_w)$ [ft^2-sec] (See Example)	ω_e [rad/sec] ③	$S_\zeta(\omega_e)$ [rad/sec] ④
0.2	0	0	0
0.3	0.02	0.40	1.0
0.4	17.80	0.57	11.0
0.5	55.97	0.76	24.8
0.6	50.68	0.97	22.5
0.7	33.22	1.21	14.5
0.8	20.17	1.46	8.5
0.9	12.25	1.76	4.0
1.0	7.61	2.06	2.2

TABLE 7.6 RESPONSE AMPLITUDE OPERATOR

① $\frac{L_w}{L}$	② $\left(\frac{s_a/L}{2\pi\zeta_a/L_w}\right)^2$	③ L_w [ft]	④ ω_w [rad/sec]	⑤ $\left(\frac{S_a}{\zeta_a}\right)^2$	⑥ ω_e [rad/sec]
0.5	0.0086	200	1.005	1.357	2.066
0.75	0.0477	300	0.821	3.344	1.528
1.00	0.2424	400	0.711	9.560	1.241
1.25	0.2500	500	0.636	6.310	1.060
1.80	0.1592	720	0.530	1.937	0.824
3.00	0.0791	1200	0.410	0.346	0.587

Description of Table 7.6

Column Number	Description
①	Ratio of Wavelength to Ship Length
②	Nondimensional RAO Values
③	Wavelength = ① × L
④	Wave Frequency, $\omega_w = \sqrt{\frac{2\pi}{L_w}}$
⑤	RAO = ② × $\left(\frac{2\pi L}{L_w}\right)^2$

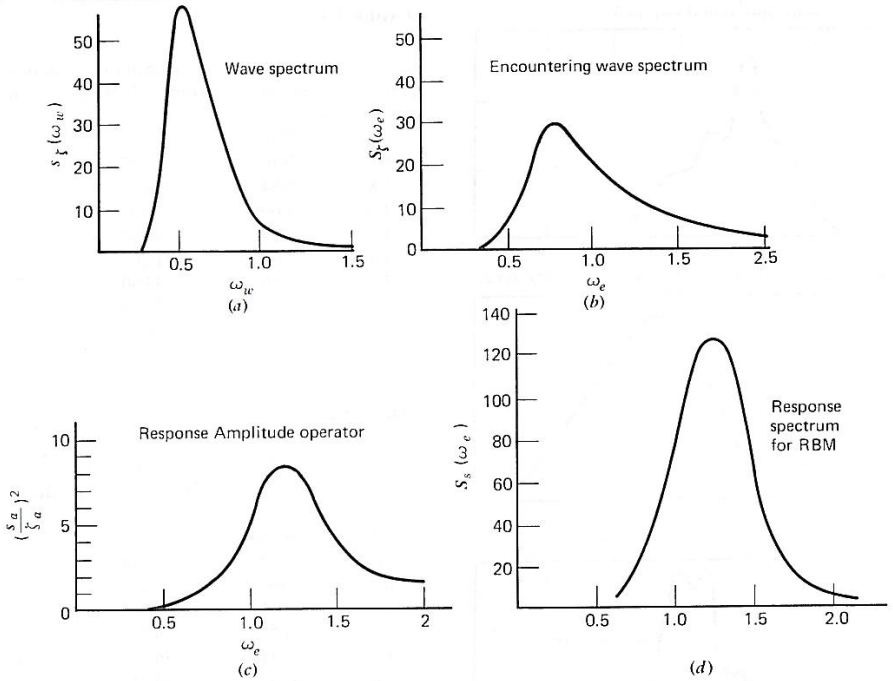


Figure 7.10 Determination of relative bow motion in an irregular seaway. (*a*) Wave spectrum. (*b*) Encountering wave spectrum. (*c*) Response spectrum operator. (*d*) Response spectrum for relative bow motion.

Thus the area under the response spectrum is

$$m_{0s} = \tfrac{1}{3} \times \Delta\omega_e \times \text{SUM} = \tfrac{1}{3} \times 0.2 \times 1095 = 73\,\text{ft}^2$$

and the significant relative bow motion amplitude is

$$(s_a)_{1/3} = 2.0 \times \sqrt{m_{0s}} \times \text{CF}$$
$$= 2.0 \times \sqrt{73} \times 1.0 = 17.00\,\text{ft}$$

assuming that the response spectrum is rather narrow. The correction factor can be calculated by taking the moments of the area of the response spectrum, as shown in Tables 7.8 and 7.9.

$$m_2 = \tfrac{1}{3} \times \Delta\omega_e \times \text{SUM}$$
$$m_2 = \tfrac{1}{3} \times 0.2 \times 1502.4 = 100.1568\,\text{ft}^2$$

Furthermore, the values in Table 7.9 result in

TABLE 7.7 RESPONSE SPECTRUM

ω_e [rad/sec]	$S_\zeta(\omega_e)$ (from Fig. 7.10*b*) [ft²-sec]	$\left(\frac{S_a}{\zeta_a}\right)^2$ (from Fig. 7.10*c*) [—]	$S_s(\omega_e)$ (see Fig. 7.10*d*) [ft² – sec] ④ = ② × ③	Simpson's Multiplier	Product
①	②	③		⑤	⑥
0.4	1	0	0	1	0
0.6	13	0.4	5.2	4	20.8
0.8	27	1.7	45	2	90
1.0	21.5	5.1	109	4	436
1.2	15	8.3	125	2	250
1.4	10	6.0	60	4	240
1.6	5.5	2.6	14.3	2	28.6
1.8	3.5	1.8	6.3	4	25.2
2.0	2.5	1.4	4	1	4
				SUM	1095

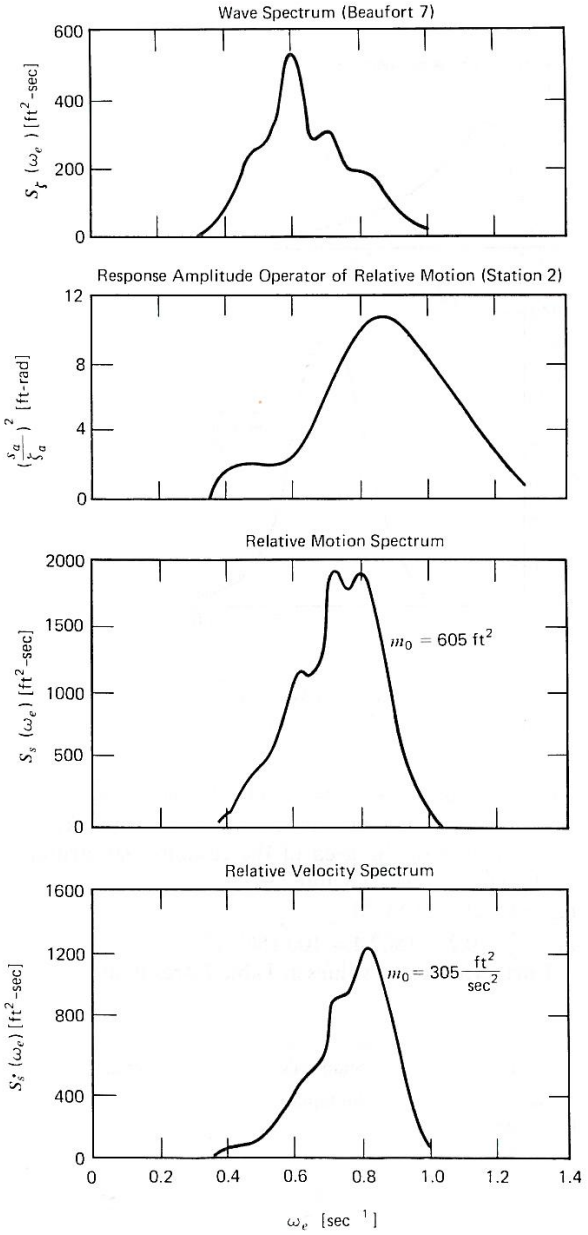


Figure 7.11 Typical response spectra for relative motion and relative velocity [167].

$$m_4 = \tfrac{1}{3} \times \Delta\omega_e \times \text{SUM}$$
$$= \tfrac{1}{3} \times 0.2 \times 2431.9 = 162.1 \text{ ft}^4$$

where $\Delta\omega_e = 0.2$ rad/sec. Thus the correction factor is obtained from (5.10):

$$\varepsilon^2 = \frac{m_0 m_4 - m_2^2}{m_0 m_4} = \frac{1799.6}{11{,}831.0}$$

TABLE 7.8

ω_e [rad/sec]	ω_e^2 [rad^2/sec^2]	$\omega_e^2 S_s(\omega_e)$ [rad^2 – ft^2/sec]	Simpson's Multiplier	Product
0.4	0.16	0	1	0
0.6	0.36	1.872	4	7.488
0.8	0.64	28.8	2	57.6
1.0	1.00	109.00	4	436.0
1.2	1.44	180.00	2	360.0
1.4	1.96	117.6	4	470.4
1.6	2.56	36.608	2	73.216
1.8	3.24	20.412	4	81.648
2.0	4.0	16.00	1	16.0
			SUM	1502.4

TABLE 7.9

ω_e [sec^{-1}]	ω_e^4 [sec^{-4}]	$\omega_e^4 S_s(\omega_e)$ [ft^2 – sec^{-3}]	Simpson's Multiplier	Product
0.4	0.0256	0	1	0
0.6	0.1296	0.674	4	2.696
0.8	0.4096	18.432	2	36.864
1.0	1.0	109.00	4	436.0
1.2	2.0736	259.2	2	518.4
1.4	3.8416	230.496	4	921.984
1.6	6.5536	93.7165	2	187.433
1.8	16.498	66.135	4	264.54
2.0	16.0	64.0	1	64.0
			SUM	2431.9

Thus

$$\varepsilon^2 = 0.152$$

and

$$\text{CF} = (1 - 0.152)^{1/2} - 0.921$$

Furthermore, from (6.10b) the value of the amplitude of significant relative bow motion is

$$(s_a)_{1/3} = 2\sqrt{m_0} \times \text{CF}$$
$$= 2\sqrt{72.9733} \times 0.921 = 15.73 \text{ ft}$$

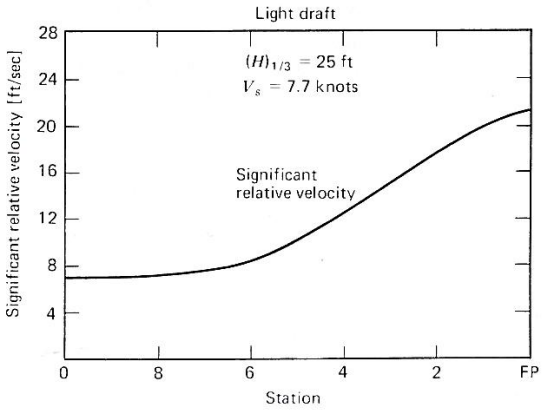


Figure 7.12 Typical significant relative velocity at different stations [170].

Typical figures for the relative bow motion and relative bow velocity spectra are shown in Fig. 7.11. Also, results for the significant relative velocity along the ship's length for a certain sea condition are given in Fig. 7.12. As can be seen, the relative velocity is about 1.7 times greater at station 2 that at station 5.

7.4 DECK WETNESS AND SLAMMING

In evaluating the seakeeping quality of a ship, the following two derived quantities are of more direct interest than the relative bow motion itself:

1. Forebody immersion, causing the shipping of green water.
2. Forefoot emergence, with a possibility of the occurrence of slamming.

If the motion of the bow relative to the water surface is such that the water rises above the deck level at the fore end, the probability of deck wetness increases, a factor that may greatly hamper a vessel in fulfilling its mission in an actual sea. Dynamic effects such as deck wetness, frequency of bow submergence, and probability of slamming cannot be determined by the characteristics of ship motions alone, since they depend also on the relative position of the ship in respect to the waves.

Let us consider a ship model moving into a train of regular waves approaching from ahead of the ship. If a pure pitching motion is assumed, the amplitude of pitching motion for two different models of the same length could be the same for a particular wavelength and wave height; however, depending on the phase relationship between the motion of the ship and the wave profile, the bow of one model may go under the water or green water may be shipped onto the deck, whereas the bow of the other model may not submerge, as illustrated in Fig. 7.13.

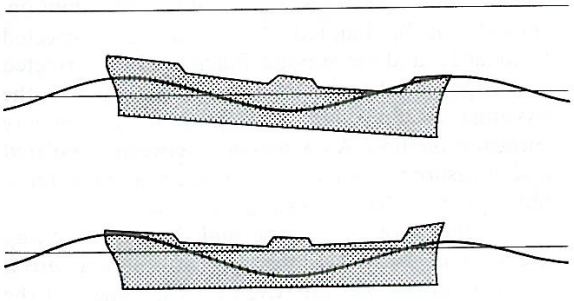


Figure 7.13 Effect of phase difference between wave and motion on bow submergence.

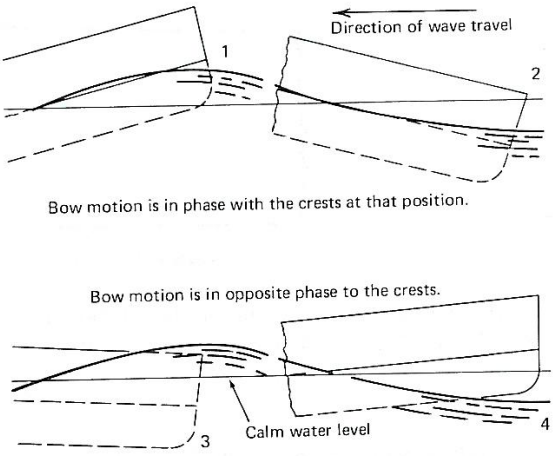


Figure 7.14 Bow motion in phase and out of phase with wave motion.

Figure 7.14 shows the two extreme positions of the bow in relation to the waves. The upper diagram shows the bow in phase with the waves; the lower diagram, the bow out of phase with the waves.

Deck Wetness

The shipping of green water is caused primarily by the relative deck motion, that is, the motion of the forward deck relative to the wave surface, but depends also on the height of the freeboard. The relative deck motion is regular in a regular wave train and irregular in an irregular seaway. If at any time the relative deck motion becomes negative, when both the deck motion and the wave motion are measured from the still whater level, green water is shipped onto the deck. This event can be predicted if the swell-up of water, both static and dynamic, is accounted for, since this phenomenon modifies the actual freeboard of the ship. The probabilities of relative deck motions can be considerably different for the actual and effective freeboards, especially at higher speeds. In any case, the greater the actual freeboard, the drier will be the ship.

Effect of Statical Swell-up of Water at the Bow

Statical swell-up of water at the bow is due to two phenomena, namely, bow waves generated by the vessel while moving in still water, and sinkage of the bow of the ship while running at a speed. The effect of

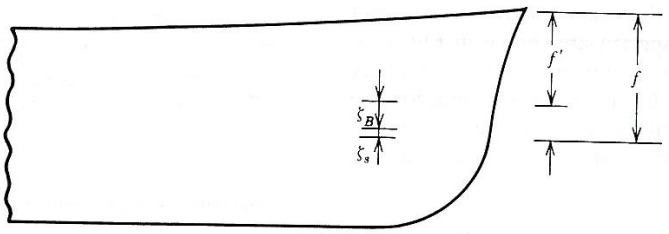


Figure 7.15 Statical swell-up and effective freeboard.

statical swell-up is reduction of the freeboard. In Fig. 7.15 the effective freeboard is, then, given as

$$f'(l) = f(l) - h_s(l) \tag{7.34}$$

where

$$\begin{aligned} f(l) &= \text{actual freeboard in still water [ft]} \\ h_s(l) &= \text{statical swell-up [ft]} \\ &= \zeta_B + \zeta_s \\ \zeta_B &= \text{elevation due to bow wave [ft]} \\ \zeta_s &= \text{sinkage due to speed [ft]} \end{aligned} \tag{7.35}$$

An approximate formula for statical swell-up is given [208] as

$$\frac{h_s}{L} = k_1' F_n^2 \tag{7.36}$$

where

$$\begin{aligned} k_1' &= k_1(B/L_E) \\ L &= \text{ship length [ft]} \\ k_1 &= 0.75 \\ B &= \text{beam} \\ L_E &= \text{length of entrance on waterplane [ft]} \\ F_n &= \text{Froude number} = V/\sqrt{gL} \end{aligned}$$

The effect of statical swell-up is a decrease in freeboard. As for example, for a series 60 ship of $C_B = 0.70$, $L = 400$ ft, $L_E = 164$ ft, and $B = 57.14$ ft, but the different values of h_s obtained from (7.36) as a function of ship speed are as follows:

V[knots]:	6.21	8.53	10.82	13.10
h_s[ft]:	1.61	3.02	4.86	7.09

Effect of Dynamic Swell-up Water at the Bow

The waves approaching the bow of a vessel cause heaving and pitching motions, and the resulting relative displacement of any point on the bow with respect to the water surface is called the *relative bow motion.* However, the relative bow motion is increased by an effect called *dynamic swell-up*, which exists because the bow, while immersing, pushes water aside and, while emerging from below, sucks in water.

From model experiments the dynamic swell-up is given by the following expression [208]:

$$h_d(l) = k_2 s(l) \omega_e \left(\frac{L}{g}\right)^{1/2} \tag{7.37a}$$

or

$$h_d(l) = k_2 L \left[\frac{s(l)}{\sqrt{gL}}\right] \tag{7.37b}$$

for $0.16 < F_n < 0.25$ and $1.6 < \omega_e^2 L/g < 2.6$, where

$$\begin{aligned} s(l) &= \text{vertical displacement} = z - l\theta - \zeta\,[\text{ft}] \\ l &= \text{distance of the CG from the forward perpendicular} \\ z &= \text{heave displacement [ft]} \\ \theta &= \text{pitch displacement [rad]} \\ \zeta &= \text{wave elevation [ft]} \\ h_d(l) &= \text{dynamic swell-up [ft]} \\ \dot{s}(l) &= \text{relative bow velocity [ft/sec]} \\ \omega_e &= \text{circular frequency of oscillation [rad/sec]} \\ k_2 &= \text{a constant depending on block coefficient} \\ &= \tfrac{1}{3}(C_B - 0.45) \text{ for } 0.6 < C_B < 0.8 \\ C_B &= \text{block coefficient} \end{aligned}$$

The phase angle between dynamic swell-up and relative bow motion is 180°; that is, maximum bow immersion takes place at the same time as maximum swell-up.

Since the magnitude of dynamic swell-up is of the same order as the amplitude of bow waves, this effect, which increases the relative bow motion, should not be ignored. Note that the corrected freeboard f' and the response function of the corrected submergence of bow immersion, considering the dynamic swell-up, are calculated by the energy spectrum method. A comparison between calculated and measured relative water surface at bow for a high-speed model is shown in Fig. 7.16.

The effects of both static and dynamic swell-up are to increase the probability of shipping green water on board the ship. Even if we assume that the average of $f'(l)$ in waves is approximately equal to that in still water, the relative freeboard in waves

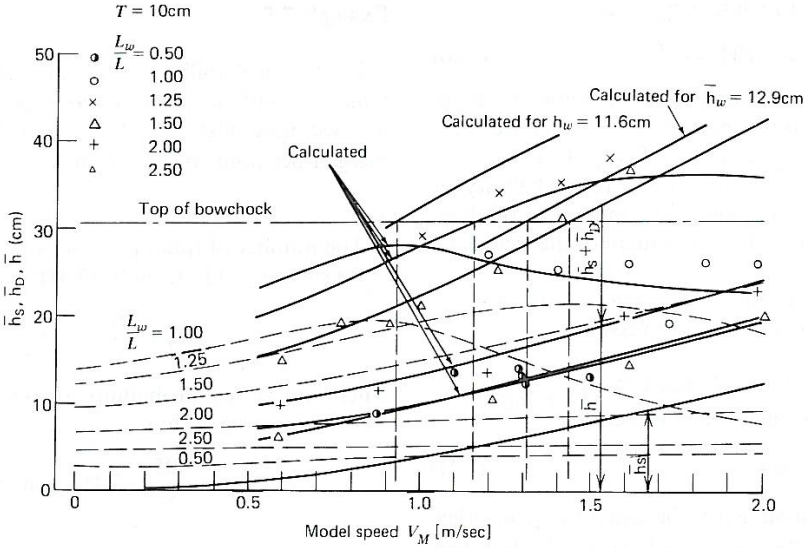


Figure 7.16 Comparison between calculated and measured water surface at bow [114].

$h'(l)$ can be expressed by the following equation:

$$h'(l) = f'(l) - h_d(l) + s(l) \tag{7.38}$$

See Fig. 7.17. After numerous experiments [208], the following conclusion can be stated: the freeboard must be increased by 10 to 15 ft if the value of the critical sea state (the sea state at which there will be a time rate of deck wetness of only 5% or less) is to be increased by one. Alternatively, for a constant sea state, if the freeboard is increased by 1 m, the critical speed (the speed at which water will be shipped not more than 5% of the time) can be increased by 3 to 4 knots.

Probability of Deck Wetness

It is often important to be able to predict the probability of deck wetness in a particular cycle of motion. From (5.17), if the histogram follows a Rayleigh distribution, the greatest value to be expected out of n observations (n should be a large number, say $n > 1000$) is $\sqrt{2 \log_e n}\ \sqrt{m_0}$. Thus, if the effective freeboard f' is put equal to the expression in (5.17), the value for n can be obtained as

$$n = e^{(f')^2/2m_0} \tag{7.39}$$

In other words, water will reach the weather deck once in n cycles. Alternatively, the percentage of cycles in which the deck will be expected to be wet can be predicted by the reciprocal of the above equation for n.

The probability that the immersion exceeds the

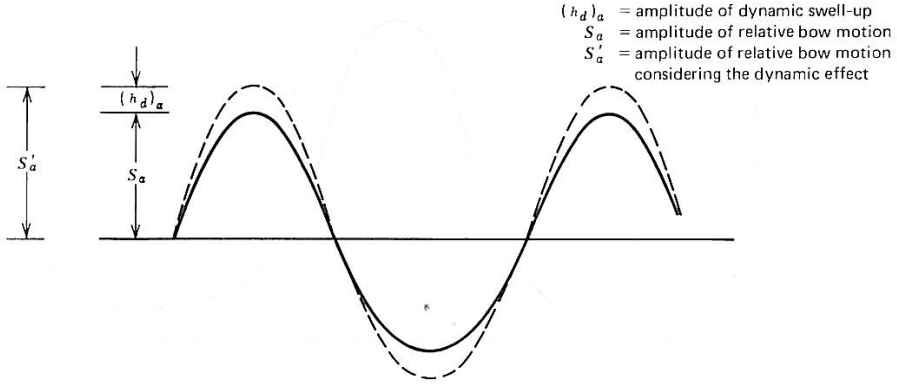


Figure 7.17 Dynamic swell-up.

effective freeboard $f^1(l)$ is defined as

$$P\{s \geqslant f^1(l)\} = e^{-[f'(l)]^2/2m_{0s}} \tag{7.40}$$

where m_{0s} is the area under the response spectrum for the relative bow motion at the forward perpendicular (FP), that is, $m_{0s} = \frac{1}{4}[(s_a)_{1/3}]^2$ and $f'(l) =$ effective freeboard at FP. Therefore probability of deck wetness is a function of the motion of the bow relative to the waves and the square of the freeboard forward.

The number of deck immersions per hour is obtained from the following expression:

$$N_T = \frac{\text{Probability of deck wetness}}{\text{Average apparent period}} \times 3600$$

$$= \frac{P_F}{T} \times 3600 \tag{7.41}$$

where T can be assumed to be equal to T_0. In other words, if the number of cycles is large, the deck will be expected to get wet N_T times per hour.

It should be noted that (7.41) is related by the formula for the expected period T, which, for a narrow band random variable having a normal distribution with zero mean, is given as

$$\bar{T} = \frac{1}{2\pi}\sqrt{\frac{2m_{0s}}{2m_{0\dot{s}}}}$$

The number of occurrences of deck wetness during each second is

$$N_w = \frac{1}{2\pi}\sqrt{\frac{2m_{0s}}{2m_{2s}}} \times \text{Probability of deck wetness} \tag{7.42a}$$

Example 7.5

Let the probability of shipping green water for a tanker be 0.05 or 5%. If the average pitching period is 5 sec, how often will the bow of the ship be submerged per hour in a sea state of 6?

Solution:

The number of times per hour the ship is expected to be submerged is given by (7.41):

$$N_T = \frac{P_F}{T} \times 3600$$

where P_F is the probability of deck wetness, and $T = T_0$ (assumed). Thus

$$N_T = \frac{0.05}{5} \times 3600 = 36\,\text{hr}^{-1}$$

Example 7.6

Assuming a relative bow motion in an irregular seaway as in Example 7.4, find the frequency of deck wetness for a 400 ft ship with an effective freeboard of 24 ft, given the area under the relative motion spectrum: $m_{0s} = 73\,\text{ft}^2$.

Solution:

From (7.42a) the number of occurrences of deck wetness during each second is

$$N_w = \frac{1}{2\pi}\sqrt{\frac{2m_{0s}}{2m_{2s}}} \times e^{-[f'(l)]^2/2m_{0s}} \tag{7.42b}$$

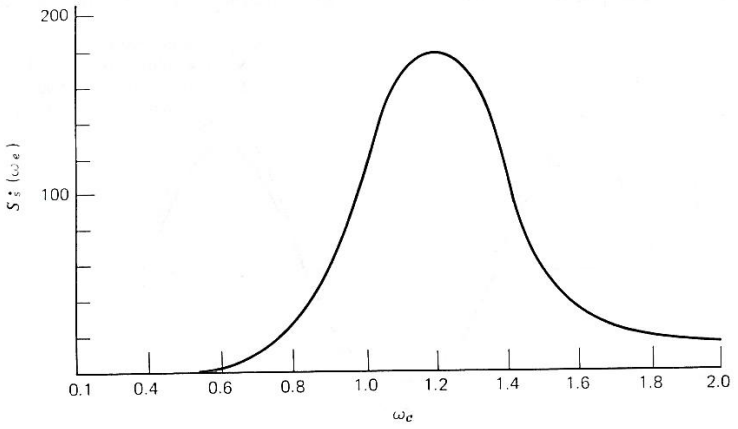


Figure 7.18 Response spectrum for relative bow velocity.

TABLE 7.10

ω_e [sec^{-1}]	$S_s(\omega_e)$ (from column of Table 7.7) [ft^2-sec]	ω_e^2 [sec^{-2}]	$S_s(\omega_e)$ (see Fig. 7.81) [ft^2/sec]	Simpson's Multiplier	Product
0.4	0	0.16	0	1	0
0.6	5.2	0.36	1.872	4	7.488
0.8	45	0.64	28.8	2	57.6
1.0	109	1.0	109	4	436.0
1.2	125	1.44	180	2	360.0
1.4	60	1.96	117.6	4	470.4
1.6	14.3	2.56	36.608	2	73.216
1.8	6.3	3.24	20.412	4	81.648
2.0	4	4.0	16.0	1	16.0
				SUM	1502.352

It has already been mentioned in Section 7.3 that m_{2s} (i.e., the area under the relative velocity spectrum) is equal to the second moment of the area under the relative motion spectrum. The second moment of the area under the relative motion spectrum is calculated in Table 7.10.

$$\text{Thus } m_{0s} = m_{2s} = \tfrac{1}{3}(S)\,(\text{SUM}) = \tfrac{1}{3}(0.2)\,(1502.352)$$
$$= 100.15 \text{ ft}^2/\text{sec}^2$$

The number of occurrences of deck wetness during each second is

$$N_w = (1/2\pi)\sqrt{2m_{0s}/2m_{2s}}\ \text{Prob}\{\text{deck wetness}\}$$

where

$$\text{Prob}\{\text{deck wetness}\} = e^{-[f'(l)]^2/2m_{0s}}$$
$$= e^{-576/176} = 0.019$$

Thus

$$N_w = \frac{1}{2\pi}\frac{146}{200.3136} \times 0.019 = 0.0026 \text{ sec}^{-1}$$

or 9.36 occurrences per hour.

It should be pointed out that frequency of deck wetness as given by (7.41) and (7.42) is in reality greater, since the correction factor $(1-\varepsilon^2)^{1/2}$ for the broadness of the spectra for relative motion and relative velocity has not been taken into account.

Using the significant amplitude of relative bow motion at any location along the length, as obtained from the spectral method, we can calculate the effective freeboard at any location for different probabilities of deck wetness, as illustrated in Fig. 7.19*a*, which shows two decklines of the constant probability of deck wetness as compared to the actual deckline. Figure 7.19*b* shows the sheer curve determined by seakeeping calculations for 1% deck wetness for the forebody of ships 200 to 1000 ft in length. It is clearly seen that the sheer should not be determined on the basis of a constant parabolic formula only. The procedure of determining sheer curve for seakeeping performance requires:

a. Selection of the maximum significant wave height for the particular route for the various weather conditions in which the ship should operate.

b. Determination of a certain percentage of deck wetness, which is an important design consideration since it assures a certain level of safety.

Figure 7.19*c* shows that the freeboard at the midship section can be reduced significantly for a Great Lakes steamer with a length greater than 550 ft. However, the freeboard determined from the seakeeping calculations is based on the selection of the value for the significant wave height.

There are two dynamic effects due to water passing over the forward deck, namely, pressure and impact. The pressure on the deck can be approximated by the static pressure due to the head of water on the deck. A formula concerning the probability for such a pressure can be expressed [62] as

$$f\{q\} = \frac{2a^2}{2m_{0s}}(q+q_*)e^{-a^2/2m_{0s}}[(q+q_*)^2 - q_*^2] \quad (7.43)$$

where $f\{q\}$ = probability of pressure due to green water on deck
q = pressure due to green water on deck [psi]
m_{0s} = variance of relative bow motion (i.e., area under the relative bow motion spectrum)

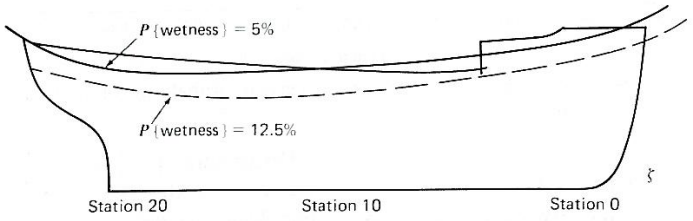


Figure 7.19*a* Deckline of constant wetness probability.

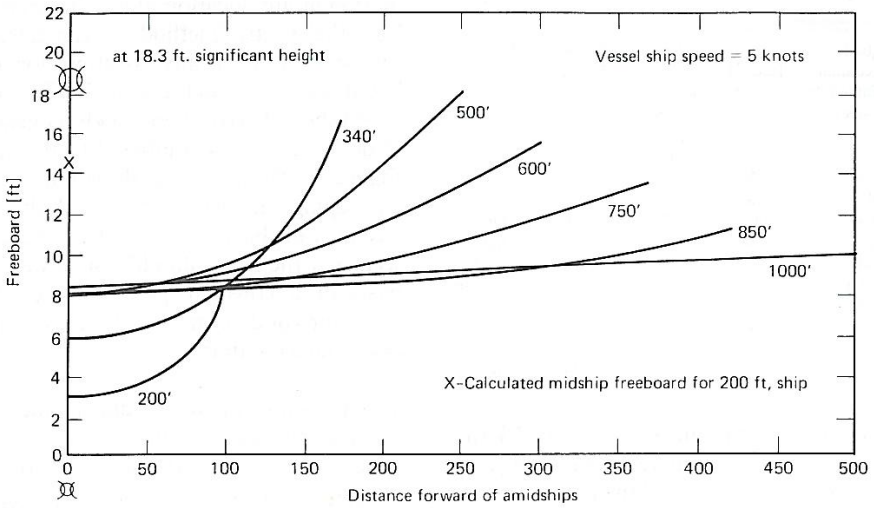


Figure 7.19*b* Typical freeboard curves for 1% deck wetness [34].

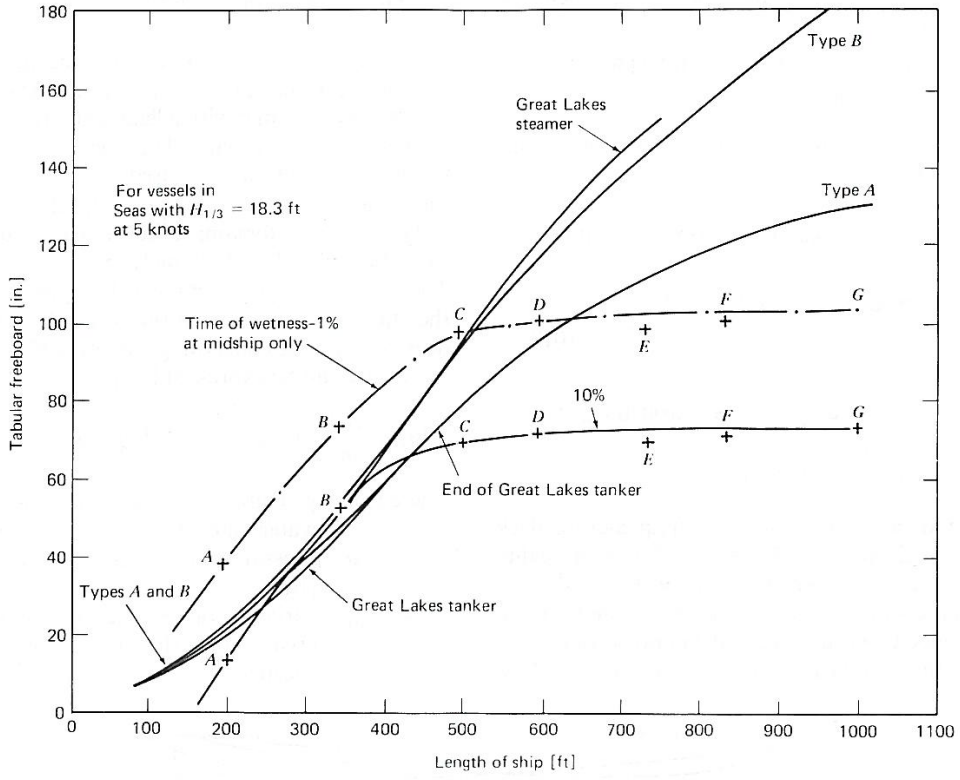


Figure 7.19*c* Midship freeboard, considering a certain probability of deck wetness, versus tabular freeboards [34].

$q_* = f/a$

f = freeboard at ship bow [ft]

a = a constant, found by experiments to be approximately 2.32 ft/psi

Ferdinande [62] has also studied the effect of impact from the many records of bow submergence and bow acceleration that he has obtained. By observing a discontinuity in the acceleration record

immediately after the bow submergence, the impact due to the shipping of green water can be detected. The time of impact from the initial bow submergence varies from observation to observation.

Slamming

Except on very large ships, the severe pitching and heaving motions in bad weather force ship operators into voluntary speed reduction. However, for large supertankers the periods of storm waves are so short compared with the natural periods of pitch and heave of the ship that such waves cause only very small motions. The effects of the impacts of large waves against the bows, however, become of greater significance. Such impacts may be the cause of severe damage to some ships in spite of speed reduction.

Not much is known about the impact forces resulting from waves hitting the bow, although the magnitude of the induced pressure may exceed 40 m of water. The physical nature of the impact is little understood, and the quantitative effects of changes in bow form, ship speed, and sea states are important considerations in preliminary ship design.

A ship moving in a seaway experiences two kinds of impact pressures:

1. Impact experienced when the forefoot hits the water surface during a severe pitching motion.
2. Impact on any part of the hull due to beam sea, astern sea, diagonal sea, and so on.

In the first kind of impact, known as *slamming*, the maximum pressure is at the edge of the surface that comes into contact with the water surface as the bow emerges and reenters the water in a heavy sea. As the ship enters further into water, the peak pressure moves outboard and its magnitude also decreases. Therefore at the time of impact the maximum pressure occurs at the keel for ship sections with a slight deadrise.

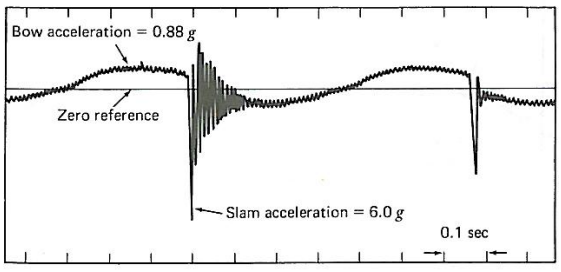


Figure 7.20 Typical slamming record.

Slamming is then defined as a hydrodynamic impact phenomenon, and it is associated with a sudden change in the acceleration of the ship. The most sudden change in the acceleration takes place at the bow and the stern, where both the acceleration and the motion are also largest.

Figure 7.20 is an example of a typical slamming record produced by an accelerometer mounted on the bow of a ship model. The graph shows changes in acceleration over a given period of time due to slamming. When the forefoot of a ship hits the water, the sudden deceleration of the ship shows up in the acceleration period. Although slamming may occur without forefoot emergence, there is a greater probability of slamming with emergence of the forefoot. When the forefoot of a ship emerges out of water and suddenly reenters an opposing wave with a relatively large velocity, slamming can occur. Thus there are three kinematic conditions to be investigated in the study of slamming:

1. *Forefoot emergence.* In general, slamming is associated with forefoot emergence, defined as a point at the intersection of the forward perpendicular and the extension of the keel, since the maximum impact force is experienced by a ship either at the instant of entry or immediately after. Therefore it is important to know whether forefoot emergence occurs for a given seaway.
2. *Phase difference between wave motion and bow motion.* If the downward-moving bow meets the upward-moving wave (i.e., if the phase difference between the wave motion and the bow motion is 180°), the critical condition for slamming is reached.
3. *Magnitude of relative bow velocity.* If the relative bow velocity is larger than a certain critical value, the ship may experience slamming. Since the critical value of the relative velocity depends on the ship's speed, a change in speed may either increase or reduce the relative bow velocity.

With the introduction of very large ships the problem of slamming and its effects is of considerable importance. This is particularly true for the full blunt bow form of the supertanker, which is very susceptible to damage due to slamming.

Slamming in an irregular seaway has two effects: (a) excessive pressure on the bottom plating, with a possibility of (b) stress in the main structure due to vibrations. The latter phenomenon is known as *whipping*, which is defined as the periodic flexural

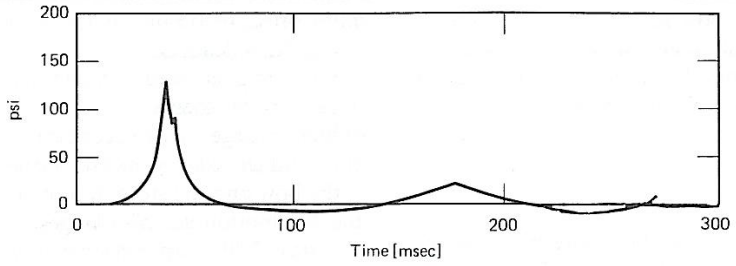


Figure 7.21 Typical time history of slamming pressure.

deformation that takes place in both the vertical and the horizontal directions. The action, once induced, continues as a dynamic phenomenon until the energy imparted by the impact force is dissipated by internal damping. The associated stress, also known as the *whipping stress*, may amount to about 20% of that due to the wave bending moment in the case of actual ships.

Slamming impact pressures are of short duration and of local origin. A full-scale measurement of a slamming pressure–time history at a point on a ship's bottom is shown in Figure 7.21.

Although sudden deceleration is rather unpleasant for the crew and passengers and may shift cargo on board, such shifting does not cause damage to the bottom of the ship. Damage is caused by the high local pressures developed on the bottom during slamming. Therefore, for design purposes, it is often necessary to predict this pressure, which is a function of the time as well as the location, and depends on both the instantaneous relative velocity and the relative acceleration. From analytical studies it has been found that the maximum pressure in every instance occurs at the edge of the instantaneous beam. As the bow enters into water, the pressure peak moves outward. In the determination of maximum pressure the slope of ship sections and the relative velocity are more important than the acceleration. Figure 7.22 gives the relationship between pressure and relative velocity, which can be calculated if the motion of the ship is known (See Chapter 4). The pressure at the keel is dependent chiefly on the relative acceleration.

The longitudinal location of the impact pressure also moves aft from the forward end when the ship's speed is increased.

The slamming force is dependent mainly on the velocity of the bow as it hits the water and the area of impact. From experimental data it has been observed that the slamming pressure is approximately proportional to the square of the relative vertical velocity, as shown in Figure 7.22. The minimum relative bow velocity at which slamming starts taking place, also known as the *threshold velocity*, is about 12 ft/sec for a 520 ft ship.

In Ref. 188 it is explained that the deformation of the water surface moves with the wave speed, which is a function of the length scale of the disturbance, and

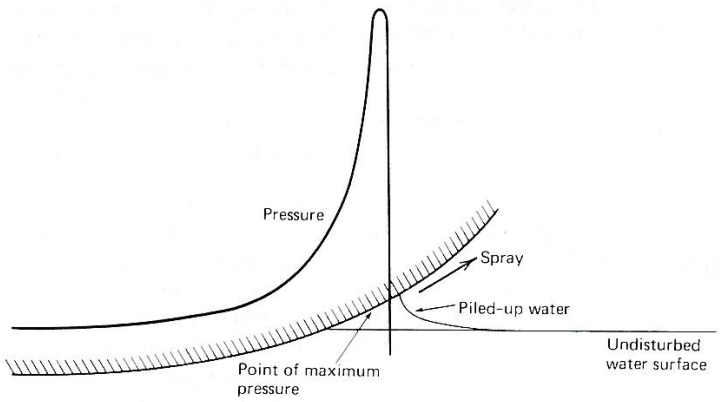


Figure 7.22*a* Schematic diagram of pressure distribution on the bottom [203].

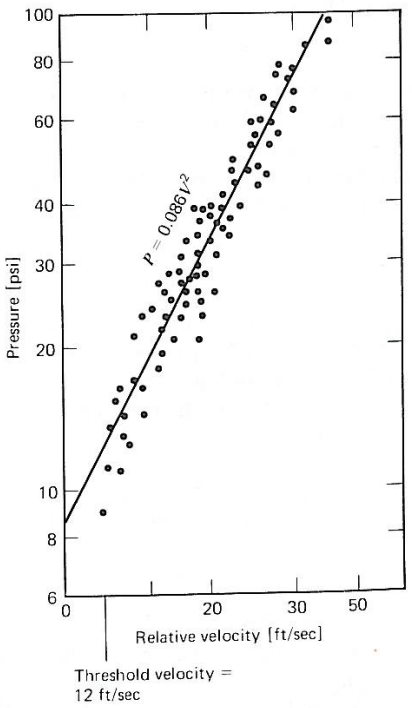


Figure 7.22*b* Effect of impact velocity on pressure [167]. Pressure on the keel plate as a function of impact velocity (*Mariner*, station 2, light draft, shipspeed 10 knots, moderate sea state 7).

so the threshold velocity can be considered as the vessel's approach speed, for which the free surface cannot move out of the way fast enough to avoid impact. If the scale of the wave disturbance is defined to be the local beam, b, at the slamming station, an analytical expression of the threshold velocity is obtained by equating the vessel's relative velocity and the velocity of the wave.

The velocity of an impulsive wave, c_w, is given [113] as

$$c_w = \sqrt{\frac{\sqrt{2}}{\pi} g \frac{b}{2}}$$

whereas the resultant speed of the approaching vessel is

$$V_r^2 = V_s^2 + \dot{s}^2$$

where V_s is ship speed, $\dot{s}$ is relative velocity, and b is width of plate panel.

When the wave velocity is equated to the resultant speed of the vessel, the threshold velocity is obtained as

$$\dot{s} = \sqrt{\frac{gb}{\sqrt{2\pi}} - V_s^2}$$

Nondimensionally, the threshold velocity can be expressed as

$$\frac{\dot{s}}{\sqrt{gL}} = \sqrt{\frac{1}{\sqrt{2}} \frac{b}{\pi L} - \frac{V_s^2}{gL}}$$

It is, therefore, clearly seen that the threshold velocity is dependent on the Froude number. However, this fact has not yet been verified experimentally.

Basic Theory [225*a*]

When a V-shaped wedge section penetrates vertically into water for a distance z, it is subject to pressures that, when integrated, will yield the inertia, damping, and buoyancy forces; thus the equation of motion can be written as

$$F_i + F_d + (F_b - F_w - F_s) = 0$$

where F_i = inertia force
F_d = damping force
F_b = buoyancy force
F_w = weight of the wedge = gM_0
F_s = force of the rest of the hull on the wedge

For the initial impact, F_d, F_b, and F_w are comparatively small, so we have

$$F_i = F_s \tag{7.44}$$

Now the inertia force F_i is determined by differentiating the momentum, that is, if

$$\text{Momentum} = (M_0 + a_z)\dot{z}$$

where M_0 is mass of section and a_z is added mass, the inertia force is

$$F_i = \frac{d}{dt}(\text{momentum}) = (M_0 + a_z)\ddot{z} + \dot{a}_z\dot{z}$$

where $\dot{a}_z$ indicates that the added mass is time dependent, since immersion itself is time dependent. Equation 7.44 can therefore be written as

$$(M_0 + a_z)\ddot{z} + \dot{a}_z\dot{z} = F_s \tag{7.46a}$$

or

$$F_s - M_0\ddot{z} = a_z\ddot{z} + \dot{a}_z\dot{z} \tag{7.46b}$$

Now, this equation can be used for the determination of the hydrodynamic impact; thus

$$P = F_s - M_0\ddot{z} = a_z\ddot{z} + \dot{a}_z\dot{z} \tag{7.47}$$

If the added mass change is considered to be due to immersion, then

$$\dot{a}_z = \frac{da_z}{dz}\cdot\frac{dz}{dt} = \frac{da_z}{dz}\cdot\dot{z} \tag{7.48}$$

Combining (7.48) and (7.46a), we have

$$(M_0 + a_z)\ddot{z} + \frac{da_z}{dz}(\dot{z})^2 = F_s \tag{7.49}$$

This equation indicates that the impact can be considered as a damping that is proportional to the square of the velocity with a damping coefficient equal to the change of added mass.

If it is assumed that the wedge is not connected to the ship, when $t = 0$, $z = 0$, $\dot{z} = V_0$,

$$\dot{z} = \frac{M_0 V_0}{M_0 + a_z}$$

and

$$\ddot{z} = \frac{M_0 V_0 \dot{a}_z}{(M_0 + a_z)^2}$$

from (7.47)

$$\text{Impact} = P = \frac{M_0 V_0 \dot{a}_z}{(M_0 + a_z)^2}$$

or

$$\frac{P}{M_0} = \frac{V_0 \dot{a}_z}{(1 + (a_z/M_0))^2} \tag{7.50}$$

Equation 7.50 indicates that, if the mass M_0 is large compared to the added mass a_z, the impact will be small; or, as $M_0 \to \infty$,

$$P \to V_0 \dot{a}_z \tag{7.51}$$

One can also see from this simplified equation that acceleration has no effect on impact. This has been found to be true with an actual ship. For the impact force therefore, a_z and a_z play the important role.

According to Ref. 230, the added mass is expressed by

$$a_z = \tfrac{1}{8}\pi^3 \rho z^2 \cot g^2\beta$$

which is obtained by treating the added mass as that of a plate of width $2b_0$ (i.e., the same width as the submerged wedge), as in Fig. 7.23.

In Fig. 7.23 the pressure distribution on the wedge has also been given [230] as

$$P = \tfrac{1}{2}\rho V_0^2\left[\frac{\pi}{\beta\sqrt{1-(x/b)^2}} - \frac{x^2b^2}{1(x^2/b^2)} + \frac{2\ddot{z}}{V^2}(\sqrt{b^2 - x^2})\right] \tag{7.52}$$

where p = pressure [psf]
x = horizontal distance from midship section [ft]
$V_0 = \dot{z}_x$ = relative vertical velocity at a distance x from the midship section [ft/sec]
$\ddot{z}_x$ = relative acceleration at a distance x [ft/sec^2]
β = deadrise angle of wedge

It is also determined in Ref. 230 that b is a function of z, given as

$$b = \frac{\pi z}{2\beta} \tag{7.53}$$

If $\ddot{z}$ is insignificant in comparison to the added mass, we have

$$\frac{p}{\frac{1}{2}\rho V^2} = \frac{\pi}{\beta\sqrt{1(x^2/b^2)}} - \frac{x^2b^2}{1-(x^2/b^2)} \tag{7.54}$$

The effect of different hull shapes (convex, concave,

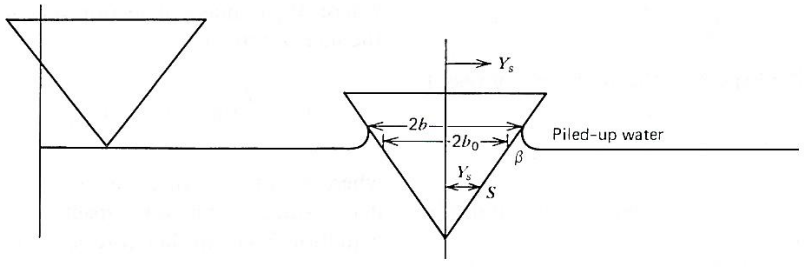


Figure 7.23 Submerged wedge.

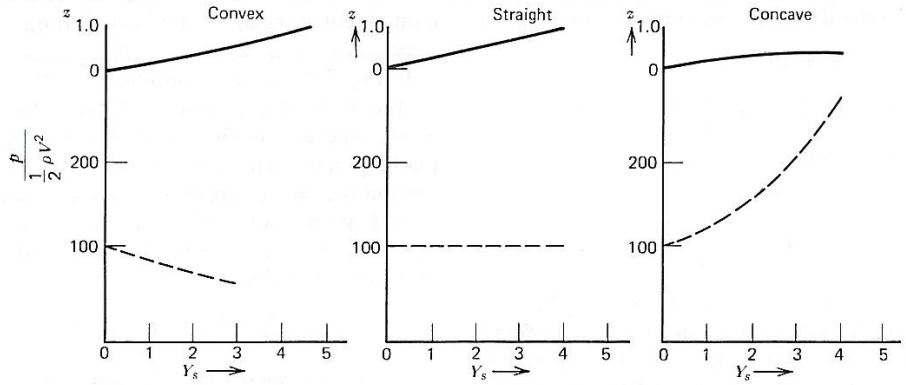


Figure 7.24*a* Distribution of pressure for different immersions of wedge-shaped sections penetrating the water surface at constant speed [225].

or straight) can be determined with the help of (7.54) and is also shown in Fig. 7.24. This figure indicates that with the convex shape (the most common shape for a ship bottom) the maximum pressure peak decreases with an increase in immersion. The opposite is true for the concave wedge.

In the case of an actual ship the pressure peak occurs in the region of the keel, and the value of this peak pressure for the first contact of the section with the water is given as

$$\frac{p_{\max}}{\frac{1}{2}\rho v^2} = 1 + \frac{\pi^2}{4\beta^2} \tag{7.55}$$

that is, the maximum pressure depends on the vertical velocity V and the angle of deadrise β. Expression 7.55 is plotted in Fig. 7.24*b*, from which we see that the smaller the value of β, the higher will be the maximum pressure.

It should be also noted that (7.55), as given in Ref. [230], yields larger values than those observed

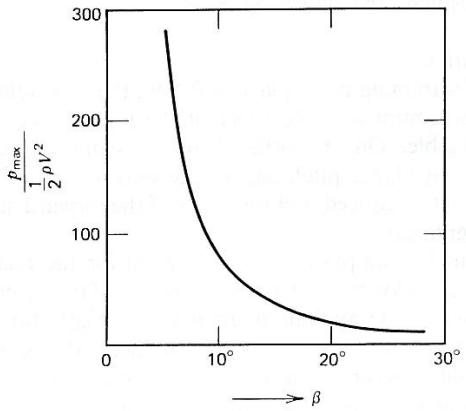


Figure 7.24*b* Maximum pressure as a function of section slope for contact with the water surface [225].

by experiments and is not valid for a flat plate (i.e., when $\beta = 0$), which should experience infinite pressure according to the equation. For a flat plate another equation is available from Ref. 225*a*; this is given as

$$\frac{p}{\frac{1}{2}\rho V^2} = \frac{2C_0}{V}$$

where C_0 is the speed of sound in water ($\simeq 15$ m/sec).

Note: The purpose of the above simple derivation is to determine the significant features of hydrodynamic impact calculations. The pressure at the forefoot of a ship depends on the relative velocity between the ship and the wave and also on the slope of the tranverse ship sections.

The relative velocity between ship and wave at any point located at a distance x from the midship section was given in Section 7.3, and the maximum pressure expressed is [203] as follows:

$$p = p_0\left[\frac{2}{\beta\sqrt{1-(Y_s/2b)^2}} + \frac{2}{\delta}\sqrt{\left(1-\frac{Y_s}{2b}\right)^2} - \frac{(Y_s/2b)^2}{1-(Y_s/2b)^2}\right] \tag{7.56}$$

where

$$p_0 = \tfrac{1}{2}\rho(\dot{z}_x)^2, \qquad \delta = \frac{(\dot{z}_x)^2}{2b\ddot{z}_x}$$

$2b$ is the modified beam, considering piled-up water; and β is the slope of the modified transverse section, also considering piled-up water (i.e., angle of deadrise). Thus the effect of the shape of the section at which the pressure is to be determined depends on the value of β for that particular section and draft.

The vertical velocity of the section is expressed by

$$\dot{z}_x = \dot{\zeta} - (\dot{z} + x\dot{\theta})$$
$$= -\omega_e \zeta_e \left(\omega_e t + \frac{2\pi x}{L_w} \right) - \dot{z} - x\dot{\theta}$$

and the acceleration is

$$\ddot{z}_x = \ddot{\zeta} - (\ddot{z} + x\ddot{\theta})$$
$$= \omega_e^2 \zeta_a \cos\left(\omega_e t + \frac{2\pi x}{L_w} \right) - \ddot{z} - x\ddot{\theta}$$

Note that at the keel (i.e., where $Y_s = 0$) the last term of (7.56) becomes zero, and since δ is much greater than β, the first term is more significant. In other words, the pressure at the forefoot is then highly dependent on the shape of the transverse section and the relative velocity. As Y_s becomes larger, the second term of (7.56) becomes rather small, and the pressure is the result of the difference between the two remaining larger terms.

The forward motion of a ship greatly influences the slamming pressure for the following reasons:

a. The motion of the bow relative to the wave may change considerably because of the change in encountering frequency, which depends on the ship's speed.

b. Pressure calculations are based on the normal component of the relative velocity (i.e., normal to the keel), and so the forward speed may make a significant contribution to this component.

If the pressure is calculated at an instant when the pitch angle is zero, the ship's speed will have no component normal to the keel. Slamming does not necessarily occur at zero pitching angle.

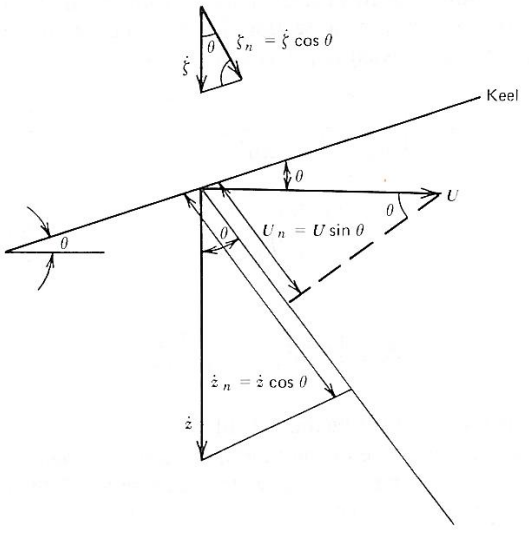


Figure 7.25 Effect of forward motion on relative velocity [203].

In Fig. 7.25 the contribution of the pitching motion to the normal component of the relative velocity is $x\dot{\theta}$, where x is the distance measured from the pitching axis. The contribution from the heaving motion is $\dot{z}_n = \dot{z} \cos\theta$, that from the forward speed is $U_n = U \sin\theta$, and that from the wave velocity is $\dot{\zeta}_n = \dot{\zeta} \cos\theta$. Therefore the total normal component of the relative velocity is

$$V_n = U_n + x\dot{\theta} + \dot{z}_n - \dot{\zeta}_n \tag{7.57a}$$

or

$$V_n = U \sin\theta + (\dot{z} - \dot{\zeta}) \cos\theta + x\dot{\theta} \tag{7.57b}$$

For small values of pitch angles, we may write

$$V_n \approx U\theta + x\dot{\theta} + \dot{z} - \dot{\zeta} \tag{7.57c}$$

It is seen that the contribution of the ship's forward motions to the normal component of the relative velocity is $U\theta$. This means that the larger the pitching angle, the greater is the significance of the forward motions.

Example 7.7

Consider a ship with the following properties:

$$L = 400 \text{ ft}$$
$$\theta_a = 10^\circ$$
$$U = 30 \text{ knots}$$
$$L_w = 400 \text{ ft}$$

Also, the maximum vertical bow velocity due to pitching at the bow is 52.6 ft/sec, and

$$U_n = 2.26 \text{ ft/sec at } \theta = 3^\circ$$

Investigate the slamming effect.

Solution:

If slamming takes place at $\theta \approx 0^\circ$, the bow velocity is maximum and the effect of the forward speed is negligible. On the other hand, if slamming takes place at higher pitch angles, the velocity of the bow is greatly reduced and the effect of the forward speed is significant.

Further simplification is obtained for the relative normal velocity if we use $\dot{z} - \dot{\zeta}$ instead of $(z - \dot{\zeta}) \cos\theta$, assuming the pitching angle is small. Neglecting the effect of the forward speed reduces the normal velocity, whereas using $\dot{z} - \dot{\zeta}$ instead of $\dot{z}_n - \dot{\zeta}_n$ increases the relative velocity. At the peak (i.e., for $Y_s = 2b\sqrt{1 - \beta^2}$) these two terms can be combined. Hence the accuracy of the numerical computation

of the peak is better than that for $Y_s > 2b\sqrt{1-\beta^2}$. For a very small value of $\beta > 0$, which describes a nearly flat-bottomed section and small draft, the positive term will be more significant, and the maximum pressure will be experienced at the instant the ship sections enter the water.

One can also see from (7.56) that the pressure is a function of the square of the relative velocity. Thus we can expect maximum pressure when there is a combination of minimum section slope and maximum relative velocity. It is rather difficult, however, to make a graphical representation of these maximum conditions, since both the minimum section slope and the maximum relative velocity depend on position along the length of the ship, as well as on time.

Hull deadrise influences the peak impact pressure significantly. The peak impact pressure may be reduced by 50% from the value for flat impacts if, for example, there is a deadrise of 20°.

Example 7.8

Given:

$$L = 400 \text{ ft}$$
$$\beta = 10^\circ$$
$$B = 65 \text{ ft}$$
$$T = 0.5 \text{ ft (instantaneous draft)}$$
$$\dot{z} = 40 \text{ ft/sec}$$
$$\beta = 0.175$$
$$Y_s = 10 \text{ ft}$$
$$2b = 30 \text{ ft}$$

Find the maximum impact pressure.

Solution:

Thus in (7.56) we have

$$p_0 = \tfrac{1}{2}\rho(\dot{z}_x)^2 = \tfrac{1}{2} \times 2 \times 40^2$$
$$= 1600 \text{ lb/ft}^2$$

and

$$\delta = \frac{z_x}{2bz_x} = \frac{40}{30 \times 64.4} = 0.02 \text{ sec/ft}$$
$$\ddot{z}_x = 2g = 64.4 \text{ ft/sec}^2$$

The maximum pressure is, then,

$$p = 1600\left[\frac{2}{0.175\sqrt{1-(10/30)^2}} + \frac{2}{0.02}\sqrt{\left(1-\frac{10}{30}\right)^2} - \frac{(10/30)^2}{1-(10/30)^2}\right]$$
$$= 1600(12.12 + 66.67 - 0.375)$$
$$= 125{,}456 \text{ psf (or 871 psi)}$$

Figure 7.26 shows the pressures experienced by the forefoot at instances immediately before and after slamming as computed in Ref. 203. The times noted on the figure are measured from the instant the wave crest is at the midship section of the ship. If we now consider station 3, we see that at $t = 1.26$ sec this station is out of water and the pressure is therefore zero; at time $t = 1.28$ sec the pressure reaches a peak value of 1300 psi and then 0.02 sec later, is reduced to 87 psi. Hence the extreme pressure acts at a station for a very short length of time and therefore is not very significant. At the particular instant when the maximum pressure is experienced by station 3, the acceleration is found to have its slamming peak (i.e., at $t = 1.28$ sec).

Probability of Slamming

The probability of forefoot emergence is expressed by

$$\text{Prob}\{\text{forefoot emergence}\} = e^{-(T^2/2m_{0s})} \quad (7.58)$$

where T is the draft at the ship's bow, and m_{0s} is the area of the spectrum for relative bow motion.

Similarly, the probability that the relative bow velocity amplitude $\dot{s}_a$ exceeds the threshold velocity v_0 is given by the expression

$$\text{Prob}\{\dot{s}_a \geq v_0\} = e^{-(v_0^2/2m_{0\dot{s}})} \quad (7.59)$$

where $m_{0\dot{s}}$ is the variance of the relative bow velocity, which is equal to the area of the response spectrum of the relative bow velocity.

If it is assumed that bow emergence and relative bow velocity are statistically independent events, the combined probability (which is the product of the probability of bow emergence and the probability that the relative bow velocity exceeds the threshold velocity) then gives the slamming probability, that is,

$$\text{Prob}\{\text{slam}\} = e^{-(T^2/2m_{0s} + v_0^2/2m_{2s})} \quad (7.60)$$

The frequency of occurrence of slamming per unit time, N_s, can now be predicted as

$$N_s = \frac{1}{2\pi}\sqrt{\frac{m_{2s}}{m_{0s}}} \times \text{Prob}\{\text{slam}\} \quad (7.61)$$

where N_s = number of slams per second
m_{0s} = area of the response spectrum of relative motion between the ship at the station considered and the water surface [ft^2]
m_{2s} = area of the response spectrum of relative velocity at the station considered [ft^2/

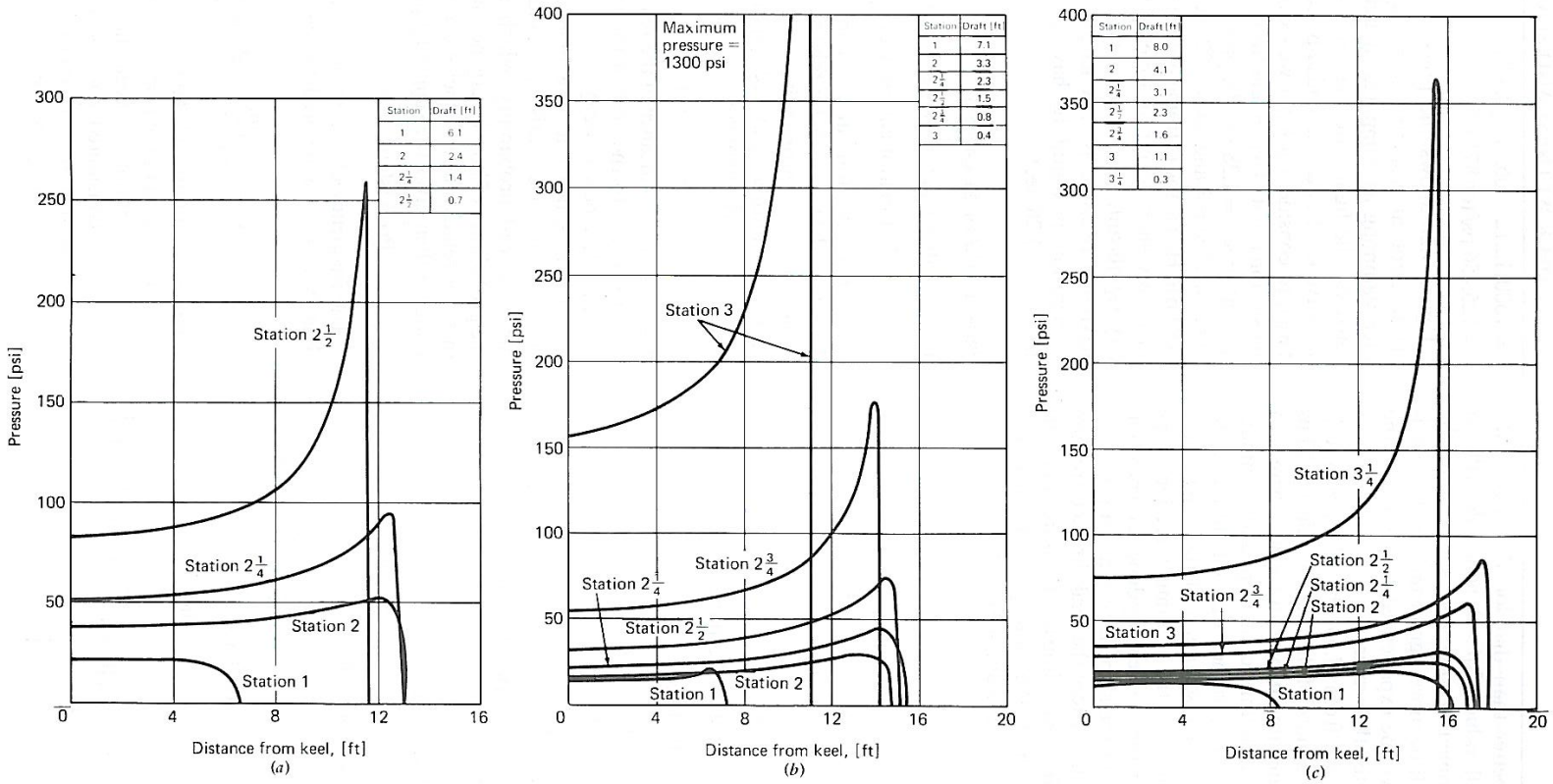


Figure 7.26 Pressure distribution at forefoot at different times [203]. (*a*) At 1.26 sec. (*b*) At 1.285 sec. (*c*) At 1.31 sec.

sec^2]; if the ordinate of the relative motion spectrum is $S_s(\omega_e)$, that of the relative velocity spectrum is $\omega_e^2 S_s(\omega_2)$

v_0 = critical value of the relative velocity above which slamming occurs [ft/sec]; this is called the *threshold velocity*, which is normally 12 ft/sec for a 520 ft vessel [ft/sec].

Equations 7.60 and 7.61 are related by the formula for the expected period $\tilde{\tilde{T}}$, which, for a narrow band random variable having a normal distribution with zero mean, is expressed as

$$\tilde{\tilde{T}} = \frac{1}{2\pi}\sqrt{\frac{2m_{0\dot{s}}}{2m_{0s}}}$$

The version of (7.60) for slamming given in Ref. 170 indicates that the probability of slamming increases with ship speed in head seas. The equation also emphasizes the importance of the relative bow vertical velocity.

Experimentally, it has been found that the threshold velocity for slamming decreases with an increase in Froude number, and Froude law is used for ships of different lengths. For a ship of 2000 ft length that is otherwise similar to a 520 ft ship, v_0 should be 24 ft/sec (i.e., 12 $\sqrt{\lambda}$), where λ, the scale factor, is equal to 4.

Tasai [208] looked for the v_0 at which the value of N_s obtained from experiments coincided with the value calculated by (7.61), and the result is shown in Fig. 7.27. The figure shows that v_0, the threshold velocity, is not constant but decreases as the Froude number becomes larger. The value for v_0 of 0.5 m/sec according to Ref. 167 seems to represent the mean value of experimental results for the ship model of [208].

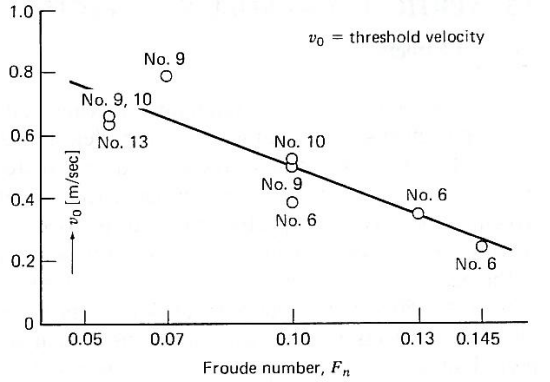


Figure 7.27 Threshold velocity as a function of speed [208].

Example 7.9

Given:

$L = 550$ ft

T = draft at station 2 = 17.1 ft

V = ship speed = 10 knots

$2m_{0s} = 605$ ft^2

$2m_{0\dot{s}} = 305$ ft^2/sec

The sea state value is a severe 7, and the wind velocity is 41 knots. Assume that the significant wave height is 35.0 ft.

Predict the number of slams for this ship during a 30 min operation.

Solution:

Since v_0, the threshold velocity, for a 520 ft ship is 12 ft/sec, for a 550 ft ship (Froude's law being valid),

$$v_0 = 12\sqrt{\lambda} = 12\sqrt{\frac{550}{520}} = 12.6 \text{ ft/sec}$$

Also, $2m_{0\dot{s}} = 2m_{2s}$ since the area under the response spectrum for relative bow velocity is considered to be equal to the second moment of the area under the relative bow motion spectrum. Therefore the number of slams per second, obtained using (7.61), is

$$N_s = \frac{1}{2\pi}\sqrt{\frac{152.5}{302.5}}\, e^{-[(17.1)^2/605 + (12.6)^2/305]}$$

$$= 0.041 \text{ sec}^{-1} \text{ or } 75 \text{ slams within a period of } 30 \text{ min}$$

The number of slam impacts in T hours is given as

$$N(T) = (3.6 \times 10^2)\frac{T}{2\pi}\sqrt{\frac{m_{2s}}{m_{0s}}}\,\text{Prob}\{\text{slam impact}\}$$

where T is ship operation time.

Interval Between Slam Impacts

The probability that a specified time t_0, or longer, will elapse before the next slam impact is given [167] by.

$$P\{\text{time interval between successive impacts} > t_0\} = e^{-N_s(t_* - t_0)} \tag{7.62}$$

where N_s is the number of slams per unit time, and t_* is the natural pitching period.

7.5 VERTICAL AND ROLLING EFFECTS

Vertical Effects

Vertical effects, such as pitching, heaving, and associated effects for regular waves, can be determined reasonably well by the strip theory and are treated in Chapter 9. To estimate the vertical effects in an irregular seaway the spectral method is used. In this analysis it is of some interest to know the position of the peak in the response spectra. It has been found that $\omega_e \approx 0.50 \text{ sec}^{-1}$ is the position for the peak for all vertical effects in bow sea conditions. When the period of the main component of the sea state is about 16 sec and the angle of encounter $\mu = 45°$, the frequency of encounter for this regular wave and a ship speed of 15 knots is about 0.48 sec^{-1}, which is very close to the position of the peak response.

Similarly, the position of the peak of the response spectrum for vertical effects in following seas has been found to be $\omega_e = 0.30 \text{ sec}^{-1}$. For an angle of $\mu = 135°$ and a main wave component having a period of 16 sec, the frequency of encounter has a value of $\omega_e = 0.30 \text{ sec}^{-1}$.

It should be remembered that for the peak frequencies of vertical effects the sea spectrum plays the dominant role in the determination of the peak position of the response spectrum, and not the response amplitude operator (RAO).

Rolling Effects

Estimates of the amplitude of rolling motion obtained by analytical means do not agree well with the results of measurements. This discrepancy appears to be due to inaccurate estimation of the roll damping in the analytical calculations.

It is also noteworthy that the peak position for the response spectrum of rolling motion occurs at the same frequency, namely, $\omega_e \approx 0.5 \text{ sec}^{-1}$, for both head and following sea conditions. For the head sea case this peak position happens to be very close to that for vertical effects; however, for the following sea case it is quite different from the vertical effect peak position. This encountering frequency value, $\omega_e = 0.50$, gives a period of $T_e = 12.6$ sec, which is quite reasonable for the rolling period of a ship.

Typical vertical and rolling effects are compared in Fig. 7.28, which shows the response spectra for both. In Fig. 7.28*a* the (RAO) for rolling is shown and is seen to be rather narrow. The peak of the response spectrum is at almost the same position as is the

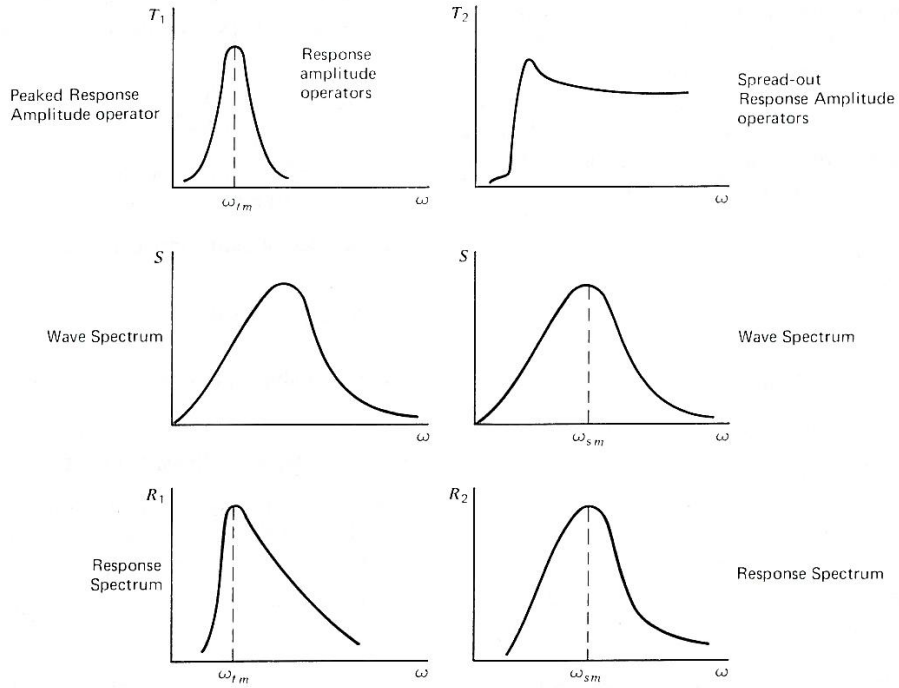


Figure 7.28 Peak position of the response spectrum.

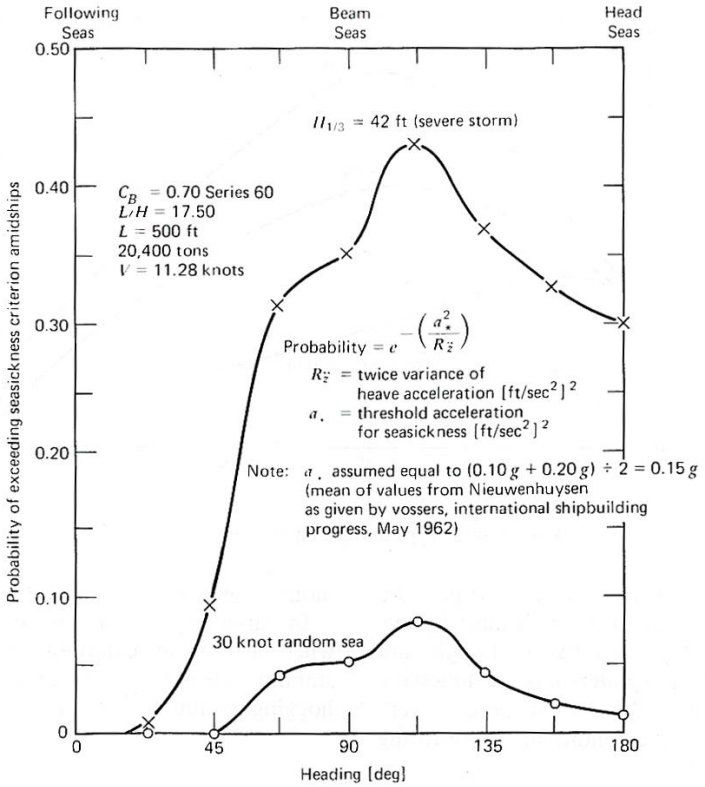


Figure 7.29 Probability of heave acceleration exceeding seasickness criterion [96].

peak for the RAO for rolling. In Fig. 7.28*b* it is the encountering wave spectrum that determines the shape of the response spectrum, and the peak of the response spectrum is at the same position as is the encountering wave spectrum. Here the RAO for heaving motion happens to be spread out, which is normally the case with this kind of motion.

7.6 SEASICKNESS

Seasickness is defined as the motion sickness experienced by the passengers and crew of a ship during travel in a seaway. One of the main reasons for such discomfort is supposed to be the fact that the vital organs of equilibrium are subjected to continuous changes in acceleration during various kinds of ship motions. Vertical acceleration values in the range of 0.10 to 0.20 g may be considered to represent the limit of human tolerance. Since vertical acceleration due to rolling seldom exceeds 0.20 g, acceleration due to pitch and heave may be considered to be the real source of seasickness.

With 0.15 g as the criterion for seasickness, Fig. 7.29 shows the effect of heading on the probability of exceeding this criterion for a certain value of $L/H = 17.5$ and at a speed of 11.28 knots.

7.7 STABILITY IN WAVES

Large motion amplitudes and large accelerations can be causes for speed reductions. In particular, large rolling amplitudes may be a reason for changing course to avoid resonance conditions. Large rolling motions occur not only at resonance, but also under certain conditions in longitudinal waves. In such waves the restoring roll moment is a time-dependent quantity, and unstable regions with large roll angles exist at or near $\omega_\phi/\omega_e = \frac{1}{2}, 1, 1\frac{1}{2}$, and so on, where ω_ϕ is the natural roll frequency and ω_e is the frequency of encounter.

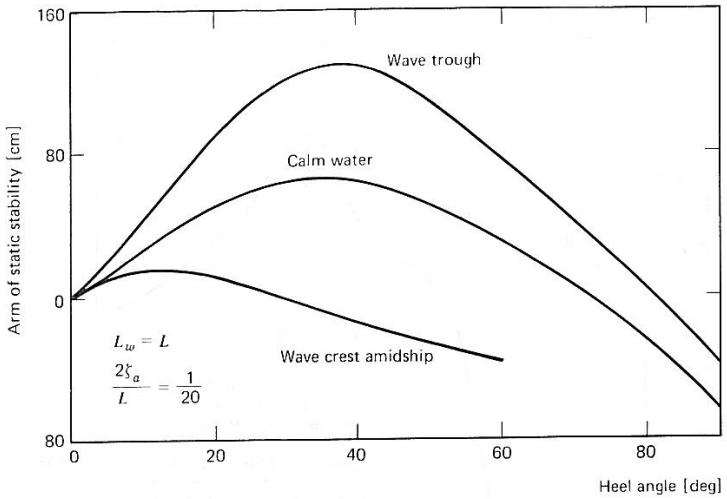


Figure 7.30 Typical righting arms in a wave.

In a following sea the danger due to these periodic changes in the roll restoring moment is most serious at $F_n = 0.20$ and $T_\phi = 5\sqrt{L/g}$. Large heel angles are also reported from fast, slender-ships in following seas when the frequency of wave encounter is very small. In such nearly static conditions the restoring moment on a wave crest can be extremely small.

In summary, maximum static stability occurs when a sagging condition exists, and minimum stability when the wave crest is amidships (i.e., a hogging condition). See Fig. 7.30.

Chapter

Eight

MOTION IN A THREE-DIMENSIONAL IRREGULAR SEAWAY

8.1 Three-Dimensional Irregular Seaway

In the preceding chapters the behavior of a ship or a model was studied for an irregular seaway having only two-dimensional irregularity. The wave heights in this case are specified for any value of wave frequency ω_w, and the waves come from only one direction of the sea. This idealized case is also known as a *long-crested seaway*, since the wave crests can be considered as uninterrupted and, therefore, very long.

In reality a seaway has a three-dimensional irregularity, in which the waves not only are of different heights and frequencies but also may approach any point from various directions. This is also sometimes referred to as the *short-crested seaway*. A seaway is seldom composed of waves traveling in one direction only. Thus the spectral energy density $S_\zeta(\omega_w)$ becomes a function not only of the frequency ω_w, but also of the direction of the component waves relative to the dominant wave direction μ_w.

In the case of a two-dimensional spectrum the cross-spectral density of the wave spectrum is obtained by summing the squares of the component wave amplitudes within both the frequency interval from ω_w to $\omega_w + d\omega_w$ and the directional interval between μ_w and $\mu_w + d\mu_w$; thus

$$S_\zeta(\omega_w, \mu_w) = \tfrac{1}{2}[(\zeta_{a_1})^2 + (\zeta_{a_2})^2 + \ldots + (\zeta_{a_n})^2] \quad (8.1)$$

for a frequency between ω_w and $\omega_w + d\omega_w$ and for a direction between μ_w and $\mu_w + d\mu_w$. The prefix "cross" indicates directional dependence.

From (8.1) we see that a larger amount of energy may be associated with one direction than another. However, at any one point the energy is approximately constant, and it is not necessary to know from which direction the energy is coming. Thus the spectral density of the waves at a point is

$$S_\zeta(\omega_w) = \int S_\zeta(\omega_w, \mu_w)\, d\mu_w \quad (8.2)$$

The area under the wave spectrum thus becomes a double integral of the form

$$m_{0\zeta} = \int_0^\infty \int_{-\pi/2}^{\pi/2} S_\zeta(\omega_w, \mu_w)\, d\mu_w\, d\omega_w$$

$$= \int_0^\infty \int_{-\pi/2}^{\pi/2} S_\zeta(\omega_w) \times f(\mu_w)\, d\mu_w\, d\omega_w \quad (8.3)$$

since it is assumed that

$$S_\zeta(\omega_w, \mu_w) \approx S_\zeta(\omega_w) \times f(\mu_w) \quad (8.4)$$

where $f(\mu_w)$ is called the *spreading function* to account for the component waves. Such an assumption is made because it is rather difficult to obtain a two-dimensional spectrum that actually represents a seaway more fully. Since both one-dimensional and two-dimensional spectra should deliver the same energy, the integral of the spreading function should be equal to 1.0. Thus

$$\int_0^\infty \int_{-\pi/2}^{\pi/2} S_\zeta(\omega_w, \mu_w)\, d\mu_w\, d\omega_w = \int_0^\infty S(\omega_w)\, d\omega_w \quad (8.5)$$

where it is assumed [105] that

$$f(\mu_w) = \frac{2}{\pi} \cos^2 \mu_w \quad (8.6)$$

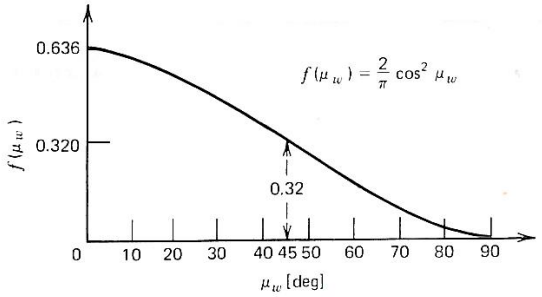


Figure 8.1 Spreading function for a short-crested seaway.

so that

$$\int_{-\pi/2}^{\pi/2} f(\mu_w) = 1.0$$

The integration for (8.3) can be easily performed by using *Simpson's rule*, first with respect to μ_w and then with respect to ω_w.

For our purposes let us define

μ_a as the *ship's course* relative to the dominant wave train or wind direction, where $0° \leqslant \mu_a \leqslant 180°$

μ_w as the angle between the component wave direction and the dominant wave direction, where $-90° \leqslant \mu_w \leqslant 90°$

also,

$$\mu = \mu_w + \mu_a \tag{8.7}$$

TABLE 8.1 WAVE SPECTRUM, $\mu_w = 45°$

ω_w [sec^{-1}] ①	$S_\zeta(\omega_w)$ (see Table 5.8) [ft^2-sec] ②	$S_\zeta(\omega_w, \mu_w) = S_\zeta(\omega_w) \times f(\mu_w)$ ② × 0.32 [ft^2-sec] ③
0.2	0	0
03	0.02	0.06
0.4	17.80	5.70
0.5	55.97	17.90
0.6	50.68	16.22
0.7	33.22	10.64
0.8	10.17	6.44
0.9	12.25	3.92
1.0	7.61	2.44

is the angle between the component wave and the ship's direction of travel. The plus sign of the μ expression signifies an angular addition, but not necessarily an algebraic addition.

The spreading function $f(\mu_w)$ of (8.6) is presented as a function of μ_w in Fig. 8.1. Table 8.1 shows the calculations for S_ζ for different values of ω_w and $\mu_w = 45°$ [i.e., $(f(\mu_w) = 0.32]$ from the ITTC formulation for wave spectra for a significant wave height of 18.5 ft.

Figure 8.2 is a typical two-dimensional spectrum, showing the spectral density as a function of both frequency ω_w and direction of the wave components μ_w as calculated by the ITTC formulation. For example, $S_\zeta(\omega_w = 0.50\,\text{sec}^{-1}, \mu_w = 45°) = 17.90\,\text{ft}^2\text{-sec}$ as shown in the figure (see also Table 8.1).

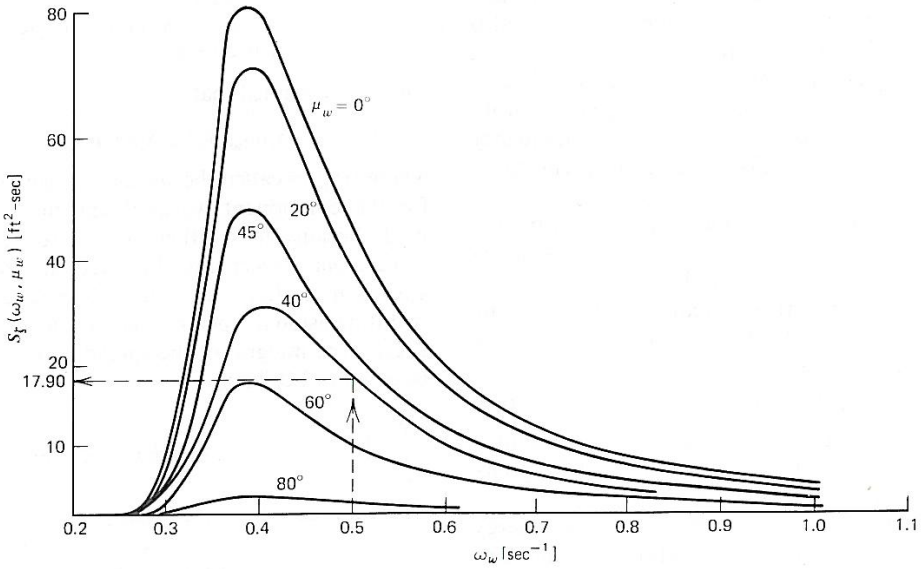


Figure 8.2 Angular components of wave spectrum.

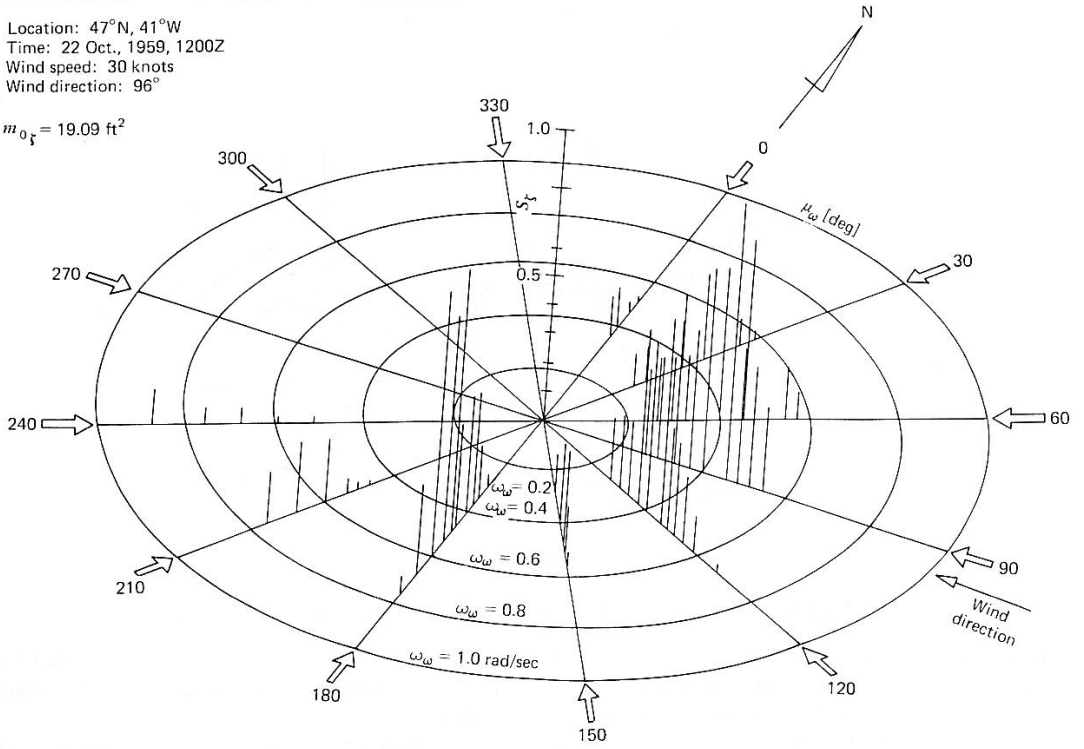


Figure 8.3 Two-dimensional sea spectrum for a three-dimensional seaway [228].

Figure 8.3 shows a typical two-dimensional sea spectrum for an actual three-dimensional seaway.

8.2 MOTION IN A SHORT-CRESTED SEAWAY

Let us now consider ship motion in a three-dimensional (or a short-crested) seaway. As before, the spectral densities of any kind of ship motion can be given as functions of the encountering wave spectra and the RAOs.

The expressions for the encountering wave spectrum, as well as the response spectrum for a short-crested seaway, are as follows:

a. The spectral density of the encountering wave spectrum is

$$S_\zeta(\omega_e,\mu_w) = S_\zeta(\omega_e) \times f(\mu_w) \tag{8.8}$$

where the frequency of encounter from (3.18a) is

$$\omega_e = \omega_w\left(1 - \frac{\omega_w}{g} V \cos\mu\right)$$

and the spectral density of the point wave spectrum is

$$S_\zeta(\omega_e) = \frac{S_\zeta(\omega_w)}{[1 - (4\omega_e/g) V \cos\mu]^{1/2}}$$

$$= \frac{S_\zeta(\omega_w)}{1 - (2\omega_w/g) V \cos\mu} \tag{8.9}$$

where μ is defined by (8.7). The area under the encountering wave spectrum is given by

$$m_{0\zeta} = \int_0^\infty \int_{-\pi/2}^{\pi/2} S_\zeta(\omega_e) f(\mu_w) d\mu_w \, d\omega_e$$

b. For the analysis of ship motion in a three-dimensional seaway, the RAOs are functions of the frequency ω_e, as well as of μ, which is the angle between the component wave and the ship's direction of travel; thus

$$\text{RAO} = \text{RAO}(\omega_e,\mu)$$

As previously mentioned, the different values for RAO are generally obtained by a series of systematic model tests in regular waves, where, for each value of the relative heading μ, various frequencies ω_e are considered.

Figure 8.4, for example, shows the *nondimensional heave response* z_a/ζ_a(= heave amplitude/wave amplitude) as a function of frequency and direction obtained from a regular wave test, while Fig. 8.5 shows the *nondimensional roll response*, that is, $\phi_a/k\zeta_a$ [= roll amplitude/(wave amplitude × wave number)]. Note that the data in Figs. 8.4 and 8.5, if extrapolated, would

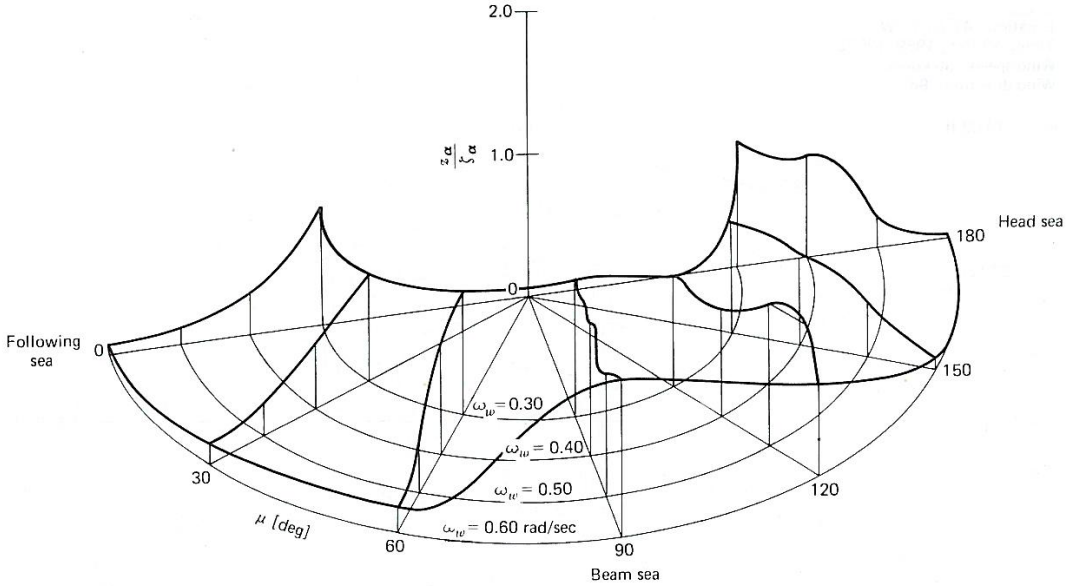


Figure 8.4 Heave response of an aircraft carrier at a speed of 25 knots [228].

be unity at zero frequency (i.e., infinite wavelength, so no dynamic effect). Ratios of roll angle to wave slope in excess of 4.0 can be obtained in beam seas, and large roll amplitudes are also experienced in quartering seas. Rolling is also observed in head and following waves at the encounter frequency.

The amplitudes of roll experienced in head waves are smaller than those in following seas. In the measurement of roll, it is observed that a model rolls at the frequency of encounter even in conditions near synchronism.

A typical *pitching motion* in nondimensionalized form, $\theta_a/k\zeta_a$ [= pitch amplitude/(wave amplitude × wave number)], is presented in Fig. 8.6. The maximum values are observed in head seas, with the dimensionless pitching response exceeding 1.00. The pitching

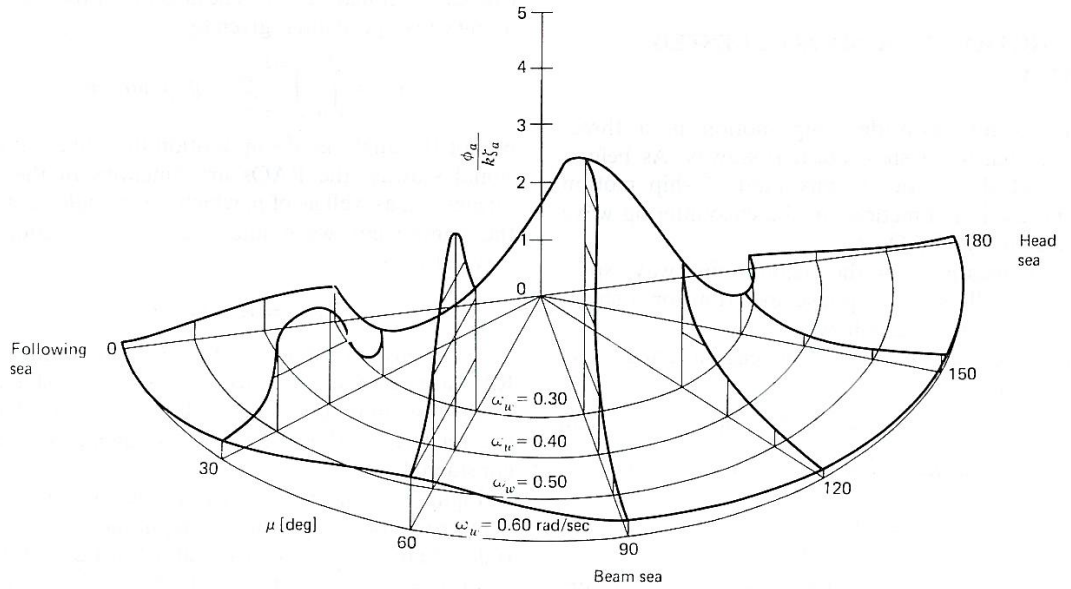


Figure 8.5 Roll response of an aircraft carrier at a speed of 25 knots [228].

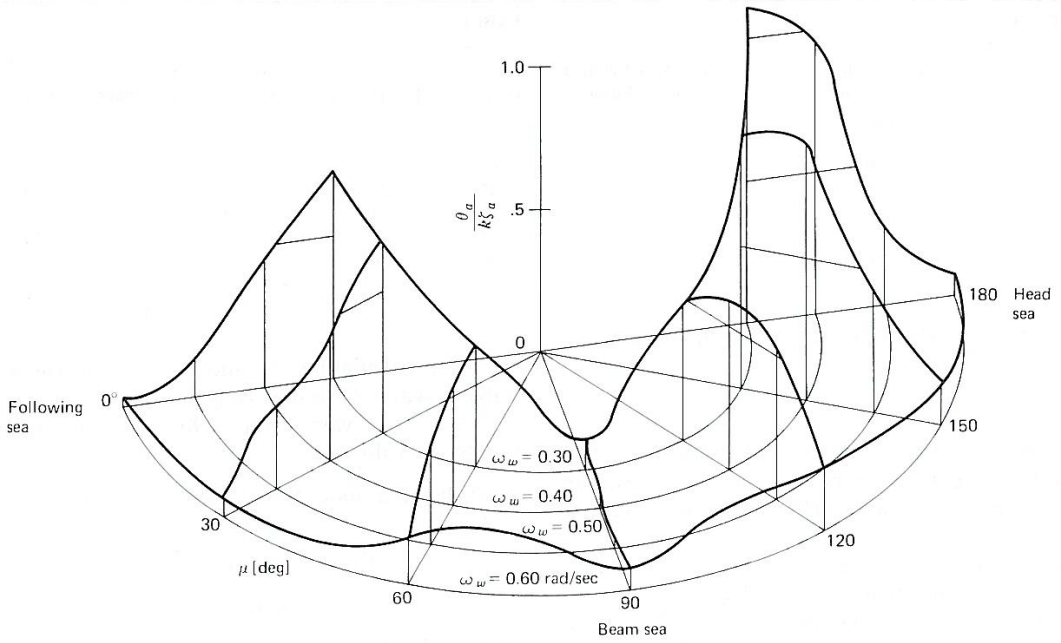


Figure 8.6 Pitch response at an aircraft carrier a speed of 25 knots [228].

gradually decreases in bow seas, and minimum motion is obtained in beam waves. Larger amplitudes of pitching motion are measured in quartering and following waves.

The test data also can be directly obtained from irregular wave tests and by analytical means, especially if computer programs for various ship motions are available.

c. The spectral density of the response, S_R, can now be expressed as

$$S_R(\omega_e,\mu_w) = [S_\zeta(\omega_e)f(\mu_w)]\,[\mathrm{RAO}(\omega_e,\mu_w)] \quad (8.10)$$

and the area under the response spectrum is given by

$$\begin{aligned} m_{0R} &= \int_{-\pi/2}^{\pi/2}\int_0^\infty S_R(\omega_e,\mu_w)\,d\omega_e\,d\mu_w \\ &= \int_{-\pi/2}^{\pi/2}\int_0^\infty [S_\zeta(\omega_e)f(\mu_w)] \\ &\quad \times [\mathrm{RAO}(\omega_e,\mu_w)]\,d\omega_e d\mu_w \end{aligned} \quad (8.11)$$

For example, the area under the relative bow motion spectrum is

$$\begin{aligned} m_{0s} &= \int_{-\pi/2}^{\pi/2}\int_0^\infty S_s(\omega_e,\mu_w)\,d\omega_e\,d\mu_w \\ &= \int_{-\pi/2}^{\pi/2}\int_0^\infty [S_\zeta(\omega_e)f(\mu_w)] \\ &\quad \times \left\{\left[\frac{s_a}{\zeta_a}(\omega_e,\mu_w)\right]^2\right\} d\omega_e d\mu_w \end{aligned} \quad (8.12)$$

Example 8.1

A ship having a length of 400 ft is heading directly into dominant waves (i.e., $\mu_a = 180°$) at a speed of 20 knots (33.78 ft/sec), and the data in Table 8.2 are available for the relative bow motion from towing tank tests for various angles between wave and ship's direction of travel.

What would be the significant amplitude of the relative bow motion of this ship when running in a short-crested seaway having a significant wave height

TABLE 8.2

		$\left(\frac{s_a/L}{2\pi\zeta_a/L_w}\right)^2$	
$\frac{L_w}{L}$	ζ_a [ft]	$\mu = 180°$	$\mu = 135°$ or $225°$
0.50	2.5438	0.0086	0.0078
0.75	3.8156	0.0477	0.1332
1.00	5.0875	0.2424	0.1345
1.25	6.3594	0.2500	0.0978
1.80	9.1575	0.1592	0.0566
3.00	15.2625	0.0791	0.0327

TABLE 8.3

μ_w [deg]	$\mu = \mu_a + \mu_w = 180^\circ + \mu_w$ [deg]	RAO for Relative Bow Motion
+90	270	$s_{a1}(\omega_e)$
+45	225	$s_{a2}(\omega_e)$
0	180	$s_{a3}(\omega_e)$
−45	135	$s_{a4} = s_{a2}(\omega_e)$
−90	90	$s_{a5} = s_{a1}(\omega_e)$

of 18.5 ft? Use the ITTC formulation for a wave spectrum in Section 5.4.

Solution:

The response amplitude operator should also vary for both different frequencies and angular positions of the component waves. The RAOs are given in Table 8.3.

The direction of ship's travel relative to the component waves is shown in Fig. 8.7. Different areas of response spectra, denoted by A's for different sea and heading conditions as shown in Fig. 8.8, are obtained from different tables. Thus the first table will provide the value for A_1, the second A_2, and so on. Since $A_1 = 0$, $A_5 = 0$, and $A_4 = A_2$, only table for calculating A_2 and A_3 are presented as Tables 8.4 and 8.5, respectively.

Now let μ_w vary from $+90^\circ$ to -90° in (8.3) to obtain Table 8.6.

TABLE 8.6

μ_w [deg]	$\mu = \mu_w + \mu_a$ [—][deg]	Area [ft²]	Simpson's Multiplier [—]	Product [ft²]
+90	270	$A_1 = 0$	1	0
+45	225	$A_2 = 18.376$	4	73.504
0	180	$A_3 = 50.283$	2	100.566
−45	135	$A_4 = 18.376$	4	73.504
−90	90	$A_5 = 0$	1	0
			SUM	247.574 ft²

Thus the area under the response spectrum

$$m_{0s} = \tfrac{1}{3} \times \frac{45^\circ}{57.3} \times 247.574$$
$$= 64.810\, ft^2$$

and the significant relative bow motion is

$$2.0\sqrt{m_{0s}} \times \text{CF} = 2.0 \times \sqrt{64.810} \times 1.0$$
$$= 16.10 \text{ ft}$$

TABLE 8.4 DETERMINATION OF RESPONSE SPECTRUM FOR $\mu_w = 45^\circ$, $\mu = 135^\circ$ OR 225°, $f(\mu_w) = \frac{2}{\pi}\cos^2 \mu_w = 0.318$

$\frac{L_w}{L}$ [—] ①	L_w [ft] ②	ω_w [sec⁻¹] ③	$S_\zeta(\omega_w)$ [ft²-sec] ④	ω_e [sec⁻¹] ⑤	$S_\zeta(\omega_e)$ [ft²-sec] ⑥	$S_\zeta(\omega_e, \mu_w)$ ⑥ × 0.318 [ft²-sec⁻¹] ⑦	$\left(\frac{s_a/L}{2\pi\zeta_a/L_w}\right)^2$ [—] ⑧	$\left(\frac{s_e}{\zeta_a}\right)^2$ [—] ⑨	$S_s(\omega_e, \mu_w)^*$ ⑦ × ⑨ [ft²-sec] ⑩
0.50	200	1.006	7.407	1.757	2.972	0.945	0.0078	1.230	1.163
0.75	300	0.821	18.145	1.321	8.182	2.602	0.1332	9.339	24.299
1.00	400	0.711	31.493	1.086	15.327	4.874	0.1345	5.304	25.851
1.25	500	0.636	44.324	0.936	22.807	7.253	0.0978	2.469	17.907
1.80	720	0.530	57.957	0.738	32.448	10.318	0.0566	0.689	7.110
3.00	1200	0.411	23.044	0.536	14.316	4.552	0.0327	0.143	0.651

*$S_s(\omega_e, \mu_w)$ values are drawn to a base of ω_e; the area can be found by Simpson's rule if the ordinates are read off at equal intervals. In this case, area = 18.376 ft².

TABLE 8.5 DETERMINATION OF RESPONSE SPECTRUM FOR $\mu_w = 0^\circ$, $\mu = 180^\circ$, $f(\mu_w) = \frac{2}{\pi}\cos^2 \mu_w = 0.637$

$\frac{L_w}{L}$ [—] ①	L_w [ft] ②	ω_w [sec⁻¹] ③	$S_\zeta(\omega_w)$ [ft²-sec] ④	ω_e [sec⁻¹] ⑤	$S_\zeta(\omega_e)$ [ft²-sec] ⑥	$S_\zeta(\omega_e, \mu_w)$ ⑥ × 0.637 [ft²-sec] ⑦	$\left(\frac{s_a/L}{2\pi\zeta_a/L_w}\right)^2$ [—] ⑧	$\left(\frac{s_a}{\zeta_a}\right)^2$ [—] ⑨	$S_s(\omega_e, \mu_w)$ ⑦ × ⑨ [ft²-sec] ⑩
0.50	200	1.006	7.407	2.068	2.381	1.517	0.0086	1.357	2.058
0.75	300	0.821	18.145	1.528	6.665	4.246	0.0477	3.344	14.197
1.00	400	0.711	31.492	1.241	12.639	8.051	0.2424	9.560	76.968
1.25	500	0.636	44.324	1.060	18.987	12.095	0.2500	6.310	76.318
1.80	720	0.530	57.957	0.825	27.442	17.481	0.1592	1.737	33.860
3.00	1200	0.411	23.044	0.588	12.374	7.882	0.0791	0.347	2.735

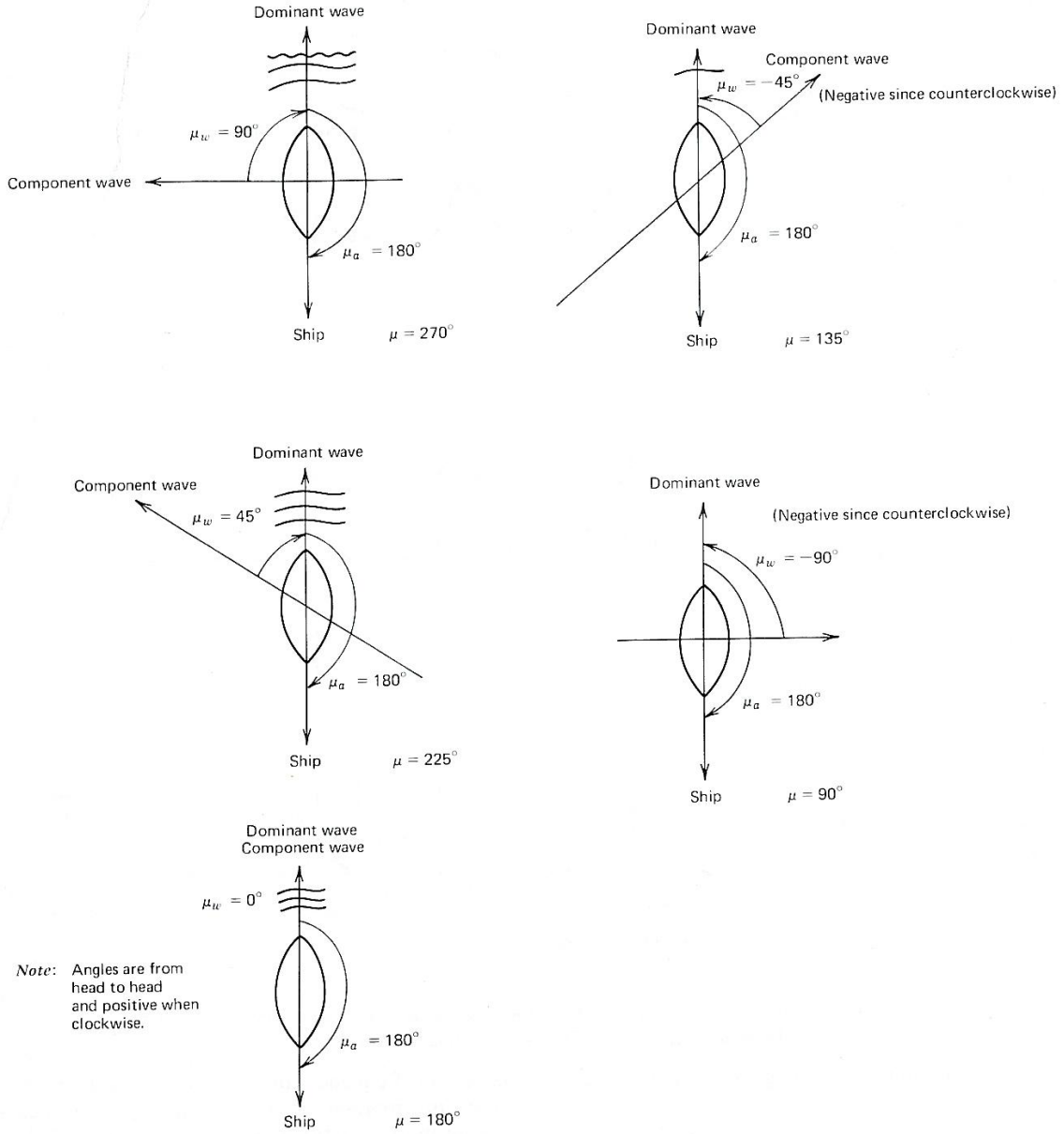


Figure 8.7 Ship's heading relative to component waves.

assuming a Rayleigh distribution (i.e., CF = 1.0).

Note the following:

1. A larger number of μ_w and ω_w values may give more accurate results.
2. Calculation with the two-dimensional wave spectrum gives a smaller significant bow motion than is obtained by using a one-dimensional wave spectrum. See Example 7.4.
3. From full-scale trials it has been found that the pitching motion predicted from model tests in irregular unidirectional head seas always exceeds the actual ship pitching motion in a three-dimensional (multidirectional) irregular seaway.
4. The directional spread of sea waves is of little importance as far as heaving motion is concerned; in other words, a change of ship course relative to the dominant waves has little effect on heaving

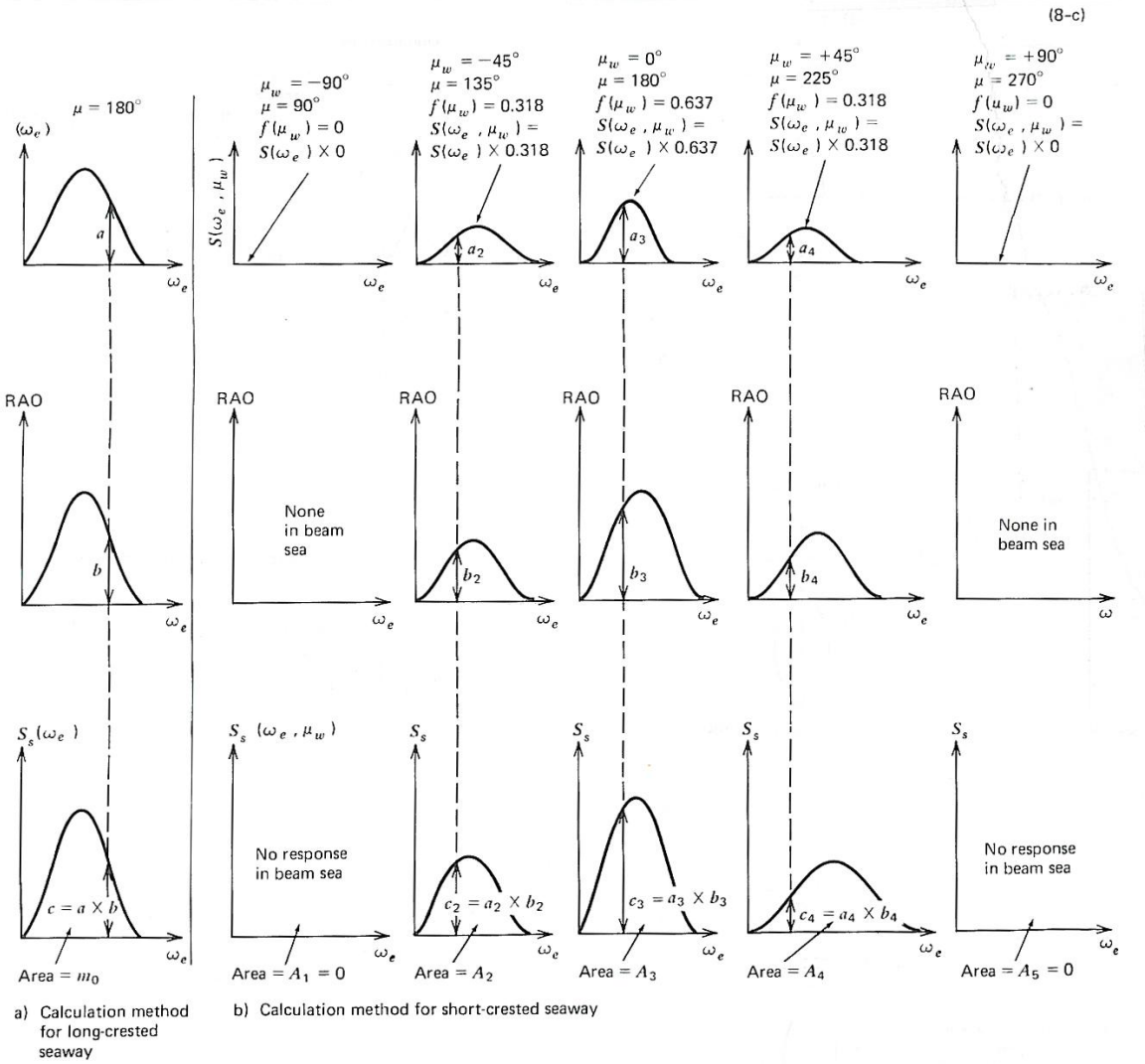
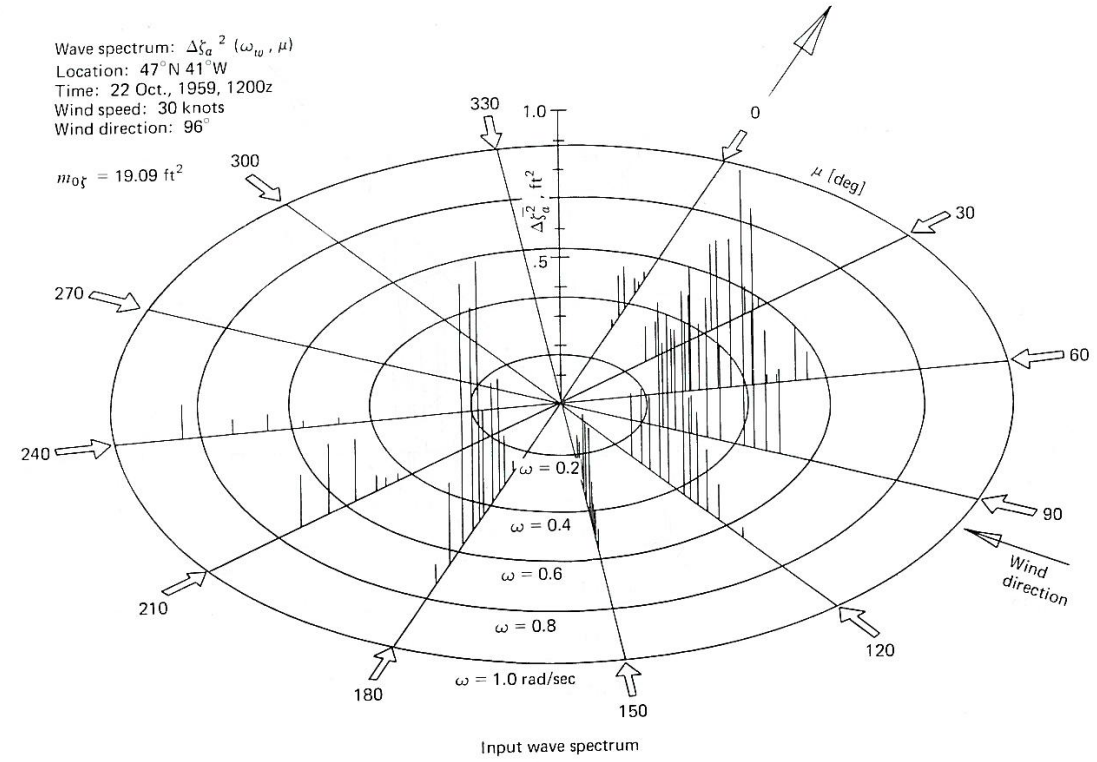


Figure 8.8 Scheme for computation of response spectrum in two-and three-dimensional seaway. (*a*) Two-dimensional seaway. (*b*) Three-dimensional seaway.

motions, although in pitching motions the effect is significant.

If wave spectra are desired from wave records, it is necessary to map both wave frequency and direction against frequency of encounter, which will result in an overlap of the various wave frequency bands in the frequency of encounter domain. For the computation the incremental meansquare values within each elemental band of wave frequency and direction are distributed uniformly in the corresponding frequency of encounter band. All such components are then redistributed into arbitrary bands of frequency of encounter, resulting in a spectrum represented by the incremental mean-square motion at the center of these bands [228].

A typical plot of the incremental meansquare pitch motion associated with each elemental wave direction and frequency band is given in Fig. 8.9, and the results, transformed to the frequency of encounter domain, are shown in Fig. 8.10 in terms of the incremental meansquare pitch motions contained in arbitrarily chosen frequency of encounter bands. The typical results shown in Fig. 8.10 are for a ship speed of 25 knots and a course angle of 60° in a seaway. The ordinate $\Delta\bar{z}^2$ in Fig. 8.10*a* is the mean square



Input wave spectrum

Figure 8.9*a* Input wave spectrum.

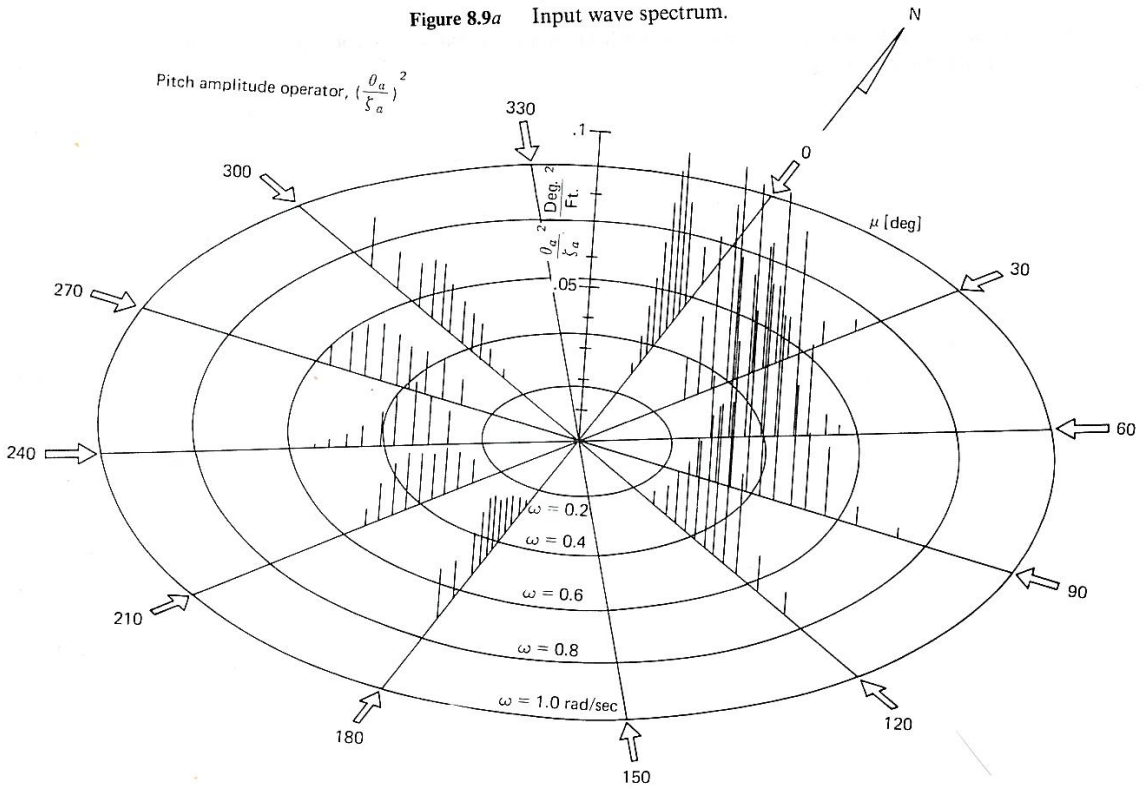


Figure 8.9*b* Pitch response operator at corresponding values of input wave spectrum.

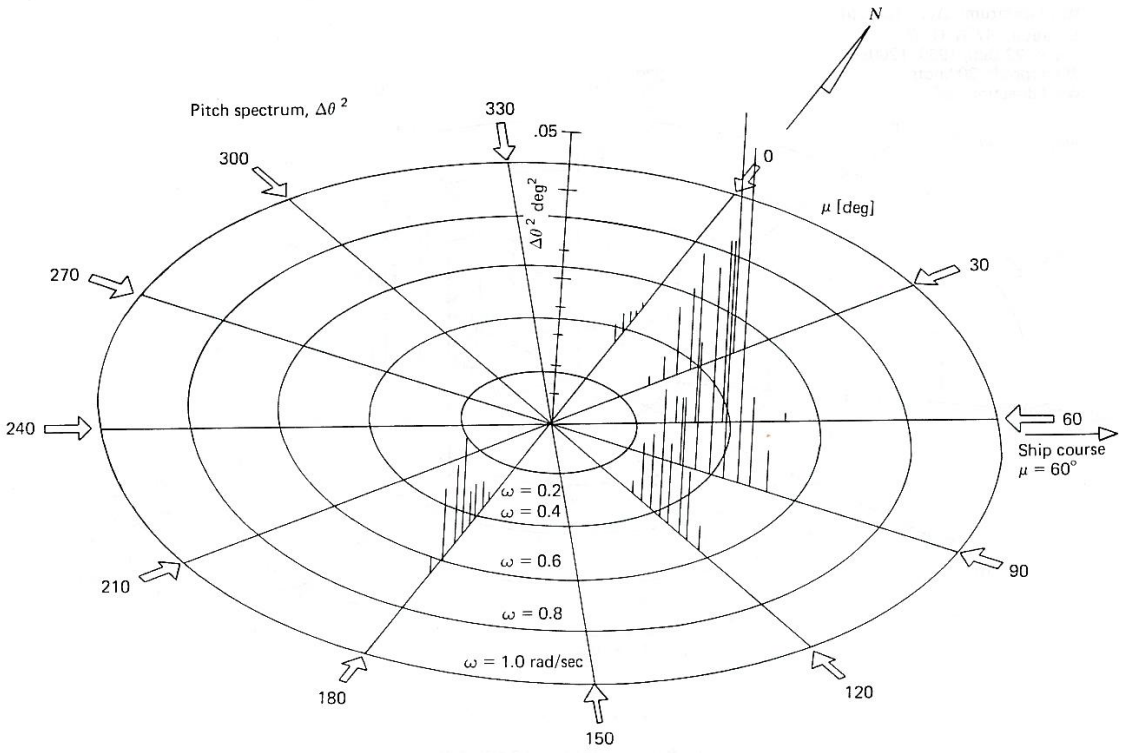


Figure 8.9*c* Incremental mean square pitch of an aircraft carrier for corresponding values of input wave spectrum [228].

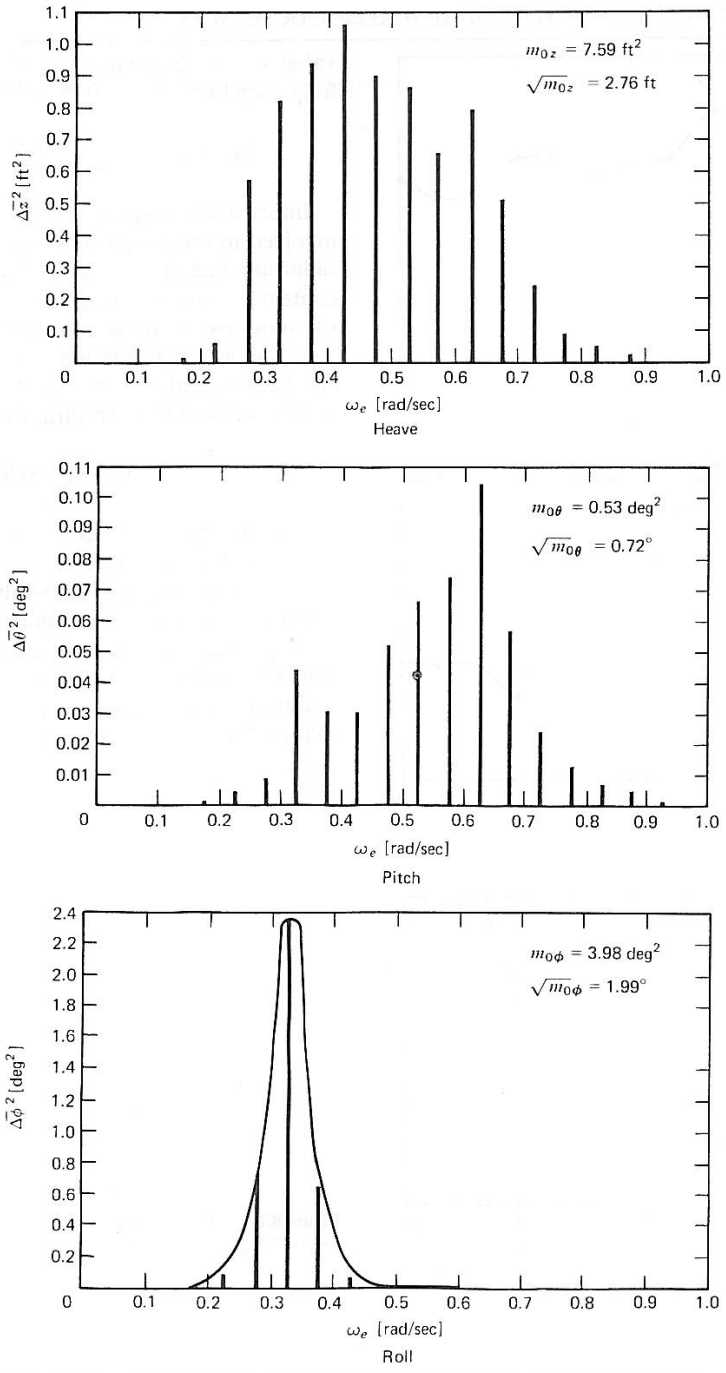
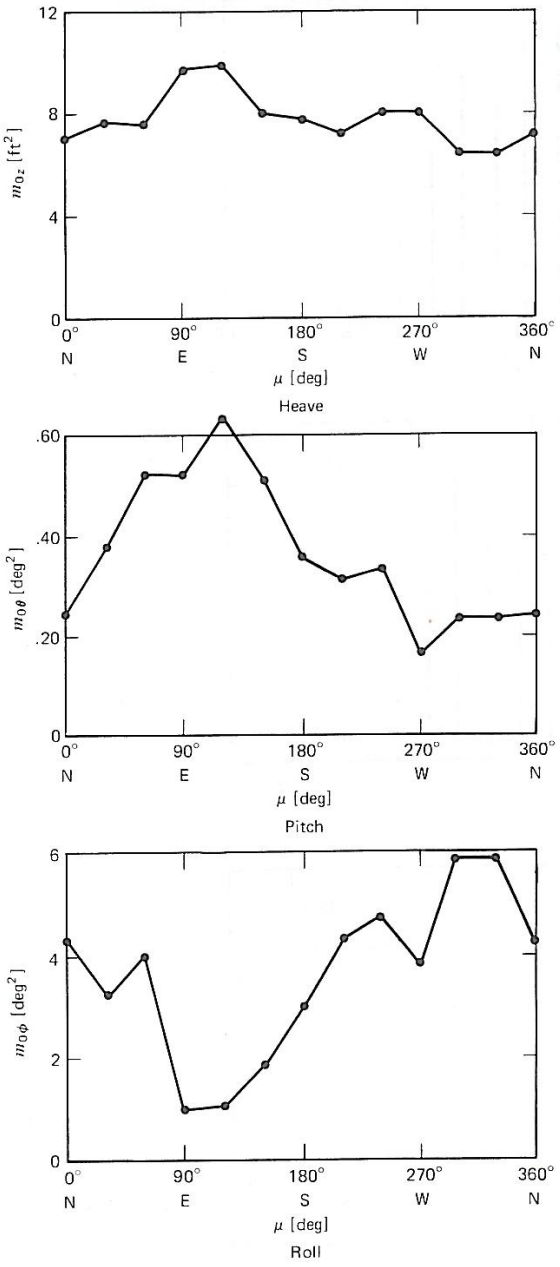


Figure 8.10 Typical heave, pitch, and roll spectra of an aircrafs carrier at a speed of 25 knots [228].



value of the heaving motion within an arbitrary frequency band $\Delta\omega_e = 0.05$ rad/sec, that is,

$$(\Delta\bar{z}^2)\,\Delta\omega_e = \sum_{\mu_w=0^\circ}^{360^\circ} = \Delta\bar{z}^2(\Delta\omega_e, \Delta\mu_w) \tag{8.13}$$

Information in spectral form is important to those involved in the design of a stabilization system for a radar antenna or in other problems where frequency content is important; other statistical averages of the motions are quite satisfactory. The meansquare value or variance (for functions with a zero mean) can be obtained by summing the incremental mean-square values of the spectra, that is,

$$m_{0z} = \sum_{\omega_e=0}^{\infty} \Delta z^2(\omega_e) \tag{8.14}$$

The variance can be used to obtain other statistical averages, if it is assumed that the motion amplitudes (double) follow a Rayleigh distribution. The statistical averages may then be computed to study the effects of ship's heading on vehicle motions, as shown in Fig. 8.11. Therefore the optimum course angle for a vessel in a particular seaway can be determined to minimize certain ship motions.

Figure 8.11 Heave, pitch, and roll as functions of heading angle [228].

Chapter

Nine

COUPLED HEAVING AND PITCHING MOTIONS

9.1 GENERAL

To simplify the study of ship motions only one degree of freedom of motion was considered in Chapter 4. Such a simplification allows us to gain a "feeling" for the forces and moments of forces involved. But in an actual seaway a ship experiences all six degrees of freedom of motion. Unfortunately, study of these coupled ship motions is rather difficult, and investigations are often restricted to the following coupled motions:

1. Heave and pitch.
2. Yaw and sway.
3. Yaw, sway, and roll.
4. Roll, yaw, and pitch.

Of these four coupled motions, the one dealing with vertical motions, namely, pitching and heaving motions, can be investigated easily in a model basin. The coupled heave and pitch for the head sea condition has been investigated analytically by the method known as the *strip theory*, and experiments have proved the validity of their approach beyond any doubt.

In the application of strip theory to coupled heaving and pitching motions two equations are derived, one for heave and the other for pitch. According to Newton's second law, at any instant all vertical forces on the ship are in dynamic equilibrium, or the sum of all the forces acting on a body at any instant is equal to the product of the body mass and its acceleration. Therefore the heaving equation is

$$m\ddot{z} = \Sigma F$$

and the pitching equation is

$$I\ddot{\theta} = \Sigma M$$

where ΣF represents the sum of various fluid forces (i.e., vertical hydrodynamic forces as well as the wave excitation force), and ΣM the sum of the corresponding moments acting on the vessel because of the relative motion of vessel and wave. When the vessel advances at a speed in calm water, the sum of vertical forces acting on the vessel is considered to be zero and there is no vertical motion of the ship.

In the study of seakeeping particular attention has been paid to the motions of pitch and heave, which are usually the factors limiting ship speed in rough weather. At high speeds a ship moving into large head seas will experience pitch and heave amplitudes that may alternately bring the bow completely out of water and submerge it. Such severe motions have considerable effects on ship structures and may require a reduction in speed and/or change of course in order to avoid damage. The ability to predict motions of pitch and heave more accurately is very helpful in improving the design for rough weather performance. A significant attempt in this area is Korvin-Kroukovsky's and Jacobs' strip theory [121]. The reader is also referred to the book by McCormick [150] for a thorough discussion of the theory. The object of the strip theory is to predict ship motions of pitch and heave for a seaway with given characteristics of amplitude and frequency. In formulating this theory Korvin-Kroukovsky was faced with reducing the phenomenon of ship–wave interaction to a workable mathematical form, a problem rendered complex because of the number of interdependent variables involved. To begin with, the motions of pitch and

heave may be *coupled* because one motion normally affects the other as the ship responds to waves. The fact that the ship is moving forward through the seaway further complicates the problem because of the added degree of motion.

9.2 BASIC APPROACH

To simplify this complex motion problem several assumptions and limitations have been made. First of all, the ship is assumed to be heading into the waves in a direction transverse to their crest line. The seaway is considered to consist of *regular harmonic* (*sinusoidal*) *waves*, and ship motions of surge, sway, yaw, and roll are neglected.

Freed by these assumptions, Korvin-Kroukovsky's[121] approach was to consider a ship's hull as a series of transverse segments, or *strips*, and to treat the flow adjacent to each as two dimensional in nature. The effect was to reduce the problem from three to two dimensions, with each strip assumed to be a part of an infinite cylinder having two-dimensional flow around it. It is, therefore, understood that there is no interaction of the flows at adjacent sections. However, there is an important difference between the assumed two-dimensional flow and the actual three-dimensional flow, particularly at both ends of the ship. The vertical motion of each strip is assumed to be composed of the combined pitching and heaving motions. After the response of each strip is calculated, the total ship response can be found by integrating the component reactions of all the strips along the ship's length. The basic mathematical equation obtained in this way is a linear second order differential equation describing the inertial, hydrodynamic, and hydrostatic components of force acting on each strip and caused by the relative vertical motion between the ship and the wave at the strip in question.

Coordinate Systems

Before embarking on a detailed analysis of the theory, it is necessary to set up a coordinate system. In Fig. 9.1*a* the primary axes are assumed to be fixed in space with their origins at a wave nodal point

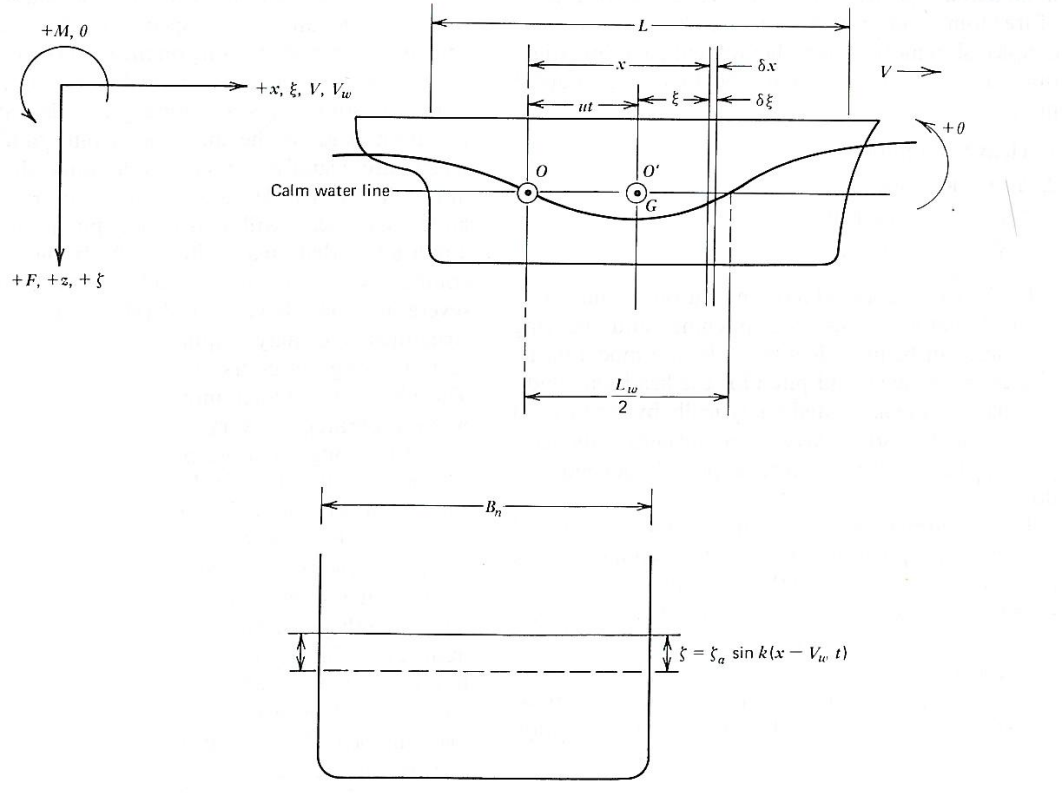


Figure 9.1*a* Coordinate system for strip theory.

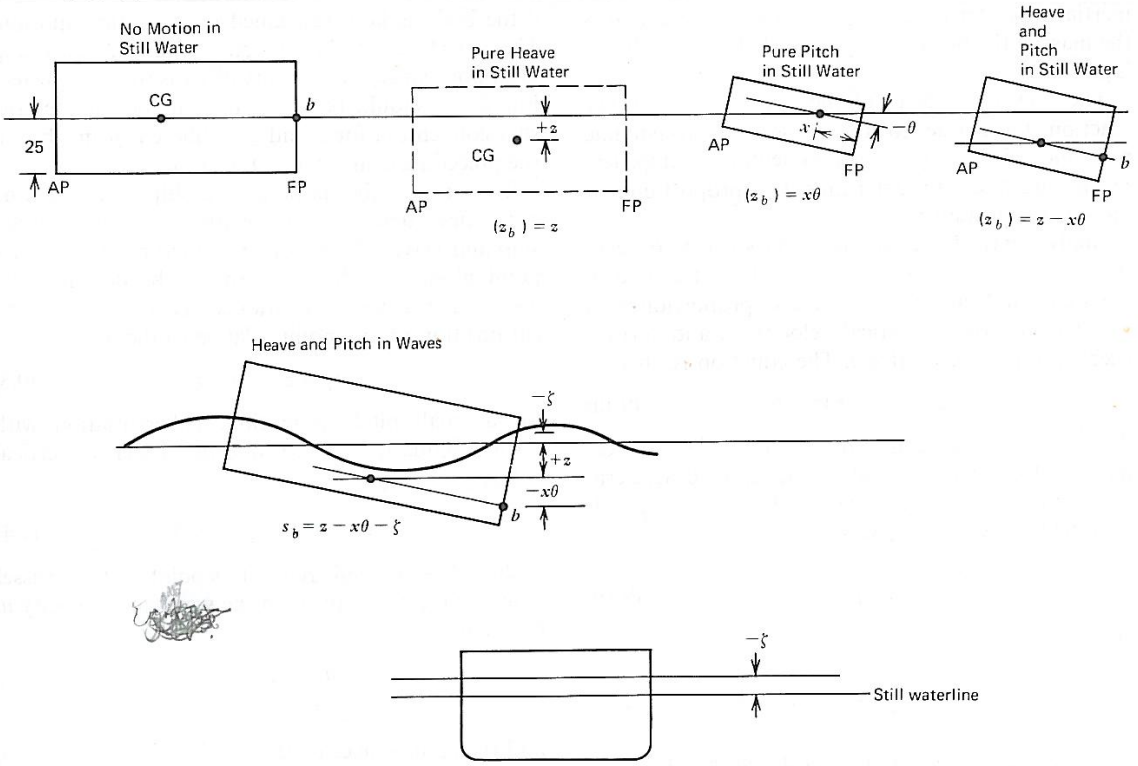


Figure 9.1*b* Wave, heaving, and pitching motions for strip theory.

(calm water level) at time zero. The horizontal plane contains the x and y-axes, while z extends vertically, with positive z downward.

A second coordinate system is created by a pair of ship reference axes whose origin, O', is at the *load waterline* on a vertical line with the ship's center of gravity. The longitudinal coordinate for this system, ξ, is positive forward.

Referring to our established coordinate system, we now have a basis for describing ship motion, the analysis of which is our objective, while it should be remembered that pitch and heave are the only degrees of freedom to be considered here. The heaving component is now z, denoting the vertical displacement of the ship's *center of gravity*. The pitching component, denoted by θ, is the angular displacement in the x-z plane about the origin of the ship's reference axes, O'. The vertical position of any point ξ along the ship's load waterline is, therefore, $z - \xi \sin\theta$, where θ is in radians. For small values of θ, $\sin\theta \simeq \theta$. Velocities and accelerations, both linear and angular, are denoted, respectively, z and $\ddot{z}$ in heave and θ and $\ddot{\theta}$ in pitch.

Basic Force Equation

At this point we are ready to discuss in further detail the basic force equations that form the backbone of strip theory analysis. When at rest in still water a strip experiences a buoyant force equal to its weight and proportional to its immersed volume. The constant of proportionality, denoted by c, is determined by the *waterplane area* of the strip and the density of the water. When displaced from its equilibrium position by some external downward force that is suddenly removed, the strip momentarily experiences buoyancy in excess of its weight, which causes an initial upward acceleration. The inertial reaction opposing this acceleration has the traditional form $F = m'\ddot{z}$, where $\ddot{z}$ is heaving acceleration and m' is greater than the mass of the strip alone. The additional mass, or *added mass* as it is called, accounts for the effort required to accelerate the water that must conform to the shape of the strip as the strip itself accelerates. This quantity, which is determined empirically or experimentally, is dependent on the shape of the body, as described earlier. The resultant

inertial force term is now $F = (m + a)\ddot{z}$, where m is the mass of the body and a_z the added mass for heaving motion.

The upward velocity of the strip causes another reaction force due to the vessel's hydrodynamic resistance. Here, again, experimental or empirical means are used to determine the proportionality (damping) constant b.

Analyzing the forces acting on the strip, we observe that they are of three types: hydrostatic, hydrodynamic, and inertial. These are proportional to vertical position, z, vertical velocity, $\dot{z}$, and vertical acceleration, $\ddot{z}$, respectively. The equation is, then,

$$cz = (m + a_z)\ddot{z} + b\dot{z} \tag{9.1a}$$

According to our sign convention of the displacement z, downward is positive and upward acceleration and velocity are negative. Incorporating this into the force equation, we have

$$cz = \left(\frac{\Delta}{g} + a_z\right)(-\ddot{z}) + b(-\dot{z}) \tag{9.1b}$$

or

$$\left(\frac{\Delta}{g} + a_z\right)\ddot{z} + b\dot{z} + cz = 0 \tag{9.1c}$$

where Δ is the vessel's weight or *displacement*. If it is assumed now that the strip is disturbed by a passing wave train of amplitude ζ_a, the initial force acting on the strip is caused by a change in water level (i.e., a buoyant force) as the first wave passes. Moreover, the fluctuating water level causes a continuous disturbing force known as the *exciting force*. The instantaneous value of this force is equal to the sum of the relative acceleration, velocity, and position between the strip and water surface times their respective constants, that is,

$$m\ddot{z} = F = a_z(-\ddot{z} + \ddot{\zeta}) + b(-\dot{z} + \dot{\zeta}) + c(-z + \zeta) \tag{9.2a}$$

or

$$m\ddot{z} + a_z(\ddot{z} - \ddot{\zeta}) + b(\dot{z} - \dot{\zeta}) + c(z - \zeta) = 0 \tag{9.2b}$$

where $\ddot{\zeta}$, $\dot{\zeta}$, and ζ are the respective instantaneous absolute vertical acceleration, velocity, and position of the water surface. It should be noted that the inertial reaction, $m\ddot{z}$, remains in terms of the fixed frame of reference.

Equation 9.2b can be further rearranged as follows:

$$(m + a_z)\ddot{z} + b\dot{z} + cz = a_z\ddot{\zeta} + b\dot{\zeta} + c\zeta \tag{9.2c}$$

where the right-hand side is known as the *exciting force*, which is exerted on the body by the waves if the body is kept restrained in its vertical motion. The wave forces in this section are analyzed assuming ideal flow, since the viscosity effect is to be neglected. Finally, it should be noted that in this chapter the sign convention for z and ζ is different from that of the preceding chapters (see Fig. 9.1*a*).

To consider the motions of a ship in waves, one must first describe the relative motion between ship and wave. The absolute vertical position of any point along the ship's length can be described by $z - \xi\theta$, as previously mentioned. Therefore the vertical position of any point relative to the wave is

$$z_r = z - \xi\theta - \zeta \tag{9.3}$$

for a small pitching motion. Differentiation with respect [equation 9.3] to time yields relative vertical velocity:

$$w_r = \dot{z}_r = \dot{z} - (\xi\dot{\theta} + \theta\dot{\xi}) - \dot{\xi} \tag{9.4}$$

It should be remembered at this point that the vessel is moving forward through the water at a velocity u. Consequently

$$\frac{d\xi}{dt} = \dot{\xi} = -u$$

and the relative acceleration is, then,

$$\begin{aligned}\dot{w}_r &= \ddot{z} - \xi\ddot{\theta} - \dot{\theta}(-u) + u\theta - \ddot{\zeta} \\ &= \ddot{z} - \xi\ddot{\theta} + 2u\dot{\theta} - \ddot{\zeta}\end{aligned} \tag{9.5}$$

Applied Force Equation

With the basic force equation and relative motion description thus derived, a specific equation for total ship response can now be developed[132]. In deriving their theory, Korvin-Kroukovsky and Jacobs considered the ship to be divided into transverse sections, or strips, along its entire length. In Fig. 9.1*a* these sections are defined by the intersection of the hull with an infinite number of vertical planes, fixed in space, positioned transversely to the ship's course, and spaced $\delta\xi$ apart.

At all times the combined vertical force contributions of the strips must be in equilibrium. However, among individual strips the force equation will probably be balanced by *shear forces* in the ship structure between adjacent imaginary strips. The incremental vertical shear force contribution of each strip is denoted by $df_n/d\xi$ and is equal to the basic force equation derived earlier, with the ship's relative motion terms inserted, that is,

$$\frac{\delta f_n}{\delta \xi} = -m_n \ddot{z}_n - (a_n \dot{w}_r + b_n w_r) - c_n z_r \qquad (9.6a)$$

in which $m_n \ddot{z}_n$ is the inertial force required to accelerate the mass of the strip, $a_n \dot{w}_r$ the hydrodynamic force required to accelerate the added mass, $b_n w_r$ the hydrodynamic damping force due to the relative velocity, and $c_n z_r$ the hydrostatic force due to the relative position.

The coefficients a_n, b_n, and c_n must be determined for each section, since they are functions of hull shape. Because a_n changes with sectional shape and therefore with time, since the linear waves slightly alter strip shape near the waterline, the derivative $d(a_n w_r)/dt$ must be considered instead of simply $a_n w_r$. Thus

$$\frac{d(a_n w_r)}{dt} = w_r \frac{da_n}{dt} + a_n \frac{dw_r}{dt}$$
$$= w_r \frac{da_n}{dt} + a_n \dot{w}_r$$

The combination of this expressions with the force equation now yields

$$\frac{\delta f_n}{d\xi} = -m_n \ddot{z}_n - a_n \dot{w}_r - \left(b_n + \frac{da_n}{dt}\right) w_r - c_n z_r \qquad (9.6b)$$

One can now sum the individual strip forces along the length of the ship. This is accomplished by integrating $\delta f_n / \delta \xi$ with respect to x; thus

$$\int \frac{\delta f_n}{\delta \xi} dx = 0$$

Here it should be noted that the horizontal displacement is

$$x = \xi + ut \qquad (9.7)$$

where ut is the displacement between the origin of fixed axes and the ship's reference origin, and ξ is the distance from the ship's reference origin to the point in the equation. For any particular time t, ut will be constant, and, therefore,

$$dx = d\xi + d(ut) = d\xi$$

Consequently the summation of forces becomes

$$\int \frac{\delta f_n}{\delta \xi} d\xi = 0$$

or, replacing the integrand as in (9.6b)

$$-\int \frac{\delta f_n}{\delta \xi} d\xi = \int m_n \ddot{z}_n \, d\xi + \int a_n \dot{w}_r \, d\xi$$
$$+ \left(\int b_n w_r \, d\xi - u \int \frac{da_n}{d\xi} w_r \, d\xi \right)$$
$$+ \int c_n z_r \, d\xi \qquad (9.8)$$

where

$$\ddot{z}_n = \ddot{z} - \xi \ddot{\theta} \qquad (9.9)$$

As previously defined, $z_r = z - \xi\theta - \zeta$. This expression should exactly be modified because of the effect of pressure attenuation. Unlike the direct variation of hydrostatic pressure with depth in still water, the dynamic water pressure beneath a wave crest decreases exponentially with depth, as shown in Chapter 3. To account for the effect of attenuation, the relative vertical position equation becomes

$$z_r = z - \xi\theta - \zeta e^{-kz} \qquad (9.10)$$

where e^{-kz} is the pressure attenuation *factor*, which approximates the net pressure of the wave through the draft of the strip. Although the use of this z value introduces a small error, it makes the analysis more manageable.

Incorporating the pressure attenuation factor in the remaining terms, we have the expressions for the relative velocity:

$$w_r = \frac{dz_r}{dt} = \dot{z} - \xi\dot{\theta} + u\theta - \dot{\zeta} e^{-kz} \qquad (9.11)$$

and the relative acceleration:

$$\dot{w}_r = \frac{dw_r}{dt} = \ddot{z} - \xi\ddot{\theta} + 2u\dot{\theta} - \ddot{\zeta} e^{-kz} \qquad (9.12)$$

9.3 MOTION EQUATION

Substitution of the expressions for $\ddot{z}_r$, $\dot{w}_r$, and w_r into the integrated force equation produces a rather long and cumbersome expression. To simplify this form it is advantageous to separate the terms dealing with *absolute ship motion* ($\ddot{z}, \dot{z}, z, \ddot{\theta}, \dot{\theta}, \theta$), and those dealing with *wave motion* ($\ddot{\zeta}, \dot{\zeta}, \zeta$). By placing all absolute ship terms on the left and all wave terms on the right of the equation, we obtain an expression analogous to the example for the uncoupled motion treated previously. In other words the left-hand side of the equation represents the natural *response* of the ship to an initial displacement in still water. The right-hand side, on the other hand, is composed of all wave terms and is therefore the *forcing function.*

Substituting the respective expressions for z_r, w_r, $\dot{w}_r$, and $\ddot{z}_n$ from (9.10), (9.11), (9.12), and (9.9),

we have

$$\int m_n(\ddot{z} - \xi\ddot{\theta})\,d\xi + \int a_n(\ddot{z} - \xi\ddot{\theta} + 2u\dot{\theta} - \ddot{\zeta}e^{-kz})d\xi + \left[\int b_n(\dot{z} - \xi\dot{\theta} + u\theta - \dot{\zeta}e^{-kz})d\xi - u\int \frac{da_n}{d\xi}(\dot{z} - \xi\dot{\theta} + u\theta - \dot{\zeta}e^{-kz})d\xi\right] + \int c_n(z - \xi\theta - \zeta e^{-kz})d\xi = 0 \tag{9.13}$$

Rearranging all the terms involving the wave on the right-hand side and equating the integrands, we have

$$\begin{aligned} &m_n(\ddot{z} - \xi\ddot{\theta}) + a_n(\ddot{z} - \xi\ddot{\theta} + 2u\dot{\theta}) + b_n(\dot{z} - \xi\dot{\theta} + u\theta) - \frac{da_n}{d\xi}(\dot{z} - \xi\dot{\theta} + u\theta) + c_n(z - \xi\theta) \\ &= \ddot{\zeta}e^{-kz}a_n + \dot{\zeta}e^{-kz}b_n - u\frac{da_n}{d\xi}\dot{\zeta}e^{-kz} + \zeta e^{-kz}c_n \end{aligned} \tag{9.14}$$

The expression on the right-hand side of this equation represents the exciting force for each strip due to the wave, dF/dx.

The assumption that the encountered wave is regular and harmonic allows us to express ζ as

$$\zeta = \zeta_a \sin k(x - V_w t)$$

Combining this expression with (9.7), we have

$$\zeta = \zeta_a \sin k(\xi + ut - V_w t)$$

or

$$\zeta = \zeta_a \sin k[\xi + (u - V_w)t]$$

But $-k(u - V_w)$ is the frequency of encounter, ω_e. Thus the free surface displacement is

$$\zeta = \zeta_a \sin(k\xi - \omega_e t) \tag{9.15}$$

while

$$\dot{\zeta} = -\zeta_a \omega_e \cos(k\xi - \omega_e t) \tag{9.16}$$

and

$$\ddot{\zeta} = -\zeta_a \omega_e^2 \sin(k\xi - \omega_e t) \tag{9.17}$$

Substitution of ζ, $\dot{\zeta}$ and $\ddot{\zeta}$ into (9.14) yields

$$\begin{aligned} &m_n\ddot{z} + a_n\ddot{z} + b_n\dot{z} - u\frac{da_n}{d\xi}\dot{z} + c_n z \\ &\quad - m_n\xi\ddot{\theta} - a_n\xi\dot{\theta} + a_n 2u\dot{\theta} - b_n\xi\dot{\theta} + b_n u\theta \\ &\quad + u\frac{da_n}{d\xi}\xi\dot{\theta} - u^2\frac{da_n}{d\xi}\theta + c_n\xi\theta \\ &= (m_n + a_n)\ddot{z} + b_n\dot{z} - u\frac{da_n}{d\xi}\dot{z} + c_n\dot{z} \\ &\quad - m_n\xi\ddot{\theta} - a_n\xi\ddot{\theta} + a_n 2u\dot{\theta} - b_n\xi\dot{\theta} + u\frac{da_n}{d\xi}\xi\dot{\theta} \\ &\quad + b_n u\theta - u^2\frac{da_n}{d\xi}\theta - c_n\xi\theta \\ &= -\zeta_a\omega_e^2 \sin(k\xi - \omega_e t)e^{-kz}a_n \\ &\quad - \zeta_a\omega_e \cos(k\xi - \omega_e t)e^{-kz}\left(b_n - u\frac{da_n}{d\xi}\right)d\xi \\ &\quad + \zeta_a \sin(k\xi - \omega_e t)e^{-kz}c_n d\xi \end{aligned} \tag{9.18}$$

Integrating this expression over the length of the ship, we obtain the general equation of motion:

$$(m + a_z)\ddot{z} + b\dot{z} + cz + d\ddot{\theta} + e\dot{\theta} + h\theta = F(t) \tag{9.19}$$

where

$$m = \int m_n\,d\xi$$

$$a_z = \int a_n\,d\xi$$

$$b = \int b_n\,d\xi$$

since u $\int (da_n/d\xi)\,d\xi = 0$ (assumed),

$$c = \int c_n\,d\xi$$

which can be expressed also as $\rho g \int B_n\,d\xi$ (B_n being the breadth of the individual section),

$$d = -\int a_n\xi\,d\xi$$

since $\int m_n\xi\,d\xi = 0$ (i.e., the moment of the total mass about its CG must be equal to zero),

$$e = -\int b_n\xi\,d\xi + 2u\int a_n d\xi + u\int \frac{da_n}{d\xi}\xi\,d\xi = -\int b_n\xi\,d\xi + ua_z \tag{9.20}$$

since $\int \xi(da_n/d\xi)\,d\xi = \int \xi\,da_n = -a_z$

$$h = -\int c_n\xi\,d\xi + u\int b_n\,d\xi = -\int c_n\xi\,d\xi + ub$$

since $u^2\int(da_n/d\xi)d\xi = 0$, and

$$F(t) = \int\frac{dF}{dx}dx = \zeta_a e^{-kz}\int(-\omega_e^2 a_n + c_n) \times \sin(k\xi - \omega_e t)\,d\xi - \zeta_a e^{-kz}\omega_e\int\left(b_n - u\frac{da_n}{d\xi}\right)\cos(k\xi - \omega_e t)d\xi$$

Since the *exciting force* F is sinusoidal in nature, it may be expressed in general form by the equation,

$$F = F_1\cos\omega_e t + F_2\sin\omega_e t = F_0\cos(\omega_e t + \sigma) \qquad (9.21)$$

where F_0 is the amplitude of the exciting force, that is,

$$F_0 = \sqrt{F_1^2 + F_2^2}$$

and σ is the *phase lag* of the exciting force relative to the wave motion, that is,

$$\sigma = -\tan^{-1}\left(\frac{F_2}{F_1}\right)$$

F_0 and σ are found from the complete forcing function solution, where the expressions for F_1 and F_2 are obtained as follows:

$$F_1 = \int\frac{dF_1}{dx}dx$$

where

$$\frac{dF_1}{dx} = \zeta_a e^{-kz}(-\omega_e^2 a_n + c_n)\sin k\xi + \zeta_a e^{-kz}\omega_e\left(b_n - u\frac{da_n}{d\xi}\right)\cos k\xi \qquad (9.21a)$$

Similarly,

$$F_2 = \int\frac{dF_2}{dx}dx$$

where

$$\frac{dF_2}{dx} = \zeta_a e^{-kz}(-\omega_e^2 a_n + c_n)\cos k\xi - \zeta_a e^{-kz}\omega_e\left(b_n - u\frac{da_n}{d\xi}\right)\sin k\xi \qquad (9.21b)$$

Note: In the above equations z is taken to be T_m, which is the *mean draft* of each section, that is,

$$T_m = \frac{S_n}{B_n} \qquad (9.22)$$

where S_n and B_n are the sectional area and sectional breadth, respectively. Equation 9.19 is referred to as the *first equation of motion* involving all the forces. The *second equation of motion* is the angular motion counterpart of the first and is written as [132]

$$(I_{yy} + A_{yy})\ddot{\theta} + B\dot{\theta} + C\theta + D\ddot{z} + E\dot{z} + Hz = M(t) \qquad (9.23)$$

where each term represents the moment of force instead of the force. The moment coefficients are defined as follows [132].

$$A_{yy} = \int a_n\xi^2\,d\xi$$

$$B = \int b_n\xi^2\,d\xi$$

since $2u\int a_n\xi d\xi = -u\int(da_n/d\xi)\xi^2 d\xi$,

$$C = \int c_n\xi^2\,d\xi - uE$$

$$D = d$$

$$E = -\int b_n\xi\,d\xi - ua_z$$

$$H = -\int c_n\xi\,d\xi$$

$$M = M_0\cos(\omega_e t + \tau) = \int\frac{dF}{d\xi}\xi\,d\xi$$

where M_0 is the amplitude of the exciting moment, that is,

$$M_0 = \sqrt{M_1^2 + M_2^2}$$

and τ is the phase lag of the exciting moment relative to wave motion, that is,

$$\tau = -\tan^{-1}\left(\frac{M_2}{M_1}\right)$$

Also,

$$M_1 = \int\frac{dM_1}{dx}d\xi$$

where $dM_1/dx = \xi(dF_1/dx)$, and

$$M_2 = \int\frac{dM_2}{dx}d\xi$$

where $dM_2/dx = \xi(dF_2/dx)$.

Note that the coefficients of (9.19) and (9.23) (i.e., a_z to h and A_{yy} to H) depend on the hull geometry, speed, and frequency. For very accurate determina-

tion of the hydrodynamic coefficients, the expressions for the coefficients b, e, and B should be derived without the assumptions made herein.

The *linearity* of (9.19) and (9.23) signifies that the motion amplitudes are linearly proportional to the amplitudes of the forcing functions. When the exciting forces, in turn, vary linearly with wave amplitude, the amplitudes of heave and pitch will also be proportional to the wave amplitude. Results of model tests in regular waves show that the assumption of linearity of motions with wave amplitude may be considered to be reasonably valid, especially in mild to moderate seas.

The coupled equations of pitching and heaving motions in *calm water* can be obtained by equating the right-hand sides of (9.19) and (9.23) to zero and assuming that the coefficients a_z to h and A_{yy} to H are the same for both calm water and waves.

Solutions of the Equation of Motion

At this point one can develop the final solution of the strip theory motion problem. The time derivatives of respective displacements provide the solution to the equation, and the displacements themselves provide the solutions of *pitch* and *heave* that we are seeking.

Because the solutions to the motion equations include both amplitudes and phase lags, they are best written in *complex form*; thus let $\bar{M}$ and $\bar{F}$ represent the forcing function in complex form:

$$\bar{F} = F_0 e^{i\sigma} \tag{9.25}$$

$$\bar{M} = M_0 e^{i\tau} \tag{9.26}$$

Let P, Q, R, and S be the complex forms of related coefficients from the equations of motion. Then from (9.19)

$$\begin{aligned} P &= -(m + a_z)\omega^2 + iB\omega + c; \\ Q &= -d\omega^2 + ie\omega + h \end{aligned} \tag{9.27}$$

and from (9.23)

$$\begin{aligned} S &= -(I_y + A_{yy})\omega^2 + iB\omega + c; \\ R &= -D\omega^2 + iE\omega + H \end{aligned} \tag{9.28}$$

If we consider $\bar{z}$ to represent all derivatives of z and $\bar{\theta}$ to represent all derivatives of θ, we may write the equations of motion in the general operator form:

$$\text{First equation (heave)} : P\bar{z} + Q\bar{\theta} = \bar{F} \tag{9.29}$$

$$\text{Second equation (pitch)} : S\bar{\theta} + R\bar{z} = \bar{M} \tag{9.30}$$

where $\bar{z}$ and $\bar{\theta}$ are the complex amplitudes of motion, that is,

$$\bar{z} = z_a e^{i\delta}$$

$$\bar{\theta} = \theta_a e^{i\varepsilon}$$

Solving for $\bar{z}$ and $\bar{\theta}$, we obtain from (9.20)

$$\bar{z} = \frac{\bar{F} - Q\bar{\theta}}{P} \tag{9.31}$$

$$\bar{\theta} = \frac{\bar{F} - P\bar{z}}{Q} \tag{9.32}$$

and in the pitch equation

$$\bar{z} = \frac{\bar{M} - S\bar{\theta}}{R} \tag{9.33}$$

$$\bar{\theta} = \frac{\bar{M} - R\bar{z}}{S} \tag{9.34}$$

The inclusion of z in the θ equations and vice versa illustrates the coupled nature of pitch and heave.

Equating $\bar{z}$ and $\bar{\theta}$ from their respective equations yields

$$\frac{\bar{F} - Q\bar{\theta}}{P} = \frac{\bar{M} - S\bar{\theta}}{R}$$

$$\frac{\bar{F} - P\bar{z}}{Q} = \frac{\bar{M} - R\bar{z}}{S}$$

Solving each equation for $\bar{z}$ or $\bar{\theta}$, we arrive at the solution for complex pitch and heave:

$$\bar{z} = \frac{\bar{M}Q - \bar{F}S}{QR - PS} \tag{9.35}$$

$$\bar{\theta} = \frac{\bar{F}R - \bar{M}P}{QR - PS} \tag{9.36}$$

This brings us to the final solution of the motion equations. Having found amplitudes and phase lags for $\bar{z}$ and $\bar{\theta}$, we can express the two motions in their final forms:

$$\bar{z} = z_a e^{i\delta} = z_a(\cos\delta + i\sin\delta) \tag{9.37}$$

$$\bar{\theta} = \theta_a e^{i\varepsilon} = \theta_a(\cos\varepsilon + i\sin\varepsilon) \tag{9.38}$$

in which z_a and δ are heave amplitude and phase lag, respectively, and θ_a and ε are the corresponding quantities for pitch.

Since the objective of the strip theory is the prediction of pitch and heave for a given seaway, it appears that Korvin-Kroukovsky's final equation is a reasonable solution; that is, one can now predict the complex motions of pitch and heave, expressed as $\theta_a e^{i\varepsilon}$ and $z_a e^{i\delta}$, respectively, in terms of a given seaway of the form $\zeta_a \sin k(x - V_w t)$ or $\zeta_a \sin \omega_e t$.

Summary

In summary, calculations of the coupled heaving and pitching motions by the strip theory are performed by following five steps:

1. Divide the ship into a finite number of sections sufficient to provide accurate representation of the underwater hull form.
2. Derive all coefficients for each section (a_n, b_n, c_n, etc.).
3. Use Simpson's integration to obtain hydrodynamic coefficients:

$$a_z = \int a_n \, d\xi \qquad A_{yy} = \int a_n \xi^2 \, d\xi$$

$$b = \int b_n \, d\xi \qquad B = \int b_n \xi^2 \, d\xi$$

and so on.

4. Calculate the exciting force and the exciting moment from wave amplitude and frequency data and ship characteristics.
5. Use the complex solution to find pitch and heave.

It should be emphasized here that the above method of determining the pitching and heaving motions can be applied for any sea other than the head sea if the wavelength L_w is replaced everywhere by the *effective wavelength* L'_w, where

$$L'_w = \frac{L_w}{\cos \mu} \tag{9.39}$$

(see Section 4.5); that is, in the calculation of exciting forces and moments the expression sin $[(2\pi/L_w)\xi]$ will be sin $[(2/L'_w)\xi]$ and cos $[(2\pi/L_w)\xi]$ will be cos $[(2\pi/L'_w)\xi]$. For oblique seas, however, the other degrees of freedom (yaw, sway, etc.) will be excited.

Although some refinements of a few of the coefficients have been obtained recently by intensive research [181], the strip theory method for coupled motions of heaving and pitching remains the same as described above. The purpose of the refinement in the analytical treatment has been to minimize the discrepancy that now exists between the computed and the measured results.

9.4 EXAMPLE ON COUPLED HEAVING AND PITCHING MOTION IN REGULAR WAVES USING STRIP THEORY

The calculations have been made for a 19.2 ft model of 0.80 *block coefficient*, running at 4.788 ft/sec in waves of model length L and height $L/48$. All tabulated dimensions and coefficients are for the hull in still water. It has been found by extensive computations that *determination of force and moment distributions at* 10 *or* 11 *stations is sufficient.*

Although this is a typical sample of the computational procedure, the results pertain only to the given vessel, speed, and wavelength. This warning is especially justified when phase angles of wave, heaving force, and pitching moment are under consideration. Theoretically, for a doubly symmetric hull form stationary in waves, the maximum heaving force due to the waves should occur when the wave crests is at midship (90° phase lag); however, the maximum pitching moment should occur when the wave node is at midship (0° phase lag). For hulls that are *asymmetric* fore and aft, maxima will occur at positions other than midship. Also, at high speeds the phase lags of the exciting force and moment, after the wave, will be larger than those at zero speed, as will the phase lag of force after moment.

Example 9.1

Given:

Length of model	L_m	=	19.2 ft
Maximum beam	$B_{\max}$	=	2.592 ft
Draft	T	=	1.144 ft
Displacement	Δ	=	2837.76 lb
Block coefficient	C_B	=	0.80
LCG		=	+0.48 ft (forward of ⊗)
LCB		=	+0.48 ft (2.5% L_{pp} forward of ⊗)
Model speed	u	=	4.788 ft/sec
Radius of gyration	k_{yy}	=	4.588 ft
Wavelength	L_w	=	19.2 ft
Wave amplitude	ζ_a	=	0.2 ft
Wave velocity	V_w	=	9.90 ft/sec

$\rho = 1.9384$ lb-sec^2/ft^4 (fresh water at 59°F)
$\mu = 180°$ (i.e., head seas)

In Fig. 9.2 the breadth, draft, and area of different stations, as well as the weight distributions for the model are as follows:

Station No.	B_n [ft]	T_n [ft]	S_n [ft^2]	Weight per Foot [lb/ft]
0	0	1.144	0	29.95
5	2.592	1.144	2.944	184.18
10	2.592	1.144	2.944	189.01
15	2.592	1.144	2.752	155.20
20	0	1.144	0	21.57

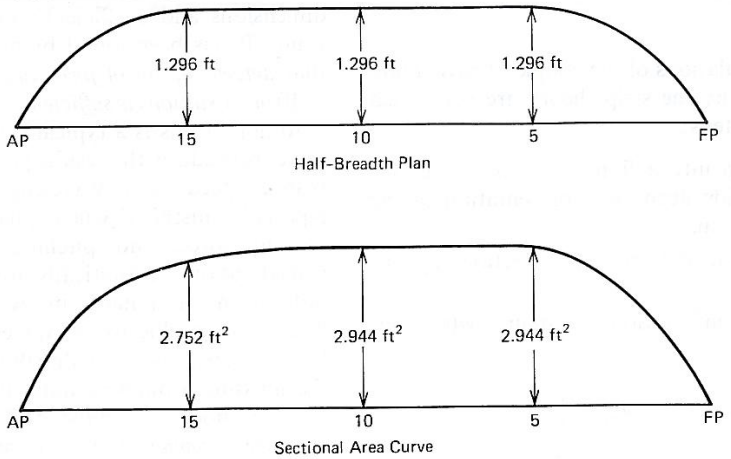


Figure 9.2 Half-breadth plan and sectional area curve of a ship model.

Find the amplitude of heaving and pitching motions of the model. In addition, determine the phase angles of both the motions in relation to the wave motion.

Solution:

The coefficients of the equations of motions are determined as shown in Tables 9.1 to 9.6.

Calculated data are as follows:

Wave frequency, ω_w

$$\omega_w = \sqrt{\frac{2\pi g}{L_w}}$$
$$= \sqrt{\frac{2 \times 3.1416 \times 32.2}{19.2}}$$
$$= 3.245 \text{ rad/sec}$$

Frequency of encounter, ω_e

$$\omega_e = \omega_w - \frac{\omega_w^2 u}{g} \cos \mu$$
$$= 3.245 - \frac{(3.245^2)(4.788)}{32.2} \cos 180^\circ$$
$$= 4.811 \text{ rad/sec}$$

Added mass for heaving, a_z

$$a_z = \int a_n \, d\xi$$
$$= \tfrac{1}{3} \times S \times \text{SUM}_1 = \tfrac{1}{3}(4.8)(47.246)$$
$$= 75.6 \text{ lb-sec}^2/\text{ft}$$

Added mass moment of inertia for pitching, A_{yy}

$$A_{yy} = \int a_n \xi^2 \, d\xi$$
$$= \tfrac{1}{3} \times S \times \text{SUM}_2$$
$$= \tfrac{1}{3}(4.8)(855.30)$$
$$= 1368.5 \text{ lb-sec}^2\text{-ft}$$

Damping coefficient for heaving, b

$$b = \int b_n \, d\xi$$
$$= \tfrac{1}{3} \times S \times \text{SUM}_1 = \tfrac{1}{3}(4.8)(66.67)$$
$$= 106.7 \text{ lb-sec/ft}$$

Damping coefficient for pitching, B

$$B = \int b_n \xi^2 \, d\xi$$
$$= \tfrac{1}{3} \times S \times \text{SUM}_2$$
$$= \tfrac{1}{3}(4.8)(1316.17)$$
$$= 2105.9 \text{ ft-lb-sec/rad}$$

Restoring force coefficient for heaving, c

$$c = \int c_n \, d\xi = (\rho g A_w)$$
$$= \tfrac{1}{3} \times S \times \text{SUM}_1 = \tfrac{1}{3}(4.8)(1617.8)$$
$$= 2588.5 \text{ lb/ft}$$

Restoring moment coefficient for pitching, C

$$C = \int c_n \xi^2 \, d\xi - uE \ (E \text{ is calculated in Table 9.4})$$
$$= (\tfrac{1}{3} \times S \times \text{SUM}_2) - uE = (\tfrac{1}{3} \times 4.8 \times 30191.4) - (4.788)(-249.65)$$
$$= 49501.6 \text{ ft-lb/rad}$$

TABLE 9.1 CALCULATIONS FOR a_z AND A_{yy}

Station No.	B_n [ft]	T_n [ft]	S_n [ft²]	ξ [ft]	$\frac{\omega_e^2}{2g} \times B_n$ [—]	$\frac{B_n}{T_n}$ [—]	$B_n \times T_n$ [ft²]	β_n [—]	C [—]
①	②	③	④	⑤	⑥	②÷③ ⑦	②×③ ⑧	④÷⑧ ⑨	⑩
0	0	1.144	0	9.12	0	0	0	0	0
5	2.592	1.144	2.944	4.32	0.932	2.266	2.965	0.993	0.98
10	2.592	1.144	2.944	−0.48	0.932	2.266	2.965	0.993	0.98
15	2.592	1.144	2.752	−5.28	0.932	2.266	2.965	0.928	0.84
20	0	1.144	0	−10.08	0	0	0	0	0

B_n^2 [ft²]	$\frac{\rho\pi}{8} \times B_n^2$ [lb-sec²/ft²]	a_n [lb-sec²/ft²]	Simpson's Multiplier	Product	ξ^2 [ft²]	$a_n \times \xi^2$ [lb-sec²]	Simpson's Multiplier	Product
②×② ⑪	⑫	⑫×⑩ ⑬	⑭	⑬×⑭ ⑮	⑤×⑤ ⑯	⑬×⑯ ⑰	⑱	⑰×⑱ ⑲
0	0	0	1	0	83.174	0	1	0
6.718	5.113	5.011	4	20.044	18.662	93.515	4	374.06
6.718	5.113	5.011	2	10.022	0.230	1.152	2	2.30
6.718	5.113	4.295	4	17.180	27.878	119.736	4	478.94
0	0	0	1	0	101.606	0	1	0
			SUM_1	47.246			SUM_2	855.8

Description of Table 9.1

Column Number	*Description*
①	Station Number
②	Beam at Station, B_n
③	Draft at Station, T_n
④	Sectional Area at Station, S_n
⑤	Lever Arm from Longitudinal Center of Buoyancy, ξ
⑥	$\frac{\omega_e^2}{2g} \times B_n$
⑦ = ②/③	Beam Draft Ratio = $\frac{B_n}{T_n}$
⑧ = ②×③	$B_n \times T_n$
⑨ = ④÷⑧	Sectional Area Coefficient, $\beta_n = \frac{S_n}{B_n \times T_n}$
⑩	Added Mass Coefficient, C, obtained from Fig. 4.4 using the values from ⑥, ⑦, and ⑨
⑪ = ②×②	Beam squared, B_n^2
⑫	$\frac{\rho\pi}{8} \times B_n^2$
⑬ = ⑫×⑩	Sectional Added Mass, $a_n = C \times \frac{\rho\pi}{8} \times B_n^2$
⑭	Simpson's Multiplier
⑮ = ⑬×⑭	Product
⑯ = ⑤×⑤	Lever Arm Squared, ξ^2
⑰ = ⑬×⑯	$a_n \times \xi^2$
⑱	Simpson's Multiplier
⑲ = ⑰×⑱	Product

Coupling terms, d, D, e, E, h, H

$$d = -\int a_n \xi \, d\xi$$

$$= -\tfrac{1}{3} \times S \times SUM_1 = -\tfrac{1}{3}(4.8)(-8.92)$$

$$= 14.27 \text{ lb-sec}^2$$

$$D = d = 14.27 \text{ lb-sec}^2$$

$$e = -\int b_n \xi \, d\xi + ua \quad (a \text{ is calculated in Table 9.1})$$

$$= (-\tfrac{1}{3} \times S \times SUM_2) + ua$$

$$= [-\tfrac{1}{3} \times 4.8 \times (-70.08)] + (4.788 \times 75.56)$$

$$= 473.9 \text{ lb-sec}^2/\text{sec}$$

$$E = -\int b_n \xi \, d\xi - ua$$

$$= 112.73 - 361.78$$

$$= -249.7 \text{ lb-sec}^2/\text{sec}$$

$$h = -\int c_n \xi \, d\xi + ub \quad (b \text{ is calculated in Table 9.2})$$

$$= (-\tfrac{1}{3} \times S \times SUM_3) + ub$$

$$= [-\tfrac{1}{3} \times 4.8 \times (-776.54)] + (4.788 \times 106.67)$$

$$= 1753.2 \text{ lb}$$

$$H = -\int c_n \xi \, d\xi$$

$$= 1242.5 \text{ lb}$$

TABLE 9.2 CALCULATIONS FOR b AND B

Station No. ①	$\frac{\omega_e^2}{2g} \times B_n$ [—] ②	$\frac{B_n}{T_n}$ [—] ③	β_n [—] ④	$\bar{A}$ ⑤	$\bar{A}^2$ ⑤ × ⑤ ⑥	b_n [lb-sec/ft^2] ⑦	Simpson's Multiplier ⑧	Product ⑦ × ⑧ ⑨	ξ^2 [ft^2] ⑩
0	0	0	0	0	0	0	1	0	83.174
5	0.932	2.266	0.993	0.57	0.325	5.866	4	23.464	18.662
10	0.932	2.266	0.993	0.57	0.325	5.866	2	11.732	0.230
15	0.932	2.266	0.928	0.66	0.436	7.852	4	31.486	27.878
20	0	0	0	0	0	0	1	0	
							SUM_1	66.67	

$b_n \times \xi^2$ [lb-sec] ⑦ × ⑩ ⑪	Simpson's Multiplier ⑫	Product ⑪ × ⑫ ⑬
0	1	0
109.47	4	437.88
1.35	2	2.70
218.89	4	875.59
0	1	0
	SUM_2	1316.17

Description of Table 9.2

Column Number	*Description*
①	Station Number
②	Nondimensional Frequency of Encounter, $\frac{\omega_e^2}{2g} \times B_n$
③	Beam Draft Ratio, $\frac{B_n}{T_n}$
④	Sectional Area Coefficient, β_n
⑤	Amplitude Ratio for Two-Dimensional Body in Heaving Motion, $\bar{A}$, found from Fig. 4.6 with the values from ②, ③, and ④
⑥ = ⑤ × ⑤	$\bar{A}^2$
⑦ = $\frac{\rho g^2}{\omega_e^3} \times$ ⑥	Sectional Damping Coefficient, $b_n = \frac{\rho g^2 \bar{A}^2}{\omega_e^3}$
⑧	Simpson's Multiplier
⑨ = ⑦ × ⑧	Product
⑩	Lever Arm Squared, ξ^2
⑪ = ⑦ × ⑩	$b_n \times \xi^2$
⑫	Simpson's Multiplier
⑬ = ⑪ × ⑫	Product

TABLE 9.3 CALCULATIONS FOR c AND C

Station No. ①	B_n [ft] ②	c_n [lb/ft^2] ③	Simpson's Multiplier ④	Product ③ × ④ ⑤	ξ^2 [ft^2] ⑥	$c_n \times \xi^2$ ③ × ⑥ ⑦	Simpson's Multiplier ⑧	Product ⑦ × ⑧ ⑨
0	0	0	1	0	83.174	0	1	0
5	2.592	161.78	4	647.12	18.662	3019.14	4	12,076.6
10	2.592	161.78	2	323.56	0.230	37.21	2	74.4
15	2.592	161.78	4	647.12	27.878	4510.10	4	18,040.4
20	0	0	1	0	101.606	0	1	0
			SUM_1	1617.8			SUM_2	30,191.4

Description of Table 9.3

Column Number	*Description*
①	Station Number
②	Beam, B_n
③ = $\rho g \times$ ②	Sectional Restoring Force Coefficient, $c_n = \rho g B_n$
④	Simpson's Multiplier
⑤ = ③ × ④	Product
⑥	Lever Arm Squared, ξ^2
⑦ = ③ × ⑥	$c_n \times \xi^2$
⑧	Simpson's Multiplier
⑨ = ⑦ × ⑧	Product

TABLE 9.4 CALCULATIONS FOR $d, e, h, D, E,$ AND H

Station No. ①	ξ [ft] ②	a_n [slugs/ft] ③	$a_n \times \xi$ [slugs] ② × ③ ④	Simpson's Multiplier ⑤	Product ④ × ⑤ ⑥	b_n [lb-sec/ft²] ⑦	$b_n \times \xi$ [lb-sec/ft] ② × ⑦ ⑧	Simpson's Multiplier ⑨	Product ⑧ × ⑨ ⑩
0	9.12	0	0	1	0	0	0	1	0
5	4.32	5.009	21.639	4	86.56	5.866	25.34	4	101.36
10	− 0.48	5.009	− 2.404	2	− 4.808	5.866	− 2.82	2	− 5.64
15	− 5.28	4.293	− 22.667	4	− 90.67	7.852	− 41.45	4	− 165.8
20	− 10.08	0	0	1	0	0	0	1	0
				SUM_1	− 8.92			SUM_2	− 70.08

c_n [lb/ft²] ⑪	$c_n\xi$ [lb/ft] ② × ⑪ ⑫	Simpson's Multiplier ⑬	Product ⑫ × ⑬ ⑭
0	0	1	0
161.78	698.89	4	2795.56
161.78	− 77.65	2	− 155.30
161.78	− 854.20	4	− 3416.8
0	0	1	0
		SUM_1	− 776.54

Description of Table 9.4

Column Number	*Description*
①	Station Number
②	Lever Arm, ξ
③ = ⑬ of Table 9.1	Sectional Added Mass Coefficient, a_n
④ = ② × ③	$a_n \times \xi$
⑤	Simpson's Multiplier
⑥ = ④ × ⑤	Product
⑦ = ⑦ of Table 9.2	Sectional Damping Coefficient, b_n
⑧ = ② × ⑦	$b_n \times \xi$
⑨	Simpson's Multiplier
⑩ = ⑧ × ⑨	Product
⑪ = ③ of Table 9.3	Sectional Restoring Force Coefficient, c_n
⑫ = ② × ⑪	$c_n \times \xi$
⑬	Simpson's Multiplier
⑭ = ⑫ × ⑬	Product

TABLE 9.5 CALCULATIONS FOR m AND I_{yy}

Station No. ①	Weight per Foot [lb/ft] ②	m_n [lb-sec²/ft²] ③	Simpson Multiplier ④	Product ③ × ④ ⑤	ξ^2 [ft²] ⑥	$m_n\xi^2$ [lb-sec²] ③ × ⑥ ⑦	Simpson Multiplier ⑧	Product ⑦ × ⑧ ⑨
0	29.95	0.93	1	0.93	83.174	77.35	1	77.35
5	184.18	5.72	4	22.88	18.662	106.75	4	427.00
10	189.01	5.87	2	21.74	0.230	1.35	2	2.70
15	155.20	4.82	4	29.28	27.878	134.37	4	537.48
20	21.57	0.67	1	0.67	101.606	68.08	1	68.07
			SUM_1	55.50			SUM_2	1112.61

Description of Table 9.5

Column Number	*Description*
①	Station Number
②	Weight per Foot
③	Mass Distribution, Weight per foot/g
④	Simpson's Multiplier
⑤ = ③ × ④	Product
⑥	Lever Arm Squared
⑦ = ③ × ⑥	$m_n \times \xi^2$
⑧	Simpson's Multiplier
⑨ = ⑦ × ⑧	Product

TABLE 9.6 CALCULATIONS FOR EXCITING FORCES AND MOMENTS (F AND M)

Station No. ①	ξ [ft] ②	$k\xi$ ③	Sin $k\xi$ ④	Cos $k\xi$ ⑤	T_m [ft] ⑥	$\frac{2\pi}{L_w}\times T_m$ ⑦	$e^{-[(2\pi/L_w)T_m]}$ ⑧	c_n ⑨	$c_n\zeta_a$ ⑩	a_n ⑪	$a_n(-\zeta_a\omega_e^2)$ ⑫
0	9.12	2.983	0.158	−0.987	0	0	1.00	0	0	0	0
5	4.32	1.413	0.987	0.157	1.136	0.371	0.69	161.78	32.36	5.011	−23.197
10	−0.48	−0.157	−0.156	0.988	1.136	0.371	0.69	161.78	32.36	5.011	−23.197
15	−5.28	−1.727	−0.988	−0.156	1.062	0.347	0.71	161.78	32.36	4.295	−19.882
20	−10.08	−3.300	0.158	−0.987	0	0	1.00	0	0	0	0

⑩ + ⑫ ⑬	$\frac{da_n}{d\xi}$ ⑭	$u\zeta_a\omega_e\frac{da_n}{d\xi}$ ⑮	$b_n\zeta_a\omega_e$ ⑯	⑯ − ⑮ ⑰	⑬ × ④ ⑱	⑰ × ⑤ ⑲	⑱ + ⑲ ⑳	⑬ × ⑤ ㉑	⑰ × ④ ㉒	㉑ − ㉒ ㉓	⑳ × ⑧ ㉔
0	−1.043	−4.805	0	4.805	0	−4.74	−4.742	0	0.760	−0.760	−4.742
9.159	−0.522	−2.405	5.64	8.045	9.040	1.263	10.303	1.440	7.944	−6.504	7.109
9.159	0.075	0.344	5.64	5.296	−1.428	5.230	3.802	9.063	−0.773	9.836	2.62
12.474	0.522	2.405	7.55	5.145	−12.324	−0.803	−13.126	−1.948	−5.105	3.157	−9.319
0	0.894	4.119	0	−4.119	0	4.065	4.065	0	−0.651	0.651	4.065

Simpson's Multiplier ㉕	Product ㉔ × ㉕ ㉖	㉓ × ⑧ ㉗	Simpson's Multiplier ㉘	Product ㉗ × ㉘ ㉙	㉔ × ② ㉚	Simpson's Multiplier ㉛	Product ㉚ × ㉛ ㉜	㉗ × ② ㉝	Simpson's Multiplier ㉞	Product ㉝ × ㉞ ㉟
1	−4.742	−0.760	1	−0.760	−43.25	1	−43.25	−6.931	1	−6.931
4	28.436	−4.488	4	−17.952	30.71	4	122.84	−19.388	4	−77.552
2	5.24	6.787	2	13.574	−1.258	2	−2.516	−3.258	2	−6.516
4	−37.28	2.240	4	8.960	49.204	4	196.816	−11.827	4	−47.308
1	4.065	0.651	1	0.651	−40.975	1	−40.975	−6.562	1	−6.562
SUM_1	−4.281		SUM_2	4.473		SUM_3	232.91		SUM_4	−144.869

Description of Table 9.6

Column Number	*Description*
①	Station Number
②	Lever Arm (i.e., distance from LCG), ξ
③	$k\xi = \frac{2\pi}{L_w}\times\xi$
④	$\mathrm{Sin}\left(\frac{2\pi}{L_w}\times\xi\right)$
⑤	$\mathrm{Cos}\left(\frac{2\pi}{L_w}\times\xi\right)$
⑥	Mean Draft, $T_m = \frac{S_n}{B_n}$
⑦ $\frac{2\pi}{L_w}\times$ ⑥	$\frac{2\pi}{L_w}\times T_m$
⑧	$e^{-[(2\pi/L_w)\times T_m]}$
⑨ = ③ of Table 9.3	Sectional Restoring Force Coefficient, c_n
⑩ = ⑨ × ζ_a	$\zeta_a \times c_n$
⑪ = ⑬ of Table 9.1	Sectional Added Mass, a_n
⑫	$a_n \times (-\zeta_a \times \omega_e^2)$
⑬ = ⑫ + ⑩	$-a_n\zeta_a\omega_e^2 + c_n\zeta_a$
⑭	Slope of the added mass curve, $da_n/d\xi$, (see sample calculation below)

Column Number	*Description*
⑮ = $u\zeta_a\omega_e\times$ ⑭	$u\times\zeta_a\omega_e\times\frac{da_n}{d\xi}$
⑯	$b_n\zeta_a\omega_e$
⑰ = ⑯ − ⑮	$b_n\zeta_a\omega_e - u\zeta_a\omega_e\frac{da_n}{d\xi}$
⑱ = ⑬ × ④	$(-a_n\zeta_a\omega_e^2 + c_n\zeta_a)\times\sin\left(\frac{2\pi}{L_w}\times\xi\right)$
⑲ = ⑰ × ⑤	$\left(b_n\zeta_a\omega_e - u\zeta_a\omega_e\frac{da_n}{d\xi}\right)\times\cos\left(\frac{2\pi}{L_w}\times\xi\right)$
⑳ = ⑱ × ⑲	$(-a_n\zeta_a\omega_e^2 + c_n\zeta_a)\sin\left(\frac{2\pi}{L_w}\times\xi\right) + \left(b_n\zeta_a\omega_e - u\zeta_a\omega_e\frac{da_n}{d\xi}\right)\cos\left(\frac{2\pi}{L_w}\times\xi\right)$
㉑ = ⑬ × ⑤	$(-a_n\zeta_a\omega_e^2 + c_n\zeta_a)\times\cos\left(\frac{2\pi}{L_w}\times\xi\right)$
㉒ = ⑰ × ④	$\left(b_n\zeta_a\omega_e - u\zeta_a\omega_e\frac{da_n}{d\xi}\right)\times\sin\left(\frac{2\pi}{L_w}\times\xi\right)$

Column Number	*Description*
㉓ = ㉑ − ㉒	$(-a_n\zeta_a\omega_e^2 + c_n\zeta_a)\cos\left(\frac{2\pi}{L_w}\times\xi\right) - \left(b_n\zeta_a\omega_e - u\zeta_a\omega_e\frac{da_n}{d\xi}\right)\sin\left(\frac{2\pi}{L_w}\times\xi\right)$
㉔ = ⑳ × ⑧	$\left[(-a_n\zeta_a\omega_e^2 + c_n\zeta_a)\sin\left(\frac{2\pi}{L_w}\times\xi\right) + \left(b_n\zeta_a\omega_e^2 - u\zeta_a\omega_e\frac{da_n}{d\xi}\right)\cos\left(\frac{2\pi}{L_w}\times\xi\right)\right] \times e^{-[(2\pi/L_w)\times T_m]} = \frac{dF_2}{dx}$
㉕	Simpson's Multiplier
㉖ = ㉔ × ㉕	Product
㉗ = ㉓ × ⑧	$\left[(-a_n\zeta_a\omega_e^2 + c_n\zeta_a)\cos\left(\frac{2\pi}{L_w}\times\xi\right) - \left(b_n\zeta_a\omega_e - u\zeta_a\omega_e\frac{da_n}{d\xi}\right)\sin\left(\frac{2\pi}{L_w}\times\xi\right)\right] \times e^{-[(2\pi/L_w)\times T_m]} = \frac{dF_2}{dx}$

Column Number	*Description*
㉘	Simpson's Multiplier
㉙ = ㉗ × ㉘	Product
㉚ = ㉔ × ②	$\left\{\left[(-a_n\zeta_a\omega_e^2 + c_n\zeta_a)\sin\left(\frac{2\pi}{L_w}\times\xi\right) + \left(b_n\zeta_a\omega_e - u\zeta_a\omega_e\frac{da_n}{d\xi}\right)\cos\left(\frac{2\pi}{L_w}\times\xi\right)\right] \times e^{-[(2\pi/L_w)\times T_m]}\right\} \times \xi = \frac{dM_1}{dx}$
㉛	Simpson's Multiplier
㉜ = ㉚ × ㉛	Product
㉝ = ㉗ × ②	$\left\{\left[(-a_n\zeta_a\omega_e^2 + c_n\zeta_a)\cos\left(\frac{2\pi}{L_w}\times\xi\right) - \left(b_n\zeta_a\omega_e - u\zeta_a\omega_e\frac{da_n}{d\xi}\right)\sin\left(\frac{2\pi}{L_w}\times\xi\right)\right] \times e^{-[(2\pi/L_w)\times T_m]}\right\} \times \xi = \frac{dM_2}{dx}$
㉞	Simpson's Multiplier
㉟ = ㉝ × ㉞	Product

The value of $da_n/d\xi$ is approximately determined at a single point by the slope equation

$$\left(\frac{da_n}{d\xi}\right)_{\text{stn } K} = \frac{1}{2}\left(\frac{a_{n_{K+1}} - a_{n_K}}{\xi_{K+1} - \xi_K} + \frac{a_{n_K} - a_{n_{K-1}}}{\xi_K - \xi_{K-1}}\right) \quad (9.40)$$

where K denotes the point in question, and K − 1 and K + 1 the points before and after K, respectively. *Note*: At end points the value of the slope to the right or left will be used, since no averaging is possible.

	Station 0	Station 5	Station 10
a_n[lb-sec^2/ft^2]	0.000	5.011	5.011
ξ [ft]	9.12	4.32	− 0.48

Thus the slope of the added mass distribution is

$$\frac{da_n}{d\xi}\text{ at station 5} = \frac{1}{2}\left(\frac{5.011 - 0.00}{4.32 - 9.12} + \frac{5.011 - 5.011}{-0.48 - 4.32}\right)$$
$$= 0.522 \text{ lb-sec}^2/\text{ft}^3$$

Ship's mass, m

$$m = \tfrac{1}{3} \times S \times \text{SUM}_1$$
$$= \tfrac{1}{3} \times 4.8 \times 55.50 = 88.8 \text{ lb-sec}^2/\text{ft}$$

Ship's mass moment of inertia, I_{yy}

$$I_{yy} = \tfrac{1}{3} \times S \times \text{SUM}_2$$
$$= \tfrac{1}{3} \times 4.8 \times 1112.61$$
$$= 1780.2 \text{ lb-sec}^2\text{-ft}$$

Note that, if the distribution of weight along the length is not known, ship mass m is obtained as

$$m = \frac{\Delta}{g}$$

and

$$I_{yy} = \frac{\Delta}{g}k_{yy}^2$$

where k_{yy}, the *radius of gyration*, is assumed to be between 0.24L and 0.26 L.

Exciting force component, F_1

$$F_1 = \tfrac{1}{3} \times S \times \text{SUM}_1$$
$$= \tfrac{1}{3} \times 4.8 \times (-4.281)$$
$$= -6.85 \text{ lb}$$

Exciting force component, F_2

$$F_2 = \tfrac{1}{3} \times S \times \text{SUM}_2$$
$$= \tfrac{1}{3} \times 4.8 \times 4.473$$
$$= 7.157 \text{ lb}$$

Amplitude of the exciting force, F_0, is given as

$$F_0 = \sqrt{F_1^2 + F_2^2} = \sqrt{(-6.85)^2 + (7.157)^2}$$
$$= 9.906 \text{ lb}$$
$$F = F_0 \cos(\omega_e t + \sigma)$$

Similarly,
Exciting moment component, M_1

$$M_1 = \tfrac{1}{3} \times S \times \text{SUM}_3$$
$$= \tfrac{1}{3} \times 4.8 \times 232.91$$
$$= 372.60 \text{ gt-lb}$$

Exciting moment component, M_2

$$M_2 = \tfrac{1}{3} \times S \times \text{SUM}_4$$
$$= \tfrac{1}{3} \times 4.8(-144.869)$$
$$= -231.79 \text{ ft-lb}$$

Amplitude of the exciting moment, M_0, is given as

$$M_0 = \sqrt{M_1^2 + M_2^2} = \sqrt{(372.60)^2 + (-231.79)^2}$$
$$= 438.81 \text{ ft-lb}$$
$$M = M_0 \cos(\omega_e t + \tau)$$

Since the exciting force and the moment are given as complex quantities,

$$\bar{F} = F_0 e^{i\sigma} = F_0(\cos\sigma + i\sin\sigma) = F_1 + iF_2$$

where

$$F_1 = F_0 \cos\sigma \quad \text{and} \quad F_2 = F_0 \sin\sigma \tag{9.41c}$$

Thus the real part of the exciting force becomes

$$\text{Re}\, F e^{i\omega_e t} = \text{Re}\, F_0 e^{i(\omega_e t + \sigma)} = F_0 \cos(\omega_e t + \sigma) \tag{9.41a}$$

Similarly, the real part of the exciting moment becomes

$$\text{Re}(\bar{M} e^{i\omega_e t}) = R_e M_0 e^{i(\omega_e t + \tau)} = M_0 \cos(\omega_e t + \tau) \tag{9.41b}$$

and

$$\bar{M} = M_1 + iM_2 = M_0 e^{i\tau} = M_0(\cos\tau + i\sin\tau) \tag{9.42}$$

where

$$M_1 = M_0 \cos\tau \quad \text{and} \quad M_2 = M_0 \sin\tau \tag{9.42a}$$

Thus

$$F_0 = (F_1^2 + F_2^2)^{1/2} \tag{9.43}$$

and

$$M_0 = (M_1^2 + M_2^2)^{1/2} \tag{9.44}$$

Also,

$$\sigma = \tan^{-1}(F_2/F_1) \tag{9.45}$$

is the phase angle of the exciting force for heaving motion in relation to wave motion, and

$$\tau = \tan^{-1}(M_2/M_1) \tag{9.46}$$

is the phase angle of the exciting moment for pitching motion in relation to wave motion. *Note*: The quadrant in which σ or τ should lie will always be determined from (9.41c) or (9.42a), respectively.

Returning to our example, we find the force and moment relations:

$$F_0 = (F_1^2 + F_2^2)^{1/2} = 9.906 \text{ lb}$$
$$\sigma = 133.7^\circ \quad \text{from (9.41c)}$$
$$M_0 = (M_1^2 + M_2^2)^{1/2} = 438.81 \text{ ft-lb}$$
$$\tau = -31.9^\circ \quad \text{from (9.42a)}$$

Thus

$$F = 9.906 \cos(\omega_e t + 133.7^\circ) \text{lb}$$
$$M = 438.81 \cos(\omega_e t - 31.9^\circ) \text{ft-lb}$$

from Table 9.6, and

$$\bar{F} = F_1 + iF_2 = F_0(\cos\sigma + i\sin\sigma) = -6.85 + 7.157i$$
$$\bar{M} = M_1 + iM_2 = M_0(\cos\tau + i\sin\tau) = 372.60 - 231.79i$$

Solution of Equations of Motion

In motion analysis, the following notation is used:

z_a = amplitude of heaving motion
θ_a = amplitude of pitching motion
δ = phase of heaving motion after wave node at CG
ε = phase of pitching motion after wave node at CG

The substitution of $z = \bar{z}e^{i\omega_e t}$ and $\theta = \bar{\theta}e^{i\omega_e t}$ and their time derivatives reduces the equations of motion to two simple algebraic equations (only the *real part* of the solution will be considered):

Heave: $z = \text{Re}\, \bar{z}e^{i\omega_e t} = \text{Re}\, z_a e^{i(\omega_e t + \delta)}$
$$= z_a \cos(\omega_e t + \delta) \tag{9.47}$$

Pitch: $\theta = \text{Re}\, \theta e^{i\omega_e t} = \text{Re}\, \theta_a e^{i(\omega_e t + \delta)}$
$$= \theta_a \cos(\omega_e t + \varepsilon) \tag{9.48}$$

Now, in our example let

$$P = -(m + a)\omega_e^2 + ib\omega_e + c = -1216.5 + 513.2i$$
$$S = -(I_{yy} + A_{yy})\omega_e^2 + iB\omega_e + C = -23{,}376.4 + 10{,}131.3i$$

$$Q = -d\omega_e^2 + ie\omega_e + h = 1422.9 + 2280.0i$$

$$R = D\omega_e^2 + iE\omega_e + H = 912.2 - 1201.1i$$

$$PS = 2.324 \times 10^7 - 2.432 \times 10^7 i$$

$$QR = 4.036 \times 10^6 + 0.371 \times 10^{6i}$$

$$PS - QR = 1.920 \times 10^7 - 2.469 \times 10^7 i$$

$$\overline{PS - QR} = 1.920 \times 10^7 + 2.469 \times 10^7 i$$

which is the complex conjugate, and

$$(PS - QR)(\overline{PS - QR}) = 9.7834 \times 10^{14} \quad (9.48a)$$

Note: When there is a complex number in the denominator, both the numerator and the denominator are multiplied by the complex conjugate of the denominator in order to obtain a simplified expression for the fraction. Thus

$$\bar{F}S = 0.876 \times 10^5 - 2.367 \times 10^5 i$$

$$\bar{M}Q = 1.059 \times 10^6 + 0.520 \times 10^6 i$$

$$\bar{F}S - \bar{M}Q = 9.710 \times 10^5 - 7.564 \times 10^5 i$$

$$(\bar{F}S - \bar{M}Q)(\overline{PS - QR}) = 3.2739 \times 10^{10} - 3.8499 \times 10^{13} i \quad (9.48b)$$

$$\bar{M}P = -3.343 \times 10^5 + 4.732 \times 10^5 i$$

$$\bar{F}R = 2347.7 + 14755.7i$$

$$\bar{M}P - \bar{F}R = -3.366 \times 105 + 4.584 \times 10^5 i$$

$$(\bar{M}P - \bar{F}R)(\overline{PS - QR}) = -1.7783 \times 10^{13} + 4.8966 \times 10^{11} i \quad (9.48c)$$

The complex heaving and pitching amplitudes are, respectively, $\bar{z}$ (taken as $z_1 + iz_2$) and θ (as $\theta_1 + i\theta_2$). For the example in question, therefore,

$$\bar{z} = \frac{(9.48b)}{(9.48a)} = z_1 + iz_2$$

$$= \frac{3.2739 \times 10^{10} - 3.8499 \times 10^{13} i}{9.7834 \times 10^{14}}$$

$$= 3.346 \times 10^{-5} - 3.935 \times 10^{-2} i$$

that is,

$$z_1 = z\,(\text{real}) = 3.346 \times 10^{-5}$$

$$z_2 = z\,(\text{imaginary}) = -3.935 \times 10^{-2}$$

and the heaving amplitude is

$$z_a = \sqrt{z_1^2 + z_2^2} = 3.935 \times 10^{-2}\ \text{ft}$$

Since $z_1 = z_a \cos\delta$ and $z_2 = z_a \sin\delta$, the phase angle is the *heave phase angle*, $\delta = -89.95°$.

Similarly, the pitching amplitude is

$$\bar{\theta} = \frac{(9.48c)}{(9.48a)} = \theta_1 + i\theta_2$$

$$= \frac{-1.7783 \times 10^{13} + 4.8966 \times 10^{11} i}{9.7834 \times 10^{14}}$$

$$= 1.818 \times 10^{-2} + 5.005 \times 10^{-4} i$$

that is,

$$\theta_1 = \theta\,(\text{real}) = 1.818 \times 10^{-2}$$

$$\theta_2 = \theta\,(\text{imaginary}) = 5.005 \times 10^{-4}$$

and the pitching amplitude is

$$\theta_a = \sqrt{\theta_1^2 + \theta_2^2} = 1.819 \times 10^{-2}\ \text{rad (or } 1.04°)$$

But

$$\theta_1 = \theta_a \cos\varepsilon \quad \text{and} \quad \theta_2 = \theta_a \sin\varepsilon$$

and so the pitching phase angle is

$$\varepsilon = 178.42°$$

The respective equations of wave, heaving, and pitching motions can therefore be expressed as

$$\zeta = \zeta_a \sin(k\xi - \omega_e t)$$

$$= -0.2 \sin\omega_e t \quad \text{since } \xi = 0 \text{ at the CG of the ship}$$

$$z = z_a \cos(\omega_e t + \delta)$$

$$= 0.03935 \cos(\omega_e t - 89.95°)\,\text{ft}$$

$$\theta = \theta_a \cos(\omega_e t + \varepsilon)$$

$$= 0.01819 \cos(\omega_e t + 178.42°)\,\text{rad}$$

The motion calculations as functions of time are presented in Table 9.7 and plotted in Fig. 9.3 and 9.4. The phase angle between the pitching and heaving motions is seen to be $178.42° - (-89.95°)$ or $+268.37°$. This lag of the heaving motion can also be interpreted as the lead of the heaving motion over the pitch by $2\pi - 268.37°$ or $\delta - \varepsilon = 91.63°$.

TABLE 9.7

$\omega_e t$ [rad]	t [sec]	ζ [ft]	F [lb]	z [ft]	M [ft-lb]	θ [rad]
0	0	0	−6.844	+0.00003	372.54	−0.0182
$\pi/4$	0.163	−0.1414	−9.903	+0.0278	427.40	−0.0132
$\pi/2$	0.327	−0.2	−7.162	+0.0393	231.88	−0.0005
$3\pi/4$	0.490	−0.1414	−0.225	+0.0278	−99.46	0.0125
1π	0.653	0	+6.844	−0.00003	−372.54	0.0182
$5\pi/4$	0.817	0.1414	+9.903	−0.0278	−427.40	0.0132
$6\pi/4$	0.980	0.2	+7.162	−0.0393	−231.88	0.0005
$7\pi/4$	1.143	0.1414	+0.225	−0.0278	99.46	−0.0125
2π	1.307	0	−6.844	+0.00003	372.54	−0.0182

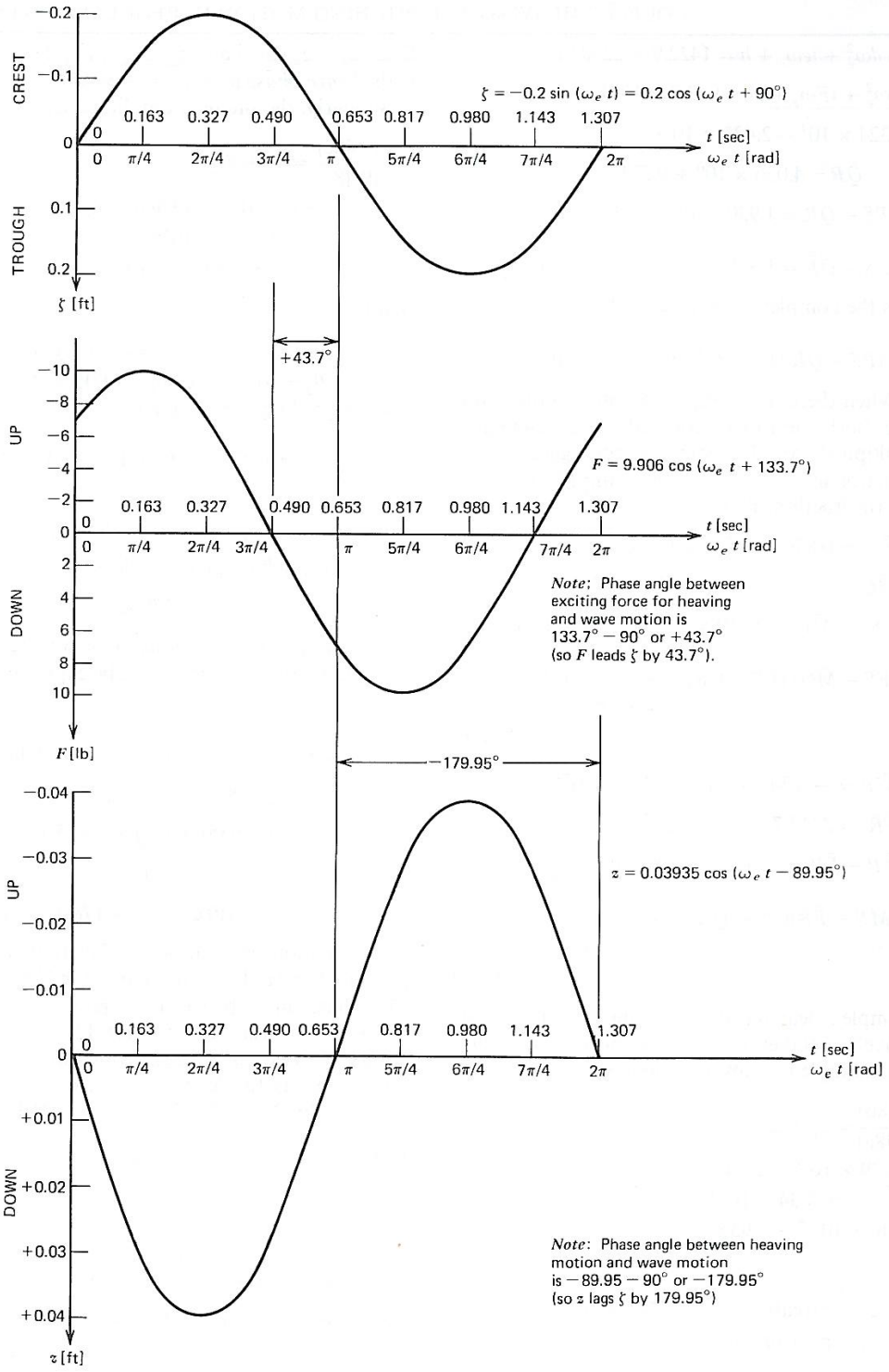


Figure 9.3 Wave motion, exciting force for heaving, and heaving motion.

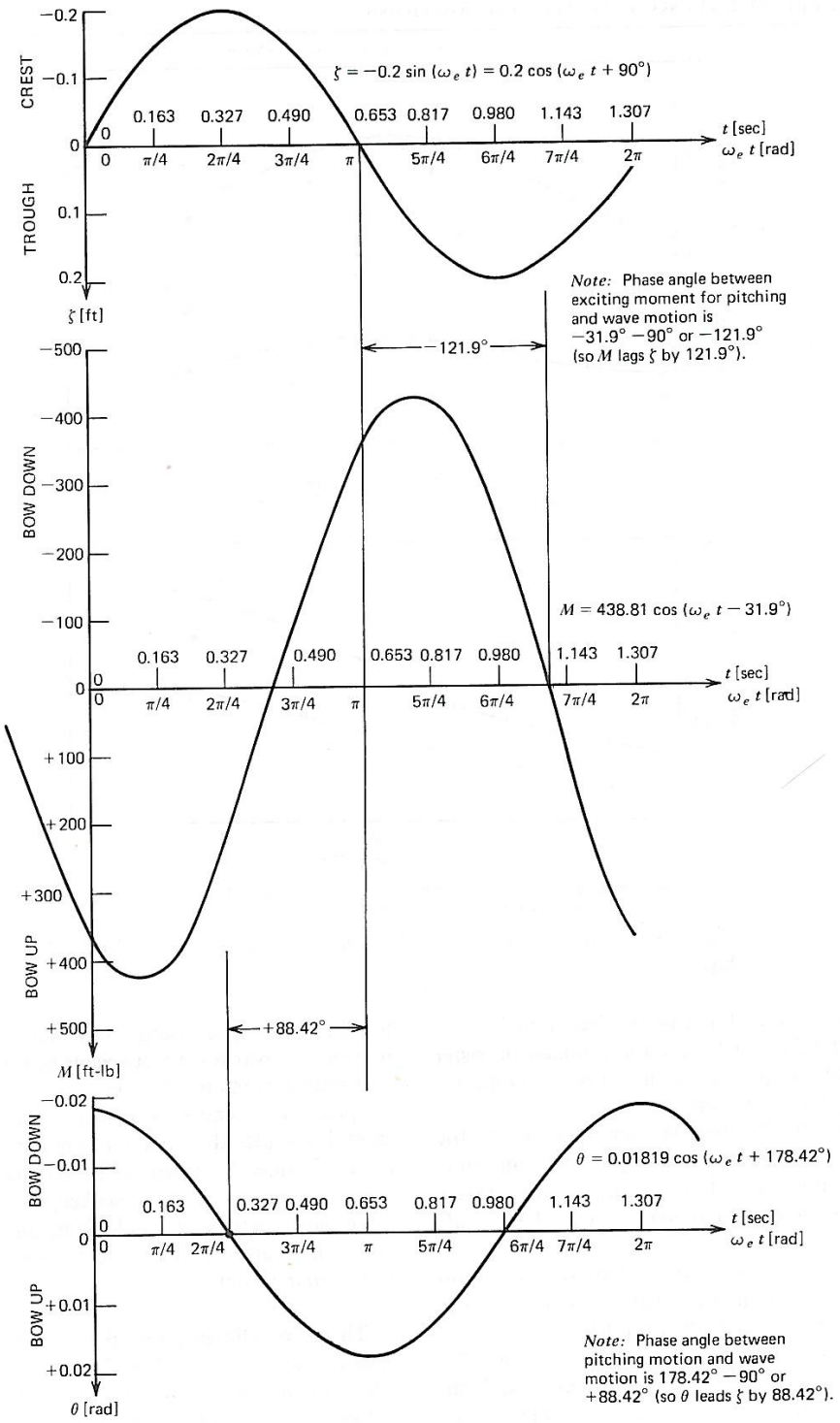


Figure 9.4 Wave motion, exciting moment for pitching, and pitching motion.

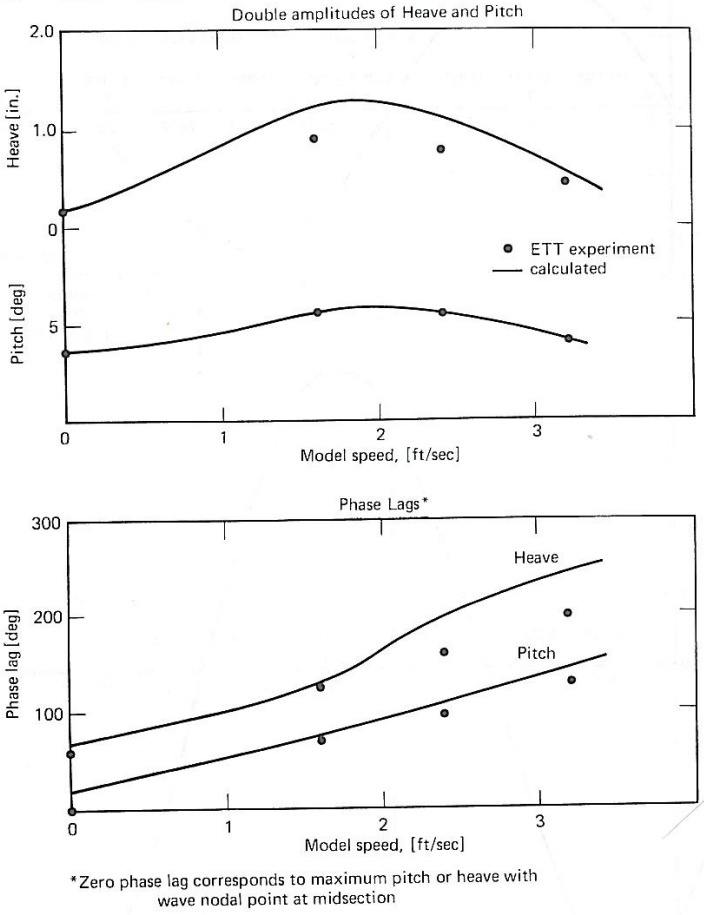


Figure 9.5 Motions of a 4.8 ft model in waves 4.8 ft long and 1.2 in high [107].

The motions of a ship can be determined easily from its model data or from data obtained on sister ship by using the proper scaling. For example, for a 480 ft ship (i.e., the scale ratio is 25), the heaving amplitude will be 25 times greater than that of the model (i.e., 0.99 ft); however, the pitching amplitude will be the same as that of the model (i.e., 1.04°), since *the angular motion is independent of the scale factor.*

Figure 9.5 shows the calculated curves of motion along with the experimental values obtained for a 4.8 ft model in head sea conditions of $L/48$ wave height. As can be seen, the agreement between the calculated and measured pitch amplitudes is excellent, whereas the calculated heave amplitudes appear to be overestimated around the synchronous speed. The agreement between calculated and measured phase lags is also satisfactory for the pitching motion for the entire speed range; however, for the heaving motion this is true only at speeds below synchronism.

It must be remembered that accurate measurement of phase differences is rather difficult. Also, one should consider that a certain amount of experimental error may be involved in the measurement of motion characteristics in seakeeping facilities. The discrepancy between the calculated and the measured values may also be attributed to three shortcomings of the *strip theory*:

1. The three-dimensional flow, especially at both ends of the ship, is neglected. The three-dimensional effect on the total damping force, which may not be considered to be large, may cause some discrepancy. At higher frequencies, but within the natural range for normal ships, three-dimensional damping in heave may be 20% higher than two-dimensional.

2. There is a question of nonlinear damping. Only wave effects have been considered in the calculation of the damping coefficients; damping due to viscosity is neglected in the calculations by the strip theory. Damping due to viscosity in the heaving motion is insignificant only at zero speed.

3. Three-dimensional effects for the calculation of added mass and added mass moment of inertia may also contribute to some extent to the discrepancy between the calculated and measured results.

For design purposes the amplitudes of heaving force and pitching moment are nondimensionalized in the following manner:

$$C_F = \frac{F_0}{\gamma' A_{WP} \zeta_a} \tag{9.49}$$

and

$$C_M = \frac{M_0}{\gamma' I_L \alpha_M} \tag{9.50}$$

where

F_0 = amplitude of heaving force in a wave of amplitude ζ_a
M_0 = amplitude of pitching moment
γ' = specific gravity of water
A_{WP} = waterplane area
I_L = longitudinal moment of inertia of waterplane area
α_M = maximum slope of a wave of amplitude ζ_a

A systematic calculation of C_F, C_M, and the *phase angles* α and β by the strip theory for various wavelengths and speeds but for a constant wave height of $\frac{1}{48} L$ (L being the model length) is presented in Ref. 73 for Series 60 forms. The results are presented in Fig. 9.6. It appears from this figure that *the influence of speed on the forcing functions is rather small.* The results of the heave and pitch calculations for a Series 60($C_B = 0.70$) hull form by the strip theory have been compared with experimental results in Fig. 9.7, and the agreement seems to be very satisfactory. The measured phase differences, $\varepsilon - \delta$ (heave after pitch), also should show good agreement with the calculated values. It is noted that the differences between the calculated and experimental results are of the same order as the experimental errors, which are approximately 10 to 20°.

To determine the effect of the *coupling* between pitching and heaving motions, the differential equations given for coupled pitch and heave is solved for the case in which all the coupling terms should be put to zero, that is,

$$d = e = h = D = E = H = 0 \tag{9.51}$$

Comparisons between the calculated and experimental results show clearly that in the prediction of pitching and heaving motions the effect of coupling between them cannot be neglected.

Example 9.2

If the heaving and pitching motions are considered as uncoupled, determine the heaving and pitching amplitudes, as well as the phase angles of motion, for the ship described in Example 9.1.

Solution:

For uncoupled heaving and pitching motions (9.51) applies. Furthermore, the following numerical are obtained.

$$P = -1212.7 + i(513.0)$$

$$S = -23298.0 + i(10141.5)$$

$$Q = R = 0$$

$$\bar{F} = -6.52368 + i(7.15482)$$

$$\bar{M} = 372.15436 - i(230.95450)$$

$$PS = 23{,}051{,}384.882 - i(24{,}251{,}807.842)$$

$$QR = 0$$

$$(PS - QR) = 23{,}051{,}384.882 - i(24{,}251{,}807.842)$$

$$\overline{(PS - QR)} = 23{,}051{,}384.882 + i(24{,}251{,}807.842)$$

$$(PS - QR)\,\overline{(PS - QR)} = 1.11951653 \times 10^{15} \tag{9.52}$$

$$\bar{F}S = 79{,}427.6 - i(232{,}853.8)$$

$$\bar{F}R = \bar{M}Q = 0$$

$$\bar{M}P = -332{,}837.2 + i(471{,}015.6)$$

$$(\bar{F}S - \bar{M}Q) = 79{,}427.6 - i(232{,}853.8)$$

$$(\bar{M}P - \bar{F}R) = -332{,}837.1 + i(471{,}015.6)$$

$$(\bar{F}S - \bar{M}Q)\overline{(PS - QR)} = 7{,}478{,}043{,}587{,}935.4 - i(3{,}441{,}339{,}213{,}753.1) \tag{9.53}$$

$$(\bar{M}P - \bar{F}R)\overline{(PS - QR)} = 19{,}095{,}339{,}080{,}069 + i(2{,}785{,}658{,}978{,}905) \tag{9.54}$$

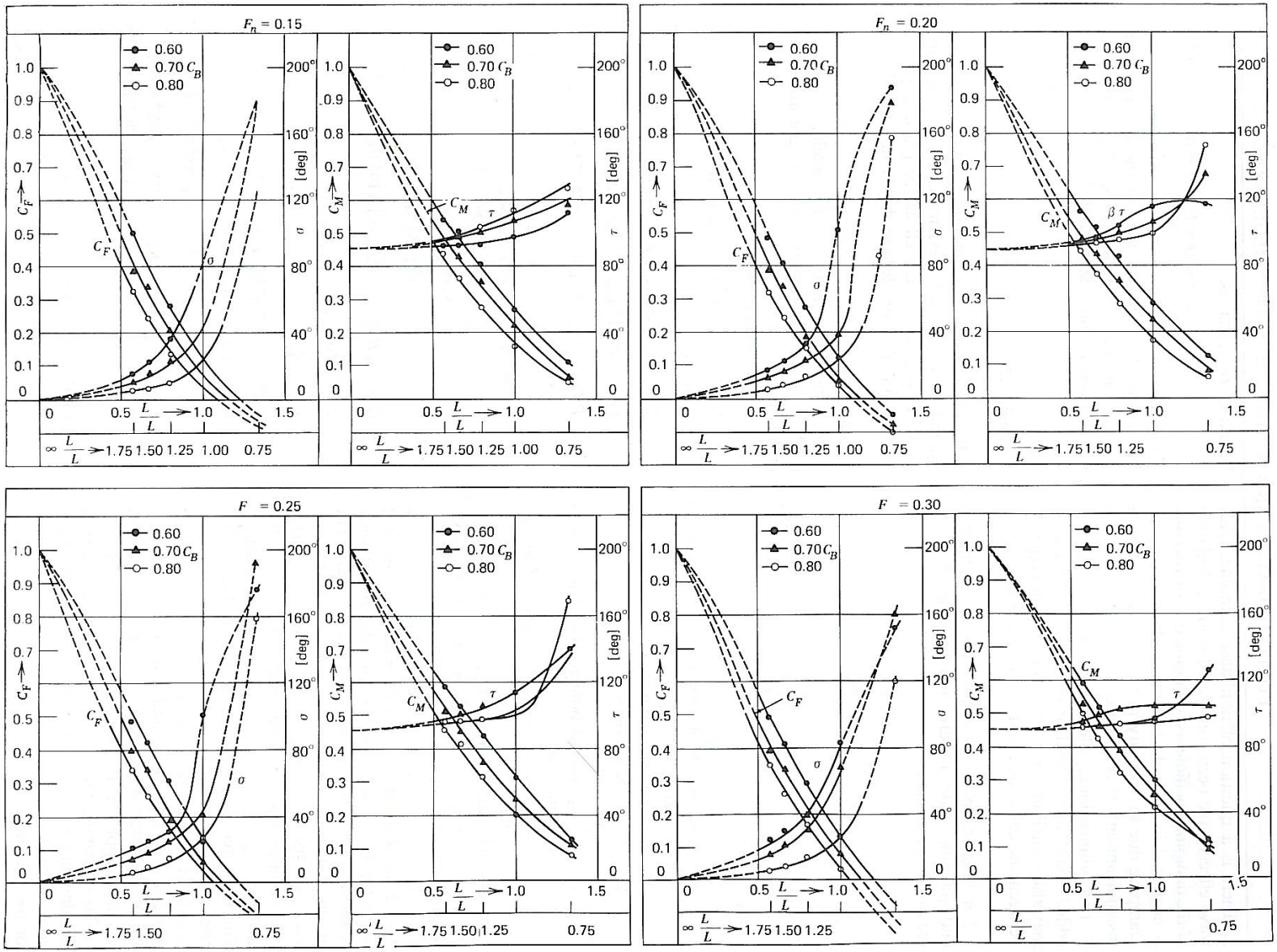


Figure 9.6 Coefficients of heave exciting force and pitch exciting moment coefficients [73].

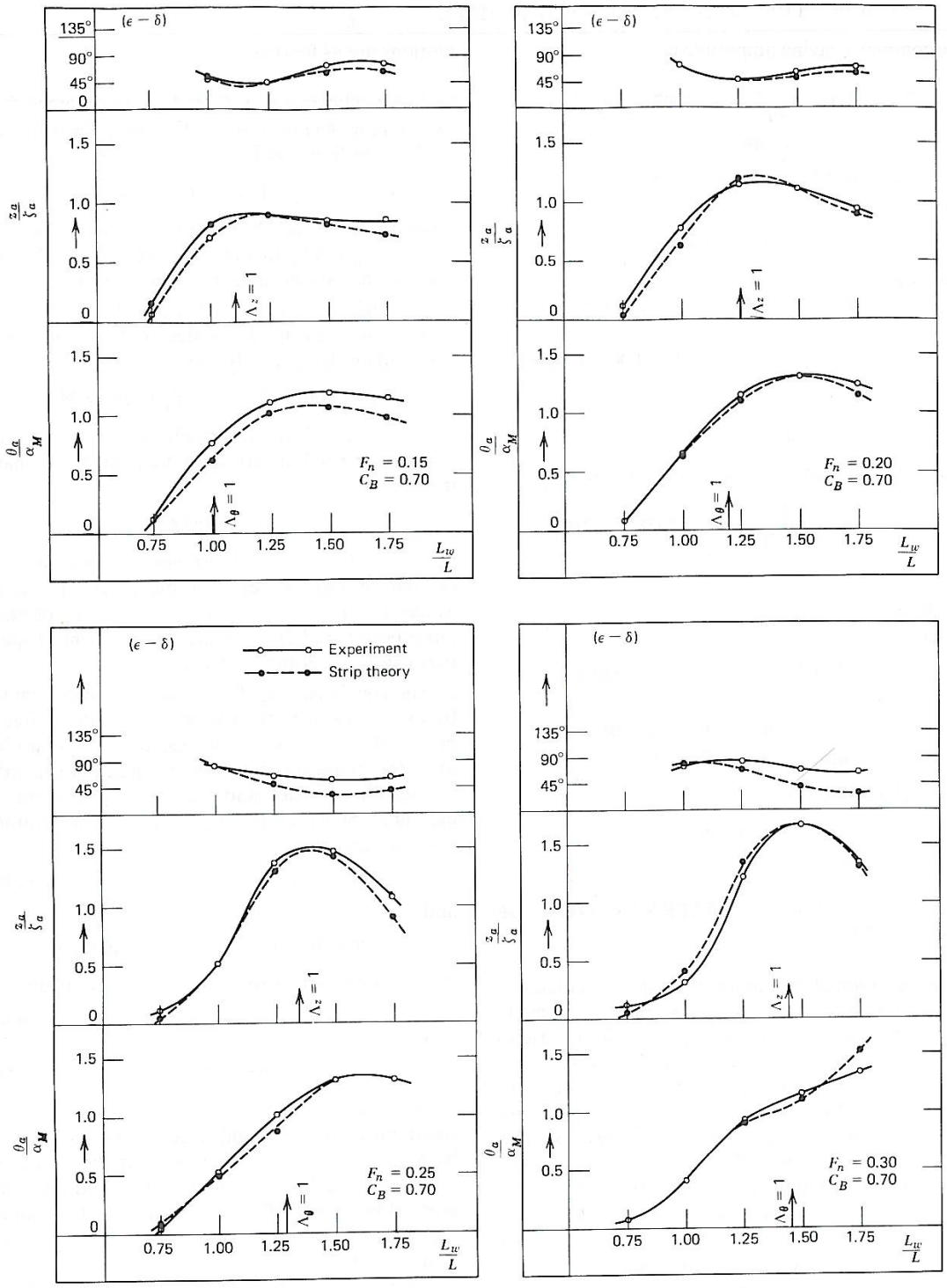


Figure 9.7 Comparison between calculated and measured motions [73].

The complex heaving amplitude is

$$\bar{z} = z_1 + iz_2 = \frac{(9.53)}{(9.52)} = 6.67971 \times 10^{-3} - i(3.07395 \times 10^{-3})$$

$$z_1 = 0.0067, \qquad z_2 = -0.0031$$

and

$$z_a = \sqrt{z_1^2 + z_2^2} = 0.0073531 \text{ ft}$$

Now, since

$$z_1 = z_a \cos\delta \quad \text{or} \quad 0.00671 = 0.0073531 \cos\delta$$

and

$$z_2 = z_a \sin\delta \quad \text{or} \quad -0.0031 = 0.0073531 \sin\delta$$

the phase angle is

$$\delta = -24.711^\circ$$

Similarly, the complex pitching amplitude is

$$\bar{\theta} = \theta_1 + i\theta_2 = \frac{(9.54)}{(9.52)} = -1.705677 \times 10^{-2} + i(2.488269 \times 10^{-3})$$

$$\theta_1 = -0.017, \qquad \theta_2 = 0.002$$

so that

$$\theta_a = \sqrt{\theta_1^2 + \theta_2^2} = 0.0172373 \text{ rad } (0.988^\circ)$$

Again, since

$$\theta_1 = \theta_a \cos\varepsilon \quad \text{or} \quad -0.017 = 0.017 \cos\varepsilon$$

$$\theta_2 = \theta_a \sin\varepsilon \quad \text{or} \quad 0.002 = 0.017 \sin\varepsilon$$

The pitching phase angle is

$$\varepsilon = 171.8^\circ$$

9.5 EXPERIMENTAL DETERMINATION OF THE COEFFICIENTS

It was mentioned in Section 9.3 that the equations for the coupled heaving and pitching motions in calm water may be obtained by equating the right-hand sides of (9.19) and (9.23) to zero. In this case we need to assume that the coefficients of the equations of motion, a_z to h and A_{yy} to H, are the same for motions both in calm water and in waves. This assumption allows us to find the coefficients experimentally by exciting the model in calm water, whereas the exciting forces and moments due to the waves can be measured with the help of a restrained model. This approach to the problem has the advantage that each of the determined coefficients can be compared directly with calculated values.

The basic principles of the experimental means for determining the coefficients of the equations of motions are as follows:

a. The coefficients c, g, C, and G are obtained from two simple *inclining tests*. For pure heaving and pitching motions, we have, when $\omega_e = 0$,

$$cz_a = F_0, \qquad C\theta_a = M_0$$

Since the force or the moment is known and the values of z_a and θ_a are measured, both the coefficients c and C can be determined as functions of speed.

b. Similarly, the coefficients h and H can be determined when the model is free to heave and pitch simultaneously. If $\omega_e = 0$, then

$$cz_a + h\theta_a = F_0, \qquad C\theta_a + Hz_a = M_0$$

where h and H are the coefficients of the statical coupling terms. For zero speed they can be calculated from

$$h = H = \gamma' l A_{WP} \tag{9.55}$$

where l is the horizontal distance between the center of floation and the center of buoyancy, A_{WP} is the waterplane area, and γ' is the specific gravity of water. Since both h and H are nearly independent of speed, they can be determined by (9.55).

c. The coefficients a_z, b, A_{yy}, and B are determined by two series of tests in which the model is free to pitch but not to heave, or vice versa. A sinusoidal force (or moment) of known frequency is generated to excite the model, and the resulting motions are measured. Since this is the case of uncoupled motion, the equations of motion are

$$a\ddot{z} + bz + cz = F_0 e^{i\omega_e t} \qquad \text{in heave} \tag{9.56a}$$

and

$$A\ddot{\theta} + B\dot{\theta} + C\theta = M_0 e^{i\omega_e t} \qquad \text{in pitch} \tag{9.56b}$$

The solutions of these equations are, respectively,

$$z = z_a e^{i(\omega_e t + \delta)} \tag{9.56c}$$

and

$$\theta = \theta_a e^{i(\omega_e t + \tau)} \tag{9.56d}$$

The values for z_a, θ_a, δ, τ, F_0, M_0, and ω_e are measured during the tests, and since c and C have already been determined, the equations can be solved for a_z, A_{yy}, b, and B by equating the real and imaginary parts of both sides. The coefficients a_{zz}, A_{yy}, b, and B depend on the frequency of motion, ship speed, and hull geometry.

Note: It has been found that because of tank wall interference measurements below a frequency of $\omega_e = 4$ rad/sec are not very reliable.

d. Now, the model is forced to oscillate in calm

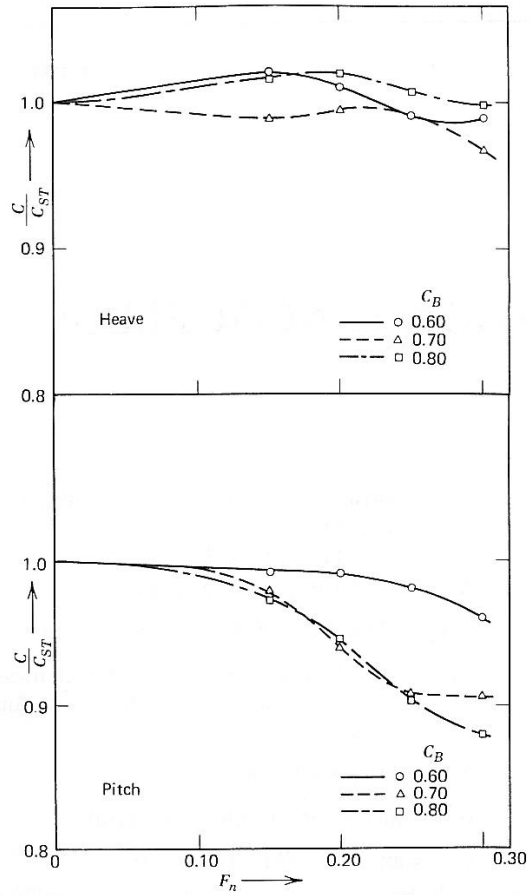


Figure 9.8 Coefficients of restoring force and moment as functions of speed [73].

water having both degrees of freedom of motion, that is, the model is free to heave and pitch simultaneously. The coupled equations of forced motion in this case are

$$a\ddot{z} + b\dot{z} + cz + d\ddot{\theta} + e\dot{\theta} + h\theta = F_0 e^{i\omega_e t} \quad \text{in heave} \tag{9.57}$$

and

$$A\ddot{\theta} + B\dot{\theta} + C\theta + Dz + E\dot{z} + Hz = M_0 e^{i\omega_e t} \quad \text{in pitch} \tag{9.58}$$

The solutions of (9.57) and (9.58) are, respectively,

$$z = z_a e^{i(\omega_e t + \delta)} \tag{9.59}$$

and

$$\theta = \theta_a e^{i(\omega_e t + \tau)} \tag{9.60}$$

Substituting these solutions into the equations of motion, we get four identities involving four unknowns, namely, d, e, D, and E, since the other coefficients, a_z, b, c, h, A_{yy}, B, C, and H, have already been found from previous tests and also since z_a, θ_a, δ, τ, F_0, and M_0 will be measured during the model tests.

Experiments have shown that both d and D have very small values, so they are highly sensitive to experimental errors. It has also been found that $d\ddot{z}$ and $D\ddot{\theta}$ can be neglected without causing any appreciable errors in the calculation of motion amplitudes and phases.

e. Finally, the forcing functions $F_0 e^{i(\omega_e t + \sigma)}$ and $M_0 e^{i(\omega_e t + \tau)}$ for models in waves are measured by making use of the *restrained model*. The experimentally obtained coefficients are presented non-dimensionally in Fig. 9.8. In that figure the *static* (for the restrained model) *restoring force coefficient* is obtained from

$$c_{st} = \gamma' A_{WP} \tag{9.61}$$

where γ' is the specific gravity of water and A_{WP} is the area of the waterplane, while the *static* (for the restrained model) *restoring moment coefficient* is

$$C_{st} = \gamma' I_L \tag{9.62}$$

where I_L is the longitudinal moment of inertia of the waterplane area.

Chapter

Ten

NONLINEAR ROLLING MOTION (UNCOUPLED)

10.1 GENERAL

In the study of vehicle motions it is usually considered sufficient to predict rolling characteristics assuming the linear equation of motions to be approximately correct. Indeed, for small angles of roll this assumption is very good. For larger angles, however, many nonlinearities become more significant, and the result of the linear approximation is doubtful.

Although the solution to nonlinear equations is rather difficult, their values are increasingly becoming the desired results in final rolling studies. According to linear theory, a sudden gust or force acting against a vessel will cause higher amplitudes momentarily, but the damping effect will return the vessel to normal oscillation. Nonlinearities, on the other hand, can magnify small variations in excitation to the point where the restoring force contributes to capsizing. The underlying reason for nonlinear studies is to avoid a design that promotes capsizing due to resonance or other nonlinear phenomena. In other words, nonlinear behavior is quite significant for predicting a vessel's maximum rolling amplitudes.

First let us consider non-linear motion in general. For the purpose of discussion and comparison, first the linear equation of motion will be presented and its terms, many of which will be included in nonlinear discussion, will be defined. (It must be remembered that linear theory is a simplification of nonlinear theory.) The equation for linear rolling is (see Chapter 4):

$$a\ddot{\phi} + b\dot{\phi} + c\phi = M(t)$$

or

$$I'_{xx}\frac{d^2\phi}{dt^2} + b\frac{d\phi}{dt} + \Delta\overline{GM}\phi = 0 \qquad (10.1)$$

where a = vertual mass moment of inertia about the longitudinal axis

$= I'_{xx} = [(\Delta + \Delta')/g]k_{xx}^2$

Δ = displacement of the vessel

Δ'/g = added mass of the vessel for rolling

k_{xx} = radius of gyration of the vessel mass plus added mass term for the rolling motion

b = damping coefficient

$\overline{GM}$ = metacentric height (transverse)

ϕ = angle of roll (in still water)

It should be noted that, when the vessel is rolling in waves, the angle of roll must include the wave slope α. The assumption is made for the linear case that the damping moment and the inertia moment are functions of ϕ alone (here a nonlinearity is avoided). The resultant equation from (10.1) is

$$I'_{xx}\ddot{\phi} + b\dot{\phi} + \Delta\overline{GM}(\phi - \alpha) = 0$$

or

$$\ddot{\phi} + \frac{bg}{\Delta_1 k_{xx}^2}\dot{\phi} + \frac{\Delta\overline{GM}\cdot g}{\Delta_1 k_{xx}^2}\phi = \frac{\Delta\overline{GM}\cdot g}{\Delta_1 k_{xx}^2}\alpha \qquad (10.2)$$

where Δ_1 is added weight $= \Delta + \Delta'$. If a sine wave is assumed for the wave excitation, then

$$\alpha = \alpha'_M \sin\omega_e t$$

where α'_M is the maximum effective wave slope, and ω_e is the frequency of encounter in waves.

Making these substitutions in (10.2), one arrives at the general equation for linear rolling in a sinusoidal seaway. Proper substitutions have been made for simplification of the coefficients:

$$\ddot{\phi} + 2\nu\phi + \omega_\phi^2\phi = \alpha'_M\omega_\phi^2 \sin\omega_e t \qquad (10.3)$$

Equation 10.3 is a linear second order differential equation that can be solved by the ordinary method for an exact solution. It is a good solution for small rolling motions, say for $\phi < 8°$.

Non linear rolling may take place as a function of many variables. For rolling motions there are four cases to be considered. First, however, let us consider the equation for nonlinear damping and restoring moment:

$$a\ddot{\phi} + b_1\dot{\phi} + b_2|\dot{\phi}|\dot{\phi} + c(\phi,t) = M(\omega_e,t) \qquad (10.4)$$

where a represents the virtual mass moment of inertia as a function of frequency of encounter, and b_1 and b_2 are damping coefficients that, when multiplied by the velocity $\dot{\phi}$ and the square of the velocity $|\dot{\phi}|\dot{\phi}$, will provide the damping moment. The square of the velocity is given by $|\dot{\phi}|\dot{\phi}$ so that, when the sign of ϕ is changed, this term also changes its sign in order that the damping moment will always oppose the motion. Also, c is the restoring moment and can be expressed as

$$c(\phi,t) = c_1(t)\phi + c_3(t)\phi^3 + c_5(t)\phi^5 + \ldots. \qquad (10.5)$$

Finally, M is the exciting moment, which varies with the frequency and time.

The four cases to be considered are as follows:

1. Linear equation of motion: $b_2 = c_3 = c_5 = 0$. Under these conditions (10.4) reduces to (10.2), and we have a linear case for the equation of rolling motion. This case has been treated extensively in Chapter 4.
2. Linear damping—nonlinear restoring moment with constant coefficients: $b_2 = 0$; c_1, c_3, c_5 not functions of time.
3. Nonlinear damping—linear restoring moment: $c_3 = c_5 = 0$; c_1 not a function of time.
4. Linear damping—linear restoring moment: $b_2 = c_3 = c_5 = 0$; c_1 a function of time.

10.2 LINEAR DAMPING: NONLINEAR RESTORING MOMENT WITH CONSTANT COEFFICIENTS

Combining (10.4) and (10.5) and using the restrictions of this case, we have for the equation of motion

$$a\ddot{\phi} + b\dot{\phi} + f(x) = M_0\cos\omega_e t$$

or

$$I'_{xx}(\omega_e)\ddot{\phi} + b\dot{\phi} + c_1\phi + c_3\phi^3 = M(\omega_e t)$$

for the rolling motion where the nonlinear restoring moment $f(x) = c_1\phi + c_3\phi^3$. Considering a cosine form for excitation and dividing all the coefficients by a, we obtain for this equation

$$\ddot{\phi} + b'\phi + c'_1\phi + c'_3\phi^3 = M'_0\cos\omega_e t \qquad (10.6)$$

The restoring moment coefficients c'_1 and c'_3 may be obtained from the approximation of the righting moment curve by a polynomial equation of the form

$$\Delta\overline{GZ} = c_1\phi + c_3\phi^3$$

The relation between the amplitude of the exciting moment M'_0, the motion amplitude A, and ω_e is obtained from the theories of nonlinear differential equations as follows [198]:

$$[(c'_1 - \omega_e^2)A + \tfrac{3}{4}c'_3A^3]^2 + b'^2A^2\omega_e^2 = M'^2_0 \qquad (10.6a)$$

It is convenient to write (10.6a) in the form

$$S^2(\omega_e,A) + b'^2A^2\omega_e^2 = M'^2_0 \qquad (10.6b)$$

in which

$$S(\omega_e,A) = (c'_1 - \omega_e^2)A + \tfrac{3}{4}c'_3A^3 \qquad (10.6c)$$

One can now draw a set of curves (called *response curves*) in an $\omega_e - A$ plane with the amplitude M'_0 of the exciting moment as a parameter; they reduce to the well-known response curves for linear forced oscillations when $c'_3 = 0$. The response curves are usually plotted with A as an ordinate, where the quantity A or, preferably, its absolute value $|A|$ is referred to as the *amplitude* of the nonlinear rolling motion; actually it is the value of the first Fourier coefficient of the oscillation. The quantity A, along with ω_e, characterizes completely a periodic solution.

In practice it is the custom to plot $|A|$ against ω_e as shown in Fig. 10.1, where response curves obtained from (10.6b) for $c'_3 \gtrless 0$ are plotted. The response curve for the free rolling motion (corresponding to $M'_0 = 0$) is drawn more heavily than the others. Also, it should be noted that the quantity A is negative on the response curves to the right of the curve for $M'_0 = 0$ and positive to the left of it, that is, the motion is in phase with the external moment or 180° out of phase with it, (strictly true only when damping is zero) according to whether the frequency is greater or less than the frequency of the free oscillation (natural frequency) as shown by the heavier line for that particular amplitude. The response curves in the nonlinear case may therefore be considered those for the linear case, twisting them to the right if $c'_3 > 0$ or to the left if $c'_3 < 0$.

The shape of the response curves in Fig. 10.1 shows some important physical phenomena. In Fig. 10.2*a* representative curves for $c'_3 > 0$ or $c'_3 < 0$ are shown. One can think of an experiment in which the ampli-

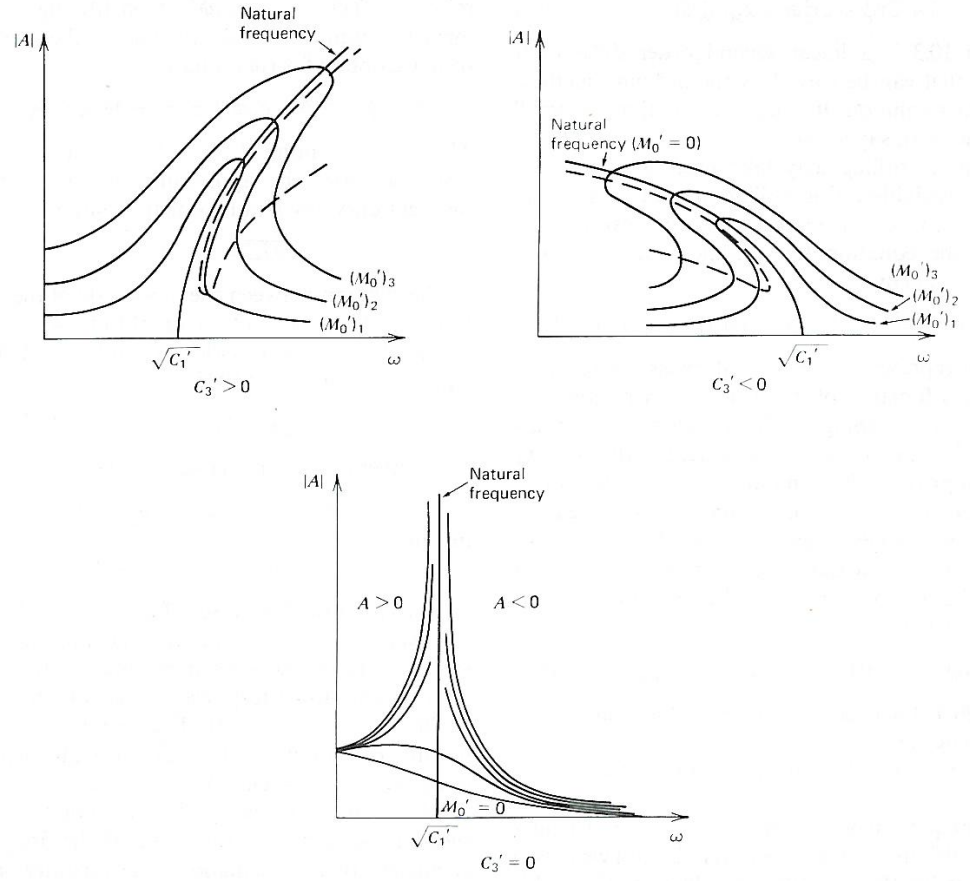


Figure 10.1 Response curves when damping is considered.

tude A of the resulting harmonic oscillation is noted. One considers first that $c_3' > 0$ and suppose that ω_e is rather large at the beginning of the experiment (i.e., one starts at point 1 on the curve). As ω_e is decreased, A slowly increases through point 2 until point 3 is reached. Since M_0' is taken to be constant, a further decrease in ω_e will require a jump from point 3 to point 4 with a corresponding increase in the amplitude A, after which A decreases with ω_e. If the experiment is conducted from the other end (i.e., starting at point 5 and increasing ω_e, the amplitude follows the 5–4–6 sequence of the curve, then jumps to point 2, and afterwards slowly decreases.

The situation is quite similar for $c_3' < 0$, although the jump in amplitude takes place in the reverse direction. It should be pointed out that, instead of conducting an experiment in which the moment amplitude M_0' is held constant, while the frequency

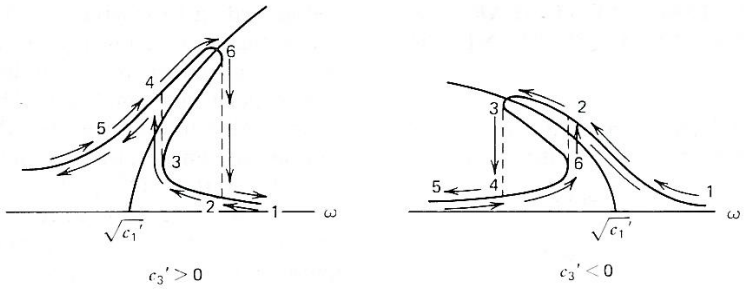


Figure 10.2*a* Jump or hysteresis phenomena.

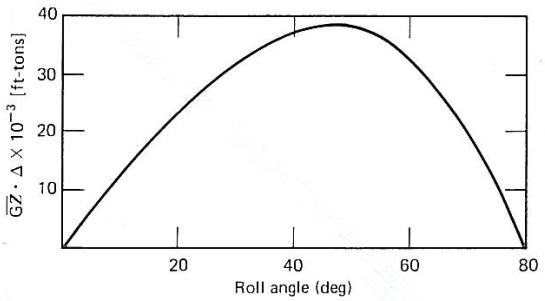


Figure 10.2*b* Stability curve: restoring moments for various angles of inclination.

ω_e is varied, one might vary M'_0 while keeping ω_e fixed. In fact, the latter experiment is easier to perform.

Analysis of (10.6a), the relation between A, ω_e, and M'_0 that results when damping is taken into account, leads to similar conclusions when the amplitude of the response is considered as a function of the moment amplitude M'_0 with ω_e held constant. These statements can easily be verified by referring either directly to (10.6a) or to the curves shown in Fig. 10.1 and considering the manner of variation of A with M'_0 along a line ω_e = constant. This analysis of the jump phenomenon shows that the rolling motions corresponding to points on the response curves between the vertical tangencies (in other words, the points lying in the regions bonded by the dotted curves of Fig. 10.1) are unstable.

The nonlinear differential equation as given by (10.6) can be solved by an iteration procedure, and the simplified solution of (10.6), without considering the damping term obtained by the first iteration, is expressed as follows [198]:

$$\phi = A\cos\omega_e t + \frac{c'_3 A^3}{32(c'_1 + \frac{3}{4}c'_3 A^2 - M'_0/A)}\cos 3\omega_e t \tag{10.6d}$$

where A is the rolling amplitude obtained from the linear equation (see Chapter 4) and

$$\omega_e^2 = c'_1 + \tfrac{3}{4}c'_3 A^2 - M'_0/\bar{A} \tag{10.6e}$$

However, by this procedure the frequency ω_e is

TABLE 10.1

```
 10 READ C1,C3,M0
 20 DEF FNG(X) = Cl + .75*C3*X*X - (MO/X)
 90 PRINT "AMP.", "FREQ."
100 FOR A = 1. TO 3.5 STEP 0.5
120 LET V = FNG(A)
140 IF V < 0 THEN 160
150 LET W = SQR(V)
155 PRINT A,W
160 LET A1 = - A
170 LET V1 = FNG(A1)
180 IF V1 < 0 THEN 210
190 LET W1 = SQR(V1)
200 PRINT A1, W1
210 NEXT A
380 DATA  .1638 , .0845 , .0257
400 END
READY
```

```
380 DATA .1638 , .0845 , .050
RUN
NL-RES.  21 FEB 76 11:06
```

```
380 DATA .1638 , .045 , 0
RUN
```

RUN	A AMP.	ω_e FREQ.	AMP.	FREQ.	AMP.	FREQ.
	0.5	0.358111	0.5	0.282212	0.5	0.423844
	− 0.5	0.48067	− 0.5	0.528814	− 0.5	0.423844
	1.	0.44886	1.	0.420922	1.	0.476629
	− 1.	0.502867	− 1.	0.526474	− 1.	0.476629
	1.5	0.537829	1.5	0.522552	1.5	0.552528
	− 1.5	0.568794	− 1.5	0.582861	− 1.5	0.553528
	2.	0.635964	2.	0.626339	2.	0.645988
	− 2.	0.655858	− 2.	0.665056	− 2.	0.645988
	2.5	0.741359	2.5	0.734775	2.5	0.748260
	− 2.5	0.755098	− 2.5	0.761508	− 2.5	0.748260
	3.	0.851826	3.	0.847059	3.	0.856840
	− 3.	0.861825	− 3.	0.866511	− 3.	0.856840
	3.5	0.965816	3.5	0.962215	3.5	0.969610
	− 3.5	0.973389	− 3.5	0.976949	− 3.5	0.969610

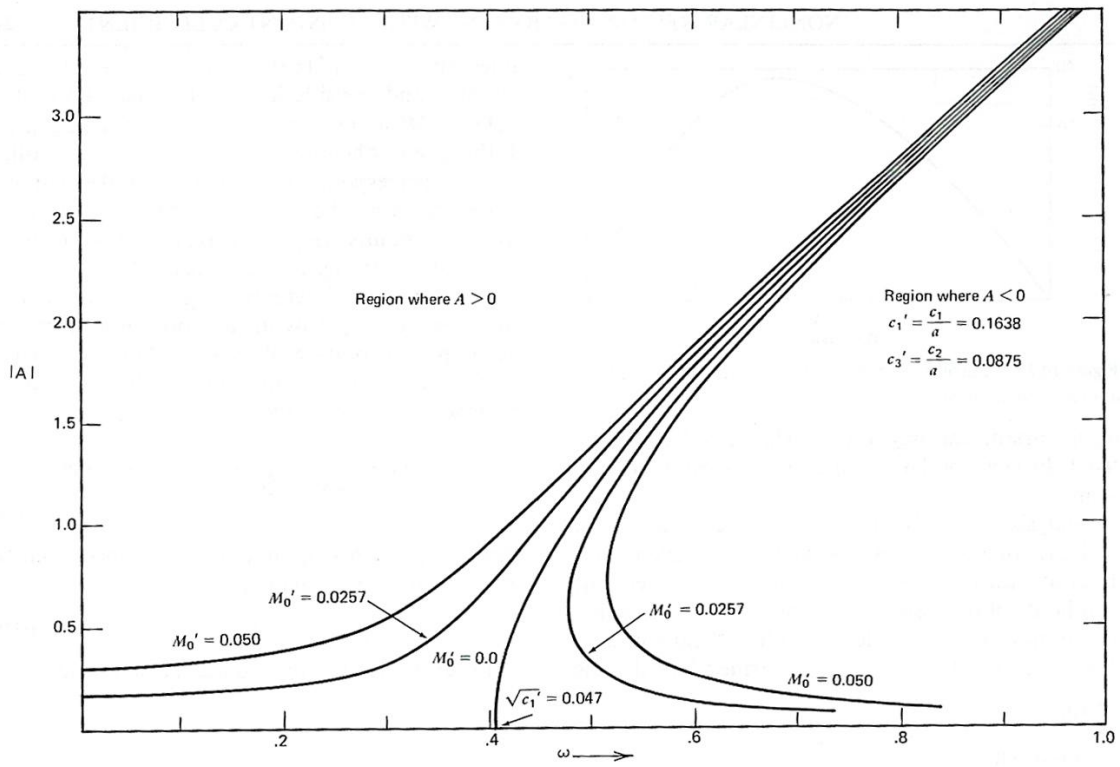


Figure 10.2*c* Amplitude response versus frequency.

```
10 READ A, B1, B2, W
40 LET S=4*B2*W/3*3.1416
50 LET V=B1/2
60 PRINT "AMPLITUDE"
65 PRINT "TIME", "NL-DAMP", "L-DAMP"
70 FOR T=0 TO 50
90 LET X=V* (A/(A*S+V)) *EXP (-V*T)/(1-S*(A/(A*S+V)) *EXP (-V*T))
100 LET X1=A*EXP(-V*T)
110 LET X2=57.3*X
120 LET X3=57.3*X1
125 PRINT T, X2, X3
130 NEXT T
140 DATA .2618, .0257, .337, .405
150 END
```

	AMPLITUDE	
TIME	NL-DAMP	L-DAMP
0	15.0011	15.0011
5	8.15594	14.0676
10	5.48633	13.1922
15	4.06684	12.3713
20	3.18742	11.6014
25	2.59016	10.8795
30	2.1588	10.2024
35	1.83323	9.56754
40	1.57926	8.97216

not decided upon in advance, but is calculated by (10.6*e*) after the value of A has been chosen.

Similarly, the first approximation of ϕ for the following undamped nonlinear equation:

$$\ddot{\phi} + c_1'\phi + c_3'\phi^5 = M_0' \cos \omega_e t$$

is given as

$$\phi(t) = A\cos\omega_e t + \frac{5c_3'A^5}{128\omega_e^2}\cos 3\omega_e t + \frac{c_3'A^5}{384\omega_e^2}\cos 5\omega_e t$$

where

$$\omega_e^2 = c_1' + \tfrac{5}{8}c_3'A^4 - \frac{M_0'}{A}$$

Example 10.1

A ship has a range of positive righting moment from 0 to 80° of roll. Also, $\Delta = 12{,}500$ tons and $\overline{GM} = 5.79$ ft. Calculate the nonlinear restoring moment coefficients.

Solution:

a. The transverse righting moment is the restoring moment for rolling motion.

b. The righting moment versus the roll angle is not linear but a polynomial function.

c. A rough approximation of the restoring moment curve is made, using the first two terms of expansion of a polynomial function, that is,

$$\text{Restoring moment} = \overline{GZ}\Delta = c_1\phi + c_3\phi^3$$

d. For small angles:

$$\overline{GZ} = \overline{GM}\sin\phi, \qquad \sin\phi \simeq \phi (\phi \text{ in radians})$$

or

$$\overline{GZ} = \overline{GM}\phi$$

e. The small angle restoring moment is linearly related to the angle of heel, that is,

$$\Delta\overline{GM}\phi = c_1\phi$$

$$c_1 = \Delta\overline{GM} = (12{,}500)(5.79) = 72{,}375 \text{ ft-tons.}$$

f. At 80° the restoring moment = 0, that is,

$$0 = c_1\phi + c_3\phi^3$$

or $$c_3 = -\frac{c_1}{\phi^2} = -\frac{72{,}375}{(1.39 \text{ rad})^2} = -37{,}124 \text{ ft-tons}$$

Thus

$$\text{Restoring moment} = 72{,}375\phi - 37{,}124\phi^3$$

where ϕ is in radians (see Fig. 10.2*b*).

ϕ [deg]	ϕ [rad]	Restoring Moment [ft-tons]
10	0.1745	12,430
15	0.2618	18,280
20	0.3491	23,670
25	0.4363	28,490
30	0.5236	32,570
35	0.6109	35,750
40	0.6981	37,890
45	0.7840	38,850
50	0.8727	38,490
55	0.960	36,635
60	1.047	33,170
65	1.134	27,940
70	1.22	20,700
75	1.304	11,470

Therefore

$$c_1' = \frac{c_1}{a} = 0.1638 \qquad \text{and} \qquad c_3' = \frac{c_3}{a} = 0.0845$$

where $a = \dfrac{\Delta_1}{g}k_{xx}^2 = 441850$

Let us now find the response curves for $M_0' = 0$, 0.0257, and 0.050.

A computer program in BASIC language, as well as the outputs, is given in Table 10.1: Figure 10.2*c* has been prepared with the output from this program. The effect of the nonlinear restoring moment is that the natural period $2\pi/\omega_\phi$ for the linear equation is not constant, but varies with the roll angle. Figure 10.3 *a* shows different nonlinear restoring moments as investigated by Vossers [225*a*], and in Fig. 10.3*b* T_ϕ'/T_ϕ is the ratio of the natural period for the nonlinear restoring moment to that for the linear restoring moment and $\bar{\phi}/\bar{\phi}_u$ is the nondimensional roll angle ratio (made dimensionless by dividing by $\bar{\phi}_u$, which is the heel angle at which the righting moment vanishes.

It should be noted that the forced rolling motion with nonlinear restoring moment may have frequencies lower than the encountering frequency ω_e. This is known as *subharmonic oscillation*. For motion with linear restoring moment, the frequencies of forced motion are always equal to the encountering frequencies.

What is important to note is that, because of the shape of the response curves (see Fig. 10.2*c*), it is possible to have several values of roll amplitude for a particular value of frequency.

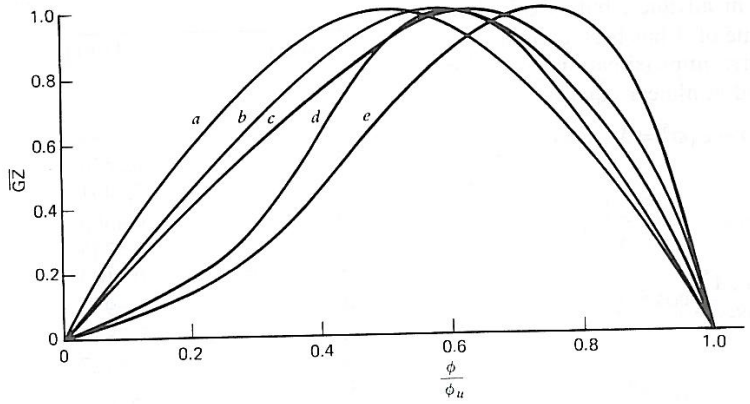


Figure 10.3*a* Curves of nonlinear restoring moment [225].

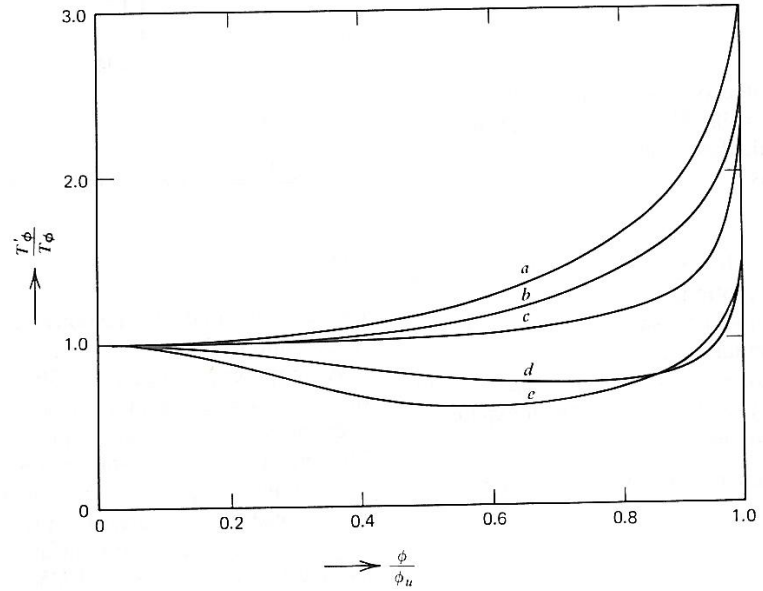


Figure 10.3*b* Roll period ratio for nonlinear rolling moment [225].

Experimental results and the phenomenon of "lurching" (a sudden increase in rolling amplitude) have shown that rolling at such a frequency is possible at many of these multivalued points. The designer must take care that his design will be safe under the most extreme values of roll for the frequency that the vessel will encounter.

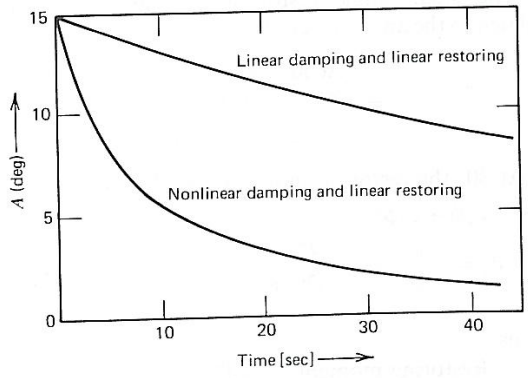


Figure 10.3*c* Amplitude versus time.

10.3 NONLINEAR DAMPING: LINEAR RESTORING MOMENT

Under the imposed conditions and a sinusoidal excitation the rolling equation is

$$a\ddot{\phi} + b_1\dot{\phi} + b_2\dot{\phi}|\dot{\phi}| + \Delta\overline{GM}\phi = M_0 \cos \omega_e t \quad (10.7)$$

For rolling in calm water, (10.7) can be written as

$$\ddot{\phi} + \omega_\phi^2 \phi + \mu f(\dot{\phi}) = 0$$

and the solution for such an equation by the method of first approximation is given [198]as

$$A = \frac{\frac{b_1}{2}\frac{\phi_a}{\phi_a S + (b_1/2)} e^{-[(b_1/2)t]}}{1 - S\frac{\phi_a}{\phi_a S + (b_1/2)} e^{-[(b_1/2)t]}}$$

where

$$A = \phi_a \text{ at } t = 0 \qquad \text{and} \qquad S = \frac{4b_2\omega_\phi}{3\pi}$$

It is easily seen that for $S = 0$ we have

$$A = \phi_a e^{-[(b_1/2)t]}$$

as should be for the case of linear damping. In other words, the quadratic damping term causes a rapid decay of amplitude because of the presence of the term

$$S\frac{\phi_a}{\phi_a S + (b_1/2)} e^{-[(b_1/2)t]}$$

in the denominator. An example has been worked out and the plots have been made in Fig. 10.3*c*.

It is possible to solve for b_1 and b_2 by use of an extinction test (see Section 4.5), and then graphical or numerical methods of approximation may be used to solve (10.7). However, through a process of linearization it has been found [132] that

$$b_1 = \frac{2K_1\Delta\overline{GM}}{\pi\omega_\phi}, \quad b_2 = \frac{3K_2\Delta\overline{GM}}{4\omega_\phi^2}$$

Analystical investigations [19] have shown that the moment of the frictional forces acting on a rolling cylinder completely submerged in a viscous fluid may be expressed by the equation

$$M(\dot{\phi}) = -b_1\dot{\phi} \qquad (10.7a)$$

where b_1 is the coefficient of proportionality, depending on the dimensions of the cylinder, the viscosity of the fluid, and the frequency or period of oscillation of the cylinder.

As the amplitude of the motions increases, the linear dependence of the resistance to the motions on the velocity is gradually replaced by a quadratic function:

$$M(\dot{\phi}) = -b_2\dot{\phi}^2 \qquad (10.7b)$$

Experiments involving ever-increasing amplitudes show that the damping moment could be the third and fourth powers of the angular velocity, for example,

$$M(\dot{\phi}) = -b_3\dot{\phi}^3 \qquad (10.7c)$$

But with intermediate amplitudes the most accurate expression may be given as

$$M(\dot{\phi}) = -b_1\dot{\phi} - b_2\dot{\phi}^2 \qquad (10.7d)$$

For small amplitudes and, hence, for small velocities of motions, the second term in (10.7d) is rather small in comparison with the first one. In other words, (10.7a) should be sufficiently accurate.

Let us take the case on p. 79 again, but consider the damping moment given in (10.7d). If the successive amplitudes of roll port and starboard are

$$15°, 11°, 8.5°, 6.5°, 5.0°, 4.1°, 3.3°, \text{and } 2.6°$$

we seek to approximate to the extinction equation.

In such a case the decrement of roll angle per swing is given as

$$-\frac{d\phi}{dn} = K_1\phi + K_2\phi^2$$

As in the example on p. 80, the following table is prepared for the determination of K_1 and K_2:

$\delta\phi$ [deg]	ϕ [deg]	ϕ_m [deg]
	15	
4		13
	11	
2.5		9.75
	8.5	
2		75
	6.5	
1.5		5.75
	5.0	
0.9		4.55
	4.1	
0.8		3.7
	3.3	
0.7		2.95
	2.6	

By using any two representative points of the curve of extinction the coefficients K_1 and K_2 can be determined. For example, let $\phi_m = 2.95°$ and $\phi_m = 13°$ be two representative points. Then

$$K_1\, 2.95 + K_2(2.95)^2 = 0.7$$

and

$$K_1\, 13 + K_2(13)^2 = 4$$

Solving, we get

$$K_1 = 0.216, \qquad K_2 = 0.00707$$

Therefore

$$-\frac{d\phi}{dn} = 0.216\phi + 0.00707\phi^2$$

For

$$\phi = 10^\circ \rightarrow -\frac{d\phi}{dn} = 2.86 \qquad \text{and}$$

$$\phi = 5^\circ \rightarrow -\frac{d\phi}{dn} = 1.26$$

The value of K_1 remains the same, independently of the value of ϕ, which may be given in either radians or degrees, but K_2 must have a value either in degrees or in radians corresponding to ϕ [11]. For example, K_2 for ϕ in radians must be multiplied by $\pi/180$ to give its equivalent.

The functional relationship concerning $\delta\phi = f(\phi)$ is known as the *law of decay* of the amplitudes. Let us consider the following cases:

a. With a linear damping law $M(\dot{\phi}) = -b_1\dot{\phi}$, the equation of motion becomes

$$\ddot{\phi} + 2\nu\dot{\phi} + \omega_\phi^2\phi = 0$$

The decay of amplitude for this case is

$$\delta\phi_{K+1} = \phi_K(1 - e^{-\nu T_\phi'/2}) = K_1\phi_K$$

where

$$K_1 = 1 - e^{-\nu T_\phi'/2}$$

and T_ϕ' is the period which is equal to the sum of two consecutive swings. Therefore a linear decay law corresponds to a linear damping law.

b. With quadratic damping, that is, $M(\dot{\phi}) = -b_2\dot{\phi}^2$, the equation of motion becomes

$$\ddot{\phi} + b_1'\dot{\phi}^2 + \omega_\phi^2\dot{\phi} = 0$$

and the decay of amplitude is then written as

$$\delta\phi_{K+1} = \tfrac{4}{3}b_2'\phi_K^2 = K_2\phi_K^2$$

where $K_2 = \frac{4}{3}b_2'$, that is, for quadratic damping there is quadratic decay.

c. With binomial damping, that is, $M(\dot{\phi}) = -b_1\dot{\phi} - b_2\dot{\phi}^2$, the equation of motion can be then written as

$$\ddot{\phi} + 2\nu\dot{\phi} + b_2'\dot{\phi}^2 + \omega_\phi^2\phi = 0$$

The decay of amplitude in this case is given by

$$\begin{aligned}\delta\phi_{K+1} &= \tfrac{2}{3}b_2'e^{-\nu T_\phi'/2}(1 + e^{-\nu T_\phi'/2})\phi_K^2 \\ &\quad + (1 - e^{-\nu T_\phi'/2})\phi_K \\ &= K_1\phi_K + K_3\phi_K^2\end{aligned}$$

where

$$K_1 \text{ (as before)} = 1 - e^{-\nu T_\phi'/2}$$

and

$$K_3 = \tfrac{2}{3}b_2'e^{-\nu T_\phi'/2}(1 + e^{-\nu T_\phi'/2})$$

Therefore, with binomial damping, binomial decay is to be expected. It is known that, if the damping to oscillation is small and is expressed [19] as

$$M(\dot{\phi}) = b_1\dot{\phi} + b_2\dot{\phi}^2 + b_3\dot{\phi}^3 + \dots$$

where b_1, b_2, ... are constants, the decay of the motion is considered as

$$\delta\phi = K_1\phi_m + K_2\phi_m^2 + K_3\phi_m^3 + \dots$$

where ϕ_m is the mean value of amplitude, and K_1, K_2, and K_3 are constants.

It is shown in Ref. 11 that for small motion (i.e., $\overline{GZ} = \overline{GM}\phi$) the decay in motion per period can be given as

$$\frac{d\phi}{dn} = K_1\phi_m + K_2\phi_m^2$$

where

$$K_1 = \frac{\pi b_1\omega_\phi}{2\Delta\overline{GM}} \qquad \text{or} \qquad b_1 = \frac{2\Delta K_1\overline{GM}}{\pi\omega_\phi}$$

and (10.8)

$$K_2 = \frac{4b_2\omega_\phi^2}{3\Delta\overline{GM}} \qquad \text{or} \qquad b_2 = \frac{3\Delta K_2\overline{GM}}{4\omega_\phi^2}$$

It has been found that b_1 and b_2 may be replaced by another constant, b, dependent only on ϕ, that is,

$$b = b_1 + b_2\phi \tag{10.9}$$

Combining (10.8) and (10.9), we have

$$b = \frac{\Delta\overline{GM}}{\pi\omega_\phi}(\delta_1 + \delta_2\phi) = \frac{\Delta\overline{GM}}{\pi\omega_\phi}\,\delta$$

Here $\delta = \delta_1 + \delta_2\phi$ is the linearized logarithmic decrement, where

$$\delta_1 = 2K_1 \qquad \text{and} \qquad \delta_2 = \frac{3\pi K_2}{4\omega_\phi}$$

Therefore, substituting these expressions back into (10.7), we get

$$I_{xx}'\ddot{\phi} + \left(\frac{\Delta\overline{GM}}{\pi\omega_\phi}\,\delta\right)\dot{\phi} + \Delta\overline{GM}\phi = M_0\cos\omega_e t \tag{10.10}$$

Equation 10.10 is linear and may be solved as in case 1 in Section 10.1. Although this solution is accurate for moderately large angles of roll, (10.7) is not adequate at extreme angles, and damping factors of the third or fourth degree (i.e., $\dot{\phi}^3$, $\dot{\phi}^4$) are needed to approximate the solution. Figure 10.4 is a curve that shows the decrease of amplitude per period for a large angle of roll. Note the increase in $-(d\phi/dn)$ for a larger angle, especially when the deck edge and bulwark are immersed. This curve may be calculated

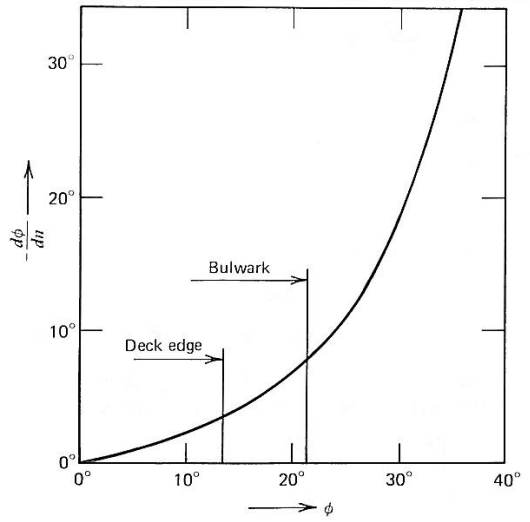


Figure 10.4 Roll decay per swing [124].

in a manner similar to that used for the former one. Here all four degrees of damping must be linearized by δ. With these solutions maximum angles of rolls can be approximated accurately and accounted for in static stability.

10.4 LINEAR DAMPING: LINEAR RESTORING MOMENT WITH TIME-DEPENDENT COEFFICIENT

In this last case to be examined, the equation of motion takes the form

$$I'_{xx}\ddot{\phi} + b\dot{\phi} + c(t)\phi = M_0 \cos \omega_e t \qquad (10.11)$$

It is a customary procedure to determine $c(t)$ in a model tank simply by heeling the model, holding it there, and measuring the restoring moment. For this condition

$c(t)\phi = M =$ heeling moment (for still water)

or

$c(t) = \Delta\overline{GM} =$ constant

Here $c(t)$ is a constant and linear theory may be applied. However, in a beam or following sea, as crests and troughs pass from bow to stern, pressure around the hull changes, and as a result of the heave caused by this pressure difference $\overline{GM}$ is no longer constant but varies. Dieudonne [48] conducted such a test and recorded $\delta\overline{KM}/\overline{KM}$ as a function of crest position along the length of the ship. Since it is because of the change in the metacenter position that $\overline{GM}$ varies, one may obtain the relative change in

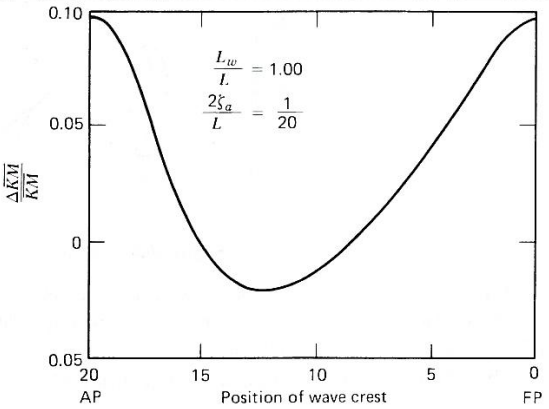


Figure 10.5 Relative change in metacentric height [48].

$\overline{GM}$ simply by multiplying $\delta\ \overline{KM}/\overline{KM}$ by $\overline{KM}/\overline{GM}$:

$$\frac{\delta\overline{KM}}{\overline{KM}} \times \frac{\overline{KM}}{\overline{GM}} = \frac{\delta\overline{KM}}{\overline{GM}} \simeq \frac{\delta\overline{GM}}{\overline{GM}}$$

Figure 10.5 shows some results reported in Ref. 48.

If one takes a simple case where the wave train is a sinusoid, $\Delta\overline{GM}/\overline{GM}$ varies with a sine curve. Thus (10.11) becomes

$$I'_{xx}\ddot{\phi} + b\dot{\phi} + \Delta\overline{GM}\left(1 + \frac{\Delta\overline{GM}}{\overline{GM}}\sin \omega_e t\right) = M_0 \sin \omega_e t \qquad (10.12)$$

In the head sea case, $M_0 = 0$ and (10.12) becomes a Mathieu equation:

$$I'_{xx}\ddot{\phi} + b\dot{\phi} + \Delta\overline{GM}\left(1 + \frac{\Delta\overline{GM}}{\overline{GM}}\sin \omega_e t\right) = 0 \qquad (10.13)$$

A characteristic of Mathieu's equation is that at certain values of frequency the solution goes to infinity in the undamped case. The value of the period for these frequencies is given by

$$T = \frac{T_\phi n}{2}, \qquad n = 1, 2, 3, \ldots$$

where T_ϕ is the natural period of the vessel. Because of the damping factor in (10.13) the solution is reduced to larger values of roll angles at the noted values of frequency. Grim [87] conducted a similar experiment in which a weight was rotated and the center of gravity systematically changed, thus simulating the change in $\overline{GM}$. These results verified the resonance roll angle predicted by Mathieu's equations. Figure 10.6 illustrates such results. Here, again, a designer should consider these peaks in roll angle in order to determine the stability of his vessel in waves.

We have thus examined the effects that nonlinearities produce in the equation of motion for rolling.

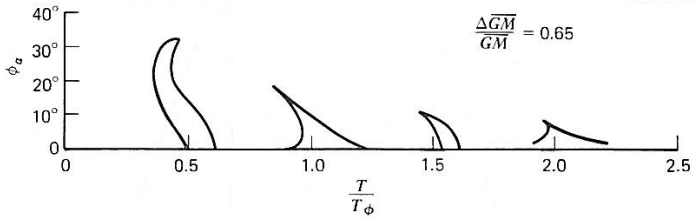


Figure 10.6 Roll angles at particular frequencies [87].

The important result of such examination is the determination of resonance points that are capable of capsizing the vessel. The final consideration will involve the effect of a sudden inclining moment.

10.5 SUDDEN INCLINING MOMENT AND CAPSIZING OF A VESSEL

When a moment is applied suddenly to the vessel, the latter takes on an acceleration $\ddot{\phi}$. For any angle of roll the resultant moment is $M_{Ke} - M_R$, where M_{Ke} = moment due to kinetic energy and M_R = restoring moment. Neglecting damping factors, it is found by summing moments that

$$I'_x\ddot{\phi} = M_{Ke}(\phi) - M_R(\phi) \tag{10.14}$$

Let us integrate (10.14) with respect to some ϕ. Recalling that $\ddot{\phi} = d\dot{\phi}/dt$ and $\dot{\phi}dt = d\phi$, we have

$$\int_0^\phi I'_{xx}\ddot{\phi}\,d\phi = \int_0^\phi [M_{Ke}(\phi) - M_R(\phi)]d\phi$$

or

$$I'_{xx}\int_0^\phi \frac{d\dot{\phi}}{dt}\dot{\phi}dt = \int_0^\phi [M_{Ke}(\phi) - M_R(\phi)]d\phi$$

or

$$I'_{xx}\int \dot{\phi}\,d\dot{\phi} = \int_0^\phi [M_{Ke}(\phi) - M_R(\phi)]d\phi$$

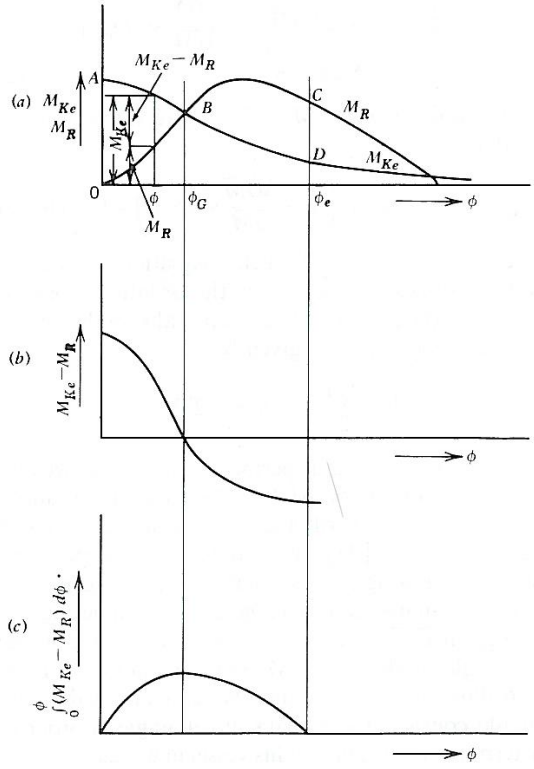


Figure 10.7 Righting and heeling moments as functions of angle of inclination.

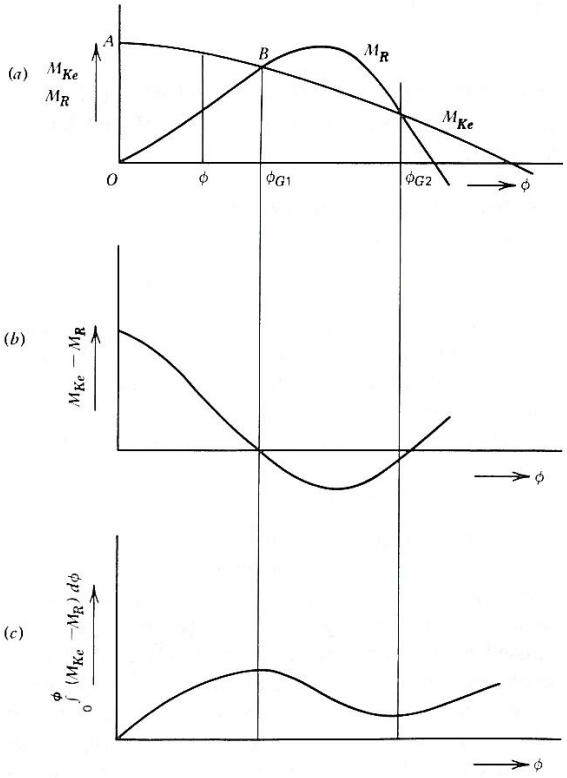


Figure 10.8 Righting and heeling moments.

or

$$I'_{xx}\frac{\dot{\phi}^2}{2} = \int_0^{\phi} [M_{Ke}(\phi) - M_R(\phi)]\,d\phi \qquad (10.15)$$

where $I_{xx}(\dot{\phi}^2/2)$ is the kinetic energy at the particular angle of inclination ϕ, and $\int_0^{\phi}[M_{Ke}(\phi) - M_R(\phi)]\,d\phi$ is the work done by the moments.

Figure 10.7 *a* shows a plot of the righting moment versus the roll angle ϕ [124]. The kinetic energy term thus increases until $\phi = \phi_G$, when the total moment becomes negative. At $\phi = \phi_G$, ϕ is maximum, but because of the momentum gained the vessel continues to roll, and the moment now becomes negative (righting moment). When the area *BCD* (Figure 10.7 *a*) is equal to *OBA*, all the kinetic energy is used up and $\phi = 0$. In Fig. 10.7*a* this occurs at $\phi = \phi_e$. The vessel will then oscillate back to $-\phi_e$ because of the potential energy of the system at ϕ_e. Because of the damping factors the vessel will roll to some angle $\phi < \phi_e$, and each corresponding oscillation will have smaller amplitude than the preceding one. The vessel will come to rest at $\phi = 0$.

The importance of this discussion is seen by examining another example. Figure 10.8*a* again shows the moments versus the roll angle. In this case, however, the moments are such that the area *BCD* can never equal *OAB*. The result can be seen in Fig. 10.8*c*, where we notice that the angular velocity $\dot{\phi}$ never reaches ϕ_{G2} and, in fact, increases after ϕ_{G2}. Hence

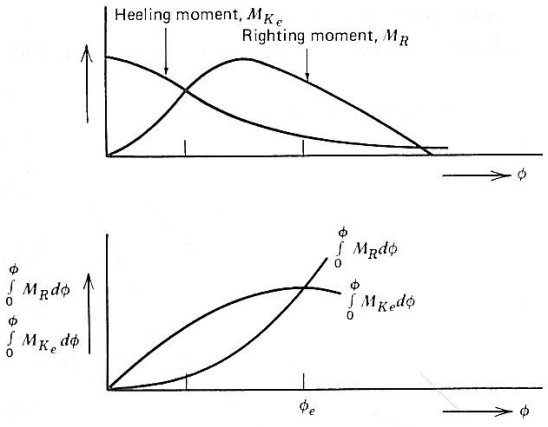


Figure 10.9 Righting moment versus angle of inclination.

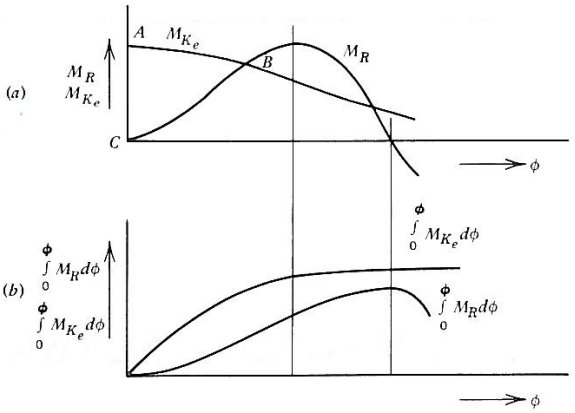


Figure 10.10 Righting and heeling moments versus angle of inclination.

the vessel never stops its roll but continues over and capsizes. This again is a most undesirable condition. To prevent this occurrence, one must investigate the problem beforehand. The first step is to plot both moments M_{Ke} (maximum expected) and M_R (Figs. 10.9*a* and 10.10*a*, respectively). The second is to integrate both moments and graph the results (Figs. 10.9*b* and 10.10*b*). From this second graph it is readily noticed that, if the two curves intersect, $\dot{\phi} = 0$ at that point, and the design is stable for that impact. The vessel will capsize, however, if the curves do not intersect.

The study of nonlinear motion of ships in waves has recently become of greater interest because of computer application. It is, however, of considerable importance for a designer to obtain approximate solutions to the nonlinear equations in order to determine maximum roll angles and points of resonance. The various categories of nonlinear response have been shown, and their solutions considered. A numerical solution for rolling motion with nonlinear damping as well as nonlinear restoring moment can easily be obtained by a computer using the fourth order Runge–Kutta method. However, nonlinear motions do not add by the superposition principle, as in the linear case; hence ordinarily, if a design will withstand the most severe roll angles of the individual nonlinear motions, the ship will not capsize. In any case, a safety factor is most desirable.

Chapter

Eleven

POWERING IN A SEAWAY

11.1 GENERAL

The capability to sustain speed in a seaway is one of the primary objectives in the design of a marine vehicle. Traditionally the power required to attain a certain speed in a seaway have been determined from the still water performance of the vessel after making an allowance of 15 to 30% for wind and waves. However, progress made in seakeeping, in both analytical methods and experimental techniques, makes it possible to determine the added resistance in a seaway with sufficient accuracy for design purposes. The added seaway resistance is often represented by either an addition of power to sustain the speed or a speed loss to maintaining the same amount of power as is used in calm water (see Fig. 11.1).

Loss of speed of a vessel in a seaway is not always due to the added resistance in waves; the speed is often voluntarily reduced in order to decrease the violent heaving and pitching motions of the vessel. The various factors responsible for loss of speed in a seaway, then, are as follows:

1. Added resistance due to wind on the vehicle's hull and superstructure.
2. Increase in resistance due to motions—heaving and pitching motions have a greater influence than rolling.
3. Added resistance due to wave reflection on the hull.
4. Increase in resistance due to drift angle or side slip or to yawing and swaying motions caused by both wind and waves, as well as rudder movement.
5. Loss in propulsive efficiency due to the fact that the conditions under which a propeller acts in a seaway are different from those in calm water. These conditions include the following:
   a. Augmentation of resistance, causing overloading of the propeller.
   b. Reduction in speed, causing a different intake velocity at the propeller disk.
   c. Motions causing changes in the intake velocity and the direction of the water flow at the propeller disk.
   d. Immersion and emergence of the propeller, causing air suction.
   e. Altered conditions affecting the characteristics of the propulsive machinery.
6. Voluntary reduction of engine power for the following reasons:
   a. Shipping of excessive green water.

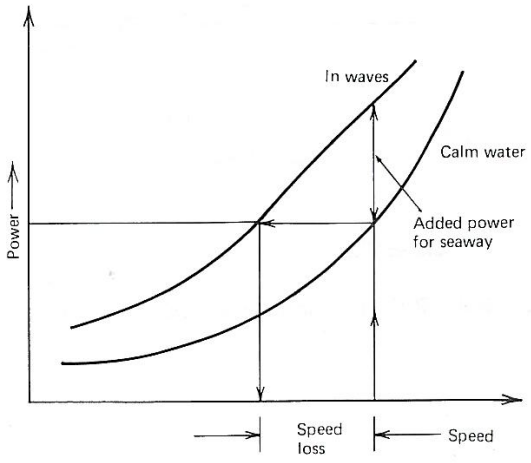


Figure 11.1 Speed loss or added power in a seaway.

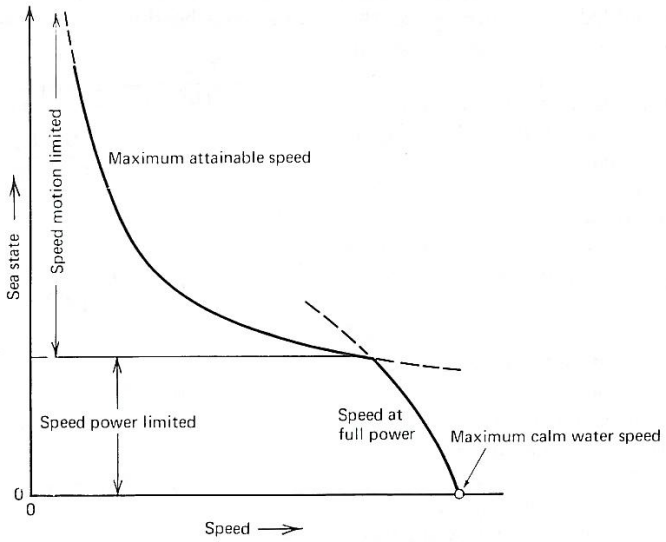


Figure 11.2 Voluntary and involuntary speed reduction.

b. Slamming.
c. Excessive acceleration that may cause cargo shifting and endanger the safety of passengers.
d. Propeller racing.
e. Difficulty in keeping on course.

Figure 11.2 illustrates the regions of voluntary and involuntary speed loss in a head sea as a function of sea state. The figure shows that a vessel's speed is power limited below a certain sea state, whereas above that sea state speed capability is motion limited. The Shipping of green water and slamming are the two most important factors that make it impossible for a ship to run at full speed in the region where speed is motion limited. In general, severe motions can be reduced only by a significant power reduction (i.e., voluntary speed loss), and added resistance is not important in such cases.

Added resistance in a seaway can be predicted either from model experiments or by analytical methods. In the case of model experiments, models are towed in regular or irregular waves, and the difference between the time-average resistance in waves and the resistance in still water for the same speed is taken to be the added resistance in a seaway. In most instances the model experiments are carried out for the head sea condition because of the fact that a vessel experiences maximum added resistance in head seas.

A number of analytical methods have been developed to predict mean added resistance in regular waves. The results of analytical methods, which are based on known ship motions, may not completely agree with experimental data; however, these methods provide adequate guidance for the designer in estimating the engine power needed in a seaway.

11.2 ADDED RESISTANCE IN REGULAR WAVES

The theoretical expression for the added resistance in regular waves as a function of pitching and heaving motions was first given by Havelock [99] as follows:

$$R_{AW} = -\frac{k}{2}(F_a z_a \sin \varepsilon_{zF} + M_a \theta_a \sin \varepsilon_{\theta M}) \quad (11.1)$$

where R_{AW} = added resistance in regular waves [lb]
k = wave number
F_a = amplitude of the exciting force for heaving [lb]
M_a = amplitude of the exciting moment for pitching [ft-lb]
z_a = amplitude of the heaving motion [ft]
θ_a = amplitude of the pitching motion [rad]
ε_{zF} = phase lag between the exciting force and the heaving motion [deg]
$\varepsilon_{\theta M}$ = phase lag between the exciting moment and the pitching motion [deg]

This equation can be considered only as the first

approximation to the added resistance, since the coupling of pitch and heave has been neglected. However, (11.1) shows that a phase relationship between motions and forcing functions is the primary cause of the added resistance. But a phase lag is possible if the damping terms are present in the equations of motion. The added resistance, therefore, can be explained as due to the energy loss associated with damping, and related to the work that must be done to keep the ship motions in a constant phase relationship with the forcing functions. This energy has to be supplied by the vessel, and it is dissipated by fluid friction and by radiation in the form of waves generated by the ship's motion. Thus the added resistance may also be determined by a knowledge of the energy content of these radiated waves.

An alternative method of finding the expression in (11.1) is to equalize the work done by the exciting force (and moment) and the work done by the force necessary to tow the ship through the given wave field. Joosen [112] derived an expression for the added resistance in waves with respect to the slenderness parameter B/L. Considering only the first order terms, he found a reasonable agreement with experiment, although this simplified treatment results in a speed-independent added resistance. In fact, use is made of the strip theory to determine the resistance force. The resulting expression is as follows:

$$R_{AW} = \frac{\omega_e^3}{2g}(b_z z_a^2 + b_\theta \theta_a^2) \tag{11.2}$$

which is equivalent to Havelock's expression, given in (11.1). In (11.2) ω_e is the encountering frequency [rad/sec], b_z is the heave damping coefficient [lb-sec/ft], and b_θ is the pitch damping coefficient [ft-lb-sec].

In (11.2) it is assumed that the vehicle is sharply pointed, that the wave and motion amplitudes are small in comparison with $L/2$, and that the frequency parameter $\omega_e^2/2g$ is of the order of unity. Furthermore, it is assumed that the speed parameter $F_n = V/\sqrt{gL}$ is of the order of $\sqrt{B/L}$. Equation 11.2 gives the expression for added resistance caused entirely by energy dissipation due to the motions. This equation shows that the added resistance can be considered as a result of the radiated waves.

The frequency of encounter is used in Ref. 112 when a ship's forward speed is considered. However, neither (11.1) nor (11.2) takes into account the relative vertical motion of the ship with respect to the water. The expression given in Ref 112 for added resistance in regular head waves is as follows:

$$\frac{R_{AW}}{\rho g \zeta_a^2 (B^2/L)} = \frac{L^2}{32B^2}\left[\left(\frac{z_a}{\zeta_a}\right)^2 P_1 + \frac{\pi^2 L^2}{L_w^2}\left(\frac{\theta_a L_w}{2\pi\zeta_a}\right)^2 P_3 - \frac{2\pi L}{L_w}\left(\frac{L_w\theta_a}{2\pi\zeta_a}\right)\left(\frac{z_a}{\zeta_a}\right) P_2 \cos\varepsilon\right] \tag{11.3}$$

where

$$P_1 = \frac{\omega_e^3}{\rho g^2}\frac{2}{L}\rho\nabla\sqrt{\frac{g}{L}}B_{33}$$

$$P_2 = \frac{\omega_e^3}{\rho g^2}\frac{2}{L}\rho\nabla\sqrt{\frac{g}{L}}(B_{35} + B_{53})$$

$$P_3 = \frac{\omega_e^3}{\rho g^2}\frac{2}{L}\rho\nabla\sqrt{\frac{g}{L}}4B_{55}$$

and

$$\varepsilon = |\varepsilon_z - \varepsilon_\theta|$$

Heave displacement, $z = z_a \cos\omega_e t$

and

Pitch displacement, $\theta = \theta_a \cos(\omega_e t + \varepsilon)$

The damping coefficients used in (11.3) are given as

$$B_{33} = \frac{1}{\omega_e \nabla}\sqrt{\frac{g}{L}}\int b_n d\xi$$

$$B_{35} + B_{53} = \frac{2}{\omega_e \nabla}\sqrt{\frac{g}{L}}\int \xi b_n d\xi$$

and

$$B_{55} = \frac{1}{\omega_e \nabla}\sqrt{\frac{g}{L}}\int \xi^2 b_n d\xi$$

where

ω_e = frequency of encounter [rad/sec]
∇ = volume of displacement [ft^3]
b_n = sectional damping coefficient
$\xi(= 2x/L)$ = nondimensional longitudinal coordinate [ft]

Thus one can see from (11.2) that the added resistance can be determined from the damping coefficients (which are frequency dependent) as well as from knowledge of the heaving and pitching motions and their phase relationships. All the quantities necessary for the prediction of added resistance by means of (11.3) can be obtained either from the computation of ship motions using the strip theory, treated in Chapter 9, or by experimentation. In other words, the added resistance may be computed by means of

(11.3) from any of the three different inputs, namely:

1. Both motion amplitudes and damping coefficients determined by the strip theory.
2. Motions determined by experimentation but B coefficients computed by the strip theory.
3. Both motions and B coefficients obtained experimentally.

The added resistance computed by (11.3) agrees satisfactorily with that obtained experimentally, especially at higher speeds. It should be pointed out that (11.3) is valid primarily for the nondimensional frequency parameter $\omega_e^2 B/2g \approx 1.0$. Any variation from a frequency parameter of unity may result in a discrepancy between computed and measured added resistance. Therefore the discrepancies found at low speeds and long waves may be due, to some extent, to this particular restriction on the theory. The experimental error may also be of considerable magnitude at low speeds. Another fact to be kept in mind is that motions are nonlinear in high waves, and in such a case lower values for the nondimensional added resistance may be expected.

Example 11.1

Given:

$L = 4.8$ ft
$B = 0.648$ ft
$V = 1.415$ knots (i.e., 2.394 ft/sec)
$\nabla = 0.7106$ ft^3
$L_w = L$(i.e., $\omega_w = 6.49$ rad/sec in deep water)
$\zeta_a = 0.05$ ft
$z_a = 0.0307$ ft
$\theta_a = 0.0404$ rad

$\int b_n(\xi)\,d\xi = 3.171$ lb-sec/ft

$\int b_n(\xi)\xi\,d\xi = 0.045$ lb-sec

$\int b_n(\xi)\xi^2\,d\xi = 8.815$ lb-sec-ft

$\cos\varepsilon = 0.0122$

$\rho = 1.9905$ lb-sec^2/ft for salt water at 59°F

Determine the added resistance of the model due to motions in a regular seaway.

Solution:

The frequency of encounter is

$$\omega_e = \omega_w - \frac{\omega_w^2}{g} V\cos\mu = 6.49 - \frac{6.49^2}{32.2}2.394(-1)$$
$$= 9.62 \text{ rad/sec}$$

From (11.3) the B coefficients are as follows:

$$B_{33} = \frac{1}{\omega_e\nabla}\sqrt{\frac{g}{L}}\int b_n\,d\xi = \frac{1}{9.62(0.7106)} \times \sqrt{\frac{32.2}{4.8}}(3.171)$$
$$= 1.201$$

$$B_{35} + B_{53} = \frac{2}{\omega_e\nabla}\sqrt{\frac{g}{L}}\int \xi b_n\,d\xi = \frac{2}{9.62(0.7106)} \times \sqrt{\frac{32.2}{4.8}}(0.045)$$
$$= 0.0341$$

and

$$B_{55} = \frac{1}{\omega_e\nabla}\sqrt{\frac{g}{L}}\int \xi^2 b_n\,d\xi = \frac{1}{9.62(0.7106)} \times \sqrt{\frac{32.2}{4.8}}(8.815)$$
$$= 3.340$$

Let

$$K_1 = \frac{\omega_e^3}{\rho g^2}\frac{2}{L}\rho\nabla\sqrt{\frac{g}{L}} = \frac{(9.62)^3}{1.9905(32.2)^2}\left(\frac{2}{4.8}\right) \times (1.9905)(0.716)(2.59)$$
$$= 0.6581$$

Then

$$P_1 = K_1(B_{33}) = 0.790$$
$$P_2 = K_1(B_{35} + B_{53}) = 0.0224$$
$$P_3 = K_1(B_{55}) = 8.792$$

Now, let

$$A = \left(\frac{z_a}{\zeta_a}\right)^2 P_1 = 0.2978$$

$$B = \frac{\pi^2 L^2}{L_w^2}\left(\frac{\theta_a L_w}{2\pi\zeta_a}\right)^2 P_3 = 33.096$$

$$C = \frac{2\pi L}{L_w}\left(\frac{L_w\theta_a}{2\pi\zeta_a}\right)\left(\frac{z_a}{\zeta_a}\right)P_2\cos\varepsilon = 0.000651$$

Finally, (11.3) yields

$$\frac{R_{AW}}{0.0140} = \frac{23.04}{13.437}(0.2978 + 33.096 - 0.000651)$$

from which the added resistance is

$$R_{AW} = 0.802 \text{ lb}$$

On the basis of analytical investigations, the following conclusions have been reached regarding the added resistance:

a. The added resistance in a seaway is proportional to the square of the wave height.

b. The added resistance is independent of the still water resistance.

c. The added resistance is a function of the motions (pitch and heave) and their phase relationships with the waves. The maximum added resistance is to be expected when there is a resonance of pitching and heaving. In other words, a marine vehicle with poor motion performance will also have a large added resistance.

d. Since added resistance is considered to be a result of the radiated waves, as mentioned earlier, it can be assumed that energy spent because of viscous damping is insignificant, and that added resistance is a nonviscous phenomenon and is due mainly to inertial and wave effects. Hence the added resistance obeys Froude's law; that is, the added resistance of a full-scale vessel can be predicted by multiplying the added resistance of the model by the cube of the scale factor.

11.3 EXPERIMENTS IN REGULAR WAVES

As mentioned earlier, the added resistance in a seaway may be obtained either analytically or by model experiments carried out in both regular and irregular waves.

Two different methods are used in the determination of added resistance in regular waves:

1. The constant thrust methods,
2. The constant velocity method.

In the first method a constant weight is applied to a pulley system to tow the model, which is not allowed to roll, yaw, or sway, but is free to pitch, heave, and surge. The system is called a *gravity towing system.* The average speed is then recorded. This enables one to determine the loss of speed associated with a constant towing force.

In the constant velocity method the model is not allowed to have any speed variation. As in the gravity towing system, the model is allowed only to heave and pitch. The time average of the resistance of the model is recorded. Since the added resistance is taken to be the difference between the calm water resistance and the resistance in waves at the same (average) speed, this method is more suitable for the prediction of added resistance. To use the linear superposition technique to predict added resistance in an irregular seaway, a knowledge of the response amplitude operator is necessary; this is obtained from the constant velocity method.

The added resistance has been found to be proportional to the square of the wave height; thus the nondimensional added resistance is expressed as

$$\sigma_{AW} = \frac{R_{AW}}{\rho g \zeta_a^2 (B^2/L)} \tag{11.4}$$

where R_{AW} = added resistance in waves [lb]
ρ = density of water [lb-sec^2/ft^4]
g = acceleration due to gravity [ft/sec^2]
B = beam [ft]
L = length [ft]
ζ_a = wave amplitude [ft]

The added resistance is due mainly to nonviscous effects; thus added resistance experiments can be carried out with small models, since no scale effect has to be considered. It should be emphasized, however, that the model experiments should be conducted with utmost care, since the added resistance is only a small fraction of the total resistance measurement in a seaway.

From theoretical studies for regular waves one can arrive at the following conclusions:

1. The pitching motion is the most important factor in resistance augmentation at low speed, but the heaving motion has a larger effect at higher speeds.
2. The reflection of waves on a ship's side is comparatively small.
3. The maximum resistance augmentation takes place at a speed slightly higher than that for pitch synchronization.

A nondimensional representation of the added resistance is presented in Fig. 11.3*a*, which shows that the added resistance increases steadily with increase in speed (as represented by the Froude number). In that figure, the dimensionless encounter frequency is

$$\omega_e \sqrt{\frac{L}{g}}$$

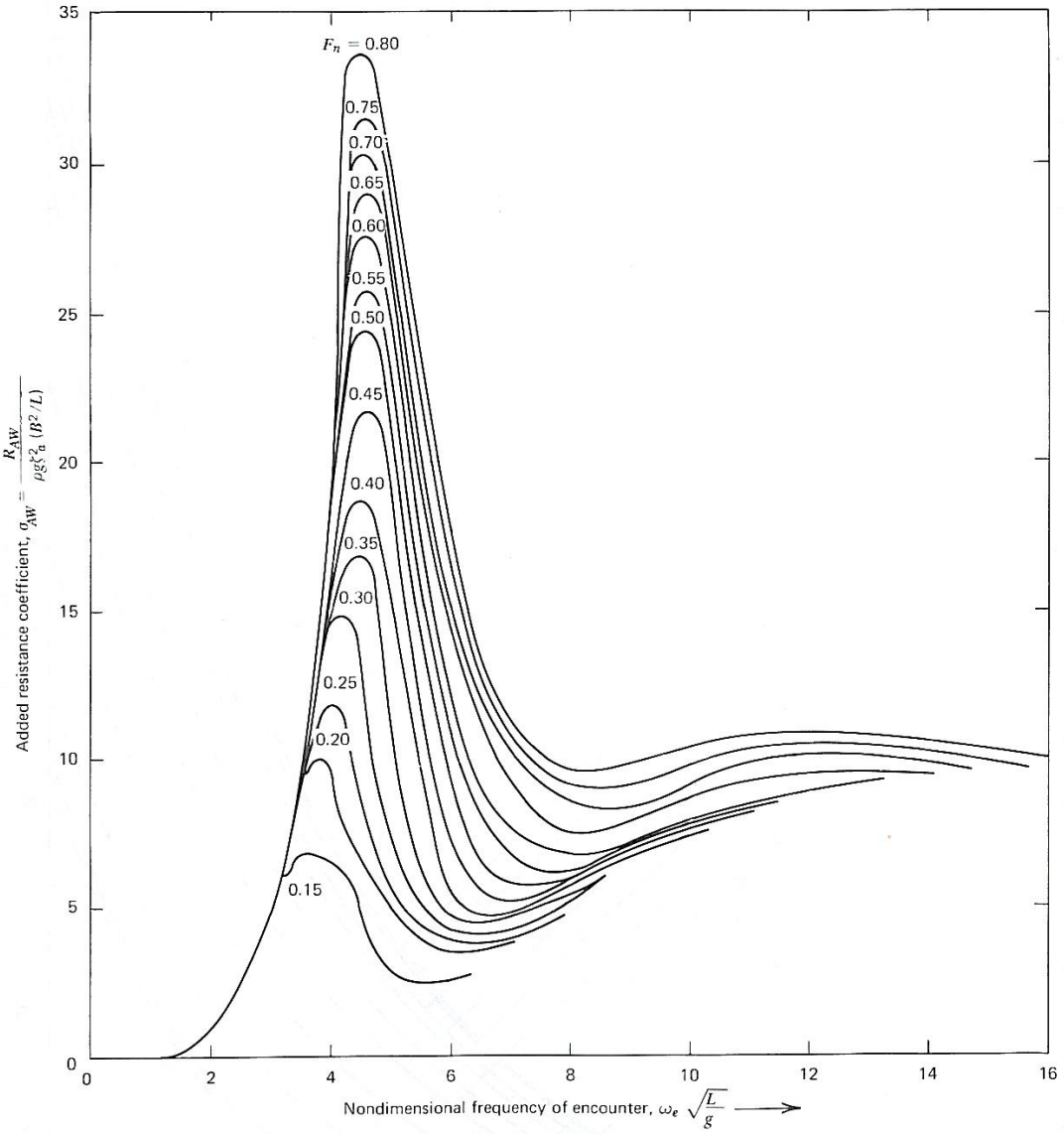


Figure 11.3*a* Coefficient of added resistance [199].

and the added resistance coefficient is defined in (11.4). Figure 11.3*c* shows typical speed losses in head seas from the calculation of effective horsepower as shown in Fig. 11.3*b* for various significant wave heights.

From the comparison between theoretical calculations and model experiments it appears that the theoretical results overestimate the added resistance for very low ship speeds and long wavelengths (rough seas) and underestimate it for short wavelengths (or mild seaways).

11.4 ADDED RESISTANCE IN AN IRREGULAR SEAWAY

The added resistance of a ship in an irregular seaway can be obtained in the same manner as in the case of regular ship motions, namely, by using the linear superposition technique as follows:

1. The wave spectrum is determined for a particular sea condition or can be assumed for a given wind condition by using ITTC standard formulation.

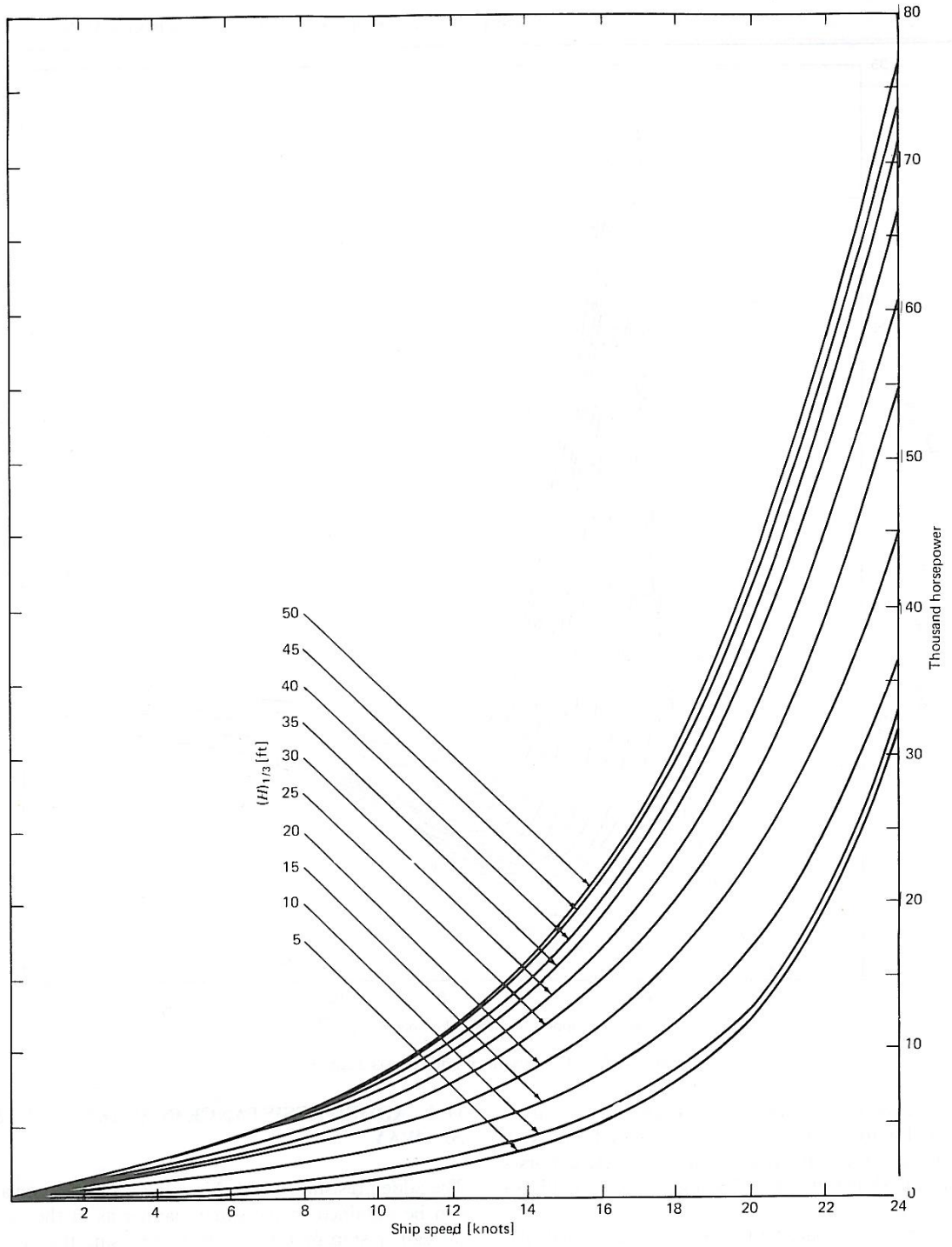


Figure 11.3*b* Typical effective horsepower in head seas.

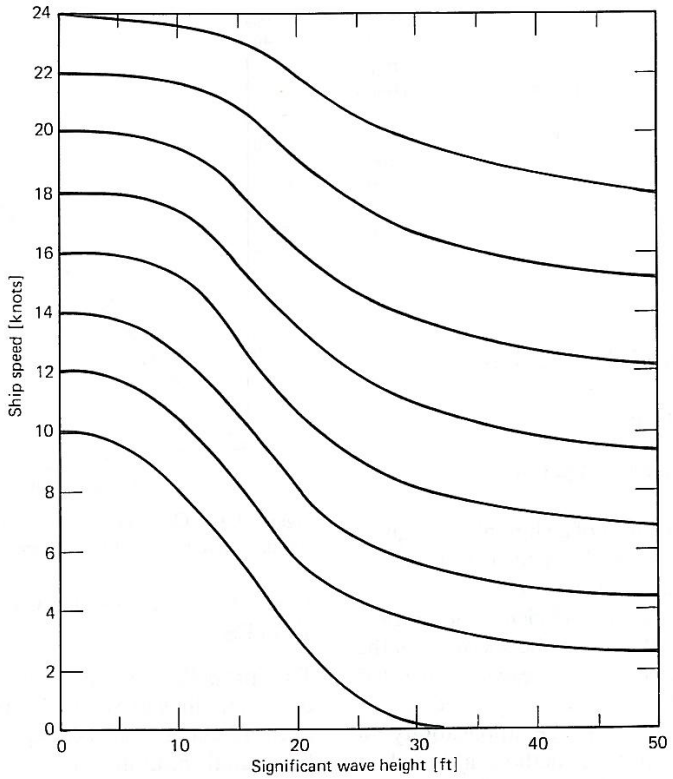


Figure 11.3c Typical speed loss in head seas.

2. The response amplitude operator (RAO) is obtained analytically or by model tests in regular waves. Note that the linear superposition technique requires that the added resistance in waves be proportional to the square of the wave amplitude, that is,

$$R_{AW} \propto \zeta_a^2 \quad \text{or} \quad \sqrt{R_{AW}} \propto \zeta_a$$

In other words, if this is true, all the curves for the square root of the added resistance of a given model tested at a constant wavelength but at various wave amplitudes can be reduced to a single value when divided by wave amplitude.

3. Then for any encountering frequency the ordinate of the response spectrum is obtained as the product of the ordinate of the encountering sea spectrum and that of the RAO for the same encountering frequency. Thus the mean added resistance is

$$R_{AW} = 2\int_0^\infty S_\zeta(\omega_e)\frac{R_{AW}}{\zeta_a^2}(\omega_e)\,d\omega_e \qquad (11.5)$$

Now, the statistical mean (or rms) of the added resistance is twice the area of the response spectrum:

$$\text{Mean } R_{AW} = 2m_0 \qquad (11.6)$$

where m_0 is the area under the response spectrum for added resistance.

If the RAO is made out of R_{AW}/h_w^2 to a base ω_e, the mean added resistance is obtained by multiplying the area under the corresponding response spectrum by 8, since

$$\frac{R_{AW}}{\zeta_a^2} = 4\frac{R_{AW}}{h_w^2} \quad \text{or} \quad \text{Mean}\sqrt{\frac{R_{AW}}{2}} = \sqrt{2m_0}$$

from which

$$\frac{R_{AW}}{4} = 2m_0 \quad \text{or} \quad R_{AW} = 8m_0$$

Example 11.2

The data in Table 11.1 are available from model experiments.

Find the mean added resistance for the irregular seaway considered.

Solution:

The ordinates of the response spectrum at various frequencies of encounter are calculated as shown in Table 11.2

TABLE 11.1

ω_e [sec^{-1}]	ζ_a [ft]	$S_\zeta(\omega_e)$ [ft^2-sec]	R_{AW} [tons]
0.2	4	0	0
0.6	5	19	100
1.0	5	20	400
1.4	5	7.5	225
1.8	2	3.5	0

From (11.6), then,

$$m_0 = \tfrac{1}{3}(0.4)(1214) = 162 \text{ tons}$$

and the mean added resistance is

$$2m_0 = 2(162) = 324 \text{ tons}$$

The mean added resistance of a ship in an irregular seaway can also be directly obtained from irregular wave tests, where the difference between the average resistance measured over a sufficiently long time and the calm water resistance for the speed gives the average added resistance for the seaway generated in the experimental basin. These experiments are conducted in order to check the applicability of the prediction by the spectral method, although it has been proved that, as in the case of ship motions, the spectral method is equally suitable for the prediction of added resistance in an irregular seaway (see Fig. 11.4). Even if the predicted values for added resistance are not as good as those for other motion characteristics, they can be quite useful for design considerations, since a reasonably good estimate of the resistance of a ship can be made for moderate seaways and for speeds less than the design speed. On the other hand, for severe seas the ship is not power-limited, voluntary power reduction is necessary, and determination of added resistance is not necessarily important.

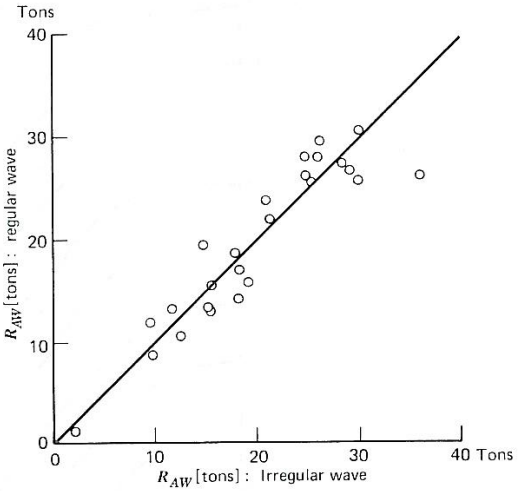


Figure 11.4 Comparison of added resistance predicted from regular wave tests and that measured in irregular waves [158].

11.5 PROPELLER OPEN WATER TESTS IN WAVES

The propeller action is greatly influenced in its operation in waves by the vertical motion due to both pitching and heaving and, in addition, the horizontal motion due to both surging and the orbital motion of the waves. Therefore a change in open water propeller characteristics is expected when a ship is in a seaway. Since the forces and moments are of a fluctuating nature, the thrust and torque of a propeller are given by the steady values only when averaged over one period. Figure 11.5 shows the experimental results for thrust increase from regular wave tests, where T_0 is the thrust in still water and T_m is the mean increase in thrust.

For resistance tests in waves a model is towed by the gravity tow system at constant thrust. In self-propulsion tests the thrust and the torque, as well as the revolutions of the propeller per unit time, do not

TABLE 11.2

ω_e [rad-sec]	ζ_a [ft]	$S_\zeta(\omega_e)$ [ft^2-sec]	R_{AW} [tons]	$\frac{R_{AW}}{\zeta_a^2}$ [tons/ft^2]	$S_\zeta(\omega_e) \times \frac{R_{AW}}{\zeta_a^2}$ [ton-sec]	Simpson's Multiplier	Product
0.2	4	0	0	0	0	1	0
0.6	5	19	100	4	76	4	304
1.0	5	20	400	16	320	2	640
1.4	5	7.5	225	9	67.5	4	270
1.8	2	3.5	0	0	0	1	0
						SUM	1214

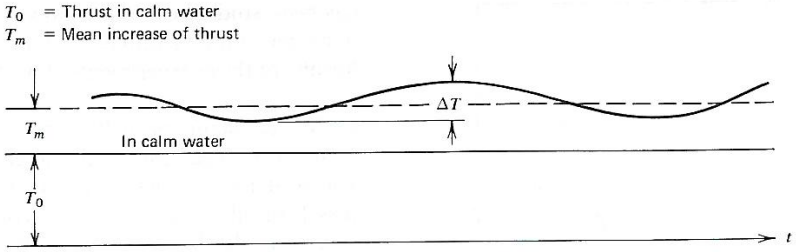


Figure 11.5 Time history of thrust in regular waves.

remain constant, but fluctuate with the model motion and with the change in water velocity at the stern due to the orbital motion of the waves.

In the case of full-scale vessels, fluctuations of thrust, torque, and revolutions occur for the same reasons as it is with the model. Hence model tests are performed to find the correlation between the resistance and self-propulsion tests.

Since the RAO is obtained from regular wave tests, the effects of wave amplitude on powering characteristics in regular waves are discussed here. The thrust increase due to the seaway is calculated by substracting the thrust of the model in still water at a particular speed from the thrust of the model at the same speed in a given seaway. Sample results of such calculations are shown in Fig. 11.6, where τ_h is the nondimensionalized form of the mean thrust increase in waves, defined as

$$\tau_h = \frac{T_{AW}}{\rho g \zeta_a^2 (B^2/L)}$$

From open water tests in calm water it is known that for a particular speed the thrust and torque are linearly proportional to each other. Therefore the torque increase due to seaway can be calculated as is done in the case of the thrust increase. It follows that for the prediction of the torque in a seaway the torque increase should be added to the toque for the calm water condition.

The effect of wave height on thrust (or torque)

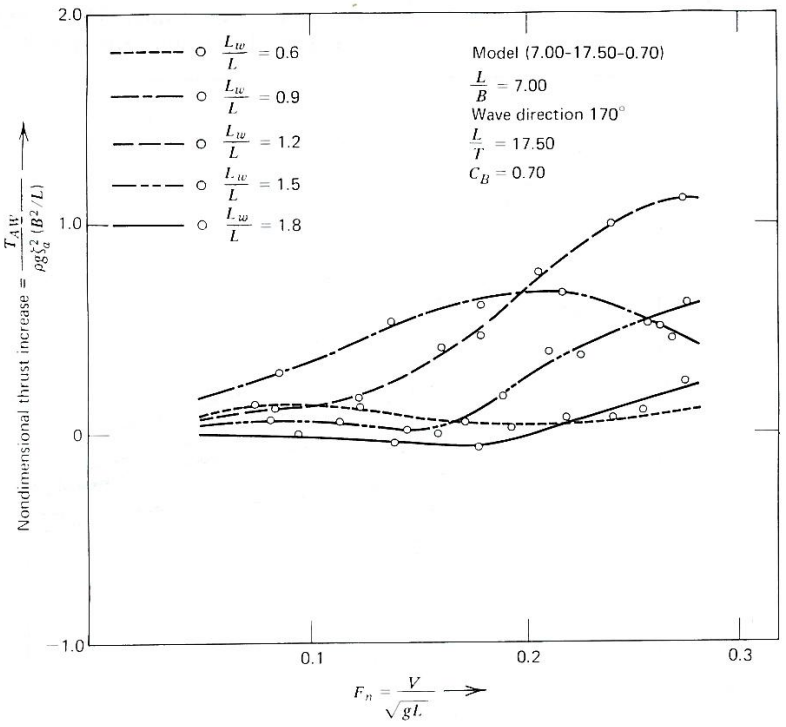


Figure 11.6 Thrust increase in regular waves [227].

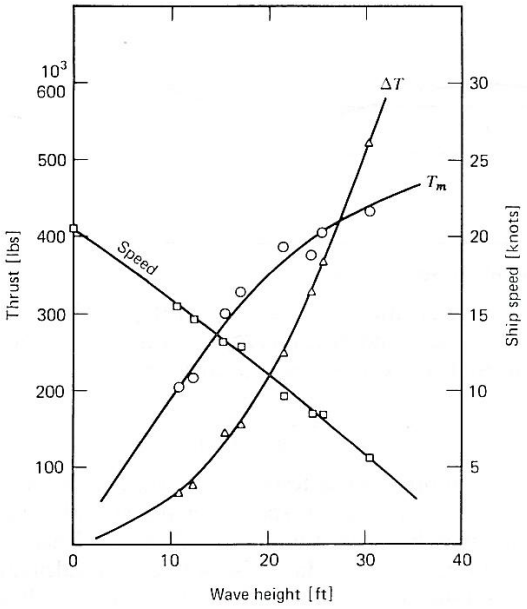


Figure 11.7 Thrust versus wave height in regular waves for constant propeller rpm (wavelength/ship length = 1, rpm = 109) [168].

has been studied experimentally for constant revolutions per minute (rpm) as well as for constant speed. Results of these experiments show the following:

1. For constant propeller rpm in regular waves, vessel speed decreases with increase in wave height. The mean increase in thrust and torque for the reduced vessel speed is linearly proportional to the wave height, while the variation in thrust and torque is proportional to the square of the wave height. This can be seen in Fig. 11.7.
2. For constant vessel speed in regular waves, the propeller rpm is increased with increase in wave height. Both the mean increase and the variation in thrust and torque for the increased rpm are proportional to the square of the wave height.
3. For constant wave height in regular waves, the amplitude of torque fluctuation is greatest for long waves. This amplitude for a given wavelength decreases as speed increases, as shown in Fig. 11.8.

11.6 SELF-PROPULSION FACTORS

The average values of the open water propeller characteristics may be considered to be the same as those in calm water. Therefore the effective wake fraction, the relative rotative efficiency, and so on

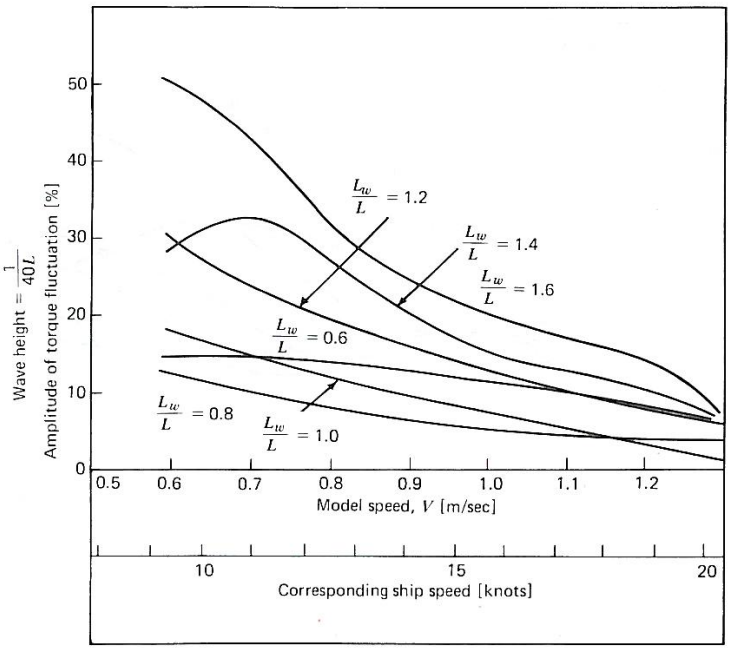


Figure 11.8 Fluctuation of torque in regular waves [77].

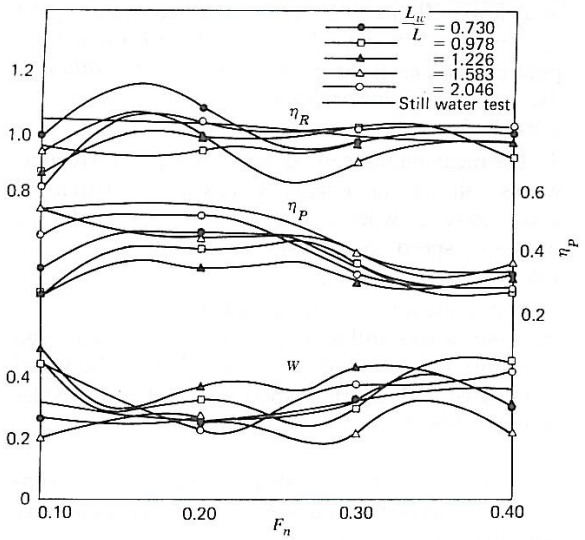


Figure 11.9 Self-propulsion factors in regular waves [114].

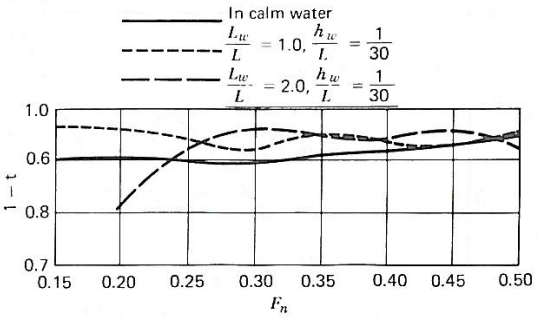


Figure 11.10 Thrust deduction factor in regular waves [114].

are obtained from the thrust, torque, number of revolutions, and mean advance speed in waves, using the open water characteristics of the propeller in calm water. A typical example of self-propulsion factors in waves is given in Fig. 11.9.

The following observations have been made regarding the propeller characteristics:

1. The relative rotative efficiency may be considered to be very close to unity in some cases or is identical with the values in calm water.
2. The wake fraction value is considered to be the same as that in calm water, except in the low speed range.
3. The propeller efficiency obtained from self-propulsion tests in waves is a little lower than that in calm water because of the change in propeller loading due to the augmentation of resistance.
4. From the results in Fig. 11.10, the thrust deduction factor seems to be slightly higher in waves than in still water, but the difference is not significant.

In Fig. 11.10 the experimental results for the thrust deduction factor in waves obtained from resistance tests and self-propulsion tests of a destroyer are presented.

It is therefore concluded that the self-propulsion factors are the same in waves as in calm water. This conclusion simplifies the analysis of propulsive performance in waves; and if the open water propeller characteristics in still water and the thrust increase coefficient curves are known, the required power and the number of revolutions in any given regular waves can be easily estimated.

11.7 THRUST AND TORQUE IN IRREGULAR WAVES

Thrust and torque in irregular waves fluctuate randomly for either constant speed or constant rpm. The thrust (or torque) is considered to be the sum of two random variables. With reference to Fig. 11.11*a* these variables are the mean increase in thrust, T_m, and the variation of thrust depending on the frequency of encounter ΔT. In regular waves both T_m and ΔT have constant values, and their magnitudes are dependent on wave amplitude and ship speed, whereas in irregular waves both T_m and ΔT fluctuate randomly.

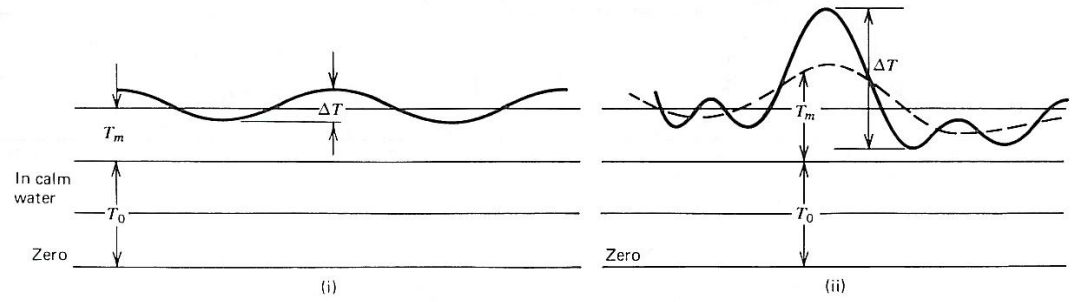


Figure 11.11*a* Time history of thrust in (i) regular and (ii) irregular waves.

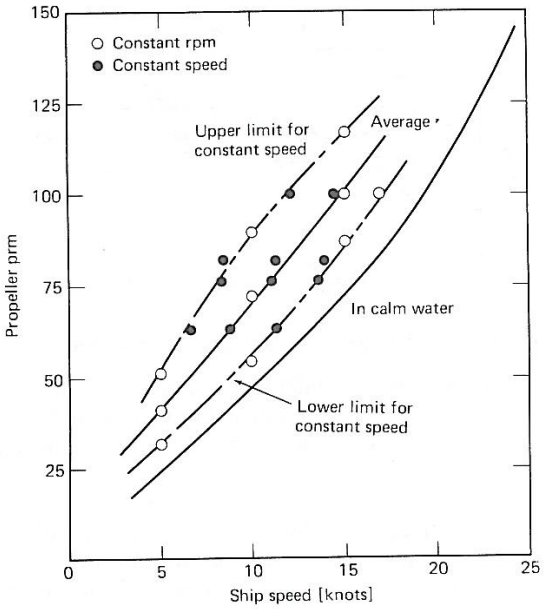


Figure 11.11*b* Ship speed and propeller rpm in irregular waves (significant wave height = 27.7 ft) [168].

The following remarks can be made about speed, thrust, torque, and rpm for irregular seaway conditions [168]:

1. Ship speed variation for constant propeller rpm, and rpm variation for constant ship speed in irregular waves, obey the normal (Gaussian) probability distribution law.
2. The average propeller rpm, as well as the upper and lower limits, obtained from constant speed tests in irregular waves agrees well with the corresponding values from constant rpm tests, although the upper and lower limit lines are reversed. See Fig. 11.11*b*.
3. The mean increase in thrust and torque in irregular waves follows the normal (Gaussian) distribution, irrespective of whether the vessel is operated with constant speed or constant propeller rpm. See Fig. 11.12*a*.
4. The variations in thrust ΔT and torque ΔQ in irregular waves follow approximately the Rayleigh distribution, again irrespective of whether the vessel is operated with constant speed or constant propeller rpm. See Fig. 11.12*b*.

Note: The probability distributions given in conclusions 3 and 4 hold for all sea states, vehicle speeds, and propeller revolutions.

11.8 PREDICTION OF ADDED POWER

As in the case of vehicle motions, the average increase in resistance, propeller thrust, torque, and number of revolutions in a specified irregular seaway can be predicted from both the RAO measured in regular waves and the measured wave spectrum by applying the linear superposition technique. The power increase necessary for sustained speed in a seaway can be predicted from the resistance increase obtained from the resistance response curve, and the increase is then added to the resistance in still water. The

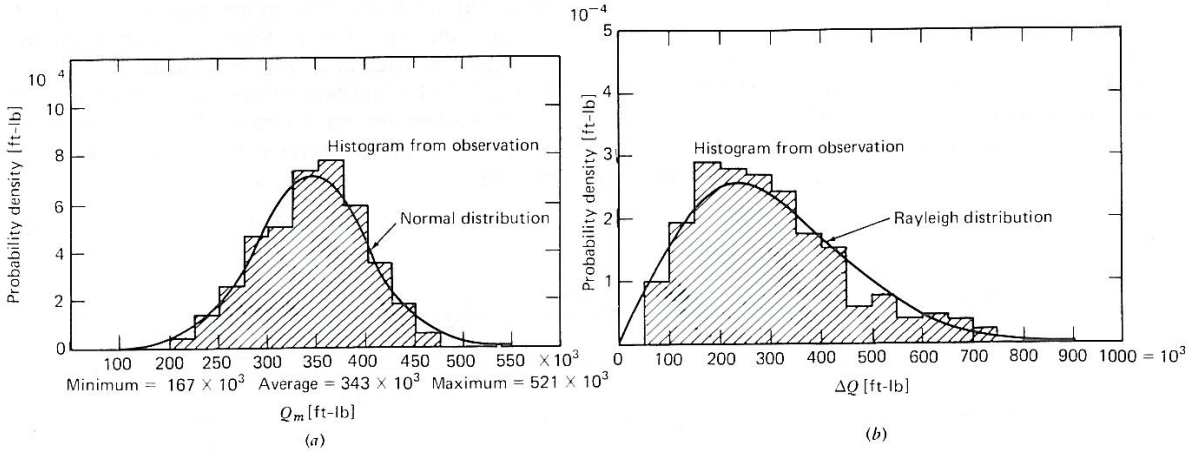


Figure 11.12 Histograms of (*a*) mean increase in torque in irregular waves (sea state 7, significant wave height = 27.7 ft, rpm = 81.5) and (*b*) variation in torque in irregular waves (sea state 7, significant wave height = 27.7 ft., rpm = 81.5) [168].

effective horsepower in irregular waves is calculated.

The self-propulsion factors in waves are obtained from the results of self-propulsion tests in regular waves at the model self-propulsion point (see Fig. 10.9) and the propeller characteristics in calm open water. The added power P_1 is then determined from the effective horsepower and propulsive efficiency in waves. The resistance increase expression is given as:

$$R_{AW} = 2\int_0^\infty \left[\frac{R_{AW}(\omega_e)}{\zeta_a^2(\omega_e)}\right] S_\zeta(\omega_e)\, d\omega_e \qquad (11.7)$$

where $R_{AW}(\omega_e)$ and R_{AW} are the resistance increases in regular and irregular waves, respectively. However, the added power in an irregular seaway can also be obtained from propulsion tests that deliver added torque, added thrust, and so on, instead of resistance tests.

The assumption that the mean added resistance is proportional to the square of wave elevation for a given wavelength is not valid for power estimation in an irregular seaway unless the vehicle in question maintains a constant speed. "Constant speed" means that the vehicle's speed, averaged in every cycle of wave encounter, is a fixed value, that is, "constant speed" means the constant mean speed [168].

It has also been shown that for a fixed wave height both the average increase and the amplitude of periodic fluctuation of different quantities will vary with wavelength. Therefore, when many wavelength components are superimposed as in an irregular seaway, one must consider the effect of superposition on both the average and the fluctuating responses.

Power increase prediction in an irregular seaway from model experiments in regular waves may be considered in two parts: prediction from response curves for the power increase of the model in irregular waves, and prediction for the full-scale vessel from the model results. In the first part the models are run in regular waves in order to obtain the RAOs. Three different methods are commonly used in predicting the power increase of a vessel from model experimentation as described below [158]:

1. Direct Power Method

It is assumed that the mean increases in delivered horsepower, propeller torque, and revolutions are proportional to the square of the wave amplitude. Therefore the mean increase in power necessary to maintain the speed of a model in irregular waves can be calculated from the regular wave tests by the formula

$${}_m\delta P_1 = 2\int_0^\infty \left[\frac{\delta P(\omega_e)}{\zeta_a^2(\omega_e)}\right]\left[S(\omega_e)\right] d\omega_e \qquad (11.8)$$

where the quantity $\delta P(\omega_e)$ is obtained from torque and revolution data from tests in waves and in still water, using the relationship

$$\delta P(\omega_e) = \frac{2\pi}{550}\left\{\left[\frac{{}_mQ_{sw} + \delta Q(\omega_e)}{Q(\omega_e)}\right]\left[\frac{{}_mn_{sw} + \delta n(\omega_e)}{n(\omega_e)}\right] - \left[\frac{{}_mQ_{sw}\,{}_mn_{sw}}{n_{sw}Q_{sw}}\right]\right\} \qquad (11.9a)$$

where $\delta P(\omega_e)$ = increase in delivered horsepower.

$$= \frac{2\pi}{550}[n(\omega_e)Q(\omega_e) - n_{sw}Q_{sw}] \qquad (11.9b)$$

n_{sw} = rate of propeller revolution in still water

Q_{sw} = propeller torque in still water

ζ_a = wave amplitude.

If δP is the power increase above the still water power, P, then the total power, $P_{\text{total}} = P + \delta P$.

Note: Experiments should be carried out in regular head and following waves with self-propelled models at the model self-propulsion point, and the propeller rpm should be kept constant during each run. For each experiment the mean torque $Q(\omega)$ and propeller revolution $n(\omega)$ should be measured.

In the case of motion experimentation it is not necessary to obtain the RAO by testing the model in uniform waves. The RAO can be obtained in a much shorter time by testing the model in irregular waves and measuring the waves as well as the motions, so that both the wave spectrum and the response spectrum can be obtained from the results. The RAO can then be derived by dividing the ordinates of the response spectrum by those of the wave spectrum at the same frequency. However, it is not possible to follow the same procedure in the case of added power because the power components for the individual frequencies in the spectrum cannot be measured and separated. Therefore the average power in the given wave condition over a sufficiently long term period is measured. This average power represents the area under the response curve; however, the actual shape of the spectrum is not defined. Therefore it is necessary to test the models in uniform waves to define the RAO for the added power.

The mean increase in propeller torque is

$$\delta Q = 2\int_0^\infty \frac{\delta Q(\omega_e)}{\zeta_a^2} S(\omega_e)\, d\omega_e \qquad (11.10)$$

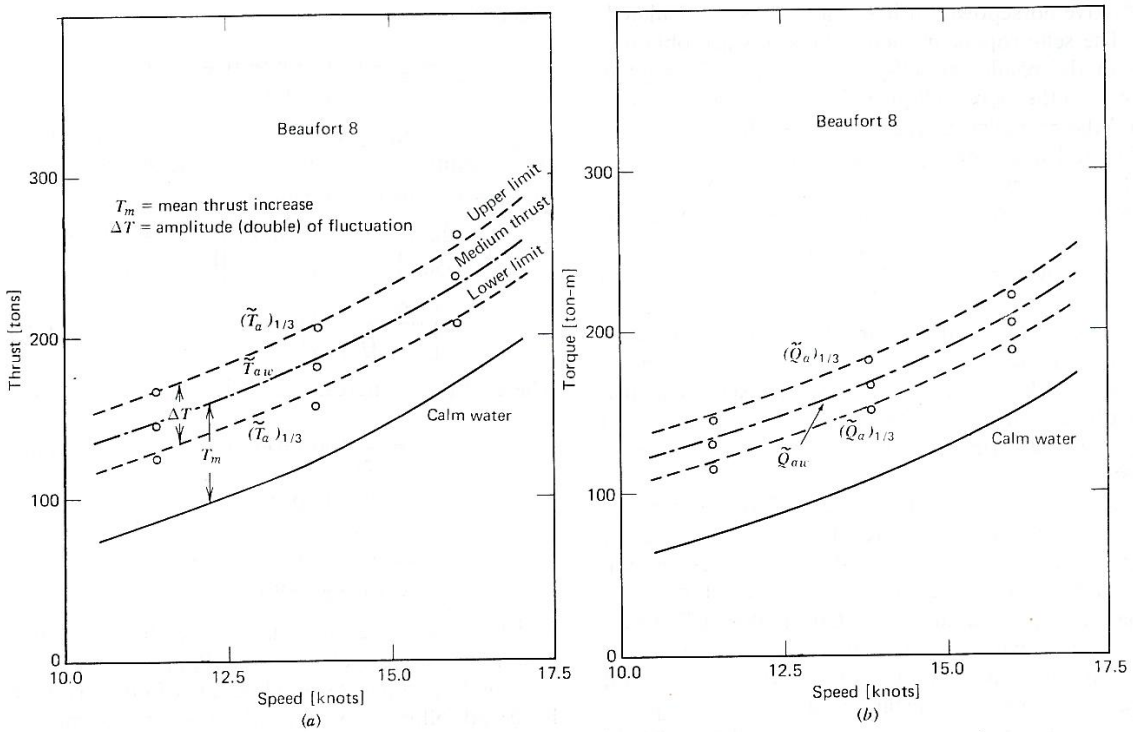


Figure 11.13 (*a*) Speed–thrust relation in head waves. [Circles show the values for irregular seaway calculated from RAO in regular waves (linear superposition principle). Dashed lines indicate values in irregular waves directly measured in the irregular sea, the power spectrum of which corresponds to the Pierson-Moscowitz formulation.] (*b*) Speed-torque relation in head waves. [221].

and the mean increase in propeller revolution is

$$\delta n = 2\int_0^\infty \frac{\delta n(\omega_e)}{\zeta_a^2} S(\omega_e)\, d\omega_e \qquad (11.11)$$

where $\delta Q(\omega_e)$ and $\delta n(\omega_e)$ are the increases in propeller torque and revolution, respectively, at the model self-propulsion point in regular waves for the particular encountering frequency ω_e in radians per second.

It appears from Figs. 11.13*a* and 11.13*b* that the agreement between the values obtained by direct measurement in irregular waves and the ones predicted by linear superposition technique is quite satisfactory. Since the experimental results were obtained from the test data at the model self-propulsion point, they should be applicable to the full-scale vessel if it is assumed that propeller loading does not influence the increase in power, and that the full-scale results can be obtained by multiplying the model results by $\lambda^{3.5}$, where λ is the scale factor.

2. Torque–Revolutions per Minute Method

In this method the ship propulsion point is considered for the calculation of power increase. For example, (11.10) and (11.11) are calculated at the model self-propulsion point and are then added to the still water values at the ship propulsion point to give a power increase, ${}_s\delta P_2$, thus

$${}_s\delta P_2 = \frac{2\pi}{550}[({}_sQ_{sw} + \delta Q)({}_sn_{sw} + \delta n) - {}_sQ_{sws}n_{sw}] \qquad (11.12)$$

where ${}_sQ_{sw}$ and ${}_sn_{sw}$ are the values obtained in still water tests at the ship propulsion point. The added power is obtained by multiplying ${}_s\delta P_2$ by $\lambda^{3.5}$, assuming that the mean increases in propeller torque and revolution are independent of propeller loading.

3. Thrust Method

Another method for calculating the added power is based on the added thrust measurements δT at the model self-propulsion point in regular waves. This added thrust is calculated from

$$\delta T = 2\int_0^\infty \frac{\delta T(\omega_e)}{\zeta_a^2} S(\omega_e)\, d\omega_e \qquad (11.13)$$

It is assumed that δT does not change with propeller loading and is added to the calm water thrust obtained from model tests at the ship self-propulsion point. By multiplying this value (calm water thrust plus added thrust) by λ^3, one obtains the full-scale thrust. The total power can then be obtained by the known thrust and torque relationship of the open water propeller efficiency in calm water (using wake fraction and rotative efficiency). In this method of calculation it is assumed that propeller performance in open water and behind the model is not affected by the waves.

Power increases may be predicted for model self-propulsion point using the direct power method [${}_m\delta P_1$ in (11.8)], or may be calculated from response curves for propeller torque and rate of rotation at the model self-propulsion point as follows:

$$ {}_m\delta P_2 = \frac{2\pi}{550}[({}_mQ_{sw} + \delta Q)({}_mn_{sw} + \delta_n) - {}_mQ_{swm}n_{sw}] \tag{11.14} $$

This equation is similar to the torque and rate of rotation method, but uses still water values at the model (not ship) propulsion point. However, ${}_m\delta P_1$ and ${}_m\delta P_2$ are not the same, since in the case of ${}_m\delta P_1$ the power increase is assumed to be proportional to ζ_a^2, whereas for ${}_m\delta P_2$ it is assumed that propeller torque and rate of rotation are each proportional to ζ_a^2. In practice, however, this inconsistency is not very significant, since none of the increases is exactly proportional to ζ_a^2.

Experimentally it has been found [158] that ${}_m\delta P_1$ is normally greater than ${}_m\delta P_2$, but the difference is within 5%. It has also been observed that the prediction from the torque and rate of rotation method is about 20% less than that from the direct power method. The power increase predicted by the thrust method may differ by up to 40% from that obtained by the direct power method. This difference is due to the assumptions of the thrust method, that is, that the propeller behaves in the same way in waves as in calm water, and that both the wake fraction and the relative rotative efficiency in still water may be used in waves. It has been found [158] that these assumptions are not justified. Predictions from the torque and rate of rotation method, however, automatically take these effects into account.

Again, the still water values used in the direct

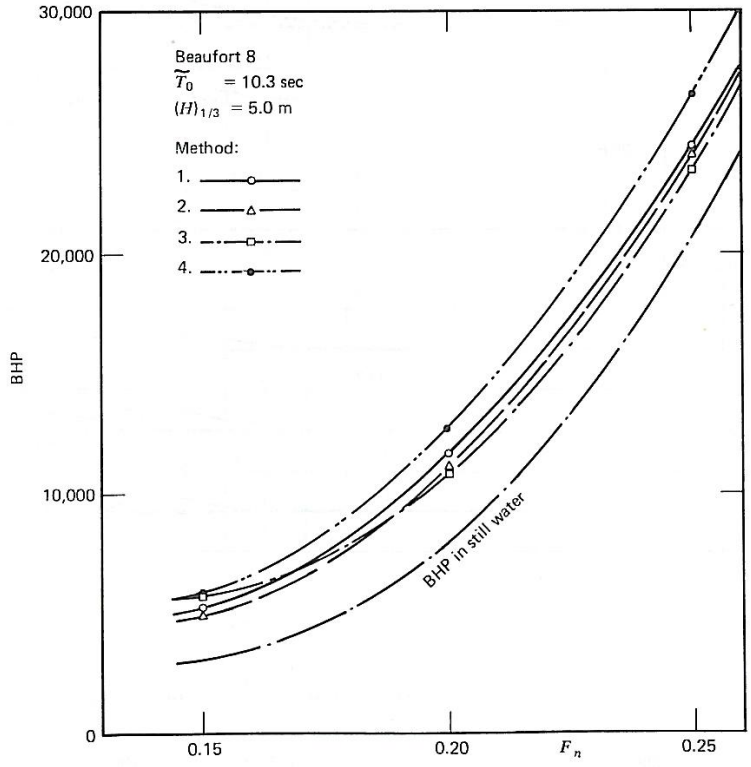


Figure 11.14 Power versus speed for an irregular seaway [84].

power method correspond to the model self-propulsion point and are therefore larger than the values to be expected at the ship propulsion point. Thus these values tend to make the power increase comparatively large. On the other hand, the increases in torque and rate of rotation measured at the model self-propulsion point are smaller than those to be expected at the ship propulsion point. Thus the power increases from the "method of torque and rate of rotation" are comparatively small.

The direct power method is often preferred to the method of torque and rate of rotation, since the assumption that power, torque, and rate of rotation are proportional to resistance is more valid for power and torque than for rate of rotation. For this reason (11.11) may be expected to be less accurate than either (11.8) or (11.10). Other advantages of the direct power method are that it gives a result that is independent of the results of overloaded self-propulsion experiments in still waters, and that estimates of the power increase based on the equation given in Ref. 155 (Section 16.3) do not depend on propeller particulars. A typical comparison of the added powers obtained by the various methods is presented in Fig. 11.14, where P_1 is obtained from the added resistance in irregular waves, P_2 from the thrust method, P_3 from the torque and rate of rotation method, and P_4 from the direct power method.

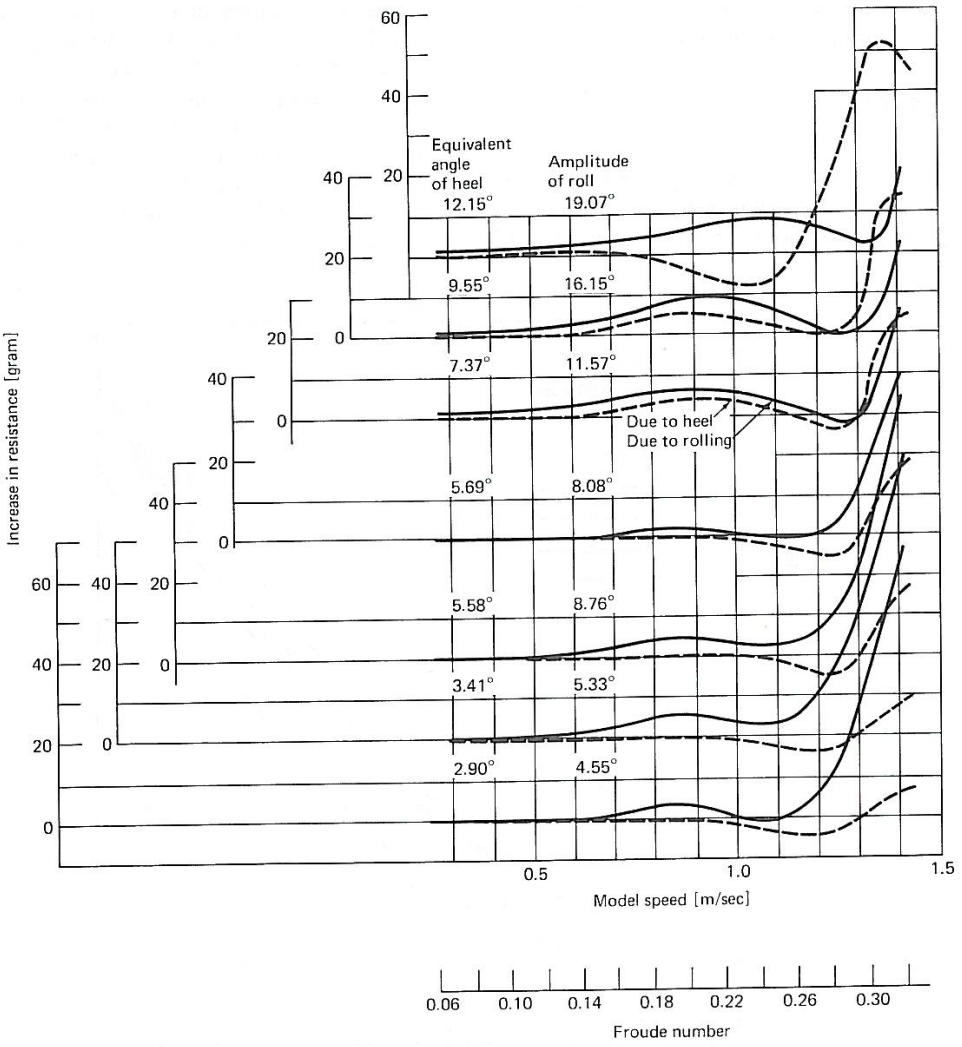


Figure 11.15 Mean increase in resistance due to rolling motion [114].

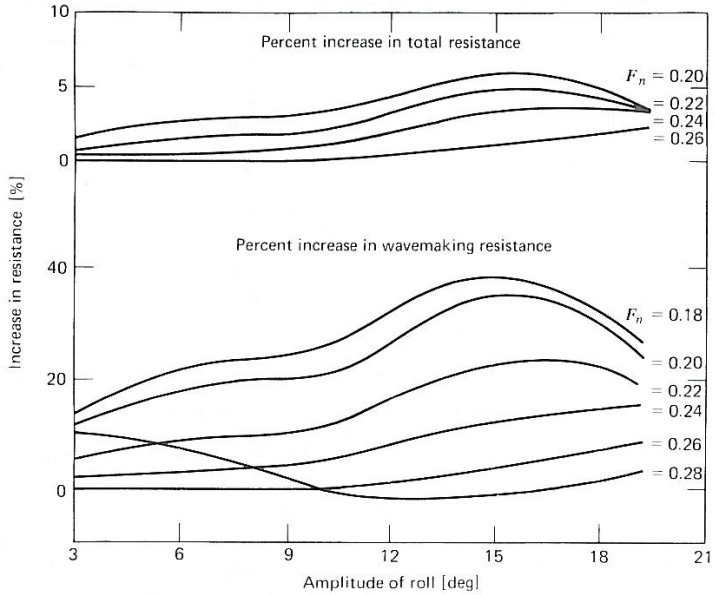


Figure 11.16 Percentage increase in resistance due to rolling motion [114].

The power increase can also be calculated for short-crested seas, and the directional spread of energy in such seas will somewhat reduce the amount of power increase. From results of actual sea trials it is concluded in Refs. 6, 7, and 8 that for long-crested seas model tests in regular waves satisfactorily predict the power increase in a sea of a given spectrum. The prediction improves if wind tunnel tests are also carried out for above-water forms of vessel. The differences between estimated and measured power are larger for short-crested seas, and, in general, the estimated power is higher than the power measured at sea. The difference increases with increasing wave heights. The directional spread of energy is the probable cause of this discrepancy.

11.9 EFFECT OF ROLLING

Forced rolling tests in still water have shown that the effect of rolling period on resistance is insignificant. In Fig. 11.15 the solid lines represent the mean curves of resistance augmentation due to the changes in rolling amplitude. It is seen that the humps and hollows of the resistance curves (particularly the humps) increase with increase in rolling amplitude.

Figure 11.16 gives the percentage increase in the total resistance and in the wavemaking resistance to a base of the rolling amplitude at various Froude numbers. One can observe from the results in this figure that the resistance augmentation due to rolling decreases with increase in speed and may be less than 3% of the total resistance when the rolling amplitude is less than 10°.

The results of self-propulsion tests of a tanker model having rolling motion are presented in Fig. 11.17. It is seen from this figure that, although the thrust and torque values fluctuate because of rolling,

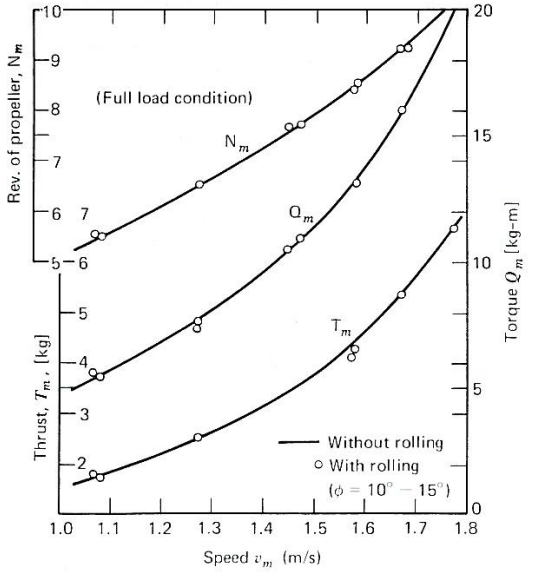


Figure 11.17 Self-propulsion test with rolling [114].

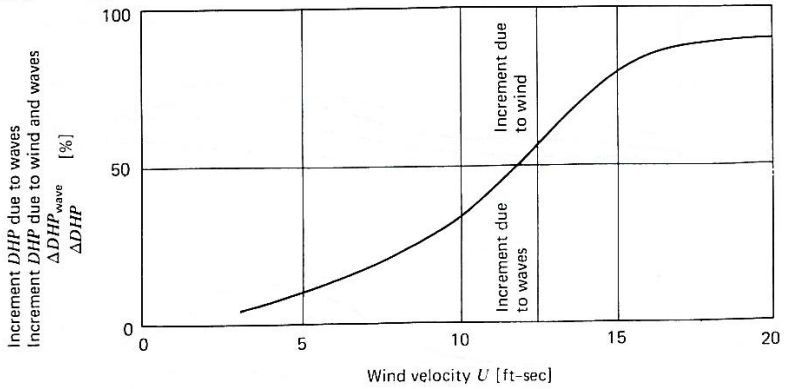


Figure 11.18 Power increase due to waves and wind [114].

the average values hardly differ from those for the still water condition.

11.10 POWER INCREASE DUE TO WIND AND WAVES

If the model experimentation methods previously described are adopted for the estimation of power increase, an increase in power due to relative wind velocity should be also included for an actual ship prediction, especially in the case of high Beaufort numbers. Figure 11.18 shows the power increase due to wind resistance in terms of the total power increase for a ship in a seaway. In this figure the drag coefficient $C_R = R_{\text{wind}}/\frac{1}{2}\rho A_R V_R^2$ has been assumed to be 1.0, where A_R is the projected area of the above-water hull form, and V_R is the wind velocity relative to the ship. Here the assumption is made that vessels can sustain a constant rate of propeller rotation at the normal depth, even in stormy weather.

An evaluation on the basis of overall operating costs could show the economic importance of the data presented in Fig. 11.19, obtained from full-scale trials. The percentage of speed loss is maximum for head seas and increases exponentially as the Beaufort number increases. Beaufort scale 6 weather is exceeded 45% of the time during the summer and 70% during the winter in the North Atlantic [4].

11.11 GENERAL CONCLUSIONS ABOUT SPEED REDUCTION

In bad weather modern vessels, in spite of their high

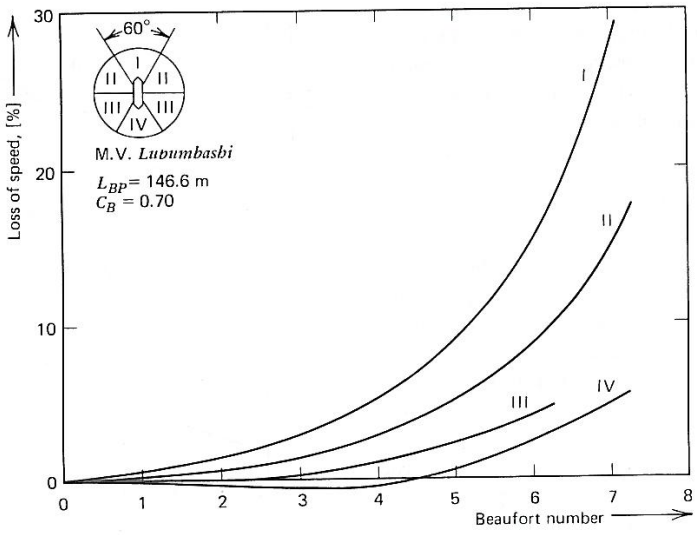


Figure 11.19 Speed loss for various weather conditions [4].

engine power, must reduce speed. Some of the main considerations are slamming, excessive shipping of green water, high accelerations, and propeller racing.

Normally, in light load conditions speed is reduced in a head sea at Beaufort 4 or 5 because of slamming or propeller racing. In full load operations, however, these phenomena occur under more severe weather conditions. In Beaufort 6 or 8, speed is reduced voluntarily either because of green water coming over the bow or because of the shifting of cargo.

Conditions for cargo ships are often optimum in medium load conditions; because of a large freeboard forward, water will not be shipped in seas up to Beaufort 7. Slamming is not considered damaging unless cargo shifting also takes place.

A bulbous bow in a large tanker is ordinarily advantageous for a gain in speed, but some vessels fitted with bulbous bows slam more and consequently lose speed. A vessel without a bulb may also maintain its speed in a seaway.

Very rough estimates of the percentages of speed loss in head seas is given in Ref. 5 for different weather conditions:

$$\text{Beaufort 5:} \quad \frac{900}{L} + 2$$

$$\text{Beaufort 6:} \quad \frac{1300}{L} + 6$$

$$\text{Beaufort 7:} \quad \frac{2100}{L} + 11$$

$$\text{Beaufort 8:} \quad \frac{3600}{L} + 18$$

where L is the vessel length in meters. These simple formulas are valid for fast or moderately fast cargo vessels without bulbs. However, since these formulas are functions of only one variable (i.e., length), they are considered as first approximations and therefore do not include the effects of the hull form.

Chapter

Twelve

LOADS DUE TO MOTION

12.1 FORCES OF COMPONENT WEIGHTS

As a ship proceeds in a seaway, each of the weights on board produces an additional load on its foundation because of the acceleration (as well as the angular velocity in the case of angular motion) developed during ship motions.

The inertial forces due to acceleration can be determined with sufficient accuracy by considering each motion separately. Thus we can classify interial forces due to (1) heaving, (2) rolling, and (3) pitching.

12.2 FORCES DUE TO HEAVING

In heaving, the motion of the ship is linear and so the inertial force is given as

$$\text{Mass} \times \text{acceleration} = m\frac{d^2z}{dt^2}$$

Depending on the direction of acceleration, the inertial force acts either upward or downward; furthermore, the force experienced by the foundation will be some factor times the weight of the component itself.

For example, when a ship is at its upwardmost position during a heaving motion in a wave, that is, at z_a, where

$$z = z_a \cos \omega t$$

the maximum acceleration

$$\ddot{z} = -\omega^2 z_a$$

acts in the downward direction, and so the total force due to cargo of mass m is the weight plus the inertial force:

$$mg + m\frac{d^2z}{dt^2} = m(g - \omega^2 z_a) \qquad (12.1)$$

From this result we see that the actual weight of the ship is reduced because the inertial force acts in the opposite direction to that of the gravitational force. On the other hand, when the ship moves downward from its equilibrium position, it experiences an upward acceleration, and so the inertial force acts downward and the total force is greater than the actual weight by an amount equal to the inertial force.

In general, the inertial force due to heaving is less than the weight of a component.

Example 12.1

If the weight of a component on board a ship is 40,000 lb, determine the maximum total force exerted on the foundation of the component due to the heaving motion of the ship if the heaving acceleration has been found to be 0.75 g.

Solution:
The maximum acceleration is

$$\frac{d^2z}{dt^2} = 0.75g = 0.75 \times 32.2 = 24.15 \text{ ft/sec}^2$$

and the component weight is 40,000 lb. Thus the inertial force is

$$\frac{w}{g}\frac{d^2z}{dt^2} = \frac{40{,}000}{32.2} \times 24.15 = 30{,}000 \text{ lb}$$

The total force on the foundation of the component, then, 70,000 lb.

12.3 FORCES DUE TO ROLLING

The rolling motion is given as

$$\phi = \phi_a \cos \omega t$$

where ϕ is the rolling displacement and ω is the circular frequency (or the angular velocity of rolling motion). Thus the angular velocity and the acceleration are, respectively,

$$\dot{\phi} = -\omega \phi_a \sin \omega t$$

and

$$\ddot{\phi} = -\omega^2 \phi_a \cos \omega t$$

For maximum acceleration, $\cos \omega t = -1$, or

$$\ddot{\phi}_{\max} = \omega^2 \phi_a$$

The linear or tangential acceleration is

$$r \times \text{angular acceleration} = r \times \frac{d^2\phi}{dt^2}$$

where r is the distance of the component from the rolling axis. Thus the maximum tangential acceleration is

$$r \times (\ddot{\phi})_{\max} = r \times \omega^2 \phi_a = \frac{4\pi^2 r \phi_a}{T^2} \quad (\phi_a \text{ in radians})$$

$$= \frac{4\pi^2 r \phi_a}{T^2 \times 57.3} \quad (\phi_a \text{ in degrees}) \qquad (12.2a)$$

since T is the period of rolling, $2\pi/\omega$,
If the weight of the component on board the ship is w, the tangential force is expressed as

$$T_R = \frac{w}{g} \times \frac{4\pi^2 r \phi_a}{T_R^2} \qquad (12.2b)$$

where ϕ_a is in radians. If ϕ_a is given in degrees,

$$T_R = \frac{w}{g} \frac{4\pi^2 r}{T^2} \times \frac{\phi_a}{57.3}$$

$$= \frac{0.0214 w \phi_a r}{T^2} \qquad (12.2c)$$

The tangential force for a component during rolling motion may be resolved into horizontal and vertical components, namely, T_{RY} and T_{RZ}, respectively, as shown in Figure 12.1*a*. In this figure

$$y_0 = r \cos \beta \qquad \text{and} \qquad z_0 = r \sin \beta$$

where y_0 and z_0 are the horizontal and vertical distances, respectively of the component from the axis of rolling motion. Thus

$$T_{RY} = \frac{w}{g} \frac{4\pi^2 z_0 \phi_a}{T^2} \quad (\phi_a \text{ in radians})$$

$$= \frac{0.0214 w \phi_a z_0}{T^2} \quad (\phi_a \text{ in degrees}) \qquad (12.3)$$

and

$$T_{RZ} = \frac{w}{g} \frac{4\pi^2 y_0 \phi_a}{T^2} \quad (\phi_a \text{ in radians})$$

$$= \frac{w}{g} \frac{4\pi^2 y_0 \phi_a}{T^2 57.3} \quad (\phi_a \text{ in degrees}) \qquad (12.4)$$

Now the centrifugal force due to angular motion is $m(v^2/r)$, where $v = \omega r$, ω is the angular velocity of the ship, and r is the distance of the CG of the component from the axis of rotation. See Fig. 12.1*b*. Hence the centrifugal force due to rolling motion is given as

$$C_R = m \frac{\omega^2 r^2}{r} = m\omega^2 r$$

$$= \frac{w}{g} (\dot{\phi})^2 r \qquad (12.5)$$

The horizontal and the vertical components respectively, of C_R can, therefore, be expressed as

$$C_{RY} = C_R \cos \beta = \frac{w}{g} (\dot{\phi})^2 r \cos \beta$$

$$= \frac{w}{g} (\dot{\phi})^2 y_0 \qquad (12.6)$$

and

$$C_{RZ} = C_R \sin \beta = -\frac{w}{g} (\dot{\phi})^2 z_0 \qquad (12.7)$$

Since the angular velocity ω is not very large (actually less than 0.15 rad/sec), the centrifugal force is rather insignificant in comparison with the gravity force. However, it should be noted that the centrifugal force is maximum when the angle of inclination of the oscillating vessel is zero, that is, when the vessel is in the upright position during rolling. The centrifugal force is absent at the maximum angle of inclination and for a rolling vessel is zero when $\phi = \phi_a$, since at this angle $\omega = 0$. Thus the total transverse force is then equal to

$$R_{RY} = w \left[\sin \phi_a + \frac{4\pi^2 z_0 \phi_a}{g T^2} + \frac{(\dot{\phi})^2 y_0}{g} \right] \qquad (12.8a)$$

Similarly, the total vertical force is obtained by adding the vertical centrifugal and inertial forces with the

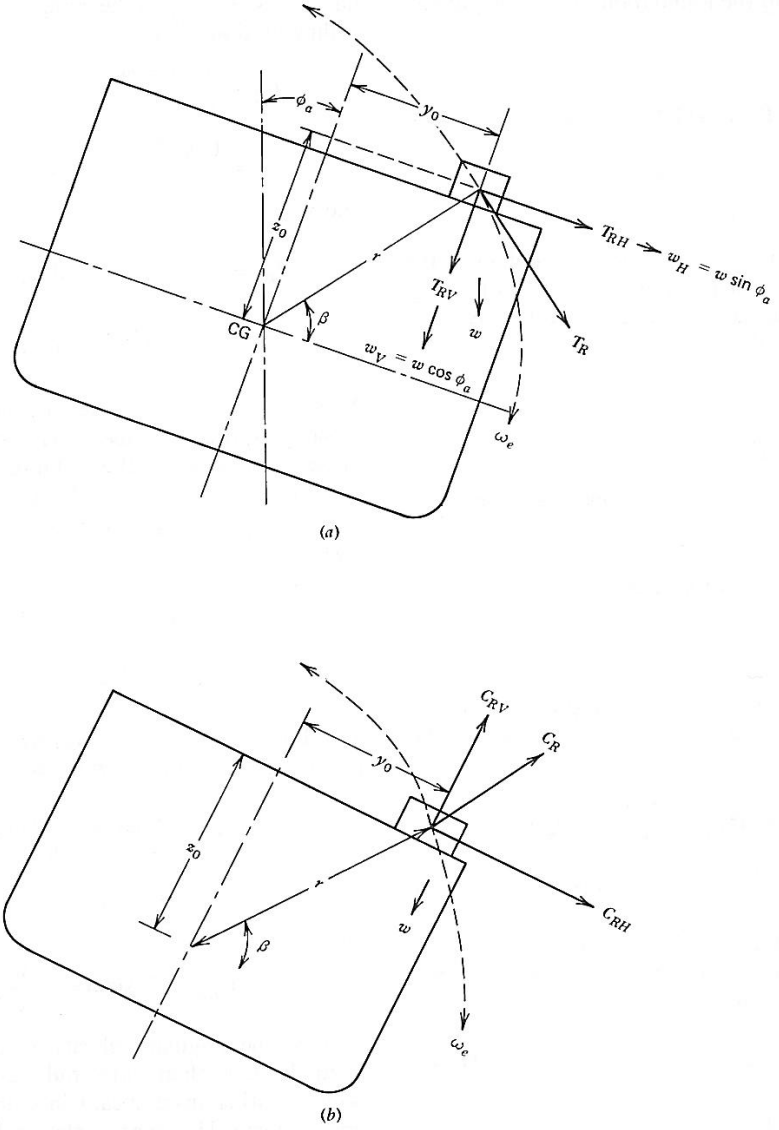


Figure 12.1 Forces during rolling motion.

gravity component:

$$R_{RZ} = w\left[\cos\phi_a + \frac{4\pi^2 y_0 \phi_a}{gT^2} - \frac{(\dot{\phi})^2 z_0}{g}\right] \quad (12.9a)$$

The general expressions for the total force in the horizontal and vertical directions are given as

$$R_{RY} = \pm w \sin\phi \pm \frac{w}{g}(\dot{\phi})^2 y_0 \pm \frac{w}{g} z_0 \frac{4\pi^2 \phi}{T^2} \quad (12.8b)$$

$$R_{RZ} = -w\cos\phi \pm \frac{w}{g}(\dot{\phi})^2 z_0 + m y_0 \frac{4\pi^2 \phi}{T^2} \quad (12.9b)$$

Figure 12.2 illustrates the components of the forces for different locations of the weight for both port and starboard rolls. The maximum resultant force during rolling motion can be determined from the analysis of different forces in this figure, where the sign conventions used are as follows: the forces in the direction of increasing positive displacements are positive,

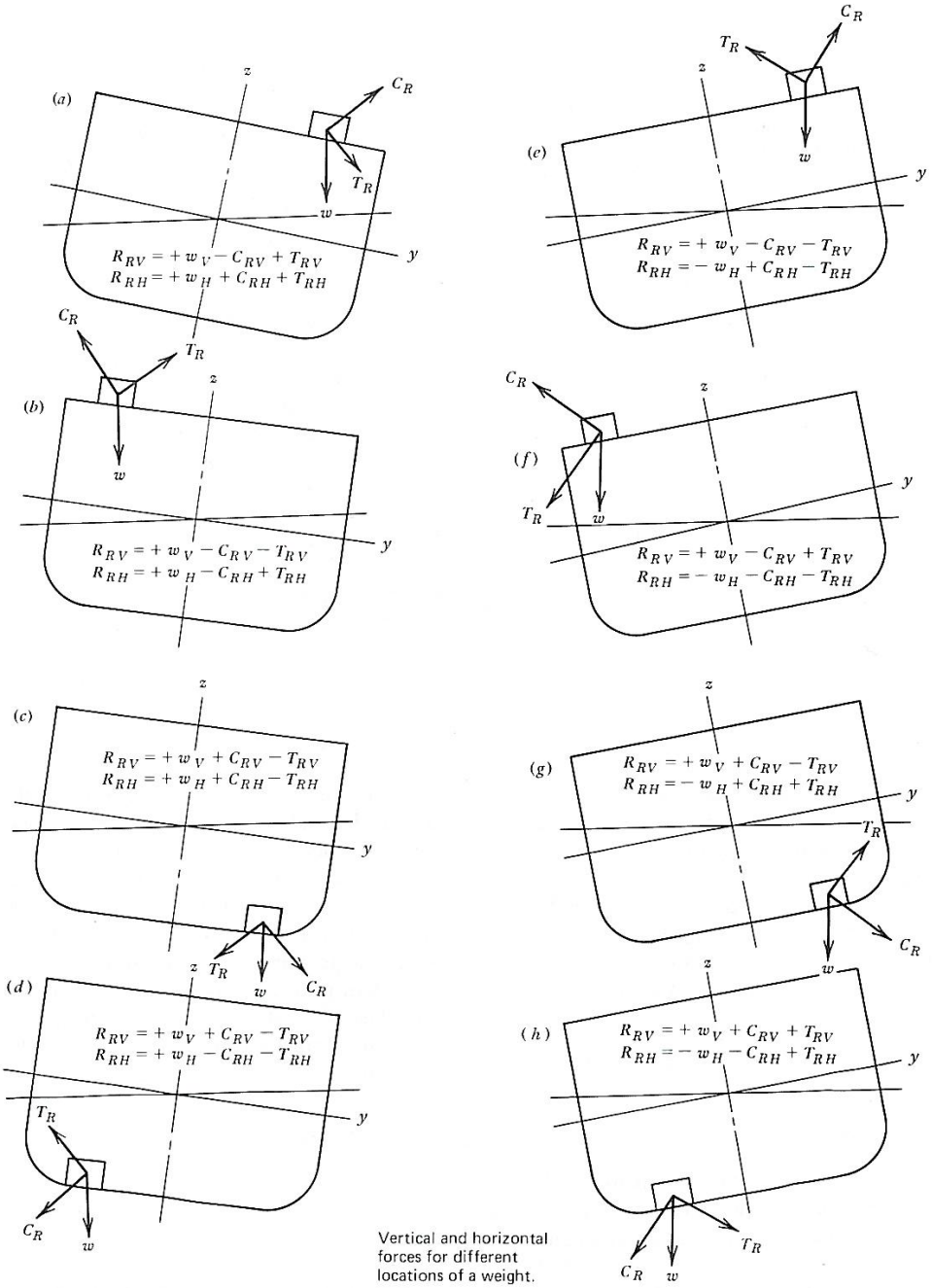
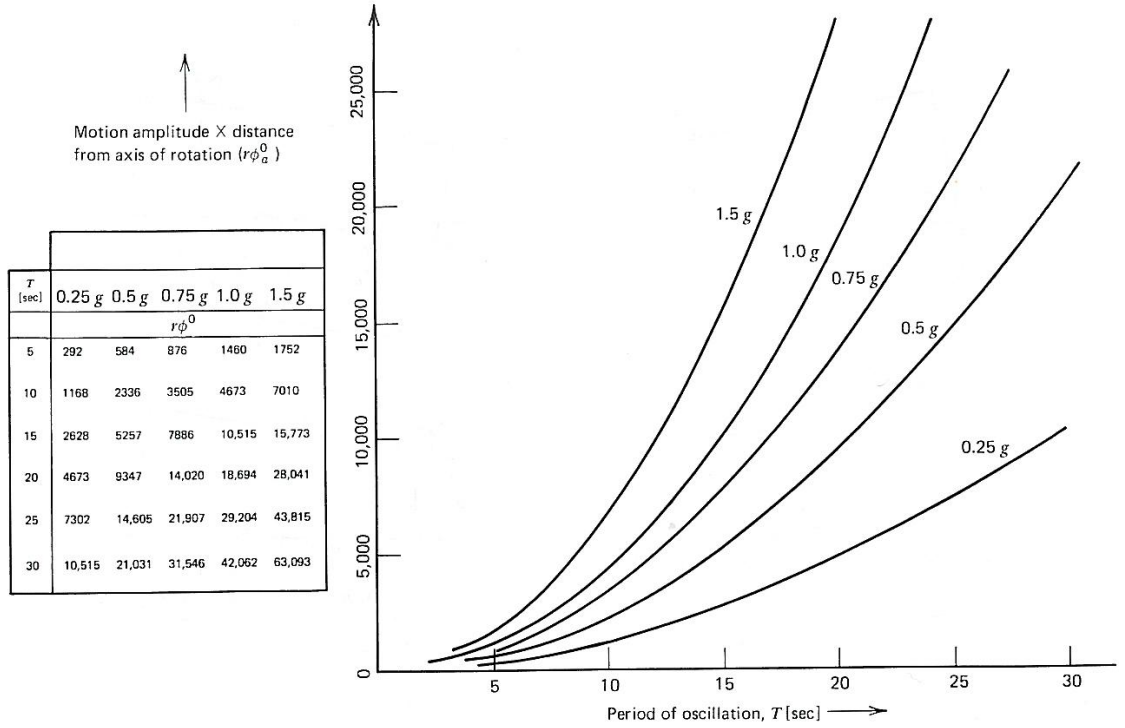


Figure 12.2 Vertical and horizontal forces for different locations of a weight [56].

and the positive sign has been used for pitch when the bow is up and for roll when the starboard side is down. To remain within the specified value for acceleration, the angle of inclination is often kept within a certain limit while at the same time the period of rolling is increased.

Figure 12.3 contains curves of the limiting tangential accelerations up to 1.0 g for practical values of rolling amplitude ϕ_a (in degrees) and period of rolling T(in seconds). These curves are obtained



T [sec]	0.25 g	0.5 g	0.75 g	1.0 g	1.5 g
	$r\phi^0$				
5	292	584	876	1460	1752
10	1168	2336	3505	4673	7010
15	2628	5257	7886	10,515	15,773
20	4673	9347	14,020	18,694	28,041
25	7302	14,605	21,907	29,204	43,815
30	10,515	21,031	31,546	42,062	63,093

Figure 12.3 Maximum acceleration for angular motion.

using the acceleration in the force expression in (12.2a). *Note*: If a weight is placed at a distance of 200 ft from the axis of rolling motion, and the maximum angle of roll is expected to be 30°, then, for a specified acceleration limit of 0.5 g, the period of roll must be at least 16 sec, referring to Fig. 12.3. From this Figure, using the value of maximum tangential acceleration of 0.5 g (16.1 ft/sec^2), we have

$$16.1 = \frac{4\pi^2 \times 200 \times 30}{T^2 \times 57.3}$$

or

$$T = 16 \text{ sec}$$

If a component is located far from the axis of rolling motion, the rolling acceleration may be as large as 1.0 g or more. A radar antenna located on a mast may thus be subject to high acceleration. For design purposes the intertial force, which is then as large as the weight itself, must be taken into consideration in order to estimate the total vertical load acting on the foundation of the component.

The maximum angular acceleration $\omega^2\phi_a$ is experienced at the end of the roll and corresponds to a maximum tangential acceleration at any part of the structure of $r\omega^2\phi_a$. For a mast, shown schematically in Fig. 12.4, of mass m per unit length, length l, and heel distance a above the axis of oscillation, the linear acceleration of an element of length δx and distance x above the hell will be $(a+x)\omega^2\phi_a$. Thus the inertial force on the element is $(w/g)(a+x)\omega^2\phi_a\,\delta x$, where w is the weight per unit run. This inertial force will produce a bending moment at the heel of the mast of $(w/g)(a+x)\omega^2 x\delta x$; thus the total inertial bending moment provided by the whole length of the mast is

$$M_b = \frac{w}{g}\omega^2\phi_a \int_0^l (a+x)x\,dx = \frac{w}{g}\omega^2\phi_a \left|\frac{ax^2}{2} + \frac{x^3}{3}\right|_0^l$$

$$= \frac{w\omega^2\phi_a l^2(3a+2l)}{3g} \tag{12.10}$$

Note that a static bending moment is to be determined in addition to the inertial bending moment. The static bending moment is given as the product of the total weight of the mast and a lever, that is,

$$(wl)\frac{l}{2}\sin\phi_a = \frac{wl^2}{2}\sin\phi_a \tag{12.11}$$

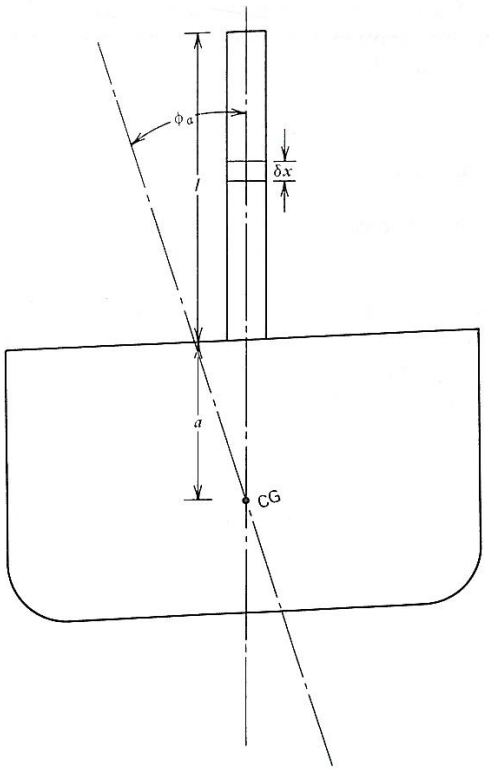


Figure 12.4 Bending moment of a ship mast due so rolling motion.

Example 12.2

A ship is rolling 35° in beam seas with a rolling period of 10 sec. A 30 ft solid mast of 6 in. diameter is attached to the deck at the midship section of the ship and along its centerline. The distance of the base of the mast from the axis of oscillation is 56 ft, and the weight density of the mast is 489 lb/ft^3.

Calculate:

a. The maximum inertial force of the mast.

b. The stress at the base of the mast.

Solution:

Recall that the maximum acceleration is at the end of the roll. The following data are given:

$$\phi_a = \frac{35^\circ}{57.3} = 0.611 \text{ rad}$$

$$T_\phi = \frac{2\pi}{\omega} = 10 \text{ sec (i.e., } \omega = 0.628)$$

$$d = 0.5 \text{ ft}$$

$$l = 30 \text{ ft}$$

$$w = \frac{\pi}{4}(0.5)^2 \times 489 \times 1 \text{ ft}$$

$$= 96 \text{ lb/ft of length}$$

W = total weight = $30 \times 96 = 2880$ lb

$a = 56$ ft

r = distance of CG of the mast from the rolling axis
$= 56 + 15 = 71$ ft

a. The inertial force is

$$\frac{w}{g} \times r\omega^2\phi_a = \frac{2880}{32.2} \times 71 \times (0.628)^2 \times 0.611$$

$$= 1530 \text{ lb}$$

Total inertial bending moment is

$$\frac{w\omega^2\phi_a l^2(3a + 2l)}{3g}$$

$$= \frac{96 \times (0.628)^2 \times 0.611(30)^2(3 \times 56 + 2 \times 30)}{3(32.2)}$$

$$= 49{,}134 \text{ ft-lb}$$

Now the bending moment due to static forces is

$$\frac{\omega l^2 \sin \phi_a}{2}$$

$$= \frac{96 \times 30^2}{2} \times 0.574$$

$$= 24{,}797 \text{ ft-lb}$$

Thus the total bending moment is 73,931 ft-lb.

b. The stress due to the bending moment is

$$\sigma = \frac{M}{I/Y}$$

where

$$I = \tfrac{1}{16} Ad^2 = \tfrac{1}{16} \times \left(\frac{\pi}{4} \times 0.5^2\right) \times (0.5)^2$$

$$= 0.0031 \text{ ft}^4$$

and

$$y = \frac{0.5}{2} = 0.25 \text{ ft}$$

Thus the maximum stress at the heel of the mast is

$$\frac{73{,}931}{0.0031/0.25} \times \frac{1}{144} = 41{,}404 \text{ psi}$$

12.4 FORCES DUE TO PITCHING

As for rolling motion, it can be shown that the maximum pitching acceleration is given as $4\pi^2 r\theta_a/T^2$ where θ_a is the pitching amplitude in radians and T is

the period of pitching. Therefore the maximum tangential (inertial) force due to pitching, T_P, is mass times pitching acceleration:

$$T_P = \frac{w}{g} \times \frac{4\pi^2 r\theta_a}{T^2} \qquad (\theta_a \text{ in radians})$$

$$T_P = \frac{0.0214wr\theta_a}{T^2} \qquad (\theta_a \text{ in degrees}) \qquad (12.12)$$

Note that Fig. 12.3 can also be used for the pitching acceleration, since both the practical pitching periods and the pitching radii are represented. For example, a component of weight is located 400 ft away from the pitching axis. If the maximum pitching amplitude and period are known to be 10° and 9 sec, respectively, we will expect the maximum acceleration to be a little above 1.0 g. The inertial force during pitching motion can also be resolved into horizontal and vertical components, respectively, which are given by

$$T_{PY} = \frac{w}{g}\frac{4\pi^2 z_0\theta_a}{57.3T^2} \qquad (12.13)$$

and

$$T_{PZ} = \frac{w}{g}\frac{4\pi^2 x_0\theta_a}{57.3T^2} \qquad (12.14)$$

where θ_a is in degrees,

$$z_0 = r\sin\delta, \qquad \text{and} \qquad x_0 = r\cos\delta$$

as shown in Figure 12.5.

The general expressions for the total force due to pitching alone in the horizontal and vertical directions are given as

$$R_{PY} = \pm w\sin\theta \pm \frac{w}{g}(\dot{\theta})^2 x_0 \pm \frac{w}{g}z_0\frac{4\pi^2\theta_a}{T^2} \qquad (12.15)$$

and

$$R_{PZ} = -w\cos\theta \pm \frac{w}{g}(\dot{\theta})^2 z_0 \pm \frac{w}{g}x_0\frac{4\pi^2\theta_a}{T^2} \qquad (12.16)$$

respectively, where T is the pitching period.

Accelerations due to pitching may reach a value of 0.75 g for a component located far from the axis of pitching motion, for example, components such as anchors, which are situated near the ends of a long ship.

Example 12.3

A ship proceeding through a rough sea experiences a roll amplitude of 35° and a pitch amplitude of 10°, where the periods of roll and pitch are 8 and 5 sec, respectively. Determine the horizontal and vertical roll and pitch inertial forces for a weight of 4000 lb located 100 ft above, 60 ft athwartships, and 250 ft aft from the CG of the ship.

Solution:

From (12.3) and (12.4) we obtain expressions for the horizontal and vertical rolling inertial forces. Thus

$$T_{RY} = \frac{w}{g}\frac{4\pi^2 z_0\phi_a}{57.3T^2}$$

$$= 0.0214\frac{\phi_a z_0 w}{T^2} = 0.0214\frac{35^\circ \times 100 \times 4000}{8^2}$$

$$= 4680 \text{ lb}$$

and

$$T_{RZ} = \frac{w}{g}\frac{4\pi^2 y_0\phi_a}{57.3T^2}$$

$$= 0.0214\frac{\phi_a y_0 w}{T^2} = 0.0214\frac{35 \times 60 \times 4000}{8^2}$$

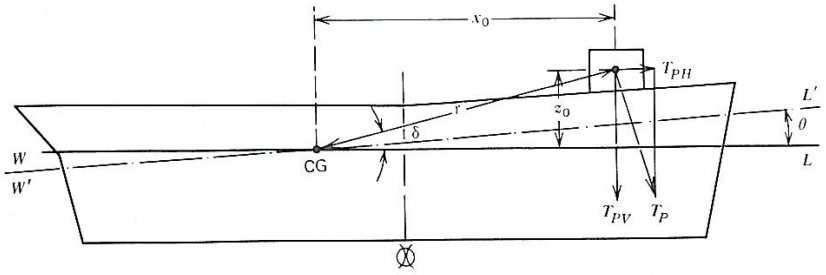
$$= 2808 \text{ lb}$$

In (12.13) and (12.14) we have the inertial forces due to pitching motion, namely,

$$T_{PY} = \frac{w}{g}\frac{4\pi^2\theta_a z_0}{57.3T^2}$$

$$= 0.0214\frac{\theta_a z_0 w}{T^2} = \frac{0.0214 \times 10 \times 100 \times 4000}{5^2}$$

$$= 3424 \text{ lb}$$



WL = original waterline; $W'L'$ = new waterline.

Figure 12.5 Inertial force during pitching motion.

TABLE 12.1 RESULTANT LOADS DURING PITCH AND ROLL [56]

		R_{PY}	R_{RY}
Weight above OX and OY-axes (Z positive)	a.	$\theta = 0$ At $\theta = 0, \ddot{\theta} = 0$ but $\dot{\theta} = \dot{\theta}_a$ $= \omega_e \theta_a$ (see Fig. 2.2) $R_{PY} = \pm \frac{w}{g} (\dot{\theta})^2 x_0$ $= \pm \frac{w}{g} x_0 \omega_e^2 \theta_a^2$ $= \pm \frac{w}{g} x_0 \frac{4\pi^2}{T_P^2} \theta_a^2$ (Negative sign to be used when the weight is located aft)	$\phi = 0$ At $\phi = 0, \ddot{\phi} = 0$ but $\dot{\phi} = \dot{\phi}_a$ $= \omega_e \phi_a$ (see Fig. 2.2) $R_{RY} = \pm \frac{w}{g} (\dot{\phi})^2 y_0$ $= \pm \frac{w}{g} y_0 \omega_e^2 \phi_a^2$ $= \pm \frac{w}{g} y_0 \frac{4\pi^2}{T_R^2} \phi_a^2$ (Negative sign to be used when the weight is located port)
	b.	$\theta = \pm \theta_a$ At $\theta = \theta_a, \dot{\theta} = 0$ and $\ddot{\theta} = \ddot{\theta}_a$ $= \omega_e^2 \theta_a$ (see Fig. 2.2) $R_{PY} = \pm \left(w \sin \theta_a + \frac{w}{g} z_0 \frac{4\pi^2}{T_P^2} \theta_a \right)$	$\phi = \pm \phi_a$ At $\phi = \phi_a, \dot{\phi} = 0$ and $\ddot{\phi} = \ddot{\phi}_a$ $= \omega_e^2 \phi_a$ (see Fig. 2.2) $R_{RY} = \pm \left(w \sin \phi_a + \frac{w}{g} z_0 \frac{4\pi^2}{T_R^2} \phi_a \right)$
Weight above OX- and OY-axes (Z negative)	a.	$\theta = 0$ $R_{PY} = \pm \frac{w}{g} x_0 \frac{4\pi^2}{T_P^2} \theta_a^2$ (Negative sign to be used when the weight is located aft)	$\phi = 0$ $R_{RY} = \pm \frac{w}{g} y_0 \frac{4\pi^2}{T_R^2} \phi_a$ (Negative sign to be used when the weight is located port)
	b.	$\theta = \pm \theta_a$ $R_{PY} = \pm \left(w \sin \theta_a - \frac{w}{g} z_0 \frac{4\pi^2}{T_P^2} \theta_a \right)$	$\phi = \pm \phi_a$ $R_{RY} = \pm \left(w \sin \phi_a - \frac{w}{g} z_0 \frac{4\pi^2}{T_R^2} \phi_a \right)$

			$R_Z = R_{PZ} + R_{RZ}$
Weight above OX- and OY-axes (Z positive)	a.	$\theta = 0, \phi = 0$	$R_Z = -w + mz_0 \frac{4\pi^2}{T_R^2} \phi_a^2 + mz_0 \frac{4\pi^2 \theta_a^2}{T_P^2}$
	b.	$\theta = \pm \theta_a, \phi = \pm \phi_a$	$R_Z = -w \cos \phi_a \cos \theta_a - \frac{w}{g} y_0 \frac{4\pi^2}{T_R^2} \phi_a - \frac{w}{g} x_0 \frac{4\pi^2}{T_P^2} \theta_a$
	c.	$\theta = \pm \theta_a, \phi = 0$	$R_Z = -\left(w \cos \theta_a + \frac{w}{g} y_0 \frac{4\pi^2}{T_R^2} \phi_a - \frac{w}{g} z_0 \frac{4\pi^2}{T_P^2} \theta_a^2 \right)$ *
	d.	$\theta = 0, \phi = \pm \phi_a$	$R_Z = -\left(w \cos \phi_a - \frac{w}{g} z_0 \frac{4\pi^2}{T_P^2} \theta_a^2 + \frac{w}{g} x_0 \frac{4\pi^2}{T_P^2} \theta_a \right)$ *
Weight above OX- and OY-axes (Z negative)	a.	$\theta = 0, \phi = 0$	$R_Z = -\left(w + \frac{w}{g} z_0 \frac{4\pi^2}{T_R^2} \phi_a^2 + \frac{w}{g} z_0 \frac{4\pi^2}{T_P^2} \theta_a^2 \right)$
	b.	$\theta = \pm \theta_a, \phi = \pm \phi_a$	$R_Z = -\left(w \cos \theta_a \cos \phi_a + \frac{w}{g} y_0 \frac{4\pi^2}{T_R^2} \phi_a + \frac{w}{g} x_0 \frac{4\pi^2}{T_P^2} \theta_a \right)$
	c.	$\theta = \pm \theta_a, \phi = 0$	$R_Z = -\left(w \cos \theta_a + \frac{w}{g} y_0 \frac{4\pi^2 \phi_a}{T_R^2} + \frac{w}{g} z_0 \frac{4\pi^2}{T_P^2} \theta_a^2 \right)$
	d.	$\theta = 0, \phi = \pm \phi_a$	$R_Z = -\left(w \cos \phi_a + \frac{w}{g} z_0 \frac{4\pi^2}{T_P^2} \theta_a^2 + \frac{w}{g} x_0 \frac{4\pi^2}{T_P^2} \theta_a \right)$

*The negative value for the centrifugal force should be neglected for rolling without pitching or for pitching without rolling motions.

Note: T_P = pitching period; T_R = rolling period.

and

$$T_{PZ} = \frac{w}{g}\frac{4\pi^2\theta_a x_0}{57.3T^2}$$

$$= 0.0214\frac{\theta_a}{T^2} \times x_0 w = 0.0214\frac{10^\circ}{5^2} \times 250 \times 4000$$

$$= 8560\,\text{lb}$$

For the combined pitching and rolling motions, the forces in the OX- and OY-directions can be determined by using (12.8b) and (12.15), respectively; the combined vertical force (i.e., in the z- direction) is expressed as

$$R_Z = R_{RZ} + R_{PZ} = -w\cos\phi\cos\theta \pm m\dot{\phi}^2 z_0 \pm my_0\frac{4\pi^2\phi_a}{T_R^2} \pm m\dot{\theta}^2 z_0 \pm mx_0\frac{4\pi^2\theta_a}{T_R^2}$$

Table 12.1 shows the expressions for R_{RY}, R_{PY}, and R_Z for various locations of the component weight.

Chapter

Thirteen

WAVE LOADS

13.1 GENERAL

To produce a successful design of a ship structure for seaway operations, it is imperative that the designer be able to determine loads that correspond to the largest actual load the vessel is expected to encounter during its entire life of service. These loads must include shear forces and bending moments along the length of the vessel in both the vertical and the athwarthship planes. Very often empirical methods based on past experience are used to predict the actual service loads the vessel will be subject to during its operation. Although an empirical approach may provide a safe design for common displacement type vessels, an efficient design must be based on proper determination of loads, including those in the athwartship plane and dynamic loads (slamming and whipping), as well as on the effect of vessel speed and other relevant factors.

Any individual section of a hull form is subject to external loads consisting mainly of the fluid pressures on the hull surface, gravity forces, and inertial forces due to the elastic and rigid body motions of the section itself. The fluid pressures are integrated over the hull surface in order to determine the hydrodynamic force, which may then be added to the gravity and inertial forces to obtain the total external forces acting on the section. The first and second integrations of these forces along the length of the vessel provide the hull girder shear forces and bending moments, respectively. The hull-girder primary stresses at the deck and bottom longitudinal plate-stiffener combinations are due to such bending moments, which are rather large at or near the midship section of a vessel and rapidly decrease to zero at both ends. It is, therefore, quite logical that from the point of view of structural design the midship section is of primary importance.

In present-day practice it is assumed that a ship is balanced statically on a trochoidal wave having a length equal to that of the ship and a height equal to either $1.1\sqrt{L_w}$ or $L_w/20$.

For the determination of seaway bending moments two extreme cases are considered, namely, hogging and sagging. In hogging the wave troughs are supposed to be at the ends, while in sagging the wave crests are placed at both ends of the ship.

To determine the load curve from the weight and buoyancy distribution along the ship's length, the buoyancy forces on the ship sections are calculated for each condition (namely, hogging and sagging), along with the Smith correction, which takes into account the orbital motions of the fluid particles in a wave. The corrected buoyancy forces are taken to be the total hydrodynamic forces on the ship sections, the effect of ship motions on the hydrodynamic pressures being neglected. The buoyancy forces so determined are then combined with the gravity (weight) forces on the sections to determine the resulting forces (loads), which are integrated successfully along the length for shear force and bending moment. In the design of the hull-girder by this conventional method the hull-girder shear forces and bending moments, as well as the impact loads and intertial forces, are generally ignored.

With the advent of large tankers, the effect of bending moments on ships has become of great importance. A study of this subject must include theoretical development, model tests in experimental tanks, and full-scale measurements in the sea.

To begin this study, we must first consider bending moments. The bending moments that a ship has to

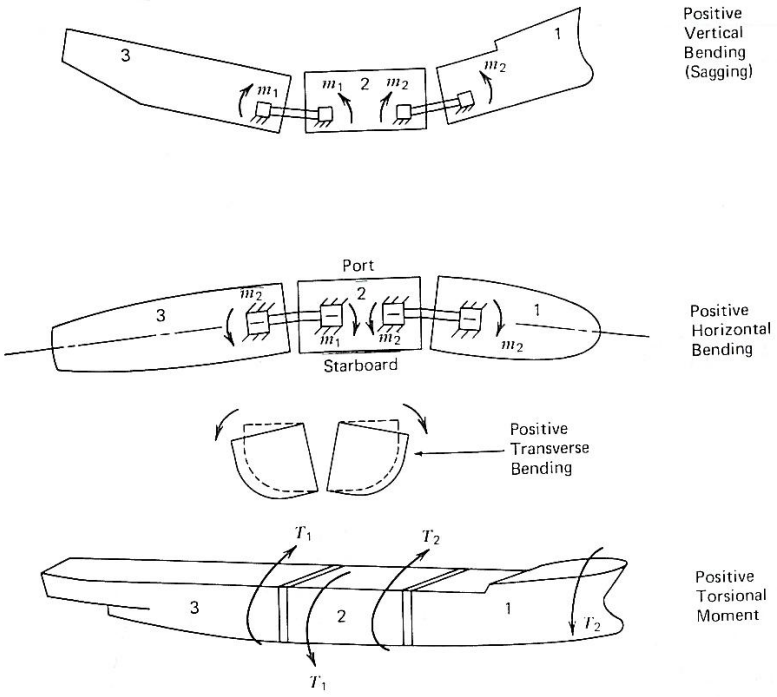


Figure 13.1 Various kinds of moments.

withstand in the seaway are of three kinds (see Fig. 13.1):

1. Vertical bending moments, producing deflections about the oy-axis.
2. Horizontal bending moments, producing deflections about the oz-axis.
3. Transverse bending moments, producing deflections about the ox-axis.

In addition, a ship may experience a torsional or twisting moment, as also shown in Fig. 13.1.

Horizontal bending moments may be caused by rolling motion and quartering seas or by wave crests on one side of the ship being in phase with troughs on the other. It can be inferred from both model tests and sea trials that horizontal bending moments may have the same magnitude as vertical bending moments. Except for catamaran vessels, hydrostatic and hydrodynamic force combinations do not produce the significant bending moments in the transverse plane. Thus the maximum resultant stress at any point of the cross section due to vertical and horizontal bending moments is given as

$$\sigma = \sqrt{\left(\frac{M_V z}{I_V}\right)^2 + \left(\frac{M_H y}{I_H}\right)^2} \qquad (13.1)$$

where M_V = vertical bending moment
M_H = horizontal bending moment
y = distance from Oz-axis (horizontal)
z = distance from Oy-axis (vertical)
I_V = moment of inertia about Oy-axis
I_H = moment of inertia about Oz-axis

Each of these bending moments can again be considered as the sum of three components:

1. That due to the difference in the distribution of weight and buoyancy when at rest in calm water.
2. That caused by ship-generated waves when in motion in calm water.
3. That induced by waves when underway in a seaway.

These three components when added together constitute the *total bending moment*; the second and third components together are known as the *wave bending moment*. The wave bending moment itself is composed of various components:

a. Loads due to changes in the distribution of underwater volume. These changes are due to the waves, as well as to heaving and pitching motions.
b. Loads due to the Smith effect, that is, due to the

modified water pressure in the wave caused by the orbital movement of the water particle.

c. Loads due to inertial forces. These forces are functions of the ship's mass as well as the added mass and their respective distribution along the ship's length.

d. Loads due to damping forces. These forces are composed mainly of two components: wave damping and viscous damping.

The calm water bending moment experienced when a ship is at rest is dependent on the arrangement and the distribution of weights within the ship. The wave bending moment, however, depends on the form of the waterplane, transverse sections, moments of weight, radius of gyration, speed, and so on.

As previously mentioned, the total bending moment M is considered to be a summation of two different kinds of bending moments:

$$M = M_S + M_W \tag{13.2}$$

where M_S is the still water bending moment, and M_W is the moment caused by the difference in the distribution of the displacement over the ship's length (i.e., between the condition in smooth water and that in waves.

The still water bending moment can be found by static calculation, whereas the wave bending moment M_W is only a function of the ship form and the wave.

Finally, the wave bending moment is expressed by

$$M_W = M_\zeta + M_z + M_\theta \tag{13.3}$$

where M_ζ is the moment produced by the wave profile, M_z is the moment produced by the heaving motion, and M_θ is the moment produced by the pitching motion.

13.2 STILL WATER LOADS

Ship in Still Water at Rest

The still water shear at any point along the ship length can be obtained from hydrostatic data (Bonjean curves) and weight distributions over the ship length as follows:

$$V_x = \int_0^x W\,dx = \int_0^x w\,dx - \int_0^x b\,dz \tag{13.4}$$

where V_x = shear force at a distance x from the bow (or stern) [lb]

w = weight per unit length [lb/ft]

b = buoyancy per unit length [lb/ft]

$W = w - b$ load per unit length [lb/ft]

Therefore the bending moment at any point is determined as

$$M_x = \int_0^x \int_0^x W\,dx\,dx = \int_0^x \int_0^x w\,dx\,dx - \int_0^x \int_0^x b\,dx \tag{13.5}$$

where M_x is the bending moment at point x.

The first step in the determination of the still water bending moment is to "balance" the ship for a certain weight distribution, so that the total weight and the longitudinal center of gravity of the ship coincide with the displacement and the longitudinal center of buoyancy. This is done by trial and error.

According to the rules of the American Bureau of Shipping, no addition of section modulus is required if the still water bending moment does not exceed

$$SCfB(C_B + 0.5) \tag{13.6}$$

where S and f are coefficients (see Table 13.1), B is the beam, C_B is the block coefficient (not less than 0.68), and $C = 1.00$ for normal cargo ships and 1.03 for oil tankers.

Ship in Calm Water at Speed

When a ship moves in calm water at a given speed, a wave pattern is generated by the underwater hull form, and this wave pattern produces an additional bending moment. At high speed a hogging moment is normally produced by the wave pattern of fast, full ships, whereas for fine ships a sagging moment is expected at high speeds due to bow and stern waves. Figure 13.2 [226] shows the dimensionless ship–wave bending moments for various block coefficients as a function of Froude number.

The bending moment caused by the ship-generated wave system can also be estimated by a method described in Section 16.3.

TABLE 13.1 BENDING MOMENT COEFFICIENTS OF THE AMERICAN BUREAU OF SHIPPING

Length [ft]	f	S	
		For Oil Carriers	For Other Ships
600	594	3.78	4.25
800	1175	3.78	4.25
1000	1921	3.90	4.38

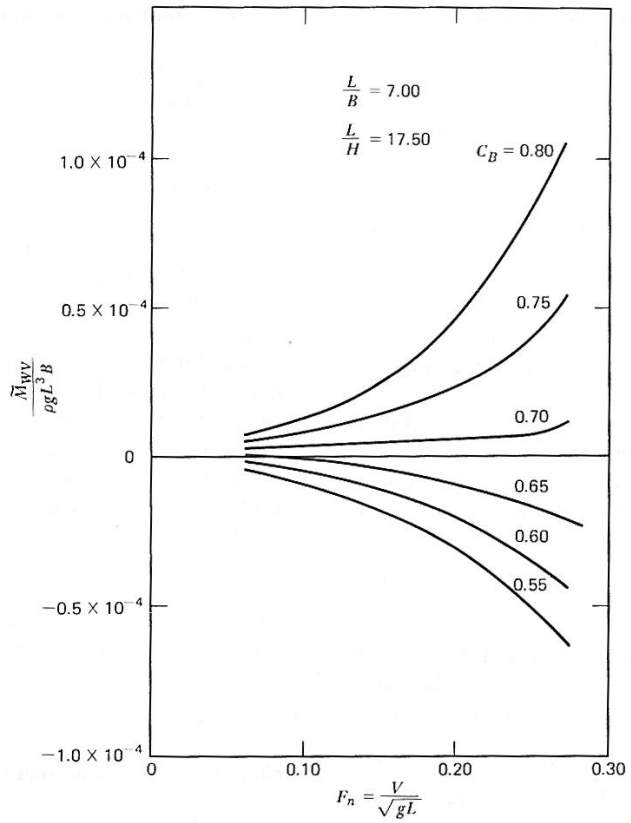


Figure 13.2 Vertical bending moment in calm water as a function of speed and block coefficient [225].

Bending Moment during Heaving Motion in Calm Water

Each item of the weight curve is subject to acceleration during heaving motion. Therefore the weight per foot is considered to be increased by the inertial force; that is, the modified weight is represented by

$$w + \frac{w'}{g}\ddot{z} = w \pm \frac{w'}{g}\omega^2 z_a \tag{13.7}$$

where $\omega^2 z_a$ is the maximum heaving acceleration [ft/sec^2], w'/g is the added mass per foot of run [lb-sec^2/ft^2], and ω is the circular frequency of heaving motion (equal to ω_e in a seaway) [rad/sec].

Similarly, the buoyancy curve is also to be modified because of the heaving motion as illustrated in Fig. 13.3. For example, if it is assumed that the ship is wall sided, the heave-induced increase of buoyancy is expressed as $\rho g A_{WP} z$. Thus the maximum increase occurs when the ship is farthest away from its equilibrium position (i.e., when $z = z_a$).

It should be noted that the areas under the heaved weight and buoyancy curves should be the same and that the centers of gravity and buoyancy must be in the same longitudinal position. Therefore the bending moment during the heaving motion is written as

$$BM = \int \left\{ \iint \left[w(x) \pm \frac{w'}{g}(x)\omega^2 z_a \right] dx \right\} dx - \int \left[\int \rho g A(x)\, dx \right] dx \pm \int \left[\int 2\rho g y(x) z_a\, dx \right] dx \tag{13.8}$$

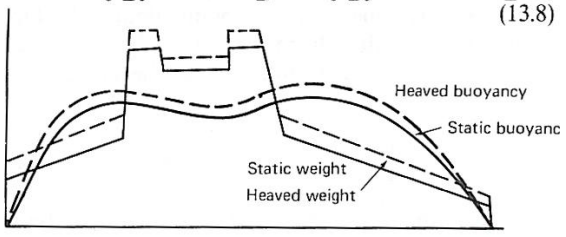


Figure 13.3 Bending moment due to heaving motion in calm water.

where $A(x)$ is the sectional area at point x in the static condition, $y(x)$ is the half-ordinate of the waterplane, and z_a is the amplitude of the heaving motion.

Therefore the change in bending moment due to heaving motion only can be expressed as

$$\delta BM = \int\left(\int \frac{w'}{g}\omega^2 z_a\,dx\right)dx \pm \int\left[\int 2\rho g y(x) z_a\,dx\right]dx \tag{13.9}$$

Bending Moment during Pitching Motion in Calm Water

Every point on a ship is not subject to the same acceleration during pitching motion, as is the case with heaving motion. The vertical acceleration at a point situated at a distance x away from the LCG of the ship is given as

$$x\frac{d^2\theta}{dt^2}$$

where θ is the pitching motion.

For the steady-state condition in a regular seaway the vertical acceleration is given as

$$\begin{aligned} x\frac{d^2\theta}{dt^2} &= -x\omega_e^2\theta \\ &= -x\omega_e^2\cdot\theta_a\sin(\omega_e t - \varepsilon_2) \end{aligned} \tag{13.10}$$

where, from (4.19m),

$$\theta = \theta_a\sin(\omega_e t - \varepsilon_2)$$

The vertical acceleration force for each item during the pitching motion is then

$$\frac{w}{g} \pm \frac{w'}{g} \times \frac{d^2\theta}{dt^2} \tag{13.11}$$

The modified weight curve is then obtained as given in Fig. 13.4.

For the buoyancy distribution during pitching motion the ship is considered to be inclined at an angle θ to the static position; therefore the increased buoyancy at any point (assuming a wall-sided ship) is

$$2\rho g x\theta y(x) \tag{13.12}$$

where $y(x)$ is the half-breadth of the waterplane at position x.

The bending moment is the same as that obtained in the case of heaving motion.

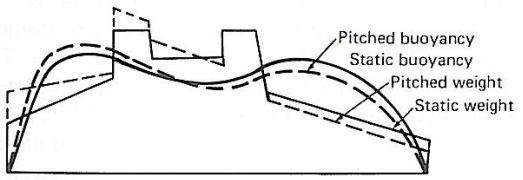


Figure 13.4 Bending moment due to pitching motion in calm water.

13.3 WAVE LOADS IN A REGULAR SEAWAY

In the preceding sections loads due to heaving and pitching motions in calm water were treated separately; however, these two motions occur simultaneously in actual seas, since the waves passing along a ship's hull generate both the exciting force for heaving and the exciting moment for pitching.

In the determination of the bending moment, therefore, the effects due to both heaving and pitching are to be considered simultaneously. In the simplest case the accelerations at any point on the ship can be considered as additive so that, for any given position of the wave, the combined effects can be obtained by adding the acceleration due to heaving and that due to pitching.

Since heaving and pitching motions are not independent of each other, but are coupled together, the theory of coupled motions as given by the strip method of Korvin-Kroukovsky and Jacobs [121] should be followed. The determination of the bending moment requires successive conditions of dynamic equilibrium; thus a complete solution to the problem cannot be found without first determining the motions. As mentioned in Chapter 9 on the strip theory of coupled pitch and heaving motions, it is necessary to determine the hydrodynamic forces and moments, which are obtained in two superimposable parts, namely, those associated with the wave passing a restrained vessel (exciting terms), and those acting on the vessel, which is forced to oscillate in calm water.

The strip theory approach for the determination of hydrodynamic forces and moments enables one to solve the equation of motions and to determine the amplitudes and phase angles of motion. The longitudinal distributions of all forces, including those that are dependent on motions, are calculated for each strip. Integration of the difference between the hydrodynamic and the gravity forces, known as the *load*, gives the shear force, and by a further integration one can determine the bending moment for any particular position of the wave along the ship's length. The shearing forces and bending

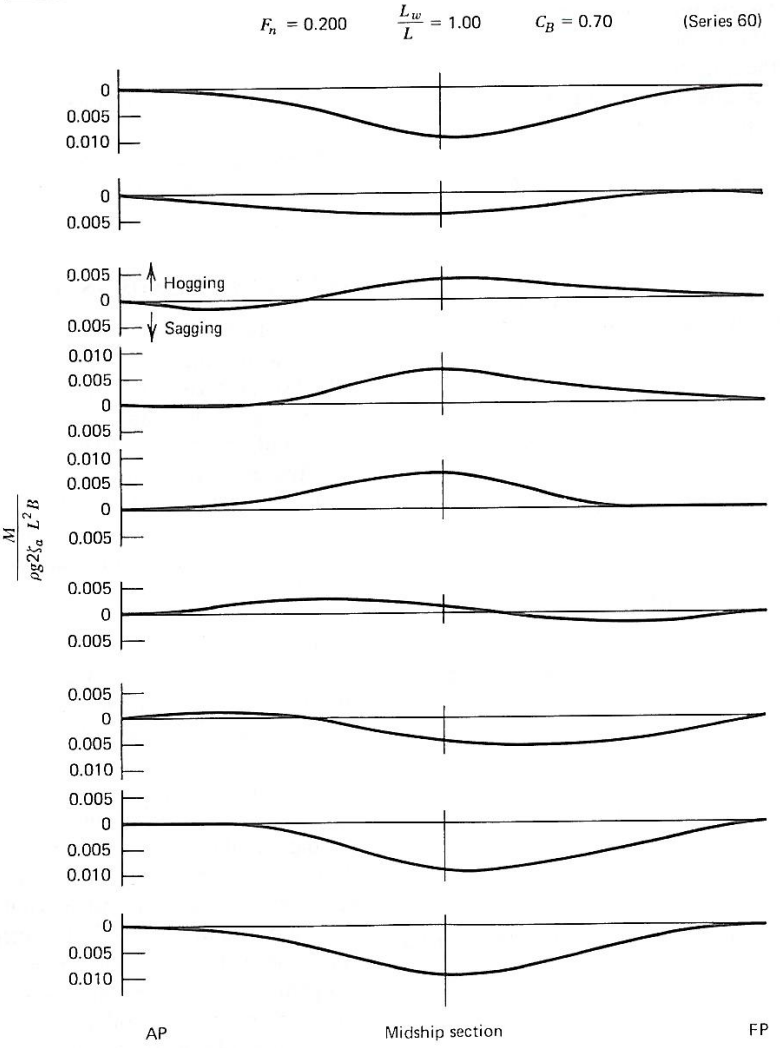


Figure 13.5 Time history of vertical bending moment [46].

moments are generally determined for the midship section for any instant in the motion cycle. The longitudinal bending moment in a regular seaway is a harmonic function of time, as illustrated in Fig. 13.5, where all the curves were obtained during a single run at a particular speed. Therefore midship bending moment can be defined as a function of time as

$$M_w = (M_w)_a \cos(\omega_e t + \beta) \tag{13.13}$$

for the condition where the wave crest is amidships and where the wave motion is expressed as

$$\zeta = \zeta_a \cos \omega_e t$$

It is also necessary to determine by systematic calculations whether the bending moment at any other section can be larger than that at the midship section; thus the computation should be performed on the basis of regular waves of various lengths.

The distribution of the maximum bending moment along the ship's length is shown in Fig. 13.6. The curves represent the envelopes of the bending moment curves occurring over one period. It should be noted that the section in which the hogging moment attains its maximum value is different from the section in which the sagging moment is maximum. However, the location where the maximum hogging or sagging

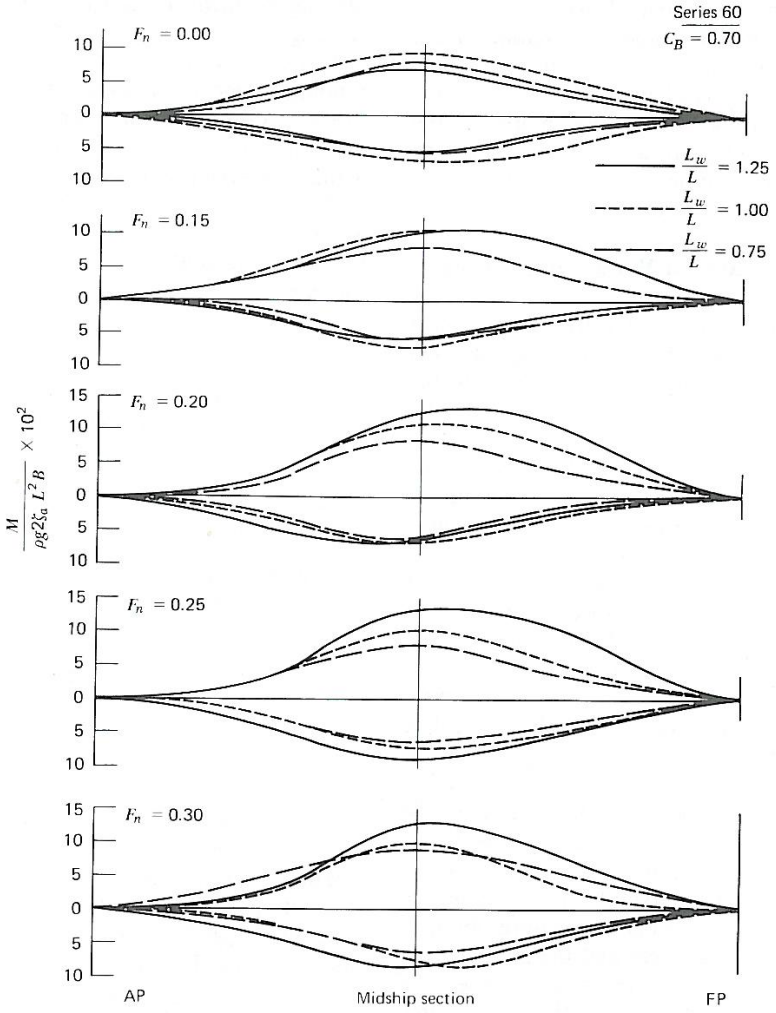


Figure 13.6 Distribution of maximum vertical bending moment in regular head waves [46].

bending moment occurs depends on the ship's speed, as well as the ratio of wavelength to ship length.

The following conclusions can be drawn from both analytical and experimental investigations:

1. There are generally two peaks in the response curve, and these peaks are higher and sharper when the ship's speed is increased and the loads within the ship are so distributed that smaller moments of weight occur in both fore- and afterbodies. On the other hand, when the loads are shifted in fore- and afterbodies, resulting in larger moments of weight in both half-bodies, the response curve has only one peak, which is sharp at higher speeds.

2. When the weight distribution is such that larger moments of weight occur in both fore- and afterbodies, the bending moment in waves is generally smaller. Alternately, when the load distribution gives a hogging bending moment in still water, the bending moment in waves is smaller than the bending moments in the load distribution, which give a sagging bending bending moment in still water.

3. The influence of weight distribution on the bending moment response is dependent to a greater degree on the moments of weight of both fore- and afterbodies than on the radius of gyration. In other words, the moments of weight or the centers of gravity of both fore- and afterbodies are better parameters

for the representation of load distribution than is the radius of gyration. The load distribution giving larger moments of weight in both fore- and afterbodies will give a larger radius of gyration; however, the bending moment response depends more on the moments of weight of both halves of the body and less on the radius of gyration.

Bending Moment in Regular Waves (Strip Theory)

For study of a ship's longitudinal strength, it is most desirable to be able to find the bending moment at any point along the length. An alternative to the standard method of balancing the ship on a trochoidal wave and computing the static bending moment is an extension of the solution of ship's motion by the strip theory of Korvin-Kroukovsky and Jacobs. In using this method one calculates the sinusoidal variation of load with a passing wave in a head sea condition. The amplitudes of the shear force and bending moment and their respective phase lags to the wave exciting force and moment are then obtained by successive integrations. In Chapter 9 the forces acting on a ship in a regular sea were analyzed by the strip method. To be able to calculate the bending moment at any station by using this method, the solution of the equation of motion should be available. For any instant of time, the bending moment is found by determining the longitudinal distribution of the total force. The distribution of both the static and the dynamic forces along the length of the ship (i.e., the load curve) are obtained from the hydrodynamic forces and the mass inertial forces acting at various ship sections, after the motions have been determined. The shear force at any point is obtained by integrating the loading over the length of the ship, while the bending moment at any station is found by integrating the shear force to that station. It should be noted that, if the model is kept restrained, that is, if it does not heave, pitch, or surge, the only forces that affect it are those due to the rise and fall of the waves and to the resulting vertical water velocities and accelerations.

The total load of the ship is a summation of the following [107]:

1. The loading due to uneven distribution of the weight and the buoyancy force in calm water, df_a/dx. This loading is ignored in the calculation here, since only the dynamic forces and moments due to the waves in a seaway are to be considered. These static moments should eventually be added to the dynamic bending moment in order to determine the total bending moment. (It should be noted, however, that this load, which is ignored in the dynamic bending moment consideration, has at any forward speed a value different from that at zero speed, since then a steady wave pattern is formed because of the ship speed in calm water.)

2. The loading caused by the change in buoyancy distribution due to wave pattern and also due to both heaving and pitching motions. The loads in this case are (see Fig. 9.1)

$$\frac{df_b}{dx} = -c_n z_r = -\rho g B_n (z - \xi\theta - \zeta) \tag{13.14}$$

where $c_n = \rho g B_n$.

3. The loading due to the Smith effect, that is, the effect of the pressure gradient in the wave,

$$\frac{df_c}{dx} = -c_n \zeta (1 - e^{-kz}) = -\rho g B_n \zeta (1 - e^{-kz}) \tag{13.15}$$

4. The loading due to the relative water velocity of wave and ship motion,

$$\begin{aligned}\frac{df_d}{dx} &= -b_n w_r + u\frac{da_n}{d\xi} w_r \\ &= \left(-b_n + u\frac{da_n}{d\xi}\right)\left(\dot{z} - \xi\dot{\theta} + u\theta - \dot{\zeta}e^{-kz}\right)\end{aligned} \tag{13.16}$$

The free surface damping effect is given by the first term, whereas the second term is obtained from the development of the potential theory.

5. Lastly, the loading due to inertial forces of the ship mass m_n per unit length, the added mass, and the inertial effect of the water flow in waves. The inertial forces are opposite in direction to the accelerations and are equal to the mass multiplied by the acceleration with opposite sign. Thus

$$\begin{aligned}\frac{df_e}{dx} &= -m_n \ddot{z}_n - a_n \dot{w}_r \\ &= -m_n(\ddot{z} - \xi\ddot{\theta}) - a_n\left(\ddot{z} - \xi\ddot{\theta} + 2u\dot{\theta} - \ddot{\zeta}e^{-kz}\right)\end{aligned} \tag{13.17}$$

The term $a_n \ddot{\zeta} e^{-kz}$ represents the inertial effect of the water flow in waves and arises from the body–wave interference. Finally, the loading is determined by adding all the terms described above as follows:

$$\sum_{i=a}^{e} \frac{df_i}{dx} = -\frac{df}{dx} = m_n \ddot{z}_n + a_n \dot{w}_r + b_n w_r - u\frac{da_n}{d\xi} w_r + c_n z_r \tag{13.17a}$$

where $z_r = z - \xi\theta - \zeta e^{-kz}$ from (9.10)

$$w_r = \frac{dz_r}{dt} = \dot{z} - \xi\dot{\theta} + u\theta - \dot{\zeta}e^{-kz}$$

$$\dot{w}_r = \frac{dw_r}{dt} = \ddot{z} - \xi\ddot{\theta} + 2u\dot{\theta} - \ddot{\zeta}e^{-kz}$$

$$\ddot{z}_n = \ddot{z} - \xi\ddot{\theta} \tag{13.18}$$

Thus

$$\frac{df}{dx} = -m_n(\ddot{z} - \xi\ddot{\theta}) - a_n(\ddot{z} - \xi\ddot{\theta} + 2u\dot{\theta} - \ddot{\zeta}e^{-kz}) - \left(b_n - u\frac{da_n}{d\xi}\right)(\dot{z} - \xi\dot{\theta} + u\theta - \dot{\zeta}e^{-kz}) - \rho g B_n(z - \xi\theta - \zeta e^{-kz}) \tag{13.19}$$

Substituting the values of ζ, $\dot{\zeta}$, and $\ddot{\zeta}$, from (9.15), (9.16) and (9.17), we have

$$\begin{aligned}\frac{df}{dx} &= -m_n(\ddot{z} - \xi\ddot{\theta}) - a_n\Big[\ddot{z} - \xi\ddot{\theta} + 2u\dot{\theta} + \zeta_a\omega_e^2 \times \sin(k\xi - \omega_e t)e^{-kz}\Big] \\ &\quad - \left(b_n - u\frac{da_n}{d\xi}\right)\Big[\dot{z} - \xi\dot{\theta} + u\theta + \zeta_a\omega_e\cos \times (k\xi - \omega_e t)e^{-kz}\Big] \\ &\quad - \rho g B_n\Big[z - \xi\theta - \zeta_a\sin(k\xi - \omega_e t)e^{-kz}\Big] \\ &= -m_n\ddot{z} - a_n\ddot{z} + m_n\xi\ddot{\theta} + a_n\xi\ddot{\theta} - 2u\dot{\theta}a_n \\ &\quad - a_n\zeta_a\omega_e^2\sin(k\xi - \omega_e t)e^{-kz} \\ &\quad - \left(b_n - u\frac{da_n}{d\xi}\right)\left(z + u\theta\right) + \left(b_n - u\frac{da_n}{d\xi}\right)\left(\xi\theta\right) \\ &\quad - \left(b_n - u\frac{da_n}{d\xi}\right)\Big[\zeta_a\omega_e\cos(k\xi - \omega_e t)e^{-kz}\Big] \\ &\quad - \rho g B_n(z) + \rho g B_n(\xi\theta) + \rho g B_n\zeta_a\sin(k\xi - \omega_e t)e^{-kz} \\ &= -(m_n + a_n)\ddot{z} + (m_n + a_n)\xi\ddot{\theta} - 2u\dot{\theta}a_n \\ &\quad - \left(b_n - u\frac{da_n}{d\xi}\right)\left(z + u\theta\right) + \left(b_n - u\frac{da_n}{d\xi}\right)\xi\dot{\theta} \\ &\quad - \rho g B_n z + \rho g B_n(\xi\theta) + \frac{dF}{dx}\end{aligned} \tag{13.20}$$

where dF/dx, the load due to waves, is expressed by (9.21).

The dynamic shear force is then given by integration of the load

$$f(x) = \int_0^x \frac{df}{dx}(x)\,dx \tag{13.21}$$

Equations 13.20 and 13.21 show that the dynamic shear force f is the sum of the hydrodynamic force F due to waves and the forces due to ship motions.

Similarly, the dynamic vertical bending moment is

$$m(x) = \int_0^x f(x)\,dx = m_0\cos(\omega_e t + \beta) \tag{13.22}$$

where m_0 is the amplitude of the bending moment.

Since the heaving displacement is

$$z = z_a\cos(\omega_e t - \delta)$$

or,

$$z = z_a(\cos\omega_e t\cos\delta + \sin\omega_e t\sin\delta)$$

the velocity and acceleration are, respectively,

$$\dot{z} = -\omega_e z_a(\sin\omega_e t\cos\delta - \cos\omega_e t\sin\delta)$$

and

$$\ddot{z} = -\omega_e^2 z_a(\cos\omega_e t\cos\delta + \sin\omega_e t\sin\delta)$$

Similarly, the pitching motion is described by

$$\theta = \theta_a\cos(\omega_e t - \varepsilon)$$

or,

$$\theta = \theta_a(\cos\omega_e t\cos\varepsilon - \sin\omega_e t\sin\varepsilon)$$

from which the velocity and acceleration are

$$\dot{\theta} = -\omega_e\theta_a(\sin\omega_e t\cos\varepsilon - \cos\omega_e t\sin\varepsilon)$$

and

$$\ddot{\theta} = -\omega_e^2\theta_a(\cos\omega_e t\cos\varepsilon + \sin\omega_e t\sin\varepsilon)$$

respectively. Using these relations, we can express the loading described by (13.20) as

$$\frac{df}{dx} = \frac{df_1}{dx}\cos\omega_e t + \frac{df_2}{dx}\sin\omega_e t \tag{13.23}$$

where

$$\begin{aligned}\frac{df_1}{dx} &= (m_n + a_n)(\omega_e^2 z_a\cos\delta - \omega_e^2\xi\theta_a\cos\varepsilon) \\ &\quad - a_n(2u\omega_e\theta_a\sin\varepsilon) \\ &\quad - \left(b_n - u\frac{da_n}{d\xi}\right)\Big(\omega_e z_a\sin\delta - \omega_e\xi\theta_a\sin\varepsilon + u\theta_a\cos\varepsilon\Big) \\ &\quad - \rho g B_n(z_a\cos\delta - \xi\theta_a\cos\varepsilon) + \frac{dF_1}{dx}\end{aligned} \tag{13.24a}$$

and

$$\begin{aligned}\frac{df_2}{dx} &= (m_n + a_n)(\omega_e^2 z_a\sin\delta - \omega_e^2\xi\theta_a\sin\varepsilon) \\ &\quad + a_n(2u\omega_e\theta_a\cos\varepsilon)\end{aligned}$$

$$+\left(b_n - u\frac{da_n}{d\xi}\right)\left(\omega_e z_a \cos\delta - \omega_e \xi\theta_a \cos\varepsilon - u\theta_a \sin\varepsilon\right)$$

$$-\rho g B_n(z_a \sin\delta - \xi\theta_a \sin\varepsilon) + \frac{dF_2}{dx} \qquad (13.24b)$$

where dF_1/dx and dF_2/dx represent the exciting forces consisting of the wave elevation terms only, as given in (9.21a) and (9.21b).

Like the exciting forces, both the shear force and the bending moment are sinusoidal. Thus we can write

$$f = f_1 \cos\omega_e t + f_2 \sin\omega_e t = f_0 \cos(\omega_e t + \alpha) \qquad (13.24c)$$

where f_0 is the amplitude of the shear force. Comparing (13.24c) with (13.23), we see that,

$$f_1 = f_0 \cos\omega_e t, \qquad f_2 = f_0 \sin\omega_e t$$

and

$$\alpha = -\tan^{-1}\left(\frac{f_2}{f_1}\right)$$

where

$$f_1 = \int \frac{df_1}{dx}\,dx, \qquad f_2 = \int \frac{df_2}{dx}\,dx$$

and the force amplitude is

$$f_0 = \sqrt{f_1^2 + f_2^2} \qquad (13.24d)$$

Similarly, the bending moment is

$$m = m_0 \cos(\omega_e t + \beta) \qquad (13.25a)$$

where m_0 is the amplitude of the bending moment, that is,

$$m_0 = \sqrt{m_1^2 + m_2^2} \qquad (13.25b)$$

and

$$\beta = -\tan^{-1}\left(\frac{m_2}{m_1}\right) \qquad (13.25c)$$

Thus

$$m_1 = \int \frac{dm_1}{dx}\,dx = m_0 \cos\omega_e t$$

where

$$\frac{dm_1}{dx} = l \times \frac{df_1}{dx} \qquad (13.26)$$

l being the lever of the force from the section at which BM is to be determined. Similarly,

$$m_2 = \int \frac{dm_2}{dx}\,dx = m_0 \sin(\omega_e t) \qquad (13.27)$$

and

$$\frac{dm_2}{dx} = l \times \frac{df_2}{dx}$$

where the positive bending moment is in the clockwise direction.

It should be pointed out that through the same process the bending moment at any point can be found simply by integrating the shear force moments upto that point. The bending moment so determined can be termed the *seaway bending moment*. The effect of the imbalance due to the initial distribution of weights and buoyancy in still water, as mentioned in item 1 above, should be determined separately and then added to the wave effects (considering both ship-generated waves at speed in calm water and the seaway effect) in order to obtain the total bending moment in a seaway. As mentioned in Section 9.3 for heaving and pitching motions, the method of determination of the wave bending moment can be applied also for oblique seas if the wavelength L_w is replaced everywhere by the effective wavelength L'_w, defined as

$$L'_w = \left|\frac{L_w}{\cos\mu}\right|$$

where μ is the direction of ship travel relative to the waves. There are some discrepancies between the calculated and the experimental bending moment results, and these can be attributed mainly to the following:

a. The difference between the two-dimensional flow (as assumed by the strip theory) and the actual three-dimensional flow, especially at both ends of the ship. The interference effects between the adjacent cross sections may be significant for certain frequency ranges.

b. The assumption that the coefficients of motion do not change throughout the motion cycle.

Example 13.1

Calculate the seaway (regular) bending moment at the midship section of a ship model described by the following data;

Length of model	$L_m = 19.2$ ft
Maximum beam	$B_{max} = 2.592$ ft
Draft	$T = 1.144$ ft
Displacement	$\Delta = 2837.76$ lb

TABLE 13.2

Station No.	B_n [ft]	T_n [ft]	S_n [ft^2]	Weight per Foot [lb/ft]	a_n [lb-sec^2/ft^2]
0	0	1.144	0	29.95	0
5	2.592	1.144	2.944	184.18	5.009
10	2.592	1.144	2.944	189.01	5.009
15	2.592	1.144	2.752	155.20	4.293
20	0	1.144	0	21.57	0

$LCG = +0.48$ ft (forward of ⊗)
Model speed $u = 4.788$ ft/sec
$\omega_e = 4.811$ rad/sec
$\rho = 1.9384$ lb-sec^2/ft^4 in fresh water at 59°F

The values for breadth, draft of individual sections, sectional areas, weight distribution, and added mass (from Fig. 4.4) for various stations are given in Table 13.2 (see also Section 9.4).

In addition, the following data are available

TABLE 13.3 CALCULATION OF THE WAVE BENDING MOMENT [109]

Station No.	ξ [ft]	l_1 [ft]	Weight per foot [lb/ft]	m_n [lb-sec^2/ft^2]	a_n [lb-sec^2/ft^2]	$m_n + a_n$ [lb-sec^2/ft^2]	$c_n = \rho g B_n$	$b_n - u\frac{da_n}{d\xi}$	$(m_n + a_n)\xi$	$c_n\xi$
①	②	③	④	⑤	⑥	⑦	⑧	⑨	⑩	⑪
0	9.12	9.6	29.95	0.93	0	0.93	0	4.99	8.482	0
5	4.32	4.8	184.18	5.72	5.009	10.729	161.78	8.36	46.349	698.89
10	− 0.48	0.0	189.01	5.87	5.009	10.879	161.78	5.15	− 5.222	− 77.65
15	− 5.28	− 4.8	155.20	4.82	4.293	9.113	161.78	5.37	− 48.117	− 854.20
20	− 10.08	− 9.6	21.57	0.67	0	0.67	0	− 4.28	− 6.754	... 0

$\left(b_n - u\frac{da_n}{d\xi}\right)\xi$ ⑫	$\omega_e^2 z_a \cos\delta \times$ ⑦ $= 0.0008 \times$ ⑦ ⑬	$\omega_e^2\theta_a \cos\varepsilon \times$ ⑩ $= -0.4209 \times$ ⑩ ⑭	$2\omega_e u\theta_a \sin\varepsilon \times$ ⑥ $= 0.0231 \times$ ⑥ ⑮	$z_a \cos\delta \times$ ⑧ $= 3.434 \times 10^{-5}$ ⑯
45.509	0.739×10^{-3}	− 3.570	0	0
36.115	8.528×10^{-3}	− 19.508	+ 0.116	$+ 5.556 \times 10^{-3}$
− 2.472	8.647×10^{-3}	2.198	0.116	5.556×10^{-3}
− 28.354	7.243×10^{-3}	20.252	0.099	5.556×10^{-3}
43.142	0.532×10^{-3}	2.843	0	0

$\theta_a \cos\varepsilon \times$ ⑪ $= -0.0182 \times$ ⑪ ⑰	$(\omega_2 z_a \sin\delta + u\theta_a \cos\varepsilon) \times$ ⑨ $= -0.2764 \times$ ⑨ ⑱	$\omega_e\theta_a \sin\varepsilon \times$ ⑫ $= 2.413 \times 10^{-3} \times$ ⑫ ⑲	$\frac{dF_1}{dx}$ ⑳
0	− 1.3792	0.110	− 4.742
− 12.708	− 2.3107	0.087	7.109
1.412	− 1.4235	− 0.006	2.620
15.532	− 1.4843	− 0.068	− 9.319
0	1.1830	0.104	4.065

$\frac{df_1}{dx}$ ㉑	Simpson's Multiplier ㉒	Product ㉑ × ㉒ ㉓	$l\frac{df_1}{dx}$ ㉔	Simpson's Multiplier ㉕	Product ㉔ × ㉕ ㉖	$\omega_e^2 z_a \sin\delta \times$ ⑦ $= -0.9108 \times$ ⑦ ㉗
0.318	1	0.318	3.053	1	3.053	− 0.847
16.194	4	64.776	77.731	4	310.924	− 9.772
3.139	2	6.278	0	2	0	− 9.908
− 12.720	4	− 50.880	61.056	4	244.224	− 8.300
0.144	1	0.144	− 1.382	1	− 1.382	− 0.610
	SUM_1	20.636		SUM_2	556.819	

TABLE 13.3 *(Continued)*

$\omega_e^2\theta_a \sin\varepsilon \times$ ⑩ $= 0.0116 \times$ ⑩ ㉘	$2\omega_e u\theta_a \cos\varepsilon \times$ ⑥ $= -0.8377 \times$ ⑥ ㉙	$z_a \sin\delta \times$ ⑧ $= -0.0393 \times$ ⑧ ㉚	$\theta_a \sin\varepsilon \times$ ⑪ $= 5.0155 \times 10^{-4} \times$ ⑪ ㉛
0.098	0	0	0
0.538	−4.196	−6.358	0.351
−0.061	−4.196	−6.358	−0.039
−0.559	−3.596	−6.358	−0.428
−0.078	0	0	0

$(\omega_e z_a \cos\delta - u\theta_a \sin\varepsilon) \times$ ⑨ $= -0.00224 \times$ ⑨ ㉜	$\omega_e\theta_a \cos\varepsilon \times$ ⑫ $= -0.0875 \times$ ⑫ ㉝	$\frac{dF_2}{dx}$ ㉞	$\frac{df_2}{dx}$ ㉟	Simpson's Multiplier ㊱	Product ㉟ × ㊱ ㊲
−0.011	−3.981	−0.760	2.265	1	2.265
−0.019	−3.159	−4.488	−9.145	4	−36.580
−0.012	0.216	6.787	−1.165	2	−2.330
−0.012	2.480	2.240	−5.659	4	−22.636
0.010	−3.774	0.651	3.903	1	3.903
				SUM_3	55.378

$l\frac{df_2}{dx}$ ㊳	Simpson's Multiplier ㊴	Product ㊳ × ㊴ ㊵
21.744	1	21.744
−43.896	4	−175.584
0	2	0
27.163	4	108.652
−37.469	1	−37.469
	SUM_4	82.657

Description of Table 13.3

Column Number	*Description*
①	Station Number
②	Lever Arm, ξ [ft], distance from LCG, positive forward
③	Distance from Station 10, l [ft]
④	Weight per Unit Length (average weight over interval $\xi - \Delta\xi/2$ to $\xi + \Delta\xi/2$)
⑤ = ④/32.2	Mass per Unit Length, m_n
⑥ = ⑬ of Table 9.1	Sectional Added Mass, a_n
⑦ = ⑤ + ⑥	Sectional Virtual Mass, $m_n + a_n$
⑧ = ③ of Table 9.3	Sectional Restoring Force Coefficient, c_n
⑨ = ⑦ Table 9.2 $- u \times$ ⑭ Table 9.6	$b_n - u\frac{da_n}{d\xi}$
⑩ = ⑦ × ②	$(m_n + a_n)\xi$
⑪ = ⑧ × ②	$c_n \times \xi$
⑫ = ⑨ × ②	$\left(b_n - u\frac{da_n}{d\xi}\right)\xi$
⑬ = $(\omega_e^2 z_a \cos\delta) \times$ ⑦	$(\omega_e^2 z_a \cos\delta) \times (m_n + a_n)$
⑭ = $(\omega_e^2\theta_a \cos\varepsilon) \times$ ⑩	$(\omega_e^2\theta_a \cos\varepsilon) \times (m_n + a_n)\xi$
⑮ = $(2\omega_e u\theta_a \sin\varepsilon) \times$ ⑥	$(2\omega_e u\theta_a \sin\varepsilon) \times a_n$
⑯ = $(z_a \cos\delta) \times$ ⑧	$(z_a \cos\delta) \times c_n$
⑰ = $(\theta_a \cos\varepsilon) \times$ ⑪	$(\theta_a \cos\varepsilon) \times (c_n \times \xi)$
⑱ = $(\omega_e z_a \sin\delta + u\theta_a \cos\varepsilon) \times$ ⑨	$(\omega_e z_a \sin\delta + u\theta_a \cos\varepsilon) \times \left(b_n - u\frac{da_n}{d\xi}\right)$

Column Number	*Description*
⑲ = $(\omega_e\theta_a \sin\varepsilon) \times$ ⑫	$(\omega_e\theta_a \sin\varepsilon) \times \left(b_n - u\dfrac{da_n}{d\xi}\right)\xi$
⑳ = ㉔ of Table 9.6	$\dfrac{dF_1}{dx}$
㉑ = ⑬ − ⑭ − ⑮ − ⑯ + ⑰ − ⑱ + ⑲ + ⑳	$\dfrac{df_1}{dx}$
㉒	Simpson's Multiplier
㉓ = ㉑ × ㉒	Product
㉔ = ③ × ㉑	$\dfrac{dm_1}{dx}$
㉕	Simpson's Multiplier
㉖ = ㉔ × ㉕	Product
㉗ = $(\omega_e^2 z_a \sin\delta) \times$ ⑦	$(\omega_e^2 z_a \sin\delta) \times (m_n + a_n)$
㉘ = $(\omega_e^2\theta_a \sin\varepsilon) \times$ ⑩	$(\omega_e^2\theta_a \sin\varepsilon) \times (m_n + a_n)\xi$
㉙ = $(2\omega_e u\theta_a \cos\varepsilon) \times$ ⑥	$(2\omega_e u\theta_a \cos\varepsilon) \times a_n$
㉚ = $(z_a \sin\delta) \times$ ⑧	$(z_a \sin\delta) \times c_n$
㉛ = $(\theta_a \sin\varepsilon) \times$ ⑪	$(\theta_a \sin\varepsilon) \times (c_n \times \xi)$
㉜ = $(\omega_e z_a \cos\delta - u\theta_a \sin\varepsilon) \times$ ⑨	$(\omega_e z_a \cos\delta - u\theta_a \sin\varepsilon) \times \left(b_n - u\dfrac{da_n}{d\xi}\right)$
㉝ $(\omega_e\theta_a \cos\varepsilon) \times$ ⑫	$(\omega_e\theta_a \cos\varepsilon) \times \left(b_n - \dfrac{da_n}{d\xi}\right)\xi$
㉞ ㉗ of Table 9.6	$\dfrac{dF_2}{dx}$
㉟ = ㉗ − ㉘ + ㉙ − ㉚ + ㉛ + ㉜ − ㉝ + ㉞	Total Loading on Each Strip, $\dfrac{df_2}{dx}$
㊱	Simpson's Multiplier
㊲ = ㉟ × ㊱	Product
㊳ = ③ × ㉟	$\dfrac{dm_2}{dx}$
㊴	Simpson's Multiplier
㊵ = ㊳ × ㊴	Product

regarding heaving and pitching motions:

Heaving amplitude	$z_a = 0.03935$ ft
Pitching amplitude	$\theta_a = 0.01819$ rad
Heave phase angle	$\delta = -89.95°$
Pitch phase angle	$\varepsilon = 178.42°$

Note that both phase angles are relative to the wave mode at the CG of the vessel.

Solution:

The calculations for the shear force and bending moment due to regular waves are performed by following (13.21) through (13.27), as shown in Table 13.3, which is based on Ref. 109.

From the tabulated values one obtains the following:

$f_1 = \frac{1}{3} \times 4.8 \times \text{SUM}_1$
$= \frac{1}{3} \times 4.8 \times 20.636$
$= 33.018$ lb

$m_1 = \frac{1}{3} \times 4.8 \times \text{SUM}_2$
$= \frac{1}{3} \times 4.8 \times 556.819$
$= 890.910$ ft-lb

$f_2 = \frac{1}{3} \times 4.8 \times \text{SUM}_3$
$= \frac{1}{3} \times 4.8 \times (-55.378)$
$= -88.605$ lb

$m_2 = \frac{1}{3} \times 4.8 \times \text{SUM}_4$
$= \frac{1}{3} \times 4.8 \times (-82.657)$
$= -132.251$ ft-lb

The force amplitude of (13.24d) is

$$f_0 = \sqrt{f_1^2 + f_2^2} = 94.557 \text{ lb}$$

Furthermore,

$$f_1 = f_0 \cos\alpha$$

or

$$33.018 = 94.557 \cos\alpha$$

and

$$f_2 = f_0 \sin\alpha$$

or

$$-88.605 = 94.557 \sin\alpha$$

Thus

$$\alpha = -69.56°$$

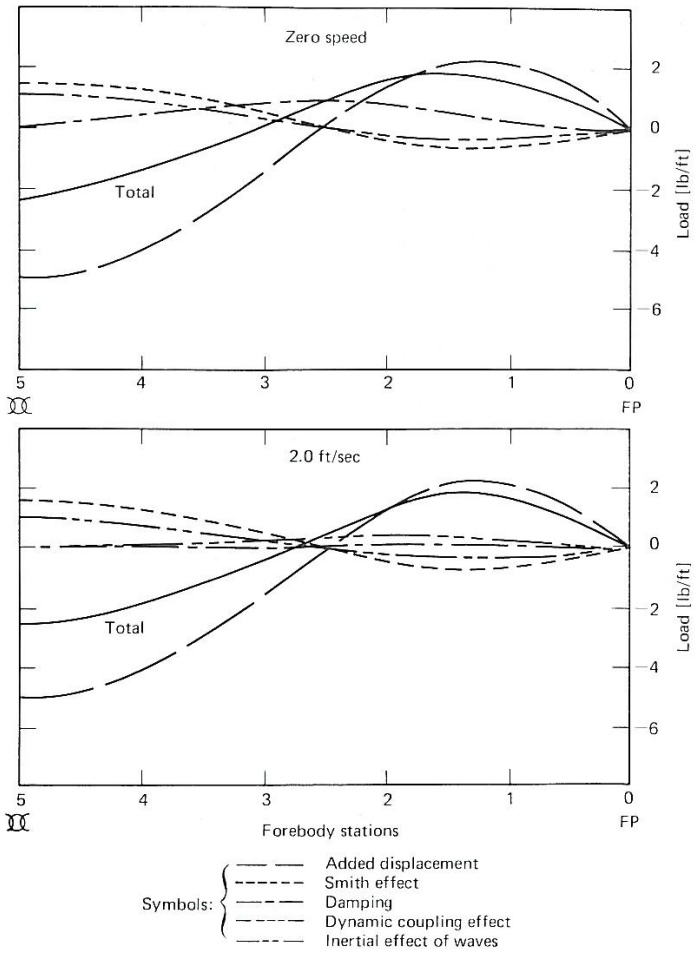


Figure 13.7 Typical example of loads on restrained model [107].

and the shear force is

$$f = f_0 \cos(\omega_e t + \alpha)$$
$$= 94.557 \cos(\omega_e t - 69.56) \text{ lb}$$

Similarly, the amplitude of the bending moment of (13.25b) is

$$m_0 = \sqrt{m_1^2 + m_2^2} = 900.673 \text{ ft-lb}$$

Furthermore,

$$m_1 = m_0 \cos \beta$$

or

$$890.910 = 900.673 \cos \beta$$

and

$$m_2 = m_0 \sin \beta$$

or

$$-132.251 = 900.673 \sin \beta$$

Thus

$$\beta = -8.44°$$

and the bending moment as a function of time is [from (13.25a)]

$$m = m_0 \cos(\omega_e t + \beta) = 900.673 \cos(\omega_e t - 8.44°)$$

In the case of a restrained model (no heaving, pitching, or surging motion) the forces acting on the model are only those due to the rise and fall of the waves, the vertical water velocities, and the relative accelerations. Such load curves are shown in Fig. 13.7.

Figure 13.8 shows the calculated as well as the measured curves of bending moments at the midship section of the restrained model.

Table 13.4 presents the theoretical and experimental results for a 4.8 ft model [107].

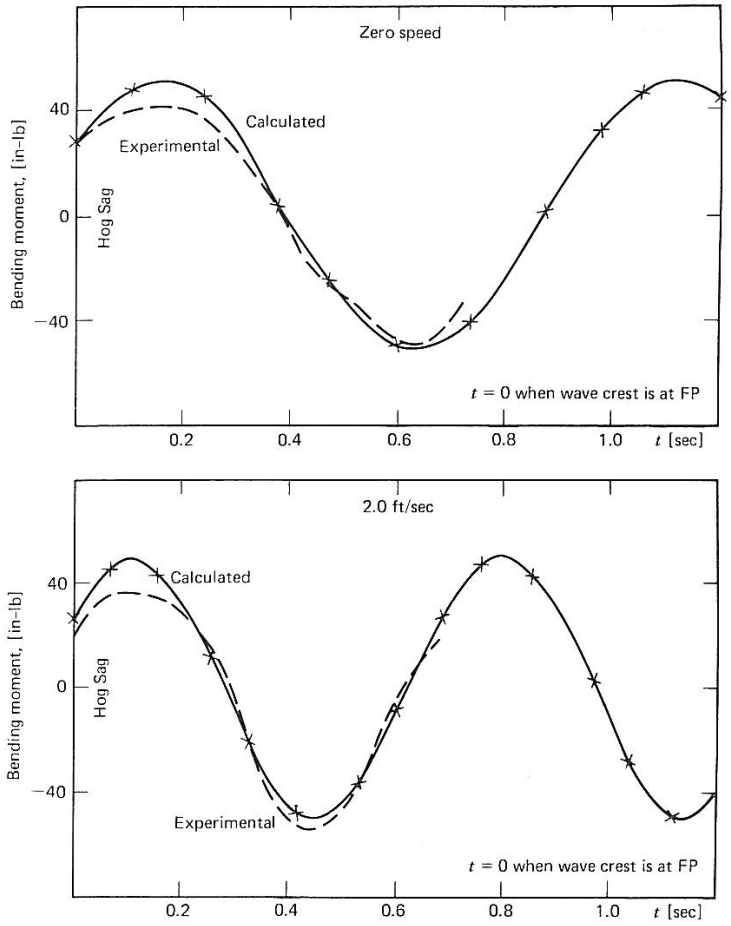


Figure 13.8 Comparison of calculated and measured bending moments for a restrained model [107].

TABLE 13.4

Model Speed [ft-sec]	Total Range of Bending Moment [lb/ft]	
	Calculated	Measured
0	101	89
2	100	88

In the table the total range of bending moments is given instead of the maximum hogging and sagging moments, because the zero line cannot be determined with certainty in either model tests or full-scale trials. It should be noted, however, that the steady wave pattern formed by the forward motion of the ship would affect the hogging and sagging moments without changing the total range.

Figures 13.9 and 13.10 show the load curves obtained by computation for a free-running model, with the wave crests at the forward and after perpendiculars. It is seen that the predominant loads, the mass inertia load, and the hydrodynamic load tend to oppose each other. Thus it can justifiably be stated that the bending moment is a second order effect and is rather sensitive to small changes in weight distribution because of the mass acceleration effects. Therefore, in the determination of the bending moment, the weight distribution should be obtained with care.

Both theoretical and experimental determinations of wave bending moments show two peaks in the midship wave bending moment response curve at two values of wavelength/LBP (length between perpendiculars), when the weight distribution is such

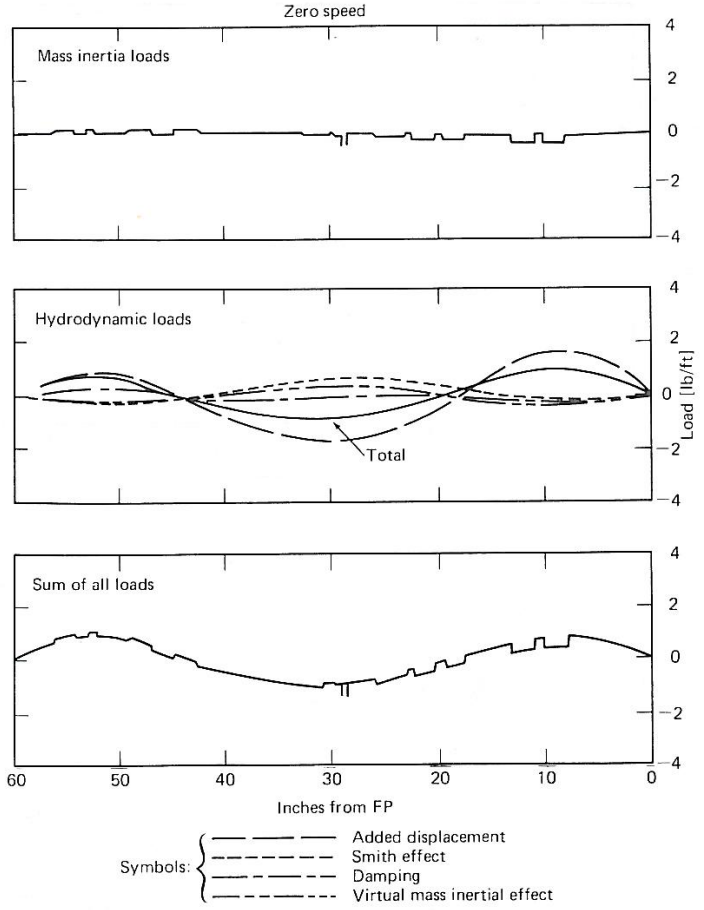


Figure 13.9 Typical example of loads on a free model at zero speed [107].

as to give small moments of weight in the fore- and afterbodies. There is, however, only one peak where the moments of weight in both halves are increased. It should be emphasized that the first moments of weight distribution for the determination of the bending moment about midship are more important than the radius of gyration.

Experiments have been conducted to determine the effect of the distribution of weight in each half of the body on the bending moment response curve while the radius of gyration is kept constant [160]. It was found that the increase in measured seaway bending moment is due almost completely to the reduction in the moments of weight in each half of the model.

Theoretically, the wave bending moment in regular waves can be calculated by summing the various hydrodynamic moments and the moments of the inertial forces due to the model mass.

The wave bending moment amidship calculated by summing the moments over the forebody will be the same as that obtained from the summation over the afterbody.

The seaway bending moment coefficient m_w can be expressed as

$$m_w = I_A + H_A = I_F + H_F \tag{13.28}$$

where

I_A = inertia moment coefficient for the afterbody
H_A = hydrodynamic moment coefficient for the afterbody
I_F = inertial moment coefficient for the forebody
H_F = hydrodynamic moment coefficient for the forebody

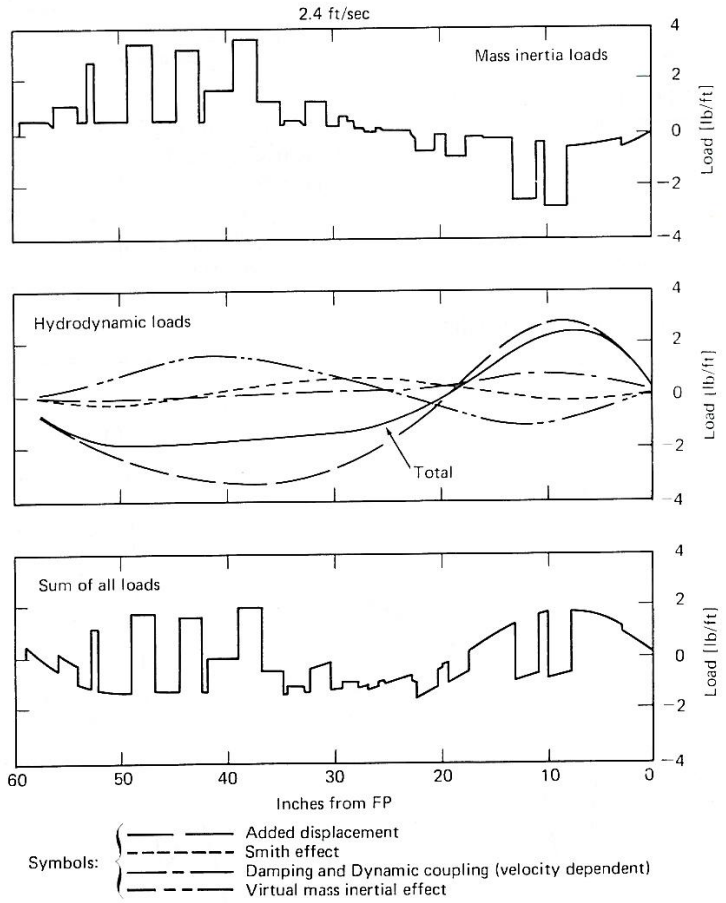


Figure 13.10 Typical example of loads on a free model at speed [107].

Thus one can also write

$$m_w - \tfrac{1}{2}(I_A + I_F) = \tfrac{1}{2}(H_A + H_F) \qquad (13.29)$$

Equation 13.29 enables one to calculate the mean hydrodynamic moment from measurements of the wave bending moment and the inertial part of the bending moment.

Inertial Bending Moment

If the pitching and heaving motions of the hull are simple harmonic, the vertical motion of a point P at a distance x from midship is given by

$$z_x(x) = z_{ax}(x)\cos(\omega_e t - \delta) \qquad (13.30)$$

where the amplitude is

$$z_{ax}(x) = (z_a \cos\varepsilon + x'\theta_a)^2 + (z_a \sin\varepsilon)^2 \qquad (13.31)$$

and

$$\delta = \tan^{-1}\left(\frac{z_a \sin\varepsilon}{z_a \cos\varepsilon + x'\theta_a}\right) \qquad (13.32)$$

where x' is the distance of P from the LCG (distance forward, considered as positive) when the heave is measured at the LCG, δ is the phase of maximum $z_x(x)$ after maximum pitch, and ε is the phase of maximum heave after pitch.

The acceleration at P is then

$$\ddot{z}_x(x) = -z_{ax}(x)\omega_e^2 \cos(\omega_e t - \delta) \qquad (13.33)$$

At the instant of wave crest at midship the acceleration at P becomes

$$\ddot{z}_x(x) = -z_{ax}(x)\omega_e^2 \cos(-\alpha - \delta) \qquad (13.34)$$

where α is the phase between the maximum pitch and the wave crest at midship.

The inertial force is then

$$F(x) = -m(x) \times \ddot{z}_x(x)$$

where $m(x)$ is the mass at position x from midship.

Thus the bending moment due to all the inertial forces is

$$M_i = \Sigma[|x|m(x)\ddot{z}_x(x)] \tag{13.35}$$

where the modulus and the change in sign give the hogging moments as positive for both the fore- and the afterbodies.

Now the inertial bending moment coefficients are obtained from the following expression:

$$I_A, I_F = \frac{1}{2\rho g L^2 B \zeta_a} \cdot \sum^{1/2LBP} [|x|m(x)\ddot{z}_x(x)] \tag{13.36}$$

where the subscripts A and F refer to "aft" and "forward," respectively.

Therefore I_A and I_F can be calculated, and the hydrodynamic bending moment can be determined from (13.29) and compared with the value obtained by the strip theory.

Curves of mean inertial and hydrodynamic bending moments, together with the wave bending moment at the instant of wave crest at midship, are plotted

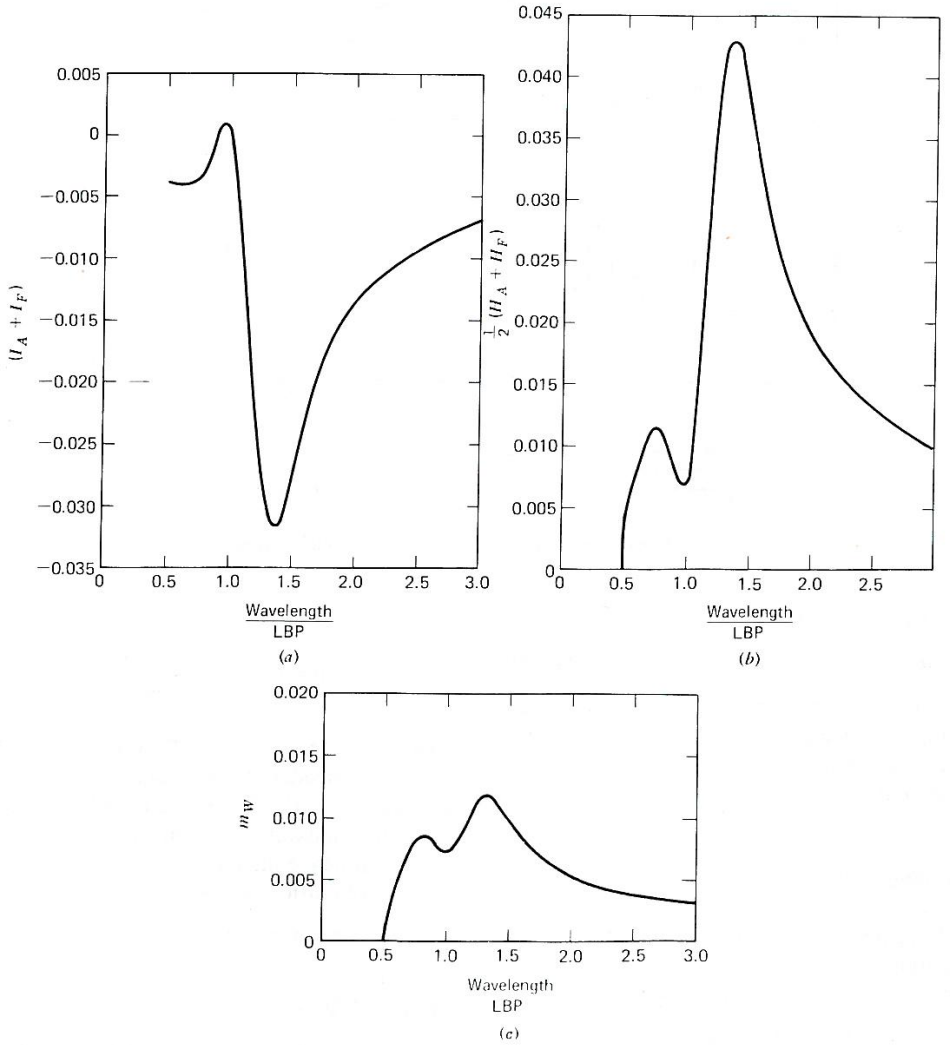


Figure 13.11 Bending moment coefficients as a function of wavelength to ship length ratios [159]. (*a*) Mean inertial bending moment. (*b*) Mean hydrodynamic bending moment. (*c*) Wave bending moment.

in Fig. 13.11 [160]. By comparing Figs. 13.11*a* and 13.11*c*, it is seen that the calculated mean inertial bending moment coefficient $\frac{1}{2}(I_A + I_F)$ is generally opposite in sign to the wave bending moment and is almost three times greater in magnitude.

This verifies the inference that the wave bending moment is a second order effect and depends on the sum of two opposite groups of forces of the same order of magnitude (i.e., the inertial and hydrodynamic forces of opposite sign). Therefore a small error in the computation of any one of these two forces may cause, as said before, a large difference in the wave bending moment. This should be an important consideration when the analytically determined bending moment is compared with the value obtained from experimentation. In any case an exact weight distribution is essential for the accurate prediction of the wave bending moment. Although the peak of the wave bending moment does not occur exactly at the maximum value of pitch or heave, since the wave bending moment is a function of both these motions and the weight distribution integrated over the length of the vessel, the location of the peak may be taken to be in the same region as that of the greatest motions.

Two peaks are found in the wave bending moment response curve when the weight distribution is such as to give the minimum inertial bending moment. There is only one peak when the distribution of weight is changed so as to increase the inertial bending moment.

One peak of the bending moment response curve occurs at approximately $L_w/L = 0.8$ and is caused by the combination of maximum inertial bending moment and minimum hydrodynamic bending moment. The second peak occurs at approximately $L_w/L = 1.4$, when the pitching and heaving motions are largest.

It has been shown [160] that the general shapes of the bending moment coefficient curves are in good agreement with the model results, although the theory overestimates the peak at about $L_w/L = 0.8$, and underestimates it at $L_w/L = 1.4$. The theoretical phase angles are also in fair agreement for $L_w/L > 1.0$ but do not agree well for $L_w/L < 1.0$ (i.e., for short waves).

The fact that reduction in the moments of weight in each half of the model increases the bending moment due to waves contributes to the following conclusions [5]:

1. For a general cargo ship which is always in the hogging condition (i.e., the moment of weights in each half of the ship does not vary significantly from the medium loaded to the deeply loaded condition), the wave bending moment remains approximately the same for a given sea state in both loading conditions.
2. For a large ore carrier which is in a hogging condition when in ballast and in a sagging condition when fully loaded, the moment of weights in each half is large in ballast and small under full load. Therefore the wave bending moment is smaller in the ballast condition than when the carrier is fully loaded.

The amplitude of the seaway bending moment is often expressed nondimensionally as

$$m_w = \frac{(M_w)_a}{2\rho g L^2 B \zeta_a} \tag{13.37}$$

13.4 LOADS IN IRREGULAR WAVES

To determine the longitudinal bending moment it is necessary to consider both static and dynamic effects. In regular waves these are comparatively easy to deal with, however, as stated in Chapter 6, one should deal with realistic sea conditions, where the total response of a vessel in an irregular seaway is the sum of the responses to the individual components. As in the case of motions, the bending moment in waves is regarded as a linear function of wave height, and the dynamic bending moment for the ship is also the sum of the bending moments due to the individual components of the irregular wave systems, that is, both the irregular waves and the bending moment can be considered as the sum of many sinusoidal functions.

There are several ways to determine the bending moment spectrum for a ship at sea. One method is to use statical strain gauges, which make it possible to obtain directly the spectrum of the bending moment for the ship. This spectrum can easily be referred to the sea state, for which can also be taken simultaneously.

A second approach is to first conduct model experiments in regular waves of varying frequencies in order to obtain the response amplitude operator (RAO). Then the linear superposition technique can be used to obtain the response spectrum, as in the case of motions, since the bending moment is also considered linearly proportional to the wave amplitude. It is also possible to estimate the RAO from the equations given in Ref. 154 for various types of ship forms. (See also Chapter 16)

A third method is to apply the strip theory for the calculation of bending moments for all wavelengths and ship headings. By applying RAOs to the wave spectrum, it is then possible to get the bending moment spectrum of the ship for the corresponding sea condition.

For an illustration, consider the following example.

Example 13.2

Calculate the significant longitudinal hogging bending moment, $(BM)_{1/3}$, of a 1000 ft ship steaming at a speed of 17.00 knots (i.e., $V/\sqrt{L} = 0.538$) into an irregular seaway caused by a wind speed of 31 knots (i.e., the significant wave height is 18.5 ft). The heading angle μ of the ship relative to the dominant waves is 180°. The model particulars of this ship are given in Example 9.1.

Solution:

The calculations are performed in very much the same manner as in the case of motion predictions. The wave spectrum for a significant wave height of 18.5 ft is obtained by the ITTC formulation for the wave spectrum, as shown in Example 5.4.

The encountering wave spectrum is obtained by the following relationships. From (6.3) the frequency of encounter is

$$\omega_e = \omega_w(1 - \eta)$$

where

$$\eta = \frac{\omega_w V}{g} \cos \mu$$

and

$$S(\omega_e) = S(\omega_w) \frac{1}{[1 - (4\omega_e V/g) \cos \mu]^{1/2}}$$

is the spectral density from (6.5a).

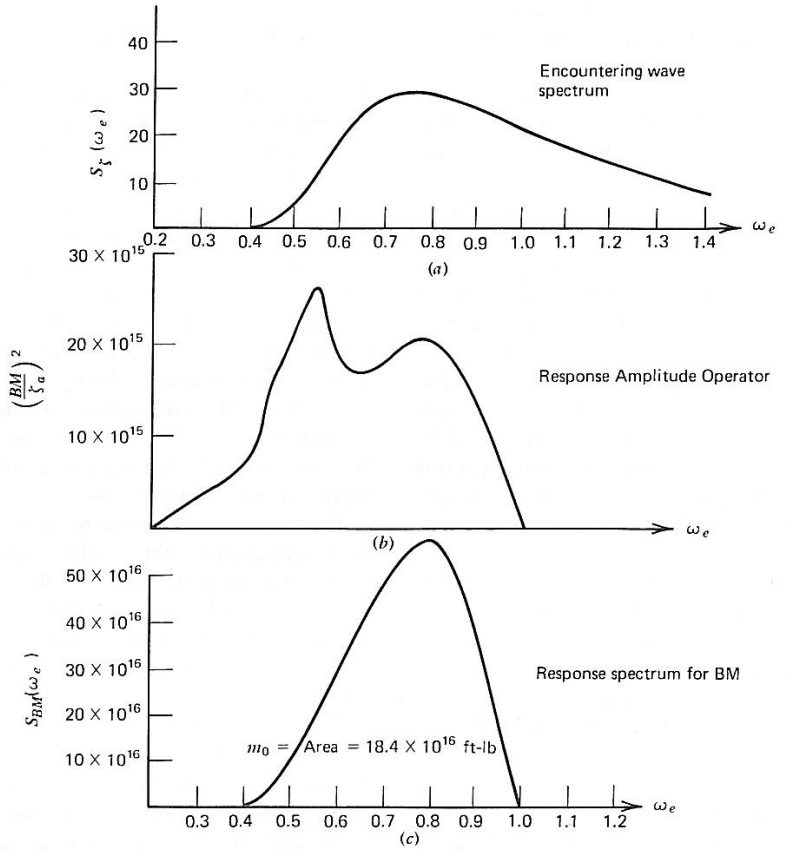


Figure 13.12 Prediction of bending moment in an irregular seaway. (*a*) Encountering wave spectrum. (*b*) Response amplitude operator. (*c*) Response spectrum for bending moment.

TABLE 13.5

ω_w [sec^{-1}] ①	$S(\omega_w)$ [ft^2-sec] ②	ω_e [sec^{-1}] ③	$S(\omega_e)$ [ft^2-sec] ④
0.2	0	0.24	0
0.3	0.02	0.38	0.01
0.4	17.80	0.54	10.41
0.5	55.97	0.72	29.63
0.6	50.68	0.92	24.49
0.7	33.22	1.14	14.76
0.8	20.17	1.37	8.31
0.9	12.25	1.62	4.71
1.0	7.61	1.89	2.74
1.1	4.88	2.18	1.65
1.2	3.22	2.48	1.03
1.3	2.19	2.81	0.66
1.4	1.52	3.15	0.43
1.5	1.09	3.51	0.30

For $V = 17.00$ knots and $\mu = 180°$, the modified spectrum is shown in Fig. 13.12 and the data are presented in Table 13.5.

Figure 13.12*a* shows the encountering wave spectrum $S_\zeta(\omega_e)$. Next, the response amplitude operator $(BM_a/\zeta_a)^2$ is obtained by using the prediction equations for the head seas. See Example 16.2 for estimating the wave bending moment.

The seaway bending moment for a ship traveling in a seaway is obtained from (13.37):

$$(M_w)_a = m_w 2\rho g L^2 B \zeta_a$$

Thus the seaway bending moment per foot of wave amplitude is

$$\frac{M_w}{\zeta_a} = 2m_w \rho g L^2 B$$

which is known as the *frequency response function*, and the RAO is then the square of this term, that is, $(M_w/\zeta_a)^2$. These data are presented in Table 13.6.

The RAO of the shear force response is obtained in the similar manner and is $(S/\zeta_a)^2$, where S is the shear force.

The response spectrum is obtained by multiplying the ordinate of the encountering wave spectrum by that of the RAO for the same encountering frequency; hence Table 13.7 is prepared in order to obtain the ordinates of the response spectrum.

TABLE 13.6

$\frac{L_w}{L}$ [—] ①	L_w [ft] ②	ω_w [rad/sec] ③	ω_e [rad/sec] ④	m_w (from Example 16.2) (hogging condition) ⑤	$\frac{M_w}{\zeta_a} = 2m_w\rho g L^2 B$ [lb] ⑥	RAO $= \left(\frac{M_w}{\zeta_a}\right)^2$ [lb^2] ⑦ = ⑥ × ⑥
0.50	500	0.636	0.997	1.3353×10^{-3}	2.4430×10^{7}	0.5968×10^{15}
0.75	750	0.519	0.760	7.9194×10^{-3}	14.489×10^{7}	20.9932×10^{15}
1.00	1000	0.450	0.630	7.0957×10^{-3}	12.982×10^{7}	16.8529×10^{15}
1.25	1250	0.402	0.546	8.8321×10^{-3}	16.159×10^{7}	26.1109×10^{15}
1.50	1500	0.367	0.487	7.6308×10^{-3}	13.961×10^{7}	19.4908×10^{15}
1.75	1750	0.340	0.443	6.3601×10^{-3}	11.636×10^{7}	13.5398×10^{15}
2.00	2000	0.318	0.408	4.8626×10^{-3}	8.896×10^{7}	7.9147×10^{15}
2.50	2500	0.284	0.357	3.8876×10^{-3}	7.113×10^{7}	5.0590×10^{15}
3.00	3000	0.260	0.320	3.4176×10^{-3}	6.253×10^{7}	3.9097×10^{15}

TABLE 13.7

ω_e ①	$S(\omega_e)$ (from Fig. 13.12*a*) ②	$\left(\frac{M_w}{\zeta_a}\right)^2$ (from Fig. 13.12*b*) ③	S_{BM} ④ = ② × ③	Simpson's Multiplier ⑤	Product ⑥ = ④ × ⑤
0.30	0	3.2×10^{15}	0	1	0
0.40	0	7.2×10^{15}	0	4	37.80×10^{16}
0.50	4.5	21.0×10^{15}	9.45×10^{16}	2	56.68×10^{16}
0.60	15.4	18.4×10^{15}	28.34×10^{16}	4	195.80×10^{16}
0.70	27.5	17.8×10^{15}	48.95×10^{16}	2	116.00×10^{16}
0.80	29.0	20.0×10^{15}	58.00×10^{16}	4	146.28×10^{16}
0.90	26.7	13.8×10^{15}	36.57×10^{16}	1	0
1.00	20.5	0×10^{15}	0×10^{16}		
				SUM	552.56×10^{16}

TABLE 13.8 [56]

Significant Wave Height [ft]	Frequency of Encountering Different Sea Conditions, p_i	Corresponding Number of Days	Expected Bending Moment, $(M_w)_i$ [ft-tons]		Corresponding Maximum Speed [knots]
			15 Knots	Maximum Speed	
①	②	③	④	⑤	⑥
7.15	0.049189761	358.10	5,582	5,998	29.0
7.80	.067984947	494.93	6,734	704,429.0	29.0
9.15	.120606773	878.02	8,328	904,629.0	29.0
10.49	.106177216	772.97	9,781	1,088,029.0	29.0
11.84	.064701734	471.03	11,031	1,252,829.0	29.0
13.18	.047364588	344.81	11,988	1,376,029.0	28.0
14.53	.029977493	218.24	12,936	14,867	28.0
15.88	.021228250	154.54	13,760	15,895	28.0
17.22	.013117869	95.50	14,442	16,807	26.5
18.56	.012201287	88.83	15,062	17,348	26.5
19.90	.002211287	16.10	15,594	18,086	26.5
21.24	.002399098	17.47	16,037	18,624	26.5
22.58	.003386110	24.65	16,444	19,164	26.5
23.93	.002733264	19.90	16,834	19,625	26.5
25.27	.001225773	8.92	17,144	19,532	24.0
26.61	.001333665	9.71	17,436	19,882	24.0
27.95	.001347152	9.81	17,720	20,192	24.0
29.29	.000592907	4.32	17.995	20,480	24.0
30.63	.000555944	4.05	18,216	20,741	24.0
31.98	.001059440	7.71	18,429	20,989	24.0
36.00	.000015485	0.11	18,928	20,755	21.0
38.68	.000025974	0.19	19,226	21,084	21.0
44.05	.000003996	0.03	19,651	21,532	21.0
46.73	.000009990	0.07	19,802	21,726	21.0
In port	.450550000	3300.00	0	0	0
SUM	1.000000000	7300.00			

Note: The maximum speed in different groups of sea conditions is determined by computing the horsepower required in addition to the calm water horsepower and comparing the total required horsepower with the available horsepower.

Figure 13.12*c* illustrates the response spectrum for the bending moment $S_{BM}(\omega_e)$. The area under the response spectrum is obtained by finding the ordinates at regular intervals of 0.10 of the abscissa and then using the Simpson rule for integration.

Thus, from the results of Table 13.8,

$$\begin{aligned} m_0 &= \tfrac{1}{3} \times \Delta\omega_e \times \text{SUM} \\ &= \tfrac{1}{3} \times 0.10 \times 552.56 \times 10^{16} \\ &= 18.4 \times 10^{16}\ \text{ft}^2\text{-lb}^2 \end{aligned}$$

and the significant bending moment (i.e., the average of the one-third highest bending moment values) is

$$\begin{aligned} 2.0\sqrt{m_0}\,\text{CF} &= 2.00\sqrt{18.4 \times 10^{16}} \times 1.0 \\ &= 2 \times 4.28 \times 10^8 \\ &= 8.56 \times 10^8\ \text{ft-lb} \end{aligned}$$

where the response spectrum is assumed to be narrow so that the CF $\simeq$ 1.0.

When the broadness parameter ε of the response spectrum for the combined load is zero (i.e., the random process is narrow band; in other words, the histogram can be presented by the theoretical Rayleigh distribution), there is a combination of low frequency loads, for example, vertical and horizontal wave bending moments, each of which has its spectral content concentrated near a center frequency ω_0. If, on the other hand, $\varepsilon \approx 1$, there is a combination of low and high frequency loads (e.g., wave bending moment and "springing" moment). The spectrum for the combined loads is then wide; and although each of the bending moments may have its spectral content around ω_i, the ω_i's are very far apart on the frequency axis [197].

To find the total bending moment due to wave action, the above result is added to M_s, that is, the bending moment in still water caused by the waves generated by the ship itself when it moves at a speed V. The value of M_s can be predicted by (16.13), obtained by regression analysis of model results.

The bending moment due to wave action may be added to the still water bending moment M_0 (for a vessel at rest), in order to determine the final bending moment of the vessel for a particular sea condition.

The short-term predictions of loads as described above are based on the Rayleigh distribution which is a special case of a more general distribution of peaks in a random process. This requires the spectrum to be narrow as stated in chapter 5.

A long-term maximum value for load may be determined in two ways; either the largest expected value in the most severe spectrum or the largest value in all spectra. The former is known as the most severe condition whereas the latter is known as the long-term distribution. Since the most severe condition is generally related to a special response and other responses may have the largest values in different conditions depending on the shape and frequency location of the transfer function the design values should be obtained from long-term distributions.

In considering structural strength in a seaway, one should examine the probability that a particular value of bending moment will be exceeded. It has been found by experience that stress reversals of the order of 600 hr^{-1} may occur. Thus, in the life of a ship for 20 years, each covering 330 days at sea, the stress reversals are in the order of 10^8, and the probability of peak sagging stresses is 10^{-8} (i.e., $p = 1/N$ for a large sample, where N is the number of records). Since seaway loads are repetitive in nature, a vessel may meet the extreme value of the load if it operates for a sufficient length of time. It should be restated that the total extreme bending moment is determined by adding the calm water bending moment to the extreme wave bending moment.

The following procedure, as given in Ref. 56, is generally followed in determining the bending moment on a long-term basis. First, the frequency of occurrence of different sea conditions (characterized by significant wave heights) is calculated on the basis of the life span of the ship as well as the geographical area of operation, as shown in column 2 of Table 13.8 [102].

The value of the bending moment, M_w, to be expected during the life of the vessel is obtained from the expression

$$M_w = \sum_i p_i (M_w)_i \tag{13.38}$$

where $(M_w)_i$ is the average or the expected value $(1.25\sqrt{m_0})$ of the wave bending moment for the ith seaway, and p_i is the probability of experiencing the ith seaway during the entire life of the vessel. From Table 13.8 the speed and the corresponding value for $\Sigma(p_i M_w)_i$ are obtained as follows:

$V = 15$ knots: $\quad \Sigma[p_i(M_w)_i] = 7{,}989$ ft-tons
$V =$ maximum: $\quad \Sigma[p_i(M_w)_i = 10{,}967$ ft-tons

If it is assumed that the maximum speed can be maintained for only 10% of the time and 15 knots for 90% of the time, the final result for M_w is determined as

$$M_w = 0.90 \times 7989 + 0.10 \times 10967$$
$$= 8290 \text{ ft-tons}$$

The most probable largest value of the total bending moment distribution is given in Ref. 145:

$$BM_n = M_s + M_w \log n \tag{13.39}$$

where M_s is the maximum still water bending moment, and n is the number of periods of time or number of encounters.

For example, the period of data collection in Ref. 102 was 7 years and the ship life is assumed to be 20 years; then the value of n is determined as

$$n = 20\sqrt{7} \simeq 3$$

Thus the most probable largest hogging bending moment during the vessel's life is given as

$$\overline{BM}_n = 7080 + 8290 \times \log 3$$
$$= 16{,}180 \text{ ft-tons}$$

where the maximum still water bending moment has been computed as 7080 ft-ton.

Now, from Ref. 145 the probability of exceeding this value is given by

$$P\{\text{extreme bending moment} > 16{,}180\}$$
$$= 1 - (1 - 1\sqrt{n})^n$$
$$= 70.4\% \tag{13.40}$$

It can be concluded, therefore, that the most probable largest bending moment (i.e., the largest bending moment of highest frequency) based on long-term analysis is not very suitable for design purposes, since the proability of exceeding it is rather high (70.4%, as shown in this example).

A ship operating in oblique seas is subject to both vertical and lateral bending moments; M_e, resulting from combined vertical and lateral bending, is expressed [20] as

$$M_e = \sqrt{M_{wv}^2 + M_{wL}^2 \left(\frac{z_v}{z_L}\right)^2 + 2M_{wv}M_{wL}\frac{z_v}{z_L}\cos\delta} \tag{13.41}$$

where M_{wv} = vertical wave bending moment
M_{wL} = lateral wave bending moment
z_v = *section modulus for vertical bending*
z_L = section modulus for lateral bending
δ = phase angle between vertical and lateral wave bending moments

In addition to the horizontal bending moment torsion is caused by oblique waves. Strictly speaking it is only for vertical bending in head sea that there is a good comparison between measurements and calculations. The effect of the unknown spreading of wave energy and the nonlinear rolling and yawing motions make such comparisons rather difficult. In the case of following oblique sea where the maximum torsional moment is expected, the calculations become unreliable because of the low and indeterminate frequencies of encounter.

Since, however, it is the vertical bending moment, which is, at a maximum in head sea conditions, that contributes most significantly to the longitudinal stresses, it may be sufficient to look at the vertical bending moment in dominating head seas when considering designs for hull scantlings and comparing the strength of various hull forms.

From the experimental results a number of conclusions have been drawn regarding wave bending moment prediction [56,134]. These include the following:

1. A peak of the bending moment exists in the region of the speed for synchronous pitching and heaving motions in regular head seas. However, the sagging wave bending moment is always greater than the hogging wave bending moment.

2. The effects of wave direction are as follows:

a. The vertical bending is generally largest in head seas and decreases as the wave direction approaches the beam.

b. The lateral moment is largest when the wave direction is about 135°; however, the magnitude of the moment is always less than the vertical bending moment at any given angle.

c. For a given wave direction both the vertical and the torsional moment slightly increase with the forward speed, the former reaching a peak value near the speeds for synchronous pitching and heaving motions.

d. In general, no appreciable decrease in wave bending moment is obtained for heading angles less than 30° off head seas, but a considerable reduction (about 50%) in vertical bending moment is expected for a heading angle 60° off head seas.

3. At a given speed in regular waves of constant height whose effective lengths are equal to the model length, the vertical bending moment is relatively constant; however, both lateral and torsional moments increase as the wave direction deviates from the head sea case. This is due to an increase in actual wave steepness on the direction of wave changes.

4. Torsional moments are relatively small and never exceed a value of 10% (and in most cases are even less than 5%) of the vertical bending moment. A large rolling moment apparently causes an increase in torsional moment.

5. An extension of the conventional head sea, static bending moment calculation to one of an oblique wave condition shows that the experimental vertical and torsional moments are approximately one half and one third of the statically calculated values, respectively.

6. The bending moments at any heading to long-crested irregular seas can be predicted in statistical terms with good accuracy using the response amplitude operator for bending moment obtained from regular wave tests.

7. The largest moments are caused by the highest waves during irregular wave tests; however, the average of the largest vertical moments is less than a value predicted from regular waves of moderate height (extrapolated to the observed height of the highest irregular waves).

8. *a.* A stress amplitude at the deck edge to leeward of the oncoming waves is higher than one at the opposite edge.

b. This lee deck-edge stress amplitude is greater than either of the respective stress amplitudes predicted from vertical and lateral moments, but is less than their sum.

9. Large tankers operating in oblique seas may experience a horizontal bending moment of the same order of magnitude as the vertical bending moment. However, because of the phase difference between them, the peak values do not occur at the same time, and so the combined effect may not be critical.

13.5 DYNAMIC LOADS

The hydrodynamic as well as the inertial forces acting on a ship due to waves and also the ship motions are generally low frequency phenomena,

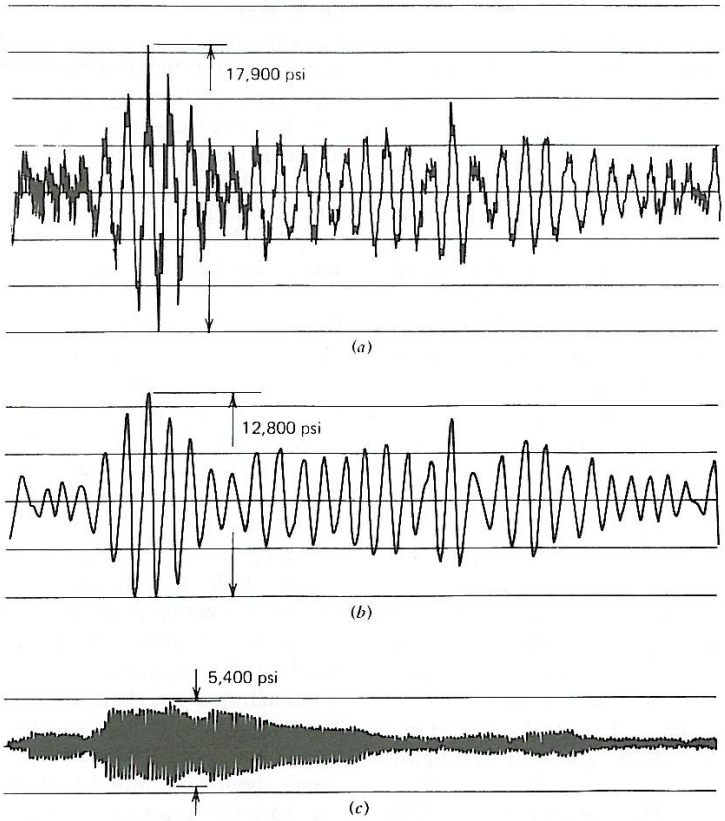


Figure 13.13 Typical record of midship stress variation [134]. (*a*) Total stress variations, including both wave-induced and first mode stress components. (*b*) Wave-induced stress variations (frequency approximatily 0.1 Hz). (*c*) First-mode (springing) stress variations (frequency approximately 0.70 Hz).

that is, the oscillating frequencies are much smaller than the natural frequency of vibration of the hull. Therefore these forces have little influence on the dynamic response; and so the hull girder stresses are determined through the laws of statics, and the slowly varying loads are called *quasi-static* or *ordinary wave loads.*

However, there are times when the ship is subject to very rapidly developed hydrodynamic loads that are of two kinds.

1. Steady-state loads: due to propeller–hull interaction, machinery–hull transmission, and seaway component excitation of hull girder response, as in springing. *Springing* is defined as a significant vibration that occurs when the ship runs into comparatively short waves that produce resonance with the natural frequency of vibration of the ship hull. The stress amidship due to this vibratory response (which continues for some length of time and fluctuates in magnitude) is superimposed on the wave bending moment. Springing loads are caused by the high frequency region of the wave spectrum and for this reason the shape of the wave spectrum is of considerable importance.

Figure 13.13 shows a typical record of midship stress, including both low frequency (due to wave bending moment) and high frequency (due to springing) stresses. The exciting forces and hence the springing bending moment acting on the springing ship in short waves may be determined by the strip theory [178]. However, springing, which is more or less a continuous vibration due to waves. does not take place in the case of normal ships.

2. Transient loads: due to slamming, deck immersion and emergence, the shipping of green water over

the forward deck, and wave impacts on structural members of the hull in a rough sea. These loads can be superimposed on other loads; however, because of their transient nature it is rather difficult to treat them statistically.

The transient loadings and the generated impacts are more pronounced in the forward portion of the ship's structure, since the relative velocities between the ship and the waves are highest in this region. These impact loads are due to rapid changes of momentum between the waves and the hull.

During slamming, large pressures are developed at the contact area of low deadrise angle. When the local elastic energy absorption capability is not adequate, structural damage results; but if the area affected is large, the energy absorbed locally is distributed through the ship structures in the form of vibratory response, such as whipping, and is dissipated through damping, structurally, by cargo and so on.

The vibratory phenomenon known as *whipping*, which is caused by the immersion of the flare, should also be determined in order to obtain a complete picture of the structural response in a seaway.

During bow flare impact the forefoot need not emerge; during ship motion the bow is rapidly immersed, thereby deflecting a large amount of water by the bow flare. This action creates a large fluid pressure covering a comparatively large area, and the strong forces so developed may also produce a whipping response of considerable magnitude. If the forward sections are of the V-form, the total hydrodynamic forces in the forebody due to impact of the bow flare are larger than those due to slamming. Figure 13.14 shows a typical record of midship bending stress with slamming and the whipping that follows.

Slamming also causes a damped high frequency stress variation that can be interpreted as an effective superimposed bending moment.

It has been observed from both model tests and full-scale trials that the hull girder bending moments due to whipping caused by impact of the bow flare may be as large as the wave-induced bending moments [49]. Unlike wave bending moments, dynamic loads acting on the hull girder cannot be considered independently of the structural response of the hull. It should be noted that the extreme structural response of the hull, such as plastic buckling or permanent set, requires a certain amount of time and a large amount of energy. As mentioned in Section 7.6, the duration of slam loads may be too short to cause any buckling of the deck or the bottom plating. The shipping of green water has been found to cause severe structural damage at the ship's bow. Green water on the deck can cause a whipping stress with a magnitude as great as that due to 40 to 70% of the sagging bending moment in regular waves.

The forces developed at the bottom plating of the bow due to slamming are caused by high pressures acting over relatively small areas of the bottom plating. The duration of this significant force is rather short (i.e., less than 100 msec). On the other hand, the forces caused by bow flare immersion are due to lesser pressures acting over larger areas and for longer durations (i.e., about 1 sec or less). These forces are significant only if there is a pronounced flare, such as that of an aircraft carrier. The initial effect of the immersion of the flare is a nonlinear addition to the wave bending moment (sagging) as the flare enters into water; however, the bending moment will be maximum at approximately the time when the wave bending moment is greatest in

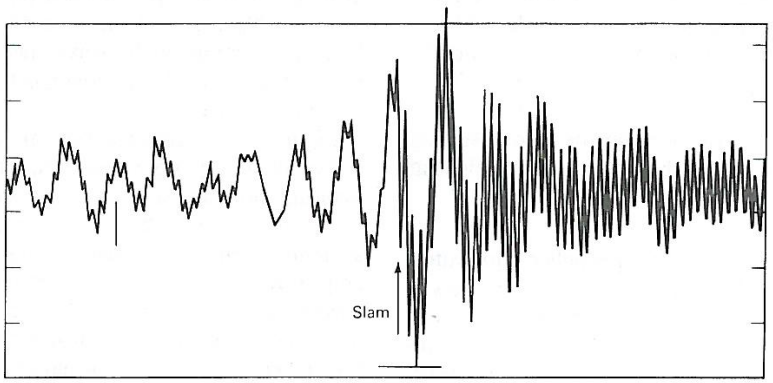


Figure 13.14 Typical record of vertical bending stress (with slamming) at midship section [134].

sagging. The total effect may be determined by adding the two maximum values, since the phase difference between the bending moment due to flare immersion and to wave loads seems to be negligible.

As mentioned in Section 7.6, the initial effect of bottom impact is the development of high local pressures that can damage the bottom structure. Reference 170 makes it possible to estimate the values of the coefficient k in the pressure expression $p = kV^2$; see Section 16.7. This expression can be used for the design of local structures; however, it is not yet possible to prescribe the slam loading of the hull girder.

To determine the effective bending moment due to slamming, one should estimate the probability function for this bending moment. This estimation involves the following steps:

a. Estimation of the local slam pressure and its variation with time and space for a particular sea condition—hence its distribution.

b. Estimation of the resulting midship stress immediately after the slam and the subsequent whipping stress—hence their distribution.

c. Translation of the distribution of (a) and (b) into effective bending moment distributions.

The local bottom pressures are estimated from ship motions by the method presented in Section 7.6. However, this estimation in space and time cannot accurately be made from the calculated motions.

The resulting midships stress can be determined from the nondestructive impact pressure over a certain bottom area. This impact load is then used in the determination of the midship slamming stress.

Finally, the stress distribution can be translated into the bending moment distribution by multiplying by the section modulus.

Full-scale strain recording on board the S.S. *Wolverine State* [142] has been made for slam and

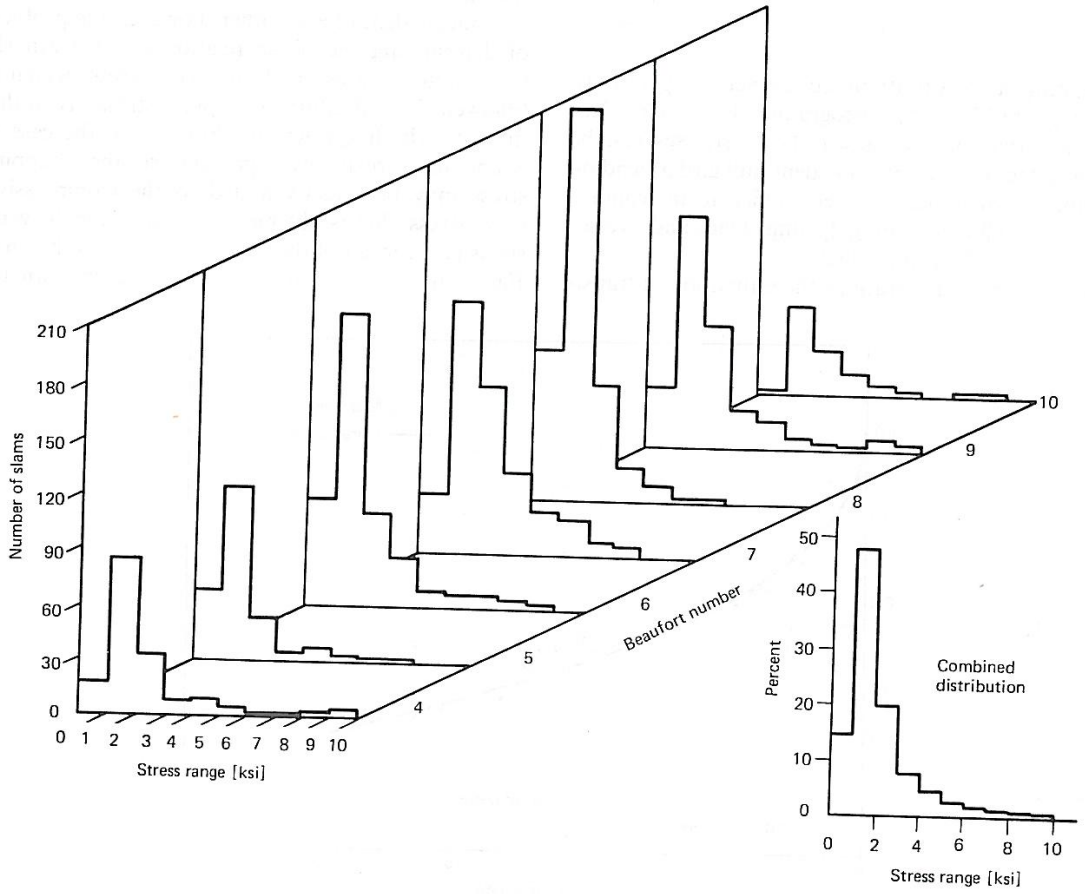


Figure 13.15 Distribution of peak-to-peak slam stress [134].

TABLE 13.9 MEASURED FULL-SCALE SLAM LOADS AND MIDSHIP STRESSES [134]

Vessel	Pressure [psi]	Peak-to-Trough Midship Slam Stress [kpsi]
USCG cutter	295 local	—
Unimak	86 ave. panel	—
Dutch destroyer	100 +	11.20
Cargo ship		
S.S. *Westboro*	—	1.90
Cargo ship		
S.S. *Wolverine State*		
Voyage	49	2.60
Voyage	69	10.00
Bulk carrier	—	15.50
Fotini L		
Container ship		
Manchester City	—	5.00
Cargo ship	—	4.50
M.V. Jordaens	19	2.04
Container ship		
Flinders Bay	—	15.60

whipping stress variations during actual operations. In Fig. 13.15 [134] histograms of midship slam stress variations are shown. These stresses can be interpreted in terms of equivalent hull girder bending moments. Such data, when sufficient in volume, can be used for estimating dynamic loads and stresses in the design of marine vehicles.

For design considerations the estimation of transient dynamic loads requires the following:

a. Prediction of the probability that slamming will occur over a certain time period, (e.g., a 20 min record).

b. Knowledge of the distribution of added stress (or equivalent bending moment) to be expected when both slamming and shipping of green water take place.

Some representative full-scale values of slam loads and midship stresses are given in Table 13.9.

It is important for the designer to determine the probability that the total stress (or equivalent bending moment) will exceed the wave bending stress due to slamming or whipping. This probability should be determined for the midship section, since the local stress is not investigated in overall vehicle dynamics.

The recent investigation reported in Ref. 134 have shown that the wave-induced stress and the slam stress are independent of each other; however, the problem of determining the phase relationship between the wave-induced stress and the slam stress, which is followed by vibratory whipping stress, is rather difficult. The frequency of vibrations in the case of whipping is relatively high, and so the whipping stress may be directly added to the (compressive) wave stress, that is, the mean increase over the wave stress is the mean of the whipping stress, as shown in Fig 13.16. This is not the case, however, with the

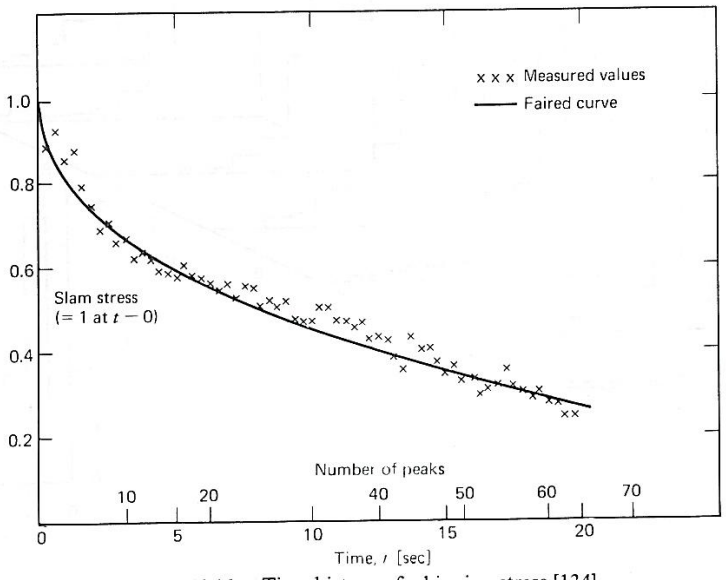


Figure 13.16 Time history of whipping stress [134].

slam stresses, which are associated with the tensile wave-induced deck stresses. In other words, any increase in bending moment due to slam is a hogging moment.

The high frequency wave loads depend most significantly on the handling of the vessel in a rough sea. More information regarding the limiting values actually allowed in service conditions is necessary before such loads are induced in seakeeping design, since the high frequency loads are very much dependent on the type and size of the vessel.

Chapter

Fourteen

MOTION STABILIZATION

14.1 INTRODUCTION

To reduce the motions of a vessel in a seaway, motion stabilization devices are often adopted that are not otherwise considered part of the vessel. With the help of stabilizers, the amplitude, rate, and acceleration of the motions, as well as the associated dynamic effects (e.g., deck wetness and slamming) can be reduced considerably. In the study of motion stabilization it is important to know the kind and magnitude of the forces that should be applied to obtain a significant reduction in amplitudes and accelerations.

Of all ship motions (heave, pitch, roll, etc.) only rolling motion has been successfully damped as yet. This is so because normal vessels have inherently low damping properties with respect to roll. Therefore in the region of resonance ($\Lambda \simeq 1.0$), where severe rolling is expected, consideration for the safety of the ship is important. On the other hand, only moderate force is necessary to induce an adequate damping moment. In comparison to rolling motion, the conditions of resonance for heave and pitch are less well defined, and the forces necessary for stabilization are rather large.

In the investigation of motion stabilization it is forced motion that is of real importance. With reference to the motion equations it can be seen that there are three different ways to reduce forced motions [242]:

1. By increasing the damping coefficient b. This is called *damping stabilization*. Since physically "damping" means a dissipation of energy, this kind of motion stabilization is effective in the case of free oscillations as well as in the region of resonance, where damping has its maximum effectiveness. The bilge keel is such a damping device for rolling motion.

2. By reducing the natural frequency of the ship (i.e., by increasing the natural period $T_\phi = 2\pi/\omega_\phi$), so that the tuning factor $\Lambda = \omega_e/\omega_\phi$ becomes much greater than unity. This type of motion stabilization, known as *tuning stabilization*, is effective only in forced oscillations, where the encountering frequency also varies in the right direction. Since, however, a seaway is composed of waves of all frequencies, it is not always proper to change the natural frequency of a vessel because the modified natural frequency may come across a different encountering frequency of the same magnitude, and resonance will still take place.

3. By reducing directly the exciting force or moment. This type is known as *equilibrium stabilization* and is, in principle, applicable to all kinds of motions; in such a case, a stabilizing moment $-M(t)$ is applied that is opposite in phase to the exciting moment, and this will result in a reduction in the exciting moment. Figure 14.1*a* shows a stabilizing moment

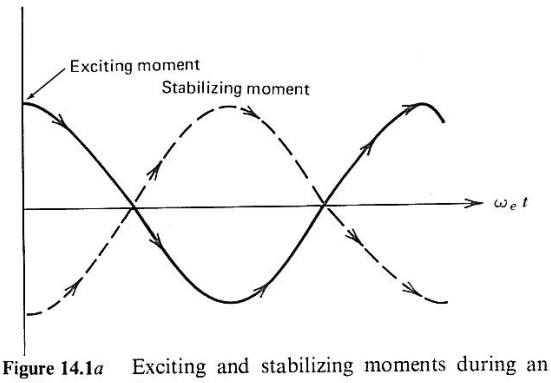


Figure 14.1*a* Exciting and stabilizing moments during an oscillatory motion.

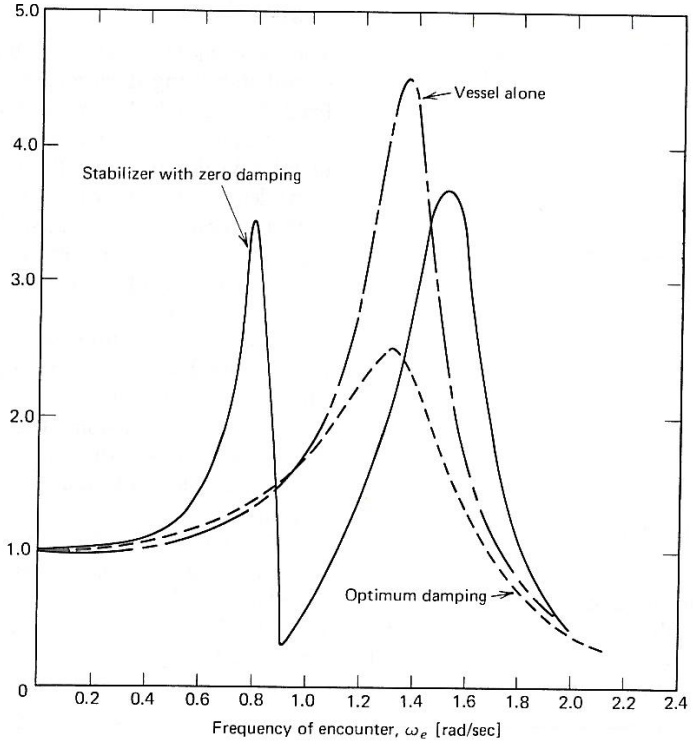


Figure 14.1*b* Effects of undamped and optimum damped stabilizers [120].

that has the same magnitude as has the exciting moment. However, the usefulness of this kind of stabilization depends entirely on the effectiveness of the control device. Although equilibrium stabilization is used mainly in the case of forced motions, it is equally effective in the case of free oscillations. Let us consider a typical example:

$\Delta = 30.00$ tons

$\overline{GM} = 2.5$ ft

α'_M = maximum effective wave slope = 6° (0.10 rad)

To nullify the exciting moment for the rolling motion a stabilizing moment of 7500 ft-tons is necessary (see Section 4.5), that is, an approximate force of 100 tons, which can reasonably be generated within the ship.

If we consider the same data for the reduction of pitch and assume the wavelength to be equal to the ship's length (i.e., say 600 ft), we get from Section 4.4 the amplitude of the exciting moment as about 600,000 ft-tons or a force of the order of 1000 tons which cannot be generated within the ship. But the angle by which pitching motion should be reduced in order to improve the seakeeping quality is not significant, and so the magnitude of the stabilizing moment need not be very large.

In the analysis of oscillatory motions with an undamped stabilizer, considerable motion reduction in the resonance zone can be achieved but new resonance peaks may appear at two other frequencies, as can be seen in Fig. 14.1*b*. This might be acceptable if the exciting force had only one particular frequency. However, since a vessel encounters wave exciting forces of various frequencies in a seaway, an undamped stabilizer is of little benefit.

14.2 ROLL STABILIZATION

As mentioned earlier, rolling motion has most successfully been controlled from the point of view of stabilization, since the forces and moments involved in rolling are comparatively small.

The stabilizers and other means used to control rolling motion have been of many kinds: the following are some examples.

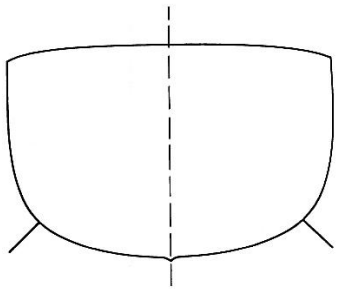


Figure 14.2 Midship section with bilge keels.

a. Bilge keels.
b. Gyroscopic stabilizers.
c. Movement of weight.
d. Rudder action.
e. Jet flaps.
f. Passive and active roll tanks.
g. Stabilizing fins.

Because of economical considerations, some of the devices mentioned above are not used at present, whereas others, although they may not be most effective technically, continue in use.

Bilge Keels

The most widely used, as well as the simplest kind of roll stabilizing devices, are bilge keels, which are fixed fins attached almost perpendicularly to the hull at or near the bilge (see Fig. 14.2). The lengths of bilge keels are normally from 25 to 50% of the ship's length, and the widths vary from 1 to 3 ft.

In the case of bilge keels, the damping moment is generated by a component supplied by the pressure resistance of the bilge keel itself and by a component due to the change in the pressure distribution on the hull. For vessels not fitted with bilge keels, roll damping is caused only by the dissipation of energy in surface waves and in viscous flow around the hull and by surface tension. The latter component is not important for the full-scale case. Bilge keels increase considerably the energy dissipation due to viscous flow.

It has been found by experience that bilge keels are also effective in heavy sea conditions. The only drawback is that hull resistance is increased when the bilge keels are fitted, although this may not be considered a serious problem for high-speed vessels.

The damping effect of bilge keels in comparison

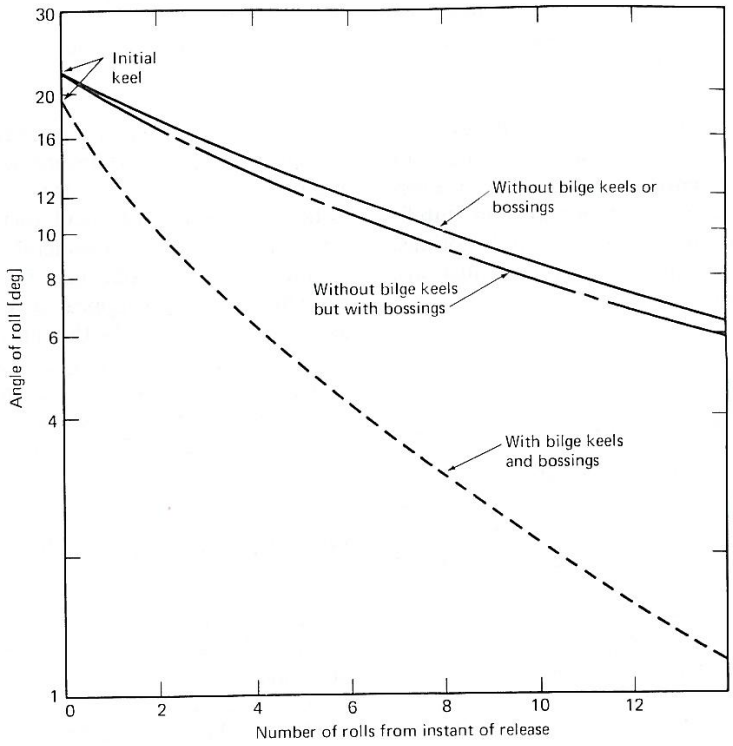


Figure 14.3*a* Typical example of roll decay for a ship with and without bilge keels [143].

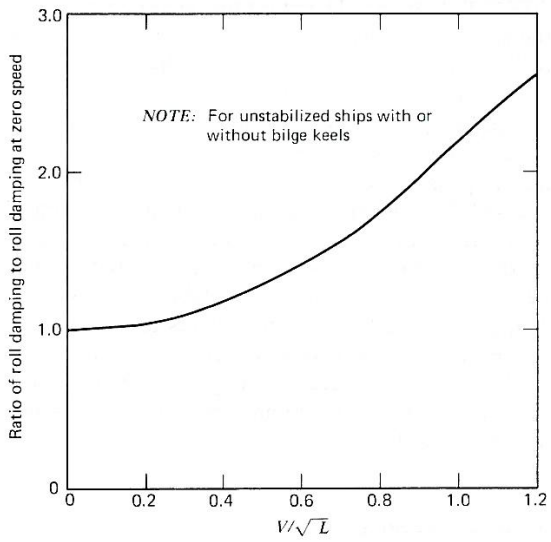


Figure 14.3*b* Typical variation of roll damping coefficient with speed/length ratio [13].

with struts and bossings is illustrated in Fig. 14.3*a*. The figure shows that roll damping is only slightly improved with bossings, while the damping effect of bilge keels is much greater. The damping effect of bilge keels increases with the speed of the vessel, since the lifting force generated by the bilge keel also increases at higher speed, thereby increasing its resistance to motion and hence providing a greater damping effect (see Fig. 14.3*b*).

If it is assumed that the resistance of a bilge keel (or a flat surface) is proportional to the square of the velocity through the water, the total force of a bilge keel [being proportional to (tangential velocity)^2] is given by

$$CA(r\omega)^2$$

along the direction perpendicular to the bilge keel where A = area of the bilge keel

r = mean distance of the area from the CG of the vessel.

C = coefficient of normal pressure acting on the bilge keel $\simeq 1.1$ to 1.7 in ft-lb-sec units, depending on the ratio of length to breadth of plate

ω = angular velocity = $d\phi/dt$

The moment of the damping force contributed by the bilge keel about the CG of the ship is

$$CAr^2 \cdot \omega^2 \cdot r = CAr^3\left(\frac{d\phi}{dt}\right)^2 = \frac{CAr^3}{2240}\left(\frac{d\phi}{dt}\right)^2 \quad \text{[ft-ton-sec]}$$

Since the damping coefficient b is expressed [132] as

$$b = \frac{16\pi^2 M}{3\Delta \overline{GM} T_\phi^2}$$

where M is the damping moment, the increase in b due to bilge keel becomes

$$\frac{16\pi^2}{3\Delta \overline{GM} T_\phi^2}\left(\frac{CAr^3}{2240}\right) = \frac{CAr^3}{1680 I'_{xx}} \quad \text{since}$$

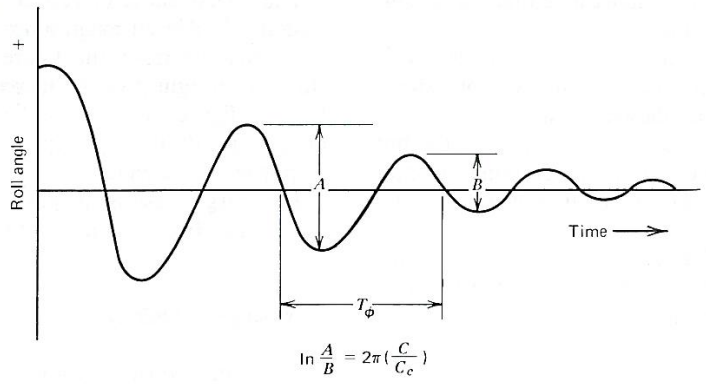
$$T_\phi = 2\pi \sqrt{\frac{I'_{xx}}{\Delta \overline{GM}}} \tag{14.1}$$

Thus one can see from (14.1) that:

a. The damping effect increases with the area of the bilge keel and also very rapidly with the distance r of the bilge keel from the rolling axis.

b. Since the decrement of rolling by the bilge keel is given by $b\phi_a^2$, bilge keels appear to be more effective for larger angles of rolling.

c. The effect of the bilge keels varies inversely with



C/C_c = effective roll damping coefficient; T_ϕ = roll period in calm water.

Figure 14.3*c* Determination of roll damping coefficients from roll decay test.

the moment of inertia of the ship about the rolling axis. Bilge keels are therefore more effective in vessels with small mass moments of inertia (i.e., when the weights are concentrated near the ship's centerline).

The following empirical expressions can be used to find the relationship between the ship particulars, bilge keel size, and roll damping at zero speed [13]:

$$\left(\frac{b}{b_c}\right)_0 = \frac{0.55(A_{BK}w^{1/2} + 0.0024LBd^{1/2})d^{5/2}\phi^{1/2}}{\Delta B^2}$$

where $(b/b_c)_0$ = ratio of the actual damping to the critical damping of the linear system
b_c = critical roll damping $= 2\sqrt{cI'_{xx}}$ of the linear system (ship)
A_{BK} = total area of bilge keel [ft^2]
L = waterline length [ft]
B = waterline beam [ft]
w = width of bilge keel [ft]
Δ = displacement [long tons]
ϕ = roll angle (zero to out) [radi]
d = distance from center line at load waterline to turn of bilge [ft]

The modification of roll damping as a function of ship speed can be also given [13] as

$$\Delta\left(\frac{b}{b_c}\right) = \left(\frac{b}{b_c}\right)_V - \left(\frac{b}{b_c}\right)_0 = 0.00085\left(\frac{L}{B}\right)\left(\frac{L}{\overline{GM}}\right)^{1/2} \times \left(\frac{F_n}{C_B}\right)\left[1 + \frac{F_n}{C_B} + 2\left(\frac{F_n}{C_B}\right)^2\right]$$

where $\Delta(b/b_c)$ = change in roll damping coefficient due to forward speed V
$(b/b_c)_V$ = damping ratio at speed V
F_n = Froude number $= V/\sqrt{gL}$
C_B = block coefficient

A typical change in damping as a function of ship speed is illustrated in Fig. 14.3*b*.

The damping coefficient can also be estimated from rolling experiments with models or similar ships in calm water, as shown in Fig. 14.3*c*.

In order not to increase the resistance of the hull during its forward motion, the longitudinal position of bilge keels should be on the flow lines along the length.

Roll stabilization by the use of bilge keels is simple and inexpensive but, as said before, is effective only in the region of resonance.

Passive Roll Stabilizers

As was mentioned earlier, normal hull forms have little roll damping. Therefore the energy imparted to the vessel by the waves is manifested by considerable rolling motions, so that the energy dissipated by the rolling motions is equal to that imparted by the waves.

A passive roll stabilizer fitted to a ship is a dynamic system having its own resonance, which is, however, not as pronounced as the ship's resonance because the stabilizer is more highly damped. A stabilizer is effective only when its resonance is nearly equal to that of the ship. To obtain adequate coupling between the vessel and the stabilization system, proper tuning of the system is necessary so that the roll energy of the vessel is successfully transferred to the stabilizer. There are, in general, two kinds of passive stabilization systems: moving weights and stabilizing tanks.

Movement of Solid Weights

By moving a large weight transversely across a vessel, a resonant system is achieved, resulting in roll damping. For effective roll damping the movement of weight should lag 90° behind the rolling motion of the ship in order to provide a moment to counteract the rolling moment.

Such a stabilizing device has proved to be effective in small vessels and can be suitably designed with a natural frequency near that predicted for the vessel. The amount of weight to be shifted on board the ship is governed not only by the decrease in the metacentric height because of the upward shift of the CG of the ship but also by the stabilizing effectiveness. A properly designed weight stabilizer should not weigh more than 5 % of the vessel displacement. The mechanical problems involved in mounting and operating a large weight may be formidable.

The effectiveness of roll stabilization by moving weights of different magnitudes is shown in Fig. 14.4. It is obvious from the figure that an increase in stabilizer weight gives an increased stabilizing effect, but the figure also shows that increases in weight do not result in any appreciable decrease in roll response over a wider range of frequencies.

For large vessels a passive tank stabilization system has been adopted with considerable success.

Gyroscopic Stabilizer

A gyroscope consists of a heavy wheel free to rotate about an axis which itself is confined within a framework that is again free to rotate about a perpendicular

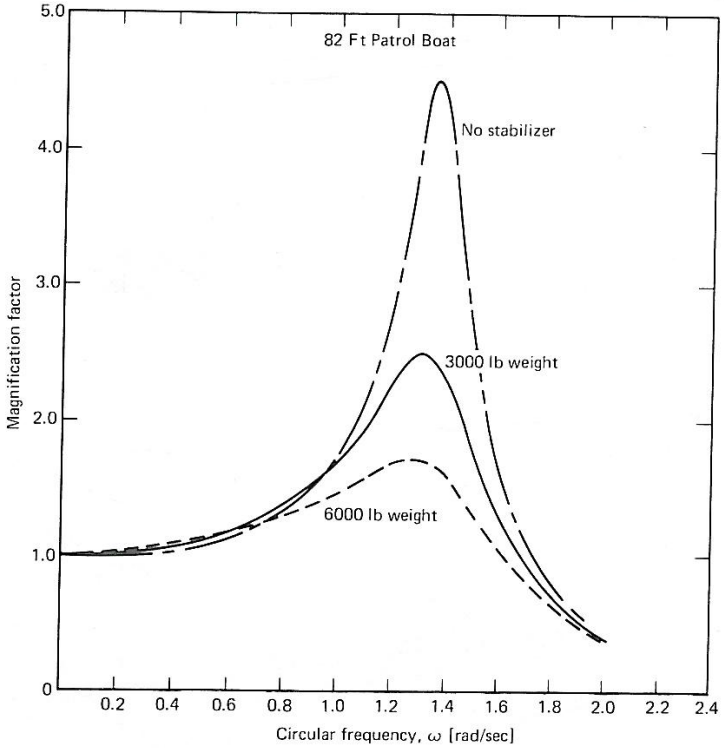


Figure 14.4 Roll stabilization by the movements of weight.

axis. A gyroscope is useful for two reasons: (a) the axis of a free gyroscope will remain fixed in space, and (b) a gyroscope can be made to deliver a torque that is proportional to the angular velocity about a perpendicular axis. The first property is known as *gyroscopic inertia* in space. When the speed of the wheel decreases, the gyroscopic inertia is also less and vanishes completely when the wheel stops rotating. When a ship rolls (so does the axis of the gyroscope, AA'), the external moment exerted on the gyroscope frame produces a rotation of the axis AA' in the fore and aft planes (see Fig. 14.5). If this motion, which is called *precession*, is resisted, the reaction at the horizontal connections of the gyroscope frame constitutes a couple which acts in an opposite direction to that of roll, and this is the stabilizing moment produced by a gyroscope, denoted by M_z. This moment originates from the conservation of angular momentum and is given as

$$M_z = I_z \omega_r \Omega \equiv \text{moment of external force with respect to the axis of spin}$$

where I_z is the mass moment of inertia of the spinning element about the axis of spin, ω_r is the angular velocity of spin, and Ω is the angular velocity of rolling motion $= d\phi/dt$.

Although a small time lag exists, the stabilizing moment is maximum when the vessel is in the upright or nearly upright position and minimum when the vessel is in the inclined position. In other words, there is a phase difference of 90° between the exciting moment and the stabilizing moment.

Although gyroscope stabilizers are very effective (60 to 80% reduction of roll), the high cost, heavy weight, and considerable amount of space required make them unattractive for modern vessels.

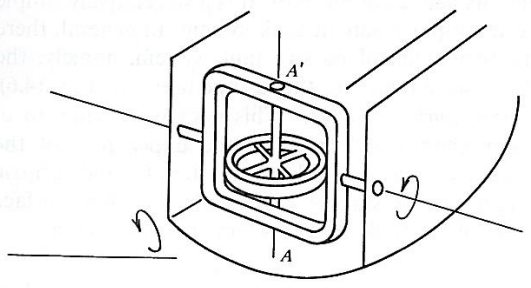


Figure 14.5 A gyroscopic stabilizer system.

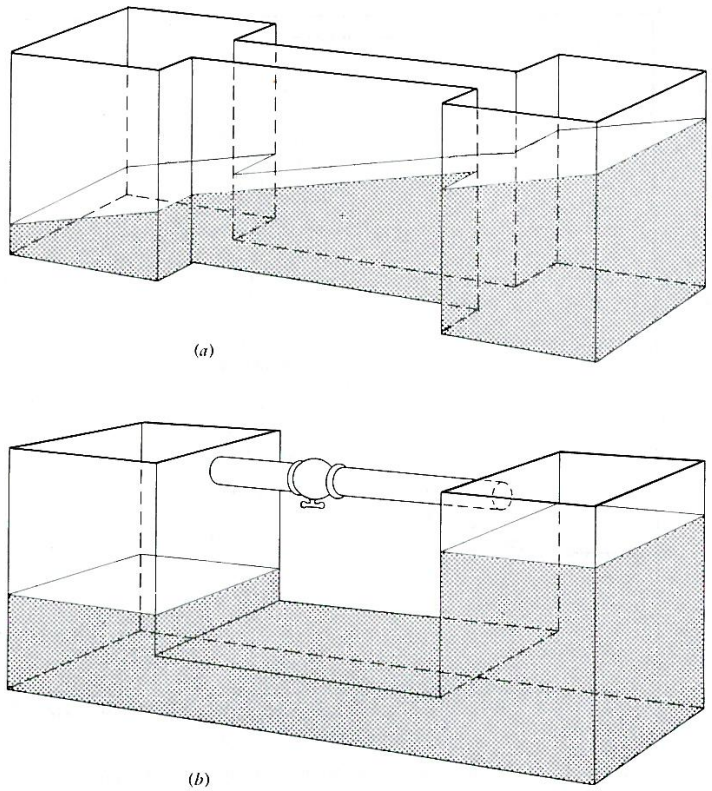


Figure 14.6 Passive tank stabilizers. (*a*) Free surface tank. (*b*) U-tube tank.

Tank Stabilizers

The free surface tank was first put to use by W. Froude in 1874 to test its effectiveness as a motion stabilizer. Later, in 1910, Frahm introduced the U-tube tank stabilization system, which was found to be more effective than the free surface tank system.

Later an active roll tank system was invented that look into consideration the amplitude of roll and controlled the size of the hull opening to achieve better motion stabilization. Also an active system was designed to put a pump in the cross connection of the U-tube tank in order to accelerate the response of the system.

The most recent development in the passive antiroll tank is the flume or diversified tank system, which has received considerable attention.

One disadvantage of tank stabilization systems is the effect of saturation, that is, sloshing of the fluid inside a tank takes place during stabilization. The sloshing motion increases with an increase in rolling motion. When the fluid in the tank slams against the tank top, there is a decrease in the tank effectiveness for motion stabilization. The height of a tank is therefore an important consideration in tank design.

Passive Tank Stabilizers

Antiroll tanks used as stabilizers are called passive when they are left alone on board except for the infrequent tuning needed for a change in the loading conditions. The sophisticated control system required in active systems is not present in the passive system, and this makes the latter often more attractive than its active counterpart. It is also relatively simple to develop a resonant tank system. In general, there are two kinds of passive tank system, namely, the free surface tank and the U-tube tank (see Fig. 14.6).

Free Surface Tanks. This system is made up of water chambers located in the upper part of the vessel (see Fig. 14.6*a*). In this system the metacentric height of the ship is reduced by the free surface effect of the tank, and this reduction is given as

$$\frac{\rho}{\rho_s}\frac{i}{\nabla}$$

where i = moment of inertia of the free surface area
∇ = volume of displacement of the ship
ρ = density of the fluid in the tank
ρ_s = density of salt water (or density of the fluid in which the vessel floats)

One should not neglect the free-surface effect of stabilizer tanks, and the following simplified formula [217] may be applied for a typical passive tank configuration (see Fig. 14.6*a*):

$$\frac{i}{\nabla} = \frac{5wB^2}{48\Delta h}$$

where i/∇ = free surface correction
w = weight of tank fluid
Δ = displacement of ship
B = beam
h = depth of fluid in tank

For example, if w/Δ is considered to be 2%, and if the fluid depth is only 5 ft, the $\overline{GM}$ loss to be expected is $0.000417B^2$. If the ship beam happens to be 75 ft, there is a $\overline{GM}$ loss of 2.25 ft, which may be a considerable portion of the actual metacentric height.

Because of the reduction in the metacentric height the natural frequency of roll is decreased, and this makes synchronous rolling motion less probable, since the chance of encountering a longer wavelength is reduced. The main effect of the free surface tank is the damping caused by the tank water lagging the rolling motion.

The disadvantage of this system is that it is not effective when a wave of shorter frequency (i.e., a longer wave) is met. Also, the reduction in the metacentric height impairs the stability characteristic of a vessel.

The simplified equation of rolling motion is given as

$$a\ddot{\phi} + b\dot{\phi} + c\phi = M$$

For free surface tank stabilizers, the rolling moment M consists of the exciting moment due to waves, as well as the moment caused by the water transfer in the tank. Both the wave moment and the tank moment can be considered to be harmonic for the purpose of analysis. When M is harmonic, the resulting steady-state motion will also be harmonic of the same frequency, but there will be a phase difference relative to the moment M. It may be assumed [217] that the steady-state rolling motion is expressed as $\phi = \phi_a \sin \omega_e t$ and the exciting moment is

$$M = M_{wa} \sin(\omega_e t + \varepsilon_w) + M_{ta} \sin(\omega_e t + \varepsilon_t)$$

where M_{wa} = amplitude of the exciting moment due to the wave
M_{ta} = amplitude of the exciting moment due to the tank
ε_w = phase angle between the wave exciting moment and the rolling motion
ε_t = phase angle between the tank exciting moment and the rolling motion (*Note*: ε_t is negative)
ϕ_a = amplitude of the rolling motion
ω_e = circular frequency of encounter

For the sake of convenience the phase angle ε_w has been used in the expression for the moment instead of that for the motion. Now, substituting the expressions for the motion and the moment, we obtain

$$(c - a\omega_e^2 - \Delta c)\sin \omega_e t + (b\omega_e - \Delta b\omega_e)\cos \omega_e t = \frac{M_{wa}}{\phi_a} \sin(\omega_e t + \varepsilon_w) \tag{14.2}$$

where

$$\Delta c = \frac{M_{ta}}{\phi_a} \cos \varepsilon_t \tag{14.3}$$

and

$$\Delta b = \frac{M_{ta}}{\omega_e \phi_a} \sin \varepsilon_t$$

As is seen, Δc can be considered to be a correction of c. Also, $-\Delta b$, which lags the motion by 90°, can be considered to be an extra damping (since ε_t is negative, $-\Delta b$ is therefore positive). Solving (14.2), we get

$$\phi_a = \frac{M_{wa}}{\sqrt{(c - a\omega_e^2 - \Delta c)^2 + (b - \Delta b)^2 \omega_e^2}} \tag{14.4}$$

and

$$\varepsilon_w = \tan^{-1} \frac{(b - \Delta b)\omega_e}{c - a\omega_e^2 - \Delta c}$$

At the natural frequency of the system, which is

$$\omega'_\phi = \sqrt{\frac{c - \Delta c}{a}} \tag{14.5}$$

the phase angle will be 90°, and the amplitude at this frequency will be

$$\phi_a = \frac{M_{wa}}{(b - \Delta b)\omega'_\phi} \tag{14.6}$$

where ω'_ϕ is the effective natural frequency, whereas the original natural frequency is known to be

$$\omega_\phi = \sqrt{\frac{c}{a}}$$

Equation 14.6 shows that the rolling amplitude is greatly influenced by the damping effect of the tank.

The following conclusions have been reached regarding free surface tank stabilization [217]:

a. The natural frequency of the tank should be equal or very near to the ship's natural frequency for proper damping of the motion.

b. The quantities Δc and Δb are considerably dependent on the frequency of motion.

c. When M_{ta} is proportional to the motion amplitude, Δc and Δb are independent of ϕ_a. In this case the stabilization system is linear, and the equation of motion can be easily determined. Otherwise, the system will be nonlinear and the solution can be found by a process of iteration.

d. As given in Section 4.5, the wave exciting moment is expressed as

$$M_{wa} = \Delta k' \zeta_a e^{-k' z_e} \overline{GM}$$

where k' = effective wave number $= 2\pi/L'_w$
L'_w = effective wavelength $= L_w/\cos\mu$
ζ_a = wave amplitude
z_e = effective mean depth below the water surface

From (14.4) the ratio of the amplitude of roll ϕ_a and the maximum effective wave slope $k'\zeta_a$ is obtained as

$$\frac{\phi_a}{\alpha'_M} = \frac{\phi_a}{k'\zeta_a} = \frac{e^{-k'z_e}}{\sqrt{(1-\Lambda^2-\Delta c/c)^2 + (\nu - \Delta\nu)^2\Lambda^2}} \tag{14.7}$$

where Λ = tuning factor $= \omega_e/\omega_\phi$
ω_ϕ = natural frequency of the ship $\sqrt{c/a}$
$\Delta\nu = \Delta b/\sqrt{ac}$

The amplitude as well as the phase of the tank moment depend on the following:

a. Frequency of encounter, ω_e.
b. Amplitude of rolling motion, ϕ_a.
c. Length of tank, l.
d. Breadth of tank, b.
e. Water height, h.
f. Vertical position of tank, s.

A typical plot of the nondimensional amplitude of tank moment μ_a (defined as $\mu_a = M_{ta}/\rho_t g b^3 l$, where ρ_t = mass density of tank fluid) and the phase angles is shown in Fig. 14.7, and the following conclusions have been reached in Ref. 217:

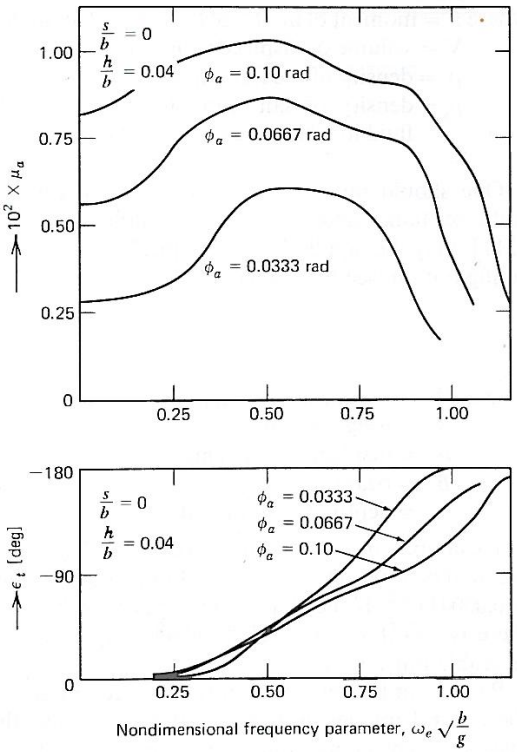


Figure 14.7 Amplitude and phase angle of tank moment for different amplitudes of motion [217].

1. The exciting moment of the tank is approximately proportional to the motion for low frequencies, whereas the plot for the phase angles becomes flatter as motion increases.
2. The tank moment is proportional to the length of the tank, l (measured in the longitudinal direction).
3. The water transfer in the tank can be considered as a wave phenomenon, that is, Froude's law of similarity can be used for scaling. Therefore the moment per unit of length is proportional to b^3 if the same h/b ratio is taken. The water height h is important for the "tuning" of the tank, and the natural frequency of the tank can be altered by changing the water depth inside it once the tank breadth is fixed. The amplitude of the tank exciting moment increases with the increase in water depth. The amplitude of tank moment (for a fixed breadth) at about the natural frequency of the tank is approximately proportional to $\sqrt{h/b}$.
4. The position of the tank (i.e., the vertical distance between the tank bottom and the axis of rotation, as denoted by s) is positive if the tank is located above the rolling axis. The amplitude of tank moment

is largest when s is the highest. Also, the plot of the phase angle to a base of frequency is flatter when the tank is situated higher. Both these qualities are preferable for motion stabilization.

U-Tube Tanks. There have been two types of U-tube tanks, one having a connection with the sea and the other completely enclosed inside the hull. The famous Frahm tank came into existence subsequently.

The principle of the Frahm tank is that the fluctuating columns of water form an oscillatory system having a natural frequency of oscillation depending on the construction of the tank. The natural frequency of the tank is made the same as that of the vessel. This is possible by having the cross section of the vertical column greater than that of the connecting tube, which lies horizontally.

However, the natural frequency of the vessel may vary for different loading conditions, and to make the natural frequency of the tanks as nearly equal as possible to that of the vessel for any particular loading condition, an air valve system is installed either on top of the tanks or in the connecting tube. In this configuration a path is provided for the air above the fluid in one wing tank to move to the space above the fluid in the other wing tank. If this air path is controlled by a valve, the amount of air flow and consequently the volume rate of water flow can be controlled. The water flow can be stopped completely by closing the valve, and this can be accomplished relatively fast.

The motion damping due to the U-tube tank is possible because there is a phase difference of 90° between the motion of the vessel and that of the water in the tank. This means that the stabilizing moment caused by the movement of water inside the tank is opposite in sign to the exciting moment.

Figure 14.8*a* shows by arrows the direction of ship movement during rolling motion, whereas the stabilizing moment is created by the weight of the tank water acting against the side of the ship, which tends to go upward. This can be seen in region A–B of Fig. 14.8*a*, which shows that the water flow in the tank is in the opposite direction to that of the ship at its extreme positions of roll; in other words, the water movement is 90° out of phase with the ship motion.

The amplitude of the tank stabilizing moment is

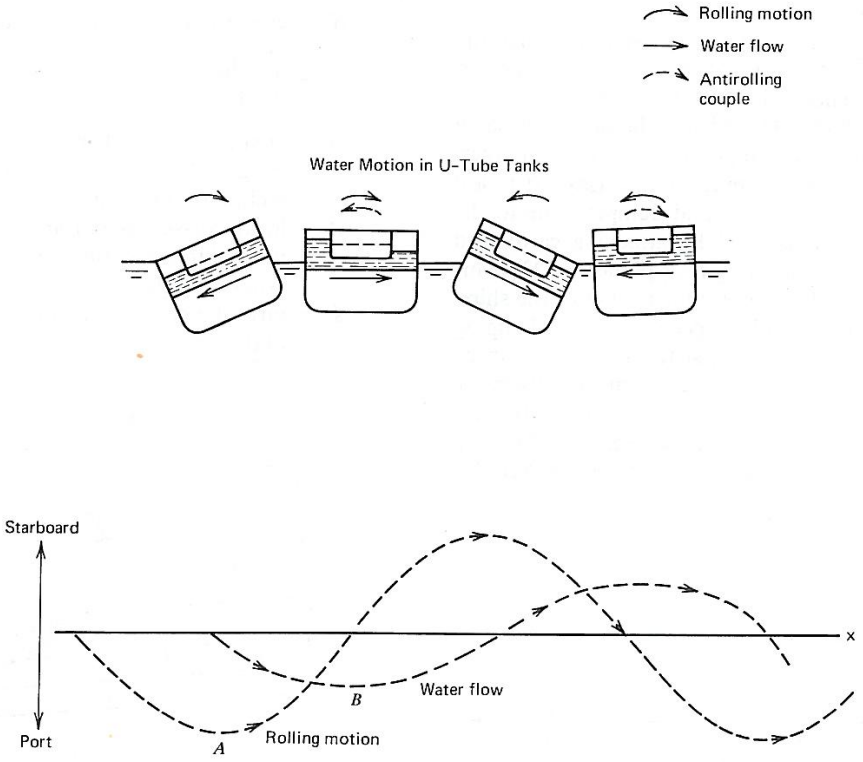


Figure 14.8*a* Water flow in stabilizer tank during rolling motion.

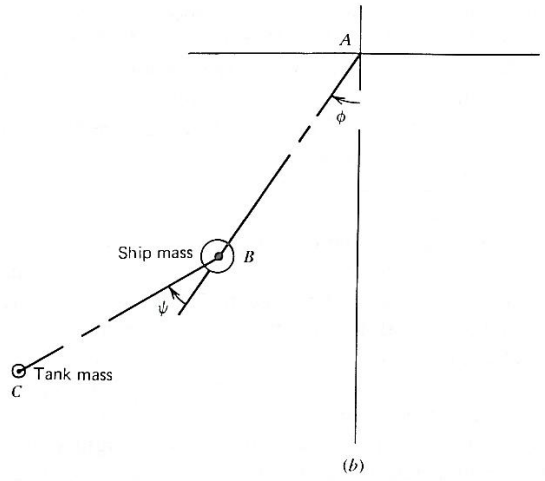


Figure 14.8*b* Pendulum analogy for ship-tank system.

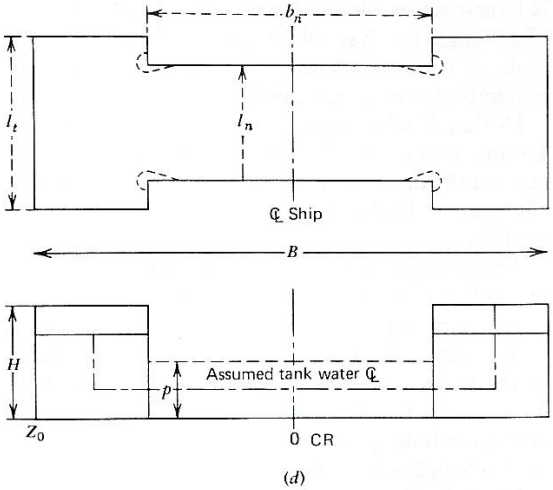


Figure 14.8*d* Schematic diagram for a U-tube tank.

characterized by the angle of heel imparted to the ship in still water under static conditions. Hence the "characteristic" of the tank is determined from the magnitude of the heeling action in still water, and greater tank volume is necessary in order to increase the characteristic of the tank and thus achieve greater tank effectiveness.

It is shown mathematically in Ref. 223 that the ship–tank system is equivalent to a compound pendulum, as shown in Fig. 14.8*b*. The lengths of the two pendulums, *AB* and *BC*, should be the same in order to make the two periods close to each other. The ship mass can be much larger (say 10 times) than the mass of the tank, and damping due to the tank can be demonstrated by attaching cardboard or paper vanes to the string near point *C* [223]. This damping, although not the same as that of the ship–tank system, is helpful in perceiving the damping effect on ship motion. At first the ship mass can be swung above, and the free oscillations are observed. When the mass of the tank is put to the ship mass, both masses can be swung and the interaction between the tank and the ship can be observed. In Ref. 223

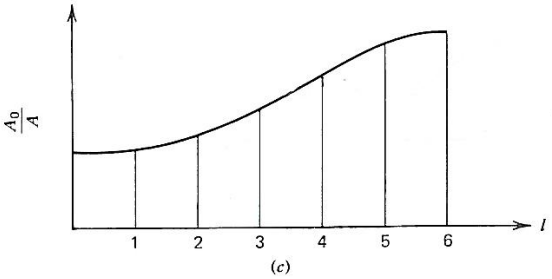


Figure 14.8*c* A_0/A versus S.

the natural frequency of the fluid in a U-tube tank of constant cross section is given as follows:

$$\omega_t = \sqrt{\frac{2g}{s}}$$

where ω_t = tank frequency
S = effective length of the U-tube

$$= \int_0^l \frac{A_0}{A(s)}\, ds$$

A_0 = area (constant) of the free surface in one wing tank of the U-tube or largest cross section of the U-tube
A = local cross-sectional area of the U-tube normal to the U-tube centerline (variable cross section)
s = girthlike coordinate along the centerline of the tank water

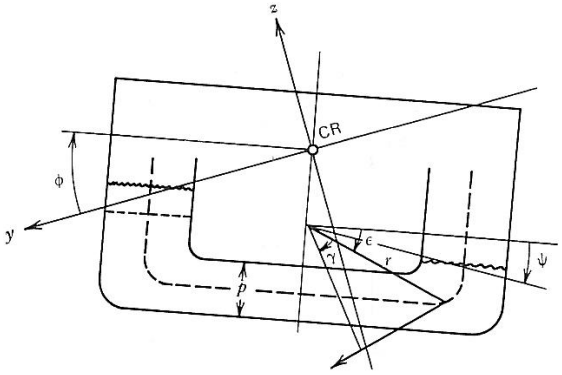


Figure 14.8*e* Tank coordinates.

l = total "girth length" of the tank water

This is illustrated in Fig. 14.8*c*.

For the tank shown in Fig. 14.8*d*, the effective length of the U-tube can be expressed as

$$S = \int_0^l \frac{A_0}{A(s)}\, ds = h + \frac{(B-b_n)^2}{4h} + \frac{(B-b)l_T b_n}{2hl_n}$$

In the nondimensionalized form the above expression is modified as

$$\tau_T^2 = \beta + \frac{(1-\gamma)^2}{4\beta} + \frac{(1-\gamma)\gamma}{2\beta C_n}$$

where

$$\tau_T^2 = \frac{S}{B} = \frac{2g}{B\omega_T^2}$$

$$\beta = \frac{h}{B}$$

$$\gamma = \frac{b_n}{B}$$

$$C_n = \frac{l_n}{l_T}$$

It should be noted that the depth of water is very important as far as tank frequency is concerned. The tank moment coefficient, K_Ψ, may be expressed in the same manner, namely, tank moment $M_t = K_\Psi \cdot \Psi$ (see Fig. 14.8*e*), where

$$K_\Psi = \rho_T g B^4 \frac{C_w}{16}(1-\gamma^2)(1+\gamma)$$

Then

$$\lambda_T = \frac{K_\Psi}{K_\phi} = \frac{\rho_T g B^4 C_w (1-\gamma^2)(1+\gamma)}{35{,}840\Delta\overline{GM}}$$

With these expressions, predictions can be made for ship roll frequency and tank and ship damping. The maximum quasi-static moment of the tank water and the maximum quasi-static heel angle caused by the tank may be obtained as follows [223]. According to Fig. 13.8*e*,

$$\tan \Psi_m = \frac{h}{2R} = \frac{\beta}{1+\gamma}$$

where Ψ_m is the maximum tank water angle before the emptying tank becomes dry. Since this angle rarely exceeds 10°, we have

$$\Psi_m = \frac{4\beta}{1+\gamma}$$

Then the maximum quasi-static moment of the tank water is

$$M_m = 2\rho g A_0 R^2 \Psi_m = \frac{\rho g B^4 (1-\gamma^2)\beta C_w}{4}$$

where

$$C_w = \frac{l_T}{B}$$

Then the maximum quasi-static heel angle due to the stabilizer is obtained as

$$\phi_m = \frac{M_m}{\Delta\overline{GM}} = \frac{\rho g B^4 (1-\gamma^2)\beta C_w}{4 \times 2240 \Delta\overline{GM}}$$

The value of ϕ_m for standard tank stabilizers is about 4°.

Example 14.1

The natural period of rolling of a ship is known to be 12 sec. Find suitable dimensions for a U-tube tank (assume a rectangular cross section for simplification of calculations).

Solution:

The period of oscillation of the mass of water within the tank should be equal to the natural period of the ship:

$$T_{\text{tank}} = T_\phi = 12\,\text{sec}$$

From this the comparative length is obtained as

$$\frac{S}{2} = \frac{g \times 12^2}{4\pi^2} = 117.5\,\text{ft}$$

The cross section should be taken as follows:

$$A_0 = ab = 25 \times 10 = 250\,\text{ft}^2$$
$$A = ac = 25 \times 2 = 50\,\text{ft}^2$$

$$\text{One-half of ship's beam} = \frac{B}{2} = 28\,\text{ft}$$

The half of the U-tube tank should be divided into a horizontal and a vertical tank. Therefore

$$\frac{S}{2} = \int_0^l \frac{A_0}{A} ds = \frac{A_0}{A} S^* + h$$

that is,

$$S^* = \frac{B}{2} - 10\,\text{ft} = 18\,\text{ft}$$

or

$$h = 5\,\text{ft}$$

or

$$\frac{S}{2} = 5 \times 18 + 5$$
$$= 95 \text{ ft}$$

But $S/2$ should be 117.5 ft. Therefore one cross section should be changed. One has to determine how much the height of C of cross section A must be changed so that $S/2$ will become 117.5 ft.

$$\frac{S}{2} = \frac{A_0}{A} S^* + h = \frac{ab}{ac} S^* + h$$

or

$$117.5 = \frac{10}{C} \times 18 + 5$$

or

$$112.5 = \frac{180}{C}$$

or

$$C = 0.625 \text{ ft}$$

This shows that the period of the mass of the tank water is 12 sec, and the length $S/2$ is 117.5 ft. For a ship breadth of 56 ft, the tank cross sections have the following dimensions:

$$A_0 = 25 \times 10 \quad = 250 \text{ ft}^2$$
$$A \quad = 25 \times 0.625 = 15.625 \text{ ft}^2$$

The advantages of a U-tube tank are as follows:

a. Relative simplicity, since it is a passive stabilizer.

b. Economical installation and operation, since no power is required for operation, and a U-tube tank can be easily installed during or after the construction of the ship.

c. Improved effectiveness, that is, the 50% or more roll stabilization obtained by a U-tube tank enhances considerably the seakeeping quality of a marine vehicle.

d. Possibility of weight reduction by emptying the tank when not used for stabilization.

e. Provision of extra storage for fresh water, reserve fuel, and other useful loads.

On the other hand, in comparison with some active roll stabilization systems, the passive U-tube tank has a few disadvantages:

a. Proper tuning for all loading variations may not be possible, since the U-tube tank is designed for only one condition, and tuning is possible for only a limited departure from the design condition.

b. This type of tank is inadequate for an irregular seaway that possesses waves of all frequencies from different directions. The quick change in rolling motion may disrupt the smooth operation of the U-tube tank, which has a comparatively large response time in relation to the active roll tank.

c. There may be an adverse effect on the stability of the vessel. The yaw–heel effects of rolling are destabilized by the passive U-tube tank system, and this is a serious drawback, especially in the case of high-speed vessels, which tend to have greater yaw–heel effects.

Diversified Tank Stabilizers. This kind of roll stabilizer has been developed from the free surface tanks. The disadvantages of the latter have been overcome by a diversified tank stabilization system, which consists of two or three transverse tanks connected by ducts, flumes, or nozzles. The flow of liquid during the rolling motion is restricted. The weight of the liquid ballast is limited to the temporarily higher side in the form of the controlled free surface effect, and the energy dissipation at the flume causes the roll damping effect. This method of control causes the free surface movement of the partially filled tanks to lag the roll of the ship by 90°, thus damping the roll of the vessel and, at the same time, counteracting the tendency to roll past the normal to the wave slope. The depth of water in the flume at the centerline of the ship remains the same throughout the transfer cycle and depends on the amount of water in the system, and not on the vessel's movement, as shown in Fig. 14.9. The angle of 90° between the free surface moment acting about the axis of roll and the normal or static position is maintained by the flume nozzles, which also prevent the movements of the water and of the vessel from synchronizing, as could occur if the system were too lightly damped. It is the introduction of this particular form of control that constitutes the main difference between the flume stabilization system and the older types of passive tank stabilizers.

Figure 14.10 shows the standard tank design for the diversified form of the flume tank stabilization system. The only method of control in this system is to change the water level in the tanks. A large tuning factor is possible if adjustable nozzles are used.

Note that the flume stabilization system is similar to both free surface tanks and U-tube tanks. The function of the center tank is similar to that of the cross-connecting tube in the U-tube tank, but the restriction of flow in this case is achieved by the nozzles. The tank itself is similar to the free surface tank in general shape. Like the U-tube tank, the

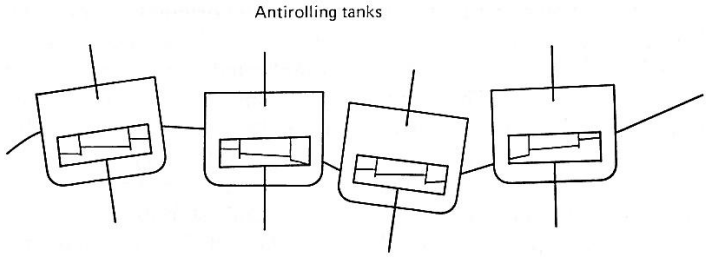


Figure 14.9 Operation of flume stabilization.

flume stabilization system can also be used as cargo or fuel space.

To obtain sufficient stability in emergency, the tanks can be emptied with the help of dump valves, thereby eliminating the free surface effects.

Because of the high effectiveness (about 75%) of flume tanks many ships have been built with them but without bilge keels in order to lessen the resistance caused by the latter.

In general, there are no real disadvantages of the flume stabilization system. Efforts are being made, however, to improve the control and tuning, in conjunction with experimental results, in order to make this system more acceptable.

To test the passive tank stabilizers, model tests are performed. The first part is the bench test, in which a large-scale tank model is oscillated on a test bench over a wide range of frequencies corresponding to varying sea conditions. The bench test is used primarily to verify the calculated values of phase lag and stabilizer moment but is also very significant for the study of the flow pattern of the water in the tank.

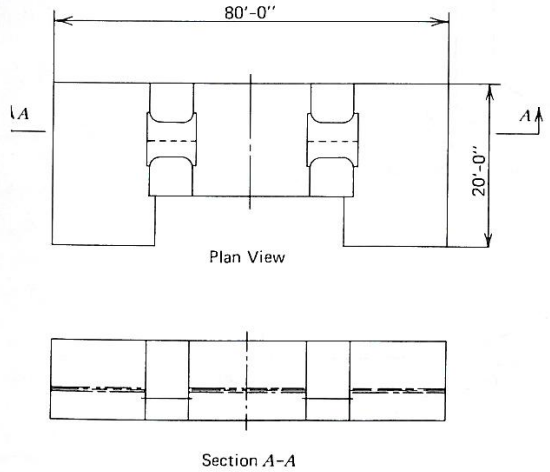


Figure 14.10 Standard tank design for flume stabilization system.

Next, a sufficiently large model is built and tested, both stabilized and unstabilized, under various sea and speed conditions.

ACTIVE ROLL STABILIZERS

Active Roll Tanks

It is self evident that active antiroll tanks can have a faster response than passive tanks to waves in an irregular seaway, as well as a greater damping effect. A further development of the active system to the Frahm U-tube is to pump water from one vertical tube to the other, thereby eliminating the dependence of the tank on resonance. Thus the stabilizing moment can be applied more quickly.

In a simplified version of an active system an accelerometer senses the rolling motions, and signals are sent from this roll sensing device to a variable pitch pump, which controls the liquid flow between the tanks.

An active version of the diversified tank system

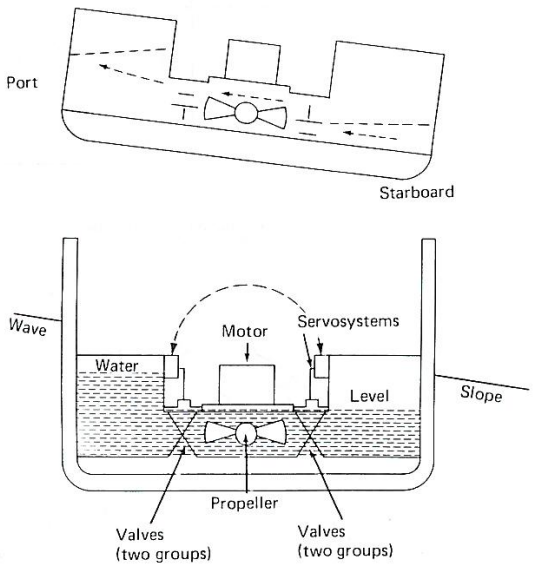


Figure 14.11 Active tank stabilizer (Muirhead-Brown type).

is the Muirhead–Brown system, shown in Fig. 14.11. In this case a propeller rotating at constant speed is put in the center channel, and the valves on either side control the direction of water flow. The pump brings the water level up high and the upper valves open on the side into which the water should flow; on the other side the upper valves close, but the lower valves open to let the water move from that side to the other one. When the ship is upright, all valves open and the water moves freely between the two tanks. This system is controlled by a servomechanism that is actuated by accelerometers.

In the Muirhead–Brown passive tank system the valves are controlled by the same type of controls as were described for the active system. The only difference is that in this controlled passive system the water is not forced to flow by a propeller. This system lies somewhere between the active and the passive system. It has better motion stabilization characteristics than ordinary passive antiroll tanks and is cheaper to install and to run than active antiroll tanks. This system is quite effective in stabilizing the roll motion of a wave train, but it cannot stabilize the ship against each single wave, as the active system will.

The main part of the active system is the sensing device that feels the change from the upright position and activates the equipments to bring the ship back to its original position. The device of the active system can be either a simple accelerometer or a complicated gyroscopic sensing system that detects even a small angle of roll by the gyroscope precession. Thus the sensing device can be used to control ship motion due to every single wave.

Depending on the sophistication of the system, active tank stabilizers have been found to have an efficiency of 80% or more in motion stabilization. Also, the fact that the system can take into account every single wave, and not just a train of waves, makes the active antiroll tank very effective in an irregular seaway.

The other advantages of the active antiroll tank are that (a) the size of the tank can be reduced because of better utilization of the weight, (b) the system can be operated even when a constant heel is present because of any particular loading of the vessel, (c) in case of damage the system can be used to correct listing, (d) an induced motion is possible for an icebreaker in its operation, and (e) there is little loss in metacentric height.

Fin Stabilization

Since World War II roll stabilization with activated fin stabilizers has been adopted for many passenger

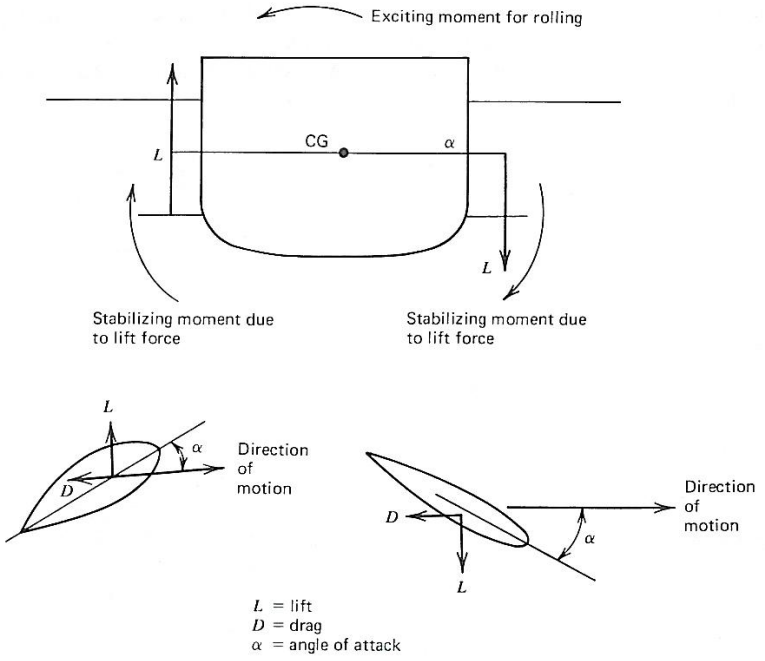


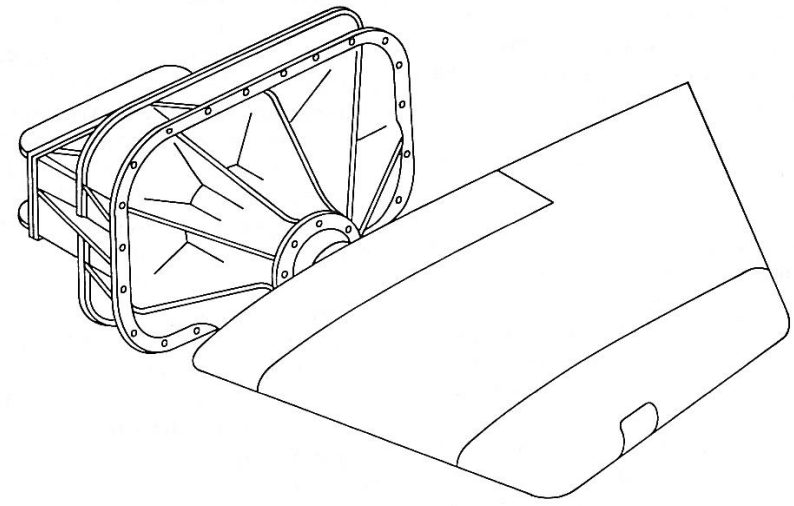
Figure 14.12*a* Location and mechanism of active fins.

liners, mainly because of the pioneering work of the Denny–Brown Company in England. However, the idea of using active fins for roll stabilization is not new, and John T. Thornycroft of England and Motora of Japan developed active fins long before World War II.

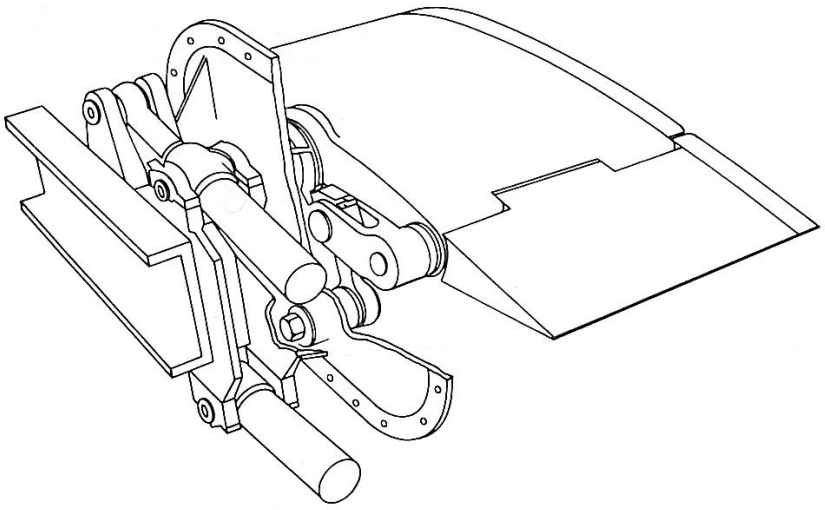
The active fin stabilization system is composed of at least one pair of moving fins, one on the port and the other on the starboard side. For rolling motion toward the port side, the port fin is tuned upward and the starboard fin is tuned downward (i.e., the angles of attack in the two fins are opposite to each other). The fins then generate a moment (couple) that opposes the moment causing the roll. The moment created by a fin is due to the lift force produced by the fin while moving at a speed (see Fig. 14.12*a*).

A typical system is shown in Fig. 14.12*b*, which describes a trapezoidal fin unit, as well as a full mechanical flap to increase the lift coefficient.

The stabilizing moment is obtained by multiplying the lift force by the appropriate lever to the rolling axis. Thus the stabilizing moment tends to heel a ship in the direction opposite to that of the exciting



Trapezoidal Fin Unit



Flapped Fin Unit

Figure 14.12*b* Typical active fin stabilizers [164].

moment for rolling. By reversing the direction of tilt, the direction of the stabilizing moment is reversed in order to oppose the exciting moment of roll, which is harmonic and therefore changes its direction after every half-period. The net effect due to the exciting and stabilizing moments is therefore a reduction in the rolling motion.

Let us say that the maximum ordinate of the exciting moment is 332 ft-tons (where $L_w = 512$ ft, $\alpha_m = 9°$, assuming $H_w = \frac{1}{20}L_w$). Then the mean ordinate of the exciting moment $= 332 \times 2/\pi = 212$ ft-tons. If it is assumed that the fin will be at full tilt for 82% of the half-period, the maximum stabilizing moment that should be applied is $212 \times (1.0/0.82) = 258$ ft-tons.

In other words, instead of seeking complete stability, the economic method will be to apply a stabilizing moment of 258 ft-tons in order to balance the exciting moments due to wave. The static list of the ship caused by this stabilizing moment may be obtained from the curve of righting moment (statical) versus angle of inclination.

To obtain the maximum stabilizing moments obtainable with fins of various shapes and sizes and at various angles of tilt, experimental investigations are necessary. In addition to the lift forces the positions of the centers of pressures also are determined to predict the torque necessary to reverse the direction of tilt for the fin.

The fin of an active fin stabilization system is almost like a horizontally placed rudder, and the problem of fin design involves the study of hydrofoils and rudders.

The main requirements for a stabilizing fin are as follows:

a. Symmetry with respect to positive and negative angles of attack.
b. High maximum lift force.
c. Low drag.
d. Low torque.
e. Retractability.
f. Adequate strength.
g. Resistance to cavitation.

These requirements determine the fin sections and the planform, which should have a geometric aspect ratio no greater than 2. There are some advantages to tapering the tips, but the tips may also be square. The thickness ratio of the fins is approximately 20% or more at the root. To obtain a higher maximum lift coefficient, a trailing edge flap is often used. (See Fig. 14.12*b*.) Flapped fins are also superior to all-movable fins where cavitation is a certainty.

According to Ref. 26, a typical "stabilized day" at sea will include a force 3 to 4 beam wind with moderate seas. Fin angles of plus and minus 8° with average lifts of 20 tons will keep the residual rolls of a typical ship of 20,000 tons to less than 0.5°. Figure 14.13 shows the motion stabilization in a moderately following sea against yaw–heel effects.

Activated fins are the most effective of all single stabilizing devices. Although the controlling equipment and machinery cost more than does a tank system, for many ships the larger expenditure may be justified by the correspondingly greater stabilization effect.

The fin system is designed to operate in up to 5° of effective wave slope and over the full rolling range of the ship. The sensitive sensing equipment allows large correcting moments to be applied for even very small rolling motions. The fin system can

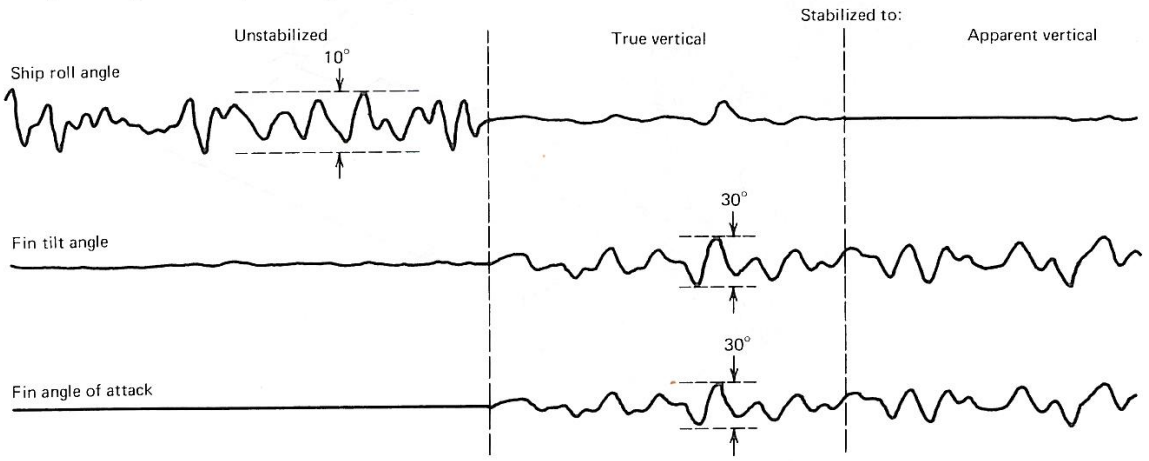


Figure 14.13 Typical record of fin movement and rolling motion [26].

therefore be used to correct any list while under way, although this represents a waste of power and an increase of drag and is generally not recommended for long terms.

For commercial ships, such as passenger liners or vessels carrying fragile cargo, active fin stabilization systems are practicable and highly desirable. The fin stabilization system is also useful in naval ships. For example, an aircraft carrier has a great need to keep a level flight deck; any loss of space incurred by the installation of stabilizing fins will be justified by the added capability of rough weather launching. Also, small ships, such as destroyers, could benefit greatly from a fin stabilizing system. The stabilizing system could be correspondingly smaller to accord with the small ships, and the increase in stabilization of the weapons platform would be worthwhile.

One serious disadvantage of fin stabilization is that the ship must be at speed for the fin to generate lift; if the vessel is at rest, the fin is ineffective, since no lift force can be generated at zero speed. The lift force (as well as the rolling moment) generated by active fins is proportional to the square of the ship speed, as shown in Fig. 14.14. At a speed below 10 knots it is seen that very little stabilizing moment is available. Also, because of the load on the activating mechanism or on the fin pivot, the maximum angular displacement for an active fin is limited for a particular speed. Hence full utilization of the system is not possible.

During the rolling motion of a vessel, the sum of the induced incidence and the imposed incidence on the active fin may add up to quite a large angle (30° or more) of attack. In addition to the structural considerations for high loading, stalling of the fin may be expected. In other words, the fin may then generate very little lift, and this means that the stabilizing moment will be insignificant.

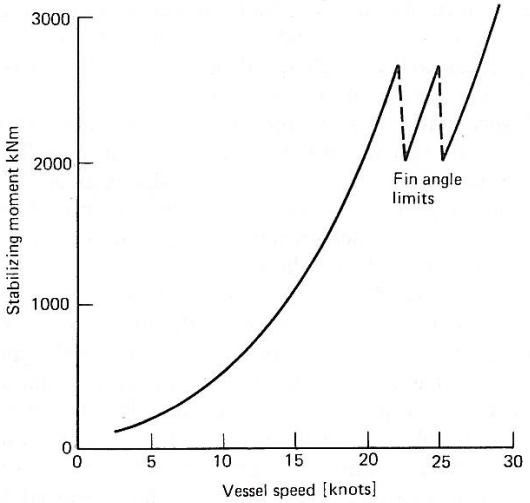


Figure 14.14 Typical active fin stabilizer characteristics.

Jet Flaps

A recent development of the fin system as a roll stabilizer is the jet flap. For warships and other vessels requiring a stable platform for helicopter operation or sonar effectiveness a low speed roll stabilization system is essential.

The jet flap system shown in Fig. 14.15 has been

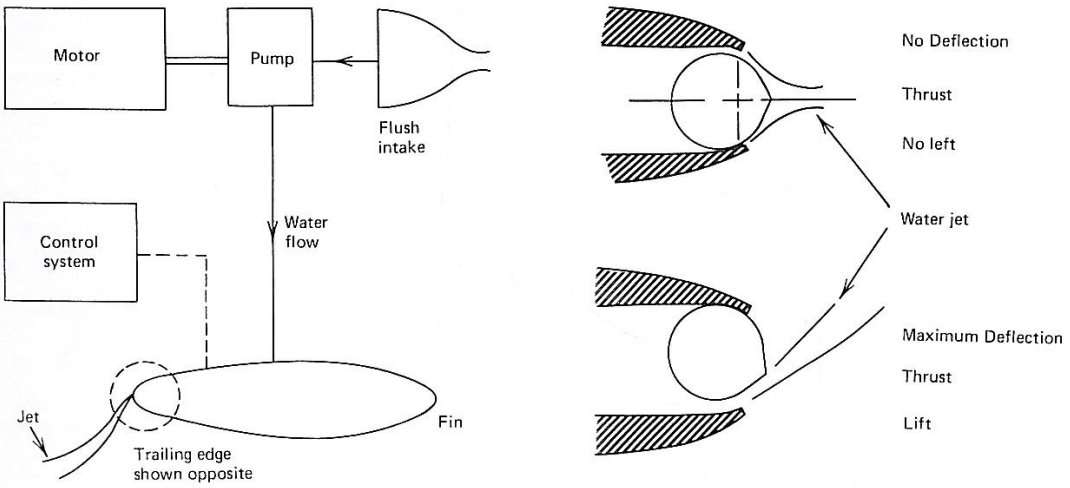


Figure 14.15 Jet flap system [164b].

developed by the Admiralty Research Laboratory of the British Navy and is very well suited for low speed as well as high speed operation. Since in the jet flap system the fin is fixed to the hull, a much higher load can be withstood by the fin than in the active fin system. In the jet flap system a jet of fluid is ejected from or near the trailing edge of an aerofoil at an angle to the mainstream. The presence of the jet produces a much greater lift force than the vertical component of the resultant thrust.

As Fig. 14.15 shows, a center body is eccentrically pivoted in the trailing edge of the fin. Water from inside the fin passes around the center body, and the relative sizes of the slots decide what quantity of water will pass through each side. Because of the Coanda effect the jets stay attached to the center body, and the individual momenta of the jets combine to form a resultant jet angle. The lift produced by the jet flap will be proportional to the square root of the momentum, as well as the angle of the jet.

The increased lift force ΔC_L is dependent on the jet strength as well as the angle at which the ejection is made. A simplified expression for ΔC_L is

$$\Delta C_L = k \sin\theta \sqrt{C_\mu} \cdot F(AR) \cdot F(t/c) \qquad (14.8)$$

where ΔC_L = lift increment due to jet flap
k = a constant depending on the geometry ≈ 3.9
θ = jet angle (maximum 60°)
C_μ = momentum coefficient $= \dot{m} V_j / \frac{1}{2}\rho S V_0^2$
$\dot{m}$ = mass of the jet flow
V_j = velocity of the jet
V_0 = speed of the ship
$F(AR)$ = finite aspect ratio correction
$F(t/c)$ = thickness correction

The increased lift thus obtained from the jet flap is added directly to the lift generated by the fin.

Rudder Stabilization

When the ship's rudder is placed off the centerline, a lift force is generated that generally acts at a point below the roll center (the CG) of the ship. This side force therefore causes both roll and yaw moments. The roll moment generated by a rudder is small in magnitude, and so its effect is also small unless its frequency is in the region of the natural roll frequency of the ship.

Model tests have shown that large roll oscillations can be generated either (a) by wave roll moments or (b) by the wave moments causing a yaw motion, which is corrected by use of the rudder. Therefore, if proper phasing can be obtained between the rudder-induced roll moment and the wave-excited roll moment, the rudder can serve as a roll stabilizer at or near the resonant roll frequency.

The rolling motion stabilized by rudder angles alone is shown in Fig. 14.16. The effectiveness of a rudder as a roll stabilizer in comparison to a passive tank stabilizer is illustrated in Fig. 14.17.

For small crafts rudder stabilization may be as effective as that due to fins, since rudder-induced

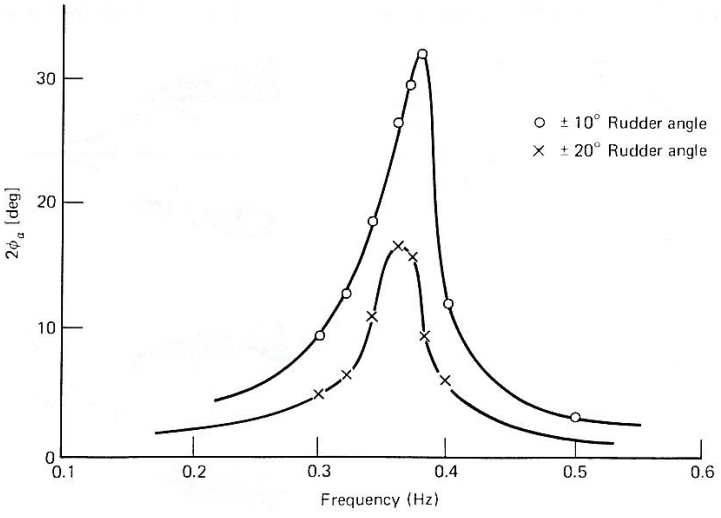


Figure 14.16 Typical record of roll stabilization due to rudder movement [36c].

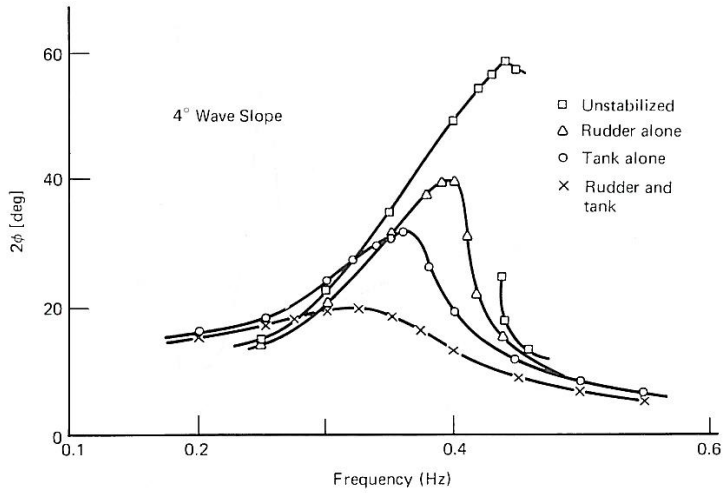


Figure 14.17 Comparison of roll responses for different stabilization systems [36c].

roll moments are as significant as the roll moments generated by fins. The comparatively shorter distance between the roll center and the lift force is offset by the increased flow velocity at the rudder due to the propeller action. It should also be noted that, because of instability in the rudder control system at larger rudder angles, due to coupling between rolling, yawing, and swaying motions, only small rudder angles can be used for stabilization. In other words, stabilization due to rudder action is rather limited.

14.3 PITCH STABILIZATION

The adverse effects of the pitching motion of ships are speed loss for a given power, slamming that may lead to severe structural damage, and motion sickness. It is therefore highly desirable that the pitching motion of a vessel be reduced. The problems of reducing pitch are quite different from those of roll stabilization. The fact that pitch is already considerably dampened by the vessel's hull, means, of course, that large forces are required for any further increase in this damping. It is quite impractical to generate these large forces by means of internal devices (i.e., tanks, gyroscopes, moving weights, etc.) as is done for roll stabilization. Also, the pitching motion is not resonance dominated, as is roll; this means that the roll spectrum is sharply tuned, whereas pitching responds to a broad range of frequencies. Hence antipitching fins operate most effectively near the synchronous range and have much less effect at higher and lower frequencies.

Thus all attempts at pitch stabilization have utilised external devices, capable of sustaining the large forces involved. These devices have been fixed bow fins, movable stern fins, and, to a lesser degree, movable bown fins and fixed stern fins. Only the fixed bow fins have been installed on ships and have been able to reduce pitch and speed loss.

Fixed Fins

Both model experimentation and full-scale trials have been undertaken to investigate the effects of fixed fins at the bow of a ship on pitching motion. It has been found that a significant reduction of motion can be achieved in shorter waves, but there is considerable doubt as to whether fixed fins can provide adequate stabilization for pitching motion. On the other hand, active fins can produce almost double the attenuation of fixed fins, but active fins and their operating machinery and controls may require excessive amounts of weight, space, and expenditure.

The importance of deep submergence of anti-pitching fins has been noticed in sea trials, but any ship fitted with bow or stern fins, however deeply submerged, faces adverse conditions when the fins emerge. This may cause a serious design problem, especially in the case of active fins, since a very large force occurs during the emergence of the fin and this must be considered in the structural design. Again, air drawing will also reduce the stabilizing forces on the upper surfaces of the fins. Although this can be improved by deeper submergence, complete correction may not be possible.

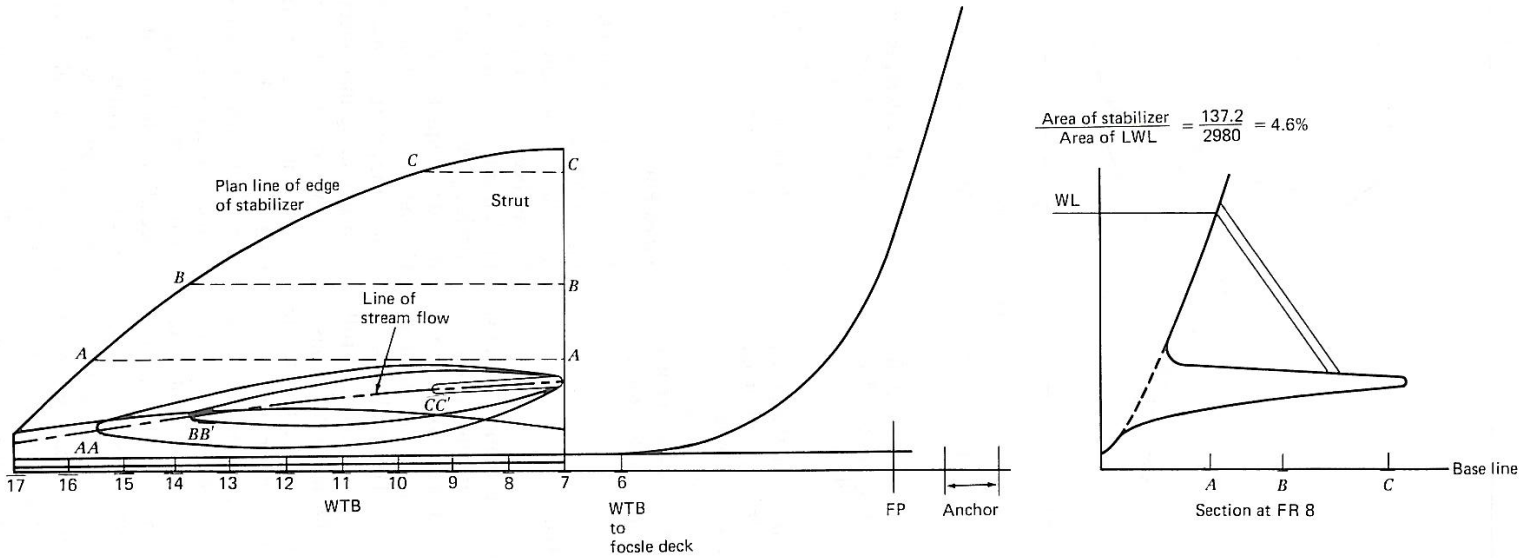


Figure 14.18 An antipitching fin [36b].

The loss of speed due to fins is not excessive in calm water, and fixed fins can even be so designed that the resistance can be decreased for a certain speed, as in the case of a bulbous bow. However, slamming occurs frequently in the stabilized ship in a rough sea when fins are fitted, and a reduction of only 20 to 25% in the pitching motion does not justify the fins in view of the adverse effects, like slamming or vibration, caused by the cavity collapse impacting against the side of the hull. Stern fins do not appear to be better than bow fins.

The fins should be as far forward as possible to give maximum stabilizing moment. A typical design of a fin with an area of 4.5% of the load waterplane area is shown in Fig. 14.18.

A systematic investigation of antipitching fins has been made [1] in order to determine both qualitatively and quantitatively the reduction they produce in the pitching motion of ships. This was done in the following manner:

a. Large lift-producing devices were placed at both ends of the ships to produce large opposing pitching moments proportional to the pitch angular velocity and thus increase the pitch damping.

b. Experimental results were obtained for the order of magnitude of the effect of resonably sized antipitching fins.

c. An analytical study was made of the equations of motions in order to predict the quantitative effect of adding the fins to the ship.

d. Model experimentation was carried out to determine also the bending moment loads at the root of the fin.

e. The adverse horizontal bow vibrations caused by bow fins were investigated.

f. An analytical approach was employed to determine the effect of automatically controlled or activated antipitching fins.

Since we are dealing here with the antipitching fin that will reduce the pitching motion of a ship, we should investigate the terms in the equation that are of considerable significance for the pitching motion.

Without any loss of qualitative significance, the equation of motion can be expressed in the form of an oscillating system having one degree of freedom as follows (see also Chapter 4):

$$a\ddot{\theta} + b\dot{\theta} + c\theta = M_0 \cos \omega_e t \qquad (14.9)$$

where a = virtual mass moment of inertia
b = linear damping coefficient
c = restoring coefficient
M_0 = exciting moment for pitching

The magnification factor is known to be

$$\mu_\theta = \frac{\text{Amplitude of pitching motions}, \theta_a}{\theta_{st}}$$

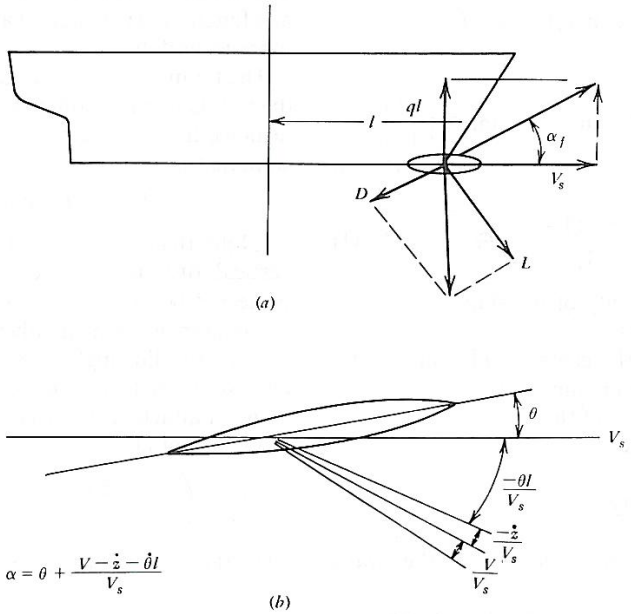


Figure 14.19 (*a*) Force diagram for an antipitching fin. (*b*) Components of angle of attack on the fin.

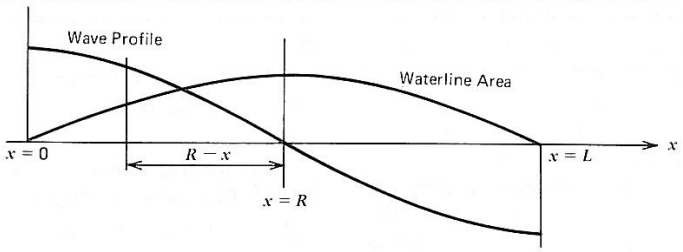


Figure 14.19*c* Wave profile and waterline area.

where

$$\theta_{st} = \frac{M_0}{c} \qquad \text{or} \qquad \theta_a = \mu_\theta \cdot \theta_{st}$$

Here c can be approximated by $\Delta\overline{GM}_L$ for normal surface ships (see Section 4.4).

A change in a typical hull design for the purpose of increasing the damping coefficient is not simple, since any alteration, say in the waterplane shape, alters each of the hydrodynamic coefficients, and the excitation often is in the opposing direction (from the point of view of contribution to the value of the damping coefficient). An appendage added to the hull, however, may significantly increase the damping coefficient for conventional ship types without significantly changing the other hydrodynamic characteristics.

An efficient large lift-producing surface is the hydrofoil (see Fig. 14.19*a*), where

$$q = \text{pitch angular velocity} = \dot{\theta}$$

For small q,

$$\text{Angle of attack at the fin} = \alpha_f = \tan^{-1}\left(\frac{ql}{V_s}\right) \tag{14.10}$$

otherwise

$$\alpha_f = \theta + \frac{-\dot{z} - \dot{\theta}l + v}{V_s} + \Theta \tag{14.11}$$

where V_s = forward velocity of the ship
C_L = lift coefficient
l = distance of the center of pressure of the fin from the pitching axis
A = projected area of the fin
C_D = drag coefficient
θ = pitch angle
$\dot{z}$ = heave velocity
$\dot{\theta}$ = pitch velocity
v = vertical orbital velocity of the wave particles at the fin
Θ = fin inclination by the control system

All angles should be in radians, and the angle of attack is then changed to degrees to enter the curve for lift coefficient versus angle of attack. A sketch showing the components of the angle of attack is given in Fig. 14.19*b*. The lift force on the fin can then be expressed as

$$L_f = \tfrac{1}{2}\rho V^2 (\text{area}) \cdot C_L(\alpha)$$

The lift produced (by angular velocity) on the fin is expressed as

$$L_f = \left(\frac{\partial C_L}{\partial \alpha}\right)_f \alpha_f \tfrac{1}{2}\rho A[V_s^2 + (ql)^2] \tag{14.12}$$

The drag on the fin is

$$D_f = C_D \tfrac{1}{2}\rho A[V_s^2 + (ql)^2] \tag{14.13}$$

It should be noted, however, that for large angles of attack the fin may approach 30°. Then the assumption of the linear slope of the lift coefficient versus angle of attack curve is not justifiable, and the lift coefficient as a function of the angle of attack should be estimated more accurately.

The fin moment produced, M_f, is given as the product of the vertical component of the lift force and the distance from the center of the fin to the CG of the ship, that is,

$$M_f = -L_f l \cos\alpha - D_f l \sin\alpha \tag{14.14}$$

(Note that the moment component due to the vertical distance between the axis and the fin is neglected because of the small force component and small moment arm involved.) The most significant part of the fin angle of attack is due to the pitch angular velocity $\dot{\theta}$; and if the lift coefficient versus angle of attack curve is assumed to be linear, $\partial C_L/\partial\alpha$ is a constant and

$$L_f = \left(\theta + \frac{-\dot{z} - \dot{\theta}l + v}{V_s} + \Theta\right)\frac{\partial C_L}{\partial \alpha}\tfrac{1}{2}\rho V^2 (\text{area})$$

Thus the major component of this force is

$$-\dot{\theta}\left[\frac{l}{V_s}\frac{\partial C_L}{\partial \alpha}\tfrac{1}{2}\rho V^2 (\text{area})\right]$$

This is a constant times $\dot{\theta}$, which is of the same form and acts in the same way as the term $b\dot{\theta}$ in (14.9) and can be considered as an extra damping for this equation. Therefore the effect of the fin is mainly to increase the damping forces, which are of considerable significance in nearly resonant conditions. When the terms are added, we have

$$M_f = -\tfrac{1}{2}\rho A l V_s^2 \left[1 + \left(\frac{ql}{V_s}\right)^2\right]^{1/2} \times \left[\left(\frac{\partial C_L}{\partial \alpha}\right)\tan^{-1}\left(\frac{ql}{V_s}\right) + C_D\left(\frac{ql}{V_s}\right)\right] \tag{14.15}$$

It is shown in Ref. 1 that, when the square root term is expressed in a binomial expansion and the inverse tangent is expressed in power series,

$$M_f = -\tfrac{1}{2}\rho A l V_s^2 \left\{\left(\frac{\partial C_L}{\partial \alpha}\right)_f \left[\left(\frac{ql}{V_s}\right) + \tfrac{1}{6}\left(\frac{ql}{V_s}\right)^3 - \frac{11}{120}\left(\frac{ql}{V_s}\right)^5 \cdots\right] + C_D\left[\frac{ql}{V_s} + \tfrac{1}{2}\left(\frac{ql}{V_s}\right)^3 - \tfrac{1}{8}\left(\frac{ql}{V_s}\right)^5 \cdots\right]\right\} \tag{14.16}$$

or the damping coefficient due to the fin is given as

$$M_f = b\frac{d\theta}{dt}$$

or

$$b = \left(\frac{\partial M_f}{\partial \theta}\right)_{\dot{\theta}=0} = -\tfrac{1}{2}\rho A V_s l^2\left[\left(\frac{\partial C_L}{\partial \alpha}\right)_f + C_D\right] \simeq -\tfrac{1}{2}\rho A V_s l^2\left(\frac{\partial C_L}{\partial \alpha}\right)_f \tag{14.17}$$

The numerical value of $\partial C_L/\partial \alpha_f$ (for α in radians) for a thin hydrofoil with elliptical distribution is given as

$$\frac{2\pi}{1 + (2/AR)} \qquad \text{(for nonviscous flow)}$$

where AR = aspect ratio of the hydrofoil = foil span/chord length, or

$$\frac{\partial C_L}{\partial \alpha_f} = \frac{5.7}{1 + (2/AR)} \qquad \text{(for real fluid)}$$

The mass of the fin can be neglected in the motion calculations, but the added mass should be taken into account. The fin added mass may be taken to be the mass of a flat plate, that is,

$$\frac{\pi\rho S^2 c^2}{4(S^2 + c^2)^{1/2}} \tag{14.18}$$

where S is the span of the fin, and C is the chord of the fin.

The fin added mass is added to the overall added mass for heaving motion a_z, whereas the fin added mass times l^2 is added to the virtual mass moment of inertia of the ship, that is, a of (14.9).

Figure 14.20*b* gives typical pitch response per unit

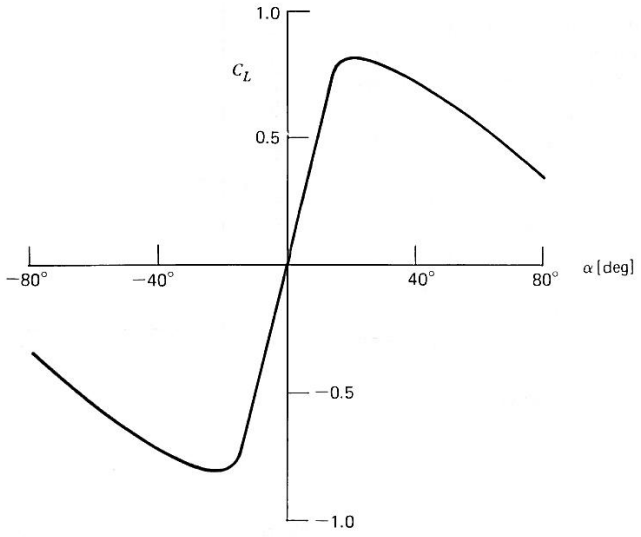


Figure 14.20*a* Lift coefficient versus angle of attack.

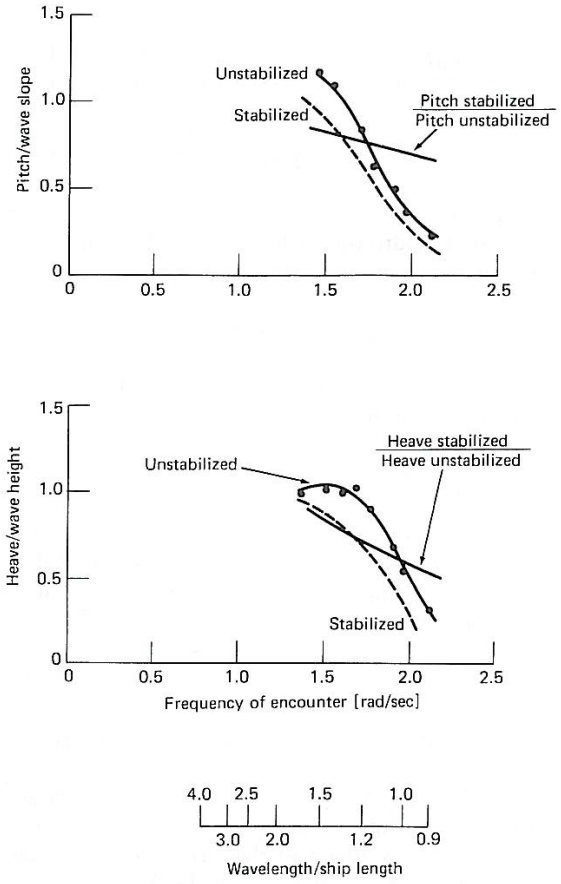


Figure 14.20*b* Pitch and heave responses from model tests [36b].

wave slope plotted against circular frequency of encounter for two ship models, one with and the other without antipitching fins. The heaving motions per foot of wave height are similarly plotted. Also, in this figure the ratios of the motion of the model with fins to that without fins are given.

The vertical accelerations of the bow converted from vertical motion are shown in Fig. 14.21.

Thus the model test results show that the pitching motion was reduced by about 25%, and the heaving by a maximum of about 40%, in the shorter waves tested. However, the effectiveness of the fins is reduced in longer waves.

Reference 37 provides the following numerical example.

Example 14.1

The following particulars of a vessel are given:

$$B = 130 \text{ ft}$$
$$T = 38 \text{ ft}$$
$$k_{yy} = 0.25L$$
$$\text{LCB from } \otimes = 7.6 \text{ ft aft}$$
$$\Delta = 84{,}000 \text{ tons}$$

Investigate the effect of an antipitching fin.

Solution:

Using a ship speed of 40.5 ft/sec and the lift curve given in Fig. 14.20*a* and multiplying by the distance from the fin to the center of gravity of the ship gives, as the maximum moment that can be exerted by the fin, 2.5×10^9 ft-lb. This must be compared with the maximum exciting moment due to the waves to be evaluated.

The order of magnitude of the exciting moment can be estimated as follows. The ship is assumed to have a sinusoidal waterline, and the wave to have a sinusoidal profile with a wavelength equal to twice the ship length and a node at the midship section. A sketch of waterline shape and wave profile is shown in Fig. 14.19*c*.

If only the added buoyancy forces due to the wave profile on the ship are taken into account, the exciting

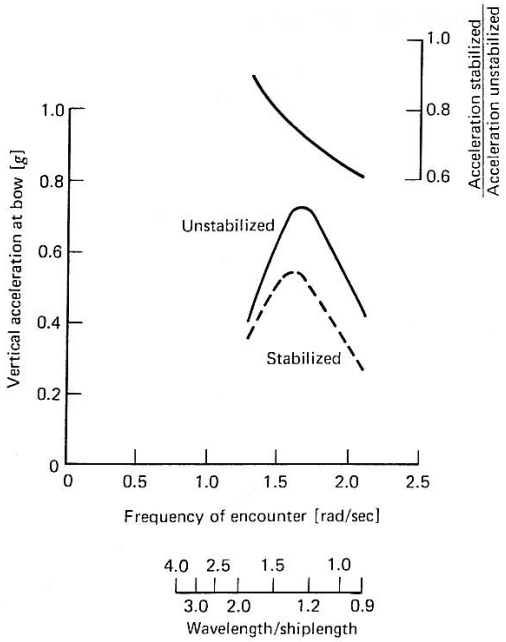


Figure 14.21 Vertical acceleration predicted from model tests [36b].

moment due to the wave is

$$M = 2 \times 64 \int_0^R A\zeta(R - x)\,dx$$

where A = waterline area per unit length
$= B \sin(\pi x/2R)$
B = maximum beam = 130 ft
ζ = wave elevation
$= \zeta_a \cos(\pi x/2R)$
$R = \frac{1}{2}$(LBP)

The maximum moment is obtained as

$$M = 2 \times 64 B\zeta_a \int_0^R \sin\left(\frac{\pi x}{2R}\right)\cos\left(\frac{\pi x}{2R}\right)(R - x)\,dx$$

$$= 64 B\zeta_a \int_0^R \sin\left(\frac{\pi x}{R}\right)(R - x)\,dx$$

$$= 64 B\zeta_a \left(\frac{R^2}{\pi}\right) = 0.645 \times 10^9 \zeta_a$$

Equating this to the maximum fin moment, we have

$$0.645 \times 10^9 \zeta_a = 2.5 \times 10^9$$

or,

$$\zeta_a \approx 4 \text{ ft}$$

The fin can therefore compensate for a wave amplitude of 4 ft and wavelength of 2000 ft. This would give a wave height/wavelength ratio of 1 : 250. Since the normal ocean wave may be assumed to have a wave height/wavelength ratio, more on the order of 1 : 40, the fin can neutralize about 20% of the exciting moment of such a wave.

Ideally the control system would measure the exciting moment and turn the fin to counteract it. The technique of measuring the moment, however, may not be easy.

An examination of the properties of an oscillation having a single degree of freedom (see Chapter 4) gives some insight into how the problem might be handled in a different way. For an uncoupled pitching motion we have (see Chapter 4)

$$a\ddot{\theta} + b\dot{\theta} + c\theta = M_0 \sin \omega_e t$$

The steady-state solution is

$$\theta = \theta_a \sin(\omega_e t - \tau)$$

$$\dot{\theta} = \theta_a \cos(\omega_e t - \tau)\omega_e$$

$$\ddot{\theta} = -\omega_e^2 \theta$$

where

$$\tan \tau = \frac{2\kappa\Lambda}{1 - \Lambda^2}$$

$$\omega_\theta = \sqrt{\frac{c}{a}}$$

$$\theta_a = \frac{\theta_{st}}{\sqrt{(1 - \Lambda^2)^2 + 4\kappa^2\Lambda^2}}$$

The resonant condition is that in which $\Lambda = 1.0$, which makes $\tau = 90°$. This means that at resonance $\dot{\theta}$ is in phase with the exciting moment.

One can now adopt one of two ways for the control problem. [1] First, an extra deflection $K_1\dot{\theta}$, can be introduced into the system. This effectively increases damping and is directly opposite in phase to the exciting moment at resonance. This should decrease the response at and near resonance. The disadvantage of this approach is that the largest component of the angle of attack is already a linear function of $\dot{\theta}$, and further θ terms will push the angle of attack over the stall angle.

The other way is to effectively change the natural frequency of the system by increasing the restoring moment with a $-K_2\theta$ term. Since the pitch angle is about 3° maximum, the largest K_2 that can be used without exceeding the stall angle is about 10.

The increase in c due to this excitation may be found as follows [37]:

$$M_r = \Delta\overline{GM}_L \cdot \theta + K_2\theta\left[\tfrac{1}{2}\rho V^2 (\text{area})\right]\frac{\partial C_L}{\partial \alpha}\frac{L}{2}$$

where

$\Delta\overline{GM}_L$ = static restoring moment coefficient
Δ = displacement [lb]
$\overline{GM}_L$ = longitudinal metacentric height, (assumed to be LBP for this calculation)
M_r = restoring moment about the center of gravity of the ship for a pitch angle θ
$\frac{\partial C_L}{\partial \alpha}$ = slope of lift coefficient curve, which is 3.5 rad^{-1}
V = velocity of ship
(area) = area of fin = 2100 ft^2

Therefore,

$$M_r = [1.88 \times 10^{11}\theta + 10 \times 2 \times \tfrac{1}{2} \times (40)^2 2100 \times 3.5 \times 500 \times \theta]$$

$$= [1.88 \times 10^{11} + 0.585 \times 10^{11}]\theta$$

The restoring moment can therefore be changed by up to 30% by activating the fin with a deflection angle proportional to θ. In other words, the natural frequency can be increased by up to 14%, If the natural frequency is greater by 14%, the resonant wave may be short enough to decrease the excitation. The

motion is also decreased at resonance as given below:

$$\theta_a = \frac{M_0/c}{\sqrt{4b^2/4ca}} = \frac{M_0\sqrt{a}}{b\sqrt{c}}$$

The square root of c is increased by 14%, and therefore the motion per unit excitation is also decreased by 14%.

The value of this type of control depends on the energy associated with the two resonant wavelengths in the energy spectrum that the ship is likely to encounter. If the natural frequency is changed considerably from the dominant wavelength, this type of control may prove useful.

Instead of placing the antipitching fins at the bow, they may be installed near the stern of a ship. But fixed stern fins have been found to be much less effective than bow fins, since the vertical component of relative velocity available to generate antipitching forces by action of a fin is considerably less at the stern than at the bow. Not only is the stern fin is at a disadvantage because of its operation in the vessel's boundary layer, but also it may increase the excitation due to waves, thus decreasing the relative damping effect. Moreover, since the pitching axis is usually located aft of amidships, a stern fin will deliver less stabilizing moment than a bow fin. It has also been found that the phase relationship between the pitching motion and the forces generated by fixed fins is more favourable at the bow than at the stern. On the other hand, although the stern fin is less effective in reducing the pitching motion than the bow fin, there may be less vibration associated with stern fins. In any case it is assumed that a combination of a fixed stern fin and a bow fin may be still less effective than a properly designed bow fin.

Active Antipitching Fins

Antipitching fins, like rudders and antirolling fins, can be operated by an automatic control, and this makes a ship behave in a much more satisfactory manner in a seaway than would be experienced by the hull alone.

If one writes the linearized equations of motion, including the automatic control terms, and regroups the terms in the form of coefficients of pitch and heave and their time derivatives, the automatic controls in effect just change the coefficients in the equation of pitching motion. In the case of antipitching fins the deflection of the fins may be made sensitive to the angle, the angular velocity, and the angular acceleration. For example, the deflection of the antipitching fin can be expressed as

$$\delta = K_1\theta + K_2\dot{\theta} + K_3\ddot{\theta}$$

where K_1, K_2, and K_3 are control constants. If the control derivatives are expressed as

$$Z_\delta = \frac{\partial Z}{\partial t} \qquad \text{(force derivative)}$$

and

$$M_\delta = \frac{\partial M}{\partial t} \qquad \text{(moment derivative)}$$

the force and moment produced on the hull due to fin activation are

$$\begin{aligned} \text{Force} &= Z_\delta \cdot \delta = Z_\delta(K_1\theta + K_2\dot{\theta} + K_3\ddot{\theta}) \\ \text{Moment} &= M_\delta \cdot \delta = M_\delta(K_1\theta + K_2\dot{\theta} + K_3\ddot{\theta}) \end{aligned} \tag{14.19}$$

Then Z_δ and M_δ can be approximated easily from the lift characteristics of the fin, namely,

$$Z_\delta \approx -\frac{\partial L_f}{\partial \alpha}, \qquad M_\delta \approx -\frac{\partial M_f}{\partial \alpha}$$

When these expressions are included in the equation of motion, equation 14.9, the coefficients are found to change.

For the sake of simplicity, let us consider the equation for pitching having one degree of freedom; when the control moment expressed by (14.19) is added to (14.9), we have [1]

$$\begin{aligned} (a - K_3M_\delta)\ddot{\theta} + (b - K_2M_\delta)\dot{\theta} + (c - K_1M_\delta)\theta \\ = M_0\cos(\omega t - \varepsilon_M) \end{aligned}$$

Therefore the coefficient of θ now has $-K_1M_\delta$ added to it. However, since $c = \Delta\overline{GM}_L$, the term K_1M_δ, which involves magnitudes of the order of $(\partial M/\partial\alpha)_f = \frac{1}{2}\rho A l u_0^2(\partial C_L/\partial\alpha)_f$ for normal ships, is very small compared to $\Delta\overline{GM}_L$ and therefore cannot appreciably affect the magnitude of the coefficient of θ. This is quite different from rolling motion, where $\overline{GM}$, the transverse metacentric height, is comparatively small and the control moment may change the coefficient significantly. Similarly, the inertia term A can be shown to be of much larger magnitude than the control term K_3M_δ. Therefore the most effective control term in the pitching equation is the term that is added to the coefficient of $\dot{\theta}$, the damping term which is increased by K_2M_δ. However, because of the pitching motion of the ship itself, an increase in the angle of attack may be caused for the antipitching fin, and breakdown of the lift may be expected. Hence a control system should be developed that may prevent an angle of attack beyond the "stall angle." However, investigations [1] have

shown that in this case the activated system does not provide any improvement over fixed antipitching fins. Moreover, serious design problems may arise in taking into account the large loads produced on the fin and in housing the activating machinery in the narrow spaces of the bow.

The activated bow fin stabilizer is not as advantageous as activated roll fins. The reason is that the fixed pitching fin automatically generates lift from the angle of attack, which arises from the combination of ship forward speed and the vertical speed of the bow due to pitching. The fixed fin resultant damping force is thus considerable and is properly phased. Activation of bow fin tail flaps may be worthwhile only for a greater lift force, particularly if pitch stabilization at low speeds is necessary. In any case, because of the need for adjusting to the pitch period instead of the roll period (e.g., 6 sec against 12 or 15 sec), the pumps and motors will still need to be of considerable size in order to produce a large amount of torque to counteract the high wave and pressure forces experienced at the bow.

The use of jet hyrofoil as an antipitching fin for partially activated, fixed fins is proposed in Ref. 79a. The jet-flapped fin would be cavitation limited, and considerably more lift would be produced before cavitation occurred.

Model results show that movable stern fins alone will perform as effectively as fixed bow fins. Moreover, whereas bow fins increase in effectiveness with increased wave height (or increased angle of attack before the breakdown), stern fins produce rather constant results irrespective of wave height [193].

Another method of pitch stabilization could be the technique of effectively reducing waterplane area by the use of open tanks. A stern tank with sides open to the sea was fitted to a ship with unusually bad pitching characteristics. Results of the model tests indicated that, although the maximum motions were not reduced by the use of the tank, these maxima were transferred to much lower speeds. This would permit the ship to operate effectively in the designed speed range [78].

14.4 EFFECTIVENESS OF MOTION STABILIZERS

There are many different methods to assess the effectiveness of motion stabilizers. As described in earlier chapters, the most complete information about ship motion characteristics is obtained from a motion spectrum. (See Chapter 6) It is also a common practice to determine the effectiveness of a passive stabilizer system from its performance in the beam sea condition, in which the most severe rolling motion is expected for unstabilized ships. Figure 14.22 shows the percentage of rolls exceeding a definite value given on the abscissa. The shaded area is then the measure of roll reduction, and the end points on the abscissa show the maximum roll angle experienced.

The spectral method may not be very suitable for full-scale work, however, because of the directional wave spread, not considered in the one-dimensional wave spectrum. Hence a frequent design practice is to use the response amplitude operators to define the effectiveness of the stabilizing system. The usual method is to find the percentage reduction in the roll response at the resonant frequency, and one generally obtains the highest figure of merit by comparing two sets of data, one stabilized and the

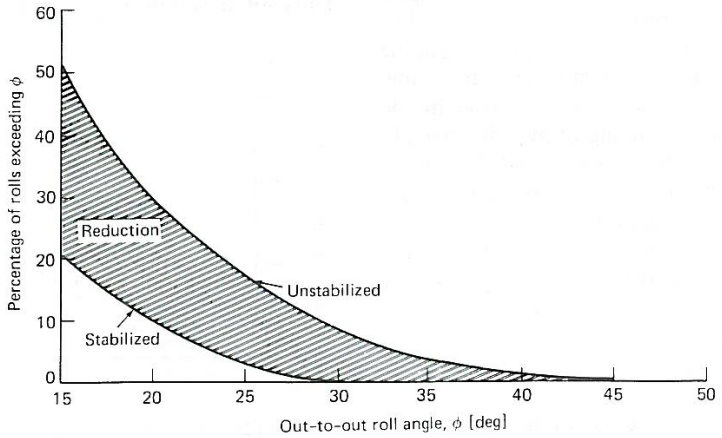


Figure 14.22 Effectiveness of a stabilizer in an irregular seaway.

other unstabilized. (Note that the resonance zone is especially preferred for roll stabilizers, since the roll response curve is very sharply tuned and therefore the resonant zone is considerably more important. In other words, ships usually roll in their natural frequencies, instead of the frequency of encounter as in the case of pitching. This fact also explains why simple damping devices that are effective for the resonance zone are also effective for roll stabilization in an irregular seaway.) The figure of merit thus obtained is suitable for the manufacturers of stabilizers, since one then obtains the highest value of the effectiveness.

The ratio of the motion responses at resonance for the stabilized and unstabilized cases indicate that under given conditions the motion is reduced by a certain percentage, but it does not identify the specific features of the motion to which this applies.

The percentage of motion reduction can then be defined as

$$R[\%] = 100\left(1 - \frac{\text{mean of one-third highest motions in the stabilized case}}{\text{mean of one-third highest motions in the unstabilized case}}\right) \tag{14.20}$$

Equation 14.20 thus describes the reduction in the overall magnitude of stabilized motion to that of unstabilized motion in a statistical manner.

But the use of an overall measure does not allow one to distinguish between small and large roll angles. For example, if there are two sets of records in which the ranges of roll angles are 0° to 10° unstabilized and 0 to 5° stabilized, (14.20) will give a percentage roll reduction of 50%, whereas it is obvious that a stabilizer is unnecessary. Again, if one takes another example, say roll angles of 0 to 30° and 0 to 15°, and supposes that a machine or a weapon works satisfactorily in roll angles up to 10° but becomes rather ineffective at higher angles of roll, the percentage of roll reduction is still 50%. It is now important, however, to know the reduction in the number of roll angles occurring above 10° brought about by the action of the stabilizer and the corresponding improvement in the effectiveness of any particular equipment or weapon.

If a Rayleigh distribution is assumed, the reduction in the number of rolls above a given angle may be expressed as follows. The cumulative probability of exceeding x is given as

$$e^{-x^2/2m_0}$$

where m_0 = mean square value of roll motions.

Then the values for the stabilized and unstabilized cases, respectively, are denoted by

$$e^{-x^2/2m_{0s}} \quad \text{and} \quad e^{-x^2/2m_{0u}}$$

where m_{0s} is the area under the stabilized motion spectrum, and m_{0u} is the area under the unstabilized motion spectrum.

The ratio of frequency of occurrence above x is then

$$\frac{e^{-x^2/2m_{0s}}}{-x^2/2m_{0u}} = e^{-Fx^2} \tag{14.21}$$

where

$$F = \frac{1}{2m_{0s}}\left(1 - \frac{2m_{0s}}{2m_{0u}}\right)$$

Clearly, from (14.21), a system becomes more effective as e^{-Fx^2} becomes smaller for a given value of x, that is, as F becomes larger. This is shown in Fig. 14.23, where the reduction in occurrence above a given roll angle is plotted against F [28].

As an example let us assume that $F = 0.002$, and accordingly the following table is made:

x [deg]	x^2	Fx^2	e^{-Fx^2}
0	0	0	1.0
2	4	0.008	0.99
4	16	0.032	0.97
6	36	0.072	0.93
8	64	0.128	0.88
10	100	0.200	0.82
12	144	0.288	0.75
14	196	0.392	0.68
16	256	0.512	0.60
18	324	0.648	0.52
20	400	0.800	0.45

Thus for a stabilizer giving $F = 0.002$, the number

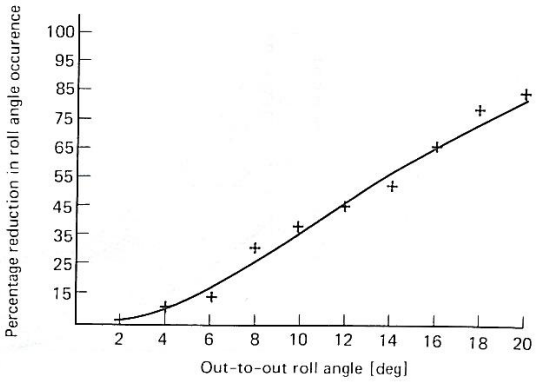


Figure 14.23 Percentage reduction in roll angle occurrence [28].

of rolls greater than 10° is reduced by 18%. If F is increased to 0.01, the reduction will be 64%.

However, F can be related to the overall measure defined in (14.20). Using the relationship

$$\frac{\bar{x}_s}{\bar{x}_u} = \frac{(x_{1/3})_s}{(x_{1/3})_u} = \sqrt{\frac{2m_{0s}}{2m_{0u}}}$$

If we define

$$r = 1 - \sqrt{\frac{2m_{0s}}{2m_{0u}}}$$

where

$$r = \frac{R}{100}$$

Then

$$F = \frac{1}{2m_{0s}}[1 - (1 - r)^{-2}]$$

or, alternatively,

$$F = \frac{1}{2m_{0u}}[(1 - r)^{-2} - 1] \qquad (14.22)$$

For a situation where $2m_{0u}$ is known (i.e., the unstabilized motion is described), F can be increased only if r is increased too. This shows that the percentage roll reduction R is the basis for obtaining such a criterion.

However, this kind of approach to establishing stabilization effectiveness (i.e., using the mean square value) is applicable only when the motion recordings are available or when the mean square value can be determined for a certain seaway. Otherwise a simpler way of determining the stabilizer effectiveness can be applied, using the ratio of the nondimensional damping coefficient of the ship with and without the stabilizer, namely,

$$R[\%] = \left(1 - \frac{\kappa_u}{\kappa_s}\right) \times 100 \qquad (14.23)$$

This expression is not dependent on the seaway and can be obtained either by simple calculation or from measurements in calm water during trials.

Chapter

Fifteen

MODEL TESTS, FULL-SCALE TRIALS, AND SCALE EFFECTS

15.1 GENERAL

Although considerable progress has been made in analytical studies of ship motions, they are still not sufficiently accurate that experimental investigations of seakeeping can be dispensed with. On the other hand, it is not only difficult but also rather expensive to conduct full-scale trials in order to obtain adequate data for design purposes. Extreme sea conditions are not always available when desired; and when they are, considerable damage may take place. Moreover, full-scale data can be useful only for vessels very similar to the one tested. Furthermore, analytical predictions of seakeeping characteristics are often not applicable to unconventional hull forms, such as catamarans, hydrofoil craft, and surface effect ships. Therefore the experimental approach to seakeeping studies in ship design is now an established fact. The main purposes of seakeeping experiments are as follows:

a. To determine the usefulness of theories and to improve the method of theoretical prediction of ship behavior in a seaway. (The strip theory has been modified after many useful experiments have been carried out in various seakeeping basins. Also, the usefulness of spectral analysis on the basis of the linear superposition technique can be shown if the seakeeping tests are performed in moderate seas.)

b. To determine the optimum hull form, not only for conventional ships, but also (and especially) when novel ship types are to be investigated, since analytical treatments for such vessels are still very limited.

c. To investigate the wave loads that a ship will encounter for the most effective design of ship structure.

Although seakeeping experiments can be conducted for any given ship form in a routine manner, it is not possible to make a systematic analysis of the influence of various parameters and wave conditions on seakeeping characteristics by experimental means alone.

One should remember when doing model testing that nonlinearity of the responses may result either from pushing the model to an excessive speed or from predicting performance in severe seaways from model tests in small waves. Again, the motion responses in moderate seas can be highly nonlinear if the model is fitted with a large bulb. Also, to predict the extreme responses in an irregular seaway the transfer functions should be obtained from model tests in severe irregular waves.

In any case, it has been seen that, although deck wetness, bow emergence, ship slamming, and other phenomena are rather nonlinear in nature, they can be predicted with sufficient accuracy from model tests by linear techniques.

Seakeeping experimentation has become standard practice in the evaluation of various seakeeping characteristics. In many establishments motions are even studied for all combined six degrees of freedom, so that a realistic picture is obtained of the actual physical phenomena. Model tests on various hull parameters are carried out in head and following seas in regular waves and in long- and short-crested irregular seas of specified spectra to predict pitch, heave, roll, surge, bending moment, bow emergence,

added drag, bow motions, slamming, deck wetness, and so on. Often the data are provided in non-dimensional form for design purposes.

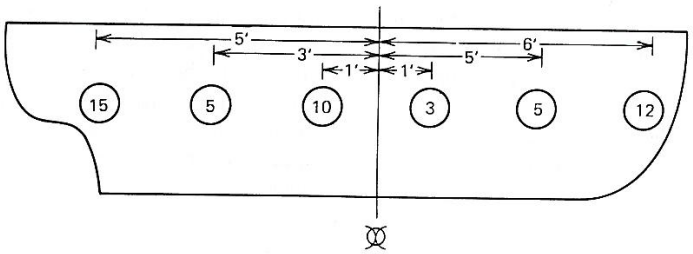
The determination of hull girder design loads from model tests is rather obvious, especially in the case of unconventional hull forms. The experimentation on ship structure can be of wide scope, since not only can severe sea conditions be investigated in a model basin, but also the influence of high-speed operation on structural loads can be simulated in a controlled laboratory environment. The hull girder deflections and accelerations can also be determined from model tests. In addition, the influence of various hull parameters (e.g., forebody section shape) on hull girder loads, as well as dynamic loads, can be investigated by model tests.

The examination of seakeeping experiments can be classified into four categories:

1. Facilities and instrumentation.
2. Testing techniques.
3. Applicability of available theories.
4. Scale effects and comparison between model and full-scale tests.

15.2 MODEL PREPARATION FOR SEAKEEPING TESTS

To be able to predict ship motion from model tests, a static as well as a dynamic similitude between the ship and the model must be achieved. For measuring



$\Sigma w = 30$ lbs

$\Sigma(wx) = 10 + 15 + 75 = 100$ ft-lb

$\Sigma(wx^2) = 10 + 45 + 375 = 430$ ft^2-lb

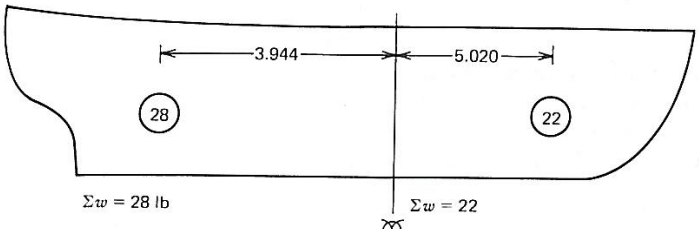
$\Sigma w = 20$ lb

$\Sigma(wx) = 3 + 25 + 72 = 100$ ft-lb

$\Sigma(wx^2) = 3 + 125 + 432 = 560$ ft^2-lb

Total weight $= \Delta = \Sigma w = 30 + 20 = 50$ lb

Total $gI_{yy} = \Delta k^2_{yy} = \Sigma(wx^2) = 430 + 560 = 990$ ft^2-lb



$\Sigma w = 28$ lb

$\Sigma(wx) = 28 \times 3.944 = 110.43$ ft-lb

$\Sigma(wx^2) = 28 \times 3.949^2 = 436$ ft^2-lb

$\Sigma w = 22$

$\Sigma(wx) = 110.5$ lb

$\Sigma(wx^2) = 554$ ft^2-lb

Total weight $= 28 + 22 = 50$ lb

Total $gI_{yy} = \Delta k^2_{yy} = \Sigma(wx^2) = 436 + 554 = 990$ ft^2-lb

Figure 15.1 Distribution of model weight.

motions as well as hull girder loads, the model hull form is so chosen that it is geometrically similar to that of the full-scale vessel, that is, the ratios of the corresponding linear dimensions, known as the scale factor λ, are constant:

$$\frac{L_s}{L_m} = \frac{B_s}{B_m} = \frac{T_s}{T_m} = \lambda$$

The static preparation of the model consists of establishing its weight distribution to correspond to that of the ship. In other words, the ratio of the masses of homologous sections of the full-scale vessel and the model should be the cube of the scale ratio. The detailed scaling relationships governed by Froude's law, which considers only inertia and gravity forces, are given in Table 4.5. Although Froude's law does not satisfy the scaling laws concerning fluid compressibility, viscosity, surface tension, and so on, the effects of these factors are insignificant as far as seakeeping characteristics are concerned.

In order to have the ship weight distribution correspond in model scale, the following four conditions must be satisfied:

1. Total weight or displacement.
2. Net longitudinal position of the center of gravity for trim purposes.
3. Radius of gyration.
4. First moment of weight.

With the weight distribution curve of the ship as a guide the model should be ballasted by arranging weights correctly to scale. However, condition 4 need be satisfied only if the hull girder bending moment is to be determined for the ship model.

Load Determination

Often it is assumed that, if the first three conditions are satisfied, the fourth one is also to scale. This assumption is not correct, however, since, if W, $\bar{X}$, and $\Sigma(wx^2)$ are correctly scaled, $\Sigma(wx)$ is not necessarily also to scale.

This point can be clearly seen in the simplified ballasting arrangement illustrated in Fig. 15.1. The arrangement of ballasting in the upper diagram of the figure shows the values of all four conditions mentioned above. The lower diagram shows that the system of weights satisfies the first three conditions of the upper diagram, but not the fourth condition, namely, the first moment of weight. This means that the weight distribution of the upper diagram is a unique case that can be properly defined by considering all four conditions.

If the bending moment is to be measured at the midship section only, a rigid wooden model jointed at the midship section with a dynamometer should be used. The dynamometer should be so calibrated that it can read the bending moment connecting both of the parts. If, on the other hand, the bending moment is to be measured at different locations along the length of the model, a segmented model consisting of a number of segments is connected as a continuous bar (usually of light material, such as aluminium alloy), known as a *strength bar*, which is equipped with strain gauges for measuring shear forces.

It should also be noted that, to measure the bending moment at any transverse plane, each section must also be properly ballasted, so that the mean moment of weight about the plane is also properly scaled. The scaling relationship between the model and the full-scale vessel for dynamic similarity of the rigid body and elastic motions is shown in Table 15.1, where λ is the ratio of prototype to model length, c is the ratio of prototype to model fluid density, e is the ratio of prototype to model modulus of elasticity, and r is the ratio of the full-scale distance from the neutral axis to the outermost fiber (deck or bottom), to the model distance from the neutral axis to the bar surface.

TABLE 15.1

Parameter	Full Scale Vessel	Model
Length	L	L/λ
Density	ρ	ρ/c
Time	t	$t/\lambda^{1/2}$
Mass	m	$m/c\lambda^3$
Velocity	V	$V/\lambda^{1/2}$
Acceleration	a	a
Force	F	$F/c\lambda^3$
Moment	M	$M/c\lambda^4$
Pressure	p	$p/c\lambda$
Frequency	ω	$\omega\lambda^{1/2}$
Bending rigidity	EI	$EI/c\lambda^5$
Modulus of elasticity	E	E/e
Section area moment of inertia	I	$Ie/c\lambda^5$
Distance from neutral axis to outermost fiber for hull girder (prototype) or strength bar (model)	Y	Y/r
Section modulus	z	$zer/c\lambda^5$
Flexure stress	σ	$\sigma\lambda/er$

Center of Gravity

The center of gravity of the model should be determined in order to correspond to the ship's center of gravity, so that

$$X_{CG} = \lambda x_{cg}, \qquad Y_{CG} = \lambda y_{cg}, \qquad Z_{CG} = \lambda z_{cg}$$

where the CG positions of the ship and the model are measured from the same fixed reference axes for both ship and model.

The longitudinal position of the model's CG can be determined by weighing the model on a scale, as shown in Fig. 15.2. One end of the model is hung on a cable (or placed on a knife edge), while the other end is put on another knife edge on the scale. Let l be the distance from the knife edge on the scale to the support; x, the distance from the CG of the model to the plane of the aft support; and p, the pressure of the model on the scale, which is determined with the aid of the weighing scale.

Using the moment equation, we have

$$\Delta x = p \times l$$

or

$$x = \frac{p}{\Delta} \times l \tag{15.1}$$

The vertical position of the CG of the model is determined by the inclining experiment. Shifting a weight athwartships along the deck of the model produces a heeling moment, $M = w \times d$ (where w is the weight, and d the distance the weight is shifted), and the angle of heel thus caused is measured. The transverse metacentric height is determined as

$$\overline{GM} = \frac{w \times d}{\Delta \tan \phi} \tag{15.2}$$

The location of the CG is determined as

$$\overline{KG} = \overline{KM} - \overline{GM}$$

where the value for $\overline{KM}$, the height of the metacenter above the base line, is computed from the lines plan of the vessel.

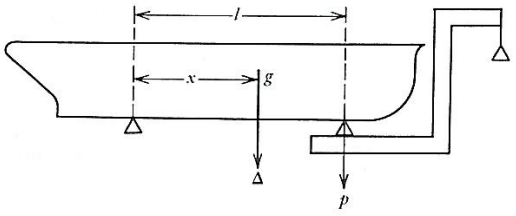


Figure 15.2 Determination of the center of gravity of a model.

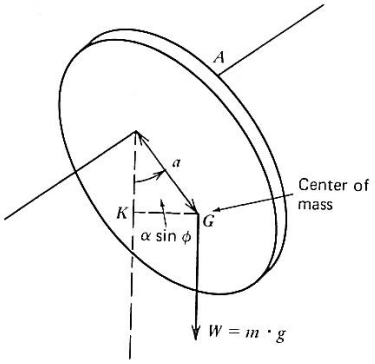


Figure 15.3 Typical physical pendulum.

Radius of Gyration

Pivotal Method

Considering a physical pendulum of continuous mass distribution (Fig. 15.3), we have

$$\sin \theta = \frac{\overline{GK}}{a}$$

or

$$\overline{GK} = a \sin \theta$$

The pendulum is subject to two external forces: (a) gravitational force, and (b) contact force from the axis at A. When we consider the torque about A, only the gravitational force contributes, and the torque is $W a \sin \theta = Mga \sin \theta$.

If the moment of inertia of the pendulum is I_a, the rate of change of angular momentum about A is

$$I_a \frac{d\omega}{dt} = I_a \frac{d^2\theta}{dt^2}$$

and we obtain

$$I_a \frac{d^2\theta}{dt^2} = -Mga \sin \theta$$

As in the case of the simple pendulum, we shall restrict our consideration to situations in which θ is small, or

$$\sin \theta \approx \theta$$

$$\therefore \; I_a \frac{d^2\theta}{dt^2} = -Wa\theta = -Mga\,\theta$$

As before, this equation describes harmonic motion, and the solution is given as $\theta = \theta_a \sin \omega_0 t$, where

$$\omega_0 = \sqrt{\frac{Mga}{I_a}} = \sqrt{\frac{ga}{k_a^2}}$$

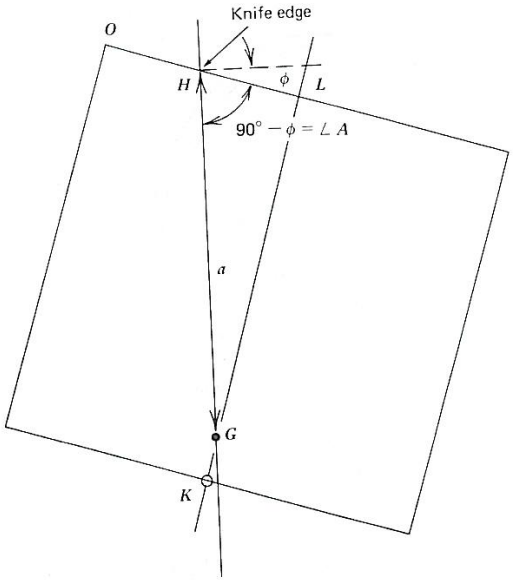


Figure 15.4 Radius of gyration about the longitudinal axis (for rolling).

since $I_a = Mk_a^2$ and

$$T = 2\pi\sqrt{\frac{I_a}{Mga}} = 2\pi\sqrt{\frac{k_a^2}{ga}}$$

where k_a is the radius of gyration of the rigid body with respect to point A, or

$$k_a^2 = \frac{g}{(2\pi)^2}T^2a$$

Now

$$I_a = Mk_a^2$$

Also,

$$I_a = I_G + Ma^2 \qquad \text{(transfer of axis)}$$
$$= M(k_G^2 + a^2)$$

since $I_G = Mk_z^2$.

$$k_a^2 = k_G^2 + a^2$$

or

$$k_G^2 = k_a^2 - a^2$$

or

$$k_G^2 = \frac{g}{(2\pi)^2}T^2a - a^2$$

In ft-lb-sec units

$$k_G^2 = 0.815T^2a - a^2 \qquad (k_G, a \text{ in feet, } T \text{ in seconds}) \tag{15.2a}$$

or

$$k_G^2 = 9.78T^2a - a^2 \qquad (k_G, a \text{ in inches, } T \text{ in seconds}) \tag{15.2b}$$

For the purpose of determining the mass moment of inertia (or the radius of gyration) the model is supported as shown in Fig. 15.4 and is set into oscillatory motion. The time for a great many full oscillations is noted, and the period for one oscillation is computed. From the formula for the period of oscillation of a physical pendulum one can compute the radius of gyration as described below.

Radius of Gyration about the Longitudinal Axis. By the analogy of the physical pendulum as explained above, the radius of gyration about the longitudinal axis through G is given as

$$k_{zz}^2 = 9.78T^2a - a^2 \tag{15.3}$$

Also,

$$\cos(90^\circ - \phi) = \frac{\overline{HL}}{a}$$

where $a = \overline{HL}/\cos(90^\circ - \phi) =$ distance from pivot point (knife edge) to CG
and

$$\overline{HL} = \frac{B}{2} - HO$$

Since ϕ is measured and HL is determined by the above expression, a can be easily computed for the determination of k_{zz}.

The vertical CG can also be found in this process;

$$\overline{GL} = \overline{HL}\cdot\tan(90^\circ - \phi)$$
$$\therefore \overline{KG} = \overline{KL} - \overline{GL}$$

In this manner one may determine both the mass moment of inertia of the vessel and the vertical location of the CG of the model.

If the values of the draft at the bow and stern of the ship are known, it is useful to mark these on the model. The ballast weights may be shifted longitudinally to bring these marks into coincidence with the waterline of the model. The resulting longitudinal location of the CG will then automatically satisfy the condition of geometric similarity.

Example 15.1

The following dimensions were obtained from the pivotal swinging of a 5 ft ship model:

$$\text{Angle } A = 90^\circ - \phi^\circ = 35^\circ$$
$$\overline{OL} = 3.313 \text{ in.}$$

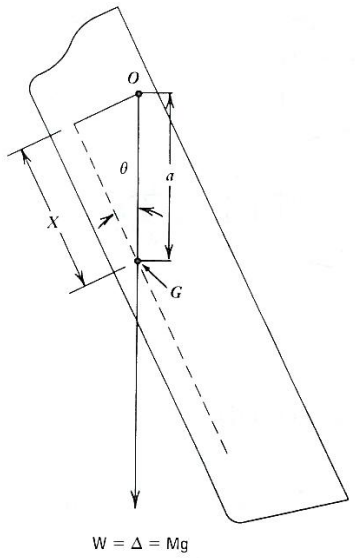


Figure 15.5 Radius of gyration about the transverse axis (for pitching).

$$\overline{OH} = 1 \text{ in.}$$
$$\overline{KL} = 4.125 \text{ in.}$$

$T = 0.68$ sec

Find k_{xx} and $\overline{KG}$.

Solution:

$$\cos 35^\circ = \frac{\overline{HL}}{a}$$

where $\overline{HL} = \overline{OL} - \overline{OH} = 3.313 - 1 = 2.313$ in.

$$\therefore\ a = \frac{2.313}{\cos 35^\circ} = 2.820 \text{ in.}$$

Substituting the values of T and a into (15.3) gives

$$k_{xx}^2 = 9.78(0.68)^2 \times 2.82 - (2.82)^2$$

or

$$k_{xx} = 2.19 \text{ in.}$$

and

$$\overline{KG} = \overline{KL} - \overline{GL}$$

where $\overline{GL} = a \tan 35^\circ = 2.82 \times 0.700 = 1.974$ in.

$$\therefore\ \overline{KG} = 4.125 - 1.974 = 2.151 \text{ in}$$

Pivotal Method for Pitching Radius of Gyration. The same equations are valid for a ship model if the model is hung and swings as in Fig. 15.5. The vertical distance of the CG of the model is given as

$$a = \frac{x}{\cos\theta}$$

where x is the longitudinal distance of the CG from the pivoting point as obtained by statical preparation of the model. The axis that goes through the pivoting point O about which the model swings and the period is measured should be the axis parallel to the pitching axis (i.e., the transverse axis through the CG).

The mass moment of inertia of the model in connection with pitching motions may also be determined with the help of a "bifilar suspension" (see the next subsection) which enables one to obtain instead of the mass moment of inertia of the model about a transverse horizontal axis, its mass moment of inertia about a transverse vertical axis, that is, instead of the moment of inertia I_{yy}, the moment of inertia I_{zz}. The fact that these two moments of inertia are normally within 1 to 2% of each other allows one, in most cases, to take the value of I_{zz} as that of I_{yy}. In fact, the expression for the moment of inertia I_{yy} is given as

$$I_{yy} = \int_M r^2\,dM = \int_M (x^2 + z^2)\,dM = \int_M x^2\,dM + \int_M y^2\,dM$$

Because of the small height of the vessel relative to its length, the second integral in this expression does not exceed 1 to 1.5% of the first. Similarly, the moment of inertia I_{zz} is expressed as

$$I_{zz} = \int_M r^2\,dM = \int_M (x^2 + y^2)\,dM = \int_M x^2\,dM + \int_M y^2\,dM$$

where the second integral is, on the average, 2 to 3% of the first. The difference between the integrals results in

$$I_{zz} - I_{yy} = \int_M y^2\,dM - \int_M z^2\,dM \approx 0.01 \text{ to } 0.02 \times \int_M x^2\,dM$$

Method of Bifilar Suspension [19]

To obtain the moment of inertia I_{zz} by the method of bifilar suspension, the model is suspended by two strings of equal length, secured in the plane of symmetry of the model so that its CG lies halfway between the strings (Fig. 15.6). Then a swinging motion in a horizontal plane about a vertical axis is imparted to the model, and the average period of a full oscillation is measured with a stopwatch.

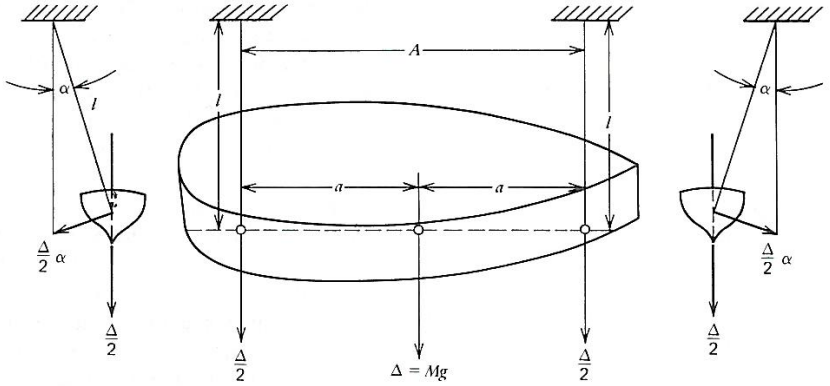


Figure 15.6 Radius of gyration about the vertical axis (for yawing).

The differential equation of the oscillatory motion of the model in the horizontal plane may be written in the form

$$I_{zz}\ddot{\psi} = M$$

where M is the restoring moment returning the model to its original position. As the model turns through an angle ψ as shown in Fig. 15.6, the bow of the model moves to the left and the stern to the right. The cables diverge from the vertical by an angle, the projection of the weight normal to the cable becomes $(\Delta/2)\alpha$, and its moment in the horizontal plane may be written as

$$M = -\frac{\Delta}{2}\alpha 2a = -\Delta a\alpha$$

From geometrical considerations

$$l\alpha = a\psi$$

where l is the length of the cable from its point of support to the point of its attachment to the model. Then

$$\alpha = \frac{a}{l}\psi$$

Substituting this into the expression for the moment, we have

$$M = -\frac{\Delta a^2}{l}\psi$$

Substituting M into the differential equation gives

$$I_{zz}\frac{d^2\psi}{dt^2} + \frac{\Delta a^2}{l}\psi = 0$$

where $I_{zz} = Mk_{zz}^2$, that is,

$$\frac{d^2\psi}{dt^2} + \frac{\Delta a^2}{l}\cdot\frac{1}{Mk_{zz}^2}\psi = 0$$

or

$$\omega^2 = \frac{\Delta a^2}{l}\cdot\frac{g}{\Delta k_{zz}^2} = \frac{ga^2}{lk_{zz}^2}$$

But

$$T = \frac{2\pi}{\omega} = \frac{2\pi}{\sqrt{ga^2/lk_{zz}^2}}$$

or

$$T^2 = \frac{4\pi^2}{ga^2/lk_{zz}^2}$$

or

$$k_{zz}^2 = \frac{T^2ga^2}{4\pi^2 l}$$

Therefore

$$k_{zz} = \frac{\sqrt{g}}{4\pi}\cdot\frac{AT}{\sqrt{l}} \tag{15.4}$$

where $A = 2a$. In ft-lb-sec units,

$$k_{zz} = 0.451\frac{AT}{\sqrt{l}} \quad (k_{zz}, l, A \text{ in feet, and } T \text{ in seconds}) \tag{15.5}$$

Note: This method is normally used in model basins in preference to the pivotal method, which is not very convenient for larger models (say 15 or 20 ft) that cannot be hung and pivoted conveniently.

Dynamic preparation of the model must be conducted with care, since any inaccuracies at this stage will cause systematic errors in seakeeping experiments with the model. In addition, some parameters of ship motions are determined as differences between large quantities. Thus relatively small errors introduced in the dynamic preparation

of the model may result in large errors in the computed values of such parameters.

Example 15.2

I. Bifilar Suspension for k_{zz}

Given:

$$l = 7 \text{ ft}$$
$$A = 43 \text{ in.}$$
$$L_{\text{Model}} = 4.76 \text{ ft}$$

For 50 swings, $T_{\text{avg}} = 1.886$ sec

Find k_{zz} by the method of bifilar suspension.

Solution:

From (15.5) we have,

$$k_{zz} = 0.451 \frac{TA}{\sqrt{l}} = \frac{0.451(1.886)(43/12)}{\sqrt{l}} = 1.151 \text{ ft}$$

where 1.151 ft is 24.1% of the length of the model.

II. Pivoted Suspension

Given:

$$a = 22.99 \text{ in.}$$

Average period, $T = 1.783$ sec

Find k_{yy} by the method of pivoted suspension.

Solution:

From (15.2a) we have,

$$k_{yy} = 0.815(1.783)^2 \frac{(22.99)}{12} - \left(\frac{22.99}{12}\right)^2$$

and, therefore,

$$k_{yy} = 1.14 \text{ ft}$$

15.3 FACILITIES AND INSTRUMENTATION

As described in Chapter 5, a seaway can be represented adequately by its wave energy spectrum, which is a function of sea state. To study the seakeeping characteristics in a seaway it is therefore essential that wave be artificially generated in a model basin in order to create model seas that generally are composed of sine waves, which may be unrealistic but are well-behaved forcing functions. Moreover, sine waves can be physically created in a model basin without much difficulty. In addition, it is rather simple to repeat sinusoidal waves, and the analysis of model test data is relatively easy. Also, the analytical results of seakeeping studies based on sinusoidal wave conditions can be easily verified in a laboratory environment.

Hence one of the most important seakeeping facilities is considered to be the wavemaker, together with its associated control mechanism. In general, four kinds of wavemakers are commonly used in seakeeping laboratories:

1. Single or multiple flap type (oscillating horizontally about a pivot).
2. Single or multiple plunger type (oscillating vertically).
3. Pneumatic type (variable air pressure).
4. Piston type (oscillating horizontally).

These are illustrated in Fig. 15.7a.

Single or multiple flap wave generators are very responsive to the input signal. They form a wave with less excitation at the tank bottom than at the surface and are not very suitable for generating waves in shallow water for this reason.

The single or multiple plunger wavemaker, on the other hand, is very effective in generating shallow water waves, since the water motion is uniform from the free surface to the bottom of the tank. However, very high power is required because of the large moving mass.

The piston type of wavemaker is not suitable for deep water waves, since the uniform horizontal displacement over the whole depth of the tank does not represent actual deep water waves, where

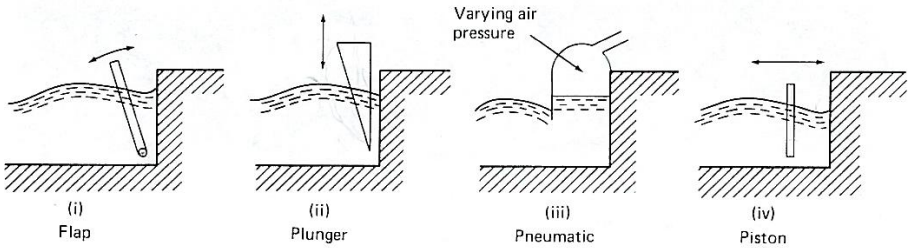


Figure 15.7a Various kinds of wavemaker. (i) Flap. (ii) Plunger. (iii) Pneumatic. (iv) Piston.

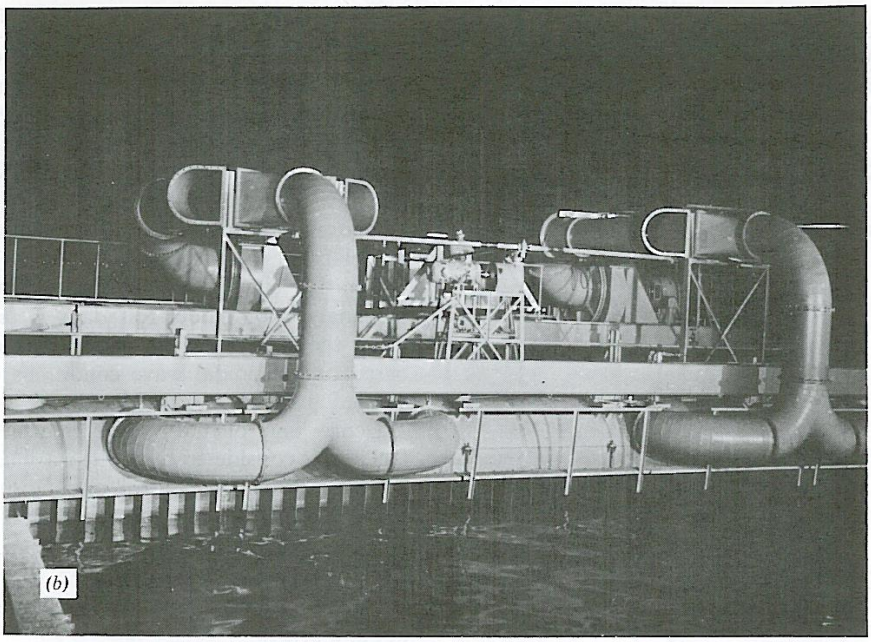


Figure 15.7*b* Pneumatic wavemaker in deep-water basin (David Taylor Naval Ships Research and Development Center).

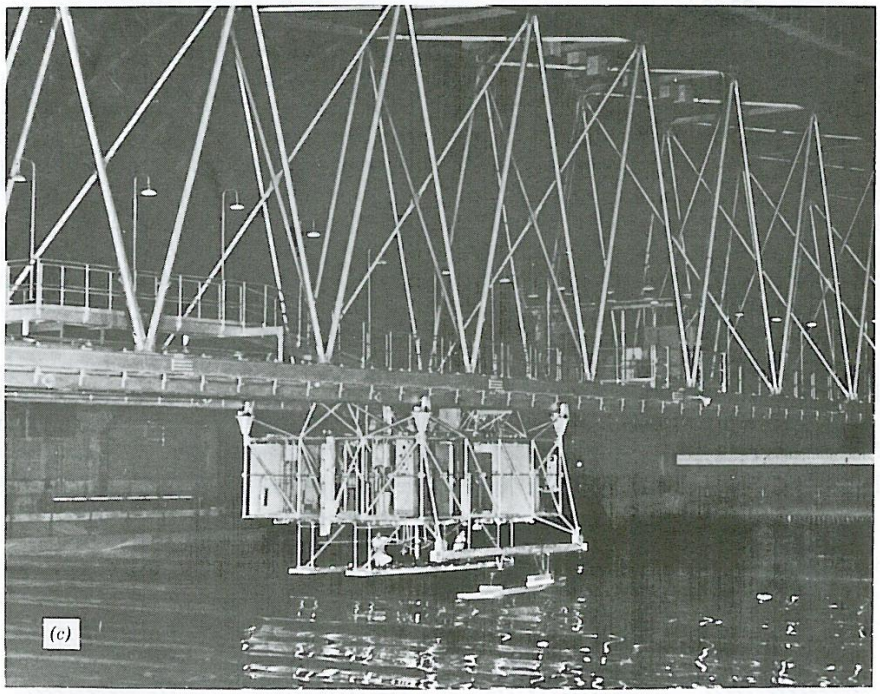


Figure 15.7*c* Test for pitching and heaving test in the maneuvering-seakeeping basin (David Taylor Naval Ship Research and Development Center).

the wave motion is decreased exponentially with the depth.

The simplest type of wavemaker is the pneumatic, which has fewer mechanical, structural, and inertial problems and is quite suitable for rapid and easy changes of wave frequencies and amplitude because of the small inertia of the moving parts. Waves are generated by varying the air pressure alternately from positive to negative in a cyclic fashion in a dome that is only partially submerged in water. The wave amplitude is regulated by controlling the blower speed, whereas the frequency of oscillating valves from pressure to suction determines the frequency and so the wavelength.

The pneumatic type of wavemaker, although it is comparatively quiet in operation and uses less power, has two significant disadvantages: (a) because of the compressibility of air the water column inside the dome does not respond fast enough to the rapid changes in air pressure necessary to produce irregular waves of shorter periods, and (b) since the water column moves vertically downward, the waves, which move in the horizontal direction, require several wavelengths down the basin before the desired wave forms can be generated; therefore repeatability of irregular wave patterns is not easy to obtain.

In conventional tow tanks only long-crested regular head and following waves can be generated, but in specially designed seakeeping basins irregular waves from any relative direction can be created. Figure 15.8 shows schematically the pneumatic wavemaker of the Naval Ship Research and Development Center of the U.S. Navy. Short-crested seaways are produced there by intersecting trains of waves generated by wavemakers situated on two adjacent walls of the rectangular basin.

The carriage for test personnel and instrumentation of this tank, supported and guided by steel guide wheels, runs underside of a bridge over the seakeeping

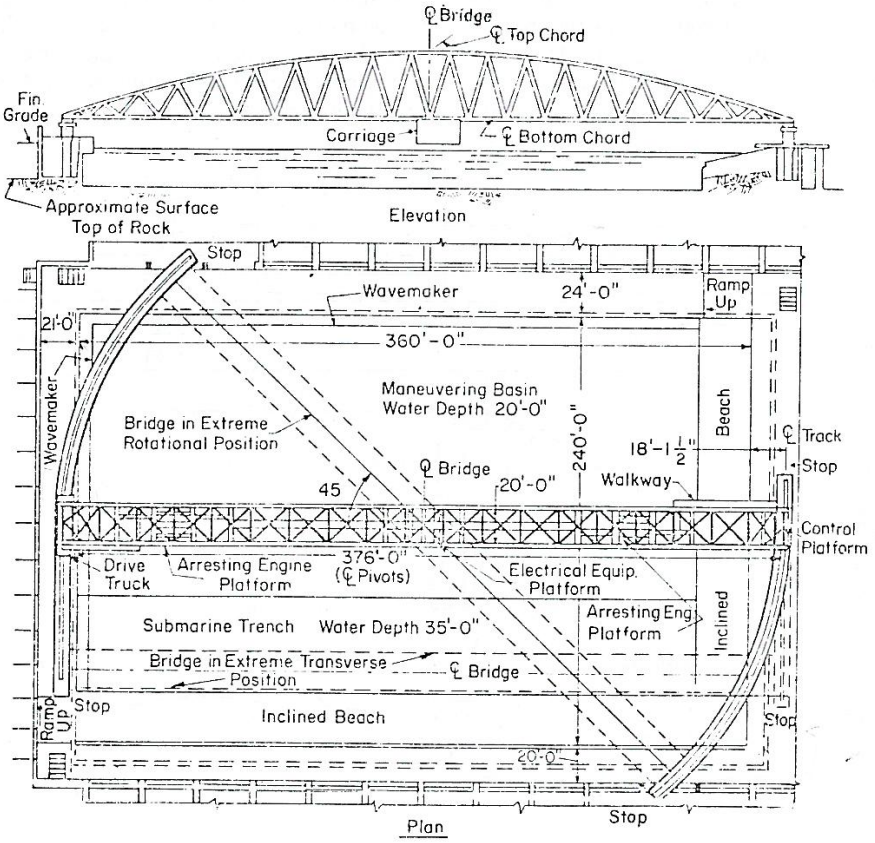


Figure 15.8 Experimental facilities for seakeeping at the Naval Ship Research and Development Center of the U.S. Navy [249].

basin and can attain an acceleration rate up to $0.4g$ and maximum speeds of 15 knots. The bridge is supported on a rail system that allows it to traverse one-half the width of the basin and to rotate through angles up to 45° from the longitudinal centerline of the basin, and this, combined with a 90° choice of wavemakers, permits the carriage to run under the bridge at any desired angle relative to the wave direction. Either free or restrained models can be tested in this seakeeping basin, which is 360 ft long, 240 ft wide, and 20 ft deep, except for one section that is 322 ft long, 50 ft wide, and 35 ft deep. The deep section is used for free-running submerged model tests.

To ensure that the generated wave form will not be unnecessarily distorted by reflections from the end of the tank, wave absorbers, known as *beaches*, are installed to damp the waves and minimize undesirable wave reflections. The beach normally extends the full width of the test basin from the free surface to the tank bottom.

It may appear that the use of a free model should be preferred to avoid any interference with the motion of the model by the guiding arrangement. However, many difficulties are associated with the free running model. The model must be fitted with its own propulsion system, power supplies, and radio control devices, as well having the capability to record much of the test data. It must be ballasted so as to possess the correct stability characteristics and scaled inertias in order that its response as a dynamic system will accurately simulate that of the ship. Furthermore, all these requirements must be met within the relatively small model normally built for seakeeping tests, since a larger model may restrict the effective length of each run, which is rather important for experiments where the test data have to be analyzed and presented in a statistical manner.

Heaving motion is normally measured using a linear potentiometer connecting to the heave rod (staff) directly above the CG of the model (see Fig. 15.9). Heaving motion can also be derived from double integration of vertical acceleration measurements. The latter method is useful when the model is not towed by attachment to a moving carriage. The resulting electrical signals are stored on magnetic tapes or oscillograph charts.

Similarly, pitching motion can be obtained with the help of a rotary potentiometer attached to rotate with the CG of the model. A rate gyroscope is also a suitable device for measuring pitch. The derivation of pitching motion from acceleration data requires

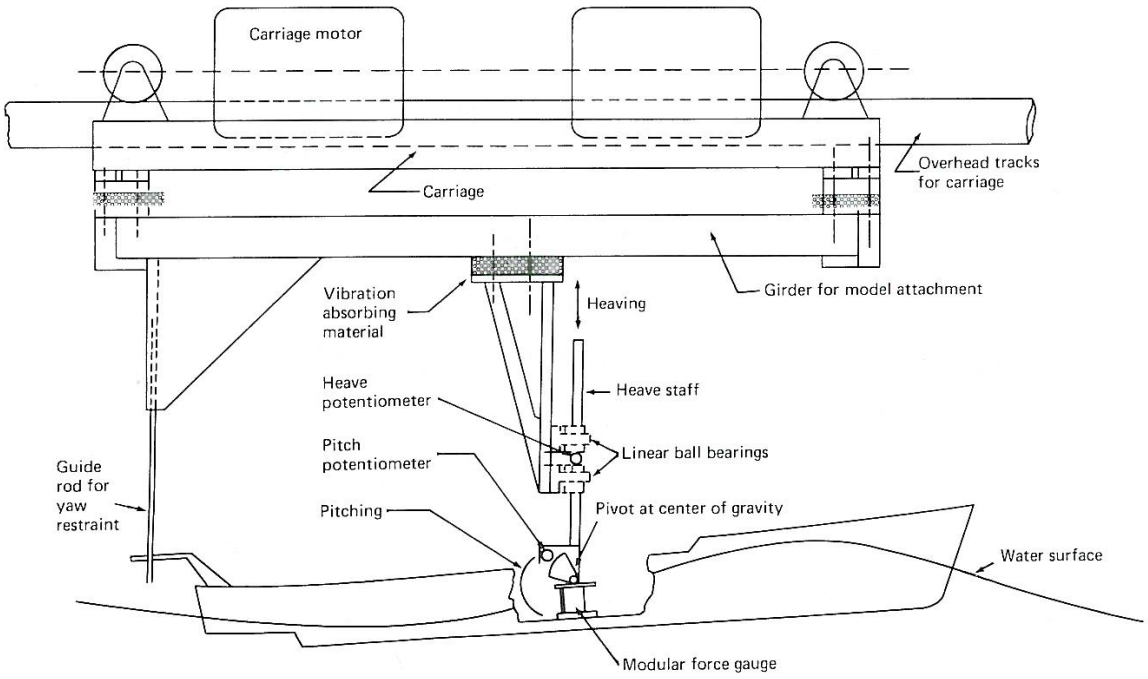


Figure 15.9 Naval Ship Research and Development Center 140 ft towing basin arrangement for regular wave experiments.

subtraction of the acceleration at the CG from the acceleration measured at the end of the model. This result is integrated twice and then divided by the distance of the second accelerometer from the CG of the model. The last two methods are used if the model is not attached to a carriage that serves as a reference.

Rolling motions are measured in ways similar to those used for pitch.

Motion pictures, taken at the normal projection speed multiplied by the square root of the scale ratio, will show the vessel motions in real time.

Resistance Tests in a Seaway

Naval and commercial ship designers are becoming more and more interested in the speed–power relationship in waves because it affects the turn-around time of vessels; hence resistance tests in a seaway are now carried out regularly in seakeeping laboratories. In general, two different procedures are followed in resistance tests in waves:

1. A constant weight is used to tow the model, and the average speed of the model is recorded.
2. The model is connected to the ordinary still water resistance dynamometer on the carriage, which moves at a given speed, and the resistance of the model is measured.

Both of these methods are illustrated in Fig. 15.10.

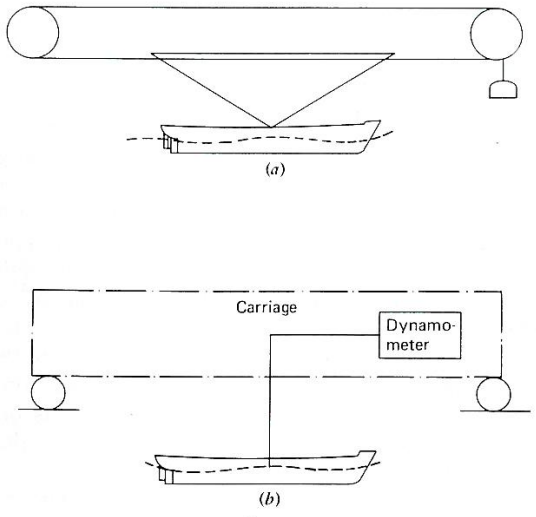


Figure 15.10 Experiments for added resistance in waves. (*a*) Constant force method. (*b*) Constant speed method.

Model experiments in waves are conducted in these major areas: ship motions and associated dynamic effects (i.e., pitching, heaving, thrust increase, vertical acceleration, etc.) as a function of, for example, the following:

a. Wave amplitude.
b. Longitudinal distribution of weight.
c. Principal dimensions.
d. Forebody section shape.
e. Bulbous bow.
f. Single or multiple propellers.
g. Following seas.

15.4 ITTC STANDARDS FOR SEAKEEPING EXPERIMENTS [106]

These standards are designed to meet the need for uniform procedures to be specified for seakeeping tests in various model basins. But it is not easy to specify such procedures in detail, since there is a great variation in the type of available equipment, as well in the kinds of experiments carried out. For example, not all test basins may have a facility to generate irregular waves, and those that do may adopt different methods to produce the irregularity and thus may require different techniques for the analysis of test data.

Model Preparation

1. Weight distribution: If the radius of gyration of the ship is known, the model gyradius should correspond to it. If it is unknown, a value of $0.25L_{pp}$ should be used for the longitudinal value. If the bending moments experienced by the model in waves are to be measured, the longitudinal weight distribution should be reproduced, and the center of gravity, both vertical and longitudinal, should be accurately determined. If, on the other hand, the vertical CG is unknown, the assumption for head sea tests should be that it is located at the still water-line.
2. Longitudinal gyradius: The model gyradius is usually determined by oscillating the model about the CG, the natural restoring force being produced by springs or by the weight of the frame supporting the model. If no oscillating frame is available, the bifilar suspension method can be used, oscillating the model about the yaw axis. This method assumes that the

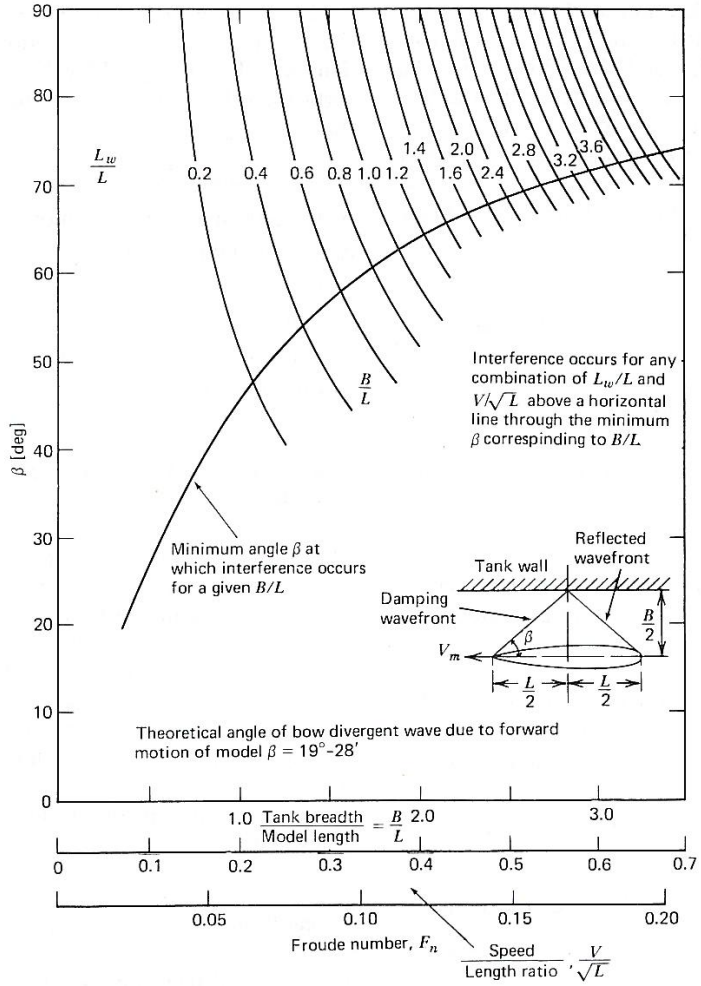


Figure 15.11 Tank wall interference in wave experiments [83].

pitch and yaw gyradii are equal; this assumption is approximately correct for normal monohull vessels.

3. Tank wall interference: The size of the tow tank usually determines the length of the model and thus its scale ratio. Reflection of the waves generated by the motions of the model has been found to influence both motion and propulsion responses. The interference effect depends mainly on the ratios of wavelength to ship length and tank width to model length, as well as the speed/length ratio. This is shown in Fig. 15.11, which is entered at the base using the tank breadth/model length ratio, B/L. Any combination of L_w/L and $V/\sqrt{L}$ that lies above a horizontal line through the minimum β value will result in a wall effect. Any experiments, therefore, that are carried out where wall effects are likely should have the limits of interference indicated on the results. It should be noted that Fig. 15.11 does not give any indication of the degree of wall effect.

The effects of tank wall interference in waves are expected, mainly for large models moving at low speeds; response curves measured at very high speeds show hardly any interference. The qualitative effects of tank wall interference may therefore be predicted by comparing the results at lower speeds with those at higher speeds. It has been found from experiments [158b] that the interference effects on the heave response are smaller than those on the pitching motion.

In Ref. 158b it is also shown that the interference effect does not cause scatter in the results, but seems to produce two jumps on the pitch response curves and

a peak on the propulsion response curves. The heave response is affected like the pitch responses, but the jumps are much smaller. The interference effects are most pronounced when the resonant responses take place in the interference region.

Experiments

1. Guidance system: The guidance system should produce the minimum restraint on the surging, pitching, and heaving motions of the model.

2. Vertical acceleration: In addition to pitching and heaving motions, measurements should be made of the vertical acceleration at two points on the model: 0.1 and 0.9 of the model length between perpendiculars.

a. Relative bow motion: The relative motion between the stem and the water surface should be measured, along with the swell-up of water at the bow.

b. Phase angles: The phase angles relative to the wave crests amidships and the pitching, heaving, and relative bow motions, should be measured whenever possible.

c. Wave amplitude: To determine the phases in item 2b accurately, the method of measuring the encountered waves should allow for the surge of the model. Wave measurements should be made with one probe fixed to the carriage and the other placed at a fixed point in the tank.

d. Propeller open water tests in waves: The mean propeller revolutions should be recorded for both regular and irregular waves throughout the train of waves used in the tests. The same is true for the mean propeller thrust and torque.

3. When a model is self-propelled, the model self-propulsion point should be used in all the tests. In addition to the propulsion experiments in waves, calm water tests should be carried out for the model propeller loading corresponding to the model self-propulsion point.

4. Tests in regular waves: For tests on models of conventional craft in regular waves at least 10 experiments should be carried out for each speed, covering a range of wavelengths from $0.5L_{pp}$ to $2.0L_{pp}$. For high-speed vessels these wavelengths should be extended to cover the resonance condition. To obtain response amplitude operators (which are necessary for seakeeping predictions in an irregular seaway by the linear superposition technique) from regular wave tests, a relatively mild seaway is generated (e.g., wave height/wavelength ratio of about 1:40).

5. Tests in irregular waves: Often the wavemaker is used first to produce waves of shorter lengths (i.e., higher frequencies), which are slowly overtaken by longer waves when the wavemaker is gradually slowed down and low-frequency waves are produced. The ship model starts in calm water, encounters first waves of shorter lengths and then longer waves, and ultimately finishes its run in calm water. A complete picture of model response can therefore be obtained by analyzing the seaway and motion records. If the length of the tank is sufficient, this method of testing provides results in a much faster manner. For tests in irregular waves where the wave and motion spectra are to be defined accurately, 200 cycles should be encountered.

If mean values of motions and waves are to be determined, between 80 and 100 cycles will suffice. To reach the required number of cycles multiple runs can be made, but care should be exercised in joining the runs together. Serious discontinuities should be avoided. The results of multiple runs should be considered separately, and the mean results taken.

6. Analysis

a. Regular waves: In determining the motions in waves, the average amplitude and period of at least 10 cycles should be obtained. Alternatively, with a digital recording system, a harmonic analysis should be made of the records to obtain the amplitudes and periods of waves and responses.

b. Oblique regular waves: The tested data in each course angle to the wave should be plotted in the dimensionless form for each wavelength as a function of the frequency of encounter. Through these experimental points mean lines should be drawn, from which the values at the circular frequencies of encounter corresponding to the desired speed are read and represented as functions of the wavelength.

c. Irregular wave tests: If the results are being recorded digitally, the response functions should be determined against the encountering frequency. If no digital analysis is carried out, the analogue records should be analyzed to give the statistics for the motions and wave height in terms of the average of the one-third highest double amplitudes or root mean squares. Alternatively, the waves or motions can be presented as a histogram, a useful form of presentation for nonlinear responses.

Presentation of Results

For wave tests the following nondimensional quantities are recommended:

a. Pitch amplitude/wave slope, $\theta_a/k\zeta_a$.
b. Heave amplitude/wave amplitude, z_a/ζ_a.
c. Vertical acceleration/wave amplitude, $aL_{pp}/g\zeta_a$.
d. Relative bow motion/wave amplitude, s_a/ζ_a.
e. Revolution increase, $n_{aw}D^3V_m/(g\zeta_a^2B^2/L)$.
f. Thrust increase, $T_{aw}/(\rho g\zeta_a^2B^2/L)$.
g. Torque increase, $Q_{aw}/(\rho g\zeta_a^2DB^2/L)$.

The results should be plotted to a base of L/L_w, where

T_{AW} = mean thrust increase or decrease
Q_{AW} = mean torque increase or decrease
n_{AW} = mean revolution increase or decrease
ζ_a = wave amplitude
D = propeller diameter
V_m = model speed
k = wave number

15.5 FULL-SCALE TESTS

This section deals with full-scale trials and implies the necessity of being able to correlate such events with theory and model tank experiments, especially in systematic parametric studies of conventional ships. Full-scale trials are a valuable source of technical information, and they are carried out for the following purposes:

a. To investigate the correlation between analytical calculations or model test results and the actual behavior of a vessel.
b. To determine whether a vessel fulfils the design specifications.
c. To predict the actual performance of a vessel in a seaway.
d. To collect data on motions, the shipping of green water, slamming, propeller racing, and wave bending moment, as well as motion stabilizers, for future ship designs. The collection of data on the structural and dynamic responses of an actual vessel structure is accomplished by an onboard instrumentation system with sensors located throughout the vessel measuring strains, stresses, accelerations, various sea characteristics, and vehicle operating parameters.

Information on induced forces and motions of marine vehicles is of little value unless the driving wave is also measured. Observations on actual vessels apply only to particular types of vessels, and the data obtained during sea trials represent only a particular sea condition and often are extremely irregular in nature. In such cases statistical methods can be used to obtain relevant solutions.

Therefore statistical analysis of full-scale data is made in vessel trials in an irregular seaway. Even then it is assumed that the irregular seaway is a long crested one, and to meet this condition as far as possible the trials are made in an area where long-crested waves are predominant. During such trials attempts have been made to obtain not only wave spectra or motion spectra, but also the response amplitude operators.

Not only motion measurements, but also wave bending moments as well as motion stabilization, are investigated during sea trials.

It should be noted that wave measurements in an actual seaway are necessary for the interpretation of full-scale test results. Important progress in collecting full-scale data has been made by the introduction of shipborne wave records [216]. Since wave data are important for the proper evaluation of seakeeping characteristics, wave measurements are collected extensively to obtain the vehicle motions as functions of the seaway. Normally the waves are measured to obtain a one-dimensional wave spectrum, but a directional spectrum (two-dimensional) is also important in certain cases.

Measurement of Sea Waves

The usual measurements of waves in a seaway are made on length, height (double amplitude), and speed. Such measurements are rather difficult and often unsatisfactory, however, since in an actual seaway both the length and the height of waves change continuously.

When a vessel proceeds directly through a regular train of waves, the wavelength can be measured with the help of a line towed astern with a buoy at the end. The length of the towline can be so adjusted that when the buoy is on top of a crest the stern of the vessel is on the next wave crest. Since, however, wave trains are seldom quite regular, the length between the wave crests may vary considerably, and it is difficult to adjust the length of the towline. In such cases the position of the wave crest along the hull is noted while the buoy is on the crest of the next wave. Since large vessels are often larger than the

waves, two successive wave crests can be noted along the hull and the length of the wave measured. If the vessel is not headed in the direction of the wave travel, the actual wavelength is obtained by multiplying the observed distance between two wave crests by the cosine of the angle of vehicle heading.

If a vessel is at rest in a regular wave train, the wave speed or celerity is determined by noting the time needed for the wave to run the entire length of the vehicle. If, however, the vessel itself moves at a speed of V ft/sec against the waves, then, during the time required by a wave crest to run the distance from the bow to the stern, the vessel will have moved a distance of Vt ft, and

$$t = \frac{L \cos \mu}{V_w - V \cos \mu} \qquad \text{[see (3.18)]}$$

or

$$V_w = \left(\frac{L}{t} - V\right) \cos \mu \tag{15.6}$$

where μ is the heading angle of the vessel relative to the wave travel. If, however, the vessel is moving with the waves, the sign of V should be reversed, and

$$V_w = \left(\frac{L}{t} + V\right) \cos \mu \tag{15.7}$$

To obtain a continuous record of waves, a device described in its simplified form as follows may be used.

A long pole or a mast is so ballasted as to float erectly, and at the lower end of the pole a disk is fitted that should act like a sea anchor to prevent any vertical oscillation of the pole. At the water surface an annular buoy surrounds the pole; the buoy is free to move up and down with the passing of the waves and is connected with a registering device (by reducing its motion properly), which actuates a pen that moves continually on a recording chart driven by clock work. The time in seconds is also recorded on the chart by the clock work. Thus the length, height, and time, as well as the continuous wave profile, can be determined.

The wave-measuring system described above is designed to obtain the point wave spectrum. As already mentioned, however, the directional spectrum is also important for seakeeping predictions.

Shipborne Wave Recorder [216]

Accurate determination of the responses of the wave recorder to waves having different frequencies and approaching from different directions is very difficult, but intelligent estimates can be made by looking at the physical phenomena involved in the problem.

Long waves, over which the vessel may ride, can be measured almost entirely by a vertical accelerometer, and short waves, which do not produce appreciable heave, are measured by pressure sensors. Thus the two types of devices utilized in shipborne wave recorders are pressure sensors and accelerometers.

Pressure Devices

In most engineering problems water is considered incompressible, and the static pressure distribution is treated as a linear function of depth, that is

$$p_z = \rho g z$$

where p_z = hydrostatic pressure
ρ = mass density of water
g = gravitational acceleration
z = depth

Since ρ and g are constant up to reasonably large depths, the relationship is linear. It is therefore a simple matter to calculate the depth of the pressure sensor once one knows the pressure at that depth; in other words, the height of the still water surface above the sensor is easily determined once the pressure is known. The relationship holds only for still water or extremely slow variation in water level.

When waves are present at the surface, this relationship does not hold. It is known that the pressure along the surface of the water is very nearly the atmospheric pressure and that the pressure at a given depth below the still water level must fluctuate in some way related to wave height. It is also known that in deep water even the largest surface disturbance does not cause significant pressure changes along the bottom. Thus pressure fluctuations near the surface attenuate in some manner with depth. This attenuation of the pressure variations is caused by viscous dissipation, as shown in Fig. 15.12, and is given by the following equation:

$$p_w = p_0 e^{-2\pi z/L_w} = p_0 e^{-4\pi^2 z/gT_w^2} \tag{15.8}$$

where p_w = wave pressure amplitude at a depth z
p_0 = wave pressure amplitude at the surface
T_w = wave period
L_w = wavelength

The total pressure at a given depth will then be

$$p = p_z + p_w$$

Two important features of this equation should be noted. The first is that the pressure attenuation

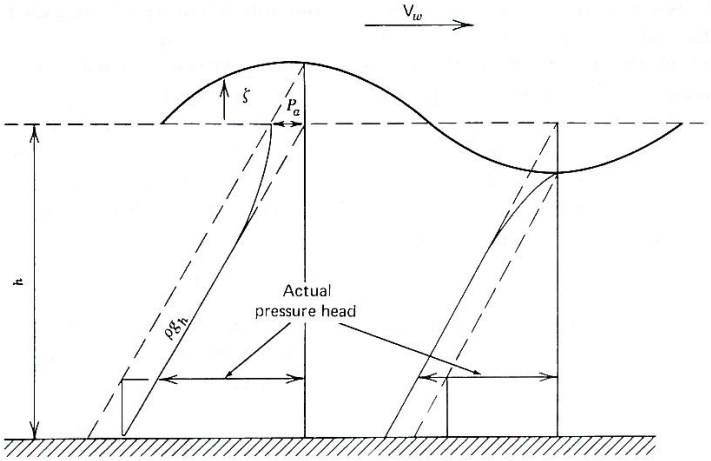


Figure 15.12 Pressure distribution under a wave.

factor, $e^{-4\pi^2 z/gT_w^2}$, is selective with wave period (or length) and waves of different periods attenuate at different rates with depth. Second, wave height does not appear in the equation as such. The term p_0 incorporates the wave height and for the present must be considered as linear. The equation is then

$$p = \rho g\left(z \pm \frac{h_w}{2} e^{-4\pi^2 z/gT_w^2}\right) \tag{15.9}$$

where h_w is the wave height. It is also to be noted here that the preceding development was based on the pressure sensor being at a fixed location.

Accelerometers

Accelerometers are basically very simple devices that measure accelerations. In general, they consist of a mass and a spring as in Fig. 15.13. If the free end of the spring is considered fixed, the force in the spring is proportional to its deflection; and, since the other end is attached to the mass, this force is also equal to the product of the mass times its acceleration. If care was taken in the selection or construction of the spring to ensure that the spring constant is linear over the expected range of deflections, the responses of the system to various forces is easily calculated. Then, by working backwards, the unknown existing forces are easily calculated from the measured responses of the accelerometer.

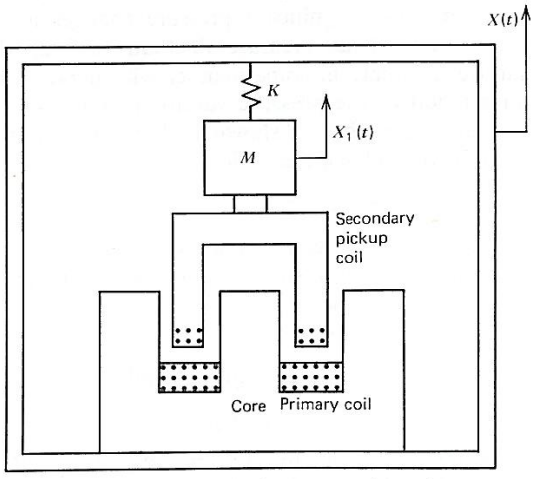


Figure 15.13 Accelerometer schematic.

If the accelerometer is fixed to a structure whose motion, $X(t)$, is unknown, this motion can be readily calculated from the measured response of the accelerometer. The method is as follows. Displacement of the mass relative to the structure, $X(t) - X_1(t)$, is measured, and the force in the spring is calculated:

$$F = k[X(t) - X_1(t)]$$

and $F = M\ddot{X}_1(t)$, since M is attached to the spring. Then

$$M\ddot{X}_1(t) = k[X(t) - X_1(t)]$$

$$\ddot{X}_1(t) = \frac{k}{M}\left[X(t) - X_1(t)\right]$$

or

$$X_1(t) = \int\int \ddot{X}_1(t) = \frac{k}{M}\int\int\left[X(t) - X_1(t)\right]$$

Therefore

$$X(t) = \left[X(t) - X_1(t)\right] + \frac{k}{M}\int\int\left[X(t) - X_1(t)\right] \tag{15.10}$$

Thus the method requires the measurement of

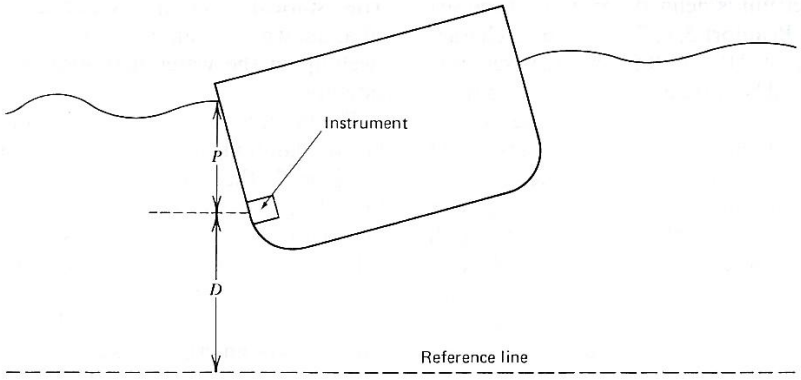


Figure 15.14 Installation of ship-borne wave recorder.

spring deflection, which should be integrated twice with time and added to or substracted from the original measurement.

The construction of the accelerometer is very similar to what would be expected from the above description. The measurement of the displacement of the mass is relative to the instrument case, which is mounted on the structure.

The shipborne wave recorder designed by Tucker [216] operates by combining these two devices. This instrument, in principle, measures the height of the water surface relative to a point on the ship's hull and adds this value to the height of the point relative to an imaginary reference surface, thus giving the height of the water surface independent of the position of the vessel (see Fig. 15.14). The first of these quantities is obtained by measuring the water pressure on the hull. Measurement of the second quantity is more difficult, and it is also not practicable to measure the absolute height of the pressure-measuring device. For the measurement of waves, however, it is necessary only to measure fluctuations in height, and this is accomplished by measuring the vertical component of acceleration and integrating it twice as described above. Therefore Tucker's design uses an accelerometer–pressure sensor pair on each side of the ship, as in Fig. 15.14. This arrangement minimizes errors induced by roll and reflected waves. If waves approach the ship on the side where the instrument is located, the wave heights may be increased because of reflection; similarly, if they approach from the other side, reduced wave heights may be recorded.

The shipborne wave recorder makes possible the simultaneous recording of waves and vehicle motions, although difficulty still remains in regard to accurate determination of the directions of the wave components. To solve this problem the vessel is steered at a constant speed along a series of courses, and waves are measured on each of the courses. From Fourier analysis of the wave records the true frequencies, as well as the directions of travel, can be determined. However, accurate results can be obtained only when the wave system either is undirectional or has most of its energy concentrated in well-separated directions and frequency bands. In other words, full-scale trials should be made only when conditions are suitable.

It will be remembered that from the pressure sensor one can find the height of the water surface above the sensor, while the accelerometer gives the vertical position of the ship with respect to the still water level or some average level. By combining the two results, one obtains a measure of wave height with respect to the reference level of the accelerometer.

Seakeeping Prediction

Information on speed, power, motions, the shipping of water, slamming, and propeller racing obtained in waves on actual vessels is of considerable value in marine vehicle design. Techniques based on spectral analyses have been developed that allow estimates to be made, not only of motions, but also of slamming and the shipping of water for a full-scale ship.

There is some difficulty in selecting wave spectra for a given wind force. For these calculations wave heights can be taken according to Table 15.2.

TABLE 15.2

Wind force [Beaufort]	5	6	7	8	9
Wind speed [knots]	18	23	30	37	44
Significant wave height [m]	3.0	3.7	5.2	8.0	11.2
Significant height of coastal waters [m]	1.5	2.3	3.0	4.3	—

The ITTC spectrum is defined, for each of the sea states denoted as Beaufort 5, 6, 7, and 8, by a characteristic period T_1 of 7.0, 7.6, 9.5, and 12.0 sec, respectively, this period being related to the first moment. The motions can be calculated according to the strip theory (see Chapter 9), assuming long-crested irregular seas. There is a power loss due to wind, wave reflection, and ship motions. This power loss depends on size, speed, and the displacement–length coefficient and is determined from the full-scale results. In the case of high-speed vessels the important speed loss is due to the shipping of water and slamming in sea states of Beaufort 7 and higher. From the calculated relative bow motion in the waves, the probability of shipping green water may be deduced. Because of the bow wave the effective freeboard is smaller than the geometric freeboard. This "statical" swell-up of water at the bow is calculated as shown in Chapter 7. Similarly, the "dynamical" swell-up of the water may also be taken into consideration.

The immersion of the bow also allows the probability of slamming to be calculated. As mentioned in Chapter 7, the threshold of relative bow velocity for a heavy slam is about 12 ft/sec for a ship 520 ft in length. For any other vessel size this threshold velocity is modified according to Froude's law.

The frequency of slamming is then calculated according to (7.61). The fact that these calculations suppose bow emergence as a prerequisite to slamming causes difficulty. It should be noted that on vessels at full draft there is another type of slamming, known as *pounding*, which, though not harmful to the ship's bottom, may induce significant whipping stresses.

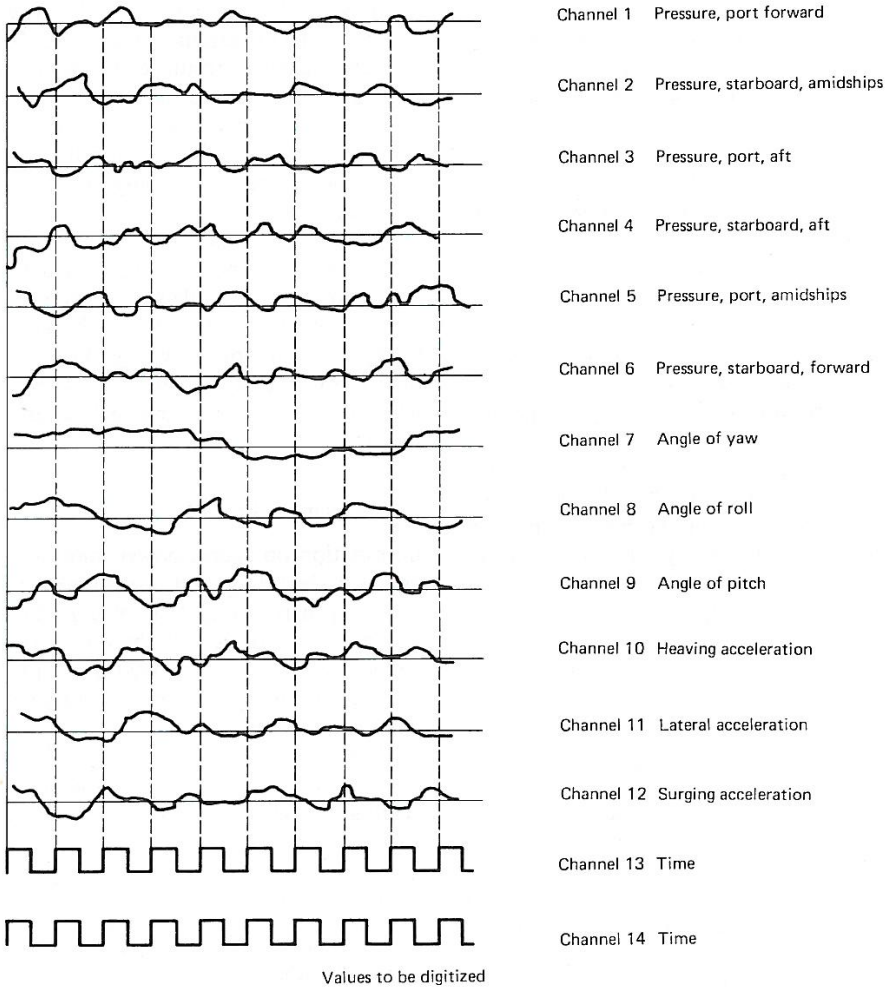


Figure 15.15 A typical record for full-scale seakeeping characteristics of a vessel in a seaway.

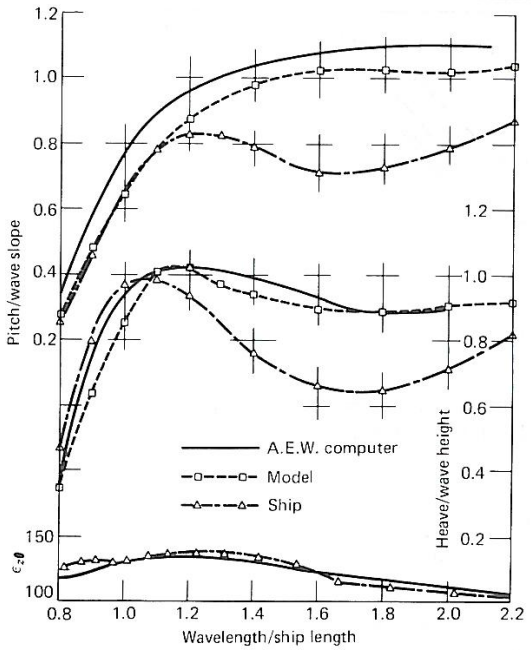


Figure 15.16 Comparison between calculated model test and full-scale results [138].

No estimates have been given as yet of these effects. Propeller emergence can be calculated in the same way as bow emergence.

Residuary resistance is calculated from standard series (e.g., Series 60) data, while frictional resistance may be calculated using the 1957 ITTC formula. As the vessels are considered to be in newly built condition, and welded, a roughness allowance c_f may be assumed, ranging from 0.0001 for a 260 m vessel to 0.00015 for a 190 m vessel and 0.0002 for a small vessel ($L = 125.4$ m). Assuming a modest propulsive efficiency gives power figures that, though high, are not excessive in modern terms.

A calculation of motions in rough water is then carried out for the vessel. A uniform radius of gyration of $0.25L$ is assumed for comparison. The vessels normally have freeboards in accord with the regulations of the Intergovernmental Maritime Consultative Organization (IMCO).

A typical record of full-scale seakeeping characteristics of a vessel in a seaway is shown in Fig. 15.15 whereas Figure 15.16 shows the results of pitching and heaving motions of a model of a frigate (at $F_n = 0.40$), obtained analytically, by model tests, and by full-scale experimentation. The analytical calculations were made by the method of strip theory as treated in Chapter 9, whereas the model tests were conducted in regular head waves and the ship trials were carried out in approximately unidirectional (i.e., long-crested) head seas. The amplitude of waves, pitch, and heave were recorded for about 20 min in order to get the appropriate spectra, from which the response amplitude operators were evaluated. It is interesting that the analytically obtained pitching and heaving motions agreed with the model results within 5%. Although the agreement was also good between the analytical results and the full-scale trials in short wavelengths, there was a discrepancy of about 25 to 30% between the analytic results and values obtained in longer waves (1.5 to 2 ship lengths). The low values of the full-scale results could be justified for two reasons: (*a*) the seaway was not exactly unidirectional, and (*b*) the seaway was not recorded at exactly the same time and the same place as the vehicle motions.

On the other hand, the calculated phase angles agree very well with the full-scale values.

For the present it can be said that [138]:

a. The analytical results are quite satisfactory.
b. There is no definite tendency in the discrepancy between theory and model tests, sometimes one produces a higher result, and sometimes the other.
c. The model results may be incorrect.
d. It does not appear that refinements in the analytical methods will produce any significant improvement in the correlation between analytical, model, and full-scale results.

Figure 15.17 shows a comparison between the observed and calculated roll angles of a trawler [8]. The maximum roll amplitude appears to occur at $L_w/L = 4.15$. This corresponds to an encountering period $T_e = 12.65$ sec, where the mean rolling period in calm water is about 13.1 sec; that is, the encountering frequency is almost the same as the natural frequency, and so it appears that resonance takes place for this particular ratio of wavelength to vessel length.

The calculated values for rolling in Fig. 15.17 are obtained as follows: from the spectra the maximum roll response is derived as 10.1° per meter of wave amplitude, and the value of the damping coefficient 0.0654, is obtained from the linear equation of rolling. The magnification factor is 7.65.

Figure 15.18 compares the maximum vertical accelerations predicted from model experiments and the actual full-scale observations. The bow and stern accelerations appear to be in agree-

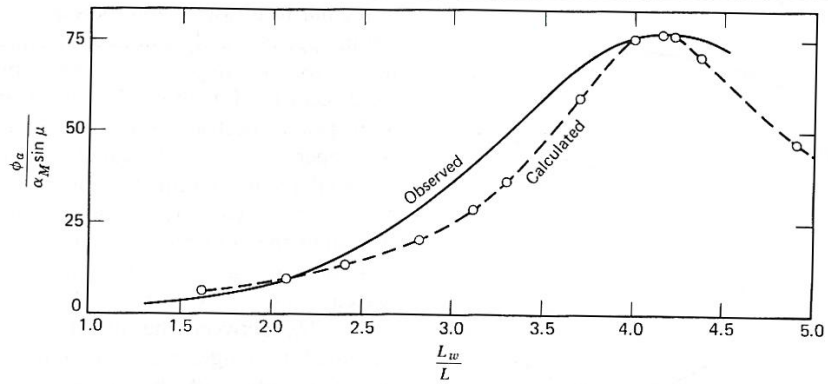


Figure 15.17 Observed and calculated roll responses [8]. Here $\mu = 95$, $\bar{H}_{1/10} = 1.80$ m, $V = 14$ knots, displacement = 1580 tons, trim = 2.0 m, $\overline{GM} = 0.48$ m.

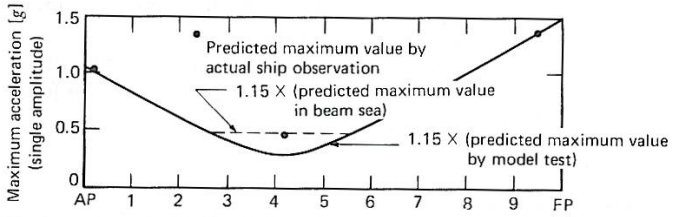


Figure 15.18 Comparison of maximum vertical acceleration predicted from actual ship observation with that from model test [114].

ment, but the value predicted from the model tests at the midship section is considerably higher than the actual observation. For a Series 60 hull form the model results appear to be as follows:

$$\sqrt{2m_0} \text{ (for a beam sea)} = 0.185\,g$$

$$\sqrt{2m_0} \text{ (for a head sea)} = 0.137\,g$$

It can be seen that the maximum acceleration for a beam sea is greater than that for a head sea condition. This is also the case in Fig. 15.18 for the maximum midship acceleration when a beam sea effect is present. However, it is assumed that the maximum vertical acceleration of an actual vessel can be estimated reasonably well from the model tests.

Figure 15.19 shows the relation between pitching motion and vertical acceleration at the bow, both of which are given in terms of a constant times the root mean square value, $\sqrt{2m_0}$. It can be deduced that vertical acceleration at the bow is proportional to pitching angle.

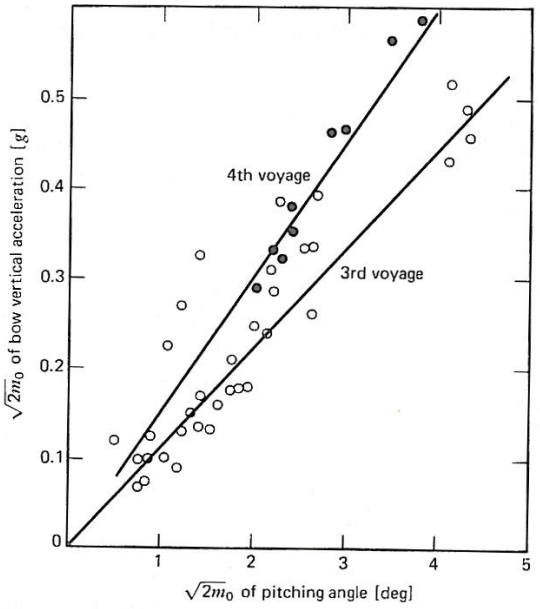


Figure 15.19 Relation between bow vertical acceleration and pitching angle [114].

Stabilizer Trials

Stabilizer trials are carried out in a seaway, where the vessel motion are recorded in both cases (i.e., when the vessel is stabilized and unstabilized). However, it is possible to conduct stabilizer trials in calm water by making the vessel heel when it is fitted with an active stabilization system. There are

two advantages to forced rolling in calm water: (a) different stabilization systems can be tested against design specifications, and (b) shipborne equipment can be studied under forced rolling conditions [the limit of acceleration is about $0.7g$ (i.e., 22.4 ft/sec^2)]. It should be noted, however, that much higher acceleration is acceptable on small ships than on larger ones.

Experimentation on stabilizing devices is actively conducted for three systems:

1. Passive antiroll tanks.
2. Active antiroll fins.
3. Antipitching tanks.

At the David W. Taylor Naval Ship Research and Development Center passive antiroll tanks are evaluated by using a sinusoidal oscillator activated over small roll angles (2 or 4°). The phase relationship between the rolling motion and the stabilizing moment of the tank is determined with this system; however, the effects of the vessel–tank system nonlinearities are not determined.

Stabilizing tanks are often installed in models to study the effects of tank location. It is understood that a considerable scale effect is present in these smaller tanks, but a comparative study using model tests should be valid.

15.6 SCALE EFFECT

The determination of scale effect, that is, the prediction from model to full-scale results, is an important consideration in seakeeping investigations. Very careful full-scale trials are essential for this kind of study, and accurate measurements of both sea waves and vehicle responses are necessary to correlate the model and full-scale results. To find the more valid transfer function the waves must be appropriate. For example, if the transfer function is to be obtained from vessel trials, the waves for the full-scale measurements should be unidirectional, and the range of frequency should be appropriate for proper correlation. On the other hand, for model tests the waves must be measured with the model present, since not only are the surrounding waves diffracted by the model, but also new waves are generated by the model motions, and both wave amplitude and phase may be distorted. The data available from full-scale trials suggest that scale effects are not important for the prediction of longitudinal motions. On the other hand, the scale effect in rolling motion is rather significant. Therefore one should be careful in the prediction of full-scale rolling.

It is therefore often suggested as in Ref. 227 that wave elevation be measured at a place where it is least vulnerable to the presence of the model, but at the same time is close enough to it for estimation of wave elevation at the CG of the model.

Other factors may also contribute significantly to the scale effect; for example, for tank tests the model is often constrained, and this may affect the motions. On the other hand, if the model is a free-running one, it is necessary to use the rudder to keep the proper course, and this rudder action may not correspond to full-scale steering. Also, the waves generated by the model are reflected by the tank, and experience is necessary to evaluate the trial results. However, it is known that, when the model is fitted with sharp-edged bilge keels, the scale effect does not cause a problem.

Similarly, in the case of slamming, if it is assumed that the impact pressure is proportional to the square of the impact velocity, the full-scale data on hull girder response and frequency of occurrence of slamming can be predicted from the model data by using the Froude number. Therefore Froude scaling is valid only for the second phase of impact, when the pressure is actually proportional to the square of the impact velocity, as seen in (7.55). Hence Froude scaling may not be applicable for ships that have wide bottom areas at the forefoot with small deadrise angles. The experimental investigations reported in Ref. 31 showed that for deadrise angle of less than 6°, the impact pressures at points away from the keel are not proportional to the second power of the impact velocity, and so Froude's law cannot be used for scaling. However, for ships with pronounced V-sections in the forebody the affected area is rather small and may contribute very little to the total hydrodynamic slamming force at the bow.

It should also be pointed out here that, if the scaling is done by using Froude's law, the scaling laws for compressibility of the fluid, viscosity, and surface tension are not fulfilled; fortunately, however, these factors appear to have very little effect [188]. Froude numbers cannot be used however, for scaling the results from the initial stage of slamming impact, since pressure is dependent on air entrapment and elastic characteristics in this part of the pressure–time history.

The dimensionless ratio of inertial force to gravity force is proportional to the Froude number, $V/\sqrt{gL}$, whereas the Cauchy number, $\rho_0 V_0^2/E = \rho_0 V_0^2/\rho_1 C_L^2$, gives the relative magnitude of inertial forces to

elastic forces and is proportional to $(V_0/C_L)^2$. If the material used for the model is the same as that of the full-scale structure, the invariance of $(V_0/C_L)^2$ makes it imperative that V_0 be the same for both the model and the full-scale structure, whereas the Froude number similarity makes it necessary that the velocity of the full-scale structure be proportional to the square root of the scale ratio. It is suggested in Ref. 188 that, since during the initial impact phase the gravitational forces associated with the reduction of body velocity V_0 (relative velocity of impact) are rather small relative to the inertial forces, instead of the Froude number the ratio V_0/C_L be applied for predicting the full-scale data of the pressure during the initial impact phase.

It appears reasonable to believe that the impact loads due to bow flare immersion (namely, pressures, forces, and moments) for full-scale vessels can be obtained with sufficient accuracy. As was mentioned in Chapter 7, the hydrodynamic impact pressure for wedges with reasonable deadrise angles is proportional to the square of the immersion velocity. In such a case Froude scaling can be applied, since p/V^2 remain constant for both model and prototype. It has been concluded, therefore, that motions determined from well-organized and carefully conducted model experiments are quite suitable for full-scale prediction.

15.7 CONCLUSIONS

Most of the theories available for the prediction of vehicle motions have been verified experimentally. The most extensive experimentation conducted in this connection involves the applicability and improvement of the strip theory for vessel motion prediction. Important improvements to the forward speed effects have become possible because of strong experimental support obtained from comparison studies of the computed motions and experiments performed for various kinds of hull forms.

As a result of such comparisons, the improved strip theory with close fit station representation (instead of just considering the B/T ratio and the sectional area coefficient of transverse sections) is now used for vessel motion predictions in regular head seas with sufficient accuracy. It has been shown that the strip theory works well, not only for common cruiser stern vessels and high-speed destroyer hulls at Froude numbers up to 0.45, but also for hulls with large bulbs and sonar domes. For prediction in following seas, however, more experimental data are needed to evaluate the accuracy of the strip theory. Presently, a strip theory with all six degrees of freedom of motion is being verified experimentally at the David W. Taylor Naval Ship Research and Development Center at Carderock, Maryland.

To satisfy design needs, many seakeeping facilities provide for calculation of vehicle response, motion, loading, and so forth in a seaway by computer as well as model seakeeping tests. Seakeeping tests in model basins have increased considerably in recent years, since seakeeping investigations are routinely performed for all conventional vessels. In addition, the potential success of unconventional vessels is determined mainly from the seakeeping performance of models. However, for more realistic prediction of seakeeping performance, experimentation should include shallow water tests, generation of multi-directional irregular seaways, more accure shipborne wave recorders, and so on.

Chapter

Sixteen

SEAKEEPING CONSIDERATIONS IN DESIGN

16.1 GENERAL

The success of a ship design depends ultimately on its performance in a seaway. However, the prediction of ship motions, resistance and propulsion characteristics, structural loads, and dynamic effects like deck wetness and slamming in a realistic seaway is such a complex problem that ship designers are generally forced to select their hull forms and ship dimensions on the basis of calm water performance without much consideration of the sea and the weather conditions. Only very recently sophisticated experimental techniques and computer applications in ship motion theories have made it possible for the designer to consider the seakeeping qualities of his ship at an early stage.

The overall seakeeping design can be divided into three areas [38]:

1. Habitability. This area deals with the environment in which the crew can perform their duties most effectively so that there is no degradation in performance due to the behavior of the ship in a seaway. Habitability is of great importance for naval ships because missions are complex and, the crew must be physically fit to perform their duties.

However, the habitability requirement depends considerably on the type of mission for the particular ship. For example, a much higher degree of habitability is to be sought for a passenger vessel than for ordinary merchant ships. Similarly, a nuclear-powered aircraft carrier is supposed to meet a variety of sea environments during its lengthy operation in different geographic locations.

2. Operability. This area of study includes the proper operation of all mechanical equipments or instrumentation systems, the safety of deck cargo, course-keeping, and the maneuvering quality of the ship in a seaway environment.

3. Survivability. This area of investigation is concerned with the factors that are of paramount importance when the ship or its major parts are damaged or destroyed, in which case both habitability and operability are no longer of concern.

From naval architectural considerations, each of the three domains described above is to be considered in the early design stage. This necessitates investigation of the following seakeeping aspects by the designer:

a. Various kinds of ship motions (heaving, pitching, rolling, etc.).

b. Accelerations due to motions.

c. Extreme motions and accelerations that the vessel may suffer.

d. Steadiness and ease in heaving, pitching, and rolling motion, and course steadiness including the consideration for broaching.

e. Motions not so severe that deck wetness, slamming, or high accelerations may result, but above a specified limit that may force a voluntary speed reduction or course change.

f. Inertial loads due to ship motions.

g. Strength of ship structures in a seaway (e.g., wave-induced stress and hull deflections.

h. Availability of adequate power to maintain ship speed in a seaway.

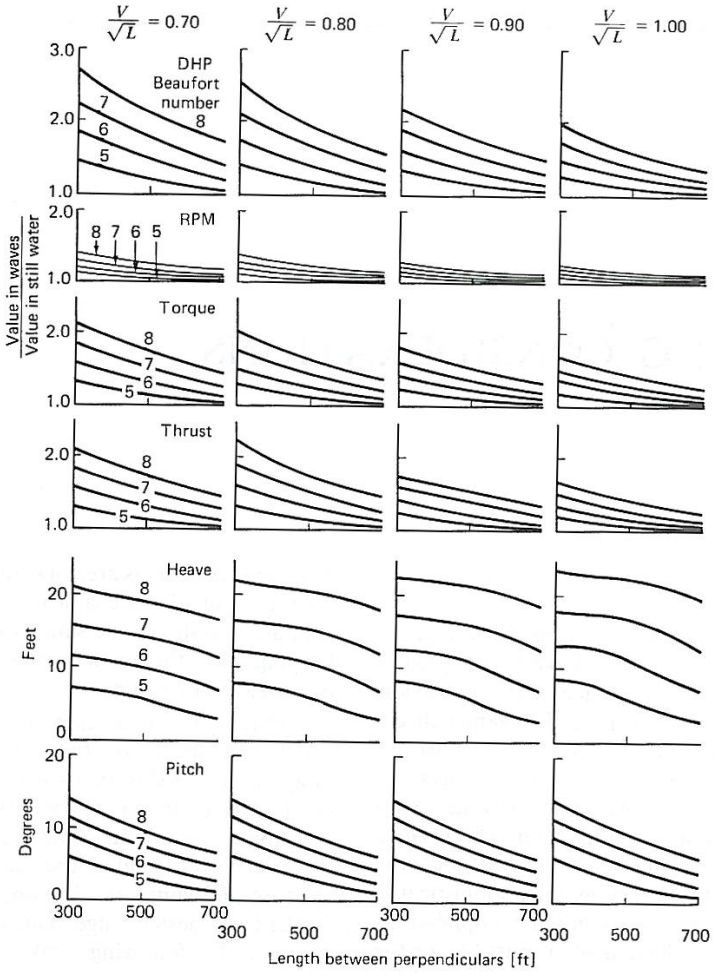


Figure 16.1 Seakeeping characteristics as functions of length [153].

i. Sufficient immersion of the propulsion devices and absence of engine racing due to propeller shaft emergence.

To assess the above items properly there are three particular considerations in regard to the seakeeping design:

1. Definition or prediction of the seaway in which the ship has to operate.
2. Qualitative or quantitative criteria of various seakeeping qualities of the ship in order for it to meet its mission.
3. Determination of whether the seakeeping criteria can be met by the ship for the particular seaway under consideration. If not, design alternatives must be sought.

However, any analysis of the seakeeping design is essentially of probabilistic nature, since the environment itself in which the ship operates (i.e., the actual seaway) can be analyzed only in a probabilistic manner by statistical methods.

16.2 DESIGN PARAMETERS

The design parameters to be considered for seakeeping design may be classified into four categories [155]:

1. The first group may consist of only the simplest parameters that must be determined before a hull form is designed (i.e., length, beam, draft, displacement, longitudinal position of the center of buoyancy, speed, etc.)

2. The second group may consist of parameters such as longitudinal moment of inertia, waterplane area, and position of the longitudinal center of flotation, which from fundamental dynamics are likely to have a significant influence.
3. The third group can include various other parameters (e.g., angle of entrance, presence or absence of bulbous bow) that might reasonably be expected to have an effect.
4. The fourth group should contain the principal parameters defining a propeller, namely, diameter, pitch, blade area ratio, number of blades, and so on.

It is not simple to determine uniquely the influence of various parameters on motions as well as dynamic effects. There is also a probability that a change in a parameter may be advantageous for the motion characteristics while degrading the dynamic effects.

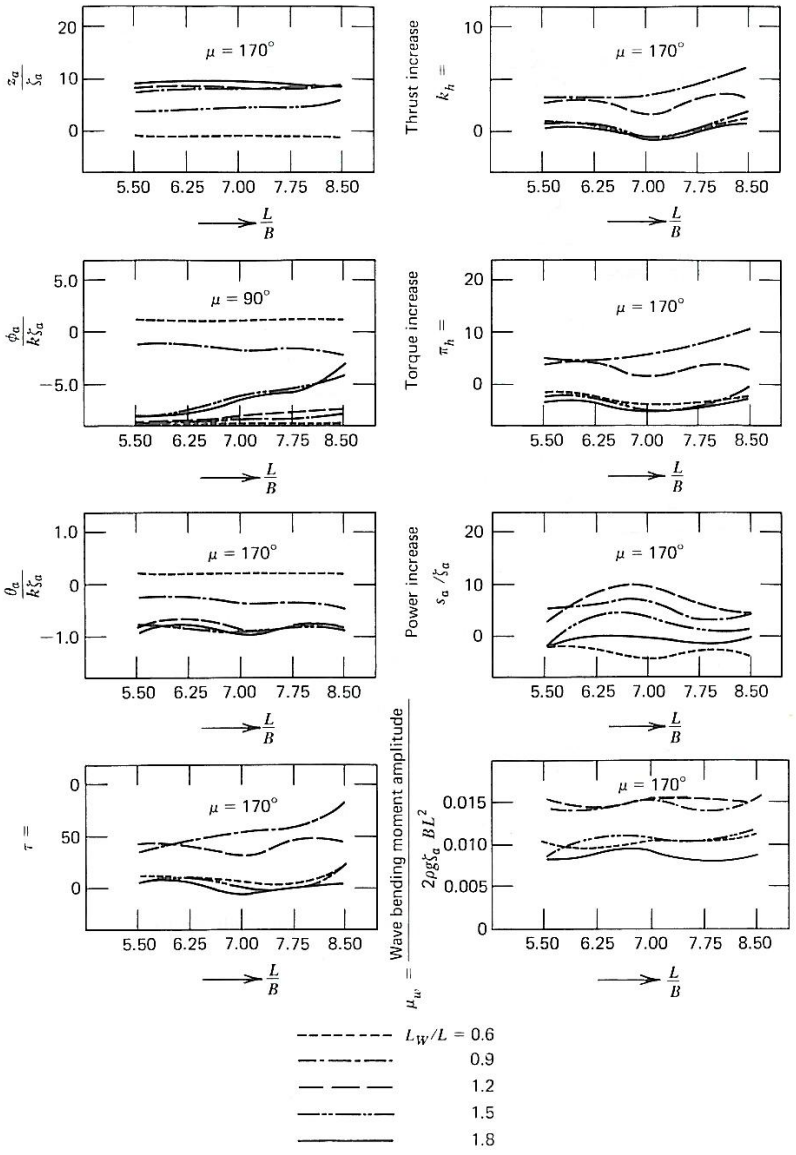


Figure 16.2 Seakeeping characteristics as functions of length/beam ratio ($F_n = 0.15$) [226].

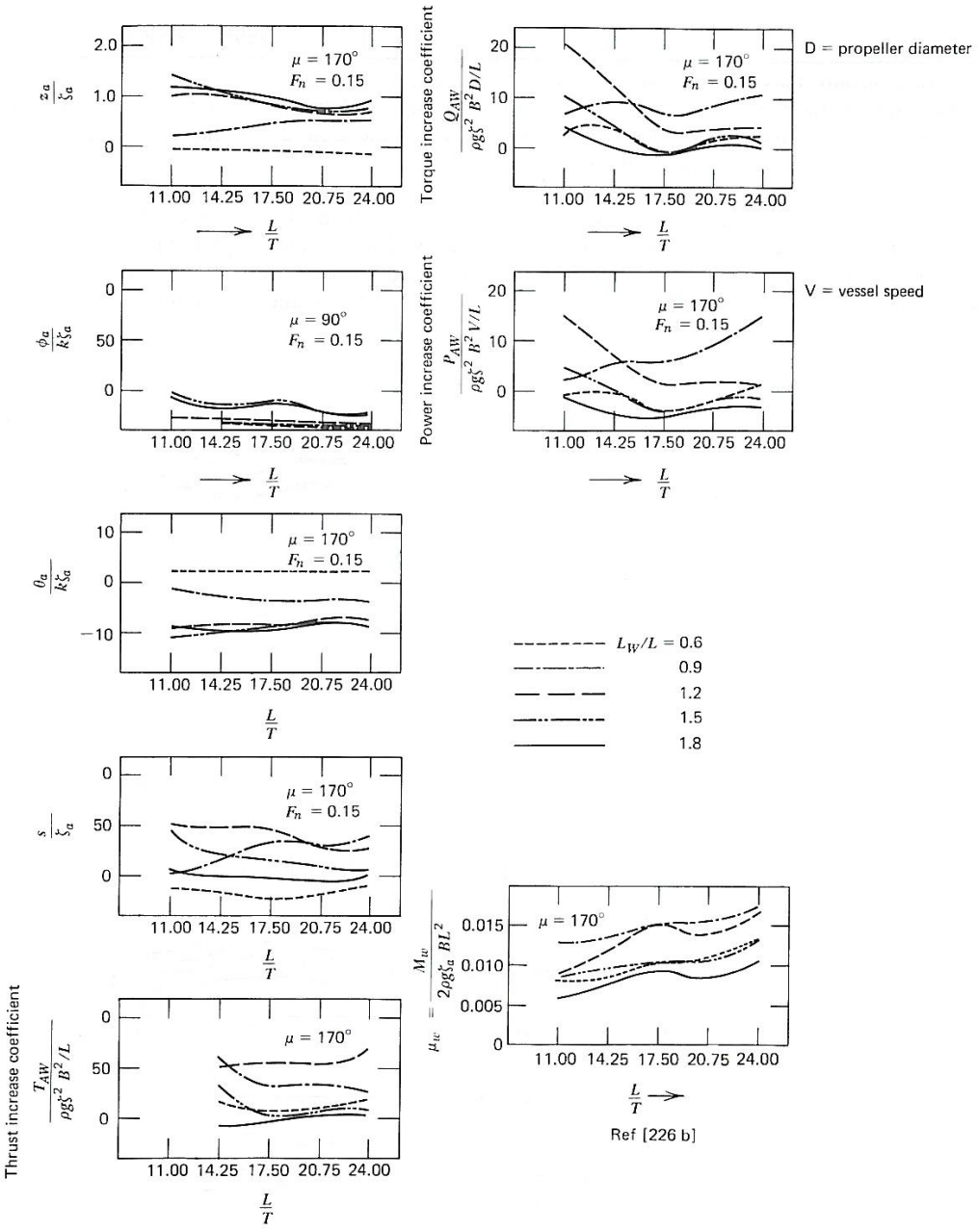


Figure 16.3 Seakeeping characteristics as functions of length/draft ratio ($F_n = 0.15$) [226].

Therefore it is imperative to make series studies systematically, either by model tests or by computer applications, in order to establish the parametric influence in the determination of seakeeping qualities of any design.

The effects of some of the significant parameters on the seakeeping performance of a ship may be described as follows.

Length. The behavior of a ship in a seaway depends to a considerable extent on the length of the ship. The exciting force, as well as the exciting moments due to waves, is relatively larger for smaller ships than for longer ones.

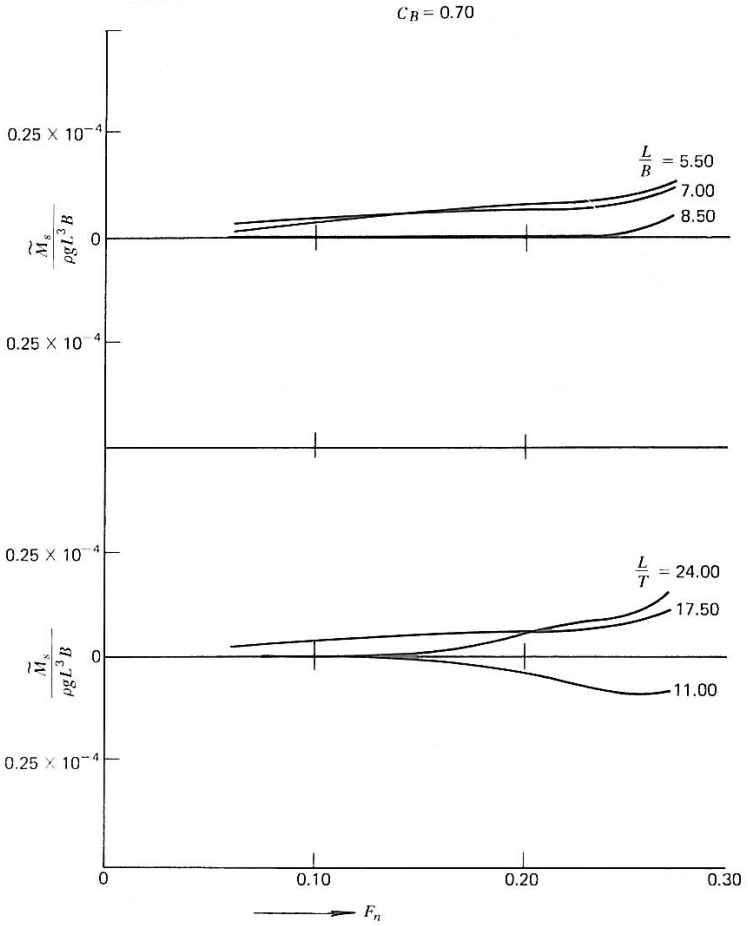
Both heaving and pitching motions are influenced considerably by the length parameter. Length is also one of the most important parameters in sustaining ship speed in a seaway. In a heavy sea speed is often reduced voluntarily to attain synchronism with waves shorter than the ship and thus avoid heavy motions. Hence the longer the ship, the less is the speed reduction necessary to do this.

Also, experience during full-scale trials has demonstrated that vertical acceleration at the bow and also the shipping of green water are much less for longer ships than for shorter ones at any particular ship speed.

In other words, for any given length, the less the displacement, the better is the seakeeping quality, provided that the draft is not reduced drastically; otherwise the probability of slamming may increase. The thrust increase coefficient is also large with a smaller displacement/length ratio (Fig. 16.1).

Beam. In spite of the fact that ship designers prefer a smaller length beam ratio, this is much less significant for seakeeping.

However, the pitching motion increases slightly



Figurd 16.4 Calm water vertical bending moment as a function of speed [226*b*].

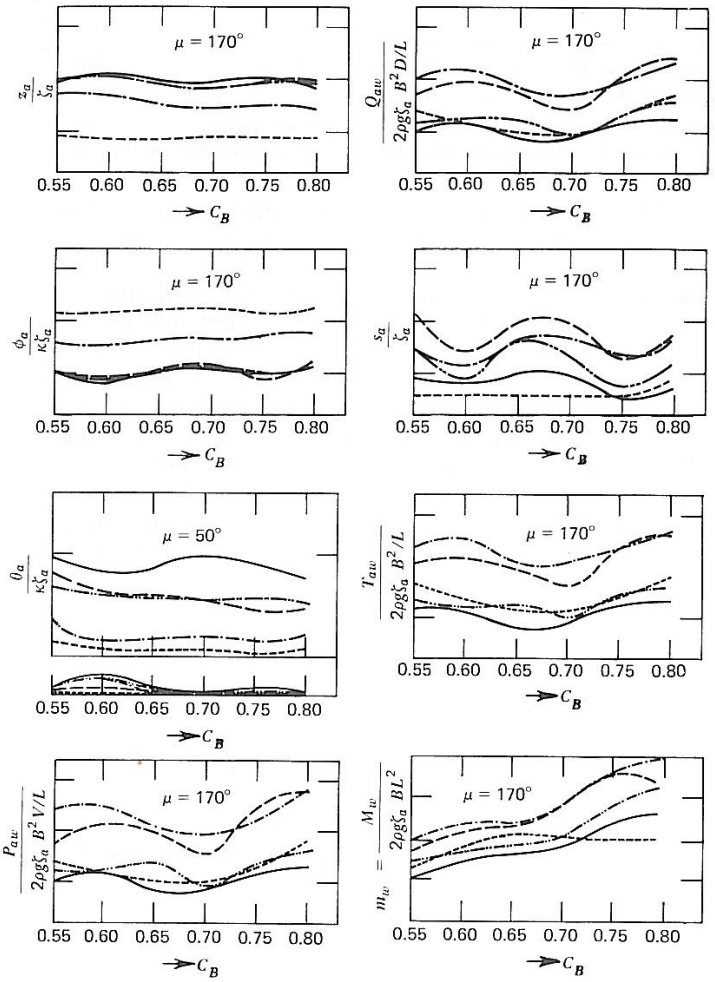


Figure 16.5 Seakeeping characteristics as functions of block coefficient ($F_n = 0.15$) [226].

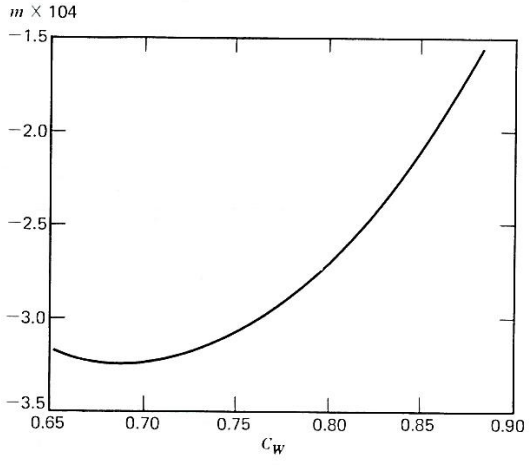


Figure 16.6 Variation of calm water bending moment coefficient with water plane area coefficient.

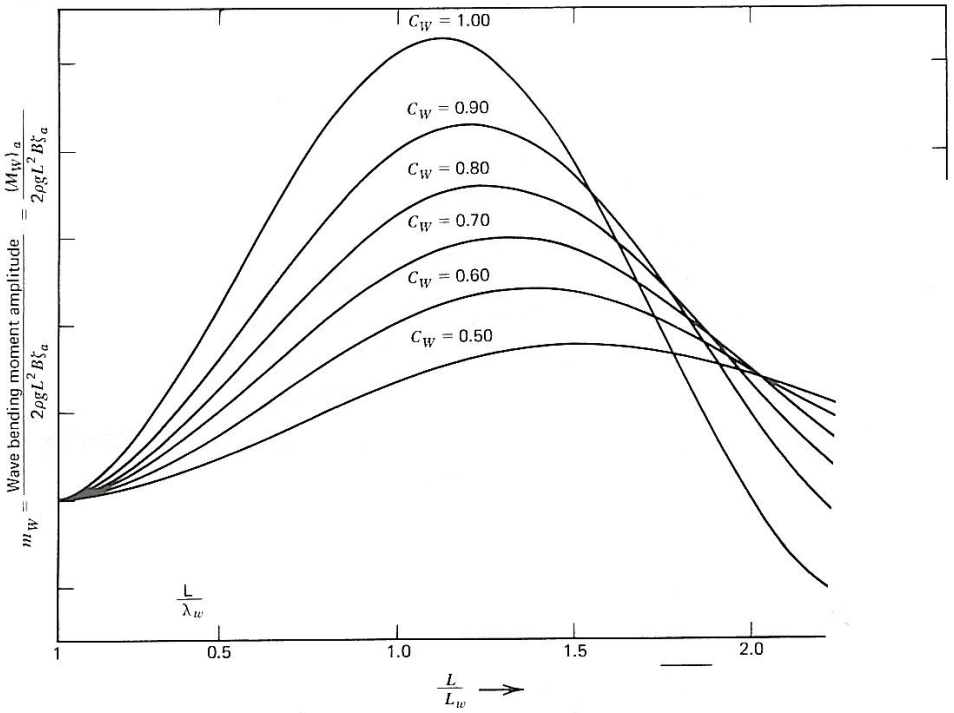


Figure 16.7 Wave bending moment as a function of wavelength (for waves of constant heights) [200].

with increase in the length/beam ratio (i.e., smaller beam). In general, this is also true for nondimensional added torque and added power increase, but the added thrust coefficient hardly differs when the length/beam ratio is varied [227] (Fig. 16.2).

Draft. Both motion and propulsion characteristics, in general, decrease with increase in the length/draft ratio for longer waves and increase for shorter waves.

The forward draft of a ship is very significant from the point of view of slamming, since a ship with a higher length draft ratio (i.e., less draft) is more prone to slamming in heavy seas. Therefore, for light ship operation, there should be sufficient ballast capacity in order to obtain an adequate draft forward (Fig. 16.3).

The magnitude of slamming is drastically decreased and also its peak location moves forward when the draft is increased. It is suggested in Ref. 167 that T/L should be more than 0.045 to avoid severe slamming in a seaway. The smooth water vertical bending moments for different length/beam and length/draft ratios are illustrated in Fig. 16.4. It has been found that the effect of draft on wave bending moment is almost insignificant, especially with large block

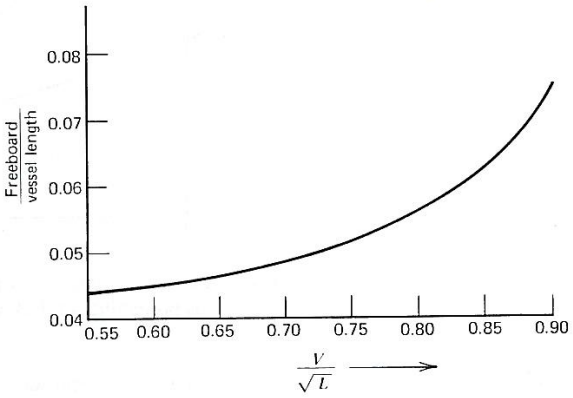


Figure 16.8 Typical freeboard/length ratio versus speed/length ratio for cargo ships.

coefficients. This is not true, however, in the case of still water bending moments [57].

Block Coefficient. In general, the block coefficient has small effect on ship motions. Although the pitching motion is almost independent of the block

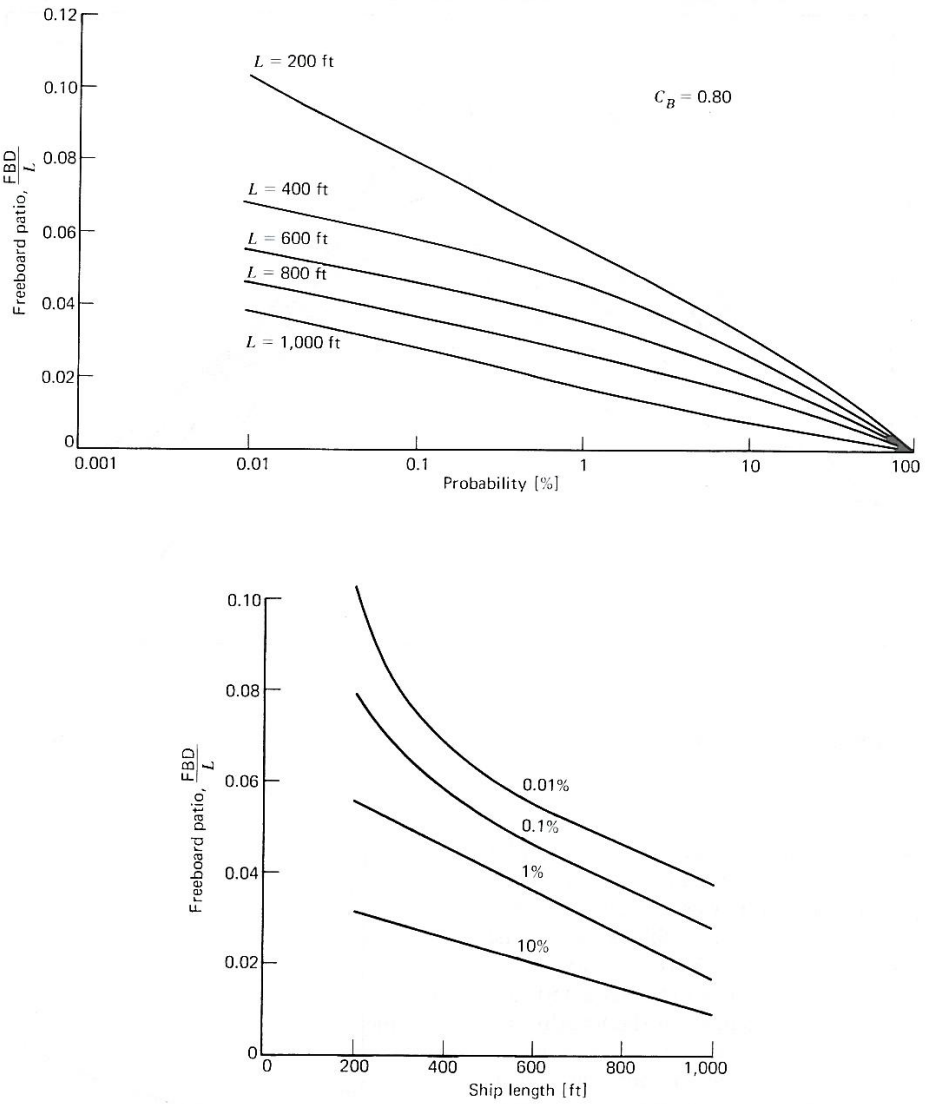


Figure 16.9 Freeboard ratio as a function of probability of deck wetness and vessel length [80]. (*a*) Freeboard ratio versus probability of deck wetness. (*b*) Freeboard ratio versus ship length.

coefficient, the heaving motion at or near resonance has been found to be larger for higher block coefficients; this is also the case for thrust increase. Experimental investigations have shown that the propulsion characteristics in a seaway are not greatly affected by the block coefficient. On the other hand, the wave bending moment increases rapidly with the block coefficient. For example, a wave bending moment is 40% greater for a 0.80 block coefficient than for a 0.60 block coefficient (see Fig. 16.5).

Prismatic Coefficient. Although from the point of view of deck wetness an increase in prismatic coefficient is not justified, the overall motion characteristics are superior with a higher prismatic coefficient. Again, when the prismatic coefficient is high, the speed loss is also greater at high speeds, but at a low Froude number the speed loss is less than that for lower prismatic coefficients.

Waterplane Area Coefficient. Both the still water and the vertical wave bending moment are proportional to the waterplane area coefficient; that is, as the waterplane area coefficient increases, so does

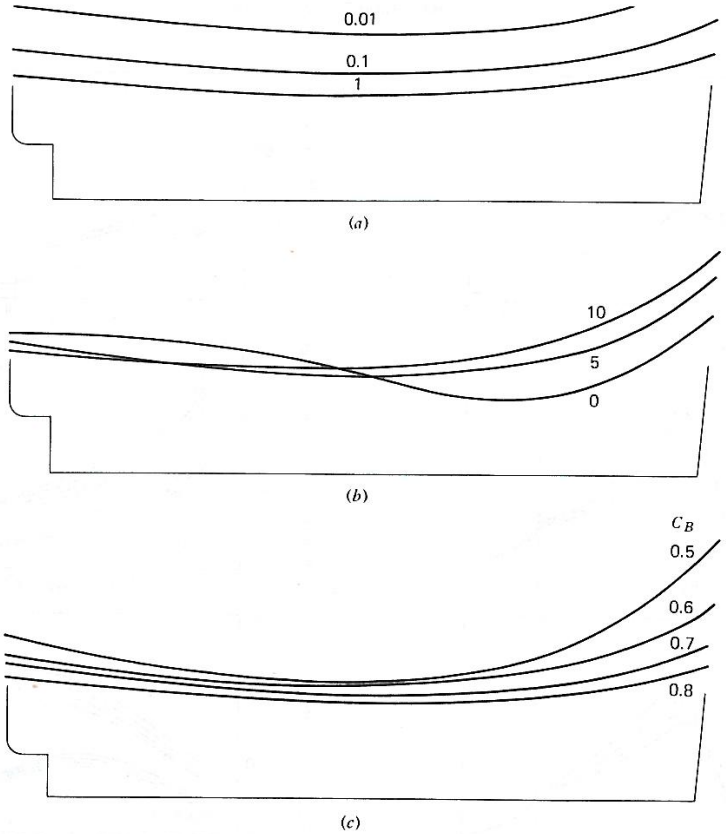


Figure 16.10 Expected trends for sheer curves developed from seakeeping analysis for ships 656 ft (200 m) long and longer [34]. (*a*) Vaxiable: probability of deck wetness in percent; constants: speed and block coefficient. (*b*) Variable: speed; constants: probability and block coefficient. (*c*) Variable: block coefficient; constants: probability and speed.

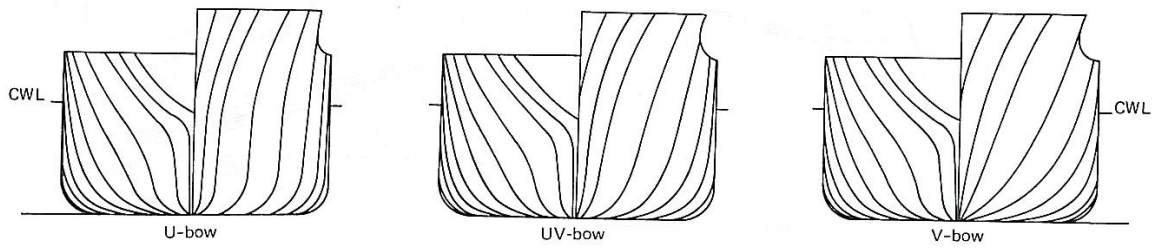


Figure 16.11 Body plans for various bow forms.

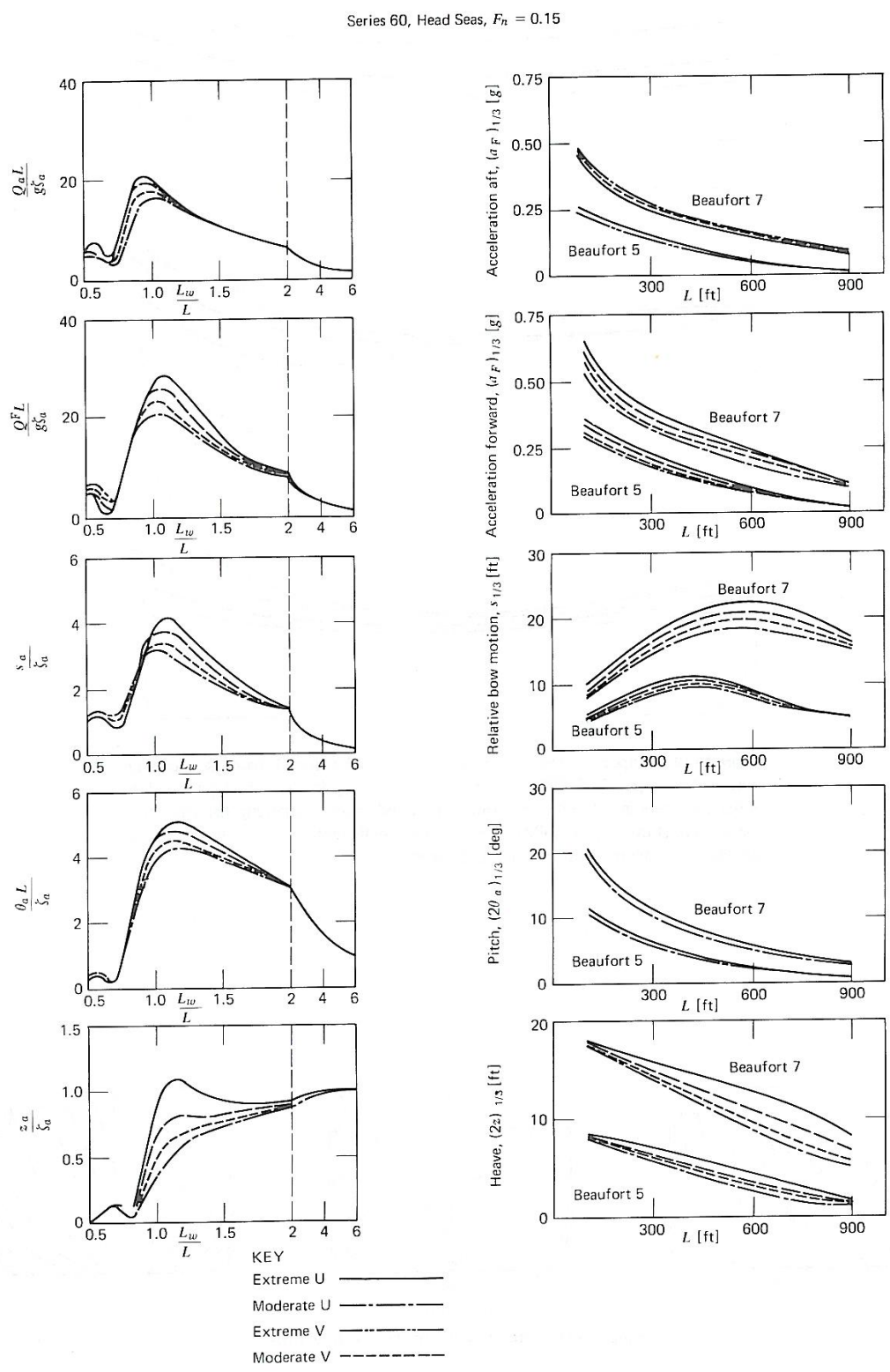


Figure 16.12 Influence of forebody shape on motions [58].

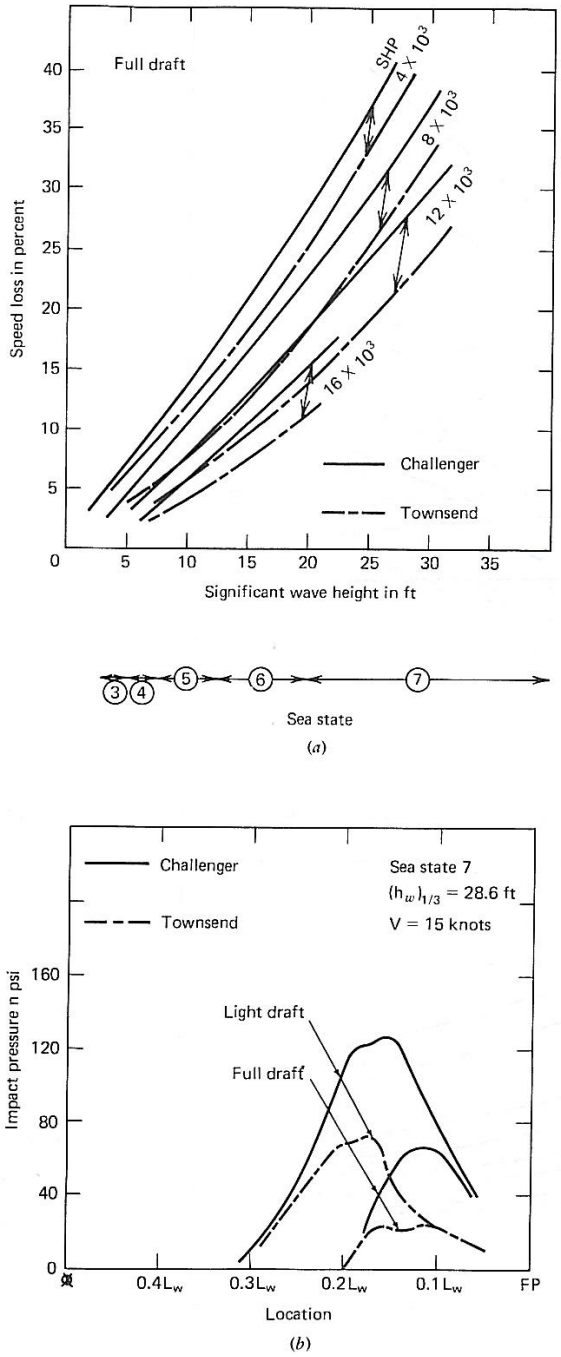


Figure 16.13 Speed loss and pressure distribution for different bow forms [213].

(*a*) Speed loss versus significant wave height with SHP as a parameter; full draft. (*b*) Comparison of pressure distribution along ship length for light and full draft; Sea State 7($(h_w)_{1/3}$ = 28.6 ft), ship speed 15 knots.

the bending moment amidships (Fig. 16.6). As far as the wave bending moment is concerned, the waterplane coefficient is a more valid parameter than the block coefficient [57]. Typical values of the wave bending moment coefficient m_W (due to both seaway waves and ship-generated waves) as functions of the waterplane area coefficient and the ship length/wavelength ratios are illustrated in Fig. 16.7. It is seen that the maximum bending moments take place when the wavelength is slightly shorter than the ship length, and also the maximum value occurs for shorter wavelengths when the waterplane area coefficient C_W decreases.

Freeboard and Flare. From a series of model tests it has been concluded that very little is gained by changing the above-water hull form, as far as the motion amplitudes of a ship are concerned.

However, both freeboard and flare at the bow are of significant importance in reducing the frequency of shipping of green water; therefore with an increase in ship speed the ratio of bow freeboard to length should be increased. Typical values for design consideration are given in Fig. 16.8.

Calculations also suggest that the frequency of occurrence of deck wetness varies with block coefficients as well as with length for a given freeboard ratio. If the nondimensional freeboard ratio is defined as the ratio of the freeboard at the forward perpendicular to the ship length, Fig. 16.9*a* is derived. It is interesting to note that the relative bow motion is almost independent of the ship length, and this means that from the point of view of deck wetness a comparatively higher freeboard and more sheer are needed for a smaller vessel than for a large ship.

The same figure can be shown in a different way as in Fig. 16.9*b*, where one can easily read the freeboard ratio required for various ship lengths for a particular probability of deck wetness. It is apparent from this figure that for a certain probability of occurrence of wetness for ship lengths above 600 ft a constant absolute freeboard is necessary.

Figure 16.10 shows the sheer curves obtained from seakeeping analysis for ships of 656 ft or larger. Such investigations produce a region of deck wetness characteristics and may tend to improve ship safety.

Also, a sufficient amount of flare is helpful in deflecting water outward as the bow moves downward into a wave. An extreme flare, however, may intensify the slamming impact and may also cause a greater speed loss.

To attain high speed in a seaway, it is important to have a clear forward weather deck so that any water collected may be shipped out quickly and

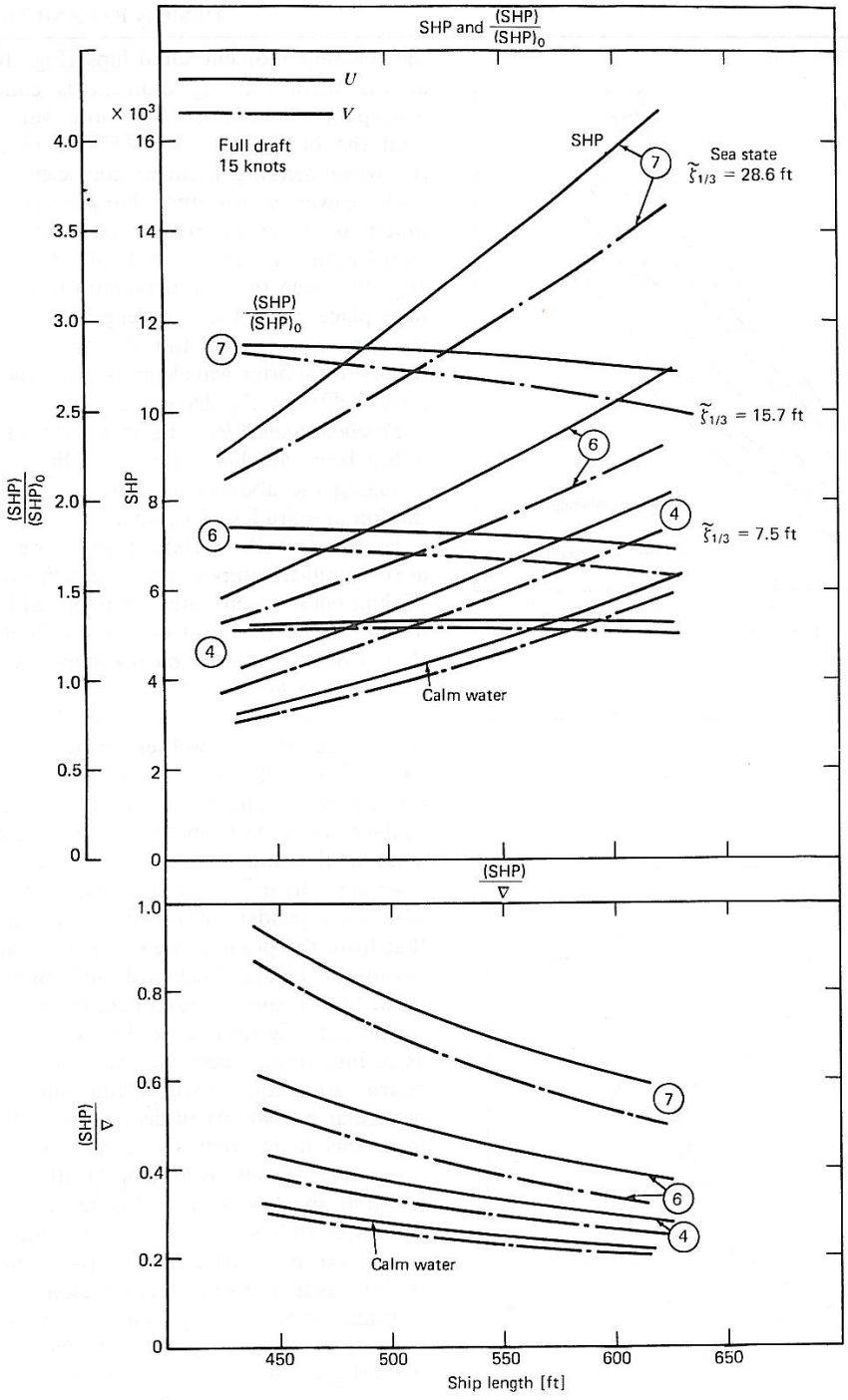


Figure 16.14 Shaft horsepower in waves as a function of ship length [213].

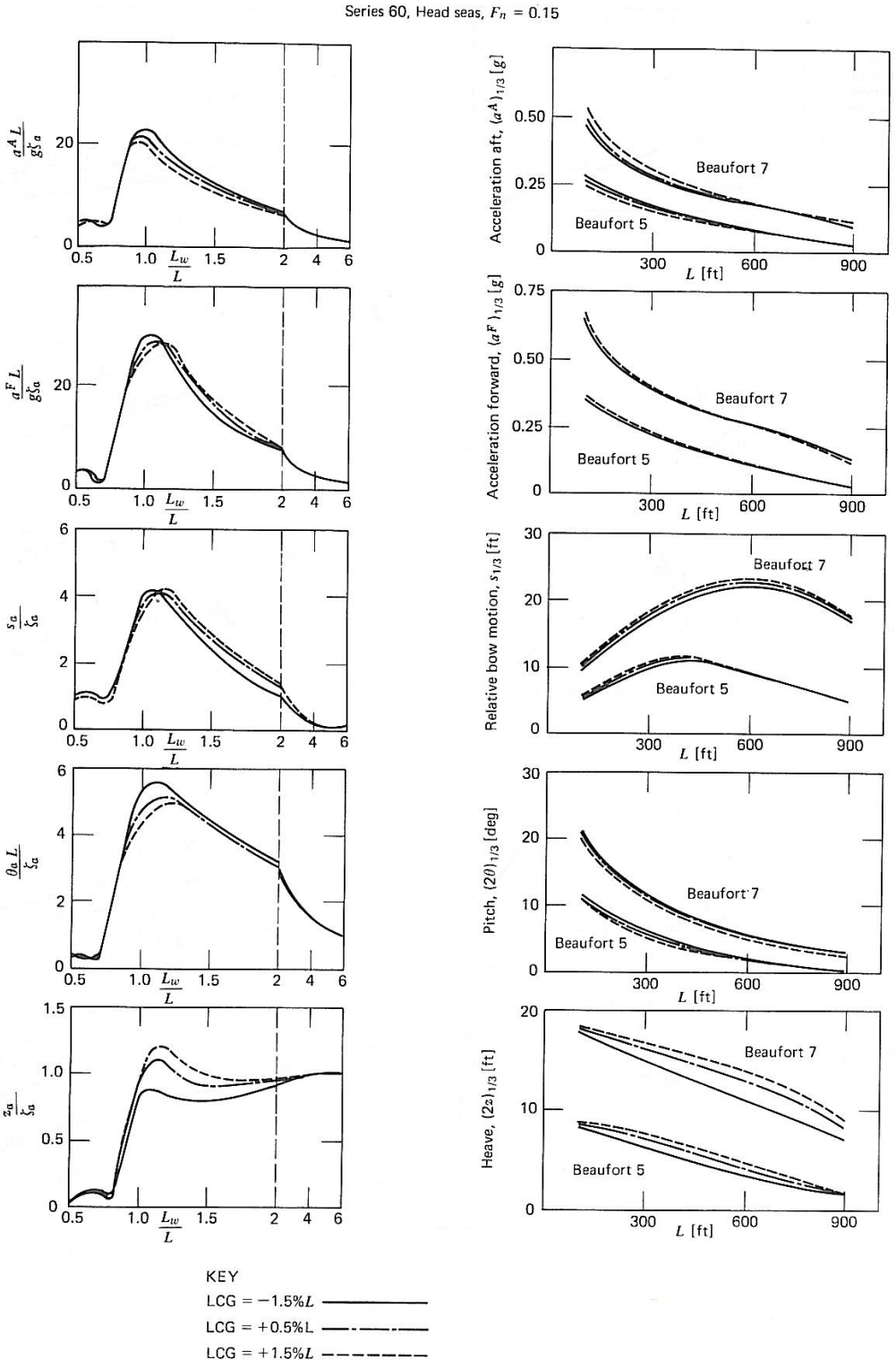


Figure 16.15 Influence of LCG on motions [58].

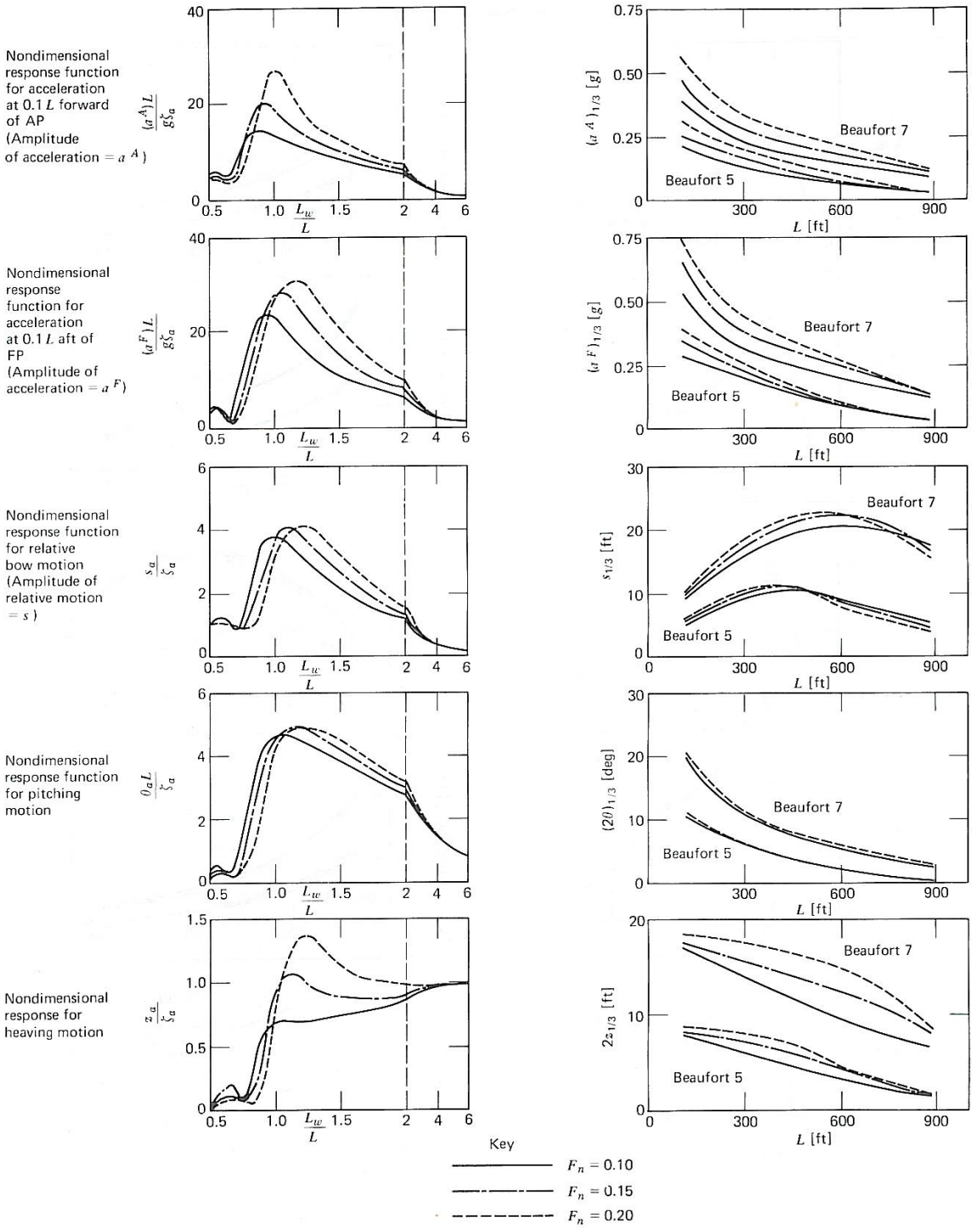


Figure 16.16 Influence of speed on motions in head waves (Series 60, extreme U-form) [58].

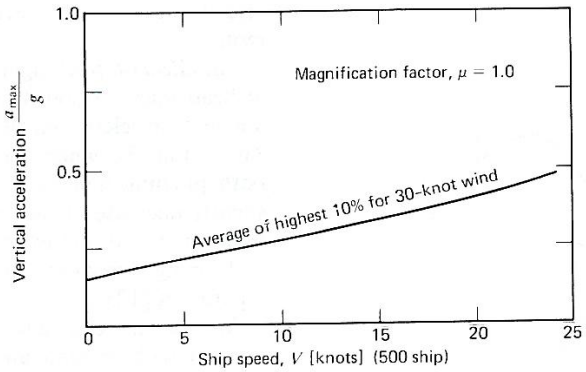


Figure 16.17 Vertical acceleration as a function of ship speed [127].

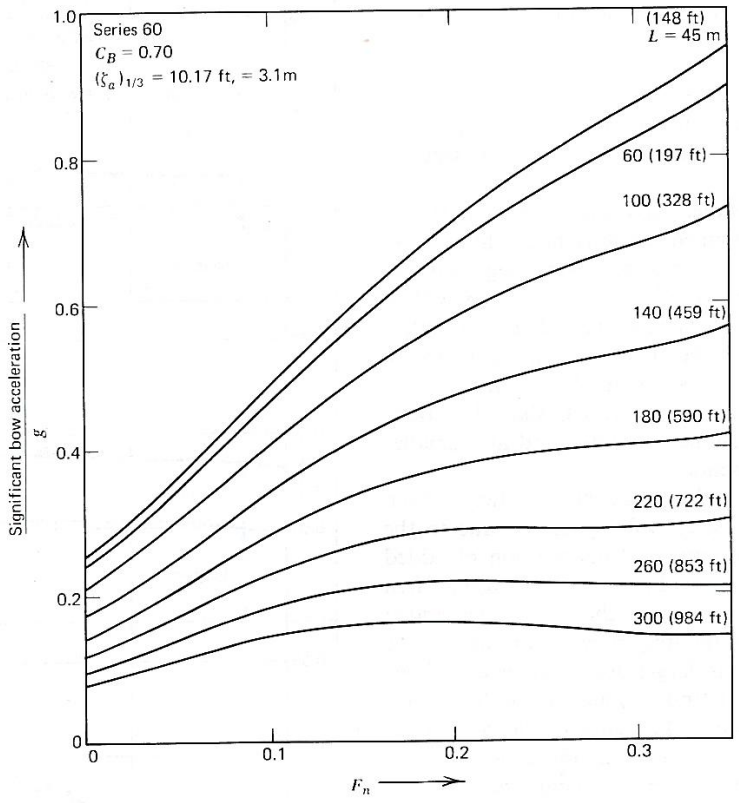


Figure 16.18 Significant bow acceleration as a function of Froude number [77].

safely. It is also important to stop water moving aft of the forecastle. That is the reason why the forecastle should be extended until it reaches the full beam of the ship.

Shape of Forebody Sections Analytical studies indicate that for the whole range of wavelengths smaller amplitudes in heaving motion are obtained when V-shaped sections are used in the forebody instead of U-shaped sections (Fig. 16.11). Pitch amplitudes are reduced by using U-shaped sections

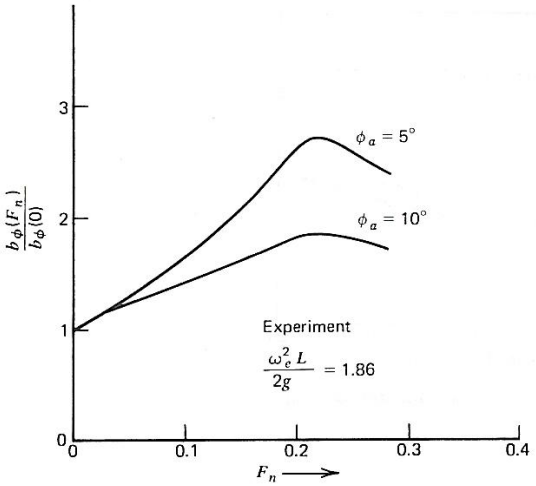


Figure 16.19 Roll damping moment as a function of Froude number [225].

only in long waves; in short waves the pitching motion actually increases for U-shaped sections (Fig. 16.12).

Experimental studies have also indicated that a forebody with V-shaped sections has a higher frequency of slamming but a lower magnitude of pressure per slam. In other words, a ship with a V-shaped forebody may run faster than one with a U-shaped forebody before the same amount of impact pressure due to slamming is experienced.

On the other hand, ships with U-shaped sections experience less resistance in waves and also smaller wave bending moments.

The difference in seakeeping characteristics between the two differently shaped forebodies is due to the difference in the longitudinal distribution of added mass and damping; although the sectional area may be the same, there is a slight difference in added mass, depending on the frequency of motion. But the sectional damping is larger for V-shaped sections, and this difference is independent of the frequency. This causes not only a difference in the coefficients b and B but also a change in the cross-coupling coefficients of the coupled heaving and pitching motions.

As is seen from Figs. 16.13 and 16.14, the V-form has better powering characteristics in waves than do U-shaped sections.

LCG Position The effect of the LCG position on ship motions is not so clear. For the head sea condition an increase in heaving motions is observed when the LCG position is located forward. This is also the case for stern acceleration and relative bow motion.

The effect on pitching motion and bow acceleration in head seas is opposite to that on heaving motion and stern acceleration, although the effect is relatively small; that is, when the LCG is moved forward, both pitching motion and relative bow motion are slightly decreased (Fig. 16.15). It has been found by both analytical and experimental investigations that seakeeping responses are sensitive to LCB–LCF separation [12].

In general, it can be said that seakeeping responses increase with sea state and Froude number, although for the lowest sea state they can decrease with increasing Froude number. This means that the vessel is then in the supercritical zone of operation.

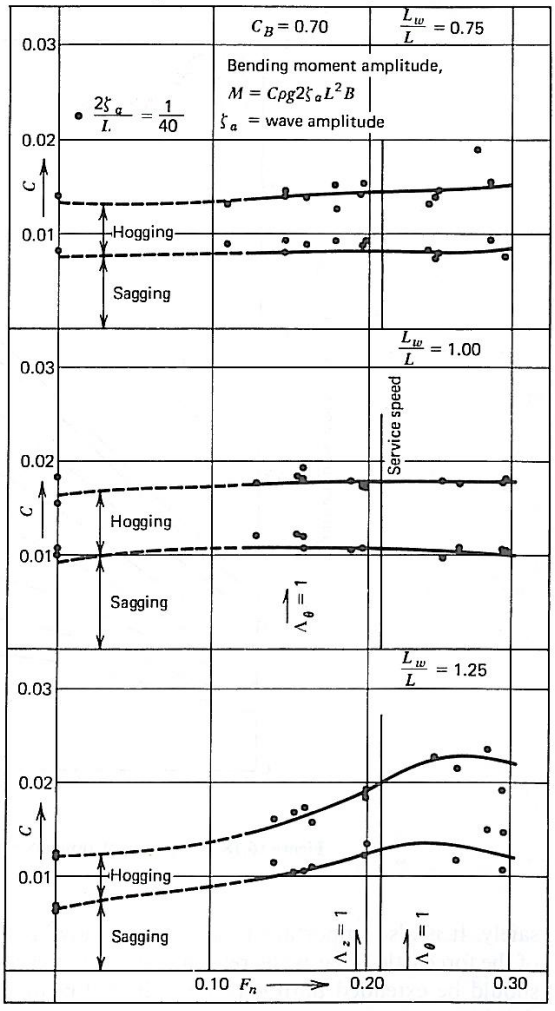


Figure 16.20 Bending moment coefficient as a function of Froude number [46].

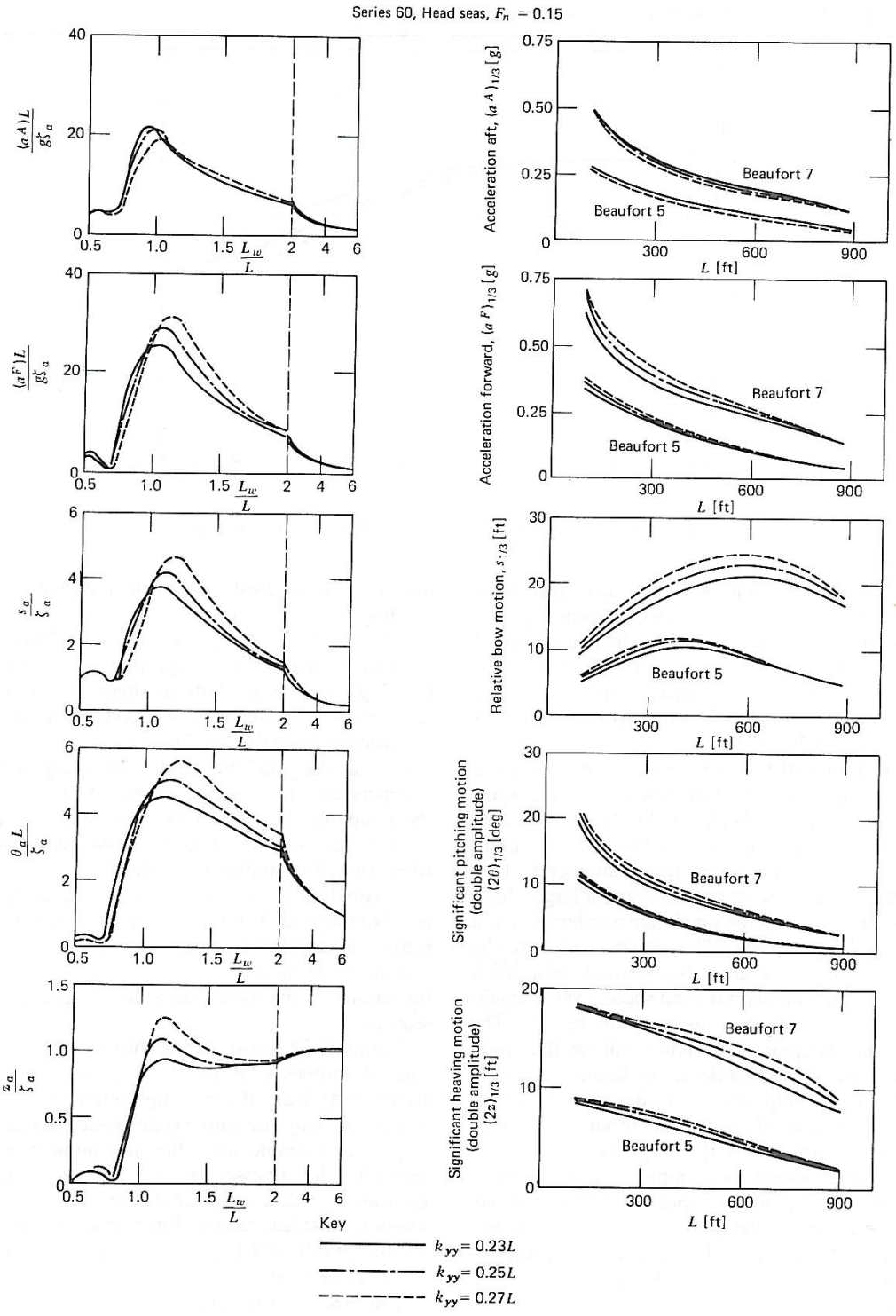


Figure 16.21 Influence of radius of gyration on motion [58].

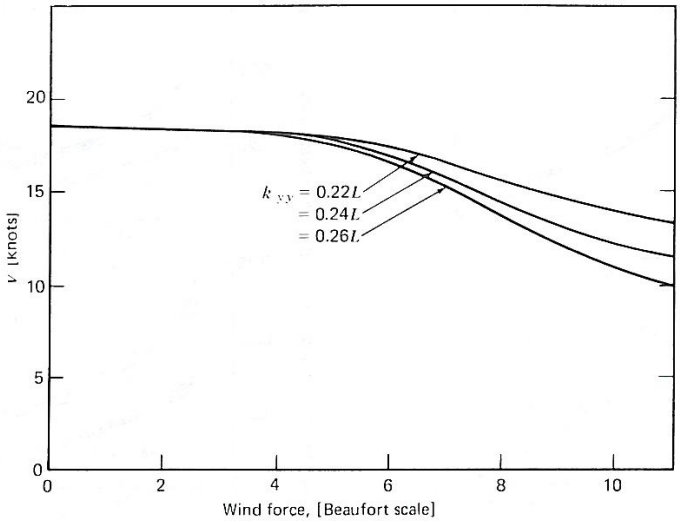


Figure 16.22 Speed loss as a function of radius of gyration [202].

Speed Heaving motion, as well as the accelerations at the bow and stern, is affected considerably by ship speed in heavy seas. On the other hand, speed has relatively small effect on pitching motion in head seas. Figure 16.16 indicates that the speed effect on heaving motion is more pronounced for a 500 ft than for a 100 ft ship.

For a given hull form in a particular seaway the effects of ship length and ship speed on the significant bow acceleration have been found to be considerable, and a typical example is shown in Fig. 16.17. It should be noted that for the same Froude number F_n bow acceleration is greater for smaller than for larger ships.

Figure 16.18 shows the maximum acceleration as a function of ship speed. The curves represent the average of the 10% highest accelerations of a 500 ft ship in a seaway of 30 knot wind speed. (The magnification factor μ has been assumed to be 1.0.) The greater the damping, the higher will be the speed attainable before the accelerations become excessive for a particular ship under consideration. However, the acceptable limit of acceleration should be specified in numerical terms for design purposes.

For rolling motion the damping coefficient b has been found to be highly dependent on ship speed. Figure 16.19 shows the damping coefficients, determined by means of an extinction curve, for various ship speeds. It is seen that roll damping increases with ship speed.

As can be seen from Fig. 16.20, there is a gradual but, in most cases, rather small increase in midship bending moment with increase in speed until a maximum is reached, and then a decrease in the bending moment is to be expected.

Longitudinal Radius of Gyration A decrease in the longitudinal radius of gyration reduces heaving, pitching, and relative bow motions, as well as bow acceleration, whereas stern acceleration may be increased slightly (Fig. 16.21).

It should be noted that, since the heaving amplitude is dependent on the longitudinal radius of gyration, the coupling effects between heaving and pitching motions are important and should be considered when analytical studies are made.

A reduction in the longitudinal radius of gyration is advantageous from the point of view of deck wetness as well as speed loss in a seaway.

A decrease in the longitudinal moment of inertia (or radius of gyration) causes less speed loss in a seaway.

Figure 16.22 shows that a ship with larger longitudinal moments of inertia (i.e., weights concentrated away from the midship section) suffers more speed loss than one with weights concentrated amidships. For example, for a Beaufort number of 7, the speed loss for a vessel with a longitudinal radius of gyration of $0.26L$ is 3.4 knots, whereas it is only 2 knots for a $0.22L$ radius of gyration. The speed loss for this 500-ft vessel was determined for a constant power in head sea operation.

The effect of change in the longitudinal moment of inertia is more pronounced for smaller vessels than for larger ones. Figure 16.23 shows the results for ships with three different lengths.

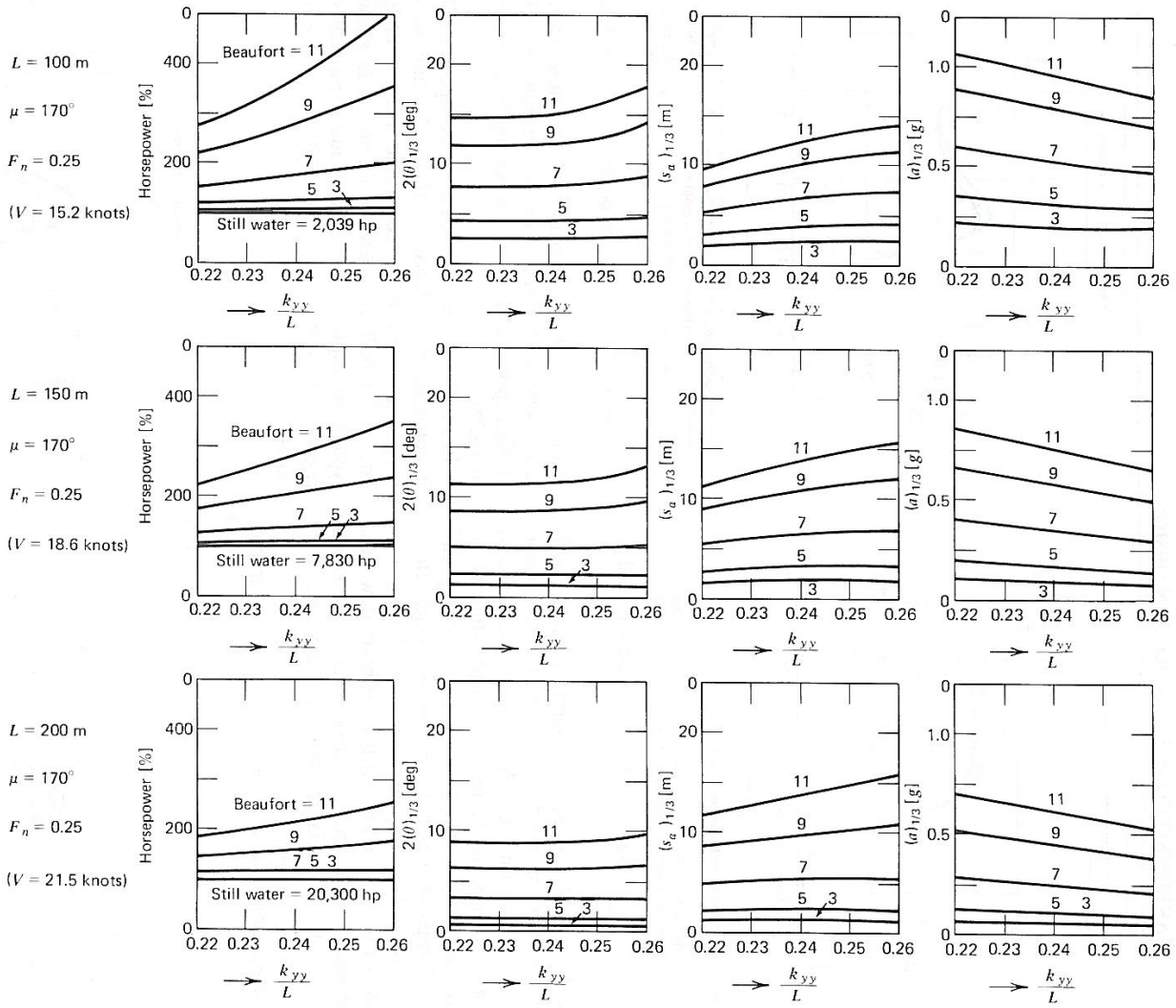


Figure 16.23 Influence of radius of gyration on seakeeping performance [202].

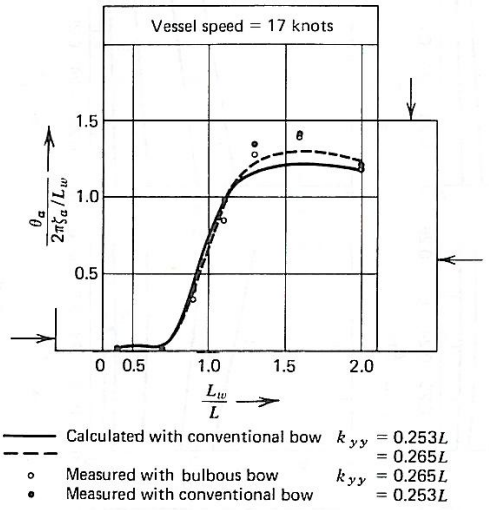


Figure 16.24 Comparison of Pitching motions [232].

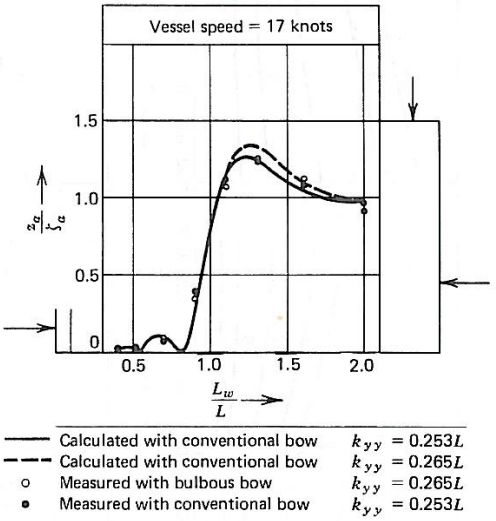


Figure 16.25 Comparison of Heaving motions [232].

As mentioned earlier, in general, a small longitudinal radius of gyration is desirable for good seakeeping performance. But in the design and operation of normal ships it is rather difficult to control the radius of gyration except for special types of ships such as bulk ore carriers, where there may be some flexibility in weight distribution.

Bulbous Bow. A model with a bulbous bow has, in general, less pitching and larger heaving in waves of $L_w/L < 1.0$ and a larger thrust increase than one with normal bow form.

Investigations have shown that a considerable reduction in both heaving and pirching motions is possible with large bulbs at the bow, especially at high speeds and in short wavelengths. (Figs. 16.24 to 16.26).

In moderate seas the effective horsepower (EHP) is considerably reduced by the bulbs, and in very rough seas there is no noticeable increase in EHP due to the bulb (Fig. 16.27). Figure 16.28 shows a typical example of vertical bending moments in regular waves for vessels with and without bulbous bows.

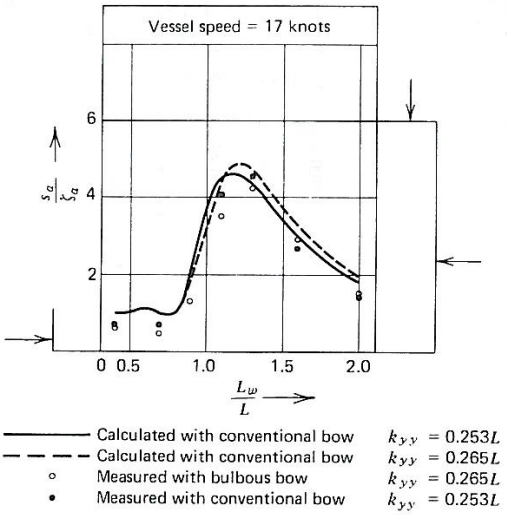


Figure 16.26 Comparison of Relative bow motions [232].

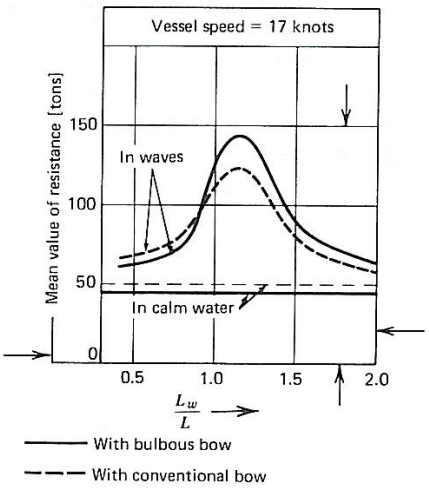


Figure 16.27 Influence of bulbous bow on added resistance [232].

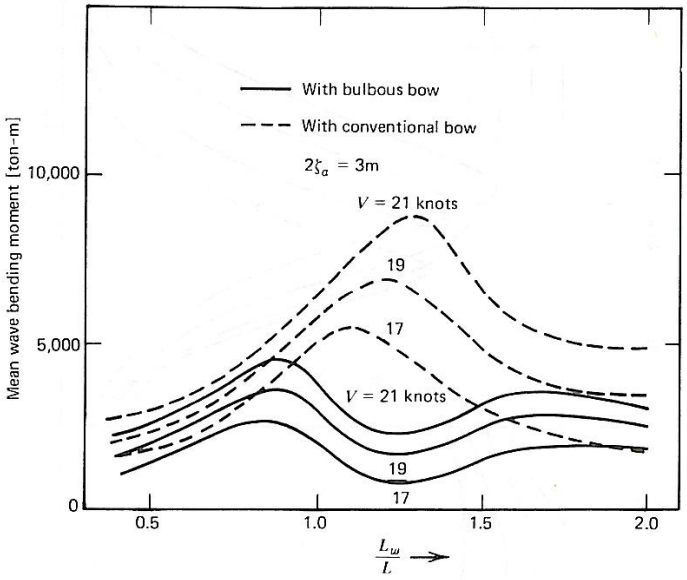


Figure 16.28 Average wave bending moment in regular waves [232].

Wave Characteristics

Wavelength

Figure 16.29 shows the experimental results for heaving, pitching, and power increase in head seas as functions of wavelength. It can be seen that the maximum amplitudes occur for wavelengths between $1.25L$ and $1.50L$. In other words, the wavelengths that have significant effects on the motions of normal ships are in the range of 1.0 to 2.5 times the length of the ship. It is also interesting that the maximum added power is not accompanied by maximum amplitude of motion, because the phase relations between motions and waves also play a part in added resistance.

Figure 16.29 also shows the effect of ship speed on various motion characteristics. Typical experimental results for thrust, torque, and revolutions per second in regular waves are illustrated in Fig. 16.30.

It should be noted that the amplitude of the bending moment is half of the sum of the maximum hogging and sagging bending moments, and that the section in which the hogging moment reaches its maximum value does not coincide with the section in which the sagging bending moment becomes maximum. Therefore the location of the section in which the hogging or sagging moment reaches a maximum is dependent on speed and on wavelength ratio (Fig. 16.31).

Wave Direction

The influence of wave direction is shown in Fig. 16.32 for two different lengths ($L_w/L = 1.00$ and 1.50).

The exciting moment for rolling is generally largest for beam seas. When resonance occurs (as shown on the figures by vertical arrows), a dynamic increase in the amplitudes takes place. Also, roll damping at high speeds is considerably larger than at lower speeds. Hence resonance occurs mainly in following seas when $L_w/L = 1.00$ and 1.50.

On the other hand, the exciting moment for pitching motion is largest in head and following seas, so pitching motion is also largest in such sea conditions. The pitching angles are, in general, larger in head waves than in following waves because resonance occurs in head seas.

The exciting forces for heaving motion are maximum in beam seas. However, because of the coupling effect between heave and pitch, appreciable heaving amplitudes may also be expected in bow seas. Figures 16.33 and 16.34 show typical examples of heaving acceleration and relative bow motion as functions of ship heading. The power increase as a function of wave direction is shown in Fig. 16.35. As this figure indicates, the maximum power increase in waves having lengths equal to or less than the ship length takes place not in head seas but in bow seas. Comparing Figs. 16.32 and 16.35, one can deduce that the maximum motion and maximum power increase

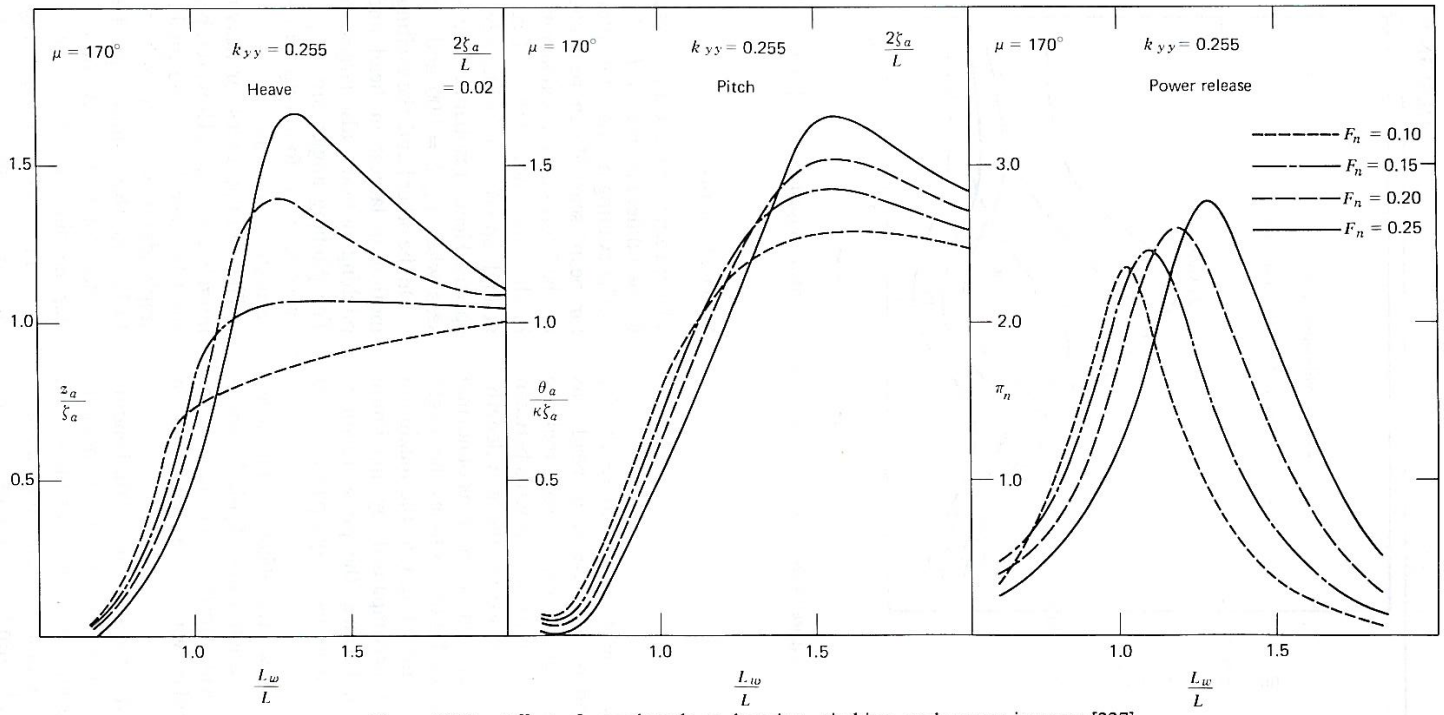


Figure 16.29 Effect of wavelength on heaving, pitching, and power increase [227].

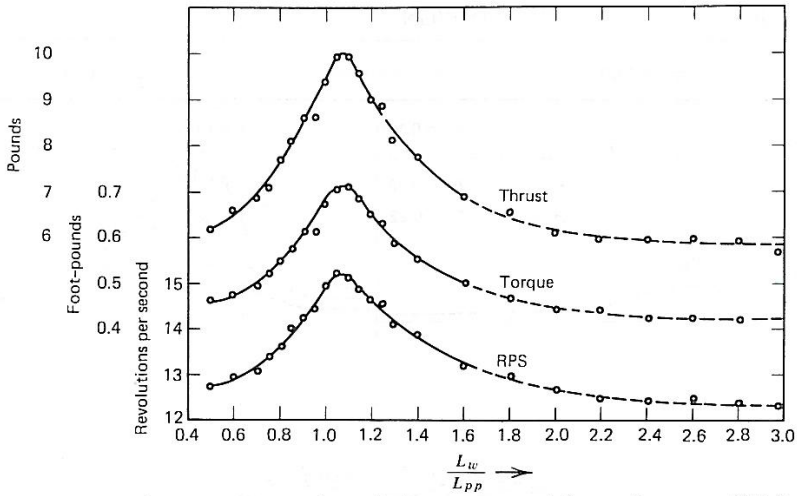


Figure 16.30 Thrust, torque, and revolutions per second in regular waves [155a].

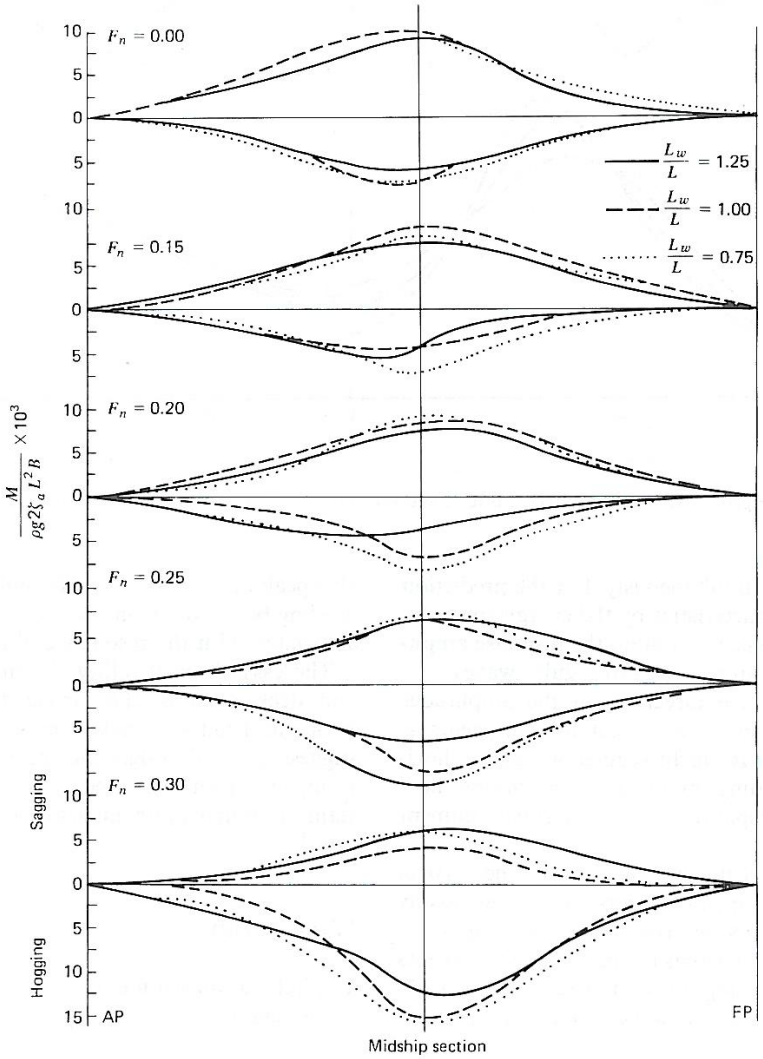


Figure 16.31 Longitudinal bending moment distribution in regular head seas [46].

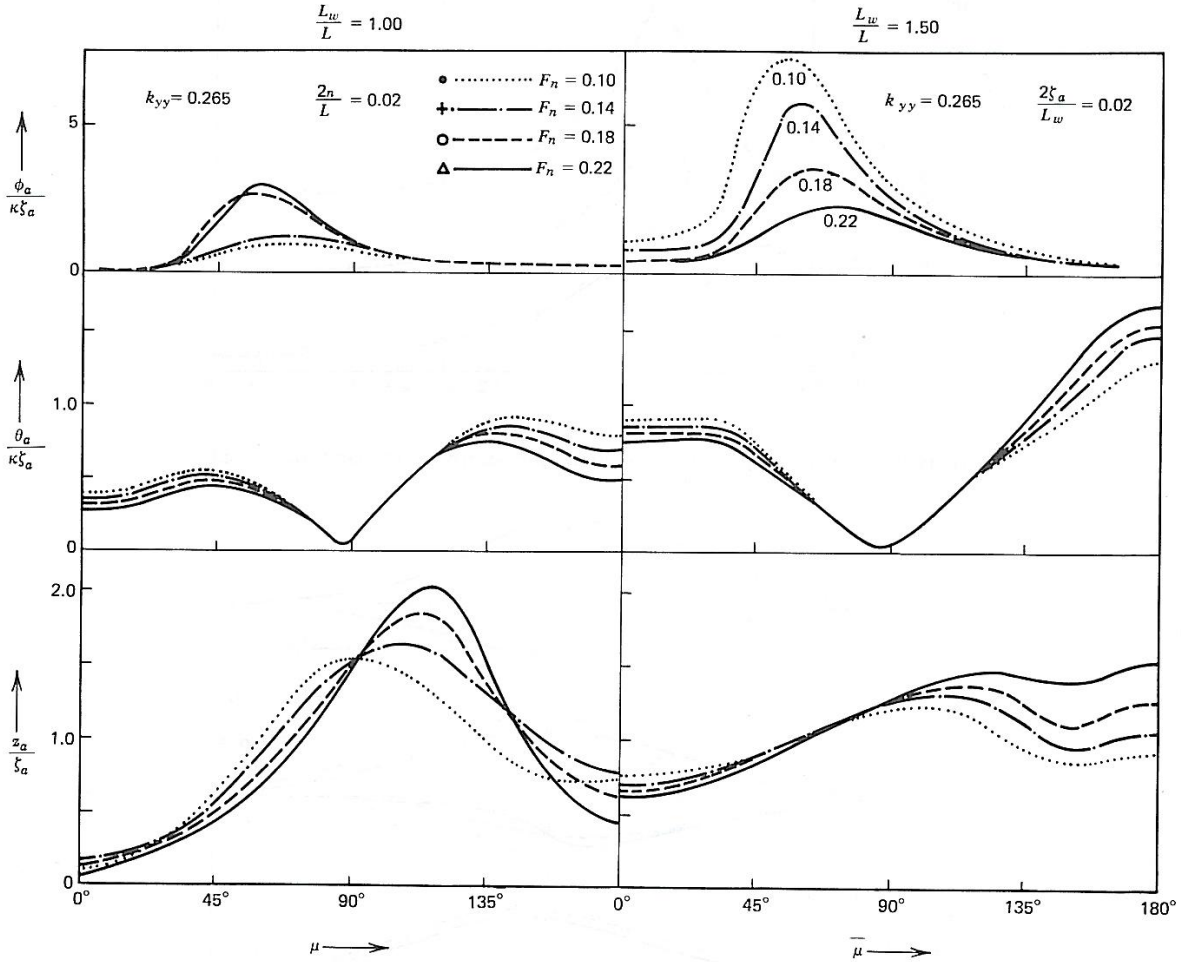


Figure 16.32 Effect of wave direction on rolling, pitching, and heaving motions [227].

do not take place simultaneously. For the prediction of seakeeping characteristics by the energy spectrum method, it is necessary to obtain the response amplitude operators at all headings to regular waves.

The effect of wave direction on the amplitudes of vertical and lateral wave bending moments is illustrated in Fig. 16.36. In regular waves the horizontal wave bending moment in quartering bow seas may be comparable to the vertical moment in head seas [57].

Model tests indicate that the peak of the vertical wave bending moment occurs at progressively shorter wavelengths as the ship's heading shifts toward beam seas, whereas the peak lateral moments are expected at headings of 60° and 120°. Figure 16.37 shows that the torsional wave moment amplitudes also peak at a heading of 120° and probably at some heading between 30° and 60° as well. These peaks are associated with the resonance of the rolling motion.

The less is the probability of occurrence of slamming and deck wetness, the further the heading angle is off the head sea angle. Experimental results also suggest that, although the frequency of slamming is higher in short-crested seas, the severity of the slams is much more intensive in long-crested seas [167].

Wave Height

1. Pitching amplitude is linearly proportional to wave height.

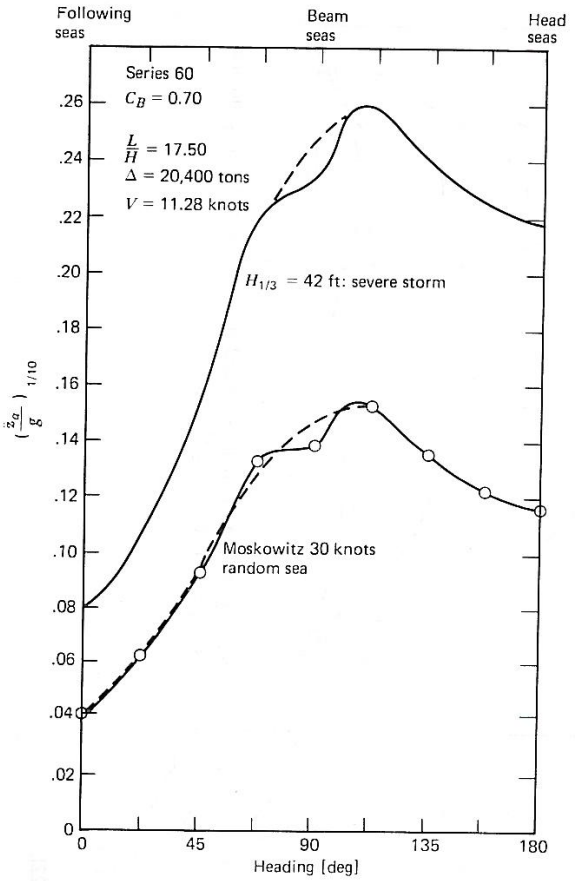


Figure 16.33 Heaving acceleration as a function of ship's heading [96].

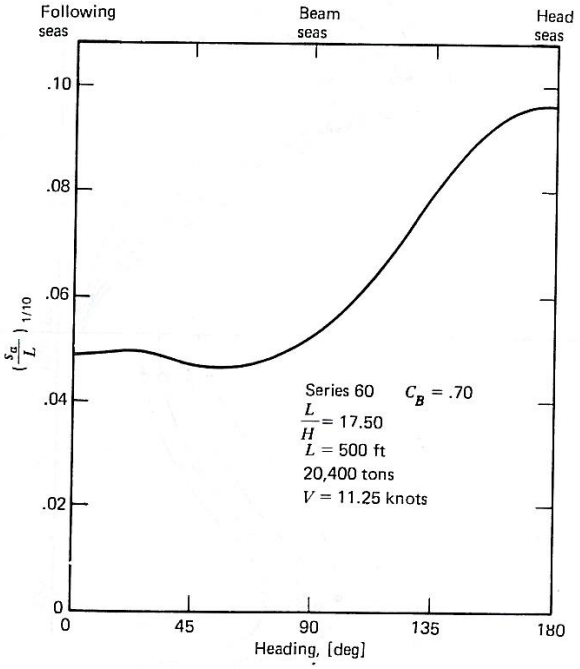


Figure 16.34 Relative bow motion as a function of heading in an irregular seaway [96].

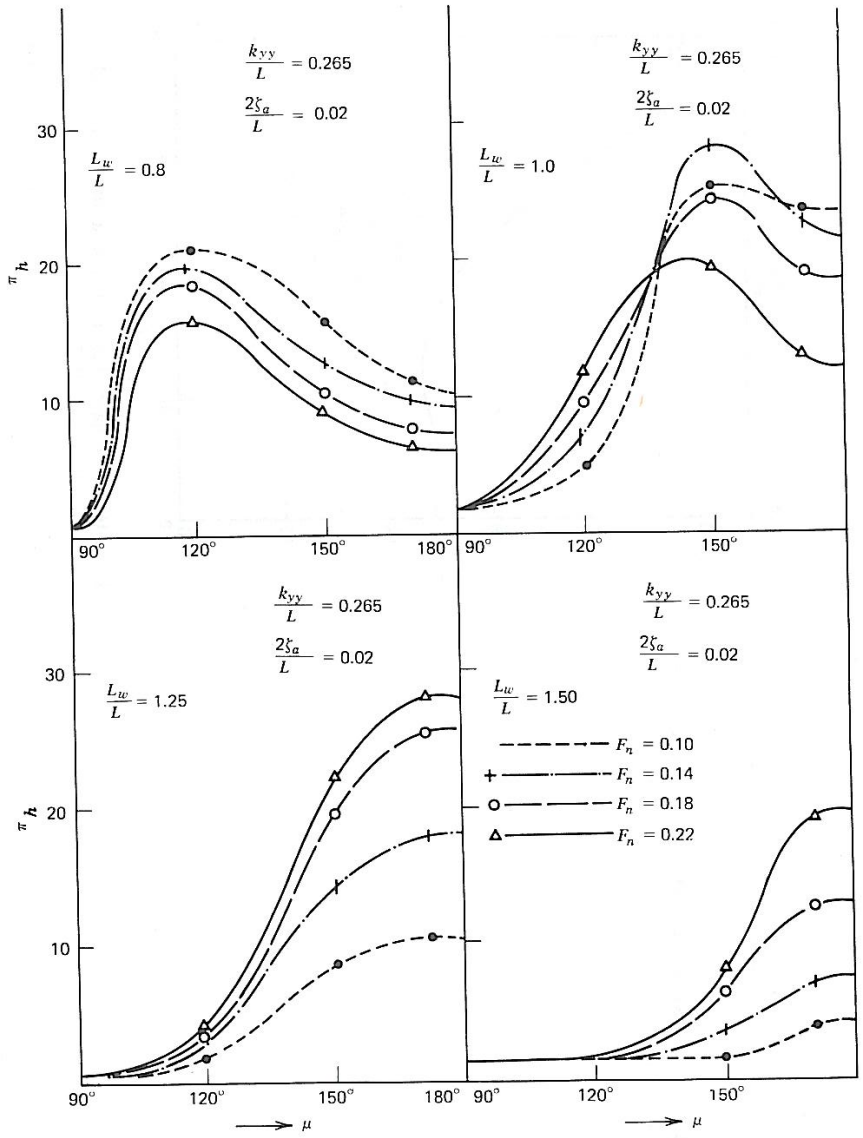


Figure 16.35 Power increase as a function of ship's heading [22].

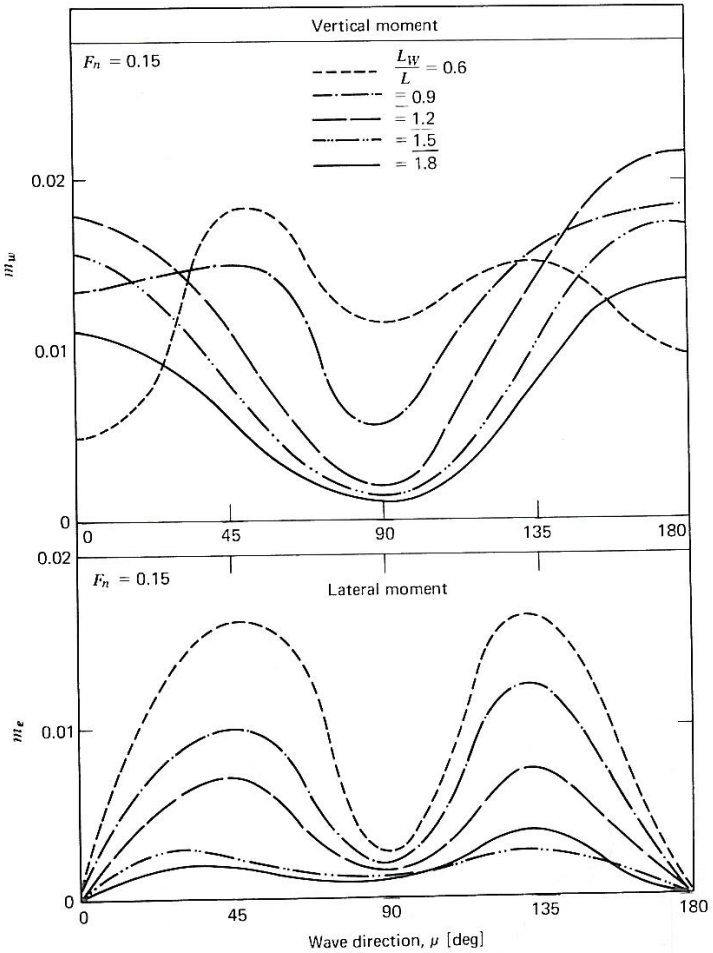


Figure 16.36 Amplitude of vertical and lateral wave bending moments as a function of heading [226*b*].

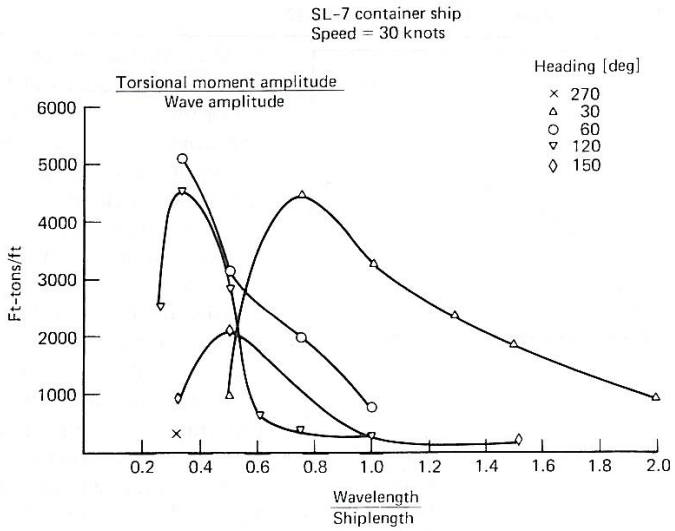


Figure 16.37 Amplitude of torsional wave bending moment at the midship section [44].

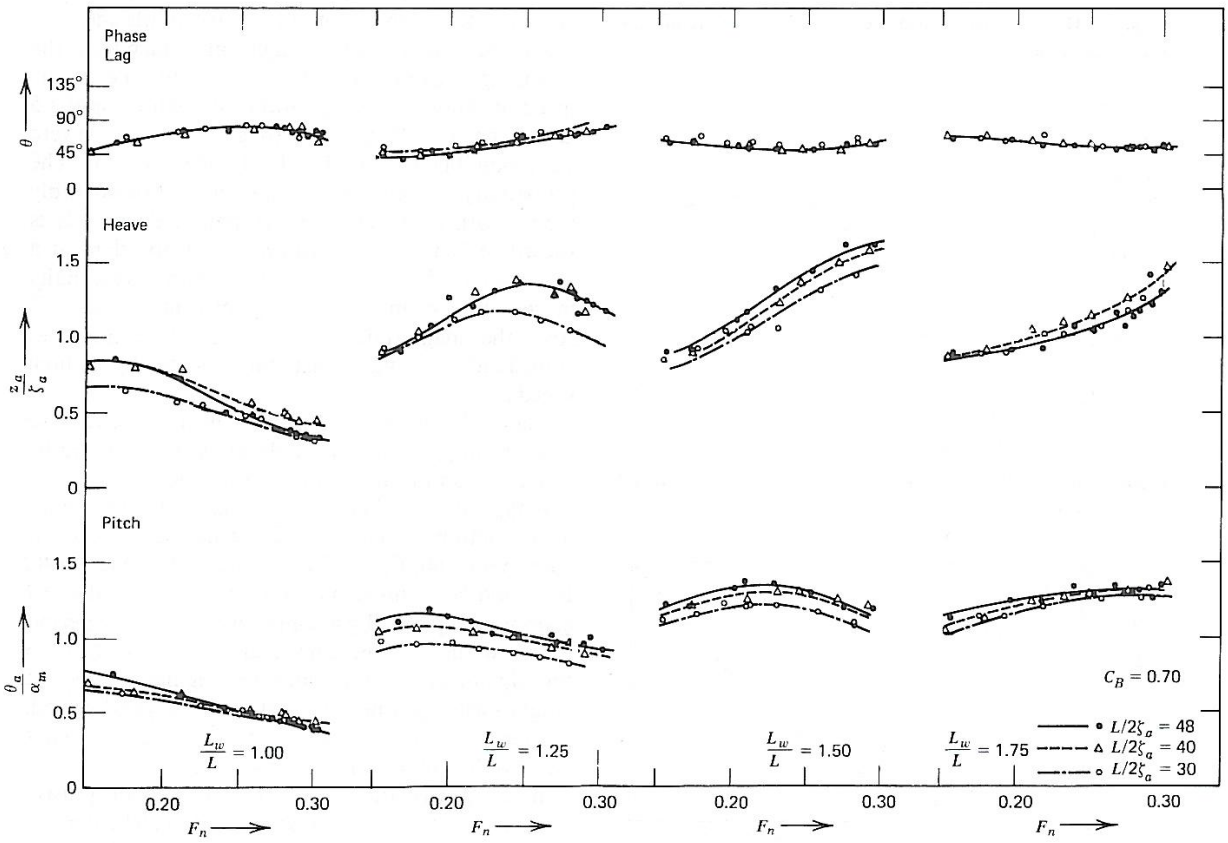


Figure 16.38 Experimental results of motion in regular waves [73].

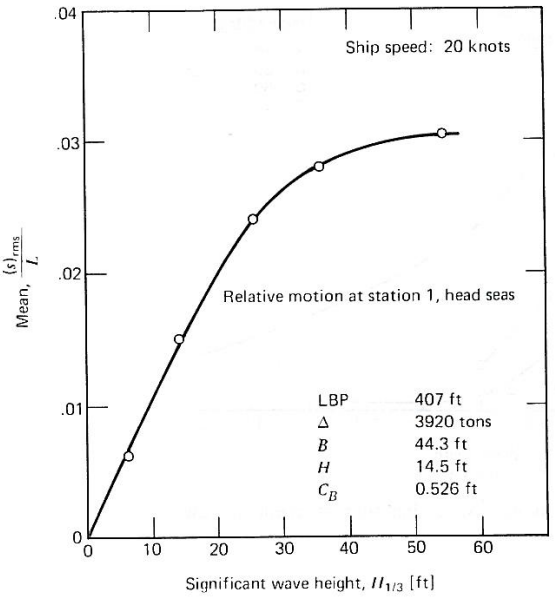


Figure 16.39 Relative motion as a function of significant wave height [96].

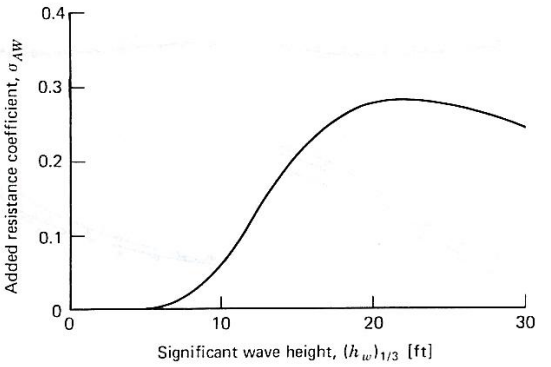


Figure 16.40 Added resistance as a function of significant wave height [199].

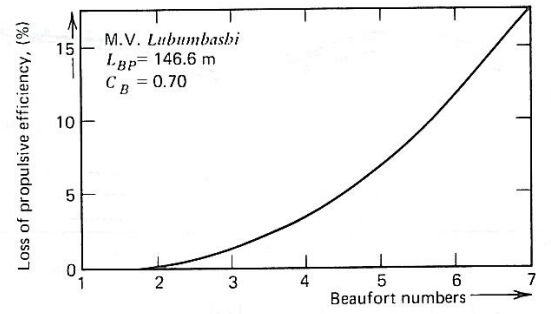


Figure 16.41 Loss of propulsion efficiency as a function of sea severity [4].

2. Also, thrust increase is approximately proportional to the square of the wave height.

For tests in very high waves the nonlinear relationship appears to be correct, because bow immersion, the shipping of green water on deck, and forefoot emergence occur in the test with high waves.

Figure 16.38 shows the experimental results of motions of hull forms tested in regular waves of three different heights ($\frac{1}{48}L, \frac{1}{40}L, \frac{1}{30}L$) and wavelengths of $1.00L$, $1.25L$, $1.50L$, and $1.75L$, where L is the length of the ship model. In general, the differences in θ_a/α_M and z_a/ζ_a for wave heights of $\frac{1}{48}L$ and $\frac{1}{40}L$ are very small; they approach the experimental error. The $\frac{1}{30}L$ wave causes some moderate nonlinearities. From Fig. 16.38 it appears to be reasonable to assume that in mild and moderate seas motions are linearly proportional to wave amplitude. However, in the case of rolling motion, nonlinearity is to be expected even in moderate seas.

It is also interesting to note that the phase angles appear to be independent of the wave amplitude.

An increase in wave height also increases the slamming pressure. The wavelengths for the occurrence of slamming are generally between 0.7 and 1.5 times the ship length, although the most severe slamming takes place for L_w/L of about 1.0. The probability of occurrence of slamming is considerably higher with an increase in severity of the sea. It is shown in Ref. 172 that *Mariner* will not slam in a sea state of 5, whereas she will slam occasionally in sea state 6 and quite frequently in sea state 7. Also the magnitude of impact pressure increases considerably at higher sea states, especially at high speeds.

Figure 16.39 shows the rms ($\sqrt{m_{0s}}$) of the relative bow motion (nondimensionalized by the ship length), as a function of the significant wave height.

A typical plot of nondimensional added resistance as a function of significant wave height for a 625 ft ship (Series 60, $C_B = 0.70$) is presented in Fig. 16.40. It should be pointed out here that the irregular sea cannot be replaced by a regular wave having a period equal to the average period and a height equal to the significant height, since for regular waves the height means just height (crest to trough) and period, whereas for irregular waves it gives the significant value of height and the average period.

In a seaway there is also a loss of propulsive efficiency as a function of sea condition. The percentage loss of propulsive efficiency for the head sea condition increases rapidly as the Beaufort number increases, as shown in Fig. 16.41.

Analytical investigations and model tests, as well as full-scale experiments, have shown that wave bending moments vary almost linearly with wave heights, except at the ship ends [57].

16.3 PREDICTION BY REGRESSION ANALYSIS

Another approach is to make statistical analyses of the data obtained from various seakeeping tests of a large number of models with different parametric values. Such a method, known as *multiple regression analysis*, provides us, for estimation purposes, with a number of equations that are functions of various important parameters, as shown in Ref. 155. To establish a good design, it is often necessary to compare it with some standards as established by these equations for heave, pitch, added torque, thrust, rate of propeller revolution, and power in a seaway.

It should be kept in mind that for conventional ship forms seakeeping characteristics do not differ much with a change in the main particulars of the ship. A drastic change in hull form is necessary to reduce motion amplitudes significantly. Hence, in that case, the main departure from the conventional ship forms should be the following:

a. Most of the volume of displacement should be as far away as possible from the load waterplane region, so that the exciting forces and moments can be reduced drastically.

b. Sophisticated motion stabilization devices should be used exclusively.

In Ref. 155 equations are given for heaving and pitching motions, as well as for increase in propeller thrust, propeller torque, rate of rotation, and power in waves. Such an estimation formula provides us not only with a quantity at an early stage in design, but also with a standard against which model performance in waves can be judged. It also provides an indication and an estimate of the effects on the performance in waves of any changes in the design parameters considered.

In the initial stage of design only a very few parameters are known (e.g., length, beam, draft); the longitudinal radius of gyration and the waterplane area coefficient may be estimated, making allowance, if necessary or desirable, for stability requirements that are greater or less than average.

Equations for Motion

Equations for the estimation of various seakeeping characteristics in regular head seas, based on the multiple regression of various model tests, are as follows [155]:

$$z_a = A_0 + A_1 C_W + A_2 C_B + A_3 \frac{L}{B} + A_4 \left(\frac{L}{T}\right)^{-1} + A_5 LCB + A_6 \frac{k_{yy}}{L} + A_7 \frac{V}{\sqrt{L}} \tag{16.1}$$

$$\theta_a = B_0 + B_1 C_W + B_2 C_B + B_3 \frac{L}{B} + B_4 \frac{L}{T} + B_5 \mathrm{LCB} + B_6 \frac{k_{yy}}{L} + B_7 \frac{V}{\sqrt{L}} + B_8 \left(\frac{V}{\sqrt{L}}\right)^2 \tag{16.2}$$

$$\frac{C_T \delta T}{L^3} = C_0 + C_1 (C_B - 0.5)^5 + C_2 \frac{L}{B} + C_3 \frac{L}{T} + C_4 \mathrm{LCB} + C_5 \frac{k_{yy}}{L} + \beta \left(C_6 + C_7 \frac{L}{T}\right) + C_8 \frac{V}{\sqrt{L}} \tag{16.3}$$

$$\frac{C_Q \delta Q}{L^4} = D_0 + D_1 \frac{L}{B} + D_2 \frac{L}{T} + D_3 \frac{k_{yy}}{L} + D_4 \frac{P}{L} + \beta \left(D_5 + D_6 \frac{L}{T}\right) + D_7 \frac{V}{\sqrt{L}} \tag{16.4}$$

$$C_N \delta N \sqrt{L} = E_0 + E_1 \frac{L}{T} + E_2 \frac{k_{yy}}{L} + E_3 \frac{P}{L} + E_4 \frac{L}{D} + E_5 \frac{P}{D} + \beta \left(E_6 + E_7 \frac{L}{T}\right) + E_8 \frac{V}{\sqrt{L}} \tag{16.5}$$

$$\frac{C_P}{L^{3.5}} \delta P = F_0 + F_1 (C_B - 0.5)^5 + F_2 \frac{L}{B} + F_3 \frac{L}{T} + F_4 \mathrm{LCB} + F_5 \frac{k_{yy}}{L} + \beta \left(F_6 + F_7 \frac{L}{T}\right) + F_8 \frac{V}{\sqrt{L}} \tag{16.6}$$

where z_a = heaving amplitude
θ_a = pitching amplitude
δT = thrust increase
δQ = torque increase

TABLE 16.1 [155a]

Beaufort Number	*LBP*	A_0	A_1	A_2	A_3	A_4	A_5	A_6	A_7
5	400	− 0.18	− 13.30	4.62	0.100	78.6	0.205	23.5	3.83
	500	0.96	− 12.54	3.63	0.175	65.4	0.204	19.2	2.50
	600	2.06	− 9.66	2.01	0.191	41.8	0.163	13.6	1.25
	800	2.38	− 5.29	0.63	0.146	13.6	0.083	6.5	0.02
	1000	2.18	− 2.67	0.04	0.097	0.3	0.035	2.4	− 0.49
6	400	1.56	− 18.19	6.52	0.066	108.0	0.262	31.5	5.79
	500	0.49	− 20.50	7.11	0.145	115.9	0.306	34.6	5.31
	600	1.69	− 18.71	5.38	0.234	97.0	0.299	29.3	3.70
	800	3.17	− 12.36	2.40	0.244	48.9	0.201	17.7	1.29
	1000	3.12	− 7.90	1.11	0.197	22.9	0.122	10.5	0.15
7	400	5.31	− 21.65	7.69	0.073	124.5	0.327	33.1	7.10
	500	1.46	− 24.91	8.91	0.140	146.5	0.371	42.8	7.75
	600	0.85	− 26.17	8.72	0.235	149.0	0.409	43.8	6.89
	800	3.41	− 20.94	5.07	0.344	100.7	0.349	31.0	3.62
	1000	3.80	− 15.18	3.08	0.307	60.3	0.244	21.6	1.72
8	400	10.92	− 24.68	8.42	0.061	135.4	0.413	33.6	7.96
	500	6.06	− 28.14	9.72	0.109	162.8	0.440	45.0	9.21
	600	2.53	− 31.72	11.36	0.180	183.6	0.473	53.4	9.65
	800	3.13	− 31.20	9.33	0.321	169.7	0.512	48.7	7.26
	1000	4.60	− 25.12	6.10	0.403	118.3	0.413	36.9	4.33

TABLE 16.2 [155a]

Beaufort Number	*LBP*	B_0	B_1	B_2	B_3	B_4	B_5	B_6	B_7	B_8
	400	3.65	− 16.19	9.10	0.222	− 0.0510	− 0.069	14.8	7.60	− 5.14
5	500	3.96	− 12.39	6.97	0.203	− 0.0329	− 0.068	5.0	5.76	− 4.24
	600	3.38	− 8.21	4.43	0.165	− 0.0167	− 0.057	0.2	3.76	− 2.99
	800	2.03	− 3.59	1.86	0.078	− 0.0037	− 0.032	− 1.7	1.40	− 1.28
	1000	1.17	− 1.61	0.85	0.038	− 0.0001	− 0.018	− 1.7	0.40	− 0.47
6	400	5.33	− 22.33	12.53	0.260	− 0.0745	− 0.095	25.2	9.09	− 5.89
	500	5.07	− 19.72	11.17	0.264	− 0.0604	− 0.093	15.7	8.86	− 6.11
	600	5.12	− 15.32	8.58	0.247	− 0.0407	− 0.085	6.1	6.94	− 5.11
	800	3.66	− 7.87	4.15	0.160	− 0.0139	− 0.058	0.9	3.38	− 2.78
	1000	2.34	− 4.25	2.25	0.090	− 0.0052	− 0.037	− 1.9	1.62	− 1.44
7	400	6.89	− 26.65	15.00	0.317	− 0.0923	− 0.110	31.3	10.41	− 6.59
	500	5.59	− 24.45	13.78	0.315	− 0.0803	− 0.104	25.5	10.79	− 7.09
	600	5.49	− 21.45	12.11	0.309	− 0.0652	− 0.101	16.5	9.93	− 6.88
	800	4.94	− 13.28	7.25	0.243	− 0.0310	− 0.083	3.1	.11	− 4.68
	1000	3.57	− 7.83	4.13	0.155	− 0.0138	− 0.057	− 0.4	3.28	− 2.70
8	400	8.74	− 30.59	17.25	0.357	− 0.1056	− 0.124	36.5	11.54	− 7.26
	500	7.17	− 28.17	15.79	0.339	− 0.0952	− 0.113	32.1	11.33	− 7.25
	600	6.16	− 25.93	14.62	0.335	− 0.0844	− 0.113	26.2	11.36	− 7.50
	800	5.95	− 19.68	11.09	0.300	− 0.0553	− 0.104	10.9	9.00	− 6.46
	1000	4.89	− 12.83	6.98	0.236	− 0.0291	− 0.082	2.8	5.77	− 4.44

δN = increase in propeller rate of rotation
δP = increase in power
C_W = waterplane area coefficient
C_B = block coefficient
L = length of the ship [ft]
B = beam of the ship [ft]
T = draft of the ship [ft]
LCB = percent of LBP as measured from ⊗
β = bulbous bow factor
= 1.0 when bulbous bow is persent
= 0 when bulbous bow is absent
V = ship speed [knots]
D = diameter of the propeller [ft]
P = pitch of the propeller [ft]
k_{yy} = radius of gyration about y-axis [ft]
C_T = a constant
$= 3.95 \times 10^6$ when the thrust is in tons
C_Q = a constant
$= 1.76 \times 10^6$ when the torque is in foot-pounds
C_N = a constant
$= 9.87 \times 10^{-3}$ when the propeller rate of rotation is in revolutions per minute
C_P = a constant
$= 5.74 \times 10^5$ when the power is in horsepower
$= 1.043 \times 10^3$ when the power in foot-pounds per second.

The coefficients

$$A_0, A_1, \ldots, A_8$$
$$B_0, B_1, \ldots, B_8$$
$$C_0, C_1, \ldots, C_8$$
$$D_0, D_1, \ldots, D_7$$
$$E_0, E_1, \ldots, E_8$$
$$F_0, F_1, \ldots, F_8$$

are given in Tables 16.1 to 16.6 as functions of length and Beaufort number.

Note that the power increase determined by the above equation is added to the still water power to determine the total power required. However, the models do not react to dynamic effects like slamming, the shipping of green water, cargo shifting, and propeller racing, which are responsible for further reductions in power on a voluntary basis, and these effects are not accounted for in the equation above.

Since the expressions derived in Ref. 155 are based on the spectrum of the British Towing Tank Panel, modification of the results is necessary if these expressions are used in connection with some other standard spectrum for predictions in an irregular seaway. The results obtained by using (16.1) to (16.6) are modified by equating the average period associated with a particular significant wave height in the ITTC wave spectrum to that of the BTTP spectrum. For example, the added thrust, computed by (16.3), is calculated for the appropriate significant wave height and then multiplied by the square of the ratio of the ITTC wave height to the BTTP wave height.

Example 16.1

Assuming the sea condition for design purposes to be Beaufort 7, find the heaving and pitching motions, as well as the increase in thrust, torque, rate of propeller rotation, and power for a ship (without bulbous bow) the particulars of which are as follows:

$L = 400$ ft

$C_B = 0.70$

$C_W = 0.785$

$k_{yy} = 0.25\,L$

$\frac{L}{B} = 7.0$

$\frac{L}{T} = 17.49$

LCB = $+0.005\,L_{pp}$ (the + sign means that LCB is forward of ⊗)
$= +0.5\%\,L_{pp}$ (i.e. + 0.5 as input in the prediction equations)

Prop. Dia., $D = 21.00$ ft

Pitch-dia, ratio, $\frac{P}{D} = 1.135$

$\frac{V}{\sqrt{L}} = 0.45, 0.60, 0.75, 0.90, 1.05,$ and 1.70

Solution:

Using (16.1):

$$z_a = 5.31 - (21.65)(0.785) + (7.69)(0.7) + (0.073)(7) + \left(\frac{124.5}{17.49}\right) + (0.327)(0.5) + (33.1)(0.25) + 7.1\frac{V}{\sqrt{L}}$$

$$= 9.76525 + 7.1\frac{V}{\sqrt{L}}$$

TABLE 16.3 [155b]

Beaufort Number	LBP	C_0	C_1	C_2	C_3	C_4	C_5	C_6	C_7	C_8
5	400	−0.089	13.8	−0.081	0.0031	0.013	2.69	0.148	−0.0053	0.540
	500	−0.054	10.2	−0.044	0.0040	0.008	1.62	0.075	−0.0026	0.258
	600	0.004	6.0	−0.025	0.0043	0.004	0.78	0.039	−0.0014	0.091
	800	0.013	2.7	−0.008	0.0025	0.001	0.19	0.017	−0.0007	0.009
	1000	0.001	1.3	−0.003	0.0011	0.000	0.06	0.008	−0.0004	0.001
6	400	−0.052	25.4	−0.178	0.0067	0.027	5.13	0.339	−0.0127	1.144
	500	−0.134	21.4	−0.117	0.0058	0.020	3.92	0.215	−0.0078	0.767
	600	−0.076	16.1	−0.071	0.0068	0.012	2.50	0.125	−0.0044	0.405
	800	0.022	7.2	−0.028	0.0059	0.004	0.77	0.047	−0.0018	0.076
	1000	0.012	3.9	−0.012	0.0033	0.002	0.28	0.024	−0.0010	0.014
7	400	0.074	40.3	−0.296	0.0118	0.039	7.72	0.535	−0.0205	1.763
	500	−0.106	31.4	−0.207	0.0086	0.032	6.20	0.390	−0.0145	1.325
	600	−0.155	26.7	−0.141	0.0079	0.024	4.76	0.258	−0.0093	0.909
	800	−0.013	14.3	−0.062	0.0090	0.010	1.98	0.107	−0.0039	0.277
	1000	0.039	7.7	−0.030	0.0065	0.004	0.74	0.053	−0.0021	0.072
8	400	0.275	62.9	−0.460	0.0186	0.055	11.34	0.746	−0.0292	2.478
	500	0.035	45.1	−0.321	0.0137	0.044	8.61	0.585	−0.0223	1.918
	600	−0.112	36.8	−0.235	0.0107	0.036	7.02	0.438	−0.0163	1.480
	800	−0.112	25.5	−0.120	0.0101	0.020	4.08	0.215	−0.0078	0.708
	1000	−0.002	14.4	−0.061	0.0098	0.009	1.91	0.108	−0.0040	0.250

TABLE 16.4 [155b]

Beaufort Number	LBP	D_0	D_1	D_2	D_3	D_4	D_5	D_6	D_7
5	400	−0.582	−0.414	−0.0041	12.07	35.4	0.754	−0.0230	2.581
	500	−0.303	−0.232	0.0059	7.00	25.6	0.341	−0.0089	1.154
	600	−0.047	−0.124	0.0114	3.24	16.8	0.151	−0.0037	0.365
	800	0.084	−0.044	0.0067	0.85	5.4	0.036	−0.0008	0.011
	1000	0.020	−0.015	0.0030	0.35	1.6	0.015	−0.0004	0.015
6	400	−0.735	−0.906	−0.0098	23.49	68.2	1.712	−0.0552	5.778
	500	−0.921	−0.606	−0.0023	17.85	53.3	1.021	−0.0299	3.772
	600	−0.599	−0.368	0.0103	11.21	40.4	0.523	−0.0132	1.957
	800	−0.035	−0.137	0.0160	3.39	18.5	0.142	−0.0031	0.347
	1000	−0.072	−0.062	0.0094	1.30	6.7	0.055	−0.0012	0.063
7	400	0.367	−1.496	−0.0151	34.01	102.8	2.773	−0.0929	8.585
	500	−0.779	−1.056	−0.0092	27.92	82.9	1.955	−0.0621	6.376
	600	−0.872	−0.732	0.0001	21.15	66.5	1.234	−0.0364	4.242
	800	−0.233	−0.310	0.0206	8.54	39.0	0.410	−0.0104	1.182
	1000	0.078	−0.143	0.0175	3.29	18.4	0.161	−0.0040	0.275
8	400	2.559	−2.316	−0.0267	47.71	140.4	3.830	−0.1301	11.894
	500	0.068	−1.621	−0.0172	38.18	115.8	2.992	−0.0990	9.300
	600	−0.814	−1.195	−0.0074	31.46	95.0	2.178	−0.0688	7.099
	800	−0.667	−0.623	0.0121	17.98	63.7	0.972	−0.0272	3.205
	1000	−0.166	−0.308	0.0238	8.22	38.0	0.410	−0.0106	1.062

TABLE 16.5 [155b]

Beaufort Number	LBP	E_0	E_1	E_2	E_3	E_4	E_5	E_6	E_7	E_8
5	400	− 7.217	0.0938	8.86	112.3	0.247	− 5.88	1.027	− 0.0379	− 0.632
	500	− 5.024	0.0692	4.76	95.1	0.186	− 4.63	0.627	− 0.0239	− 0.787
	600	− 3.081	0.0517	1.41	72.8	0.126	− 3.34	0.416	− 0.0170	− 0.752
	800	− 1.298	0.0222	− 0.02	37.3	0.056	− 1.60	0.186	− 0.0082	− 0.373
	1000	− 0.583	0.0086	− 0.03	17.3	0.024	− 0.72	0.078	− 0.0036	− 0.151
6	400	− 14.357	0.2030	16.83	223.7	0.491	− 11.87	2.410	− 0.0914	− 1.173
	500	− 10.976	0.1436	12.86	178.7	0.382	− 9.19	1.515	− 0.0563	− 1.121
	600	− 7.944	0.1116	7.19	152.6	0.296	7.39	1.015	− 0.0389	− 1.283
	800	− 3.612	0.0629	0.90	93.1	0.152	− 4.16	0.511	− 0.0216	− 0.971
	1000	− 1.828	0.0303	0.09	51.5	0.077	− 2.21	0.260	− 0.0115	− 0.503
7	400	− 21.464	0.3378	24.85	319.5	0.730	− 17.41	4.156	− 0.1624	− 1.936
	500	− 17.252	0.2397	20.40	270.1	0.592	− 14.23	2.755	− 0.1040	− 1.535
	600	− 13.434	0.1804	15.28	223.4	0.473	− 11.42	1.869	− 0.0702	− 1.515
	800	− 7.299	0.1167	4.37	161.3	0.289	− 7.51	0.989	− 0.0397	− 1.576
	1000	− 3.898	0.0669	0.72	102.8	0.164	− 4.54	0.555	− 0.0237	− 1.037
8	400	− 29.137	0.5085	37.96	363.6	0.957	− 21.55	6.371	− 0.2542	− 2.881
	500	− 24.083	0.3708	27.64	364.3	0.823	− 19.62	4.465	− 0.1736	− 2.258
	600	− 19.782	0.2775	22.92	314.5	0.683	− 16.47	3.148	− 0.1195	− 1.883
	800	− 12.568	0.1770	11.97	232.2	0.462	− 11.41	1.699	− 0.0651	− 1.871
	1000	− 7.390	0.1202	3.93	168.8	0.295	− 7.79	1.027	− 0.0417	− 1.662

TABLE 16.6 [155b]

Beauofrt Number	LBP	F_0	F_1	F_2	F_3	F_4	F_5	F_6	F_7	F_8
5	400	− 0.615	41.4	− 0.115	0.0091	0.040	2.91	0.209	− 0.0073	1.528
	500	− 0.408	28.5	− 0.063	0.0086	0.026	1.68	0.109	− 0.0037	0.891
	600	− 0.194	16.5	− 0.034	0.0074	0.015	0.70	0.060	− 0.0021	0.454
	800	− 0.044	6.6	− 0.011	0.0034	0.005	0.11	0.023	− 0.0009	0.128
	1000	− 0.016	2.8	− 0.004	0.0014	0.002	0.03	0.009	− 0.0004	0.041
6	400	− 1.044	80.0	− 0.247	0.0179	0.076	5.44	0.470	− 0.0172	3.111
	500	− 0.919	63.2	− 0.166	0.0149	0.059	4.22	0.297	− 0.0104	2.235
	600	− 0.626	45.0	− 0.101	0.0140	0.042	2.59	0.175	− 0.0060	1.400
	800	− 0.185	19.0	− 0.037	0.0092	0.017	0.61	0.069	− 0.0026	0.472
	1000	− 0.066	9.4	− 0.015	0.0047	0.007	0.17	0.032	− 0.0013	0.179
7	400	− 1.358	126.0	− 0.394	0.0285	0.110	7.77	0.753	− 0.0283	4.761
	500	− 1.308	97.1	− 0.288	0.0223	0.092	6.59	0.539	− 0.0195	3.675
	600	− 1.113	78.1	− 0.201	0.0191	0.073	5.08	0.357	− 0.0125	2.702
	800	− 0.496	... 39.9	− 0.085	0.0159	0.037	1.89	0.153	− 0.0054	1.156
	1000	− 0.179	20.4	− 0.039	0.0098	0.017	0.58	0.075	− 0.0029	0.482
8	400	− 1.630	191.8	− 0.585	0.0413	0.150	10.58	1.061	− 0.0405	6.721
	500	− 1.586	140.0	− 0.431	0.0326	0.125	8.76	0.820	− 0.0306	5.253
	600	− 1.481	112.2	− 0.326	0.0264	0.105	7.41	0.605	− 0.0219	4.157
	800	− 0.984	72.4	− 0.171	0.0211	0.067	4.23	0.301	− 0.0105	2.320
	1000	− 0.459	39.5	− 0.084	0.0166	0.036	1.73	0.152	− 0.0055	1.113

Using (16.2):

$$\theta_a = 6.89 - (0.785)(26.65) + (0.7)(15) + (0.317)(7) - (0.0923)(17.49) - (0.11)(0.5) + (31.3)(0.25) + 10.41\frac{V}{\sqrt{L}} - 6.59\left(\frac{V}{\sqrt{L}}\right)^2$$

$$= 4.844 + 10.41\frac{V}{\sqrt{L}} - 6.59\left(\frac{V}{\sqrt{L}}\right)^2$$

Using (16.3):

$$\delta T = \frac{(400)^3}{(3.95 \times 10^6)}\left[0.074 + (40.3)(0.2)^5 - (0.296)(7) + (0.0118)(17.49) + (0.039)(20) + (7.72)(0.25) + 0 + 1.763\frac{V}{\sqrt{L}}\right]$$

$$= 3.7987 + 28.565\frac{V}{\sqrt{L}}$$

Using (16.4):

$$\delta Q = \frac{(400)^4}{(1.76 \times 10^6)}\left(367 - 10.472 - 0.262 + 8.5 + 6.126 + 0 + 8.585\frac{V}{\sqrt{L}}\right)$$

$$= 6.575 \times 10^4 + 1.248 \times 10^5\frac{V}{\sqrt{L}}$$

Using (16.5):

$$\delta N = \frac{1}{(20)(9.87 \times 10^{-3})}\left(-21.464 + 5.91 + 6.21 + 19.038 + 12.77 - 19.76 + 0 - 1.936\frac{V}{\sqrt{L}}\right)$$

$$= 13.7 - 9.8\frac{V}{\sqrt{L}}$$

Using (16.6):

$$\delta P = \frac{(400)^{3.5}}{5.74 \times 10^5}\left(1.358 + 0.04 - 2.758 + 0.359 + 0.22 + 1.94 + 0 + 4.761\frac{V}{\sqrt{L}}\right)$$

$$= -3472 + 10.6 \times 10^3\frac{V}{\sqrt{L}}$$

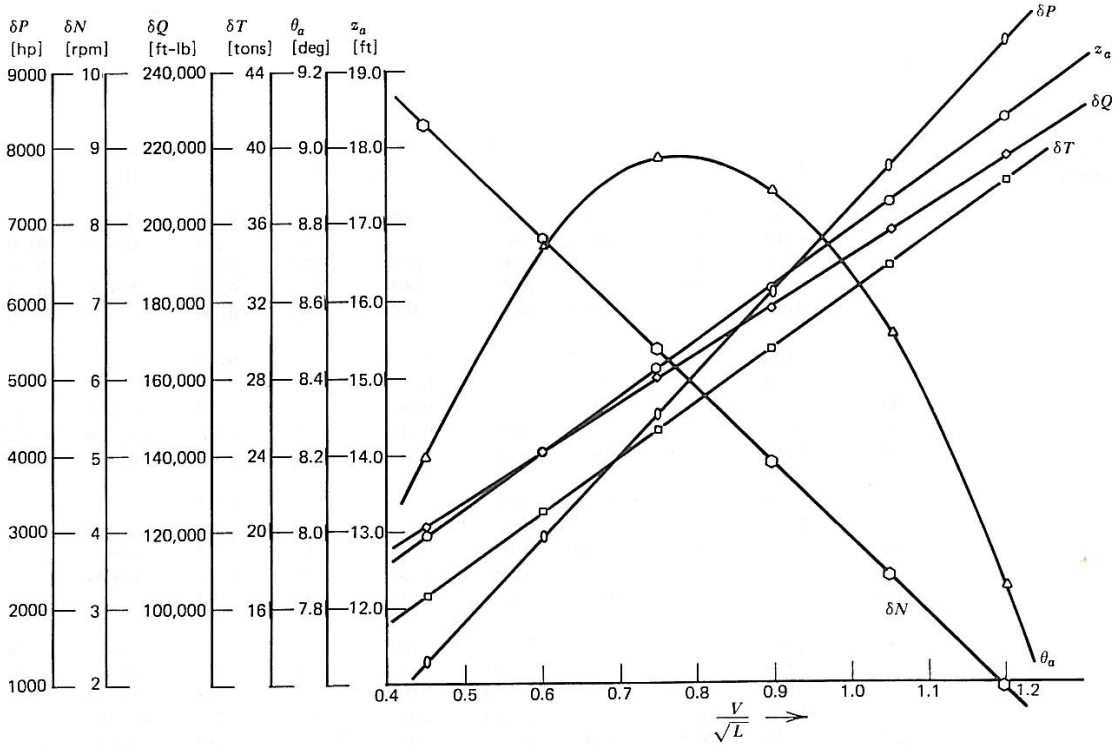


Figure 16.42 Seakeeping characteristics as functions of speed.

TABLE 16.7

$\frac{V}{\sqrt{L}}$	z_a [ft]	θ_a [deg]	δT [tons]	δQ [ft-lbs]	δN [rpm]	δP [hp]
0.45	12.9603	8.19402	16.5629	121910	9.29	1298
0.60	14.0252	8.7176	20.8477	140630	7.82	2888
0.75	15.0902	8.94463	25.135	159350	6.35	4478
0.90	16.1552	8.8751	29.4172	178070	4.88	6068
1.05	17.2202	8.50902	33.702	196790	3.41	7658
1.20	18.2852	7.8464	37.9867	215510	1.94	9248

These results are shown in Fig. 16.42.

Longitudinal Bending Moments in Head Seas

In Ref. 154 formulas are also presented for estimating the vertical bending moment at midships in head seas from experimental results on models of widely differing form, representing typical ships with block coefficients from 0.59 to 0.80. The ordinates of the bending moment response curves and the location of the peak or peaks for any vessel of similar type may be estimated from the principal dimensions of the hull and its waterplane area coefficient, longitudinal radius of gyration, and speed.

The total bending moment M_T can be divided into three different parts:

$$M_T = M_0 + M_s + M_w \tag{16.7}$$

where M_0 is the bending moment in still water at rest, M_s is the additional bending moment in still water when the ship is at speed, and M_w is the additional bending moment due to the action of seaway waves only.

The total bending moment due to wave action alone is expressed as

$$M_W = M_T - M_0 = M_s + M_w \tag{16.8}$$

The nondimensional form of M_W is m_W, which is defined as

$$m_W = \frac{\text{bending moment in addition to the moment experienced by the ship at rest in still water, } M_W}{\rho g (L_{pp})^2 B h_w}$$

$$= \frac{M_s + M_w}{2\rho g L^2 B \zeta_a} \tag{16.9}$$

whereas the nondimensional forms of M_s and M_w were expressed separately as

$$m_s = \frac{M_s}{\rho g (L_{pp})^3 B} \tag{16.10}$$

and

$$m_w = \frac{M_w}{2\rho g (L_{pp})^2 B \zeta_a} \tag{16.11}$$

In the case of hogging or sagging in waves, m_w is given in terms of m_W as follows:

$$m_w = m_W - m_s \frac{L}{2\zeta_a} \quad \text{(for hogging in waves)} \tag{16.12a}$$

or

$$m_w = m_W + m_s \frac{L}{2\zeta_a} \quad \text{(for sagging in waves)} \tag{16.12b}$$

Therefore the combined values of m_w for both hogging and sagging conditions is obtained as

$$(m_w)_{\text{hog + sag}} = (m_w)_{\text{hog}} + (m_w)_{\text{sag}} = 2m_W$$

In other words the coefficient m_W is the mean of hogging and sagging moments divided by $2\rho g L^2 B \zeta_a$.

According to the prediction equation, based on the multiple regression analysis presented in Ref. 154, m_s is given as follows:

$$m_s = 10^{-4}\left(\frac{V}{\sqrt{L}}\right)^2 \left(45.4C_w^2 - 62.7C_w + 0.0851\frac{L}{T} + 0.119\frac{L}{B} + 18.38\right) \tag{16.13}$$

whereas m_w at a particular value of L_w/L is determined by the equation

$$m_w = A_1 C_w + A_2 \frac{L}{T} + A_3 \frac{k_{yy}}{L} + A_4 \frac{L}{B} + A_5 \frac{V}{\sqrt{L}} + A_6 \tag{16.14}$$

where the values of the coefficients A_1, A_2, A_3, A_4, A_5, and A_6 are given in Table 16.8 as functions of the wavelength to ship length ratio L_w/L for hogging, sagging, and hogging + sagging conditions. The curve for m_w to a base of L_w/L generally has two peaks, and the peaks in hog and sag do not occur at the same L_w/L values, nor are their absolute values the same.

The magnitudes of the peak bending moments are obtained by using the coefficient values given in Table 16.9, whereas Table 16.10 makes it possible to determine the location of the peaks of the response curve at the proper value of L_W/L.

Although the strip theory method is more nearly correct theoretically for bending moment prediction, the empirical equation may be preferred by a practicing engineer because more accurate results are obtained for various parameters that are accepted as the factors influencing the performance of a ship in waves.

TABLE 16.8 COEFFICIENTS OF BENDING MOMENT RESPONSE CURVES [154]

$$m_w = A_1 C_w + A_2 \frac{L}{T} + A_3 \frac{k_{yy}}{L} + A_4 \frac{L}{B} + A_5 \frac{V}{\sqrt{L}} + A_6$$

$\frac{L_w}{L}$	A_1	A_2	A_3	A_4	A_5	A_6
			Hog			
0.50	0.0008	0.000220	0.0209	0.00099	− 0.0003	− 0.0143
0.75	0.0251	0.000235	0.0089	0.00034	0.0031	− 0.0225
1.00	0.0200	0.000200	− 0.0510	0.00096	0.0022	− 0.0066
1.25	0.0203	− 0.000199	− 0.1383	− 0.00082	0.0016	0.0354
1.50	0.0284	− 0.000087	− 0.0764	− 0.00079	0.0021	0.0093
1.75	0.0214	− 0.000074	− 0.0551	− 0.00021	0.0006	0.0051
2.00	0.0144	− 0.000079	− 0.0594	0.00018	0.0001	0.0083
2.50	0.0097	− 0.000094	− 0.0527	0.00003	− 0.0005	0.0110
3.00	0.0078	− 0.000088	− 0.0456	− 0.00014	− 0.0009	0.0115
			Sag			
0.50	− 0.0088	0.000025	0.0039	0.00305	0.0002	− 0.0130
0.75	0.0112	0.000057	0.0427	0.00220	0.0027	− 0.0298
1.00	0.0003	0.000036	0.0545	0.00538	− 0.0007	− 0.0408
1.25	0.0161	− 0.000238	0.0431	0.00210	0.0044	− 0.0255
1.50	0.0345	− 0.000140	0.0177	0.00028	0.0072	− 0.0272
1.75	0.0206	− 0.000129	− 0.0385	− 0.00015	0.0019	0.0021
2.00	0.0175	− 0.000092	− 0.0430	0.00022	0.0004	0.0020
2.50	0.0125	− 0.000059	− 0.0363	0.00017	− 0.0000	0.0028
3.00	0.0108	− 0.000025	− 0.0234	− 0.00007	− 0.0002	0.0013
			Hog + Sag			
0.50	− 0.0080	0.000245	0.0247	0.00403	− 0.0001	− 0.0273
0.75	0.0363	0.000292	0.0516	0.00254	0.0058	− 0.0513
1.00	0.0202	0.000236	0.0034	0.00634	0.0015	− 0.0474
1.25	0.0364	− 0.000437	− 0.0952	0.00128	0.0061	0.0099
1.50	0.0629	− 0.000227	− 0.0587	− 0.00051	0.0093	− 0.0179
1.75	0.0420	− 0.000203	− 0.0936	− 0.00036	0.0025	0.0072
2.00	0.0320	− 0.000171	− 0.1025	0.00041	0.0005	0.0103
2.50	0.0222	− 0.000153	− 0.0891	0.00020	− 0.0005	0.0138
3.00	0.0186	− 0.000113	− 0.0690	− 0.00022	− 0.0011	0.0127

TABLE 16.9 [154]

$$m_w = A_1 C_w + A_2 \frac{L}{T} + A_3 \frac{K_{yy}}{L} + A_4 \frac{L}{B} + A_5 \frac{V}{\sqrt{L}} + A_6$$

	A_1	A_2	A_3	A_4	A_5	A_6
First peak, hog	0.0262	0.000294	0.0347	0.00187	0.0026	− 0.0408
First peak, sag	0.0144	0.000188	0.0813	0.00254	0.0032	− 0.0461
First peak, hog + sag	0.0396	0.000487	0.0667	0.00338	0.0074	− 0.0679
Second peak, hog	0.0303	(0.000015	− 0.1011	− 0.00096	0.0011	+ 0.0163
Second peak, sag	0.0211	− 0.000110	0.0873	0.00268	0.0035	− 0.0455
Second peak, hog + sag	0.0526	− 0.000042	− 0.0614	0.00036	0.0068	− 0.0115

TABLE 16.10 [154]

$$\frac{L_w}{L} = B_1 \frac{L}{T}\left(\frac{1}{C_w}\right) + B_2 \frac{V}{\sqrt{L}}\left(\frac{K_{yy}}{L}\right) + B_3$$

	B_1	B_2	B_3
First peak, hog	0.0018	(0.04)	0.75
First peak, sag	0.0048	0.69	0.60
First peak, hog + sag	0.0029	(−0.06)	0.76
Second peak, hog	−0.0198	2.12	1.24
Second peak, sag	−0.0158	2.10	1.17
Second peak, hog + sag	−0.0179	2.17	1.19

Example 16.2

The data for a ship model are as follows:

$L = 16$ ft
$B = 2.439$ ft
$T = 1.098$ ft
$\Delta = 1851$ lb
$C_B = 0.693$
$C_W = 0.828$
$k_{yy} = 0.260L$

Using the expressions given by the regression analysis of Ref. 154, find the total longitudinal bending moment of the model in the nondimensional form (excluding the bending moment in still water at rest) for wavelength/ship length ratios $L_w/L = 0.5$, 0.75, 1.0, 1.25, 1.75, 2.0, 2.5, and 3.0 if the speed/length ratio $V/\sqrt{L}$ is 0.538. Also determine the location and the magnitude of the peaks of the bending moment curves. Consider the wave height to be a constant for all the wavelengths, namely, $h_w = 0.232\,L$. Also find the bending moment of the prototype which is 1000 ft long (i.e., $\lambda = 62.5$).

Solution:

The locations of peaks and the peak bending moments are as follows:

$$\text{First peak (hog):} \frac{L_w}{L} = B_1 \times \frac{L}{T} \times \frac{1}{C_w} + B_2 \times \frac{V}{\sqrt{L}} \times \frac{k_{yy}}{L} + B_3$$

$$= 0.0018 \frac{16}{1.098} \times \frac{1}{0.828} + 0.04 \times 0.538 \times 0.26 + 0.75$$

$$= 0.787$$

The corresponding peak bending moment is obtained as

$$m_w = A_1 C_w + A_2 \frac{L}{T} + A_3 \frac{k_{yy}}{L} + \frac{L}{B} + A_5 \frac{V}{\sqrt{L}} + A_6$$

$$= 0.0262 \times 0.828 + 0.000294 \times \frac{16}{1.098} + 0.0347 \times 0.26 + 0.00187 \times \frac{16}{2.439} + 0.0026 \times 0.538 - 0.0408$$

$$= 7.866 \times 10^{-3}$$

The values obtained for the other peaks are shown in Table 16.11.

Ship moving in calm water:

$$m_s = 10^{-4}\left(\frac{V}{\sqrt{L}}\right)^2 \left(45.4 C_w^2 - 62.7 C_w + 0.0851 \frac{L}{T} + 0.119 \frac{L}{B} + 18.38\right)$$

$$= 10^{-4}(0.538)^2 \left[45.4 \times (0.828)^2 - 62.7 \times 0.828 + 0.0851 \times \frac{16}{1.098} + 0.119 \times \frac{16}{2.439} + 18.38\right]$$

$$= -1.127 \times 10^{-5}$$

Ship moving in waves:

$$m_w = A_1 C_w + A_2 \frac{L}{T} + A_3 \frac{k_{yy}}{L} + A_4 \frac{L}{B} + A_5 \frac{V}{\sqrt{L}} + A_6$$

Hogging for $L_w/L = 0.5$;

$$m_w = 0.0008 \times 0.828 + 0.00022 \times \frac{16}{1.098} + 0.0209 \times 0.26 + 0.00099 \times \frac{16}{2.439} - 0.0003 \times 0.538 - 0.0143$$

$$= 1.335 \times 10^{-3}$$

Sagging for $L_w/L = 0.5$:

$$m_w = -0.0088 \times 0.828 + 0.000025 \times \frac{16}{1.098} + 0.0039 \times 0.26 + 0.00305 \times \frac{16}{2.439} + 0.0002 \times 0.538 - 0.0130$$

$$= 1.208 \times 10^{-3}$$

TABLE 16.11

Peaks	$\frac{L_W}{L}$	m_w
1st, hog	0.787	7.866×10^{-3}
1st, sag	0.781	8.085×10^{-3}
1st, hog + sag	0.803	9.629×10^{-3}
2nd, hog	1.188	15.102×10^{-3}
2nd, sag	1.186	12.530×10^{-3}
2nd, hog + sag	1.179	35.711×10^{-3}

TABLE 16.12 VALUES FOR HOGGING

$\frac{L_w}{L}$	m_s (16.13)	m_w (16.14)	m_W (16.12a)	Bending Moment Due to Wave Action [ft-lb] (16.8)
0.50	-1.127×10^{-5}	1.335×10^{-3}	0.850×10^{-3}	0.446×10^{7}
0.75	-1.127×10^{-5}	7.919×10^{-3}	7.434×10^{-3}	4.043×10^{7}
1.00	-1.127×10^{-5}	7.096×10^{-3}	6.610×10^{-3}	3.595×10^{7}
1.25	-1.127×10^{-5}	8.832×10^{-3}	8.346×10^{-3}	4.539×10^{7}
1.50	-1.127×10^{-5}	7.631×10^{-3}	7.145×10^{-3}	3.886×10^{7}
1.75	-1.127×10^{-5}	6.360×10^{-3}	5.874×10^{-3}	3.195×10^{7}
2.00	-1.127×10^{-5}	4.863×10^{-3}	4.377×10^{-3}	2.380×10^{7}
2.50	-1.127×10^{-5}	3.888×10^{-3}	3.402×10^{-3}	1.850×10^{7}
3.00	-1.127×10^{-5}	3.417×10^{-3}	2.932×10^{-3}	1.594×10^{7}

TABLE 16.13 VALUES FOR SAGGING

$\frac{L_w}{L}$	m_s (16.13)	m_w (16.14)	m_W (16.12b)	Bending Moment of the prototype Due to Wave Action [ft-lb] (16.8)
0.50	-1.127×10^{-5}	1.208×10^{-3}	1.693×10^{-3}	0.921×10^{7}
0.75	-1.127×10^{-5}	7.791×10^{-3}	8.277×10^{-3}	4.501×10^{7}
1.00	-1.127×10^{-5}	9.060×10^{-3}	9.545×10^{-3}	5.191×10^{7}
1.25	-1.127×10^{-5}	11.712×10^{-3}	12.198×10^{-3}	6.633×10^{7}
1.50	-1.127×10^{-5}	9.638×10^{-3}	10.124×10^{-3}	5.506×10^{7}
1.75	-1.127×10^{-5}	7.305×10^{-3}	7.791×10^{-3}	4.237×10^{7}
2.00	-1.127×10^{-5}	5.628×10^{-3}	6.114×10^{-3}	3.325×10^{7}
2.50	-1.127×10^{-5}	3.967×10^{-3}	4.453×10^{-3}	2.422×10^{7}
3.00	-1.127×10^{-5}	3.227×10^{-3}	3.713×10^{-3}	2.019×10^{7}

Therefore

$$(m_W)_{h3g} = m_w + m_s \frac{L}{2\zeta_a}$$

$$= 1.335 \times 10^{-3} - 1.127 \times 10^{-5} \frac{L}{0.0232\,L}$$

$$= 0.850 \times 10^{-3}$$

Similarly,

$$(m_W)_{sag} = m_w - m_s \frac{L}{2\zeta_a}$$

$$= 1.208 \times 10^{-3} + 1.127 \times 10^{-5} \frac{L}{0.0232\,L}$$

$$= 1.693 \times 10^{-3}$$

Tables 16.12 and 16.13 are prepared for the bending moments at various wavelength/ship length ratios (see also Figs. 16.43 and 16.44).

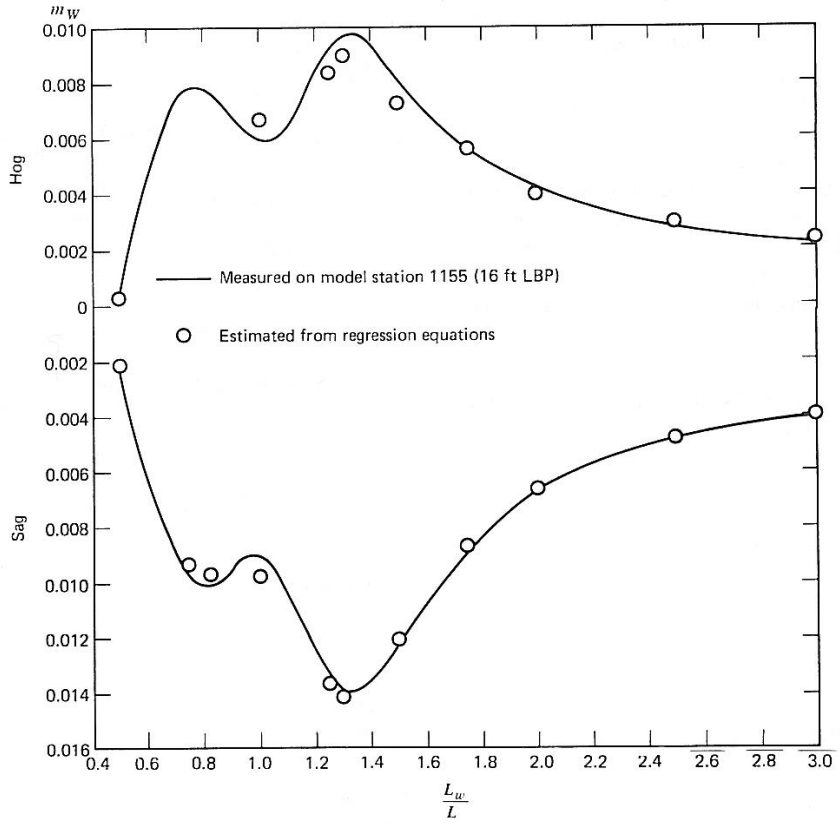


Figure 16.43 Bending moment coefficients in hog and sag [154].

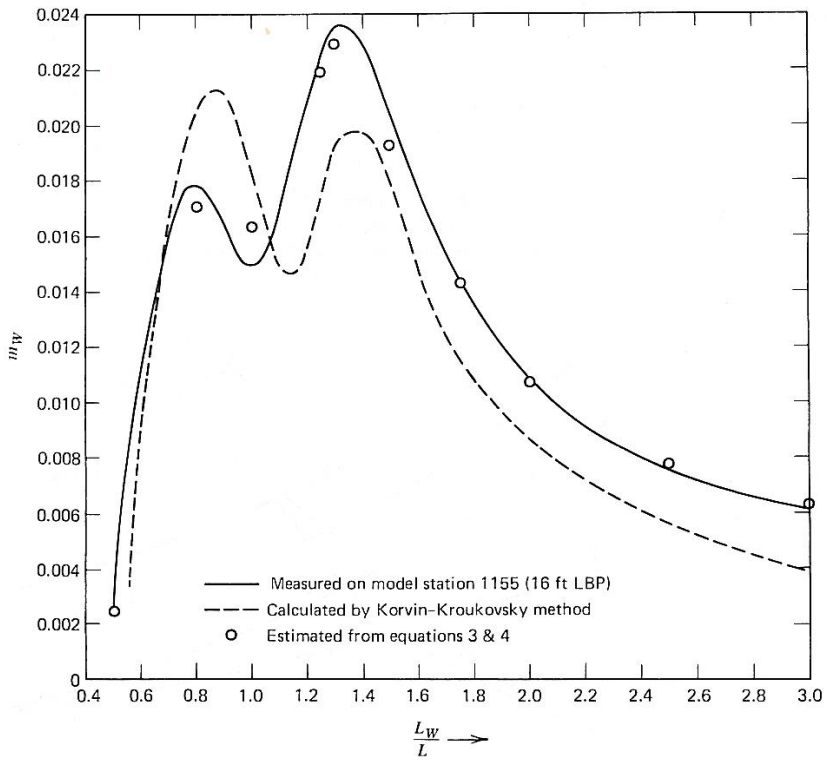


Figure 16.44 Bending moment coefficients in hog plus sag [154].

16.4 DESIGN CRITERIA

Before the seakeeping performance of a ship in a particular seaway is analyzed in the design office, the following should be at the designer's disposal:

a. Information on existing and new seakeeping test techniques.

b. Improved theoretical predictions of the behavior of ships in waves, including nonlinear effects.

c. A set of design spectra describing various representative seaways, since ship response is highly dependent on the spectral distribution of the seaway energy. However, if information on a particular seaway is not available, the ITTC standard spectral formulations should be used both for prediction and for experiments.

d. A review of the problem of determining ship propulsive performance in a seaway, supplemented, if possible, with trial data.

e. An analysis of the problem of predicting sustained sea speed from available seakeeping data.

Similarly, the statistical approach enables a designer to predict the seakeeping characteristics of a ship in numerical terms as follows:

1. Number of times that green water may be shipped over the bow per 100 pitch oscillations or during half an hour of operation in a particular seaway.
2. Number of slams that the vessel may have to endure per 100 pitching oscillations or during any specified amount of time.
3. Largest vertical acceleration at the bow of the ship.
4. Best capability of sustaining speed in rough water.

On the other hand, the specified design limits from the point of view of seakeeping criteria may also be defined at an early design stage, as given in Ref. 7 (Fig. 16.45). For example, a frequency of green water shipping of 8 per 100 pitching oscillations may be considered as the limit for a conventional ship. In general, the standard deck wetness consideration is only 5%. However, the term *deck wetness* is normally used in a very general sense, although this condition may be divided into zones of spray,

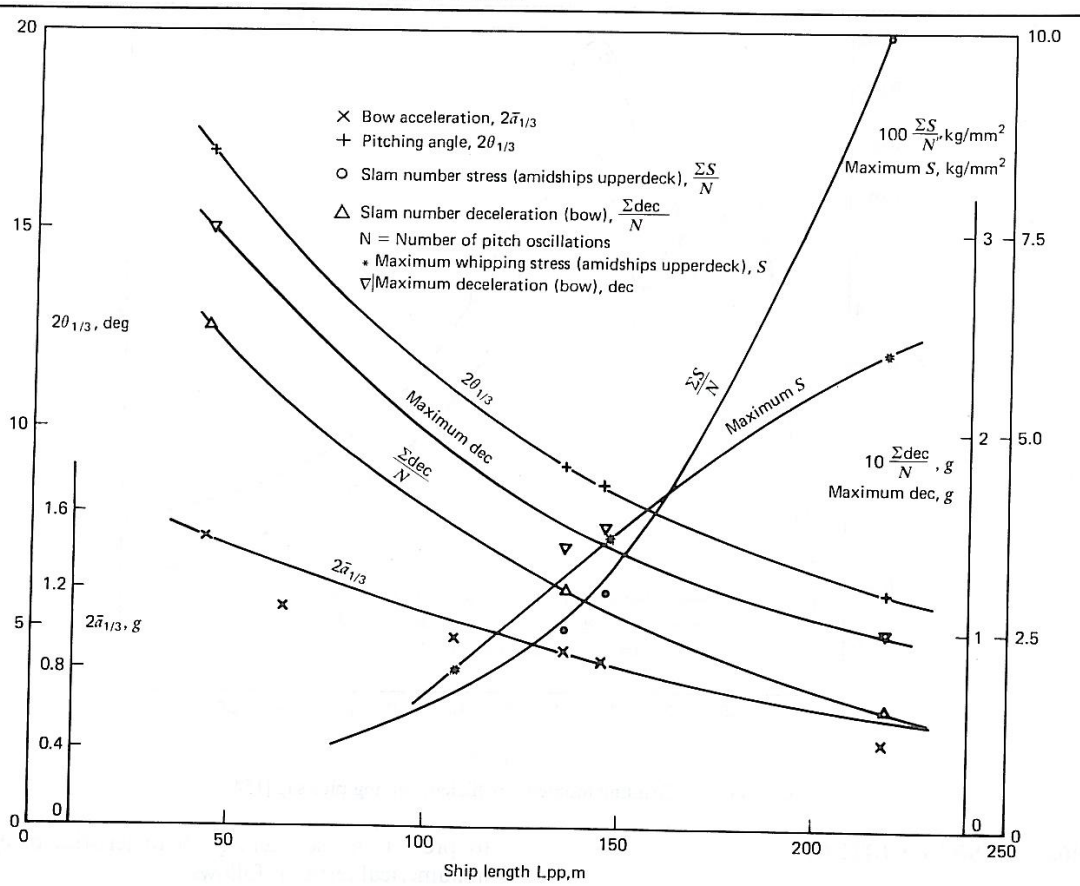


Figure 16.45 Design plots for various ship lengths [7].

wet, and very wet; and it is only when the deck is very wet that voluntary speed reduction is necessary in order to avoid damage to deck fittings and superstructures. The limit between the spray and the wet conditions corresponds shipping water about 2 times per 100 pitch oscillations, whereas at the boundary between wet and very wet green water is shipped 5 times per 100 pitch oscillations.

Again, for a conventional ship, more than 1 or 2 slams per 100 pitching oscillations is not acceptable. However, modern ships having strong reinforcement in the forebody may take 3 or even 4 slams per 100 pitching oscillations before any voluntary speed reduction is necessary.

A maximum relative velocity of 18 ft/sec (5.5 m/sec) at $0.10L_{pp}$ from the bow is a good criterion, provided that the number of slams is limited to 2 or 3.

A different criterion for slamming may be the limitation of whipping stress amidships in the main decks. For example, an amount of 850 psi (i.e., 60 kg/cm)^2 is applicable only for ships 500 ft in length. This limit can be higher for larger bulk carriers. Another criterion may be deceleration at the bow, which may reach $0.5g$ for a severe slam. However, a more direct criterion may be the dynamic pressure at the bottom of the forebody, and this is about 15 psi (i.e., 1 kg/cm^2) for a slam.

In Ref. 7 it is suggested that an impact should be called a slam when the whipping stress double amplitude on the upper deck amidships is in excess of 0.4 kg/mm^2 on 110 m cross-channel ships, 0.6 kg/mm^2 on 140 m cargo liners, and 2.0 kg/mm^2 on 220 m bulk carriers. The threshold of 0.6 kg/mm^2 for a cargo liner of 140 m length corresponds to a relative bow velocity of 18 ft/sec (5.5 m/sec).

Propeller racing becomes critical for 25 emergences of the propeller per 100 pitch oscillations, with a propeller being considered as emergent on each occasion that the decrease in torque exceeds 25%. (*Note*: In extreme sea conditions, propeller emer-

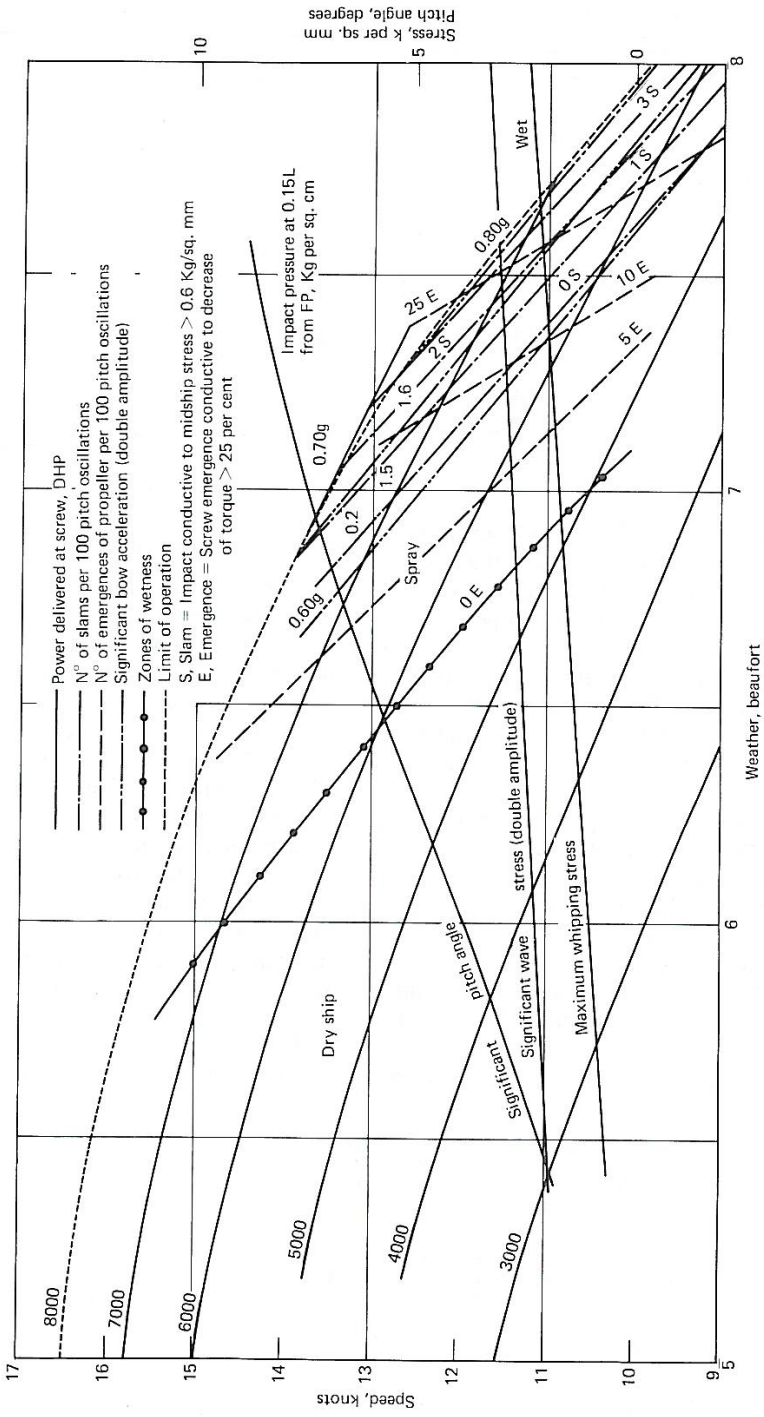


Figure 16.46 Dynamic effects as functions of sea states [6].

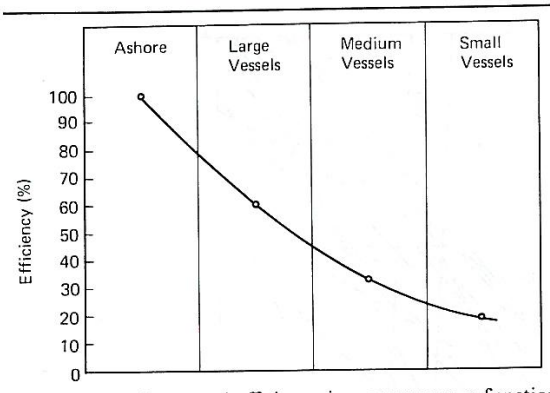


Figure 16.47 Personnel efficiency in a seaway as a function of ship size

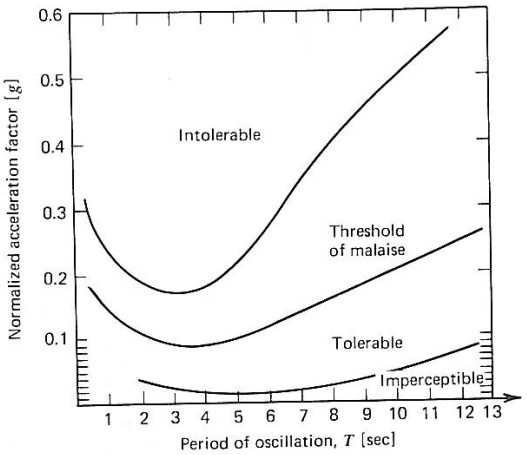


Figure 16.48 Human tolerance as a function of a period of oscillation and acceleration [94].

gences may be as frequent as 70 per 100 oscillations.) However, it should be remembered that while establishing criteria one should distinguish between design criteria and those used in actual operation in a seaway.

In Fig. 16.46 curves are plotted representing a given bow acceleration, a given number of slams, and a given number of screw emergences for different sea conditions (or Beaufort numbers) for any particular design.

The performances of human operators for different ship motions have been evaluated, and the figures given later in the paragraph can be used for establishing design criteria from the point of view of habitability. Figure 16.47 is a typical illustration of the performance efficiency of ship personnel in general, depending on the size of the vessel—the smaller the vessel, the lower is the efficiency. The primary factor in producing seasickness, which is a psychophysiological phenomenon, has been found to be random multidirectional acceleration. Either linear or angular acceleration may lead to motion sickness; in most locations aboard ship, there is a combination of both types of acceleration. Human endurance as a function of acceleration for different periods of oscillation can be read from Fig. 16.48. For a pitching period of 6 sec an acceleration of $0.3g$ may be considered as intolerable for prolonged periods, whereas the same amount of acceleration may be acceptable for a pitching period of 8 sec. Similarly, Fig. 16.49 shows that even a roll amplitude of 10° may reduce human effectiveness to 50%. In the design of unconventional ships, figures like 16.48 and 16.49 may serve as guidelines for the performance of their mission. Before new ships, including hydrofoils, Surface Effect Ships, and Hovercrafts, can be used in their design environment (open sea and at speed), the human habitability factor must be addressed.

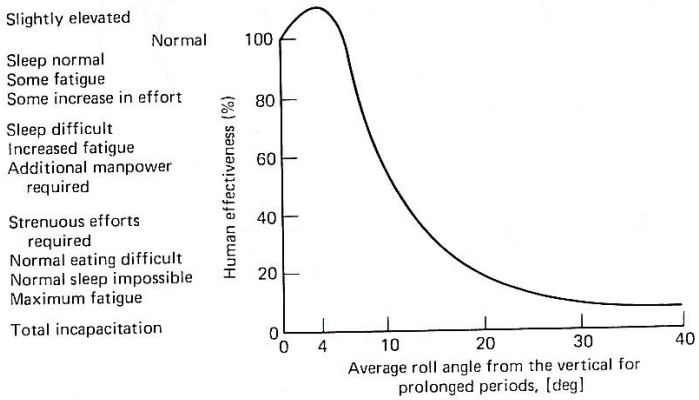


Figure 16.49 Human effectiveness as a function of roll amplitudes [94].

16.5 DATA FOR SEAKEEPING DESIGN

As mentioned earlier, seakeeping characteristics are an important consideration during the preliminary ship design stage, when the designer is in a position to change the principal characteristics in order to improve the seakeeping performance. The design data for the hull form are important when both the speed and the size of the ship are chosen as significant variables, whereas small changes in other ship particulars do not produce any appreciable change in seakeeping quality. However, for any unconventional vessel (i.e., hydrofoil crafts, air cushion vehicles, etc.) seakeeping quality may be the most important criterion in its design.

From the designer's point of view, the most important seakeeping characteristics of a ship to be considered are the following:

a. Heaving motion at the midship section.
b. Pitching motion.
c. Rolling motion.
d. Relative motion and relative velocity at stations 1, 2, 3, 4, and 20.
e. Vertical acceleration at stations 0, 5, 10, 15, and 20.
f. Wave bending moment amidships.
g. Added resistance.

For a particular type of hull form the nondimensional seakeeping characteristics in an irregular head sea of various nondimensional sea states can be made available as design data, as shown in the tables of Appendix A, and the values for any given vessel can be readily determined by interpolation (or extrapolation) from such tables when the specific ship data are available (see Table 16.14).

The tables in Appendix A show various seakeeping characteristics of extended Series 60 hull forms with ranges of $0.55 \leqslant C_B \leqslant 0.90$, $5.5 \leqslant L/B \leqslant 8.5$, and $2.0 \leqslant B/T \leqslant 4.0$ [29b]. It should be pointed out that the values of LCB, LCF, and radius of gyration and the weight distribution of the forebody are constant for a given C_B. The radius of gyration value has been taken to be $0.24L_{PP}$, and the longitudinal radius of gyration for the forebody about the CG of the vessel (i.e., k'_{yy}) has been assumed to be $0.125L_{pp}$. In addition, the following relationships have been used for the calculation of seakeeping series:

$$\frac{W_F}{W_T} = 0.2C_B + 0.36 \tag{16.15}$$

and

$$\frac{\text{LCG}_F}{L_{PP}} = 0.10C_B + 0.13 \tag{16.16}$$

where W_F is the weight of the forebody of the vessel (i.e., forward of the midship section), W_T is the total weight of the vessel, and LCG_F is the distance of the forebody CG from amidships.

For the determination of bending moment, a change in k_{yy} was accomplished by changing LCG_F position while keeping W_F and k'_{yy} constant.

The seakeeping tables (Tables A1 to A24) have been prepared with the average weight distribution as mentioned above. The bending moment predicted for a design on the basis of this weight distribution should be sufficiently accurate, since the wave bending moment for the midship section does not change appreciably with a moderate change in weight distribution. This may be explained as follows.

A larger radius of gyration will cause an increase in motions and hence an increase in the hydrodynamic bending moment, however, such an increase in radius of gyration is obtained by moving weights away from amidships. The increased distance of the weight from amidships and the larger motions together will produce a larger inertial bending moment, which counteracts the increased hydrodynamic bending moment. The net result may be even a slight decrease in total wave bending moment [140].

The results are given in Tables A1 to A24 in terms of $\sqrt{m_0}$ values as functions of the ship particulars, the ship speed, and the significant wave height. These results for heaving and pitching motions, as well as responses resulting from them, have been obtained for long-crested head seas by the linear superposition technique, for which the ITTC formulation (see Chapter 5) has been used for wave spectra and the response amplitude operators have been determined analytically by the strip theory (see Chapter 9). It should be pointed out that the theoretical calculations and model tests are quite satisfactory for ship motions and loads. Thus the theoretical results may be considered adequate for design purposes. Although the rolling motion is important for seakeeping performance, these values have not been presented because of their nonlinearity and the difficulty in estimating viscous damping for the rolling motion. For more accurate prediction of motion, the correction factor $(1 - \varepsilon^2)^{1/2}$ should be applied, where ε is the broadness parameter and may have a value between 0.3 and 0.70. The tables of Appendix A can be used successfully for feasibility studies and preliminary ship design. Since seakeeping qualities do not differ appreciably with a change in hull form, the seakeeping tables of Appendix A can be considered as relative standards for seakeeping design. However, the tabulated results are made

TABLE 16.14 SEAKEEPING TABLES: U.S.S. Annapolis

$L = 400$ ft, $\frac{L}{B} = 7.0$, $\frac{B}{T} = 3.0$, $C_B = 0.60$,
$LCB = 0.5\%$ of LBP aft of ⊗
Heaving Motion

	RMS Heave Amidships / Length between Perpendiculars $= \frac{\sqrt{m_{0z}}}{L_{pp}}$		
Nondimensional Sea State $= (h_w)_{1/3}/L_{pp}$	$F_n = 0.10$	$F_n = 0.20$	$F_n = 0.30$
0.025	0.0020	0.0040	0.0050
0.050	0.0090	0.0120	0.0150
0.075	0.0160	0.0180	0.0210
0.100	0.0220	0.0240	0.0270

Pitching Motion

	RMS Pitch [deg], $\sqrt{m_{00}}$		
Nondimensional Sea State $= (h_w)_{1/3}/L_{pp}$	$F_n = 0.10$	$F_n = 0.20$	$F_n = 0.30$
0.025	1.00	1.10	1.05
0.050	2.30	2.50	2.70
0.075	3.00	3.40	3.60
0.100	3.50	3.90	4.10

Relative Motion at Station 1

	RMS Relative Motion at Station 1 / L_{pp}		
Nondimensional Sea State $= \frac{(h_w)_{1/3}}{L_{pp}}$	$F_n = 0.10$	$F_n = 0.20$	$F_n = 0.30$
0.025	0.0120	0.0140	0.0135
0.050	0.0210	0.0261	0.0290
0.075	0.0250	0.0315	0.0360
0.100	0.0270	0.0330	0.0390

Added Resistance

	(Mean Added Resistance) $\times 10^3$ / $\rho g(L_{pp})^3$		
Nondimensional Sea State $= \frac{(h_w)_{1/3}}{L_{pp}}$	$F_n = 0.10$	$F_n = 0.20$	$F_n = 0.30$
0.025	0.0050	0.0060	0.0065
0.050	0.0140	0.0210	0.0290
0.075	0.0180	0.0310	0.0450
0.100	0.0200	0.0400	0.0600

TABLE 16.14 (*Contd.*)
Wave bending Moment

	(RMS Bending Moment Amidships) $\times 10^3$ / $\rho g(L_{pp})^4$		
Nondimensional Sea State $= \frac{(h_w)_{1/3}}{L_{pp}}$	$F_n = 0.10$	$F_n = 0.20$	$F_n = 0.30$
0.025	0.0140	0.0160	0.0170
0.050	0.0250	0.0300	0.0350
0.075	0.0300	0.0350	0.0420
0.100	0.0320	0.0390	0.0450

nondimensional with respect to ship length. In other words, to compare the seakeeping performances of vessels having different lengths but encountering the same sea state, different nondimensional sea states should be considered. It should be noted that the root mean square values given in the tables are the mean values as used in statistics, and the significant values or other averages may be obtained from the rms values. However, for the added resistance the mean values has been presented; this is equal to $2m_0$, where m_0 is the area under the response spectrum obtained from the response amplitude operators, defined as R_{aw}/ζ_a^2 (see Chapter 11). It is suggested in Ref. 140 that the propeller efficiency may be obtained satisfactorily from standard propeller design charts, estimating the mean thrust (calm water value plus the mean added thrust and the thrust necessary for wind resistance) from the mean resistance and using the calm water values for thrust deduction fraction as well as wake fraction. The response spectrum for the bending moment is wider than heaving and pitching motions and also acceleration; the spectra for the relative motion and the relative velocity are the widest, the spectrum for the relative motion being wider than that for the relative velocity.

Since the seakeeping tables have been prepared for the extended Series 60, they should be sufficiently accurate for a ship having constant draft along its length (except in the region of the aft perpendicular), and a beam maximum near amidships and tapering to zero at both ends. Also, the LCB and LCF are close to the midship section. Hull forms with transom sterns or bulbous bows do not come into this category, although small bulbs may not alter the seakeeping characteristics significantly. Finally, it should be stressed that the theoretical calculations given in Tables A1 to A24 do not consider the effects of the above-water hull form.

Example 16.3

For U.S.S. *Annapolis* the following data are given:

$L = 400$ ft

$\frac{L}{B} = 7.0$

$\frac{B}{T} = 3.0$

$C_B = 0.60$

LCB = 0.5% of LBP aft of ⊗

$F_n = 0.20$

Nondimensional sea state $= \frac{(h_w)_{1/3}}{L_{pp}} = 0.025$, 0.075, 0.050, 0.100

Find:

a. Heaving.

b. Pitching.

c. Wave bending moment.

d. Relative motion, relative velocity, and acceleration at stations 0, 5, 10, 15, 20.

e. Added resistance in a seaway.

Solution:

a. Heaving: $\left(\frac{\text{RMS heave}}{L_{pp}} \times 10^4\right) \times \frac{L_{pp}}{10^4}$

$= \text{RMS heave}$

(Heave from tables) × 0.04 = RMS heave

From Tables A.1 through A.24 the following values have been obtained.

$\frac{(h_w)_{1/3}}{L_{pp}}$	$\frac{\text{RMS Heave}}{L_{pp}} \times 10^4$ [−]	RMS Heave at ⊗ [ft]	Significant Heave [ft]
0.025	41	1.64	3.28
0.050	113	4.52	9.04
0.075	178	7.12	14.24
0.100	242	9.68	19.36

b. Pitching:

$\frac{(h_w)_{1/3}}{L_{pp}}$	[RMS ° × 10²]	RMS Pitch [deg]	Significant Roll [deg]
0.025	115	1.15	2.30
0.050	264	2.64	5.28
0.075	346	3.46	6.92
0.100	398	3.98	7.96

c. Wave bending moment

$\frac{(h_w)_{1/3}}{L_{pp}}$	$\frac{\text{RMS Bending} \times 10^7}{\rho g(L_{pp}^4)}$	RMS Bending Moment	Significant Bending Moment [lb-ft]
0.025	146	2.394×10^7	4.789×10^8
0.050	268	4.396×10^7	8.792×10^8
0.075	314	5.150×10^7	1.030×10^8
0.100	335	5.495×10^7	1.099×10^8

d. Relative velocity, motion, and acceleration at Station 0

$\frac{(h_w)_{1/3}}{L_{pp}}$	$\frac{\text{RMS Relative Motion} \times 10^4}{L_{pp}}$	RMS Relative Motion [ft]	Significant Relative Motion [ft]
0.025	145	5.8	11.6
0.050	280	11.2	22.4
0.075	332	13.28	26.56
0.100	355	14.2	28.4
	$\frac{\text{RMS Relative Velocity} \times 10^4}{\sqrt{gL_{pp}}}$	RMS Relative Velocity [ft/sec]	Significant Relative Velocity [ft/sec]
0.025	545	6.75	13.50
0.050	946	10.73	21.46
0.075	1059	12.01	24.02
0.100	1100	12.48	24.96
	$\frac{\text{RMS Relative Acceleration} \times 10^4}{g}$	RMS Relative Acceleration [ft/sec² × 10⁻¹]	Significant Relative Acceleration [ft/sec²]
0.025	1587	0.507	10.14
0.050	2999	0.965	19.30
0.075	3518	1.132	22.64
0.100	3751	1.207	24.14

e. Added resistance in a seaway

$\frac{(h_w)_{1/3}}{L_{pp}}$	$\frac{\text{Mean Added Resistance} \times 10^7}{\rho g L_{pp}^3}$	Mean Added Resistance [lb]	Significant Added Resistance [lb]
0.025	57	23,370	46,740
0.050	198	81,180	162,360
0.075	294	120,540	241,080
0.100	377	154,570	309,140

16.6 EXTREME VALUES AS DESIGN CONSIDERATIONS

It is often of considerable interest to the designer to find the most probable largest value that can be

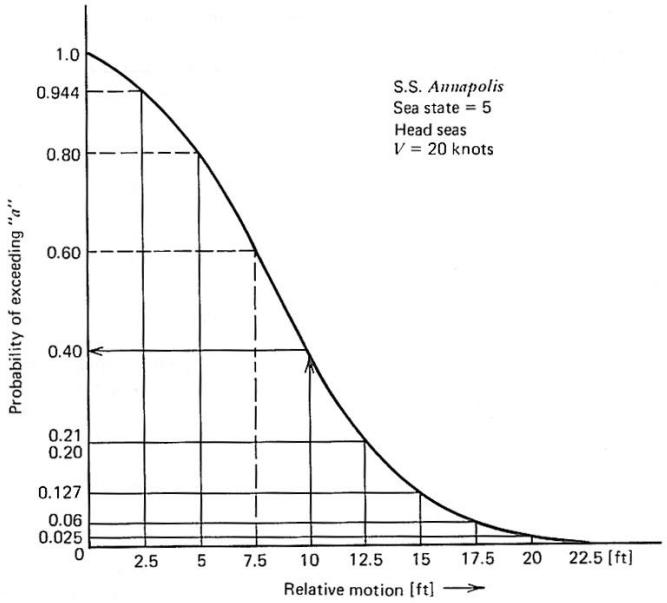


Figure 16.50 Probability of relative motion.

predicted by statistical theory. It has been shown that the largest probable value out of n observations is $\sqrt{m_0}$ times a constant if the response has the Rayleigh distribution, where the constant is a function of n only. For large n this constant becomes approximately equal to $\sqrt{2\log_e n}$. But the chance that the extreme value will exceed the most probable largest value (obtained by statistical formulation) is high, so that the most probable largest value cannot be justified for design consideration. Therefore the extreme value for a particular α (where α is the probability that the extreme value will be exceeded) should be used by the designer in establishing the criteria for the seakeeping characteristics of his ship.

Hence spectral analysis is not performed to predict seakeeping characteristics on a long-term basis. The probability function as given by the following equation is used to estimate the long-term ship response:

$$\text{Probability}\{\text{extreme value amplitude} > a\} = e^{-a^2/2m_0} = \alpha \qquad (16.17)$$

where α is the probability that the extreme value amplitude will be exceeded, m_0 is the area under the response spectrum, and a is the design value amplitude. [169].

(Note that, in order to predict the double amplitude, $2m_0$ in the above equation should be replaced by $8m_0$.) For example, if m_0, the area under the response spectrum for relative motion amplitude at Station 1 is known to be 54.5 ft^2, Fig. 16.50 can be obtained for various relative motions along with their probabilities; for example, a value of 10 ft of relative motion will be exceeded with a probability of $e^{-10^2/2\times 54,5} = 0.40$ (i.e., 40%).

For design considerations, an extreme value (for n observations for which the probability that the extreme value will exceed the predicted largest value is α) is determined for a desired probability of being exceeded. Although the decision regarding which probability value should be taken for design purposes depends on the designer's own judgment, a probability of 0.01 to 0.05 (i.e., 1 to 5%) is often considered as a standard in design practice.

The extreme values of a random process are given as a function of the number of observations, n. For practical design purposes, however, it is sometimes more significant to obtain the extreme value in terms of time instead of the number of observations n, where n can be expressed as a function of time, and the most probable largest value as a function of time T is given [169] as

$$\sqrt{2\log_e\left[\frac{60^2T}{2\pi}\left(\frac{m_2}{m_0}\right)^{1/2}\right]}\sqrt{m_0} \qquad (16.18)$$

where T is time in hours, and m_0 and m_2 are the area and second moment of the area under the response spectrum of the random process under consideration.

If α is selected as 0.01, this means that only one among 100 sister ships operating in similar sea

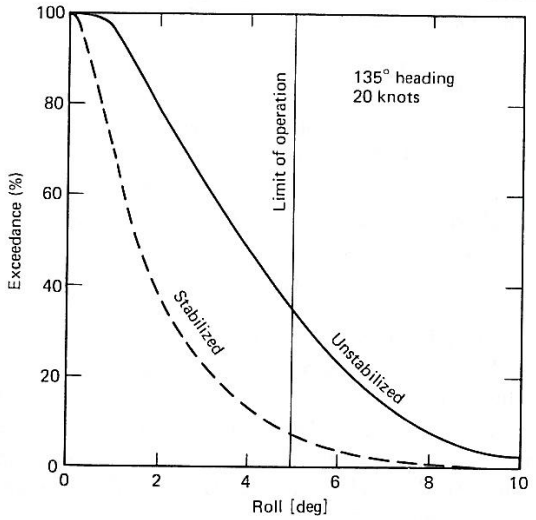


Figure 16.51 Exceedance of roll motion [94].

conditions may have a motion (or bending moment) greater than the predicted value in a specified period of time.

The usefulness of prediction for existence can also be illustrated as shown in Fig. 16.51. Assume that a helicopter landing is possible only if the angle of roll is no more than 5°. Then this figure shows that, in case of an unstabilized ship in a particular seaway, a roll amplitude of 5° will be exceeded 35% of the time. The fact that only 65% of the time is available for helicopter operation may not be acceptable, since for 75% of the time the ability to land is essential for this particular design. But when the ship is stabilized, a 5° angle of roll will be exceeded only 8% of time, that is, during 92% of the time the landing operation can be conducted safely.

16.7 SPECIFIC DESIGN REQUIREMENTS

Ship Speed in a Seaway

Since speed is the basis of preliminary ship design, it is important that speed be determined not only considering the seaway characteristic but also taking into account the dynamic effects due to ship motions. To be able to predict ship speed correctly in a seaway, it is also necessary to have sufficient knowledge concerning realistic performance of a ship propeller in a seaway, as propulsive efficiency may be significantly different in a seaway from what it is in calm water.

In Fig. 16.52 the reduction of ship speed in different sea states has been illustrated for the leading wave components coming from different directions.

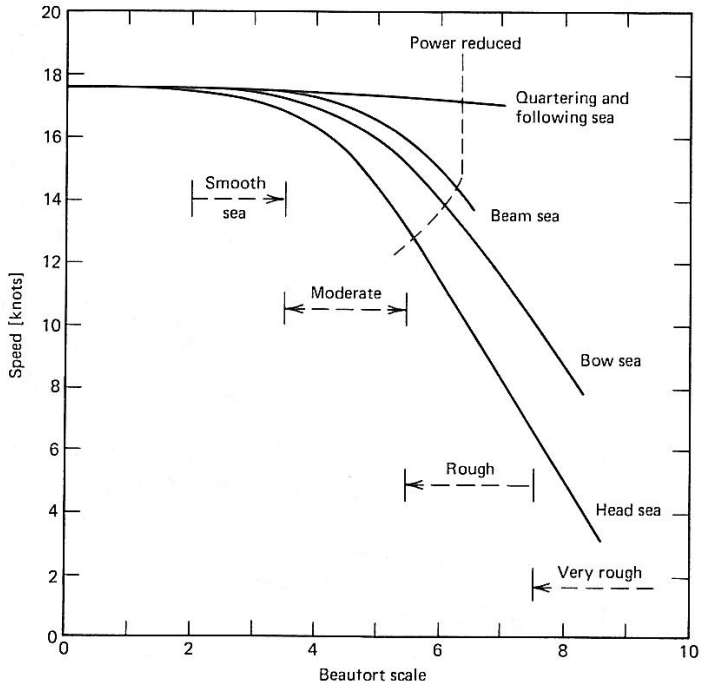


Figure 16.52 Attainable ship speeds for various sea conditions [127].

1. Determination of speed (without considering motion, i.e., considering involuntary speed loss). The average ship speed for a specified engine output can be determined in the following way if there is no limitation due to motion effects [29a]:

a. The most efficient propeller, (e.g., B.4.55 of the Wageningen series) is selected after the curve of K_T/J^2 is calculated and plotted on the propeller diagram:

$$\frac{K_T}{J^2} = \frac{EHP \times 326}{\rho D^2 V^3 \times (1.689)^3 \times (1-w)^2 \times (1-t)} \tag{16.19}$$

where EHP and V are determined from Fig. 16.53 for a particular sea state, and the propeller diameter D, the wake fraction w, and the thrust deduction fraction t are estimated from open water test results available, assuming that they are valid also for rough water. Thus the open water efficiency η_o is computed.

b. The propulsive efficiency is

$$\eta_P = \eta_O \eta_H \eta_R \eta_S \tag{16.20}$$

where η_O = open water efficiency.

$$\eta_H = \frac{1-t}{1-w}$$

η_R = relative rotative efficiency, assumed to be 1.026 for all sea states

η_S = shaft transmission efficiency

c. Therefore the power required for a given ship speed and sea state is

$$\text{SHP}_r = \frac{EHP}{\eta_p} \tag{16.21}$$

where SHP_r is the required shaft horsepower, EHP is the effective horsepower, and η_p is the propulsive efficiency.

d. The above calculation is repeated by selecting pairs of values of EHP and V for a given sea state until $\text{SHP}_r = \text{SHP}_a$, where SHP_a is the available shaft horsepower.

e. All the calculations are now repeated for a different sea state (the propeller, however, is selected for one particular sea state).

f. After the speeds have been determined for all the

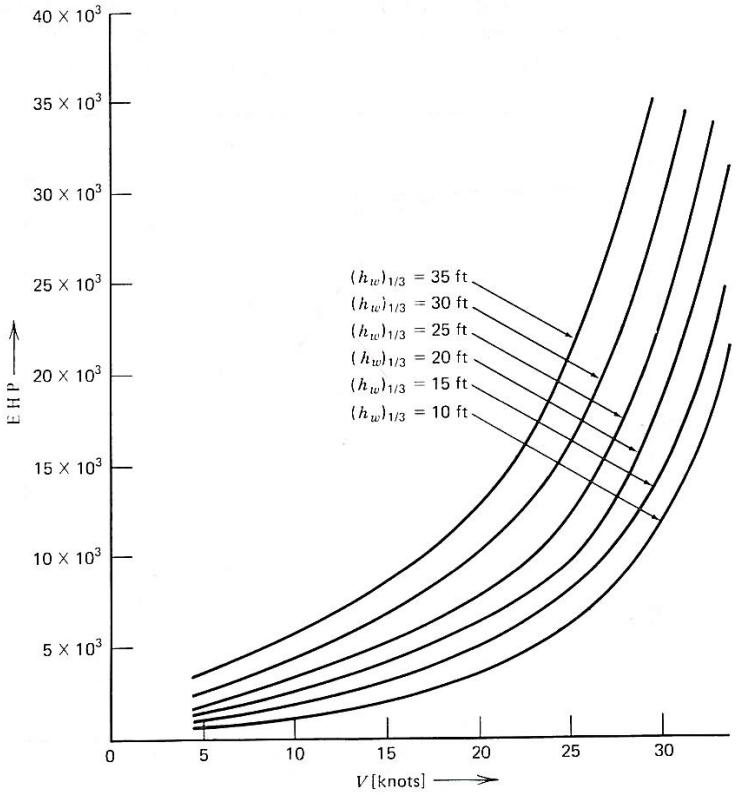


Figure 16.53 Effective horsepower curves for various sea conditions.

sea states for a given engine output, SHP_a, the average speed V_a is calculated using the following expression:

$$V_a = \frac{1}{100} \sum_{i=1}^{N} (F_i V_i) \qquad (16.22)$$

where V_a = average speed
F_i = frequency of occurrence in percentage of the ith state [i.e., $(h_w)_{1/3}$], which is obtained from the table for a wave height histogram, as shown in Table 16.15 for a given sea
V_i = ship speed in the ith sea state obtained after step e
N = number of sea states [i.e., number of $(h_w)_{1/3}$ used to describe the seaway (*note*: $N = 6$ in Fig. 16.53)]

2. Determination of speed (considering the dynamic effects due to motion or after voluntary speed

TABLE 16.15 A TYPICAL HISTOGRAM FOR SIGNIFICANT WAVE HEIGHT (FOR THE NORTH ATLANTIC ROUTE)

Significant Wave Height [ft]	Percentage of Time [%]
4	3.0
6	10.0
8	32.0
10	20
12	14
14	11
16	6
18	2.0
20	1.0
22	0.5
24	0.3
26	0.1
28	0.06
30	0.03
32	0.01

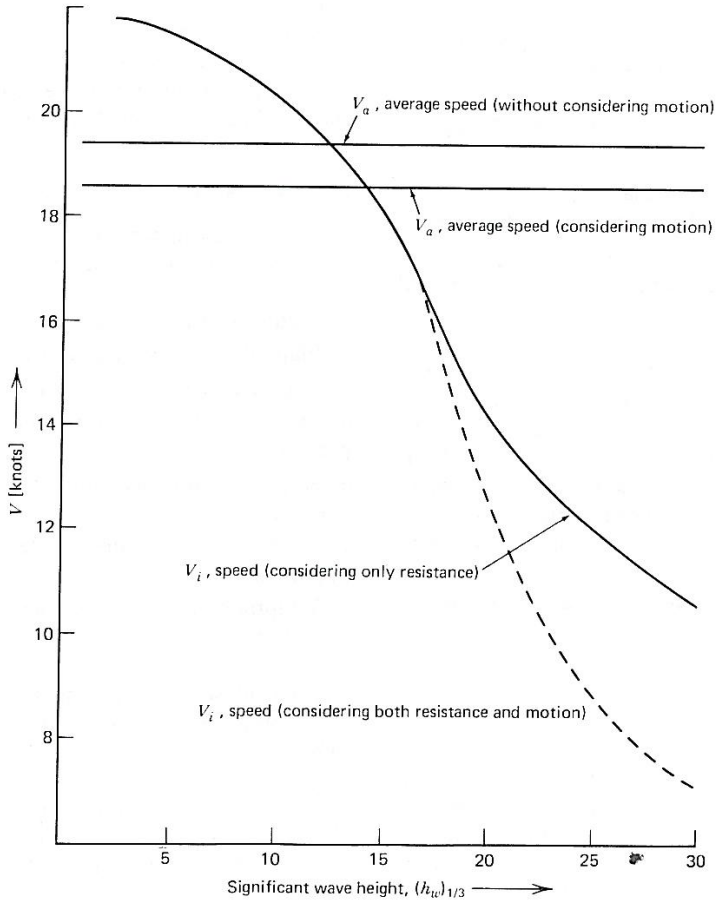


Figure 16.54 Speed curves for a particular design [29a].

reduction). The ship speed V_i as a function of the sea state $(h_w)_{1/3}$ is determined as shown in case 1, but is subject to possible reduction if motion considerations are to be made [29a].

The following factors influence voluntary speed reduction:

a. The upper limit of vertical acceleration, which is important for the crew and passengers, should be no more than $0.125g$.

b. Safety of the cargo entails three considerations:

(i) The average of the one-tenth highest vertical acceleration amplitudes $\ddot{z}_{1/10}$ at any point along the ship's length must not exceed $0.50g$ or 16.1 ft/sec^2, that is,

$$\ddot{z}_{1/10} = 2.55\sqrt{m_{0\ddot{z}}}(1-\varepsilon^2)^{1/2} \qquad (16.23)$$

where $m_{0_{\ddot{z}}}$ is the area under the response spectrum for the vertical acceleration.

Note: the values tabulated in the seakeeping table are rms $(=\sqrt{m_{0\ddot{z}}})$ i.e., the statistical average values. ε can be assumed to be 0.60 for design purposes.

It is suggested in Ref. 29a that, in order to ensure that $\ddot{z}_{1/10}$ will not exceed $0.50g$, the value for $m_{0\ddot{z}} \leq 0.25\ g$.

(ii) The probability that the relative motion amplitude at station 1 will exceed the freeboard at station 1 should be less than 0.01 (i.e. less than 1%).

(iii) The probability of slamming at station 2 should not exceed 0.01.

The speed determined from the resistance consideration alone (case 1) should be reduced until the criteria for dynamic effects are duly satisfied. The average ship speed in an actual seaway is determined in the same way as in case 1, the only difference now is that V_i is the ship speed in the ith sea state after the dynamic effects have been taken into account.

The results of such computations are then obtained as shown in Fig. 16.54.

Deck Wetness and Slamming

There are two ways to improve the situation as far as deck wetness is concerned. The first is to increase the freeboard and employ the optimum amount and shape of flare to keep water off the foredeck. The other means is to design the foredeck in such a manner that a large quantity of water can be shipped out quickly and safely, that is, using adequate camber (or turtleback), breakwaters to throw water overboard, protected and structurally sound hatch covers, minimum deck fittings subject to damage, and a strong forecastle deck to withstand heavy pressure due to the shipping of green water. The second approach can be idealized in the case of a surfaced submarine.

Similarly, slamming may also be treated during the design stage; for example, the shape of the forward sections should be so designed as to reduce the flatness of the bottom as much as possible. If possible, the draft of the ship should be increased in order to lessen the chance of forefoot emergence, as well as to permit better section shapes. (It should be noted that, if the load waterline and sectional area curves are not changed, the ratio of S_n/B_n, also known as the *mean draft*, does not change if the draft is increased; accordingly the hydrodynamic characteristics, such as added mass, and damping, differ very little).

It has often been the case that the hull form has been designed specifically to reduce deck wetness and slamming while accepting large amplitudes of motion and accelerations at high speed in rough water.

Design Considerations for Slamming

For the design in regard to slamming, the following information should be available:

a. Frequency of occurrence of slam impact.

b. Elapsed time between successive slam impacts.

c. Intensity of impact pressure.

d. Most probable largest pressures as well as extreme pressure to be expected.

e. Ship speed at which damage may occur on bottom plating.

f. Distribution of impact pressure and resulting impact force.

g. Whipping stress and acceleration change due to slamming.

The following points should be considered in seakeeping design from the point of view of slamming [170]:

1. It may not be correct to compare the two-dimensional results of slamming pressure with those for the three-dimensional case. In two-dimensional drop tests, pressures for a given impact velocity may be many times larger than those measured in waves

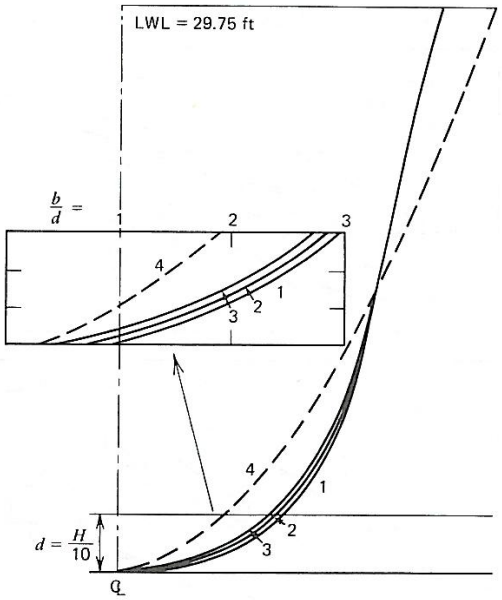


Figure 16.55 Charts for k_1 values [170]. b is half-width of station at one-tenth of design draft waterline, d is one-tenth of design draft, k is dimensional constant associated with impact pressure k_1 is nondimensional k value.

	Estimation of k_1 Values			
	①	②	③	④
b, [ft]	8.81	8.50	8.17	5.63
$d = H/10$, [ft]	2.975	2.975	2.975	2.975
b_*, [ft]	2.60	1.95	1.30	0.96
b/d	2.96	2.86	2.75	1.89
b_*/b	0.30	0.23	0.16	0.17
C_a	0.73	0.70	0.68	0.63
k_1	18.1	16.4	15.0	10.4

for the same impact velocity. Therefore predictions should be based on three-dimensional tests in regular or irregular waves.

2. It is reasonably correct to assume that the pressure increases with the second power of the impact velocity [170]:

$$p = kV_r^n \tag{16.24}$$

where p = impact pressure [psi]
k = coefficient, not dimensionless since it includes the density ρ of liquid
V_r = impact velocity [ft/sec], which is relative velocity between wave and ship bottom at the station considered, or
= s_b when slamming at the bow is under consideration
n = exponent (experimentally determined) as very close to 2.

Values of k have been given in Ref. 170 for various section shapes and are at the present time, determined by model tests. The value of k is a constant depending on the hull section shape, particularly that of the bottom portion. The k value for a given ship section can be evaluated by a regression equation that is established through available data from seakeeping model tests. Since k is not dimensionless, another coefficient can be introduced:

$$k_1 = \frac{2k}{\rho} \quad \text{or} \quad p = \tfrac{1}{2}\rho k_1 V_r^2 \tag{16.25}$$

This type of equation will take into consideration the difference in density between fresh and salt water. *Note*: Pressure is still given per square inch, whereas velocity is in feet per seconds.

Values for k_1 are given in Fig. 16.55 as functions of the width/draft ratio b/d, nondimensional flat-bottom width b_*/b, and sectional area coefficient, where $C_a = A_*/2bd$, b_* is the half-width of the flat bottom, and A_* is the sectional area below the one-tenth of the design draft. These symbols are clearly explained in Fig. 16.56.

3. Ochi's [170] introduction of the coefficient k can be applied to estimate the slamming pressures for all kinds of hull forms. According to Ochi, k varies from 0.21 to 0.145 for various ship hulls and locations on these hulls.

4. Results also indicate that there is no difference between test results in regular or irregular waves (i.e., model tests can be made in regular waves, thereby simplifying the test procedures).

Other statistical quantities can also be obtained as follows [170]:

a. Average pressure $= k(V_0^2 + 2m_{0\dot{s}})$. (16.26a)
b. Significant pressure $= k(V_0^2 + 2.1 \times 2m_{0\dot{s}})$. (16.26b)
c. Average of the one-tenth highest pressures $= k(V_0^2 + 3.3 \times 2m_{0\dot{s}})$. (16.26c)
d. Most probable extreme pressure in n slams $= k(V_0^2 + 2m_{0\dot{s}} \ln n)$. (16.26d)
e. Extreme pressure in n slams for which the probability of being exceeded is

$$\alpha = k\{V_0^2 - 2m_{0\dot{s}} \times \ln[1 - (1-\alpha)^{1/n}]\} \tag{16.26e}$$

where V_0 = threshold relative velocity
= 12 ft/sec for a 520 ft vessel
n = number of slams

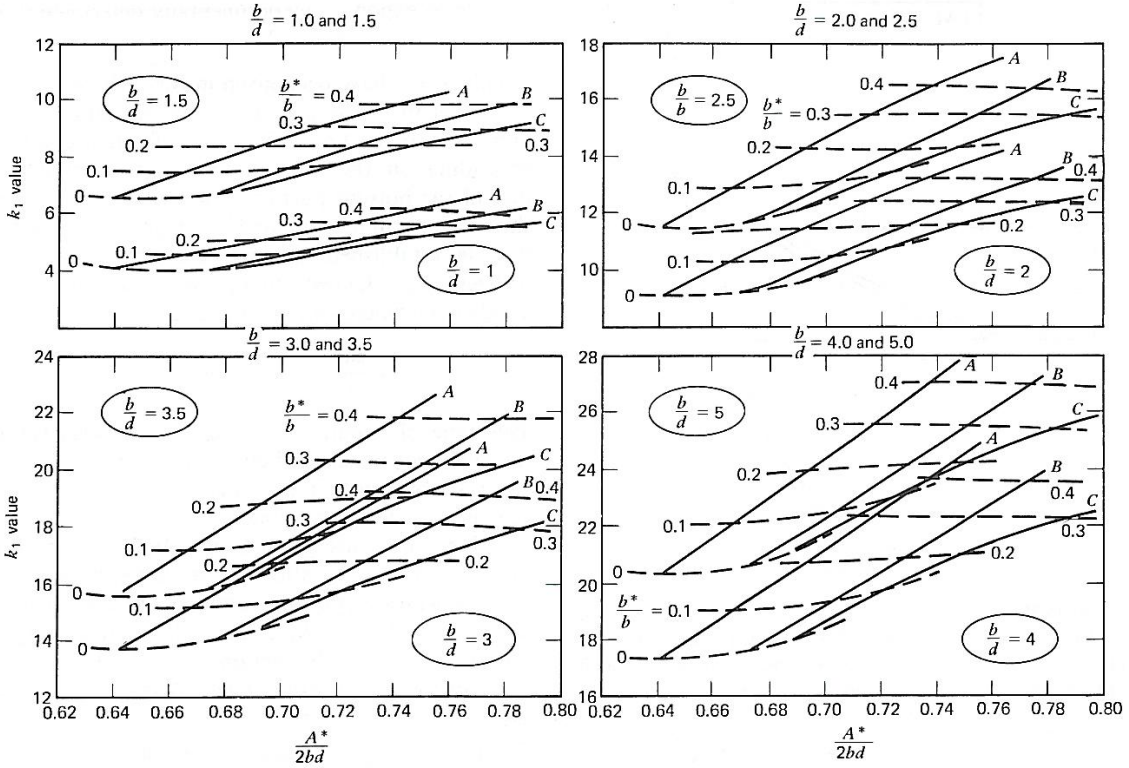


Figure 16.56 Station 3 of a *Mariner* ship and three modifications [170].

$k = \frac{1}{2}\rho k_1$ (Fig. 16.56 can be used to estimate k_1)

α = constant (small number)
= 0.01 for 99% assurance; that is, one out of 100 ships may experience a value higher than the extreme value determined by this formula (16.26*e*). If a greater assurance of safety is desired, a smaller value for α should be considered

$m_{0\dot{s}}$ = variance of the relative velocity
= m_{2s} = second moment of the area under the response spectrum for relative bow motion

The extreme pressures in terms of time in rough seas can be calculated by substituting for n in the above equations the value given below:

$$n = \frac{3600T}{2\pi}\sqrt{\frac{2m_{0\dot{s}}}{2m_{0s}}} \times \text{Prob}\{\text{slam}\} \qquad (16.27)$$

where T is ship operation time in hours.

Figure 16.57 and 16.58 give the results of extreme pressures calculated using equations (16.26d) and (16.26e) for a *Mariner* (light draft condition) doing 10 knots in sea state 7 (significant wave height 30.2 ft) at several forward locations. Also shown in the figures are the numbers of slams per hour at various locations along the ship length.

The bottom plate damage is generally limited to the forward part of the ship, at a distance between $0.10L$ and $0.30L$ from the forward perpendicular (see Fig. 16.59) and at a breadth of 0 to $0.25B$ on both sides of the keel, especially when the angle of deadrise, β, is small. The maximum pressure peak coefficients under normal operating conditions on ships amount to about $P/\rho gL = 0.5$ to 1.0.

Figure 16.60 shows the location of damage on a hull due to slamming. The location is a function of the buttock height and the distance above the keel. The graph axes represent the distance from the forward perpendicular (in percent of ship's length) versus corresponding deadrise angle (in degrees).

The effect of changing sea state on maximum pressure is shown in Fig. 16.61. The effect of an increase in significant wave height on the maximum pressure is much less than might be expected. The figure shows that the high pressure due to wave

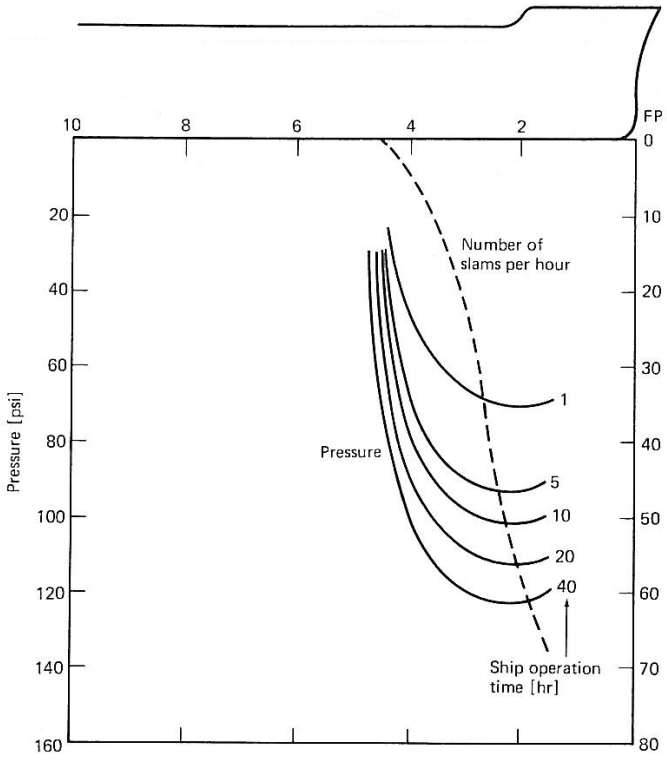


Figure 16.57 Number of slams per hour and most probable extreme pressure [170].

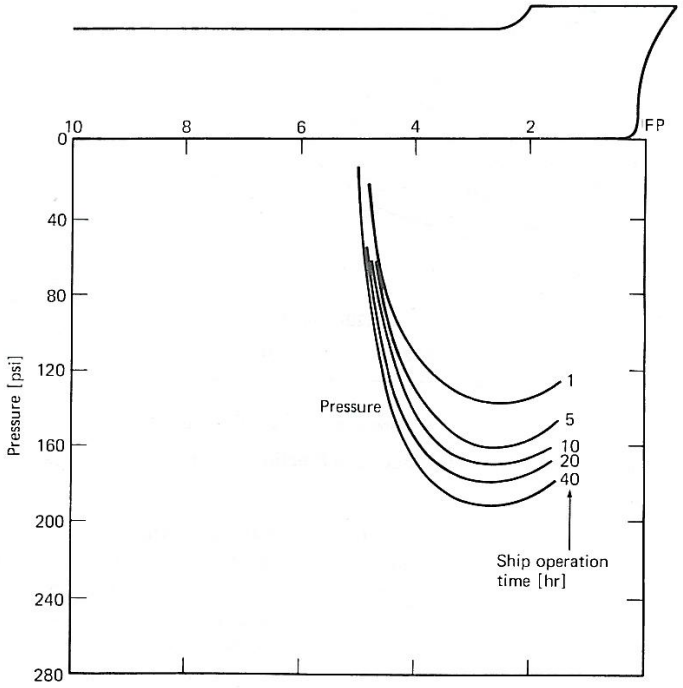


Figure 16.58 Extreme pressure for which the probability of being exceeded is 1% [170].

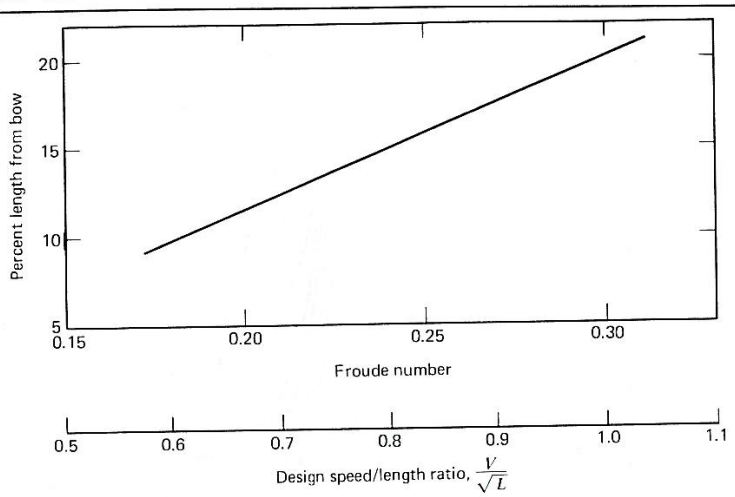


Figure 16.59 Location of bottom damage as a function of speed [19a].

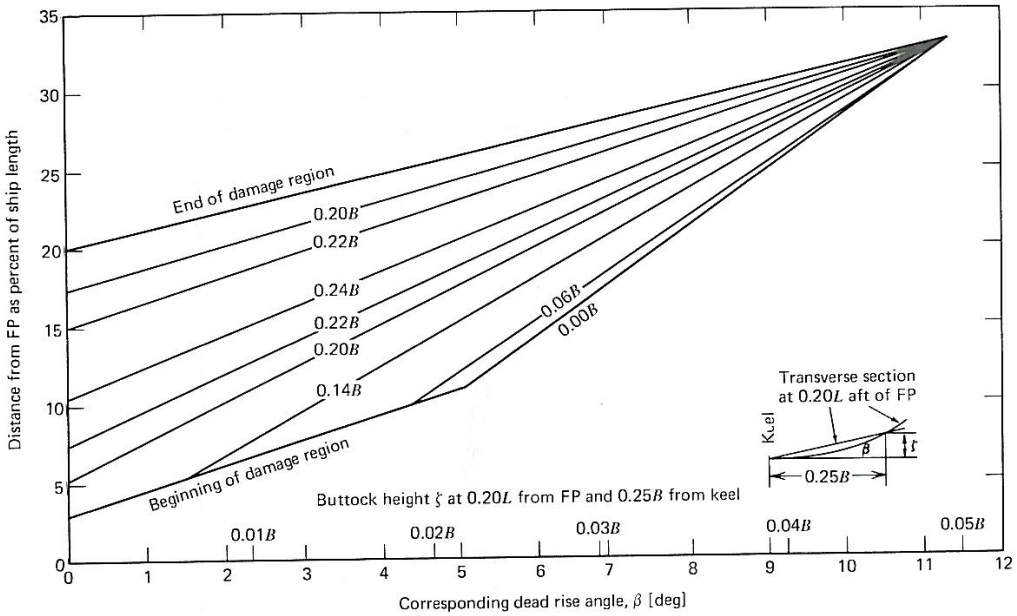


Figure 16.60 Bottom damage as a function of deadrise angle [126a].

impact is caused by the particular phasing between the ship motion and the wave and by the steepness of the waves, and hence the maximum pressure may occur over a wide range of significant wave height.

Figure 16.62 shows the important dependence of maximum pressure on speed. For example, a decrease in speed from 14 to 11 knots reduces the maximum pressure by about 35%.

Model experimentation shows that the magnitude and nature of the impact pressures depend on ship speed and sea state, and the results of such experiments make possible the prediction of the maximum safe speed for any selected design limit of impact pressure for a particular ship form and sea state. A possible redesign of the hull shape above water

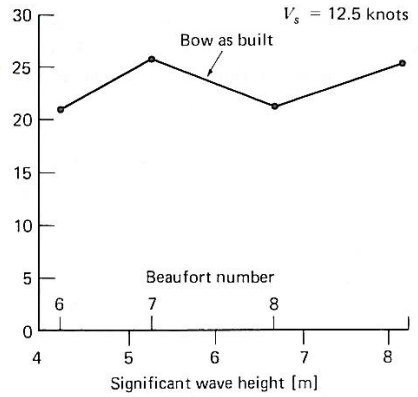


Figure 16.61 Maximum pressure increase as a function of sea state [161].

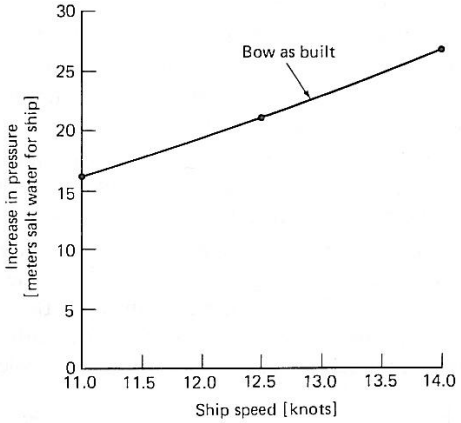


Figure 16.62 Maximum pressure increase as a function of speed [161].

may also result, experimentally, in a drastic reduction in the severity of the impacts.

It has been found by experiments that the natural pitching period is the minimum time interval between two successive slams. It is maintained that consideration of the peak pressure is not very important in the actual design, since the peak pressure has a very short duration and travels outboard at a very high speed. However, the peak pressure is important in studying the effects of ship form, speed, wave height, and wave length.

Figure 16.63 shows the results for damage most likely to occur for various sea states and ship speeds. The following conclusions can be drawn from this figure:

a. Slamming damage is not likely to occur in sea state 5 or lower for any ship speed up to 20 knots.

b. For sea state 6 or higher, voluntary reduction of speed is necessary to avoid damage to bottom plating and crew discomfort.

c. The tolerable speed is approximately the same as the speed free from slam damage in almost all sea states.

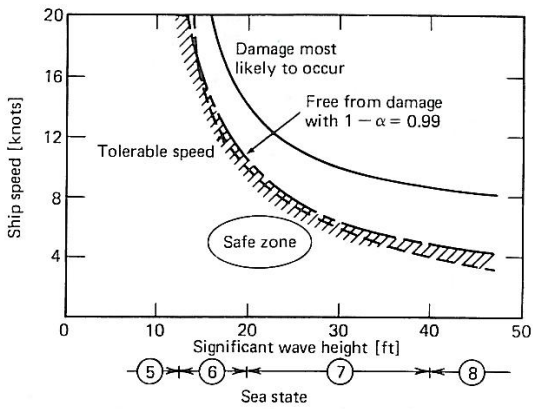


Figure 16.63 Attainable ship speeds for various sea states from the point of view of slam (*Mariner*, light draft) [170].

Loads

To obtain the maximum bending moment at the midship section, the combined bending moments from various loads that cause excessive deflection should be determined.

Still Water Loads

The still water bending moment is different for different loading conditions, which may vary from voyage to voyage, depending on density or distribution of cargo and/or ballast. During a long voyage there may also be a considerable change in bending moment as fuel is consumed and ballast tanks are filled with sea water. The probabilities of different levels of bending moment can be obtained after histograms of still water bending moments are available, as shown in Fig. 16.64. This figure shows the frequency of occurrence of different values of still water bending moment for outbound and inbound (or ballasted) voyages. Note that the "maximum" shown in the histogram is the maximum value along the ship's length, which may or may not occur exactly in the midship section.

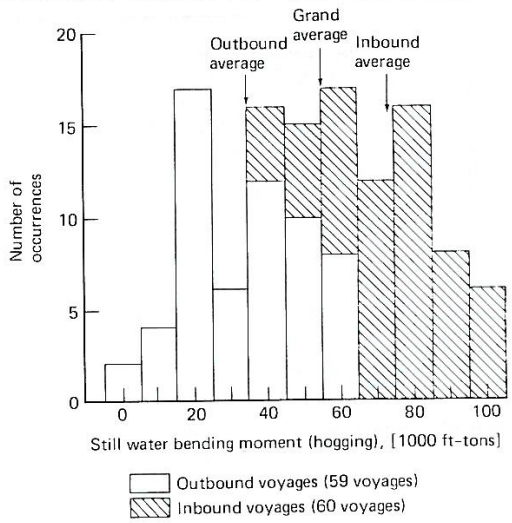


Figure 16.64 Histogram of calm water bending moments [134].

Wave Loads

The bending moment due to the wave system generated by the ship for forward speed in calm water should also be estimated for design purposes. The response amplitude operators for the vertical bending moment (at midship) and the vertical shear (at quarter length) should be determined for a range of wavelengths, headings, and speeds, although speed is not a very important factor for the wave bending moment for ships of normal displacement. If there is any chance of the maximum bending moment occurring at any other place other than the midship section, this should be taken into consideration. The next step would be to determine the bending moment responses for various sea conditions for the same route and to derive thereby probability density functions for both the vertical bending moment and the vertical shear. To determine the bending moments in irregular waves, the vertical and the lateral (horizontal) bending moments should be combined.

Stabilizer

Motion stabilization has become a significant development in recent years, particularly for passenger and naval vessels. An antirolling device not only provide comfort to the crew and passengers but also is useful for attaining a higher rough water speed. A ship fitted with an antirolling device need not slow down or change its course because of heavy rolling.

There is also a secondary effect of an antirolling device. When a ship encounters severe head sea conditions, heavy pitching is caused; this can be improved by changing course by even a few degrees. Often, however, a course change may produce excessive rolling. This means that the solution is, not course changing, but speed reduction. If an antirolling device is fitted, however, a course change may be possible without loss of speed.

Free Surface Tank

The following recommendations for the design of a free surface tank are given in Ref. 217:

a. Satisfactory results have been obtained for $\overline{GM}/B$ values between 0.03 and 0.18.

b. Free surface in the tank must be considered in the calculation of the static stability of the ship.

c. The tank should be as broad as possible and should be located as high as possible.

d. From the point of view of large yawing motions in the following seas, the tank should be located neither far forward nor aft of the midship section.

e. The depth of the tank should allow the water to rise to a height of approximately three times its height at rest. For the design purposes the tank depth may be estimated as $D_t > 2GM$. Although the optimum tuning of the tank is not possible for

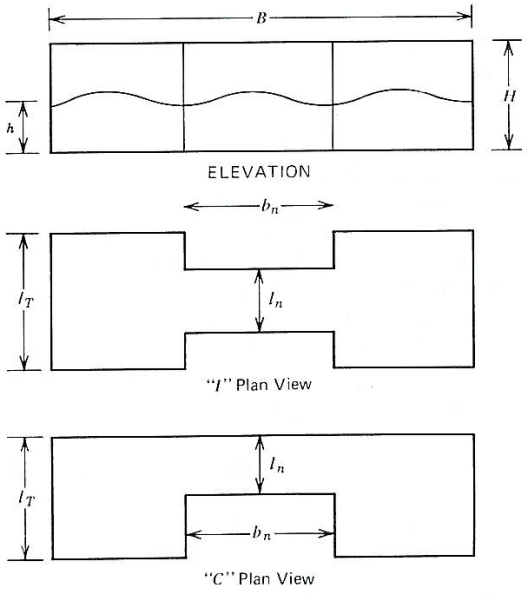


Figure 16.65 Nomenclature for a free surface tank.

every condition of loading, for large ships the water level can be adapted for the loading condition since in most cases $\overline{GM}$ is known.

f. After the breadth and length of the tank are settled, the water depth can be determined from the diagrams for

$$\mu_a \sin \varepsilon_t \text{ and } \mu_a \cos \varepsilon_t$$

given by Ref (217) for $\phi_a = 0.1$ radian (i.e. 5.7°) which is reasonable for normal design purposes (See Fig. 16.65). The figures for the nearest s/b (s is distance from tank bottom to rolling axis, b is tank breadth) ratios are selected, for the required s/b value is obtained by interpolation.

g. The range of frequency that is of interest lies between $0.75\omega_\phi$ and $1.25\omega_\phi$, since the roll amplitude within this frequency range is of most significance. In other words, extra damping is necessary only in this frequency region.

h. By estimation or graphical interpolation, it is first necessary to determine the h/b (h is water depth in the tank at rest) ratios that give the highest quadrature component at the natural frequency of the ship.

For the obtained h/b ratio, Δc (equation 14.3) and the corrected natural frequency ω'_ϕ (equation 14.5) are calculated, using the in-phase component $\mu_a \cos \varepsilon_t$, which is read from Fig. 16.67. The process is repeated until the difference between the "input" and the "output" is considered to be insignificant. If the same water depth is used for different loading conditions, the entire frequency range (from 0.75 times the lowest corrected natural frequency to 1.25 times the highest value) should be covered by the quadrature component of the tank moment.

Equation 14.7 is used to calculate the ratio of roll amplitude to wave slope, which can give information about the effectiveness of the tank.

To keep the tank weight at a minimum, the tank has to run the full beam of the ship. The loss of metacentric height is less, given as [13]

$$\delta\overline{GM} = \frac{(\rho_f/\rho_s)[l_T(B^3 - b_n^3) + l_n b_n^3]}{420\Delta} \tag{16.28}$$

If b_n is small compared to B, we can simplify this expression as follows:

$$\delta\overline{GM} \approx \frac{(\rho_f/\rho_s) l_T B^3}{420\Delta} \tag{16.29}$$

The typical value of $\overline{GM}$ can be considered to be 15 to 30% of the uncorrected $\overline{GM}$. With such an approximation one can reduce the value of l_T (the fore-and-aft dimension of the tank), since the beam and displacement of the ship are known during the preliminary design.

To obtain the maximum capacity for the tank, it should be half full, that is, $h = H/2$. Then

$$\tau_{sat} = \tan^{-1}\left(\frac{H}{B}\right) \approx 57\frac{H}{B}\text{deg} \tag{16.30}$$

whereas

$$\tau_{sat} \approx 114\frac{h}{B}\text{deg}$$

or

$$\tau_{sat} \approx 114\frac{H-h}{B}\text{deg}$$

whichever is smaller, if h is not equal to $H/2$. The value of τ_{sat} should be greater than 10°. When the tank is half full (i.e., $h = H/2$), $H = 0.2B$, and this corresponds to $\tau_{sat} = 11.4°$

The value of b_n and l_n should be properly chosen for the desired timing. If

$$B' = B + \frac{b(l_T - 0.9l_n)}{0.9l_n} \tag{16.31}$$

(the factor 0.9 can be considered to take into account the damping structures within the tank), then, from Ref. 13,

$$\omega_t = \left[\left(\frac{\pi g}{B'}\right)\tanh\left(\frac{\pi h}{B'}\right)\right]^{1/2} \tag{16.32}$$

If $h/B < 0.10$, the natural frequency of the tank is obtained as

$$\omega_t = \pi\sqrt{\frac{gh}{B'}}$$

Equating this to the desired tank frequency, we have

$$B' = 1.05B\sqrt{\frac{h}{\overline{GM}_{\text{uncorrected}}}} \tag{16.33}$$

Since the right-hand side is known, l_n and b_n should be properly chosen to obtain the right value of B'.

Now the volume and weight of the tank fluid are obtained as

$$V_f = [l_T(B - b_n) + l_n b_n]h \tag{16.34}$$

and

$$W_f = \rho_f g V_f \tag{16.35}$$

and the total tank volume is known to be

$$V_t = V_f\frac{H}{h} \tag{16.36}$$

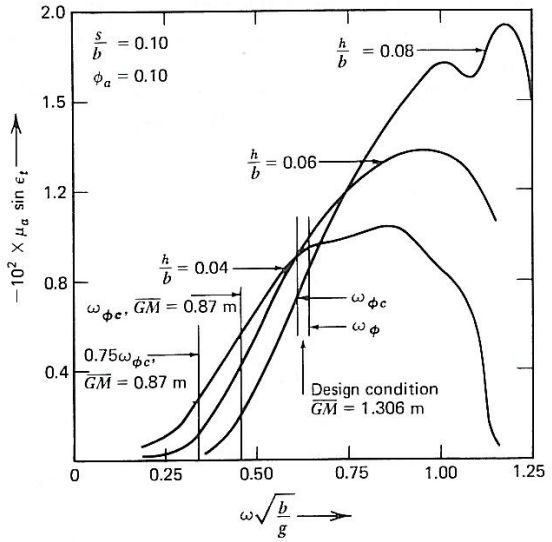


Figure 16.66 Tank water depth for the design condition [217].

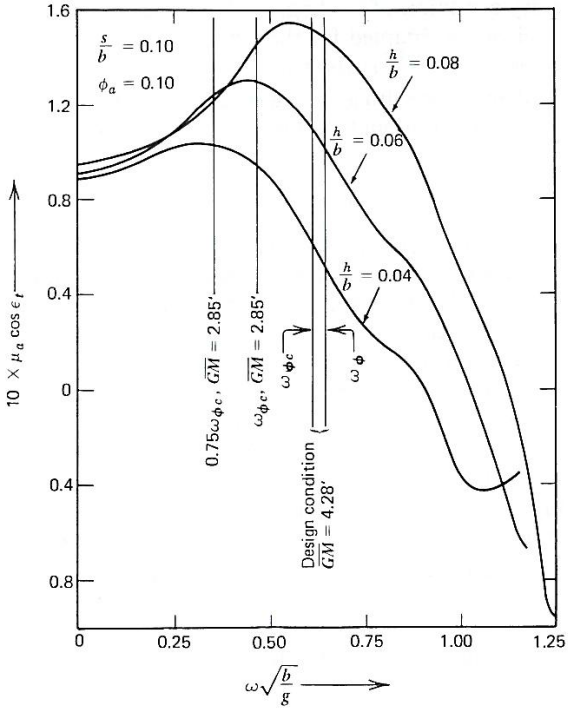


Figure 16.67 Determination of in-phase component for design condition [217].

Example 16.4

Given:

$L_{pp} = 500$ ft
$B = 71.42$ ft
$D = 44.42$ ft
$T = 28.58$ ft
$\nabla = 20{,}410$ tons in Salt water
$\frac{\overline{GM}}{B} = 0.06$
$\overline{KG} = 24.52$ ft
$\frac{k_{xx}}{B} = 0.38$
$T_\phi = 14.52$ sec
$\omega_\phi = 0.4327 \text{ sec}^{-1}$
$\nu = 0.069$ (obtained from model experiments)
b = breadth of tank available = 70.87 ft
l = length of tank available = 13.12 ft
$\frac{s}{b} = \frac{\text{distance from tank bottom to rolling axis}}{\text{tank breadth}}$
$= 0.10$ (should be as high as possible)

Perform the design calculation for a free-surface tank.

Solution:

Values of $\mu_a \cos \varepsilon_t$ and $\mu_a \sin \varepsilon_t$ are obtained for $s/b = 0.10$ by interpolation and are shown in Figs. 16.66 and 16.67. For $\omega_\phi = 0.4327$ (given), the non-dimensional frequency parameter

$$\omega_\phi \sqrt{\frac{b}{g}} = 0.642$$

From the figure for $\mu_a \sin \varepsilon_t$, the optimum value for h/b (where h is water depth in the tank at rest) lies between 0.04 and 0.06. Since the natural frequency corrected for $\mu_a \cos \varepsilon_t$ is lower than the original natural frequency, the value for h/b is chosen as 0.04. The corrected natural frequency is obtained by the iterative method as

$$\omega'_\phi = 0.412$$

and

$$\omega'_\phi \sqrt{\frac{h}{g}} = 0.611 \text{ with } \mu_a \sin \varepsilon_t = 0.913 \times 10^{-2}$$

The last value is very nearly the optimum.

Note that, if h/b had been chosen as 0.05, the performance of the tank would have been greatly inferior, while the gain in the design condition would have been insignificant.

Figure 16.68 shows ϕ_a/ϕ_{st} against nondimensional frequency values, obtained with $\nu = 0.069$ determined from the measured peak value of ϕ_a/ϕ_{st}. The rolling motion with the tank is calculated using (13.4).

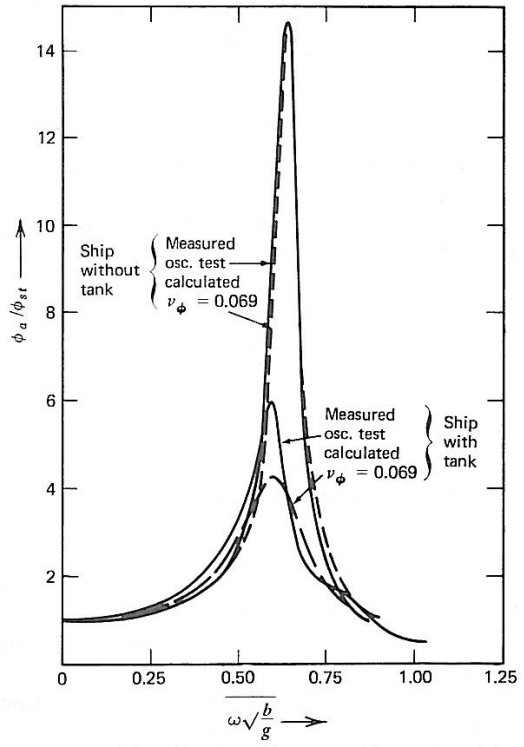


Figure 16.68 Magnification factors with and without stabilization tank in calm water [217].

U-Tube Tank

A simplified method for the design of a U-tube tank is given in Ref. 13. If the tank runs the full beam of the ship (see Fig. 14.8*e*) the loss of metacentric height due to the free surface within the tank is given by

$$\delta\overline{GM} = \frac{\rho_f}{\rho_s} l_T \frac{B^3 - b_n^3}{420\Delta} \tag{16.37}$$

A further simplification can be made if b_n is small compared to B; then

$$\delta\overline{GM} \approx \frac{\rho_f}{\rho_s} \frac{l_T B^3}{420\Delta}$$

When the wing tanks are half full, the beginning of saturation is given by

$$\tau_{sat} = \tan^{-1}\left(\frac{H}{B}\right) \approx 57\frac{H}{B}\text{deg}$$

whereas, if h is not $H/2$, then

$$\tau_{sat} \approx 114\frac{h}{B}\text{deg}$$

or

$$\tau_{sat} \approx 114\frac{H-h}{B}\text{deg}$$

whichever is smaller.

Since it is the designer's aim to have τ_{sat} greater than 10°, the value of H is obtained as

$$H = 0.2B$$

The tank frequency is given as (see also Section 14.2)

$$\omega_t = \sqrt{\frac{2g}{S}}$$

where, for the configuration shown in Fig. 14.8*e*, S, the effective tank length, is expressed by

$$S = h + B - b_n + b_n\frac{l_T(B-b_n)}{2l_n p} \tag{16.38}$$

Equating this expression to the required tank frequency, one obtains

$$S = 0.223\frac{B^2}{\overline{GM}_{\text{uncorrected}}} \tag{16.39}$$

Since the right-hand side of this expression is already known to the designer, the value of S can be easily determined in an early stage; hence b_n, p, and l_n are selected in accordance with the value of S.

Furthermore, the fluid volume of the U-tube tank and the weight of the tank fluid, respectively, are obtained from the following expressions:

$$V_f = l_T(B-b_n)h + b_n l_n p \tag{16.40}$$

and

$$W_f = \rho_f g V_f \tag{16.41}$$

whereas the total volume of the tank is given by

$$V_t = l_T(B-b_n)H + b_n l_n p \tag{16.42}$$

Active Antiroll Tanks

As a result of both the theoretical and the experimental study reported in Ref. 238, the following are some of the conclusions reached in regard to the design of active antiroll tanks:

1. The tank should have a natural frequency as large as possible; this amounts to a frequency that is about 1.2 to 1.7 times that of the ship.
2. The free surface area also should be as large as possible if stability considerations permits; this normally amounts to a loss of metacentric height of about 20 to 40%.

3. Roll stabilization by active roll tanks can be as high as 80%, depending on the ship characteristics and speed, the heading of the wind, and the dominant waves of the seaway. The most beneficial effect takes place for a following quartering sea, whereas the least effect is found for low sea states in head seas.

Although a passive antiroll tank may not be as effective as an active system, both tank systems, active and passive, are effective even when the ship is moving at a very slow speed or has stopped.

In principle, the active antiroll tank has a configuration similar to that of a U-tube tank. The significant difference between an active and a passive tank system is that the natural frequency of the active tank is about 30 to 40% greater than the vessel's natural frequency when the air valve is open, and it is also necessary that an active tank have an equivalent linear damping ratio a little less than that of a passive tank. To obtain the proper tuning the following expression is used for the equivalent length of the tank [13] (see also Section 14.2):

$$S = 0.178 \frac{B^2}{\overline{GM}_{\text{uncorrected}}} \tag{16.43}$$

ANTIROLL FINS

For an antiroll fin stabilization system it is necessary to determine the fin size and the resulting weight of fins. The size of fins is generally defined in terms of the static roll angle to be generated per degree of fin angle at a design speed (e.g., speed/length ratio of 1.2) which is expressed as

$$\phi_{\text{static}} = \arcsin\left(\frac{K_{\text{fin}}}{\Delta GM}\right) \tag{16.44}$$

where ϕ_{static} = static roll angle
K_{fin} = total roll moment of fins
Δ = vehicle displacement
GM = metacentric height

The total roll moment caused by the fins is obtained as follows:

$$K_{\text{fin}} = (\tfrac{1}{2}\rho u^2 A_{\text{fin}} C_{L_\alpha} \alpha_F) \cos\gamma d_{\text{fin}} \tag{16.45}$$

where ρ = density of water
u = vehicle speed (e.g., for a speed/length ratio of 1.2, $u = 1.2\sqrt{L_{WL}} \times 1.689$ ft/sec)
A_{fin} = area of all fins
C_{L_α} = effective slope of the lift curve when plotted to the base of angle of attack
α_F = effective angle of attack for the fin (for this method of design, α_F is considered to be 1°
γ = angle between the fin and the CG of the ship (see Fig. 14.12*a*)
d_{fin} = distance between the center of area of the fin and the ship CG
L_{WL} = waterline length

To account for the effects of the hull boundary layer, hull curvature near the fin, and interference from bilge keels, it is permissible to ignore image effect. The geometric aspect ratio is used to determine the lift curve slope.

Table 16.16 is a useful guide for the preliminary design [13], especially since design data for active fins are rather scarce.

ANTIPITCHING FIN

The following general conclusions have been reached from model experiments [195] regarding antipitching fin location, size, and configuration:

1. Maximum reduction in pitching motion is obtained if the fin is fitted in the forward 10% of the hull.
2. The farther forward the fin is located on the ship, the more hull vibration is to be expected.
3. Reductions in pitching and heaving motions, as well as in bow acceleration, increase approximately linearly with fin area.
4. The magnitude of induced vibrations is proportional to fin area and impact force.
5. A fin having properly sized holes and appropriate shape may be more effective in reducing vibrations.

The optimum location which depends on fin configuration and vessel speed may also be presented in tabular form (see Table 16.17 as a guide for the appropriate location of a rectangular fin.) In addition, model test results have provided the following design information:

1. Fins operate most effectively near the synchronous range and have little influence at higher or lower frequencies.
2. Fins have little effect on the phase lag of heave and pitch, but it should be remembered that a slight change in phase can have a marked effect on relative motions.
3. The area of fin planform does not have significant effect on motions. Although an increase in planform area is helpful in obtaining increased pitch reduction, this increase is not in direct proportion to the increase in area.
4. Loadings caused by the vorticity effect can be

TABLE 16.16 SHIP DESIGN IMPACT DATA FOR ACTIVE FIN SYSTEM

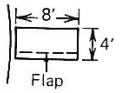
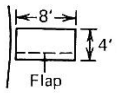
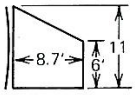
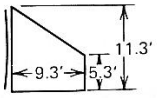
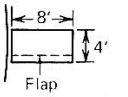
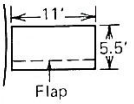
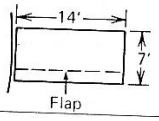
Installation	Fin Planform	Fin Area 1 Side [ft²]	Total System Weight [long tons]	Weight Group 518 [long tons]	Weight Group 113 [long tons]	Internal Volume, 1 Side [ft³]	Control Lower [hp]	Maximum Angle/ Flap Angle [deg]	Time Stop to Stop [sec]	Maximum Design Lift [long tons]	Comments
DE 1040 Class Sperry		32	(Manual) 13.5	—	—	134	20	± 25	~ 2	23	
DE 1040 Class Denny-Brown		32	16.5	~ 17.7	4.4	277	20	± 23 – 23	1.3	23	
DE 1052 Class Sperry		74	20.5	—	–	226	50	± 30	2	38.4	
DE 1052 Class Denny-Brown		77	27.7	25.4	6.0	308	75	± 30	1.6	38.4	
Sperry Gyro Fin		32	34				25			16.5	Retractable Lost Buoyancy = 14 Total
Sperry Gyro Fin		60.5	54				40			31	Retractable Lost Buoyancy = 26 Total
Sperry Gyro Fin		98	96				75			50	Retractable Lost Buoyancy = 34 L.T. Total

TABLE 16.17 [166]

Effects	Location of Fin Aft of Forward Perpendicular				
	Forward Perpendicular	0.05*L*	0.10*L*	0.15*L*	0.20*L*
Increase of Resistance [%]	0	1.9	9.2	16.0	
Reduction of Pitching [%]	22.8	21.9	18.5	12.4	
Reduction of Heave [%]	31.5	20.7	12.9	8.0	
Reduction of Bow Vertical Acceleration [%]	24.5	19.0	15.5	11.8	
Reduction of Slamming [%]	85.0	85.0	81.8	67.7	
Intensity of Induced vibration	1	0.66	0.35	0.10	0.02

lessened by deeper submergence, greater fin span, tip fences, and relief mechanisms such as slots and holes.

5. Fins with greatly increased aspect ratio should provide more effective pitch stabilization and better flow conditions in the vicinity of the hull.

6. Fins should be placed as low as possible. Fins mounted about 10 ft below the keel line should ensure adequate submergence under all operating conditions. However, such configurations require special devices to permit the use of most docking facilities and to allow for other shallow water operations.

7. The aspect ratio is a significant parameter in the design of fins. The pitch reduction is 30% less for a fin with an aspect ratio of 0.5 than for a fin with an aspect ratio of 2.0.

8. The horizontal vibration at the bow due to the large angle of attack on the fin during the downward motion gives rise to a low pressure on the upper fin surface. Just before the downward stroke begins, the fin is near the surface and the low-pressure area causes suction and possible ventilation. As the fin goes deeper, the bubble collapses, causing a large pressure impact. Since port and starboard fins do not ventilate uniformly, a differential pressure impact situation is created.

16.8 DESIGN PLOT

A simplified method of presenting the seakeeping performance of a specific design is to plot a polar diagram, as given in Fig. 16.69, which shows the maximum attainable speed for all headings in a seaway, obtained simply by calculating the included area. In seaway operation, if speed is the main criterion for seakeeping performance, the included area of a polar diagram may be considered as the measure of merit for seakeeping design. A polar diagram may be obtained in the following manner [35].

If the maximum significant roll for the effective operation of a certain equipment on board a vessel is 15°, the vessel's maximum attainable speed for all heading angles is represented by plot *A* on Fig. 16.69. Similar plots may be obtained for other limitations. For example, the generally accepted design criterion for maximum speed in still water can be modified to take into account the added resistance in a seaway (see plot *B* of Fig. 16.69); on the other hand, plot *C* of the same figure takes into account a specified number of slams per hour. Thus the shaded area of Fig. 16.69 is the effective measure of merit for the seaway performance of the ship.

It can be said, therefore, that a large number of variables and limitations may be taken into account with the help of a polar diagram, which in the end delivers a simple, well-defined measure of merit.

However, the polar diagram is determined for a particular sea state, which also varies with season and region of operation. Therefore statistical data similar to those given in Ref. 102 may be adopted; these data indicate the percentage of time that a vessel will experience a specific sea state (Fig. 16.70*a*), and this percentage of time is then multiplied by the included area (measure of merit) of the polar diagram for the sea state in question, as shown by a single

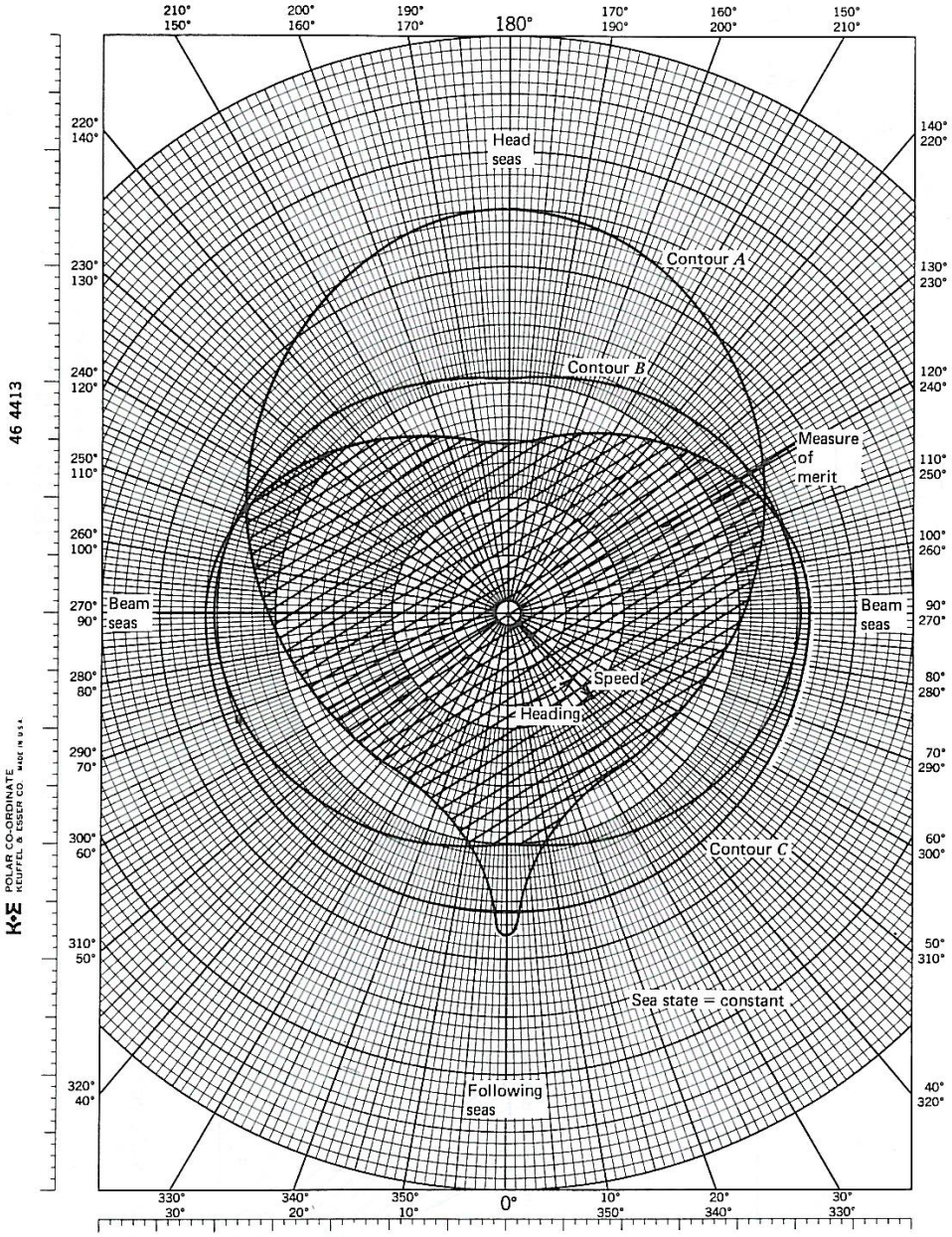


Figure 16.69 Seakeeping speed polar diagram [35].

point on Fig. 16.70*b*. The area under this figure obtained for various sea states will be the measure of merit and should be maximum for a particular design. The seakeeping performance efficiency may then be considered to be the ratio of this area to that obtained by multiplying the ordinates of Fig. 16.70*a* by the area of the polar diagram for calm water conditions (see Fig. 16.71).

Figure 16.72 illustrates the complete flow chart for the calculation of seakeeping performance design [35].

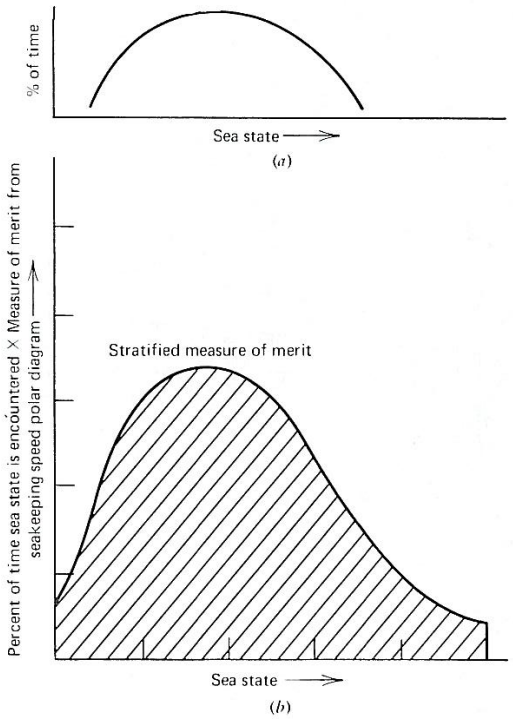


Figure 16.70 Seakeeping performance diagram [35].

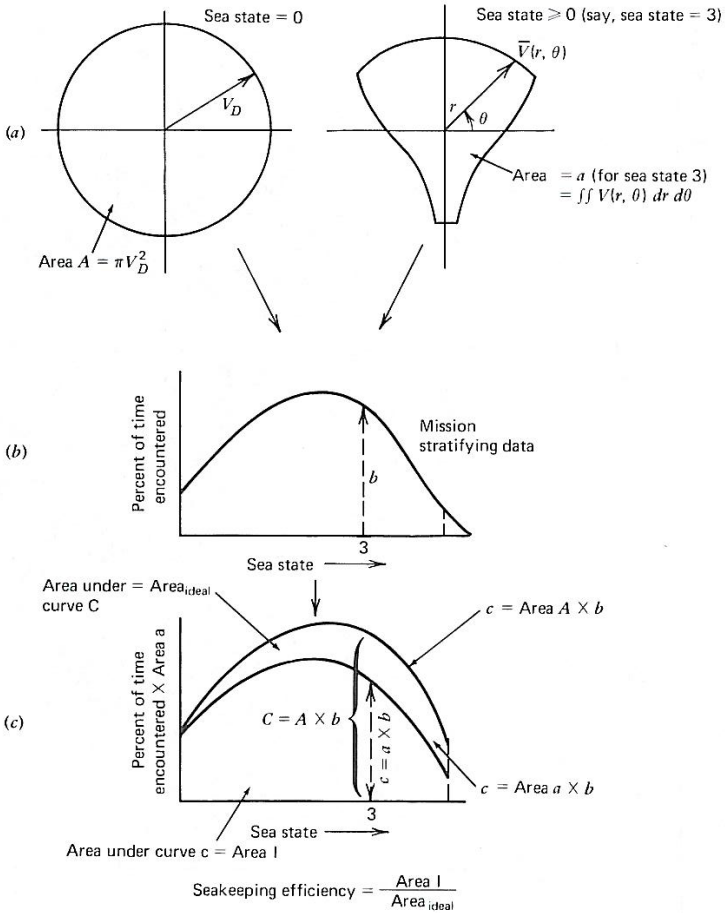


Figure 16.71 Seakeeping performance efficiency [35].

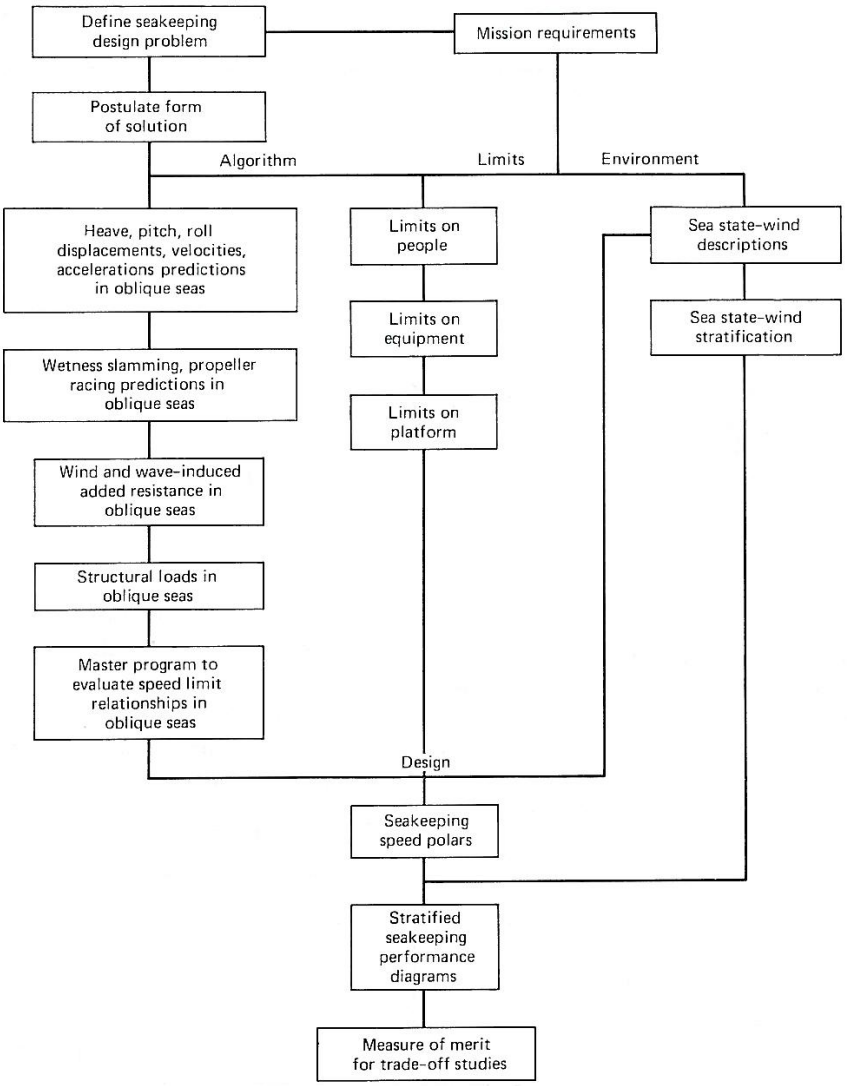


Figure 16.72 Flow chart for seakeeping design [35].

Chapter

Seventeen

SEAKEEPING OF ADVANCED MARINE VEHICLES

17.1 GENERAL

Recently there has been considerable development in regard to high-performance vessels. The problems related to the seakeeping investigation of advanced marine vehicles are considerably different from those for conventional surface vessels. The types of vehicles of main interest in this respect are as follows:

a. Catamarans, low waterplane and conventional.
b. Ocean engineering vehicles.
c. Planing crafts.
d. Hydrofoil boats.
e. Air cushion vehicles and surface effect ships.
f. Submarines.

Figure 17.1 illustrates some concepts of advanced

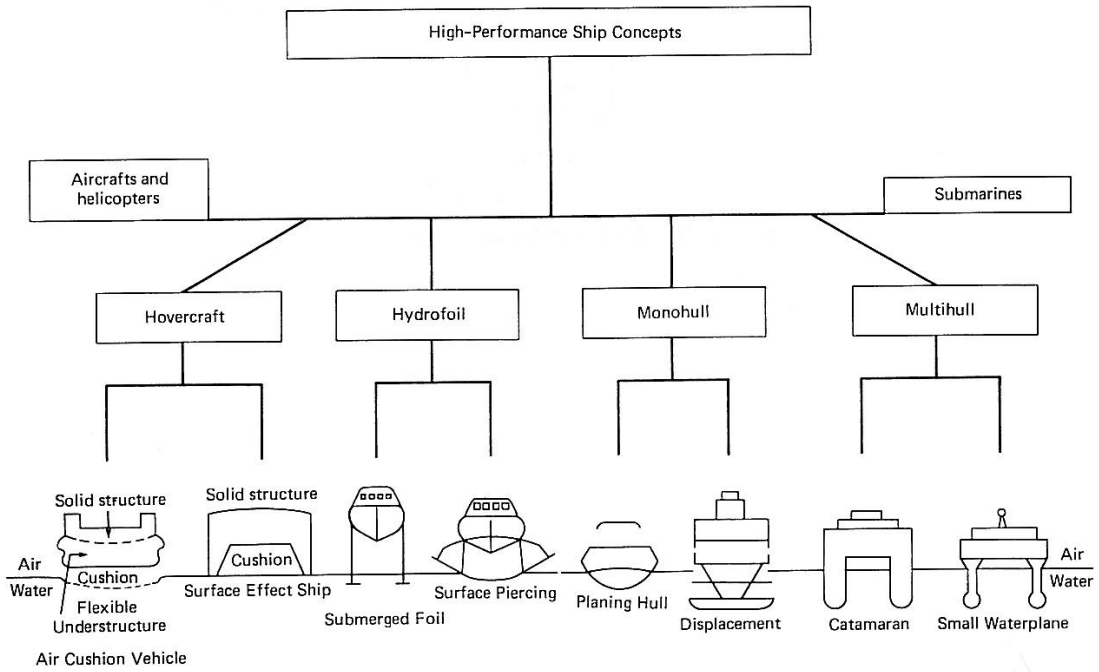


Figure 17.1 Concepts of advanced marine vehicles.

marine vehicles, mainly of four categories, namely, Hovercraft, hydrofoils, monohulls, and multihull vehicles. Again, the monohull vehicles can be classified into two groups: displacement vehicles and planing crafts. Also, the multihull vehicles can be of two types, namely, normal catamaran forms and the small waterplane area twin hull (SWATH). The air-cushioned vehicles are classified as hovercrafts and surface-effect ships with sidewalls, whereas the hydrofoil boats can be grouped as either fully submerged foil system or surface piercing foil system.

Advanced marine vehicles have two basic disadvantages when compared to conventional displacement type surface ships, namely, high cost per ton and low endurance, which may be expressed either in nautical miles or in hours. However, advanced marine vehicles are designed for different missions and tasks, which may require either high-speed operation or, in some cases, a more stable platform.

17.2 CATAMARANS

Considerable interest has been manifested in the design of twin-hull or catamaran ships for special uses, such as oceanographic research, ferries, and oil-drilling platforms.

The main advantage of a catamaran ship is the large internal volume, the large useful deck area (20 to 40% greater than that of a corresponding single-hull vehicle of the same displacement), and the large transverse stability, which, however, can be used effectively only if the catamaran hull forms possess good seaworthiness characteristics.

Until recently catamarans were often regarded as inferior to monohull surface ships. Although less rolling motion is to be expected from catamarans, accelerations are often excessive, and other motions are almost the same for normal catamaran hulls. A significant improvement in the catamaran form is the recent introduction of the low-waterplane (LWP) catamarans.

The significant motions of catamarans in waves are generally heaving and pitching in head seas since both the wave impacts at the bottom of the cross structure and deck wetness and slamming at the forefoot are caused by these two motions.

Typical body plans are shown in Fig. 17.2*a*, and particular dimensions in Table 17.1. Results of seakeeping tests in regular head waves for some

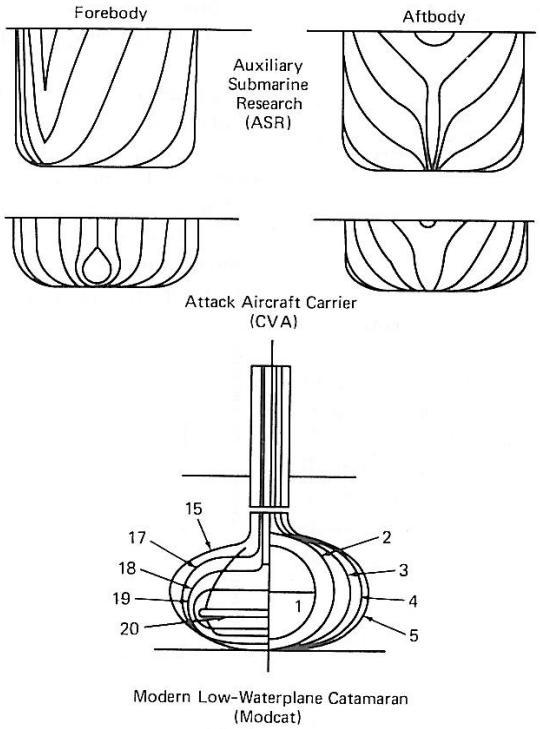


Figure 17.2*a* Typical catamaran body plan [196].

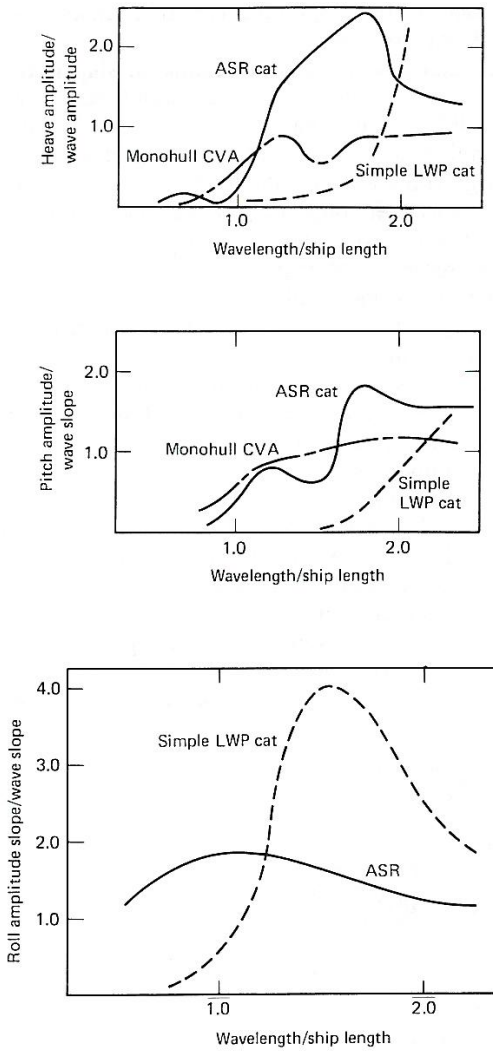


Figure 17.2*b* Heaving, pitching, and rolling motions.

different kinds of catamaran forms are given in in Fig. 17.2*b*. Both heaving and pitching motions are given for a symmetric catamaran, a simple LWP catamaran, and (for comparison) a monohull CVA. All ships were of equal length. The favourable pitch and heave response in head seas of the catamaran in comparison to the other forms is most encouraging.

The rise in the response curves at $L_W/L = 2$ indicates the onset of resonance. Up to the point of resonance, however, both heave and pitch are insignificant and considerably less than for monohulls.

An improved LWP catamaran had considerably less waterplane area than the simple LWP catamaran.

TABLE 17.1 PARTICULAR DIMENSIONS [196]

Particular	ASR	CVA	Modcat
Beam (each hull) at the Waterline [ft]	24.0	95.8	30.42
Draft [ft] (station 10)	18.0	36.5	69.5
Length at the waterline [ft]	210.0	820.0	850.0
Displacement of each hull [long tons] (salt water)	1386	47,400	50,500
Hull spacing [ft]	38.0	141.2	207.0
Longitudinal center of Gravity Aft of FP [ft]	105.6	419.0	420.0
Longitudinal Radius of gyration [ft]	0.233*L*	0.23*L*	0.26*L*
Block coefficient	0.55	0.59	0.964
Scale ratio	16.89	54.67	50.0
Vertical height of neutral axis from mean waterline [ft]	23.0	61.5	68.2

Motion experiments on this improved form demonstrated still less pitch and heave response and, in addition, a shift of resonance to $L_W/L = 4$. This means that a substantial latitude in the selection of ship length is possible with little effect on ship motions.

An analytical method has been developed to calculate the hydrodynamic coefficients and exciting force by strip theory, taking into consideration the interaction between both hulls [126]. Because of the basic geometry of the catamaran the magnitude of the radiated waves is relatively smaller, and so the linear portion of hydrodynamic damping, which is ordinarily influenced considerably by the waves generated during ship motions (except roll), is significantly smaller.

The rolling motion of catamarans is also significantly different from that of a conventional monohull vehicles, since catamarans invariably have a greater value for the metacentric height. Thus catamarans

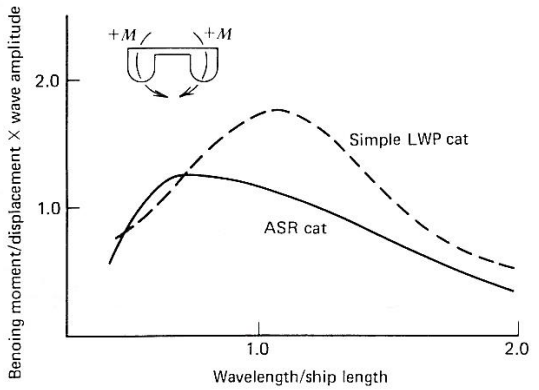


Figure 17.2*c* Vertical wave bending moment in regular beam seas [196].

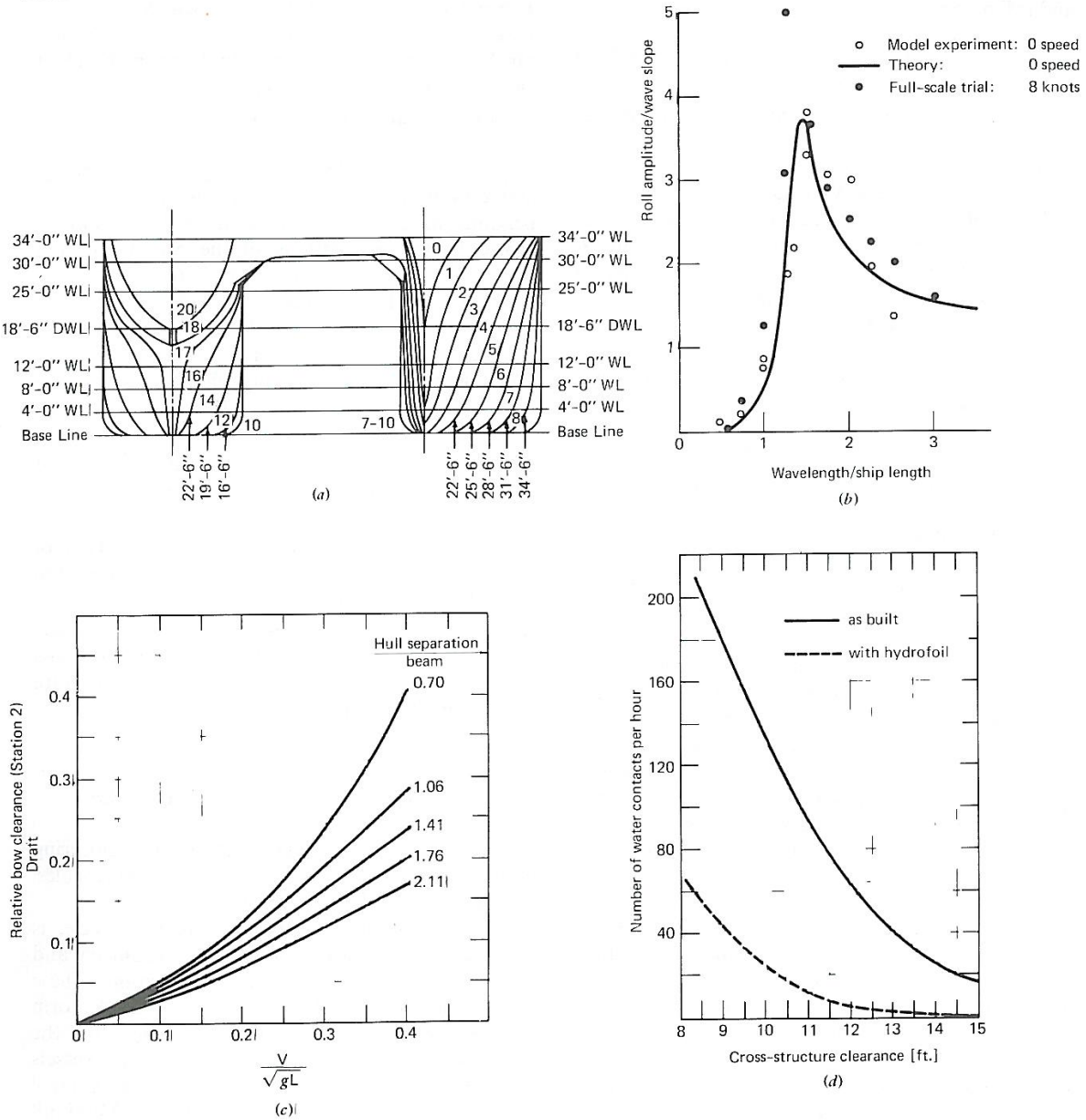


Figure 17.3 Body plan and seakeeping characteristics of U.S.N.S. *Hayes* [95]. (*a*) Body plan. (*b*) Comparison of roll motion in beam waves. (*c*) Elevation of water surface relative to bow at centerline of catamaran $0.1L$ aft of FP, preliminary design model of ASR 21–22. (*d*) Number of water contacts of cross structure versus clearance at 12 knots in head seas.

have comparatively decreased roll angles, natural periods of rolling, and also lateral accelerations. These values, when associated with the natural pitching period, produce a different effect on the crew from the habitability point of view. The random variation of the plane in which the predominant angular motions, known as "corkscrew" motion occur, may, along with the linear and angular accelerations, cause severe seasickness. The corkscrew motion tends to become severe as the natural pitching

and rolling periods become closer to each other.

Comparative rolling motions for two catamarans are also shown in Fig. 17.2. The roll response indicated for the LWP catamaran is somewhat higher in amplitude than that for the ASR. The use of flare in the upper portions of the struts and active antiroll or motion damping devices may help to reduce the roll amplitude for the LWP catamaran.

The problem of slamming on the cross structure of a catamaran is rather unique. For the determination of slamming pressures both the relative motion and the clearance of the cross structure above water are important considerations.

Seaway loadings (obtained from model experiments in regular sea) on catamaran bridging structures are illustrated in Fig. 17.2*c*. These loads are a result of hydrodynamic forces on the hulls and do not include the inertial effects of bridge mass. Of the sea-induced moments applied to LWP catamarans (i.e., longitudinal bending, transverse bending, and torsion), the dominant load appears to be in the transverse rather than the longitudinal direction. In the longitudinal direction LWP catamarans tend to have a uniform distribution of weight, and this, coupled with their reduced waterplane area, produces low hogging and sagging moments. Longitudinal moments are resisted by deep structural sections of high modulus, and, consequently, low primary bending stresses are developed. In the transverse direction, however, large moments are resisted by shallow bridging structure sections of relatively low modulus. Stress levels produced by sea-induced loading therefore tend to be greater in the transverse than in the longitudinal structure; in the case of monohulls our experience is just the opposite.

To predict the magnitude and distribution of the impact pressure acting on this type of structure, it is convenient to treat the components separately. This approach assumes that there is hydrodynamic independence of the components. The cross structure is then treated as a flat plate with its two ends restricted, and the twin hulls are modeled as two-dimensional wedges with appropriate trim and deadrise angles.

The motions of the vessel in regular and irregular seas are critical factors if an accurate estimate of the impact pressure is desired. This pressure is highly dependent on the relative velocity at impact between the vessel and the surface of the water.

The seakeeping characteristics of U.S.N.S. *Hayes* are shown in Fig. 17.3.

The following recommendations are made in Ref. 95 for the seakeeping design of a catamaran:

a. For the necessary advantages, such as large deck area and greater stability, the catamaran configuration can be designed very successfully from the point of view of overall seakeeping qualities.

b. For any catamaran design the installation of a hydrofoil forward should be considered very favorably; a hydrofoil helps in reducing rolling, pitching, and corkscrew motions, as well as cross-structure bending moments and cross-structure slamming. However, the proportions of the catamaran hull form, especially the beam/draft ratio (i.e., the separation between the two hulls) should be different if a hydrofoil is fitted. Also, the hydrofoil should be so located that it does not broach the free surface under operating conditions; broaching may be expected in the case of very steep, regular waves at pitch resonance.

c. The prediction of seakeeping characteristics should be confirmed by model tests in order to ensure satisfactory seaway performance.

d. A study of the effect of the corkscrew type of motion on human endurance should be made from the habitability point of view.

e. In addition to motion prediction, a realistic assessment of the impact pressures on the cross structure, as well as the velocity for cross-structure slamming, should be made.

17.3 OCEAN ENGINEERING VEHICLES

There are three general classes of Ocean engineering vehicles: (a) floating vehicles, (b) semisubmersibles, and (c) submersibles (Fig. 17.4).

The first of these types, the floating vehicle, is defined as having a fixed underwater geometry and waterline with a free surface penetration. These vessels may take one of two forms. Single form floating vehicles are the most conventional and the most often used in ocean engineering. These vessels are also most readily subject to motion control and least affected by extreme wind and sea. Multihull vehicles (catamarans or trimarans) have begun to take on some tasks in ocean engineering and are well known for their high initial stability and large deck area for a given displacement.

The second type, the semisubmersible vehicles, is a configuration with waterplane and an underwater geometry that is variable to satisfy particular requirements. These vessels protrude both in the air and in the water and are affected by wind, currents, and sea states. Stability can be achieved by either spacing

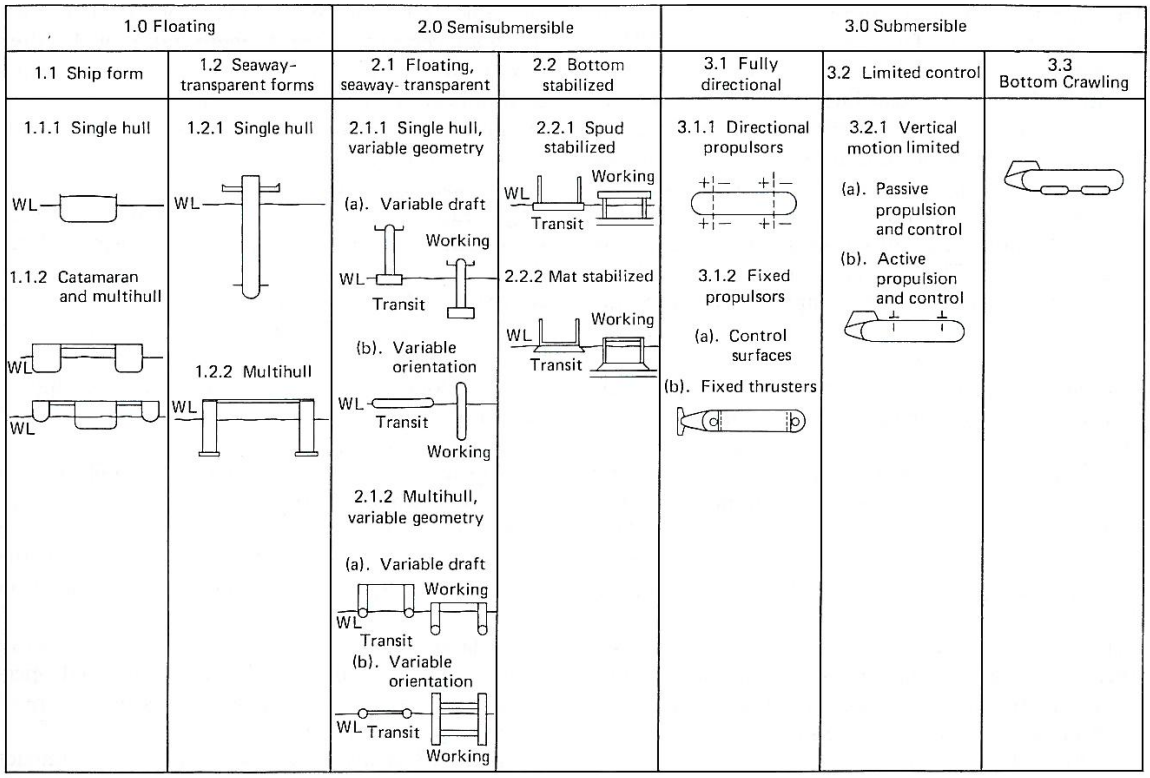


Figure 17.4 Classification of ocean engineering vehicles [179].

the segments of the water plane area far enough apart or designing a "pendulum" effect with the VCG below the center of buoyancy. Semisubmersibles may be further classified as single hull and multihull.

For the single hull there are two general designs, variable draft and variable operation systems. The former system generally has a high-stability waterplane to move about and then ballasts down to a deep draft. The variable orientation system generally moves from place to place horizontally and then flips to an upright position when working. This is achieved through ballasting.

Multihull variations of the variable hull are used mainly in offshore drilling platforms. When moving, the vessel rests on two or more pontoons of very shallow draft. When the vessel reaches its destination, it is ballasted down to working depth.

Comparison between normal hull forms and semisubmersible floating structures is not difficult. The conventional hulls have greater mobility, reduced vulnerability, and lower construction cost, whereas semisubmersibles are less affected by the seaway and fewer working hours are lost during rough weather operation.

The ship form is particularly useful in near-shore operations, where there is a preferred wave direction. If the ship is headed into the seas, it has a small longitudinal motion. In the open ocean environment, however, the situation is considerably different. Waves of the same order as the ship's beam or longer, combine and cause large motions. On the other hand, the ship forms have small roll damping characteristics, and around the roll resonance frequency considerable rolling motion may be expected. However, this motion can be reduced by the use of stabilizers.

The catamaran differs from conventional ships in three ways. First, it has much greater roll stability because of the spacing between the two hulls. Secondly, the roll resonance is well damped. Third, the beam is larger and the length shorter than in the ship form, thus altering motion characteristics considerably. The open ocean response is characterized by slightly greater motions arising from bow or stern waves but fewer motions from beam seas. Rolling motions are reduced for a catamaran because of cancellation effects. However, the general nature of all motions is basically the same. The same holds

true for the trimaran, although it has somewhat less motion because of increased cancellation [179].

The spar vehicle is different from the other forms mentioned. It has exceedingly low resonant frequencies for heave, roll, and pitch. Normal operating seaways generally do not have wave components at these frequencies to produce exciting forces for these motions. It is the larger draft of the spar that is responsible for the small motions, which are mainly pitch and roll. These remain small for small sea states. When the wavelength approaches twice the draft of the spar, the pitching and rolling motions become significant [179].

In summary, it can be seen that the spar vehicle is least likely to develop serious motions, followed by the trimaran. The ship form and catamaran are useful in sheltered water. However, one should always keep in mind that the selection of a vessel is dependent mainly on the task and limitations of the operation. The motions that an ocean engineering vehicle must go through are the most important factors in determining its usefulness for certain tasks. Whether the mission is to lay pipe or drill wells, there is a certain magnitude of motions beyond which the required performance cannot be achieved.

In principle, there are three kinds of submersibles, namely, fully directional, submersibles with limited control, and bottom crawling submersibles. For the motions of submersibles, the reader is referred to Section 17.7 which is a discussion of submarine motions.

17.4 PLANING CRAFTS

The seakeeping qualities of a planing craft are, in general, based on three different factors: (a) resistance increment, (b) heaving and pitching motions, and (c) acceleration.

Figure 17.5*a* shows the relationship between the speed/length ratio and the rough water resistance characteristics of a planing craft in regular head seas, whereas Fig. 17.5*b* shows the increase in resistance for the following sea condition.

Of the various kinds of ship motions, examination of the pitching motion of planing boats is most important. Typical pitch amplitude is plotted against speed/length ratios in Fig. 17.6. This figure indicates that pitch amplitude per foot of wave height increases as speed is increased, reaches a maximum value, and then decreases rapidly to a nearly constant value as the speed/length ratio increases [183a].

The rough water heaving motions are essentially the same as the pitching motions of Fig. 17.6 until the boat reaches a speed/length ratio of 4. After this point the hull flies from wave crest to wave crest in head seas, even though the measured heaving motions are no larger than those for a speed/length ratio of 2 or 3.

The heaving motion is maximum at low speed/length ratios, at which the encountering frequency is the same as the natural heaving frequency. After the resonant speed is reached, the heaving motion is greatly reduced.

It should be noted that the absolute value of the acceleration depends mainly on the hull form, trim, and sea condition. Figure 17.7*a* shows the impact acceleration as a function of speed and sea state for head sea conditions.

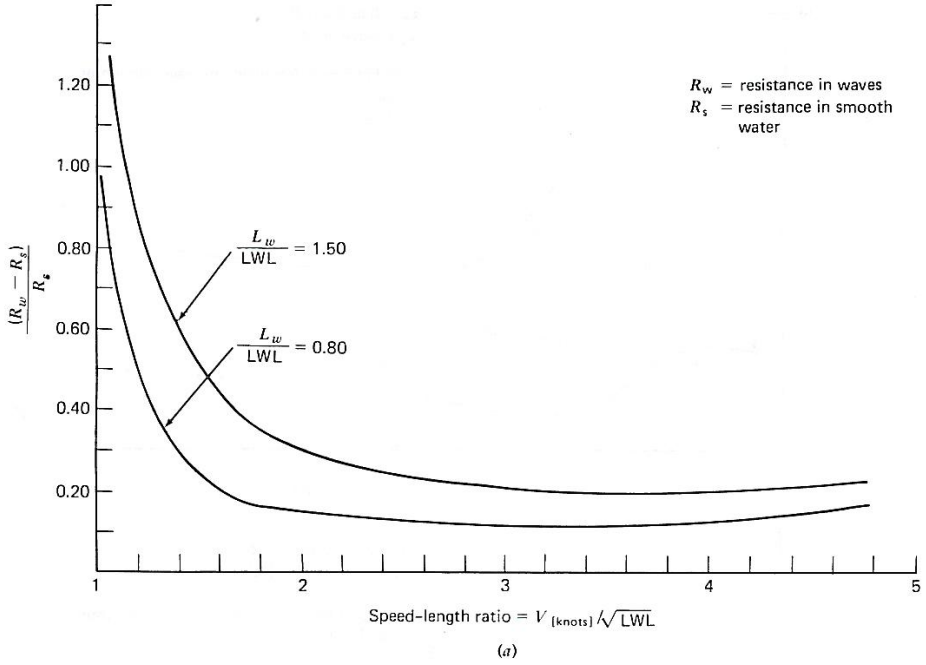
In general, the acceleration is not significant up to a speed/length ratio of 2.0 and is linearly proportional to the speed. For speed/length ratios greater than 2.0, the acceleration increases as the square of the speed. Furthermore, the acceleration in sea state 5 (average wavelength = 5.5 ft) is about 5 times larger than that in sea state 3 (average wave height = 2.5 ft), indicating that for high-speed operation the impact accelerations vary as the square of the average wave height.

Figure 17.7*a* also shows clearly that the impact accelerations can attain a value that is intolerable in a seaway. Therefore, for a planing craft in rough water operation, the impact acceleration becomes the limiting factor in the design.

Figure 17.7*b* shows the variation in the acceleration of the CG of a planing craft in following sea operation. Comparison with Fig. 17.7*a* for the head sea condition indicates that the acceleration in the following sea is much less pronounced, especially for speed/length ratios larger than 3.5. Also, the acceleration in sea state 5 is only slightly greater than that in sea state 3, since in following sea operations the increased wave speed improves the hull–wave impact effect. The difference in head sea operation, on the other hand, is much larger, since both wave height and wave speed increase in a higher sea state, increasing the impact acceleration.

Considering different combinations of hull loading, trim, speed, and sea conditions, designers prefer various configurations for planing hulls, namely, (*a*) round-bottom hulls, (*b*) hard-chine hulls, and (*c*) deep-vee hulls.

For slower operation (i.e., for speed/length ratios less than 2.5) the seakeeping characteristics of planing hulls are similar to those of displacement hull forms, namely [183a]:



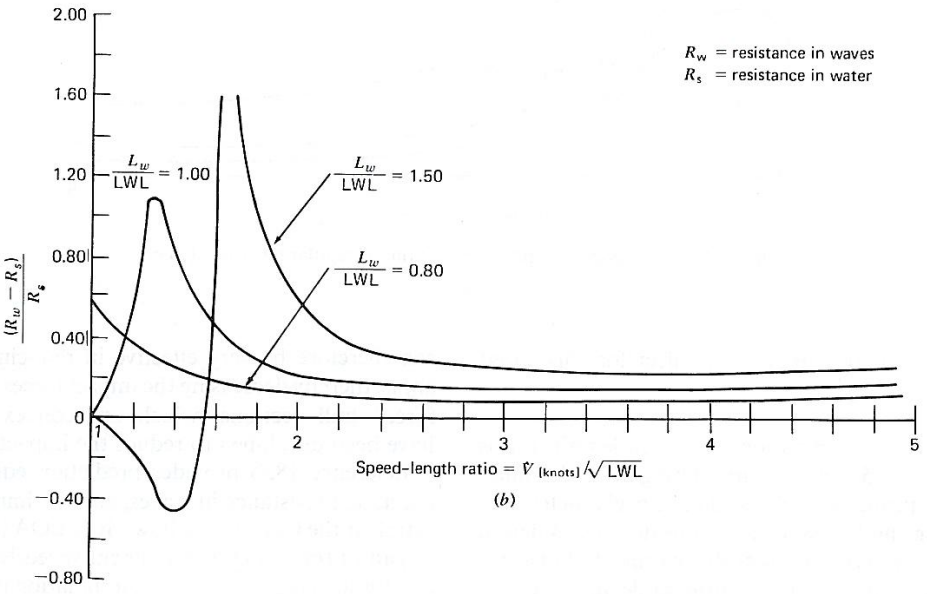


Figure 17.5 Added resistance in regular (*a*) head and (*b*) following seas [183a].

a. All other conditions being the same, the different hull section shapes (i.e., concave sections, convex sections, or straight V) have relatively little effect on motions.

b. An increase in length beam ratio means a decrease in both heaving and pitching motions.

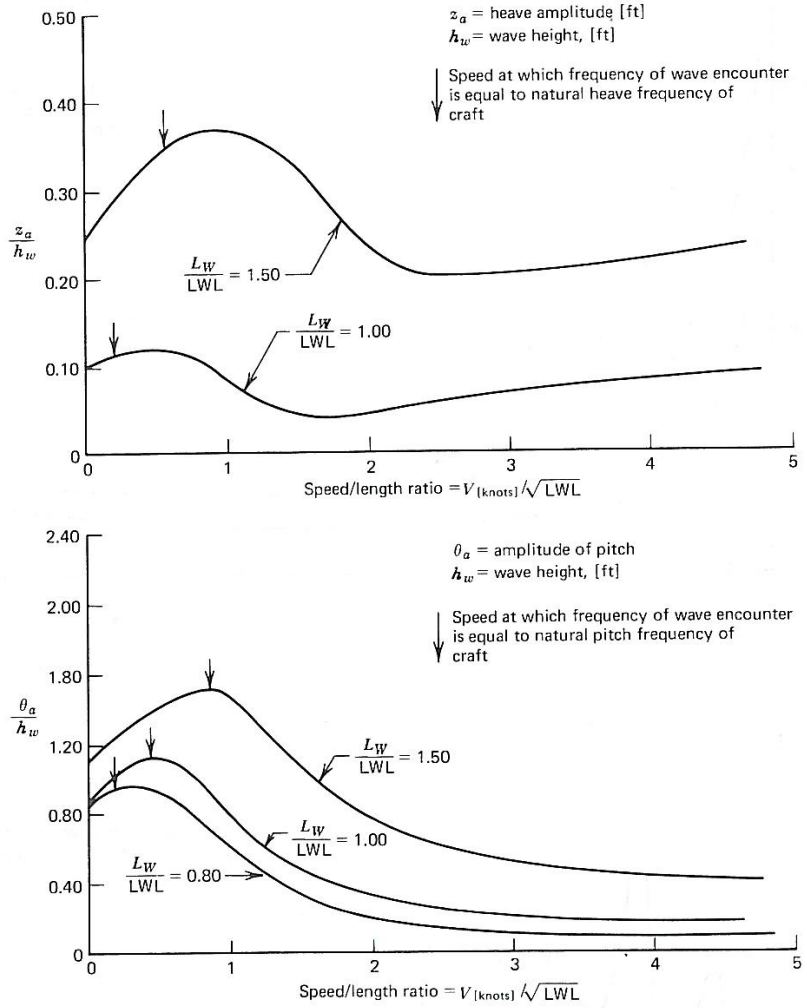


Figure 17.6 Heaving and pitching motions in regular head seas [183a].

c. The trim angle has a small effect for this speed range.

However, for operation at speed/length ratios higher than 2.5, the dynamic lifting force becomes most significant, and the seakeeping characteristics of planing hull vessels are considerably different from those of conventional displacement ships.

The trim angle has a considerable influence on seakeeping quality, since the impact force on a bow section of unit length is proportional to the square of the local effective trim angle of that section. Hence a small reduction in trim angle may reduce the impact acceleration significantly. The small transom flaps can therefore be very effective in reducing the trim angle, thereby decreasing the impact forces. "Constant force" hull sections, which are convex in shape, have been developed to reduce the impact force.

Reference 183b provides prediction equations for the added resistance in waves, and the impact acceleration at the CG and the bow [10% LOA (length over all) aft of the stem]. For different speed/length ratios and for intermediate speeds interpolation is necessary. In the case of acceleration the average value is given. This is obtained by measuring all the peaks of the positive upward accelerations in the time-history record and then taking the average value. The ranges of applicability for these equations are given as

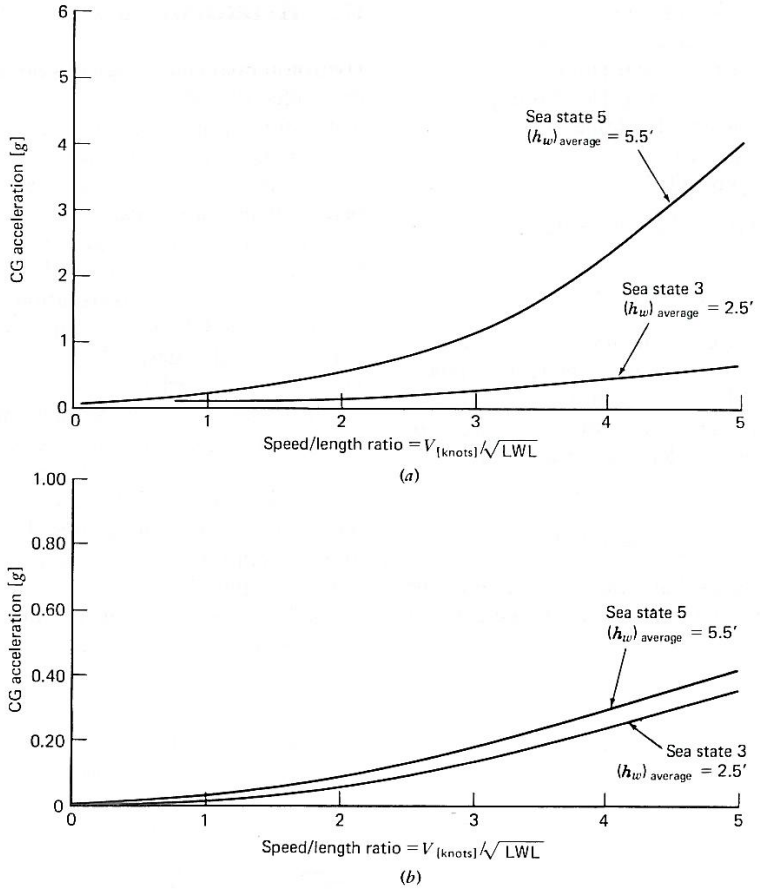


Figure 17.7 Acceleration in irregular (*a*) head and (*b*) following seas [183a].

follows:

Parameter	Range
$\Delta_{LT}/(0.01L)^3$	100 –250
L/b	3 –5
Trim [deg]	3 –7
Deadrise [deg]	10 –30
$H_{1/3}/b$	0.2–0.7
$V_k/\sqrt{L}$	2 –6

Added resistance

For $V_k/\sqrt{L} = 2$:

$$\frac{R_{AW}}{wb^3} = 66 \times 10^{-6}\left(\frac{H_{1/3}}{b} + 0.5\right)\frac{(L/b)^3}{C_\Delta} + 0.0043(\tau - 4)$$

For $V_K/\sqrt{L} = 4$:

$$\frac{R_{AW}}{\Delta} = \frac{0.3H_{1/3}/b}{1 + 2H_{1/3}/b}(1.76 - \frac{\tau}{6} - 2\tan^3\beta)$$

For $V_K/\sqrt{L} = 6$:

$$\frac{R_{AW}}{wb^3} = \frac{0.158H_{1/3}/b}{1 + (H_{1/3}/b)[0.12\beta - 21C_\Delta(5.6 - L/b) + 7.5(6 - L/b)]}$$

Average impact acceleration [g units].

$$\bar{n}_{CG} = 0.85\left(\frac{H_{1/3}}{b} + 0.07\right)\frac{\tau}{4}\left(\frac{5}{3} - \frac{\beta}{30}\right)\left(\frac{L/b}{3} - \frac{2}{3}\right) \times \frac{(V/4\sqrt{L})^{1.4}}{C_\Delta}$$

$$\bar{n}_{bow} = 0.2 + \left[0.45 + 0.16\left(\frac{4}{V/\sqrt{L}} - 1\right)\right]\left(2.25 + \frac{L}{b}\right)\bar{n}_{CG}$$

where b = beam [ft]
C_Δ = static beam-loading coefficient, ∇/B_x^3
B_X = maximum waterline beam
w = specific weight of water [lb/ft^3]
β = deadrise angle [deg]

τ = trim angle of planing area [deg]
R_{AW} = added resistance in waves [lb]
Δ = Craft displacement [lbs]
Δ_{LT} = Craft displacement [long tons]
∇ = Craft displaced volume [ft^3]
V = speed [ft/sec]
V_K = speed [knots]

The average one-Nth highest acceleration, $\bar{n}_{1/N}$, is obtained as

$$\bar{n}_{1/N} = \bar{n}(1 + \log_e N)$$

where $\bar{n}$ is the average acceleration. This indicates that the average one-third and one-tenth highest accelerations are 2.1 and 3.3 times the average acceleration, respectively. Also, the probability of exceeding a specified acceleration is determined by the expression

$$P[n > n_{\text{specified}}] = e^{-(n/\bar{n})}$$

This means that the probabilities of exceeding the one-third and one-tenth highest average accelerations are 12 and 4% respectively.

17.5 HYDROFOIL BOATS

Hydrofoil boats have been developed mainly because they offer the advantage of achieving higher speed while still maintaining good seakeeping quality in a rough sea, namely, lower vertical acceleration. From planing hulls evolved hydrofoils, which have much better lift per unit area.

One of the other major differences in hydrofoil boats is the distribution of the lifting surface area along the hull. The distribution of hydrofoil area relative to the CG of the craft is an important consideration in the design of these boats, since long lengths of hull overhanging the foils are to be avoided; for example, long bow overhang may cause the bow to dip into the wave in rough water operation. It is not the actual impact, but the sudden forward shift of the center of lateral area, that is particularly undesirable, since this causes directional instability and the craft may trip on its nose. In the canard type of configuration (see Fig. 17.8) the major portion of the load is on the large aft foils. A smaller, lightly loaded foil is placed forward. The opposite, or conven-

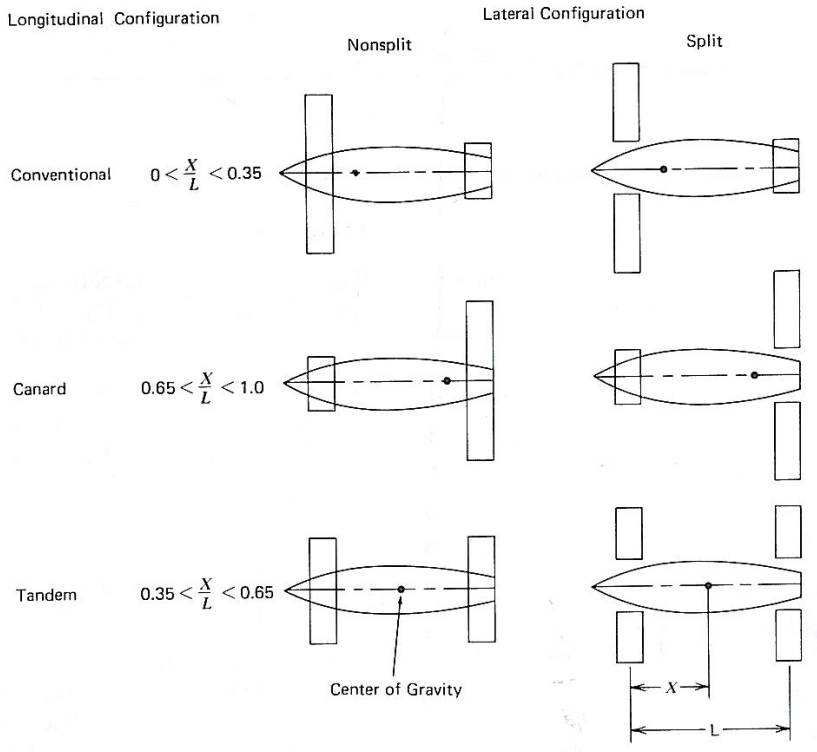


Figure 17.8 Definition of foil area distribution.

tional, type has the most weight on the forward foil and about 35% aft. The tandem type falls in between, with the load distributed evenly in a seaway.

The bow foil is sensitive to a change in immersion but insensitive to the angle of attack, thereby setting the vessel to the required trim and enabling the main foil to anticipate the oncoming wave. There is, therefore, a canard configuration that seems to be very effective. Another advantage of the canard configuration is that it enables the hull to have very fine bow lines; these are suitable to reduce pounding due to wave impact when the vessel is foilborne and quite significant for improved seakeeping when it is hullborne [55].

There are two basic types of hydrofoil systems:

1. Surface-piercing foils.
2. Fully submerged foils.

In the case of surface-piercing foils the lifting surfaces penetrate the free surface, whereas they are completely under water in the fully submerged foil system. The surface-piercing system is self stabilizing, since the lift varies in relation to the depth of the foil submergence. A deviation from equilibrium position brings a change in the wetted, lift-producing foil area, thereby creating the restoring force automatically, although the vessel's ability to remain foilborne in a following sea is rather limited. One of the problems with the surface-piercing foil system is how to avoid ventilation on foil parts positioned near the free surface during transit; this can be accomplished by carefully selecting the foil configuration and foil sections.

The fully submerged foil system experiences the same problem and thereby suffers a loss in lift when it comes rather close to the free surface. In the fully

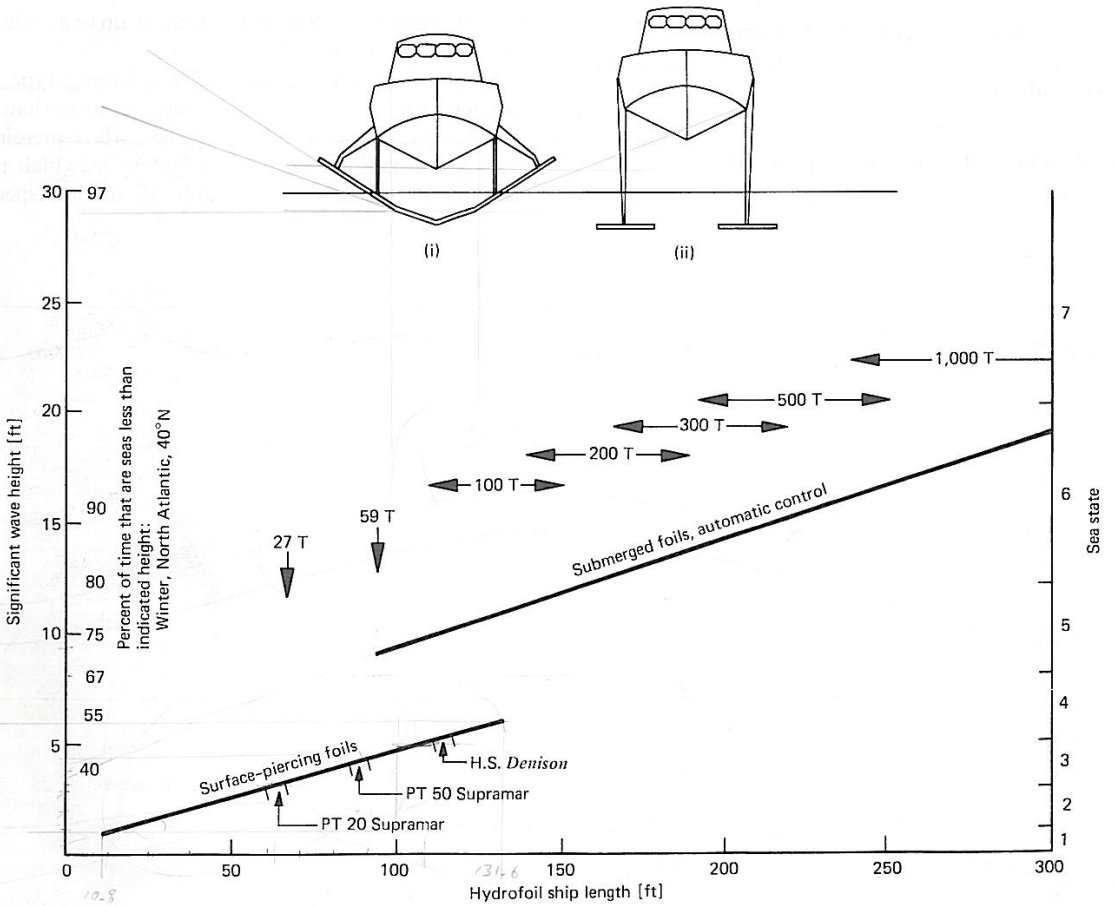


Figure 17.9*a* Significant wave height for unrestricted operation [55]. (i) Surface piercing and (ii) fully submerged foil systems.

submerged system the lifting surface is located, by means of struts, completely below the free surface, where the wave disturbance and orbital motions of the water particles are considerably less. Since the fully submerged foil system is not inherently as stable as the surface-piercing system, it is necessary to maintain immersion depth and roll and pitch stability for fully submerged foils by means of an automatic lift control system, which is complicated as well as expensive, involving boat position and motion-sensing devices and servomechanisms. However, the fully submerged foil system offers superior seakeeping qualities due to its smaller and smoother heaving and pitching responses in waves and also its more effective stabilization, as compared with the V-foil configuration of the surface-piercing type.

Both kinds of foil systems are being developed simultaneously. The surface-piercing type has the following advantages:

a. Better seakeeping quality at hullborne speeds.
b. Greater ability to remain foilborne in extreme sea conditions.
c. Inherent stability without controls.
d. A wider range of foilborne speeds.
e. Greater tolerance off-design loads.

The fully submerged foil system, on the other hand, is superior to the surface-piercing type in the following respects:

a. A more comfortable ride in moderate seas.
b. A higher lift/drag ratio.
c. Lower weight of the foil system.
d. Retraction capability, especially for shallow water operation.
e. Better foilborne maneuverability (e.g., very high turning rates), thereby making it especially suitable for naval missions.

A combined foil system consisting of a surface-piercing front foil system with an air-ventilated submerged rear foil system has proved to be an improvement over the surface-piercing tandem system from the point of view of riding quality in a seaway. The completely submerged foil system, however, is most suitable for operation in a seaway up to a certain sea state (see Fig. 17.9*a*).

A hydrofoil craft of the surface-piercing type is simpler as well as more rugged in operation than a fully submerged hydrofoil ship. The surface-piercing type is a comparatively simple system in which no movable part is involved. In addition, at slow speed

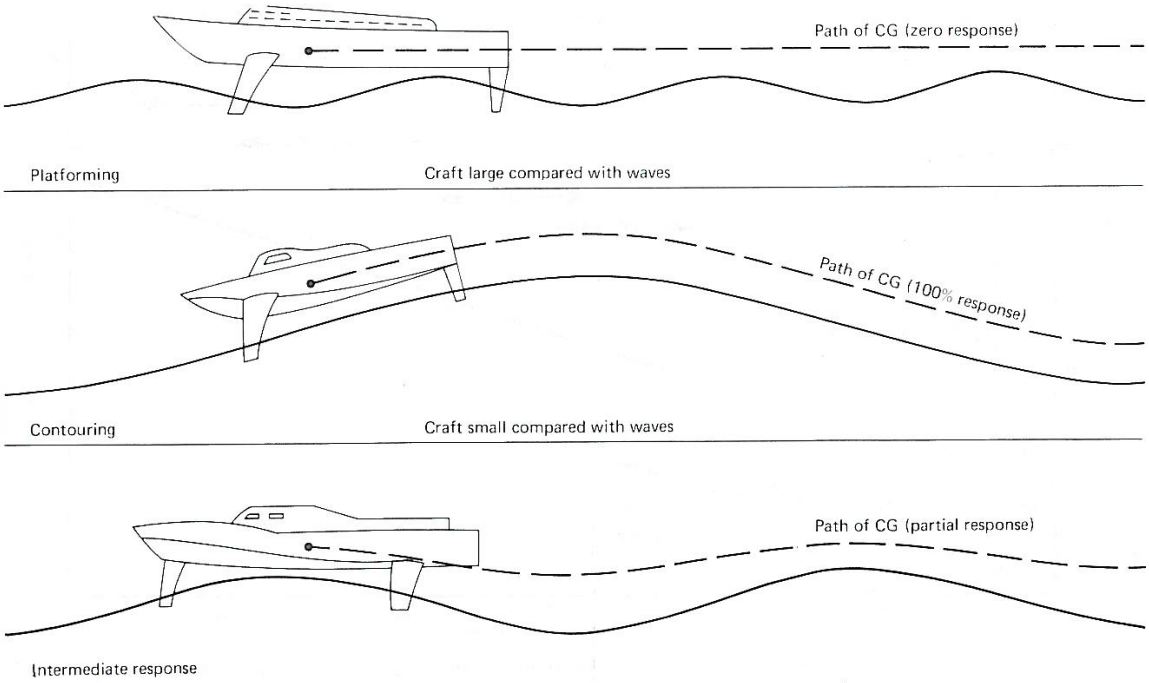


Figure 17.9*b* Comparison of platforming and contouring modes.

a high amount of damping is available because the large foil area makes the craft a sufficiently stable platform even when the vessel is hullborne.

In foilborne operation in a seaway there are two possible modes by which a hydrofoil boat can move forward: (a) platforming and (b) contouring, as shown in Fig. 17.9*b*. It has been observed with full-scale operation that the forces and motions caused by cutting through waves are more acceptable than those experienced because of contouring in wave heights up to about 1.5 times the hull clearance.

Proper damping and restoring properties of the foil can make a hydrofoil boat with the surface-piercing foil system quite seaworthy; a deviation from equilibrium condition produces a change in the lift-generating foil area, and so the restoring force is controlled accordingly. However, the autopilot system is superior in most sea conditions. The vertical

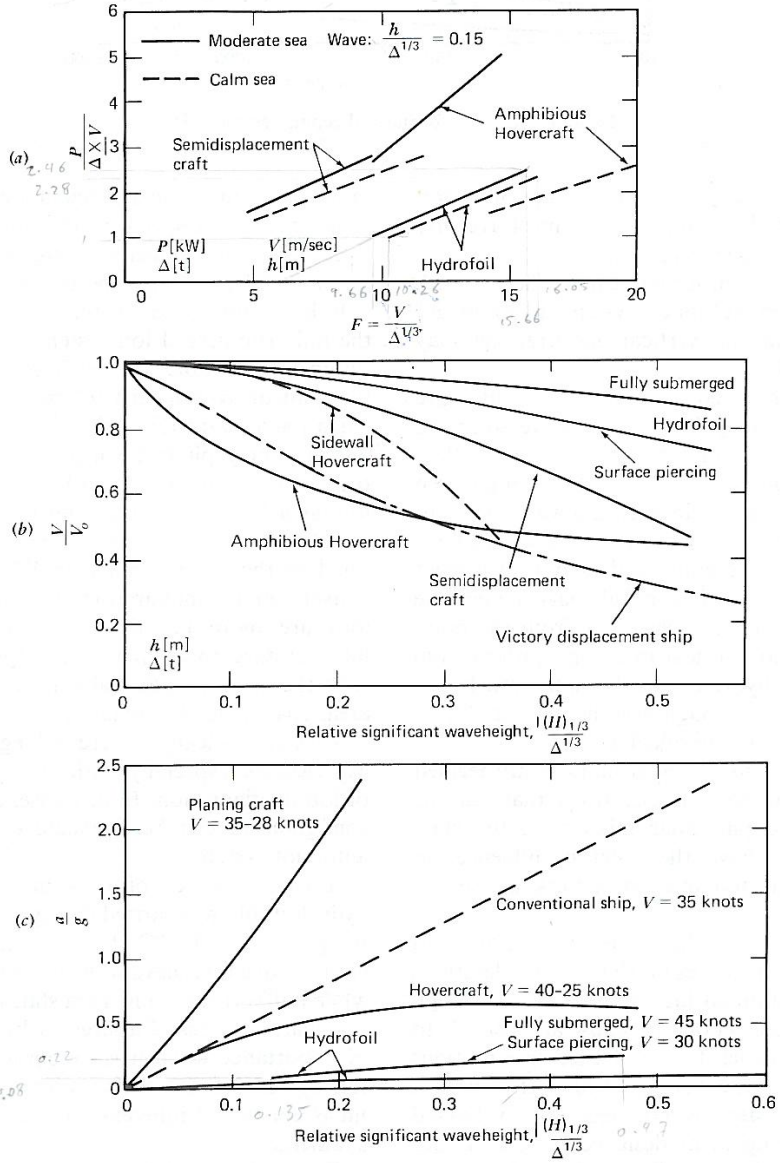


Figure 17.10 Speed and acceleration of hydrofoil crafts [225]. (*a*) Specific power requirements of the Hovercraft. (*b*) Speed drop in a seaway. (*c*) Induced vertical mean acceleration versus relative significant wave height.

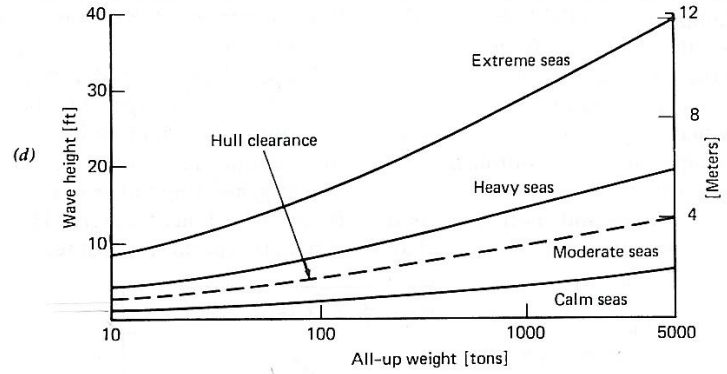


Figure 17.10*d* Foilborne seakeeping regions [53].

acceleration of a fully submerged autopilot foil system is half of the value for the most recently developed surface-piercing vessels.

In heavier seas "contouring" cannot be avoided. A fully submerged autopilot system is no longer advantageous, and the vertical accelerations may become intolerable.

When contouring becomes more significant, wave height becomes less significant, and wave steepness influences motion characteristics much more than wave height. Figure 17.10*a* shows a comparison of the specific power (defined as kilowatts per ton-knots) to a base of the speed/length coefficient for hydrofoil boats, hovercraft, and semidisplacement vessels. The superiority of hydrofoil boats in moderate sea conditions is clearly seen. Also, from the point of view of speed loss in a seaway, one gathers from Fig. 17.10*b* that hydrofoil boats suffer much less speed reduction in a rough sea than do the other kinds of advanced marine vehicles.

The limits of motion for a hydrofoil ship are decided mainly by the limiting accelerations that can be withstood for the particular mission of the ship. The accelerations have the greatest influence on structural strength and mission success, as well as human comfort.

Figure 17.10*c* shows that a hydrofoil craft with submerged foils experiences much lower accelerations than other conventional high-speed ships. In rough sea operations conventional ships are forced to reduce speed in order to avoid excessive motions and accelerations, whereas a hydrofoil craft with a submerged foil system is not acceleration limited in sea conditions up to its designed wave clearance height. For example, according to Fig. 17.10*c*, at a relative significant wave height of 0.3 (i.e., an absolute wave height of 1.3 m for a craft of 70 tons displacement), a mean vertical acceleration of only 0.1 g is experienced at a speed of 45 knots for a hydrofoil craft with fully submerged foils, whereas an acceleration of 0.7 g is to be expected for a hovercraft.

It has been found by recent experience that for the fully submerged foil system the canard configuration is preferable for rough sea operation. When the control system fails to prevent broaching (i.e., when the forward foils drive out the side of a wave), the bow may pitch down abruptly. In the case of the canard configuration with a single lightly loaded foil, at a long lever arm from the CG of the craft, a sufficient righting moment may be quickly generated as the foil resubmerges. With the tandem or conventional configuration, in which the forward foils are more heavily loaded, the instantaneous lift necessary to prevent hull impact can be more than the maximum available from a foil of constant area. Also, since broaching normally does not take place symmetrically, severe rolling motion may be experienced, especially with the conventional type of foil configuration. In any case, every kind of foil configuration can be adequately controlled by an autopilot system.

A routine series of tests on a surface-piercing hydrofoil ship was carried out by the Canadian Navy. Its specific ship, HMCS *Bras d'Or*, a 200 ton hydrofoil craft, proved successful in its seakeeping quality while hullborne, even in a sea state of 5. The seakeeping characteristics of a large hydrofoil craft are also of importance when it is foilborne. *Bras d'Or* has a foil system of the surface-piercing type, in which lift is controlled inherently by the varying foil area submerged.

Figure 17.10*d* defines four regions of foilborne operation for a hydrofoil craft with the surface-piercing system. The following information regarding

hydrofoil operation in a seaway is useful for design consideration [53]:

a. For calm sea operation, because of the damping of the foil system and the inertia of the craft, there is no significant motion whether the surface-piercing type or the fully submerged foil system is used. It is true that the fully submerged system will provide a smoother ride, but the frequencies of encounter are such that, instead of motion, only a vibration is felt in the case of the surface-piercing hydrofoil crafts.

b. In moderate seas the differences between the control systems is noticeable. A fully submerged autopilot system is needed so that the craft can be controlled to ignore the seas, and therefore a motion-sensing rather than a surface-sensing system is preferred.

The surface-piercing foil system may be adequate if proper damping and inertia are chosen, but the ride will be less comfortable than that offered by a fully submerged foil system which uses an autopilot. Vertical acceleration may be double in the case of the surface-piercing type.

c. In the heavy sea condition, contouring through waves cannot be avoided, and the ride becomes uncomfortable, since a significant amount of vertical acceleration results. When contouring becomes pronounced, wave height is no longer significant, since motions then become dependent on wave steepness rather than wave height.

d. In the extreme sea condition, foilborne operation may not be feasible, although the surface-piercing system may have a higher potential because of its greater reserves of lift. The vertical acceleration may be endured by the crew for a short run, but may be unacceptable for any routine operation.

e. The region of a hydrofoil boat most subject to impact lies midway between the forward and aft foils, and in a normal hydrofoil configuration this position is well ahead of the midship section. Therefore the canard configuration is a satisfactory one, since the deadrise increases more toward the bow and the impact will not be as severe because of the deadrise.

In conclusion it can be said that the fully submerged foil system is preferable in moderate seas, whereas in the extreme sea condition the surface-piercing type is more seaworthy.

In the design of hydrofoil boats for predominantly hullborne operation a proper combination of foil configuration and hull form is important. In calm water operation the conventional hull form with the tandem configuration may have lower resistance, but in seaway operation the canard configuration (i.e., the finer form at the bow) is advantageous, both from the resistance and from the seakeeping points of view. In addition, because of the long lever arm exerted by the foils in both pitch and roll, a surface-piercing canard foil system is better suited to damp rolling and pitching motions during hullborne conditions. Also, a predominantly hullborne hydrofoil boat should have a foil system that allows a low take-off speed, so that a conventional round-bilged or soft-chine hull can be adopted.

On the other hand, the hull form of ferry-type hydrofoil craft, which is mainly foilborne except during maneuvers in calm harbor areas, should be designed primarily from the point of view of foilborne requirements; that is, it may be of the hard-chine or stepped form, depending on the take-off speed. For example, in case of inland water operation, ease of take-off is of paramount importance in the design of hydrofoil boats, whereas for rough water operation foilborne impact against waves, depending on craft speed and sea conditions, may necessitate a high deadrise all along the length of the hull and also may dictate a soft-chine form as the best design.

From the point of view of seakeeping considerations the following information is necessary for the design of hydrofoil ships:

a. The relative motion of the foil, as well as that of the main hull, all along the length. Both the immersion and the emergence of the bow, foil, and propeller are important design considerations.

b. The speed loss in the actual seaway in which the hydroil craft will operate.

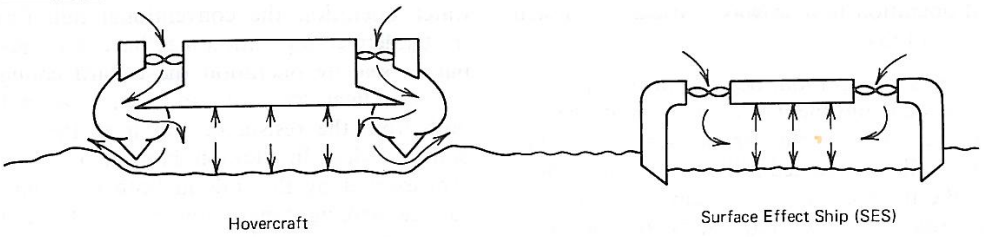
c. The loadings due to water impact, slamming, and so on, especially when the craft is hullborne.

17.6 AIR CUSHION VEHICLES

The discovery that a ship can run with much less resistance if it operates on a cushion of air has opened up a whole new concept of ship design. There are basically two types of craft using the air cushion principle; one is the hovercraft, and the other the surface effect ship (see Fig. 17.11*a*).

Hovercraft

During its operation, no parts of the hovercraft are immersed in the water. Air is forced under the



Figre 17.11*a* Types of air-cushioned vehicles.

craft and escapes around the whole undersurface.

Hovercraft static stability is maintained by a change in the geometric shape of the cushion area. When the craft rolls or pitches, the cushion moves outward on the downgoing side, providing a restoring moment. Stability differs over different types of surfaces and varies with forward speed and small changes in skirt geometry, principally the angle of the cushion section to the surface.

The pitching motion is the initial cause of the rollover of the Hovercraft, which is a constant danger.

Tests have shown that headwinds cause a nose-down attitude, with a tail-up attitude in tailwinds. Also experiments with different Hovercraft configurations indicate that, as suction ports are moved farther forward, pitching moments become progressively nose-up. A plot of pitching moment characteristics is shown in Fig. 17.11*b*. It can be assumed that, as the sea state increases, the action of waves against the hull increases the pitch and therefore the chance of rollover.

Also, from full-scale tests, it has been found that, up to 40 knots, the pitching moment per unit wave height is generally much larger than that experienced by conventional small craft as well as large displacement vessels.

It has been observed that pitch is linearly related to wave height. While moving forward over water, however, the flared bow of a Hovercraft reduces the downward pitch in waves by acting as a lifting surface.

Operation of the hovercraft at the design speed of about 70 knots is supercritical for pitching. It has been found that the natural frequency for this supercritical pitching is about 1.85 rad/sec.

Because there is no immersed portion to give restoring moments, the peak pitch amplitude/wave slope ratios of the hovercraft are, in general, considerably higher than those of planing and round-bottom crafts and large displacement vessels. Tests conducted in model basins have also shown that the largest pitching motions are obtained. Also, the heaving motion per wave height is greater than that of

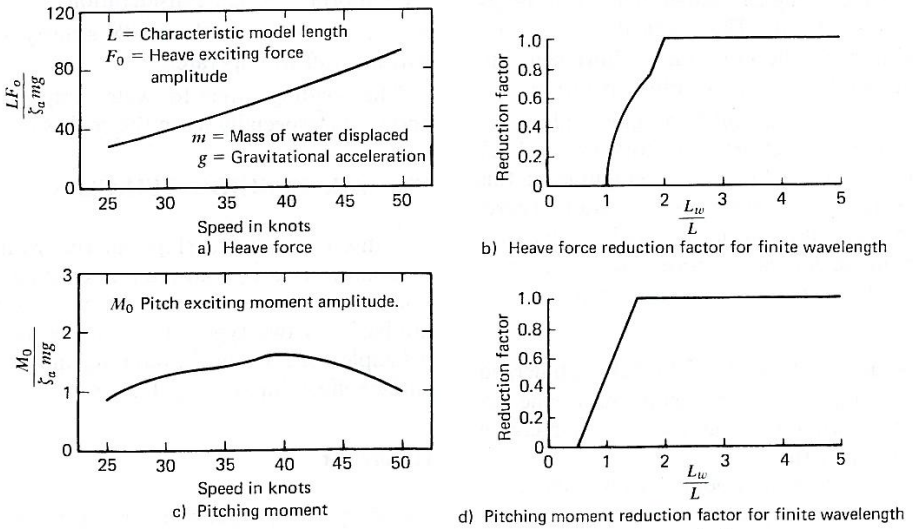


Figure 17.11*b* Exciting moment for pitching and rolling [10].

conventional ships. In fact, the heaving motion of hovercraft is as bad in following seas as is the heaving motion of regular ships in head seas.

Like pitching, heaving is also linearly proportional to wave height and is found to increase as speed increases, so that at a cruising speed of 70 knots large heaving motions can be experienced. When frequencies lower than the natural heaving frequency are encountered, the minimum motion equals the mean displacement of the surface and corresponds, for long waves with these lower frequencies, to contouring these waves, which is done by increasing damping. When frequencies above the natural heaving frequency are encountered, the opposite or small values of damping must be used.

The length/beam ratio is less for Hovercraft than for normal displacement ships, and this decreases the rolling moment. However, the problem of having no displacement restoring force is persent here also.

As stated previously, the danger of rollover is a serious problem in Hovercraft operation. Because of the great speed of the Hovercraft, as plough-in occurs, a strong drag force is applied, causing yaw.

Any small angle of yaw will cause an uneven force and produce a 90° angle. The craft then goes sideways and essentially has a wide, straight bow. The rolling moment, or what has now become the pitching moment, increases. Moreover, the motion is further increased because of huge jets of air escaping from the side that is angled up. Rollover may then take place.

The principle used in a certain type of multicushion craft design to obtain stability in pitch and roll is to employ the heave stiffness of individual cushions. When the craft tilts, the air gaps on the downgoing side reduce, thus decreasing the air flow requirement and raising the pressure of the cushions affected. On the upgoing side the pressure decreases.

Several means have been employed for controlling pitch, roll, and heave. Certain types of Hovercraft use a fuel ballast system and a movable tailpiece surface situated in the propeller slipstream to help regulate trim and keep drag to a minimum. Also, a certain degree of control over pitch has been achieved in some Hovercraft by using two fans in tandem arrangement. Cable-operated skirt-lifting systems are employed in controlling roll attitude. Cushion air is allowed to escape from part of the skirt periphery, causing the vehicle to tilt down in that direction. Heave is normally controlled by varying the fan revolutions per minute.

Typical results obtained from model tests of a Hovercraft are shown in Fig. 17.12. The curves of

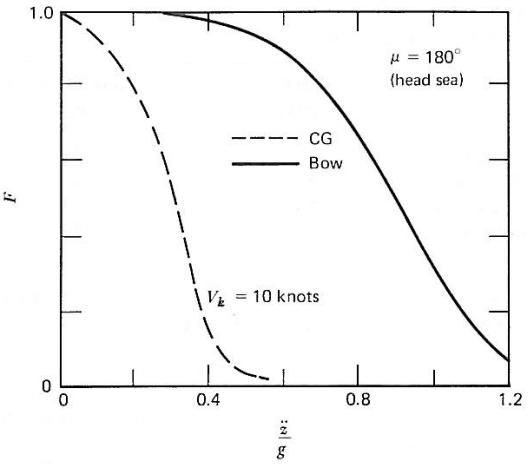


Figure 17.12 Comparison of accelerations at bow and center of gravity [205].

this figure, obtained statistically, show the vehicle acceleration levels at the bow in comparison with those at the CG of the ship. The curves pertain to the maximum of the acceleration–time histories, the ordinates F of the curves giving the probability that an arbitrarily chosen maximum will exceed the corresponding abscissas. Thus the abscissa corresponding to $F = 0.5$ is the median of all the maxima; the abscissa corresponding to $F = \frac{1}{2}(\frac{1}{3}) = 0.167$ is the median of the one-third highest maxima; and so on.

The resonance amplitude operators in the figures were obtained by dividing the ordinates of the response spectrum by those of the encountering wave spectrum. In the case of the heaving motion the encountering spectrum was taken as the wave height spectrum, whereas for the pitching and rolling motions the encountered wave slope spectrum was used instead of the standard half-wave amplitude spectrum [where the ordinates are designated as $S_\zeta(\omega_e)$]. This type of encountering wave spectra makes it possible to have nondimensional RAOs for various vehicle motions.

Table 17.2 shows the undamped natural frequencies as well as the nondimensional damping ratios, k. It is noticed that the observed roll RAO given in Fig. 17.13 may have been influenced by wave energy coming in at oblique angles as well as the coupling effect between heaving and pitching motions.

Until now, seakeeping design for air cushion vehicles has been based on small-scale model investigations and theoretical studies. However, the results shown in Fig. 17.13 indicate that the statistical approach to seakeeping performance may also be

TABLE 17.2 [60]

a. Seakeeping Trial Runs

Run	Speed [knots]	Compass Heading [deg]
Head seas	52	135
Following seas	55	315
Beam seas (1)	56	0
Beam seas (2)	61	180

b. RMS Values for Craft Motions in a Seaway RMS wave Height = 0.159 m (0.522 ft); significant wave height = 0.637m (2.09 ft)

	Types of seas			
Run	Head	Following	Beam (1)	Beam (2)
CG acceleration [g]	0.125	0.0652	0.0655	0.0933
Bow Acceleration [g]	0.208	0.120	0.105	0.144
Pitch angle [deg]	0.735	1.48	0.515	0.948
Roll angle [deg]	0.792	0.976	1.025	1.096

c. Damping Ratios and Natural Frequencies

Test Conditions	ω_n [rad/sec]	Damping Ratio κ
Heave, head seas (52 knots)	2.84	0.46
Pitch, head seas (52 knots)	2.50	0.42
Pitch, following seas (55 knots)	1.97	0.40

valid for air cushion vehicles. The RAOs derived from response and input spectra give useful information and can be applied as a reliable design tool.

SURFACE EFFECT SHIPS

Another kind of air cushion vehicle is the surface effect ship (SES), which has sidewalls on each side

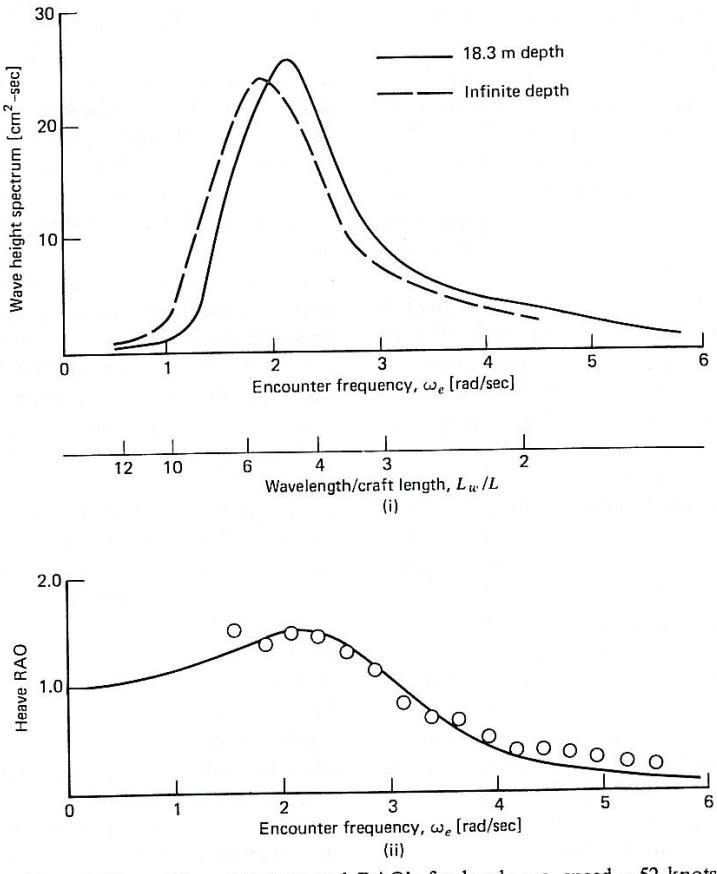


Figure 17.13*a* Wave spectrum and RAO's for head seas, speed = 52 knots [60]. (i) Wave height spectrum. (ii) Heave RAO.

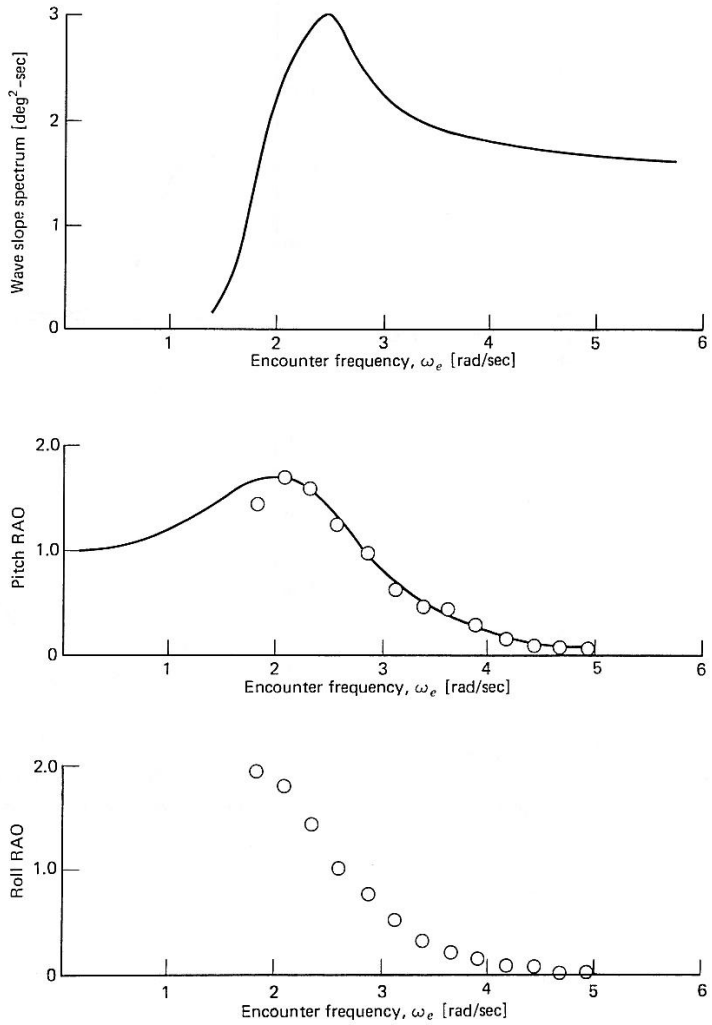


Figure 17.13*b* Wave spectrum and RAO's for head seas, speed = 52 knots [60]. (i) Wave slope spectrum. (ii) Pitch RAO. (iii) Roll RAO.

that penetrate the water to a moderate draft and lend some buoyancy force, but mainly provide a complete seal on the sides to the air cushion when moving in water. This reduces leakage and thus the lift power requirements. Because of the sidewalls, water screw or water jet propulsion is applicable for SESs.

It is claimed in Ref. 54 that the SES is the only advanced marine vehicle that does not suffer from either size or speed limitations.

It is rather difficult to obtain quantitative motion data and operational information for such vehicles. The motions of SESs in regular waves are not typically sinusoidal, as one might expect from a linear model excited by a sinusoidal forcing function. Harmonics are present that distort the wave form of the time history and sometimes make the motion response difficult to analyze.

In obtaining the data each time history has to be examined and compared with the statistical averages, and for responses that are more or less sinusoidal the average of the crests and troughs is taken as the value that most nearly represents the motion. On the other hand, when higher frequencies are present, the smaller crests and troughs are ignored, the

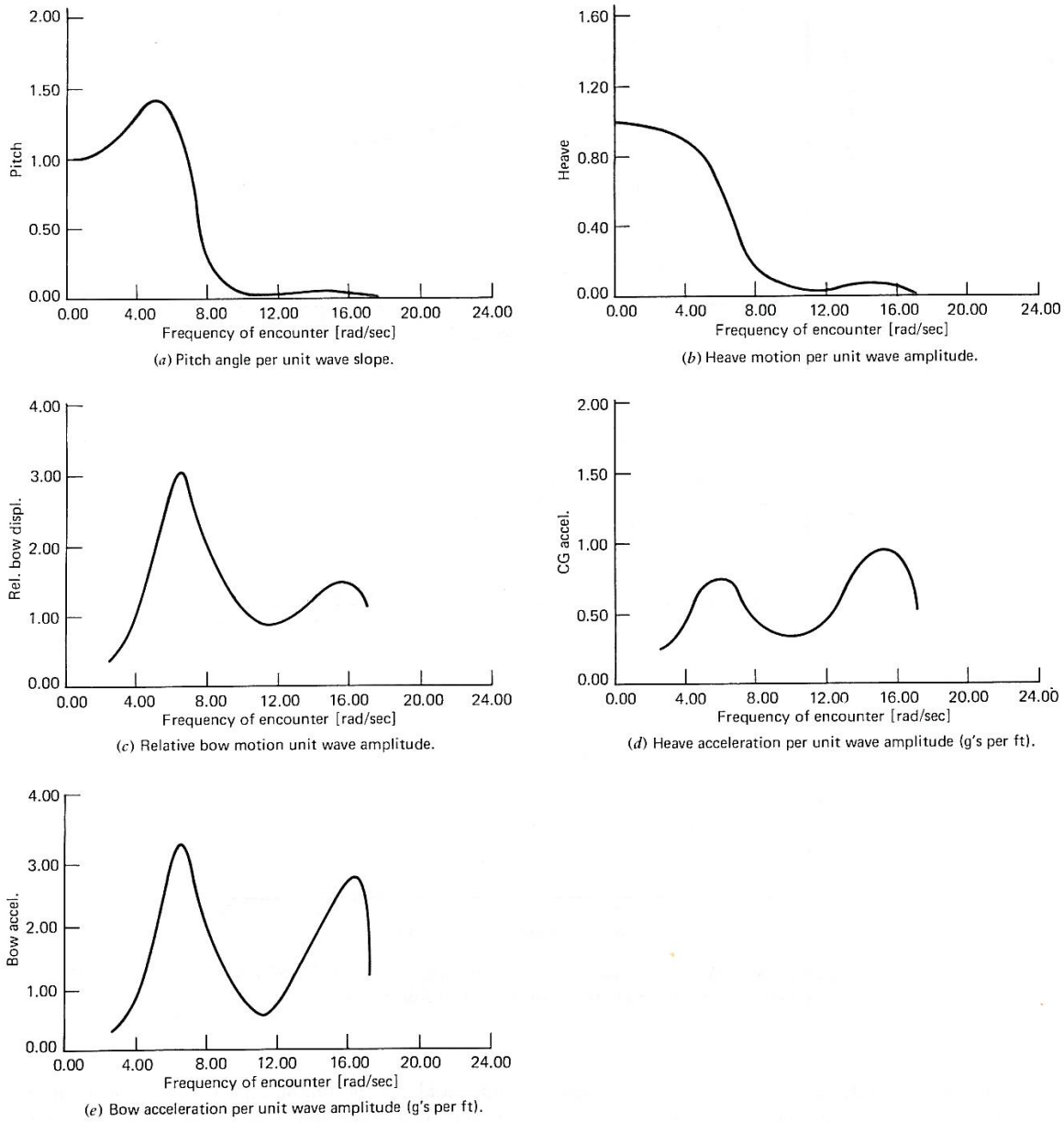


Figure 17.14 Accelerations in regular head seas [67].

significant value (the average of the one-third highest) being taken as representative of the primary response.

Linearity can be shown by plotting the motion responses as a function of wave height. It is clear that at some wave lengths linearity is good; at others, however, the response is different from the straight line relationship, particularly near resonance. From the faired lines of these plots, averaged RAOs can be calculated and presented against frequency of encounter, as shown in Fig. 17.14.

The acceleration–time histories are also seldom truly sinosoidal in regular waves. In the majority of cases the responses are found to occur at twice the encountering frequency. Typically the acceleration pattern appears to be that of small crest (up acceleration) followed by larger crest. The troughs remain

almost the same. The bow acceleration is less prone to the double frequency response than are the CG and stern accelerations. For the most part the accelerations appear to be motion induced, the crests being about equal to the troughs in magnitude. Not until the craft is tested in larger waves can the accelerations be considered slams or impact spikes. For this reason the stable amplitude values are presented in the figures for regular waves.

Typical double amplitude accelerations are plotted against L/L_w in Fig. 17.14. The maximum value occurs at about a wavelength of about 2.5 cushion lengths.

An immediate benefit of the high speed of an SES is a substantial decrease in pitch motion. The ship comes into contact with more waves per unit time than a normal displacement ship; this means that the pitch amplitude decreases. But the pitching accelerations appear to be a serious problem. The methods for improving this situation are basically developed from heave damping techniques.

As speed increases, there is also a shift in the mean pitch angle toward a permanent bow-down orientation. In other words, the ship exhibits a trimming of the bow. This characteristic also becomes noticeable with increasing wave amplitude. The use of ballast tanks in the stern can improve this situation.

Tests made in selecting proper seals for SESs have shown that a hard, spring-actuated stern seal is the best type. The forward seal should be relatively soft, because the impact of waves can be damped to a great extent by a soft seal. Another feature of the forward seal is a pressurized air bag at the upper part. This bag is needed because the only initial trim-restoring force without it would be given by the sidewalls, which are made to have a minimum thickness in order to allow higher speed. When the pitching motion is too large, the bag, which is situated in the foremost part of the ship, enters the water and generates a very large retoring force.

Fins may also be used to reduce motions, but there is a possibility that an active horizontal fin may increase the pitching motion. It is also believed that superventilated foils located at the stern of each sideboard could be used for pitch damping. Such devices could be retractable with variable areas and angle-of-attack capabilities.

Computer calculations have been made using variables of fan blade pitch and louver controls. The fans force air into the bubble. The computations show that decreasing the pitch of the blade, while keeping the volume of air flow constant, decreases the pitching of the ship. However, a disadvantage is that the power needed for the fan also increases at a very high rate. It has also been found that increasing the inflow of air reduces motion.

As the vehicle speed increases, the heaving motion amplitude decreases. However, the number of wave crests also increases, and the accelerations of the ship in a vertical direction become a very real problem.

The main damping force, not only for heave but also for accelerations at the CG of the vehicle, consists of louvers. The restoring force for heave of an SES is composed of two parts, the displacement hulls of the sideboards and the air chamber itself. The latter is the main force. As the ship sinks into the water during heave, the pressure in the chamber increases, causing the ship to rise. Then the pressure drops, causing the ship to fall. A "spring cycle" develops, similar to that in displacement ships. To keep a constant pressure inside the plenum chamber, louvers are needed to release air. Although there is a constant leakage, it has been found that varying the air exhaust in response to motions, while keeping the pressure constant, reduces motion. By using a pressure sensor, louvers can be opened and closed in an attempt to decrease the rate of change in pressure. On the SES 100A (a 100 ton test craft), the vertical accelerations were reduced by 50 to 70% with the help of a heave attenuation system (see Fig. 17.15*a*).

Rolling is not a major problem in a SES that has displacement sidewalls for restoring forces, plus longitudinal rigid seals in the plenum chamber. These partitions keep the sides under different pressures as the ship rolls and provide restoring forces. Since the beam of the ship is relatively wide, the sidewalls provide ample stability.

A 45° deadrise angle for the sideboards has been found to give good roll stability. Superventilated foils at the sideboard sterns, used collectively for pitch control, can also be employed differentially for roll control.

Very little has been done in terms of experimental

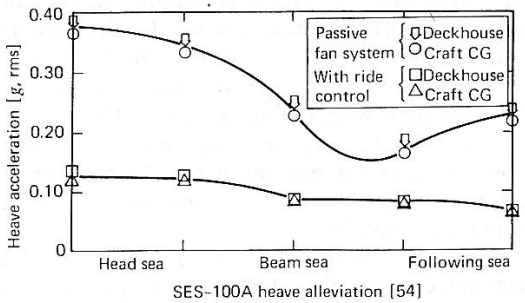


Figure 17.15*a* SES 100A heave alleviation [54].

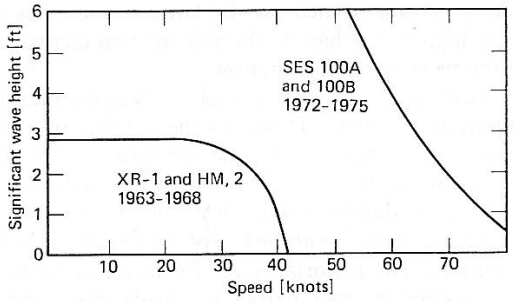


Figure 17.15*b* Surface effect ships operating envelope [54].

measurements of impact pressures due to slamming of SESs. The theories presented in Refs. 31 and 32 can be applied to predict the magnitude and distribution of the impact pressure of a V-shaped hull against a water surface of known geometry. However, since data are not available to verify the validity of the prediction, the results should be used with reservations.

The methods outlined in Section 17.2 for catamarans may provide other guidelines, especially in the early stages of design, although the operational speeds and impact velocities may be higher for SES vehicles. However, until full-scale data on impact pressures are available, the validity of the analytical methods will not be known, and consequently they must be used with caution.

The speed capabilities of SES vessels developed over the last 12 years in various sea states are shown in Fig. 17.15*b*.

Many characteristics of captured air vehicles (both Hovercraft and SES) have been calculated by computers, and enough Hovercraft have now been built to provide adequate data. However, an actual seagoing surface effect ship large enough for other than just experimental data acquisition has not been built.

At the moment it seems as if the only real danger in regard to the SES is the severe accelerations. The high speed plus the large accelerations may require that new instrumentation systems be designed for such vessels. Also, there may have to be selection for a crew, as it is the case with astronauts, so that they can cope with the accelerations. Crew spaces will probably have to be at the stern of the ship, where motions are less, and it may be necessary to spring-damp all the living compartments to make them more habitable.

Also, model preparation for seakeeping tests of such vehicles is rather difficult, since part or most of the lift of air cushion vehicles and surface effect ships is obtained with the help of an air cushion that is contained at least partly with flexible skirts. A typical model is fitted with lift fans, often its own propulsion, sundry ducts, plenums, and pressure gauges to measure the cushion pressure. In spite of the geometric scaling of cushion dimensions and ambient atmospheric pressure, the compressibility of the air cushion is still out of scale. Hence in the prediction of full-scale performance from model tests there is an error due to the scaling discrepancy in air cushion compressibility. However, this error may be significant only for SESs and not for air cushion vehicles. In addition, the following points may be made regarding the difficulty of full-scale prediction [43]:

a. Motion, acceleration, and wave loads do not possess zero mean lines.

b. Super- and subharmonic responses are often present in regular wave tests.

c. Motion responses are not linear in regular wave tests.

The seakeeping design information for air cushion vehicles should then include the following items:

1. Energy spectrum of the realistic seas in which the vessel has to operate (including the surf conditions on a sloping beach).
2. Relative motion of the vehicle along the sidewalls and seals causing deck wetness and water impact, as well as loadings due to water impact on the underside of the deck structure and on seals. Also propeller emergence causing a high degree of vibration of the sidewalls.
3. Speed loss in a seaway.
4. Seaway loads on the deck and sidewalls, especially at the junctions of the sidewall and deck.
5. Motion stabilization.
6. Loadings, such as slamming and green water on deck and in the off-cushion condition in heavy seas.

17.7 SUBMARINES

The study of submarine motions includes roll, pitch, heave, and suction forces. As in the case of surface ships, the motions of a submarine are rather complex. The shape of the submarine's hull and the fact that it operates at different depths complicate matters even more. It has to functions efficiently at great depths, where little motion is present, but it must

also have the capability of operating efficiently on or near the surface.

To obtain the most efficient submarine possible, the design has to be such as to produce the least magnitude of all the various motions combined with the longest possible periods. This reduces the adverse effects of the submarine's motion. In particular, a submarine should have small angles of trim and list combined with long periods of time between oscillations.

The roll of a submarine in a seaway can be calculated by the use of differential equations as discussed in Chapter 4. The rolling motion of a submarine in a seaway is the sum of the free and forced harmonic oscillations. As it has been found with surface ships, the forced oscillations of submarines are also proportional to the wave slope.

The other important submarine motion is pitch. When a submarine pitches, it alternately trims by the bow and by the stern. The period of pitch can be calculated in the same manner as the rolling period (see Chapter 4). An approximation for the free pitching period is $T_\theta = \frac{1}{2}T_\phi$ sec.

Since heave, roll, and pitch are harmonic motions, they are subject to resonance. When waves strike a submarine so that the resonance effect occurs in the ship's roll or pitch, the amplitude increases by a factor of 3 to 10. This phenomenon is of great importance for a submarine because it tends to increase the oscillatory amplitudes which cause complications in the overall operation of this type of vessel. Comparing the ratios of snap roll to steady roll, a submarine with sail and one without sail it is found that roll damping is much less when there is no sail [253]. Also the modern submarines are fitted with dual sets of hydroplanes to control the motions in the vertical plane, one pair at the bow and the other at the stern. The stern planes are far more effective than the bow planes since the interaction between the stern planes and the hull is much more favourable and so the lift generated by the stern planes is considerably larger. In modern submarines the bow planes have been replaced by the sail planes, although the sail planes cannot be used for fast diving, but this requirement is no longer important [253].

In order to damp or control these motions, stabilizers can be employed to set up moments to counter the induced motions and thus reduce their magnitude. As discussed in Chapter 14, stabilizers are normally of two types, active and passive. The stabilizing moment is not controlled in the passive stabilizers but is created and controlled in the active ones.

Rolling chocks and tank stabilizers may be considered as two of the more common passive stabilizers for submarines. Rolling chocks increase the resistance of the water to rolling, thereby reducing rolling amplitudes by a factor of 1.5 to 2. However, they have little effect when the rolling amplitude is small. Both the active and passive systems are not normally found on modern submarines.

Suction forces acting always upwards are of considerable importance in regard to the motions of a submarine. A submarine traveling just below the surface is subject to forces and moments as a result of the motion in relation to the free surface. These are due to the Venturi effect, that is, due to the accelerated flow of water between the submarine and the free surface. The pressure in a moving fluid is reduced below the hydrostatic pressure by an amount proportional to the square of the fluid velocity. The suction force decreases exponentially as the distance to the free surface increases. If the submarine had fore and aft symmetry, no moment would be produced. Since this is not the case, the water flow is accelerated to a greater degree over the bow than over the stern, causing the ship to have a bow-up moment, and this produces a destabilizing effect. These forces and moments become significant when the submarine is about three diameters below the surface or less. In order to maintain constant depth the hydrodynamic vertical force and the vertical moment are counterbalanced by having a hull angle of attack as well as stern plane angle which are called neutral angles and must be large, especially at low speed when the asymmetry is extensive [253]. When the submarine reaches a depth of three-quarters of a diameter, it is near enough to the free surface to produce a surface wave, causing in a bow-down moment. At high speeds the attractive forces have a stabilizing effect, but the speeds necessary to produce this effect are rather too high for present-day submarines [257].

The submarine also experiences suction in a seaway. The cause of these suction forces is water particle motion. Water particles near the hull are affected by wave motion and move in circular paths. Since the orbital velocities of these particles decrease with depth, velocities over the deck are greater than those under the keel. Taking the horizontal components of these velocities, a high negative pressure is created over the deck with respect to the keel, and an upward suction force results. (See Fig 17.16). Although the suction force oscillates with time, it always remains positive. The oscillation does not take place at wave frequency, but rises and falls as groups of high and

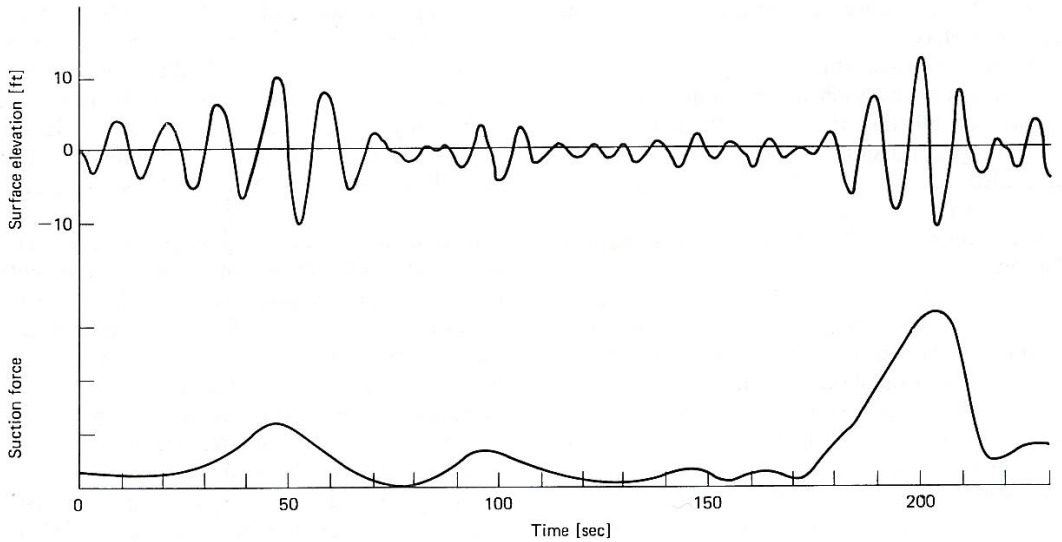


Figure 17.16 Typical time history of a sample wave record and the corresponding suction force at 60 ft. keel depth in head seas.

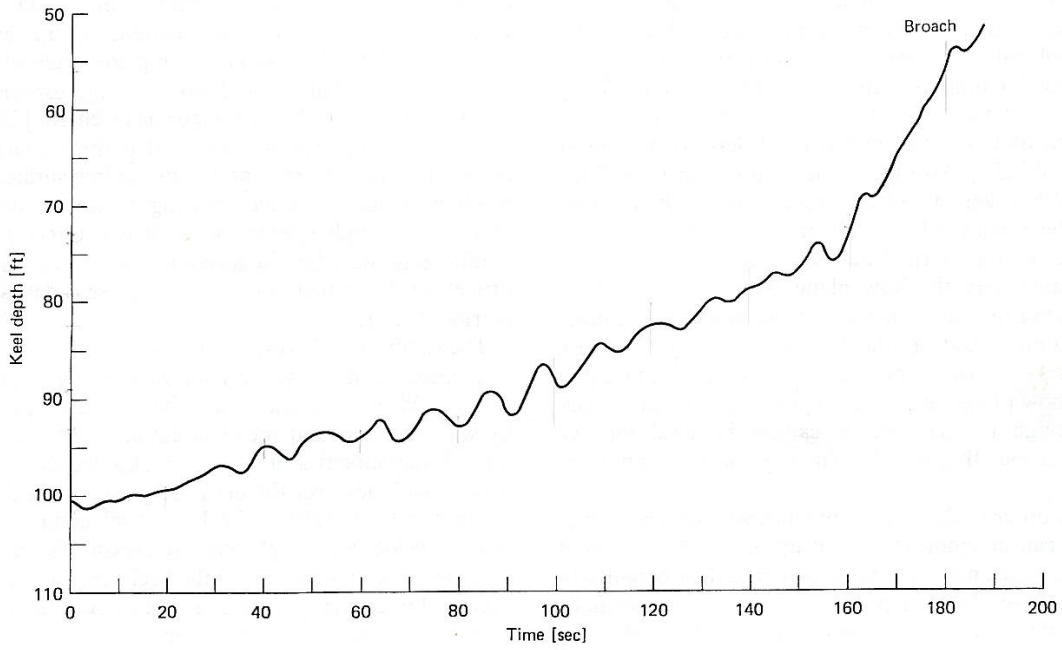


Figure 17.17 Depth record showing effect of suction force on submarine under waves. Quartering sea, wave height = 18 ft., vessel speed = 0 knot.

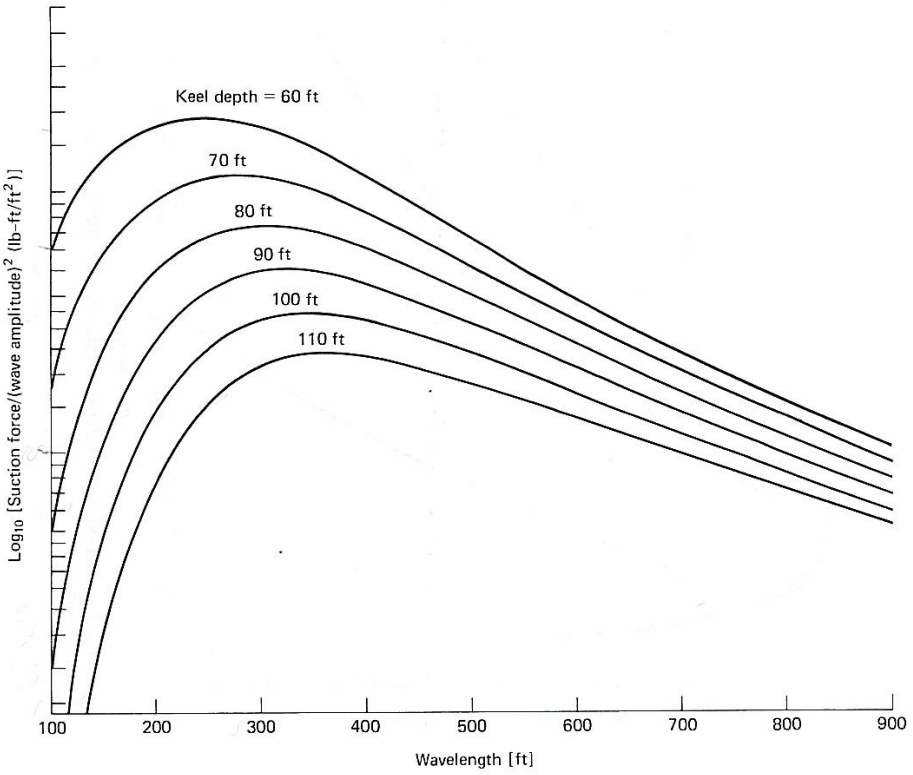


Figure 17.18*a* The suction force in regular head or following waves. The ship speed is zero.

low waves are encountered by the submarine. Since the suction force is approximately proportional to the square of wave height, relatively high, narrow peaks separated by wide, low valleys are noticed for the suction force as shown in Fig. 17.16. With the help of this figure one is able to understand the regions of pronounced curvature followed by the regions of relatively steady rise of the plot for the typical depth record of an uncontrolled vessel (see Fig. 17.17). Suction forces are found to be proportional to the wave height squared for a given wavelength, and the magnitude decreases exponentially with depth. (See Fig 17.18).

Suction forces are greatly affected by oscillatory motions. When the submarine is in a beam sea, it rolls, heaves, and pitches with the waves, closely following the motion of the water particles around the ships. The Venturi effect is minimum, and so are the suction forces. In a head or following sea, however, the vessel does not move simultaneously with the water particles near it. Here the Venturi effect is maximum. In regular waves the suction forces for head and following seas may be an order of magnitude more than the value for the beam sea of the same wave height. (See Fig. 17.19). An increase in speed also increases suction forces [257].

For a fixed depth and changing sea conditions, the suction forces increase as the wavelength decreases until a maximum is reached; then the suction drops off rapidly. The reason for this is a change in force due to the rate of change in particle velocity increasing with respect to the depth. This is shown in Fig. 17.19. Fig. 17.20 is a typical illustration of average suction force in irregular head and following seas and Fig. 17.21 shows the uncontrolled pitching motion of a submarine in head seas due to suction force.

Since waves seldom move past a submarine in a regular manner, the magnitude of suction forces vary as various combinations and groups of low and high waves pass over the vessel. The average suction force is constant over a long period of time, but there may be instances when the force is several

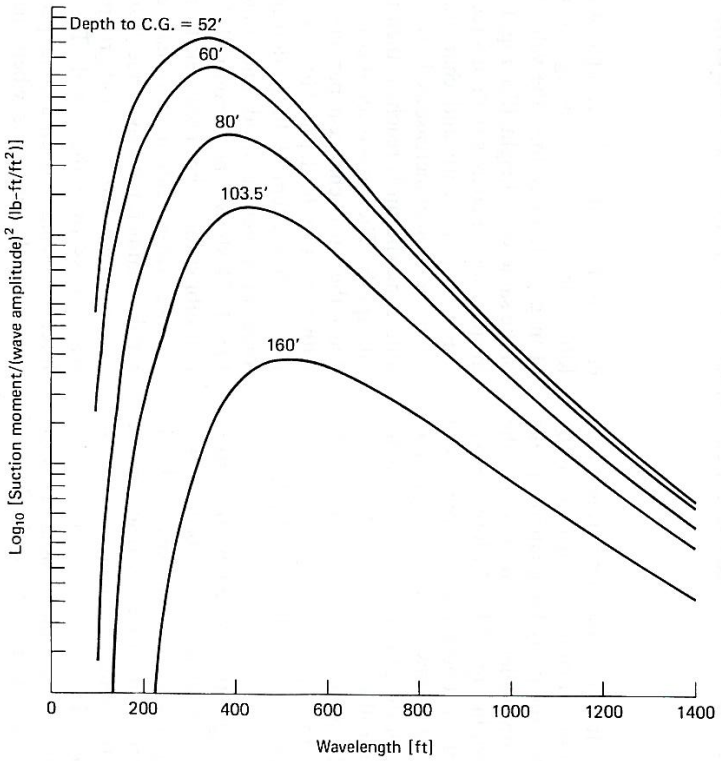


Figure 17.18*b* Suction moment for the unrestrained vessel in head seas.

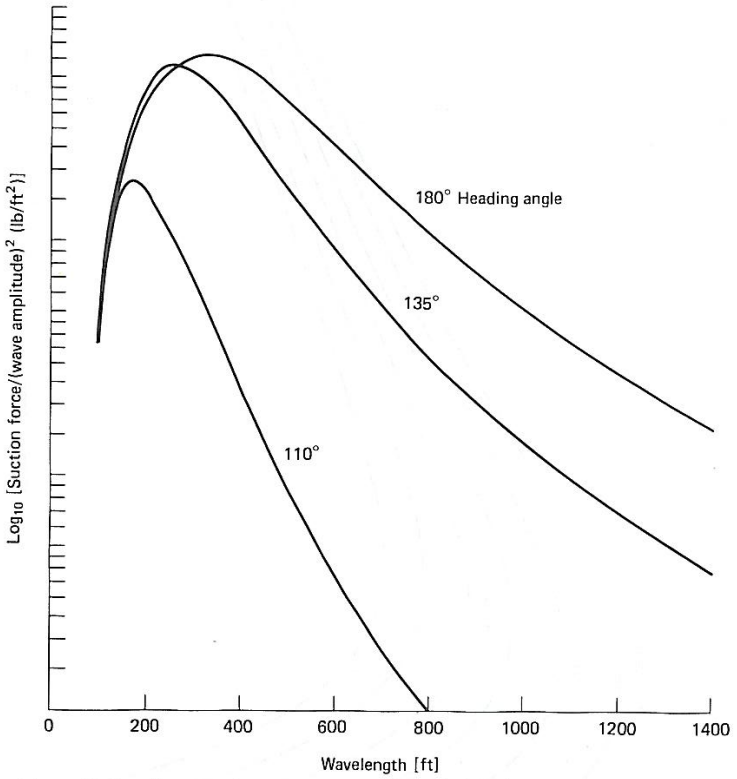


Figure 17.19 Suction force versus wavelength for the unrestrained vessel. Depth = 60 ft.

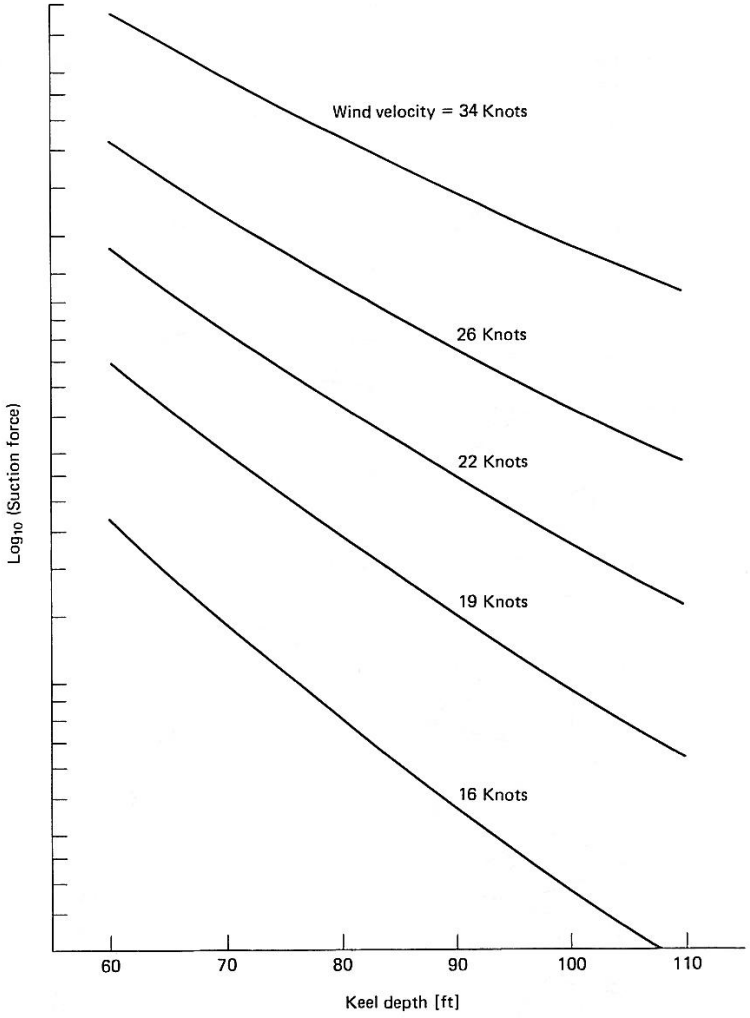


Figure 17.20 The average suction force in irregular head or following seas.

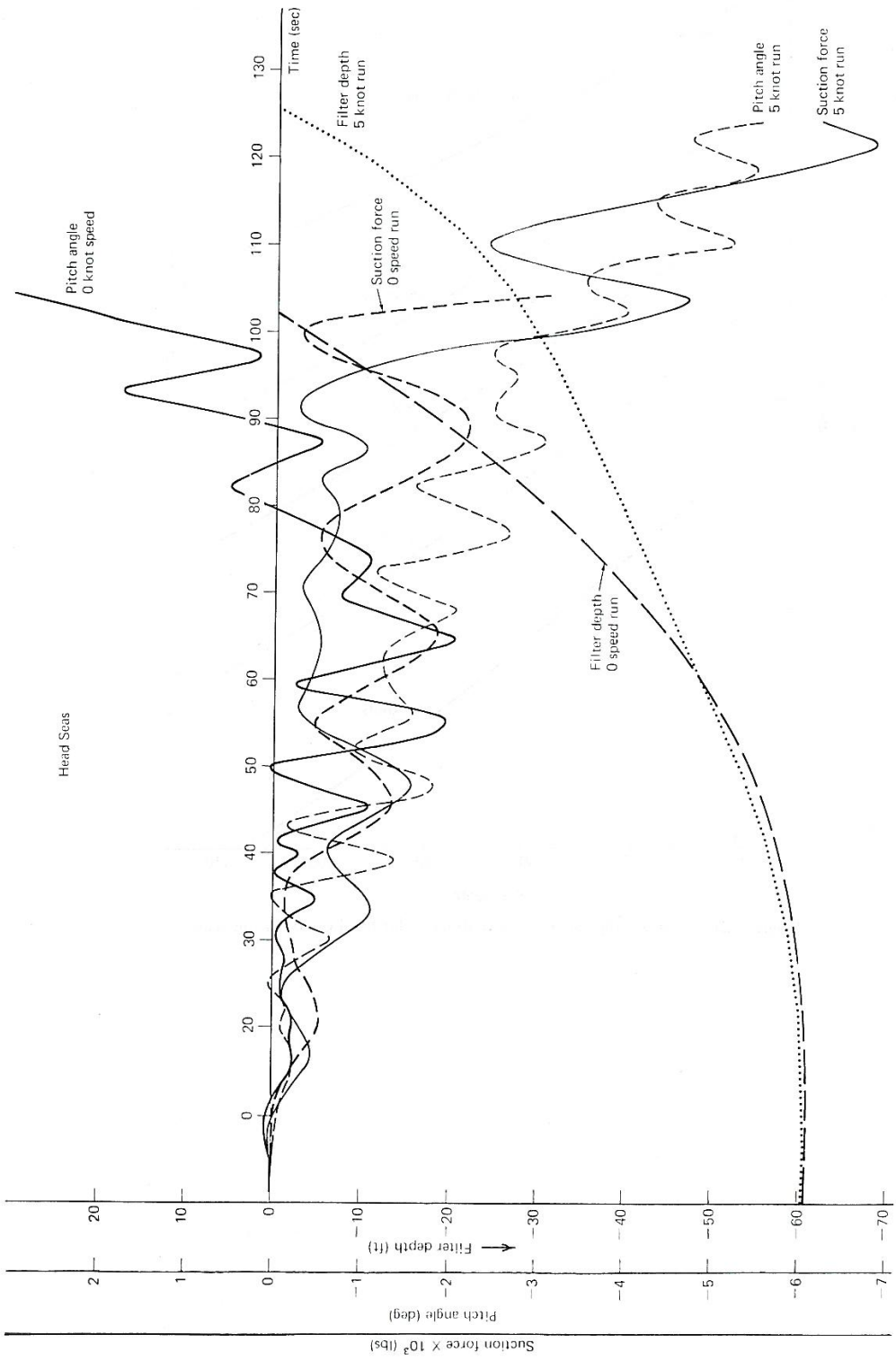


Figure 17.21 Typical uncontrolled motions of a submarine due to suction force.

times greater than the average suction force.

Because suction forces make depth maintenance difficult and may cause broaching in near-surface operations, countermeasures are often necessary. To optimize course for minimum suction forces it is necessary to determine the direction and severity of the sea as closely as possible. If the seas are, irregular, the component waves should be considered and the dominant component should be compensated. It is advantageous to meet the dominant sea on the beam, since the head and following seas are least desirable. The use of diving planes and ballasting by an amount equal to the suction force are also recommended.

The suction forces experienced near the free surface are also present near the bottom or a fixed boundary. Near the bottom the Venturi effect produces a bow-down moment which is known as squatting. The similar forces are experienced by submarines when operating in a narrow channel; here they originate from both sides of the channel and act in a lateral direction. If the submarine sails directly down the center of a channel, the suction forces and moments are equal in magnitude but opposite in sign and so cancel each other. If, however, the submarine is closer to one side of the channel, it experiences a bow-towards moment. When the submarine operates near another ship a similar effect is also to be expected.

Appendix

A

SEAKEEPING TABLES FOR EXTENDED SERIES 60 SHIPS IN HEAD SEAS

Seakeeping Tables for Extended Series 60 *Ships in Head Seas* [29*b*]

The following nondimensional relationships have been used in the seakeeping tables, Tables A.1 to A.24, that follows:

Froude number	(ship speed/$\sqrt{g\text{LWL}}$) $\times 10^2$
Nondimensional sea state	significant wave height/LBP
Heaving motion	(rms heave at amidships/LBP) $\times 10^4$
Pitching motion	(rms pitch in degrees) $\times 10^2$
Bending moment	[(rms bending moment at amidships) $\times 10^7$]/$pg(\text{LBP})^4$
Added resistance	[(mean added resistance) $\times 10^7$]/$pg(\text{LBP})^3$
Relative motion	(rms relative motion/LBP) $\times 10^4$
Relative velocity	(rms relative velocity/$\sqrt{g\text{LBP}}$) $\times 10^4$
Acceleration	(rms acceleration/g) $\times 10^4$

The rms values are the root mean squares of the responses in an irregular seaway, that is, $\sqrt{m_0}$, which is the square root of the area under the response spectrum for a particular ship motion characteristic.

TABLE A-1 SEAKEEPING RESPONSES FOR $C_B = 0.55$, $L/B = 5.5$, LCB $= -1.5\%$

		Froude No.	$B/T = 2$								$B/T = 3$								$B/T = 4$							
			Significant Wave Height/LBP								Significant Wave Height/LBP								Singificant Wave Height/LBP							
		[%]	0.015	0.020	0.025	0.030	0.040	0.050	0.075	0.100	0.015	0.020	0.025	0.030	0.040	0.050	0.075	0.100	0·015	0.020	0.025	0.030	0.040	0.050	0.075	0.100
Heave		10	10	31	51	71	105	135	199	262	10	22	36	49	75	101	166	231	8	18	29	41	65	91	156	222
		15	9	27	55	81	126	158	229	290	9	26	44	61	90	117	183	246	9	22	35	49	75	102	167	231
		20	6	23	55	83	137	177	256	320	9	27	48	68	104	134	201	264	9	24	40	57	86	114	179	243
		25	4	21	50	82	142	192	280	347	8	25	49	73	115	149	220	283	8	25	44	62	96	125	193	257
		30	3	19	41	82	146	206	301	372	6	21	50	76	124	161	238	302	8	24	45	66	104	137	206	270
Pitch		10	27	70	119	166	240	297	389	444	34	77	119	156	216	263	343	394	34	71	107	140	195	239	315	365
		15	20	58	107	153	235	295	396	457	29	72	117	158	224	275	360	414	31	71	110	145	204	251	331	382
		20	16	48	94	142	227	291	399	462	24	65	111	154	225	279	370	427	27	67	108	147	209	258	342	395
		25	11	39	87	132	220	287	402	470	20	58	104	149	224	281	377	436	23	63	105	145	211	262	349	404
		30	8	35	76	125	215	292	409	480	16	49	97	144	225	283	384	444	20	58	101	142	211	265	355	412
Bending Moment		10	37	72	106	137	183	215	257	279	53	97	136	167	213	245	287	307	62	108	147	179	225	256	298	319
		15	37	68	106	140	195	229	280	304	51	98	141	178	230	265	314	336	62	112	157	192	244	279	326	348
		20	37	68	106	140	200	241	302	330	50	96	144	185	246	287	342	369	60	115	164	206	264	304	358	383
		25	37	70	107	143	207	255	323	357	50	96	146	192	262	308	373	404	59	117	170	216	284	329	392	421
		30	38	72	109	149	218	273	349	388	49	96	150	199	279	330	406	442	59	117	175	226	303	356	427	462
Added Resistance		10	7	29	63	104	176	236	314	359	11	32	61	91	148	191	248	282	13	34	60	88	140	179	231	262
		15	5	23	59	105	203	278	412	496	9	32	65	103	175	234	332	405	12	34	65	99	161	214	305	377
		20	3	17	56	107	229	321	509	632	7	31	70	116	202	277	416	528	11	35	70	110	182	249	379	491
		25	2	13	45	97	229	358	590	745	6	26	68	121	233	325	507	643	9	34	73	121	212	296	458	597
		30	1	9	34	88	229	394	670	859	4	21	65	126	265	373	598	757	8	33	76	131	242	343	538	703
Acceleration	Sta. 0	10	268	673	1072	1436	1940	2301	2751	2975	408	834	1201	1492	1896	2181	2535	2703	438	813	1130	1370	1736	1972	2287	2444
		15	214	578	1057	1475	2147	2549	3160	3444	376	885	1343	1736	2262	2623	3109	3331	463	941	1355	1683	2154	2476	2886	3081
		20	177	515	1008	1453	2220	2729	3482	3834	344	878	1401	1869	2540	2990	3594	3884	445	1004	1507	1940	2508	2915	3447	3689
		25	148	459	944	1427	2274	2888	3767	4191	312	826	1413	1957	2771	3297	4042	4382	412	1026	1601	2107	2820	3298	3952	4261
		30	127	424	857	1404	2326	3071	4052	4546	271	744	1409	2007	2978	3565	4463	4872	391	1013	1653	2233	3081	3656	4428	4801
	Sta. 5	10	158	426	687	925	1257	1496	1798	1958	241	503	729	909	1161	1344	1579	1699	259	486	675	824	1050	1200	1411	1525
		15	127	363	693	984	1450	1722	2146	2345	222	548	840	1095	1431	1665	1992	2150	278	574	831	1038	1334	1542	1816	1956
		20	98	314	676	983	1535	1889	2434	2693	205	552	894	1202	1649	1949	2361	2568	267	622	943	1224	1589	1855	2215	2388
		25	78	285	626	972	1587	2042	2688	3003	187	516	910	1280	1838	2194	2713	2955	248	642	1016	1347	1821	2137	2585	2806
		30	67	265	549	967	1638	2204	2930	3303	158	458	918	1325	2002	2407	3043	3342	236	636	1057	1445	2018	2407	2942	3208
	Sta. 10	10	93	262	413	550	740	882	1076	1194	109	221	326	410	541	646	805	905	102	190	270	338	455	544	699	801
		15	89	256	469	667	967	1147	1428	1568	111	288	442	582	763	905	1113	1231	125	256	381	482	638	759	945	1058
		20	69	224	504	728	1130	1367	1759	1951	115	326	528	711	980	1167	1436	1588	128	314	484	638	839	1001	1234	1366
		25	52	211	498	754	1233	1571	2069	2313	115	327	580	822	1184	1419	1771	1947	128	357	571	764	1047	1244	1539	1703
		30	43	205	435	783	1323	1786	2358	2658	98	295	620	901	1373	1649	2099	2320	133	375	633	875	1238	1491	1853	2049
	Sta. 15	10	150	334	495	633	818	957	1160	1274	158	288	403	497	654	765	942	1050	137	243	340	428	569	675	851	960
		15	145	368	581	778	1053	1244	1512	1654	175	359	522	661	850	999	1214	1335	163	307	435	542	719	847	1048	1170
		20	129	345	639	894	1300	1531	1907	2087	175	419	636	823	1085	1271	1543	1693	183	378	552	702	912	1076	1315	1451
		25	106	316	676	954	1475	1797	2315	2560	176	449	719	970	1323	1571	1913	2092	186	439	666	865	1140	1338	1634	1795
		30	91	309	631	1002	1617	2105	2713	3020	164	432	777	1094	1581	1864	2313	2525	191	482	760	1011	1371	1626	1984	2181
	Sta. 20	10	257	559	834	1072	1395	1630	1948	2104	313	596	837	1032	1324	1521	1792	1934	303	553	765	942	1206	1386	1644	1779
		15	235	585	912	1204	1620	1914	2312	2516	321	665	967	1221	1571	1825	2160	2328	334	644	910	1125	1454	1675	1980	2140
		20	213	553	958	1333	1895	2235	2747	2984	306	717	1083	1400	1835	2136	2555	2763	348	721	1049	1325	1705	1983	2350	2533
		25	178	498	1009	1403	2118	2540	3234	3554	297	744	1170	1560	2103	2485	2988	3240	343	783	1178	1520	1981	2305	2755	2974
		30	153	481	963	1452	2297	2929	3738	4132	277	712	1227	1706	2418	2841	3478	3762	334	826	1284	1690	2260	2658	3188	3460

Relative Motion	Sta. 1	10	48	99	153	204	276	328	392	424	55	103	147	184	235	271	317	338	57	99	135	165	209	239	278	297
		15	43	83	144	199	290	344	427	465	50	100	150	194	255	296	354	380	54	99	142	177	228	264	311	332
		20	40	74	132	187	285	351	449	494	46	94	146	194	266	314	381	413	50	97	143	185	242	282	337	363
		25	39	68	119	176	278	355	463	515	44	85	139	191	273	326	404	439	47	92	141	185	251	296	359	389
		30	38	64	106	167	272	360	475	533	41	76	133	186	277	334	421	462	45	87	137	184	257	307	376	410
	Sta. 2	10	48	95	144	189	253	298	353	380	55	97	136	167	210	241	279	296	56	92	123	148	185	210	241	255
		15	43	81	136	186	268	316	389	421	49	95	139	178	231	267	315	337	53	94	131	161	205	235	273	290
		20	41	72	126	176	266	325	412	452	46	90	137	180	243	286	343	370	50	92	133	170	219	254	300	321
		25	39	67	115	167	261	330	428	474	44	82	131	179	252	299	366	396	47	89	132	172	229	268	322	347
		30	39	63	103	159	256	336	441	493	42	74	126	175	257	307	385	420	45	84	129	172	236	280	340	369
	Sta. 3	10	47	90	133	173	228	267	314	336	53	90	123	149	185	210	240	253	53	84	110	130	160	179	203	214
		15	43	78	128	173	245	287	351	378	49	90	128	162	206	237	277	294	52	87	119	144	180	205	235	249
		20	41	70	120	165	246	298	376	411	46	86	127	165	220	257	305	328	49	87	122	154	195	225	263	279
		25	40	66	110	158	243	306	393	435	44	79	123	165	230	271	329	355	46	84	123	157	207	240	285	306
		30	39	63	99	151	240	313	408	455	42	72	119	163	236	281	349	379	45	80	121	158	214	252	304	328
	Sta. 4	10	46	84	122	157	204	237	276	294	50	82	109	130	160	180	202	212	49	75	95	111	134	148	166	173
		15	43	75	119	159	223	260	314	337	47	83	116	145	182	207	239	253	49	79	105	126	155	175	198	208
		20	41	68	113	154	226	272	341	371	45	80	117	150	197	228	268	287	47	80	111	137	171	195	226	239
		25	39	64	105	148	225	282	360	397	43	75	114	152	208	243	293	314	45	79	112	142	184	212	249	265
		30	39	61	95	143	224	291	377	419	41	69	111	151	216	255	314	339	44	76	111	144	193	225	268	288
	Sta. 20	10	35	50	68	87	115	136	169	184	35	51	68	84	109	127	154	167	37	55	72	87	111	128	153	165
		15	37	55	75	96	129	153	188	206	34	48	64	80	105	124	152	166	35	49	65	79	102	119	144	156
		20	38	57	84	110	154	180	223	243	35	50	67	84	110	130	159	175	34	47	61	76	97	114	140	153
		25	38	57	93	121	177	211	268	295	37	53	73	93	124	146	179	195	35	48	63	77	100	118	144	158
		30	38	59	93	131	198	251	318	351	37	54	79	104	144	168	207	225	36	50	66	83	109	128	156	171
Relative Velocity	Sta. 1	10	260	364	487	607	771	890	1024	1084	279	392	501	591	712	796	887	921	286	388	480	552	658	722	794	822
		15	294	370	499	627	839	961	1141	1214	308	422	546	659	807	908	1031	1079	320	431	540	631	758	843	937	971
		20	334	393	510	632	858	1006	1222	1313	344	445	572	697	877	996	1146	1208	353	464	585	697	840	942	1062	1107
		25	375	423	522	642	873	1045	1284	1389	382	465	592	726	933	1066	1245	1315	388	492	618	739	911	1024	1168	1226
		30	417	459	538	657	889	1085	1338	1455	422	488	614	749	982	1122	1330	1413	428	520	646	774	967	1098	1261	1330
	Sta. 2	10	261	357	466	572	715	819	932	983	280	380	474	550	653	723	794	819	286	375	452	513	599	650	703	722
		15	296	367	482	597	784	892	1047	1108	310	413	521	619	746	831	933	970	322	420	514	590	697	766	839	864
		20	335	392	498	607	808	938	1128	1206	346	439	551	660	815	918	1043	1094	355	455	560	656	777	863	960	993
		25	376	424	513	620	826	978	1189	1280	384	462	574	692	872	987	1139	1196	391	486	596	701	847	943	1062	1107
		30	418	460	532	638	845	1019	1243	1344	424	487	598	717	921	1043	1221	1290	430	515	626	738	904	1015	1151	1206
	Sta. 3	10	261	347	443	534	657	745	839	881	277	363	442	504	589	645	699	715	281	356	418	466	534	571	608	618
		15	297	363	464	565	728	820	953	1002	309	399	492	575	680	751	832	859	319	403	481	543	630	685	738	753
		20	336	389	484	580	757	869	1033	1099	346	429	526	619	750	837	939	979	354	441	530	610	710	779	854	876
		25	377	422	502	597	778	911	1096	1173	385	456	553	654	808	906	1031	1077	391	475	569	657	779	858	952	985
		30	419	459	524	618	799	952	1148	1235	424	483	580	683	858	961	1111	1166	430	507	602	697	836	929	1038	1081
	Sta. 4	10	259	335	417	493	597	670	746	779	271	342	406	454	522	564	601	609	272	331	379	414	463	489	510	512
		15	296	355	442	530	670	748	859	898	306	382	459	528	612	668	730	747	313	381	444	491	559	99	634	641
		20	335	384	467	551	704	800	940	995	344	416	498	575	683	753	833	863	350	423	496	559	638	692	746	759
		25	376	419	490	571	729	844	1003	1068	383	446	528	613	741	822	923	958	388	460	538	610	707	770	841	863
		30	418	456	514	596	754	887	1056	1131	423	476	559	646	793	879	1002	1044	428	494	574	652	765	840	924	955
	Sta. 20	10	237	261	288	317	358	388	426	436	233	256	282	306	342	367	394	400	237	267	297	322	359	383	406	413
		15	284	315	349	384	436	474	518	534	276	296	317	338	367	389	411	413	276	296	317	335	363	381	397	395
		20	329	364	411	462	544	591	657	677	323	344	368	392	425	447	472	474	319	335	352	368	386	400	410	403
		25	373	408	472	531	648	713	822	862	369	396	427	460	507	540	573	579	365	382	399	416	437	450	459	451
		30	417	453	518	592	743	857	994	1052	415	445	487	533	607	649	705	716	411	432	455	477	508	528	543	539

TABLE A-2 SEAKEEPING RESPONSES FOR $C_B = 0.55$, $L/B = 7.0$, LCB $= -1.5\%$

		Froude No	$B/T = 2$								$B/T = 3$								$B/T = 4$							
			Significant Wave Height/LBP								Significant Wave Height/LBP								Significant Wave Height/LBP							
		[%]	0.015	0.020	0.025	0.030	0.040	0.050	0.075	0.100	0.015	0.020	0.025	0.030	0.040	0.050	0.075	0.100	0.015	0.020	0.025	0.030	0.040	0.050	0.075	0.100
Heave		10	13	31	47	64	89	116	178	241	9	19	30	42	66	92	157	222	8	16	26	37	61	86	152	217
		15	12	36	58	78	111	140	204	265	12	25	39	52	78	105	169	233	9	20	31	43	68	93	158	224
		20	12	35	62	88	130	163	231	291	11	29	47	64	92	120	184	247	11	24	37	51	77	103	168	232
		25	9	30	63	93	146	182	257	318	10	32	52	72	106	135	201	263	10	26	43	59	87	115	179	243
		30	6	25	63	94	154	197	280	345	10	31	55	78	117	150	218	280	10	28	47	65	97	126	192	255
Pitch		10	38	90	138	182	245	296	378	429	40	80	117	150	206	249	325	374	35	69	103	133	185	227	301	351
		15	32	81	131	178	252	308	397	452	38	82	124	161	221	268	347	397	36	73	110	143	198	242	318	368
		20	25	69	121	170	251	309	407	464	34	79	124	165	229	279	363	415	34	74	113	148	207	253	331	383
		25	21	61	111	160	244	307	410	472	28	74	120	164	232	285	373	427	31	72	114	151	212	260	342	394
		30	16	50	102	153	242	306	414	478	24	68	115	160	233	288	379	436	27	69	112	152	215	265	349	402
Bending Moment		10	39	73	103	128	161	186	219	234	50	86	117	141	177	201	233	249	54	90	122	146	182	206	239	256
		15	37	73	105	132	173	199	236	254	50	90	125	151	191	218	253	269	56	97	131	158	197	223	258	275
		20	37	71	104	135	182	212	254	274	49	92	130	162	205	236	275	294	57	102	139	169	213	242	281	299
		25	37	69	105	137	190	223	272	295	48	93	134	169	219	252	298	319	56	104	146	181	229	262	306	326
		30	37	69	106	139	196	234	289	316	47	93	136	174	231	269	321	346	55	106	152	191	244	281	331	354
Added Resistance		10	8	26	51	77	120	155	199	222	10	25	44	63	99	124	158	178	12	27	44	63	96	120	153	172
		15	6	25	54	88	147	196	272	322	9	27	51	76	120	157	217	262	11	28	49	71	112	146	203	250
		20	5	25	58	99	174	237	344	421	8	29	57	88	141	190	275	346	10	29	53	79	128	171	254	328
		25	3	19	54	99	197	273	417	514	7	29	61	99	169	230	340	430	9	30	59	92	151	205	309	400
		30	2	13	50	99	220	308	489	607	6	28	65	110	196	270	405	513	9	31	65	106	174	240	365	472
Acceleration	Sta. 0	10	438	965	1410	1795	2209	2557	2955	3129	523	939	1280	1530	1910	2145	2457	2612	483	830	1112	1339	1667	1882	2180	2327
		15	396	984	1515	1961	2599	3016	3555	3824	576	1127	1592	1936	2452	2789	3199	3391	586	1063	1460	1754	2200	2481	2850	3030
		20	347	906	1506	2062	2860	3359	4061	4364	547	1216	1795	2282	2888	3334	3882	4126	636	1237	1745	2126	2702	3073	3538	3756
		25	296	809	1482	2077	3026	3606	4468	4856	503	1243	1910	2487	3263	3780	4477	4793	644	1344	1962	2464	3134	3614	4200	4467
		30	248	717	1437	2067	3145	3823	4836	5310	472	1229	1967	2618	3558	4185	5007	5404	600	1402	2117	2740	3526	4090	4822	5146
	Sta. 5	10	267	596	877	1123	1377	1606	1868	1988	308	558	762	914	1147	1295	1501	1613	288	493	660	797	997	1133	1330	1442
		15	234	630	979	1275	1694	1966	2332	2520	353	688	977	1190	1516	1732	2007	2138	352	642	884	1064	1342	1520	1765	1895
		20	213	588	995	1376	1921	2266	2746	2963	332	759	1130	1449	1832	2126	2495	2664	385	760	1078	1317	1683	1923	2233	2388
		25	176	510	990	1414	2094	2490	3105	3379	301	788	1225	1606	2122	2464	2938	3163	391	838	1232	1560	1989	2305	2704	2889
		30	138	442	976	1414	2198	2680	3423	3778	288	784	1275	1714	2352	2780	3346	3630	362	883	1349	1759	2277	2651	3151	3382
	Sta. 10	10	144	303	443	559	694	823	984	1077	119	213	294	363	479	566	716	817	118	190	254	316	419	503	655	757
		15	138	382	588	763	998	1157	1390	1518	163	313	449	546	716	837	1014	1122	142	260	361	446	587	691	864	975
		20	144	411	671	915	1256	1487	1796	1956	173	398	597	770	972	1153	1378	1503	178	346	500	614	807	945	1151	1273
		25	129	374	715	1027	1503	1773	2200	2391	166	463	718	945	1247	1455	1760	1920	193	424	634	809	1042	1229	1486	1626
		30	97	321	754	1085	1683	2021	2572	2842	174	497	805	1083	1488	1766	2140	2346	187	486	752	991	1290	1522	1844	2013
	Sta. 15	10	210	375	513	615	794	910	1084	1190	173	289	391	482	623	728	902	1008	155	258	348	433	569	672	844	949
		15	220	465	673	846	1062	1228	1458	1575	213	375	512	622	807	931	1128	1248	177	306	420	523	685	807	1004	1125
		20	213	535	808	1042	1358	1582	1882	2047	250	477	671	824	1052	1222	1452	1582	217	391	540	663	866	1007	1229	1362
		25	209	544	888	1219	1667	1959	2358	2543	253	566	832	1061	1341	1554	1853	2005	255	490	692	853	1102	1283	1538	1684
		30	179	487	956	1345	1974	2305	2845	3098	253	635	967	1249	1644	1913	2283	2485	268	580	849	1083	1371	1603	1916	2080
	Sta. 20	10	374	708	987	1208	1532	1743	2028	2173	377	653	881	1066	1338	1520	1774	1910	340	579	779	949	1199	1371	1618	1750
		15	378	780	1131	1424	1807	2095	2453	2624	423	777	1070	1300	1649	1875	2180	2339	396	702	956	1166	1475	1683	1978	2128
		20	346	836	1264	1624	2120	2454	2913	3141	454	884	1251	1537	1960	2250	2617	2800	444	823	1138	1388	1771	2019	2360	2534
		25	335	853	1345	1813	2439	2878	3435	3698	445	972	1424	1810	2288	2644	3105	3317	484	939	1327	1629	2084	2392	2789	2988
		30	294	774	1410	1972	2833	3297	4017	4341	428	1042	1575	2024	2646	3060	3619	3898	489	1039	1512	1914	2414	2797	3276	3502

Relative Motion																														
Sta. 1	10	56	115	167	214	267	310	362	384	60	105	143	173	218	247	285	304	59	96	129	155	194	220	255	272
	15	51	109	167	218	291	340	404	435	59	109	154	190	243	279	325	346	58	102	139	170	215	245	285	304
	20	46	96	158	216	304	358	437	471	53	107	130	203	260	303	358	383	57	103	146	181	233	268	314	335
	25	43	83	148	208	306	367	459	500	49	102	156	204	274	320	384	414	53	102	149	190	245	286	339	363
	30	40	74	138	197	302	371	474	523	46	96	151	203	280	333	404	439	49	99	149	194	255	299	359	387
Sta. 2	10	56	108	155	196	241	278	321	339	59	98	130	155	193	216	247	261	57	89	116	138	169	190	217	231
	15	50	104	156	201	266	309	364	390	58	102	142	173	218	248	286	303	57	95	127	153	191	215	247	262
	20	46	93	149	202	280	329	397	426	53	101	147	186	236	273	319	340	56	98	135	165	209	238	276	293
	25	43	81	141	195	284	338	420	456	49	98	146	189	250	290	346	371	53	97	138	174	222	257	301	321
	30	41	73	132	186	282	344	437	480	46	92	143	189	258	304	366	396	49	95	139	179	233	270	322	345
Sta. 3	10	54	101	141	177	214	246	281	295	56	89	116	136	167	185	208	219	53	80	102	119	143	159	180	189
	15	49	98	145	184	241	277	324	346	56	95	128	154	192	217	247	260	55	87	114	135	165	185	209	220
	20	46	89	139	187	256	299	358	383	52	95	134	169	211	242	281	297	54	90	122	147	184	208	238	251
	25	43	79	133	182	262	310	382	413	48	92	135	173	226	260	307	328	51	91	127	157	198	227	263	279
	30	41	71	126	175	262	318	400	439	46	88	133	174	235	275	329	354	48	89	128	163	209	242	284	303
Sta. 4	10	52	92	127	157	187	214	241	252	52	79	100	116	140	153	170	177	48	69	86	99	117	128	142	148
	15	48	92	132	167	215	246	285	303	53	86	114	135	166	186	208	218	51	77	99	115	139	154	171	179
	20	45	85	129	171	231	269	319	340	50	88	121	150	186	212	242	255	51	82	108	128	158	177	200	210
	25	43	76	125	169	241	283	345	372	47	86	124	157	201	231	269	286	49	84	114	140	173	197	226	238
	30	41	69	119	164	243	292	365	399	45	83	123	159	212	247	292	313	47	83	117	147	185	213	247	262
Sta. 20	10	35	54	75	93	121	141	171	185	38	59	78	95	121	139	164	177	41	61	80	96	121	138	162	174
	15	35	54	74	94	121	144	175	190	36	53	71	87	113	131	157	170	38	56	74	89	113	130	154	166
	20	37	58	80	101	134	157	191	209	35	51	68	85	109	128	155	168	36	52	68	82	105	122	146	158
	25	38	61	88	115	155	182	221	239	35	52	70	87	113	131	160	175	35	49	65	79	101	118	142	155
	30	38	60	96	129	183	212	260	282	36	55	75	94	123	144	174	190	35	49	65	80	102	119	144	157
Relative Velocity																														
Sta. 1	10	279	416	550	673	796	904	1013	1051	295	409	506	581	692	755	825	854	295	391	472	537	627	681	743	767
	15	308	439	585	715	902	1022	1168	1233	331	459	581	676	815	904	999	1034	335	449	550	630	746	814	889	919
	20	342	446	594	746	969	1107	1292	1361	359	492	632	759	911	1024	1151	1196	371	495	615	710	850	939	1034	1069
	25	379	458	605	756	1009	1160	1381	1470	392	518	666	804	993	1116	1273	1335	404	531	665	783	936	1046	1166	1209
	30	419	481	618	762	1031	1201	1451	1558	430	541	689	835	1052	1196	1374	1451	438	562	705	841	1012	1134	1281	1335
Sta. 2	10	280	402	520	626	732	825	914	944	294	393	475	539	629	679	732	751	294	375	442	495	566	707	651	665
	15	309	429	559	673	837	940	1064	1119	331	445	550	630	749	822	896	921	335	434	519	586	681	734	790	810
	20	344	441	572	708	903	1026	1184	1242	361	480	603	712	842	939	1042	1076	372	482	585	664	783	854	928	952
	25	381	456	588	722	947	1079	1272	1348	394	509	639	760	922	1028	1159	1208	407	520	636	737	866	958	1054	1085
	30	421	481	604	732	971	1121	1341	1434	432	535	665	794	982	1106	1256	1319	441	553	678	795	941	1044	1164	1205
Sta. 3	10	278	385	486	576	664	743	813	834	289	371	438	489	560	597	634	645	286	351	403	444	496	525	553	558
	15	308	415	529	628	768	855	959	1003	328	425	514	578	677	735	789	806	330	412	481	534	608	648	686	696
	20	345	433	548	666	835	942	1075	1123	360	464	568	660	768	848	929	953	369	463	548	612	708	764	816	831
	25	382	451	567	686	883	997	1163	1225	394	496	608	711	848	936	1042	1080	405	503	601	684	791	865	937	958
	30	422	478	587	700	910	1040	1232	1310	432	525	638	748	907	1013	1136	1186	440	539	645	744	864	949	1043	1072
Sta. 4	10	274	364	448	521	594	658	710	724	279	344	395	434	485	511	533	535	272	321	359	386	421	439	452	447
	15	306	399	496	580	697	768	853	886	321	401	472	522	600	643	680	688	320	384	437	476	530	556	578	579
	20	343	422	521	622	765	856	966	1004	356	443	529	604	690	754	814	829	362	437	505	554	628	668	702	707
	25	382	444	544	647	817	914	1054	1104	392	478	572	658	769	841	924	950	400	481	561	626	710	767	817	828
	30	422	473	569	666	848	959	1123	1188	430	511	606	698	830	917	1015	1053	437	520	607	687	783	850	920	937
Sta. 20	10	233	262	294	324	371	401	437	447	237	273	309	339	384	411	439	449	243	282	320	349	393	419	446	456
	15	279	306	337	370	409	443	479	485	275	300	328	351	389	413	435	438	279	308	339	363	400	422	441	444
	20	325	360	399	436	490	526	569	583	318	338	361	383	412	437	452	449	318	339	362	379	408	425	435	431
	25	372	413	462	516	591	647	704	721	363	386	411	437	465	486	507	503	360	377	395	410	429	443	447	436
	30	416	456	523	596	717	778	869	897	410	438	470	500	544	571	598	602	405	422	439	458	473	485	489	474

TABLE A-3 SEAKEEPING RESPONSES FOR $C_B = 0.55$, $L/B = 8.5$, LCB $= -1.5\%$

		Froude No. [%]	$B/T = 2$ Significant Wave Height/LBP 0.015	0.020	0.025	0.030	0.040	0.050	0.075	0.100	$B/T = 3$ Significant Wave Height/LBP 0.015	0.020	0.025	0.030	0.040	0.050	0.075	0.100	$B/T = 4$ Significant Wave Height/LBP 0.015	0.020	0.030	0.040	0.050	0.075	0.075	0.100
Heave		10	14	26	39	61	76	101	165	229	9	17	26	37	61	87	152	218	8	15	24	35	58	84	149	215
		15	15	35	53	70	96	124	185	247	11	22	33	45	70	95	160	225	9	18	28	39	63	89	154	219
		20	13	40	63	84	117	146	209	270	13	28	42	55	82	108	172	236	10	21	33	45	70	96	161	226
		25	13	40	67	93	134	168	234	294	13	32	50	67	95	123	186	249	12	25	39	53	79	105	170	234
		30	12	36	68	100	150	186	258	318	12	34	55	76	108	137	202	264	12	28	44	60	88	116	180	244
Pitch		10	48	95	139	175	236	281	357	406	39	75	110	141	193	235	309	358	34	66	97	127	177	218	291	340
		15	41	94	143	188	253	304	386	437	41	83	122	155	212	256	331	381	36	71	106	137	190	232	306	356
		20	35	86	138	185	259	314	403	457	40	85	127	164	225	271	350	400	37	75	112	145	200	244	320	371
		25	28	77	129	179	259	316	412	468	36	82	127	168	232	282	364	416	36	76	115	150	208	254	332	383
		30	24	69	121	171	253	316	416	476	31	79	125	169	235	287	373	427	34	75	116	153	213	261	341	393
Bending Moment		10	39	68	93	112	142	161	186	199	45	74	100	120	149	169	196	210	46	77	103	123	153	173	201	215
		15	38	70	97	121	150	173	201	215	46	79	107	129	161	181	209	223	49	82	110	131	163	184	212	227
		20	36	70	99	125	161	184	216	232	47	83	114	138	173	196	226	241	51	88	118	141	176	198	228	243
		25	36	69	100	127	168	195	231	248	46	85	119	147	184	211	245	261	52	92	125	151	189	214	247	263
		30	36	67	100	130	175	204	246	265	45	86	123	154	196	225	264	282	52	94	131	160	202	230	267	284
Added Resistance		10	7	21	37	53	83	103	129	144	9	20	33	46	69	86	109	122	10	21	34	47	70	86	108	120
		15	7	23	45	67	107	138	186	219	8	22	38	55	86	110	150	182	10	23	38	53	82	105	145	178
		20	6	25	52	82	131	173	244	294	8	24	44	64	102	134	192	242	9	24	41	60	94	124	183	236
		25	5	23	52	89	153	210	302	366	7	26	50	78	124	166	241	303	9	25	47	69	112	149	221	287
		30	4	21	52	96	176	246	360	438	7	27	57	92	146	198	290	363	9	27	52	78	129	174	260	337
Acceleration	Sta. 0	10	609	1122	1536	1809	2288	2552	2883	3043	542	914	1211	1447	1783	2000	2300	2446	490	804	1061	1272	1577	1780	2062	2205
		15	583	1261	1829	2312	2827	3263	3740	3944	682	1220	1656	1969	2444	2732	3102	3282	625	1071	1439	1711	2117	2377	2730	2900
		20	520	1288	1956	2509	3277	3760	4409	4710	745	1433	2004	2414	3049	3445	3922	4142	742	1333	1818	2174	2710	3042	3473	3679
		25	476	1233	1971	2638	3561	4172	4967	5328	728	1549	2250	2819	3540	4069	4689	4961	807	1539	2147	2594	3278	3704	4233	4480
		30	424	1134	1949	2693	3795	4488	5451	5883	675	1599	2411	3112	3975	4590	5380	5719	828	1683	2414	2978	3780	4324	4978	5273
	Sta. 5	10	372	677	930	1094	1394	1558	1772	1885	319	539	713	854	1059	1194	1394	1502	293	476	626	752	937	1065	1257	1363
		15	363	792	1155	1466	1787	2076	2391	2528	407	735	999	1191	1485	1666	1910	2037	375	642	855	1027	1276	1440	1676	1800
		20	313	832	1276	1649	2152	2468	2912	3119	463	884	1242	1497	1902	2157	2478	2625	449	812	1110	1330	1666	1877	2162	2309
		25	294	811	1312	1764	2397	2820	3362	3625	450	974	1427	1801	2257	2609	3028	3214	493	953	1335	1616	2054	2329	2682	2856
		30	264	736	1306	1838	2617	3101	3782	4083	406	1019	1554	2023	2591	2999	3537	3778	515	1054	1523	1892	2406	2767	3212	3415
	Sta. 10	10	165	291	405	471	616	708	851	944	130	206	268	332	434	516	668	768	130	194	246	306	401	482	633	733
		15	206	422	611	759	934	1098	1284	1386	165	297	404	493	637	739	907	1017	154	252	335	414	539	636	808	919
		20	190	512	778	1007	1282	1476	1753	1889	221	417	592	707	920	1061	1261	1379	186	339	466	571	741	861	1055	1178
		25	194	562	888	1174	1577	1849	2200	2393	242	520	765	965	1211	1419	1677	1812	233	442	632	763	994	1155	1383	1517
		30	193	546	942	1324	1851	2197	2658	2873	229	598	915	1197	1519	1775	2114	2281	261	539	790	984	1266	1479	1760	1912
	Sta. 15	10	226	370	489	591	739	846	1017	1122	191	301	394	482	617	720	890	991	177	277	363	447	578	679	847	948
		15	279	494	668	788	1014	1148	1343	1459	220	362	484	591	755	877	1074	1192	194	316	422	523	679	798	993	1110
		20	297	609	869	1086	1333	1541	1798	1923	273	474	638	767	982	1122	1340	1472	223	376	509	629	814	951	1173	1305
		25	282	701	1045	1328	1703	1949	2299	2479	327	603	834	1001	1280	1468	1719	1862	273	482	655	797	1028	1185	1430	1576
		30	288	748	1161	1542	2033	2404	2829	3059	339	717	1034	1305	1607	1866	2187	2345	327	605	839	1013	1309	1504	1781	1939
	Sta. 20	10	455	784	1051	1256	1562	1758	2023	2161	403	661	872	1048	1305	1478	1724	1854	362	588	779	940	1183	1349	1590	1716
		15	488	907	1251	1511	1913	2159	2486	2652	478	819	1096	1319	1643	1857	2151	2304	429	723	964	1167	1465	1665	1949	2097
		20	502	1008	1441	1793	2243	2591	2992	3181	536	967	1316	1588	1997	2254	2598	2777	494	860	1160	1407	1766	2004	2339	2506
		25	460	1089	1622	2065	2643	3019	3554	3795	588	1108	1542	1860	2370	2692	3098	3300	556	1008	1375	1665	2103	2382	2762	2954
		30	453	1150	1756	2291	2995	3533	4137	4469	592	1227	1765	2215	2745	3172	3668	3894	616	1157	1606	1939	2476	2812	3245	3463

Relative Motion	Sta. 1	10	67	118	163	196	250	283	325	344	61	101	134	161	200	226	261	278	58	93	122	146	182	206	239	255
		15	58	120	175	225	279	324	377	400	62	109	149	180	227	258	297	316	60	99	133	161	202	229	265	283
		20	52	115	175	227	302	349	415	455	61	112	158	195	249	286	333	354	59	104	143	174	221	251	292	312
		25	49	105	167	226	311	367	443	478	55	111	162	208	265	308	363	388	58	106	149	184	236	272	317	339
		30	45	92	158	220	316	377	464	504	50	107	162	212	278	324	387	416	55	105	152	192	248	288	340	364
	Sta. 2	10	64	111	150	177	224	251	284	299	59	93	121	143	175	196	223	236	56	85	109	129	157	176	202	214
		15	58	113	163	206	252	292	336	355	60	102	136	162	202	227	258	273	58	92	121	144	177	199	227	241
		20	52	110	164	210	276	317	374	400	59	106	146	177	225	255	293	311	58	97	131	157	196	221	254	269
		25	48	101	158	211	287	337	403	433	55	105	151	191	240	278	324	344	57	100	138	167	212	242	279	297
		30	45	90	150	207	294	348	425	459	50	102	152	196	254	294	348	373	55	100	141	176	224	259	302	322
	Sta. 3	10	61	102	135	158	197	218	244	256	56	83	106	123	148	164	185	194	52	75	94	109	131	145	164	172
		15	56	106	149	186	225	259	296	310	58	93	122	143	176	195	219	231	55	83	106	125	151	168	189	199
		20	51	103	152	193	250	285	334	355	57	98	133	159	199	224	254	267	56	89	117	139	171	190	216	227
		25	48	96	148	195	262	306	363	389	54	98	139	173	215	247	285	301	55	93	125	150	187	211	241	255
		30	45	87	141	193	270	319	387	416	50	96	140	179	229	264	310	329	53	93	130	159	200	229	264	280
	Sta. 4	10	57	91	119	137	169	185	204	213	50	72	89	103	121	132	147	153	46	63	78	89	104	114	126	131
		15	54	97	134	165	198	227	255	266	54	83	106	123	148	163	181	189	50	72	90	104	124	136	151	158
		20	49	96	139	175	224	254	294	312	54	89	118	139	172	192	215	225	52	80	102	119	144	159	178	186
		25	47	91	137	179	237	276	324	346	52	91	125	154	190	216	246	258	52	84	111	131	162	181	203	213
		30	45	83	132	178	247	290	349	374	48	90	128	162	204	234	272	287	51	86	117	141	175	199	227	238
	Sta. 20	10	38	61	83	101	129	149	176	190	42	64	85	101	127	145	169	182	43	64	84	100	125	142	166	178
		15	37	56	78	95	125	145	174	189	38	59	78	95	121	138	164	177	40	60	79	95	119	136	160	172
		20	36	56	78	99	126	149	179	194	36	55	73	89	114	132	158	171	38	56	74	89	113	129	153	165
		25	37	61	85	106	139	161	195	212	36	53	71	87	111	130	156	169	36	53	69	83	107	123	146	158
		30	39	65	92	119	156	185	221	240	35	54	72	91	114	134	161	175	35	51	67	81	103	120	143	155
Relative Velocity	Sta. 1	10	305	442	562	643	787	862	943	976	301	404	488	557	650	705	767	793	297	385	458	518	598	646	702	723
		15	327	483	635	774	912	1034	1154	1195	343	471	582	667	792	863	939	970	342	449	540	614	715	775	841	868
		20	354	505	671	817	1021	1146	1308	1374	380	522	657	759	915	1011	1111	1148	382	507	618	706	833	907	988	1019
		25	389	516	682	848	1081	1237	1426	1505	409	557	711	846	1010	1134	1265	1311	420	555	685	786	939	1032	1131	1168
		30	426	526	690	863	1131	1297	1522	1611	440	584	748	903	1094	1228	1392	1452	455	593	738	860	1027	1143	1265	1309
	Sta. 2	10	303	424	528	597	720	780	844	868	300	387	457	513	586	628	674	690	295	368	427	474	535	571	610	618
		15	328	467	601	722	840	947	1045	1076	343	455	548	620	723	779	837	858	342	433	508	568	648	694	742	757
		20	355	493	640	769	948	1055	1194	1248	380	506	623	709	843	921	1000	1026	383	492	585	659	763	821	880	901
		25	391	509	656	803	1008	1145	1308	1374	411	543	678	794	935	1040	1146	1181	421	540	652	737	866	941	1017	1042
		30	428	521	668	823	1060	1206	1402	1476	442	573	717	853	1016	1132	1268	1315	457	581	706	809	952	1048	1144	1176
	Sta. 3	10	297	401	488	545	647	694	741	757	292	362	417	460	515	545	574	580	284	341	386	420	464	487	509	508
		15	326	448	563	665	765	855	932	955	337	431	508	566	647	689	729	741	334	408	467	513	572	605	635	640
		20	355	477	606	718	870	961	1077	1120	377	485	582	652	764	825	883	900	378	468	544	603	684	727	767	777
		25	391	498	627	754	932	1051	1187	1243	410	525	639	736	854	941	1023	1047	418	519	611	680	785	842	897	911
		30	429	514	643	779	986	1113	1280	1341	442	557	681	797	934	1031	1141	1176	455	562	667	751	870	946	1018	1038
	Sta. 4	10	287	374	444	489	569	604	635	644	277	330	371	401	437	456	471	468	267	306	337	359	386	398	404	394
		15	321	424	521	603	686	760	818	832	327	401	461	505	564	593	617	621	320	375	418	450	490	510	524	519
		20	352	458	568	663	790	865	959	991	369	457	536	591	679	725	764	772	367	438	496	540	598	627	649	650
		25	390	483	595	703	853	954	1066	1112	405	501	595	673	768	837	897	912	409	492	564	617	697	738	773	778
		30	428	504	615	733	909	1018	1158	1207	439	537	641	736	847	926	1011	1035	449	537	622	688	781	839	889	898
	Sta. 20	10	236	276	316	350	402	434	468	480	244	287	330	362	410	439	469	481	247	291	333	365	410	437	466	477
		15	276	306	342	369	419	449	480	488	278	313	348	377	420	446	470	477	282	319	356	384	426	449	472	479
		20	322	352	386	422	461	498	530	534	317	343	370	393	430	452	469	469	320	349	378	402	436	455	469	470
		25	368	406	450	492	548	581	627	637	360	381	405	425	456	477	490	484	360	381	404	421	449	463	468	460
		30	414	462	516	571	644	706	758	783	405	428	455	483	506	531	546	537	403	419	437	451	472	483	482	467

TABLE A-4 SEAKEEPING RESPONSES FOR $C_B = 0.60$, $L/B = 5.5$, LCB $= -0.5\%$

		Froude No.	$B/T=2$								$B/T=3$								$B/T=4$							
			Significant Wave Height/LBP								Significant Wave Height/LBP								Significant Wave Height/LBP							
		[%]	0.015	0.020	0.025	0.030	0.040	0.050	0.075	0.100	0.015	0.020	0.025	0.030	0.040	0.050	0.075	0.100	0.015	0.020	0.025	0.030	0.040	0.050	0.075	0.100
Heave		10	9	26	45	63	95	124	190	253	8	19	31	44	70	96	161	227	7	16	26	37	62	88	154	219
		15	8	24	49	72	114	146	217	280	8	22	38	54	83	110	176	241	7	19	31	44	70	97	163	228
		20	5	20	50	75	126	164	243	307	8	24	42	61	95	125	193	257	7	21	36	51	80	108	174	239
		25	3	19	46	75	132	180	266	334	7	22	44	66	106	139	210	274	7	22	39	56	89	118	186	251
		30	2	17	37	76	137	194	287	359	5	19	45	69	115	151	227	292	7	21	40	60	97	129	199	264
Pitch		10	26	67	113	157	227	280	369	423	31	70	109	144	202	248	327	378	30	64	99	130	184	227	303	353
		15	20	58	104	149	226	284	380	439	26	66	108	147	209	259	342	396	28	64	101	135	192	237	316	368
		20	15	47	95	142	225	285	389	451	22	61	104	145	212	264	353	408	24	61	100	136	195	243	325	379
		25	11	39	89	133	221	286	399	465	19	55	98	141	214	269	361	419	21	57	97	135	198	247	332	387
		30	8	36	76	128	220	299	414	483	15	46	93	138	217	272	371	430	18	53	93	133	199	251	339	395
Bending Moment		10	42	83	123	160	216	255	308	335	58	107	151	187	239	275	324	349	66	117	160	195	246	281	330	354
		15	41	78	123	164	232	275	339	370	56	109	158	201	260	302	359	386	67	123	172	212	270	310	364	390
		20	40	76	123	165	239	291	368	405	55	109	163	210	281	329	396	428	66	126	181	228	295	341	403	433
		25	40	78	122	167	246	308	395	437	55	108	166	219	301	356	435	471	65	128	189	241	319	372	444	479
		30	41	80	122	173	257	328	424	474	54	107	170	228	322	384	476	519	64	130	196	254	343	404	488	529
Added Resistance		10	6	29	64	107	182	242	325	372	11	32	62	95	155	201	263	300	14	35	64	94	152	194	253	289
		15	5	23	60	107	208	287	427	516	9	32	66	106	181	244	352	434	12	35	67	103	172	230	334	418
		20	3	16	56	108	234	331	528	660	7	31	70	117	208	288	441	568	11	35	71	113	192	266	414	546
		25	2	13	44	98	233	368	611	777	6	26	67	121	238	335	533	685	9	33	73	123	221	313	496	655
		30	1	9	33	88	232	405	694	895	4	21	65	126	269	383	625	802	8	32	75	132	250	359	578	764
Acceleration	Sta. 0	10	241	603	963	1288	1744	2066	2486	2692	353	728	1056	1321	1694	1957	2296	2460	378	715	1001	1226	1567	1793	2100	2254
		15	199	541	966	1343	1942	2318	2877	3142	332	777	1188	1538	2020	2357	2809	3023	397	818	1187	1492	1925	2227	2620	2812
		20	166	480	935	1351	2056	2519	3209	3535	303	777	1249	1669	2281	2693	3259	3532	385	872	1319	1710	2237	2615	3116	3352
		25	135	427	896	1338	2132	2691	3520	3918	278	739	1268	1759	2501	2988	3681	4004	359	892	1408	1862	2516	2959	3573	3868
		30	116	399	811	1330	2201	2912	3832	4297	242	668	1272	1816	2705	3251	4086	4473	341	882	1454	1979	2757	3285	4011	4362
	Sta. 5	10	136	366	594	803	1100	1311	1594	1743	204	430	628	793	1022	1190	1417	1537	224	423	592	730	940	1084	1289	1404
		15	113	322	608	864	1274	1525	1914	2101	190	468	724	949	1256	1473	1779	1932	234	491	718	909	1180	1374	1640	1778
		20	88	280	601	879	1374	1696	2192	2434	176	473	775	1049	1454	1727	2113	2309	225	530	812	1062	1401	1645	1988	2158
		25	70	256	568	877	1437	1850	2449	2743	161	446	795	1123	1627	1953	2436	2668	209	546	875	1170	1603	1896	2318	2531
		30	61	241	498	883	1498	2024	2697	3048	137	398	807	1169	1780	2155	2746	3030	201	540	912	1259	1782	2137	2642	2895
	Sta. 10	10	78	219	352	473	649	778	968	1083	87	181	273	352	474	574	736	839	88	163	235	299	411	500	657	761
		15	77	221	412	588	861	1031	1297	1435	91	240	375	500	671	803	1008	1129	101	214	323	419	566	683	870	987
		20	59	195	449	653	1023	1246	1615	1801	97	276	455	620	869	1044	1305	1455	105	265	414	553	746	898	1129	1264
		25	45	188	448	683	1127	1445	1919	2153	98	278	508	724	1060	1281	1618	1791	108	300	491	667	933	1120	1407	1571
		30	38	185	389	718	1221	1662	2205	2494	84	254	547	800	1235	1497	1928	2145	112	316	551	770	1110	1349	1699	1891
	Sta. 15	10	141	327	490	631	821	962	1170	1286	148	274	388	483	639	752	930	1040	131	234	329	417	557	664	841	950
		15	138	358	573	774	1058	1254	1528	1673	163	343	503	643	834	983	1202	1325	153	291	417	526	701	831	1035	1158
		20	120	328	628	886	1303	1539	1925	2111	163	399	612	799	1064	1252	1528	1681	168	356	528	678	888	1053	1296	1434
		25	97	302	662	939	1468	1800	2333	2584	165	425	691	941	1299	1546	1894	2076	172	413	634	831	1108	1307	1607	1771
		30	83	297	605	988	1606	2113	2728	3042	152	405	748	1058	1546	1831	2287	2505	177	451	721	970	1330	1586	1949	2147
	Sta. 20	10	245	557	837	1081	1403	1637	1959	2116	291	558	789	977	1263	1457	1727	1869	278	513	714	886	1144	1322	1578	1716
		15	228	584	921	1228	1661	1965	2370	2577	300	633	928	1180	1521	1773	2108	2275	307	598	852	1062	1381	1600	1905	2064
		20	201	537	970	1360	1961	2308	2846	3092	287	689	1051	1366	1800	2102	2522	2732	324	674	990	1260	1631	1905	2275	2457
		25	165	483	1016	1420	2173	2622	3360	3695	280	713	1138	1531	2082	2464	2975	3227	316	735	1118	1452	1908	2229	2680	2901
		30	142	469	945	1470	2348	3035	3876	4289	259	676	1197	1675	2400	2826	3476	3768	310	775	1220	1621	2189	2584	3117	3388

Relative Motion																													
Sta. 1	10	47	92	141	187	252	297	357	385	53	96	136	169	216	250	293	313	54	92	126	154	195	223	261	279
	15	43	80	134	183	264	314	389	424	48	93	138	178	234	272	326	350	52	93	131	164	211	245	289	310
	20	41	72	125	176	265	324	412	453	45	88	135	179	245	289	351	380	48	90	132	170	223	261	313	337
	25	39	66	116	167	261	330	430	477	43	58	130	177	252	301	372	405	46	86	130	171	232	273	332	360
	30	39	63	104	160	258	339	445	499	41	73	125	173	256	309	390	428	44	82	127	170	238	284	349	380
Sta. 2	10	46	88	132	172	229	268	319	343	52	90	124	153	193	221	256	272	53	86	114	138	172	194	224	238
	15	43	78	126	171	243	287	352	382	48	88	128	163	211	244	288	309	51	87	121	149	189	216	252	269
	20	41	70	119	165	245	298	376	412	45	84	126	165	223	261	314	339	48	86	123	156	201	234	277	297
	25	39	65	111	157	243	305	395	437	43	78	122	165	231	274	336	364	46	83	122	158	211	247	297	320
	30	39	63	100	152	241	315	411	459	42	71	118	162	237	283	355	387	44	79	120	158	217	258	314	340
Sta. 3	10	46	83	122	157	205	239	282	301	50	83	112	136	168	191	219	231	50	78	101	120	147	165	187	197
	15	43	75	118	158	221	260	316	341	47	83	117	147	187	215	252	268	49	81	109	132	165	188	216	228
	20	41	68	112	154	226	272	341	373	45	80	117	151	201	234	278	299	47	80	112	140	179	206	241	256
	25	39	64	105	148	225	281	361	399	43	75	114	152	210	247	301	324	45	78	113	144	189	220	261	280
	30	39	61	96	143	225	292	379	422	41	69	111	151	217	258	320	348	43	75	111	145	197	231	279	301
Sta. 4	10	44	78	111	141	182	211	245	261	47	75	99	118	144	161	182	191	47	69	87	101	122	135	151	157
	15	42	71	109	145	200	233	281	301	45	76	105	130	164	186	215	228	46	73	96	115	141	159	180	189
	20	40	66	105	142	206	247	308	335	43	75	107	136	178	206	243	259	45	74	101	124	156	178	205	217
	25	39	62	100	138	208	258	329	362	42	71	106	139	189	221	266	286	43	73	103	129	167	193	227	242
	30	39	60	92	135	209	270	348	386	41	66	104	139	197	233	286	310	42	71	103	132	176	206	245	264
Sta. 20	10	36	52	71	90	119	140	173	189	35	50	67	83	107	125	152	166	37	54	71	85	109	126	151	163
	15	37	57	79	102	137	162	198	217	34	49	64	81	104	123	152	166	35	49	64	78	100	117	142	155
	20	38	58	88	117	165	193	239	261	36	51	68	84	111	131	161	177	35	47	61	75	96	113	139	153
	25	38	58	96	127	188	226	288	317	37	53	73	94	126	149	182	199	35	48	62	76	100	117	144	158
	30	38	60	94	136	209	268	340	375	38	54	80	105	146	172	212	232	36	50	66	82	109	128	157	172
Relative Velocity																									
Sta. 1	10	259	351	459	565	710	812	933	984	275	374	470	550	660	735	817	847	282	373	455	521	616	675	741	766
	15	295	366	478	591	774	885	1042	1107	307	406	514	614	746	837	947	989	317	413	510	592	706	782	868	898
	20	334	391	495	606	807	937	1126	1204	343	433	544	654	814	919	1053	1108	351	447	553	651	781	872	980	1020
	25	376	422	515	622	830	979	1195	1287	383	458	569	686	869	988	1146	1209	388	478	588	694	847	948	1077	1127
	30	418	459	534	642	853	1030	1257	1361	423	484	594	713	920	1045	1230	1302	428	509	618	731	902	1018	1164	1223
Sta. 2	10	260	344	439	531	656	744	844	886	275	362	444	511	603	664	727	748	281	359	428	482	559	604	653	667
	15	296	363	462	561	721	817	951	1004	308	397	491	576	688	763	852	883	318	402	485	552	647	708	773	794
	20	336	389	483	580	756	870	1033	1099	345	426	524	618	755	844	955	997	353	439	530	613	721	796	881	910
	25	377	422	505	599	782	913	1100	1179	384	454	551	653	810	912	1044	1094	390	472	567	658	786	871	975	1013
	30	419	459	527	622	807	962	1161	1248	424	482	579	683	861	968	1124	1183	430	504	599	696	841	939	1058	1104
Sta. 3	10	259	334	416	494	600	674	755	788	272	346	413	467	541	589	635	647	275	340	394	436	495	528	559	565
	15	296	357	443	529	666	748	860	902	307	384	463	533	625	686	755	776	314	386	453	507	582	629	675	686
	20	336	385	468	552	705	801	940	995	344	416	499	579	692	766	854	886	351	425	500	568	656	716	779	797
	25	377	419	492	575	733	846	1007	1072	383	446	530	616	748	833	940	978	389	460	540	616	721	789	869	895
	30	419	457	517	600	760	895	1065	1139	424	477	560	649	799	889	1018	1064	428	494	575	656	776	856	950	983
Sta. 4	10	256	321	391	455	542	602	666	690	265	325	379	420	476	511	540	545	265	315	355	385	426	447	464	462
	15	294	348	422	495	610	678	770	801	302	367	431	488	559	607	656	669	307	364	416	457	513	546	575	577
	20	334	379	451	523	653	734	850	894	341	402	471	536	627	686	753	775	345	406	467	520	587	632	675	683
	25	376	415	479	549	684	780	916	970	381	436	506	577	685	753	837	864	385	445	510	570	652	705	763	779
	30	418	453	506	577	714	829	973	1035	421	469	539	613	737	810	913	946	425	481	548	614	709	771	841	863
Sta. 20	10	239	266	296	328	371	402	442	454	234	257	282	305	341	365	391	397	236	264	293	316	353	376	399	405
	15	285	319	358	398	458	501	550	568	278	297	319	341	369	391	414	415	277	296	317	335	361	379	394	393
	20	330	366	419	477	573	625	703	728	324	347	372	396	431	453	479	482	320	337	353	369	387	401	411	403
	25	374	410	479	543	675	750	877	924	370	398	430	464	515	549	586	593	366	383	401	417	439	451	460	452
	30	417	455	521	603	770	904	1054	1121	416	446	490	537	617	660	721	735	412	433	456	478	510	529	545	541

TABLE A-5 SEAKEEPING RESPONSES FOR $C_B = 0.60$, $L/B = 7.0$, LCB $= -0.5\%$

		Froude No.	$B/T = 2$								$B/T = 3$								$B/T = 4$							
			Significant Wave Height/LBP								Significant Wave Height/LBP								Significant Wave Height/LBP							
		[%]	0.015	0.020	0.025	0.030	0.040	0.050	0.075	0.100	0.015	0.020	0.025	0.030	0.040	0.050	0.075	0.100	0.015	0.020	0.025	0.030	0.040	0.050	0.075	0.100
Heave		10	10	25	40	55	80	107	171	235	8	17	27	38	63	88	154	220	7	15	24	35	58	84	149	215
		15	10	31	50	69	101	129	194	256	9	21	34	47	73	99	164	229	8	17	28	40	64	90	156	221
		20	10	31	55	79	119	151	219	280	9	25	41	57	85	113	178	242	9	20	33	46	72	99	164	229
		25	8	26	57	85	134	169	244	305	9	27	46	65	98	126	193	256	9	23	38	53	81	109	174	239
		30	5	22	58	86	143	184	266	332	9	27	49	71	108	140	209	272	8	24	42	59	90	119	186	250
Pitch		10	37	83	128	168	230	278	359	409	36	73	108	140	194	237	312	362	32	64	96	126	177	218	292	342
		15	30	77	125	169	238	292	379	432	34	75	114	149	207	253	331	382	32	67	102	134	187	230	306	357
		20	24	69	118	164	241	297	391	448	31	73	115	153	215	264	346	398	31	67	104	138	195	239	318	369
		25	21	61	110	159	240	301	400	459	26	69	113	154	219	270	356	410	28	66	105	140	199	246	326	378
		30	16	49	104	154	244	304	409	472	23	65	109	151	221	274	363	419	25	64	104	141	202	250	333	386
Bending Moment		10	44	83	118	148	187	216	255	274	54	95	128	155	196	223	260	279	57	97	131	158	198	225	263	282
		15	42	83	121	154	202	234	279	301	56	100	138	169	214	245	285	305	60	105	142	172	216	245	285	305
		20	42	80	121	158	215	252	304	328	54	103	146	183	232	267	314	335	62	111	153	186	236	269	312	334
		25	41	77	121	160	225	266	327	356	53	104	151	191	250	289	342	368	61	115	162	200	255	293	343	366
		30	40	77	122	162	232	279	349	383	52	104	154	199	265	310	371	401	60	117	169	213	274	317	374	401
Added Resistance		10	8	26	51	77	122	158	203	229	10	26	46	67	106	134	172	194	13	29	49	69	107	135	173	195
		15	6	25	54	88	149	200	279	334	9	27	52	78	126	166	233	285	12	29	52	76	122	160	228	283
		20	4	24	58	99	176	242	355	439	8	29	57	89	146	198	294	377	10	30	55	83	137	186	283	372
		25	3	18	54	99	200	279	430	537	7	28	61	100	173	238	360	462	9	30	60	95	160	220	340	447
		30	2	13	50	100	223	315	505	634	6	28	65	110	200	279	426	547	8	31	65	107	182	254	397	522
Acceleration	Sta. 0	10	395	857	1251	1583	1982	2289	2662	2832	457	829	1138	1370	1724	1950	2254	2405	437	754	1014	1228	1540	1748	2034	2182
		15	361	885	1362	1773	2340	2729	3228	3471	498	988	1405	1725	2195	2510	2904	3091	511	938	1299	1574	1992	2262	2621	2797
		20	317	838	1386	1881	2606	3066	3712	4005	487	1071	1587	2025	2591	2999	3518	3751	546	1080	1537	1893	2422	2773	3220	3436
		25	278	763	1373	1929	2794	3337	4133	4490	447	1102	1705	2226	2935	3417	4066	4366	553	1172	1723	2184	2804	3247	3811	4067
		30	231	669	1351	1946	2956	3579	4520	4967	419	1097	1766	2358	3220	3796	4567	4940	521	1224	1868	2424	3156	3678	4366	4681
	Sta. 5	10	230	512	756	967	1209	1408	1656	1774	264	486	670	809	1026	1168	1370	1481	260	446	599	726	917	1047	1241	1351
		15	205	546	853	1117	1489	1737	2076	2250	298	591	846	1045	1338	1540	1805	1936	301	560	775	946	1205	1377	1615	1745
		20	188	520	881	1215	1704	2019	2460	2668	284	653	979	1263	1618	1887	2234	2400	326	654	936	1161	1494	1721	2021	2176
		25	159	459	884	1267	1879	2243	2809	3064	260	680	1068	1406	1876	2192	2635	2850	328	717	1067	1365	1760	2051	2433	2617
		30	124	397	883	1283	1998	2440	3124	3459	249	680	1116	1510	2091	2482	3012	3279	307	756	1167	1532	2014	2357	2830	3056
	Sta. 10	10	115	248	367	470	596	717	874	971	103	182	255	319	430	516	669	772	112	176	236	294	393	475	628	731
		15	116	326	504	661	873	1022	1245	1370	132	258	378	470	625	742	922	1034	123	223	316	395	530	632	808	922
		20	125	356	590	808	1121	1335	1628	1786	140	337	508	664	855	1020	1245	1373	146	290	428	537	715	851	1059	1185
		25	113	328	638	923	1363	1615	2020	2202	140	394	621	823	1106	1301	1595	1755	155	357	543	707	925	1107	1357	1502
		30	84	283	683	986	1540	1861	2381	2645	149	427	704	957	1332	1592	1952	2152	155	415	650	865	1152	1368	1683	1855
	Sta. 15	10	199	363	501	604	783	902	1078	1184	167	278	377	467	608	713	888	995	158	256	342	427	560	663	836	941
		15	207	453	662	842	1057	1227	1462	1582	199	356	490	601	784	911	1110	1231	171	295	406	509	670	792	991	1112
		20	202	521	796	1032	1358	1586	1891	2061	232	453	645	800	1025	1196	1431	1564	202	369	516	639	842	985	1210	1344
		25	199	525	871	1208	1669	1963	2375	2559	234	538	800	1027	1310	1524	1827	1983	235	461	660	823	1068	1251	1512	1660
		30	166	462	941	1328	1970	2307	2858	3124	236	603	929	1210	1606	1878	2252	2457	246	545	808	1039	1330	1559	1879	2048
	Sta. 20	10	362	687	960	1169	1495	1703	1983	2127	347	607	822	1002	1267	1447	1701	1837	323	549	738	904	1149	1319	1566	1697
		15	361	774	1132	1437	1810	2101	2463	2633	393	728	1007	1230	1571	1793	2097	2256	364	652	893	1097	1399	1605	1896	2050
		20	333	839	1278	1647	2161	2505	2971	3208	425	840	1197	1481	1890	2180	2546	2728	409	765	1064	1307	1680	1925	2264	2440
		25	325	844	1356	1852	2513	2962	3546	3806	415	932	1379	1763	2237	2589	3053	3267	445	877	1250	1548	1988	2294	2691	2889
		30	277	748	1426	2005	2918	3398	4152	4501	403	1005	1532	1981	2605	3024	3585	3869	455	975	1433	1828	2321	2695	3181	3405

Relative Motion	Sta. 1	10	54	106	153	194	244	283	330	352	58	98	133	161	203	230	266	284	57	92	122	146	183	208	241	258
		15	49	102	154	200	266	310	370	398	56	101	142	176	224	258	301	322	56	95	130	159	201	230	268	286
		20	46	92	147	200	278	329	400	432	51	99	145	186	240	280	332	355	54	96	136	168	216	250	293	314
		25	43	81	139	194	283	339	423	461	47	95	144	189	252	295	355	383	51	95	138	175	227	265	315	339
		30	40	73	132	187	284	346	440	485	46	90	141	188	259	308	374	407	48	92	137	179	236	277	334	360
	Sta. 2	10	53	100	141	177	219	252	291	308	56	91	120	144	178	200	229	242	55	84	109	129	159	178	204	216
		15	49	97	143	184	242	280	331	355	55	95	130	159	200	229	264	279	55	89	118	142	178	201	231	245
		20	46	88	138	185	255	300	362	389	51	94	135	170	217	250	294	313	53	91	125	152	193	221	256	273
		25	43	79	132	182	262	312	386	418	47	91	135	174	230	267	318	341	50	90	128	160	205	237	279	298
		30	41	71	126	176	264	320	404	444	45	87	132	174	237	280	338	365	47	88	128	165	215	250	298	320
	Sta. 3	10	52	92	128	158	194	221	253	266	53	82	106	125	153	170	191	201	51	75	95	110	133	148	167	175
		15	48	91	132	168	217	250	292	312	53	87	117	141	175	198	226	238	52	81	105	124	153	171	194	204
		20	45	84	129	171	232	271	324	347	49	88	123	153	193	221	256	271	51	84	112	135	169	191	219	232
		25	43	76	124	169	240	284	349	377	47	86	124	159	206	238	281	300	49	84	117	144	182	208	242	257
		30	41	69	119	164	244	294	369	403	45	82	123	160	215	252	301	325	47	83	118	150	192	222	262	279
	Sta. 4	10	50	84	114	139	168	190	214	224	49	72	91	106	126	139	154	160	46	64	79	91	107	117	130	135
		15	46	84	120	151	193	220	255	270	49	79	103	122	150	168	188	197	48	71	91	105	127	140	157	164
		20	44	80	119	156	209	242	287	306	47	81	111	136	168	191	219	231	48	75	99	117	144	162	183	192
		25	42	73	116	156	219	257	314	337	45	80	113	143	183	209	245	260	47	77	104	127	158	180	206	217
		30	40	67	112	153	224	268	335	365	44	78	113	146	193	225	266	285	45	77	107	134	169	194	226	240
	Sta. 20	10	36	55	75	93	121	142	171	185	38	57	76	93	118	136	162	175	39	59	78	94	118	135	160	172
		15	36	56	77	98	125	147	180	195	36	53	71	86	111	130	156	169	37	55	72	87	111	127	152	164
		20	38	60	84	107	141	166	200	219	35	51	68	85	108	128	155	169	36	51	67	81	104	121	145	158
		25	39	63	92	122	165	194	236	254	35	52	70	88	114	133	162	177	35	49	64	79	100	117	142	154
		30	39	61	100	135	194	226	278	303	37	55	75	95	125	147	177	194	35	49	64	80	102	118	144	157
Relative Velocity	Sta. 1	10	276	395	512	616	734	826	923	958	289	390	477	546	646	705	770	795	291	378	452	512	595	645	702	723
		15	306	422	550	668	830	938	1068	1123	325	437	546	632	756	837	923	954	330	431	522	595	700	763	833	859
		20	342	437	568	701	898	1021	1184	1248	357	472	595	706	845	946	1059	1100	366	475	581	668	794	874	961	993
		25	380	456	585	720	943	1080	1276	1353	391	501	631	754	921	1033	1172	1226	401	511	629	734	872	971	1079	1118
		30	420	479	604	736	979	1129	1351	1445	429	528	659	788	981	1109	1268	1336	436	544	669	788	943	1052	1184	1231
	Sta. 2	10	276	382	484	572	672	750	828	854	289	375	448	505	585	630	678	694	289	362	422	470	534	572	611	621
		15	308	412	525	627	767	859	967	1012	325	424	516	588	693	757	823	845	330	417	492	552	637	686	736	751
		20	344	431	547	663	834	941	1080	1132	358	461	567	662	779	863	954	983	367	462	552	624	728	792	858	878
		25	382	452	567	686	882	1001	1169	1233	393	492	605	711	854	948	1063	1104	403	501	602	690	806	886	971	997
		30	422	478	589	705	918	1049	1241	1321	431	522	636	748	913	1022	1155	1208	439	535	643	745	875	966	1071	1106
	Sta. 3	10	274	365	451	525	607	671	731	748	282	353	412	456	517	550	582	589	280	338	384	419	465	491	514	514
		15	307	398	496	582	701	777	865	900	321	405	481	539	623	673	720	732	324	395	455	501	566	601	633	638
		20	343	422	522	622	768	860	974	1015	356	445	534	612	708	776	845	864	363	443	516	573	656	704	750	760
		25	382	446	546	650	818	919	1061	1113	392	479	575	664	782	859	950	980	400	484	568	639	733	796	858	874
		30	422	474	571	672	855	968	1132	1198	431	511	608	703	841	932	1038	1079	437	521	611	695	801	874	954	977
	Sta. 4	10	269	344	415	473	538	589	632	641	271	326	370	402	445	466	482	482	265	307	339	362	391	405	413	405
		15	303	382	463	535	632	693	763	787	313	381	441	484	549	584	614	618	312	367	411	444	489	511	527	524
		20	341	410	495	579	700	777	869	900	351	424	496	558	633	686	734	744	354	418	475	517	578	612	639	640
		25	380	437	522	611	754	838	955	995	388	462	541	613	707	768	836	855	394	462	529	583	655	702	743	749
		30	421	468	551	637	793	887	1025	1078	428	496	577	655	767	840	922	951	432	502	575	641	723	779	836	848
	Sta. 20	10	236	265	299	327	375	406	441	451	236	270	304	333	376	403	431	441	239	275	312	340	383	408	435	445
		15	281	311	346	383	424	460	498	506	276	301	328	350	388	411	433	436	277	306	334	358	394	415	434	437
		20	327	366	410	452	513	555	603	621	319	341	364	386	414	440	456	453	318	339	361	379	406	423	433	428
		25	373	417	472	535	623	684	753	772	365	388	414	441	471	493	515	512	362	378	396	412	430	444	448	437
		30	417	458	533	614	752	821	925	962	411	440	473	505	551	581	610	616	406	423	441	459	475	486	491	477

TABLE A-6 SEAKEEPING RESPONSES FOR $C_B = 0.60$, $L/B = 8.5$, LCB $= -0.5\%$

		Froude No.	$B/T = 2$								$B/T = 3$								$B/T = 4$							
			Significant Wave Height/LBP								Significant Wave Height/LBP								Significant Wave Height/LBP							
		[%]	0.015	0.020	0.025	0.030	0.040	0.050	0.075	0.100	0.015	0.020	0.025	0.030	0.040	0.050	0.075	0.100	0.015	0.020	0.025	0.030	0.040	0.050	0.075	0.100
Heave		10	11	22	34	45	70	95	160	225	8	15	25	35	59	84	150	216	8	14	23	33	56	82	147	213
		15	12	29	46	61	87	114	177	240	9	19	30	41	66	92	157	222	8	16	26	37	61	86	151	217
		20	11	34	55	75	107	134	199	261	11	24	37	50	76	102	167	232	9	19	30	42	67	92	158	223
		25	12	36	60	84	123	156	222	283	11	28	44	60	88	115	180	243	10	22	35	48	74	101	166	230
		30	11	32	62	91	138	174	245	306	10	30	49	68	100	128	194	257	10	24	40	55	83	110	175	239
Pitch		10	43	87	128	162	221	265	341	390	36	70	103	133	184	226	299	349	31	62	93	121	171	211	284	334
		15	39	87	133	174	238	287	367	418	37	75	112	145	200	243	318	368	33	66	99	129	181	223	297	347
		20	33	82	131	176	245	299	385	438	36	77	117	152	211	257	335	385	33	69	104	136	190	233	309	359
		25	27	76	126	173	249	304	397	452	33	76	118	157	218	267	347	399	32	69	106	140	196	241	318	369
		30	24	70	120	169	248	309	405	464	29	73	117	159	222	273	357	410	30	69	107	142	200	247	326	378
Bending Moment		10	43	77	105	127	161	183	213	228	48	80	108	130	163	185	216	232	49	82	110	132	165	188	219	235
		15	42	79	112	139	174	200	234	250	51	87	118	142	178	201	233	249	52	88	118	142	177	201	233	249
		20	40	80	115	145	187	215	255	273	52	92	127	154	194	220	255	272	55	95	128	154	193	218	252	269
		25	40	78	115	148	197	230	274	296	51	95	133	165	208	239	279	297	56	100	137	166	209	237	275	293
		30	40	76	115	151	207	242	294	317	50	96	138	174	223	256	302	323	57	104	145	178	225	257	299	319
Added Resistance		10	7	21	38	54	85	106	135	151	9	21	36	50	77	96	122	137	11	24	38	53	80	99	125	139
		15	6	22	44	68	108	141	193	229	9	23	40	58	92	119	165	203	11	24	41	58	92	118	167	206
		20	5	24	51	82	131	175	251	307	8	24	45	66	107	142	208	268	10	25	44	64	104	138	208	273
		25	4	22	52	89	154	213	311	382	7	25	50	79	128	173	258	330	9	26	48	73	120	162	248	326
		30	4	20	52	96	177	251	371	457	6	26	56	92	149	205	308	391	9	27	53	81	136	187	288	379
Acceleration	Sta. 0	10	535	989	1361	1619	2045	2295	2614	2769	488	828	1101	1323	1642	1851	2142	2285	465	757	994	1195	1488	1684	1960	2098
		15	534	1125	1631	2050	2548	2933	3380	3578	596	1077	1472	1764	2206	2481	2842	3017	561	969	1307	1565	1951	2202	2547	2712
		20	483	1165	1767	2278	2960	3419	4018	4292	646	1259	1773	2157	2734	3106	3565	3779	647	1178	1620	1953	2456	2775	3194	3395
		25	434	1136	1815	2417	3268	3820	4563	4904	649	1368	1997	2510	3183	3667	4259	4518	696	1347	1897	2314	2944	3349	3861	4102
		30	398	1069	1817	2500	3502	4164	5051	5463	599	1421	2157	2787	3584	4157	4891	5218	723	1471	2125	2651	3386	3894	4527	4808
	Sta. 5	10	310	583	806	959	1224	1380	1588	1699	287	485	646	777	970	1101	1293	1403	279	448	586	705	881	1005	1193	1297
		15	314	685	1002	1272	1576	1832	2126	2262	350	640	877	1054	1327	1501	1739	1865	335	577	773	934	1170	1329	1556	1681
		20	277	727	1120	1454	1900	2195	2602	2796	392	763	1080	1319	1683	1923	2231	2378	384	710	975	1185	1498	1702	1980	2126
		25	259	718	1166	1567	2145	2523	3027	3274	384	841	1246	1578	2000	2323	2717	2902	418	823	1164	1427	1827	2090	2432	2605
		30	238	663	1174	1653	2354	2804	3432	3717	350	884	1360	1775	2300	2674	3177	3411	434	906	1324	1665	2133	2474	2898	3099
	Sta. 10	10	132	235	332	395	526	615	763	861	127	193	252	310	408	489	641	741	133	192	241	297	388	466	617	716
		15	166	350	511	645	806	960	1138	1244	144	251	348	428	566	667	842	951	144	231	308	381	502	598	770	882
		20	160	441	672	878	1126	1308	1570	1705	181	347	501	610	803	940	1143	1264	160	292	408	505	668	787	984	1108
		25	169	492	783	1040	1414	1663	1997	2183	197	438	655	838	1065	1266	1514	1652	193	374	544	671	885	1040	1271	1408
		30	171	484	843	1194	1679	2003	2441	2648	190	515	792	1045	1351	1586	1914	2083	213	457	681	865	1124	1327	1609	1764
	Sta. 15	10	212	352	469	569	718	825	998	1103	194	300	388	474	608	711	881	982	182	280	362	445	574	674	842	942
		15	265	476	650	770	996	1133	1331	1448	210	346	464	571	735	856	1054	1173	197	314	415	514	670	788	984	1100
		20	279	591	853	1077	1320	1533	1795	1923	254	447	608	736	951	1093	1315	1447	214	362	490	610	795	932	1155	1288
		25	266	683	1028	1310	1699	1944	2303	2487	303	571	798	969	1240	1432	1689	1833	254	454	624	765	996	1156	1404	1551
		30	276	726	1139	1527	2023	2406	2838	3070	313	680	992	1262	1566	1822	2150	2312	301	568	798	975	1263	1463	1746	1906
	Sta. 20	10	426	740	993	1195	1489	1681	1942	2080	382	626	824	996	1247	1418	1665	1793	357	573	751	912	1148	1313	1553	1677
		15	473	883	1220	1466	1874	2117	2438	2601	440	761	1022	1240	1555	1766	2059	2212	407	684	912	1111	1401	1600	1884	2030
		20	482	1000	1441	1811	2243	2600	3006	3192	498	906	1239	1501	1902	2155	2498	2675	454	799	1083	1323	1674	1910	2239	2410
		25	440	1091	1638	2088	2694	3069	3619	3870	552	1052	1473	1788	2283	2606	3010	3210	512	936	1285	1565	1993	2269	2645	2840
		30	443	1148	1771	2335	3061	3632	4250	4590	553	1176	1706	2157	2677	3099	3600	3826	568	1080	1511	1840	2357	2692	3126	3343

Relative Motion	Sta. 1	10	62	109	150	181	230	260	299	318	59	95	126	151	188	213	246	263	57	89	117	140	173	196	228	243
		15	56	111	161	204	256	297	346	368	59	102	138	168	212	241	278	297	58	94	126	152	191	216	251	268
		20	51	107	162	210	276	321	381	409	57	104	146	181	231	266	310	330	57	98	134	163	207	236	275	294
		25	47	99	156	209	287	338	408	441	53	103	150	191	245	285	337	360	55	99	139	171	220			319
		30	45	90	149	206	293	350	430	466	49	100	150	195	257	300	359	386	53	98	141	178	231	268	318	341
	Sta. 2	10	60	102	137	163	204	229	260	275	57	88	113	134	164	183	209	221	54	81	103	122	149	166	190	201
		15	55	105	148	186	231	265	306	324	57	95	126	151	187	210	240	254	56	87	113	135	166	187	214	227
		20	50	102	151	193	251	290	342	365	56	98	135	164	207	236	271	288	55	91	122	146	183	207	238	253
		25	47	95	147	194	263	308	369	397	53	98	139	175	222	256	299	318	54	93	128	155	197	225	261	277
		30	45	87	141	192	270	321	392	423	49	95	140	180	234	271	321	344	52	93	131	163	208	240	281	300
	Sta. 3	10	57	93	123	144	178	197	221	232	53	78	98	114	137	152	171	179	50	71	88	102	122	135	153	160
		15	54	97	135	167	205	234	267	280	54	86	112	132	161	180	202	213	52	78	99	116	140	156	176	185
		20	49	96	139	176	226	259	303	322	54	90	122	146	182	205	233	246	53	83	108	128	158	177	200	211
		25	47	90	137	179	239	279	331	354	51	91	127	158	197	226	261	276	52	86	115	138	173	195	223	236
		30	44	83	132	178	248	293	354	381	48	90	129	164	210	242	284	302	51	87	119	147	185	211	244	259
	Sta. 4	10	53	83	107	124	151	165	183	190	47	67	82	94	110	121	133	139	44	59	72	82	96	104	116	120
		15	51	89	121	148	178	202	228	238	50	76	97	112	135	148	165	172	47	67	84	96	114	125	139	145
		20	48	89	126	159	201	228	264	280	51	82	108	127	156	174	196	205	49	74	94	109	132	146	163	171
		25	46	85	126	163	215	249	293	313	49	83	114	140	172	196	224	235	49	77	102	120	148	165	187	196
		30	44	79	123	164	226	265	318	341	47	83	118	148	186	213	247	262	48	79	107	129	161	182	208	219
	Sta. 20	10	38	60	82	100	128	147	175	188	40	62	82	98	124	142	167	180	41	62	82	98	123	140	164	177
		15	37	57	78	96	126	146	175	190	38	58	77	93	118	136	162	175	39	58	77	93	117	134	158	170
		20	37	59	81	103	130	154	185	200	36	54	72	88	113	131	157	170	37	55	72	87	111	127	151	163
		25	38	63	89	111	147	169	204	222	36	53	71	87	111	131	157	170	36	52	68	82	105	122	145	158
		30	40	67	96	126	166	197	235	255	36	54	73	92	115	135	163	177	35	50	66	80	102	119	143	155
Relative Velocity	Sta. 1	10	296	417	524	600	725	794	868	897	296	390	467	530	615	665	723	745	295	377	444	499	573	618	670	686
		15	324	459	593	710	843	948	1055	1092	337	450	549	627	740	806	876	903	338	435	518	586	679	734	796	818
		20	353	486	632	764	940	1056	1199	1256	373	498	618	711	850	937	1029	1062	377	488	588	668	784	852	926	954
		25	388	504	652	798	1007	1143	1314	1383	405	534	669	789	939	1049	1167	1208	414	532	648	741	878	963	1055	1087
		30	427	521	667	821	1057	1210	1408	1489	438	564	708	846	1017	1139	1284	1338	450	571	699	809	959	1063	1174	1213
	Sta. 2	10	295	401	491	555	660	715	771	792	294	373	436	486	552	590	631	642	292	359	412	454	511	543	577	582
		15	324	444	561	661	774	863	949	977	336	434	517	581	673	724	776	793	336	418	486	540	613	654	697	708
		20	354	474	602	717	870	969	1088	1134	374	483	585	663	780	851	921	943	377	473	556	622	715	768	821	837
		25	390	495	626	754	936	1054	1198	1256	407	521	638	739	867	959	1052	1082	415	519	617	694	807	875	943	964
		30	428	515	645	780	986	1119	1290	1357	441	554	679	797	943	1046	1165	1205	452	559	669	760	887	971	1057	1084
	Sta. 3	10	289	379	453	505	590	631	671	683	285	347	396	433	481	507	532	534	280	330	370	400	438	459	476	471
		15	322	425	524	608	701	775	841	859	330	411	478	528	599	636	670	678	328	393	445	485	538	566	591	592
		20	353	458	568	667	795	877	975	1009	369	462	547	609	704	758	807	820	371	449	515	567	638	675	710	715
		25	390	484	596	706	861	962	1081	1127	405	503	601	684	789	863	933	952	411	498	578	638	729	779	826	836
		30	428	507	619	736	913	1027	1170	1224	440	538	644	743	863	948	1042	1070	449	540	631	705	807	873	935	950
	Sta. 4	10	279	351	410	450	515	544	569	573	270	315	349	374	405	420	429	422	261	295	321	339	360	370	371	358
		15	316	402	483	550	624	683	730	741	319	381	431	469	519	543	561	560	313	359	396	423	456	472	480	472
		20	349	439	531	613	718	784	861	885	361	435	502	549	622	660	691	695	359	419	468	505	554	578	594	591
		25	387	468	564	656	784	868	963	999	399	479	559	624	706	763	812	822	401	470	532	577	644	678	705	706
		30	426	495	590	690	839	934	1051	1093	435	517	605	685	780	847	917	934	441	516	587	643	722	770	810	815
	Sta. 20	10	237	275	314	348	399	430	464	475	239	280	320	352	399	427	457	470	243	283	324	355	400	427	456	467
		15	279	310	346	373	425	456	488	495	277	310	343	371	413	438	462	469	279	313	348	375	415	439	461	468
		20	324	358	397	438	477	518	554	558	318	343	370	392	429	451	468	467	319	346	374	397	430	449	462	462
		25	369	413	462	508	575	612	664	679	362	383	408	429	459	484	494	488	360	381	403	420	447	461	466	458
		30	416	467	528	592	676	748	808	836	407	431	459	488	513	537	555	547	404	420	439	453	472	484	484	468

TABLE A-7 SEAKEEPING RESPONSES FOR $C_B = 0.65$, $L/B = 5.5$, LCB = $+0.5\%$

		Froude No.	$B/T = 2$								$B/T = 3$								$B/T = 4$							
			Significant Wave Height/LBP								Significant Wave Height/LBP								Significant Wave Height/LBP							
		[%]	0.015	0.020	0.025	0.030	0.040	0.050	0.075	0.100	0.015	0.020	0.025	0.030	0.040	0.050	0.075	0.100	0.015	0.020	0.025	0.030	0.040	0.050	0.075	0.100
Heave		10	8	23	41	59	90	119	185	249	6	17	29	41	66	93	158	224	6	14	24	35	59	85	151	217
		15	7	21	45	67	108	140	211	275	7	20	35	50	79	106	172	237	6	17	29	42	67	94	160	225
		20	4	18	46	70	119	158	237	302	7	21	39	57	91	121	189	253	6	19	33	48	76	104	170	236
		25	3	18	41	71	126	174	259	327	6	19	41	62	102	134	206	270	6	20	36	53	85	114	182	248
		30	2	15	33	71	130	187	280	352	4	17	42	64	109	145	222	288	6	19	37	57	93	124	195	260
Pitch		10	23	62	106	147	213	264	351	404	28	64	101	134	190	235	313	364	27	59	92	122	174	217	292	342
		15	19	55	99	142	215	271	364	421	24	61	100	137	198	246	328	381	25	58	94	126	181	226	304	356
		20	14	44	92	137	218	276	376	437	20	56	97	136	201	252	338	393	22	56	92	127	185	232	313	366
		25	10	37	87	130	217	281	391	456	17	50	92	134	204	257	348	404	19	53	90	126	188	236	320	374
		30	7	34	72	127	217	297	411	479	13	42	88	131	208	262	358	417	17	48	87	125	190	240	326	382
Bending Moment		10	45	89	136	180	247	294	360	394	61	115	164	205	264	307	366	395	70	124	172	211	269	309	366	394
		15	43	83	135	182	262	314	394	434	59	117	171	219	288	336	404	437	70	130	184	229	295	341	404	435
		20	42	82	133	180	267	330	423	470	58	116	175	228	310	365	444	482	68	133	194	246	321	374	446	482
		25	42	84	130	182	273	346	449	501	57	114	178	237	331	393	486	529	67	135	201	260	347	407	491	532
		30	43	85	131	187	282	363	477	537	56	113	182	245	351	422	528	580	67	136	208	273	373	442	539	586
Added Resistance		10	6	29	65	109	187	249	336	385	11	32	63	96	159	207	271	310	14	36	65	97	159	204	267	306
		15	4	22	61	109	214	297	446	541	9	31	66	107	186	252	366	455	12	35	68	106	178	240	352	445
		20	3	15	56	109	242	344	555	697	7	31	70	118	213	298	461	599	10	34	71	115	197	276	437	584
		25	2	12	43	99	239	382	642	820	5	25	67	122	244	347	559	724	9	33	73	124	228	325	523	699
		30	1	9	31	88	235	420	729	943	4	20	64	126	275	396	656	849	7	31	75	134	258	373	610	813
Acceleration	Sta. 0	10	207	524	848	1145	1564	1854	2255	2445	306	639	936	1185	1531	1778	2108	2267	329	633	893	1107	1427	1644	1941	2094
		15	173	481	859	1195	1736	2090	2611	2866	285	680	1052	1374	1824	2140	2571	2779	345	718	1057	1342	1747	2033	2418	2602
		20	144	424	832	1216	1861	2289	2928	3235	260	679	1107	1494	2064	2447	2986	3248	328	763	1175	1533	2029	2383	2866	3098
		25	117	377	807	1207	1941	2457	3234	3609	237	643	1125	1576	2267	2721	3379	3689	306	778	1247	1666	2280	2698	3284	3571
		30	101	354	724	1211	2014	2683	3547	3987	206	580	1132	1628	2454	2969	3759	4134	289	764	1286	1772	2502	2996	3691	4028
	Sta. 5	10	114	307	510	699	973	1164	1436	1575	173	371	551	704	916	1074	1296	1414	192	370	525	653	850	988	1189	1303
		15	93	273	527	751	1123	1357	1723	1907	159	403	633	837	1125	1328	1621	1773	200	425	633	811	1063	1248	1508	1644
		20	74	240	518	770	1218	1521	1981	2212	148	404	676	927	1304	1559	1928	2118	186	457	713	943	1263	1492	1822	1991
		25	59	221	492	772	1282	1665	2222	2502	134	378	695	993	1462	1766	2228	2452	76	469	767	1038	1445	1722	2126	2335
		30	51	206	430	784	1343	1829	2463	2797	113	338	708	1034	1598	1953	2515	2793	69	459	798	1118	1610	1942	2428	2672
	Sta. 10	10	69	194	316	431	601	725	914	1028	73	160	242	319	435	535	695	800	77	142	209	270	378	466	623	729
		15	67	193	373	537	799	962	1227	1366	79	212	337	453	621	747	951	1074	85	187	288	380	520	637	822	941
		20	51	173	407	597	949	1170	1530	1716	86	243	412	567	808	979	1235	1384	89	233	372	502	691	836	1066	1203
		25	39	171	401	628	1049	1363	1820	2051	85	243	460	665	991	1201	1535	1708	95	266	443	609	866	1048	1332	1496
		30	34	164	343	665	1139	1565	2099	2384	72	222	500	734	1150	1408	1832	2052	99	277	498	707	1037	1266	1614	1803
	Sta. 15	10	133	322	488	633	828	973	1185	1304	141	265	378	472	628	742	922	1032	126	225	319	405	545	652	830	940
		15	131	345	566	774	1071	1272	1555	1703	152	331	493	634	827	977	1200	1325	145	279	405	513	688	818	1025	1149
		20	110	310	619	877	1309	1553	1955	2151	153	384	597	786	1056	1248	1529	1685	157	341	512	663	874	1039	1286	1426
		25	88	289	639	922	1461	1814	2362	2619	154	401	669	923	1292	1539	1898	2080	160	394	613	809	1090	1291	1595	1763
		30	76	281	568	974	1592	2121	2756	3081	139	376	725	1031	1528	1818	2286	2514	165	425	693	943	1309	1566	1936	2135
	Sta. 20	10	228	541	820	1065	1386	1618	1942	2101	269	522	745	927	1206	1398	1667	1809	258	478	670	837	1089	1265	1521	1660
		15	215	565	906	1224	1669	1978	2390	2597	276	598	887	1137	1470	1720	2057	2224	287	557	802	1007	1318	1536	1844	2001
		20	185	506	960	1353	1881	2332	2894	3153	265	655	1010	1322	1758	2059	2481	2694	295	630	938	1205	1567	1840	2210	2393
		25	149	460	993	1402	2179	2659	3426	3771	259	671	1093	1489	2050	2429	2949	3200	285	690	1061	1389	1844	2162	2613	2839
		30	128	445	895	1460	2349	3083	3954	4387	235	625	1153	1625	2364	2790	3454	3759	285	723	1157	1555	2123	2517	3054	3325

Relative Motion																															
Sta. 1	10	45	85	130	172	232	273	329	355	51	90	126	157	201	232	273	292	52	87	118	144	183	209	244	261
	15	42	76	125	169	242	289	359	392	47	87	128	165	217	254	304	327	50	87	123	154	198	229	271	291
	20	40	69	116	163	245	300	381	420	44	82	126	166	228	269	328	356	47	65	124	159	209	245	294	317
	25	39	64	109	156	243	306	399	444	43	76	121	165	235	281	348	380	45	81	122	160	217	257	312	339
	30	39	62	98	151	241	317	417	467	41	70	117	162	240	289	366	402	43	77	119	160	223	266	329	358
Sta. 2	10	45	81	121	158	210	246	293	314	50	84	115	142	178	204	237	252	51	80	107	128	160	181	208	221
	15	42	74	117	157	222	263	324	352	46	83	119	151	195	226	268	287	49	82	112	138	176	202	235	251
	20	40	67	110	153	226	275	347	381	44	79	117	153	207	243	293	316	46	80	114	145	188	218	259	277
	25	39	63	104	147	225	283	366	406	42	74	114	153	215	255	314	340	44	78	114	147	197	231	278	300
	30	39	61	95	143	225	294	384	429	41	68	111	151	221	265	332	363	43	74	112	148	204	241	295	320
Sta. 3	10	44	77	111	143	188	218	258	275	48	77	103	125	155	176	201	212	48	72	94	111	136	152	172	181
	15	42	71	109	145	202	237	289	313	45	77	108	135	173	199	232	247	47	75	101	122	153	174	200	212
	20	40	65	104	142	207	251	314	343	43	75	108	140	186	216	258	277	45	75	104	130	166	191	224	239
	25	39	62	99	138	209	260	334	369	42	70	106	141	195	230	280	302	43	73	105	134	176	205	244	262
	30	38	59	91	134	209	272	353	393	40	66	104	140	202	240	299	326	42	71	104	136	184	216	262	282
Sta. 4	10	43	72	101	129	166	191	223	237	45	69	91	108	132	148	166	174	44	64	80	93	112	123	138	143
	15	41	67	101	132	182	213	257	276	43	71	97	120	151	172	198	209	44	68	89	106	130	146	166	174
	20	39	63	98	131	190	228	283	308	42	70	99	126	165	190	225	240	43	69	94	115	144	164	190	201
	25	39	60	94	129	192	238	304	335	41	67	98	129	175	205	248	266	42	68	96	120	156	179	211	225
	30	38	58	87	126	194	251	324	360	40	63	97	129	183	217	267	290	41	67	96	123	164	192	230	247
Sta. 20	10	36	54	73	92	121	143	175	192	35	50	66	81	106	124	151	165	36	52	69	84	107	124	149	162
	15	38	58	82	106	143	169	206	225	35	49	65	80	104	123	152	167	35	49	63	77	99	116	142	155
	20	38	58	91	121	172	202	252	275	36	51	68	85	113	133	163	180	35	47	61	75	96	113	139	153
	25	38	59	97	130	195	238	304	335	37	53	74	95	129	152	187	204	36	48	62	76	100	117	145	159
	30	38	60	93	140	216	281	358	397	38	54	81	106	149	175	218	239	37	50	66	82	110	129	159	175
Relative Velocity																									
Sta. 1	10	257	337	432	527	657	747	858	901	271	358	444	517	616	684	759	786	278	359	433	493	580	633	693	714
	15	295	359	457	554	715	816	958	1016	305	391	488	577	697	780	879	917	313	399	486	560	663	733	811	838
	20	335	386	476	576	753	871	1038	1106	342	421	519	617	762	858	980	1028	349	434	528	616	735	817	916	951
	25	376	419	502	595	781	913	1107	1189	382	449	547	651	816	923	1068	1123	387	466	564	659	798	890	1007	1052
	30	418	457	524	619	808	968	1171	1263	423	478	575	680	866	980	1147	1213	427	498	595	696	852	956	1090	1142
Sta. 2	10	257	330	413	495	606	683	773	807	270	346	419	480	561	616	673	690	275	345	405	454	523	564	606	618
	15	295	354	440	526	665	752	871	919	305	382	465	540	641	709	788	815	313	387	460	521	605	661	719	736
	20	335	384	464	550	705	806	949	1006	343	413	499	583	705	785	884	921	349	424	505	578	676	744	820	844
	25	376	418	491	573	734	849	1015	1084	382	444	529	619	759	850	969	1013	387	459	542	623	739	815	908	941
	30	418	456	516	599	763	901	1077	1153	423	474	559	650	809	906	1046	1098	428	492	576	662	793	880	988	1027
Sta. 3	10	256	320	391	460	552	616	688	714	266	330	389	437	502	543	583	593	268	324	372	408	460	489	515	518
	15	294	348	422	495	614	686	784	822	302	369	438	499	581	635	695	712	308	370	429	477	543	584	623	631
	20	334	379	449	523	655	741	861	907	341	403	475	545	645	711	788	815	346	410	476	536	613	666	721	735
	25	376	414	478	549	687	785	926	982	381	435	508	584	701	775	871	903	385	446	516	582	676	736	807	828
	30	418	453	506	578	718	835	984	1048	421	468	541	618	750	831	944	984	425	482	552	624	730	801	884	912
Sta. 4	10	253	308	368	424	499	550	605	623	259	310	356	393	440	470	494	496	258	300	335	360	395	412	424	419
	15	292	339	402	464	563	622	700	728	298	353	408	457	520	560	602	611	300	349	394	430	477	506	528	528
	20	333	373	433	496	606	678	776	812	337	390	449	506	585	636	693	710	340	392	445	490	549	587	623	628
	25	374	410	465	525	641	724	840	886	378	425	486	547	641	701	774	796	380	432	488	540	612	658	706	718
	30	417	449	496	557	674	773	897	949	419	460	521	584	692	757	845	874	421	469	527	584	667	722	782	799
Sta. 20	10	240	269	302	334	379	411	452	465	235	257	282	304	338	362	388	393	235	261	289	311	347	369	393	398
	15	287	322	364	408	475	521	575	593	279	300	322	344	371	393	417	418	278	297	317	334	359	377	392	390
	20	331	367	426	487	593	650	739	769	326	350	375	400	437	461	487	491	322	338	355	371	389	402	412	405
	25	375	411	483	551	693	780	921	974	372	400	434	470	524	560	600	608	368	386	404	420	443	455	465	457
	30	418	456	520	611	789	941	1104	1179	417	447	493	542	626	672	739	757	414	435	459	481	515	535	552	548

TABLE A-8 SEAKEEPING RESPONSES FOR $C_B = 0.65$, $L/B = 7.0$, LCB $= +0.5\%$

		Froude No.	$B/T = 2$								$B/T = 3$								$B/T = 4$							
			Significant Wave Height/LBP								Significant Wave Height/LBP								Significant Wave Height/LBP							
		[%]	0.015	0.020	0.025	0.030	0.040	0.050	0.075	0.100	0.015	0.020	0.250	0.030	0.040	0.050	0.075	0.100	0.015	0.020	0.025	0.030	0.040	0.050	0.075	0.100
Heave		10	9	23	37	51	76	103	167	232	7	15	25	36	60	85	151	217	7	13	22	32	56	81	147	213
		15	9	28	46	64	96	124	189	252	8	19	31	44	69	95	161	226	7	15	26	37	61	87	153	219
		20	9	28	51	74	113	145	213	275	8	23	38	54	81	108	174	238	7	18	31	43	69	95	161	226
		25	7	24	53	80	128	163	238	300	8	25	43	61	93	122	189	253	7	21	35	50	78	105	171	236
		30	4	21	54	81	136	178	260	326	8	25	46	67	104	136	204	268	7	22	39	55	86	115	182	246
Pitch		10	34	76	118	156	216	263	341	392	32	67	101	131	184	226	300	350	29	59	90	119	169	210	283	333
		15	28	72	117	160	225	277	361	414	31	68	106	140	196	241	318	369	29	62	95	126	178	221	296	346
		20	23	66	113	156	229	284	375	431	28	67	107	144	203	251	332	384	28	62	97	130	185	229	306	357
		25	20	58	105	154	233	291	388	444	23	64	106	145	208	257	342	395	25	61	98	132	189	235	314	366
		30	14	46	102	151	239	297	400	463	21	60	103	144	211	263	350	406	22	59	97	133	192	239	321	374
Bending Moment		10	47	91	131	166	212	246	294	317	58	102	139	170	216	247	290	313	60	104	141	171	216	246	290	312
		15	45	90	134	172	229	268	322	350	59	108	151	185	236	272	319	343	64	112	153	186	236	269	315	338
		20	44	86	132	175	243	286	350	380	57	110	158	199	256	296	351	377	65	118	164	202	257	295	345	370
		25	42	82	132	176	251	300	374	409	55	111	163	208	275	320	383	413	64	122	173	217	278	321	379	407
		30	42	82	131	176	256	312	396	437	55	110	166	215	291	343	414	449	63	124	181	229	299	347	413	445
Added Resistance		10	7	25	50	76	123	158	205	231	10	26	47	68	110	139	179	204	13	30	51	73	115	145	186	210
		15	6	25	54	88	151	203	286	344	9	27	52	79	129	171	243	300	12	30	53	79	128	169	243	306
		20	4	24	57	100	180	249	368	457	8	28	57	90	148	203	307	397	10	29	55	84	141	193	300	401
		25	3	18	54	100	204	287	448	563	7	27	60	100	176	246	376	487	9	30	60	96	164	228	359	479
		30	2	12	50	100	227	325	528	668	5	27	64	111	204	288	446	577	8	30	65	108	187	262	419	558
Acceleration	Sta. 0	10	346	753	1107	1406	1788	2065	2424	2588	401	738	1020	1239	1572	1788	2083	2231	388	680	920	1122	1418	1618	1897	2043
		15	316	779	1212	1590	2103	2472	2940	3170	437	873	1252	1557	1992	2291	2676	2855	444	836	1162	1428	1821	2081	2427	2603
		20	275	742	1241	1688	2359	2781	3388	3672	420	945	1421	1820	2352	2737	3231	3462	480	955	1374	1713	2206	2541	2982	3188
		25	245	682	1232	1743	2538	3046	3793	4130	386	971	1521	2001	2666	3118	3737	4027	474	1033	1546	1972	2552	2974	3516	3769
		30	200	593	1222	1769	2704	3286	4167	4595	364	966	1577	2125	2930	3472	4205	4562	445	1077	1666	2180	2874	3362	4024	4332
	Sta. 5	10	192	441	661	849	1078	1259	1497	1616	229	428	593	725	929	1065	1261	1373	231	399	539	659	839	964	1154	1264
		15	176	469	742	983	1321	1557	1875	2042	253	515	748	935	1204	1396	1654	1784	261	494	691	851	1095	1260	1493	1622
		20	158	443	770	1070	1523	1810	2228	2428	238	567	866	1123	1459	1707	2043	2208	282	572	831	1042	1351	1569	1865	2015
		25	133	394	775	1119	1679	2019	2553	2798	221	590	940	1249	1691	1988	2410	2621	275	625	948	1223	1593	1869	2238	2422
		30	104	344	777	1138	1790	2208	2850	3170	211	586	982	1347	1888	2255	2762	3018	258	657	1031	1366	1825	2146	2602	2826
	Sta. 10	10	97	218	327	426	545	660	819	918	91	160	228	287	395	480	635	739	102	160	216	270	366	447	600	704
		15	102	290	455	601	805	950	1168	1295	111	226	335	426	570	685	867	981	107	196	282	356	486	588	764	880
		20	111	316	537	742	1045	1251	1537	1691	119	299	457	605	790	946	1171	1301	123	255	380	487	656	787	996	1124
		25	97	288	584	849	1274	1513	1913	2097	123	352	563	752	1027	1216	1505	1666	132	319	489	646	855	1029	1279	1426
		30	71	253	627	907	1433	1751	2263	2525	133	380	642	882	1244	1499	1851	2047	134	370	589	790	1073	1278	1590	1764
	Sta. 15	10	191	354	494	600	777	900	1077	1183	161	268	364	453	593	699	874	981	157	252	335	419	551	653	826	932
		15	195	446	659	844	1064	1237	1478	1602	190	343	477	585	770	898	1098	1219	165	285	394	495	655	777	977	1099
		20	193	509	787	1031	1370	1606	1919	2092	218	437	630	791	1011	1186	1426	1559	192	354	500	622	823	968	1195	1331
		25	186	499	857	1202	1689	1980	2413	2599	218	520	781	1008	1301	1513	1824	1984	220	441	640	806	1047	1232	1497	1646
		30	151	435	928	1309	1965	2317	2892	3177	223	579	903	1188	1589	1871	2249	2458	228	521	782	1013	1309	1536	1862	2034
	Sta. 20	10	342	655	920	1121	1443	1649	1926	2069	324	567	770	945	1204	1381	1635	1771	309	522	699	861	1101	1268	1516	1647
		15	337	752	1111	1421	1789	2076	2445	2614	364	682	951	1166	1501	1720	2023	2182	340	610	839	1038	1334	1537	1828	1982
		20	316	822	1262	1637	2162	2518	2986	3231	394	795	1144	1428	1823	2113	2481	2662	378	714	1003	1238	1603	1847	2186	2362
		25	305	808	1335	1851	2551	2994	3605	3860	381	888	1328	1708	2184	2529	2999	3217	415	821	1184	1482	1905	2211	2615	2810
		30	253	702	1417	1991	2938	3434	4226	4604	375	958	1477	1926	2551	2980	3540	3831	413	917	1364	1753	2241	2611	3098	3327

Relative Motion	Sta. 1	10	52	98	141	178	226	261	306	326	55	92	124	150	189	215	249	266	55	87	114	138	172	195	226	241
		15	48	94	142	185	245	287	342	369	53	94	132	164	209	241	282	301	54	90	122	149	189	216	252	269
		20	44	86	137	184	258	304	371	402	49	93	136	173	225	261	310	333	52	91	127	158	203	234	276	296
		25	42	78	130	180	263	315	394	429	46	89	135	176	236	276	333	360	49	89	129	165	214	249	297	319
		30	40	70	124	175	265	323	411	454	45	85	132	176	243	289	352	383	46	87	129	167	222	261	315	340
	Sta. 2	10	51	92	130	162	202	231	268	284	53	85	112	133	165	186	212	225	52	79	102	120	148	166	190	201
		15	47	90	132	170	222	258	305	327	52	88	121	148	186	212	245	260	52	83	111	133	166	187	215	229
		20	44	83	128	171	236	276	334	360	49	88	125	158	202	233	274	292	51	85	117	143	180	206	240	255
		25	42	75	123	168	242	289	358	388	46	85	126	162	214	249	297	319	48	85	119	150	192	222	261	279
		30	40	68	118	164	245	298	376	414	44	81	123	163	222	262	316	342	46	83	120	154	201	234	280	301
	Sta. 3	10	49	85	117	144	177	202	231	243	50	77	98	115	140	156	176	185	48	70	88	102	123	136	153	161
		15	46	84	121	154	199	229	268	286	50	81	109	131	162	183	209	220	49	75	98	115	141	158	179	189
		20	44	78	119	157	214	249	298	320	47	82	114	142	179	205	238	252	49	78	105	126	157	178	204	215
		25	42	72	115	156	222	262	323	349	45	80	116	147	192	221	261	280	47	79	109	134	169	194	226	240
		30	40	66	111	153	226	273	342	375	44	77	115	149	201	235	282	303	45	78	110	140	180	207	245	262
	Sta. 4	10	47	77	104	126	153	172	195	203	46	67	84	97	115	126	140	146	43	59	72	83	97	106	118	122
		15	45	78	110	138	175	201	232	247	47	73	95	113	138	154	173	181	45	66	84	97	117	129	144	150
		20	43	74	110	143	192	222	264	281	45	75	102	125	155	176	202	213	46	70	92	109	133	149	169	177
		25	41	69	107	144	202	237	289	311	43	75	105	132	169	194	227	241	45	72	97	118	147	167	191	202
		30	40	64	105	142	207	249	310	339	42	73	105	136	180	209	248	266	43	72	100	125	158	181	211	224
	Sta. 20	10	36	55	75	93	120	141	170	185	37	56	74	90	116	134	160	173	38	57	75	91	116	133	158	171
		15	36	57	79	100	128	150	183	199	36	52	70	85	110	128	155	169	36	53	70	85	109	126	150	163
		20	38	62	87	111	147	173	208	227	35	51	68	85	108	128	155	169	36	50	66	80	103	120	144	157
		25	39	63	94	127	175	204	248	267	36	53	71	88	115	134	164	179	35	49	64	78	100	117	142	155
		30	39	61	104	139	202	237	293	321	37	55	76	96	127	150	181	198	35	49	65	79	102	119	145	159
Relative Velocity	Sta. 1	10	271	376	480	571	681	762	851	882	284	374	453	516	607	660	719	740	287	366	432	487	562	608	659	676
		15	305	404	518	625	767	868	984	1033	320	420	517	597	708	782	861	888	325	416	498	564	660	718	781	803
		20	341	425	541	657	835	945	1093	1150	354	455	565	665	793	883	987	1023	362	459	555	634	748	822	901	928
		25	380	448	561	681	879	1004	1181	1249	389	486	601	712	864	966	1093	1141	398	495	601	697	823	912	1012	1046
		30	421	475	584	702	919	1056	1254	1339	429	515	631	747	922	1039	1184	1244	435	529	641	748	891	989	1109	1152
	Sta. 2	10	271	363	453	530	622	689	760	782	282	359	424	474	547	587	629	641	283	348	401	444	502	535	568	575
		15	305	395	493	585	707	793	888	926	319	406	488	554	646	705	764	781	324	401	468	521	598	641	685	697
		20	342	418	530	621	774	868	993	1039	354	444	538	622	729	803	885	910	362	445	526	590	684	742	800	816
		25	381	444	543	648	820	927	1077	1133	390	477	576	671	799	884	987	1023	398	484	574	653	757	830	906	928
		30	421	472	568	672	860	978	1148	1218	429	508	608	708	857	955	1074	1121	435	520	615	705	824	905	1000	1030
	Sta. 3	10	268	347	421	485	559	614	666	680	275	337	388	426	480	509	535	539	272	322	362	393	433	454	472	470
		15	303	382	466	542	644	714	790	819	314	387	454	505	579	623	663	672	316	378	431	471	528	558	584	587
		20	340	409	496	582	711	790	892	927	351	428	506	574	660	719	780	796	356	425	490	540	613	656	695	701
		25	380	437	523	612	759	849	974	1019	388	463	547	625	730	799	878	904	394	467	540	604	686	742	796	808
		30	421	468	551	639	799	899	1043	1100	427	496	581	665	788	869	963	998	432	505	584	658	753	817	887	906
	Sta. 4	10	262	327	387	438	495	537	573	579	263	310	347	375	411	428	439	436	257	292	319	338	361	372	375	365
		15	299	366	436	498	580	636	693	713	306	364	415	454	508	539	562	563	304	351	389	417	454	472	482	477
		20	338	397	470	542	648	713	793	818	345	408	470	523	589	634	675	681	347	401	450	487	539	568	588	586
		25	378	428	501	576	698	772	874	908	384	446	514	577	659	712	770	785	387	446	503	551	613	653	686	689
		30	419	461	532	606	740	823	941	986	424	483	552	620	718	782	852	876	427	486	549	607	679	727	775	783
	Sta. 20	10	237	267	300	329	375	407	441	451	234	266	299	326	368	395	422	432	236	269	304	331	373	398	425	435
		15	282	315	353	391	435	470	511	520	277	301	327	349	385	408	430	432	276	303	330	353	387	408	427	429
		20	329	370	418	463	530	577	629	649	321	343	366	390	416	439	459	456	319	339	361	378	404	420	431	425
		25	375	418	479	549	650	713	793	813	367	391	418	445	478	499	524	522	363	380	398	414	431	445	450	438
		30	418	458	542	625	777	853	972	1019	413	443	477	511	560	592	624	631	408	426	444	462	479	490	495	482

TABLE A-9 SEAKEEPING RESPONSES FOR $C_B = 0.65$, $L/B = 8.5$, LCB $= +0.5\%$

		Froude No.	$B/T = 2$								$B/T = 3$								$B/T = 4$							
			Significant Wave Height/LBP								Significant Wave Height/LBP								Significant Wave Height/LBP							
		[%]	0.015	0.020	0.025	0.030	0.040	0.050	0.075	0.100	0.015	0.020	0.025	0.030	0.040	0.050	0.075	0.100	0.015	0.020	0.025	0.030	0.040	0.050	0.075	0.100
Heave		10	9	19	30	41	66	91	156	222	7	14	23	33	56	82	147	214	7	13	21	31	54	79	145	211
		15	11	27	42	57	82	109	173	237	8	17	27	38	63	88	154	220	7	14	24	34	58	83	149	215
		20	10	31	51	70	101	129	193	256	9	21	34	47	72	98	163	228	8	17	28	39	64	89	155	220
		25	11	32	56	79	118	149	216	278	9	25	41	57	84	111	176	240	8	20	32	45	71	97	162	227
		30	10	29	58	86	133	167	239	300	9	27	46	64	95	124	190	253	8	22	37	52	79	106	172	236
Pitch		10	39	80	118	151	208	251	325	375	32	64	96	125	176	216	290	339	29	58	88	115	164	204	276	326
		15	36	81	124	162	224	272	351	401	33	69	105	136	190	232	307	357	30	61	93	123	173	214	288	338
		20	31	77	124	167	232	284	369	421	33	71	109	143	200	245	322	373	30	63	97	128	181	223	299	349
		25	25	72	121	165	239	291	381	437	30	70	111	147	207	254	334	385	29	64	99	132	187	231	308	359
		30	23	67	116	164	240	300	393	450	26	68	110	150	211	260	344	396	27	63	100	134	190	236	315	366
Bending Moment		10	47	84	116	141	181	206	243	261	51	87	117	142	178	204	240	258	51	87	118	143	179	205	240	259
		15	45	87	124	156	196	227	268	288	54	94	128	155	196	222	260	279	55	94	127	154	193	219	256	275
		20	43	87	127	161	211	244	291	315	55	99	138	168	213	244	285	305	58	101	138	167	210	239	278	297
		25	43	84	126	164	222	260	313	339	54	102	145	181	230	265	311	333	59	107	148	180	228	260	303	324
		30	42	81	125	166	231	272	334	363	52	103	149	189	245	284	337	362	59	110	155	192	245	282	330	353
Added Resistance		10	7	20	37	53	85	107	136	153	10	22	37	53	82	102	131	147	12	25	41	57	87	108	137	154
		15	6	22	44	68	108	142	196	235	9	23	41	59	95	124	174	216	11	25	43	61	97	127	181	226
		20	5	24	51	82	132	178	257	317	8	23	44	66	108	145	218	284	10	25	45	66	108	146	224	299
		25	4	22	51	90	157	218	322	397	7	25	50	79	130	178	269	349	9	26	49	74	123	169	264	353
		30	3	19	52	97	182	259	387	477	6	26	56	92	152	210	321	413	8	27	53	82	139	193	304	407
Acceleration	Sta. 0	10	467	875	1213	1454	1847	2086	2394	2545	436	748	1007	1209	1511	1712	1995	2135	425	694	913	1105	1383	1572	1842	1978
		15	464	995	1451	1832	2307	2660	3088	3277	523	960	1322	1597	2014	2278	2627	2799	502	874	1186	1431	1798	2040	2370	2538
		20	426	1033	1583	2052	2672	3114	3670	3934	570	1117	1586	1952	2486	2842	3292	3496	564	1052	1459	1775	2250	2557	2964	3161
		25	378	1009	1632	2182	2979	3480	4187	4509	560	1212	1795	2268	2897	3357	3921	4178	615	1197	1700	2098	2687	3076	3580	3811
		30	352	960	1642	2270	3193	3816	4651	5045	518	1260	1932	2514	3268	3802	4505	4823	623	1302	1916	2404	3087	3577	4184	4464
	Sta. 5	10	267	508	710	851	1095	1245	1448	1558	256	436	582	705	888	1013	1201	1310	253	408	535	648	815	934	1118	1222
		15	263	594	883	1126	1411	1642	1927	2063	302	565	779	946	1204	1370	1602	1727	297	517	697	849	1072	1224	1447	1571
		20	238	631	982	1285	1695	1976	2356	2546	335	668	959	1185	1519	1753	2048	2194	334	628	873	1068	1364	1560	1830	1975
		25	221	619	1024	1391	1928	2274	2754	2987	323	735	1104	1414	1808	2108	2491	2674	366	723	1037	1286	1658	1910	2249	2416
		30	202	572	1037	1470	2120	2535	3131	3405	297	772	1204	1583	2083	2430	2913	3143	367	794	1183	1501	1935	2257	2671	2872
	Sta. 10	10	115	203	292	349	475	564	714	814	119	179	234	288	382	462	613	715	127	182	228	280	367	444	594	694
		15	141	309	457	587	735	882	1062	1170	123	220	311	385	518	617	790	904	131	209	282	349	465	560	732	846
		20	140	395	609	798	1041	1213	1469	1608	155	304	446	552	732	868	1071	1195	140	257	365	456	612	729	927	1053
		25	152	440	713	957	1316	1557	1884	2065	166	395	590	768	982	1172	1421	1562	166	329	486	608	810	963	1195	1334
		30	151	428	772	1104	1577	1882	2315	2516	165	462	721	955	1258	1478	1803	1975	180	405	613	794	1036	1239	1514	1672
	Sta. 15	10	202	338	452	551	700	807	980	1086	194	296	380	467	598	700	870	971	188	284	359	442	569	667	836	936
		15	255	465	642	766	988	1132	1332	1448	202	333	448	554	716	838	1037	1156	196	309	407	506	658	776	972	1088
		20	262	581	848	1080	1328	1541	1814	1945	242	430	589	715	932	1075	1298	1431	206	349	474	592	776	914	1137	1271
		25	254	670	1018	1304	1708	1965	2329	2522	285	550	778	957	1220	1417	1679	1823	242	435	603	742	973	1133	1383	1531
		30	263	699	1118	1523	2042	2427	2880	3107	290	657	968	1242	1552	1805	2142	2308	283	544	772	953	1234	1438	1725	1887
	Sta. 20	10	395	691	931	1127	1411	1599	1858	1996	369	598	780	949	1193	1361	1609	1736	348	554	721	879	1109	1272	1513	1636
		15	450	846	1175	1412	1815	2058	2375	2537	410	712	959	1171	1477	1685	1978	2131	390	651	863	1060	1342	1538	1822	1969
		20	451	973	1417	1800	2218	2574	2990	3173	463	851	1171	1423	1818	2068	2409	2586	425	749	1019	1253	1595	1828	2157	2328
		25	416	1072	1622	2071	2697	3080	3634	3900	513	996	1409	1725	2199	2526	2931	3130	473	874	1212	1482	1902	2176	2551	2746
		30	424	1115	1744	2338	3089	3674	4314	4645	514	1121	1643	2096	2610	3024	3535	3763	533	1012	1432	1757	2256	2594	3036	3246

Relative Velocity																													
		10	15	20	25	30	10	15	20	25	30	10	15	20	25	30	10	15	20	25	30	10	15	20	25	30	10	15	20	25	30
		58	53	49	46	44	57	53	49	46	44	54	51	49	47	44	50	48	46	44	42	38	38	37	38	40	289	319	351	387	426
	Sta. 1	102	103	100	93	85	94	97	95	89	82	86	90	89	84	78	76	82	82	79	74	59	58	60	65	68	396	437	466	488	510
		139	149	150	145	139	127	137	139	136	131	113	124	128	126	123	98	111	116	114	114	80	79	83	92	99	492	556	595	619	640
		168	188	194	194	192	150	171	179	180	179	132	153	162	165	165	112	135	145	150	152	98	96	106	115	131	561	660	715	750	776
		213	238	255	267	272	188	213	232	245	251	163	188	208	221	230	137	163	184	199	208	125	125	133	152	174	674	784	871	941	986
		242	274	298	314	326	211	245	268	286	298	181	214	239	257	271	150	184	210	229	245	145	146	157	176	207	737	876	981	1060	1127
		278	321	354	380	401	240	283	316	343	365	202	245	278	306	329	166	208	242	270	294	172	176	189	212	247	805	975	1108	1218	1307
		295	342	380	411	436	253	299	338	369	395	212	257	296	328	354	172	217	256	288	316	186	190	204	231	267	830	1008	1159	1278	1381
		246	278	310	339	364	205	237	269	297	323	164	196	228	257	282	125	156	188	217	244	178	173	170	171	179	696	843	991	1127	1248
		231	261	291	316	338	194	224	253	279	301	157	187	216	243	265	120	150	180	207	230	165	160	156	157	165	678	820	962	1090	1200
		199	225	249	267	281	170	196	220	239	254	139	166	190	210	225	109	136	160	181	198	139	134	130	131	136	626	756	878	982	1067
		176	198	216	230	241	152	174	193	207	219	126	149	168	183	196	100	123	144	160	173	121	116	112	111	117	580	696	798	882	956
		142	157	169	179	183	124	140	153	163	168	105	122	135	147	153	86	103	117	129	137	95	91	87	87	92	503	593	673	745	799
		118	130	137	140	140	105	117	126	130	131	91	104	113	118	120	75	89	99	106	109	79	75	71	71	73	445	522	587	636	675
		90	96	98	97	94	82	89	91	91	89	72	80	84	85	84	62	70	76	78	78	59	56	53	53	54	376	433	478	515	547
		56	56	54	51	48	54	55	53	50	47	50	52	51	49	46	45	47	48	47	45	38	37	36	36	36	291	331	368	402	436
		55	55	54	53	50	52	53	53	52	50	47	49	50	50	48	41	44	46	47	46	39	37	37	36	35	291	333	372	410	446
		85	89	92	93	92	76	82	86	87	87	66	73	78	80	81	54	62	68	72	74	60	56	54	52	50	366	421	471	515	553
		110	119	126	130	133	97	106	114	120	123	82	92	101	107	112	65	77	87	94	100	79	75	71	68	66	426	496	562	620	669
		131	143	153	161	168	114	126	137	146	153	94	108	119	129	137	74	88	101	112	121	95	90	85	81	80	476	558	635	704	769
		163	179	195	207	217	138	155	171	185	195	112	130	147	161	172	86	104	122	137	149	120	114	109	104	102	544	643	741	829	905
		184	203	222	239	253	155	174	193	211	225	124	144	164	182	197	94	114	134	153	169	138	131	126	121	119	584	693	804	908	1001
		214	236	259	281	300	177	200	223	245	264	140	163	186	208	228	104	127	150	173	193	162	156	150	145	143	630	748	871	991	1103
		228	252	277	301	322	187	211	236	260	282	146	171	196	220	242	107	131	157	181	204	175	169	162	157	155	643	766	894	1019	1137
		252

TABLE A-10 SEAKEEPING RESPONSES FOR $C_B = 0.70$, $L/B = 5.5$, LCB = + 1.0%

		Froude No.	$B/T = 2$								$B/T = 3$								$B/T = 4$							
			Significant Wave Height/LBP								Significant Wave Height/LBP								Significant Wave Height/LBP							
		[%]	0.015	0.020	0.250	0.030	0.040	0.050	0.075	0.100	0.015	0.020	0.025	0.030	0.040	0.050	0.075	0.100	0.015	0.020	0.025	0.030	0.040	0.050	0.075	0.100
Heave		10	7	21	38	55	87	115	182	246	6	15	26	39	64	90	156	222	5	13	22	33	57	83	149	215
		15	6	19	42	63	103	135	207	271	6	18	33	47	75	103	169	235	5	15	27	39	64	91	157	223
		20	3	17	42	66	114	153	231	298	6	19	36	54	87	117	185	250	6	17	31	45	73	101	168	233
		25	2	16	37	66	120	168	253	322	5	17	38	59	98	130	202	267	6	18	34	50	82	111	179	245
		30	2	14	30	67	125	180	274	347	4	15	39	61	105	141	218	285	5	17	35	54	89	121	192	257
Pitch		10	21	59	100	139	204	252	337	390	25	59	94	126	181	225	301	352	24	54	86	115	166	208	283	333
		15	18	53	95	137	208	263	353	409	21	56	94	130	188	235	316	369	22	54	87	119	173	216	294	345
		20	12	41	90	134	215	271	370	430	18	53	91	129	193	242	327	382	19	52	86	120	176	222	302	355
		25	8	36	85	128	215	281	390	453	15	47	87	128	197	249	338	394	17	49	84	119	179	226	309	363
		30	6	33	68	128	217	300	414	482	12	39	85	126	202	255	350	409	15	45	81	119	182	231	317	372
Bending Moment		10	45	88	134	178	248	296	368	405	61	116	165	208	270	316	380	413	70	126	175	216	279	322	383	415
		15	44	83	134	179	260	313	398	440	59	117	172	220	293	343	416	452	70	131	187	234	303	352	420	454
		20	43	85	133	179	264	329	424	473	59	116	176	230	314	372	455	496	68	134	196	250	330	385	462	501
		25	44	87	133	183	272	344	447	501	58	116	180	239	335	400	497	544	68	137	204	265	356	419	509	553
		30	45	89	137	191	284	362	477	537	58	116	186	249	357	431	542	597	68	138	212	279	384	456	559	609
Added Resistance		10	6	29	65	110	192	255	346	397	10	32	63	97	163	213	281	322	14	37	68	101	167	216	283	325
		15	4	21	60	109	218	303	460	561	8	31	66	108	190	259	380	475	12	35	69	108	185	251	372	475
		20	2	14	54	108	244	351	573	725	7	29	68	118	216	305	479	628	10	34	71	116	202	286	461	626
		25	2	11	41	97	238	388	662	851	5	24	65	121	247	355	580	759	8	31	72	124	233	335	551	744
		30	1	8	27	87	233	424	751	977	4	18	62	123	277	404	680	890	7	29	73	133	263	385	640	863
Acceleration	Sta. 0	10	178	464	762	1035	1428	1691	2077	2259	266	567	845	1073	1400	1637	1955	2113	288	565	807	1009	1313	1522	1813	1964
		15	154	435	776	1088	1585	1924	2415	2658	247	603	945	1246	1669	1968	2383	2587	298	637	956	1220	1602	1878	2251	2435
		20	125	376	760	1119	1725	2125	2729	3026	224	601	996	1355	1894	2259	2774	3029	281	675	1055	1390	1862	2197	2665	2893
		25	101	339	742	1111	1807	2298	3040	3399	206	566	1013	1434	2089	2518	3150	3449	263	686	1117	1510	2093	2493	3056	3336
		30	88	318	651	1132	1884	2536	3368	3793	177	508	1025	1484	2265	2755	3515	3882	251	669	1152	1608	2302	2771	3442	3767
	Sta. 5	10	95	263	446	618	875	1049	1311	1446	147	325	491	632	832	983	1199	1317	166	327	471	591	778	911	1109	1223
		15	80	238	464	666	1005	1228	1577	1755	136	351	560	749	1022	1214	1497	1646	170	373	565	732	970	1146	1401	1537
		20	62	209	457	689	1100	1386	1820	2044	126	350	600	831	1187	1429	1784	1969	158	400	635	848	1153	1371	1691	1860
		25	50	194	435	693	1166	1529	2054	2323	114	326	618	892	1335	1622	2066	2285	151	408	682	934	1320	1586	1976	2181
		30	44	180	376	714	1229	1688	2295	2617	95	291	633	929	1457	1799	2339	2612	144	396	709	1007	1475	1790	2261	2499
	Sta. 10	10	60	170	285	393	559	680	867	980	63	141	218	292	404	501	663	769	67	125	188	247	351	439	597	704
		15	58	168	338	491	744	901	1164	1304	69	187	304	413	578	701	903	1028	73	167	260	349	483	597	784	903
		20	42	152	369	547	881	1101	1453	1640	76	215	373	521	755	921	1175	1323	78	208	337	460	645	785	1014	1153
		25	33	155	356	577	978	1291	1731	1959	73	212	419	612	929	1132	1464	1637	84	236	404	560	810	991	1269	1433
		30	29	144	300	617	1065	1475	2005	2288	60	195	458	675	1074	1329	1748	1970	87	244	453	653	974	1195	1541	1730
	Sta. 15	10	122	308	474	621	823	970	1186	1307	131	250	362	457	610	725	907	1018	119	214	306	390	529	636	814	925
		15	120	323	547	760	1067	1269	1563	1713	139	314	473	616	809	959	1185	1313	134	264	387	496	667	799	1007	1132
		20	97	283	599	851	1292	1545	1961	2167	141	362	571	760	1035	1229	1513	1672	143	321	488	639	850	1014	1265	1407
		25	77	271	602	889	1433	1808	2362	2625	139	370	637	892	1269	1513	1881	2064	147	369	583	776	1060	1262	1568	1739
		30	66	257	518	947	1556	2101	2756	3091	123	341	692	988	1490	1783	2261	2499	150	392	656	904	1274	1530	1905	2104
	Sta. 20	10	207	517	795	1038	1364	1593	1920	2083	246	485	700	877	1149	1340	1609	1751	238	444	629	790	1036	1210	1467	1605
		15	200	533	878	1204	1664	1976	2397	2603	249	560	842	1089	1417	1662	2001	2171	262	516	753	953	1255	1471	1780	1938
		20	164	463	936	1324	1974	2334	2918	3193	241	614	961	1269	1706	2009	2430	2648	261	585	882	1145	1501	1767	2138	2326
		25	131	431	947	1362	2157	2674	3459	3813	235	618	1037	1434	2005	2379	2909	3158	258	640	999	1319	1773	2089	2539	2769
		30	112	411	823	1433	2319	3093	4000	4450	209	566	1099	1558	2306	2734	3412	3731	258	664	1086	1480	2049	2439	2980	3249

| Relative Motion | | |

TABLE A-11 SEAKEEPING RESPONSES FOR $C_B = 0.70$, $L/B = 7.0$, LCB $= +1.0\%$

		Froude No. [%]	$B/T = 2$ Significant Wave Height/LBP 0.015	0.020	0.025	0.030	0.040	0.050	0.075	0.100	$B/T = 3$ Significant Wave Height/LBP 0.015	0.020	0.025	0.030	0.040	0.050	0.075	0.100	$B/T = 4$ Significant Wave Height/LBP 0.015	0.020	0.025	0.030	0.040	0.050	0.075	0.100
	Heave	10	8	21	34	48	73	99	164	229	6	10	23	34	57	83	149	215	6	12	21	31	54	79	145	211
		15	8	25	43	60	91	119	185	249	7	18	29	42	66	93	158	224	6	14	24	35	59	85	150	216
		20	8	25	47	70	108	140	208	271	7	21	36	51	78	105	171	236	6	17	28	41	66	92	158	224
		25	6	21	50	75	123	157	232	296	7	23	40	58	90	119	185	250	7	19	33	47	75	102	168	233
		30	4	19	50	76	130	172	254	321	7	23	43	64	100	132	201	265	7	20	36	52	83	112	179	244
	Pitch	10	31	71	111	146	204	250	328	378	29	62	94	124	175	217	291	341	26	55	85	113	162	202	275	325
		15	25	68	111	153	215	265	349	401	28	63	99	132	187	231	307	358	26	57	89	119	170	212	287	337
		20	22	64	109	151	222	276	364	420	25	62	101	137	194	241	321	372	25	57	91	123	176	220	297	348
		25	18	55	102	152	231	286	382	436	21	60	100	138	200	248	331	384	23	56	92	125	180	225	304	356
		30	13	43	102	149	237	295	398	461	19	57	98	137	203	255	340	396	20	54	91	126	184	230	311	364
	Bending Moment	10	47	91	131	167	216	252	304	331	58	103	143	175	224	257	305	330	61	106	145	177	226	259	307	331
		15	46	90	133	171	231	271	329	359	59	109	153	189	243	280	332	358	64	114	157	192	245	280	330	356
		20	45	86	132	175	243	288	355	387	57	111	160	202	262	304	363	391	65	120	168	207	266	306	361	388
		25	44	84	133	176	251	301	378	415	56	111	164	210	280	327	393	427	64	124	177	222	287	332	394	425
		30	44	86	133	178	256	314	399	442	56	111	168	219	297	350	426	463	63	126	184	235	308	359	430	464
	Added Resistance	10	7	25	50	75	123	159	207	233	10	27	48	70	114	145	188	214	14	32	54	78	123	156	201	228
		15	6	24	53	87	152	206	292	353	9	26	50	76	127	174	263	322	12	30	55	82	135	179	261	332
		20	4	23	56	99	181	253	377	472	8	27	56	90	150	208	319	419	10	29	56	86	146	202	321	436
		25	3	17	53	98	204	291	461	583	6	27	61	102	179	249	387	502	9	29	60	97	169	237	382	518
		30	2	11	49	97	226	329	544	695	5	26	62	110	207	296	464	607	8	30	65	108	192	272	443	600
Acceleration	Sta. 0	10	306	672	1000	1264	1634	1892	2235	2398	351	663	923	1132	1450	1659	1944	2092	352	620	842	1035	1318	1512	1785	1929
		15	277	697	1096	1454	1927	2272	2722	2939	381	779	1140	1421	1830	2121	2492	2672	392	750	1056	1306	1681	1932	2272	2445
		20	244	674	1135	1544	2170	2573	3147	3428	365	843	1284	1660	2164	2528	3007	3234	419	852	1251	1565	2030	2358	2784	2990
		25	217	616	1125	1611	2365	2842	3554	3869	334	867	1375	1825	2458	2885	3482	3766	409	920	1396	1801	2348	2751	3278	3529
		30	174	528	1135	1643	2530	3083	3929	4350	316	860	1426	1942	2704	3226	3926	4274	384	959	1504	1985	2650	3111	3752	4057
	Sta. 5	10	164	386	585	753	975	1140	1372	1490	200	381	535	658	852	984	1177	1288	206	360	491	604	776	898	1085	1194
		15	151	409	656	880	1192	1415	1719	1879	216	456	674	849	1100	1286	1537	1668	228	440	624	774	1005	1165	1395	1523
		20	135	387	686	959	1380	1650	2047	2245	203	500	774	1014	1334	1568	1895	2060	243	506	746	947	1237	1449	1738	1888
		25	114	345	692	1008	1530	1851	2359	2595	188	519	840	1128	1549	1833	2238	2445	234	552	849	1109	1460	1721	2083	2266
		30	88	301	700	1030	1635	2033	2647	2958	183	512	878	1220	1733	2083	2572	2821	219	579	924	1234	1676	1979	2421	2644
	Sta. 10	10	82	194	292	387	503	611	772	874	82	143	207	263	368	452	608	713	94	146	200	251	344	425	578	682
		15	90	258	410	547	745	886	1101	1229	96	201	303	393	528	646	824	940	95	174	255	325	451	552	729	847
		20	98	279	487	683	975	1173	1456	1609	102	268	417	557	739	887	1113	1245	107	226	344	448	608	741	947	1076
		25	83	251	534	782	1194	1423	1818	2003	110	318	515	693	964	1148	1433	1595	113	285	444	595	798	964	1215	1363
		30	60	226	576	835	1335	1651	2158	2419	120	340	588	821	1172	1420	1769	1962	118	332	537	726	1005	1202	1512	1687
	Sta. 15	10	178	339	478	587	759	886	1066	1172	153	255	350	436	574	680	856	964	155	245	327	408	538	639	813	918
		15	178	429	643	830	1056	1228	1475	1603	178	325	458	565	748	877	1079	1201	158	271	378	476	635	757	958	1080
		20	181	486	763	1012	1359	1605	1921	2097	199	415	607	772	988	1164	1408	1543	180	335	478	598	797	943	1172	1308
		25	169	460	827	1176	1686	1969	2422	2609	199	494	752	976	1277	1488	1803	1968	201	416	611	780	1014	1201	1469	1620
		30	132	398	901	1267	1930	2295	2896	3197	207	546	864	1151	1556	1845	2227	2438	206	491	746	973	1274	1497	1828	2004
	Sta. 20	10	319	618	877	1074	1387	1595	1870	2012	301	529	724	892	1144	1319	1573	1708	296	496	665	822	1055	1221	1468	1599
		15	306	721	1079	1393	1760	2042	2417	2590	336	636	896	1103	1431	1649	1952	2110	315	569	790	981	1270	1471	1762	1915
		20	297	791	1229	1610	2143	2516	2984	3235	358	745	1087	1374	1752	2042	2413	2594	353	662	942	1170	1526	1769	2113	2284
		25	279	752	1294	1825	2568	2997	3638	3888	344	837	1267	1640	2122	2458	2933	3157	375	764	1116	1412	1820	2129	2530	2726
		30	223	644	1390	1946	2916	3430	4266	4676	345	900	1407	1856	2479	2919	3478	3773	366	854	1288	1669	2156	2513	3005	3240

Relative Motion																														
Sta. 1	10	50	92	132	165	211	243	286	305	53	87	117	142	179	203	236	251	53	82	108	130	163	184	214	229
	15	46	89	133	174	229	269	321	346	51	89	125	155	198	228	267	285	52	85	116	141	179	205	239	255
	20	44	82	129	173	242	286	349	379	48	88	128	164	212	247	294	316	50	86	120	150	192	222	262	281
	25	42	74	123	171	248	298	372	405	45	85	127	166	223	262	316	342	47	85	122	156	203	237	283	304
	30	40	67	119	166	251	307	391	432	44	81	124	166	230	274	335	364	45	83	122	158	211	248	300	325
Sta. 2	10	49	86	121	150	188	215	250	265	51	80	105	125	155	175	200	211	50	75	96	113	139	156	178	189
	15	46	84	123	159	207	241	285	305	50	83	114	139	175	200	231	245	50	79	104	125	156	176	203	216
	20	43	78	121	160	220	259	313	338	47	83	118	149	190	220	259	276	49	80	110	135	170	195	227	242
	25	42	72	116	159	228	272	337	366	45	81	118	153	202	235	281	303	47	80	113	142	181	210	248	265
	30	40	66	113	156	232	282	356	393	43	77	117	154	210	248	301	326	45	79	114	145	191	222	266	286
Sta. 3	10	47	80	109	133	165	187	214	225	48	72	92	108	131	146	164	172	46	65	82	95	114	127	143	150
	15	45	79	113	144	184	213	249	266	47	76	102	123	152	171	196	206	47	71	92	108	132	148	168	177
	20	42	74	112	147	199	232	279	300	45	77	107	133	168	192	224	237	46	74	98	118	147	167	192	203
	25	41	69	109	147	208	246	303	328	43	76	109	138	181	209	247	264	45	74	102	127	160	183	213	227
	30	40	64	106	145	213	257	323	355	42	73	108	141	190	223	267	288	43	74	104	132	170	196	232	248
Sta. 4	10	45	72	96	116	141	159	179	187	44	63	78	90	107	117	129	134	41	55	67	77	90	98	108	112
	15	43	73	102	128	162	186	215	228	45	68	89	106	128	144	161	168	43	62	78	91	109	120	133	139
	20	41	70	103	133	179	207	246	263	43	71	96	118	146	165	190	200	44	66	86	102	125	140	158	166
	25	40	66	101	135	189	222	271	292	42	71	99	124	160	183	214	227	43	68	91	111	138	157	180	190
	30	39	61	99	134	195	234	293	320	41	69	100	128	170	198	235	252	42	68	94	117	149	171	200	212
Sta. 20	10	37	55	74	92	119	141	169	184	36	54	72	87	112	130	156	169	36	54	72	88	112	129	154	167
	15	37	58	80	101	131	152	186	202	36	51	68	83	108	126	153	166	36	52	68	82	106	122	147	160
	20	39	63	89	114	152	179	216	235	36	51	68	84	107	126	154	169	36	50	65	78	100	117	142	155
	25	39	63	97	131	183	213	260	280	36	53	71	88	116	135	165	180	35	49	63	77	98	115	140	153
	30	39	61	106	142	209	246	308	339	38	56	77	97	129	152	184	201	36	49	64	78	101	118	144	158
Relative Velocity																									
Sta. 1	10	268	361	455	535	640	712	794	822	279	361	433	491	575	624	678	697	283	355	415	466	535	577	624	638
	15	303	391	494	593	720	814	921	963	316	406	494	568	670	739	812	836	321	403	478	539	628	682	740	758
	20	340	416	521	625	787	888	1023	1078	351	442	541	633	751	835	931	964	359	445	533	606	711	779	853	877
	25	380	442	543	654	836	950	1113	1172	388	474	578	679	821	914	1033	1077	395	483	579	667	783	865	958	988
	30	421	470	571	679	879	1004	1187	1267	428	505	609	716	877	986	1121	1176	433	518	618	716	849	939	1051	1090
Sta. 2	10	267	349	428	496	583	642	706	725	276	345	404	450	516	553	590	600	277	336	384	423	475	504	534	538
	15	302	381	470	554	662	741	827	860	314	392	466	526	610	664	717	732	318	387	448	496	566	606	645	653
	20	340	409	500	590	729	814	926	969	350	430	515	591	689	757	832	854	356	431	504	563	647	701	754	767
	25	380	437	525	621	777	875	1011	1059	387	464	553	639	757	835	929	962	394	470	551	624	719	785	854	874
	30	421	467	555	648	820	927	1082	1147	427	497	587	677	814	905	1014	1056	432	507	593	674	784	858	944	971
Sta. 3	10	263	332	398	454	523	569	616	627	268	323	368	403	451	477	498	500	265	310	345	372	407	426	439	435
	15	300	369	443	513	602	666	733	756	308	373	432	479	544	585	620	626	309	364	411	447	497	524	546	546
	20	338	399	476	552	668	739	829	861	346	414	483	545	623	676	730	744	350	411	469	514	579	617	651	655
	25	378	430	505	586	717	799	911	948	384	450	525	595	691	753	825	847	389	453	519	576	650	700	749	758
	30	419	462	537	616	760	851	979	1031	424	485	561	636	748	821	907	937	428	492	562	628	715	773	836	852
Sta. 4	10	258	314	366	410	462	496	527	531	257	298	331	354	386	400	407	402	251	281	304	320	339	347	346	334
	15	296	354	415	470	541	591	640	655	300	351	396	431	478	505	524	523	298	338	371	396	428	442	448	441
	20	335	388	452	515	608	665	735	757	340	395	450	498	556	595	630	635	341	389	432	464	509	534	550	546
	25	376	421	485	551	659	725	814	842	380	435	495	550	624	672	722	734	382	433	484	527	581	616	644	644
	30	417	456	519	584	703	777	881	921	421	472	534	594	682	740	802	821	423	475	530	581	646	688	729	734
Sta. 20	10	240	269	302	331	374	409	441	449	234	262	293	318	358	383	410	418	233	263	295	320	360	385	410	419
	15	285	320	359	398	446	480	524	534	278	301	326	347	380	403	424	425	276	301	326	347	379	399	416	417
	20	331	374	425	474	547	599	654	677	323	345	369	393	417	440	459	456	321	340	360	376	400	415	425	418
	25	376	420	485	561	676	740	832	853	369	395	422	449	485	505	530	530	365	382	400	416	431	444	449	436
	30	419	459	549	634	797	881	1015	1073	415	446	482	517	568	604	637	644	411	429	447	464	483	492	497	484

TABLE A-12 SEAKEEPING RESPONSES FOR $C_B = 0.70$, $L/B = 8.5$, LCB = $+1.0\%$

		Froude No.	$B/T = 2$								$B/T = 3$								$B/T = 4$							
			Significant Wave Height/LBP								Significant Wave Height/LBP								Significant Wave Height/LBP							
		[%]	0.015	0.020	0.025	0.030	0.040	0.050	0.075	0.100	0.015	0.020	0.025	0.030	0.040	0.050	0.075	0.100	0.015	0.020	0.025	0.030	0.040	0.050	0.075	0.100
Heave		10	8	17	28	38	63	88	154	220	7	13	21	31	55	80	145	212	7	12	20	30	52	77	143	209
		15	9	24	38	53	78	105	169	233	7	15	25	36	60	86	151	217	6	13	22	32	56	81	147	213
		20	9	29	48	65	96	125	189	252	8	19	31	44	69	95	160	226	7	15	26	37	61	87	152	218
		25	10	29	52	75	113	144	211	273	8	23	38	53	80	107	172	237	7	18	30	43	68	94	160	225
		30	8	26	54	81	128	161	234	296	8	25	43	60	92	120	186	250	7	21	34	49	76	103	169	234
Pitch		10	35	73	110	142	196	239	313	362	30	60	91	119	168	208	281	331	27	55	83	110	158	198	270	319
		15	33	75	117	153	213	259	337	388	30	64	98	129	181	223	297	347	27	57	88	117	166	207	281	331
		20	28	73	118	161	223	274	357	408	30	66	103	135	191	235	312	362	27	59	91	121	173	215	290	341
		25	24	70	117	159	231	283	371	427	28	66	104	140	197	244	323	375	26	59	94	125	178	222	299	350
		30	22	65	112	162	237	295	387	442	24	64	105	143	203	251	333	386	25	59	94	127	182	227	305	357
Bending Moment		10	48	85	118	144	186	214	254	275	51	89	121	147	187	214	254	274	52	90	123	149	189	216	256	276
		15	46	87	125	158	200	232	277	299	55	96	131	160	203	232	273	294	56	97	131	160	202	230	271	291
		20	44	87	127	161	214	249	298	324	55	101	141	173	220	253	297	319	59	104	142	173	218	249	292	313
		25	44	85	127	165	224	264	320	347	54	103	147	185	236	273	323	347	60	109	151	185	236	271	317	340
		30	43	82	127	167	233	275	340	370	53	105	152	193	252	292	348	376	60	112	159	198	254	293	345	370
Added Resistance		10	7	20	36	53	85	107	137	155	10	23	39	56	87	110	140	158	13	27	44	62	95	118	151	170
		15	6	21	43	67	108	143	200	241	9	23	42	61	99	129	185	231	11	26	45	65	104	136	197	249
		20	5	23	50	82	131	179	262	327	8	23	44	66	110	149	229	304	10	25	46	68	113	154	243	329
		25	4	20	50	89	158	221	331	410	7	24	49	79	132	182	282	371	9	26	49	76	128	178	284	386
		30	3	18	50	96	186	263	400	493	6	25	55	91	155	215	335	438	8	26	52	83	143	202	326	444
Acceleration	Sta. 0	10	409	783	1095	1324	1688	1919	2217	2365	402	686	923	1117	1405	1598	1870	2013	397	647	847	1031	1297	1481	1746	1881
		15	413	893	1319	1656	2119	2443	2856	3045	460	864	1197	1460	1857	2113	2451	2622	453	799	1082	1322	1673	1907	2230	2396
		20	376	931	1440	1888	2455	2879	3410	3661	501	1001	1449	1786	2288	2636	3068	3273	499	948	1324	1628	2081	2379	2775	2972
		25	335	919	1498	2004	2764	3232	3906	4224	490	1087	1629	2076	2670	3107	3655	3907	540	1073	1556	1922	2479	2862	3348	3580
		30	318	877	1509	2107	2976	3572	4373	4744	451	1132	1756	2304	3022	3525	4206	4517	541	1165	1737	2204	2847	3316	3909	4186
	Sta. 5	10	236	450	634	769	993	1138	1340	1446	230	395	531	648	821	943	1128	1236	234	377	494	602	761	876	1058	1162
		15	227	524	786	1007	1282	1492	1770	1905	265	504	704	860	1104	1265	1492	1618	265	467	636	779	993	1141	1359	1483
		20	207	556	875	1158	1537	1806	2167	2352	289	593	868	1079	1389	1613	1903	2051	293	561	790	974	1256	1446	1712	1856
		25	192	546	918	1255	1761	2085	2542	2768	277	652	992	1284	1656	1939	2312	2494	317	643	942	1173	1522	1771	2099	2268
		30	176	505	932	1334	1944	2333	2907	3168	256	685	1082	1433	1914	2241	2707	2934	313	705	1065	1369	1777	2085	2491	2691
	Sta. 10	10	98	178	256	314	434	521	674	776	112	166	221	271	362	440	591	694	121	171	218	265	350	426	575	676
		15	119	277	411	536	677	815	998	1108	110	196	281	350	479	578	752	868	121	191	261	324	437	530	702	817
		20	122	355	552	728	965	1132	1383	1524	133	270	400	507	674	813	1012	1138	125	229	331	417	567	684	882	1010
		25	137	394	652	883	1229	1467	1783	1961	142	353	536	708	914	1094	1344	1487	143	293	438	559	750	899	1132	1274
		30	132	377	706	1023	1488	1771	2205	2399	145	417	659	877	1179	1388	1709	1883	154	368	558	734	965	1161	1437	1596
	Sta. 15	10	188	319	430	525	675	781	955	1062	192	291	373	457	585	685	856	957	192	284	356	439	561	659	826	926
		15	238	445	622	751	965	1116	1318	1434	192	316	429	531	692	814	1013	1133	194	302	398	493	643	760	955	1072
		20	238	559	828	1064	1317	1527	1809	1944	227	407	564	686	902	1047	1272	1405	197	332	456	569	751	888	1113	1247
		25	238	645	989	1277	1692	1960	2325	2527	262	521	748	933	1184	1386	1653	1798	226	410	575	711	940	1101	1353	1502
		30	245	656	1078	1496	2038	2415	2892	3109	263	623	931	1202	1520	1766	2112	2283	260	512	737	921	1192	1400	1690	1853
	Sta. 20	10	361	641	872	1059	1336	1520	1777	1914	356	572	745	908	1144	1310	1555	1682	348	544	695	853	1075	1234	1475	1597
		15	422	803	1126	1358	1750	1998	2313	2473	380	662	900	1103	1402	1607	1899	2052	373	619	822	1011	1286	1480	1763	1909
		20	410	935	1380	1774	2184	2534	2962	3146	427	793	1104	1343	1733	1980	2322	2498	394	699	959	1183	1518	1748	2077	2248
		25	388	1039	1586	2031	2676	3073	3625	3909	477	935	1339	1660	2109	2441	2853	3047	435	813	1138	1398	1811	2082	2458	2652
		30	398	1058	1691	2315	3098	3681	4354	4665	457	1057	1571	2021	2535	2936	3457	3689	486	942	1359	1674	2152	2497	2934	3149

Relative Motion	Sta. 1	10	56	95	130	157	199	227	261	277	54	86	112	134	167	189	218	233	53	81	105	125	154	175	203	216
		15	52	97	139	175	223	257	301	321	54	90	123	148	187	213	247	263	53	85	113	136	170	193	224	240
		20	48	94	141	183	239	280	333	358	52	92	129	160	204	235	276	294	53	88	119	145	185	211	247	264
		25	45	88	138	183	252	296	359	388	49	92	133	169	218	253	300	322	51	88	124	153	197	227	268	287
		30	44	81	132	182	258	309	381	414	46	89	133	173	229	267	321	346	49	88	126	160	206	241	286	308
	Sta. 2	10	54	88	118	140	175	197	224	237	52	78	99	117	143	159	182	192	50	72	91	107	130	145	166	175
		15	50	91	128	159	199	228	264	280	52	84	110	132	164	184	211	223	51	78	100	119	146	164	188	199
		20	47	89	130	168	216	252	296	317	51	86	118	144	181	207	239	254	51	81	108	129	162	183	211	224
		25	45	84	128	169	230	268	323	347	48	86	122	154	195	226	264	282	50	83	113	138	175	200	232	247
		30	43	78	124	169	237	282	345	373	46	85	123	159	207	240	286	306	48	83	116	145	185	214	251	268
	Sta. 3	10	51	80	105	122	151	167	188	197	47	68	85	98	117	130	145	152	45	62	76	88	105	116	130	136
		15	49	84	115	142	175	199	228	240	49	75	97	114	139	155	174	183	47	69	86	101	121	135	152	160
		20	46	83	119	152	193	223	260	277	49	79	106	127	158	178	203	214	48	73	95	112	138	154	175	184
		25	44	80	119	155	208	241	287	308	47	80	111	138	172	198	229	242	47	76	101	122	152	172	197	208
		30	42	75	116	156	216	255	310	334	45	79	113	144	185	213	251	267	46	77	105	130	163	186	216	230
	Sta. 4	10	47	71	90	104	126	138	152	158	42	58	70	79	92	100	110	114	39	51	61	69	80	86	95	98
		15	46	76	103	124	151	170	192	201	45	66	83	96	115	126	139	145	42	59	72	82	97	106	117	121
		20	44	77	108	135	170	195	225	238	46	71	93	110	134	150	168	175	44	64	81	94	114	126	140	146
		25	43	75	109	140	186	214	253	270	45	73	99	121	150	170	194	204	45	68	89	105	128	144	162	170
		30	41	71	108	143	196	230	277	297	43	74	103	129	163	186	217	230	44	70	94	114	141	160	183	192
	Sta. 20	10	38	57	78	95	122	142	169	183	37	56	75	92	117	135	160	174	38	57	76	92	116	134	159	172
		15	38	58	78	97	124	147	175	189	36	54	72	88	113	131	156	170	36	54	72	87	111	128	152	165
		20	38	61	85	108	136	159	192	207	36	53	70	85	110	128	154	167	36	52	69	83	106	122	147	159
		25	39	66	94	119	157	183	219	239	36	53	70	87	110	130	156	170	36	51	66	80	102	118	142	155
		30	40	68	101	136	183	216	259	278	36	54	73	92	118	136	166	180	36	50	65	79	100	117	141	154
Relative Velocity	Sta. 1	10	283	380	467	531	633	692	754	776	287	364	427	480	552	594	641	656	288	356	410	457	519	556	598	608
		15	315	421	528	620	739	821	912	942	326	418	500	565	660	716	775	794	329	409	478	535	613	660	710	725
		20	349	451	568	680	819	923	1039	1084	363	463	562	642	756	831	909	934	368	458	541	608	706	764	826	845
		25	386	477	596	713	892	999	1145	1201	398	500	611	710	837	929	1030	1063	406	501	596	675	790	863	940	965
		30	426	503	619	745	936	1068	1235	1301	434	533	650	763	910	1011	1135	1179	443	539	644	738	863	951	1047	1077
	Sta. 2	10	280	364	436	489	572	618	663	676	282	345	395	436	489	520	550	555	280	334	376	410	455	481	504	503
		15	314	407	498	576	675	742	813	834	323	401	468	520	595	637	677	688	324	390	444	488	547	580	612	616
		20	348	440	541	636	754	841	935	970	361	448	530	596	689	748	805	820	365	441	508	562	638	682	723	732
		25	385	467	571	672	824	916	1036	1080	397	487	580	664	769	844	921	944	404	486	565	628	721	777	833	846
		30	426	495	597	705	870	982	1121	1175	434	522	622	717	840	924	1022	1054	441	526	614	691	793	864	935	954
	Sta. 3	10	274	342	400	441	507	540	569	575	270	318	355	384	420	439	454	450	265	303	332	355	383	397	405	395
		15	310	388	464	528	607	660	713	725	315	377	429	468	524	553	576	578	312	362	402	433	473	494	509	504
		20	345	424	509	588	686	756	829	854	355	427	493	544	617	661	698	704	356	416	468	508	563	593	616	615
		25	383	455	543	628	754	830	927	960	393	468	545	612	696	754	810	822	396	464	526	575	646	686	721	725
		30	424	485	572	663	802	895	1009	1050	430	505	589	667	766	833	907	927	436	506	578	638	718	771	819	828
	Sta. 4	10	264	318	362	391	439	460	475	474	255	288	312	330	349	357	358	346	246	270	287	298	310	314	307	290
		15	303	367	428	478	537	578	612	617	303	350	387	414	451	467	475	469	297	331	357	376	398	407	405	393
		20	341	407	476	539	617	671	725	741	346	402	453	490	543	572	591	590	344	388	424	451	487	502	508	500
		25	380	441	513	583	685	746	820	842	386	447	507	558	621	664	699	702	387	438	485	519	569	594	610	605
		30	421	474	546	621	735	810	900	930	425	487	554	615	691	741	793	803	428	484	538	583	641	678	705	704
	Sta. 20	10	237	271	307	337	384	414	445	455	232	265	300	328	372	399	428	440	234	268	304	332	375	401	430	441
		15	283	315	351	381	426	464	493	498	276	304	333	358	396	420	442	446	274	302	332	356	393	415	436	441
		20	328	367	411	458	503	542	586	592	321	344	369	389	423	443	460	457	318	341	366	386	416	433	445	442
		25	374	423	480	531	612	661	719	743	366	389	413	438	462	484	499	492	363	382	402	417	440	453	458	447
		30	420	473	542	623	730	811	893	919	411	437	467	497	528	549	571	565	407	424	442	458	472	484	484	467

TABLE A-13 SEAKEEPING RESPONSES FOR $C = 0.75$, $L/B = 5.5$, LCB = $+1.5\%$

		Froude No.	$B/T = 2$								$B/T = 3$								$B/T = 4$							
			Significant Wave Height/LBP								Significant Wave Height/LBP								Significant Wave Height/LBP							
		[%]	0.015	0.020	0.025	0.030	0.040	0.050	0.075	0.100	0.015	0.020	0.025	0.030	0.040	0.050	0.075	0.100	0.015	0.020	0.025	0.030	0.040	0.050	0.075	0.100
Heave		10	6	18	34	51	82	110	178	242	5	14	24	36	61	87	153	219	5	11	20	31	54	80	146	213
		15	5	17	38	58	98	130	202	267	5	16	30	44	72	99	166	232	5	14	24	36	62	88	154	220
		20	3	15	38	61	107	146	225	292	5	17	33	51	83	113	181	247	5	15	28	42	70	97	164	230
		25	2	15	34	62	114	161	246	316	4	16	35	55	93	125	197	263	5	16	31	47	78	107	176	241
		30	2	12	27	63	118	172	266	340	3	14	36	57	100	136	213	280	4	15	32	50	86	117	188	254
Pitch		10	19	55	94	131	192	239	321	373	22	53	86	117	169	212	288	339	22	49	79	107	157	197	271	322
		15	17	49	90	131	200	252	340	394	19	52	87	121	177	223	302	354	20	49	80	111	162	205	282	333
		20	11	38	88	130	209	263	360	419	16	49	85	121	182	231	314	368	17	47	80	112	166	211	290	342
		25	7	35	81	124	210	277	383	445	14	42	82	121	188	238	326	381	15	44	78	111	169	215	297	351
		30	5	30	63	126	214	297	411	479	10	35	80	119	193	245	339	397	13	40	76	111	173	220	305	359
Bending Moment		10	46	87	134	178	252	302	381	423	61	116	168	213	280	328	400	437	70	128	180	224	291	338	407	443
		15	45	85	134	178	259	315	406	453	60	117	173	223	300	353	432	473	70	132	190	240	314	366	441	480
		20	45	88	133	180	261	329	427	479	59	117	177	232	320	380	470	515	69	136	199	255	339	398	482	525
		25	45	91	136	186	272	342	447	504	59	118	183	242	340	408	510	561	69	138	208	269	365	432	529	577
		30	47	94	144	196	287	361	475	537	59	120	189	254	363	440	556	614	69	140	216	285	394	470	580	635
Added Resistance		10	6	28	66	111	197	261	358	411	10	32	64	99	169	221	295	340	14	38	70	106	178	231	307	355
		15	4	21	60	109	222	312	478	588	8	30	66	108	195	268	401	508	12	35	70	111	193	265	404	525
		20	2	14	54	107	247	362	599	765	6	28	67	118	221	315	507	676	10	33	70	117	209	300	500	695
		25	2	10	40	97	241	398	691	896	5	23	64	120	251	366	612	814	8	31	71	125	240	351	594	818
		30	1	7	26	86	235	433	783	1027	4	17	62	122	281	417	718	951	7	28	72	134	272	402	688	942
Acceleration	Sta. 0	10	152	410	681	926	1290	1533	1896	2073	227	496	749	961	1267	1489	1796	1952	252	494	718	906	1191	1395	1679	1825
		15	137	392	697	986	1441	1760	2220	2449	210	528	839	1118	1513	1794	2191	2390	253	557	848	1096	1453	1714	2075	2257
		20	109	332	693	1023	1588	1957	2526	2812	193	527	888	1218	1723	2066	2557	2804	236	589	934	1246	1691	2006	2456	2681
		25	88	305	678	1017	1672	2137	2836	3177	178	496	906	1295	1910	2312	2915	3203	225	598	993	1355	1904	2282	2822	3094
		30	78	285	584	1051	1751	2373	3169	3577	153	442	922	1341	2072	2537	3263	3620	216	581	1024	1446	2101	2541	3185	3500
	Sta. 5	10	79	224	388	542	780	939	1190	1322	123	281	431	561	749	891	1101	1219	140	283	415	528	703	831	1026	1140
		15	68	207	405	587	895	1106	1434	1605	113	303	492	665	920	1103	1374	1521	140	323	497	653	876	1044	1291	1428
		20	53	180	403	613	989	1255	1663	1878	107	302	528	740	1073	1300	1642	1822	132	346	559	755	1044	1252	1560	1726
		25	43	171	385	619	1056	1394	1886	2144	96	280	546	796	1210	1480	1907	2121	128	352	601	834	1197	1449	1826	2026
		30	38	157	330	645	1118	1545	2122	2431	80	251	561	831	1322	1647	2164	2431	122	339	627	901	1342	1638	2094	2326
	Sta. 10	10	53	148	255	356	518	632	819	931	54	124	194	265	373	467	629	737	61	112	169	225	326	412	570	678
		15	49	147	305	447	687	840	1100	1239	60	165	274	374	534	656	854	980	63	147	232	317	447	557	744	865
		20	36	135	333	500	814	1031	1374	1559	67	189	336	476	702	862	1114	1261	68	183	305	418	598	736	961	1101
		25	29	140	317	530	910	1215	1638	1863	63	185	380	561	866	1061	1389	1562	74	209	365	512	754	929	1205	1368
		30	25	126	266	570	992	1382	1902	2181	51	174	417	619	998	1250	1662	1883	75	213	410	599	911	1123	1466	1653
	Sta. 15	10	112	290	452	597	802	947	1165	1287	120	232	339	433	582	697	879	991	112	199	288	369	505	611	789	901
		15	110	298	522	733	1044	1244	1545	1695	125	291	446	585	777	925	1152	1282	122	244	363	469	636	767	976	1102
		20	86	260	571	817	1256	1515	1937	2149	129	335	537	723	997	1191	1475	1635	128	297	458	605	814	975	1227	1371
		25	69	254	563	852	1391	1779	2327	2593	126	336	599	848	1227	1466	1838	2022	133	340	546	734	1016	1217	1522	1694
		30	60	235	475	910	1507	2050	2717	3055	109	309	653	935	1430	1725	2208	2452	137	357	613	856	1225	1475	1853	2051
	Sta. 20	10	188	486	755	991	1317	1541	1865	2029	222	442	646	817	1077	1264	1531	1673	215	404	580	732	970	1141	1396	1535
		15	183	495	838	1164	1629	1936	2363	2566	222	515	784	1024	1343	1581	1918	2089	230	468	694	887	1176	1389	1693	1854
		20	146	424	899	1276	1929	2296	2890	3176	218	566	899	1198	1629	1929	2346	2564	232	533	817	1070	1416	1674	2043	2232
		25	117	404	892	1311	2106	2647	3430	3789	212	561	970	1358	1931	2292	2825	3072	231	584	927	1234	1680	1993	2435	2666
		30	102	377	757	1389	2261	3043	3974	4433	186	509	1035	1471	2211	2637	3321	3648	233	601	1007	1390	1952	2331	2870	3136

Relative Motion																														
Sta. 1	10	43	76	113	148	201	235	285	307	47	79	110	138	176	204	240	257	48	77	104	127	161	184	216	231
	15	41	70	110	148	209	252	313	341	44	78	113	145	191	223	268	289	46	78	108	136	173	203	241	259
	20	40	64	105	145	216	264	335	370	43	74	111	147	201	238	291	317	44	76	110	140	186	217	262	284
	25	39	61	100	139	217	273	356	395	41	69	108	146	209	250	312	340	43	73	109	142	194	229	280	305
	30	38	59	90	139	217	287	378	423	40	64	105	144	214	259	329	363	42	70	106	142	200	239	296	324
Sta. 2	10	42	72	105	136	181	210	252	270	45	74	100	123	155	177	207	220	46	71	93	112	139	158	182	193
	15	41	68	103	137	191	228	280	304	43	73	104	132	171	198	235	252	45	72	99	122	154	177	207	221
	20	39	62	99	135	199	241	303	333	42	71	104	135	182	214	259	279	43	72	101	128	166	193	229	246
	25	39	59	95	139	200	250	324	359	41	67	101	136	191	227	279	303	42	70	101	130	175	205	248	268
	30	38	58	86	139	202	265	346	386	40	62	100	135	196	236	298	327	41	67	100	131	182	216	265	288
Sta. 3	10	41	68	96	123	161	185	220	234	43	68	90	108	134	151	173	183	43	64	81	96	117	131	149	157
	15	40	65	96	125	173	204	249	269	42	68	94	118	150	173	202	216	43	66	88	107	133	151	175	185
	20	39	60	93	125	181	219	273	299	41	67	96	122	163	190	227	244	42	67	92	114	146	168	197	210
	25	38	58	90	122	184	229	295	325	40	64	95	125	173	203	248	268	41	66	93	118	156	182	217	233
	30	38	56	83	122	187	243	316	352	39	60	93	125	179	214	267	292	40	64	93	120	164	193	234	253
Sta. 4	10	40	63	88	110	142	162	189	200	41	61	79	93	113	126	142	148	40	56	70	80	96	106	117	122
	15	39	61	89	114	155	182	220	236	40	63	85	104	131	149	171	181	41	60	78	92	113	127	143	150
	20	38	58	87	116	165	198	245	267	40	63	88	110	144	167	197	210	40	62	83	101	127	144	167	177
	25	38	56	85	114	170	210	268	294	39	61	88	114	155	181	219	236	39	62	85	106	138	159	187	200
	30	38	55	79	115	173	224	290	321	38	58	88	115	163	193	239	260	39	60	86	110	147	171	206	221
Sta. 20	10	38	55	75	93	124	145	177	194	35	49	63	78	100	118	144	158	35	49	64	78	100	116	141	154
	15	39	58	84	110	151	178	218	237	36	49	64	78	102	120	148	163	35	48	61	74	94	110	135	148
	20	39	58	94	124	181	215	270	297	37	52	68	85	113	133	163	180	36	47	60	72	93	109	135	148
	25	39	60	96	133	204	255	326	360	38	54	74	96	131	154	191	208	37	49	62	75	98	115	142	157
	30	39	59	89	144	224	296	385	428	38	54	81	106	151	179	225	247	38	50	66	82	109	128	159	174
Sta. 1	10	254	317	394	469	578	647	741	774	264	333	403	463	545	602	665	685	269	334	394	444	516	562	611	626
	15	293	347	424	502	630	716	831	878	301	369	446	519	619	688	772	801	307	374	445	507	592	651	716	737
	20	334	377	451	533	680	775	910	967	340	402	481	560	681	761	863	903	345	411	487	560	659	728	811	839
	25	376	413	483	557	713	821	984	1051	380	434	512	597	736	825	947	992	384	446	524	602	719	796	894	931
	30	418	453	508	590	745	886	1058	1134	422	466	545	630	785	881	1023	1079	425	481	558	641	772	860	973	1014
Sta. 2	10	253	309	375	440	530	588	663	688	261	320	378	427	494	538	583	596	264	318	367	406	462	495	528	535
	15	292	342	408	475	583	656	751	788	298	358	424	485	566	623	686	707	303	361	419	469	537	582	629	641
	20	333	374	438	508	633	714	827	872	338	393	461	528	629	694	775	804	341	400	464	523	604	659	721	739
	25	375	410	471	535	668	759	897	950	378	427	495	567	683	757	856	889	381	436	503	567	663	726	802	827
	30	417	450	499	569	701	819	965	1027	419	461	529	601	732	812	929	972	422	472	539	608	717	788	878	908
Sta. 3	10	250	300	356	409	482	529	587	603	255	305	351	389	440	472	502	506	256	299	336	364	404	426	443	443
	15	290	335	391	448	538	597	673	701	294	346	399	448	513	556	602	613	297	345	390	429	480	512	541	545
	20	331	369	424	483	587	654	746	780	334	383	439	494	575	627	688	707	336	386	437	484	547	588	631	639
	25	373	406	459	514	624	700	813	855	375	418	476	535	630	689	766	790	377	424	479	531	607	655	710	725
	30	415	446	490	548	659	757	877	926	417	454	512	572	679	744	836	868	418	462	517	574	661	717	784	803
Sta. 4	10	248	291	336	379	436	473	514	523	250	289	324	352	388	409	424	421	248	280	305	324	349	360	363	355
	15	289	327	375	421	494	541	599	618	291	333	375	413	461	492	520	524	291	328	363	390	425	445	458	453
	20	330	364	410	459	544	599	671	696	332	373	419	462	524	563	605	615	332	372	412	447	492	521	545	545
	25	372	403	447	493	584	646	736	768	373	411	458	505	580	626	681	695	374	413	457	497	553	588	623	628
	30	415	443	481	530	621	700	796	834	415	448	496	545	630	681	750	771	416	453	497	542	608	650	695	705
Sta. 20	10	245	276	309	341	390	422	464	477	238	259	281	301	329	351	374	376	236	258	281	300	330	350	370	372
	15	290	326	372	422	498	547	610	630	284	305	327	347	374	392	413	414	281	299	317	333	353	368	380	374
	20	333	369	434	497	617	683	787	828	330	356	382	406	445	469	495	499	327	344	360	374	392	401	408	398
	25	376	413	484	556	712	820	977	1038	376	404	440	477	537	572	617	624	373	392	411	426	449	461	467	458
	30	419	456	514	619	799	970	1169	1265	420	450	498	546	635	684	759	783	418	441	465	488	523	542	560	553

TABLE A-14 SEAKEEPING RESPONSES FOR $C_B = 0.75$, $L/B = 7.0$, LCB = $+1.5\%$

		Froude No.	$B/T = 2$								$B/T = 3$								$B/T = 4$							
			Significant Wave Height/LBP								Significant Wave Height/LBP								Significant Wave Height/LBP							
		[%]	0.015	0.020	0.025	0.030	0.040	0.050	0.075	0.100	0.015	0.020	0.025	0.030	0.040	0.050	0.075	0.100	0.015	0.020	0.025	0.030	0.040	0.050	0.075	0.100
Heave		10	6	18	31	44	69	95	160	226	5	12	21	31	55	80	146	213	6	11	19	29	52	77	142	209
		15	7	23	39	56	86	114	180	244	6	16	26	39	63	89	155	221	5	13	22	33	56	82	148	214
		20	7	22	44	65	103	134	203	266	6	19	33	47	74	101	167	232	6	15	26	38	63	89	155	221
		25	5	19	46	70	116	151	226	290	7	21	37	54	85	114	181	246	6	17	30	44	71	98	164	230
		30	3	18	46	71	123	165	247	314	7	20	40	60	96	127	196	261	6	19	34	49	80	108	175	240
Pitch		10	28	65	102	135	191	235	311	361	26	56	86	115	165	206	279	329	23	50	79	106	154	193	266	316
		15	23	63	104	143	204	251	333	384	25	57	91	122	176	219	294	345	23	52	82	111	161	202	276	327
		20	20	60	103	144	212	265	250	405	22	57	93	128	183	228	307	359	22	52	84	114	166	209	285	336
		25	17	51	99	147	225	278	371	425	19	55	93	129	189	236	318	371	20	51	85	117	170	214	292	344
		30	11	40	100	144	231	288	391	453	18	52	92	130	194	244	328	383	17	50	84	118	174	219	299	351
Bending Moment		10	47	92	133	170	222	261	320	350	60	106	147	182	235	272	325	354	62	110	151	186	238	275	329	357
		15	47	90	133	172	235	278	340	374	60	110	156	195	252	293	350	380	65	116	162	199	256	295	351	379
		20	46	87	133	175	245	291	363	399	58	112	163	206	270	315	379	411	65	122	172	214	276	319	380	410
		25	45	88	135	177	250	303	383	424	57	113	167	214	288	338	409	445	65	125	180	228	297	345	413	447
		30	45	90	136	181	257	316	403	447	57	114	171	223	305	361	441	481	64	128	188	240	318	372	449	486
Added Resistance		10	7	24	49	74	123	160	210	238	10	27	50	73	120	154	202	231	14	33	57	83	134	170	223	255
		15	5	23	52	86	153	209	300	367	9	27	52	81	136	184	271	345	12	31	57	85	143	192	288	375
		20	4	22	55	98	183	258	390	495	7	26	55	90	152	214	340	458	10	29	56	87	151	214	354	494
		25	3	16	52	97	205	298	479	613	6	26	58	100	182	260	416	555	9	29	60	98	175	250	417	579
		30	2	10	48	96	228	337	569	731	5	25	61	110	211	307	492	652	7	29	64	108	198	285	480	664
Acceleration	Sta. 0	10	269	593	888	1126	1475	1713	2039	2198	304	583	822	1017	1314	1514	1792	1938	309	552	758	938	1207	1393	1661	1803
		15	239	618	982	1314	1751	2072	2498	2702	328	685	1014	1278	1658	1932	2292	2468	345	660	943	1177	1530	1771	2108	2274
		20	216	608	1028	1402	1977	2364	2899	3174	314	744	1146	1496	1966	2309	2769	2990	358	749	1115	1412	1845	2158	2572	2776
		25	192	553	1021	1479	2188	2630	3304	3599	287	767	1233	1647	2245	2649	3216	3491	348	809	1244	1624	2139	2518	3029	3275
		30	151	470	1048	1513	2347	2864	3675	4082	277	763	1282	1762	2477	2970	3640	3974	325	843	1340	1786	2418	2857	3469	3767
	Sta. 5	10	140	334	511	661	873	1024	1246	1365	172	333	473	588	769	896	1086	1196	179	318	439	544	707	825	1009	1119
		15	128	353	575	780	1069	1276	1566	1719	183	396	594	758	991	1167	1411	1541	195	384	554	694	912	1066	1292	1420
		20	116	338	607	852	1238	1493	1868	2062	172	436	684	904	1205	1425	1739	1902	204	441	664	850	1121	1323	1605	1756
		25	98	302	613	903	1385	1685	2164	2391	161	452	744	1008	1404	1671	2060	2262	194	481	751	994	1326	1572	1923	2105
		30	75	264	627	927	1485	1859	2442	2741	157	447	781	1096	1577	1906	2376	2616	186	505	820	1105	1525	1815	2239	2459
	Sta. 10	10	69	169	258	346	460	561	724	828	75	129	187	240	340	424	580	686	87	133	185	232	323	402	554	660
		15	79	227	369	494	685	824	1032	1159	82	178	268	355	482	596	776	893	85	155	229	297	416	516	694	812
		20	86	245	440	624	903	1092	1370	1522	88	236	372	501	679	819	1044	1178	93	202	307	408	559	689	895	1026
		25	71	220	486	716	1109	1331	1716	1901	98	280	466	629	889	1071	1347	1509	98	252	400	541	739	897	1148	1297
		30	51	203	525	766	1238	1548	2045	2300	106	299	531	752	1089	1326	1671	1860	104	295	489	662	934	1129	1430	1606
	Sta. 15	10	162	315	450	559	724	851	1032	1138	145	238	329	411	546	650	827	936	151	235	314	392	518	618	791	897
		15	161	404	613	795	1023	1193	1441	1573	163	299	426	531	708	837	1041	1163	148	253	356	450	606	726	927	1050
		20	168	456	728	976	1324	1572	1889	2066	179	384	569	732	942	1115	1361	1498	165	309	446	564	757	902	1132	1269
		25	152	421	789	1132	1650	1926	2387	2578	180	458	706	923	1224	1432	1746	1915	181	383	571	738	966	1150	1420	1573
		30	117	367	862	1213	1868	2241	2857	3163	190	504	811	1094	1495	1783	2185	2375	185	453	699	918	1218	1436	1768	1947
	Sta. 20	10	290	570	817	1008	1304	1510	1782	1922	275	482	667	825	1068	1238	1491	1626	278	462	622	772	996	1158	1405	1535
		15	275	678	1026	1332	1695	1968	2342	2518	303	578	825	1022	1337	1551	1852	2010	287	518	728	910	1189	1385	1675	1829
		20	276	747	1174	1555	2084	2463	2926	3178	319	684	1011	1293	1652	1936	2306	2487	311	602	867	1086	1427	1666	2004	2180
		25	253	692	1240	1767	2529	2942	3598	3848	308	775	1187	1544	2024	2350	2820	3048	328	696	1032	1321	1709	2008	2408	2609
		30	198	592	1341	1874	2841	3366	4232	4653	315	832	1319	1760	2374	2812	3366	3658	325	782	1195	1560	2040	2384	2873	3111

Relative Motion																									
Sta. 1																									
	10	48	86	122	152	196	225	265	283	50	82	109	132	166	189	220	235	50	78	102	122	152	173	201	215
	15	45	83	124	162	213	249	299	321	49	34	117	145	184	213	250	267	50	80	109	132	168	192	225	240
	20	43	78	121	161	225	266	325	354	46	83	120	153	198	231	276	297	48	81	113	140	180	209	247	265
	25	41	71	116	161	233	279	249	380	44	80	119	156	210	246	298	322	46	80	115	147	191	223	267	287
	30	40	65	114	157	237	289	369	408	43	76	117	156	217	258	316	344	44	78	115	149	199	234	284	307
Sta. 2	10	47	80	111	137	174	198	230	244	48	75	98	116	144	162	185	196	47	70	89	105	129	145	166	176
	15	44	79	114	147	192	223	264	282	47	78	106	129	162	186	215	228	47	74	97	117	145	165	190	201
	20	42	75	113	149	204	241	291	315	45	78	110	139	177	205	241	258	46	76	103	126	159	182	213	227
	25	41	69	109	149	214	254	315	341	43	76	111	143	189	220	264	284	45	75	106	133	170	197	233	250
	30	39	63	107	147	218	264	335	369	42	73	110	144	197	233	283	307	43	74	107	136	180	209	251	270
Sta. 3	10	45	74	100	122	151	171	196	206	45	67	85	99	121	134	151	158	43	61	76	88	105	117	131	138
	15	43	74	105	133	170	197	230	245	45	71	94	113	140	158	181	190	44	66	85	100	123	137	156	164
	20	41	71	105	136	184	215	258	278	44	72	100	124	156	179	208	221	44	69	92	110	137	156	179	189
	25	40	66	102	137	194	230	283	305	42	72	102	129	169	195	231	247	43	70	96	119	149	171	200	213
	30	39	61	101	136	200	241	303	333	41	69	102	132	178	209	251	270	42	70	98	123	160	184	218	234
Sta. 4	10	43	67	89	106	129	145	163	170	41	58	72	83	98	107	118	122	39	52	62	71	83	90	99	102
	15	42	68	95	118	149	171	198	209	42	64	83	98	118	132	148	154	41	58	73	84	100	111	123	128
	20	40	66	96	124	165	191	227	243	42	66	89	109	135	153	176	185	42	62	80	95	116	130	147	153
	25	39	63	95	126	176	207	253	271	41	67	93	116	149	170	199	212	41	64	86	104	129	146	168	177
	30	38	59	94	126	183	219	274	300	40	65	94	120	159	185	220	236	41	65	89	110	140	160	187	199
Sta. 20	10	37	55	73	90	116	137	165	179	35	52	68	83	107	125	150	164	35	52	69	83	107	124	148	161
	15	38	58	80	100	130	151	184	200	36	50	66	81	104	122	148	162	35	50	66	79	102	118	142	155
	20	40	63	89	115	153	181	217	237	36	50	66	82	105	123	151	165	36	49	63	76	97	113	138	150
	25	40	62	97	131	186	215	265	285	37	53	70	87	114	133	162	178	36	48	62	76	96	112	137	150
	30	39	60	107	142	210	249	315	346	38	55	76	96	128	151	183	200	36	49	63	77	99	116	141	155
Sta. 1	10	265	346	429	499	597	660	734	759	274	347	411	463	539	584	633	648	277	342	396	442	505	542	584	595
	15	300	379	470	560	674	757	855	891	312	391	470	537	629	691	757	778	316	389	457	512	592	641	693	708
	20	339	408	501	593	738	832	952	1003	348	428	517	600	706	783	870	899	355	431	510	576	671	733	801	821
	25	380	436	525	627	792	895	1043	1093	386	462	555	646	775	860	968	1007	392	469	555	635	740	815	900	927
	30	420	465	558	655	837	950	1117	1191	427	495	588	684	831	931	1053	1103	431	505	595	683	805	887	989	1024
Sta. 2	10	263	334	404	462	542	593	650	666	269	330	382	423	481	514	546	553	270	322	364	398	444	470	495	497
	15	299	369	447	523	618	687	765	792	308	376	442	496	570	618	666	677	311	372	426	469	531	566	600	606
	20	338	400	480	559	682	760	859	898	345	416	491	559	646	708	774	793	350	416	480	534	609	657	704	714
	25	378	430	508	594	734	822	944	984	384	451	531	607	714	783	868	896	389	456	528	593	678	737	800	816
	30	419	462	541	624	779	875	1015	1074	424	486	566	647	770	852	951	988	428	493	569	642	742	808	886	909
Sta. 3	10	259	319	376	422	485	524	564	573	261	309	348	378	420	441	458	457	258	296	326	350	379	395	404	398
	15	296	356	421	483	561	617	675	693	302	358	410	451	508	543	573	576	302	349	390	422	465	488	505	503
	20	335	390	458	524	625	688	766	795	341	400	461	515	584	631	677	687	343	397	447	487	543	577	605	607
	25	376	423	489	560	676	749	848	878	380	438	503	566	651	706	768	786	383	439	497	548	613	657	699	705
	30	417	456	523	593	722	802	915	961	421	474	541	608	707	773	848	874	423	479	541	599	676	727	782	795
Sta. 4	10	254	302	347	383	429	457	482	483	252	287	314	334	359	370	373	365	245	271	289	303	317	322	317	304
	15	293	343	396	445	505	548	589	599	295	339	378	407	447	469	483	478	292	327	355	375	402	413	414	404
	20	333	379	435	489	570	619	678	697	336	384	431	472	523	556	584	585	336	377	414	442	480	500	511	504
	25	374	415	470	528	622	680	756	778	373	425	477	525	590	630	672	680	378	422	466	503	549	579	601	599
	30	416	451	507	564	668	733	822	858	418	463	517	570	647	697	750	765	419	464	513	557	614	649	683	686
Sta. 20	10	242	271	301	330	368	402	432	438	234	260	287	310	347	370	394	400	231	258	286	309	346	369	392	399
	15	287	322	361	398	447	480	522	533	281	302	325	344	374	395	414	412	277	299	322	341	370	387	402	401
	20	333	376	427	477	552	606	662	684	326	347	370	393	416	435	453	448	323	341	360	375	395	409	416	407
	25	377	420	487	563	685	748	846	868	372	397	424	449	485	505	527	526	368	385	402	417	430	440	443	428
	30	420	460	551	634	800	888	1033	1095	418	448	483	518	569	605	637	643	413	432	450	465	484	491	493	478

TABLE A-15 SEAKEEPING RESPONSES FOR $C_B = 0.75$, $L/B = 8.5$, LCB = $+1.5\%$

		Froude No.	$B/T = 2$								$B/T = 3$								$B/T = 4$							
			Significant Wave Height/LBP								Significant Wave Height/LBP								Significant Wave Height/LBP							
		[%]	0.015	0.020	0.025	0.030	0.040	0.050	0.075	0.100	0.015	0.020	0.025	0.030	0.040	0.050	0.075	0.100	0.015	0.020	0.025	0.030	0.040	0.050	0.075	0.100
Heave		10	7	15	25	36	60	85	151	217	7	12	20	30	52	77	143	209	7	11	19	28	51	75	140	207
		15	8	21	35	49	74	100	165	230	6	14	23	34	57	83	148	215	6	12	21	31	54	79	144	210
		20	8	26	44	60	91	119	184	248	7	17	29	41	66	92	157	223	6	14	23	34	58	84	149	215
		25	9	26	48	70	107	138	205	268	7	21	35	50	76	103	169	233	6	16	28	40	65	91	156	222
		30	7	24	50	76	121	154	228	290	7	23	40	56	87	116	182	246	6	19	32	46	73	99	165	230
Pitch		10	31	66	100	131	183	225	298	347	27	55	84	111	159	199	271	321	25	51	77	104	151	189	261	311
		15	30	69	108	142	200	245	321	371	27	58	90	120	171	212	286	335	24	52	81	109	158	198	271	321
		20	25	68	111	152	211	260	341	392	27	60	95	126	180	223	299	349	24	54	85	113	164	205	280	330
		25	22	67	112	152	221	273	357	412	24	60	97	131	186	232	310	361	23	54	86	117	169	211	287	338
		30	21	61	108	157	231	287	377	430	21	59	98	135	193	239	320	372	22	54	87	119	172	216	294	345
Bending Moment		10	49	87	121	149	194	225	270	294	53	92	126	155	198	228	273	296	54	94	129	158	201	232	276	299
		15	46	88	126	160	206	240	290	315	56	98	136	166	213	244	290	314	57	100	137	167	213	244	289	313
		20	45	88	128	162	218	255	308	337	56	103	144	178	228	264	313	337	60	106	146	179	229	262	310	334
		25	45	85	128	167	227	268	328	357	55	105	150	189	244	283	337	364	60	111	155	192	246	283	335	360
		30	44	85	129	169	234	278	346	379	54	106	155	196	259	302	362	392	60	114	163	204	263	305	362	390
Added Resistance		10	7	19	36	52	85	109	141	160	10	24	42	60	94	119	154	175	13	29	47	67	105	132	170	193
		15	6	21	42	66	108	144	205	251	9	23	42	63	103	137	201	256	12	27	47	69	112	149	221	286
		20	4	22	48	80	131	180	270	343	7	22	43	66	112	155	247	337	10	25	47	70	119	166	272	380
		25	4	20	49	88	160	224	344	430	6	23	48	78	135	189	302	406	9	25	49	77	134	190	315	440
		30	3	17	49	96	190	269	418	518	5	24	54	91	158	222	356	475	8	25	52	84	148	213	358	500
Acceleration	Sta. 0	10	361	688	970	1187	1519	1739	2032	2172	352	614	826	1013	1286	1471	1738	1877	360	589	773	948	1199	1376	1635	1769
		15	363	792	1177	1482	1920	2218	2612	2797	407	763	1070	1315	1687	1933	2263	2431	398	711	974	1199	1532	1758	2075	2238
		20	327	831	1296	1716	2236	2632	3138	3375	432	883	1295	1611	2079	2409	2829	3030	441	837	1186	1470	1897	2184	2577	2765
		25	296	830	1364	1825	2535	2978	3610	3922	421	963	1459	1880	2434	2845	3373	3621	465	945	1390	1737	2257	2624	3098	3326
		30	284	794	1375	1939	2753	3314	4076	4422	388	1005	1578	2086	2766	3237	3891	4195	462	1028	1553	1996	2597	3040	3616	3889
	Sta. 5	10	202	392	563	686	889	1032	1225	1333	201	351	476	585	749	866	1048	1156	210	339	448	548	700	812	990	1095
		15	194	457	692	889	1153	1343	1611	1745	228	442	625	770	1000	1155	1377	1502	231	414	570	703	906	1049	1264	1387
		20	178	485	773	1033	1382	1637	1977	2154	246	519	770	969	1256	1469	1752	1899	252	493	704	876	1141	1324	1586	1730
		25	166	478	817	1123	1593	1894	2328	2548	234	572	881	1152	1503	1768	2129	2310	269	563	837	1056	1382	1619	1941	2109
		30	152	444	832	1200	1768	2130	2677	2926	217	601	963	1286	1742	2053	2497	2721	264	617	947	1234	1617	1908	2303	2502
	Sta. 10	10	86	156	226	283	394	481	635	739	106	156	208	254	342	419	569	673	114	160	206	250	332	406	554	656
		15	100	142	364	480	617	744	930	1041	100	176	253	319	441	538	713	830	112	174	241	299	408	499	671	787
		20	107	313	495	658	885	1044	1290	1432	114	241	356	461	616	751	951	1078	112	205	298	379	522	637	835	965
		25	122	350	589	808	1137	1365	1674	1849	121	313	482	643	842	1012	1261	1406	124	259	392	509	689	839	1067	1210
		30	115	331	643	939	1389	1653	2082	2272	128	372	596	797	1093	1293	1608	1783	133	326	502	670	893	1079	1353	1515
	Sta. 15	10	172	292	398	487	634	739	913	1021	190	282	363	441	565	664	834	936	191	279	350	427	545	641	809	908
		15	217	414	585	715	917	1070	1274	1390	180	295	403	500	657	777	977	1098	189	290	384	474	620	734	930	1047
		20	215	527	788	1020	1273	1478	1762	1902	208	374	525	643	852	997	1224	1358	185	309	429	537	715	850	1075	1211
		25	222	608	943	1228	1641	1915	2277	2481	236	482	700	886	1125	1326	1595	1742	207	377	536	667	889	1050	1303	1453
		30	224	607	1025	1443	1997	2358	2850	3058	235	579	876	1137	1458	1695	2043	2218		471	687	871	1130	1336	1628	1792
	Sta. 20	10	325	580	796	971	1237	1415	1670	1806	339	538	701	855	1082	1243	1488	1613	338	521	663	813	1026	1182	1422	1542
		15	385	742	1051	1278	1646	1894	2206	2364	346	604	829	1020	1309	1509	1799	1951	351	577	770	949	1214	1403	1685	1831
		20	368	879	1312	1700	2103	2440	2869	3056	386	722	1016	1243	1618	1862	2201	2377	359	637	884	1097	1420	1645	1973	2144
		25	361	986	1517	1955	2596	3003	3545	3835	420	858	1245	1564	1983	2312	2718	2916	391	738	1046	1294	1691	1958	2333	2527
		30	368	987	1614	2246	3051	3609	4305	4597	406	978	1470	1903	2415	2796	3317	3554	432	858	1246	1565	2015	2350	2789	3002

Relative Motion	Sta. 1	10	53	89	121	146	184	210	242	258	52	81	105	126	156	176	204	218	51	76	98	117	145	164	190	203
		15	50	91	129	162	207	238	280	299	52	85	115	139	175	199	232	247	51	80	106	127	160	181	211	225
		20	46	88	131	171	223	261	311	334	50	87	121	150	191	221	259	276	50	83	112	136	173	199	232	249
		25	44	84	129	171	236	277	336	364	47	86	124	158	204	238	283	303	49	83	116	144	185	214	253	271
		30	43	78	125	171	242	290	359	389	45	84	125	162	215	251	303	327	47	83	118	150	195	227	271	291
	Sta. 2	10	51	82	109	130	161	182	207	218	49	73	92	109	132	148	169	178	47	68	85	100	121	135	154	163
		15	48	85	118	146	184	211	244	259	49	78	103	122	152	171	196	208	48	73	94	111	136	153	176	186
		20	45	83	121	156	201	233	275	294	49	81	110	134	169	193	223	237	48	76	101	121	151	171	197	209
		25	43	80	120	157	214	250	301	324	46	81	114	144	183	211	248	264	48	78	106	129	164	187	218	232
		30	42	75	117	159	222	264	324	350	44	80	116	149	194	225	269	288	46	78	109	136	174	201	237	253
	Sta. 3	10	48	74	96	112	138	153	172	180	45	63	78	91	108	119	133	140	42	58	70	81	96	106	119	124
		15	46	78	107	130	161	183	209	220	46	70	90	105	129	143	161	169	44	64	80	93	112	125	140	147
		20	44	78	111	141	179	206	240	256	46	74	99	118	146	165	189	199	45	68	88	104	128	143	162	171
		25	42	75	111	144	193	224	267	286	45	75	104	129	161	184	213	226	45	71	95	114	141	160	184	194
		30	41	71	109	146	202	239	290	312	43	75	106	134	173	199	235	251	44	72	99	121	152	175	203	216
	Sta. 4	10	44	66	83	95	114	125	138	143	40	53	64	73	84	91	100	103	37	47	56	63	73	79	86	88
		15	44	71	94	114	139	155	175	183	43	61	77	88	105	115	127	132	40	55	66	76	89	97	107	111
		20	43	72	100	125	157	180	207	219	44	66	86	102	124	138	155	162	42	60	76	88	105	116	129	134
		25	41	70	102	130	172	199	234	250	43	69	93	113	139	158	180	190	43	64	83	98	119	134	151	158
		30	41	67	101	134	183	214	258	277	42	69	96	120	152	174	203	215	42	66	88	107	131	149	171	180
	Sta. 20	10	37	55	74	90	117	136	163	176	35	53	71	87	111	129	154	168	36	54	72	87	111	128	153	166
		15	38	57	77	95	121	143	171	185	36	52	69	84	108	125	151	164	35	52	68	83	106	123	147	160
		20	38	61	84	106	136	157	190	206	36	51	68	82	106	123	149	163	36	51	66	80	102	118	142	154
		25	40	66	94	119	157	184	220	240	36	52	68	85	107	126	153	166	36	50	64	77	98	114	138	150
		30	41	67	101	136	186	218	264	282	37	54	73	89	116	134	163	177	36	49	63	77	97	113	138	150
Relative Velocity	Sta. 1	10	277	362	440	499	589	643	698	717	281	351	407	455	519	557	599	611	282	344	392	435	491	524	561	568
		15	312	404	500	580	690	763	845	872	321	402	476	534	621	671	724	740	323	395	457	508	579	621	666	677
		20	346	437	541	644	767	862	967	1006	359	446	535	608	711	779	850	872	363	442	517	578	667	720	776	791
		25	384	466	573	677	840	936	1068	1121	395	485	584	674	789	873	965	995	401	485	571	643	746	813	884	905
		30	425	495	599	713	886	1007	1159	1217	432	519	624	726	861	953	1066	1106	439	524	619	704	817	898	985	1012
	Sta. 2	10	273	346	410	457	531	571	610	621	274	330	374	411	458	484	510	512	272	320	356	387	426	448	467	465
		15	309	390	471	538	629	687	750	768	316	384	444	490	557	594	629	636	316	374	422	461	514	543	569	571
		20	345	425	514	601	704	783	866	895	355	431	504	563	646	699	750	762	357	424	484	532	600	639	675	681
		25	383	456	548	637	774	855	963	1003	392	471	554	629	723	791	860	879	397	469	539	597	679	730	779	789
		30	424	487	577	674	821	923	1049	1095	430	507	596	681	793	868	957	984	436	510	588	658	749	813	877	892
	Sta. 3	10	266	326	376	412	468	497	521	524	262	304	335	360	391	406	416	411	256	289	314	333	356	367	371	360
		15	304	372	438	492	564	609	654	663	307	361	406	440	489	513	532	530	304	347	381	408	442	459	469	462
		20	341	410	484	555	639	702	765	785	348	410	468	513	577	615	647	650	348	400	445	480	528	553	571	568
		25	380	443	521	595	708	774	859	887	387	453	520	579	654	705	753	763	389	447	502	545	607	643	671	672
		30	421	477	553	633	756	839	940	975	426	491	564	634	722	782	847	864	429	491	553	607	677	724	766	771
	Sta. 4	10	258	304	341	366	406	423	433	429	249	277	296	310	325	330	326	313	240	259	273	282	290	290	279	261
		15	299	353	405	447	499	532	560	561	297	337	368	391	421	433	436	427	291	319	341	356	373	378	372	357
		20	338	395	454	509	575	623	667	678	341	389	432	464	509	533	547	542	337	375	406	428	457	469	470	459
		25	378	431	494	554	643	695	758	776	381	434	486	530	585	621	649	650	381	425	465	495	536	557	567	559
		30	419	466	529	595	693	759	836	861	422	475	533	587	653	697	740	747	423	471	518	557	607	638	659	655
	Sta. 20	10	239	270	302	328	373	400	429	436	230	258	289	315	355	381	407	416	230	260	292	318	358	382	409	419
		15	285	317	350	381	420	457	484	488	277	302	328	350	385	406	426	427	273	297	324	345	379	399	417	419
		20	330	369	413	458	505	540	584	592	323	345	368	386	416	435	449	444	319	340	363	380	406	421	431	424
		25	376	425	482	534	615	668	725	749	368	390	414	438	458	479	492	483	365	383	402	415	435	446	448	434
		30	421	473	543	626	740	819	908	931	414	440	468	496	528	546	566	560	410	427	444	459	470	479	477	457

TABLE A-16 SEAKEEPING RESPONSES FOR $C_B = 0.80$, $L/B = 5.5$, LCB $= +2.0\%$

		Froude No.	$B/T = 2$								$B/T = 3$								$B/T = 4$							
			Significant Wave Height/LBP								Significant Wave Height/LBP								Significant Wave Height/LBP							
		[%]	0.015	0.020	0.025	0.030	0.040	0.050	0.075	0.100	0.015	0.020	0.025	0.030	0.040	0.050	0.075	0.100	0.015	0.020	0.025	0.030	0.040	0.050	0.075	0.100
Heave		10	5	16	31	47	77	105	173	238	4	12	22	33	58	83	150	216	4	10	18	29	52	77	143	210
		15	4	15	35	54	92	123	196	261	5	15	27	41	68	95	162	228	4	12	22	34	58	84	151	217
		20	3	14	35	57	101	139	218	285	5	15	31	47	79	108	177	242	4	14	26	39	66	93	160	227
		25	2	13	31	57	107	153	238	308	4	14	32	51	88	120	192	258	4	14	28	44	74	103	172	238
		30	1	11	25	57	111	162	256	330	3	13	33	53	94	130	207	275	4	13	30	47	81	112	183	249
Pitch		10	17	50	85	119	176	221	300	352	19	47	77	106	156	197	272	322	19	44	71	98	145	185	258	308
		15	15	45	83	122	186	235	320	373	16	46	78	110	163	207	284	336	17	43	72	101	150	192	267	318
		20	10	35	82	121	196	248	341	398	14	43	77	111	169	215	296	349	15	42	72	102	154	197	274	327
		25	7	32	75	117	199	263	365	425	12	38	75	111	175	223	308	362	13	39	71	102	157	201	281	334
		30	5	28	59	119	203	282	393	459	9	32	73	110	180	230	321	378	12	36	68	102	160	206	288	342
Bending Moment		10	49	90	137	183	262	318	408	457	63	119	173	221	294	348	429	473	71	131	187	234	308	361	439	482
		15	47	89	137	182	266	328	428	483	61	119	176	228	311	369	458	505	70	135	195	248	329	387	472	516
		20	47	94	137	185	267	339	445	504	60	119	180	237	328	393	492	543	69	137	204	262	353	417	511	559
		25	48	96	143	193	278	349	460	523	60	121	185	246	347	419	529	587	69	140	212	276	378	450	556	610
		30	49	99	154	203	295	365	484	550	61	124	193	259	370	451	573	637	69	143	220	292	406	487	607	668
Added Resistance		10	6	28	65	111	198	263	371	427	11	33	66	102	175	231	323	376	15	40	76	114	196	258	356	417
		15	4	20	59	109	224	318	499	620	8	30	66	110	201	280	436	566	13	36	73	116	208	290	462	621
		20	2	13	53	107	250	372	627	812	6	27	66	117	226	328	549	756	10	33	70	118	219	323	569	825
		25	2	10	39	96	245	408	722	949	5	22	64	120	257	382	661	899	8	30	71	127	252	376	667	949
		30	1	7	25	85	239	443	818	1086	4	17	61	123	288	436	772	1042	7	27	72	135	285	429	766	1073
Acceleration	Sta. 0	10	130	357	596	814	1143	1365	1706	1878	191	424	650	842	1126	1333	1628	1781	211	423	630	799	1064	1258	1534	1681
		15	122	348	614	875	1285	1580	2005	2222	176	453	730	983	1347	1610	1985	2177	210	475	737	964	1297	1541	1890	2069
		20	97	293	618	916	1429	1764	2292	2562	165	456	777	1074	1538	1856	2320	2558	199	504	814	1097	1511	1809	2236	2455
		25	79	271	609	913	1510	1936	2585	2905	154	429	795	1146	1710	2083	2651	2927	192	514	866	1195	1704	2056	2571	2834
		30	71	254	524	949	1588	2157	2896	3281	134	383	813	1190	1858	2292	2974	3315	186	497	896	1277	1884	2292	2905	3209
	Sta. 5	10	65	188	333	468	686	832	1072	1202	101	238	371	489	664	798	1002	1120	116	241	360	464	627	750	942	1056
		15	58	179	348	509	786	984	1292	1458	94	256	424	581	817	989	1249	1394	115	274	430	572	782	940	1181	1317
		20	46	155	347	537	875	1120	1500	1707	90	256	458	648	955	1167	1494	1670	110	293	484	662	933	1128	1426	1591
		25	37	147	337	543	938	1246	1707	1952	81	238	475	699	1079	1333	1738	1947	108	299	522	733	1072	1309	1671	1867
		30	34	136	290	568	997	1384	1923	2217	68	216	489	732	1180	1488	1977	2234	103	287	546	794	1204	1482	1920	2147
	Sta. 10	10	46	128	225	320	475	583	769	881	47	107	171	237	342	432	596	705	55	99	151	205	301	385	544	652
		15	43	130	273	403	629	778	1032	1171	53	144	243	336	490	608	804	930	55	127	205	284	410	516	703	825
		20	32	121	297	454	748	958	1289	1471	59	164	301	431	647	800	1049	1195	59	160	271	375	550	683	906	1046
		25	26	125	284	483	839	1128	1537	1758	55	163	343	510	799	988	1308	1482	65	182	326	464	696	864	1136	1299
		30	23	112	240	517	916	1281	1782	2054	45	154	375	563	921	1166	1567	1785	65	185	369	545	842	1046	1383	1570
	Sta. 15	10	102	265	418	557	757	897	1113	1234	108	210	310	399	541	653	835	947	105	183	266	342	473	576	754	866
		15	101	274	488	688	991	1187	1485	1635	113	265	409	541	728	871	1096	1226	110	220	332	433	593	721	928	1055
		20	79	240	534	769	1194	1452	1866	2076	117	304	495	673	940	1128	1409	1568	115	268	419	558	762	918	1167	1312
		25	63	235	522	805	1324	1706	2242	2506	114	304	555	791	1160	1392	1760	1945	121	307	500	679	953	1149	1450	1622
		30	56	216	441	857	1436	1957	2612	2948	99	280	605	872	1349	1640	2118	2360	123	320	562	793	1153	1394	1768	1965
	Sta. 20	10	171	445	696	918	1230	1444	1758	1919	197	393	580	741	983	1163	1425	1567	194	360	523	665	890	1055	1306	1445
		15	169	455	782	1093	1543	1837	2256	2457	196	462	712	936	1240	1466	1795	1965	202	415	624	806	1078	1282	1581	1742
		20	133	391	843	1202	1833	2195	2777	3058	197	511	822	1105	1519	1806	2212	2425	204	475	737	974	1305	1551	1912	2100
		25	107	374	831	1241	2007	2542	3303	3658	191	504	893	1260	1813	2158	2680	2924	207	522	840	1128	1556	1854	2286	2514
		30	94	347	703	1313	2158	2912	3827	4280	167	458	956	1365	2075	2491	3161	3485	209	535	916	1276	1818	2178	2706	2967

Relative Motion																														
Sta. 1	10	42	71	105	136	184	215	262	283	45	74	102	127	163	188	223	239	46	72	97	118	149	171	201	216
	15	41	67	102	136	192	232	288	314	43	73	104	134	176	207	249	269	44	72	101	126	162	189	225	242
	20	39	61	98	135	200	243	309	341	41	70	104	136	186	221	271	295	43	71	102	130	173	203	245	265
	25	38	59	95	130	201	252	329	366	40	66	101	136	194	232	290	317	42	69	101	132	180	214	262	286
	30	38	57	86	130	202	266	350	392	39	62	99	135	199	241	307	339	41	66	99	133	187	223	278	304
Sta. 2	10	41	67	97	125	165	192	230	248	43	69	93	113	143	163	190	203	44	66	86	103	128	146	169	179
	15	40	65	96	126	175	209	257	280	42	68	96	121	157	183	217	233	43	67	91	112	143	164	193	206
	20	39	60	93	126	183	222	279	307	41	66	96	125	168	198	240	260	41	67	94	118	154	179	214	230
	25	38	58	90	122	186	231	300	332	40	63	95	126	177	210	260	283	41	66	94	121	163	191	232	251
	30	38	56	83	122	188	245	320	358	39	60	93	126	183	220	278	305	40	63	93	123	170	202	248	270
Sta. 3	10	40	64	89	113	147	169	201	214	41	63	83	99	123	139	159	168	41	59	75	88	108	121	137	144
	15	39	62	89	116	158	187	228	247	40	64	88	109	138	159	187	199	41	62	82	99	123	140	161	171
	20	38	58	87	117	167	201	251	275	40	63	89	113	151	175	210	226	40	63	85	106	135	156	183	196
	25	38	56	85	114	171	212	272	300	39	61	89	116	160	189	231	250	40	62	87	110	145	169	202	218
	30	38	55	79	115	174	225	292	326	38	58	88	116	167	200	249	273	39	60	87	113	153	180	220	237
Sta. 4	10	39	60	82	101	130	148	173	183	40	57	73	86	104	116	130	136	38	53	65	75	88	97	108	112
	15	39	59	83	106	142	167	201	217	39	60	79	97	121	137	158	167	39	57	73	86	104	117	132	139
	20	38	56	82	108	153	182	226	246	39	59	82	103	134	154	182	195	39	58	77	94	118	134	155	164
	25	38	55	81	107	158	194	247	272	38	58	83	106	144	169	204	219	39	59	80	99	129	148	175	187
	30	37	54	76	108	161	208	268	298	38	56	83	108	152	180	223	243	38	58	81	103	138	160	193	207
Sta. 20	10	38	54	72	89	118	138	169	185	36	48	61	74	95	111	136	150	35	48	61	74	94	110	133	145
	15	39	57	82	106	145	171	210	229	37	49	62	75	97	114	140	155	36	47	59	71	90	105	128	141
	20	39	58	91	120	174	208	262	288	38	51	66	82	108	127	156	172	36	47	58	70	89	104	128	141
	25	39	59	93	129	197	247	317	351	38	53	73	92	126	148	183	200	37	48	61	73	94	110	136	149
	30	39	59	87	139	217	287	374	417	39	54	79	102	144	172	217	239	38	50	64	79	105	123	152	167
Relative Velocity																														
Sta. 1	10	252	307	375	441	536	597	680	709	260	320	381	433	507	557	614	631	264	320	373	418	482	522	567	579
	15	292	341	407	476	587	665	766	806	298	357	424	489	577	639	713	739	302	361	423	478	554	606	665	682
	20	333	373	438	510	639	722	842	890	337	392	461	531	638	709	800	835	341	399	466	529	619	680	754	778
	25	375	410	472	537	674	768	913	971	379	426	494	569	691	771	880	919	382	436	504	572	676	746	834	865
	30	417	450	500	571	709	832	985	1051	420	460	529	603	740	826	953	1002	423	471	539	612	729	807	909	945
Sta. 2	10	250	300	357	413	492	542	608	629	255	307	357	400	458	497	536	546	257	304	346	380	429	458	487	491
	15	290	335	392	451	544	609	691	722	294	346	403	456	528	577	633	650	297	347	398	442	501	541	582	591
	20	331	369	425	487	595	665	763	801	334	383	442	500	589	646	717	742	337	387	443	495	566	614	668	683
	25	373	406	461	517	632	711	832	877	376	418	477	540	642	708	794	823	377	425	483	539	624	680	746	767
	30	416	446	491	552	668	770	898	950	417	454	513	577	691	762	865	902	419	462	520	581	677	740	819	844
Sta. 3	10	248	292	340	385	449	489	538	551	251	293	333	365	409	436	461	463	250	287	318	343	376	395	408	405
	15	289	329	377	426	502	554	619	641	291	335	381	423	479	516	555	563	292	333	372	405	449	477	500	501
	20	330	364	412	464	553	611	690	717	332	374	423	470	540	585	637	652	332	375	419	460	514	550	585	591
	25	372	403	449	497	593	657	754	789	373	411	461	512	594	646	712	731	374	415	462	507	573	615	662	673
	30	414	443	483	533	630	713	816	857	415	449	498	551	644	701	780	806	415	453	501	551	626	675	733	748
Sta. 4	10	246	284	323	359	408	439	473	478	247	281	311	334	364	381	390	385	244	272	293	309	329	337	336	326
	15	288	323	364	403	464	505	553	567	288	325	362	393	434	460	482	482	288	320	350	372	402	418	425	418
	20	329	361	401	444	516	562	622	641	330	366	406	443	496	529	563	568	330	365	399	429	467	491	508	505
	25	372	400	440	480	557	610	685	710	372	405	446	487	551	590	636	646	372	407	444	479	527	556	584	586
	30	414	441	476	518	597	663	744	774	414	444	486	528	601	645	703	719	414	447	486	525	582	617	654	659
Sta. 20	10	247	276	307	335	380	408	445	456	241	260	280	298	321	339	358	358	237	257	277	294	320	336	352	351
	15	291	326	369	414	486	531	590	608	286	307	327	344	368	382	398	396	283	301	317	331	348	359	367	358
	20	334	369	430	488	602	666	766	804	332	357	381	403	438	459	479	479	329	347	362	373	389	395	396	384
	25	377	413	478	548	696	802	952	1012	377	405	438	472	527	558	598	603	374	394	412	425	445	454	455	442
	30	420	456	510	609	782	946	1140	1235	420	451	495	539	621	668	737	758	419	442	465	486	517	533	545	535

TABLE A-17 SEAKEEPING RESPONSES FOR $C_B = 0.80$, $L/B = 7.0$, LCB $= +2.0\%$

		Froude No.	$B/T = 2$								$B/T = 3$								$B/T = 4$							
			Significant Wave Height/LBP								Significant Wave Height/LBP								Significant Wave Height/LBP							
		[%]	0.015	0.020	0.025	0.030	0.040	0.050	0.075	0.100	0.015	0.020	0.025	0.030	0.040	0.050	0.075	0.100	0.015	0.020	0.025	0.030	0.040	0.050	0.075	0.100
Heave		10	5	16	27	40	65	90	156	222	5	11	19	29	52	77	143	210	5	10	18	27	50	74	140	206
		15	6	20	35	51	81	109	175	239	5	14	24	36	60	85	151	218	5	11	20	30	54	79	145	211
		20	6	20	40	60	96	127	196	260	5	17	30	43	70	97	163	228	5	13	24	35	60	86	152	218
		25	4	17	42	64	109	143	218	283	6	18	34	50	81	109	176	241	5	15	28	41	68	94	161	226
		30	3	16	42	66	115	157	239	306	6	18	36	55	90	121	191	256	5	17	31	46	75	103	171	236
Pitch		10	24	57	91	122	174	217	291	341	22	49	78	105	153	192	265	314	21	45	72	97	144	182	254	304
		15	20	57	95	131	188	233	312	363	21	51	82	111	162	204	278	329	20	46	75	102	150	190	263	314
		20	19	55	95	133	197	248	330	384	19	51	84	116	169	213	290	341	19	46	76	105	155	196	271	322
		25	15	46	92	137	212	261	351	404	17	50	85	118	175	220	300	353	17	45	76	107	158	201	277	329
		30	10	37	94	135	218	273	372	432	16	47	84	120	180	229	310	364	15	45	76	108	162	205	283	336
Bending Moment		10	49	94	137	176	235	278	344	380	61	110	154	191	250	291	353	387	64	114	159	197	255	297	358	391
		15	49	92	136	176	244	291	362	401	60	113	161	203	265	310	375	410	66	120	168	209	271	315	378	412
		20	47	89	136	179	252	302	381	422	59	114	166	212	281	330	401	438	66	124	177	222	290	338	406	441
		25	47	92	138	180	255	312	397	444	58	115	170	220	297	351	430	470	65	127	185	235	310	363	438	477
		30	47	95	140	187	263	324	415	463	58	116	175	228	313	373	461	505	64	130	193	247	331	389	474	516
Added Resistance		10	7	23	47	73	122	159	217	248	11	28	53	78	129	167	230	267	15	36	63	92	151	195	265	309
		15	5	22	50	84	153	210	312	388	9	27	53	83	142	195	303	397	13	32	60	91	157	216	341	459
		20	4	21	54	96	183	261	406	528	7	25	54	89	156	224	376	528	10	29	57	90	162	236	416	609
		25	3	16	51	96	207	304	502	653	6	25	57	100	187	273	456	626	9	28	60	100	185	272	480	694
		30	2	10	48	96	231	348	598	777	5	24	60	111	218	321	536	725	7	28	64	110	208	308	545	778
Acceleration	Sta. 0	10	230	510	771	983	1304	1525	1833	1989	264	501	724	896	1172	1367	1637	1780	265	479	668	834	1087	1265	1529	1669
		15	203	535	859	1159	1559	1849	2253	2447	276	589	883	1125	1477	1732	2078	2253	291	568	832	1041	1370	1604	1928	2095
		20	189	539	911	1244	1765	2124	2623	2886	264	640	1000	1318	1753	2079	2510	2726	299	643	973	1248	1651	1944	2345	2546
		25	171	491	909	1325	1970	2378	3003	3283	245	666	1080	1457	2009	2384	2921	3187	288	694	1084	1433	1915	2274	2759	3001
		30	134	416	940	1362	2124	2599	3355	3738	239	663	1129	1564	2224	2681	3315	3634	276	729	1173	1578	2168	2579	3163	3454
	Sta. 5	10	118	284	439	572	769	909	1123	1242	144	284	411	517	685	807	994	1105	152	274	385	482	636	750	932	1042
		15	107	299	495	680	945	1133	1412	1558	151	338	514	665	881	1046	1284	1415	162	329	482	613	815	963	1186	1314
		20	98	290	528	743	1094	1330	1685	1875	142	372	592	792	1074	1282	1581	1742	166	376	575	750	1002	1191	1468	1618
		25	84	262	533	793	1227	1510	1957	2175	136	387	647	887	1254	1504	1876	2073	161	411	654	875	1188	1422	1759	1939
		30	65	230	548	819	1324	1671	2214	2498	133	381	682	967	1414	1719	2169	2401	157	433	715	975	1369	1642	2050	2266
	Sta. 10	10	59	144	225	304	416	510	675	781	70	118	170	220	315	397	553	660	82	126	172	217	303	380	532	638
		15	70	197	325	442	622	755	960	1086	71	154	236	318	440	548	729	848	79	139	205	269	383	480	658	777
		20	75	214	393	562	826	1004	1277	1429	76	204	329	447	620	753	975	1111	80	175	271	366	511	635	841	974
		25	62	196	437	648	1014	1231	1602	1787	86	246	415	568	815	990	1261	1422	84	219	354	485	677	827	1076	1227
		30	45	183	470	698	1138	1438	1914	2161	93	261	477	683	1006	1229	1569	1755	92	258	436	597	858	1046	1342	1518
	Sta. 15	10	145	282	408	512	667	789	970	1077	138	221	305	382	510	612	787	896	146	223	299	371	491	588	759	865
		15	146	370	564	737	957	1122	1365	1497	147	269	387	487	653	780	983	1107	140	233	330	418	567	684	884	1007
		20	154	417	676	914	1253	1491	1805	1978	159	346	519	673	876	1041	1286	1424	148	277	406	518	701	844	1073	1211
		25	139	387	739	1063	1564	1834	2288	2481	163	417	648	853	1146	1348	1656	1826	160	344	520	678	897	1074	1343	1497
		30	107	340	805	1141	1771	2141	2745	3045	172	457	747	1019	1409	1686	2064	2269	166	409	638	843	1136	1347	1673	1854
	Sta. 20	10	258	508	734	914	1185	1382	1647	1786	251	433	603	749	977	1141	1390	1525	259	423	573	711	924	1081	1323	1453
		15	247	618	941	1227	1573	1833	2194	2369	269	512	738	923	1216	1422	1718	1875	259	463	658	826	1090	1280	1566	1720
		20	253	685	1090	1454	1966	2327	2778	3021	280	611	913	1178	1517	1785	2147	2328	275	532	778	983	1303	1534	1866	2042
		25	231	634	1162	1661	2399	2797	3440	3691	275	699	1082	1415	1875	2187	2642	2869	286	618	928	1201	1567	1851	2243	2443
		30	180	547	1257	1765	2697	3215	4065	4476	285	752	1209	1629	2219	2638	3178	3460	286	699	1080	1419	1881	2214	2683	2921

Relative Motion												Relative Velocity										
Sta. 1	10	46	80	112	139	179	206	243	261	48	76	101	122	154	175	204	218	48	72	94	113	141	161	187	200
	15	43	77	114	148	196	229	275	296	47	78	108	133	170	197	232	248	47	75	101	123	156	179	210	224
	20	42	74	113	149	206	245	300	327	44	77	111	141	184	215	257	276	46	76	105	131	168	195	231	248
	25	41	68	108	149	215	258	323	351	43	75	111	144	195	268	277	301	44	75	107	136	178	208	250	270
	30	39	62	107	147	220	267	342	378	42	72	109	145	202	341	295	322	43	74	107	139	186	219	266	289
Sta. 2	10	45	74	102	125	158	181	210	223	46	69	90	107	132	149	170	181	44	65	82	97	119	134	153	162
	15	43	73	105	135	175	204	242	259	45	72	98	119	150	171	199	211	45	69	90	108	134	152	176	187
	20	41	70	105	137	187	221	268	290	43	73	102	128	164	189	224	239	44	70	95	117	147	169	198	211
	25	40	66	102	138	197	235	291	315	42	71	103	132	175	204	245	264	43	71	98	123	158	183	218	233
	30	39	61	100	137	202	245	310	342	41	69	102	134	183	217	264	286	42	70	99	127	167	195	235	253
Sta. 3	10	43	68	92	111	138	155	178	188	43	62	78	91	110	122	138	144	41	56	70	81	97	107	120	126
	15	41	69	96	122	155	179	210	224	43	66	87	104	129	145	166	175	42	62	79	92	113	126	143	151
	20	40	67	97	125	169	197	237	255	42	68	92	114	144	165	192	204	42	64	85	102	127	144	166	175
	25	39	63	95	127	179	212	260	281	41	67	95	120	156	180	214	229	41	66	89	110	139	159	186	198
	30	38	59	94	127	185	223	280	308	40	65	95	123	165	194	233	252	41	65	91	115	149	172	204	219
Sta. 4	10	41	62	81	96	117	131	148	154	39	54	67	76	89	98	107	111	37	49	58	65	76	82	90	92
	15	40	64	87	109	136	156	180	190	41	60	76	90	108	121	135	141	39	55	67	78	92	102	113	117
	20	40	63	90	114	151	175	208	223	40	62	83	101	124	141	161	170	40	58	75	88	107	120	135	142
	25	39	60	89	117	162	190	232	250	40	63	86	108	138	158	184	196	40	61	80	97	120	136	156	165
	30	38	57	89	118	169	203	253	277	39	62	88	112	148	172	205	219	39	61	83	103	131	150	175	186
Sta. 20	10	37	53	69	86	109	128	155	169	35	49	64	78	101	117	142	154	34	49	64	78	100	116	140	152
	15	38	57	76	95	123	143	174	190	36	49	63	77	98	115	140	153	35	48	62	75	96	111	134	147
	20	40	61	85	110	147	173	209	227	36	50	64	79	100	117	143	157	36	48	61	73	92	107	131	143
	25	40	61	94	126	178	207	255	276	37	52	68	83	108	126	154	169	36	48	60	72	91	106	130	142
	30	39	60	103	137	202	241	305	336	38	54	73	92	122	144	175	191	37	49	61	73	95	110	134	147
Sta. 1	10	262	331	404	463	551	607	673	694	268	331	388	434	501	541	585	597	271	327	375	416	471	505	542	550
	15	298	366	445	525	625	698	786	816	307	375	445	503	586	641	700	717	310	374	433	482	553	597	644	656
	20	337	398	480	560	687	770	877	923	345	414	491	564	659	728	805	830	349	416	485	544	628	684	744	761
	25	378	429	507	596	741	834	964	1007	383	449	531	611	726	802	898	932	388	455	530	601	695	762	838	861
	30	419	461	542	627	789	888	1036	1100	424	484	565	650	781	870	980	1023	428	492	571	648	758	832	923	953
Sta. 2	10	258	319	379	429	500	544	593	606	262	314	359	395	446	474	502	506	261	306	342	373	413	435	456	456
	15	296	356	423	490	573	633	701	722	302	361	417	464	530	571	612	621	303	356	402	440	494	525	554	558
	20	335	390	460	528	634	703	789	824	341	401	466	525	602	657	714	730	344	400	456	503	569	611	652	659
	25	376	423	490	565	686	765	871	905	380	438	507	574	668	729	804	827	383	441	503	560	636	688	743	756
	30	418	456	525	599	734	818	940	990	421	474	544	615	723	796	883	914	423	480	545	609	698	756	825	844
Sta. 3	10	254	305	354	393	448	481	513	519	254	295	328	354	389	406	419	415	250	283	308	328	352	364	370	362
	15	293	345	400	454	520	568	618	630	296	344	388	424	472	502	525	526	295	336	370	397	434	453	465	460
	20	333	381	440	496	583	637	703	727	336	387	439	486	545	585	624	631	337	383	426	461	508	537	560	559
	25	374	416	473	535	634	698	781	806	377	426	483	537	610	658	711	724	378	426	475	519	576	614	648	652
	30	416	451	509	571	682	751	847	885	418	464	522	580	666	723	788	808	419	467	520	570	638	682	729	738
Sta. 4	10	250	292	329	358	398	420	438	437	247	277	299	316	336	343	342	331	241	263	278	289	299	301	292	276
	15	291	334	378	420	470	506	539	544	291	329	361	386	418	436	444	437	288	318	341	357	378	386	382	370
	20	331	372	420	466	534	575	623	637	333	374	414	449	491	518	539	537	332	367	398	422	453	469	474	464
	25	373	410	457	507	586	636	698	715	374	416	460	502	557	591	624	628	375	413	450	482	521	545	560	554
	30	415	447	495	545	634	689	763	790	416	456	502	548	614	656	699	709	417	456	497	535	583	613	639	638
Sta. 20	10	244	270	297	323	355	382	410	414	236	258	281	301	332	352	372	374	231	253	277	297	329	349	368	371
	15	289	322	356	389	434	462	499	507	283	303	323	340	364	382	396	391	279	298	318	334	358	373	383	377
	20	335	375	421	468	538	587	638	657	328	349	369	389	409	423	436	428	325	343	359	372	388	399	401	388
	25	378	419	482	552	667	726	819	841	374	399	423	444	476	492	508	503	370	387	402	415	426	432	429	411
	30	421	459	544	621	778	865	1005	1063	419	449	481	512	559	589	616	617	416	434	451	463	479	483	479	460

TABLE A-18 SEAKEEPING RESPONSES FOR $C_B = 0.80$, $L/B = 8.5$, LCB = + 2.0%

		Froude No.	$B/T = 2$								$B/T = 3$								$B/T = 4$							
			Significant Wave Height/LBP								Significant Wave Height/LBP								Significant Wave Height/LBP							
		[%]	0.015	0.020	0.025	0.030	0.040	0.050	0.075	0.100	0.015	0.020	0.025	0.030	0.040	0.040	0.075	0.100	0.015	0.020	0.025	0.030	0.040	0.050	0.075	0.100
Heave		10	6	13	22	33	56	82	147	214	6	11	19	28	50	75	140	207	6	11	18	27	48	73	138	204
		15	6	19	31	44	69	95	160	226	6	12	21	31	54	80	145	212	6	11	19	29	51	76	141	208
		20	7	23	39	55	85	113	178	242	6	15	26	38	62	88	153	219	5	12	21	32	55	81	146	212
		25	8	23	44	64	100	131	198	262	6	18	32	46	72	98	164	229	5	14	25	37	61	87	153	219
		30	6	21	46	70	113	146	219	283	6	21	36	52	82	110	177	241	6	17	29	43	69	95	161	227
Pitch		10	27	58	89	118	168	208	280	329	23	49	76	102	149	187	259	308	22	46	71	96	142	180	251	301
		15	26	61	97	129	183	226	301	351	24	52	82	109	158	198	271	321	22	47	74	101	148	187	260	310
		20	22	61	101	139	195	241	320	371	23	53	85	115	166	208	283	333	21	48	77	104	153	193	267	318
		25	20	61	103	141	206	255	337	391	21	54	87	120	173	217	293	344	20	48	78	107	157	199	274	325
		30	19	56	100	146	217	270	357	409	18	53	89	123	179	224	303	355	19	48	79	109	160	203	279	331
Bending Moment		10	50	90	127	158	207	242	294	322	54	96	133	164	213	247	298	326	56	98	136	168	217	252	303	330
		15	47	90	130	166	217	254	310	340	57	102	141	174	226	261	314	341	58	104	143	177	228	263	315	342
		20	47	90	131	166	226	267	326	358	57	105	149	186	240	279	334	363	60	109	152	188	242	280	334	362
		25	46	87	131	170	234	278	344	377	56	107	154	194	255	297	357	388	61	114	160	200	259	300	358	387
		30	45	88	133	172	239	286	359	397	55	108	158	202	269	315	381	415	61	117	168	211	276	321	384	417
Added Resistance		10	7	19	36	53	86	111	151	173	11	26	45	65	105	134	180	208	14	31	52	75	120	153	206	239
		15	5	20	41	65	108	146	216	271	9	24	44	66	111	150	231	305	12	28	50	75	125	171	268	361
		20	4	21	46	77	129	180	281	370	7	22	42	66	116	166	281	403	10	26	48	74	131	188	329	483
		25	4	19	47	86	161	228	360	462	6	22	48	78	139	200	337	471	9	25	50	80	144	211	373	543
		30	3	17	48	95	192	275	439	554	5	23	53	90	162	233	392	539	8	25	52	86	157	233	416	603
Acceleration	Sta. 0	10	306	590	851	1042	1343	1555	1832	1974	306	536	729	901	1157	1334	1595	1732	317	521	689	852	1090	1260	1516	1649
		15	311	683	1025	1296	1702	1976	2349	2530	346	657	945	1160	1505	1744	2066	2229	341	619	859	1067	1380	1597	1907	2068
		20	281	722	1137	1519	1994	2362	2834	3059	364	761	1130	1424	1854	2161	2566	2765	373	721	1049	1302	1700	1980	2357	2547
		25	256	731	1210	1623	2271	2680	3272	3571	355	831	1276	1660	2175	2556	3061	3303	389	815	1216	1542	2022	2366	2826	3052
		30	251	707	1226	1738	2481	3001	3711	4039	328	871	1384	1846	2480	2923	3536	3831	385	885	1359	1768	2328	2742	3297	3566
	Sta. 5	10	169	334	487	601	785	920	1109	1217	173	305	419	519	674	787	966	1074	183	299	399	492	636	744	921	1026
		15	163	390	597	771	1018	1193	1449	1584	196	379	545	678	891	1039	1261	1383	197	358	501	624	815	953	1165	1288
		20	150	414	668	904	1223	1458	1783	1952	204	444	669	854	1118	1318	1593	1740	211	423	615	775	1022	1198	1455	1598
		25	140	410	713	985	1415	1692	2103	2316	195	490	766	1012	1342	1593	1936	2114	223	482	730	935	1237	1461	1776	1943
		30	131	386	729	1057	1573	1911	2424	2666	184	519	841	1134	1559	1850	2274	2493	216	529	825	1091	1451	1727	2106	2304
	Sta. 10	10	78	137	199	254	357	443	598	703	102	151	198	243	325	399	548	652	107	150	195	235	314	386	532	635
		15	85	207	316	421	555	672	858	973	93	159	227	290	405	500	676	793	106	165	224	279	381	470	642	758
		20	95	273	440	585	800	958	1191	1332	98	209	313	413	558	686	887	1017	104	183	266	343	479	590	789	920
		25	107	305	525	728	1040	1252	1555	1725	104	272	425	573	766	925	1173	1319	108	229	346	458	627	771	1000	1144
		30	100	292	580	849	1272	1523	1938	2129	113	326	535	716	999	1196	1498	1673	113	283	445	601	815	991	1264	1427
	Sta. 15	10	159	262	358	440	579	682	856	965	188	272	350	422	540	635	802	904	186	268	336	408	521	613	779	878
		15	192	369	527	653	840	986	1190	1308	171	272	373	462	612	729	928	1049	185	277	366	450	588	699	892	1010
		20	193	480	723	940	1185	1383	1659	1802	188	335	474	587	782	925	1151	1286	175	285	397	498	667	800	1023	1159
		25	203	557	873	1146	1546	1810	2165	2363	208	432	635	813	1040	1231	1499	1648	187	338	486	610	820	978	1231	1382
		30	205	555	957	1353	1894	2237	2723	2930	211	525	801	1045	1359	1586	1927	2105	207	421	622	798	1043	1242	1533	1699
	Sta. 20	10	292	512	707	866	1114	1284	1535	1670	323	500	652	794	1007	1162	1403	1526	320	487	619	758	961	1111	1348	1468
		15	341	660	943	1158	1493	1731	2035	2191	315	541	748	923	1194	1387	1672	1824	328	529	710	875	1126	1308	1587	1731
		20	328	799	1201	1562	1947	2264	2679	2867	342	638	907	1120	1468	1703	2036	2211	325	570	799	996	1301	1519	1841	2012
		25	330	906	1404	1823	2436	2829	3352	3632	367	763	1120	1423	1812	2124	2523	2719	346	651	936	1169	1539	1798	2167	2361
		30	336	904	1507	2109	2896	3421	4105	4390	359	881	1337	1738	2232	2590	3096	3333	370	758	1117	1420	1838	2159	2587	2803

Relative Motion																														
Sta. 1	10	50	82	111	134	169	193	223	238	49	75	97	116	144	163	190	202	48	71	91	109	135	152	177	189
	15	48	84	119	148	190	219	258	275	49	79	106	128	162	185	215	230	49	75	98	118	148	169	197	211
	20	45	82	121	157	205	240	287	308	48	81	112	139	177	205	241	258	48	77	104	127	161	185	217	233
	25	43	78	120	157	217	255	310	337	46	80	115	147	190	221	263	283	47	78	108	134	173	200	237	254
	30	42	74	116	159	224	269	332	361	44	79	116	150	200	234	283	306	45	78	110	140	182	212	254	274
Sta. 2	10	48	76	100	118	147	166	189	200	46	67	85	100	121	136	155	164	44	63	78	92	111	124	143	151
	15	46	78	108	133	169	192	224	237	47	72	95	113	140	158	181	192	46	68	86	102	126	142	163	172
	20	44	77	111	143	184	214	253	270	46	75	102	124	156	178	207	220	46	71	93	112	140	159	183	195
	25	42	75	112	145	197	230	277	299	44	76	106	133	169	195	230	246	45	73	98	120	152	174	203	217
	30	41	71	109	147	204	244	299	324	43	75	107	138	180	209	250	269	44	73	101	127	162	187	221	237
Sta. 3	10	45	68	88	102	125	139	156	163	42	58	72	83	98	108	121	127	39	53	64	74	88	97	109	113
	15	44	72	97	118	147	166	190	200	44	65	83	97	118	131	147	155	42	59	74	86	103	114	129	135
	20	43	72	102	129	163	188	220	234	44	69	91	109	134	152	173	183	43	64	82	96	118	132	150	158
	25	41	70	103	132	177	205	245	263	43	70	96	118	148	170	197	209	43	66	88	105	131	148	170	180
	30	41	67	101	135	186	220	267	288	42	70	99	124	160	185	218	233	42	68	92	113	142	162	189	201
Sta. 4	10	42	61	76	86	103	113	124	128	38	50	59	66	73	83	90	92	35	44	52	58	66	72	78	79
	15	42	66	86	103	126	141	159	166	41	57	71	81	96	105	116	120	38	51	61	70	81	89	97	100
	20	41	67	92	115	143	164	189	199	42	62	80	94	113	127	142	148	40	56	70	81	97	107	118	123
	25	40	66	94	120	158	182	215	229	41	64	86	104	128	145	166	175	41	60	77	91	110	123	139	146
	30	40	64	94	123	168	197	238	255	40	65	90	111	141	161	188	199	41	62	82	99	122	138	159	167
Sta. 20	10	37	53	70	84	109	127	153	166	34	50	66	80	104	121	145	158	34	50	67	81	104	121	144	157
	15	38	55	73	90	113	134	161	175	35	50	65	79	101	118	142	155	34	49	64	77	99	115	138	151
	20	38	59	80	100	128	148	180	196	36	50	65	78	100	116	141	154	35	49	63	75	96	111	134	146
	25	40	64	89	113	150	176	211	230	37	51	66	81	101	119	145	158	36	48	62	74	93	108	131	143
	30	40	65	97	130	179	209	254	272	37	53	69	85	110	127	154	169	36	48	61	74	92	107	130	142
Relative Velocity																														
Sta. 1	10	271	344	412	465	544	592	641	656	275	335	385	427	484	518	555	564	275	329	372	410	459	489	521	525
	15	307	387	470	539	638	702	775	798	314	385	450	501	578	623	670	683	316	379	434	479	542	580	619	627
	20	343	421	512	603	711	796	890	922	353	429	507	571	663	724	787	805	356	426	492	546	624	672	722	734
	25	382	454	548	638	782	868	985	1032	391	468	555	634	738	813	895	920	396	469	544	608	700	760	824	841
	30	424	486	576	676	828	938	1072	1123	429	504	596	686	806	889	990	1024	435	508	591	667	768	841	919	942
Sta. 2	10	266	329	384	425	488	523	557	564	266	314	351	383	424	447	467	468	263	304	335	362	395	414	429	425
	15	304	373	442	499	580	630	685	699	308	367	418	458	517	549	578	582	307	357	398	433	478	503	525	524
	20	341	410	487	563	652	721	794	817	348	413	476	528	601	647	691	699	349	406	458	500	560	594	624	627
	25	380	443	524	601	721	791	886	920	387	454	526	591	675	734	794	810	390	451	513	563	635	680	722	730
	30	421	477	555	639	767	858	968	1008	425	492	569	644	742	809	887	909	429	493	561	623	703	759	815	827
Sta. 3	10	259	310	352	384	430	454	472	472	254	290	315	336	361	373	379	371	248	275	295	311	330	338	338	325
	15	299	357	413	458	521	558	595	601	300	345	383	412	453	473	486	482	296	332	361	383	411	424	430	421
	20	338	396	460	520	592	647	700	714	342	394	444	483	537	569	594	594	340	385	423	452	493	513	526	520
	25	377	432	499	563	660	716	789	812	382	438	496	546	610	654	694	700	383	432	479	516	568	599	621	619
	30	419	468	533	603	707	781	866	896	422	478	540	600	677	728	784	796	424	476	530	576	637	677	711	713
Sta. 4	10	253	291	322	343	374	387	392	385	244	267	282	293	304	306	297	281	236	252	262	269	273	271	256	236
	15	295	341	384	417	463	488	509	507	292	325	351	369	393	401	399	387	286	310	337	339	351	352	342	324
	20	335	383	433	480	534	575	609	615	336	377	413	439	476	494	502	494	333	364	390	408	430	438	434	420
	25	375	422	475	526	602	645	696	709	378	422	467	504	549	578	599	596	377	414	448	473	506	522	526	515
	30	417	459	513	568	651	708	771	791	419	465	514	559	616	652	686	688	419	460	500	534	574	599	613	606
Sta. 20	10	241	267	295	317	355	379	404	408	229	253	278	300	335	357	379	385	227	252	279	302	337	359	381	389
	15	287	315	345	373	404	433	459	459	279	300	323	341	370	388	403	400	273	293	315	333	362	379	391	390
	20	332	368	407	445	489	519	556	561	326	346	366	382	405	421	430	421	321	340	359	373	394	406	410	400
	25	378	423	474	522	597	645	696	716	371	392	413	433	449	465	472	460	368	384	401	412	427	435	432	414
	30	422	470	536	612	722	793	877	898	416	441	466	489	517	531	544	534	413	429	444	457	464	470	462	439

TABLE A-19 SEAKEEPING RESPONSES FOR $C_B = 0.85$, $L/B = 5.5$, LCB = $+2.5\%$

		Froude No.	$B/T = 2$								$B/T = 3$								$B/T = 4$							
			Significant Wave Height/LBP								Significant Wave Height/LBP								Significant Wave Height/LBP							
		[%]	0.015	0.020	0.025	0.030	0.040	0.050	0.075	0.100	0.015	0.020	0.025	0.030	0.030	0.040	0.075	0.100	0.015	0.020	0.025	0.030	0.040	0.050	0.075	0.100
Heave		10	5	14	29	44	74	102	170	236	4	11	20	31	55	81	147	214	4	9	17	27	50	75	141	208
		15	4	14	32	50	87	119	192	258	4	13	25	38	65	92	159	226	3	11	21	32	56	82	148	215
		20	2	12	32	53	96	134	213	281	4	14	28	44	75	104	173	239	4	12	24	37	64	91	158	224
		25	2	12	28	53	102	147	232	302	3	12	30	48	84	116	188	255	4	13	26	41	71	100	168	235
		30	1	9	23	53	105	155	249	324	2	12	30	50	90	126	203	271	3	12	28	44	78	108	180	246
Pitch		10	15	45	78	109	164	207	283	335	16	42	70	98	145	185	258	309	16	39	65	90	136	175	247	298
		15	13	40	77	114	176	222	304	356	14	41	71	101	152	194	270	322	14	38	66	93	141	181	255	306
		20	9	32	77	114	185	235	326	383	13	39	70	102	158	202	281	334	13	37	65	94	144	186	262	314
		25	6	30	69	111	190	254	351	410	11	34	69	103	164	210	293	347	11	35	64	94	147	190	268	321
		30	4	25	53	113	195	271	381	445	8	28	68	102	169	218	307	363	10	31	62	94	150	194	275	328
Bending Moment		10	49	89	137	183	266	327	427	483	61	119	173	223	302	360	451	501	70	132	190	240	320	377	465	513
		15	47	91	138	183	267	335	444	506	60	118	176	229	316	379	476	529	68	134	197	252	338	401	494	545
		20	48	96	139	189	271	345	458	523	59	118	180	238	332	401	508	565	68	137	204	265	361	429	532	586
		25	48	99	149	199	286	355	473	542	60	122	187	248	350	427	544	607	68	139	212	280	386	463	577	637
		30	49	102	162	213	307	377	500	570	61	126	196	264	376	460	589	657	68	143	222	296	415	501	630	696
Added Resistance		10	6	27	64	109	198	263	375	433	11	33	68	106	183	242	343	399	17	42	81	123	211	277	395	465
		15	4	20	57	106	221	315	501	625	9	30	66	110	203	286	453	592	13	37	75	120	217	305	501	683
		20	2	12	50	102	243	368	627	817	6	26	63	114	224	329	563	785	10	32	69	117	223	333	607	901
		25	2	9	37	92	237	399	720	952	5	21	61	116	253	383	676	931	8	29	69	125	255	386	707	1024
		30	1	7	23	81	231	431	813	1088	3	16	58	118	282	436	789	1076	7	26	69	133	287	439	807	1148
Acceleration	Sta. 0	10	110	311	523	715	1019	1225	1547	1717	157	363	565	743	1008	1203	1488	1640	174	363	551	711	959	1143	1413	1559
		15	106	302	538	778	1154	1428	1827	2031	147	390	637	868	1207	1453	1813	2001	172	407	642	854	1166	1400	1733	1911
		20	83	251	552	817	1290	1598	2097	2357	141	392	679	950	1380	1678	2121	2352	166	433	710	969	1358	1638	2050	2265
		25	68	239	540	817	1368	1773	2376	2681	131	364	697	1016	1540	1889	2428	2695	164	438	755	1056	1532	1863	2357	2613
		30	61	221	456	862	1446	1975	2678	3047	114	326	716	1054	1671	2081	2729	3059	159	420	783	1129	1696	2080	2666	2960
	Sta. 5	10	53	158	287	407	608	746	976	1107	82	201	320	429	594	720	921	1039	94	204	313	409	563	681	871	986
		15	49	152	298	446	698	886	1178	1339	78	217	367	510	732	893	1146	1290	94	232	373	504	702	854	1088	1225
		20	38	131	302	472	780	1008	1371	1573	74	216	397	570	856	1057	1373	1546	91	249	421	583	839	1024	1314	1477
		25	31	128	292	479	841	1131	1564	1801	67	200	414	617	970	1211	1599	1805	91	252	454	648	966	1190	1542	1734
		30	29	116	250	507	898	1254	1768	2053	57	184	427	647	1060	1355	1823	2074	87	240	477	702	1086	1350	1773	1997
	Sta. 10	10	40	112	205	294	445	551	735	849	41	94	154	217	320	409	571	682	47	87	135	187	281	364	522	632
		15	37	115	248	370	586	733	984	1123	47	128	220	308	458	573	769	895	46	111	185	259	383	487	672	795
		20	27	108	268	417	696	902	1227	1408	51	144	272	397	605	753	1001	1147	51	141	244	343	513	643	865	1006
		25	22	113	253	444	783	1065	1461	1681	46	143	312	468	746	931	1247	1422	57	159	295	426	650	814	1084	1246
		30	20	98	215	475	855	1200	1692	1963	38	138	340	517	857	1100	1494	1711	55	163	335	502	788	985	1320	1507
	Sta. 15	10	92	243	390	523	723	860	1076	1198	98	193	289	376	514	624	806	920	96	169	250	324	451	553	730	843
		15	90	247	455	648	949	1139	1440	1590	100	242	380	506	693	833	1057	1189	99	202	309	408	564	690	898	1025
		20	68	216	497	722	1135	1395	1809	2022	105	275	458	631	894	1080	1361	1519	103	244	388	521	724	877	1125	1272
		25	55	216	476	756	1261	1647	2170	2435	100	270	514	739	1104	1330	1699	1885	108	277	461	634	904	1097	1397	1569
		30	49	192	397	806	1367	1871	2527	2863	85	250	559	811	1274	1566	2043	2288	109	284	517	739	1094	1329	1703	1901
	Sta. 20	10	152	405	642	853	1160	1366	1675	1835	174	354	530	684	915	1090	1349	1491	173	324	479	615	831	992	1241	1381
		15	150	409	725	1024	1469	1751	2170	2366	172	417	651	864	1160	1378	1702	1872	179	373	569	744	1005	1203	1499	1660
		20	115	350	785	1125	1738	2100	2680	2964	175	459	752	1023	1427	1706	2105	2316	179	426	672	896	1219	1456	1812	2001
		25	93	343	757	1163	1908	2451	3189	3543	168	445	819	1167	1711	2042	2560	2803	184	467	764	1039	1455	1745	2170	2395
		30	83	309	631	1237	2053	2785	3700	4154	145	405	879	1261	1946	2359	3025	3350	185	472	833	1176	1705	2050	2573	2830

Relative Motion		Relative Velocity																											
Sta. 1		Sta. 1																											
10	40	67	98	126	170	199	243	264	43	69	95	118	151	175	208	224	44	67	90	110	139	160	189	202
15	40	64	95	127	179	216	268	293	41	68	97	125	165	193	233	252	42	68	94	117	152	177	211	228
20	39	59	93	127	187	227	289	320	40	66	97	127	174	207	254	277	41	67	95	122	162	190	231	250
25	38	57	90	123	188	237	309	344	40	62	95	127	182	219	273	299	40	65	95	124	169	201	248	270
30	38	56	82	123	190	250	330	370	39	59	93	126	186	227	290	321	40	62	93	124	176	210	263	288
Sta. 2		Sta. 2																											
10	40	64	91	115	153	177	214	230	41	64	86	105	133	152	177	189	41	62	80	96	120	136	157	167
15	39	62	90	118	162	194	239	260	40	64	90	113	147	157	203	218	41	63	85	105	133	153	180	193
20	38	57	88	118	171	207	261	287	39	63	90	116	157	185	225	244	40	63	88	111	144	168	201	216
25	38	56	86	115	174	217	281	311	39	60	89	118	166	197	244	266	39	62	88	113	153	180	219	237
30	38	55	79	116	176	230	302	337	38	57	88	118	171	207	262	288	39	60	88	115	160	190	235	256
Sta. 3		Sta. 3																											
10	39	60	84	105	136	157	186	199	40	59	78	93	114	129	148	157	39	56	71	83	101	113	128	134
15	39	59	84	108	147	174	212	230	39	61	82	102	129	149	174	186	39	59	77	93	115	131	151	160
20	38	56	83	110	156	188	235	257	39	60	84	106	141	164	197	212	39	60	80	100	127	146	172	184
25	37	55	81	108	160	199	255	282	38	58	84	109	150	177	217	235	39	59	82	104	137	159	191	206
30	37	54	76	109	164	212	276	308	38	56	83	110	157	188	235	258	38	58	82	106	145	170	208	225
Sta. 4		Sta. 4																											
10	39	57	77	95	121	138	161	171	39	55	69	81	98	109	122	127	38	51	62	71	84	92	101	105
15	38	57	79	100	133	156	188	202	39	57	75	91	113	128	148	156	38	54	69	81	99	110	125	130
20	38	55	78	102	143	171	211	231	38	57	78	97	126	145	171	183	38	56	74	89	111	126	146	155
25	37	54	78	102	148	183	232	256	38	56	79	101	136	159	193	207	38	56	76	94	122	140	165	177
30	37	53	73	103	152	196	253	281	38	54	79	102	144	171	211	230	38	56	77	98	131	152	183	197
Sta. 20		Sta. 20																											
10	38	54	70	87	115	134	164	180	36	47	60	72	91	107	132	144	35	47	59	71	91	105	128	140
15	39	56	80	103	142	167	206	225	37	49	61	73	94	110	136	150	36	47	58	69	87	101	124	136
20	39	57	89	117	170	204	258	285	38	51	65	80	105	123	152	167	37	47	58	68	87	100	124	136
25	39	58	90	126	193	244	313	347	39	53	71	90	123	144	179	196	38	48	60	71	92	107	132	145
30	39	58	84	136	212	281	370	414	39	54	77	99	140	168	212	235	38	50	64	77	102	119	148	162
Sta. 1		Sta. 1																											
10	249	299	358	416	501	555	630	657	255	307	361	408	475	520	571	587	257	307	354	394	452	489	529	539
15	290	334	392	453	552	623	712	747	294	345	405	462	542	598	665	687	297	348	403	452	521	568	621	636
20	331	367	426	489	605	678	786	830	334	382	443	504	601	665	747	778	336	387	445	502	583	638	705	726
25	373	406	461	518	642	727	857	907	376	417	477	543	654	726	824	858	377	424	484	545	639	702	781	809
30	416	446	490	556	677	789	929	988	417	453	514	579	702	780	895	939	419	461	521	585	691	761	854	886
Sta. 2		Sta. 2																											
10	248	292	342	391	461	505	564	582	251	296	340	378	430	464	499	507	251	292	329	360	403	429	453	456
15	289	329	379	430	512	571	643	669	290	336	386	433	497	541	590	604	292	336	380	419	472	507	543	550
20	330	364	414	468	565	626	713	747	331	374	426	477	556	607	670	691	332	376	425	471	534	577	625	638
25	372	402	451	500	603	673	780	820	373	411	462	518	608	667	745	769	373	415	465	515	591	641	700	718
30	414	443	483	538	640	732	847	893	415	448	500	555	657	721	813	845	415	453	504	557	643	699	771	792
Sta. 3		Sta. 3																											
10	246	285	327	367	423	458	500	511	248	285	320	348	387	410	430	430	246	279	306	328	357	372	382	377
15	287	324	366	409	476	522	578	596	288	327	368	405	454	486	519	524	288	325	359	388	426	450	469	468
20	329	361	403	449	528	578	646	670	330	367	410	452	513	553	598	609	330	367	406	442	489	520	550	553
25	371	400	442	483	568	625	710	739	372	406	449	494	567	613	670	685	372	408	449	489	547	584	624	632
30	414	441	476	522	607	681	772	807	414	444	488	534	616	666	736	758	414	447	489	533	600	643	693	704
Sta. 4		Sta. 4																											
10	245	279	314	346	389	415	443	446	245	276	302	322	348	362	368	361	243	268	287	301	318	324	320	308
15	287	320	356	390	443	479	520	530	287	321	353	380	416	438	455	452	287	316	342	362	387	400	404	394
20	329	358	394	432	495	536	587	602	329	362	397	430	476	504	532	535	329	361	391	417	451	470	483	477
25	371	398	434	470	538	584	649	669	372	402	439	475	531	565	603	610	372	403	436	467	509	534	556	554
30	414	440	471	509	579	637	708	732	414	442	479	517	581	619	669	681	414	444	479	513	563	594	624	626
Sta. 20		Sta. 20																											
10	248	276	305	331	375	401	435	444	243	262	280	297	318	333	349	347	239	258	277	291	314	329	342	338
15	292	325	367	409	480	522	581	597	288	309	327	343	366	378	390	386	285	303	318	331	346	355	359	348
20	334	368	426	481	591	656	755	794	333	358	381	402	435	454	472	469	331	349	363	374	388	393	390	376
25	377	412	472	541	684	792	938	998	377	405	437	469	522	551	589	593	376	396	413	426	444	452	450	434
30	419	454	504	601	768	928	1124	1221	421	451	493	534	612	658	725	746	420	444	466	485	515	529	530	526

TABLE A-20 SEAKEEPING RESPONSES FOR $C_B = 0.85$, $L/B = 7.0$, LCB = $+2.5\%$

		Froude No.	$B/T = 2$								$B/T = 3$								$B/T = 4$							
			Significant Wave Height/LBP								Significant Wave Height/LBP								Significant Wave Height/LBP							
		[%]	0.015	0.020	0.025	0.030	0.040	0.050	0.075	0.100	0.015	0.020	0.025	0.030	0.040	0.050	0.075	0.100	0.015	0.020	0.025	0.030	0.040	0.050	0.075	0.100
Heave		10	5	14	25	37	62	88	154	220	4	10	18	27	50	75	141	208	5	9	17	26	48	72	137	204
		15	6	18	32	48	77	105	171	236	4	12	22	33	57	83	149	215	4	10	18	28	51	77	142	209
		20	6	18	37	56	92	122	192	257	5	15	27	40	67	93	160	225	4	12	22	33	57	83	149	215
		25	4	16	39	60	103	138	213	278	5	17	31	47	77	105	173	238	4	14	26	38	65	91	158	224
		30	2	15	38	62	110	151	233	301	5	16	34	52	87	117	187	252	5	15	29	43	72	100	168	233
Pitch		10	21	51	82	112	162	203	276	325	20	44	71	97	143	182	254	303	18	41	66	91	136	174	245	295
		15	18	52	87	121	175	218	296	346	19	45	75	103	151	192	266	316	18	41	68	94	141	180	253	303
		20	17	51	88	125	185	234	314	367	17	46	77	107	158	201	276	327	16	41	69	97	145	186	260	311
		25	13	42	86	129	201	248	336	388	15	45	77	109	164	208	286	338	15	41	70	99	148	190	266	317
		30	9	34	88	127	207	261	359	417	14	42	77	111	170	216	296	349	13	40	70	99	152	194	271	323
Bending Moment		10	49	94	138	179	242	288	362	404	61	111	157	197	260	306	376	414	64	116	164	205	269	314	383	420
		15	49	92	136	177	248	299	377	420	60	113	163	207	273	322	395	434	65	121	172	215	282	330	401	439
		20	47	90	137	180	255	307	394	440	58	114	167	214	288	340	418	460	65	125	180	227	300	351	427	467
		25	47	95	140	183	256	318	408	459	58	115	171	222	303	360	445	490	64	128	187	239	319	376	458	501
		30	48	98	143	192	269	332	425	477	57	116	176	231	319	381	475	524	64	130	195	251	340	402	494	541
Added Resistance		10	7	23	46	72	121	159	219	252	12	30	56	82	138	179	251	292	16	38	69	100	166	214	303	355
		15	5	21	48	82	150	208	312	392	9	27	54	85	147	203	322	429	13	33	63	96	167	232	381	524
		20	4	20	51	92	178	257	405	532	7	24	52	87	156	227	393	565	10	28	57	91	168	250	459	693
		25	3	15	48	92	201	300	504	660	6	23	55	97	187	276	475	664	9	28	59	100	190	285	524	776
		30	2	10	45	92	224	343	602	788	5	22	58	108	218	325	557	763	7	27	62	108	213	321	589	860
Acceleration	Sta. 0	10	196	440	675	868	1164	1373	1668	1822	223	434	638	800	1058	1243	1508	1650	223	415	591	746	986	1159	1417	1557
		15	170	468	757	1028	1402	1665	2052	2241	231	508	775	999	1328	1569	1905	2078	242	490	733	931	1239	1462	1779	1945
		20	166	475	807	1111	1585	1927	2397	2649	219	553	878	1172	1578	1882	2298	2510	249	554	854	1112	1489	1767	2158	2357
		25	147	426	808	1193	1794	2169	2757	3024	208	576	951	1294	1812	2163	2677	2936	240	599	953	1275	1729	2066	2535	2774
		30	115	362	848	1225	1930	2372	3098	3464	206	573	994	1395	2011	2439	3045	3351	234	628	1030	1401	1958	2344	2906	3190
	Sta. 5	10	98	242	380	501	685	818	1025	1144	122	244	360	458	616	735	919	1029	126	235	338	428	575	685	865	976
		15	88	254	429	596	845	1018	1288	1432	124	289	448	588	791	947	1180	1311	134	281	422	544	734	877	1096	1225
		20	83	249	461	655	975	1200	1539	1724	118	320	517	700	966	1161	1452	1612	137	322	503	666	903	1083	1354	1505
		25	71	224	466	703	1104	1369	1792	2005	114	331	566	786	1131	1366	1725	1918	133	354	572	775	1073	1293	1622	1801
		30	54	198	484	728	1192	1517	2037	2309	112	324	598	860	1278	1566	2000	2226	132	371	626	864	1238	1497	1892	2105
	Sta. 10	10	51	127	202	275	387	478	642	750	64	106	154	202	294	375	531	639	76	115	157	200	284	360	511	618
		15	61	174	293	403	580	707	911	1036	61	134	211	289	408	511	694	814	69	123	184	245	356	451	629	749
		20	66	188	358	515	768	941	1212	1364	66	181	299	406	576	708	926	1063	68	152	243	333	474	593	800	935
		25	52	173	398	595	944	1158	1519	1705	77	219	375	521	760	930	1197	1358	72	193	321	440	629	778	1022	1174
		30	39	166	427	641	1058	1352	1820	2062	81	230	433	629	941	1155	1493	1677	81	230	394	546	799	982	1275	1452
	Sta. 15	10	130	258	378	480	630	749	931	1039	128	206	288	361	486	586	761	871	138	210	284	352	471	566	736	844
		15	131	340	525	691	911	1072	1314	1447	133	247	360	459	618	744	947	1072	130	217	310	395	540	656	855	980
		20	140	381	631	863	1196	1431	1744	1917	141	317	481	631	830	991	1237	1377	135	255	378	488	665	806	1035	1174
		25	122	347	692	1001	1496	1761	2213	2411	146	381	601	797	1087	1287	1592	1763	142	314	481	635	851	1023	1292	1448
		30	93	310	752	1070	1681	2052	2662	2959	155	412	691	956	1341	1610	1989	2190	148	372	589	785	1076	1283	1607	1789
	Sta. 20	10	228	459	671	845	1100	1291	1553	1692	229	393	554	692	911	1071	1318	1454	237	387	532	662	868	1022	1262	1394
		15	219	565	870	1140	1482	1729	2085	2260	239	461	674	852	1129	1331	1624	1782	232	419	605	764	1018	1204	1487	1642
		20	230	626	1011	1366	1863	2220	2662	2901	245	552	836	1091	1416	1673	2032	2213	243	479	711	909	1213	1438	1768	1944
		25	203	567	1084	1561	2293	2675	3313	3568	244	634	992	1307	1759	2062	2506	2735	251	555	847	1109	1461	1734	2123	2324
		30	157	494	1176	1652	2556	3074	3933	4341	255	675	1108	1515	2091	2496	3030	3304	253	629	986	1305	1757	2073	2539	2778

| Relative Motion | | |

TABLE A-21 SEAKEEPING RESPONSES FOR $C_B = 0.85$, $L/B = 8.5$, LCB $= +2.5\%$

		Froude No.	$B/T = 2$								$B/T = 3$								$B/T = 4$							
			Significant Wave Height/LBP								Significant Wave Height/LBP								Significant Wave Height/LBP							
		[%]	0.015	0.020	0.025	0.030	0.040	0.040	0.075	0.100	0.015	0.020	0.025	0.030	0.040	0.050	0.075	0.100	0.015	0.020	0.025	0.030	0.040	0.050	0.075	0.100
Heave		10	5	12	21	31	54	79	145	211	6	11	18	27	48	73	138	204	6	10	17	25	47	71	136	202
		15	6	17	28	41	66	92	157	223	5	11	19	29	52	77	143	209	5	10	18	27	49	74	139	205
		20	7	21	36	51	81	108	174	239	5	14	24	35	59	85	150	217	5	11	20	30	53	78	144	210
		25	7	21	41	60	95	126	193	258	5	17	29	43	69	95	161	226	5	13	23	35	59	84	150	216
		30	5	19	43	66	108	141	214	278	6	19	34	49	79	107	173	238	5	15	27	40	66	92	158	224
Pitch		10	24	52	81	108	156	195	267	316	21	44	70	95	140	178	249	299	20	42	66	90	135	172	243	293
		15	23	55	88	119	170	212	286	335	21	46	75	101	149	188	260	310	19	43	69	94	140	179	251	301
		20	19	56	93	128	183	227	304	355	20	48	78	106	156	197	271	321	18	43	71	97	144	184	257	308
		25	19	57	95	132	193	242	321	374	18	48	80	111	162	205	280	331	18	43	72	99	148	188	263	314
		30	17	51	93	138	207	257	343	393	16	48	82	114	168	211	289	341	16	43	72	101	151	192	268	319
Bending Moment		10	51	91	130	163	215	254	313	345	55	98	138	172	224	262	320	351	57	102	142	177	230	269	325	356
		15	47	91	131	168	223	263	326	360	57	103	145	180	235	275	333	364	59	106	148	184	239	278	336	367
		20	48	89	131	167	230	274	339	375	56	106	151	190	248	290	351	384	60	111	156	194	253	294	353	385
		25	46	88	132	172	237	283	355	392	55	107	155	197	262	306	372	407	60	114	163	205	268	313	376	410
		30	46	91	135	174	241	292	368	411	55	108	159	205	275	324	396	433	60	117	170	216	285	333	403	439
Added Resistance		10	7	19	36	53	88	114	157	180	12	28	49	70	113	145	202	235	15	33	57	83	133	170	240	281
		15	5	19	39	63	106	145	219	278	9	24	45	68	116	158	252	341	13	30	53	80	136	187	308	425
		20	4	19	43	73	125	176	281	376	7	21	42	66	118	172	303	446	10	26	49	77	138	204	375	569
		25	3	17	44	83	158	224	363	471	6	21	46	77	141	205	358	514	9	25	50	82	151	226	419	628
		30	3	15	46	92	191	272	445	565	5	22	51	87	163	238	413	581	7	24	51	87	163	248	463	688
Acceleration	Sta. 0	10	261	513	749	930	1205	1406	1676	1816	263	469	650	809	1051	1223	1478	1615	273	457	616	768	995	1160	1412	1545
		15	265	593	901	1151	1524	1784	2140	2318	294	572	835	1039	1361	1588	1902	2065	289	538	764	957	1254	1463	1768	1929
		20	235	634	1005	1356	1800	2134	2589	2805	306	660	995	1270	1672	1962	2356	2552	315	627	927	1168	1541	1807	2177	2366
		25	224	649	1079	1453	2049	2440	2994	3287	295	721	1123	1482	1962	2328	2806	3045	325	705	1072	1379	1829	2155	2604	2828
		30	219	621	1092	1570	2267	2743	3421	3725	278	761	1224	1645	2246	2657	3246	3534	319	766	1196	1580	2106	2503	3034	3299
	Sta. 5	10	141	288	426	535	704	831	1017	1126	146	264	370	463	610	719	896	1005	156	259	353	440	578	683	858	965
		15	137	335	520	678	910	1079	1322	1456	164	327	482	603	802	948	1163	1288	165	309	442	556	738	871	1081	1205
		20	125	356	583	798	1098	1314	1629	1793	168	382	586	759	1006	1195	1465	1612	176	364	541	690	922	1092	1346	1490
		25	119	354	627	872	1269	1532	1923	2133	160	423	672	899	1211	1445	1778	1957	182	415	638	834	1117	1329	1638	1806
		30	111	332	641	942	1421	1737	2227	2459	155	447	739	1007	1410	1684	2094	2308	179	456	725	971	1314	1573	1943	2141
	Sta. 10	10	69	122	179	233	330	415	570	677	96	141	185	227	307	380	528	632	100	139	183	222	297	368	513	616
		15	73	181	283	379	512	621	809	926	84	143	205	265	375	469	645	764	100	151	205	258	357	444	615	732
		20	84	242	395	531	740	892	1123	1263	84	183	280	375	514	638	840	971	93	162	239	313	443	552	751	883
		25	95	270	477	668	965	1171	1469	1639	89	239	382	519	710	860	1107	1256	92	201	309	416	578	718	947	1093
		30	86	257	528	780	1187	1427	1836	2026	100	290	483	653	928	1119	1417	1592	96	248	400	546	755	922	1196	1361
	Sta. 15	10	147	241	333	410	545	647	821	931	180	259	336	404	519	613	779	882	178	255	323	392	502	593	757	858
		15	172	337	488	612	790	933	1139	1258	160	254	351	436	582	698	896	1018	176	262	350	430	565	674	866	985
		20	172	442	673	879	1126	1316	1591	1736	170	306	439	551	737	879	1105	1242	163	265	374	470	636	766	989	1126
		25	186	512	814	1081	1471	1736	2084	2282	184	395	588	762	982	1168	1437	1588	170	310	451	573	775	932	1184	1337
		30	183	501	892	1276	1819	2141	2635	2836	188	481	742	972	1288	1507	1846	2027	183	384	575	747	984	1179	1471	1638
	Sta. 20	10	265	462	644	791	1029	1194	1442	1578	302	463	612	743	948	1100	1338	1463	299	453	583	713	909	1057	1292	1414
		15	302	596	862	1074	1384	1616	1917	2072	288	492	688	852	1113	1301	1584	1737	302	486	661	817	1059	1238	1513	1660
		20	289	732	1111	1452	1834	2133	2542	2733	305	574	828	1032	1361	1592	1922	2097	292	516	736	921	1215	1428	1748	1920
		25	302	833	1305	1710	2303	2698	3203	3482	322	689	1025	1320	1687	1988	2384	2580	308	586	855	1078	1431	1684	2051	2244
		30	301	816	1401	1987	2778	3265	3958	4227	316	799	1227	1603	2094	2433	2931	3171	325	682	1019	1314	1709	2020	2445	2661

Relative Motion																															
Sta. 1	10	47	76	103	124	157	179	208	221	47	70	91	108	135	153	177	189	46	67	85	102	126	142	166	177
	15	46	78	110	137	176	203	240	257	47	74	99	120	151	173	202	216	46	70	92	111	139	158	185	198
	20	43	77	112	146	191	223	268	288	46	76	105	130	166	192	226	242	46	72	98	119	151	174	205	219
	25	42	74	112	146	202	238	290	316	44	75	108	137	178	207	248	267	45	73	101	126	162	188	223	240
	30	41	70	109	149	210	252	312	339	42	74	109	140	188	220	267	289	43	73	104	132	171	200	240	259
Sta. 2	10	45	70	92	110	136	153	175	185	44	63	79	93	113	126	144	152	42	59	73	85	103	116	132	140
	15	44	73	100	123	156	178	207	220	44	68	88	105	130	147	169	179	43	63	81	95	117	132	152	161
	20	42	72	104	133	171	199	235	252	44	70	95	116	145	166	193	206	44	66	87	105	131	148	172	183
	25	41	71	104	135	183	214	258	280	43	71	99	124	158	183	216	231	43	68	92	113	142	163	191	204
	30	40	67	102	137	191	228	281	303	41	70	101	129	169	196	235	253	42	69	95	119	152	176	209	224
Sta. 3	10	43	64	81	95	115	128	143	150	40	55	67	77	91	100	112	117	38	50	60	69	81	90	100	104
	15	43	67	90	109	136	153	176	185	42	61	77	90	109	121	137	143	40	56	69	80	96	106	120	125
	20	41	68	95	120	152	175	204	217	42	64	85	102	125	141	162	170	41	60	77	90	110	123	140	147
	25	40	67	96	123	165	191	228	246	41	66	90	111	139	159	185	196	41	63	82	99	123	139	160	169
	30	40	64	95	126	174	206	250	270	40	66	93	116	150	173	205	219	41	64	86	106	133	153	178	189
Sta. 4	10	40	57	71	80	95	104	114	117	37	47	56	62	71	77	83	85	34	43	50	55	63	67	72	73
	15	41	62	81	95	116	130	146	153	39	54	66	76	89	98	107	111	37	49	58	66	76	83	90	93
	20	40	63	86	107	133	152	175	185	40	59	75	88	106	118	132	137	39	54	66	76	91	100	110	115
	25	40	63	89	112	147	169	200	214	40	61	81	98	120	136	155	163	40	57	73	86	104	116	131	136
	30	39	61	89	116	157	185	223	239	40	62	85	105	133	151	176	187	40	59	78	94	115	130	149	157
Sta. 20	10	37	52	67	81	104	121	147	160	33	48	63	77	99	115	139	152	33	48	64	77	99	115	139	151
	15	38	54	70	87	109	128	155	169	36	49	63	76	97	113	137	149	34	47	61	74	95	110	133	145
	20	38	58	78	96	124	144	174	190	37	49	63	76	96	112	136	149	36	48	61	72	92	107	129	141
	25	40	62	87	110	146	172	206	224	37	50	64	78	98	115	139	152	36	48	60	72	90	104	126	138
	30	40	63	94	127	176	204	250	268	38	52	67	82	106	123	149	164	36	48	60	73	89	103	126	137
Sta. 1	10	265	329	390	437	507	550	595	607	267	321	365	403	454	485	517	524	267	315	352	387	431	457	485	488
	15	303	372	445	506	595	653	718	738	307	369	427	473	542	583	625	635	308	364	412	453	510	544	578	585
	20	340	408	488	570	667	741	827	854	347	413	482	540	623	678	735	750	349	410	469	517	588	631	676	686
	25	379	443	525	605	734	812	916	960	385	453	530	601	694	762	836	859	389	452	520	578	660	715	772	787
	30	421	476	555	645	783	881	1003	1046	425	490	571	651	761	835	927	957	428	493	566	635	726	791	863	883
Sta. 2	10	260	314	363	400	454	486	515	519	258	301	333	361	397	416	433	432	255	290	317	341	370	386	397	392
	15	299	359	420	469	541	586	633	645	301	352	397	433	484	512	537	539	299	343	379	409	448	470	488	485
	20	337	397	464	532	611	672	737	755	342	398	454	500	564	605	643	650	342	391	437	474	526	556	582	583
	25	377	433	503	570	677	740	824	855	381	440	503	561	635	688	741	754	383	436	490	535	599	639	676	681
	30	419	468	536	611	725	807	905	937	421	478	546	612	701	760	829	849	423	478	538	593	665	715	764	774
Sta. 3	10	254	298	335	362	402	422	436	434	249	280	302	320	340	349	351	341	243	267	283	297	311	317	313	300
	15	295	345	394	432	487	519	550	553	295	334	367	392	426	443	451	445	291	322	346	366	389	399	400	389
	20	335	386	441	495	556	604	649	659	337	383	426	460	506	534	553	551	335	374	407	432	466	483	491	483
	25	375	424	482	537	622	671	734	753	378	427	477	521	577	615	648	652	378	421	462	495	539	565	582	578
	30	417	461	518	579	671	735	810	833	419	467	522	574	642	687	734	743	420	465	512	553	605	640	668	668
Sta. 4	10	249	283	309	328	353	363	363	354	242	262	275	284	292	291	279	261	235	249	258	263	266	262	243	221
	15	292	332	369	397	437	457	472	467	289	318	340	356	374	380	373	359	284	305	320	329	338	337	323	303
	20	333	375	419	460	506	540	567	569	334	369	400	423	453	468	471	460	331	358	380	395	413	418	409	392
	25	374	415	462	506	571	608	650	659	376	415	453	485	524	548	563	556	375	408	437	458	485	498	497	483
	30	417	455	501	550	621	670	724	737	418	458	501	540	589	620	646	645	418	454	489	518	552	572	580	570
Sta. 20	10	243	268	293	313	347	369	391	392	231	252	274	294	325	345	364	367	227	248	273	293	325	345	364	369
	15	289	316	343	370	397	422	445	444	281	301	322	338	364	379	391	385	274	293	312	328	353	368	377	372
	20	333	368	403	437	481	508	541	545	328	348	367	382	400	414	420	408	323	341	358	370	389	399	399	385
	25	379	421	469	515	587	634	681	699	373	394	413	432	446	458	462	447	370	387	402	413	424	430	423	403
	30	423	467	530	603	713	777	864	881	418	442	466	485	513	524	532	521	415	432	445	457	463	466	454	428

TABLE A-22 SEAKEEPING RESPONSES FOR $C_B = 0.90$, $L/B = 5.5$, LCB $= +2.5\%$

		Froude No	$B/T = 2$								$B/T = 3$								$B/T = 4$							
			Significant Wave Height/LBP								Significant Wave Height/LBP								Significant Wave Height/LBP							
		[%]	0.015	0.020	0.025	0.030	0.040	0.050	0.075	0.100	0.015	0.020	0.025	0.030	0.040	0.050	0.075	0.100	0.015	0.020	0.025	0.030	0.040	0.050	0.075	0.100
Heave		10	4	14	29	44	75	103	172	238	3	11	20	31	55	81	147	214	3	9	17	27	49	74	140	207
		15	3	13	31	50	87	121	194	260	4	13	25	38	66	93	160	226	3	10	20	31	56	82	148	215
		20	2	12	30	52	95	135	215	283	4	13	28	44	76	105	174	240	4	12	23	36	63	90	158	224
		25	1	11	25	52	101	148	234	305	3	12	29	47	84	116	189	256	4	12	26	41	71	100	169	235
		30	1	7	21	51	105	153	250	326	2	11	29	48	89	126	204	272	3	11	27	43	77	108	180	247
Pitch		10	14	43	75	105	160	202	278	329	15	40	67	94	141	181	253	303	15	37	62	87	132	171	243	293
		15	11	36	73	110	174	218	301	352	13	39	68	97	148	190	265	317	13	36	63	90	137	177	251	301
		20	7	29	74	109	181	233	326	382	12	36	67	99	154	199	277	329	11	35	62	90	140	181	257	309
		25	5	29	61	109	187	258	353	413	9	30	66	99	162	207	290	344	10	32	61	90	143	186	264	316
		30	3	21	47	111	195	268	382	449	6	26	64	97	164	215	305	361	9	28	59	90	147	190	271	324
Bending Moment		10	45	81	122	162	232	287	381	435	56	107	156	202	278	333	422	473	65	123	178	228	305	363	451	500
		15	45	90	129	168	234	296	391	449	56	108	159	207	286	345	437	489	64	125	184	235	319	379	471	522
		20	46	95	138	186	257	317	410	466	56	112	168	219	303	366	464	518	64	128	191	248	339	405	504	557
		25	47	98	158	205	289	343	447	504	58	119	180	238	328	398	504	561	65	133	203	266	366	439	549	607
		30	48	104	170	232	329	405	516	576	60	124	196	263	369	444	561	623	68	140	216	289	401	483	606	670
Added Resistance		10	6	26	64	110	205	274	392	454	11	34	70	110	189	249	354	410	17	43	84	128	218	287	410	479
		15	4	19	55	102	219	317	510	634	8	29	65	111	206	290	459	594	13	37	76	122	221	311	511	693
		20	2	11	46	95	233	360	628	814	6	24	61	112	224	331	563	778	9	31	68	117	225	335	611	906
		25	2	8	33	85	226	382	708	940	5	19	58	111	248	380	676	926	8	27	67	123	256	387	712	1031
		30	1	5	19	74	219	404	788	1066	3	14	54	110	272	429	789	1074	6	24	67	130	287	439	814	1155
Acceleration	Sta. 0	10	96	281	480	659	957	1162	1478	1652	136	332	525	701	958	1153	1433	1586	152	332	514	670	913	1093	1362	1509
		15	89	258	487	725	1102	1357	1755	1952	127	353	589	810	1148	1385	1744	1932	151	373	597	805	1109	1338	1670	1848
		20	65	214	514	749	1210	1513	2025	2287	125	349	624	887	1308	1603	2042	2271	147	393	658	907	1292	1564	1973	2189
		25	56	218	467	762	1294	1729	2298	2604	112	314	641	946	1467	1804	2341	2610	148	393	696	987	1455	1781	2270	2525
		30	53	183	385	818	1381	1878	2598	2979	98	287	659	974	1576	1986	2641	2972	142	369	720	1053	1614	1987	2571	2864
	Sta. 5	10	46	142	264	376	573	712	942	1076	71	184	298	405	568	694	893	1012	82	186	291	386	537	654	843	959
		15	41	132	270	415	665	848	1138	1298	68	196	341	479	700	858	1111	1255	82	212	348	475	671	820	1054	1191
		20	30	114	280	435	736	960	1328	1530	66	192	368	536	818	1017	1332	1505	81	227	391	548	802	984	1273	1437
		25	26	117	255	448	797	1099	1518	1756	57	175	384	579	927	1165	1553	1761	82	226	422	610	923	1146	1496	1689
		30	26	97	217	481	861	1195	1716	2009	50	165	394	603	1008	1304	1776	2027	77	213	442	659	1040	1300	1722	1948
	Sta. 10	10	36	103	198	288	441	551	738	854	35	89	151	213	319	408	570	681	38	77	126	178	273	356	515	625
		15	29	101	233	354	575	725	979	1121	42	120	212	301	455	570	768	895	39	104	178	251	377	481	666	790
		20	21	99	248	393	669	881	1215	1398	45	133	260	385	596	745	997	1144	46	132	234	333	505	635	858	1000
		25	18	103	218	421	752	1048	1440	1664	37	126	297	449	728	916	1236	1416	51	146	281	413	638	802	1075	1238
		30	16	78	188	446	825	1148	1652	1933	30	127	317	490	827	1078	1479	1698	47	145	318	481	770	967	1306	1496
	Sta. 15	10	81	225	373	507	717	859	1077	1203	85	181	278	368	505	617	800	914	83	155	234	310	437	539	716	830
		15	73	212	426	620	938	1124	1439	1590	87	227	364	491	684	825	1052	1186	86	189	296	397	553	679	887	1016
		20	53	190	461	675	1087	1360	1800	2018	93	249	432	608	878	1066	1353	1511	90	228	370	503	711	864	1114	1262
		25	44	195	407	714	1210	1632	2144	2417	83	233	483	703	1077	1304	1682	1876	97	254	435	610	883	1079	1382	1555
		30	39	154	337	756	1314	1787	2468	2823	69	220	520	759	1220	1525	2020	2270	95	251	485	705	1067	1299	1681	1881
	Sta. 20	10	135	374	607	816	1134	1345	1653	1819	151	328	503	659	885	1060	1320	1462	151	298	450	584	798	958	1207	1347
		15	123	349	674	974	1445	1712	2152	2345	149	387	616	825	1129	1343	1669	1843	156	346	538	714	970	1167	1463	1625
		20	90	303	730	1046	1657	2036	2656	2949	155	415	702	976	1384	1666	2069	2279	157	395	634	854	1180	1414	1770	1961
		25	75	310	648	1094	1824	2429	3141	3507	140	383	763	1102	1659	1984	2513	2764	164	425	714	987	1404	1695	2121	2347
		30	68	249	531	1162	1969	2657	3611	4092	119	353	815	1172	1852	2279	2971	3304	162	415	773	1110	1648	1985	2516	2774

Relative Motion																														
Sta. 1																														
	10	40	65	95	122	166	195	239	261	42	67	92	115	148	172	205	221	42	65	88	107	136	157	186	199
	15	39	61	91	124	176	212	265	289	40	66	94	121	162	189	230	249	41	66	91	115	149	173	208	224
	20	38	57	91	122	182	222	287	318	40	63	94	123	171	204	251	274	40	65	92	119	159	187	227	247
	25	38	56	85	119	185	237	307	342	39	60	92	124	179	215	271	297	40	63	92	120	166	198	245	267
	30	38	54	78	122	188	246	329	372	38	57	91	122	182	224	288	320	39	60	91	121	173	207	261	286
Sta. 2	10	39	62	88	112	150	175	211	229	41	63	84	103	131	150	176	188	41	60	79	94	118	134	155	165
	15	39	59	86	115	160	192	237	258	39	63	87	111	145	168	201	216	40	62	84	103	131	151	178	191
	20	38	56	86	114	167	203	259	287	39	61	88	114	155	183	223	242	39	62	86	108	142	165	199	214
	25	37	55	82	112	171	218	280	311	38	58	87	115	164	195	243	265	39	60	86	111	150	178	217	235
	30	37	53	75	115	174	227	302	340	38	56	86	115	168	205	261	288	38	58	85	113	158	188	233	254
Sta. 3	10	39	59	82	102	135	155	185	199	39	59	77	92	114	129	148	156	39	55	70	82	100	112	127	134
	15	38	57	81	106	146	173	212	229	39	59	81	100	128	147	174	185	39	58	76	92	114	130	150	160
	20	38	55	82	107	154	185	234	258	38	59	82	105	140	163	196	212	39	58	79	98	126	145	171	183
	25	37	54	78	106	158	200	255	282	38	56	82	107	149	176	217	236	38	58	80	102	135	158	190	205
	30	37	53	73	108	162	210	277	310	37	55	82	107	155	187	236	259	38	56	81	104	144	169	207	225
Sta. 4	10	38	57	76	94	121	137	161	172	39	55	69	81	98	109	123	128	38	51	62	71	84	92	102	106
	15	38	56	77	98	133	156	189	203	38	56	74	91	113	129	149	157	38	54	69	81	99	111	125	131
	20	38	54	77	100	142	169	212	232	38	56	77	96	126	145	172	184	38	56	73	89	111	126	147	155
	25	37	53	75	100	147	184	233	257	38	55	78	100	136	159	194	209	38	56	75	94	122	140	166	177
	30	37	52	71	103	152	194	255	285	37	54	78	101	143	170	213	233	38	55	76	97	130	152	184	198
Sta. 20	10	39	54	71	88	117	137	167	183	37	48	59	71	90	105	129	141	36	47	59	70	88	103	125	136
	15	39	56	81	105	147	172	214	233	38	49	61	73	94	110	135	149	37	47	57	68	85	98	121	133
	20	39	57	89	118	174	211	270	298	38	51	66	81	107	125	154	169	37	48	58	68	86	99	122	135
	25	39	58	87	127	197	256	327	363	39	53	73	91	126	148	184	202	38	49	60	72	92	107	132	145
	30	38	56	81	136	217	285	382	430	39	54	78	100	143	173	220	243	38	50	65	78	104	121	150	165
Relative Velocity																														
Sta. 1	10	247	293	349	402	487	541	614	644	251	300	353	399	463	508	559	575	253	299	346	384	440	477	517	527
	15	289	328	381	442	541	608	698	729	290	338	395	450	530	583	650	673	292	341	393	441	508	554	607	623
	20	330	362	419	477	589	660	771	817	332	375	432	492	586	650	731	762	333	379	435	489	569	623	689	711
	25	372	403	452	507	627	720	841	892	373	410	467	531	641	710	808	842	374	417	473	531	624	686	765	793
	30	415	443	481	549	664	773	918	981	415	448	505	565	685	762	880	926	416	454	510	571	677	744	837	869
Sta. 2	10	246	287	336	380	451	494	552	573	248	291	334	371	422	456	491	499	248	287	324	353	395	421	445	448
	15	287	324	370	422	504	559	632	655	288	331	378	424	488	530	580	594	289	330	373	411	463	498	533	541
	20	329	360	409	458	553	612	702	737	329	369	418	467	544	596	658	680	330	371	417	462	525	566	614	627
	25	371	400	444	491	592	668	768	808	371	405	455	508	599	655	733	757	371	410	457	506	580	629	688	706
	30	414	440	476	532	629	720	839	888	413	443	493	545	644	707	802	836	413	448	496	547	633	687	759	780
Sta. 3	10	245	282	323	360	417	450	493	506	247	283	317	345	383	406	427	427	246	277	305	326	354	370	379	375
	15	287	321	361	403	470	515	571	587	287	325	364	400	449	480	513	519	288	323	356	385	422	446	465	464
	20	329	358	400	442	519	568	639	664	329	364	405	446	507	546	591	603	329	365	403	437	484	514	544	548
	25	371	399	437	477	560	621	702	731	371	403	444	488	561	605	663	678	371	405	445	484	541	577	617	625
	30	414	439	472	519	599	673	768	804	413	442	484	527	608	658	730	753	413	445	485	527	594	636	686	697
Sta. 4	10	245	278	312	342	387	412	441	446	246	276	302	323	349	364	371	364	244	270	289	303	321	327	323	311
	15	287	318	352	387	441	476	517	526	288	320	351	379	415	437	455	452	288	317	342	363	388	401	405	396
	20	329	357	393	428	491	531	584	601	330	361	395	427	474	503	531	534	330	361	391	417	450	470	483	478
	25	371	398	432	466	534	583	645	665	372	401	436	472	529	562	602	609	372	403	435	465	508	533	555	554
	30	414	439	469	507	574	633	707	733	414	441	478	513	577	616	667	682	415	443	477	511	562	592	623	625
Sta. 20	10	249	278	308	336	382	411	445	455	245	265	283	299	318	332	346	342	243	262	279	294	314	327	338	332
	15	292	325	369	414	493	536	602	620	290	312	330	345	370	382	393	388	288	306	321	333	347	354	355	343
	20	334	368	426	482	596	668	781	826	334	360	385	407	442	463	483	480	333	352	366	376	391	395	391	375
	25	377	412	465	540	688	815	963	1029	378	406	440	473	531	562	605	612	377	399	417	430	450	458	457	441
	30	419	452	497	599	769	928	1143	1253	421	451	495	535	618	668	745	770	421	445	469	490	523	538	550	539

TABLE A-23 SEAKEEPING RESPONSES FOR $C_B = 0.90$, $L/B = 7.0$, LCB = $+2.5\%$

		Froude No.	$B/T = 2$								$B/T = 3$								$B/T = 4$							
			Significant Wave Height/LBP								Significant Wave Height/LBP								Significant Wave Height/LBP							
		[%]	0.015	0.020	0.025	0.030	0.040	0.050	0.075	0.100	0.015	0.020	0.025	0.030	0.040	0.050	0.075	0.100	0.015	0.020	0.025	0.030	0.040	0.050	0.075	0.100
Heave		10	5	14	26	38	63	89	154	220	4	9	17	27	50	75	140	207	4	9	16	25	47	71	137	203
		15	5	17	32	48	78	106	173	238	4	12	22	33	57	83	149	215	4	10	18	28	51	76	141	208
		20	5	16	36	56	92	123	194	259	5	15	27	40	67	94	160	226	4	12	21	33	57	83	149	215
		25	3	14	38	59	103	139	215	281	5	16	31	47	77	106	173	239	4	13	25	38	65	91	157	223
		30	2	15	36	60	109	151	235	303	4	15	33	52	87	117	188	253	4	14	28	43	72	100	168	233
Pitch		10	19	49	80	109	158	199	271	320	18	42	68	94	140	178	249	299	17	39	64	88	132	170	241	291
		15	16	50	84	116	172	214	291	342	17	43	72	100	148	188	261	311	16	39	66	91	137	176	249	299
		20	16	47	84	123	184	232	312	363	15	44	74	104	155	197	272	323	15	39	67	94	141	182	256	306
		25	11	36	85	126	201	248	335	389	14	43	75	106	161	205	282	334	13	39	67	96	145	186	261	313
		30	7	33	85	122	204	259	363	420	13	39	73	109	168	214	294	346	12	38	67	96	148	190	267	319
Bending Moment		10	45	84	122	156	218	261	333	376	57	104	148	187	249	295	365	404	61	113	160	201	265	311	382	420
		15	46	83	122	158	218	266	338	380	55	104	150	191	255	302	374	413	61	115	164	206	273	321	392	431
		20	45	88	129	164	227	273	350	394	55	106	154	196	265	315	389	430	61	118	170	216	286	337	412	452
		25	46	96	136	178	239	292	370	413	55	109	161	207	280	334	414	456	61	121	177	227	304	359	440	482
		30	46	97	149	198	269	321	400	446	55	114	171	221	300	359	445	492	62	125	186	241	325	385	474	521
Added Resistance		10	7	23	47	74	124	164	226	258	12	30	57	85	142	184	259	300	17	39	71		173	224	319	373
		15	5	20	48	82	151	211	317	393	9	27	54	86	150	207	328	434	13	34	64	98	172	239	395	544
		20	3	18	48	91	178	259	409	529	6	24	52	87	157	229	396	568	10	28	56	92	170	254	471	715
		25	2	13	45	87	196	296	508	658	5	22	53	97	189	278	481	669	8	27	59	100	193	291	537	798
		30	1	9	41	84	213	334	606	788	5	20	55	107	221	328	566	770	7	26	61	108	216	327	604	882
Acceleration	Sta. 0	10	170	404	628	826	1104	1321	1607	1762	197	401	600	760	1012	1196	1459	1602	199	379	554	704	941	1112	1371	1510
		15	147	427	707	958	1343	1588	1976	2169	203	469	727	948	1270	1507	1843	2016	215	453	688	883	1184	1404	1720	1887
		20	151	430	743	1050	1507	1853	2317	2559	191	513	822	1110	1511	1805	2222	2435	218	513	800	1056	1424	1702	2085	2286
		25	119	359	755	1123	1730	2089	2665	2947	187	527	887	1217	1731	2079	2586	2849	213	556	892	1206	1655	1982	2451	2690
		30	93	322	795	1131	1825	2262	3034	3389	184	512	920	1317	1928	2345	2954	3250	211	576	962	1319	1872	2251	2807	3094
	Sta. 5	10	86	222	355	475	653	790	994	1114	108	225	340	435	591	709	893	1005	109	214	315	404	549	658	838	950
		15	76	230	400	558	811	976	1248	1394	108	267	421	560	760	915	1146	1279	118	259	396	516	703	844	1064	1193
		20	75	225	425	617	930	1155	1494	1676	104	294	485	664	929	1120	1411	1572	121	298	473	633	867	1047	1315	1466
		25	57	193	436	663	1059	1322	1738	1960	104	303	530	744	1086	1321	1678	1873	118	326	537	735	1032	1247	1575	1756
		30	45	181	452	677	1134	1456	1993	2260	100	290	558	816	1233	1514	1952	2174	120	340	587	818	1189	1446	1839	2054
	Sta. 10	10	46	123	200	274	389	482	647	755	53	94	142	192	284	366	522	631	66	102	143	186	271	347	500	607
		15	56	163	283	394	579	705	914	1040	52	127	205	284	404	507	691	812	58	111	171	234	344	440	618	739
		20	58	171	340	499	758	929	1211	1361	60	174	290	397	572	704	923	1061	58	143	233	324	465	583	792	927
		25	40	151	380	569	917	1141	1503	1702	71	205	360	508	749	922	1193	1354	64	183	310	427	620	768	1013	1166
		30	30	157	395	603	1019	1320	1804	2043	71	209	412	609	929	1139	1486	1669	74	216	378	530	785	970	1264	1442
	Sta. 15	10	115	249	372	481	629	751	936	1045	111	186	268	341	467	568	743	855	120	189	264	331	449	546	716	826
		15	116	323	508	671	914	1070	1320	1457	118	233	348	450	608	735	939	1064	113	198	291	376	522	638	837	963
		20	126	345	597	841	1184	1423	1751	1918	122	301	466	618	824	983	1233	1375	119	239	363	475	651	792	1022	1161
		25	96	294	659	956	1467	1740	2195	2420	132	357	575	771	1070	1277	1583	1759	125	297	463	618	837	1008	1280	1438
		30	73	281	699	998	1609	1995	2656	2947	137	371	651	923	1322	1587	1981	2176	133	349	563	758	1056	1265	1590	1776
	Sta. 20	10	201	434	648	833	1076	1272	1537	1675	198	358	518	654	872	1032	1278	1416	206	351	497	624	829	983	1223	1357
		15	192	533	834	1093	1469	1704	2068	2250	212	431	643	823	1094	1298	1590	1748	205	385	568	726	978	1163	1445	1601
		20	208	567	950	1324	1829	2194	2651	2879	212	518	800	1056	1384	1636	1999	2183	216	447	675	874	1172	1397	1726	1903
		25	162	477	1029	1486	2247	2632	3272	3567	219	591	941	1251	1712	2022	2464	2700	220	519	806	1067	1419	1692	2078	2281
		30	124	443	1096	1534	2437	2973	3920	4318	228	608	1035	1452	2043	2441	2992	3253	226	586	933	1244	1705	2022	2484	2729

Relative Motion	Sta. 1	10	43	72	101	127	162	189	223	240	44	69	92	111	141	161	188	201	44	66	86	103	129	147	172	184
		15	41	70	103	133	179	208	253	273	43	71	98	122	156	181	215	230	44	68	92	112	143	164	194	208
		20	40	68	102	135	187	226	277	302	41	70	101	129	169	198	238	257	43	69	96	120	155	180	215	231
		25	39	61	99	136	200	239	300	328	41	68	101	131	179	211	258	281	41	68	98	125	164	193	233	252
		30	38	58	99	133	201	246	322	357	40	65	99	133	187	224	277	302	40	67	98	127	172	203	249	271
	Sta. 2	10	42	68	92	114	144	165	193	206	42	63	82	98	121	136	157	166	41	59	75	89	109	122	141	149
		15	40	67	95	122	161	186	223	239	42	66	89	109	137	157	184	195	42	63	82	99	123	140	163	173
		20	40	65	95	125	170	203	247	269	41	66	93	117	151	175	208	223	41	65	87	107	136	156	184	196
		25	39	60	93	127	183	217	270	295	40	65	94	121	162	189	228	247	40	65	90	113	147	170	203	218
		30	38	57	94	124	186	225	292	323	39	63	93	123	170	202	248	269	40	64	91	116	155	182	220	238
	Sta. 3	10	41	63	84	101	126	143	164	173	40	58	72	84	102	113	127	133	39	53	65	75	89	99	111	116
		15	40	63	88	111	144	164	194	207	41	61	80	96	119	134	154	162	40	57	73	86	104	117	133	139
		20	39	62	89	115	154	182	219	237	40	63	85	105	133	153	179	190	40	60	79	95	118	134	154	163
		25	38	58	88	117	167	197	243	263	39	62	87	110	145	168	200	215	39	61	83	102	129	148	174	186
		30	38	56	88	116	171	206	265	291	39	61	87	114	154	182	220	237	39	61	85	106	139	161	192	206
	Sta. 4	10	40	59	76	89	109	122	137	143	38	52	63	72	84	92	100	103	37	47	56	63	72	78	84	86
		15	39	60	81	100	127	144	168	177	39	57	72	84	102	113	127	132	38	52	64	74	87	96	106	109
		20	39	59	83	105	139	163	194	208	39	59	78	94	117	132	152	160	39	56	71	83	101	113	127	133
		25	38	57	83	109	152	178	218	235	39	59	81	100	129	148	174	185	39	57	75	91	113	128	147	156
		30	38	55	84	109	157	189	240	263	39	58	82	105	139	163	194	208	39	58	78	97	124	141	166	177
	Sta. 20	10	38	52	67	83	104	122	148	162	36	49	62	74	95	110	133	145	35	48	61	73	93	108	131	143
		15	39	56	75	92	122	141	172	188	37	49	61	74	93	108	132	145	36	48	60	71	90	104	126	138
		20	40	59	84	110	148	175	212	230	37	50	63	75	96	111	137	150	37	48	59	70	87	101	123	134
		25	39	58	93	125	180	211	261	286	38	52	67	81	106	124	151	165	37	48	59	69	87	100	123	135
		30	39	59	100	133	200	244	317	348	39	54	72	91	123	143	176	191	38	49	60	71	91	106	129	141
Relative Velocity	Sta. 1	10	254	311	372	426	500	553	610	630	257	310	360	399	459	495	534	544	258	305	347	382	431	461	493	500
		15	292	347	414	479	575	632	714	740	297	353	413	465	537	586	640	655	298	351	402	445	507	547	589	599
		20	333	383	449	519	625	706	798	838	336	392	458	522	606	666	736	759	338	393	452	505	577	628	682	697
		25	374	414	480	558	691	769	883	922	376	429	497	564	669	736	822	854	378	432	496	558	642	700	769	790
		30	416	450	521	587	728	813	964	1021	418	465	532	606	722	802	903	939	419	470	536	602	701	767	848	877
	Sta. 2	10	251	301	352	396	456	497	539	550	253	296	335	366	410	435	458	461	251	288	319	345	379	399	415	414
		15	290	339	396	451	528	575	638	656	293	342	390	431	487	524	561	568	293	336	377	409	455	483	507	509
		20	331	376	434	492	580	646	719	750	333	382	437	489	556	603	655	668	334	381	428	470	525	563	599	604
		25	373	410	466	532	642	707	800	828	374	421	478	534	619	672	738	759	375	422	474	524	590	635	684	695
		30	414	446	507	564	682	752	874	919	415	458	516	577	672	737	815	841	416	461	516	570	649	700	761	778
	Sta. 3	10	250	292	333	367	414	443	470	474	249	284	312	334	364	379	387	382	246	274	295	312	332	341	342	333
		15	289	332	379	424	485	521	566	575	291	331	369	400	441	466	485	484	290	324	354	377	407	423	431	424
		20	331	371	419	467	538	590	645	666	332	374	418	459	510	544	577	581	332	371	407	438	478	502	519	516
		25	372	407	454	508	598	650	722	741	373	414	462	507	573	613	658	669	374	414	456	494	542	574	602	604
		30	414	444	495	544	640	697	791	824	415	453	501	551	627	677	733	749	415	455	500	542	602	639	679	685
	Sta. 4	10	248	283	316	340	375	394	408	404	246	273	293	307	324	330	325	311	242	262	276	285	293	294	281	263
		15	289	326	364	399	445	472	501	502	290	322	351	372	400	414	418	409	288	314	335	349	366	372	364	349
		20	331	366	406	444	501	540	578	589	332	367	402	432	468	491	506	502	332	362	390	410	436	449	449	437
		25	373	404	444	488	558	600	652	663	374	409	447	482	531	560	586	587	374	407	440	467	500	520	530	522
		30	415	443	486	526	603	648	718	742	416	450	489	529	587	623	660	665	416	450	486	518	561	586	605	601
	Sta. 20	10	247	273	298	324	350	373	397	399	242	263	284	300	326	342	357	354	236	256	276	293	319	335	348	346
		15	292	324	358	387	436	462	496	505	288	308	326	343	360	374	383	374	285	304	321	334	353	364	368	357
		20	336	374	420	470	543	594	649	665	332	354	373	389	410	420	427	417	330	348	363	375	386	392	389	371
		25	378	415	480	548	672	734	831	864	377	403	427	447	478	496	507	501	375	393	407	417	428	430	421	399
		30	421	458	538	608	765	859	1029	1089	421	451	483	515	565	594	623	621	420	440	456	467	483	486	476	455

TABLE A-24 SEAKEEPING RESPONSES FOR $C_B = 0.90$, $L/B = 8.5$, LCB = $+2.5\%$

		Froude No.	$B/T = 2$								$B/T = 3$								$B/T = 4$							
			Significant Wave Height/LBP								Significant Wave Height/LBP								Significant Wave Height/LBP							
		[%]	0.015	0.020	0.025	0.030	0.040	0.050	0.075	0.100	0.015	0.020	0.025	0.030	0.040	0.050	0.075	0.100	0.015	0.020	0.025	0.030	0.040	0.050	0.075	0.100
Heave		10	5	12	21	31	54	79	145	211	5	10	17	26	48	72	137	204	6	10	16	25	46	70	135	201
		15	5	17	29	41	67	92	158	223	5	11	19	29	52	77	142	209	5	10	17	26	48	73	138	204
		20	6	20	36	52	82	109	175	240	5	13	24	35	59	85	150	216	4	11	19	29	52	77	143	209
		25	6	20	40	60	96	127	195	260	5	16	29	42	69	95	161	227	4	13	23	34	58	84	150	216
		30	4	17	42	65	109	142	216	280	6	18	33	49	79	107	174	239	5	15	27	39	66	92	158	224
Pitch		10	22	49	78	105	152	191	262	311	19	42	68	92	137	174	245	294	19	40	64	88	131	169	239	289
		15	21	53	85	117	166	209	282	331	19	44	72	98	145	184	256	306	18	41	66	91	136	175	247	297
		20	18	54	91	125	181	223	301	351	19	46	75	104	152	193	267	317	17	41	68	94	141	180	253	304
		25	19	55	93	131	190	241	319	372	17	47	78	109	159	201	277	327	16	41	69	97	144	185	259	310
		30	15	45	90	136	211	256	344	393	15	46	79	111	166	208	286	338	15	41	70	99	147	189	264	315
Bending Moment		10	46	83	119	151	201	239	298	332	53	95	134	168	221	260	319	351	56	101	142	177	232	271	330	362
		15	44	82	117	148	202	239	299	334	53	97	137	172	226	265	324	356	57	103	145	181	237	276	335	367
		20	45	82	118	151	204	246	306	340	52	98	140	177	233	274	334	367	57	106	150	188	246	287	347	380
		25	44	85	125	158	216	254	320	354	53	101	145	183	244	287	350	384	58	109	156	197	258	302	366	400
		30	45	93	133	169	223	271	336	375	53	103	151	193	257	304	372	408	58	112	163	207	274	321	390	426
Added Resistance		10	7	19	36	54	89	116	159	182	12	28	50	72	117	150	210	243	16	35	60	87	141	182	258	302
		15	5	19	39	63	109	147	221	279	9	24	46	69	118	162	260	350	13	30	55	82	141	196	325	452
		20	4	18	42	72	128	177	283	376	7	21	41	66	119	174	309	456	10	26	49	77	141	210	392	601
		25	3	16	43	80	162	225	368	472	6	21	46	77	143	208	366	525	8	25	50	82	154	232	436	660
		30	2	13	43	89	195	273	453	569	5	21	50	87	167	243	423	594	7	24	51	88	167	255	481	718
Acceleration	Sta. 0	10	232	477	706	886	1156	1354	1624	1765	232	431	613	767	1007	1178	1431	1569	241	417	577	724	949	1112	1363	1499
		15	235	550	847	1101	1453	1726	2070	2249	262	531	788	990	1306	1532	1845	2008	262	495	725	906	1199	1411	1714	1875
		20	202	584	945	1275	1741	2042	2507	2724	273	614	939	1212	1604	1891	2284	2482	281	581	874	1111	1477	1740	2108	2299
		25	210	602	1010	1382	1942	2365	2897	3196	259	675	1059	1416	1885	2242	2722	2961	290	655	1010	1314	1752	2076	2523	2748
		30	186	538	1007	1492	2223	2647	3345	3621	249	704	1151	1553	2162	2559	3147	3439	284	712	1126	1505	2021	2409	2940	3206
	Sta. 5	10	125	268	402	512	676	804	991	1101	129	244	349	439	585	694	870	980	137	236	329	414	550	655	830	938
		15	121	313	489	647	871	1042	1284	1421	147	304	456	577	771	916	1132	1257	146	284	415	526	706	839	1048	1173
		20	109	326	547	752	1062	1264	1584	1748	149	357	553	727	969	1160	1426	1574	157	338	510	658	885	1054	1308	1452
		25	111	326	588	829	1209	1484	1869	2082	142	395	635	858	1169	1398	1732	1912	162	387	603	798	1074	1288	1593	1762
		30	93	290	595	895	1385	1681	2176	2402	141	414	697	956	1362	1631	2040	2257	159	427	685	926	1266	1520	1891	2090
	Sta. 10	10	60	116	173	230	326	412	568	675	85	126	169	211	292	366	515	621	91	131	171	209	284	355	502	606
		15	64	176	279	376	513	624	812	931	73	130	192	253	363	459	635	754	87	136	188	241	341	429	600	719
		20	78	231	382	518	740	888	1126	1266	73	172	271	369	507	629	835	967	79	148	224	299	428	538	737	870
		25	87	253	456	653	949	1162	1465	1636	80	229	376	507	705	859	1103	1253	80	188	296	405	566	703	935	1082
		30	69	224	502	751	1175	1407	1825	2018	94	277	466	636	917	1110	1410	1588	85	236	386	531	744	914	1185	1351
	Sta. 15	10	130	225	318	395	533	635	810	920	156	231	310	376	491	586	754	859	164	237	307	373	483	574	738	841
		15	153	326	482	618	790	939	1148	1267	140	231	327	413	560	675	874	998	154	236	325	403	539	649	841	962
		20	152	423	655	856	1134	1313	1601	1751	152	290	425	541	724	870	1096	1233	143	243	351	447	613	744	966	1105
		25	174	478	779	1061	1442	1741	2085	2290	161	377	573	754	974	1160	1434	1586	152	291	433	558	757	915	1168	1321
		30	151	431	840	1230	1824	2113	2641	2833	168	456	716	940	1277	1494	1837	2026	162	364	555	732	968	1162	1457	1626
	Sta. 20	10	235	430	611	755	995	1160	1407	1543	265	418	569	697	902	1053	1291	1421	273	419	551	678	873	1020	1253	1379
		15	269	568	838	1068	1357	1598	1903	2057	252	450	645	807	1067	1255	1537	1691	264	441	619	769	1011	1189	1464	1614
		20	252	696	1074	1399	1830	2106	2528	2728	274	539	792	998	1320	1554	1884	2059	260	476	692	874	1167	1379	1698	1871
		25	283	778	1242	1668	2237	2692	3178	3469	280	650	986	1292	1648	1956	2350	2548	276	548	814	1038	1382	1637	2002	2197
		30	251	701	1310	1910	2786	3206	3959	4199	280	753	1174	1534	2055	2388	2886	3138	287	640	973	1274	1659	1968	2395	2613

Relative Motion																														
Sta. 1	10	46	74	101	122	154	176	205	219	45	68	89	106	132	150	174	186	44	65	83	99	123	139	163	174
	15	44	76	107	135	173	201	237	254	45	72	97	117	149	170	199	213	45	68	90	108	136	155	182	195
	20	42	74	109	142	189	219	265	285	44	73	102	127	163	189	223	240	44	70	95	117	149	171	202	216
	25	41	72	109	144	197	236	287	314	42	73	105	135	175	204	245	264	43	71	99	124	159	185	221	238
	30	40	66	105	146	210	249	312	337	41	72	106	137	186	217	264	287	42	71	101	129	168	197	238	257
Sta. 2	10	44	69	91	108	134	152	173	183	43	62	78	91	111	124	142	150	41	57	71	83	101	113	130	137
	15	43	71	98	121	153	176	205	219	43	66	87	103	128	145	167	177	42	62	79	94	115	130	149	158
	20	41	70	101	130	170	196	234	250	43	69	93	114	143	164	192	204	43	65	86	103	129	146	170	180
	25	41	69	102	132	179	213	256	279	41	69	97	122	156	181	214	229	42	67	90	111	140	161	189	202
	30	40	64	99	135	192	226	281	302	40	68	98	126	167	194	234	252	41	67	93	117	150	174	207	222
Sta. 3	10	42	63	81	94	114	127	143	149	40	54	66	76	90	99	111	116	37	50	60	68	81	89	99	103
	15	42	66	89	108	134	152	175	185	41	60	76	89	108	121	136	142	40	55	68	79	95	105	118	124
	20	40	66	93	117	151	173	204	216	41	63	84	101	124	141	161	170	41	59	76	89	109	122	139	146
	25	40	65	95	121	162	190	227	245	41	65	88	110	138	158	184	195	41	62	81	98	121	138	159	168
	30	39	62	93	125	174	204	251	269	40	65	91	115	150	172	204	219	40	63	85	105	132	152	177	189
Sta. 4	10	40	57	71	81	96	105	115	118	37	48	56	63	72	78	84	85	35	44	50	56	63	68	72	73
	15	41	61	80	95	116	130	147	153	39	54	67	76	90	98	108	111	37	49	59	66	77	83	90	93
	20	40	62	85	106	133	151	176	185	40	58	75	88	106	118	132	138	39	54	66	76	91	100	111	114
	25	39	62	88	111	145	169	200	215	40	61	80	98	120	136	156	164	40	57	73	86	104	116	131	136
	30	39	60	87	115	158	184	224	239	39	61	84	104	133	151	177	188	39	59	77	94	115	130	150	158
Sta. 20	10	38	52	67	80	103	119	144	157	35	48	62	76	97	113	136	148	33	47	62	75	96	112	135	147
	15	38	54	70	87	109	127	154	168	37	49	63	75	95	111	134	146	35	48	61	73	93	107	130	141
	20	39	59	79	97	127	146	177	193	37	49	62	75	94	110	133	146	36	48	60	71	90	104	126	137
	25	40	63	88	114	150	179	213	232	37	51	64	77	98	114	138	151	37	48	59	71	88	102	123	134
	30	40	61	95	129	184	212	261	279	38	53	68	82	107	124	150	164	37	48	59	71	88	101	123	134
Sta. 1	10	260	322	381	427	496	539	584	596	262	313	357	394	444	474	506	512	261	307	344	377	420	446	473	476
	15	299	364	434	496	580	640	704	725	303	361	418	463	530	571	613	623	303	355	403	442	498	531	565	571
	20	336	399	476	553	656	722	811	838	342	405	472	529	609	664	721	737	344	401	458	505	574	618	662	672
	25	377	436	514	591	711	799	896	944	381	444	518	590	679	746	821	843	384	443	509	566	645	700	757	772
	30	418	467	541	632	777	864	992	1025	421	482	558	634	747	817	910	941	423	483	554	622	710	775	846	867
Sta. 2	10	256	309	356	393	446	478	507	512	255	296	328	355	390	409	425	424	251	286	312	334	362	378	389	384
	15	296	352	411	461	529	576	622	635	297	346	391	425	475	504	529	531	296	338	373	401	440	461	479	476
	20	334	390	455	520	602	656	725	742	338	392	446	491	554	595	633	640	338	386	430	466	517	547	572	573
	25	375	427	494	558	659	729	807	842	378	433	494	552	623	676	730	743	379	430	482	527	588	628	665	670
	30	417	461	525	600	720	792	896	920	418	472	536	599	690	746	816	837	420	472	530	584	653	702	752	762
Sta. 3	10	253	295	332	359	398	419	433	430	248	279	301	318	339	348	349	339	243	267	283	296	310	315	311	297
	15	294	341	389	427	480	513	543	547	293	332	365	389	423	440	448	441	290	321	345	364	386	396	396	385
	20	333	381	434	487	551	593	642	650	336	380	422	456	501	528	549	546	334	372	404	429	462	479	487	478
	25	375	420	476	528	609	663	721	745	376	423	472	517	570	608	642	645	377	418	458	491	534	559	576	572
	30	416	456	510	571	667	725	804	820	417	464	516	567	636	678	726	736	419	462	508	549	599	633	661	661
Sta. 4	10	249	283	309	328	353	365	365	356	243	264	278	287	295	295	283	265	238	253	262	267	270	266	247	225
	15	292	331	367	395	434	456	470	466	290	319	341	357	376	382	376	361	286	307	322	332	341	341	325	305
	20	332	373	416	456	504	535	565	565	334	369	400	423	453	468	472	460	332	359	382	397	415	420	411	393
	25	374	414	459	501	564	604	643	656	376	414	452	485	522	547	562	556	376	408	437	459	485	498	497	483
	30	416	452	497	545	620	665	722	730	418	457	499	537	587	617	644	643	418	454	488	518	551	572	580	569
Sta. 20	10	247	272	296	315	347	368	389	389	236	257	278	297	326	344	360	359	230	250	272	290	320	339	354	356
	15	290	318	346	375	400	424	447	445	286	306	326	341	365	379	388	380	279	298	316	331	353	366	372	364
	20	335	371	408	441	493	518	553	560	331	351	369	385	401	413	417	403	328	346	362	374	390	398	396	379
	25	380	423	473	525	597	656	704	725	375	397	416	434	451	460	462	447	373	390	405	416	425	429	420	397
	30	423	465	531	610	738	797	899	913	420	446	470	489	520	533	540	530	417	435	449	460	466	466	452	425

Appendix B

SYMBOLS

A_{yy}	coefficient of added mass moment of inertia for pitching motion
a	virtual mass, or virtual mass moment of inertia
a_z	added mass for heaving
B	coefficient of pitch damping moment
B_n	waterline breadth for nth section
b	coefficient for damping force or damping moment
b_n	damping coefficient per unit length
C	coefficient for pitch restoring moment
c	coefficient for restoring force or restoring moment
E	wave energy per unit area of free surface
E_K	kinetic energy per unit area of wave surface
E_P	potential energy per unit area of wave surface
f	frequency, $1/T$
h_w	height of wave
$\tilde{h}_w$	apparent wave height
I_{xx}	mass moment of inertia for rolling
I_{yy}	mass moment of inertia for pitching
I_{zz}	mass moment of inertia for yawing
k	wave number
k_{xx}	radius of gyration for rolling
k_{yy}	radius of gyration for pitching
k_{zz}	radius of gyration for yawing
L_{pp}	length between perpendiculars
L_w	wavelength from crest to crest
$\tilde{L}_w$	apparent wavelength (according to zero crossings)
M_L	horizontal or lateral wave bending moment
M_s	still water vertical bending moment
M_T	torsional wave bending moment
M_V	vertical wave bending moment
M_W	total wave bending moment
m_n	spectrum moment (where n is an integer)
m_s	still water vertical bending moment coefficient
m_w	wave bending moment amplitude coefficient
n_{AW}	increase in mean rate of revolution in waves
P_{AW}	mean power increase in waves
$Q_{1/3}$	significant torque in irregular waves
Q_{AW}	mean torque increase in waves
R_{AW}	mean resistance increase in waves, that is, resistance in waves minus resistance in still water
RAO	response amplitude operator
S_n	area of nth section
$S_\zeta(\omega)$, $S_\theta(\omega)$, etc.	one-dimensional spectral density
$S_\zeta(\omega,\mu)$, $S_\theta(\omega,\mu)$, etc.	two-dimensional spectral density
s	relative vertical motion of bow with respect to wave surface
T_{AW}	mean thrust increase in waves
T_e	period of encounter
T_w	wave period
T_z	natural period (in smooth water) for heaving
T_θ	natural period (in smooth water) for pitching
T_ϕ	natural period (in smooth water) for rolling
$\tilde{T}$	apparent wave period (according to zero crossings)
u	horizontal component of water velocity

v	vertical component of water velocity
V_w	wave velocity or celerity
z	heaving motion
z_a	heaving amplitude
α	wave slope
α_M	maximum wave slope
α'_M	maximum effective wave slope
β	sectional area coefficient
ε	phase angle between motions and waves
ε_1	phase angle between wave motion and exciting force (or moment)
ε_2	phase angle between exciting force (or moment) and motions
ζ	instantaneous wave elevation
ζ_a	wave amplitude
$\tilde{\zeta}_a$	apparent wave amplitude
θ	pitch angle
θ_a	pitch amplitude
κ	damping factor
Λ_z	tuning factor for heaving, ω_e/ω_z
Λ_θ	tuning factor for pitching, ω_e/ω_θ
Λ_ϕ	tuning factor for rolling, ω_e/ω_ϕ
μ	heading angle
μ_w	angle between component wave and wind (dominant wave direction)
μ_z	magnification factor for heaving
μ_θ	magnification factor for pitching
μ_ϕ	magnification factor for rolling
ϕ	roll angle
ϕ_a	roll amplitude
ϕ_m	mean roll angle
ω_e	frequency of encounter (circular), $2\pi/T_e$
ω_z	natural (circular) frequency for heaving, $2\pi/T_z$
ω_θ	natural (circular) frequency for pitching, $2\pi/T_\theta$
ω_ϕ	natural (circular) frequency for rolling, $2\pi/T_\phi$

Glossary of Seakeeping Terms

(After American and International Towing Tank Conferences)

Added Mass Coefficient. A nondimensional coefficient expressing added mass in relation to the geometry of a body.

Amplitude. The magnitude of the extreme of a sinusoidal quantity with respect to the mean value. The double amplitude is the magnitude of the difference of the extreme.

Apparent. With reference to wave characteristics, a visible property of an irregular wave record as distinguished from a property of the component waves. Thus an apparent wave height is a particular peak-to-trough distance. Apparent values are indicated by a tilde (˜) above the symbol, for example, apparent wave amplitude $= \tilde{\zeta}_a$.

Broaching. An involuntary and dangerous change in heading produced by a severe following sea.

Celerity. See *Wave Speed.*

Coupling. The influence of one mode of motion on another, for instance, coupling between heave and pitch.

Damping. A characteristic property of a dynamic system, which dissipates energy and reduces motion.

Damping Coefficient. The ratio of damping force or moment amplitude to velocity amplitude as a function of frequency.

Emergence (s) $[L]$. The relative vertical distance of an oscillating ship above the water surface; opposite to *Submergence.*

Factor, Magnification. The ratio of output amplitude at a certain frequency to static response.

Factor, Tuning $(\Lambda)[—]$. The ratio of excitation frequency to natural frequency (or the ratio of natural period of a motion to period of encounter). The tuning factors in heave, pitch, and roll have the symbols $\Lambda_z = \omega_e/\omega_z$, $\Lambda_\theta = \omega_e/\omega_\theta$, $\Lambda_\phi = \omega_e/\omega_\phi$, respectively.

Force, Damping. A force that tends to reduce motion and, if assumed to be linear, is proportional to the velocity.

Force, Exciting. A fluctuating external force that causes motion of a body, for instance, a ship when encountering a train of waves.

Force, Restoring. A force tending to return a body to its equilibrium position when it has been displaced by an external force.

Frequency, Characteristic (f) $[T^{-1}]$. The number of cycles occurring per unit of time: $f = 1/T$, where T is the period.

Frequency, Circular (ω) $[T^{-1}]$. In any cyclic motion, or in any periodic motion that may be represented by a cyclic motion, the circular frequency is the angular velocity. If ω is in radians per second, $\omega = 2\pi/T$, where T is the period.

Frequency of Encounter, Circular $(\omega_e)[T^{-1}]$. Here $\omega = 2\pi/T$, where T is the period.

Frequency of Heave, Pitch, or Roll of a Ship. The frequency of the periodic heaving, pitching, or rolling motion of a ship.

Frequency, Natural Circular, of Heave, Pitch, or Roll. Natural circular frequency has the following definitions for heave, pitch, and roll, respectively: $\omega_z = 2\pi/T_z$, $\omega_\theta = 2\pi/T_\theta$, $\omega_\phi = 2\pi/T_\phi$.

Green Water. Water shipped on the deck of a ship in heavy seas, as distinct from spray.

Group Velocity. The average rate of advance of the energy of a finite train of gravity waves.

Gyradius (Radius of Gyration) (k_{xx}, k_{yy}, k_{zz})$[L]$. The square root of the ratio of the mass moment of inertia to the mass of a body.

Harmonic. Sinusoidal, in referring to a function or motion.

Heading. A direction assumed by the forward axis or centerline of a body or the bow of a ship in a horizontal plane.

Heaving. The vertical oscillatory motion of a specified point in a vessel, usually the center of gravity.

Impact. The forcible, sudden contact of a body or ship, or any part thereof, with the surface of a liquid.

Long-Crested Seas. A wave system in which all components advance in the same direction.

Mass, Added. The total hydrodynamic force, per unit acceleration, exerted on a ship or other body in phase with and proportional to the acceleration.

Moment, Lateral Wave Bending $(M_L)[L^2MT^{-2}]$. The part of the internal lateral bending moment acting on a cross section of a hull that is caused by the action of waves and ship motions.

Moment, Torsional Wave Bending $(M_T)[L^2MT^{-2}]$. The part of the internal torsional or twisting moment acting on a cross section of a hull that is caused by the action of waves and ship motions.

Moment, Vertical Wave Bending $(M_V)[L^2MT^{-2}]$. The part of the internal vertical bending moment acting on a cross section of a hull that is caused by the action of waves and ship motions.

Moment, Damping. A moment resulting from damping action, which tends to reduce the motion.

Moment, Exciting. A fluctuating external moment that causes motion of a body or ship, for example, when encountering a train of regular waves.

Moment, Heaving. Exciting moment in heave.

Moment of Intertia $(I_{xx}, I_{yy}, I_{zz})[L^2M]$. The summation of products of elementary masses and the squares of their distances from axes through the center of gravity. Equal to the mass times the gyradius squared.

Moment, Pitching. Exciting moment in pitch.

Moment, Restoring or Righting. A moment tending to return a body to its initial condition after it has been displaced by an external moment.

Moment, Rolling. Exciting moment in roll.

Moment, Stabilizing. Moment associated with a displacement from a position of equilibrium and tending to decrease this displacement.

Natural Period of Motions: Heave, Pitch, Roll (T_z, T_θ, T_ϕ) $[T]$. The time for one complete cycle of the motion resulting when a body is displaced in calm water from its equilibrium position by an external force and then is released.

Period. The length of time for one complete cycle of a periodic quantity or phenomenon, such as the rolling of a ship from port to starboard and back to port.

Period of Encounter of a Ship in Waves (T_e) $[T]$. The time interval between successive crests of a train of waves passing a fixed point in a ship, at a fixed angle of encounter μ.

Phase Angle (ε) $[-]$. The angle between two vectors representing two harmonically varying quantities having the same frequency.

Pitching. The angular component of the oscillatory motion of a vessel, about a transverse axis.

Porpoising. The oscillation of a high-speed craft, primarily in calm water, in which heaving motion is combined with pitching motion. The motion is sustained by energy drawn from the thrust.

Pounding. The impact of a water surface against the side or bottom of a ship hull, whether caused by ship velocity, water velocity, or both. Pounding is differentiated from slamming in that the impact, although heavy, is not in the nature of a shock.

Power, Mean Increase in Waves $(P_{AW})[L^3MT^{-3}]$. The absolute mean increase in power, as compared with the power in smooth water, necessary to maintain speed in a seaway.

Pressure, Impact. A local pressure sustained by a hull when subjected to impact with the water. Usually associated with slamming or pounding.

Radius of Gyration. See *Gyradius.*

Resistance, Mean Increase in Waves $(R_{AW})[LMT^{-2}]$. The mean absolute increase in resistance, as compared with the resistance in smooth water, that occurs when speed is maintained in wind and waves.

Resonance. The dynamic condition of a simple, uncoupled system in which the excitation frequency is equal to the natural frequency. *Note*: In a coupled system, the dynamic condition in which the excitation frequency corresponds to the frequency of maximum response to unit exciting force over a range of frequencies.

Response Amplitude Operator. The square of the ratio of response amplitude to excitation amplitude of a forced harmonic motion applied to a linear system, as a function of frequency.

Revolutions per Minute, Mean Increase in Waves. The mean absolute increase in revolutions per minute, as compared with those in calm water, necessary to maintain speed in wind and waves.

Rolling. The angular component of the oscillatory motion of a ship measured about a longitudinal axis.

Sea direction

1. BEAM SEA. A condition in which a ship and the waves, or the predominant wave components, advance at right angles, or nearly so.

2. BOW SEA. A condition in which a ship and the waves, or the predominant wave components, advance at oblique angles. This condition covers the direction between a head sea and a beam sea.

3. FOLLOWING SEA. A condition in which a ship and the waves, or the predominant wave components, advance in the same, or nearly the same, direction.

4. HEAD SEA. A condition in which a ship and the waves, or the predominant wave components, advance in opposite, or nearly opposite directions.

5. QUARTERING SEA. A condition in which a ship and the waves, or the predominant wave components, advance at oblique angles. This condition covers the direction between a beam sea and a following sea.

Shearing Force, Wave. The part of the internal shearing force acting on a cross section of a hull that is caused by the action of waves and ship motions.

Short-Crested Seas. An irregular wave system in which the components advance in various directions.

Significant Height. The average apparent height of the one-third highest waves in an irregular pattern.

Slamming. A phenomenon described broadly as severe impacting between a water surface and the side or bottom of a hull, where the impact causes a shocklike blow. See also *Pounding*.

Smith Effect. The difference between the actual pressure at a point under a wave profile and the static pressure corresponding to the actual distance below the surface.

Spectral Density, One-Dimensional (S). A function of frequency whose integral over any interval represents the energy contribution of all the component waves of a random function in that interval: $S_\zeta(\omega)\,d\omega = \sum_{d\omega} \frac{1}{2}\zeta_{an}^2$, $S_\theta(\omega)\,d\omega = \sum_{d\omega} \frac{1}{2}\theta_{an}^2$, etc., where the subscript n denotes a particular component amplitude.

Spectral Density, Two-Dimensional ($S_{\omega,\mu}$). A function of frequency and wave direction whose integral over any interval represents the energy contributions of all the component waves of a random function in that interval.

Spectrum, Amplitude, Wave (or Motion). A function of frequency whose integral over any interval represents the squared amplitude of a wave (or motion) at the central frequency having the same energy as all the component waves (or motions) in that interval.

Speed Loss. The decrease in speed, as compared with the speed in smooth water, caused directly by wind and waves at a constant setting of the main propulsion plant. Usually speed loss is determined at constant power (turbine plant) or constant torque (diesel plant).

Speed Reduction. The decrease in speed, as compared with the speed in smooth water, caused mainly by reducing the setting of the main propulsion plant in order to minimize the adverse effects on the ship of wind and waves.

Stabilizer. Equipment to reduce the rolling (or pitching) motion of a ship.

Submergence (s) $[L]$. The relative verticle distance of a part of an oscillating ship below the water surface.

Surging. The longitudinal oscillatory motion of a specified point in a ship, usually the center of gravity.

Swaying. The transverse oscillatory motion of a specified point in the ship, usually the center of gravity.

Thrust, Mean Increase in Waves (T_{AW}) $[LMT^{-2}]$. The mean absolute increase in thrust, as compared with the thrust in smooth water, necessary to maintain speed in wind and waves.

Torque, Mean Increase in Waves (Q_{AW})$[L^2MT^{-2}]$. The mean absolute increase in torque, as compared with the torque in smooth water, necessary to maintain speed in wind and waves.

Transient. Irregular or nonharmonic, as the free oscillation of a damped motion.

Virtual Mass. The combined effect of the mass of the ship and the hydrodynamic forces in phase and proportional to the accelerations.

Wave. A disturbance of the surface of a fluid that usually progresses across the surface as the result of circular or other local motions of the fluid components. A standing wave is a special case of a wave that does not advance.

1. AMPLITUDE (ζ_a)$[L]$. The radius of orbital motion of a surface wave particle, equal to one-half of the wave height.

2. COMPONENTS. The infinity of infinitesimal waves of different frequencies and directions that are found by spectral analysis to compose an irregular sea, or the large number of finite waves used to approximate such an irregular sea.

3. CREST. The position of maximum positive disturbance in a progressive wave, that is, in any wave other than a standing wave.

4. FREQUENCY (f) $[T^{-1}]$. The reciprocal of a wave period $= 1/T_w$ (or circular frequency $\omega_w = 2\pi/T_w$).

5. HEIGHT (h_w)$[L]$. The vertical distance from wave crest to wave trough, or twice the wave amplitude of a harmonic wave.

6. HEIGHT, APPARENT ($\tilde{h}_w$)$[L]$. The vertical distance between a successive crest and trough.

7. INSTANTANEOUS ELEVATION (ζ) $[L]$. The instantaneous elevation of a point in a wave system above the level of the undisturbed surface.

8. LENGTH(L_w) $[L]$. The horizontal distance between adjacent wave crests in the direction of advance.

9. LENGTH, APPARENT($\tilde{L}$]. The horizontal distance between adjacent wave crests of an irregular sea in the direction of advance.

10. NUMBER (k) $[1/L]$. Here $k = 2\pi/L_w$.

11. PERIOD (T_w)$[T]$. The time between the passages of two successive wave crests past a fixed point.

12. PERIOD, APPARENT($\tilde{T}_w$)$[T]$. The time elapsing between the occurrences of two successive crests in an irregular sea, or between two successive upward crossings of zero in a record.

13. PROFILE. The elevation of the surface particles of a wave plotted as a function of space in fixed time.

14. SLOPE OF SURFACE. The surface slope of a wave profile perpendicular to the crest in space coordinates. The maximum wave slope of a regular harmonic or trochoidal wave is $\pi \times$ steepness ratio.

15. SPEED OR CELERITY (V_w)$[LT^{-1}]$. The phase velocity of a surface gravity wave in deep water.

16. STEEPNESS RATIO. The ratio of wave height to length.

17. TRAIN. A continuous sequence of wave crests and troughs.

18. TROCHOIDAL. A profile closely approximating that of a regular surface gravity wave in a fluid; it can be geometrically constructed by tracing the path of a point on the radius of a circle as the circle rolls along the underside of a horizontal line.

19. TROUGH. A point of minimum (algebraic) value of the disturbance in a progressive wave. Opposite of *Wave Crest.*

Wave, Harmonic. A wave for which the disturbance at any point in space through which the wave is propagated varies sinusoidally with time. Specifically, if the wave is a plane harmonic wave in the x-direction, the disturbance ζ is given by $\zeta = \zeta_a \sin(\omega_w t - kx)$, where ζ_a is the wave amplitude, $\omega_w = 2\pi/T_w$ (where T_w is the wave period), and $k = \omega_w/V_w$ (where V_w is the wave velocity).

Wave Periodic. A wave for which the disturbance repeats itself in equal intervals of time at each point of space, and at equal intervals of space at each given instant of time

Wave, Standing. A wave for which the disturbance is not progressive; that is, any component of the field can be specified as a function of position multiplied by a sinusoidal function of time. A standing wave results from the superposition of two waves traveling in opposite directions but having identical amplitudes and frequencies. The wave disturbance is maximal at certain points occurring periodically, called *loops* or *antinodes*, and is zero at points between them, called *nodes.*

Wetness. The quality of a part of the ship, usually the weather deck forward, with respect to its likelihood of being wet as a result of motions of ship and waves.

Yawing. The angular components of the oscillatory motion of a hull measured about a vertical axis.

Conversion Table

Multiply	*by*	*to obtain*
atmospheres	33.90	feet of water
atmospheres	10.333	kgs. per sq. meter
atmospheres	14.70	pounds per sq. inch
centimeters	0.3397	inches
centimeters	0.01	meters
centimeters	10	millimeters
centimeters per second	0.6	meters per minute
centimeters per second	0.02237	miles per hour
cubic centimeters	3.531×10^{-5}	cubic feet
cubic centimeters	6.102×10^{-3}	cubic inches
cubic centimeters	10^{-4}	cubic meters
cubic centimeters	2.642×10^{-4}	gallons
cubic centimeters	10^{-3}	liters
cubic feet	62.43	pounds of water
cubic feet	2.832×10^{4}	cubic cms.
cubic feet	1728	cubic inches
cubic feet	0.02832	cubic meters
cubic feet	7.481	gallons
cubic feet	28.32	liters
cubic feet per minute	472.0	cubic cms. per sec.
cubic feet per minute	0.1247	gallons per sec.
cubic feet per minute	62.4	lbs. of water per min.
cubic inches	16.39	cubic centimeters
cubic inches	5.787×10^{-4}	cubic feet
cubic inches	1.639×10^{-3}	cubic meters
cubic inches	4.329×10^{-3}	gallons
cubic inches	1.639×10^{-3}	liters
degrees (angle)	60	minutes
degrees (angle)	0.01745	radians
feet	0.3048	meters
feet of water	0.02950	atmospheres
feet of water	304.8	kgs. per sq. meter
feet of water	62.43	pounds per sq. ft.
foot-pounds	5.050×10^{-7}	horse-power-hours
foot-pounds	0.1383	kilogram-meters
foot-pounds per min.	3.030×10^{-5}	horse-power
foot per second	0.592	knots
gallons	0.1337	cubic-feet
gallons	3.785×10^{-3}	cubic meters
gallons	3.785	liters
grams	10^{3}	kilograms

Multiply	*by*	*to obtain*
grams	10^{3}	milligrams
grams	0.03527	ounces
grams	0.03215	ounces (troy)
grams	0.07093	poundals
grams	2.205×10^{-3}	pounds
horse-power	44.44	B. t. units per min.
horse-power	33.000	foot-pounds per min.
horse-power	550	foot-pounds per sec.
horse-power	745.7	watt (w)
horse-power	1.014	horse-power (metric)
horse-power	735.50	watt (W)
inches	2.540	centimeters
inches of water	25.40	kgs. per sq. meter
inches of water	5.204	pounds per sq. ft.
kilograms	10^{3}	grams
kilograms	2.2046	pounds
kilogram force (kgf)	9.807	Newton (N)
kilogram-force per square meter	9.807	pascals (Pa)
kilogram-force per square centimeter	9.8067×10^{4}	pascals (Pa)
kilometers	10^{5}	centimeters
kilometers	3281	feet
kilometers	10^{3}	meters
kilometers	0.6214	miles
knot	1.689	ft per sec
$\log_{10} N$	2.303	$\log_e N$ or $\ln N$
$\log_e N$ or $\ln N$	0.4343	$\log_{10} N$
meters	100	centimeters
meters	3.2808	feet
meters	39.37	inches
meters	10^{-2}	kilometers
meters	10^{2}	millimeters
miles	1.609×10^{5}	centimeters
miles	5280	feet
miles	1.6093	kilometers
miles	1760	yards
miles (nautical)	1852	meters (m)
miles per hour	44.70	centimeters per sec.
miles per hour	88	feet per minute
miles per hour	1.467	feet per second

Multiply	*by*	*to obtain*
miles per hour	1.6093	kilometers per hour
miles per hour	0.8684	knots
miles per hour	26.82	meters per minute
Newtons (N)	0.2248	pound-force
Newtons (N)	0.1020	kilogram-force
pascals (Pa)	0.0209	pound-force per square foot
pascals (Pa)	1.450×10^{-4}	pound-force per sq. inch (psi)
pascals (Pa)	0.102	kilogram-force per square meter
pascals (Pa)	0.102×10^{-4}	kilogram-force per square centimeter
pounds	453.6	grams
pounds of water	0.01602	cubic feet
pounds of water	27.68	cubic inches
pounds of water per min.	2.569×10^{-4}	cubic feet per sec.
pounds per cubic foot	16.02	kgs. per cubic meter
pounds per cubic foot	5.787×10^{-4}	pounds per cubic in.
pounds per square foot	0.01602	feet of water
pounds per square foot	4.882	kgs. per sq. meter
pounds per square inch	703.1	kgs. per sq. meter
pounds per square inch	144	pounds per sq. foot
pound-force	4.448	Newtons (N)
pound-force per square foot	47.88	pascal (Pa)
pound-force per square inch (psi)	6895	pascals (Pa)
slug	14.594	kilogram (kg)
square centimeters	0.1550	square inches
square centimeters	10^{-4}	square meters
square centimeters	100	square millimeters
square feet	144	square inches
square feet	0.09290	square meters
square inches	6.452	square centimeters
square inches	6.944×10^{-2}	square feet
temp. (degs. C.) + 17.8	1.8	temp. (degs. Fahr.)
temp. (degs. F.) − 32	5/9	temp. (degs. Cent.)
tons (long)	2240	pounds
tons (long)	1016	kilograms (kg)
tons (short)	2000	pounds
tons (metric)	1000	kilograms (kg)
watts (W)	1.341×10^{-3}	horse-power
watts (W)	1.360×10^{-3}	horse-power (metric)
yards	0.9144	meters (m)

Abbreviations for References

ATMA	Association Technique Maritime et Aeronautique
ATTC	American Towing Tank Conference
DL	Davidson Laboratory (Stevens Institute of Technology)
DTNSRDC	David Taylor Naval Ship Research and Development Center
HSVA	Hamburgische Schiffbauversuchsanstalt, Hamburg
IfS	Institut für Schiffbau
I Mar. E	Institute of Marine Engineers
ISP	*International Shipbuilding Progress*
ISSC	International Ship Structure Congress
ITTC	International Towing Tank Conference
J. SNAJ	*Journal of the Society of Naval Architects of Japan*
JSR	*Journal of Ship Research*
MIT	Massachusetts Institute of Technology
MT	*Marine Technology*
NA	*Naval Architect*
NAVSEC	Naval Ship Engineering Center (U.S. Navy)
NECIES	Northeast Coast Institute of Engineers and Shipbuilders
NEJ	*Naval Engineers Journal*
NSMB	Netherlands Ship Model Basin
ONR	Office of Naval Research (U.S. Navy)
RINA	Royal Institution of Naval Architects
SNAJ	Society of Naval Architects of Japan
SNAME	Society of Naval Architects and Marine Engineers
SSC	Ship Structure Committee (An interagency of the U.S. government)
STG	Schiffbautechnische Gesellschaft

References

1. Abkowitz, M. A., "The Effect of Anti-Pitching Fins on Ship Motions," *Trans. SNAME*, 1959.
2. Abkowitz, M. A., L. A. Vassilopoulos, and F. H. Sellars, IV, "Recent Developments in Seakeeping Research and Its Application to Design," *Trans. SNAME*, 1966.
3. Abkowitz, M. A., "Applications of the Spectral Techniques to Design and Operation," *Proc. SNAME Seakeeping Symposium*, 1973.
4. Aertssen, G., "Service Performance and Seakeeping Trials on *M. V. Lubumbashi*," *Trans. RINA*, 1957.
5. Aertssen, G., "Discussion on 'Longitudinal Bending Moments on Models in Head Seas,'" *Trans. RINA*, 1967.
6. Aertssen, G., "Laboring of Ships in Rough Seas, with Special Emphasis on the Fast Ship," *Proc. SNAME Spring Meeting*, 1968.
7. Aertssen, G., "Limiting speed in Rough Seas," *Proc. Van Lammeren Jubilee Memorials*, NSMB, 1970.
8. Aertssen, G. et al., "Service Performance and Seakeeping Trials on a Stern Trawler," *Trans. NECIES*, 1966–67.
9. Allan, J. F., "The Stabilization of Ships by Activated Fins," *Trans. RINA*, 1945.
10. Magnuson, A. H., Messalle, R. F. "The Prediction of the Motion of the JEFF (B) Amphibious Assault Landing Craft in Head Seas," *DTNSRDC—SPD* 647–01, 1975.
11. Atwood, E. L. and H. S. Pengelly, *Theoretical Naval Architecture*, Longmans, Green & Co., 1953.
12. Bales, N. K. and W. E. Cummins, "The Influence of Hull Form on Seakeeping," *Trans. SNAME*, 1970.
13. Miller, E. R., Slager, J. J., Webster, W. C. "Development of a Technical Practice for Roll Stabilization System Selections," NAVSEC Report 6136–74–280, 1974.
14. Baumann, H., "Rollzustände grosser Amplitude in seitlicher Dünung," *Schiffstechnik*, 1955.
15. Beck, Robert F., "The Added Resistance of Ships in Waves," M.I.T. Report 67–9, 1967.
16. Bell, J., "Ship Stabilization Controls and Computation," *Trans. RINA*, 1957.
17. Bell, John, "Stabilization to the Apparent Vertical Measurement of Sway," *Trans. RINA*, 1965.
18. Bell, John and W. P. Walker, "Activated and Passive Controlled Fluid Tank System for Ship Stabilization," *Trans. SNAME*, 1966.
19. Blagoveschensky, S. N., *Theory of Ship Motions*, Dover, 1962.

19a. Bledsoe, M. P., "Series Investigation of Slamming Pressures," DTNSRDC Report 1043, 1956.

20. Blight, G. J., "Discussion on 'Longitudinal Bending Moments on Models in Head Seas,'" *Trans. RINA*, 1967.
21. Lloyd, A. R. J. M., (a) "Roll Stabilizer Fins: A Design Procedure," *Trans. RINA* 1974 and (b) "Recent Developments in Roll Stabilization," *NA*, 1977.
22. Boese, P., "Eine einfache Methode zur Berechnung der Widerstanserhohung eines Schiffes im Seegang," *Schiffstechnik*, 1970.
23. Bridges, T. F., B. A. Hilliard, and J. J. McMullen, "The Influence of Bilge Keels and Rolling in Waves on Sea Speed and Horsepower," *Trans. SNAME*, 1964.
24. Brunsel, P. A., S. B. Field, J. P. Martin, and F. V. A. Pangalila, "Correlation of Full Scale and Model Basin Stabilization Test Results for the Canadian Weatherships," *Trans. RINA*, 1969.
25. Canham, H. J. S., D. E. Cartwright, G. J. Goodrich, and N. Hogben, "Seakeeping Trials on O.W.S. *Weather Reporter*," *Trans. RINA*, 1962.
26. Chadwick, J. H., "On the Stabilization of Roll," *Trans. SNAME*, 1955.
27. Chaplin, H. R. and A. G. Ford, "Some Design Principles of Ground Effect Machines (Seakeeping)," DTNSRDC Report 2121G, 1966.
28. Chaplin, P. D., "The Effectiveness of Roll Stabilizers," *Trans. RINA*, 1972.
29. Chryssostomidis, C., (a) "Seakeeping Considerations in a Total Design Methodology," 9th ONR Symposium on Naval Hydrodynamics, Paris, 1972 and (b) "Ship Motion Prediction and Control," Maritime Administration Contract 35466, 1971.
30. Chuang, S. L., "Experiments on Flat-Bottom Slamming, *JSR*, 1966.
31. Chuang, S. L., "Slamming of Rigid Wedge-Shaped Bodies

with Various Deadrise Angles," DTNSRDC Report 2268, 1966.

32. Chuang, S. L., "Investigation of Rigid and Elastic Bodies with Water," DTNSRDC Report 3248, 1970.
33. Bhattacharyya, R., "On the Application of Seakeeping Research," *Proc. Symposium on Seakeeping*, Shipbuilding Design and Research Institute, Varna, Bulgaria, 1974.
34. Cleary, W. A., Jr., "Loadlines—The lever of Safety," *Trans. SNAME*, 1975.
35. Comstock, E. N. and P. M. Covich, "Seakeeping Performance Design Program," NAVSEC Report 6136–75–2, 1975.

36a. Conolly, J. E., "Rolling and its Stabilization by Active Fins," *Trans. RINA*, 1969.

36b. Conolly, J. E. and G. J. Goodrich, "Sea Trials of Antipitching Fins," *Trans. RINA*, 1970.

36c. Cowley, W. E. and T. H. Lambert, "The Use of the Rudder as a Roll Stabilizer," *Proc. 3rd Ship Control Systems Symposium*, 1972.

37. Cummings, D. E., "The Effect of Antipitching Fins on the Motions and Vibration of a Large Aircraft Carrier," M.I.T. Report 64–16, 1964.
38. Cummins, W. E., "Ship Motions or Design for Seakeeping," Report, Dept. of Naval Architecture and Marine Engineering, University of Michigan, 1972.
39. Cummins, W. E., "Pathologies of the Transfer Functions," SNAME Symposium on Seakeeping, 1973.
40. Dalzell, J. F., "Cross-Spectral Analysis of Ship-Model Motions; Some Experimental and Computational Problems," DL Report 853, November 1961.
41. Dalzell, J. F., "Some Notes on the Design of Irregular Wave Experiments in the Towing Tank with Respect to Spectral Analysis," DL Report 659, 1962.
42. Dalzell, J. F., "Some Further Experiments on the Application of Linear Superposition Techniques to the Responses of a Destroyer Model in Extreme Irregular Long-Crested Head Seas," DL Report 918, September 1962.
43. Dalzell, J. F., "High Speed Vehicles and Unusual Ship Forms," *Proc. 17th ATTC*, 1974.
44. Dalzell, J. F. and M. J. Chiocco, "Wave Loads in a Model of the SL-7 Containership Running at Oblique Headings in Regular Waves," SSC-Report 239, 1974.
45. Davis, M. C. and E. E. Zarnick, "Testing Ship Models in Transient Waves," *Proc. 5th ONR Symposium on Naval Hydrodynamics*, 1964.
46. De Does, J. Ch., "Experimental Determination of Bending Moments for Three Models of Different Fullness in Regular Waves," *ISP* 1960.
47. De Herre, R. F. S. and A. R. Bakker, *Buoyancy and Stability of Ships*, H. Stam, Holland, 1969.
48. Dieudonne, J., "Remarques sur la Tenue a la Mer," *Trans. ATMA*, 1949.
49. Dinsenbacher, A. L. and J. N. Andrews, "Vertical and Transverse Loads and Motions of a Segmental Model in Regular Waves," DTNSRDC Report 3152, 1969.
50. Draper, L. and E. M. Squire, "Waves at Ocean Weather Ship Station *India*," *Trans. RINA*, 1967.
51. DuCane, P., "Discussion on 'The Brave' Class Fast Patrol Boats," *Trans. Rina*, 1960.
52. Dyne, G., "An Investigation Concerning the Motions of a Hovercraft in Regular Head Seas," *Trans RINA*, October 1968.
53. Eames, M. C. and T. G. Drummond, "H.M.C.S. *Bras d'Or*: Sea Trials and Future Prospects," *Trans. RINA*, 1973.
54. Eggington, W. J. and N. Kobitz, "The Domain of the Surface-Effect Ship," *Trans. SNAME*, 1975.
55. Ellsworth, W. M., "The U.S. Navy Hydrofoil Development Program—a Status Report," AIAA/SNAME Advanced Marine Vehicles Meetings, 1967.
56. Evans, J. H., "Ship Structural Design Concepts," U.S. Coast Guard Headquarters, Washington, 1974.
57. Evans, J. H., "Structural Design Criteria," SSC Report 200, U.S. Coast Guard Headquarters, Washington, 1974.
58. Ewing, J. A., "The Effect of Speed, Forebody Shape and Weight Distribution on Ship Motions," *Trans. RINA*, 1967.
59. Ewing, J. A. and J. G. Goodrich, "The Influence on Ship Motions of Different Wave Spectra and of Ship Length," *Trans. RINA*, 1967.
60. Fein, J., A. H. Magnuson, and D. D. Moran, "Dynamic Performance of an Air Cushion Vehicle in a Marine Environment," AIAA/SNAME Symposium on Advanced Marine Vehicles, 1974.
61. Ferdinande, V., "Model Tests in Regular and Irregular Waves at the Davidson Laboratory," *Trans. RINA*, 1963.
62. Ferdinande, V., "Some Notes on the Shipping of Water on a Model of a Cargo Ship in Irregular Waves," *ISP*, 1969.
63. Flipse, J. E., "Stabilizer Performance on the S.S. *Mariposa* and S.S. *Montery*," *Trans. SNAME*, 1957.
64. Frahm, H., "Neuartige Schlingertanks zur Abdämpfung von Schiffsrollbewegungen und ihre erfolgreiche Anwendung in der Praxis," *Trans. STG*, 1911.
65. Frankland, L. H., "Discussion on Longitudinal Bending Moments on Models in Head Seas," *Trans. RINA*, 1967.
66. Freakes, W. and Keay, K. L., "Effects of Shallow Water on Ship Motion Parameters in Pitch and Heave," M.I.T. Report 66-F, 1966.
67. Magnuson, A. H. and K. K. Wolff, "Seakeeping Characteristics of the XR-5," *DTNSRDC-SPD* 616–01, 616–02, 1975.
68. Fukuda, J., "Discussion on Longitudinal Bending Moments in Head Seas," *Trans. RINA*, 1967.
69. Fukuda, J., "Computer Program Results for Ship Behavior in Regular Oblique Waves," *Proc. 12th ITTC*, 1969.
70. Gadd, G. E., "Some Experiments on the Incremental Resistance Due to Rolling with and without Bilge Keels and Vanes," *Trans. RINA*, 1967.
71. Gerritsma, J., "Experimental Determination of Damping, Added Mass and Added Mass Moment of Inertia of a Ship Model," *ISP*, 1957.
72. Gerritsma, J., "An Experimental Analysis of Ship Motions in Lontitudinal Regular Waves," *ISP*, 1958.
73. Gerritsma, J., "Ship Motions in Longitudinal Waves," *ISP*, 1960.
74. Gerritsma, J. and W. Beukelman, "Distribution of the Hydrodynamic Forces on a Heaving and Pitching Ship Model in Still Water," *ISP*, 1964.
75. Gerritsma, J., "The Purposes of Seakeeping Experiments," *Proc. 11th ITTC*, Tokyo, 1966.
76. Gerritsma, J. and W. Smith, "Full-Scale Destroyer-Motion Measurements," *JSR*, 1967.
77. Gerritsma, J., "Sustained Sea Speed," Report of the Post-Graduate Course, 1969.
78. Giddings, A. J., "A Survey of Ship Motion Stabilization,"

Proc. 5th ONR Symposium on Naval Hydrodynamics, 1964.

79. Goldberg, J. H., *Automatic Controls: Principles of Systems Dynamics*, Allyn and Bacon, Boston, 1964.

79a. Kaplan, P. and T. R. Goodman, "Use of Jet-flapped hydrofoils as Ship's Anti-pitching Fins" Oceanic Inc. Report 64–13, 1964.

80. Goodrich, G. J., "The Influence of Freeboard on Wetness," *Proc. 5th ONR Symposium on Naval Hydrodynamics*, 1964.

81. Goodrich, J. G., "Prediction of the Long Term Distribution of Ship Bending Moments from Model Tests," NECIES, 1966.

82. Goodrich, J. G., "Development and Design of Passive Roll Stabilizers," *Trans. RINA*, 1969.

83. Goodrich, G. J., "Proposed Standards of Seakeeping Experiments in Head and Following Seas," *Proc. 12th ITTC*, 1969.

84. Kitagawa, H., Discussion of "On Predicting Power Increase in Irregular Waves from Model Experiments in Regular Waves," *Proc. 13th ITTC*, 1972.

85. Grim, O., "Das Schiff in von Achtern Auflaufender See," *Trans. STG*, 1951.

86. Grim, O., "Berechnung der durch Schwingungen eines Schiffskorpers erzeugten hydrodynamischen Kräfte," *Trans. STG*, 1953.

87. Grim, O., "Rollschwingungen, Stabilität und Sicherheit im Seegang," *Schiffstechnik*, 1952/53.

88. Grim, O., "Die hydrodynamischen Kräfte beim Rollversuch," *Schhiffstechnik*, 1956.

89. Grim, O., "Die Schwingungen von Schwimmenden, Zweidimensionalen Körpern," HSVA Report 1171, 1959.

90. Grim, O., "Beitrag zu dem Problem der Sicherheit des Schiffes im Seegang," *Schiff und Hafen*, 1961.

91. Grim, O., "A Method for a More Precise Computation of Heaving and Pitching Motions Both in Smooth Water and in Waves," *Proc. 3rd ONR Symposium on Naval Hydrodynamics*, 1960.

92. Grim, O., "Die Bewegungen und Belastungen des Schiffes im Seegang," *Trans.* STG, 1967.

93. Hoffman, D., J. Williamson, and E. V. Lewis, "Correlation of Model and Full Scale Results in Predicting Wave Bending Moment Trends," SSC Report 233, 1972.

94. Hadler, J. B. and T. H. Sarchin, "Seakeeping Criteria and Specifications," SNAME Seakeeping Symposium, 1973.

95. Hadler, J. B., C. M. Lee, J. T. Birmingham, and H. D. Jones, "Ocean Catamaran Seakeeping Design, Based on the Experience of U.S.N.S. *Hays*," *Trans. SNAME*, 1974.

96. Hamlin, N. A. and R. H. Compton, "Assessment of Seakeepability," *MT*, 1966.

97. ISSC, "Loads Induced by Wind, Waves and Motions," *Proc. 6th ISSC*, 1976.

98. Harbaugh, K. H. and W. H. G. Fitzgerald, "Hydrofoil Operations and Development Experience, 1952–64," SNAME Hydrofoil Symposium, 1965.

99. Havelock, T. H., "The Effect of Speed of Advance upon Damping of Heave and Pitch," *Trans. RINA*, 1958.

100. Henschke, W., *Schiffbautechnisches Handbuch*, VEB Verlag Technik, Berlin, 1958.

101. Hoffman, D. and W. M. Meclean, "Ship Model Study of Incidence of Shipping Water Forward," *MT*, 1970.

102. Hogben, N. and F. E. Lumb, "Ocean Wave Statistics," Her Majesty's Stationary Office, London, 1967.

103. Hooft, J. P., "The Behavior of a Ship in Head Waves at Restricted Water Depths," *ISP*, 1974.

104. Hort, H., "Beschreibung und Versuchsergebnisse ausgeführter Schiffsstabilisierungsanglagen," *Trans. STG*, 1934.

105. ITTC, "Recommendations of the 11th International Towing Tank Conference," *Proc. 11th ITTC*, Tokyo, 1966.

106. ITTC, "Technical Decisions and Recommendations of the Seakeeping Committee," *Proc. 12th and 13th ITTC*, Rome, 1969, Berlin, 1972.

107. Jacobs, W. R., "The Analytical Calculation of Ship Bending Moments in Regular Waves," *JSR*, June 1958.

108. Jacobs, W. R. and J. F. Dalzell, "Theory and Experiment in the Evaluation of Bending Moments Acting on a Ship in Waves," *ISP*, September 1960.

109. Jacobs, W. R., J. Dalzell, and P. Lalangas, "Guide to Computational Procedure for Analytical Evaluation of Ship Bending-Moments in Regular Waves," DL Report 791, October 1960.

110. Jasper, N. H., "Statistical Distribution Patterns of Ocean Waves and of Wave-Induced Ship Stresses and Motions with Engineering Applications," *Trans. SNAME*, 1956.

111. Jens, J., "Die Periodenbestimmung freier, ungedämpfter Schlingerschwingnungen," *Schiffstechnik*, 1958.

112. Joosen, W. P. A., "Added Resistance of Ships in Waves," *Proc. 6th ONR Symposium on Naval Hydrodynamics*, 1966.

113. Jordaan, J. M., "Impulsive Waves: Model and Prototype Correlations," *Advances in Hydroscience*, Vol. 8, Academic Press, 1972.

114. Kans, S., *Researches on Seakeeping Qualities of Ships in Japan*, 60th Anniversary Series, Vol. 8, SNAJ, 1963.

115. Kato, H., "On the Approximate Calculation of Ship's Rolling Period," *J. SNAJ*, 1956.

116. Kato, H., S. Motora, and K. Ishikawa, "On the Rolling of a Ship in Irregular Wind and Wave," *Proc. Symposium on the Behaviour of Ships in a Seaway*, Wageningen, 1957.

117. Keil, H., "Untersuchungen über das Seeverhalten von Schiffen," *Schiff und Hafen*, 1967.

118. Kent, J. L., "The Design of Seakindly Ships," *Trans. NECIES*, 1949–50.

119. Kilgore, U., "Hydrodynamic Aspects of Tracked Amphibians," *NEJ*, 1969.

120. Kirkman, K. L., "Development and Testing of a Passive Moving-Weight Roll Stabilizer for the U.S.C.G. 82-ft Class Patrol Boat," SNAME, Chesapeake Section, 1972.

121. Korvin-Kroukovsky, B. V. and W. R. Jacobs, "Pitching and Heaving Motions of a Ship in Regular Waves," *Trans. SNAME*, 1957.

122. Korvin-Kroukovsky, B. V., *Theory of Seakeeping, SNAME*, 1961.

123. Krappinger, O., "Über Rollschwingungen von Schiffen," *Hansa*, 1958.

124. Krappinger, O., "Schiffsschwingungen," *Handbuch der Werften*, 1960.

125. Kriloff, A., "A General Theory of the Oscillation of a Ship in Waves," *Trans. RINA*, 1898.

126. Lee, C. M., H. D. Jones, and R. M. Curphey, "Prediction of Motion and Hydrodynamic Loads of Catamarans," SNAME, Chesapeake Section, 1973.

126a. Lehmann, G., "Bodenschäden im Vorschiff und die neuen Vorschriften der Klassifikationsgesellschaften," *Schiffbau*, 1936.

127. Lewis, E. V., "Ship Speeds in Irregular Seas," *Trans. SNAME*, 1955.

128. Lewis, E. V., "Log Analyses," DL Report 708.

129. Lewis, E. V., "Increasing the Sea Speed of Merchant Ships," *Trans. SNAME*, 1959.

130. Lewis, E. V. and E. Numata, "Ship Motions in Oblique Seas," *Trans. SNAME*, 1960.

131. Lewis, E. V., "Research toward More Efficient Transportation by Sea," *Trans. SNAME*, 1961.

132. Lewis, E. V., chapter entitled "Ship Motion," *Principles of Naval Architecture, SNAME*, 1967.

133. Lewis, E. V., "Predicting Long-Term Distributions of Wave-Induced Bending Moment on Ship Hulls, SNAME Spring Meeting, 1967.

134. Lewis, E. V., D. Hoffman, W. M. Maclean, R. Van Hoof, R. B. Zubaly, "Load Criteria for Ship Structural Design," SSC Report 240, U.S. Coast Guard Headquarters, Washington, 1973.

135. Lewis, F. M., "The Inertia of the Water Surrounding a Vibrating Ship," *Trans. SNAME*, 1929.

136. Lewis, F. M., chapter entitled "Hull Vibration of Ships," *Principles of Naval Architecture, SNAME*, 1967.

137. Lindgren, H. and N. H. Norrbin, "Model Tests and Ship Correlation for a Cargo Liner," *Trans. RINA*, 1962.

138. Lofft, R. F., "Comparison of Computed Ship Motions with Model and Ship Results," *Proc. 11 ITTC*, Tokyo, 1966.

139. Longuet-Higgins, M. S., "On the Statistical Distribution of the Heights of Sea Waves," *J. Marine Research*, 1952.

140. Loukakis, T. A. and C. Chryssostomidis, "Seakeeping Standard Series for Cruiser-Stern Ships," *Trans. SNAME*, 1975.

141. I SSC, "Design Loads," *Proc. 6th ISSC*, 1976.

142. Maclean, W. and E. V. Lewis, "Analysis of Slamming on the S.S. *Wolverine State*," *MT*, 1973.

143. Mandel, P., "Some Hydrodynamic Aspects of Appendage Design," *Trans. SNAME*, 1953.

144. Mandel, P., "Subcritical and Supercritical Operation of Ships in Waves and the Coincidence of Maximum Damping," *JSR*, 1960.

145. Mansour, A. E., "Methods of Computing the Probability of Failure under Extreme Values of Bending Moment," *JSR*, 1972.

146. Mansour, A. and J. M. d'Oliveria, "Hull Bending Moment Due to Ship Bottom Slamming in Regular Waves," *JSR*, 1975.

147. Marks, W., T. R. Goodman, W. J. Pierson, Jr., L. J. Trick, and L. A. Vassilopoulos, "An Automated System for Optimum Ship Routing," *Trans. SNAME*, 1968.

148. Marsich, S. and F. Merega, "Strip Theory and Power Spectral Density Function: Application to the Study of Ship Geometry and Weight Distribution Influence on Wave Bending Moment," *Proc. 7th ONR Symposium on Naval Hydrodynamics*, 1968.

149. Maruo, H., "The Excess of Resistance for a ship in Rough Seas," *ISP*, 1957.

150. McCormick, M. E., "Ocean Engineering Wave Mechanics," John Wiley & Sons, 1973.

151. Meyerhoff, W. K., "Übersicht über grundlegende theoretische und experimentelle Arbeiten zum Problem der Bodenstösse bei Schiffen," *Trans. STG*, 1967.

152. Michell, W. H., "Sea Spectra Simplified," *MT*, 1968.

153. Moor, D. I., "Resistance Propulsion and Motions of High-Speed Single-Screw Cargo Liners," *Trans. NECIES*, 1966.

154. Moor, D. I., "Longitudinal Bending Moments on Models in Head Seas," *Trans. RINA*, 1967.

155. Moor, D. I. and D. C. Murdey, (a) "Motions and Propulsion of Single Screw Models in Head Seas," *Trans. RINA*, 1968 and (b) Motions and Propulsion of Single Screw Models in Head Seas, *Trans, RINA*, 1970.

156. Motora, S. and P. A. Lalangas, "Experimental Study of a Passive Anti-rolling Tank Installation in a Ship Model Running in Oblique Seas," DL Report 961, 1963.

157. Muckle, W., "A Note on the Buoyancy of a Ship amongst Waves," *Trans. RINA*, 1965.

158. Murdey, D. C., (a) "On Predicting Power Increase in Irregular Waves from Model Experiments in Regular Waves," and (b) "Some Effects of Tank Wall Interference on the Results of Experiments in Waves," *Proc. 13th ITTC*, Berlin-Hamburg, 1972.

159. Murdey, D. C., "Discussion on 'Longitudinal Bending Moments on Models in Head Seas,'" *Trans. RINA*, 1967.

160. Murdey, D. C., "On the Double Peaks in Wave Bending Moment Response Curves," *Trans. RINA*, 1969.

161. Murdey, D. C., "Pressures on the Bow Due to Wave Impacts," *NA*, 1972.

162. Nakamura, S., R. Hosoda, and A. Shintani, "Propulsive Performance of a Series 60, $C_B = 0.70$, Ship Model in Regular Head Waves," *Proc. 12th ITTC*, Rome, 1969.

163. Newton, R. N., "Wetness Related to Freeboard and Flare," *Trans. RINA*, 1960.

164. Norman, D. W., "Roll Stabilization Using Jet Flaps," *Proc. 3rd Ship Control Systems Symposium*, 1972.

165. Numata, E., "Longitudinal Bending and Torsional Moments Acting on a Ship Model at Oblique Headings to Waves," *JSR*, 1960.

166. Ochi, K. M., "Hydroelastic Study of a Ship Equipped with an Anti-pitching Fin," *Trans. SNAME*, 1961.

167. Ochi, M. K., "Extreme Behaviour of a Ship in Rough Seas," *Trans. SNAME*, 1964.

168. Ochi, M. K., "Statistical Properties of Powering Characteristics in Waves," *Proc. 15th TTC*, Ottawa, 1968.

169. Ochi, M. K., "On Prediction of Extreme Values," *JSR*, 1973.

170. Ochi, M. K. and L. E. Motter, "Prediction of Slamming Characteristics and Hull Response for Ship Design," *Trans. SNAME*, 1973.

171. Parker, M. N., "Brief Review of Ship Stabilizing Systems," *Shipping World and Shipbuilder*, 1964.

172. Patrick, D. A. and R. L. Wiegel, "Amphibian Tractors in the Surf," *Proc. 1st* Conference on *Ships and Waves*, 1954.

173. Planeix, J. M., "Wave Loads—A Correlation between Calculations and Measurements at Sea," *ISP*, 1972.

174. Pournaras, U. A., "A Study of the Sea Behavior of a Mariner Class Ship Equipped with Anti-pitching Bow Fins," DTNSRDC Report 1084, 1958.

175. Rawson, K. J. and E. C. Tupper, *Basic Ship Theory*, American Elsevier, New York, 1968.

176. Robb, A. M., *Theory of Naval Architecture*, C. Griffin and Co. Ltd., London, 1952.
177. Robb, A. M., "A Note on the Rolling of Ships," *Trans. RINA*, 1958.
178. Goodman, R. A., "Wave-Excited Main Hull Vibration in Large Tankers and Bulk Carriers," *Trans. RINA*, 1970.
179. Roseman, D. P., V. E. Johnson, and W. C. Webster, "Vehicles for Ocean Engineering," *Trans. SNAME*, Diamond Jubilee Meeting, 1968.
180. Russ, J. E., "Roll Computer," *Proc. 16th ATTC*, 1971.
181. Salvesen, N., E. O. Tuck, and O. Faltinsen, "Ship Motions and Sea Loads," *Trans. SNAME*, 1970.
182. Saunders, H. E., *Hydrodynamics in Ship Design*, SNAME, 1957.
183a. Savitsky, D., "On the Seakeeping of Planing Hulls," M.T. 1968.
183b. Savitsky, D. and P. W. Brown, "Procedures for Hydrodynamic Evaluation of Planing Hulls in Smooth and Rough Water." *Hampton Roads Section, SNAME*, 1975.
184. Scott, J. R., "Some Average Sea Spectra," *Trans. RINA*, 1968.
185. Scott, J. R., "A Sea Spectrum for Model Tests and Long-Term Ship Predictions," *JSR*, 1965.
186. Sellars, F. H., "The Limiting Height of Ocean Waves," Report 67–10, Ocean Engineering Dept., M.I.T., Cambridge, Mass., 1967.
187. Sellars, F. H., "Discussion on 'The Influence on Ship Motions of Different Wave Spectra and of Ship Length,'" *Trans. RINA*, 1967.
188. Sellars, F. H., "Water Impact Loads," SNAME, Chesapeake Section, 1975.
189. Sellars, F. H. and T. A. Loukakis, "The Analysis and Modelling of Irregular Waves," Report 66–5, Ocean Engineering Dept., M.I.T., Cambridge, Mass., 1966.
190. Silverleaf, A., "Discussion on 'Known and Unknown Properties of the Two-Dimensional Wave Spectrum and Attempts to Forecast the Two-Dimensional Wave Spectrum for the North Atlantic Ocean," *Proc. 5th ONR Symposium on Naval Hydrodynamics*, 1964.
191. Smiley, R. F., "A Semi-empirical Procedure for Computing the Water Pressure Distribution on Flat and V-Bottom Prismatic Surfaces during Impact or Planing," NACA Tech. Note 2583, 1951.
192. Smith, W., "Pitch and Heaving Motions for Arbitrary Ship Forms," *ISP*, 1967.
193. Spens, P. G., "Research on the Reduction of Pitching Motions of Ships by Controllable Fins," DL Report 913, 1962.
194. St. Denis, M. and W. J. Pierson, Jr., "On the Motions of Ships in Confused Seas," *Trans. SNAME*, 1953.
195. Stefun, George P., "Model Experiments with Fixed Bow Anti-pitching Fins," *JSR*, 1959.
196. Stevens, R. M., "New Dimensions for Naval Catamarans," *NEJ*, 1972.
197. Stiansen, S. G., and A. E. Mansour, "Ship Primary Strength Based on Statistical Data Analysis," *Trans. SNAME*, 1975.
198. Stoker, J. J., *Nonlinear Vibrations*, Interscience Publishers, New York, 1950.
199. Strom-Tejsen, J., H. Y. H. Yeh, and D. D. Moran, "Added Resistance in Waves," *Trans. SNAME*, 1973.
200. Swaan, W. A., "Amidships Bending Moments for Ships in Waves," *ISP*, 1959.
201. Swaan, W. A. and G. Vossers, "The Effect of Forebody Section Shape on Ship Behavior in Waves," *Trans. RINA*, 1961.
202. Swaan, W. A. and H. Rijken, "Speed Loss at Sea as a Function of Longitudinal Weight Distribution," *Trans. NECIES*, 1964.
203. Szebehely, V. G. and M. A. Todd, "Ship Slamming in Head Seas," DTNSRDC Report 913, 1955.
204. Takezawa, S., "A Study on the Large Bulbous Bow of High Speed Displacement Ships," *Trans. SNAJ*, 1962.
205. Tamiya, S. and S. Motora, *Advances in Research on Stability and Rolling of Ships*, 60th Anniversary Series, Vol. 6, SNAJ, 1960.
206. Tamiya, S., "A Calculation of Non-linear Non-symmetric Rolling of Ships," *Proc. 12th ITTC*, 1969.
207. Conolly, J. E., "Standards of Good Seakeeping for Destroyers and Frigates in Head Seas," *Proc. International Symposium on The Dynamics of Marine Vehicles and Structures in Waves*, Institution of Mechanical Engineers, London, 1974.
208. Tasai, F., "On the Deck Wetness and Slamming of Full Ship Forms," *Proc. 12th ITTC*, Rome, 1969.
209. Tasaki, R., "On Shipment of Water in Head Seas," *Proc. 10th ITTC*, London, 1963.
211. Thode, H., "*Messungen zur Stabilitätskontrolle im Bordbetrieb*," Hansa, 1954.
212. "Ship Power Prediction in Waves," *Proc. 12th ITTC*, Rome, 1969.
213. Ochi, M. K., "Performance of Two Hull Forms (U and V) in Irregular Waves," SNAME T and R Symposium, 1967.
214. Trillo, R. S., *Marine Hovercraft Technology, Leonard Hill Books*, London, 1971.
215. Truax, R. C., "Surface Effect Ships in the Surface Navy," *Proc. Naval Institute*, 1973.
216. Tucker, M. J., "A Shipborne Wave Recorder," *Trans. RINA*, 1956.
217. Van Den Bosch, J. J. and J. H. Vugts, "On Roll Damping by Free-Surface Tanks," *Trans. RINA*, 1966.
218. Van Dyck, R. L., "Seakeeping Characteristics of Four Members of Hydrofoil Hull Series 65," DL Report, 1973.
219. Van Oortmerssen, G., "The Motions of a Ship in Shallow Water," *Ocean Engineering*, Pergamon Press, 1976.
220. Van Sluijs, M. F. and T. S. Gie, "Behavior and Performance of Compact Frigates in Head Seas," *ISP*, 1972.
221. Van Sluijs, M. F., "Propeller Load Fluctuations and Performance in Regular and Irregular Waves," *Proc. 13th ITTC*, Berlin-Hamburg, 1972.
222. Vassilopolus, L. and P. Mandel, "A new Appraisal of Strip Theory," *Proc. 5th ONR Symposium on Naval Hydrodynamics*, 1964.
223. J. Vasta, A. J. Giddings, A. Taplin, and J. J. Stilwell, "Roll Stabilization by Means of Passive Tanks," *Trans. SNAME*, 1961.
224. Volpich, H., J. Rorke, and A. Tann, "Nähre Untersuchungen über Schlingertank-Anlagen," *Trans, STG*, 1968.
225. Von Schertel, B. H., "The Design and Application of Hydrofoils and Their Future Prospects," *Trans. I Mar. E.*, 1974.
225a. Vossers, G., "Behaviour of Ships in Waves," *ISP*, 1961.
226. Vossers, G., W. A. Swaan, and H. Rijken, (a) "Experiments with Series 60 Models in Waves," *Trans. SNAME*, 1960 and (b) "Vertical and Lateral Bending Moment Measurement on Series 60 Models," *ISP*, 1961.

227. Vossers, G. and W. A. Swaan, "Some Seakeeping Tests with a Victory Model," *ISP*, 1960.
228. Wachnik, Z. G. and E. E. Zarnick, "Ship Motions Prediction in Realistic Short-Crested Seas," *Trans. SNAME*, 1965.
229. Wachnik, Z. G., "Pitch and Heave Motions Prediction for the XR-3 Configuration," DTNSRDC Report 2920.
230. Wagner, H. "Ueber Stoss- und Gleitvorgänge an der Oberfläche von Flüssigkeiten," *Zeitschrift Angewandte Mathematik und Mechanik*, 1932.
231. ISSC, "Design Procedure," Report of Committee V. 1, 6th ISSC, Boston, 1976.
232. Wahab, R., "Das Verhalten eines schnellen Frachtschiffes mit konvenventionellem Bug und mit Wulstbug im Seegang," *Trans. STG*, 1966.
233. Wahab, R., Moss, L. W. "On the Added Drag of Destroyers in Regular Head Waves" DTNSRDC Report 3704, 1971.
234. Wahab, R., C. Pritchett, and L. C. Ruth, "On the Behavior of the ASR Catamaran in Waves," *MT*, 1971.
235. Ward, G., "Model Experiments in Regular Waves with Particular Reference to Wave Bending Moments Amidships," *Trans. RINA*, 1963.
236. Ward, G., "Cairndhu—Model Experiments in Regular Head Waves," *Trans. RINA*, 1964.
237. Webster, A. R., "The Design of the Canadian Weatherships," *Trans. RINA*, 1964.
238. Webster, W. C., "Analysis of the Control of Activated Anti-roll Tanks," *Trans. SNAME*, 1967.
239. Weinblum, G., *Die Bewegungsgleichungen des Schiffes im Seegang*, Schiffbau, 1931.
240. Weinblum, G., *Über den Einfluss der Schiffsform auf die Bewegungen eines Schiffes im Seegang*, Werft-Reederei-Hafen, 1933.
241. Murdey, D. C., "An Analyses of Longitudinal Bending Moments Measured on Models in Head Waves," *Trans. RINA*, 1972.
242. Weinblum, G. and M. St. Denis, "On the Motion of Ships at Sea," *Trans. SNAME*, 1950.
243. Weib, G., *Erfahrungen Mit der Stabilitätsprüfung durch Rollversuche*, Hansa, 1953.
244. Weib, G., "Ein Verfahren zur werftseitigen Vorausberechnung der Rollzeit," *Schiffstechnik*, 1955.
245. Wendel, K., *Rollschwingungen und Hebelarmkurve*, Schiffbau, 1940.
246. Wendel, K., "Hydrodynamische Massen und hydrodynamische Massenträgheitsmomente," *Trans. STG*, 1950.
247. Van Sluijs, M. F., "Ship Relative Motions and Related Phenomena," *Proc. International Symposium on the Dynamics of Marine Vehicles and Structures in Waves*, Institution of Mechanical Engineers, London, 1974.
248. Woollard, L., *Macrow's Naval Architect's and Shipbuilder's Pocket Book*, Technical Press, London, 1954.
249. Wright, E. A., "New Research Resources at the David Taylor Model Basin," *Trans. SNAME*, 1958.
250. Yamanouchi, Y., "On the Analysis of Ship Oscillations among Waves, Part I," *J. Zosen Kiokai* (*J. SNAJ*), 1961.
251. Yamanouchi, Y. and S. Ando, Experiments on a Series 60, $C_B = 0.70$, Ship Model in Oblique Regular Waves," *Proc. 11th ITTC*, Tokyo, 1966.
252. Yourkov, N., "Vertical Motions of Ships with Different Forms of Forebody," *ISP*, 1973.
253. Arentzen, E. S. and P. Mandel, "Naval Architectural Aspects of Submarine Design," *Trans. SNAME*, 1960.
254. Van Sluijs, M. F. and T. S. Gie, "The Effect of Water Depth on Ship Motions" *Proc. 14th ITTC*, Ottawa.
255. Tasaki, R. "Propulsion Factors and Fluctuating Propeller Load in Waves" *Proc. 14th ITTC*, Ottawa.
256. Beukelman, W. and M. Buitenhck, "Full-Scale Measurements and Predicted Seakeeping Performance of the Container Ship '*Atlantic Crown*'," ISP, 1974.
257. U. S. Navy, "Fundamentals of Submarine Hydrodynamics, Motion and Control" NAVSHIPS 0911-003-6010, 1971.
258. Cummins, W. E., "A Review of Free Surface Attraction on a Submerged Submarine," DTNSRDC Report C-1578, 1963.

INDEX

Accelerated motion, 39
  rotational, 55
Acceleration effects, 137
Acceleration spectrum, 150
Accelerometer, 159, 291, 292, 319, 323, 324, 325
Active antipitching fins, 304
Active antiroll tank, 329, 389, 390
Active fin, 293, 294, 295, 297
Active roll stabilizer, 291
Active roll tank, 290, 291, 390
Added mass, 36, 39, 40, 42, 43, 52, 64, 81, 100, 161, 162, 185, 186, 187, 203, 208, 251, 252, 256, 301, 346, 380
Added mass moment of inertia, 64, 67, 75, 77, 82, 83, 100, 203
Added power, 233, 234, 236, 335, 351
Added resistance, 53, 137, 220, 221, 222, 223, 224, 225, 227, 351, 373, 392, 404, 406
  in irregular seaway, 225, 228
Added resistance coefficient, 225
Added thrust, 233, 234, 235, 361, 374
Added torque, 233, 335, 359
Addition:
  of simple harmonic motions, 9
  of wave trains, 20
Advanced marine vehicles, 2, 396, 397
Advantages:
  of active antiroll tank, 292
  of U-tube tank, 290
Ahead sea, 31, 96
Air cushion vehicles, 2, 126, 373, 396, 411, 413, 414, 418
Amplitude, 5, 6, 7, 8, 10, 27, 36, 38, 39, 50, 87, 89, 148, 208, 230, 253, 265, 278, 372, 419
  of bending moment, 257, 258, 351
  of encountering force, 36
  of exciting force, 50, 52, 221
  of exciting moment, 70, 209, 221, 285
  of extreme value, 135
  of heaving motion, 36, 221, 253
  of motion, 6, 37, 45, 351
  of nonlinear rolling, 209
  of pitching moment, 72
  of pitching motion, 72, 153, 221, 299
  of resultant motion, 10
  of roll, 284
  of seaway bending moment, 267
  of shear force, 258
  of wave, 14, 17, 43, 115
Amplitude ratio, 43
Angular acceleration, 6, 63, 75, 241, 244, 304, 372, 399
Angular amplitude, 6
Angular displacement, 6, 75
Angular frequency, 5
Angular motion, 6, 202, 241, 399
Angular velocity, 6, 8, 10, 55, 63, 64, 75, 215, 219, 240, 241, 281, 283, 304
Antipitching fin, 297, 299, 302, 304, 305, 390
Antiroll fins, 390
Anti-roll tanks, 284
Aperiodic, 37, 67
Apparent period, 101
Apparent wave amplitude, 101
Apparent wave height, 101
Apparent wavelength, 101, 117
Apparent wave period, 107
Apparent zero-crossing period, 101
Aspect ratio, 294, 301, 390, 392
Astern sea, 159
Average:
  of one-hundredth highest rolls, 121
  of one-hundredth highest, 106
  of one-tenth highest, 124, 380
  of one-tenth highest rolls, 121
  of one-tenth highest waves, 106, 109
  of one-third highest, 416
Average apparent wavelength, 117
Average height:
  of one-third highest waves, 109
  of one-tenth highest waves, 109
Average increase in resistance, 232
Average period, 361
Average roll, 121, 131
Average wave height, 101, 109, 110
Average zero-crossing period, 116

Basic theory of slamming, 161
Beach, 318, 418
Beam, 335
Beam sea, 49, 50, 70, 90, 159, 174, 328, 351, 354, 401, 421
Beaufort number, 101, 238, 348, 358, 361, 372
Bench test, 291
Bending moment, 136, 244, 249, 250, 251, 252, 253, 254, 255, 256, 258, 262, 263, 264, 265, 266, 267, 268, 270, 271, 274, 275, 276, 277, 299, 308, 310, 319, 341, 348, 365, 373, 377, 385, 386, 400
  during heaving, 252
  during pitching, 253
  in regular waves, 256
Bending moment spectrum, 267, 268
Bifilar suspension, 313, 319
Bilge keel, 2, 77, 79, 278, 280, 281, 282, 291, 329, 390
Body accelerating force, 40
Bow acceleration, 158, 346, 348, 372, 390, 417
Bow-down moment, 419, 425
Bow emergence, 131, 138, 144, 145, 165, 308, 326, 327
Bow immersion, 143, 358

Bow motion, 138, 139, 143, 144, 309
Bow planes, 419
Bow sea, 168, 175, 351
Bow submergence, 153, 158, 159
Bow-towards moment, 425
Bow-up moment, 419
British towing tank panel (BTTP), 361
Broaching, 331, 400, 410, 425
Broadness parameter, 116, 135, 270, 373
BTTP spectrum, 361
Bulbous bow, 239, 299, 319, 332, 350, 374
Buoyancy distribution, 249, 253
Buoyancy force, 161, 249, 256, 415

Calculation:
  of added mass, 40
  of coupled motions, 191
Canard configuration, 410
Catamaran, 250, 308, 396, 397, 398, 400, 401, 402, 418
Cauchy number, 329
Celerity, 17, 18, 19, 323
Center of gravity, 36, 311, 319
  of histogram, 107
Centrifugal force, 241
Characteristic frequency, 5, 14
Characteristic of tank, 288
Characteristic wave height, 101
Circular frequency, 8, 15, 25, 30, 36, 37, 38, 40, 117, 241, 252, 321
Classification of seas, 101
Coefficients:
  for pitching motion, 64
  for rolling, 75
Compound pendulum, 288
Constant revolution, 230
Constant rpm, 232
Constant speed, 230, 231, 232, 233
Constant thrust, 224, 228
Constant velocity, 224
Contouring, 409, 410
Corkscrew motion, 399, 400
Correction factor, 116, 117, 119, 120, 131, 132, 133, 148, 157, 373
Coupled heaving and pitching, 183, 206, 253, 346
Coupling effect, 144, 348, 351, 413
Crest-to-crest period, 116, 117
Critical zone, 96, 97
Curve:
  of declining angles, 79
  of extinction of rolling, 80

Damped frequency, 67
Damped oscillation, 36
Damped period, 37, 81
Damped pitching period, 67
Damped rolling period, 81, 82
Damping coefficient, 43, 45, 46, 52, 64, 65, 72, 77, 80, 100, 162, 203, 208, 209, 222, 223, 278, 299, 300, 301, 307, 327, 348
  from experiment, 79
Damping constant, 36, 186
Damping factor, 38, 46, 52, 89, 90, 216, 217, 218, 219
Damping force, 36, 43, 45, 77, 161, 187, 202, 250, 281, 301, 305
Damping force coefficient, 46, 65
Damping moment, 63, 64, 69, 75, 77, 81, 83, 208, 215, 278, 280, 281
  rolling, 77
Damping moment coefficient, 75, 77
Damping stabilization, 278
Data for seakeeping design, 373
Deadrise angle, 162, 329, 330, 382, 400, 405, 417
Decaying constant, 37
Deck wetness, 53, 68, 131, 137, 153, 278, 308, 309, 331, 338, 341, 348, 354, 369, 380, 397, 418
Deep-vee hulls, 402
Deep water wave, 315
Definitions of sea conditions, 104
Depth effects in waves, 22
Depth maintenance, 425
Design considerations for slamming, 380
Design criterion, 369, 372, 392
Design parameters, 332
Design plot, 392, 393
Determination of coefficients for rolling motion, 75
Directional spectrum, 322, 323
Direct power method, 233, 235, 236
Displacement-length ratio, 68
Diversified tank stabilizer, 290
Draft, 335
Dynamic effects, 1, 2, 68, 137, 145, 153, 174, 267, 278, 319, 331, 332, 361, 377, 379, 380
Dynamic loads, 249, 272, 274, 276, 309
Dynamic preparation of model, 314
Dynamic response, 38, 45
Dynamic similarity, 310
Dynamic swell-up, 154, 326
Dynamometer, 310, 319

Effect:
  of damping, 43
  of dynamic swell-up, 154
  of impact, 158
  of rolling, 237
  of shallow water on ship motion, 98
  of statical swell-up, 154
Effective freeboard, 155, 156, 326
Effective horsepower, 225, 233, 350, 378
Effective length of U-tube, 289
Effective maximum wave slope, 34
Effectiveness of motion stabilizers, 305
Effective wavelength, 31, 49, 50, 51, 70, 71, 191, 258, 286
Effective wave number, 49, 139, 286
Effective wave profile, 49, 50
Emergence of forefoot, 1
Encountering angle, 30
Encountering force, 36
Encountering frequency, 30, 31, 38, 40, 43, 64, 75, 86, 89, 95, 127, 131, 148, 164, 213, 222, 227, 234, 278, 321, 327, 402, 416
Encountering period, 30, 33, 327
Encountering sea spectrum, 227
Encountering wavelength, 50
Encountering wave spectrum, 125, 130, 148, 169, 173, 413
Energy per unit wave surface, 18
Energy spectrum, 111, 112, 113, 114, 115, 131, 304, 315, 354, 418

Equation of heaving motion, 39
Equation of motion, 36, 43, 67, 71, 161, 190, 206, 216, 217, 222, 285, 286, 299, 304
  for rolling, 75, 81, 217
Equation of pitching motion, 73
Equation of rolling, 209
Equation of wave motion, 73
Equilibrium stabilization, 278, 279
Even moments, 116
Exciting force, 35, 36, 38, 45, 47, 49, 50, 52, 96, 98, 186, 188, 189, 190, 191, 206, 222, 256, 258, 273, 278, 279, 333, 359, 398, 402
  for heaving, 50, 52, 253, 351
Exciting force coefficient, 50
Exciting moment, 63, 64, 75, 98, 189, 209, 256, 278, 279, 283, 285, 286, 287, 294, 333
  for pitching, 69, 70, 72, 73, 253, 299, 351
  for rolling, 84, 351
Experimental determination:
  of coefficients, 206
  of damping, 45
Extinction curve, 45, 348
Extinction equation, 80, 215
Extreme value, 115, 134, 135, 136, 376
  as design consideration, 375

Facilities and instrumentation, 315
Factors responsible for loss of speed, 220
Fin stabilization, 292
First moment of weight, 310
Fixed fins, 297
Floating vehicle, 400
Flume tank stabilization, 290
Following sea, 28, 31, 96, 125, 168, 170, 174, 217, 294, 308, 319, 330, 351, 402, 407, 421, 425
Forced heaving motion, 38
  damped, 37
Forced oscillation, 36, 38, 45, 46, 87, 89, 90, 419
Forced rolling, 329
Forces:
  due to heaving, 240
  due to pitching, 245
  due to rolling, 241
Forcing function, 187, 189, 190, 203, 222
Forebody immersion, 153
Foredeck immersion, 141
Forefoot emergence, 139, 141, 144, 153, 159, 165, 358, 380
Frahm tank, 287
Frahm U-tube, 291
Freeboard and flare, 341
Free damped heaving motion, 37
Free oscillation, 36, 38, 39, 45, 279
  damped, 37
Free Racing, 137
Free surface tank, 284, 285, 290, 386
Free undamped heaving motion, 37
Frequency of encounter, 30, 31, 38, 53, 95, 123, 124, 125, 127, 131, 150, 168, 169, 173, 174, 178, 188, 208, 209, 222, 231, 272, 285, 286, 302, 321, 416
Frequency of occurrence of slamming, 165, 329
Frequency response function, 129, 269
Froude's law, 167, 224, 286, 310, 326, 329
Full-scale slam loads and midship stress, 276
Full-scale tests, 322, 412
Full-scale thrust, 235
Full-scale trials, 2, 3, 148, 177, 238, 263, 274, 297, 308, 322, 325, 327, 329, 335
Fully developed sea, 112, 113
Fully-submerged foil, 397, 407, 408, 410, 411

Gaussian law, 116
Gaussian or normal distribution, 106
Girth length of tank, 289
Glossary of seakeeping terms, 478
Gravity towing system, 224, 228
Green water, 137
Group velocity, 26, 27, 28
Group wave, 28
Gyradius, 319, 320
Gyroscope, 283, 297, 318
Gyroscopic inertia, 283
Gyroscopic sensing system, 292
Gyroscopic stabilizer, 280, 282

Habitability, 331, 372, 399, 400
Hard-chine hulls, 402
Harmonic motion, 4, 9, 21, 311, 419
Head sea, 28, 40, 97, 125, 144, 145, 167, 177, 183, 202, 221, 225, 238, 239, 256, 272, 319, 328, 330, 346, 348, 351, 354, 358, 359, 365, 390, 397, 398, 402, 421
Heading angle, 49, 89, 323, 354
Heaving, 35, 36, 37, 39, 47, 48, 137, 145, 148, 154, 220, 222, 223, 228, 240, 250, 256, 257, 258, 262, 319, 331, 333, 348, 350, 351, 359, 373, 374, 397, 398, 402, 403
Heaving acceleration, 49, 53, 185, 351
Heaving amplitude, 52, 202, 348, 351, 359
Heaving force, 50, 191, 203
Heaving motion, 159, 169, 177, 182, 183, 184, 203, 221, 224, 252, 253, 265, 267, 272, 302, 318, 321, 327, 338, 345, 346, 348, 373, 390, 402, 412, 413, 417
Heaving period, 36, 37, 47, 49, 68
Histogram, 106, 109, 110, 115, 120, 121, 123, 148, 155, 321, 385
  of midship slam stress, 276
  of wave elevations, 106
Hogging, 170, 249, 251, 254, 255, 263, 266, 267, 277, 351, 365, 400
Hogging wave bending moment, 272
Horizontal motion, 228
  bending, 250, 272, 386
Hovercraft, 3, 372, 397, 410, 411, 413, 418
Hull girder bending moment, 276, 310
Hull girder deflections, 309
Hull girder loads, 309, 310
Human habitability factor, 3, 372
Hydrodynamic coefficient, 190, 191, 300, 398
Hydrofoil boats, 2, 396, 397, 406, 409, 410, 411
Hysteresis phenomena for nonlinear motion, 210

IMCO, 327
Impact acceleration, 402
Impact due to shipping of green water, 159
Impact load, 249, 330

Impact pressure, 137, 159, 160, 329, 330, 346, 358, 380, 381, 384, 400, 418
Inertia force, 2, 36, 39, 40, 48, 49, 52, 161, 186, 187, 240, 241, 244, 246, 249, 251, 252, 256, 264, 266, 272, 329, 330
Inertial bending moment, 244, 265, 266, 267, 373
Inertial coefficient, 40
Inertial moment, 63, 75
Interval between slam impacts, 167
Irregular seaway, 17, 148, 224, 228, 232, 233, 267, 290, 291, 292, 306, 308, 321, 322
Irregular waves, 101
Irregular wave test, 228, 272, 321
ISSC, 134
ITTC, 117, 125, 134, 172, 225, 327, 361, 369, 373
ITTC spectrum, 125, 326
ITTC standards for seakeeping experiments, 319

Jet flap, 280, 295, 296
Jump phenomenon, motion, 210, 211

Kinetic energy, 6, 14, 24, 218, 219

Lateral bending moment, 271, 386
Law of decay, 216
LCG-LCF separation, 346
Length, 333
Lewis form, 40
Lewis sections, 77
Lift force, 293, 294, 295, 296, 297, 300, 305
Linear acceleration, 244
Linear damping, 209, 215, 216, 217, 390
Linear equation of motion, 209
Linear restoring moment, 209
Linear restoring moment with time dependent coefficient, 217
Linear rolling, 208
Linear superposition technique, 128, 134, 224, 225, 227, 232, 234, 267, 308, 321, 373
Linear theory of ship motion, 136
Linearity of motion, 190
Liquid accelerating force, 40
Load, 253, 385
Load determination, 310
Load waterline, 50
Loads, 385
  due to motion, 240
  in irregular waves, 267
Long crested, 14, 101, 171, 237, 272, 317, 326, 327, 354, 373
Longitudinal bending moment, 267
  in head sea, 365
Longitudinal gyradius, 319
Longitudinal radius of gyration, 68, 348, 359, 365, 373
Long term distribution, 271
Loss of propulsive efficiency, 358
Loss of speed, 2, 220, 224, 299, 386
Low waterplane (LWP) catamarans, 397
Lurching, 214

Magnification factor, 38, 45, 71, 87, 89, 96, 134, 299, 327, 348
Mass moment of inertia, 59, 64, 67, 82, 282, 283, 312, 313
Mathieu's equation, 217
Maximum acceleration, 240, 241, 246, 328, 348
Maximum effective wave slope, 208, 279
Maximum heaving acceleration, 252
Maximum pitching acceleration, 245
Maximum wave slope, 33
Mean added resistance, 221, 227, 228, 233
Mean draft, 189, 380
Mean increase:
  in power, 233
  in propeller revolution, 234
  in propeller torque, 233, 234
  in thrust, 228, 230, 231, 232
Mean propeller revolution, 321
Mean propeller thrust, 321
Measure of merit, 392, 393
Measurement of seawaves, 322
Metacentric height, 311, 387, 389, 398
Method of bifilar suspension, 313
Model preparation, 309, 319
Model tests, 2, 3, 13, 42, 145, 148, 177, 190, 207, 227, 229, 235, 237, 249, 250, 263, 274, 291, 296, 305, 308, 309, 327, 328, 329, 333, 341, 354, 359, 373, 381, 413, 418
Modulus of elasticity, 310
Moment of inertia, 250, 282, 285, 311, 332, 348
Most probable largest amplitude, 119
Most probable largest value, 135, 136, 271, 375, 376
Most probable largest wave amplitude, 119
Motion:
  in short-crested seaway, 173
  in shallow water, 98
Motion equation, 187
Motion prediction in an irregular seaway, 123
Motion sickness, 169, 297
Motion spectrum, 131, 150, 305, 322
Motion stabilization, 2, 3, 39, 278, 284, 287, 292, 294, 322, 359, 386, 418
Movement of weight, 280, 282
Muirhead-Brown system, 292
Multicushion craft, 413
Multi-directional irregular seaway, 330
Multiple regression analysis, 359, 365

Narrow frequency spectrum, 116
Natural circular frequency, 67, 82
Natural frequency, 36, 37, 38, 45, 53, 67, 75, 82, 96, 209, 273, 278, 282, 285, 286, 287, 304, 306, 327, 387, 389, 390, 412, 413
Natural period, 36, 82, 159, 213, 217, 278
  heaving, 37, 47, 49
  of rolling, 399
Natural pitching period, 67, 68, 167, 385, 399
Natural roll frequency, 169
Node, 21, 28
Nondimensional added resistance, 224, 358
Nondimensional amplitude of exciting moment, 70, 85
  of pitching moment, 72
Nondimensional damping coefficient, 46, 66, 71, 72, 80, 87, 89
Nondimensional damping factor, 38
Nondimensional exciting moment, 86
Nondimensional frequency parameter, 96, 223
Nondimensional heave response, 173
Nondimensional heaving force, 51
Nondimensional roll response, 173
Nonlinear damping, 203, 209, 214, 219

Nonlinear motion, 208, 219
Nonlinear restoring moment, 209, 213, 219
Nonlinear rolling, 208, 209, 272
Normal distribution, 106, 167
Normal (Gaussian) probability distribution, 232
Number of deck immersions, 156
Number of occurrences of deck wetness, 156

Ocean engineering vehicles, 396, 400, 402
Ocean waves, 1
One degree of freedom of motion, 183
One-dimensional spectrum, 171
One-dimensional wave spectrum, 177, 305, 322
Open water propeller characteristics, 228, 230, 231
Operability, 331
Orbital motion, 228, 229, 408
Oscillator, 45, 329
Oscillatory rotational motion, 6
Oscillatory translational motion, 6
Overtaking sea, 31, 96, 97

Passive roll stabilizer, 282
Passive tank stabilizer, 284, 290, 291
Peak bending moment, 365
Period of encounter, 30
Period of motion, 4
Period of oscillation, 6
Period of pitching, 246
Period of roll, 244
Period of waves, 18
Phase angle, 7, 8, 9, 10, 11, 15, 16, 37, 38, 50, 53, 54, 70, 71, 72, 85, 87, 90, 138, 144, 154, 191, 203, 253, 267, 285, 286, 287, 321, 327, 358
Phase difference, 7, 9, 25, 72, 87, 144, 145, 159, 202, 203, 272, 275, 285, 287
Phase lag, 45, 53, 127, 189, 190, 191, 202, 221, 222, 256, 291, 390
Phase relationship, 53, 73, 222, 223, 276, 304, 329
Phase shift, 7, 8
Phase velocity, 14, 17
Physical pendulum, 311, 312
Pitch angular velocity, 299, 300
Pitch stabilization, 297, 305, 392
Pitching, 35, 63, 145, 148, 153, 159, 202, 221, 223, 228, 240, 262, 265, 267, 272, 319, 321, 327, 331, 348, 350, 351, 386, 390, 397, 400, 402, 417
Pitching acceleration, 246, 417
Pitching amplitude, 245, 246, 354, 359
Pitching moment of inertia, 57, 72
Pitching motion, 67, 72, 136, 154, 159, 174, 177, 178, 186, 202, 220, 222, 224, 246, 250, 253, 256, 258, 279, 297, 299, 304, 313, 318, 328, 333, 335, 337, 346, 348, 350, 351, 359, 373, 374, 390, 398, 402, 403, 411, 412, 417, 421
Pitching period, 68, 246, 372, 419
Pitching radius of gyration, 58
Pitching in waves, 71
Pivotal method, 311, 313, 314
  for pitching radius of gyration, 313
Planing crafts, 2, 396, 397, 402
Platforming, 409
Point spectrum, 125
Point wave spectrum, 323
Polar diagram, 392, 393
Potential energy, 6, 24, 219
Pounding, 326
Power increase, 233, 234, 235, 236, 237, 238, 351, 361
  due to wind and waves, 238
Powering in seaway, 220
Precession, 283, 292
Prediction:
  of added power, 232
  in irregular seaway, heaving, 114
  by regression analysis, 359
Presentation of results, 322
Pressure, 18, 19, 25, 26, 161, 162, 163, 164, 165, 187, 217, 249, 274, 275, 280, 305, 317, 323, 325, 329, 330, 346, 380, 381, 382, 413, 417, 418, 419
  on deck, 157
  in wave, 23
Pressure attenuation factor, 187, 323
Pressure devices, 323
Pressure distribution, 162, 280
Pressure gradient, 256
Pressure peak, 163
Pressure sensor, 323, 324, 325
Probability:
  of deck wetness, 153, 155, 156, 157, 341
  of occurrence of different wave heights, 109
  of peak sagging stress, 271
  of pressure, 157
  of shipping green water, 154, 326
  of slamming, 153, 159, 165, 167, 326, 335, 380
Probability density per foot, 107
Progressive wave, 14, 22
Propeller efficiency, 231, 235, 374
Propeller emergence, 327, 370, 418
Propeller loading, 231, 234, 235, 321
Propeller open water tests in waves, 228, 321
Propeller racing, 221, 239, 322, 361, 370
Propulsive efficiency, 220, 233, 327, 377, 378

Quartering sea, 250
Quasi-static or ordinary wave load, 273

Radius of gyration, 56, 57, 58, 61, 64, 75, 81, 208, 251, 256, 264, 310, 311, 312, 313, 319, 327, 348, 350, 361, 373
RAO, 130, 131, 134, 148, 150, 168, 169, 173, 227, 229, 232, 233, 267, 268, 413, 414, 416
Ratio of response amplitude to wave amplitude, 93
Rayleigh distribution, 107, 108, 109, 110, 113, 115, 116, 119, 120, 123, 131, 132, 135, 141, 148, 155, 177, 182, 232, 270, 271, 306, 376
Rayleigh law, 110, 116
Regular seaway, 137, 253
Regular wave test, 229, 233, 272, 321, 418
Relative acceleration, 160, 162, 186, 187, 262
Relative bow acceleration, 141
Relative bow motion, 141, 143, 148, 153, 154, 156, 157, 165, 175, 321, 322, 326, 341, 346, 348, 351, 358
Relative bow velocity, 145, 147, 148, 153, 159, 160, 165, 326, 370
Relative bow vertical velocity, 167
Relative motion, 53, 54, 167, 183, 373, 374, 376, 380, 390, 400, 411, 418

Relative motion spectrum, 157
Relative rotative efficiency, 230, 231, 235, 378
Relative velocity, 1, 148, 153, 160, 161, 163, 164, 165, 167, 187, 274, 304, 330, 370, 373, 374, 381, 382, 400
Relative velocity spectrum, 157
Relative vertical motion, 150, 184
Relative vertical velocity, 141, 148, 150, 162, 186
Resistance augmentation, 237
Resistance experiments in regular waves, 224
Resistance test, 228, 319
Resonance, 39, 46, 47, 53, 66, 68, 72, 87, 89, 96, 169, 208, 217, 218, 219, 223, 273, 278, 279, 282, 291, 306, 321, 327, 338, 351, 354, 398, 400, 416, 419
Response amplitude operator, 123, 127, 129, 224, 227, 267, 272, 305, 321, 322, 327, 354, 373, 374, 386
Response curve, 209, 211, 233, 235, 255, 306, 365, 398
Response in irregular seaway, 121
Response spectrum, 121, 123, 130, 131, 132, 148, 150, 151, 156, 165, 168, 169, 173, 175, 227, 233, 267, 270, 374, 376, 380, 413
  for relative bow motion, 382
Restoring force, 4, 5, 6, 35, 36, 47, 208, 319, 407, 409, 417
  heaving, 47
Restoring force coefficient, 47, 52, 207
Restoring moment, 6, 63, 64, 66, 75, 170, 209, 217, 218, 412
Restoring moment coefficient, 64, 66, 67, 75, 80, 207, 209
Resultant loads during pitch and roll, 247
Resultant motion, 10, 11
Resultant stress, 250
Revolution increase, 322
RMS, 131, 132, 227, 374
Rolling, 35, 75, 148, 168, 169, 211, 220, 237, 240, 241, 243, 250, 278, 279, 284, 287, 290, 291, 293, 294, 331, 386, 400, 411, 417
  in calm water, 81
  in regular seaway, 86
Rolling chocks, 419
Rolling effects, 137, 168
Rolling motion, 294, 295, 296, 304, 305, 319, 329, 331, 348, 354, 373, 397, 398, 400, 401, 402, 410, 419
Rolling period, 68, 82, 237, 400, 419
Rollover, 412, 413
Roll stabilization, 279, 282, 293, 297, 390
Root mean square (rms), 108, 116, 122, 321, 374
Rough estimates of the percentage of speed loss, 239
Round-Bottom hulls, 402
Rudder, 220, 294, 296, 297, 304, 329
Rudder action, 280, 297, 329
Rudder induced roll moment, 296
Rudder stabilization, 296
Runge-kutta method, 219

Sagging, 170, 249, 251, 254, 255, 263, 267, 365
Sagging bending moment, 274, 351
Sagging wave bending moment, 272
Scale effect, 2, 224, 308, 309, 329
Scale factor, 49, 55, 167, 202, 234, 310
Seakeeping, of advanced marine vehicles, 396
Seakeeping criteria, 332
Seakeeping design, 124
Seakeeping prediction, 325
Seakeeping tables for extended series, 60, 427
Seasickness, 169, 372, 399
Sea state, 101, 168, 267, 315, 326, 346, 358, 373, 374, 377, 378, 379, 380, 382, 384, 385, 392, 393, 400, 402, 412
Sea trial, 250
Seaway bending moment, 249, 258, 264
Seaway bending moment coefficient, 264
Section modulus, 251, 272, 275
Self-propulsion factors, 230, 231, 233
Self propulsion test, 228, 229, 231, 233, 237
Semi-submersibles, 400, 401
Series 60 hull forms, 373
SES, 414, 415, 417, 418
Shallow water, 17, 20, 28, 315, 330, 392, 408
Shape of forebody sections, 345
Shear force, 186, 249, 251, 253, 256, 257, 258, 310
Shipborne wave recorder, 322, 323, 325, 330
Ship heading, 49, 351, 354
Ship model correlation, 55
Shipping of green water, 137, 153, 221, 239, 273, 274, 276, 322, 335, 341, 358, 361, 380
Ship speed in seaway, 377
Ship speed zones, 95
Ship in waves, 28
Short crested seaway, 171, 173, 237, 317, 354
Significant roll, 121, 133, 392
Significant wave amplitude, 119
Significant wave height, 105, 117, 119, 125, 134, 157, 225, 271, 358, 361, 373, 382, 384, 410
Significant wave period, 117
Simple harmonic, 128, 137, 265
Simple harmonic motion, 4, 5, 7, 9, 10, 15, 16, 36, 63, 140
Simple harmonic wave, 33
Simpson's rule, 172
Single or multiple flap wave generators, 315
Sinusoidal water waves, 13
Sinusoidal wave, 14, 15, 17, 18, 23, 24, 110, 111, 128, 184
Six-degrees of freedom, 183, 308, 330
Slamming, 1, 2, 137, 141, 159, 160, 164, 239, 249, 273, 274, 276, 278, 308, 309, 325, 326, 329, 335, 346, 354, 358, 361, 380, 381, 382, 400, 411, 418
Slamming of SES, 418
Slamming pressure, 160, 164, 358, 380, 381, 400
Slam stress, 276
Ship in waves, 28
Short-crested seaway, 171
Simple harmonic motion, 4, 5, 6, 14
Sinusoidal water waves, 13
Slamming, 68, 131, 153, 159, 165, 221, 273, 275, 297, 299, 308, 322, 331, 370, 397
Slamming pressure, 160, 164
Slamming probability, 165
Small waterplane area twin hull (Swath), 397
Smith correction, 69, 249
Smith effect, 26, 250, 256
Snap roll, 419
Solution of coupled heaving and pitching, 190
Spar vehicle, 402
Specific design requirements, 377
Spectral density, 113, 114, 115, 123, 125, 129, 131, 148, 171, 172, 173, 175
Speed loss, 137, 220, 221, 225, 238, 239, 297, 326, 338, 341, 348, 410, 411, 418

Speed reduction, 169, 335, 386
Speed zones, 95
Spreading function, 171, 172
Spring constant, 36
Springing, 270, 273
Springing bending moment, 273
Springing load, 273
Squatting, 425
Stability in waves, 169
Stabilizer trials, 328
Stabilizing fins, 280
Stabilizing moment, 278, 279, 283, 287, 291, 293, 294, 295, 299, 304, 329, 419
Stabilizing tanks, 282, 329
Standard wave spectrum, 117, 125
Standing wave, 14, 20, 21
Static bending moment, 244, 256, 272
Static heave, 52
Static heaving amplitude, 38, 52
Static pitch angle, 71
Static pitch deflection, 72
Static restoring force coefficient, 207
Static roll angle, 390
Static stability, 170, 386
Statical swell-up, 153, 154, 326
Stationary point spectrum, 125
Statistical average, 116
Steady-state load, 273
Steady-state oscillation, 36
Stern acceleration, 346, 348, 417
Stern planes, 419
Still water bending moment, 251, 271, 337, 385
Still water loads, 251, 385
Stochastic nature, 128
Strength bar, 310
Strip theory, 43, 45, 64, 98, 128, 168, 183, 190, 191, 202, 203, 222, 223, 253, 256, 258, 266, 268, 273, 308, 326, 327, 330, 365, 373, 398
Subcritical zone, 96, 97
Subharmonic oscillation, 213
Subharmonic responses, 418
Submarine, 396, 418, 419, 421
Submersibles, 400, 402
Suction force, 418, 419, 421, 425
Sudden inclining moment and capsizing, 218
Supercritical zone, 96, 346
Superposition principle, 131
Superposition technique, 131
Surface effect ship, 2, 308, 372, 396, 397, 411, 414, 418
Surface piercing foil, 397, 407, 409, 411
Surging, 35, 47, 228, 262, 321
Survivability, 331
SWATH, 397
Swaying, 35, 47, 220
Swell, 116
Swell-up of water, 153, 321
Synchronism, 38, 45, 87, 89, 174, 202, 333

Tandem or conventional configuration, 410
Tangential acceleration, 241, 243, 244
Tangential force, 241, 246
Tank moment, 286, 387
Tank moment coefficient, 289
Tank stabilizers, 284, 419
Tank wall interference, 206, 320
Tests in regular waves, 321
Three-dimensional effect, 202, 203
Three-dimensional irregular seaway, 171, 177
Threshold velocity, 160, 161, 165, 167, 326
Thurst and torque, 228
  in irregular waves, 231
Thrust deduction factor, 231
Thrust deduction fraction, 374, 378
Thrust increase, 229, 231, 319, 322, 338, 350, 358, 359
Thrust increase coefficient, 335
Thrust method, 234, 236
Time-dependent coefficient, 218
Time history of whipping stress, 276
Time interval between successive impacts, 167
Thrust increase, 228, 229
Torque increase, 229, 322, 359
Torque-RPM method, 234, 235, 236
Torsional (or twisting) moment, 250, 272
Total bending moment, 250, 251, 258, 270, 365
Total energy, 24, 25, 111, 112, 115, 125
Total extreme bending moment, 271
Total power, 235
Total resistance, 237
Total transverse force, 241
Total vertical force, 241
Transfer function, 271, 308, 329
Transform spectrum, 123
Transient loads, 273
Transient motion, 38, 39
Transient oscillation, 36
Transverse bending moment, 250
Trim angle, 404
Trimaran, 400, 402
Trochoidal wave, 14, 249, 256
Trough, 14, 23, 24, 26
Tuning factor, 38, 39, 52, 87, 90, 95, 96, 278, 290
Tuning stabilization, 278
Two-dimensional spectrum, 171, 172
Two-dimensional wave spectrum, 177
Typical rolling periods, 85

U-tube tank, 284, 287, 288, 290, 389, 390
U-type ship, 46
Uncoupled heaving, 35, 203
Uncoupled pitching, 35, 203
Uncoupled rolling, 35
Undamped heaving, 38, 48
Undamped nonlinear equation, 213

V-Type section, 46
Variance, 115, 120, 141, 157, 165, 182, 382
Vector representation, 9
Velocity of oscillation, 43
Velocity spectrum, 150
Venturi effect, 419, 421, 425
Vertical acceleration, 1, 36, 68, 116, 141, 169, 186, 253, 302, 318, 319, 321, 322, 327, 328, 335, 369, 373, 380, 406, 410, 417
Vertical bending moment, 250, 257, 272, 337, 350, 365, 386

Vertical effects, 137, 168
Vertical motion, 49, 50, 137, 150, 183, 184, 186, 228, 265, 302
Vertical velocity, 116, 140, 145, 150, 163, 164
Virtual mass, 36, 47, 49, 52
Vritual mass moment of inertia, 63, 64, 75, 208, 209, 299
Virtual radius of gyration, 75, 76
Viscous damping, 251, 373
Voluntary and involuntary speed loss, 221
Voluntary power reduction, 228
Voluntary speed reduction, 159, 331, 370, 379

Wake fraction, 230, 231, 235, 374, 378
Wall effect, 320
Water wave, 13
Waterplane area coefficient, 47, 50, 51, 70, 338, 341, 359, 361, 365
Wave:
  properties of harmonic waves in deep water, 18
  properties of harmonic waves in water of any depth, 19
Wave amplitude, 15, 52, 95, 110, 116, 124, 127, 129, 173, 174, 190, 224, 227, 229, 231, 233, 267, 286, 317, 319, 321, 322, 327, 329, 358, 417
Wave bending moment, 123, 160, 250, 251, 258, 263, 264, 265, 266, 267, 270, 271, 272, 273, 274, 322, 337, 338, 338, 354, 359, 373, 386
Wave bending stress, 276
Wave characteristics, 351
Wave crest, 14, 19, 23, 33, 171, 187, 191, 249, 250, 254, 263, 265, 266, 321, 322, 323, 402, 417
Wave damping, 251
Wave direction, 351, 354, 401
Wave elevation, 101, 115, 116, 233, 258, 329
Wave energy, 6, 24
Wave energy spectrum, 110
Wave frequency, 16, 30, 31, 40, 145, 171, 178, 317, 419
Wave height, 33, 105, 111, 131, 171, 224, 229, 230, 233, 237, 267, 302, 305, 321, 323, 324, 325, 354, 358, 359, 402, 410, 412, 416, 421
Wavelength, 14, 17, 18, 22, 25, 27, 28, 33, 49, 110, 111, 112, 127, 191, 203, 225, 230, 233, 255, 263, 268, 285, 304, 317, 320, 321, 323, 327, 341, 345, 350, 351, 358, 365, 386, 402, 416, 417, 421
Wave loads, 249, 277, 308, 386, 418
  in regular seaway, 253
Wavemaker, 315, 317, 318, 321
Wave motion, 72, 419
Wave number, 16, 18, 49, 50, 174, 221, 322
Wave period, 17, 18, 30, 90, 105, 111, 323, 324
Wave propagation, 14
Wave reflection, 220
Wave slope, 18, 33, 208, 290, 294, 387, 412, 419
Wave spectrum, 110, 113, 114, 115, 116, 120, 123, 125, 130, 131, 132, 171, 178, 225, 232, 233, 268, 273, 322, 325, 373
Wave trough, 249
Wave velocity, 17, 18, 19, 145
Weight distribution, 251, 255, 263, 264, 267, 310, 319, 350, 373
Whipping, 159, 249, 274, 276
Whipping stress, 160, 274, 275, 276, 326, 370, 380
Wind generated seas, 116
Wind speed, 25, 112, 117

Yaw-heel effect, 294
Yaw moment, 296
Yawing, 35, 47, 220, 272, 386
Yawing moment of inertia, 57

Zero-crossing period, 116, 117
Zero up-crossing, 116